Overcoming Limitations in Carbonyl-Olefin Metathesis Through Novel Catalytic Approaches

by

Ashlee J. Davis

A dissertation submitted in partial fulfillment
of the requirements for the degree of
Doctor of Philosophy
(Chemistry)
in the University of Michigan
2022

Doctoral Committee:

Associate Professor Corinna S. Schindler, Chair
Professor Anne J. McNeil
Professor Peter J. H. Scott
Professor John P. Wolfe

Ashlee J. Davis

dashlee@umich.edu

ORCID iD: 0000-0003-3347-7537

Dedication

To my mom, Lisa, who has supported me endlessly.

Acknowledgements

The work presented in this dissertation was achieved through the unending support of a large community of colleagues, friends, and family. I would like to thank my dissertation committee, Professor Corinna S. Schindler, Professor Anne J. McNeil, Professor John P. Wolfe, and Professor Peter J. H. Scott, for the outstanding advice and encouragement they have provided over the last five years. Your guidance has helped shaped the outcome of my graduate studies. I would also like to thank Professor Brian P. Coppola, who I had the pleasure of teaching Chem 220 with. It was such a pleasure learning how to engage and connect with students on a deeper level.

I would also like to thank my colleagues and labmates that I have worked with over the years. My fondest memories of my time in Michigan are centered around the friends that I have made. Particularly, I would like to thank Dr. Rebecca Watson and Dr. Lara Cala Alvarez. You two started as mentors to me when I first joined the group, and truly taught me how to succeed as a woman in chemistry. I continue to be inspired by you, and thank you for the friendship, love, and support you have given. I would also like to thank Hannah Vonesh. I am beyond grateful for your friendship and am so glad that we will continue to work together as we transition out of graduate school.

I would also like to acknowledge the support system that I had coming into the University of Michigan. First, I would like to thank Professor Suzanne A. Blum and Dr. Darius Faizi. You both took a chance on me as an undergraduate, and my time in the Blum lab is where I truly fell in love with organic chemistry. I would not be here had I not had that opportunity. Additionally, I would like to thank my best friend, Stephanie Watson. Your friendship has meant so much to me over the years, and although we do not see each other every day, I am still so glad to have you in my life.

I would also like to thank my family. To my aunt Lori, and my cousin Jacob, you have been so supportive of me, and I love you both. My mom, Lisa, has been my rock, my idol, my role model from day one. You have worked so hard to make my dreams come true, and I hope that one day I can be half the mother you have been to me.

Finally, I would like to thank my partner, Lily. I could not imagine getting to this point without you. Having you in my life has been such a blessing, and I could not have made it to the finish line without your love and support.

Table of Contents

List of Figures

List of Tables

List of Abbreviations

° C	degree Celsius
Ac	acetyl
AllylOH	allyl alcohol
AllylTMS	allyltrimethylsilane
aq.	aqueous
Ar	aryl
BF_4	tetrafluoroborate anion
Bn	benzyl
BnBr	benzyl bromide
BnOH	benzyl alcohol
BPR	back pressure regulator
Bu	butyl
cm	centimeters
$CDCl_3$	deuterated chloroform
COM	carbonyl−olefin metathesis
DCE	1,2-dichloroethane
DCM	dichloromethane
DFT	density functional theory
δ	chemical shift in parts per million
d	doublet

dd	doublet of doublets
DIBAL	diisobutylaluminium hydride
DMAP	4-(Dimethylamino)pyridine
DMF	N,N'-dimethylformamide
DMP	1,1,1-Tris(acetyloxy)-1,1-dihydro-1,2-benziodoxol-3-(1H)-one
DMSO	dimethyl sulfoxide
EDG	electron donating group
ee	enantiomeric excess
eq.	equation
equiv.	equivalents
Et	ethyl
Et_2O	diethyl ether
EtOAc	ethyl acetate
EtOH	ethanol
EWG	electron withdrawing group
$FeCl_3$	iron(III) chloride
FT-IR	Fourier Transform-infrared spectroscopy
g	grams
h	hours
H_2	hydrogen
HCl	hydrogen chloride
HRMS	high resolution mass spectroscopy
hν	light

Hz	hertz
IBX	2-iodoxybenzoic acid
iPr	iso-propyl
iPrOH	isopropanol
J	coupling constant
KIE	kinetic isotope effect
K_2CO_3	potassium carbonate
LDA	lithium diisopropylamine
LED	light-emitting diode
Li	lithium
$LiAlH_4$	lithium aluminum hydride
m	multiplet
M	molar concentration
mCPBA	meta-chloroperoxybenzoic acid
Me	methyl
MeCN	acetonitrile
MeLi	methyl lithium
MeOH	methanol
MeOD	deuterated methanol
mg	milligrams
$MgSO_4$	magnesium sulfate
MHz	megahertz
min	minutes

μL	microliters
mL	milliliters
mM	millimolar concentration
mmol	millimoles
mol	moles
mol%	mole percent
MW	molecular weight
N_2	nitrogen
Na_2SO_4	sodium sulfate
NaH	sodium hydride
$NaHCO_3$	sodium bicarbonate
Na_2CO_3	sodium carbonate
n-BuLi	n-butyllithium
NH_4Cl	ammonium chloride
NH_4OH	ammonium hydroxide
NMR	nuclear magnetic resonance
OTf	triflate anion
p	pentet
PFR	plug-flow reactor
Ph	phenyl
PhCl	1-chlorobenzene
PhH	benzene
PhMe	toluene

$PhSiMe_3$	phenyltimethylsilane
ppm	parts per million
q	quartet
R	alkyl group
rt	temperature
s	singlet
t	triplet
TBAF	tetra-n-butylammonium fluoride
TBSCl	tert-butyldimethylsilyl chloride
TEA	triethylamine
TfOH	triflic acid
THF	tetrahydrofuran
TLC	thin layer chromatography
TMEDA	N,N,N′,N′-tetramethylethylenediamine
TMSCN	trimethylsilyl cyanide
TPP	triphenyl phosphine
TPPO	triphenyl phosphineoxide
t_R	residence time
TsOH	p-toluenesulfonic acid

Abstract

Carbon−carbon bond forming reactions are among the most desirable transformations to synthetic organic chemists. Olefin−olefin metathesis is one of the most strategic methods available for the direct formation of carbon−carbon double bonds through the use metal alkylidene catalysts. The relative abundance of feedstocks available for this mode of reactivity has garnered olefin−olefin metathesis relevance in a wide range of applications from pharmaceuticals to materials. More recently, carbonyl−olefin metathesis has emerged as a key alternative to traditional olefin metathesis, with catalytic protocols relying on Lewis, Brønsted, and organocatalysts promoting renewed interest in the field.

Chapter 1 provides a detailed look at the current methods available for carbonyl−olefin metathesis using Lewis acids. Early approaches relied on stoichiometric amounts of Lewis acids to promote the desired reactivity, while newer methods achieve the same reactivity in a catalytic fashion using a range of Lewis acids and mild reaction conditions. Chapter 2 presents the first general catalyst for the synthesis of larger ring systems from unreactive starting materials. The Al(III)-ion pair catalyst promotes ring-closing carbonyl−olefin metathesis through a unique and unprecedented carbonyl-ene/hydroalkoxylation pathway, as supported by NMR, KIE, and computational studies.

Chapter 3 investigates the development and employment of metal complexes for carbonyl−olefin metathesis. The tunability of the Lewis acidic metal center promotes the ring-closing reaction on substrates that are sensitive to traditional catalytic systems such as bis-olefinic aryl ketones, and precursors to ring-closed products that are prone to isomerization under Lewis acidic conditions. NMR and IR studies demonstrate the formation of the active catalysts and quantify their Lewis acidic character. Chapter 4 expands the use of the metal complexes for ring-closing carbonyl−olefin metathesis for the synthesis of 7-membered rings. The increased potency of the Lewis acid catalyst is demonstrated on previously studied substrate classes, highlighting its superb catalytic activity.

Lastly, chapter 5 focuses on the use of continuous flow reactors as enabling technology of the synthesis of 6-membered rings. This work restores the use of simple monomeric $FeCl_3$ as the Lewis acid catalyst, eliminating the need for Ag(I) additives and costly air-free equipment and techniques. Mechanistic investigations reveal the reaction conditions promote a reversible carbonyl-ene reaction, followed by an unprecedented stepwise hydroalkoxylation reaction to form the desired products.

Chapter 1 An Introduction to Carbonyl-Olefin Metathesis
1.1 Introduction

Carbon-carbon forming reactions are the among the most sought-after modes of reactivity available to synthetic chemists. Catalytic carbonyl-olefin metathesis has emerged as a particularly powerful strategy in recent years for the direct formation of carbon-carbon double bonds, a functional group pertinent to a wide range of industrial applications from pharmaceuticals to materials.[1] While the analogous olefin-olefin metathesis is well documented using catalytic amounts of metal alkylidenes,[2,3] catalytic carbonyl-olefin metathesis has thus far failed to be realized under these conditions (Error! Reference source not found.**, top**).[4] The metal-oxo b yproducts formed from these reactions are inert and therefore unable to turnover, rendering the reactions stoichiometric. Alternatively, the use of Lewis and Brønsted acids as the active catalyst is appealing as the Lewis basic carbonyl moiety could coordinate to the acid activator reversibly, allowing for catalyst turnover (**Figure 1.1, bottom**). The first example of Lewis acid promoted carbonyl-olefin metathesis was reported in 1971.[5] Despite this important discovery, a catalytic approach to carbonyl-olefin metathesis remained elusive for over 40 years. In 2016, the Schindler group reported the first examples of catalytic carbonyl-olefin metathesis employing Earth-abundant and environmentally-benign $FeCl_3$ as the Lewis acid catalyst.[6] Aryl ketones bearing pendant olefins were readily converted to the ring-closed products under the mild reaction conditions. This advancement has spurred further innovation in both catalyst design and scope

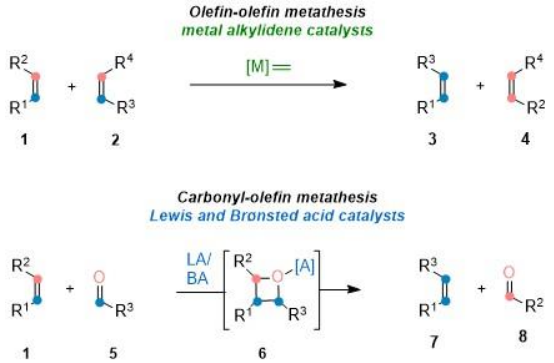

Figure 1.1. Metathesis reactions employing carbonyls and olefins.

expansion. This chapter will focus on the initial development of Lewis-acid promoted carbonyl-olefin metathesis reactions, as well as more recent advances in catalytic approaches.

1.2 Stoichiometric Lewis Acid Approaches

As previously mentioned, early examples of carbonyl-olefin metathesis relied on stoichiometric amounts of Lewis acids. The reactions proceed *via* activation of the Lewis basic carbonyl functionality through Lewis acid/base interactions to promote a [2+2]-cycloaddition between the carbonyl and olefin moieties to form an oxetane intermediate. Fragmentation of the oxetane leads to the desired olefinic product and carbonyl byproduct.

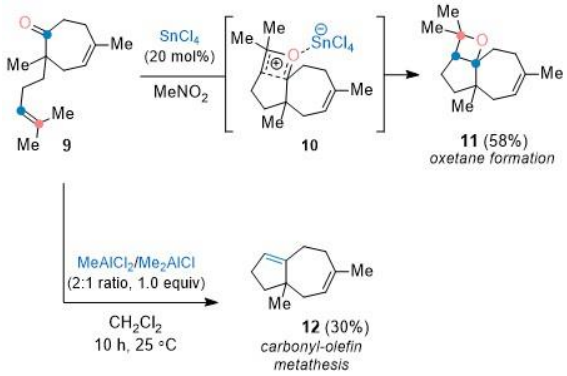

Figure 1.2. First examples of Lewis acid carbonyl activation.

The first known example was reported in 1971, in which Demole, Enggist and Borer reported a series of stepwise cyclizations towards the synthesis of α-cedrene, a sesquiterpene that has a role as a metabolite.[5] Early on into the synthesis, a $SnCl_4$-catalyzed intramolecular [2+2]-cycloaddition of cycloheptenone **9** was employed to yield 58% of *cis*-oxetane **11**, compound closely related to the sesquiterpene carotol (**Figure 1.2.** First examples of Lewis acid carbonyl activation.). Motivated by a simple route to carotol, in 1984 Snider reexamined the reaction of substrate **9** with different alkylaluminum halides to promote an intramolecular ene reaction.[7] The treatment of cycloheptenone **9** with a 2:1 mixture of $MeAlCl_2$ and Me_2AlCl led to the formation of metathesis product **12** in 30% yield. Snider proposed a stepwise cycloaddition to form the intermediate oxetane **3** and a subsequent retro-cycloaddition to provide **12** and acetone. The mixture of Lewis acids proved crucial; the reaction did not proceed in the presence of $Me_{1.5}AlCl_{1.5}$. In contrast, a complex mixture of products was obtained with $MeAlCl_2$, indicating the importance of tuning the Lewis acidity to promote the carbonyl-olefin metathesis reaction.

Ten years later, Bickelhaupt, van Schaik, and Vijn investigated the intermolecular carbonyl-olefin reaction of benzaldehyde **13** with olefins (**14a-b**) catalyzed by a solid Lewis acid, EPZ-10, consisting of clay-supported $ZnCl_2$ (**Figure 1.3.** Intermolecular carbonyl-olefin metathesis using a solid-supported Lewis acid.).[8] The one-pot reaction afforded metathesis products **15a** and **15b** in low yields. Modification of the reaction conditions to increase the yields, including longer reaction times and higher temperatures, resulted in the formation of more byproducts. The limitation of the olefination process resides in the carbonyl compounds, where compounds with α-hydrogen substituents prefer to undergo aldol condensation reactions. Furthermore, no reaction was observed when benzophenone was used instead of **5** probably due to the cation stability.

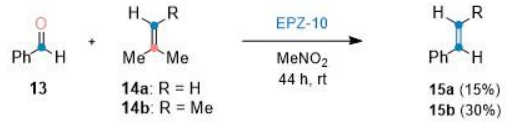

Figure 1.3. Intermolecular carbonyl-olefin metathesis using a solid-supported Lewis acid.

The Khirpach group discovered the intramolecular rearrangement of 5,10-seco steroid **16** to **18** in 60% yield using excess of $BF_3 \cdot OEt_2$ as part of their attempts to protect the carbonyl moiety as a dithioketal (**Figure 1.4**).[9] The transannular carbonyl-olefin metathesis reaction is determined by the stereochemistry of compound **16**; (*E*)-enone led to the formation of **18** while (*Z*)-isomer was unreactive under identical reaction conditions. DFT calculations of conformational analysis of **16** revealed a possible reaction mechanism consisting of an intramolecular Lewis acid promoted [2+2]-cycloaddition to oxetane **17**, followed by a cycloreversion to give fragmentation product **18**.

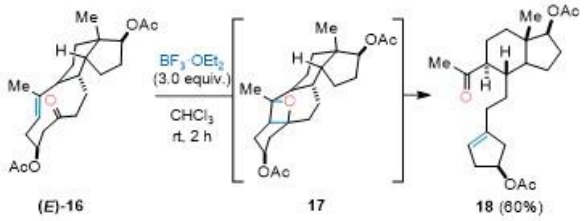

Figure 1.4. BF_3-promoted transannular carbonyl-olefin metathesis.

The efforts of Schmalz and co-workers toward the total synthesis of marine natural product pestalone unexpectedly led them to obtain a carbonyl-olefin metathesis product.[10] In an attempt to perform a selective deprotection of methylether moieties in *ortho*-prenylated benzophenone compounds with $BF_3 \cdot SMe_2$, Schmalz and coworkers instead observed the formation of a carbonyl-olefin metathesis product in 20% yield, resembling the results previously reported by the Khirpach

group.[9] Optimization of the reaction conditions revealed that 1.5 equivalents of $BF_3 \cdot OEt_2$ could efficiently convert aryl ketone **19** to ring-closed product **20** in 87% (**Figure 1.5**).

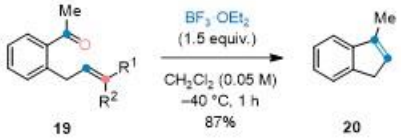

Figure 1.5. Ring-closing carbonyl-olefin metathesis.

1.3 Lewis Acid-Catalyzed Ring-Closing Carbonyl-Olefin Metathesis for 5- and 6-Membered Rings

The use of an environmentally friendly Lewis acid in catalytic amounts for ring-closing carbonyl-olefin metathesis was reported by Schindler and co-workers in 2016.[6] The mild reaction conditions developed by this group includes $FeCl_3$ in 5 mol% and 1,2-dichloroethane as solvent allowing for the formation of cyclopentene and cyclohexene metathesis products **22** in up to 99% yield starting from aryl ketone substrate **21** (**Figure 1.6**). The substrate scope of this transformation was expanded to include aromatic β-ketoesters electronically differentiated substrates, as well as aryl ketones with different β-substitution, heteroatom incorporation and different structural motifs. Furthermore, it was found that although less sterically incumbering olefins were well tolerated in the reaction, substrates with more sterically congested olefin units inhibited product formation.

Figure 1.6. $FeCl_3$-catalyzed carbonyl-olefin metathesis.

Both the Schindler and Devery groups followed up on this report with extensive mechanistic investigations including both computational and experimental studies.[11–13] It was found that prenylated ketones likely undergo a concerted, asynchronous [2+2]-cycloaddition pathway, while styrenyl substrates prefer a stepwise cycloaddition *via* a Prins-like carbocation. Additionally, the Schindler group demonstrated that the Fe(III)-catalyzed reaction was scalable, with 15 grams of material converted to the ring-closed product in 97%.[14]

Both the Li[15] and Schindler[16] groups expanded the substrate scope of $FeCl_3$-catalyzed ring-closing metathesis reaction to include the synthesis of sulfonate-protected *N*-heterocycles **25** and

27 (**Figure 1.7**). The established optimized reaction conditions[6,13] failed to perform the metathesis reaction, while stoichiometric amounts of $FeCl_3$ provided the product in only 20% yield. The Li group solved this lack of reactivity with the addition of excess of allyltrimethylsilane yielding up to 91% of the desired metathesis products (**Figure 1.7a**). Allyltrimethylsilane was proposed to coordinate to the iron catalyst to promote the formation and fragmentation of the oxetane. An alternative approach was presented by the Schindler group, who reported that using strongly electron-deficient sulfonate protecting groups such as the trifluoromesylate on the nitrogen atom (**26**) could successfully promote the desired reaction (**Figure 1.7b**). These electron-withdrawing groups limited the Lewis acid/base interaction between the catalyst and the nitrogen atom of the starting material, thereby promoting carbonyl-olefin metathesis and catalyst turnover. The optimized reaction conditions for this transformation allowed the synthesis of a wide variety of commercially available chiral and racemic amino acid-derived 3-pyrrolines **27** in up to 99% yield and >98% *ee*. This strategy was also successful in access tetrahydropyridine scaffolds, as

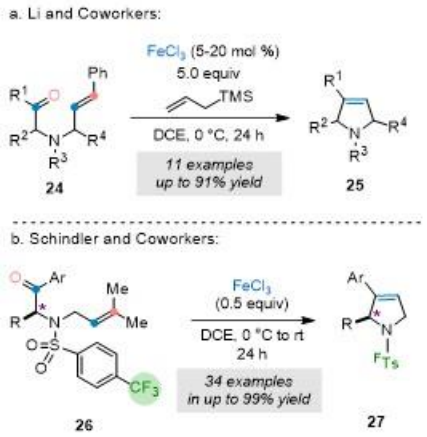

Figure 1.7. Synthesis of pyrrolines.

demonstrated by the Schindler group in 2020.[17]

Several other Lewis acid catalysts have been reported for ring-closing carbonyl-olefin metathesis (**Figure 1.8**). For example, the Franzén group reported an aldehyde-olefin ring-closing metathesis reaction as a general protocol to obtain a variety of functionalized indene products in up to 84% yield.[18] Several Lewis acids including $FeCl_3$ were tested to perform this transformation; however, little to no indene product was obtained. The use of an Au(III)-catalyst for ring-closing carbonyl-olefin metathesis was reported by the Lin group in 2020.[19] The reactivity was amenable to both aryl ketone and aldehyde starting materials **28** to produce the desired metathesis products containing 5-membered cycloalkene subunits (**29**). Additionally, $AuCl_3$ could also be used to

access larger ring systems, as well as convert *N*-tosyl containing starting materials in good to moderate yields. Finally, the Nguyen group reported that both molecular iodine[20] and tropylium

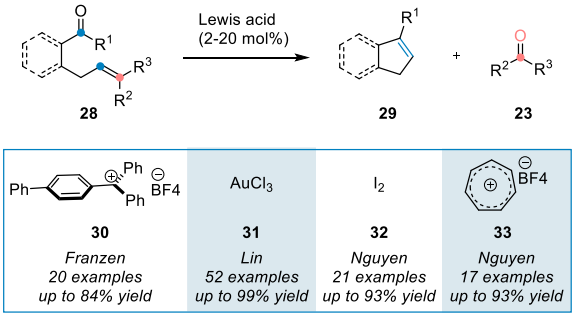

Figure 1.8. Other Lewis acid catalysts for ring-closing carbonyl-olefin metathesis.

salts[21] serve as Lewis acid catalysts, providing cyclopentenes **29** in up to 96%.

Gandon and Bour reported in 2019 the first example of a tandem process consisting of a ring-closing carbonyl-olefin metathesis and transfer hydrogenation.[22] The cationic Ga(III) complex (**35**) was employed as catalyst and 1,4-cyclohexadiene (1,4-CHD) as the hydrogen donor, performing the reductive cyclization of β-ketoesters (**34**) to give saturated carbocycle products **36** in up to 95% yield (**Figure 1.9**). The presence of carbonyl-olefin metathesis product at the end of the reaction confirmed its participation as an active intermediate. Interestingly, the established catalysts[6] for carbonyl-olefin metathesis of aryl ketones, $FeCl_3$ and $GaCl_3$, provided moderate yields of metathesis product but both failed at inducing the hydrogenation step. In general, the *cis*/*trans* diastereomeric ratios of the products were 4:1 when β-ketoesters were used as substrates, and 20:1 when aryl ketones were used.

The Schindler lab was able to expand their $FeCl_3$-catalyzed COM protocol to include the synthesis of polycyclic aromatic compounds (PAC, **Figure 1.10**).[23] PACs are structural motifs predominant in various subfields of chemistry, such as natural product synthesis, materials science, and asymmetric catalysis. Notably, when starting materials containing either a prenyl- (**37**) or crotyl-derived (**38**) olefin fragments were utilized, competing carbonyl-ene reactivity resulted in

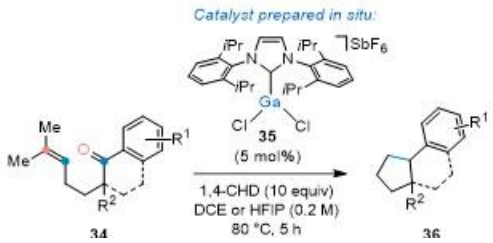

Figure 1.9. Tandem metathesis/hydrogenation reaction catalyzed by Ga(III)-complex.

diminished yields of the desired metathesis product. However, it was found that utilizing 5 mol% $FeCl_3$ could efficiently convert aryl ketones containing a styrenyl olefin subunit **43** to exclusively the desired metathesis product.

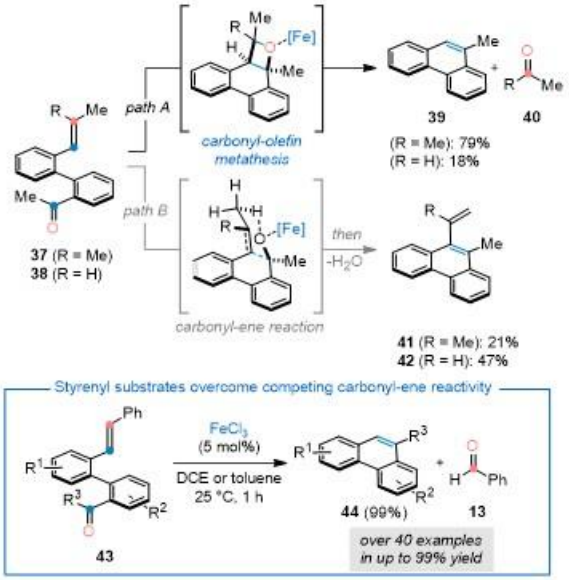

Figure 1.10. $FeCl_3$-catalyzed PAC formation.

1.4 Superelectrophilic Lewis Acid Catalyst for Challenging Ring-Closing Carbonyl-Olefin Metathesis of Aliphatic Ketones

The Schindler group reported the first general protocol for the ring-closing carbonyl-olefin metathesis reaction of aliphatic ketones **45**.[24] Higher catalysts loadings of the Lewis acid $FeCl_3$ were required to promote the transformation, which was demonstrated on 40 examples with yields of up to 94% (**Figure 1.11**). Mechanistic investigations revealed a distinct pathway requiring the *in-situ* formation of an Fe(III)dimer species. Kinetic, computational, and spectroscopic experiments determined that initial coordination of the $FeCl_3$ with the carbonyl moiety of the aliphatic ketone substrates **45**, which served as the catalyst resting state. However, monomeric $FeCl_3$[6] does not activate the carbonyl moiety effectively for metathesis. A second coordination event to form the active homodimer complex **48** is required to promote oxetane formation and subsequent fragmentation to furnish the desired metathesis products and catalyst turnover. Homobimetallic interaction to form bridged dimeric species **48** is consistent with the experimentally determined rate order of 1.7 for $FeCl_3$ and is supported by DFT calculations, IR, EPR, and Raman spectroscopy studies. Furthermore, this discovery aligns with literature reports

from over 60 years ago that Lewis acid activation through association can lead to reactive superelectrophiles as more potent catalysts.[25,26]

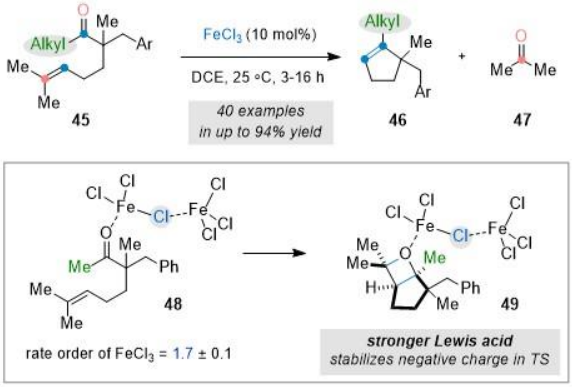

Figure 1.11. Homobimetallic dimer as superelectrophilic Lewis acid catalyst.

1.5 Ring-Opening Carbonyl-Olefin Metathesis

Ring-opening carbonyl-olefin metathesis was first reported by the Schindler group in 2018.[27] In contrast to its ring-closing counterpart, which relies on catalytic amounts of $FeCl_3$,[6,13] this intermolecular ring-opening methodology utilizes $GaCl_3$ as the optimal catalyst (**Figure 1.12**). The reaction conditions furnished 22 products (**51**) in yields up to 47%. Interestingly, ring-strain of starting material **50** was found to have no effect on reactivity, as cycloalkenes with higher ring-strain values did not undergo the desired transformation, while 5- and 6-membered rings could be converted readily to the extended aryl ketone products. The Nguyen group also demonstrated that both their molecular iodine[20] and tropylium salt[21] catalysts could also promote ring-opening carbonyl-olefin metathesis.

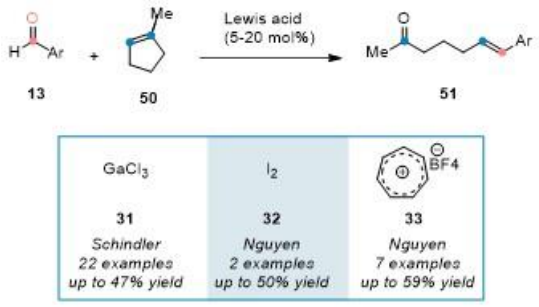

Figure 1.12. Catalysts for ring-opening carbonyl-olefin metathesis.

1.6 Intermolecular Cross Metathesis

The first report of cross-metathesis between aryl aldehydes **13** and olefins **52** was published by The Franzén lab in 2015.[28] Catalytic amounts of the organic Lewis acid trityl tetrafluoroborate (**54**) effectively promoted the intermolecular reaction, providing 18 examples in up to 85% yield (**Figure 1.13**). Importantly, the reaction selectively produced the (*E*)-isomer as the exclusive product in all cases. This methodology was further expanded by the Schindler lab to include a Lewis acid-catalyzed intermolecular cross-metathesis variant (**Figure 1.13**).[29] Thorough optimization provided the optimal reaction conditions of 10 mol% of $FeCl_3$, 30 mol% of the silver salt $AgBF_4$, and superstoichiometric amounts of aldehyde substrate **13**. Although the starting materials could produce up to four different regiomeric oxetane intermediates, extensive experimental and NMR studies determined that the reaction proceeds exclusively through a [2+2]-cycloaddition to form a *trans*-oxetane intermediate. [2+2]-cycloreversion was found to be stereoselective for the (*E*)-isomer as the exclusive olefinic product (**53**). The Nguyen group also demonstrated this mode of reactivity using their molecular iodine[20] and tropylium salt[21] catalysts for a small subset of substrates.

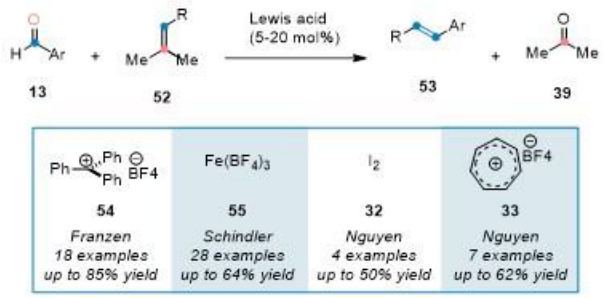

Figure 1.13. Catalysts for intermolecular cross metathesis of carbonyls and olefins.

1.7 Transannular Carbonyl-Olefin Metathesis

The catalytic, transannular carbonyl-olefin metathesis of steroid natural products utilizing $FeCl_3$ as the Lewis acid catalyst was published by the Schindler group.[30] Mechanistic investigations determined that the choice of Lewis acid employed can selectively promote either carbonyl-ene, metathesis, or a cyclization reactivity to form molecular scaffolds A, B, or C, respectively (**Figure 1.14**). Additionally, computational studies support a distinct mechanism for transannular carbonyl-olefin metathesis reactions relying on an initial -but reversible- carbonyl-ene step as a competing pathway for the [2+2]-cycloaddition to form an oxetane intermediate. Once formed, the oxetane

can then fragment to the metathesis product (**57**) or undergo an elimination and subsequent addition to form tetrahydrofuran **59**.

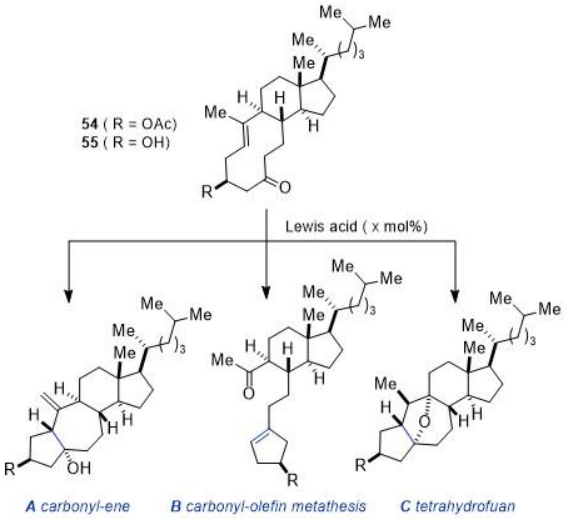

Entry	Lewis acid (mol %)	R	Yield A (%)	Yield B (%)	Yield C (%)
1	Me_2AlCl (100)	OAc	85	-	-
2	$FeCl_3$ (10)	OH	-	75	-
3	$SnCl_4$ (10)	OAc	-	65	44

Figure 1.14. Divergent Lewis acid-catalyzed reactions of carbonyls and olefins.

1.8 Conclusion

In recent years, carbonyl-olefin metathesis has emerged as an effective strategy for the formation of high-value olefinic motifs from simple, readily available building blocks. Early efforts revealed that stoichiometric Lewis acids could promote the desired carbon-carbon bond-forming reaction, albeit in low yields. More recent advances have focused on the unique ability of Lewis acids to catalyze carbonyl-olefin metathesis under mild conditions. The scope of this transformation has seen a significant expansion over the last decade to include the synthesis of heterocyclic and polycyclic motifs, intramolecular variations, and applications on natural product derivatives. Despite these important improvements, there still exists many unmet challenges within the metathesis paradigm. Future developments focused on addressing the inherent limitations within the field are expected to spur further innovation in translating this chemistry to industrially relevant processes. This dissertation will explore four unique catalytic strategies aimed at addresses several of these limitations and provide insight for overcoming unseen future challenges.

1.9 References

(1) Albright, H.; Davis, A. J.; Gomez-Lopez, J. L.; Vonesh, H. L.; Quach, P. K.; Lambert, T. H.; Schindler, C. S. Carbonyl-Olefin Metathesis. *Chemical Reviews*. American Chemical Society August 11, 2021, pp 9359–9406. https://doi.org/10.1021/acs.chemrev.0c01096.

(2) Angew Chem Int Ed Engl - October 2 1995 - Schwab - A Series of Well-Defined Metathesis Catalysts Synthesis of RuCl2 .

(3) Scholl, M.; Trnka, T. M.; Morgan, J. P.; Grubbs, R. H. *Increased Ring Closing Metathesis Activity of Ruthenium-Based Oiefin Metathesis Catalysts Coordinated with Imidazolin-2-Ylidene Ligands*; 1999; Vol. 40.

(4) Ho, T.-L.; Mcmurry, J. E.; Clive, D. L. J.; Zhang, C.; Murthy, K. S. K.; Hayward, W. D.; Daigneault, S.; Grubbs, R. H.; Turnas, W.; Hartley, F.; Pine, S. H. *C) Feast, W. J.; Gibson, V. C. In The Chemistry of the Metal-Carbon Bond*; UTC, 1993; Vol. 89.

(5) Helvetica Chimica Acta - 1 November 1971 - Demole - Applications Synth Tiques de La Cyclisation d Alcools Tertiaires -.

(6) Ludwig, J. R.; Zimmerman, P. M.; Gianino, J. B.; Schindler, C. S. Iron(III)-Catalysed Carbonyl-Olefin Metathesis. *Nature* **2016**, *533*, 374–379. https://doi.org/10.1038/nature17432.

(7) Jackson, A. C.; Goldman, B. E.; Snider, B. B. *Intramolecular and Intermolecular Lewis Acid Catalyzed Ene Reactions Using Ketones as Enophiles*; 1984; Vol. 49.

(8) *COM M UNlCATlONS.*

(9) Khripach, V. A.; Zhabinskii, V. N.; Kuchto, A. I.; Zhiburtovich, Y. Y.; Gromak, V. v.; Groen, M. B.; van der Louw, J.; de Groot, A. Intramolecular Cycloaddition/Cycloreversion of (E)-3β,17β-Diacetoxy-5,10-Secoandrost-1(10)-En-5-

One. *Tetrahedron Letters* **2006**, *47* (38), 6715–6718. https://doi.org/10.1016/j.tetlet.2006.07.096.

(10) Soicke, A.; Slavov, N.; Neudörfl, J. M.; Schmalz, H. G. Metal-Free Intramolecular Carbonyl-Olefin Metathesis of Ortho-Prenylaryl Ketones. *Synlett* **2011**, No. 17, 2487–2490. https://doi.org/10.1055/s-0030-1260320.

(11) Malakar, T.; Hanson, C. S.; Devery, J. J.; Zimmerman, P. M. Combined Theoretical and Experimental Investigation of Lewis Acid-Carbonyl Interactions for Metathesis. *ACS Catalysis* **2021**, *11* (8), 4381–4394. https://doi.org/10.1021/acscatal.0c05277.

(12) Hanson, C. S.; Psaltakis, M. C.; Cortes, J. J.; Devery, J. J. Catalyst Behavior in Metal-Catalyzed Carbonyl-Olefin Metathesis. *J Am Chem Soc* **2019**, *141* (30), 11870–11880. https://doi.org/10.1021/jacs.9b02613.

(13) Ludwig, J. R.; Phan, S.; McAtee, C. C.; Zimmerman, P. M.; Devery, J. J.; Schindler, C. S. Mechanistic Investigations of the Iron(III)-Catalyzed Carbonyl-Olefin Metathesis Reaction. *J Am Chem Soc* **2017**, *139* (31), 10832–10842. https://doi.org/10.1021/jacs.7b05641.

(14) Becker, M. Carbonyl-Olefin Metathesis for the Synthesis of Cyclic Olefins. *Organic Syntheses* **2018**, *95*, 472–485. https://doi.org/10.15227/orgsyn.095.0472.

(15) Ma, L.; Li, W.; Xi, H.; Bai, X.; Ma, E.; Yan, X.; Li, Z. FeCl 3 -Catalyzed Ring-Closing Carbonyl-Olefin Metathesis . *Angewandte Chemie* **2016**, *128* (35), 10566–10569. https://doi.org/10.1002/ange.201604349.

(16) Groso, E. J.; Golonka, A. N.; Harding, R. A.; Alexander, B. W.; Sodano, T. M.; Schindler, C. S. 3-Aryl-2,5-Dihydropyrroles via Catalytic Carbonyl-Olefin Metathesis. *ACS Catalysis* **2018**, *8* (3), 2006–2011. https://doi.org/10.1021/acscatal.7b03769.

(17) Rykaczewski, K. A.; Groso, E. J.; Vonesh, H. L.; Gaviria, M. A.; Richardson, A. D.; Zehnder, T. E.; Schindler, C. S. Tetrahydropyridines via FeCl3-Catalyzed Carbonyl-Olefin Metathesis. *Organic Letters* **2020**, *22* (7), 2844–2848. https://doi.org/10.1021/acs.orglett.0c00918.

(18) Ni, S.; Franzén, J. Carbocation Catalysed Ring Closing Aldehyde-Olefin Metathesis. *Chemical Communications* **2018**, *54* (92), 12982–12985. https://doi.org/10.1039/C8CC06734A.

(19) Wang, R.; Chen, Y.; Shu, M.; Zhao, W.; Tao, M.; Du, C.; Fu, X.; Li, A.; Lin, Z. AuCl3-Catalyzed Ring-Closing Carbonyl–Olefin Metathesis. *Chemistry - A European Journal* **2020**, *26* (9), 1941–1946. https://doi.org/10.1002/chem.201905199.

(20) Tran, U. P. N.; Oss, G.; Breugst, M.; Detmar, E.; Pace, D. P.; Liyanto, K.; Nguyen, T. v. Carbonyl-Olefin Metathesis Catalyzed by Molecular Iodine. *ACS Catalysis* **2019**, *9* (2), 912–919. https://doi.org/10.1021/acscatal.8b03769.

(21) Tran, U. P. N.; Oss, G.; Pace, D. P.; Ho, J.; Nguyen, T. v. Tropylium-Promoted Carbonyl-Olefin Metathesis Reactions. *Chemical Science* **2018**, *9* (23), 5145–5151. https://doi.org/10.1039/c8sc00907d.

(22) Djurovic, A.; Vayer, M.; Li, Z.; Guillot, R.; Baltaze, J. P.; Gandon, V.; Bour, C. Synthesis of Medium-Sized Carbocycles by Gallium-Catalyzed Tandem Carbonyl-Olefin Metathesis/Transfer Hydrogenation. *Organic Letters* **2019**, *21* (19), 8132–8137. https://doi.org/10.1021/acs.orglett.9b03240.

(23) McAtee, C. C.; Riehl, P. S.; Schindler, C. S. Polycyclic Aromatic Hydrocarbons via Iron(III)-Catalyzed Carbonyl-Olefin Metathesis. *J Am Chem Soc* **2017**, *139* (8), 2960–2963. https://doi.org/10.1021/jacs.7b01114.

(24) Albright, H.; Riehl, P. S.; McAtee, C. C.; Reid, J. P.; Ludwig, J. R.; Karp, L. A.; Zimmerman, P. M.; Sigman, M. S.; Schindler, C. S. Catalytic Carbonyl-Olefin Metathesis of Aliphatic Ketones: Iron(III) Homo-Dimers as Lewis Acidic Superelectrophiles. *J Am Chem Soc* **2019**, *141* (4), 1690–1700. https://doi.org/10.1021/jacs.8b11840.

(25) Olah, G. A. *International Edition in English Superelectrophiles***; 1993; Vol. 32.

(26) Negishi, E. *CONCEPTS*; 1999; Vol. 5.

(27) Albright, H.; Vonesh, H. L.; Becker, M. R.; Alexander, B. W.; Ludwig, J. R.; Wiscons, R. A.; Schindler, C. S. GaCl3-Catalyzed Ring-Opening Carbonyl-Olefin Metathesis. *Organic Letters* **2018**, *20* (16), 4954–4958. https://doi.org/10.1021/acs.orglett.8b02086.

(28) Naidu, V. R.; Bah, J.; Franzén, J. Direct Organocatalytic Oxo-Metathesis, a Trans-Selective Carbocation-Catalyzed Olefination of Aldehydes. *European Journal of Organic Chemistry* **2015**, *2015* (8), 1834–1839. https://doi.org/10.1002/ejoc.201403651.

(29) Albright, H.; Vonesh, H. L.; Schindler, C. S. Superelectrophilic Fe(III)-Ion Pairs as Stronger Lewis Acid Catalysts for (E)-Selective Intermolecular Carbonyl-Olefin Metathesis. *Organic Letters* **2020**, *22* (8), 3155–3160. https://doi.org/10.1021/acs.orglett.0c00917.

(30) Riehl, P. S.; Nasrallah, D. J.; Schindler, C. S. Catalytic, Transannular Carbonyl-Olefin Metathesis Reactions. *Chemical Science* **2019**, *10* (44), 10267–10274. https://doi.org/10.1039/c9sc03716k.

(31) Ni, S.; Franzén, J. Carbocation Catalysed Ring Closing Aldehyde-Olefin Metathesis. *Chemical Communications* **2018**, *54* (92), 12982–12985. https://doi.org/10.1039/C8CC06734A.

(32) Tran, U. P. N.; Oss, G.; Pace, D. P.; Ho, J.; Nguyen, T. v. Tropylium-Promoted Carbonyl-Olefin Metathesis Reactions. *Chemical Science* **2018**, *9* (23), 5145–5151. https://doi.org/10.1039/c8sc00907d.

(33) Naidu, V. R.; Bah, J.; Franzén, J. Direct Organocatalytic Oxo-Metathesis, a Trans-Selective Carbocation-Catalyzed Olefination of Aldehydes. *European Journal of Organic Chemistry* **2015**, *2015* (8), 1834–1839. https://doi.org/10.1002/ejoc.201403651.

(34) Hanson, C. S.; Psaltakis, M. C.; Cortes, J. J.; Devery, J. J. Catalyst Behavior in Metal-Catalyzed Carbonyl-Olefin Metathesis. *J Am Chem Soc* **2019**, *141* (30), 11870–11880. https://doi.org/10.1021/jacs.9b02613.

(35) Ma, L.; Li, W.; Xi, H.; Bai, X.; Ma, E.; Yan, X.; Li, Z. FeCl 3 -Catalyzed Ring-Closing Carbonyl-Olefin Metathesis . *Angewandte Chemie* **2016**, *128* (35), 10566–10569. https://doi.org/10.1002/ange.201604349.

(36) Riehl, P. S.; Nasrallah, D. J.; Schindler, C. S. Catalytic, Transannular Carbonyl-Olefin Metathesis Reactions. *Chemical Science* **2019**, *10* (44), 10267–10274. https://doi.org/10.1039/c9sc03716k.

(37) Albright, H.; Vonesh, H. L.; Becker, M. R.; Alexander, B. W.; Ludwig, J. R.; Wiscons, R. A.; Schindler, C. S. GaCl3-Catalyzed Ring-Opening Carbonyl-Olefin Metathesis. *Organic Letters* **2018**, *20* (16), 4954–4958. https://doi.org/10.1021/acs.orglett.8b02086.

(38) Groso, E. J.; Golonka, A. N.; Harding, R. A.; Alexander, B. W.; Sodano, T. M.; Schindler, C. S. 3-Aryl-2,5-Dihydropyrroles via Catalytic Carbonyl-Olefin Metathesis. *ACS Catalysis* **2018**, *8* (3), 2006–2011. https://doi.org/10.1021/acscatal.7b03769.

(39) Ludwig, J. R.; Phan, S.; McAtee, C. C.; Zimmerman, P. M.; Devery, J. J.; Schindler, C. S. Mechanistic Investigations of the Iron(III)-Catalyzed Carbonyl-Olefin Metathesis

Reaction. *J Am Chem Soc* **2017**, *139* (31), 10832–10842. https://doi.org/10.1021/jacs.7b05641.

(40) Ludwig, J. R.; Schindler, C. S. Lewis Acid Catalyzed Carbonyl-Olefin Metathesis. *Synlett* **2017**, *28* (13), 1501–1509. https://doi.org/10.1055/s-0036-1588827.

(41) Ludwig, J. R.; Zimmerman, P. M.; Gianino, J. B.; Schindler, C. S. Iron(III)-Catalysed Carbonyl-Olefin Metathesis. *Nature* **2016**, *533*, 374–379. https://doi.org/10.1038/nature17432.

(42) Albright, H.; Riehl, P. S.; McAtee, C. C.; Reid, J. P.; Ludwig, J. R.; Karp, L. A.; Zimmerman, P. M.; Sigman, M. S.; Schindler, C. S. Catalytic Carbonyl-Olefin Metathesis of Aliphatic Ketones: Iron(III) Homo-Dimers as Lewis Acidic Superelectrophiles. *J Am Chem Soc* **2019**, *141* (4), 1690–1700. https://doi.org/10.1021/jacs.8b11840.

(43) McAtee, C. C.; Riehl, P. S.; Schindler, C. S. Polycyclic Aromatic Hydrocarbons via Iron(III)-Catalyzed Carbonyl-Olefin Metathesis. *J Am Chem Soc* **2017**, *139* (8), 2960–2963. https://doi.org/10.1021/jacs.7b01114.

(44) Rykaczewski, K. A.; Groso, E. J.; Vonesh, H. L.; Gaviria, M. A.; Richardson, A. D.; Zehnder, T. E.; Schindler, C. S. Tetrahydropyridines via FeCl3-Catalyzed Carbonyl-Olefin Metathesis. *Organic Letters* **2020**, *22* (7), 2844–2848. https://doi.org/10.1021/acs.orglett.0c00918.

(45) Catti, L.; Tiefenbacher, K. Brønsted-Säure-Katalysierte Carbonyl-Olefin-Metathese in Einer Selbstorganisierten Supramolekularen Wirtstruktur. *Angewandte Chemie* **2018**, *130* (44), 14797–14800. https://doi.org/10.1002/ange.201712141.

(46) Zhu, Y.; Rebek, J.; Yu, Y. Cyclizations Catalyzed inside a Hexameric Resorcinarene Capsule. *Chemical Communications* **2019**, *55* (25), 3573–3577. https://doi.org/10.1039/c9cc01611b.

(47) Griffith, A. K.; Vanos, C. M.; Lambert, T. H. Organocatalytic Carbonyl-Olefin Metathesis. *J Am Chem Soc* **2012**, *134* (45), 18581–18584. https://doi.org/10.1021/ja309650u.

(48) Hong, X.; Liang, Y.; Griffith, A. K.; Lambert, T. H.; Houk, K. N. Distortion-Accelerated Cycloadditions and Strain-Release-Promoted Cycloreversions in the Organocatalytic Carbonyl-Olefin Metathesis. *Chemical Science* **2014**, *5* (2), 471–475. https://doi.org/10.1039/c3sc52882k.

(49) Zhang, Y.; Jermaks, J.; MacMillan, S. N.; Lambert, T. H. Synthesis of 2 H-Chromenes via Hydrazine-Catalyzed Ring-Closing Carbonyl-Olefin Metathesis. *ACS Catalysis* **2019**, *9* (10), 9259–9264. https://doi.org/10.1021/acscatal.9b03656.

(50) Zhang, Y.; Jermaks, J.; MacMillan, S. N.; Lambert, T. H. Synthesis of 2 H-Chromenes via Hydrazine-Catalyzed Ring-Closing Carbonyl-Olefin Metathesis. *ACS Catalysis* **2019**, *9* (10), 9259–9264. https://doi.org/10.1021/acscatal.9b03656.

(51) Albright, H.; Davis, A. J.; Gomez-Lopez, J. L.; Vonesh, H. L.; Quach, P. K.; Lambert, T. H.; Schindler, C. S. Carbonyl-Olefin Metathesis. *Chemical Reviews*. American Chemical Society August 11, 2021, pp 9359–9406. https://doi.org/10.1021/acs.chemrev.0c01096.

(52) Soicke, A.; Slavov, N.; Neudörfl, J. M.; Schmalz, H. G. Metal-Free Intramolecular Carbonyl-Olefin Metathesis of Ortho-Prenylaryl Ketones. *Synlett* **2011**, No. 17, 2487–2490. https://doi.org/10.1055/s-0030-1260320.

(53) Schopov, I. *A Carbonyl-Olefin Exchange Reaction-New Route to Polyconjugated Polymers, 1 A New Synthesis of Polyphenylacetylene*; 1983; Vol. 4.

(54) Ho, T.-L.; Mcmurry, J. E.; Clive, D. L. J.; Zhang, C.; Murthy, K. S. K.; Hayward, W. D.; Daigneault, S.; Grubbs, R. H.; Turnas, W.; Hartley, F.; Pine, S. H. *C) Feast, W. J.; Gibson, V. C. In The Chemistry of the Metal-Carbon Bond*; UTC, 1993; Vol. 89.

(55) Valiulin, R. A.; Arisco, T. M.; Kutateladze, A. G. Photoinduced Intramolecular Cyclopentanation vs Photoprotolytic Oxametathesis in Polycyclic Alkenes Outfitted with Conformationally Constrained Aroylmethyl Chromophores. *Journal of Organic Chemistry* **2013**, *78* (5), 2012–2025. https://doi.org/10.1021/jo301909j.

(56) Valiulin, R. A.; Arisco, T. M.; Kutateladze, A. G. Double-Tandem [4π+2π]·[2 Π+2π]·[4π+2π] ·[2π+2π] Synthetic Sequence with Photoprotolytic Oxametathesis and Photoepoxidation in the Chromone Series. *Journal of Organic Chemistry* **2011**, *76* (5), 1319–1332. https://doi.org/10.1021/jo102221q.

(57) Valiulin, R. A.; Kutateladze, A. G. Harvesting the Strain Installed by a Paternò-Büchi Step in a Synthetically Useful Way: High-Yielding Photoprotolytic Oxametathesis in Polycyclic Systems. *Organic Letters* **2009**, *11* (17), 3886–3889. https://doi.org/10.1021/ol901456m.

(58) Pérez-Ruiz, R.; Miranda, M. A.; Alle, R.; Meerholz, K.; Griesbeck, A. G. An Efficient Carbonyl-Alkene Metathesis of Bicyclic Oxetanes: Photoinduced Electron Transfer Reduction of the Paternò–Büchi Adducts from 2,3-Dihydrofuran and Aromatic Aldehydes. *Photochemical and Photobiological Sciences* **2006**, *5* (1), 51–55. https://doi.org/10.1039/b513875b.

(59) Pérez-Ruiz, R.; Gil, S.; Miranda, M. A. Stereodifferentiation in the Photochemical Cycloreversion of Diastereomeric Methoxynaphthalene-Oxetane Dyads. **2005**. https://doi.org/10.1021/jo048708.

(60) D'Auria, M.; Racioppi, R.; Viggiani, L. Paternò-Büchi Reaction between Furan and Heterocyclic Aldehydes: Oxetane Formation vs. Metathesis. *Photochemical and Photobiological Sciences* **2010**, *9* (8), 1134–1138. https://doi.org/10.1039/c0pp00076k.

(61) Guilford Jones, B.; Acquadro, M. A.; Carmody, M. A. *Long-Chain Enals Oia Carbonyl-Olefin Metathesis. An Application in Pheromone Synthesis*; 1975.

(62) Guilford Jones, B. I.; Schwartz, S. B.; Marton, M. T. *Regiospecific Thermal Cleavage of Some Oxetan Photoadducts : Carbonyl-Olefin Metathesis in Sequential Photochemical and Thermal Steps*; 1973.

(63) Albright, H.; Vonesh, H. L.; Schindler, C. S. Superelectrophilic Fe(III)-Ion Pairs as Stronger Lewis Acid Catalysts for (E)-Selective Intermolecular Carbonyl-Olefin Metathesis. *Organic Letters* **2020**, *22* (8), 3155–3160. https://doi.org/10.1021/acs.orglett.0c00917.

(64) Olah, G. A. *International Edition in English Superelectrophiles***; 1993; Vol. 32.

(65) Negishi, E. *CONCEPTS*; 1999; Vol. 5.

(66) Stephan, D. W.; Erker, G. Chemie Frustrierter Lewis-Paare: Entwicklung Und Perspektiven. *Angewandte Chemie* **2015**, *127* (22), 6498–6541. https://doi.org/10.1002/ange.201409800.

(67) Denmark, S. E.; Eklov, B. M.; Yao, P. J.; Eastgate, M. D. On the Mechanism of Lewis Base Catalyzed Aldol Addition Reactions: Kinetic and Spectroscopic Investigations Using

Rapid-Injection NMR. *J Am Chem Soc* **2009**, *131* (33), 11770–11787. https://doi.org/10.1021/ja902474j.

(68) Tomifuji, R.; Maeda, K.; Takahashi, T.; Kurahashi, T.; Matsubara, S. FeCl 3 as an Ion-Pairing Lewis Acid Catalyst. Formation of Highly Lewis Acidic FeCl 2+ and Thermodynamically Stable FeCl 4- to Catalyze the Aza-Diels-Alder Reaction with High Turnover Frequency. *Organic Letters* **2018**, *20* (23), 7474–7477. https://doi.org/10.1021/acs.orglett.8b03249.

(69) Ic00256a033.

(70) Davis, A. J.; Watson, R. B.; Nasrallah, D. J.; Gomez-Lopez, J. L.; Schindler, C. S. Superelectrophilic Aluminium(Iii)–Ion Pairs Promote a Distinct Reaction Path for Carbonyl–Olefin Ring-Closing Metathesis. *Nature Catalysis* **2020**, *3* (10), 787–796. https://doi.org/10.1038/s41929-020-00499-5.

(71) Strauss, S. H. *The Search for Larger and More Weakly Coordinating Anions*; 1993; Vol. 93.

(72) Beck, W.; Sunkel, K. Metal Complexes of Weakly Coordinating Anions. Precursors of Strong Cationic Organometallic Lewis Acids1^.

(73) Schottel, B. L.; Chifotides, H. T.; Shatruk, M.; Chouai, A.; Pérez, L. M.; Bacsa, J.; Dunbar, K. R. Anion-π Interactions as Controlling Elements in Self-Assembly Reactions of Ag(I) Complexes with π-Acidic Aromatic Rings. *J Am Chem Soc* **2006**, *128* (17), 5895–5912. https://doi.org/10.1021/ja0606273.

(74) Om50006a014.

(75) Mayfield, H. G.; Bull, W. E. *SECTION A I Norgan Ic, P Hysica I, and T Heoret Ica 1 Chemistry Co-Ordinating Tendencies of the Hexaf Luorophosphate Ion*.

(76) *Chapman et Al*.

(77) Bini, R.; Chiappe, C.; Marmugi, E.; Pieraccini, D. The “Non-Nucleophilic” Anion [Tf2N]- Competes with the Nucleophilic Br-: An Unexpected Trapping in the Dediazoniation Reaction in Ionic Liquids. *Chemical Communications* **2006**, No. 8, 897–899. https://doi.org/10.1039/b514988f.

(78) Hanson, C. S.; Psaltakis, M. C.; Cortes, J. J.; Siddiqi, S. S.; Devery, J. J. Investigation of Lewis Acid-Carbonyl Solution Interactions via Infrared-Monitored Titration. *Journal of Organic Chemistry* **2020**, *85* (2), 820–832. https://doi.org/10.1021/acs.joc.9b02822.

(79) Hanson, C. S.; Psaltakis, M. C.; Cortes, J. J.; Devery, J. J. Catalyst Behavior in Metal-Catalyzed Carbonyl-Olefin Metathesis. *J Am Chem Soc* **2019**, *141* (30), 11870–11880. https://doi.org/10.1021/jacs.9b02613.

(80) Malakar, T.; Hanson, C. S.; Devery, J. J.; Zimmerman, P. M. Combined Theoretical and Experimental Investigation of Lewis Acid-Carbonyl Interactions for Metathesis. *ACS Catalysis* **2021**, *11* (8), 4381–4394. https://doi.org/10.1021/acscatal.0c05277.

(81) Hull, S.; Keen, D. A. *Pressure-Induced Phase Transitions in AgCl, AgBr, and AgI*.

(82) Rodriguez-Ruiz, V.; Carlino, R.; Bezzenine-Lafollée, S.; Gil, R.; Prim, D.; Schulz, E.; Hannedouche, J. Recent Developments in Alkene Hydro-Functionalisation Promoted by Homogeneous Catalysts Based on Earth Abundant Elements: Formation of C-N, C-O and C-P Bond. *Dalton Transactions*. Royal Society of Chemistry July 21, 2015, pp 12029–12059. https://doi.org/10.1039/c5dt00280j.

(83) Ozawa, T.; Kurahashi, T.; Matsubara, S. Manganese Porphyrin Catalyzed Cycloisomerization of Enynes. *Organic Letters* **2012**, *14* (12), 3008–3011. https://doi.org/10.1021/ol301416f.

(84) Ic00219a025.

(85) Honeychuck, R. v; Hersh, W. H. *) And 1.954 (11) A (3b), 2.186 (3) and 1.979 (3) A (3c), 2.168 (7) and 1.500 (14) A (5*; 1989; Vol. 28.

(86) Gowik, P.; Klapiitke, T.; Thewalt, U. *Metallocen-Chemie Hochfluorierter Ligand-Systeme XI *. Synthese Und Charakterisierung von Cp,Ti(SbF,) 2 Und Cp,Ti(Sb, F,) 2; Struktur von Cp,Ti(SbF,) 2 Und Cp2V(SbF,) 2*; Elsevier Sequoia S.A, 1990.

(87) Dash, C.; Das, A.; Yousufuddin, M.; Dias, H. V. R. Isolable, Copper(I) Dicarbonyl Complexes Supported by N-Heterocyclic Carbenes. *Inorganic Chemistry* **2013**, *52* (3), 1584–1590. https://doi.org/10.1021/ic302455y.

(88) Smirnova, E. S.; Muñoz Molina, J. M.; Johnson, A.; Bandeira, N. A. G.; Bo, C.; Echavarren, A. M. Polynuclear Gold [Au I] 4 , [Au I] 8 , and Bimetallic [Au I 4 Ag I] Complexes: C−H Functionalization of Carbonyl Compounds and Homogeneous Carbonylation of Amines . *Angewandte Chemie* **2016**, *128* (26), 7613–7617. https://doi.org/10.1002/ange.201603200.

(89) Bour, C.; Monot, J.; Tang, S.; Guillot, R.; Farjon, J.; Gandon, V. Structure, Stability, and Catalytic Activity of Fluorine-Bridged Complexes IPr·GaCl2(μ-F)EFn -1 (EFn- = SbF6-, PF6-, or BF 4-). *Organometallics* **2014**, *33* (2), 594–599. https://doi.org/10.1021/om4012054.

(90) Kavoosi, A.; Fillion, E. Synthesis and Characterization of Tricarbastannatranes and Their Reactivity in B(C 6 F 5) 3 -Promoted Conjugate Additions . *Angewandte Chemie* **2015**, *127* (18), 5578–5582. https://doi.org/10.1002/ange.201500983.

(91) Michelet, B.; Colard-Itté, J. R.; Thiery, G.; Guillot, R.; Bour, C.; Gandon, V. Dibromoindium(Iii) Cations as a π-Lewis Acid: Characterization of [IPr·InBr2][SbF6] and

Its Catalytic Activity towards Alkynes and Alkenes. *Chemical Communications* **2015**, *51* (34), 7401–7404. https://doi.org/10.1039/c5cc00740b.

(92) Cornella, J.; Martin, R. Ni-Catalyzed Stereoselective Arylation of Inert C-O Bonds at Low Temperatures. *Organic Letters* **2013**, *15* (24), 6298–6301. https://doi.org/10.1021/ol4031815.

(93) Kshirsagar, U. A.; Regev, C.; Parnes, R.; Pappo, D. Iron-Catalyzed Oxidative Cross-Coupling of Phenols and Alkenes. *Organic Letters* **2013**, *15* (12), 3174–3177. https://doi.org/10.1021/ol401532a.

(94) Bao, L.-L.; Iu, Z.-Q. Tetrahydropyrrolization of Resveratrol and Other Stilbenes Improves Inhibitory Effects on DNA Oxidation. https://doi.org/10.1002/cmdc.201600205:NMR.

(95) Konishi, H.; Ueda, T.; Muto, T.; Manabe, K. Remarkable Improvement Achieved by Imidazole Derivatives in Ruthenium-Catalyzed Hydroesterification of Alkenes Using Formates. *Organic Letters* **2012**, *14* (18), 4722–4725. https://doi.org/10.1021/ol301850y.

(96) Yoo, K. S.; Yoon, C. H.; Jung, K. W. Oxidative Palladium(II) Catalysis: A Highly Efficient and Chemoselective Cross-Coupling Method for Carbon-Carbon Bond Formation under Base-Free and Nitrogenous-Ligand Conditions. *J Am Chem Soc* **2006**, *128* (50), 16384–16393. https://doi.org/10.1021/ja063710z.

(97) Kobayashi, K.; Ueno, M.; Kondo, Y. Phosphazene Base-Catalyzed Condensation of Trimethylsilylacetate with Carbonyl Compounds. *Chemical Communications* **2006**, No. 29, 3128–3130. https://doi.org/10.1039/b606056k.

(98) Charette, A. B.; Molinaro, C.; Brochu, C. Catalytic Asymmetric Cyclopropanation of Allylic Alcohols with Titanium-TADDOLate: Scope of the Cyclopropanation Reaction. *J Am Chem Soc* **2001**, *123* (49), 12168–12175. https://doi.org/10.1021/ja0108382.

(99) Hodgson, D. M.; Ying, K. C.; Nuzzo, I.; Freixas, G.; Kulikiewicz, K. K.; Cleator, E.; Paris, J. M. Intramolecular Cyclopropanation of Unsaturated Terminal Epoxides and Chlorohydrins. *J Am Chem Soc* **2007**, *129* (14), 4456–4462. https://doi.org/10.1021/ja0672932.

(100) Usui, I.; Schmidt, S.; Breit, B. Dual Palladium-and Proline-Catalyzed Allylic Alkylation of Enolizable Ketones and Aldehydes with Allylic Alcohols. *Organic Letters* **2009**, *11* (6), 1453–1456. https://doi.org/10.1021/ol9001812.

(101) Oppolzer, W.; Spivey, A. C.; Bochet, C. G. *1991,56, 2988 and References Mentioned Therein. Cf.\ Martin, S. F. The Amaryllidaceae Alkaloids*; Academic Press, 1994; Vol. 116.

(102) Daniel Little, R.; Carroll, G. L.; Petersen, J. L.; Tetrahedron Symp, K. Total Synthesis of the Marine Natural Product A9(12)-Capnellene. Reversal of Regiochemistry in the Intramolecular 1,3-Diyl Trapping Reaction. *Marine Natural Products, Chemical and Biological Perspectives* **1983**, *105* (2), 7129–7130.

(103) le Nôtre, J.; Touzani, R.; Lavastre, O.; Bruneau, C.; Dixneuf, P. H. Homologation of Monoterpenoids into New Sesquiterpenoids via Tandem Isomerisation/Claisen Rearrangement Reactions with Three-Component Ruthenium Catalysts, and Ru(Methallyl)2 (COD) Revealed by High Throughput Screening Techniques. *Advanced Synthesis and Catalysis* **2005**, *347* (6), 783–791. https://doi.org/10.1002/adsc.200404391.

(104) Aebi, J. D.; Deyo, D. T.; Sun, C. Q.; Guillaume, D.; Dunlap, B.; Rich, D. H. *Synthesis, Conformation, and Immunosuppressive Activities of Three Analogues of Cyclosporin A Modified in the 1-Position1 Both Conformations Have a Type IT 0-Tum for Residues 2-*·*5 and a Cis Amide Bond Between*; 1990; Vol. 33.

(105) Casey, C. P.; Bertz, S. H.; Burkhardt, T. J. *REACTION OF METAL-CARBENE COMPLEXES WITH OIAZOALKANES. A VERSATILE VINYL ETHER SYNTHESIS*; PequDon Pram, 1973.

(106) Banks, J. L.; Beard, H. S.; Cao, Y.; Cho, A. E.; Damm, W.; Farid, R.; Felts, A. K.; Halgren, T. A.; Mainz, D. T.; Maple, J. R.; Murphy, R.; Philipp, D. M.; Repasky, M. P.; Zhang, L. Y.; Berne, B. J.; Friesner, R. A.; Gallicchio, E.; Levy, R. M. Integrated Modeling Program, Applied Chemical Theory (IMPACT). *Journal of Computational Chemistry*. December 2005, pp 1752–1780. https://doi.org/10.1002/jcc.20292.

(107) Shao, Y.; Gan, Z.; Epifanovsky, E.; Gilbert, A. T. B.; Wormit, M.; Kussmann, J.; Lange, A. W.; Behn, A.; Deng, J.; Feng, X.; Ghosh, D.; Goldey, M.; Horn, P. R.; Jacobson, L. D.; Kaliman, I.; Khaliullin, R. Z.; Kuš, T.; Landau, A.; Liu, J.; Proynov, E. I.; Rhee, Y. M.; Richard, R. M.; Rohrdanz, M. A.; Steele, R. P.; Sundstrom, E. J.; Woodcock, H. L.; Zimmerman, P. M.; Zuev, D.; Albrecht, B.; Alguire, E.; Austin, B.; Beran, G. J. O.; Bernard, Y. A.; Berquist, E.; Brandhorst, K.; Bravaya, K. B.; Brown, S. T.; Casanova, D.; Chang, C. M.; Chen, Y.; Chien, S. H.; Closser, K. D.; Crittenden, D. L.; Diedenhofen, M.; Distasio, R. A.; Do, H.; Dutoi, A. D.; Edgar, R. G.; Fatehi, S.; Fusti-Molnar, L.; Ghysels, A.; Golubeva-Zadorozhnaya, A.; Gomes, J.; Hanson-Heine, M. W. D.; Harbach, P. H. P.; Hauser, A. W.; Hohenstein, E. G.; Holden, Z. C.; Jagau, T. C.; Ji, H.; Kaduk, B.; Khistyaev, K.; Kim, J.; Kim, J.; King, R. A.; Klunzinger, P.; Kosenkov, D.; Kowalczyk, T.; Krauter, C. M.; Lao, K. U.; Laurent, A. D.; Lawler, K. v.; Levchenko, S. v.; Lin, C. Y.; Liu, F.; Livshits, E.; Lochan, R. C.; Luenser, A.; Manohar, P.; Manzer, S. F.; Mao, S. P.; Mardirossian, N.; Marenich, A. v.; Maurer, S. A.; Mayhall, N. J.; Neuscamman, E.; Oana, C. M.; Olivares-Amaya, R.; Oneill, D. P.; Parkhill, J. A.; Perrine, T. M.; Peverati, R.;

Prociuk, A.; Rehn, D. R.; Rosta, E.; Russ, N. J.; Sharada, S. M.; Sharma, S.; Small, D. W.; Sodt, A.; Stein, T.; Stück, D.; Su, Y. C.; Thom, A. J. W.; Tsuchimochi, T.; Vanovschi, V.; Vogt, L.; Vydrov, O.; Wang, T.; Watson, M. A.; Wenzel, J.; White, A.; Williams, C. F.; Yang, J.; Yeganeh, S.; Yost, S. R.; You, Z. Q.; Zhang, I. Y.; Zhang, X.; Zhao, Y.; Brooks, B. R.; Chan, G. K. L.; Chipman, D. M.; Cramer, C. J.; Goddard, W. A.; Gordon, M. S.; Hehre, W. J.; Klamt, A.; Schaefer, H. F.; Schmidt, M. W.; Sherrill, C. D.; Truhlar, D. G.; Warshel, A.; Xu, X.; Aspuru-Guzik, A.; Baer, R.; Bell, A. T.; Besley, N. A.; Chai, J. da; Dreuw, A.; Dunietz, B. D.; Furlani, T. R.; Gwaltney, S. R.; Hsu, C. P.; Jung, Y.; Kong, J.; Lambrecht, D. S.; Liang, W.; Ochsenfeld, C.; Rassolov, V. A.; Slipchenko, L. v.; Subotnik, J. E.; van Voorhis, T.; Herbert, J. M.; Krylov, A. I.; Gill, P. M. W.; Head-Gordon, M. Advances in Molecular Quantum Chemistry Contained in the Q-Chem 4 Program Package. *Molecular Physics* **2015**, *113* (2), 184–215. https://doi.org/10.1080/00268976.2014.952696.

(108) Zimmerman, P. M. Single-Ended Transition State Finding with the Growing String Method. *Journal of Computational Chemistry* **2015**, *36* (9), 601–611. https://doi.org/10.1002/jcc.23833.

(109) Zimmerman, P. M. Growing String Method with Interpolation and Optimization in Internal Coordinates: Method and Examples. *Journal of Chemical Physics* **2013**, *138* (18). https://doi.org/10.1063/1.4804162.

(110) Jafari, M.; Zimmerman, P. M. Reliable and Efficient Reaction Path and Transition State Finding for Surface Reactions with the Growing String Method. *Journal of Computational Chemistry* **2017**, *38* (10), 645–658. https://doi.org/10.1002/jcc.24720.

(111) Zimmerman, P. Reliable Transition State Searches Integrated with the Growing String Method. *Journal of Chemical Theory and Computation* **2013**, *9* (7), 3043–3050. https://doi.org/10.1021/ct400319w.

(112) Metz, B.; Stoll, H.; Dolg, M. Small-Core Multiconfiguration-Dirac-Hartree-Fock-Adjusted Pseudopotentials for Post-d Main Group Elements: Application to PbH and PbO. *Journal of Chemical Physics* **2000**, *113* (7), 2563–2569. https://doi.org/10.1063/1.1305880.

(113) Peterson, K. A.; Figgen, D.; Goll, E.; Stoll, H.; Dolg, M. Systematically Convergent Basis Sets with Relativistic Pseudopotentials. II. Small-Core Pseudopotentials and Correlation Consistent Basis Sets for the Post-d Group 16-18 Elements. *Journal of Chemical Physics* **2003**, *119* (21), 11113–11123. https://doi.org/10.1063/1.1622924.

(114) Leininger, T.; Nicklass, A.; Kiichle, W.; Stoll, H.; Dolg, M.; Bergner, A. *PHYSICS LETTERS ELSEVIER The Accuracy of the Pseudopotential Approximation: Non-Frozen-Core Effects for Spectroscopic Constants of Alkali Fluorides XF (X = K, Rb, Cs)*; 1996; Vol. 255.

(115) Kaupp, M.; Schleyer, P. V. R.; Stoll, H.; Preuss, H. Pseudopotential Approaches to Ca, Sr, and Ba Hydrides. Why Are Some Alkaline Earth MX2 Compounds Bent? *The Journal of Chemical Physics* **1991**, *94* (2), 1360–1366. https://doi.org/10.1063/1.459993.

(116) Marenich, A. v.; Cramer, C. J.; Truhlar, D. G. Universal Solvation Model Based on Solute Electron Density and on a Continuum Model of the Solvent Defined by the Bulk Dielectric Constant and Atomic Surface Tensions. *Journal of Physical Chemistry B* **2009**, *113* (18), 6378–6396. https://doi.org/10.1021/jp810292n.

(117) Djurovic, A.; Vayer, M.; Li, Z.; Guillot, R.; Baltaze, J. P.; Gandon, V.; Bour, C. Synthesis of Medium-Sized Carbocycles by Gallium-Catalyzed Tandem Carbonyl-Olefin Metathesis/Transfer Hydrogenation. *Organic Letters* **2019**, *21* (19), 8132–8137. https://doi.org/10.1021/acs.orglett.9b03240.

(118) Catti, L.; Tiefenbacher, K. Brønsted-Säure-Katalysierte Carbonyl-Olefin-Metathese in Einer Selbstorganisierten Supramolekularen Wirtstruktur. *Angewandte Chemie* **2018**, *130* (44), 14797–14800. https://doi.org/10.1002/ange.201712141.

(119) Lambert, T. H. Development of a Hydrazine-Catalyzed Carbonyl-Olefin Metathesis Reaction. *Synlett* **2019**, *30* (17), 1954–1965. https://doi.org/10.1055/s-0039-1689924.

(120) Ohkubo, K.; Menon, S. C.; Orita, A.; Otera, J.; Fukuzumi, S. Quantitative Evaluation of Lewis Acidity of Metal Ions with Different Ligands and Counterions in Relation to the Promoting Effects of Lewis Acids on Electron Transfer Reduction of Oxygen. *Journal of Organic Chemistry* **2003**, *68* (12), 4720–4726. https://doi.org/10.1021/jo034258u.

(121) Evans, D. A.; Lectka, T.; Miller, S. J.; Murry, J. A.; Matt, P.; Norcross, R. D.; Johnson, J. S.; Kozlowski, M. C.; Ghosh, A. K.; Mathivanan, P.; Cappiello, J.; Krishnan, K.; Johannsen, M.; Jørgensen, K. A. *C 2-Symmetric Copper(II) Complexes as Chiral Lewis Acids. Enantioselective Catalysis of the Glyoxylate-Ene Reaction*; 1993; Vol. 115.

(122) Johnson, J. S.; Evans, D. A. Chiral Bis(Oxazoline) Copper(II) Complexes: Versatile Catalysts for Enantioselective Cycloaddition, Aldol, Michael, and Carbonyl Ene Reactions. *Accounts of Chemical Research* **2000**, *33* (6), 325–335. https://doi.org/10.1021/ar960062n.

(123) Hilt, G.; Pünner, F.; Möbus, J.; Naseri, V.; Bohn, M. A. A Lewis Acidity Scale in Relation to Rate Constants of Lewis Acid Catalyzed Organic Reactions. *European Journal of Organic Chemistry* **2011**, No. 30, 5962–5966. https://doi.org/10.1002/ejoc.201101029.

(124) *INFRARED SPECTRA OF XANTH0NE:LEWIS ACID COMPLEXES*?*

(125) Tran, U. P. N.; Oss, G.; Breugst, M.; Detmar, E.; Pace, D. P.; Liyanto, K.; Nguyen, T. v. Carbonyl-Olefin Metathesis Catalyzed by Molecular Iodine. *ACS Catalysis* **2019**, *9* (2), 912–919. https://doi.org/10.1021/acscatal.8b03769.

(126) Wang, R.; Chen, Y.; Shu, M.; Zhao, W.; Tao, M.; Du, C.; Fu, X.; Li, A.; Lin, Z. AuCl3-Catalyzed Ring-Closing Carbonyl–Olefin Metathesis. *Chemistry - A European Journal* **2020**, *26* (9), 1941–1946. https://doi.org/10.1002/chem.201905199.

(127) Jermaks, J.; Quach, P. K.; Seibel, Z. M.; Pomarole, J.; Lambert, T. H. Ring-Opening Carbonyl-Olefin Metathesis of Norbornenes. *Chemical Science* **2020**, *11* (30), 7884–7895. https://doi.org/10.1039/d0sc02243h.

(128) Lambert, T. H. Development of a Hydrazine-Catalyzed Carbonyl-Olefin Metathesis Reaction. *Synlett* **2019**, *30* (17), 1954–1965. https://doi.org/10.1055/s-0039-1689924.

(129) Zhang, Y.; Jermaks, J.; MacMillan, S. N.; Lambert, T. H. Synthesis of 2 H-Chromenes via Hydrazine-Catalyzed Ring-Closing Carbonyl-Olefin Metathesis. *ACS Catalysis* **2019**, *9* (10), 9259–9264. https://doi.org/10.1021/acscatal.9b03656.

(130) Hong, X.; Liang, Y.; Griffith, A. K.; Lambert, T. H.; Houk, K. N. Distortion-Accelerated Cycloadditions and Strain-Release-Promoted Cycloreversions in the Organocatalytic Carbonyl-Olefin Metathesis. *Chemical Science* **2014**, *5* (2), 471–475. https://doi.org/10.1039/c3sc52882k.

(131) Griffith, A. K.; Vanos, C. M.; Lambert, T. H. Organocatalytic Carbonyl-Olefin Metathesis. *J Am Chem Soc* **2012**, *134* (45), 18581–18584. https://doi.org/10.1021/ja309650u.

(132) Musacchio, A. J.; Nguyen, L. Q.; Beard, G. H.; Knowles, R. R. Catalytic Olefin Hydroamination with Aminium Radical Cations: A Photoredox Method for Direct C-N Bond Formation. *J Am Chem Soc* **2014**, *136* (35), 12217–12220. https://doi.org/10.1021/ja5056774.

(133) Fernández-Mateos, A.; Madrazo, S. E.; Teijón, P. H.; González, R. R. Radical Cyclization of Epoxy Vinyl- and Allylsulfones Promoted by Titanocene Chloride. *Journal of Organic Chemistry* **2015**, *80* (9), 4378–4391. https://doi.org/10.1021/acs.joc.5b00206.

(134) Kuriyama, Y.; Sasano, Y.; Hoshino, Y.; Uesugi, S. ichiro; Yamaichi, A.; Iwabuchi, Y. Highly Regioselective 5-Endo-Tet Cyclization of 3,4-Epoxy Amines into 3-Hydroxypyrrolidines Catalyzed by La(OTf)3. *Chemistry - A European Journal* **2021**, *27* (6), 1961–1965. https://doi.org/10.1002/chem.202004455.

(135) Johnson, L. A.; Dunbabin, A.; Benton, J. C. R.; Mart, R. J.; Allemann, R. K. Modular Chemoenzymatic Synthesis of Terpenes and Their Analogues. *Angewandte Chemie - International Edition* **2020**, *59* (22), 8486–8490. https://doi.org/10.1002/anie.202001744.

(136) Lucke, A. J.; Young, D. J. Electrophilic Cleavage of Cyclopropylmethystannanes: An Experimental Comparison of σ-σ and σ-π Conjugation. *Journal of Organic Chemistry* **2005**, *70* (9), 3579–3583. https://doi.org/10.1021/jo047822p.

(137) Cai, Z.; Yongpruksa, N.; Harmata, M. Total Synthesis of the Terpenoid Buddledone A: 11-Membered Ring-Closing Metathesis. *Organic Letters* **2012**, *14* (7), 1661–1663. https://doi.org/10.1021/ol300400x.

(138) Anderson, T. E.; Woerpel, K. A. Strain-Promoted Oxidation of Methylenecyclopropane Derivatives Using N-Hydroxyphthalimide and Molecular Oxygen in the Dark. *Organic Letters* **2020**, *22* (14), 5690–5694. https://doi.org/10.1021/acs.orglett.0c02075.

(139) Xu, B.; Shi, M. Ring-Opening Reactions of Methylenecyclopropanes Promoted by Metal Halides. *Organic Letters* **2003**, *5* (9), 1415–1418. https://doi.org/10.1021/ol034142k.

(140) Labes, R.; Battilocchio, C.; Mateos, C.; Cumming, G. R.; de Frutos, O.; Rincón, J. A.; Binder, K.; Ley, S. v. Chemoselective Continuous Ru-Catalyzed Hydrogen-Transfer Oppenauer-Type Oxidation of Secondary Alcohols. *Organic Process Research and Development* **2017**, *21* (9), 1419–1422. https://doi.org/10.1021/acs.oprd.7b00190.

(141) Labes, R.; González-Calderón, D.; Battilocchio, C.; Mateos, C.; Cumming, G. R.; de Frutos, O.; Rincón, J. A.; Ley, S. v. Rapid Continuous Ruthenium-Catalysed Transfer Hydrogenation of Aromatic Nitriles to Primary Amines. *Synlett* **2017**, *28* (20), 2855–2858. https://doi.org/10.1055/s-0036-1589096.

(142) Köckinger, M.; Hone, C. A.; Gutmann, B.; Hanselmann, P.; Bersier, M.; Torvisco, A.; Kappe, C. O. Scalable Continuous Flow Process for the Synthesis of Eflornithine Using Fluoroform as Difluoromethyl Source. *Organic Process Research and Development* **2018**, *22* (11), 1553–1563. https://doi.org/10.1021/acs.oprd.8b00318.

(143) Mata, A.; Hone, C. A.; Gutmann, B.; Moens, L.; Kappe, C. O. Continuous-Flow Pd-Catalyzed Carbonylation of Aryl Chlorides with Carbon Monoxide at Elevated Temperature and Pressure. *ChemCatChem* **2019**, *11* (3), 997–1001. https://doi.org/10.1002/cctc.201801974.

(144) Labes, R.; Mateos, C.; Battilocchio, C.; Chen, Y.; Dingwall, P.; Cumming, G. R.; Rincón, J. A.; Nieves-Remacha, M. J.; Ley, S. v. Fast Continuous Alcohol Amination Employing a

Hydrogen Borrowing Protocol. *Green Chemistry* **2019**, *21* (1), 59–63. https://doi.org/10.1039/c8gc03328e.

(145) Sagmeister, P.; Kaldre, D.; Sedelmeier, J.; Moessner, C.; Püntener, K.; Kummli, D.; Williams, J. D.; Kappe, C. O. Intensified Continuous Flow Synthesis and Workup of 1,5-Disubstituted Tetrazoles Enhanced by Real-Time Process Analytics. *Organic Process Research and Development* **2021**, *25* (5), 1206–1214. https://doi.org/10.1021/acs.oprd.1c00096.

(146) Sambiagio, C.; Ferrari, M.; van Beurden, K.; Ca', N. della; van Schijndel, J.; Noel, T. Continuous-Flow Synthesis of Pyrylium Tetrafluoroborates: Application to Synthesis of Katritzky Salts and Photoinduced Cationic RAFT Polymerization. *Organic Letters* **2021**, *23* (6), 2042–2047. https://doi.org/10.1021/acs.orglett.1c00178.

(147) Quesnel, J. S.; Kayser, L. v.; Fabrikant, A.; Arndtsen, B. A. Acid Chloride Synthesis by the Palladium-Catalyzed Chlorocarbonylation of Aryl Bromides. *Chemistry - A European Journal* **2015**, *21* (26), 9550–9555. https://doi.org/10.1002/chem.201500476.

(148) Schröder, N.; Wencel-Delord, J.; Glorius, F. High-Yielding, Versatile, and Practical [Rh(III)Cp*]-Catalyzed Ortho Bromination and Iodination of Arenes. *J Am Chem Soc* **2012**, *134* (20), 8298–8301. https://doi.org/10.1021/ja302631j.

(149) Mukhopadhyay, S.; Batra, S. Direct Transformation of Arylamines to Aryl Halides via Sodium Nitrite and N-Halosuccinimide. *Chemistry - A European Journal* **2018**, *24* (55), 14622–14626. https://doi.org/10.1002/chem.201803347.

(150) Moreira, J. A.; Corrêa, A. G. Enantioselective Synthesis of Three Stereoisomers of 5,9-Dimethylpentadecane, Sex Pheromone Component of Leucoptera Coffeella, from (-)-

Isopulegol. *Tetrahedron Asymmetry* **2003**, *14* (23), 3787–3795.

https://doi.org/10.1016/j.tetasy.2003.09.030.

Chapter 2 Superelectrophilic Aluminum(III)-Ion Pairs Promote A Distinct Reaction Path for Carbonyl-Olefin Metathesis

*This work has been published in:

Davis, A. J.; Watson, R. B.; Nasrallah, D. J.; Gomez-Lopez, J. L.; Schindler, C. S. *Nature Catalysis*, **2020**, *3*, 787-796.

2.1 Introduction

Catalytic carbonyl-olefin metathesis has seen a recent surge in the literature, with a broad range of catalyst systems – including Lewis acids,[31–44] Brønsted acids,[45,46] and organocatalysts[47–50] - being reported in the last 10 years.[51] This strategy employs carbonyls and olefins as coupling partners to provide value-added olefinic products through an operationally simplistic regime.[52–62]

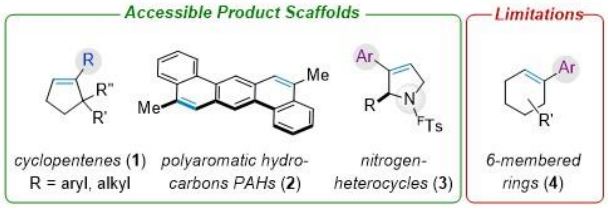

Figure 2.1. Examples of ring-closing carbonyl-olefin metathesis product scaffolds and limitations.

Furthermore, current methods for this reaction paradigm rely on a [2+2]-cycloaddition to form oxetanes as key intermediates, which then can readily fragment to the desired products. Our group first pioneered efforts to develop a Lewis acid-catalyzed protocol for ring-closing carbonyl-olefin metathesis or aryl ketones.[41] The use of catalytic amounts of $FeCl_3$ to promote the reaction served as an environmentally benign and cost-efficient strategy for cyclic olefin formation. Since this initial report, we have expanded the role of $FeCl_3$ as a potent catalyst to transform a wide variety of substrates into the corresponding ring-closing products, including cyclopentenes (**1**),[42] polyaromatic scaffolds (**2**),[43] and *N*-heterocyclic structures[38,44] (**3, Figure 2.1**). Additional efforts have focused on developing general protocols for ring-opening[37] and cross metathesis variations.[63] Despite these advances, there still exists certain limitations within the field that simple Lewis acids alone have not been able to overcome. Specifically, ring-closing variations generally remain limited to 5-membered ring formation, while access to 6-membered rings **4** requires the formation

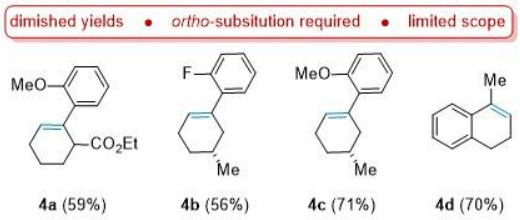

Figure 2.2. Limited scope of $FeCl_3$-catalyzed 6-membered ring formation.

of highly conjugated polyaromatic systems[43] or require high loadings of catalysts[44] to achieve synthetic useful yields. General protocols for cyclohexene formation using catalytic $FeCl_3$ require the use of *ortho*-substituted aryl ketones, and was limited to just four examples in moderate yields of 56-71% (**Figure 2.2**).[41] Additionally, competing carbonyl-ene reactivity have proven detrimental to metathesis pathways, resulting in diminished yields of the desired products. Efforts within our group have been aimed at overcoming these limitations. The use of superelectrophilic[64,65] $FeCl_3$-homodimers **7**, which can be formed via *in situ* coordination of two monomeric units of $FeCl_3$ **(6)**, have proven effective in overcoming challenges associated with activating less reactive aliphatic ketones as substrates for ring-closing carbonyl-olefin metathesis to form trialkyl substituted cyclopentenes **10** (**Figure 2.3**).[42] The polarization of the metal center induced by the coordination event results in a net increase of the Lewis acidity of the metal center. We hypothesized that further polarization could result in the formation of ion pair **8** with further

enhanced Lewis acidic character (**Figure 2.3**, bottom panel).[66–69] The formation of the ion pair species could result in more potent catalyst systems to activate metathesis substrates currently inactive under available protocols. Specifically, we envisioned employing this catalyst to efficiently convert aryl ketones into the corresponding 6- and 7-membered ring-closing products through carbonyl-olefin metathesis. The results discussed in this chapter focus on the development of such a catalyst, its employment across a broad scope of substrates, and the mechanistic insights gained.[70] This includes the identification of a new and distinct reaction pathway for carbonyl-olefin metathesis in direct competition with the previously accepted [2+2]-cycloaddition route.

2.2 Results and Discussion

Initial efforts into this investigation were focused on the identification of optimal conditions for ring-closing carbonyl-olefin metathesis to access 6-membered rings. Lewis acids such as $FeCl_3$,[35,41] $GaCl_3$,[37] $InCl_3$, and $AlCl_3$ were all evaluated, but resulted diminished yields of no more than 25% of the desired cyclohexene **12** (**Figure 2.4**, entries 1-4). Importantly, higher loadings of $FeCl_3$ (10 mol%) did not result in increased yields, indicating that superelectrophilic[64,65] $FeCl_3$

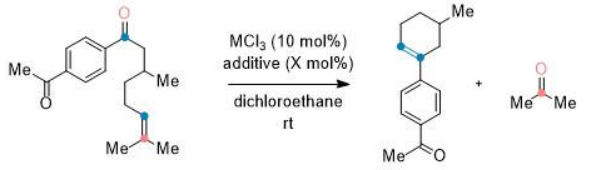

11 **12** **13**

entry	Lewis acid	additive	mol %	yield **14** (%)	conv. (%)
1	$FeCl_3$	-	-	25	46
2	$GaCl_3$	-	-	17	44
3	$InCl_3$	-	-	10	41
4	$AlCl_3$	-	-	0	0
5	$FeCl_3$	$AgSbF_6$	10	69	92
6	$GaCl_3$	$AgSbF_6$	10	71	99
7	$InCl_3$	$AgSbF_6$	10	72	99
8	**$AlCl_3$**	**$AgSbF_6$**	**10**	**90**	**99**
9	$AlCl_3$	$AgBF_4$	10	0	8
10	$AlCl_3$	$AgPF_6$	10	0	11
11	$AlCl_3$	$AgAsF_6$	10	71	81
12	$AlCl_3$	AgOTf	10	0	19
13	$AlCl_3$	$AgNTf_2$	10	43	58
14	$AlCl_3$	$AgBPh_4$	10	0	38
15	$AlCl_3$	$AgBAr^F{}_4$	10	75	94
16	$AlCl_3$	$AgSbF_6$	20	86	99
17	$AlCl_3$	$AgSbF_6$	30	84	99
18	-	$Ph_3C^+BF_4^-$	20	0	37
19	-	$C_7H_7^+BF_4^-$	15	4	63
20	-	$C_7H_7^+BF_4^-$	10	0	19
21	-	I_2	10	7	82

Conditions: Reactions were performed on 0.10 mmol of **11** in DCE (0.02M) at room temperature for 5-24 hours. Yields and conversions determined by ^{1}H NMR against mesitylene as internal standard. For entried 18-21, reported

Figure 2.4. Optimization of reaction conditions.

homodimers, which have been demonstrated to form under these conditions,[42] are unsuited for the formation of larger ring systems. This led us to evaluate ion pairs as potential catalysts for this transformation. We hypothesized that the increased electrophilic character of the metal center could be better suited for activating these less reactive substrates. Specifically, we envisioned forming these ion pair catalysts via *in situ* chloride abstraction from the neutral Lewis acid by an Ag(I).[71,72] Indeed, when $FeCl_3$ was employed as the active catalyst along with $AgSbF_6$, a sharp increase in yield from 25% to 69% was observed (entry 1 vs. entry 5). When other Lewis acids were evaluated as ion pairs, such as $GaCl_3$ and $InCl_3$, similarly improved yields were observed (entries 6-7). The ion pair $[AlCl_2][SbF_6]$ proved to be the superior catalytic system, providing the metathesis product in 90% yield (Figure 2.1, entry 8). Other Ag(I) salts bearing weakly coordinating anions[73–75] such as $[BF_4]^-$, $[PF_6]^-$, and $[AsF_6]^-$ were also evaluated. While both $AgBF_4$ and $AgPF_6$ resulted in only slight decomposition of starting ketone **11**, $AgAsF_6$ did provide metathesis product **12** in good yields of 71% (entries 9-11). Silver salts bearing more strongly coordinating anions, such as AgOTf[76] and $AgNTf_2$[77] also proved inferior, providing respective yields of 0% and 71% of cyclohexene **11** (entries 12-13). Similarly, noncoordinating anions were evaluated for their ability to promote the metathesis reaction. While $AgBPh_4$ proved ineffective due to its poor solubility in DCE, $AgBArF_4$ yielded **12** in 75% yield (entries 14-15). Next, the loading of silver salt was evaluated. Increasing the amount to 20 and 30 mol% in combination with 10 mol% of $AlCl_3$, which would promote additional halide abstraction from the metal center, did not promote any increased reactivity relative to the optimal conditions and ultimately provided yields of 86% and 84% of **12**, respectively (entries16-17).

With the optimal catalyst system in hand, we next turned our attention to the overall scope of the transformation. Generally, the conditions were well suited to both electron-rich and -poor substituents at the *ortho, meta,* and *para* positions of the aryl ketone moiety to smoothly access the corresponding cyclohexene metathesis products **16** in excellent yields of 54-99% (**Figure 2.5**). Substrates bearing electron-donating groups such as dimethoxy substrates **30**, and **36** provided 61% and 57% of the metathesis products, respectively. Cyclohexenes containing chlorinated rings **25**, **28**, **33**, and **40** could be easily accessed in up to 85%, while aryl bromides **20** and **31** were formed in 75%, enabling the formation of cyclohexenes capable of further functionalization through cross coupling reactions. Strongly electron-deficient systems such as acetylated trifluoromethylated aryl fragments (**19**, **22**, **34**) could also be employed providing up to 90% of

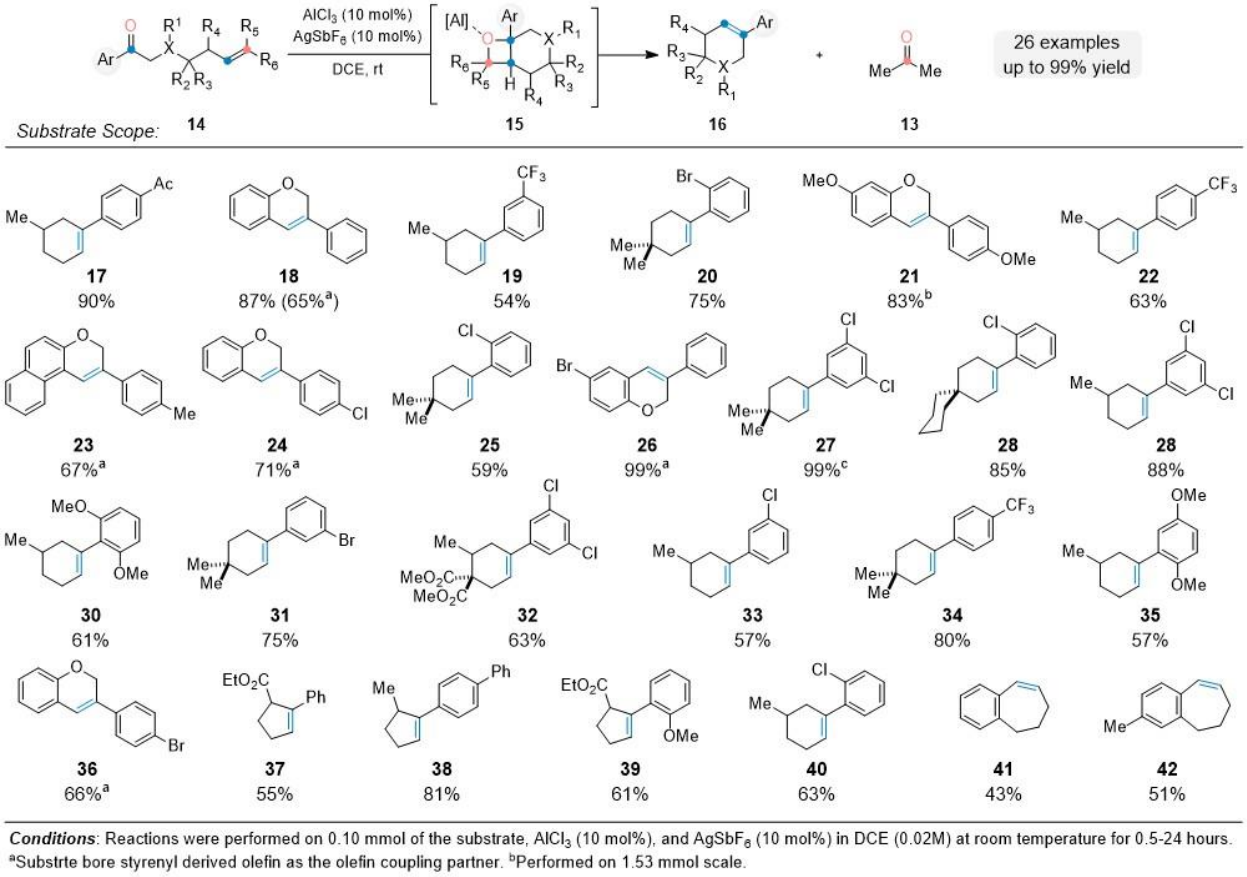

Figure 2.5. Reaction scope of Al(III)-ion pairs as superelectrophilic catalysts for metathesis.

the desired product. The substitution of the aliphatic backbone was also well tolerated, providing up to 99% of the metathesis products. Specifically, dimethyl (**20**, **25**, **27**, **34**) and diester (**32**) substituted aryl ketones were efficiently converted into the functionalized cyclohexene products. Additionally, spirocycle **28** was formed in excellent yield of 85% under the optimized reaction conditions. Cyclic motifs bearing Lewis basic heteroatoms could also be accessed using the ion pair catalyst.[36–39,41,43,44] Chroman-derived scaffolds were especially well tolerated, broadening the scope of oxygen atom incorporation for the carbonyl-olefin metathesis paradigm. Specifically, electron-poor chromans (**24**, **26**, **38**) were formed in up to 99% yield, and incorporated halide functionality, which could serve as handles for further reactivity. Electron-rich chromans were also well suited for this transformation, with dimethoxy **21** and methylated **23** accessed in 83% and 67% yield, respectively. Importantly, both styrenyl and prenyl derived olefin subunits could be employed to provide efficient yields of 87% or 65%, respectively, of **18**. Finally, 5-membered rings (**37**, **38**, **39**) could be accessed in 55-81% yield using the ion pair catalyst, while 7-membered rings (**41**, **42**) could be formed from the corresponding aryl aldehydes in up to 51%.

The scope of alkene tolerance was also examined as part of this study by subjecting trifluoromethyl ketone **43** bearing various olefin substituents to the optimized reactions conditions (**Figure 2.6**). The prenylated variant **43a** was well tolerated, providing 80% of the metathesis product, styrenyl olefin **43b** resulted in slightly diminished yields of 44%. Additionally, substrate **43c**, which would produce acetophenone as the carbonyl byproduct upon metathesis, provided just 27% of cyclohexene **34**. These two results are most likely caused by catalyst inhibition by the carbonyl byproducts upon formation.[39,78–80] Terminal olefin **43d** provided 68% of the metathesis product via *in situ* isomerization to the corresponding prenyl olefin. Finally, diphenyl olefin **43e** remained unreactive, likely due to the increased steric strain of the oxetane intermediate, while crotyl- and allylic olefins **43f** and **43g** were unreactive due to their inherent lack of nucleophilicity.

entry	alkene		yield (%)	entry	alkene		yield (%)
1		**44a**	80	4		**44d**	68
2		**44b**	44	5		**44e**	0
3		**44c**	27	6		**44f:** R = Me	0
				7		**44g:** R = H	0

Conditions: All reactions were performed using 0.10 mmol of the substrate in DCE (0.02 M) at room temperature for 7-24 h.

Figure 2.6. Alkene scope.

2.3 Mechanistic Investigations

Our mechanistic investigations into this transformation began with obtaining experimental evidence for the formation of the active ion pair catalyst. We hypothesized that up to 5 distinct Lewis acids could be operative under the reaction conditions. Specifically, $AlCl_3$ (A) or $AgSbF_6$ (B) prior to halide abstraction, the proposed ion pair catalyst $[AlCl_2][SbF_6]$ (C), or $AlCl_2F$ (D) or SbF_5 (E), which could be formed upon fluoride transfer of the ion pair, were all theorized as potential catalysts (**Figure 2.7**). To test this, dichlorinated aryl ketone **45**, which was selected as

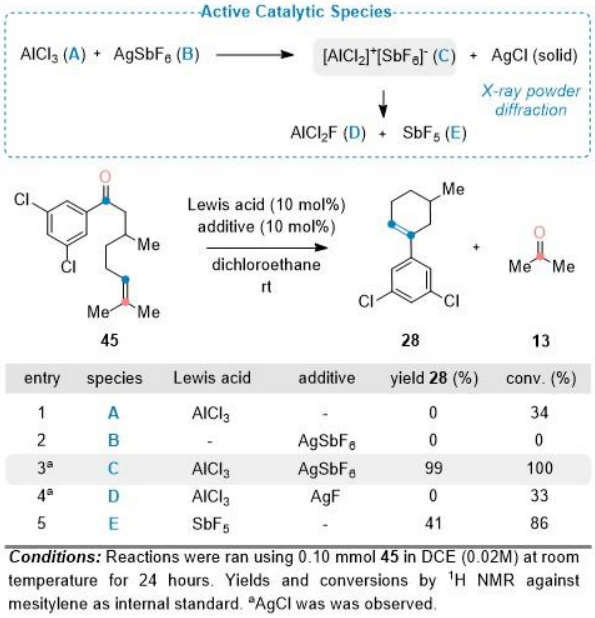

entry	species	Lewis acid	additive	yield **28** (%)	conv. (%)
1	A	$AlCl_3$	-	0	34
2	B	-	$AgSbF_6$	0	0
3[a]	C	$AlCl_3$	$AgSbF_6$	99	100
4[a]	D	$AlCl_3$	AgF	0	33
5	E	SbF_5	-	41	86

Conditions: Reactions were ran using 0.10 mmol **45** in DCE (0.02M) at room temperature for 24 hours. Yields and conversions by ^1H NMR against mesitylene as internal standard. [a]AgCl was was observed.

Figure 2.7. Evaluation of possible catalytic species.

the mechanistic probe due to its high reactivity **(Figure 2.5**, 88% yield) was subjected to each catalytic regime. Neither $AlCl_3$ nor $AgSbF_6$ alone resulted in any of the desired product **28** (entries 1-2). Under optimal reaction conditions, **28** was quantitatively converted to the metathesis adduct (entry 3), Additionally, AgCl was observed as a solid precipitate throughout the course of the reaction. By utilizing AgF for halide abstraction, $AlCl_2F$ could be formed *in situ*, although this did not provide any of the desired product, despite observed AgCl formation. Finally, although commercially available SbF_5 did result in metathesis, it was in a reduced yield of just 41%, supporting it was indeed not the active catalyst. Furthermore, the observed AgCl precipitate which was observed throughout the reaction was recovered, was both qualitatively and quantitatively identified. 1.5 mg of the white solid was recovered from the reaction of ketone **45**, consistent with quantitative formation of AgCl, and analyzed by X-ray powder diffraction, which confirmed its identity when compared to literature precedent (**Figure 2.8**).[81] Together, these two results provide experimental support for the formation and employment of $[AlCl_2][SbF_6]$ as the active catalytic species for ring-closing carbonyl-olefin metathesis for 6-membered rings.

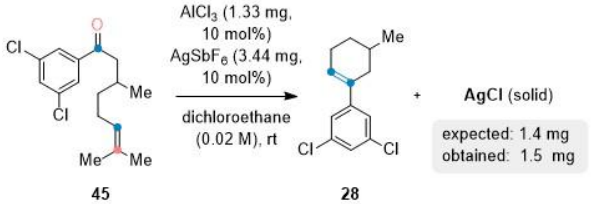

Figure 2.8. AgCl identification under the optimized reaction conditions.

With the active catalyst identified, we next sought to understand why the ion pair catalyst serves as a more potent system for 6-membered ring formation. To this end we opted to follow the reaction progress by ^{1}H NMR, a technique which could not be employed for the analogous Fe(III)-catalyzed transformation, due it the paramagnetic nature of $FeCl_3$.[39,41] When subjected to the optimized reaction conditions, mechanistic probe **46** was converted into corresponding metathesis product **27 (Figure 2.9**, left panel). Interestingly, a third species, marked in red, was initially formed, but was also consumed throughout the course of the reaction. Independent synthesis and characterization confirmed this new species as carbonyl-ene adduct **47**. Interestingly, this carbonyl-ene product **47** reached its maximum of 20% at roughly 45 minutes, with 31% total conversion of aryl ketone **46**. The added complexity of formation and depletion of **47** led us to explore whether carbonyl-ene was simply reacting in a reversible pre-equilibrium with substrate **46** before funneling into the metathesis product, or if it was in fact serving as an active intermediate along the reaction pathway. To gain insight into the role of **47** in the carbonyl-olefin metathesis reaction, we independently synthesized alcohol **47**, subjected it to the optimized reaction conditions, and again followed the reaction by ^{1}H NMR spectroscopy (**Figure 2.9**, right panel). Carbonyl-ene adduct **47** was quickly converted to aryl ketone **46**, which reached its maximum formation of 47% at 102 minutes, while only 19% of the metathesis product was produced. This rapid isomerization suggests the ion pair catalyst promotes a reversible equilibrium reaction

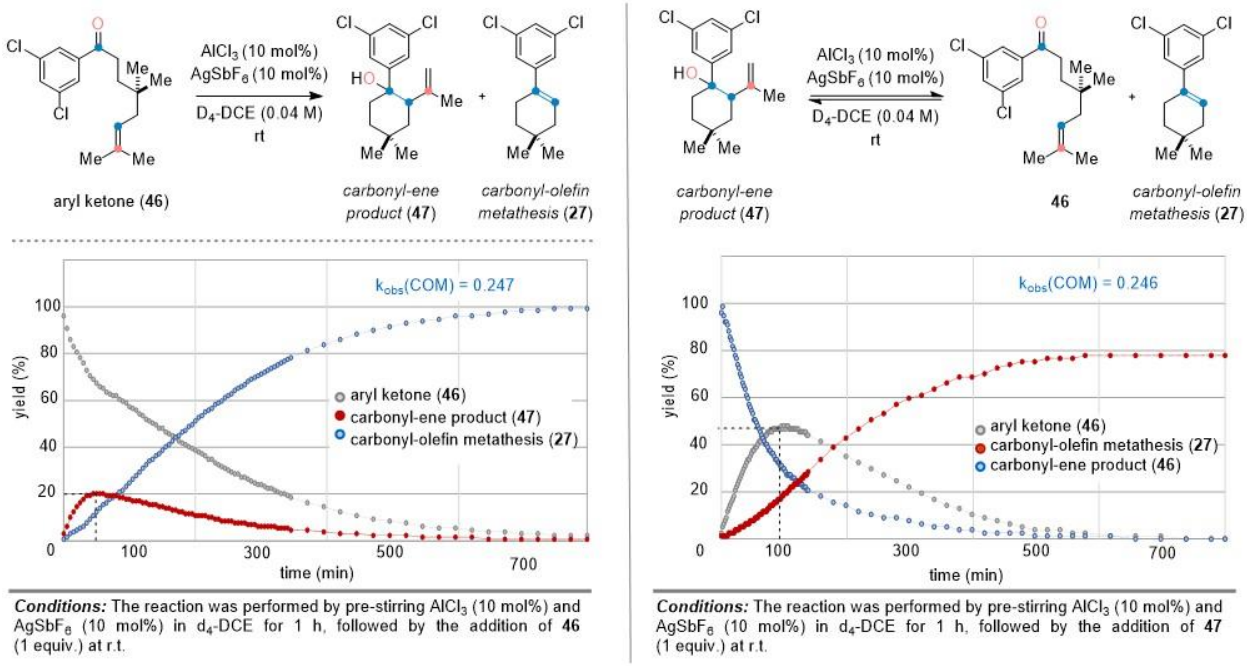

Figure 2.9. ^{1}H NMR analysis of carbonyl-olefin metathesis.

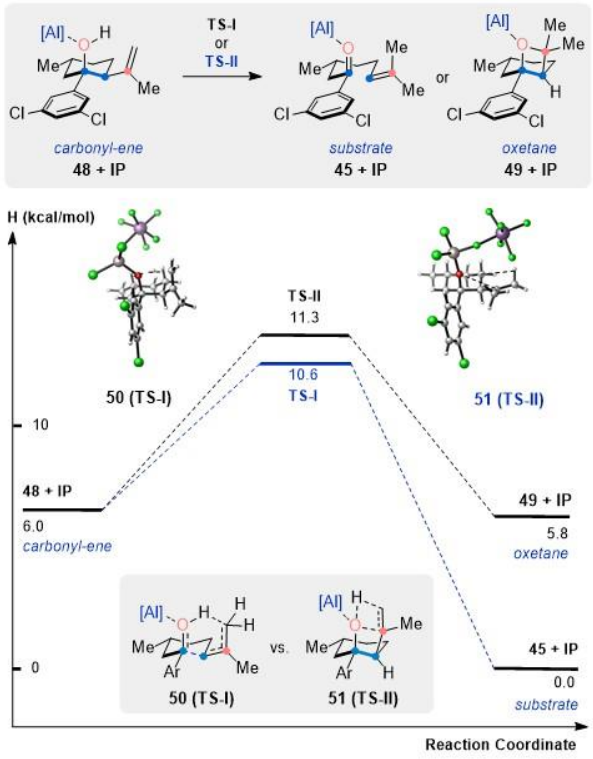

Figure 2.10. Computational reactive pathways from **48**.

between starting material **46** and carbonyl-ene **47**, favoring the ketone. Further analysis also revealed that once this equilibrium point was established, the rate of metathesis product formation was nearly identical and independent of the initial concentrations of the two species; starting from aryl ketone **46** provided a product formation rate of 0.247. while carbonyl-ene was converted to **27** at a rate of 0.246 From these results, we hypothesized that the Al(III)-ion pair catalyst could be promoting one of two distinct reaction pathways for carbonyl-olefin metathesis. Specifically, either aryl ketone **46** is reversibly converted to carbonyl-ene **47**, but does not proceed forward towards metathesis, or the resulting alcohol intermediate can then undergo a subsequent hydroalkoxylation[82] event to form an intermediate oxetane. Either pathway would serve as an important advancement for carbonyl-olefin metathesis, as previous methods relying on Lewis acid catalysis have activated competing carbonyl-ene pathways as a detrimental side reaction.[36,37] To distinguish which pathway is operative for metathesis, we employed computational modelling. The results revealed that both pathways are active for tertiary alcohol **48** in the presence of the ion pair catalyst (**Figure 2.10**). Retro carbonyl-ene, which provides aryl ketone starting material **45**, is promoted via TS-I and proceeds with an enthalpic barrier of 11.3 kcal/mol. Once formed, activated aryl ketone **45** is thermodynamically more stable than the corresponding carbonyl-ene

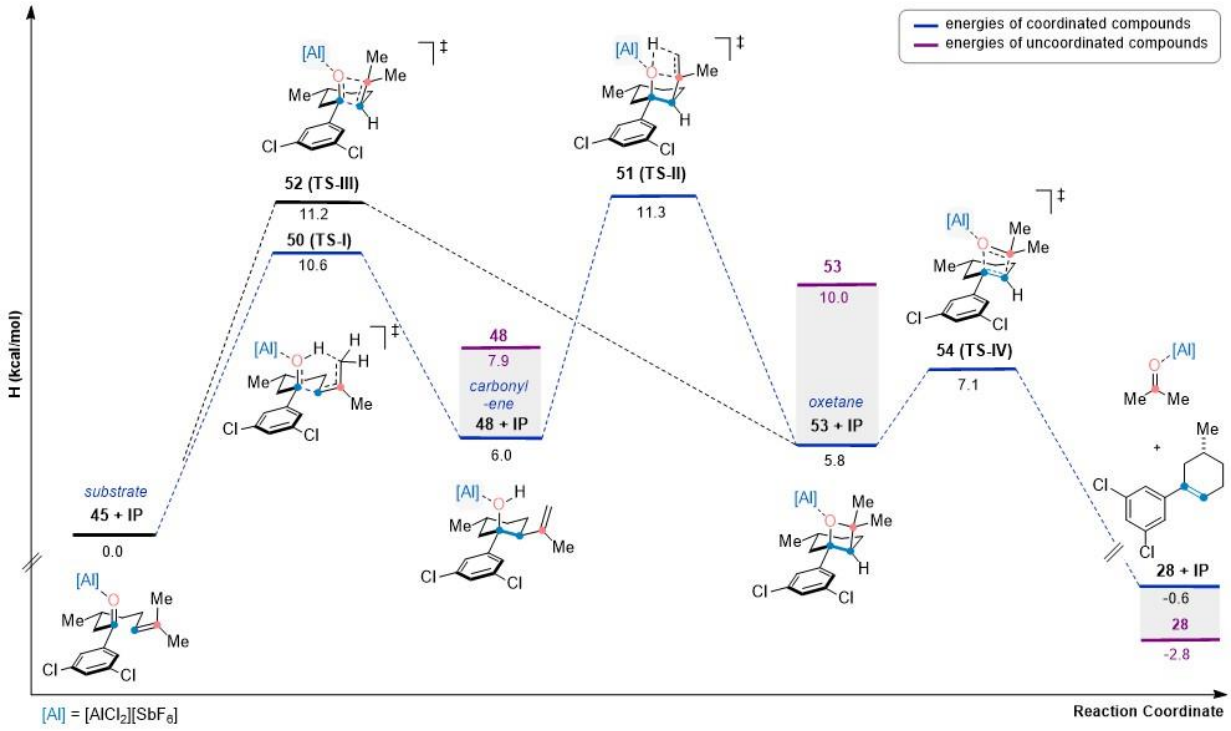

Figure 2.11. Full computational reaction profile.

adduct **48** by 6.0 kcal/mol, supporting the predominant formation of aryl ketone **45** observed as the favored isomer during ^{1}H NMR analysis (**Figure 2.9**, right panel). Interestingly, activated carbonyl-ene **48** can also undergo a direct hydroalkoxylation to form oxetane **49** via TS-I. The enthalpic barrier for this mode of reactivity is 10.6 kcal/mol, roughly 0.7 kcal/mol lower in energy than the retro carbonyl-ene pathway, supporting our unprecedented hypothesis that carbonyl-ene **48** is active intermediate for carbonyl-olefin metathesis. This set of computations led us to next investigate the full reaction pathway for carbonyl-olefin metathesis using the Al(III)-ion pair (**Figure 2.11**). Catalyst-bound aryl ketone **46** can undergo a reversible carbonyl-ene reaction to form tertiary alcohol **48** via TS-I with an enthalpic barrier of 10.6 kcal/mol, or directly undergo an asynchronous, concerted [2+2]-cycloaddition form oxetane **53** via TS-III, requiring traversing an enthalpic barrier 11.2 kcal/mol. Oxetane formation from activated carbonyl-ene **48** can then proceed through a barrier of 11.3 kcal/mol, energetically similar to the direct [2+2]-addition step. Once formed, oxetane **53** can then fragment through a retro-[2+2]-cycloaddition to furnish metathesis product **28** and acetone as the carbonyl byproduct. Importantly, as part of the computational investigations, we also explored the relative energies of the reactive intermediates when unbound from the Al(III)-ion pair catalyst. The liberated carbonyl-ene intermediate **48** was

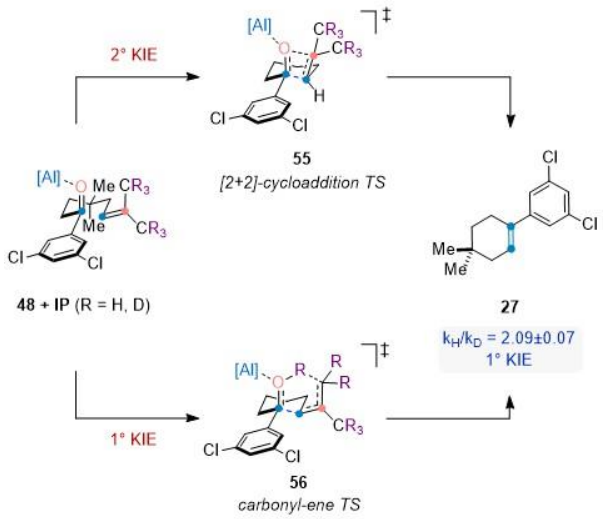

Figure 2.12. Kinetic isotope effects on carbonyl-olefin metathesis pathways.

7.9 kcal/mol higher in energy that that of the activated aryl ketone, again supporting the observed equilibrium (**Figure 2.9**, right panel). The unbound oxetane **53** was significantly higher in energy at 10.0 kcal/mol. This supported why oxetane species were not observed or isolated over the course of this study and is consistent with previous results. Subsequent efforts focused on identifying experimental support for carbonyl-olefin metathesis via a carbonyl-ene pathway. We envisioned that deuterated **43** could provide key insight through kinetic isotope effect (KIE) experiments (**Figure 2.12**). Specifically, we hypothesized that if aryl ketone **43** was exclusively forming

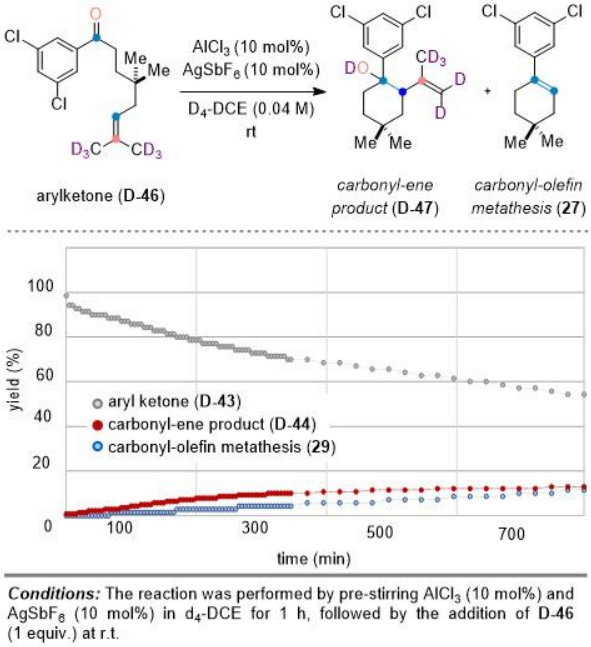

Figure 2.13.[1]H NMR analysis of KIE experiment.

metathesis product **27** through a direct [2+2]-cycloaddition pathway, this would result in a β-secondary KIE caused by the proximity of the deuterium isotope relative to the C–C π bond involved in the transition state and would ultimately have little effect on the overall rate of the reaction.[39,41] However, if carbonyl-ene is playing an active role in the formation of **27**, then a primary KIE would be expected, as the C-H/D bond is directly involved in both transition states forming the key oxetane intermediate, and the rate would be significantly impacted by the isotope. Mechanistic probe **D-46** independently synthesized, subjected to the optimized reaction conditions, and the reaction was monitored by ^{1}H NMR spectroscopy (**Figure 2.13**). A primary KIE of k_H/k_D = 2.09 ± 0.07 was calculated based on consumption of the aryl ketone starting material and suggests carbonyl-ene formation is vital for carbonyl-olefin metathesis of 6-membered ring precursors bearing prenylated olefins.

From the combined computational and experimental results, we were able to propose carbonyl-ene reactivity as an unprecedented pathway for ring-closing carbonyl-olefin metathesis of 6- and 7-membered rings (**Figure 2.14**). When prenylated aryl ketones **57** are subjected to catalytic amounts of [$AlCl_2$][SbF_6], a reversible carbonyl-ene reaction leads to unsaturated alcohol **59**. This alcohol can either revert back to aryl ketone, or funnel toward oxetane **61** via hydroalkoxylation of the terminal olefin. Once formed, oxetane **61** can then fragment via a retro-[2+2]-cycloaddition to provide the cyclohexene product **63** along with acetone (**13**) as the corresponding carbonyl

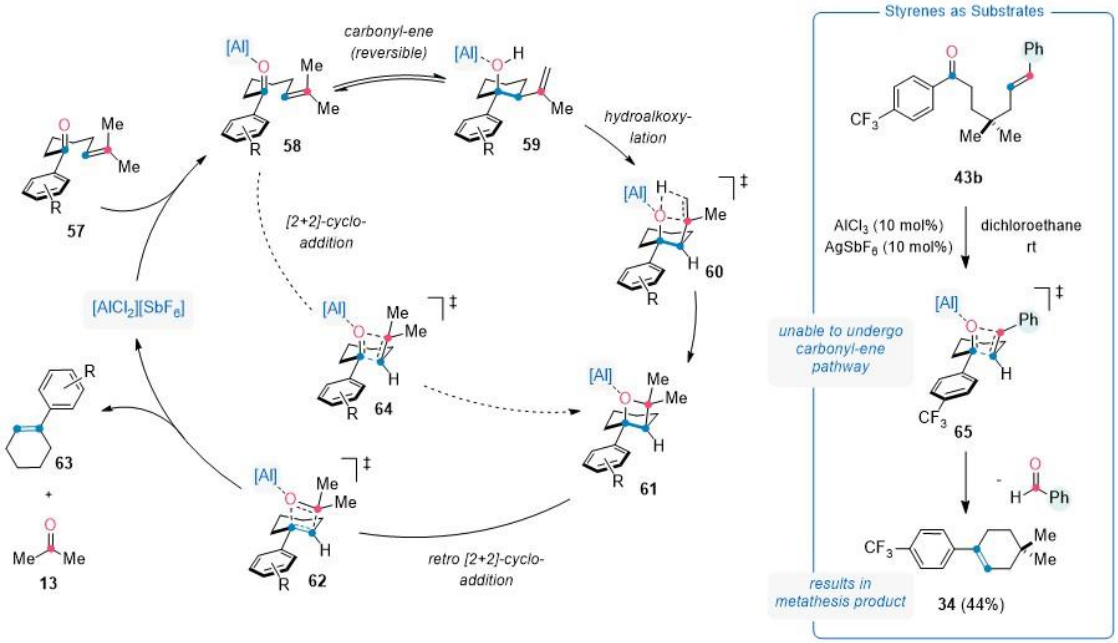

Figure 2.14. Proposed catalytic cycle for carbonyl-olefin metathesis relying in Al(III)-ion pairs.

byproduct. Interestingly, when styrenyl derived substrates such as **43b** are employed, it is still able to form the metathesis product, albeit in diminished yield of 44% despite lacking the β-hydrogens necessary to promote a carbonyl-ene reaction. This suggests that direct [2+2]-cycloaddition via transition state **64** is still operative as a secondary pathway in some instances. In comparison, when the olefin subunit is replaced with a prenylated fragment the yield increases to 80%, supporting carbonyl-ene and subsequent hydroalkoxylation as the predominant pathway for metathesis.

2.4 Conclusions

The work presented in this chapter represents a new reaction protocol for ring-closing carbonyl-olefin metathesis to form 6- and 7-membered rings, a class of products previously which were previously generally inaccessible under traditional Lewis acid catalysis. It relies on the *in-situ* formation of a heterobimetallic ion pair generated from $AlCl_3$ and $AgSbF_6$ upon halide abstraction. Once formed, this ion pair functions as a superelectrophilic Lewis acid which can activate olefinated aryl ketones to form the desired metathesis products in up to 99%. Computational and experimental results support a distinct reaction pathway relying on carbonyl-ene and subsequent hydroalkoxylation as the active path for metathesis, although direct [2+2]-cycloaddition may still be operative in some cases, such as when styrenyl-derived olefins are used as the starting material.

2.5 Experimental Procedures and Supplemental Information

2.5.1 General Information

All moisture-sensitive reactions were performed in a nitrogen-filled glovebox or using Schlenk techniques in oven or flame-dried round bottom flasks fitted with rubber septa. Stainless steel syringes were used to transfer air or moisture-sensitive liquids. Flash chromatography was performed using silica gel SiliaFlash® 40-63 micron (230-400 mesh) from SiliCycle. All chemicals were purchased from commercial suppliers and were used as received unless otherwise stated. 2,2,5-trimethylhex-5-en-1-ol2, (1-(4-bromophenyl)ethoxy)(tert-butyl)dimethylsilane3, and dimethyl 2-(3-methylbut-2-en-1-yl)malonate4 were prepared according to a literature procedure. Proton Nuclear Magnetic Resonance (1H NMR) spectra and Carbon Nuclear Magnetic Resonance (13C NMR) spectra were recorded on a Varian Unity Plus 400, Varian MR400, Varian vnmrs 500,

Varian Inova 500, Varian Mercury 500, and Varian vnmrs 700 spectrometers. Chemical shifts for protons are reported in parts per million and are referenced to the NMR solvent peak (CDCl3: δ 7.26). Chemical shifts for carbons are reported in parts per million and are referenced to the carbon resonances of the NMR solvent (CDCl3: δ 77.16). Data is represented as follows: chemical shift, integration, multiplicity (br = broad, s = singlet, d = doublet, t = triplet, q = quartet, p = pentet, m = multiplet), and coupling constants in Hertz (Hz). Mass spectroscopic (MS) data was recorded at the Mass Spectrometry Facility at the Department of Chemistry of the University of Michigan in Ann Arbor, MI on an Agilent Q-TOF HPLC-MS with ESI high resolution mass spectrometer. Infrared (IR) spectra were obtained using either an Avatar 360 FT-IR or Perkin Elmer Spectrum BX FT-IR spectrometer. IR data are represented as frequency of absorption (cm^{-1}).

2.5.2 Additional Optimization

Table 2.1 Solvent evaluation for reactivity.

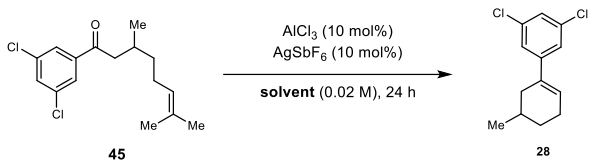

45 28

entry	solvent	conversion (%)	28 (%)
1	DCE	100	99
2	DCM	100	85
3	benzene	77	55
4	toluene	83	53
5	chlorobenzene	39	10

Conditions: All reactions were performed using 0.10 mmol of **45** in solvent (0.02 M) at room temperature for 24 h. Yields and conversions are reported as 1H-NMR yields with mesitylene as internal standard.

Table 2.2. Evaluation of various additives.

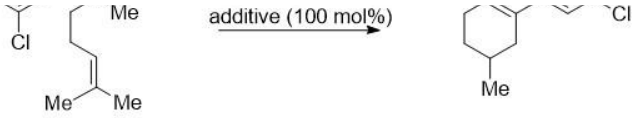

45 **28**

entry	additive (100 mol%)	yield (%)	converion (%)
1	benzoic acid	88	100
2	acetic acid	70	100
3	methanol	35[a]	61
4	isopropanol	7[a]	22
5	allyltrimethylsilane	10[a]	41
6	allyltrimethylsilane (500 mol%)	0[a]	10
7	nitromethane	27	86
8	phenylacetylene	22	82
9	triethylamine	0	28
10	acetonitrile	0	38

Conditions: All reactions performed using 0.1 mmol of the substrate in DCE (0.02 M) at room temperature for 24 h. Yields are reported as NMR yields with mesitylene as internal standard.[a]No other products observed.

Table 2.2 Details: In a flame-dried flask, $AlCl_3$ (10 mol%) and $AgSbF_6$ (10 mol%) were collected in the glovebox. The reaction flask was sealed and brought out of the glovebox. Aryl ketone substrate (**45**) (1.0 eq) and appropriate additive were dissolved in DCE (0.02 M) and added to the reaction flask under nitrogen via a syringe. The reaction was allowed to stir for 24 hours at room temperature. At the end of this time, the reaction was filtered through a silica plug eluting with DCM. The filtrate was concentrated under reduced pressure to remove all volatile components. Yield and conversion were determined by ^{1}H-NMR using mesitylene as an internal standard. In all cases, the metathesis product (**28**) was the exclusive product and none of the corresponding nucleophilic addition products were observed.

Table 2.3 Details: We also considered the possibility that this heterobimetallic ion pair $[AlCl_2]^+[SbF_6]^-$ could fragment to form $AlCl_2F$ and SbF_5. Both are considered strong Lewis acids and could function as the active catalytic species. The following experiments were conducted as controls (see table below). Based on these results, we postulate the heterobimetallic ion pair $[AlCl_2]^+[SbF_6]^-$ is the active catalytic species. Yields and conversions were determined by 1H-NMR using mesitylene as an internal standard. $AlCl_2^+$ is an extremely Lewis acidic species and will coordinate to the most accessible Lewis base. In our system, this potent Lewis acid will be

Table 2.3. Support for active catalyst.

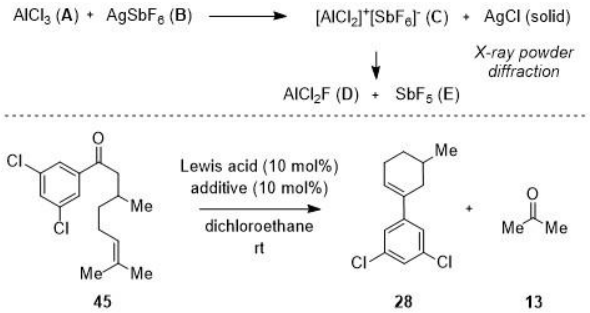

entry	species	Lewis acid	additive	yield **17** (%)	conv. (%)
1	A	$AlCl_3$	-	0	34
2	B	-	$AgSbF_6$	0	0
3[a]	C	$AlCl_3$	$AgSbF_6$	99	100
4[a]	D	$AlCl_3$	AgF	0	33
5	E	SbF_5	-	41	86

Conditions: Reactions were ran using 0.10 mmol XX in DCE (0.02M) at room temperature for 24 hours. Yields and conversions by ^{1}H NMR against mesitylene as internal standard. [a]AgCl was was observed.

quenched by a carbonyl and/or a fluoride lone pair (from SbF_6-) to form Cl_2-Al … F-SbF_5 and R_2C=O … $AlCl_2$ … F-SbF_5 as the reactive Lewis acid-base complex in our chemistry. Aluminum is known to be either 3-coordinate trigonal-planar or 4-coordinate tetrahedral. Both of our explanations for coordination compounds (Cl_2-Al … F-SbF_5 and R_2C=O … $AlCl_2$ … F-SbF_5) put forth satisfy these requirements. Additionally, our experiments shown in Table 1 of our manuscript corroborate this hypothesis.

As noted, the combination of $AlCl_3$ and $AgSbF_6$ provide the best results. It is known that the SbF_6 anion can act as an "L" type donor in certain instances. This is established for a variety of Lewis acidic transition metals including Mn,[83] Fe,[84] W,[85] Ti,[86] Cu,[87] and Au.[88] Particularly relevant to our manuscript is that SbF6 anions are established to act as "L" type donors for more traditional main group Lewis acids (including cationic species).[89–91] Note that the Lewis acids in these examples

Figure 2.15. Spectrum of isolated AgCl crystals.

[87]are described as cationic. These systems serve as synthons for the cationic Lewis acid. Our system is analogous to these, except for the supporting (ancillary) ligands.

Figure 2.15 Details: AgCl crystals were collected from reaction flask and washed three times with cold DCE. The obtained spectra match previously reported data.[81]

2.5.3. Synthesis of Substrates and Intermediates

General Grignard addition and IBX oxidation procedure for the synthesis of aryl ketone substrates:

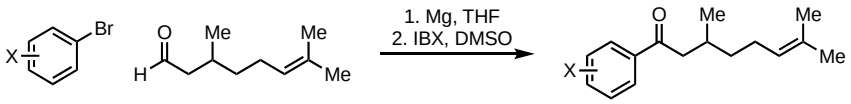

A flame-dried flask was charged with activated magnesium (2.0 eq). Dry THF (0.2 M) was added, followed by aryl bromide (2.5 eq). The resulting mixture was stirred until the activated magnesium dissolved. Citronellal (1.0 eq) was added dropwise, and the mixture was stirred until judged complete by TLC analysis. The resulting reaction mixture was quenched slowly with saturated ammonium chloride. The aqueous layer was extracted with ethyl acetate (x3), and the combined organics were washed with saturated sodium chloride, dried over Na_2SO_4, and concentrated under reduced pressure. The crude alcohol was used without further purification. The crude alcohol was dissolved in DMSO (0.3 M), and IBX (1.3 eq) was added to the reaction mixture. The resulting mixture was stirred at room temperature until judged complete by TLC analysis, quenched with water, and filtered through celite eluting with ethyl acetate. The filtrate was then transferred to a separatory funnel. The aqueous layer was extracted with ethyl acetate (x3) and the combined organics were washed with saturated sodium chloride, dried over Na_2SO_4, and concentrated under reduced pressure. The crude ketone was purified by column chromatography eluting with the indicated solvent to give the pure aryl ketone substrate.

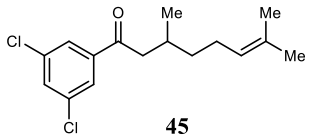

45

1-(3,5-dichlorophenyl)-3,7-dimethyloct-6-en-1-one (**45**): The Grignard addition and IBX oxidation protocol was performed on 5.40 mmol scale. Purification by flash column

chromatography eluting with hexanes/EtOAc (90:10) provided 1.11 g (69% yield) of **16** as a yellow oil. **^{1}H NMR** (500 MHz; $CDCl_3$) δ 7.78 (s, 2H), 7.53 (s, 1H), 5.09 (t, *J* = 6.8 Hz, 1H), 2.90 (dd, *J* = 16.1, 5.5 Hz, 1H), 2.69 (dd, *J* = 16.1, 8.1 Hz, 1H), 2.15 (dq, *J* = 13.3, 6.7 Hz, 1H), 2.02 (ddt, *J* = 22.5, 14.5, 7.4 Hz, 2H), 1.68 (s, 3H), 1.60 (s, 3H), 1.45 – 1.35 (m, 1H), 1.34 – 1.23 (m, 1H), 0.96 (d, *J* = 6.6 Hz, 3H); **^{13}C NMR** (125 MHz; $CDCl_3$) δ 197.8, 139.9, 135.7, 132.6, 131.9, 126.7, 124.3, 46.1, 37.2, 29.4, 25.8, 25.6, 20.0, 17.8; **IR** (Neat) 2963, 2914, 1690, 1565, 1433, 1417, 1377, 1283, 1203, 1098, 1031, 984, 868, 853, 800, 703, 670, 615; **HRMS:** calcd for $C_{16}H_{21}Cl_2O^+$: 299.0964 found 299.0893.

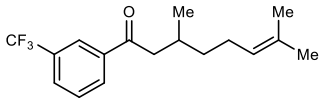

S19

3,7-dimethyl-1-(3-(trifluoromethyl)phenyl)oct-6-en-1-one (**S19**): The Grignard addition and IBX oxidation protocol was performed on 5.60 mmol scale. Purification by flash column chromatography eluting with hexanes/EtOAc (93:7) provided 0.70 g (42% yield) of **S21** as a clear oil. **^{1}H NMR** (500 MHz; $CDCl_3$) δ 8.19 (s, 1H), 8.12 (d, *J* = 7.8 Hz, 1H), 7.81 (d, *J* = 7.7 Hz, 1H), 7.60 (t, *J* = 7.8 Hz, 1H), 5.10 (t, *J* = 7.0 Hz, 1H), 2.98 (dd, *J* = 16.0, 5.5 Hz, 1H), 2.78 (dd, *J* = 16.0, 8.1 Hz, 1H), 2.26 – 2.13 (m, *J* = 6.8 Hz, 1H), 2.03 (ddp, *J* = 21.9, 14.6, 7.3 Hz, 2H), 1.68 (s, 3H), 1.60 (s, 3H), 1.49 – 1.38 (m, 1H), 1.36 – 1.26 (m, 1H), 0.98 (d, *J* = 6.6 Hz, 3H); **^{13}C NMR** (175 MHz; $CDCl_3$) δ 199.0, 138.0, 131.9, 131.4, 131.3 (q, *J* = 32.8 Hz), 129.42 (q, *J* = 3.9 Hz), 129.38, 125.1 (q, *J* = 3.9 Hz), 124.3, 123.9 (q, *J* = 272.5 Hz), 46.1, 37.2, 29.5, 25.8, 25.7, 20.1, 17.8; **IR** (Neat) 2964, 2916, 1689, 1611, 1437, 1377, 1329, 1282, 1257, 1199, 1166, 1125, 1096, 1071, 1001, 927, 799, 759, 694, 679, 654; **HRMS:** calcd for $C_{17}H_{21}F_3OK^+$: 337.1176 found: 337.1385.

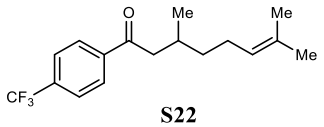

S22

3,7-dimethyl-1-(4-(trifluoromethyl)phenyl)oct-6-en-1-one (**S22**): The Grignard addition and IBX oxidation protocol was performed on 8.32 mmol scale. Purification by flash column chromatography eluting with hexanes/EtOAc (95:5) provided 1.93 g (78% yield) of **S24** as a clear oil. **^{1}H NMR** (500 MHz; $CDCl_3$) δ 8.04 (d, *J* = 8.1 Hz, 2H), 7.73 (d, *J* = 8.2 Hz, 2H), 5.09 (t, *J* =

7.1 Hz, 1H), 2.98 (dd, *J* = 16.0, 5.5 Hz, 1H), 2.77 (dd, *J* = 16.0, 8.1 Hz, 1H), 2.28 – 2.11 (m, *J* = 6.5 Hz, 1H), 2.01 (ddt, *J* = 21.9, 14.6, 7.2 Hz, 2H), 1.68 (s, 3H), 1.60 (s, 3H), 1.48 – 1.36 (m, 1H), 1.36 – 1.24 (m, 1H), 0.97 (d, *J* = 6.6 Hz, 3H); **^{13}C NMR** (175 MHz; $CDCl_3$) δ 199.5, 140.2, 134.3 (q, *J* = 32.6 Hz), 131.8, 128.6, 125.8 (q, *J* = 3.7 Hz), 124.4, 123.8 (q, *J* = 272.6 Hz), 46.3, 37.2, 29.6, 25.9, 25.7, 20.0, 17.8; **IR** (Neat) 2962, 2920, 1690, 1581, 1510, 1452, 1409, 1377, 1322, 1284, 1211, 1167, 1127, 1108, 1064, 1012, 898, 827, 760, 722; **HRMS:** calcd for $C_{17}H_{21}F_3O^+$: 298.1545 found: 298.1549.

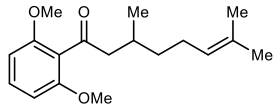

S30

1-(2,6-dimethoxyphenyl)-3,7-dimethyloct-6-en-1-one (**S30**): The Grignard addition and IBX oxidation protocol was performed on 3.42 mmol scale. Purification by flash column chromatography eluting with hexanes/EtOAc (95:5) provided 0.68 g (68% yield) of **S31** as a clear oil. **^{1}H NMR** (500 MHz; $CDCl_3$) δ 7.41 – 7.15 (m, 1H), 6.54 (d, *J* = 8.4 Hz, 2H), 5.09 (t, *J* = 7.1 Hz, 1H), 3.78 (s, 6H), 2.75 (dd, *J* = 16.8, 5.3 Hz, 1H), 2.57 (dd, *J* = 16.8, 8.1 Hz, 1H), 2.11 (dq, *J* = 13.5, 6.9 Hz, 1H), 1.98 (dq, *J* = 16.9, 7.4 Hz, 2H), 1.67 (s, 3H), 1.59 (s, 3H), 1.46 – 1.33 (m, 1H), 1.29 – 1.15 (m, 1H), 0.97 (d, *J* = 6.6 Hz, 3H); **^{13}C NMR** (125 MHz; $CDCl_3$) δ 205.1, 156.9, 131.3, 130.5, 124.8, 121.0, 104.1, 55.9, 52.3, 37.1, 28.8, 25.9, 25.6, 20.0, 17.8; **IR** (Neat) 2913, 2840, 1703, 1592, 1471, 1432, 1401, 1376, 1287, 1251, 1173, 1004, 937, 909, 777, 732, 716, 620; **HRMS:** calcd for $C_{18}H_{27}O_3^+$: 291.1955 found: 291.1955.

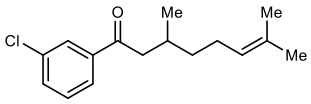

S33

1-(3-chlorophenyl)-3,7-dimethyloct-6-en-1-one (**S33**): The Grignard addition and IBX oxidation protocol was performed on 4.86 mmol scale. Purification by flash column chromatography eluting with hexanes/EtOAc (95:5) provided 1.06 g (82% yield) of **S34** as a yellow oil. **^{1}H NMR** (700 MHz; $CDCl_3$) δ 7.91 (s, 1H), 7.81 (d, *J* = 7.8 Hz, 1H), 7.52 (d, *J* = 8.0 Hz, 1H), 7.40 (t, *J* = 7.9 Hz, 1H), 5.09 (t, *J* = 7.0 Hz, 1H), 2.93 (dd, *J* = 15.9, 5.5 Hz, 1H), 2.72 (dd, *J* = 15.9, 8.1 Hz, 1H), 2.17 (dq, *J* = 13.7, 6.9 Hz, 1H), 2.02 (ddq, *J* = 37.5, 14.7, 7.3 Hz, 2H), 1.68 (s, 3H), 1.60 (s, 3H), 1.46

– 1.37 (m, 1H), 1.35 – 1.24 (m, 1H), 0.96 (d, *J* = 6.6 Hz, 3H); **^{13}C NMR** (175 MHz; $CDCl_3$) δ 199.1, 139.1, 135.0, 132.9, 131.8, 130.0, 128.4, 126.3, 124.4, 46.1, 37.3, 29.6, 25.9, 25.7, 20.1, 17.8; **IR** (Neat) 2961, 2915, 1685, 1570, 1453, 1421, 1376, 1287, 1258, 1205, 1113, 1076, 999, 973, 903, 713, 680, 652; **HRMS:** calcd for $C_{16}H_{21}ClO^+$: 264.1281 found: 264.1281.

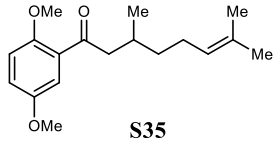

S35

1-(2,5-dimethoxyphenyl)-3,7-dimethyloct-6-en-1-one (**S35**): The Grignard addition and IBX oxidation protocol was performed on 3.89 mmol scale. Purification by flash column chromatography eluting with hexanes/EtOAc (95:5) provided 0.71 g (63% yield) of **S35** as a clear oil. **^{1}H NMR** (500 MHz; $CDCl_3$) δ 7.18 (d, *J* = 3.2 Hz, 1H), 7.00 (dd, *J* = 9.0, 3.2 Hz, 1H), 6.89 (d, *J* = 9.0 Hz, 1H), 5.08 (t, *J* = 7.1 Hz, 1H), 3.85 (s, 3H), 3.79 (s, 3H), 3.00 (dd, *J* = 15.9, 5.5 Hz, 1H), 2.75 (dd, *J* = 15.9, 8.2 Hz, 1H), 2.09 (dq, *J* = 13.7, 6.9 Hz, 1H), 1.98 (dq, *J* = 15.3, 7.6 Hz, 2H), 1.67 (s, 3H), 1.59 (s, 3H), 1.46 – 1.31 (m, 1H), 1.29 – 1.11 (m, 1H), 0.92 (d, *J* = 6.7 Hz, 3H); **^{13}C NMR** (175 MHz; $CDCl_3$) δ 203.0, 153.6, 152.8, 131.4, 129.5, 124.7, 119.5, 114.1, 113.1, 56.2, 56.0, 51.3, 37.4, 29.5, 25.9, 25.7, 20.0, 17.8; **IR** (Neat) 2913, 1671, 1609, 1582, 1493, 1463, 1409, 1376, 1275, 1177, 1021, 874, 810, 724, 656; **HRMS:** calcd for $C_{18}H_{27}O_3^+$: 291.1955 found: 291.1955.

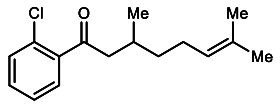

S40

1-(2-chlorophenyl)-3,7-dimethyloct-6-en-1-one (**S40**): The Grignard addition and IBX oxidation protocol was performed on 1.00 mmol scale. Purification by flash column chromatography eluting with hexanes/EtOAc (93:7) provided 0.10 g (39% yield) of **S40** as a clear oil. **^{1}H NMR** (700 MHz; $CDCl_3$) δ 7.41 (t, *J* = 6.9 Hz, 2H), 7.37 (t, *J* = 7.6 Hz, 1H), 7.31 (t, *J* = 7.4 Hz, 1H), 5.07 (t, *J* = 7.0 Hz, 1H), 2.95 (dd, *J* = 16.4, 5.6 Hz, 1H), 2.76 (dd, *J* = 16.4, 8.1 Hz, 1H), 2.12 (dt, *J* = 13.2, 6.8 Hz, 1H), 2.05 – 1.93 (m, 2H), 1.67 (s, 3H), 1.59 (s, 3H), 1.43 – 1.34 (m, 1H), 1.31 – 1.19 (m, 1H), 0.97 (d, *J* = 6.7 Hz, 3H); **^{13}C NMR** (175 MHz; $CDCl_3$) δ 203.8, 140.2, 131.7, 131.5, 130.8, 130.6, 128.9, 127.0, 124.4, 50.5, 37.1, 29.5, 25.9, 25.6, 20.0, 17.8; **IR** (Neat) 2962, 2914, 1695, 1590,

1432, 1400, 1376, 1288, 1208, 1062, 1036, 1002, 947, 829, 735, 700, 644, 606; **HRMS:** calcd for $C_{16}H_{21}ClOK^{+}$: 303.0913 found: 303.1119.

General Horner-Wadsworth-Emmons procedure for the synthesis of intermediate alcohols:

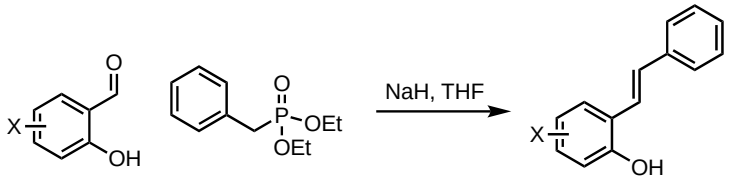

In a flame-dried flask, NaH (4.0 eq, 60% dispersion in mineral oil) was dissolved in dry THF (0.3 M). The reaction flask was cooled to 0 °C, and phosphonate ester (2.0 eq) was added dropwise. After stirring for 30 minutes at this temperature, aldehyde (1.0 eq) dissolved in THF (5 mL) was added slowly. The reaction mixture was allowed to slowly warm to room temperature and stirred until judged complete by TLC analysis. The reaction was quenched slowly with saturated ammonium chloride, the aqueous layer was extracted with ethyl acetate (x3), and the combined organics were washed with saturated sodium chloride, dried over Na_2SO_4, and concentrated under reduced pressure. The crude alcohol was purified by column chromatography eluting with the indicated solvent to give the pure intermediate alcohol

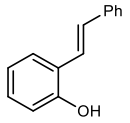

IA20

(*E*)-2-styrylphenol (**IA20**): The Horner-Wadsworth-Emmons protocol was performed on 16.4 mmol scale. Purification by flash column chromatography eluting with hexanes/EtOAc (90:10) provided 2.55 g (79% yield) of **IA20** as a white solid. Spectral data was found to be in accordance with literature data.[92]

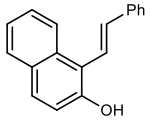

IA25

(*E*)-1-styrylnaphthalen-2-ol (**IA25**): The Horner-Wadsworth-Emmons protocol was performed on 5.81 mmol scale. Purification by flash column chromatography eluting with hexanes/EtOAc

(95:5) provided 0.91 g (63% yield) of **IA25** as a white solid. Spectral data was found to be in accordance with literature data.[93]

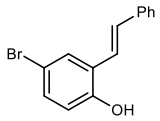

IA28

(*E*)-4-bromo-2-styrylphenol (**IA28**): The Horner-Wadsworth-Emmons protocol was performed on 9.95 scale. Purification by flash column chromatography eluting with hexanes/EtOAc (90:10) provided 1.72 g (63% yield) of **IA28** as a white solid. Spectral data was found to be in accordance with literature data.[94]

General Wittig olefination procedure for the synthesis of intermediate alcohols:

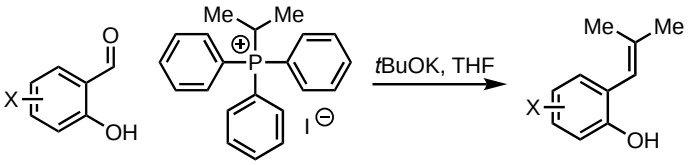

In a flame-dried flask, wittig salt (2.3 eq) was dissolved in dry THF (0.3 M) and *t*BuOK (2.33 eq) was added in one portion. After stirring for 1 hour at room temperature, the reaction flask was cooled to -78 °C. At this temperature, aldehyde (1.0 eq) dissolved in THF (5 mL) was added slowly. The reaction mixture was allowed to slowly warm to room temperature and stirred until judged complete by TLC analysis. The reaction was quenched slowly with saturated ammonium chloride, the aqueous layer was extracted with ethyl acetate (x3), and the combined organics were washed with saturated sodium chloride, dried over Na_2SO_4, and concentrated under reduced pressure. The crude alcohol was purified by column chromatography eluting with the indicated solvent to give the pure intermediate alcohol.

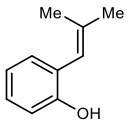

IA20-2

2-(2-methylprop-1-en-1-yl)phenol (**IA20-2**): The Wittig olefination protocol was performed on 16.4 mmol scale. Purification by flash column chromatography eluting with hexanes/EtOAc (95:5) provided 1.43 g (59% yield) of **IA20-2** as a yellow solid. Spectral data was found to be in accordance with literature data.[95]

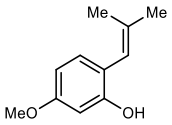

IA23

5-methoxy-2-(2-methylprop-1-en-1-yl)phenol (**IA23**): The Wittig olefination protocol was performed on 6.57 mmol scale. Purification by flash column chromatography eluting with hexanes/EtOAc (90:10) provided 0.75 g (64% yield) of **IA23** as a clear oil. **^{1}H NMR** (500 MHz; $CDCl_3$) δ 6.94 (d, *J* = 8.3 Hz, 1H), 6.61 – 6.38 (m, 2H), 6.05 (s, 1H), 5.05 (s, 1H), 3.78 (s, 3H), 1.93 (s, 3H), 1.67 (s, 3H); **^{13}C NMR** (125 MHz; $CDCl_3$) δ 160.0, 153.9, 140.4, 130.5, 118.5, 117.3, 106.4, 100.5, 55.4, 26.0, 19.5; **IR** (Neat) 3418, 2910, 2836, 1616, 1577, 1502, 1466, 1443, 1376, 1304, 1274, 1237, 1199, 1177, 1055, 983, 955, 832, 786, 732, 629; **HRMS:** calcd for $C_{11}H_{14}O_2^+$: 178.0994 found: 178.1002.

General Horner-Wadsworth-Emmons procedure for the synthesis of intermediate esters:

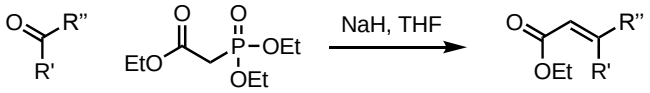

In a flame-dried flask, NaH (1.2 eq, 60% dispersion in mineral oil) was dissolved in dry THF (0.3 M). The reaction flask was cooled to 0 °C, and phosphonate ester (1.2 eq) was added dropwise. The reaction mixture was warmed to room temperature, and after stirring for 30 minutes, ketone (1.0 eq) dissolved in THF (5 mL) was added slowly. The reaction stirred until judged complete by TLC analysis. The reaction was quenched with saturated sodium bicarbonate, the aqueous layer was extracted with ethyl acetate (x3), and the combined organics were washed with saturated sodium chloride, dried over Na_2SO_4, and concentrated under reduced pressure. The crude ester was purified by column chromatography eluting with the indicated solvent to give the pure intermediate ester.

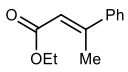

IE18c

Ethyl (*E*)-3-phenylbut-2-enoate (**IE18c**): The Horner-Wadsworth-Emmons protocol was performed on 50.0 mmol scale. Purification by flash column chromatography eluting with hexanes/EtOAc (90:10) provided 8.18 g (86% yield) of **IE18c** as a clear oil. Spectral data was found to be in accordance with literature data.[96]

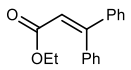

IE18e

Ethyl 3,3-diphenylacrylate (**IE18e**): The Horner-Wadsworth-Emmons protocol was performed on 45.0 mmol scale. Purification by flash column chromatography eluting with hexanes/EtOAc (90:10) provided 9.41 g (83% yield) of **IE18e** as a clear oil. Spectral data was found to be in accordance with literature data.[97]

General DIBAL reduction procedure for the synthesis of intermediate allylic alcohols:

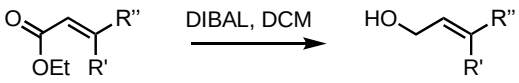

In a flame-dried flask, intermediate ester (1.0 eq) was dissolved in dry DCM (0.1 M). The reaction flask was cooled to -78 °C, and DIBAL (2.24 eq, 1 M solution in DCM) was added dropwise using an addition funnel. After the DIBAL was added, the reaction mixture was allowed to slowly warm to room temperature over 2 hours. At the end of this time, the reaction mixture was cooled to -78 °C, and was quenched with saturated Rochelle's salt. The aqueous layer was extracted with DCM (x3), and the combined organics were washed with saturated sodium chloride, dried over Na_2SO_4, and concentrated under reduced pressure. The crude alcohol was purified by column chromatography eluting with the indicated solvent to give the pure intermediate allylic alcohol.

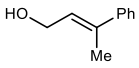

IAA18c

(*E*)-3-phenylbut-2-en-1-ol (**IAA18c**): The DIBAL reduction protocol was performed on 14.50 mmol scale. Purification by flash column chromatography eluting with hexanes/EtOAc (85:15) provided 1.90 g (89% yield) of **IAA18** as a clear oil. Spectral data was found to be in accordance with literature data.[98]

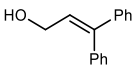

IAA18e

3,3-diphenylprop-2-en-1-ol (**IAA18e**): The DIBAL reduction protocol was performed on 17.8 mmol scale. Purification by flash column chromatography eluting with hexanes/EtOAc (90:10)

provided 2.56 g (68% yield) of **IAA20** as a white solid. Spectral data was found to be in accordance with literature data.

General bromination procedure for the synthesis of intermediate allylic bromides:

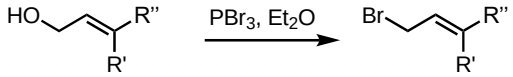

In a flame-dried flask, intermediate allylic alcohol (1.0 eq) was dissolved in dry Et_2O (0.1 M). The reaction flask was cooled to 0 °C, and PBr_3 (0.5 eq) was added dropwise. The reaction was allowed to slowly warm to room temperature and stirred until judged complete by TLC analysis. The reaction was quenched with water, the aqueous layer was extracted with Et_2O (x3), and the combined organics were washed with saturated sodium chloride, dried over Na_2SO_4, and concentrated under reduced pressure. The crude intermediate allylic bromide was used without further purification.

General alkylation procedure for the synthesis of aryl ketone substrates:

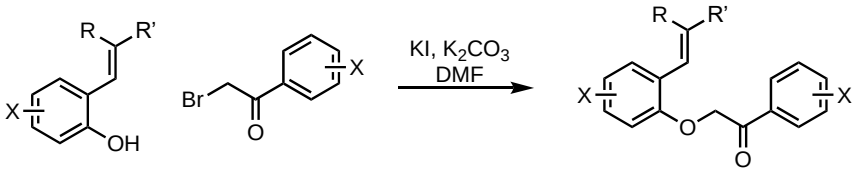

In a flame-dried flask, intermediate phenol (1.0 eq) was dissolved in dry DMF (0.2 M). KI (0.8 eq) and K_2CO_3 (1.5 eq) were added, followed by corresponding bromide (1.2 eq). The reaction mixture was stirred until judged complete by TLC analysis. The reaction was quenched with water, the aqueous layer was extracted with ethyl acetate (x3), and the combined organics were washed with saturated sodium chloride, dried over Na_2SO_4, and concentrated under reduced pressure. The crude ketone was purified by column chromatography eluting with the indicated solvent to give the pure aryl ketone substrate.

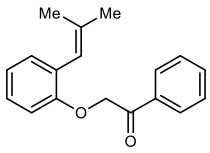

S18-2

2-(2-(2-methylprop-1-en-1-yl)phenoxy)-1-phenylethan-1-one (**S18-2**): The alkylation protocol was performed on 1.01 mmol scale. Purification by flash column chromatography eluting with hexanes/dichloromethane (60:40) provided 0.18 g (68% yield) of **S20-2** as a white solid. **^{1}H NMR** (700 MHz; $CDCl_3$) δ 8.01 (d, *J* = 7.6 Hz, 2H), 7.61 (t, *J* = 7.4 Hz, 1H), 7.49 (t, *J* = 7.7 Hz, 2H),

7.21 (d, *J* = 7.2 Hz, 1H), 7.14 (t, *J* = 7.8 Hz, 1H), 6.96 (t, *J* = 7.4 Hz, 1H), 6.78 (d, *J* = 8.2 Hz, 1H), 6.38 (s, 1H), 5.26 (s, 2H), 1.91 (s, 3H), 1.80 (s, 3H); **^{13}C NMR** (175 MHz; $CDCl_3$) δ 195.1, 155.7, 136.0, 134.9, 133.9, 130.9, 128.9, 128.4, 128.4, 127.4, 121.3, 120.5, 112.3, 71.7, 26.8, 19.7; **IR** (Neat) 2965, 1688, 1594, 1576, 1485, 1447, 1355, 1300, 1274, 1219, 1205, 1163, 1117, 1070, 1000, 967, 938, 840, 810, 750, 730, 688, 676, 629; **HRMS:** calcd for $C_{18}H_{18}O_2Na^+$: 289.1199 found: 289.1199.

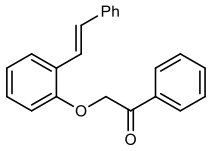

S18

(*E*)-1-phenyl-2-(2-styrylphenoxy)ethan-1-one (**S18**): The alkylation protocol was performed on 4.08 mmol scale. Purification by flash column chromatography eluting with hexanes/EtOAc (95:5) provided 0.87 g (68% yield) of **S20** as a white solid. **^{1}H NMR** (500 MHz; $CDCl_3$) δ 8.03 (d, *J* = 7.1 Hz, 2H), 7.62 (t, *J* = 7.5 Hz, 2H), 7.57 – 7.47 (m, 5H), 7.34 (t, *J* = 7.6 Hz, 2H), 7.25 – 7.14 (m, 3H), 7.02 (t, *J* = 7.5 Hz, 1H), 6.88 – 6.81 (m, 1H), 5.33 (s, 2H); **^{13}C NMR** (125 MHz; $CDCl_3$) δ 194.8, 155.6, 138.0, 134.9, 133.9, 129.8, 129.0, 128.7, 128.7, 128.4, 127.6, 127.3, 127.0, 126.8, 123.4, 122.0, 112.7, 71.7; **IR** (Neat) 2957, 1688, 1594, 1578, 1485, 1447, 1337, 1316, 1302, 1279, 1218, 1239, 1208, 1162, 1114, 1069, 1000, 984, 962, 834, 846, 689, 676, 636; **HRMS:** calcd for $C_{22}H_{18}O_2Na^+$: 337.1199 found: 337.1204.

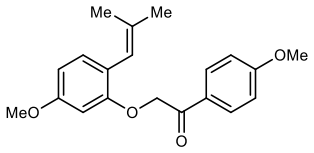

S21

2-(5-methoxy-2-(2-methylprop-1-en-1-yl)phenoxy)-1-(4-methoxyphenyl)ethan-1-one (**S21**): The alkylation protocol was performed on 3.09 mmol scale. Purification by flash column chromatography eluting with hexanes/EtOAc (90:10) provided 0.92 g (91% yield) of **S23** as a white solid. **^{1}H NMR** (500 MHz; $CDCl_3$) δ 8.00 (d, *J* = 8.9 Hz, 2H), 7.11 (d, *J* = 8.4 Hz, 1H), 6.95 (d, *J* = 8.9 Hz, 2H), 6.49 (dd, *J* = 8.4, 2.3 Hz, 1H), 6.37 (d, *J* = 2.4 Hz, 1H), 6.31 (s, 1H), 5.18 (s, 2H), 3.88 (s, 3H), 3.76 (s, 3H), 1.89 (s, 3H), 1.79 (s, 3H); **^{13}C NMR** (125 MHz; $CDCl_3$) δ 193.3, 164.1, 159.2, 156.6, 134.8, 131.2, 130.8, 127.9, 121.1, 120.1, 114.0, 105.2, 100.1, 71.5, 55.6, 55.5,

26.7, 19.7; **IR** (Neat) 2967, 2931, 1575, 1499, 1445, 1422, 1371, 1308, 1126, 1110, 1070, 1054, 1039, 1024, 1000, 968, 933, 917, 836, 822, 785, 732, 715, 642, 632, 620; **HRMS:** calcd for $C_{20}H_{22}O_4Na^+$: 349.1410 found: 349.1414.

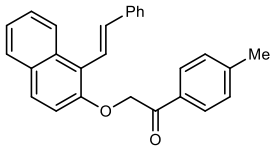

S23

(*E*)-2-((1-styrylnaphthalen-2-yl)oxy)-1-(*p*-tolyl)ethan-1-one (**S23**): The alkylation protocol was performed on 3.67 mmol scale. Purification by flash column chromatography eluting with hexanes/EtOAc (95:5) provided 0.84 g (60% yield) of **S25** as a yellow solid. **^{1}H NMR** (500 MHz; $CDCl_3$) δ 8.26 (d, *J* = 8.6 Hz, 1H), 7.91 (d, *J* = 8.0 Hz, 2H), 7.79 (d, *J* = 8.1 Hz, 1H), 7.74 (d, *J* = 9.0 Hz, 1H), 7.60 (d, *J* = 16.6 Hz, 1H), 7.55 (d, *J* = 7.8 Hz, 2H), 7.52 – 7.45 (m, 1H), 7.43 – 7.33 (m, 3H), 7.32 – 7.16 (m, 5H), 5.38 (s, 2H), 2.39 (s, 3H); **^{13}C NMR** (175 MHz; $CDCl_3$) δ 194.6, 153.5, 144.9, 138.2, 135.6, 132.9, 132.3, 130.1, 129.6, 129.0, 128.7, 128.52, 128.52, 127.7, 126.8, 126.7, 124.7, 124.2, 122.02, 121.98, 114.9, 72.6, 21.9; **IR** (Neat) 3032, 2889, 1703, 1620, 1605, 1590, 1573, 1511, 1494, 1471, 1447, 1428, 1402, 1294, 1230, 1211, 1181, 1150, 1120, 1074, 1029, 970, 929, 905, 855, 817, 687, 642, 610; **HRMS:** calcd for $C_{27}H_{22}O_2Na^+$: 401.1512 found: 401.1513.

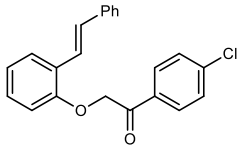

S24

(*E*)-1-(4-chlorophenyl)-2-(2-styrylphenoxy)ethan-1-one (**S24**): The alkylation protocol was performed on 2.55 mmol scale. Purification by flash column chromatography eluting with hexanes/dichloromethane (70:30) provided 0.43 g (48% yield) of **S26** as a white solid. **^{1}H NMR** (700 MHz; $CDCl_3$) δ 7.97 (d, *J* = 8.4 Hz, 2H), 7.63 (d, *J* = 7.6 Hz, 1H), 7.54 – 7.45 (m, 5H), 7.35 (t, *J* = 7.6 Hz, 2H), 7.26 (t, *J* = 7.3 Hz, 1H), 7.21 (t, *J* = 7.8 Hz, 1H), 7.16 (d, *J* = 16.5 Hz, 1H), 7.03 (t, *J* = 7.5 Hz, 1H), 6.83 (d, *J* = 8.2 Hz, 1H), 5.25 (s, 2H); **^{13}C NMR** (175 MHz; $CDCl_3$) δ 194.0, 155.4, 140.4, 137.9, 133.2, 130.0, 129.9, 129.3, 128.8, 128.7, 127.7, 127.3, 127.0, 126.7, 123.2, 122.2, 112.6, 71.8; **IR** (Neat) 2833, 1677, 1595, 1581, 1483, 1453, 1433, 1397, 1360, 1318,

1292, 1276, 1245, 1222, 1175, 1161, 1113, 1091, 1066, 1052, 1013, 991, 974, 966, 849, 836, 801, 754, 692, 658, 628, 620; **HRMS:** calcd for $C_{22}H_{17}ClO_2Na^+$: 371.0809 found: 371.0807.

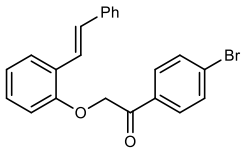

S36

(*E*)-1-(4-bromophenyl)-2-(2-styrylphenoxy)ethan-1-one (**S36**): The alkylation protocol was performed on 2.55 mmol scale. Purification by flash column chromatography eluting with hexanes/EtOAc (95:5) provided 0.61 g (61% yield) of **S36** as a yellow solid. **^{1}H NMR** (700 MHz; $CDCl_3$) δ 7.90 (d, *J* = 8.4 Hz, 2H), 7.67 – 7.58 (m, 3H), 7.53 – 7.43 (m, 3H), 7.35 (t, *J* = 7.6 Hz, 2H), 7.26 (d, *J* = 5.5 Hz, 1H), 7.21 (t, *J* = 7.8 Hz, 1H), 7.15 (d, *J* = 16.5 Hz, 1H), 7.03 (t, *J* = 7.5 Hz, 1H), 6.83 (d, *J* = 8.2 Hz, 1H), 5.25 (s, 2H); **^{13}C NMR** (175 MHz; $CDCl_3$) δ 194.2, 155.4, 137.9, 133.6, 132.3, 130.1, 130.0, 129.2, 128.8, 128.7, 127.7, 127.3, 127.0, 126.7, 123.2, 122.2, 112.7, 71.8; **IR** (Neat) 2935, 1677, 1596, 1579, 1481, 1453, 1433, 1395, 1319, 1293, 1277, 1244, 1220, 1178, 1161, 1113, 1073, 1051, 1010, 989, 974, 966, 848, 833, 801, 691, 653, 625; **HRMS:** calcd for $C_{22}H_{17}BrO_2Na^+$: 415.0304 found: 415.0302.

General alkylation procedure for the synthesis of aldehyde intermediates:

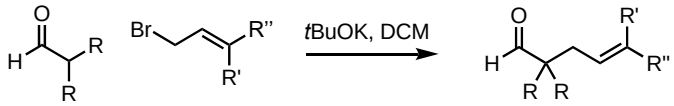

In a flame-dried flask, allylic bromide (1.2 eq) was dissolved in dry DCM (0.2 M). Aldehyde (1.0 eq) was added, and the reaction flask was cooled to 0 °C. At this temperature, *t*BuOK (1.2 eq) was added in one portion. The reaction mixture was allowed to slowly warm to room temperature and was stirred until judged complete by TLC analysis. The reaction was quenched with saturated ammonium chloride, the aqueous layer was extracted with DCM (x3), and the combined organics were washed with saturated sodium chloride, dried over Na_2SO_4, and concentrated under reduced pressure. The crude aldehyde was purified by column chromatography eluting with the indicated solvent to give the pure aldehyde intermediate.

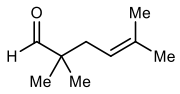

A18a

2,2,5-trimethylhex-4-enal (**A18a**): The alkylation protocol was performed on 20.0 mmol scale. Purification by flash column chromatography eluting with hexanes/EtOAc (95:5) provided 1.30 g (47% yield) of **A18a** as a clear oil. Spectral data was found to be in accordance with literature data.[99]

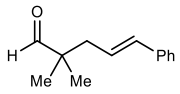

A18b

(*E*)-2,2-dimethyl-5-phenylpent-4-enal (**A18b**): The alkylation protocol was performed on 15.2 mmol scale. Purification by flash column chromatography eluting with hexanes/EtOAc (95:5) provided 2.30 g (80% yield) of **A18b** as a yellow oil. Spectral data was found to be in accordance with literature data.[100]

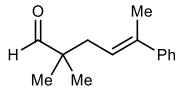

A18c

(*E*)-2,2-dimethyl-5-phenylhex-4-enal (**A18c**): The alkylation protocol was performed on 12.2 mmol scale. Purification by flash column chromatography eluting with hexanes/EtOAc (93:7) provided 1.40 g (57% yield) of **A18c** as a green oil. Spectral data was found to be in accordance with literature data.[101]

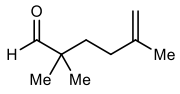

A18d

2,2,5-trimethylhex-5-enal (**A18d**): The alkylation protocol was performed on 3.66 mmol scale. Purification by flash column chromatography eluting with pentanes/Et_2O (10:90) provided 0.373 g (73% yield) of **A18d** as a clear oil. Spectral data was found to be in accordance with literature data.[102]

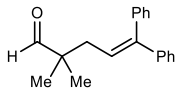

A18e

2,2-dimethyl-5,5-diphenylpent-4-enal (**A18e**): The alkylation protocol was performed on 2.28 mmol scale. Purification by flash column chromatography eluting with hexanes/EtOAc (90:10) provided 0.59 g (98% yield) of **A18e** as a clear oil. Spectral data was found to be in accordance with literature data.[103]

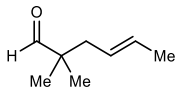

A18f

(*E*)-2,2-dimethylhex-4-enal (**A18f**): The alkylation protocol was performed on 4.48 mmol scale. Purification by flash column chromatography eluting with hexanes/EtOAc (93:7) provided 0.47 g (42% yield) of **A18f** as a yellow oil. Spectral data was found to be in accordance with literature data.[104]

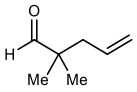

A18g

2,2-dimethylpent-4-enal (**A18g**): The alkylation protocol was performed on 20 mmol scale. Purification by flash column chromatography eluting with pentanes/Et_2O (90:10) provided 1.18 g (53% yield) of **A18g** as a yellow oil. Spectral data was found to be in accordance with literature data.[105]

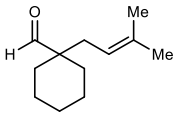

A30

1-(3-methylbut-2-en-1-yl)cyclohexane-1-carbaldehyde (**A30**): The alkylation protocol was performed on 60.0 mmol scale. Purification by flash column chromatography eluting with hexanes/DCM (65:35) provided 4.59 g (51% yield) of **A30** as a clear oil. **^{1}H NMR** (500 MHz; $CDCl_3$) δ 9.44 (s, 1H), 5.02 (t, *J* = 7.7 Hz, 1H), 2.10 (d, *J* = 7.7 Hz, 2H), 1.97 – 1.84 (m, 2H), 1.68 (s, 3H), 1.63 – 1.50 (m, 6H), 1.37 – 1.18 (m, 5H); **^{13}C NMR** (125 MHz; $CDCl_3$) δ 207.5, 134.7,

118.3, 50.7, 35.3, 31.0, 26.1, 25.9, 22.9, 18.0; **IR** (Neat) 2927, 2853, 2695, 1725, 1450, 1377, 1113, 964, 936, 877, 829, 771, 741, 632; **HRMS:** calcd for $C_{14}H_{23}NO^+$: 221.1774 found: 221.1536.

General Horner-Wadsworth-Emmons procedure for the synthesis of enone intermediates:

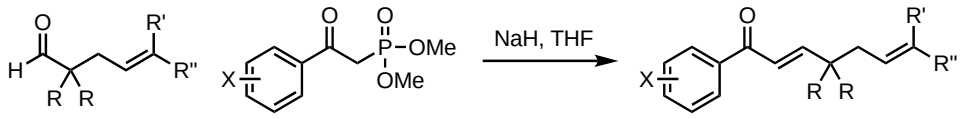

In a flame-dried flask, phosphonate ester (1.13 eq) was dissolved in dry THF (0.2 M). The reaction flask was cooled to 0 °C, and NaH (1.25 eq, 60% dispersion in mineral oil) was added carefully. The reaction mixture was allowed to stir at room temperature for 30 minutes, and then was cooled to 0 °C. At this temperature, aldehyde (1.0 eq) dissolved in 5 mL of THF was added slowly. The reaction mixture was allowed to slowly warm to room temperature, and then was heated to 70 °C until judged complete by TLC analysis. The reaction was quenched with saturated ammonium chloride, the aqueous layer was extracted with EtOAc (x3), and the combined organics were washed with saturated sodium chloride, dried over Na_2SO_4, and concentrated under reduced pressure. The crude enone was purified by column chromatography eluting with the indicated solvent to give the pure enone intermediate.

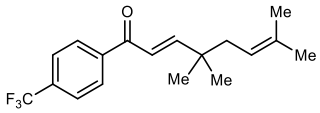

E18a

(*E*)-4,4,7-trimethyl-1-(4-(trifluoromethyl)phenyl)octa-2,6-dien-1-one (**E18a**): The Horner-Wadsworth-Emmons protocol was performed on 4.25 mmol scale. Purification by flash column chromatography eluting with hexanes/EtOAc (85:15) provided 0.90 g (69% yield) of **E18a** as a yellow oil. **^{1}H NMR** (400 MHz; $CDCl_3$) δ 7.99 (d, *J* = 8.2 Hz, 2H), 7.73 (d, *J* = 8.3 Hz, 2H), 7.04 (d, *J* = 15.8 Hz, 1H), 6.70 (d, *J* = 15.8 Hz, 1H), 5.11 (t, *J* = 7.5 Hz, 1H), 2.11 (d, *J* = 7.6 Hz, 2H), 1.72 (s, 3H), 1.60 (s, 3H), 1.13 (s, 6H); **^{13}C NMR** (175 MHz; $CDCl_3$) δ 190.8, 160.6, 141.3, 134.4, 134.0 (q, *J* = 32.6 Hz), 129.0, 125.7 (q, *J* = 3.7 Hz), 123.8 (q, *J* = 272.5 Hz), 122.1, 120.0, 40.5, 38.4, 26.3, 26.2, 18.1; **IR** (Neat) 2966, 1673, 1613, 1512, 1410, 1319, 1167, 1014, 991, 820, 775, 743, 727, 690, 676; **HRMS:** calcd for $C_{18}H_{22}F_3O^+$: 311.1617 found: 311.1618.

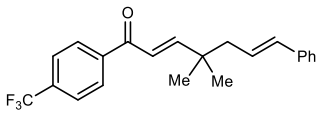

E18b

(2*E*,6*E*)-4,4-dimethyl-7-phenyl-1-(4-(trifluoromethyl)phenyl)hepta-2,6-dien-1-one (**E18b**): The Horner-Wadsworth-Emmons protocol was performed on 3.93 mmol scale. Purification by flash column chromatography eluting with hexanes/EtOAc (95:5) provided 1.18 g (84% yield) of **E18b** as a yellow oil. **^{1}H NMR** (500 MHz; $CDCl_3$) δ 7.97 (d, *J* = 8.1 Hz, 2H), 7.69 (d, *J* = 8.1 Hz, 2H), 7.31 (dt, *J* = 15.1, 7.5 Hz, 4H), 7.22 (t, *J* = 7.1 Hz, 1H), 7.08 (d, *J* = 15.8 Hz, 1H), 6.74 (d, *J* = 15.8 Hz, 1H), 6.42 (d, *J* = 15.7 Hz, 1H), 6.16 (dt, *J* = 15.4, 7.5 Hz, 1H), 2.35 (d, *J* = 7.5 Hz, 2H), 1.20 (s, 6H); **^{13}C NMR** (125 MHz; $CDCl_3$) δ 190.8, 159.7, 141.1, 137.4, 134.0 (q, *J* = 32.5 Hz), 133.4, 129.0, 128.7, 127.4, 126.3, 126.0, 125.7 (q, *J* = 3.7 Hz), 123.7 (q, *J* = 272.6 Hz), 122.5, 45.9, 38.2, 26.5; **IR** (Neat) 2967, 1672, 1622, 1611, 1578, 1510, 1496, 1448, 1410, 1385, 1364, 1320, 1296, 1245, 1159, 1110, 1066, 1030, 1011, 966, 873, 849, 827, 777, 751, 693, 685; **HRMS:** calcd for $C_{22}H_{21}F_3ONa^+$: 381.1437 found: 381.1441.

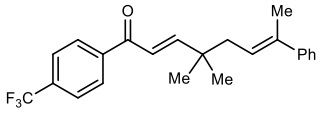

E18c

(2*E*,6*E*)-4,4-dimethyl-7-phenyl-1-(4-(trifluoromethyl)phenyl)octa-2,6-dien-1-one (**E18c**): The Horner-Wadsworth-Emmons protocol was performed on 2.79 mmol scale. Purification by flash column chromatography eluting with hexanes/DCM (65:35) provided 0.68 g (73% yield) of **E18c** (9:1 mixture of alkene isomers) as a yellow oil. **^{1}H NMR** (500 MHz; $CDCl_3$) δ 7.98 (d, *J* = 8.1 Hz, 2H), 7.70 (d, *J* = 8.1 Hz, 2H), 7.35 (d, *J* = 8.2 Hz, 2H), 7.30 (t, *J* = 7.5 Hz, 2H), 7.23 (t, *J* = 7.6 Hz, 1H), 7.10 (d, *J* = 15.8 Hz, 1H), 6.75 (d, *J* = 15.8 Hz, 1H), 5.75 (t, *J* = 7.6 Hz, 1H), 2.36 (d, *J* = 7.6 Hz, 2H), 2.03 (s, 3H), 1.22 (s, 6H); **^{13}C NMR** (175 MHz; $CDCl_3$) δ 190.7, 159.9, 144.0, 141.2, 137.6, 134.0 (q, *J* = 32.7 Hz), 129.0, 128.4, 127.0, 125.9, 125.7 (q, *J* = 3.8 Hz), 123.9, 123.80 (q, *J* = 272.7 Hz), 122.4, 41.1, 38.7, 26.5, 16.3; **IR** (Neat) 2962, 1672, 1613, 1580, 1511, 1494, 1445, 1409, 1384, 1365, 1318, 1218, 1166, 1029, 1013, 994, 976, 936, 909, 870, 830, 760, 740, 694, 646; **HRMS:** calcd for $C_{25}H_{26}F_3NO^+$: 413.1961 found: 413.2123.

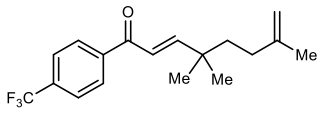

E18d

(*E*)-4,4,7-trimethyl-1-(4-(trifluoromethyl)phenyl)octa-2,7-dien-1-one (**E18d**): The Horner-Wadsworth-Emmons protocol was performed on 2.41 mmol scale. Purification by flash column chromatography eluting with hexanes/DCM (65:35) provided 0.19 g (35% yield) of **E18d** (3:1 mixture of alkene isomers) as a green oil. **^{1}H NMR** (for the mixture of isomers; 500 MHz; $CDCl_3$) δ 8.00 (t, *J* = 8.1 Hz, 2H), 7.74 (d, *J* = 8.1 Hz, 2H), 7.09 – 6.98 (m, 1H), 6.72 (dd, *J* = 19.6, 15.8 Hz, 1H), 5.11 (t, *J* = 7.6 Hz, 0.25H), 4.68 (d, *J* = 14.0 Hz, 1.5H), 2.14 – 2.08 (m, 0.5H), 2.02 – 1.88 (m, 1.5H), 1.72 (s, 3H), 1.63 – 1.53 (m, 2.25H), 1.16 (s, 4.5H), 1.12 (s, 1.5H); **^{13}C NMR** (for the mixture of isomers; 125 MHz; $CDCl_3$) δ 190.51, 190.46, 160.6, 160.5, 160.2, 160.1, 146.0, 141.2, 134.0 (q, *J* = 32.8 Hz), 128.97, 128.95, 125.7 (q, *J* = 3.7 Hz), 123.9 (q, *J* = 272.5 Hz), 122.2, 122.1, 120.0, 109.9, 40.5, 38.4, 37.43, 37.42, 33.0, 26.5, 26.3, 26.2, 22.8, 18.1; **IR** (Neat) 2964, 2925, 1671, 1613, 1511, 1409, 1319, 1128, 1167, 1110, 1032, 1014, 992, 887, 831, 779, 723, 689; **HRMS**: calcd for $C_{18}H_{22}F_3O^+$: 311.1617 found 311.1613.

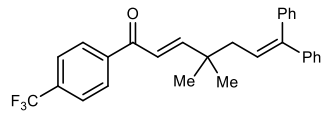

E18e

(*E*)-4,4-dimethyl-7,7-diphenyl-1-(4-(trifluoromethyl)phenyl)hepta-2,6-dien-1-one (**E18e**): The Horner-Wadsworth-Emmons protocol was performed on 2.28 mmol scale. Purification by flash column chromatography eluting with hexanes/EtOAc (90:10) provided 0.59 g (98% yield) of **E18e** as a yellow oil. **^{1}H NMR** (700 MHz; $CDCl_3$) δ 7.98 (d, *J* = 8.1 Hz, 2H), 7.71 (d, *J* = 8.2 Hz, 2H), 7.36 (t, *J* = 7.4 Hz, 2H), 7.31 (t, *J* = 7.4 Hz, 1H), 7.28 – 7.20 (m, 3H), 7.18 (d, *J* = 6.9 Hz, 2H), 7.13 (d, *J* = 7.1 Hz, 2H), 7.04 (d, *J* = 15.8 Hz, 1H), 6.72 (d, *J* = 15.8 Hz, 1H), 6.06 (t, *J* = 7.5 Hz, 1H), 2.29 (d, *J* = 7.5 Hz, 2H), 1.16 (s, 6H); **^{13}C NMR** (175 MHz; $CDCl_3$) δ 190.6, 159.9, 144.1, 142.7, 141.1, 140.0, 134.0 (q, *J* = 32.6 Hz), 130.1, 129.0, 128.4, 128.3, 127.31, 127.30, 127.2, 125.7 (q, *J* = 3.7 Hz), 125.1, 123.8 (q, *J* = 272.5 Hz), 122.4, 41.7, 38.4, 26.6; **IR** (Neat) 3024, 2962, 1672, 1613, 1511, 1494, 1466, 1409, 1385, 1318, 1218, 1167, 1126, 1110, 1066, 1031, 1013, 992, 908, 870, 830, 760, 696, 646; **HRMS**: calcd for $C_{30}H_{28}F_3NO^+$: 475.2118 found 475.1473.

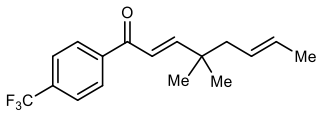

E18f

(2*E*,6*E*)-4,4-dimethyl-1-(4-(trifluoromethyl)phenyl)octa-2,6-dien-1-one (**E18f**): The Horner-Wadsworth-Emmons protocol was performed on 3.96 mmol scale. Purification by flash column chromatography eluting with hexanes/EtOAc (90:10) provided 0.50 g (42% yield) of **E18f** (3:1 mixture of alkene isomers) as a yellow oil. **^{1}H NMR** (for the mixture of isomers; 700 MHz; $CDCl_3$) δ 7.99 (d, *J* = 8.0 Hz, 2H), 7.73 (d, *J* = 8.1 Hz, 2H), 7.04 (t, *J* = 16.2 Hz, 1H), 6.71 (t, *J* = 16.0 Hz, 1H), 5.60 (dq, *J* = 13.6, 6.8 Hz, 0.25H), 5.47 (dq, *J* = 12.7, 6.4 Hz, 0.75H), 5.36 (dt, *J* = 14.6, 6.6 Hz, 1H), 2.18 (d, *J* = 7.6 Hz, 0.5H), 2.10 (d, *J* = 7.3 Hz, 1.5H), 1.67 (d, *J* = 6.3 Hz, 2.25H), 1.61 (d, *J* = 6.8 Hz, 0.75H), 1.15 (s, 1.5H), 1.11 (s, 4.5H); **^{13}C NMR** (for the mixture of isomers; 175 MHz; $CDCl_3$) δ 190.9, 190.7, 160.5, 160.2, 141.2, 134.0 (q, *J* = 32.7 Hz), 128.99, 128.97, 128.8, 126.8, 126.7, 125.9, 125.7 (q, *J* = 3.6 Hz), 123.8 (q, *J* = 272.6 Hz), 122.2, 122.1, 45.5, 39.1, 38.2, 37.8, 26.30, 26.29, 18.2, 13.1; **^{13}C NMR** (signals corresponding to the major isomer; 175 MHz; $CDCl_3$) δ 190.9, 160.5, 141.2, 134.0 (q, *J* = 32.7 Hz), 129.0, 128.8, 126.7, 125.7 (q, *J* = 3.6 Hz), 123.8 (q, *J* = 272.6 Hz), 122.2, 45.5, 37.8, 26.3, 18.2; **IR** (Neat) 2964, 1673, 1613, 1580, 1511, 1450, 1409, 1385, 1365, 1318, 1219, 1127, 1167, 1033, 1014, 993, 967, 927, 870, 831, 755, 727, 689, 675; **HRMS:** calcd for $C_{17}H_{20}F_3O^+$: 297.1461 found 297.1462.

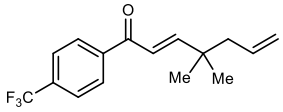

E18g

(*E*)-4,4-dimethyl-1-(4-(trifluoromethyl)phenyl)hepta-2,6-dien-1-one (**E18g**): The Horner-Wadsworth-Emmons protocol was performed on 4.46 mmol scale. Purification by flash column chromatography eluting with hexanes/EtOAc (93:7) provided 0.40 g (32% yield) of **E18g** as a yellow oil. **^{1}H NMR** (700 MHz; $CDCl_3$) δ 7.99 (d, *J* = 8.1 Hz, 2H), 7.73 (d, *J* = 8.2 Hz, 2H), 7.04 (d, *J* = 15.8 Hz, 1H), 6.71 (d, *J* = 15.8 Hz, 1H), 5.74 (td, *J* = 17.4, 7.4 Hz, 1H), 5.11 – 5.03 (m, 2H), 2.19 (d, *J* = 7.4 Hz, 2H), 1.14 (s, 6H); **^{13}C NMR** (175 MHz; $CDCl_3$) δ 190.7, 159.9, 141.2, 134.3, 134.0 (q, *J* = 32.8 Hz), 129.0, 125.7 (q, *J* = 3.8 Hz), 123.8 (q, *J* = 272.6 Hz), 122.3, 118.2, 46.6, 37.6, 26.3; **IR** (Neat) 2965, 1673, 1614, 1581, 1512, 1468, 1410, 1386, 1366, 1318, 1219, 1167, 1127, 1110, 1066, 1032, 1014, 992, 917, 831, 778, 752, 728, 690; **HRMS:** calcd for $C_{16}H_{18}F_3O^+$: 283.1304 found 283.1307.

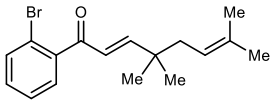

E22

(*E*)-1-(2-bromophenyl)-4,4,7-trimethylocta-2,6-dien-1-one (**E22**): The Horner-Wadsworth-Emmons protocol was performed on 4.03 mmol scale. Purification by flash column chromatography eluting with hexanes/dichloromethane (80:20) provided 0.17 g (15% yield) of **E22** as a yellow oil. **^{1}H NMR** (700 MHz; $CDCl_3$) δ 7.60 (d, *J* = 7.8 Hz, 1H), 7.37 (t, *J* = 7.4 Hz, 1H), 7.30 (d, *J* = 7.9 Hz, 2H), 6.63 (d, *J* = 16.1 Hz, 1H), 6.34 (d, *J* = 16.1 Hz, 1H), 5.07 (t, *J* = 7.4 Hz, 1H), 2.04 (d, *J* = 7.5 Hz, 2H), 1.68 (s, 3H), 1.55 (s, 3H), 1.07 (s, 6H); **^{13}C NMR** (175 MHz; $CDCl_3$) δ 195.9, 161.9, 141.4, 134.3, 133.4, 131.2, 129.1, 127.3, 126.7, 120.0, 119.5, 40.5, 38.4, 26.2, 26.1, 18.0; **IR** (Neat) 2962, 2927, 1658, 1615, 1588, 1564, 1465, 1429, 1384, 1364, 1289, 1251, 1214, 1096, 1066, 1023, 987, 910, 847, 760, 699, 639, 621, 606; **HRMS:** calcd for $C_{17}H_{21}BrONa^{+}$: 343.0668 found: 343.0666.

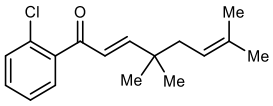

E27

(*E*)-1-(2-chlorophenyl)-4,4,7-trimethylocta-2,6-dien-1-one (**E27**): The Horner-Wadsworth-Emmons protocol was performed on 3.57 mmol scale. Purification by flash column chromatography eluting with hexanes/dichloromethane (93:7) provided 0.56 g (57% yield) of **E27** as a green oil. **^{1}H NMR** (700 MHz; $CDCl_3$) δ 7.42 (d, *J* = 7.4 Hz, 1H), 7.38 (td, *J* = 8.0, 7.6, 1.9 Hz, 1H), 7.35 (dd, *J* = 7.6, 1.8 Hz, 1H), 7.32 (t, *J* = 7.3 Hz, 1H), 6.66 (d, *J* = 16.1 Hz, 1H), 6.37 (d, *J* = 16.1 Hz, 1H), 5.07 (t, *J* = 7.6 Hz, 1H), 2.05 (d, *J* = 7.6 Hz, 2H), 1.69 (s, 3H), 1.55 (s, 3H), 1.07 (s, 6H); **^{13}C NMR** (175 MHz; $CDCl_3$) δ 195.0, 161.5, 139.4, 134.2, 131.3, 131.2, 130.3, 129.3, 126.8, 126.8, 120.0, 40.5, 38.3, 26.2, 26.1, 18.0; **IR** (Neat) 2963, 2928, 1657, 1615, 1593, 1468, 1432, 1384, 1364, 1295, 1213, 1100, 1072, 1042, 1021, 988, 910, 847, 761, 733, 702, 678, 642, 622; **HRMS:** calcd for $C_{17}H_{22}ClO^{+}$: 277.1354 found 277.1354.

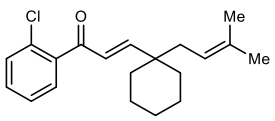

E30

(*E*)-1-(2-chlorophenyl)-3-(1-(3-methylbut-2-en-1-yl)cyclohexyl)prop-2-en-1-one (**E40**): The Horner-Wadsworth-Emmons protocol was performed on 2.77 mmol scale. Purification by flash column chromatography eluting with hexanes/DCM (65:35) provided 0.14 g (16% yield) of **E40** as a yellow oil. **^{1}H NMR** (500 MHz; $CDCl_3$) δ 7.44 – 7.28 (m, 4H), 6.56 (d, *J* = 16.4 Hz, 1H), 6.39 (d, *J* = 16.4 Hz, 1H), 5.04 (t, *J* = 7.6 Hz, 1H), 2.05 (d, *J* = 7.6 Hz, 2H), 1.67 – 1.63 (m, 5H), 1.55 – 1.51 (m, 6H), 1.45 – 1.35 (m, 5H); **^{13}C NMR** (125 MHz; $CDCl_3$) δ 194.9, 160.9, 139.4, 134.1, 131.2, 131.1, 130.3, 129.2, 129.0, 126.8, 119.4, 41.9, 39.5, 35.3, 26.3, 26.2, 22.6, 18.1; **IR** (Neat) 2927, 2853, 1655, 1611, 1592, 1450, 1432, 1377, 1298, 1216, 1105, 1072, 1040, 1021, 987, 951, 909, 837, 820, 762, 731, 678, 640, 621, 603; **HRMS:** calcd for $C_{20}H_{25}ClO^+$: 316.1594 found: 316.1597.

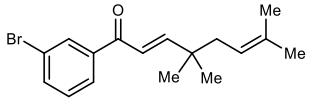

E32

(*E*)-1-(3-bromophenyl)-4,4,7-trimethylocta-2,6-dien-1-one (**E32**): The Horner-Wadsworth-Emmons protocol was performed on 4.03 mmol scale. Purification by flash column chromatography eluting with hexanes/EtOAc (95:5) provided 0.46 g (40% yield) of **E32** as a yellow oil. **^{1}H NMR** (700 MHz; $CDCl_3$) δ 8.03 (t, *J* = 1.7 Hz, 1H), 7.83 (d, *J* = 7.8 Hz, 1H), 7.68 (d, *J* = 7.9 Hz, 1H), 7.35 (t, *J* = 7.8 Hz, 1H), 7.04 (d, *J* = 15.7 Hz, 1H), 6.68 (d, *J* = 15.7 Hz, 1H), 5.11 (t, *J* = 7.6 Hz, 1H), 2.11 (d, *J* = 7.6 Hz, 2H), 1.72 (s, 3H), 1.60 (s, 3H), 1.12 (s, 6H); **^{13}C NMR** (175 MHz; $CDCl_3$) δ 190.1, 160.1, 140.2, 135.5, 134.3, 131.7, 130.2, 127.2, 123.0, 121.8, 120.0, 40.5, 38.4, 26.4, 26.2, 18.1; **IR** (Neat) 2962, 2927, 1670, 1615, 1564, 1450, 1420, 1363, 1383, 1303, 1265, 1210, 1104, 1067, 1029, 989, 908, 853, 790, 718, 688, 669, 646, 630, 610; **HRMS:** calcd for $C_{17}H_{21}BrONa^+$: 343.0668 found: 343.0670.

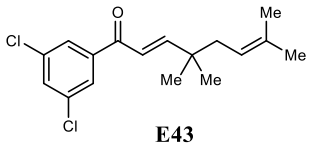

E43

(E)-1-(3,5-dichlorophenyl)-4,4,7-trimethylocta-2,6-dien-1-one (E43): The Horner-Wadsworth-Emmons protocol was performed on 4.99 mmol scale. Purification by flash column chromatography eluting with hexanes/EtOAc (85:15) provided 1.10 g (73% yield) of **E43** as a yellow oil. **^{1}H NMR** (400 MHz; $CDCl_3$) δ 7.75 (d, *J* = 2.0 Hz, 2H), 7.54 (t, *J* = 1.9 Hz, 1H), 7.06

(d, *J* = 15.7 Hz, 1H), 6.63 (d, *J* = 15.7 Hz, 1H), 5.17 – 4.90 (m, 1H), 2.11 (d, *J* = 7.6 Hz, 2H), 1.73 (s, 3H), 1.60 (s, 3H), 1.13 (s, 6H).; **^{13}C NMR** (175 MHz; $CDCl_3$) δ; **IR** (Neat) 3076, 2962, 2929, 1736, 1672, 1616, 1562, 1416, 1384, 1303, 1282, 1239, 1210, 1098, 1055, 989, 841, 801, 726, 659, 642; **HRMS:** calcd for $C_{17}H_{21}Cl_2O^+$: 311.0964 found 311.096.

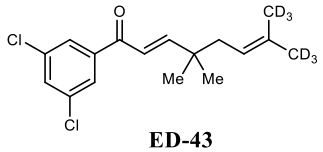

ED-43

(E)-1-(3,5-dichlorophenyl)-4,4-dimethyl-7-(methyl-d3)octa-2,6-dien-1-one-8,8,8-d3 (ED-43)

The Horner-Wadsworth-Emmons protocol was performed on 2.91 mmol scale. Purification by flash column chromatography eluting with hexanes/EtOAc (85:15) provided 0.135 g (15% yield) of **ED-43** as a yellow oil. **^{1}H NMR** (400 MHz; $CDCl_3$) δ 7.74 (d, *J* = 1.9 Hz, 2H), 7.54 (t, *J* = 1.9 Hz, 1H), 7.06 (d, *J* = 15.7 Hz, 1H), 6.63 (d, *J* = 15.7 Hz, 1H), 5.10 (t, *J* = 7.6 Hz, 1H), 2.11 (d, *J* = 7.6 Hz, 2zzH), 1.12 (s, 6H); **^{13}C NMR** (175 MHz; $CDCl_3$) δ 188.8, 161.0, 140.9, 135.6, 134.3, 132.3, 127.1, 121.4, 119.9, 40.5, 38.5, 26.3; **IR** (Neat) 3076, 2961, 2713, 2224, 2191, 2064, 1673, 1563, 1431, 1303, 1210, 1048, 991, 974, 889, 801, 724, 694, 650, 642; **HRMS:** calcd for C17H15D6Cl2O$^+$: 3171.1341 found 317.1346.

General 1,4-reduction procedure for the synthesis of aryl ketone substrates:

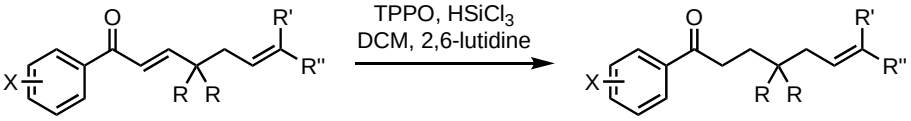

In a flame-dried flask, enone (1.0 eq) was dissolved in dry DCM (0.1 M). Triphenylphosphine oxide (0.2 eq) was added, and the reaction flask was cooled to 0 °C. At this temperature, 2,6-lutidine (2.0 eq) was added followed by trichlorosilane (2.0 eq). The reaction was allowed to slowly warm to room temperature and stirred until judged complete by TLC analysis. The reaction was quenched with saturated sodium bicarbonate, the aqueous layer was extracted with DCM (x3), and the combined organics were washed with saturated sodium chloride, dried over Na_2SO_4, and concentrated under reduced pressure. The crude aryl ketone was purified by column chromatography eluting with the indicated solvent to give the pure aryl ketone substrate.

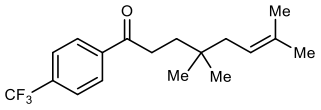

43a

4,4,7-trimethyl-1-(4-(trifluoromethyl)phenyl)oct-6-en-1-one (**43a**): The 1,4-reduction protocol was performed on 1.37 mmol scale. Purification by flash column chromatography eluting with hexanes/EtOAc (93:7) provided 0.33 g (76% yield) of **43a** as a clear oil. **^{1}H NMR** (500 MHz; $CDCl_3$) δ 8.05 (d, *J* = 8.1 Hz, 2H), 7.73 (d, *J* = 8.3 Hz, 2H), 5.19 (t, *J* = 7.5 Hz, 1H), 2.99 – 2.90 (m, 2H), 1.95 (d, *J* = 7.5 Hz, 2H), 1.73 (s, 3H), 1.67 – 1.62 (m, 2H), 1.61 (s, 3H), 0.92 (s, 6H); **^{13}C NMR** (125 MHz; $CDCl_3$) δ 200.1, 139.9, 134.4 (q, *J* = 32.6 Hz), 133.4, 128.6, 125.8 (q, *J* = 3.8 Hz), 123.8 (q, *J* = 272.5 Hz), 120.9, 40.1, 35.9, 34.4, 33.9, 27.0, 26.2, 18.1; **IR** (Neat) 2959, 2929, 1691, 1582, 1511, 1470, 1410, 1386, 1366, 1323, 1213, 1167, 1128, 1016, 986, 899, 848, 777, 730, 674; **HRMS:** calcd for $C_{18}H_{24}F_3O^+$: 313.1774 found: 313.1774.

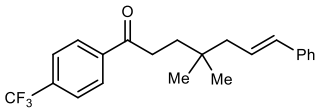

43b

(*E*)-4,4-dimethyl-7-phenyl-1-(4-(trifluoromethyl)phenyl)hept-6-en-1-one (**43b**): The 1,4-reduction protocol was performed on 1.95 mmol scale. Purification by flash column chromatography eluting with hexanes/dichloromethane (70:30) provided 0.22 g (31% yield) of **43b** as a white solid. **^{1}H NMR** (700 MHz; $CDCl_3$) δ 8.05 (d, *J* = 8.1 Hz, 2H), 7.68 (d, *J* = 8.1 Hz, 2H), 7.35 (d, *J* = 7.8 Hz, 2H), 7.30 (t, *J* = 7.5 Hz, 2H), 7.21 (t, *J* = 7.3 Hz, 1H), 6.42 (d, *J* = 15.7 Hz, 1H), 6.26 (dt, *J* = 15.4, 7.5 Hz, 1H), 3.06 – 2.94 (m, 2H), 2.19 (d, *J* = 7.5 Hz, 2H), 1.81 – 1.65 (m, 2H), 1.00 (s, 6H); **^{13}C NMR** (175 MHz; $CDCl_3$) δ 199.9, 139.8, 137.7, 134.3 (q, *J* = 32.6 Hz), 132.7, 128.7, 128.6, 127.2, 127.1, 126.2, 125.8 (q, *J* = 3.7 Hz), 123.7 (q, *J* = 272 Hz), 45.7, 36.1, 34.3, 33.8, 27.1; **IR** (Neat) 2962, 1689, 1598, 1510, 1495, 1471, 1448, 1411, 1387, 1368, 1328, 1277, 1221, 1198, 1163, 1065, 1030, 987, 967, 898, 914, 862, 842, 814, 768, 725, 694, 674, 637, 627, 613, 602; **HRMS:** calcd for $C_{22}H_{23}F_3ONa^+$: 383.1593 found: 383.1593.

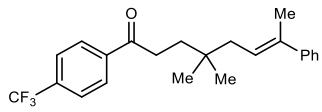

43c

(*E*)-4,4-dimethyl-7-phenyl-1-(4-(trifluoromethyl)phenyl)oct-6-en-1-one (**43c**): The 1,4-reduction protocol was performed on 1.21 mmol scale. Purification by flash column chromatography eluting with hexanes/EtOAc (93:7) provided 0.19 g (42% yield) of **43c** as a green oil. **^{1}H NMR** (500 MHz; $CDCl_3$) δ 8.05 (d, *J* = 8.1 Hz, 2H), 7.69 (d, *J* = 8.2 Hz, 2H), 7.38 (d, *J* = 7.2 Hz, 2H), 7.31 (t, *J* = 7.6 Hz, 2H), 7.23 (t, *J* = 7.3 Hz, 1H), 5.85 (t, *J* = 7.6 Hz, 1H), 3.04 – 2.93 (m, 2H), 2.18 (d, *J* = 7.6 Hz, 2H), 2.05 (s, 3H), 1.79 – 1.65 (m, 2H), 1.01 (s, 6H); **^{13}C NMR** (125 MHz; $CDCl_3$) δ 200.0, 144.2, 139.8, 136.7, 134.4 (q, *J* = 32.7 Hz), 128.5, 128.3, 126.8, 125.84, 125.82 (q, *J* = 3.8 Hz), 124.9, 123.7 (q, *J* = 272.6 Hz), 40.8, 36.1, 34.4, 34.3, 27.1, 16.3; **IR** (Neat) 2960, 1687, 1600, 1582, 1511, 1495, 1448, 1410, 1368, 1323, 1266, 1212, 1166, 1125, 1109, 1065, 1015, 985, 849, 730, 699; **HRMS:** calcd for $C_{23}H_{26}F_3O^+$: 375.1930 found: 375.1916.

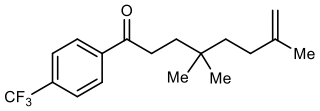

43d

4,4,7-trimethyl-1-(4-(trifluoromethyl)phenyl)oct-7-en-1-one (**43d**): The 1,4-reduction protocol was performed on 0.61 mmol scale. Purification by flash column chromatography eluting with hexanes/EtOAc (93:7) provided 0.09 g (63% yield) of **43d** (2:1 mixture of alkene isomers) as a green oil. **^{1}H NMR** (for the mixture of isomers; 500 MHz; $CDCl_3$) δ 8.06 (d, *J* = 8.2 Hz, 2H), 7.73 (d, *J* = 8.2 Hz, 2H), 5.19 (t, *J* = 7.5 Hz, 0.33 H), 4.69 (d, *J* = 5.1 Hz, 1.33 H), 3.02 – 2.87 (m, 2H), 2.04 – 1.88 (m, 2H), 1.73 (d, *J* = 5.2 Hz, 3H), 1.71 – 1.60 (m, 3H), 1.46 – 1.34 (m, 1.33 H), 0.94 (d, *J* = 13.0 Hz, 6H); **^{13}C NMR** (for the mixture of isomers; 125 MHz; $CDCl_3$) δ 200.2, 200.0, 146.8, 139.8, 134.4 (q, *J* = 32.6 Hz), 133.4, 128.6, 128.5, 125.8 (q, *J* = 3.5 Hz), 123.8 (q, *J* = 272.9 Hz), 120.8, 109.5, 40.1, 40.0, 35.9, 35.8, 34.4, 34.2, 32.6, 32.4, 27.03, 26.98, 26.2, 22.9, 18.1; **IR** (Neat) 2959, 1691, 1649, 1582, 1511, 1471, 1410, 1387, 1367, 1323, 1211, 1167, 1016, 984, 886, 848, 779, 731, 672; **HRMS:** calcd for $C_{18}H_{23}F_3ONa^+$: 335.1593 found: 335.1589.

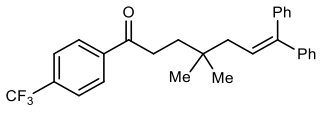

43e

4,4-dimethyl-7,7-diphenyl-1-(4-(trifluoromethyl)phenyl)hept-6-en-1-one (**43e**): The 1,4-reduction protocol was performed on 0.68 mmol scale. Purification by flash column chromatography eluting with hexanes/EtOAc (95:5) provided 0.93 g (37% yield) of **43e** as a clear oil. **^{1}H NMR** (500 MHz; $CDCl_3$) δ 7.94 (d, *J* = 8.2 Hz, 2H), 7.68 (d, *J* = 8.3 Hz, 2H), 7.35 – 7.19

(m, 8H), 7.15 – 7.12 (m, 2H), 6.16 (t, *J* = 7.6 Hz, 1H), 2.82 – 2.66 (m, 2H), 2.13 (d, *J* = 7.6 Hz, 2H), 1.72 – 1.62 (m, 2H), 0.97 (s, 6H); **^{13}C NMR** (125 MHz; $CDCl_3$) δ 199.71, 143.46, 143.00, 140.31, 139.75, 134.3 (q, *J* = 32.8 Hz), 130.2, 128.5, 128.31, 128.27, 127.4, 127.2, 127.1, 126.2, 125.7 (q, *J* = 3.8 Hz), 123.6 (q, *J* = 272.5 Hz), 40.8, 35.4, 34.2, 34.1, 27.5; **IR** (Neat) 2959, 1692, 1494, 1444, 1410, 1368, 1325, 1265, 1170, 1131, 1109, 1066, 1016, 908, 850, 733, 701, 627; **HRMS:** calcd for $C_{28}H_{27}F_3ONa^+$: 249.1906 found 459.1904.

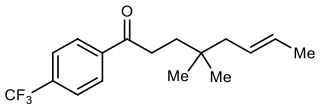

43f

(*E*)-4,4-dimethyl-1-(4-(trifluoromethyl)phenyl)oct-6-en-1-one one (**43f**): The 1,4-reduction protocol was performed on 0.85 mmol scale. Purification by flash column chromatography eluting with hexanes/EtOAc (95:5) provided 0.16 g (62% yield) of **43f** (3:1 mixture of alkene isomers) as a clear oil. **^{1}H NMR** (for the mixture of isomers; 700 MHz; $CDCl_3$) δ 8.05 (d, *J* = 8.1 Hz, 2H), 7.72 (d, *J* = 8.2 Hz, 2H), 5.62 – 5.53 (m, 0.25H), 5.49 – 5.40 (m, 1.75H), 3.00 – 2.90 (m, 2H), 2.01 (d, *J* = 7.6 Hz, 0.5H), 1.94 (d, *J* = 4.8 Hz, 1.5H), 1.69 – 1.65 (m, 3H), 1.65 – 1.58 (m, 2H), 0.94 (s, 1.5H), 0.91 (s, 4.5H); **^{13}C NMR** (for the mixture of isomers; 175 MHz; $CDCl_3$) δ 200.1, 200.0, 139.8, 134.3 (q, *J* = 32.6 Hz), 128.54, 128.52, 127.8, 127.6, 126.7, 126.0, 125.8 (q, *J* = 3.7 Hz), 123.8 (q, *J* = 272.6 Hz), 45.1, 38.8, 35.9, 35.8, 34.3, 34.2, 33.7, 33.2, 27.0, 26.9, 18.2, 13.1; **^{13}C NMR** (signals corresponding to the major isomer; 175 MHz; $CDCl_3$) δ 200.1, 139.8, 134.3 (q, *J* = 32.6 Hz), 128.5, 127.8, 127.6, 125.8 (q, *J* = 3.7 Hz), 123.8 (q, *J* = 272.6 Hz), 45.1, 35.8, 34.2, 33.2, 27.0, 18.2; **IR** (Neat) 2959, 1690, 1582, 1512, 1471, 1410, 1387, 1323, 1211, 1167, 1127, 1065, 1016, 968, 923, 849, 776, 721, 670, 625; **HRMS:** calcd for $C_{17}H_{22}F_3O^+$: 299.1617 found 299.1617.

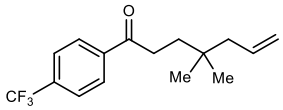

43g

4,4-dimethyl-1-(4-(trifluoromethyl)phenyl)hept-6-en-1-one (**43g**): The 1,4-reduction protocol was performed on 0.90 mmol scale. Purification by flash column chromatography eluting with hexanes/EtOAc (95:5) provided 0.11 g (43% yield) of **43g** as a clear oil. **^{1}H NMR** (700 MHz; $CDCl_3$) δ 8.05 (d, *J* = 8.2 Hz, 2H), 7.73 (d, *J* = 8.2 Hz, 2H), 5.83 (ddt, *J* = 17.5, 10.2, 7.4 Hz, 1H), 5.14 – 4.99 (m, 2H), 2.99 – 2.91 (m, 2H), 2.03 (d, *J* = 7.4 Hz, 2H), 1.71 – 1.61 (m, 2H), 0.94 (s,

6H); **^{13}C NMR** (175 MHz; $CDCl_3$) δ 199.9, 139.8, 135.2, 134.4 (q, *J* = 32.7 Hz), 128.5, 125.8 (q, *J* = 3.8 Hz), 123.8 (q, *J* = 272.6 Hz), 117.4, 46.5, 35.9, 34.2, 33.1, 26.9; **IR** (Neat) 2960, 1691, 1512, 1471, 1410, 1387, 1367, 1324, 1211, 1167, 1127, 1108, 1065, 1016, 995, 914, 849, 777, 741, 731, 680; **HRMS:** calcd for $C_{17}H_{23}ClONa^+$: 301.1330 found 301.1332.

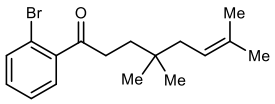

S20

1-(2-bromophenyl)-4,4,7-trimethyloct-6-en-1-one (**S20**): The 1,4-reduction protocol was performed on 0.78 mmol scale. Purification by flash column chromatography eluting with hexanes/EtOAc (95:5) provided 0.15 g (61% yield) of **S20** as a yellow oil. **^{1}H NMR** (700 MHz; $CDCl_3$) δ 7.60 (d, *J* = 8.0 Hz, 1H), 7.41 – 7.32 (m, 2H), 7.31 – 7.27 (m, 1H), 5.17 (t, *J* = 7.6 Hz, 1H), 3.04 – 2.74 (m, 2H), 1.90 (d, *J* = 7.5 Hz, 2H), 1.71 (s, 3H), 1.66 – 1.60 (m, 2H), 1.59 (s, 3H), 0.88 (s, 6H); **^{13}C NMR** (175 MHz; $CDCl_3$) δ 205.4, 142.4, 133.7, 133.3, 131.4, 128.4, 127.5, 120.9, 118.7, 40.1, 38.4, 35.6, 33.8, 26.9, 26.2, 18.1; **IR** (Neat) 2957, 2927, 1700, 1588, 1466, 1428, 1385, 1364, 1301, 1212, 1105, 1067, 1026, 982, 898, 847, 810, 725, 673, 654, 638, 611; **HRMS:** calcd for $C_{17}H_{23}BrONa^+$: 345.0824 found: 345.0821.

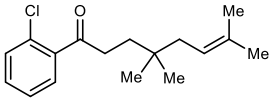

S25

1-(2-chlorophenyl)-4,4,7-trimethyloct-6-en-1-one (**S25**): The 1,4-reduction protocol was performed on 1.16 mmol scale. Purification by flash column chromatography eluting with hexanes/EtOAc (93:7) provided 0.13 g (41% yield) of **S25** as a yellow oil. **^{1}H NMR** (700 MHz; $CDCl_3$) δ 7.41 (td, *J* = 7.2, 6.7, 1.3 Hz, 2H), 7.37 (td, *J* = 7.7, 1.7 Hz, 1H), 7.31 (td, *J* = 7.4, 1.2 Hz, 1H), 5.16 (t, *J* = 7.6 Hz, 1H), 3.02 – 2.77 (m, 2H), 1.90 (d, *J* = 7.6 Hz, 2H), 1.71 (s, 3H), 1.65 – 1.60 (m, 2H), 1.59 (s, 3H), 0.88 (s, 6H); **^{13}C NMR** (175 MHz; $CDCl_3$) δ 204.6, 140.1, 133.3, 131.5, 130.8, 130.6, 128.8, 127.0, 120.9, 40.1, 38.6, 35.7, 33.8, 26.9, 26.2, 18.1; **IR** (Neat) 2956, 2868, 1699, 1591, 1469, 1432, 1387, 1369, 1299, 1209, 1097, 1074, 1037, 983, 814, 693, 641, 610; **HRMS**: calcd for $C_{17}H_{23}ClOK^+$: 317.1069 found: 317.1101.

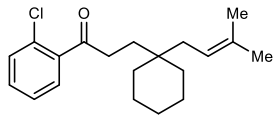

S28

1-(2-chlorophenyl)-3-(1-(3-methylbut-2-en-1-yl)cyclohexyl)propan-1-one (**S28**): The 1,4-reduction protocol was performed on 0.43 mmol scale. Purification by flash column chromatography eluting with hexanes/EtOAc (93:7) provided 0.69 g (51% yield) of **S28** as a yellow oil. **^{1}H NMR** (500 MHz; $CDCl_3$) δ 7.44 – 7.29 (m, 4H), 5.12 (t, *J* = 7.4 Hz, 1H), 2.95 – 2.77 (m, 2H), 1.94 (d, *J* = 7.4 Hz, 2H), 1.73 – 1.62 (m, 5H), 1.59 (s, 3H), 1.50 – 1.24 (m, 10H); **^{13}C NMR** (175 MHz; $CDCl_3$) δ 204.9, 140.2, 133.1, 131.5, 130.8, 130.5, 128.7, 127.0, 120.2, 37.6, 35.72, 35.71 (two carbons as observed by HMBC), 31.2, 26.5, 26.3, 21.8, 18.1; **IR** (Neat) 2923, 2851, 1698, 1591, 1454, 1432, 1376, 1306, 1271, 1210, 1111, 1066, 1036, 988, 909, 849, 752, 732, 690, 643; **HRMS:** calcd for $C_{20}H_{27}ClO^{+}$: 318.1750 found: 318.1743.

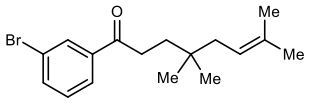

S31

1-(3-bromophenyl)-4,4,7-trimethyloct-6-en-1-one (**S31**): The 1,4-reduction protocol was performed on 0.78 mmol scale. Purification by flash column chromatography eluting with hexanes/EtOAc (95:5) provided 0.15 g (61% yield) of **S31** as a yellow oil. **^{1}H NMR** (700 MHz; $CDCl_3$) δ 8.07 (s, 1H), 7.87 (d, *J* = 7.7 Hz, 1H), 7.68 (d, *J* = 7.9 Hz, 1H), 7.34 (t, *J* = 7.8 Hz, 1H), 5.19 (t, *J* = 8.0 Hz, 1H), 3.03 – 2.76 (m, 2H), 1.94 (d, *J* = 7.5 Hz, 2H), 1.73 (s, 3H), 1.63 (d, *J* = 8.2 Hz, 2H), 1.61 (s, 3H), 0.92 (s, 6H); **^{13}C NMR** (175 MHz; $CDCl_3$) δ 199.7, 139.0, 135.9, 133.4, 131.3, 130.3, 126.7, 123.1, 120.9, 40.1, 35.9, 34.2, 33.9, 27.0, 26.2, 18.1; **IR** (Neat) 2957, 2927, 1686, 1566, 1469, 1450, 1417, 1384, 1364, 1296, 1204, 1125, 1104, 1067, 996, 900, 847, 764, 659, 645, 615; **HRMS:** calcd for $C_{17}H_{23}BrO^{+}$: 323.2679 found: 323.0959.

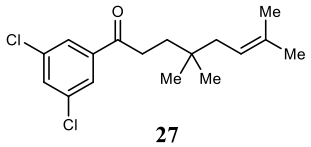

27

1-(3,5-dichlorophenyl)-4,4,7-trimethyloct-6-en-1-one (27): The 1,4-reduction protocol was performed on 1.64 mmol scale. Purification by flash column chromatography eluting with hexanes/EtOAc (93:7) provided 0.246 g (49% yield) of **27** as a clear oil. **^{1}H NMR** (500 MHz; $CDCl_3$) δ 7.79 (d, *J* = 1.9 Hz, 2H), 7.54 (t, *J* = 1.9 Hz, 1H), 5.26 – 5.09 (m, 1H), 3.00 – 2.70 (m, 2H), 1.99 – 1.89 (d, *J* = 7.6 Hz, 1H), 1.73 (s,f 1H), 1.64 (m, 2H),1.62 (s, 3H), 0.92 (s, 3H); **^{13}C NMR** (125 MHz; $CDCl_3$) δ 198.5, 139.6, 135.8, 133.5, 132.7, 126.7, 120.8, 40.07, 35.7, 34.3, 33.9, 27.0, 26.2, 18.1. ; **IR** (Neat) 3075, 2956, 2927, 2753, 1691, 1565, 1417, 1385, 1364, 1294, 1204, 1098, 1066, 985, 898, 866, 801, 682, 668, 625, 604, 602; **HRMS:** calcd for $C_{17}H_{23}Cl_2O^+$: 313.1120CD3 found 313.1129.

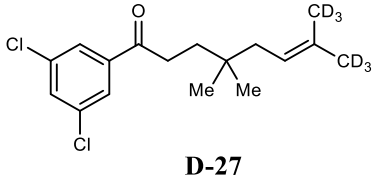

D-27

1-(3,5-dichlorophenyl)-4,4-dimethyl-7-(methyl-d3)oct-6-en-1-one-8,8,8-d3 (D-27): The 1,4-reduction protocol was performed on 4.10 mmol scale. Purification by flash column chromatography eluting with hexanes/EtOAc (93:7) provided 0.113 g (86% yield) of **D-27** as a clear oil. **^{1}H NMR** (500 MHz; $CDCl_3$) (d, *J* = 1.0 Hz, 2H), 7.54 (d, *J* = 0.9 Hz, 1H), 5.18 (t, *J* = 7.5 Hz, 1H), 2.99 – 2.76 (m, 2H), 1.94 (d, *J* = 7.6 Hz, 2H), 1.82 – 1.43 (m, 2H), 0.92 (s, 6H); **^{13}C NMR** (125 MHz; $CDCl_3$) δ 198.6, 139.6, 135.8, 133.3, 132.7, 126.7, 120.8, 40.1, 35.7, 34.3, 33.9, 27.0; **IR** (Neat); **HRMS:** calcd for $C_{17}H_{17}D_6Cl_2O^+$: 319.1497 found 319.1498.

General procedure for the alkylation of aryl aldehydes for aldehyde substrates:

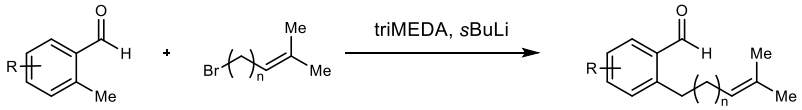

A flame-dried flask equipped with a stir bar was charged with dry THF (0.4 M) and N,N,N'-trimethylethylenediamine (1.1 eq). The solution was cooled to -20 °C, and *s*BuLi (1.05 eq) was

added slowly via syringe, followed by the corresponding aldehyde (1 eq). The reaction mixture was allowed to stir at this temperature for 15 minutes before a second portion of *s*BuLi (3 eq) was added slowly via syringe. The flask was then further cooled to -78 °C, and the corresponding alkyl bromide reagent (4 eq) was added dropwise. The reaction was allowed to slowly warm to room temperature and stirred until judged complete by TLC analysis. The reaction was quenched with saturated ammonium chloride, the aqueous layer was extracted with ethyl acetate (x3), and the combined organics were washed with saturated sodium chloride, dried over Na_2SO_4, and concentrated under reduced pressure. The crude aryl aldehyde was purified by column

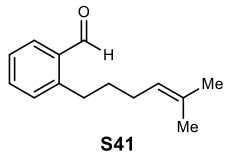

S41

chromatography eluting with the indicated solvent to give the pure aryl aldehyde substrate.

2-(5-methylhex-4-en-1-yl)benzaldehyde (**S41**): The alkylation was performed on a 2.0 mmol scale. Purification by flash column chromatography eluting with hexanes: EtOAc (93:7) provided 154 mg (38% yield) as a clear oil. **^{1}H NMR** (500 MHz; $CDCl_3$) δ 10.29 (s, 1H), 7.83 (d, *J* = 7.7 Hz, 1H), 7.54 – 7.45 (m, 1H), 7.28 (s, 1H), 5.14 (t, *J* = 7.2 Hz, 1H), 3.02 (dd, *J* = 9.1, 6.7 Hz, 2H), 2.07 (q, *J* = 7.3 Hz, 2H), 1.72-1.62 (m, 5H), 1.59 (s, 3H); **^{13}C NMR** (175 MHz; $CDCl_3$) δ 192.4, 145.8, 133.9, 133.8, 132.4, 131.4, 131.1, 126.6, 124.1, 32.6, 32.1, 27.9, 25.9, 17.9; **IR** (Neat) 2925, 2856, 2737, 1694, 1599, 1573, 1450, 1376, 1188, 834, 803, 750, 635; **HRMS:** calcd for $C_{14}H_{19}O^+$: 203.1430 found 203.1426.

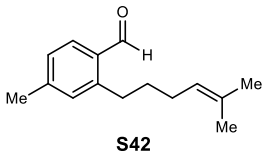

S42

4-methyl-2-(5-methylhex-4-en-1-yl)benzaldehyde (**S42**): The alkylation was performed on a 2.0 mmol scale. Purification by flash column chromatography eluting with hexanes: EtOAc (93:7) provided 281 mg (69% yield) as a clear oil. **^{1}H NMR** (500 MHz; $CDCl_3$) δ 10.22 (s, 1H), 7.73 (d, *J* = 7.8 Hz, 1H), 7.15 (d, *J* = 7.8 Hz, 1H), 7.07 (s, 1H), 5.15 (t, *J* = 7.0 Hz, 1H), 2.97 (dd, *J* = 9.1, 6.7 Hz, 2H), 2.39 (s, 3H), 2.06 (q, *J* = 7.4 Hz, 2H), 1.70 (s, 3H), 1.69 – 1.55 (m, 5H); **^{13}C NMR** (175 MHz; $CDCl_3$) δ 192.0, 145.8, 144.8, 132.3, 131.8, 131.7, 131.6, 127.4, 124.2, 32.6, 32.1,

28.0, 25.9, 21.9, 17.9; **IR** (Neat) 2925, 2857, 2733, 1693, 1599, 1450, 1376, 1189, 1058, 833, 751; **HRMS:** calcd for $C_{15}H_{21}O^+$: 217.1587 found 217.1231.

General procedure for the alkylation of β-keto-esters for five-membered ring precursors:
A 25 mL round bottom flask equipped with a magnetic stir bar was charged with K_2CO_3 (470 mg, 3.4 mmol) and KI (300 mg, 1.8 mmol). Dry DMF (11.0 mL) was then added, followed by starting ketone (2.2 mmol) and alkyl halide/ pseudo halide (2.6 mmol). The resulting mixture was heated to 55 ˚C and stirred until judged complete by TLC analysis (12-24 h). The reaction flask was allowed to cool to room temperature, and then partitioned between diethyl ether (20 mL) and water (10 mL). The organic phase was washed with water (2 × 10 mL) and saturated sodium chloride (1 × 10 mL), dried over MgSO4 and concentrated under reduced pressure to remove all volatile components. The crude product was purified via column chromatography eluting with the indicated solvent to give the pure alkylated ketone (S) in 13%-60% yield.

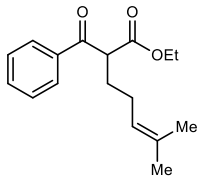

S37

ethyl 2-benzoyl-6-methylhept-5-enoate (S37): The alkylation was performed on a 3.4 mmol scale. Purification by flash column chromatography eluting with hexanes:EtOAc (90:10%) provided **S37** as a clear oil. Spectral data was found to be in accordance with literature data.[41]

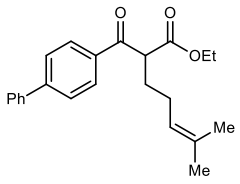

S38

ethyl 2-([1,1'-biphenyl]-4-carbonyl)-6-methylhept-5-enoate (S38): The alkylation was performed on a 3.4 mmol scale. Purification by flash column chromatography eluting with hexanes:EtOAc (90:10%) provided **S38** as a clear oil. Spectral data was found to be in accordance with literature data.[41]

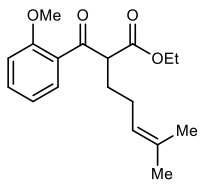

S39

ethyl 2-(2-methoxybenzoyl)-6-methylhept-5-enoate (S39): The alkylation was performed on a 3.4 mmol scale. Purification by flash column chromatography eluting with hexanes:EtOAc (90:10%) provided **S39** as a clear oil. Spectral data was found to be in accordance with literature data.[41]

Miscellaneous procedures for the synthesis of all other intermediates and aryl ketone substrates:

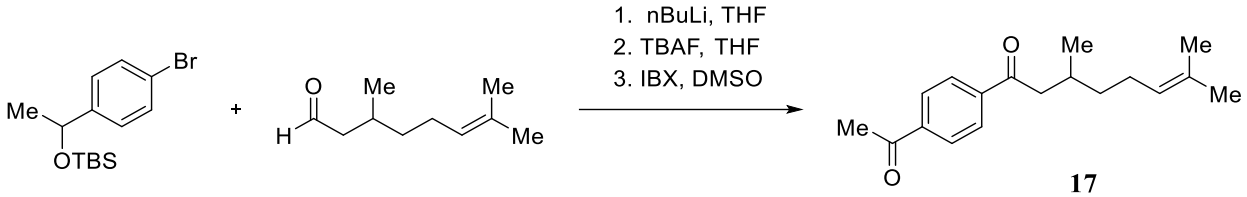

17

1-(4-acetylphenyl)-3,7-dimethyloct-6-en-1-one (**17**): A flame-dried flask was charged with (1-(4-bromophenyl)ethoxy)(*tert*-butyl)dimethylsilane (1.35 g, 1.1 eq) and dry THF (19 mL, 0.2 M). The reaction flask was cooled to -78 °C, and *n*BuLi (2.0 mL, 1.3 eq, 2.5 M solution in hexanes) was added slowly via a syringe. The reaction flask stirred at this temperature for 30 minutes before citronellal (0.7 mL, 1.0 eq) was added. The reaction mixture was allowed to slowly warm to room temperature and was stirred until judged complete by TLC analysis. The resulting reaction mixture was quenched slowly with saturated ammonium chloride. The aqueous layer was extracted with ethyl acetate (x3), and the combined organics were washed with saturated sodium chloride, dried over Na_2SO_4, and concentrated under reduced pressure. The crude alcohol was used without further purification. The crude alcohol was dissolved in THF (13 mL, 0.3 M), and the reaction flask was cooled to 0 °C. At this temperature, TBAF (4.7 mL, 1.2 eq, 1 M solution in THF) was added slowly via a syringe. The resulting mixture was allowed to slowly warm to room temperature and stirred until judged complete by TLC analysis. The reaction mixture was quenched with saturated ammonium chloride. The aqueous layer was extracted with ethyl acetate (x3), and the combined organics were washed with saturated sodium chloride, dried over Na_2SO_4, and concentrated under reduced pressure. The crude diol was used without further purification. The

crude diol was dissolved in DMSO (13 mL, 0.3 M), and IBX (2.83 g, 2.6 eq) was added to the reaction mixture. The resulting mixture was stirred at room temperature until judged complete by TLC analysis, quenched with water, and filtered through celite eluting with ethyl acetate. The filtrate was then transferred to a separatory funnel. The aqueous layer was extracted with ethyl acetate (x3) and the combined organics were washed with saturated sodium chloride, dried over Na_2SO_4, and concentrated under reduced pressure. Purification by flash column chromatography eluting with hexanes/EtOAc (95:5) provided 0.68 g (64% yield) of **17** as a clear oil. **^{1}H NMR** (700 MHz; $CDCl_3$) δ 8.22 – 7.90 (m, 4H), 5.09 (t, *J* = 7.1 Hz, 1H), 2.98 (dd, *J* = 15.9, 5.5 Hz, 1H), 2.77 (dd, *J* = 15.9, 8.1 Hz, 1H), 2.64 (s, 3H), 2.17 (dq, *J* = 13.6, 6.9 Hz, 1H), 2.02 (ddq, *J* = 37.2, 14.6, 7.4 Hz, 2H), 1.68 (s, 3H), 1.60 (s, 3H), 1.45 – 1.39 (m, 1H), 1.34 – 1.26 (m, 1H), 0.97 (d, *J* = 6.7 Hz, 3H); **^{13}C NMR** (175 MHz; $CDCl_3$) δ 200.0, 197.6, 140.7, 140.1, 131.8, 128.6, 128.4, 124.4, 46.4, 37.3, 29.6, 27.0, 25.9, 25.7, 20.1, 17.8; **IR** (Neat) 2962, 2915, 1682, 1569, 1500, 1435, 1402, 1356, 1306, 1262, 1210, 1111, 1074, 1008, 956, 900, 822, 721, 641; **HRMS:** calcd for $C_{18}H_{24}O_2Na^+$: 295.1669 found: 295.1671.

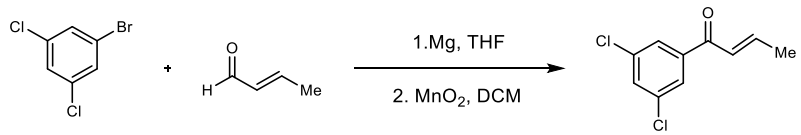

E32

(*E*)-1-(3,5-dichlorophenyl)but-2-en-1-one (**E32**): A flame-dried flask was charged with activated magnesium (0.16 g, 1.5 eq). Dry THF (9 mL, 0.5 M) was added, followed by aryl bromide (1.45 g, 1.5 eq). The resulting mixture was stirred until the activated magnesium dissolved. Crotonaldeyde (0.36 mL, 1.0 eq) was added dropwise, and the mixture was stirred until judged complete by TLC analysis. The resulting reaction mixture was quenched slowly with saturated ammonium chloride. The aqueous layer was extracted with ethyl acetate (x3), and the combined organics were washed with saturated sodium chloride, dried over Na_2SO_4, and concentrated under reduced pressure. The crude alcohol was used without further purification. The crude alcohol was dissolved in DCM (17 mL, 0.25 M), and activated MnO_2 (5.58 g, 15.0 eq) was added to the reaction mixture. The resulting mixture was stirred at room temperature until judged complete by TLC analysis. The mixture was filtered through celite, eluting with DCM, and concentrated under reduced pressure. Purification by flash column chromatography eluting with hexanes/EtOAc (95:5) provided 0.39 g (42% yield) of **E32** as a white solid. **^{1}H NMR** (700 MHz;

$CDCl_3$) δ 7.76 (d, *J* = 1.9 Hz, 2H), 7.53 (t, *J* = 1.9 Hz, 1H), 7.19 – 7.02 (m, 1H), 6.80 (dd, *J* = 15.3, 1.6 Hz, 1H), 2.02 (dd, *J* = 6.9, 1.6 Hz, 3H); **^{13}C NMR** (175 MHz; $CDCl_3$) δ 188.1, 147.2, 140.6, 135.7, 132.4, 127.0, 126.8, 18.9; **IR** (Neat) 3073, 1674, 1620, 1581, 1564, 1415, 1391, 1369, 1295,

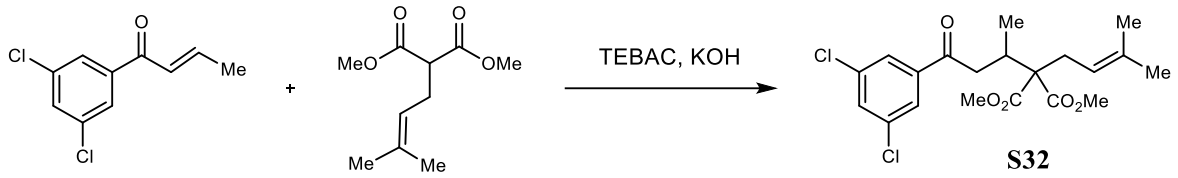

S32

1216, 1115, 1097, 1061, 962, 935, 904, 867, 823, 802, 720, 701, 655; **HRMS:** calcd for $C_{10}H_{18}Cl_2O^+$: 215.0759 found: 215.9933.

dimethyl 2-(4-(3,5-dichlorophenyl)-4-oxobutan-2-yl)-2-(3-methylbut-2-en-1-yl)malonate (**S32**): A flame-dried scintillation vial was charged with enone intermediate (0.25 g, 1.0 eq), dimethyl 2-(3-methylbut-2-en-1-yl)malonate (0.70 g, 3.0 eq), KOH (3.9 mg, 6 mol%), and TEBAC (16 mg, 6 mol%). The resulting reaction mixture was allowed to stir at room temperature until judged complete by TLC analysis. The reaction mixture was quenched with water, the aqueous layer was extracted with DCM (x3), and the combined organics were washed with saturated sodium chloride, dried over Na_2SO_4, and concentrated under reduced pressure. Purification by flash column chromatography eluting with hexanes/EtOAc (95:5) provided 0.17 g (35% yield) of **S32** as a clear oil. **^{1}H NMR** (500 MHz; $CDCl_3$) δ 7.84 (d, *J* = 1.6 Hz, 2H), 7.54 (s, 1H), 5.05 (t, *J* = 7.2 Hz, 1H), 3.78 (s, 3H), 3.72 (s, 3H), 3.32 (d, *J* = 16.6 Hz, 1H), 3.05 – 2.87 (m, 1H), 2.79 – 2.58 (m, 3H), 1.71 (s, 3H), 1.62 (s, 3H), 0.93 (d, *J* = 6.8 Hz, 3H); **^{13}C NMR** (125 MHz; $CDCl_3$) δ 196.7, 171.6, 171.2, 139.5, 135.7, 135.6, 132.8, 126.8, 118.0, 61.7, 52.5, 52.4, 43.1, 32.4, 32.2, 26.2, 18.0, 15.7; **IR** (Neat) 2953, 1720, 1691, 1565, 1406, 1386, 1294, 1275, 1240, 1167, 1115, 1096, 1051, 1015, 990, 954, 933, 910, 866, 852, 799, 787, 707, 686, 670; **HRMS:** calcd for $C_{20}H_{25}Cl_2O_5^+$:415.1074 found: 415.1075.

1-(3,5-dichlorophenyl)-4,4-dimethyl-2-(prop-1-en-2-yl)cyclohexan-1-ol (47): In a flame-dried flask, aryl ketone **43** (1.0 eq.) was dissolved in DCE. The flask was sealed with a septum and flushed with nitrogen. The solution was cooled to 0 °C, and $AlMe_2Cl$ (40 mol%) was added via

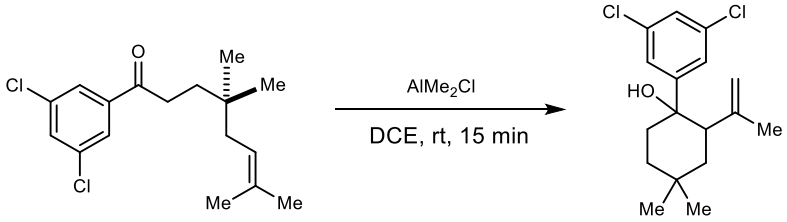

46 **47**

syringe. The reaction was warmed to room temperature and stirred for 15 minutes. The reaction was filtered through a silica plug, eluting with DCM. The solution was concentrated under reduced pressure. Purification by flask column chromatography eluting with pentanes/Et_2O (95:5) provided 5.0 mg (10% yield) of **47** as a clear oil. **^{1}H NMR** (500 MHz; C_6D_6) δ x7.38 (d, *J* = 1.9 Hz, 2H), 7.08 (t, *J* = 1.9 Hz, 1H), 4.61 (s, 1H), 4.55 (s, 1H), 2.39 (dd, *J* = 13.2, 3.6 Hz, 1H), 1.70 (t, *J* = 13.2 Hz, 1H), 1.67 – 1.61 (m, 2H), 1.56 (td, *J* = 13.5, 3.8 Hz, 1H), 1.32 (ddd, *J* = 14.0, 3.9, 2.6 Hz, 1H), 1.25 (s, 3H), 1.07 (dt, *J* = 13.2, 2.7 Hz, 1H), 1.01 (m, 1H), 0.90 (s, 3H), 0.77 (s, 3H).; **^{13}C NMR** (125 MHz; C_6D_6) δ 153.0, 146.5, 135.1, 126.9, 124.3, 113.7, 74.3, 49.2, 40.7, 36.8, 34.2, 33.0, 30.3, 24.3, 24.0.; **IR** (Neat) 3529, 2952, 2853, 1708, 1635, 1585, 1411, 1385, 1365, 1335, 1283, 1206, 1100, 1105, 995, 900, 854, 795, 773, 687; **HRMS**: calcd for $C_{17}H_{22}Cl_2O^+$: 312.1048 found:312.1055.

2.5.4. Synthesis of products

General procedure for the Al(III)-ion pair catalyzed carbonyl-olefin metathesis reaction:

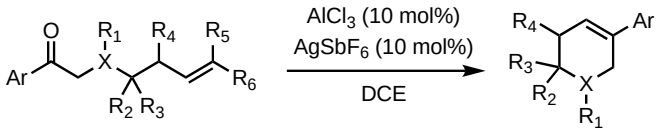

In a flame-dried flask, $AlCl_3$ (10 mol%) and $AgSbF_6$ (10 mol%) were collected in the glovebox. The reaction flask was sealed and brought out of the glovebox. Aryl ketone substrate (1.0 eq) dissolved in DCE (0.02 M) was added to the reaction flask under nitrogen and via a syringe. The reaction was allowed to react at room temperature and stirred until judged complete by TLC analysis. The reaction was filtered through a plug of silica, eluting with DCM, and the resulting filtrate was concentrated under reduced pressure. The crude material was purified by column chromatography eluting with the indicated solvent to give the pure metathesis product.

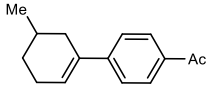

17

1-(3'-methyl-2',3',4',5'-tetrahydro-[1,1'-biphenyl]-4-yl)ethan-1-one (**17**): The cyclization of **S17** was performed on 0.10 mmol scale with a total reaction time of 24 hours. Purification by flash column chromatography eluting with 100% pentanes provided 19 mg (90% yield) of **17** (9:1 mixture of alkene isomers) as a clear oil. **^{1}H NMR** (400 MHz; $CDCl_3$) δ 7.90 (d, *J* = 8.5 Hz, 2H),

7.46 (d, *J* = 8.5 Hz, 2H), 6.25 (s, 0.9H), 6.10 (s, 0.1H), 2.59 (s, 3H), 2.47 (dd, *J* = 16.7, 3.8 Hz, 1H), 2.35 – 2.23 (m, 2H), 2.12 – 1.99 (m, 1H), 1.88 – 1.71 (m, 2H), 1.34 – 1.16 (m, 1H), 1.07 (d, *J* = 6.5 Hz, 3H); **^{13}C NMR** (175 MHz; $CDCl_3$) δ 197.9, 147.3, 135.6, 135.3, 128.6, 127.2, 125.1, 35.8, 30.3, 29.0, 26.7, 26.3, 22.1; **IR** (Neat) 2926, 1682, 1607, 1456, 1406, 1359, 1268, 1012, 958, 826, 610; **HRMS**: calc for $C_{15}H_{19}O^+$: 215.1430 found 215.1425.

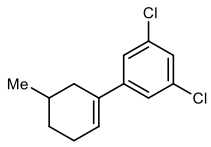

28

3',5'-dichloro-3-methyl-2,3,4,5-tetrahydro-1,1'-biphenyl (**28**): The cyclization of **S28** was performed on 0.10 mmol scale with a total reaction time of 12 hours. Purification by flash column chromatography eluting with 100% hexanes provided 21 mg (88% yield) of **28** as a clear oil. **^{1}H NMR** (700 MHz; $CDCl_3$) δ 7.24 (d, *J* = 1.8 Hz, 2H), 7.19 (t, *J* = 1.8 Hz, 1H), 6.16 – 6.12 (m, 1H), 2.40 – 2.35 (m, 1H), 2.33 – 2.19 (m, 2H), 2.01 – 1.93 (m, 1H), 1.85 – 1.68 (m, 2H), 1.29 – 1.18 (m, 1H), 1.05 (d, *J* = 6.6 Hz, 3H); **^{13}C NMR** (175 MHz; $CDCl_3$) δ 145.7, 134.8, 134.4, 127.1, 126.4, 123.7, 35.9, 30.2, 29.0, 26.1, 22.0; **IR** (Neat) 2950, 2922, 1583, 1558, 1454, 1432, 1411, 1376, 1349, 1122, 1097, 851, 833, 796, 778, 704, 687, 676; **HRMS**: calcd for $C_{13}H_{14}Cl_2^+$: 240.0473 found: 240.0480.

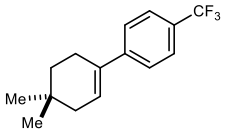

18

4,4-dimethyl-4'-(trifluoromethyl)-2,3,4,5-tetrahydro-1,1'-biphenyl (**18**): The cyclization of **18a** was performed on 0.10 mmol scale with a total reaction time of 24 hours. Purification by flash column chromatography eluting with 100% pentanes provided 20 mg (80% yield) of **18** as a clear oil. **^{1}H NMR** (700 MHz; $CDCl_3$) δ 7.55 (d, *J* = 8.2 Hz, 2H), 7.49 (d, *J* = 8.2 Hz, 2H), 6.16 (s, 1H), 2.49 – 2.34 (m, 2H), 2.18 – 1.98 (m, 2H), 1.55 (t, *J* = 6.4 Hz, 2H), 0.98 (s, 6H); **^{13}C NMR** (175 MHz; $CDCl_3$) δ 145.8, 134.3, 128.6 (q, *J* = 32.3 Hz), 126.3, 125.3, 124.5 (q, *J* = 3.5 Hz), 124.3 (q, *J* = 272.5 Hz), 40.1, 35.8, 28.5, 28.3, 25.1; **IR** (Neat) 2962, 1666, 1411, 1325, 1265, 1168, 1126, 1068, 1016, 896, 837, 703; **HRMS**: calcd for $C_{15}H_{17}F_3^+$: 254.1285 found 254.1291.

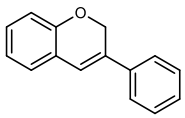

18

3-phenyl-2*H*-chromene (**18**): The cyclization of **S18-2** (prenyl-derived substrate) was performed on 0.19 mmol scale with a total reaction time of 1 hour. Purification by flash column chromatography eluting with hexanes/EtOAc (97:3) provided 34 mg (87% yield) of **20** as a white solid. The cyclization of **S18** (styrene-derived substrate) was performed on 0.16 mmol scale with a total reaction time of 1 hour. Purification by flash column chromatography eluting with hexanes/EtOAc (97:3) provided 22 mg (65% yield) of **18** as a white solid. Spectral data was found to be in accordance with literature data.[30] **^{1}H NMR** (500 MHz; $CDCl_3$) δ 7.47 – 7.43 (m, 2H), 7.40 (t, *J* = 7.6 Hz, 2H), 7.32 (t, *J* = 7.2 Hz, 1H), 7.19 – 7.06 (m, 2H), 6.92 (td, *J* = 7.4, 1.1 Hz, 1H), 6.86 (d, *J* = 8.0 Hz, 1H), 6.82 (s, 1H), 5.18 (s, 2H).

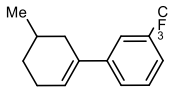

19

3-methyl-3'-(trifluoromethyl)-2,3,4,5-tetrahydro-1,1'-biphenyl (**19**): The cyclization of **S19** was performed on 0.10 mmol scale with a total reaction time of 24 hours. Purification by flash column chromatography eluting with 100% pentanes provided 13 mg (54% yield) of **19** as a clear oil. **^{1}H NMR** (500 MHz; $CDCl_3$) δ 7.62 (s, 1H), 7.55 (d, *J* = 7.7 Hz, 1H), 7.46 (d, *J* = 7.6 Hz, 1H), 7.40 (t, *J* = 7.7 Hz, 1H), 6.17 (s, 1H), 2.54 – 2.41 (m, 1H), 2.37 – 2.14 (m, 2H), 2.09 – 1.96 (m, 1H), 1.90 – 1.72 (m, 2H), 1.35 – 1.21 (m, 1H), 1.07 (d, *J* = 6.5 Hz, 3H); **^{13}C NMR** (125 MHz; $CDCl_3$) δ 143.4, 135.4, 130.7 (q, *J* = 32.1 Hz), 128.7, 128.4, 126.2, 124.5 (q, *J* = 272.3 Hz), 123.2 (q, *J* = 3.9 Hz), 121.9 (q, *J* = 3.9 Hz), 36.0, 30.3, 29.1, 26.1, 22.1; **IR** (Neat) 2952, 2913, 1457, 1434, 1326, 1298, 1238, 1218, 1161, 1121, 1098, 1072, 1007, 898, 840, 796, 781, 759, 697, 680, 652; **HRMS**: calcd for $C_{17}H_{21}F_3O^+$: 240.1126 found: 240.1125.

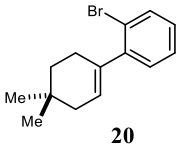

20

2'-bromo-4,4-dimethyl-2,3,4,5-tetrahydro-1,1'-biphenyl (**20**): The cyclization of **S20** was performed on 0.10 mmol scale with a total reaction time of 2 hours. Purification by flash column chromatography eluting with 100% pentanes provided 20 mg (75% yield) of **20** as a clear oil. **^{1}H**

NMR (500 MHz; $CDCl_3$) δ 7.53 (d, *J* = 8.0 Hz, 1H), 7.36 – 7.21 (m, 1H), 7.15 (dd, *J* = 7.5, 1.5 Hz, 1H), 7.08 (td, *J* = 7.9, 1.7 Hz, 1H), 5.56 (s, 1H), 2.44 – 2.25 (m, 2H), 1.96 (d, *J* = 3.2 Hz, 2H), 1.51 (t, *J* = 6.4 Hz, 2H), 1.02 (s, 6H); **^{13}C NMR** (125 MHz; $CDCl_3$) δ 145.4, 138.0, 132.7, 130.3, 128.1, 127.3, 126.3, 122.8, 39.4, 35.8, 28.5, 28.4, 27.3; **IR** (Neat) 2949, 2911, 2865, 1466, 1431, 1384, 1363, 1262, 1235, 1177, 1154, 1065, 1045, 1024, 940, 924, 725, 689, 846; **HRMS:** calcd for $C_{14}H_{17}Br^+$: 264.0514 found: 264.0505.

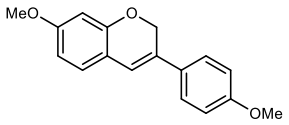

21

7-methoxy-3-(4-methoxyphenyl)-2*H*-chromene (**21**): The cyclization of **S21** was performed on 1.53 mmol scale with a total reaction time of 30 minutes. Purification by flash column chromatography eluting with hexanes/EtOAc (80:20) provided 0.34 g (83% yield) of **21** as a white solid. **^{1}H NMR** (700 MHz; $CDCl_3$) δ 7.36 (d, *J* = 8.2 Hz, 2H), 6.99 (d, *J* = 8.2 Hz, 1H), 6.92 (d, *J* = 8.2 Hz, 2H), 6.69 (s, 1H), 6.48 (d, *J* = 8.3 Hz, 1H), 6.45 (s, 1H), 5.12 (s, 2H), 3.83 (s, 3H), 3.79 (s, 3H); **^{13}C NMR** (175 MHz; $CDCl_3$) δ 160.5, 159.3, 154.4, 129.7, 128.5, 127.5, 125.9, 118.2, 116.6, 114.2, 107.5, 101.5, 67.4, 55.53, 55.48; **IR** (Neat) 2915, 2838, 1611, 1583, 1514, 1502, 1465, 1443, 1419, 1286, 1265, 1248, 1194, 1179, 1157, 1113, 1026, 957, 914, 831, 818, 806, 797, 756, 722, 705, 629; **HRMS**: calcd for $C_{17}H_{15}O_2^+$: 267.1016 found 267.1015.

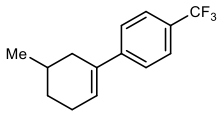

22

3-methyl-4'-(trifluoromethyl)-2,3,4,5-tetrahydro-1,1'-biphenyl (**22**): The cyclization of **S22** was performed on 0.10 mmol scale with a total reaction time of 24 hours. Purification by flash column chromatography eluting with 100% hexanes provided 15 mg (63% yield) of **22** (9:1 mixture of alkene isomers) as a clear oil. **^{1}H NMR** (for the mixture of isomers; 500 MHz; $CDCl_3$) δ 7.55 (d, *J* = 8.3 Hz, 2H), 7.47 (d, *J* = 8.2 Hz, 2H), 6.19 (s, 0.9H), 6.04 (s, 0.1H), 2.51 – 2.41 (m, 1H), 2.40 – 2.20 (m, 2H), 2.11 – 2.00 (m, 1H), 1.90 – 1.70 (m, 2H), 1.36 – 1.19 (m, 1H), 1.07 (d, *J* = 6.6 Hz, 3H); **^{13}C NMR** (for the mixture of isomers; 125 MHz; $CDCl_3$) δ 146.1, 135.5, 133.3, 128.6 (q, *J* = 32.4 Hz), 126.8, 125.4, 125.3, 125.2 (q, *J* = 4.0 Hz), 124.5 (q, *J* = 271.6 Hz), 36.0, 31.1, 30.8, 30.3, 29.9, 29.1, 27.4, 26.2, 22.1, 22.0, 21.8; **^{13}C NMR** (signals corresponding to the major isomer; 125 MHz; $CDCl_3$) δ 146.1, 135.5, 128.6 (q, *J* = 32.4 Hz), 126.8, 125.3, 125.2 (q, *J*

= 4.0 Hz), 124.5 (q, *J* = 271.6 Hz), 36.0, 30.3, 29.1, 26.2, 22.1; **IR** (Neat) 2925, 1614, 1457, 1434, 1412, 1322, 1281, 1247, 1162, 1111, 1067, 1015, 971, 953, 911, 856, 824, 780, 761, 735, 677; **HRMS**: calcd for $C_{14}H_{15}F_3^+$: 240.1126 found 240.1128.

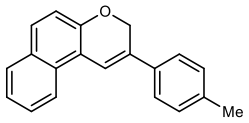

23

2-(*p*-tolyl)-3*H*-benzo[*f*]chromene (**23**): The cyclization of **S23** was performed on 0.10 mmol scale with a total reaction time of 20 minutes. Purification by flash column chromatography eluting with hexanes/EtOAc (98:2) provided 18 mg (67% yield) of **23** as a white solid. **^{1}H NMR** (700 MHz; $CDCl_3$) δ 8.07 (d, *J* = 8.4 Hz, 1H), 7.78 (d, *J* = 8.1 Hz, 1H), 7.67 (d, *J* = 8.8 Hz, 1H), 7.51 (t, *J* = 8.2 Hz, 1H), 7.48 (s, 1H), 7.45 (d, *J* = 8.1 Hz, 2H), 7.37 (t, *J* = 7.4 Hz, 1H), 7.25 (d, *J* = 8.0 Hz, 2H), 7.14 (d, *J* = 8.8 Hz, 1H), 5.23 (s, 2H), 2.40 (s, 3H); **^{13}C NMR** (175 MHz; $CDCl_3$) δ 151.6, 138.1, 134.5, 130.5, 130.2, 129.73, 129.65, 129.3, 128.8, 126.8, 125.0, 123.9, 121.6, 117.4, 116.3, 115.6, 67.3, 21.4; **IR** (Neat) 2918, 2849, 1628, 1588, 1510, 1467, 1436, 1392, 1230, 1188, 1158, 1094, 1048, 1016, 979, 939, 859, 805, 773, 740, 691, 672, 637; **HRMS:** calcd for $C_{20}H_{16}O^+$: 272.1201 found: 272.1189.

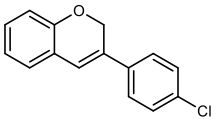

24

3-(4-chlorophenyl)-2*H*-chromene (**24**): The cyclization of **S24** was performed on 0.10 mmol scale with a total reaction time of 30 minutes. Purification by flash column chromatography eluting with hexanes/EtOAc (98:2) provided 20 mg (83% yield) of **24** as a white solid. **^{1}H NMR** (500 MHz; $CDCl_3$) δ 7.36 (s, 4H), 7.15 (t, *J* = 8.2 Hz, 1H), 7.09 (d, *J* = 7.4 Hz, 1H), 6.92 (t, *J* = 7.4 Hz, 1H), 6.86 (d, *J* = 8.0 Hz, 1H), 6.80 (s, 1H), 5.13 (s, 2H); **^{13}C NMR** (125 MHz; $CDCl_3$) δ 153.4, 135.3, 133.9, 130.7, 129.5, 129.1, 127.3, 126.1, 122.8, 121.9, 120.8, 115.7, 67.1; **IR** (Neat) 2919, 2847, 1602, 1486, 1456, 1413, 1336, 1211, 1122, 1096, 1053, 1008, 974, 960, 934, 898, 881, 813, 750, 719, 631; **HRMS:** calcd for $C_{15}H_{10}ClO^+$: 241.0415 found: 241.0416.

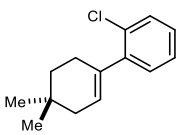

25

2'-chloro-4,4-dimethyl-2,3,4,5-tetrahydro-1,1'-biphenyl (**25**): The cyclization of **S25** was performed on 0.10 mmol scale with a total reaction time of 2 hours. Purification by flash column chromatography eluting with 100% pentanes provided 20 mg (75% yield) of **25** as a clear oil. **^{1}H NMR** (700 MHz; $CDCl_3$) δ 7.33 (d, *J* = 7.7 Hz, 1H), 7.18 (dt, *J* = 25.3, 7.6 Hz, 3H), 5.59 (s, 1H), 2.34 – 2.30 (m, 2H), 1.99 – 1.94 (m, 2H), 1.51 (t, *J* = 6.3 Hz, 2H), 1.01 (s, 6H); **^{13}C NMR** (175 MHz; $CDCl_3$) δ 143.4, 136.5, 132.7, 130.3, 129.6, 127.9, 126.7, 126.5, 39.5, 35.8, 28.4 (two carbons as observed by HMBC), 27.1; **IR** (Neat) 2949, 2912, 2866, 1470, 1429, 1384, 1363, 1154, 1121, 1069, 1050, 1034, 1013, 924, 818, 732, 700, 654; **HRMS**: calcd for $C_14H_{17}Cl^+$: 220.1019 found: 220.1210.

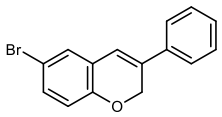

26

6-bromo-3-phenyl-2*H*-chromene (**28**): The cyclization of **S26** was performed on 0.10 mmol scale with a total reaction time of 2 hours. Purification by flash column chromatography eluting with hexanes/EtOAc (93:7) provided 14 mg (99% yield) of **26** as a white solid. **^{1}H NMR** (400 MHz; $CDCl_3$) δ 7.47 – 7.36 (m, 4H), 7.39 – 7.31 (m, 1H), 7.21 (d, *J* = 7.2 Hz, 2H), 6.73 (d, *J* = 8.9 Hz, 2H), 5.17 (d, *J* = 1.2 Hz, 2H); **^{13}C NMR** (175 MHz; $CDCl_3$) δ 152.4, 136.4, 133.2, 131.6, 129.5, 129.0, 128.6, 125.01, 125.00, 119.1, 117.3, 113.7, 67.4; **IR** (Neat) 2923, 2858, 1496, 1479, 1448, 1404, 1336, 1250, 1216, 1120, 1073, 1047, 1015, 998, 964, 913, 899, 858, 812, 758, 730, 690, 613; **HRMS**: calcd for $C_{15}H_{10}BrO^+$: 284.9910 found: 284.9906.

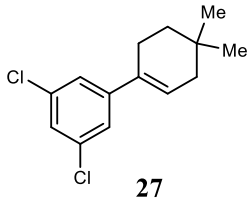

27

3',5'-dichloro-4,4-dimethyl-2,3,4,5-tetrahydro-1,1'-biphenyl (27): The cyclization of **46** was performed on 0.08 mmol scale with a total reaction time of 17 hours. Purification by flash column chromatography eluting with 100% hexane provided 18 mg (99% yield) of **29** as a clear oil. **^{1}H NMR** (500 MHz; $CDCl_3$) δ 7.25 (d, J = 1.9 Hz, 2H), 7.19 (t, J = 1.9 Hz, 1H), 6.10 (m, 1H), 2.35 (m, 2H), 2.00 (m, 2H), 1.52 (t, J = 6.4 Hz, 1H), 0.96 (s, 3H); **^{13}C NMR** (125 MHz; $CDCl_3$) δ 145.3, 134.8, 133.3, 126.6, 126.4, 123.7, 40.0, 35.7, 28.5, 28.2, 25.0.; **IR** (Neat) 2950, 2914, 2865, 1583,

1557, 1431, 1411, 1383, 1363, 1251, 1217, 1154, 1122, 1096, 1067, 1016, 988, 941, 867, 850, 797, 744, 700, 675; **HRMS**: calcd for $C_{14}H_{16}Cl_2^+$: 254.0629 found: 254.0625.

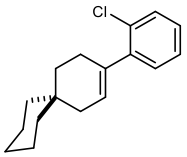

28

3-(2-chlorophenyl)spiro[5.5]undec-2-ene (**28**): The cyclization of **S28** was performed on 0.10 mmol scale with a total reaction time of 17 hours. Purification by flash column chromatography eluting with 100% pentanes provided 22 mg (85% yield) of **28** as a clear oil. **^{1}H NMR** (500 MHz; $CDCl_3$) δ 7.33 (d, *J* = 7.4 Hz, 1H), 7.23 – 7.08 (m, 3H), 5.59 – 5.57 (m, 1H), 2.39 – 2.22 (m, 2H), 2.02 (d, *J* = 3.3 Hz, 2H), 1.59 (t, *J* = 6.4 Hz, 2H), 1.55 – 1.36 (m, 10H); **^{13}C NMR** (125 MHz; $CDCl_3$) δ 143.4, 136.7, 132.7, 130.3, 129.6, 127.8, 126.7, 126.2, 37.2, 36.7, 33.3, 30.9, 27.0, 26.1, 22.1; **IR** (Neat) 2914, 2846, 2822, 1469, 1429, 1125, 1067, 1054, 1034, 973, 938, 923, 873, 845, 815, 750, 731, 716, 689, 651; **HRMS**: calcd for $C_{17}H_{21}Cl^+$: 260.1332 found 260.1343.

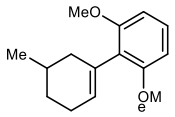

30

2',6'-dimethoxy-3-methyl-2,3,4,5-tetrahydro-1,1'-biphenyl (**30**): The cyclization of **S30** was performed on 0.10 mmol scale with a total reaction time of 3 hours. Purification by flash column chromatography eluting with hexanes/EtOAc (99:1) provided 14 mg (61% yield) of **30** (3:1 mixture of alkene isomers) as a clear oil. **^{1}H NMR** (for the mixture of isomers; 500 MHz; $CDCl_3$) δ 7.15 (t, *J* = 8.3 Hz, 1H), 6.56 (d, *J* = 8.3 Hz, 2H), 5.53 (s, 0.75H), 5.40 (s, 0.25H), 3.77 (d, *J* = 2.7 Hz, 6H), 2.42 – 2.03 (m, 3H), 1.97 – 1.63 (m, 3H), 1.41 – 1.20 (m, 1H), 1.02 (dd, *J* = 18.1, 6.7 Hz, 3H); **^{13}C NMR** (for the mixture of isomers; 125 MHz; $CDCl_3$) δ 157.92, 157.86, 133.0, 131.2, 130.6, 127.57, 127.55, 126.1, 122.7, 122.5, 104.7, 104.5, 56.33, 56.26, 37.6, 31.2, 30.7, 30.5, 29.1 29.0, 25.7, 22.2, 22.04, 22.02; **^{13}C NMR** (signals corresponding to the major isomer; 125 MHz; $CDCl_3$) δ 157.9, 133.0, 131.2, 127.6, 126.1, 104.5, 56.3, 37.5, 30.5, 29.1, 25.7, 22.0; **IR** (Neat) 2921, 2833, 1585, 1468, 1431, 1301, 1279, 1241, 1171, 1039, 968, 946, 906, 873, 837, 813, 777, 721, 627; **HRMS**: calcd for $C_{15}H_{21}O_2^+$: 233.1536 found 233.1533.

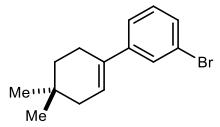

31

3'-bromo-4,4-dimethyl-2,3,4,5-tetrahydro-1,1'-biphenyl (**31**): The cyclization of **S31** was performed on 0.10 mmol scale with a total reaction time of 24 hours. Purification by flash column chromatography eluting with 100% pentanes provided 20 mg (75% yield) of **31** as a clear oil. **^{1}H NMR** (700 MHz; $CDCl_3$) δ 7.54 (s, 1H), 7.32 (dd, *J* = 12.7, 7.9 Hz, 2H), 7.17 (t, *J* = 7.9 Hz, 1H), 6.08 (t, *J* = 4.0 Hz, 1H), 2.46 – 2.32 (m, 2H), 2.00 (d, *J* = 3.5 Hz, 2H), 1.52 (t, *J* = 6.4 Hz, 2H), 0.96 (s, 6H); **^{13}C NMR** (175 MHz; $CDCl_3$) δ 144.6, 134.2, 129.8, 129.5, 128.3, 125.3, 123.7, 122.7, 40.0, 35.8, 28.5, 28.3, 25.2; **IR** (Neat) 2949, 2917, 2864, 1591, 1558, 1473, 1455, 1431, 1383, 1363, 1243, 1074, 994, 874, 816, 685, 653; **HRMS**: calcd for $C_{14}H_{17}Br^+$: 264.0514 found 264.0508.

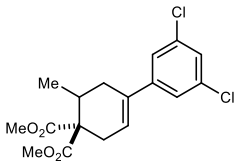

32

Dimethyl 3',5'-dichloro-3-methyl-2,5-dihydro-[1,1'-biphenyl]-4,4(3*H*)-dicarboxylate (**32**): The cyclization of **S33** was performed on 0.10 mmol scale with a total reaction time of 24 hours. Purification by flash column chromatography eluting with hexanes/EtOAc (98:2) provided 22 mg (63% yield) of **32** as a clear oil. **^{1}H NMR** (700 MHz; $CDCl_3$) δ 7.23 – 7.20 (m, 3H), 6.08 (dt, *J* = 4.1, 2.3 Hz, 1H), 3.73 (d, *J* = 4.2 Hz, 6H), 2.86 – 2.82 (m, 2H), 2.77 – 2.67 (m, 2H), 2.27 – 2.17 (m, 1H), 1.07 (d, *J* = 6.9 Hz, 3H); **^{13}C NMR** (175 MHz; $CDCl_3$) δ 171.7, 170.9, 144.3, 134.9, 133.1, 126.9, 123.8, 123.0, 56.5, 52.9, 52.7, 32.8, 32.3, 29.6, 17.0; **IR** (Neat) 2953, 1721, 1586, 1559, 1434, 1413, 1382, 1258, 1222, 1197, 1096, 1052, 962, 853, 796, 730; **HRMS**: calcd for $C_{17}H_{18}Cl_2ONa^+$: 379.0474 found 379.0471.

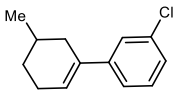

33

3'-chloro-3-methyl-2,3,4,5-tetrahydro-1,1'-biphenyl (**33**): The cyclization of **S33** was performed on 0.10 mmol scale with a total reaction time of 24 hours. Purification by flash column chromatography eluting with 100% pentanes provided 12 mg (57% yield) of **33** (4:1 mixture of

alkene isomers) as a clear oil. **^{1}H NMR** (for the mixture of isomers; 500 MHz; $CDCl_3$) δ 7.36 (s, 1H), 7.31 – 7.12 (m, 3H), 6.12 (s, 0.8H), 5.98 (s, 0.2H), 2.47 – 2.39 (m, 1H), 2.36 – 2.16 (m, 2H), 2.09 – 1.95 (m, 1H), 1.92 – 1.70 (m, 2H), 1.33 – 1.15 (m, 1H), 1.06 (d, *J* = 6.4 Hz, 3H); **^{13}C NMR** (for the mixture of isomers; 125 MHz; $CDCl_3$) δ 144.6, 135.3, 135.0, 134.3, 132.4, 129.5, 126.63, 126.57, 125.8, 125.5, 125.4, 123.3, 123.2, 36.0, 31.1, 30.9, 30.4, 29.1, 27.4, 26.1, 22.1, 22.0, 21.9; **^{13}C NMR** (signals corresponding to the major isomer; 125 MHz; $CDCl_3$) δ 144.6, 135.3, 134.3, 129.5, 126.6, 125.8, 125.4, 123.2, 36.0, 30.4, 29.1, 26.1, 22.1; **IR** (Neat) 2951, 2922, 2869, 2832, 1593, 1565, 1478, 1455, 1433, 1375, 1329, 1243, 1165, 1127, 1097, 1078, 997, 883, 839, 772, 734, 718, 685; **HRMS**: calcd for $C_{13}H_{15}Cl^{+}$: 206.0862 found 206.0860.

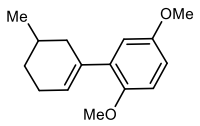

35

2',5'-dimethoxy-3-methyl-2,3,4,5-tetrahydro-1,1'-biphenyl (**35**): The cyclization of **S35** was performed on 0.10 mmol scale with a total reaction time of 3 hours. Purification by flash column chromatography eluting with hexanes/EtOAc (98:2) provided 13 mg (57% yield) of **35** (2:1 mixture of alkene isomers) as a clear oil. **^{1}H NMR** (for the mixture of isomers; 500 MHz; $CDCl_3$) δ 6.78 (d, *J* = 8.2 Hz, 1H), 6.74 – 6.69 (m, 2H), 5.77 (s, 0.66H), 5.64 (s, 0.33H), 3.78 – 3.75 (m, 6H), 2.43 – 2.29 (m, 2H), 2.27 – 2.20 (m, 1H), 2.10 – 1.98 (m, 1H), 1.89 – 1.68 (m, 2H), 1.36 – 1.20 (m, 1H), 1.05 (d, *J* = 6.9 Hz, 1H), 1.01 (d, *J* = 6.6 Hz, 2H); **^{13}C NMR** (for the mixture of isomers; 125 MHz; $CDCl_3$) δ 153.68, 153.66, 151.2, 151.1, 137.0, 136.8, 134.89, 134.87, 132.8, 126.1, 115.9, 115.7, 112.5, 112.3, 112.08, 112.05, 56.5, 56.4, 55.84, 55.83, 37.4, 31.1, 30.9, 30.5, 29.0, 28.8, 26.0, 22.2, 22.1; **^{13}C NMR** (signals corresponding to the major isomer; 125 MHz; $CDCl_3$) δ 153.7, 151.1, 137.0, 134.9, 126.1, 115.7, 112.3, 112.1, 56.4, 55.8, 37.4, 30.5, 29.0, 25.9, 22.1; **IR** (Neat) 2919, 2833, 1585, 1468, 1431, 1375, 1301, 1279, 1242, 1171, 1107, 1039, 969, 907, 837, 778, 722, 628; **HRMS**: calcd for $C_{15}H_{21}O_2^{+}$: 233.1536 found: 233.1529.

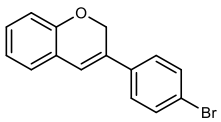

36

3-(4-bromophenyl)-2*H*-chromene (**36**): The cyclization of **S36** was performed on 0.10 mmol scale with a total reaction time of 3 hours. Purification by flash column chromatography eluting with hexanes/EtOAc (98:2) provided 19 mg (66% yield) of **36** as a white solid. **^{1}H NMR** (400 MHz; $CDCl_3$) δ 7.51 (d, *J* = 8.5 Hz, 2H), 7.30 (d, *J* = 8.5 Hz, 2H), 7.15 (t, *J* = 8.2 Hz, 1H), 7.09 (d, *J* = 7.4 Hz, 1H), 6.92 (t, *J* = 7.4 Hz, 1H), 6.86 (d, *J* = 8.0 Hz, 1H), 6.81 (s, 1H), 5.13 (s, 2H); **^{13}C NMR** (125 MHz; $CDCl_3$) δ 153.4, 135.8, 132.0, 130.7, 129.5, 127.3, 126.4, 122.8, 122.1, 121.9, 120.9, 115.7, 67.0; **IR** (Neat) 2919, 2850, 1601, 1574, 1486, 1456, 1410, 1334, 1291, 1210, 1122, 1087, 1073, 1052, 1004, 958, 933, 897, 880, 810, 670, 640, 629; **HRMS:** calcd for $C_{15}H_{10}BrO^+$: 284.9910 found: 284.9909.

37

ethyl 2-phenylcyclopent-2-ene-1-carboxylate (37): The cyclization of **S37** wa**s** performed on a 0.1o mmol scale with a total reaction time of 1 hour. Purification by flash column chromatography eluting with hexanes/DCM (75:25) provided 12 mg (55%) of **37** as a clear oil. Spectral data was found to be in accordance with literature data.[96]

ethyl 2-([1,1'-biphenyl]-4-yl)cyclopent-2-ene-1-carboxylate (38): The cyclization of **S38** wa**s** performed on a 0.1o mmol scale with a total reaction time of 2 hours. Purification by flash column

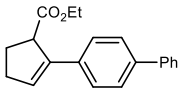

38

chromatography eluting with hexanes/DCM (75:25) provided 12 mg (81%) of **38** as a clear oil. Spectral data was found to be in accordance with literature data.[1996]

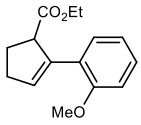

39

ethyl 2-(2-methoxyphenyl)cyclopent-2-ene-1-carboxylate (39): The cyclization of **S39** wa**s** performed on a 0.1o mmol scale with a total reaction time of 1.5 hours. Purification by flash

column chromatography eluting with hexanes/DCM (75:25) provided 15 mg (61%) of **39** as a clear oil. Spectral data was found to be in accordance with literature data.[96]

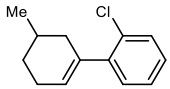

40

2'-chloro-3-methyl-2,3,4,5-tetrahydro-1,1'-biphenyl (**40**): The cyclization of **S40** was performed on 0.10 mmol scale with a total reaction time of 24 hours. Purification by flash column chromatography eluting with 100% pentanes provided 13 mg (63% yield) of **40** (9:1 mixture of alkene isomers) as a clear oil. **^{1}H NMR** (for the mixture of isomers; 500 MHz; $CDCl_3$) δ 7.33 (d, *J* = 7.3 Hz, 1H), 7.22 – 7.08 (m, 3H), 5.65 (s, 0.9H), 5.61 (s, 0.1H), 2.32 (dd, *J* = 17.0, 3.7 Hz, 1H), 2.27 – 2.19 (m, 2H), 2.04 – 1.93 (m, 1H), 1.91 – 1.80 (m, 1H), 1.80 – 1.71 (m, 1H), 1.37 – 1.24 (m, 1H), 1.03 (d, *J* = 6.6 Hz, 3H); **^{13}C NMR** (for the mixture of isomers; 125 MHz; $CDCl_3$) δ 143.4, 137.3, 132.8, 132.6, 130.3, 129.6, 128.1, 127.8, 127.3, 127.0, 126.8, 126.7, 37.9, 37.7, 30.3, 28.9, 25.6, 21.8; **^{13}C NMR** (signals corresponding to the major isomer; 125 MHz; $CDCl_3$) δ 143.4, 137.3, 132.6, 130.3, 129.6, 127.8, 127.0, 126.7, 37.7, 30.3, 28.9, 25.6, 21.8; **IR** (Neat) 2949, 2922, 2870, 1468, 1455, 1434, 1126, 1068, 1054, 1035, 750, 729, 704, 646; **HRMS**: calcd for $C_{13}H_{15}Cl^+$: 206.0862 found: 206.0870.

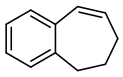

41

6,7-dihydro-5*H*-benzo[7]annulene (**41**): The cyclization of **S41** was performed on a 0.10 mmol scale with a total reaction time of 40 minutes. Purification by flash column chromatography eluting with 100% pentanes provided 6 mg (43% yield) of **41** as a clear oil. **^{1}H NMR** (700 MHz; $CDCl_3$) δ 7.17 – 7.14 (m, 2H), 7.10 (t, *J* = 3.6 Hz, 2H), 6.41 (dt, *J* = 12.2, 2.2 Hz, 1H), 5.90 (dt, *J* = 12.2, 4.5 Hz, 1H), 2.87 – 2.83 (m, 2H), 2.43 (dt, *J* = 6.6, 4.5 Hz, 2H), 1.97 (dt, *J* = 10.9, 6.4 Hz, 2H); **^{13}C NMR** (125 MHz; $CDCl_3$) δ 141.8, 136.4, 132.4, 131.0, 129.9, 129.1, 126.7, 126.0, 36.3, 32.6, 27.1; **IR** (Neat) 3015, 2924, 1911, 1489, 1448, 1288, 967, 932, 778, 740, 704, 679; **HRMS**: calcd for $C_{11}H_{13}^+$: 144.0939 found 144.0944.

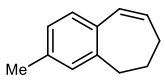

42

3-methyl-6,7-dihydro-5*H*-benzo[7]annulene (**42**): The cyclization of **S42** was performed on a 0.10 mmol scale with a total reaction time of 40 minutes. Purification by flash column chromatography eluting with 100% pentanes provided 8 mg (51% yield) of **42** as a clear oil. **^{1}H NMR** (700 MHz; $CDCl_3$) δ 7.05 (d, *J* = 7.7 Hz, 1H), 6.96 (dd, *J* = 7.8, 1.8 Hz, 1H), 6.92 (s, 1H), 6.38 (d, *J* = 12.2 Hz, 1H), 5.83 (dt, *J* = 12.2, 4.5 Hz, 1H), 2.96 – 2.74 (m, 2H), 2.49 – 2.35 (m, 2H), 2.30 (s, 3H), 1.95 (dt, *J* = 10.8, 6.3 Hz, 2H); **^{13}C NMR** (125 MHz; $CDCl_3$) δ 141.7, 136.4, 133.6, 131.3, 131.0, 130.0, 129.7, 126.6, 36.3, 32.7, 27.0, 21.1; **IR** (Neat) 3011, 2922, 2856, 1610, 1503, 1423, 948, 822, 712, 684; **HRMS**: calcd for $C_{12}H_{14}^+$: 158.1096 found 158.1092.

2.5.5 Computational Data

Conformational searches were performed with MacroModel version 11.7 and the OPLS_2005 force field[106] in order to sample potential reactive conformers. After running the program, conformers 10 kJ mol^{-1} above the minimum were carried forward into Q-Chem for density functional theory (DFT) calculations with a higher level of theory. Using a 10 kJ mol^{-1} threshold in our system allowed for around 10 unique conformers to be analyzed. Increasing the threshold above 10 kJ mol^{-1} did not seem to lead to additional unique conformers. All quantum chemical calculations utilized DFT as implemented in the Q-Chem 4.3 quantum chemistry package.[107] The unrestricted B97-D density functional with singlet spin was used in combination with the Def2-SVP basis set[37] to acquire solvent phase geometries for the intermediates discussed. The unrestricted density function was used in order to not prematurely eliminate open shell species as is our standard practice. Optimizations were conducted in the solvent phase in order to incorporate any solvent effects on the ion pair catalysts employed. The reaction discovery tools developed by the Zimmerman group, specifically the Growing String Method (GSM),[108–111] were used to probe potential reaction paths and determine the exact transition state and minimum energy reaction path for each proposed elementary step. By optimizing the reaction path, GSM provides verification that the saddle point connects the reactant to product geometries through a single transition state. Frequency calculations were performed on all structures at the same level of theory to confirm that optimizations led to stable minima (intermediates) or transition states. Stable intermediates were characterized by all real frequencies, and transition states were identified by a single imaginary frequency. The B97-D[102] density functional and the def2-TZVP basis set[112–115] were used to calculate energies with the SMD solvent model[116] using 1,2-dichloroethane as the implicit solvent,

in the ORCA software package. Thermodynamic corrections were applied to the solvated energies at a temperature of 296.15 K. For these corrections, low frequencies (<50 cm^{-1}) were set to 50 cm^{-1}. Energies are reported as enthalpies (H).

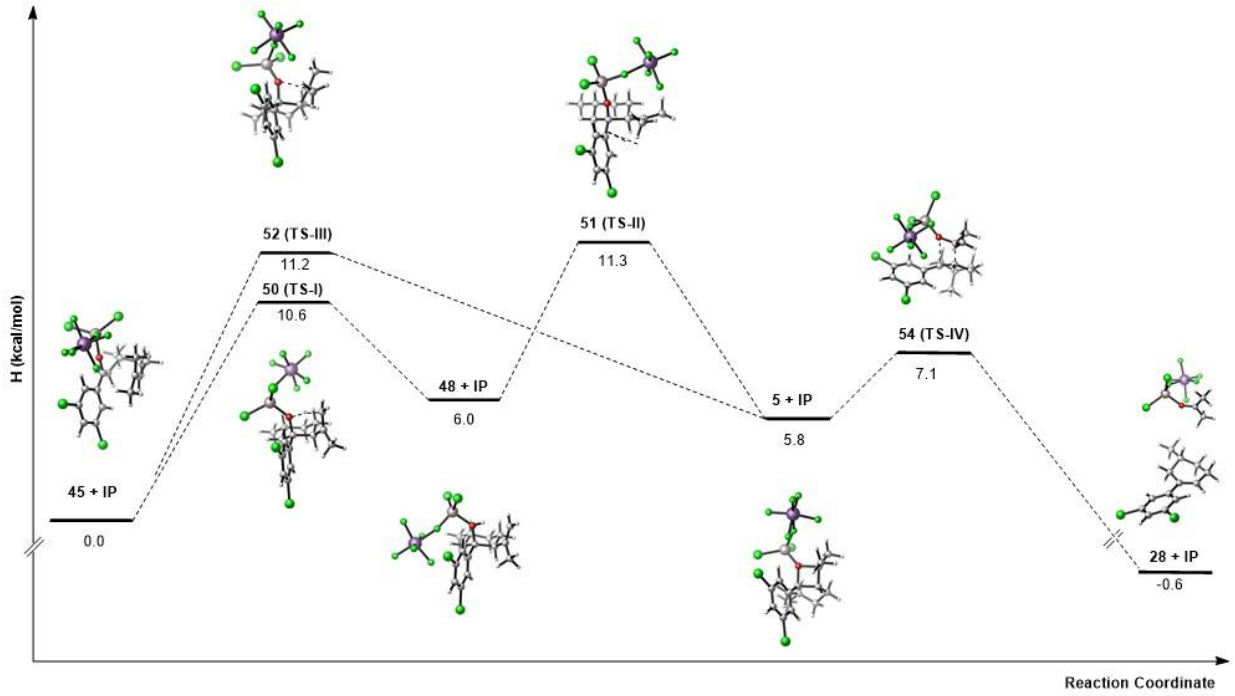

Figure 2.16. Full computational reaction profile.

Table 2.4. Computational values.

Compound name	E(solv) (B97-D/Def2-TZVP) (Hartree)	S(cal/molK) (B97-D/Def2-SVP)	H(kcal/mol) (B97-D/Def2-SVP)	G(hartree)	H + Esolv	ΔG(kcal/mol)	ΔH(kcal/mol)
45 + IP	−3620.27331554296	216.15	232.606	-2271564	-2271500	0.0	0.0
48 (TS-I)	−3620.25228141201	212.591	230.057	-2271552	-2271489	11.7	10.6
60 (TS-III)	−3620.25386015591	215.148	231.615	-2271552	-2271489	11.5	11.2
46 + IP	−3620.26495803941	209.778	233.376	-2271556	-2271494	7.9	6.0
49 (TS-II)	−3620.25327722577	216.254	231.322	-2271553	-2271488	11.3	11.3
47 + IP	−3620.26569889475	208.858	233.627	-2271556	-2271494	8.0	5.8
61 (TS-IV)	−3620.26183303084	207.963	232.493	-2271554	-2271493	9.5	7.1
cyclohexene compounent	−1424.11423847803	119.236	153.486	-893518	-893482		
acetone + IP	−2196.15636736654	152.168	76.802	-1378063	-1378018		
62 + IP				-2271581	-2271500	-17.0	-0.6
45	−1617.22869373320	145.613	210.419	-1014649	-1014605	0.0	0.0
46	−1617.21757555311	138.633	211.307	-1014639	-1014598	9.9	7.9
47	−1617.21375575935	138.204	211.055	-1014636	-1014595	12.2	10.0
cyclohexene compounent	−1424.11423847803	119.236	153.486	-893518	-893482		
acetone	−193.11530911161	75.802	54.802	-121148	-121126		
62				-1014666	-1014608	-17.3	-2.7

XYZ coordinates for all reported structures

Structure **45 + IP**

C	-4.66302187	5.93899897	-1.59004292
C	-4.72708766	5.04492461	-2.76254905
C	-3.56576612	6.94882643	-1.44889404
C	-3.24151508	7.50169763	-0.04450802
C	-2.29866625	6.57669868	0.74788331
C	-2.89631540	5.22368649	1.17337294
H	-1.98912219	7.11875269	1.66197319
H	-1.37749843	6.40969102	0.15074053
C	-3.11714432	4.24980494	0.04429579
H	-3.83037104	5.39883101	1.73727073
H	-2.19038364	4.75515824	1.89333698
C	-4.12255801	3.33413647	-0.05151271
O	-5.69635964	6.03814218	-0.85952275
C	-2.61784225	8.90065423	-0.19012566
H	-4.18615121	7.60045720	0.52108917
H	-2.39033196	9.32749714	0.80456006
H	-3.30440323	9.58817941	-0.72066123
H	-1.67177377	8.84616702	-0.76493484
C	-5.99480161	4.60368641	-3.20922874
C	-6.07380341	3.76802260	-4.33031561
C	-4.92047458	3.34926566	-5.01612954
C	-3.66883666	3.79935627	-4.55526687
C	-3.55555409	4.64669368	-3.44778039
H	-6.90433544	4.92135006	-2.69978639
Cl	-7.63865593	3.22275091	-4.88560318
Cl	-2.22055757	3.27255141	-5.38133824
H	-2.56413872	4.94798679	-3.10201247
C	-5.24504112	3.22784998	0.95052180
H	-5.41627141	4.15996792	1.51498266
H	-5.00617653	2.43477966	1.69073970
H	-6.18392634	2.92642188	0.45928840
C	-4.16396308	2.32246971	-1.16553661
H	-3.29146000	2.39822858	-1.83759086
H	-5.09362218	2.45165401	-1.75533534
H	-4.20587157	1.29569692	-0.74590670
H	-2.64646897	6.61857407	-1.95809086
H	-3.96767343	7.77956049	-2.07638438
Cl	-8.21278081	7.98581992	-0.91101578
F	-7.95415680	5.01549865	0.31561049
F	-7.59102301	2.83315500	-1.42453776
F	-8.84770180	2.53478778	0.95803169
Al	-7.05532196	6.56901854	0.17179713
Sb	-9.20376942	3.56621709	-0.63065225
Cl	-6.48669693	7.07761209	2.16208777
F	-10.62720579	4.50449889	0.26699931
F	-9.27194665	4.84617180	-2.07835067
F	-10.35384881	2.26430326	-1.44700973
H	-4.99469345	2.68671984	-5.88432187
H	-2.32530994	4.21652586	-0.72033623

Structure **52 (TS-III)**

C	-4.79471792	4.93291033	-1.85498338
C	-3.98882572	4.53251777	-3.10108765
C	-5.15071508	6.42693014	-2.02117379
C	-5.67847144	7.13530494	-0.76708966
C	-4.64645225	6.96299543	0.35790648
C	-4.49202067	5.47779227	0.70424535
H	-4.97780339	7.50509354	1.26309970
H	-3.67861890	7.40238586	0.03773074
C	-4.04613567	4.60788933	-0.49183580
H	-5.47014831	5.14366938	1.07863607
H	-3.76642419	5.32958018	1.52552621
C	-4.38566961	3.14762171	-0.36223313
O	-5.93956330	4.07950140	-1.74538853
C	-5.99079304	8.60548126	-1.06711648
H	-6.61773909	6.65958638	-0.44087647
H	-5.07725560	9.14042119	-1.39564832
H	-6.74858821	8.68746742	-1.86977209
H	-6.38521323	9.10855608	-0.16390273
C	-4.58639527	3.75630779	-4.10778102
C	-3.85361577	3.45291645	-5.26734566
C	-2.53701834	3.90219508	-5.45450186
C	-1.96336496	4.68017195	-4.43305558

C	-2.67133344	5.00318889	-3.26621456
H	-5.60710981	3.38618710	-3.98507218
Cl	-4.60219670	2.47360235	-6.51692491
Cl	-0.31523683	5.25034489	-4.62096506
H	-2.19438312	5.61314484	-2.49169497
C	-5.21260191	2.61914097	0.73558505
H	-5.47245246	1.55792832	0.59487960
H	-6.09657536	3.23376352	0.96423696
H	-4.55443111	2.71264570	1.63286468
C	-3.67695286	2.15274775	-1.18890366
H	-2.99689252	2.57882471	-1.93816905
H	-4.41150132	1.45893604	-1.64324922
H	-3.10105296	1.52808644	-0.46791381
H	-4.23961135	6.96048502	-2.35138922
H	-5.87629308	6.48141746	-2.85480112
Cl	-8.52115000	2.22686232	-1.62664389
F	-7.80344359	4.69798393	0.19566882
F	-7.21833545	5.91287531	2.60358708
F	-8.70560461	7.23418962	0.77082056
Al	-7.67789681	4.19114256	-1.55609398
Sb	-8.92164226	5.58065580	1.74984004
Cl	-8.68402597	5.70610848	-2.68485756
F	-10.45973330	5.14672911	0.66581735
F	-8.92064607	3.79200302	2.47574409
F	-9.96030058	6.35113230	3.16993324
H	-1.97882740	3.65582824	-6.36229355
H	-2.95352121	4.69896939	-0.64411012

Structure **48 + IP**

C	-3.22996276	3.35329126	-1.22984617
C	-4.23611373	2.62961988	-0.35049718
C	-1.78532151	3.11040274	-0.79836837
C	-0.78332773	4.11775528	-1.37664526
C	-1.19996242	5.51837263	-0.90180236
C	-2.58499953	5.95261703	-1.43747969
H	-0.44531087	6.26664435	-1.20907038
H	-1.20790373	5.50788501	0.20748335
C	-3.63521961	4.82288377	-1.60945459
H	-2.44750005	6.45077831	-2.41290239
H	-3.00854452	6.71776670	-0.76361794
C	-3.95322705	4.31939523	-3.05457973
O	-3.39559800	2.93609392	-2.67160365
C	0.64039869	3.74584656	-0.94599802
H	-0.82798334	4.08065695	-2.48178761
H	1.37736779	4.45836184	-1.36290898
H	0.89651214	2.72710226	-1.29414594
H	0.72665841	3.76479281	0.15877125
C	-5.12181506	1.65997099	-0.84537651
C	-5.99069575	1.00510306	0.04288901
C	-6.01859010	1.30696977	1.41229499
C	-5.14719659	2.30831414	1.87582755
C	-4.25889246	2.96962045	1.01699603
H	-5.14899052	1.40115178	-1.90454764
Cl	-7.06763383	-0.22683002	-0.58210387
Cl	-5.16942690	2.73626768	3.57661127
H	-3.58744763	3.73916478	1.41156005
C	-5.43453436	4.17469665	-3.35586411
H	-5.97407749	3.74269709	-2.49589200
H	-5.58752074	3.53932485	-4.24629047
H	-5.84100556	5.18323646	-3.55833421
C	-3.15797724	4.86213022	-4.22312269
H	-2.07488393	4.85865579	-4.01921267
H	-3.47982607	5.90099678	-4.41897528
H	-1.74086243	3.17235634	0.30420023
H	-1.51658477	2.06857221	-1.03991710
Cl	-0.69482962	1.75443544	-4.18888063
F	-2.86509270	0.32473485	-2.30001796
F	-3.86399822	-1.77816967	-0.87994303
F	-1.70028940	-2.12541664	-2.51690357
Al	-2.72822052	1.50561913	-3.63432577
Sb	-2.06044314	-1.10460612	-0.92347504
Cl	-4.09965470	1.01208928	-5.17822570
F	-0.41599623	-0.12158397	-1.19824466
F	-2.53405996	0.15138707	0.47110014

F	-1.30934963	-2.40074170	0.27492501
H	-6.69761941	0.78657576	2.09410475
H	-4.56846692	5.10536013	-1.09824569
H	-3.36804131	4.26200484	-5.12786476

Structure **50 (TS-I)**

C	-4.33613905	5.46129384	-1.20313717
C	-4.50793446	4.83438079	-2.59494402
C	-3.70723010	6.86877539	-1.30763432
C	-3.40974452	7.53915843	0.04158953
C	-2.45225860	6.64178177	0.84194393
C	-3.06576673	5.25438099	1.06484904
H	-2.22552503	7.10557509	1.82084980
H	-1.49426412	6.55356929	0.28848446
C	-3.40086755	4.53211955	-0.25937484
H	-3.98558726	5.38283323	1.66095704
H	-2.38412439	4.60393866	1.64372698
C	-4.17962608	3.25945988	-0.11174814
O	-5.59993488	5.53137014	-0.54048086
C	-2.84669382	8.94887764	-0.17802595
H	-4.35639947	7.62432547	0.61315489
H	-2.63876173	9.44237397	0.79065001
H	-3.56191615	9.57580954	-0.74465798
H	-1.89939435	8.90221261	-0.75156803
C	-5.73984528	4.29037268	-2.99366915
C	-5.86050577	3.68690221	-4.25588489
C	-4.77628346	3.59733578	-5.14163028
C	-3.54893619	4.13584880	-4.71619451
C	-3.40162828	4.75136909	-3.46418566
H	-6.60417711	4.30075714	-2.33270403
Cl	-7.41417801	3.02461227	-4.72686408
Cl	-2.15739489	4.02479403	-5.77804056
H	-2.42315704	5.14235626	-3.17059385
C	-5.29518011	3.25163181	0.72075327
H	-5.31857304	3.85354948	1.64079716
H	-5.97579430	2.39322578	0.68843665
H	-5.70352566	4.33153740	0.00951757
C	-3.92461342	2.13404804	-1.05914774
H	-3.45096932	2.46785685	-1.99694928
H	-4.84503822	1.55874470	-1.26236877
H	-3.20616512	1.45431851	-0.54886450
H	-2.75658837	6.77261863	-1.86195421
H	-4.38189372	7.48919673	-1.92383073
Cl	-7.09738269	7.94314615	-2.24997340
F	-8.31709847	5.39180182	-0.92010835
F	-10.09484233	3.72691352	-2.06902247
F	-7.82753550	2.61422224	-1.07551977
Al	-7.03339913	6.62118850	-0.57602970
Sb	-9.31000728	3.60781420	-0.31429871
Cl	-7.39564126	7.41825593	1.36597206
F	-8.27367527	3.81107514	1.30991995
F	-10.64374348	4.79771963	0.40162253
F	-10.24907776	2.01778046	0.21131889
H	-4.88023401	3.12596174	-6.12400228
H	-2.47970923	4.35838921	-0.84118855

Structure **53 + IP**

C	-2.97293073	3.36519287	-1.54450705
C	-4.13976795	2.55633006	-0.97204761
C	-1.70801075	3.23696714	-0.68009558
C	-0.52391928	4.10298236	-1.14218618
C	-0.97145826	5.57043096	-1.22736559
C	-2.14885244	5.71825032	-2.20030640
H	-0.12662896	6.20431341	-1.55829019
H	-1.27064258	5.91817027	-0.21661090
C	-3.36632059	4.86717844	-1.77471218
H	-1.81590529	5.41114961	-3.20893069
H	-2.48028475	6.77045712	-2.27297777
C	-4.55768653	4.97001702	-2.72824455
O	-2.62222225	2.81493657	-2.89936339
C	0.67056648	3.89123525	-0.20468909
H	-0.22668626	3.78414685	-2.15871155
H	0.41190750	4.19652949	0.82895363
H	1.54040009	4.49018272	-0.53551848

H	0.96384483	2.82388636	-0.18505944
C	-4.86701243	1.63849277	-1.74720031
C	-5.93364852	0.93329042	-1.16942113
C	-6.32554404	1.13889167	0.16041216
C	-5.60145414	2.08100169	0.90889080
C	-4.51706360	2.78379040	0.36598787
H	-4.62886906	1.45027751	-2.79573934
Cl	-6.78142113	-0.25621421	-2.13712638
Cl	-6.06016933	2.37068060	2.57515461
H	-3.98241219	3.50737463	0.98822913
C	-5.92434666	5.05599296	-2.09638716
H	-6.72535828	5.07462524	-2.85693246
H	-5.98657631	5.97992144	-1.48512291
H	-6.10059526	4.21176829	-1.40456016
C	-4.39317410	4.95945633	-4.07323198
H	-3.40228340	4.98776375	-4.54813343
H	-5.26606432	4.98333058	-4.74009461
H	-1.98633585	3.55783560	0.33916914
H	-1.42597332	2.17328160	-0.59530869
Cl	0.31990792	1.33747675	-3.53912854
F	-2.21011933	0.28741221	-1.92806017
F	-3.46555407	-2.07128997	-1.46286657
F	-0.74277183	-1.99671889	-1.56131023
Al	-1.78647077	1.20487995	-3.38372550
Sb	-2.08698753	-1.22385060	-0.41632533
Cl	-2.90406257	0.53198496	-5.05888616
F	-0.73290070	-0.08481177	0.36018900
F	-3.43601465	-0.19451901	0.49827510
F	-1.99468600	-2.59229903	0.92530223
H	-7.15790777	0.58215553	0.60216674
H	-3.68823417	5.20939065	-0.77374714
H	-3.25729888	3.19707112	-3.56170550

Structure **51 (TS-II)**

C	-3.10174098	3.33674827	-1.43715962
C	-4.27942697	2.65190606	-0.71961424
C	-1.83906820	3.16529976	-0.56743201
C	-0.66291193	4.08862636	-0.90688318
C	-1.15349135	5.54034977	-0.80251126
C	-2.20832551	5.80319474	-1.88322527
H	-0.31218236	6.24562636	-0.94101568
H	-1.56913565	5.71543633	0.21174165
C	-3.43923332	4.87343592	-1.77679389
H	-1.70494032	5.66827960	-2.85516340
H	-2.57183380	6.84729501	-1.84876070
C	-4.19342855	4.66355424	-3.05373311
O	-2.91724499	2.80235416	-2.73906123
C	0.52256398	3.78594715	0.01840057
H	-0.35242486	3.90350490	-1.95484075
H	1.38821766	4.43227627	-0.22272844
H	0.83208719	2.72800748	-0.07992232
H	0.24222888	3.96360710	1.07611383
C	-4.93151471	1.54264457	-1.28045759
C	-5.94601320	0.89779178	-0.55546293
C	-6.34790761	1.33704546	0.71422951
C	-5.69956380	2.46681129	1.24431224
C	-4.67663942	3.12379841	0.54761178
H	-4.68067753	1.17988758	-2.27789470
Cl	-6.74493690	-0.49306651	-1.26283004
Cl	-6.17893580	3.05366023	2.82678707
H	-4.18509583	3.99355949	0.99605355
C	-5.61276208	4.27619854	-3.00186394
H	-5.97779245	4.01559553	-1.99906446
H	-5.82894390	3.49020580	-3.75033913
H	-6.15662873	5.18195827	-3.36088723
C	-3.63773295	5.01874449	-4.37148429
H	-2.56900941	4.76239425	-4.44905016
H	-3.69499996	6.13213632	-4.42119214
H	-2.10165630	3.32477698	0.49403164
H	-1.54899374	2.10451737	-0.65409194
Cl	-0.09188310	1.59973643	-3.93463416
F	-2.39555851	0.04593129	-2.35837351
F	-3.39354209	-2.08687752	-0.98477120
F	-0.87789700	-2.19651667	-2.03849987

Al	-2.18650535	1.42114665	-3.53068329
Sb	-1.75522435	-1.11158055	-0.70828580
Cl	-3.40587353	0.90110409	-5.21888353
F	-0.22338371	0.07637437	-0.68128128
F	-2.69939066	0.16165308	0.40091348
F	-1.16144738	-2.17528489	0.77881582
H	-7.13949822	0.82281779	1.26785348
H	-4.13475599	5.24831083	-1.00346428
H	-4.22490171	4.59285777	-5.20107204

Structure **54 (TS-IV)**

C	-3.62803918	3.44961118	-0.20349988
C	-4.45724914	2.31683653	0.14062917
C	-2.20719414	3.27228288	-0.60295032
C	-1.23701395	4.27026431	0.09146656
C	-1.71645054	5.70330443	-0.17630567
C	-3.18030879	5.90680993	0.23767225
H	-1.57969561	5.92609083	-1.24829953
H	-1.08562820	6.41913310	0.38517729
C	-4.18181327	4.81280376	-0.24630729
H	-3.53939897	6.89495239	-0.09404074
H	-3.24604875	5.90626559	1.34147380
C	-4.85254939	5.17417393	-1.75973365
O	-5.60885779	4.09569208	-2.18518980
C	-1.11428508	3.93245196	1.58547502
H	-0.24958217	4.13052652	-0.38600273
H	-0.38160536	4.60275453	2.07344937
H	-0.78076003	2.88646608	1.72474207
H	-2.08680972	4.04660041	2.10385646
C	-5.88135073	2.44186071	0.18142528
C	-6.67123859	1.31479850	0.41577397
C	-6.09761249	0.05188998	0.65320088
C	-4.69338757	-0.06039334	0.66580181
C	-3.87636473	1.03846899	0.40915906
H	-6.37060464	3.39581104	-0.00883681
Cl	-8.40850484	1.46815020	0.43236405
Cl	-3.97159120	-1.61192152	0.99431858
H	-2.79630510	0.89996012	0.43323003
C	-3.76891650	5.56240181	-2.77018164
H	-4.27336323	5.79003651	-3.72660115
H	-3.05335543	4.74403811	-2.96340687
H	-3.21838873	6.45998468	-2.44650557
C	-5.81240430	6.35266419	-1.50944884
H	-6.28207823	6.60750288	-2.47744343
H	-5.29052560	7.24522018	-1.12602762
H	-6.60094135	6.05178986	-0.79683981
H	-1.84812640	2.24234144	-0.50049251
H	-2.19244008	3.48352995	-1.69456959
Cl	-5.12112859	3.43274325	-5.38858115
F	-4.07610848	1.84476827	-2.84523188
F	-4.44764094	-0.79948025	-2.29898340
F	-4.32832672	0.04059694	-4.89327963
Al	-5.54084936	2.82110824	-3.37460791
Sb	-3.10718946	0.04804202	-3.39851428
Cl	-7.23203056	1.52346962	-3.16927211
F	-1.90122342	1.20643761	-4.36342201
F	-2.00412777	0.29878940	-1.82494158
F	-2.23007393	-1.58879458	-3.88911285
H	-6.72953746	-0.82380903	0.83509803
H	-5.06919148	4.86414971	0.40014153

Structure **28 + IP**

Cyclohexene component

C	-3.67762981	3.28117082	0.24987082
C	-4.59899268	2.13635457	0.48514465
C	-2.21515542	2.96625724	-0.03956855
C	-1.43662510	4.14342596	-0.65978712
C	-1.72351819	5.43009553	0.13325291
C	-3.22373633	5.77213339	0.10648102
H	-1.13170429	6.27321305	-0.27268065
H	-1.39478350	5.27635256	1.18242232
C	-4.10651348	4.56865416	0.32453291
H	-3.48800813	6.22812641	-0.87410232
H	-3.46444173	6.54747974	0.86196546

C	0.06391404	3.83303619	-0.73303574
H	-1.81866342	4.29145413	-1.69236978
H	0.61545372	4.65642338	-1.22710748
H	0.25221418	2.89878368	-1.29751296
H	0.47959607	3.70528425	0.28692295
C	-4.08511865	0.88144881	0.89756792
C	-4.95638882	-0.19267628	1.13464884
C	-6.34587306	-0.07818178	0.96903603
C	-6.84037234	1.16845100	0.54404777
C	-5.99927426	2.25975464	0.29649676
H	-3.01074619	0.74133421	1.04619348
Cl	-4.29493598	-1.73760765	1.65273606
Cl	-8.57321293	1.34647954	0.30327361
H	-6.43206399	3.19869394	-0.06125322
H	-1.71527999	2.66101821	0.90559943
H	-2.15058846	2.08417338	-0.70713819
H	-7.01623953	-0.92314983	1.15553144
H	-5.16001974	4.77431272	0.56058265
Acetone component			
C	-5.62330188	4.89184070	-1.70623667
O	-5.14247310	3.80289208	-2.12539231
C	-5.55669851	6.11780480	-2.55079190
H	-5.97615179	5.88695870	-3.55032367
H	-4.48390873	6.35776549	-2.70467628
H	-6.07634172	6.97378460	-2.09344156
C	-6.23606914	4.93280813	-0.35772224
H	-6.18977921	3.95597214	0.14893233
H	-7.28253074	5.28632432	-0.46212705
H	-5.71647096	5.71844448	0.22937870
Cl	-2.39304768	4.37008451	-3.68295244
F	-3.92815286	1.57236206	-3.09949664
F	-4.34360211	-0.49790778	-4.89500652
F	-2.35172031	1.29282413	-5.26442359
Al	-4.20548908	3.26199745	-3.63904043
Sb	-2.75112064	-0.04355524	-3.91245700
Cl	-5.50519932	3.28660938	-5.31569216
F	-1.34969405	0.68378454	-2.81019747
F	-3.38928512	-1.07651454	-2.41971140
F	-1.66345304	-1.42327994	-4.679681

The following data contains the optimized geometries and energies of structures without $AlCl_2SbF_6$

XYZ coordinates for structures without $AlCl_2SbF_6$

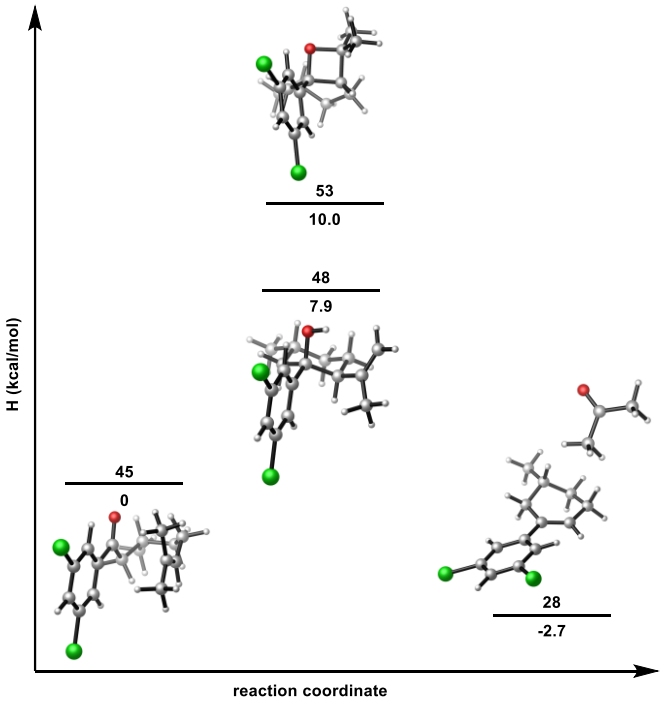

Figure 2.17. Computational values for uncoordinated species.

Structure **45**

C	-4.70066947	6.12111898	-1.55010440
C	-4.85584015	5.13674194	-2.69156203
C	-3.38864060	6.89238948	-1.43450421
C	-3.14657636	7.58924905	-0.08068713
C	-2.54257508	6.64731142	0.98358977
C	-3.32037573	5.34669719	1.28208081
H	-2.44506671	7.22785076	1.92190308
H	-1.50903780	6.38206468	0.67293029
C	-3.11584548	4.26845636	0.24459909
H	-4.39486145	5.57535449	1.40965943
H	-2.96525310	4.96483873	2.26427737
C	-3.99735431	3.32924877	-0.17579045
O	-5.64887967	6.34289221	-0.80320244
C	-2.23065421	8.81116266	-0.26996242
H	-4.12910092	7.93927202	0.29107183
H	-2.04902118	9.32163631	0.69568653
H	-2.67739947	9.54073620	-0.97325246
H	-1.24825181	8.49939984	-0.67910555
C	-6.09817108	4.48125373	-2.82603212
C	-6.27727762	3.53883822	-3.84514182
C	-5.25398910	3.24012462	-4.76273699
C	-4.02872670	3.91245898	-4.61968387
C	-3.81431466	4.85177235	-3.59912733
H	-6.90226891	4.71012883	-2.12098676
Cl	-7.80521710	2.68553570	-3.96985520
Cl	-2.72544461	3.55209981	-5.73780803
H	-2.83815023	5.33603474	-3.51748076
C	-5.40828929	3.19418197	0.34191854
H	-5.72061625	4.03929513	0.97803262
H	-5.50978654	2.25809639	0.93086656
H	-6.11811877	3.10832686	-0.50501432
C	-3.61230305	2.31341948	-1.22638965
H	-2.56330716	2.43303901	-1.55488449
H	-4.27021875	2.41679395	-2.11245598
H	-3.75311726	1.27890061	-0.84829384
H	-2.52965168	6.24750130	-1.69067041
H	-3.44209705	7.65087807	-2.24650605
H	-5.40358520	2.50398902	-5.55857019
H	-2.10924567	4.24536278	-0.20512536

Structure **48**

C	-2.94337739	3.31542130	-1.61786764
C	-4.11205289	2.51615103	-1.01035471
C	-1.70359799	3.19230780	-0.69876487
C	-0.50984164	4.05181827	-1.14976814
C	-0.94748743	5.52199277	-1.27001151
C	-2.14017296	5.67336820	-2.22389003
H	-0.09736906	6.14065662	-1.61949260
H	-1.22850486	5.89338614	-0.26139820
C	-3.35492027	4.83909579	-1.76216827
H	-1.83560274	5.34044850	-3.23337769
H	-2.45055084	6.73225597	-2.30657889
C	-4.58129142	5.00529181	-2.65661693
O	-2.56006202	2.78966683	-2.88362050
C	0.67474045	3.88373287	-0.18898189
H	-0.20724809	3.70413520	-2.15750982
H	0.39530987	4.22114292	0.82982172
H	1.54300843	4.48548344	-0.52168373
H	0.98932147	2.82384820	-0.12272831
C	-4.74443498	1.49921165	-1.74682210
C	-5.85377624	0.83230578	-1.20091414
C	-6.35550858	1.14099847	0.07324044
C	-5.69643278	2.14965981	0.79855756
C	-4.58790817	2.83220571	0.27927367
H	-4.37450277	1.23141511	-2.74013091
Cl	-6.64273372	-0.42644431	-2.14161242
Cl	-6.28881159	2.57157116	2.39854768
H	-4.11448131	3.62307076	0.86967442
C	-5.92060591	5.10894097	-1.96352793
H	-6.73871993	5.29683736	-2.68331612
H	-5.90168587	5.93052373	-1.21842941
H	-6.14829324	4.18395503	-1.40031914

C	-4.48744472	5.04402873	-4.00553298
H	-3.52037311	5.00764411	-4.52482322
H	-5.38977583	5.13819141	-4.62666571
H	-1.99357751	3.50092764	0.32310460
H	-1.41809505	2.12342475	-0.65286068
H	-7.22342842	0.61765401	0.48619022
H	-3.62488385	5.17510344	-0.74332765
H	-3.25534826	3.03704474	-3.52139583

Structure **53**

C	-3.76870021	3.31648584	-0.38524707
C	-4.85636043	2.45272917	0.23487014
C	-2.37767920	2.70635578	-0.13536295
C	-1.25667042	3.61178321	-0.66680848
C	-1.25053575	4.98974245	0.04554592
C	-2.63663042	5.49341958	0.54787683
H	-0.79346435	5.73209261	-0.63602757
H	-0.57714236	4.92672845	0.92329105
C	-3.88343082	4.83965135	-0.06305178
H	-2.71096335	6.59099303	0.42467576
H	-2.70150267	5.30470057	1.63655152
C	-4.23771320	4.99513228	-1.57172615
O	-3.98699503	3.55907511	-1.80209624
C	0.11518049	2.93041939	-0.56990441
H	-1.48254001	3.77618765	-1.73691140
H	0.91267309	3.59188245	-0.96223110
H	0.13313560	1.98461852	-1.14597459
H	0.35744849	2.69515407	0.48631665
C	-5.75959429	1.73143684	-0.56568642
C	-6.74072869	0.93812473	0.05251475
C	-6.84810764	0.83825749	1.44960921
C	-5.93308035	1.57231972	2.22546755
C	-4.94319902	2.37346323	1.63943144
H	-5.69793233	1.80708455	-1.65496949
Cl	-7.88461470	0.05036722	-0.94508305
Cl	-6.03726459	1.48983457	3.97871332
H	-4.24746329	2.93715773	2.27029267
C	-3.34068922	5.86949119	-2.44243666
H	-3.58112833	5.69752402	-3.50927431
H	-2.27270587	5.65402061	-2.28116974
H	-3.52439814	6.93634817	-2.21415925
C	-5.71630298	5.30837639	-1.81472553
H	-6.35696340	4.65193076	-1.19750813
H	-5.96761973	5.15380892	-2.88190206
H	-5.92813876	6.36258147	-1.55106987
H	-2.25318705	2.53706649	0.95275128
H	-2.34273316	1.71535780	-0.62964307
H	-7.61829815	0.21677396	1.91567833
H	-4.74904443	5.07402539	0.58092063

Structure **28**

Cyclohexene component

C	-3.67762981	3.28117082	0.24987082
C	-4.59899268	2.13635457	0.48514465
C	-2.21515542	2.96625724	-0.03956855
C	-1.43662510	4.14342596	-0.65978712
C	-1.72351819	5.43009553	0.13325291
C	-3.22373633	5.77213339	0.10648102
H	-1.13170429	6.27321305	-0.27268065
H	-1.39478350	5.27635256	1.18242232
C	-4.10651348	4.56865416	0.32453291
H	-3.48800813	6.22812641	-0.87410232
H	-3.46444173	6.54747974	0.86196546
C	0.06391404	3.83303619	-0.73303574
H	-1.81866342	4.29145413	-1.69236978
H	0.61545372	4.65642338	-1.22710748
H	0.25221418	2.89878368	-1.29751296
H	0.47959607	3.70528425	0.28692295
C	-4.08511865	0.88144881	0.89756792
C	-4.95638882	-0.19267628	1.13464884
C	-6.34587306	-0.07818178	0.96903603
C	-6.84037234	1.16845100	0.54404777
C	-5.99927426	2.25975464	0.29649676
H	-3.01074619	0.74133421	1.04619348

Cl	-4.29493598	-1.73760765	1.65273606	C	-4.51324352	5.82942889	-2.68833017
Cl	-8.57321293	1.34647954	0.30327361	H	-4.91170813	6.51604572	-1.91527376
H	-6.43206399	3.19869394	-0.06125322	H	-5.02758002	6.08634566	-3.63616622
H	-1.71527999	2.66101821	0.90559943	H	-3.42406106	5.96992020	-2.80031057
H	-2.15058846	2.08417338	-0.70713819	C	-6.29865333	4.07430480	-2.07536211
H	-7.01623953	-0.92314983	1.15553144	H	-6.89461893	4.35367446	-2.96684043
H	-5.16001974	4.77431272	0.56058265	H	-6.67611104	4.69128593	-1.23530617
Acetone component				H	-6.43265978	3.00271067	-1.84655666
C	-4.82900000	4.38809322	-2.31555132				
O	-3.95720614	3.53595943	-2.21618658				

2.5.6. ^{1}H NMR Kinetic Analysis

Monitoring the Al(III)-ion pair catalyzed carbonyl-olefin metathesis reaction by ^{1}H-NMR

To a screw-top NMR tube was added AlCl3 (10 mol%) and AgSbF6 (10 mol%) in the glovebox. The NMR tube was sealed and brought out of the glovebox. Aryl ketone starting material 41 or carbonyl-ene product 2 (0.075 mmol), deuterated dichloroethane (1.88 mL, 0.04 M), and mesitylene (3 □L, 0.0215 mmol) were added to the tube quickly and immediately prior to when the tube was placed in a 700 MHz or 500 MHz NMR instrument. A 1H NMR spectrum was collected immediately, and every five minutes following for 13 hours. From these spectra, percent yield of the aryl ketone starting material 41, carbonyl-ene product 42, and metathesis product 34 were calculated utilizing mesitylene as an internal standard.

Comparison of product formation rates

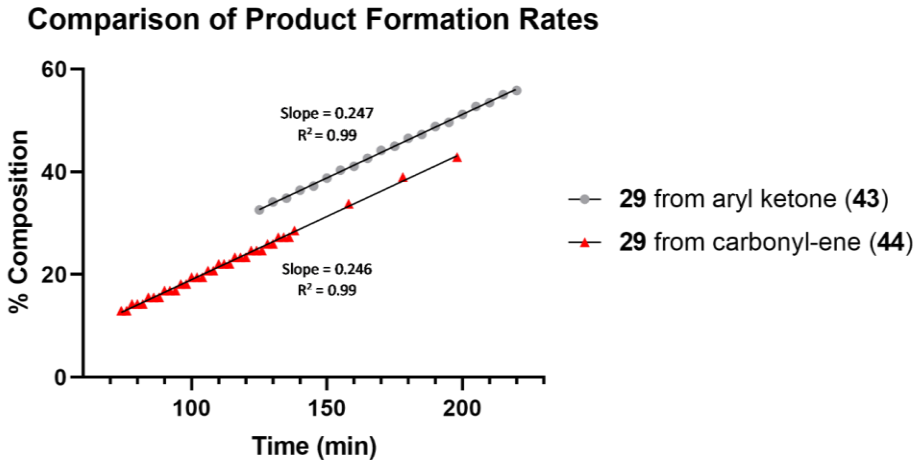

Figure 2.18. ^{1}H-NMR analysis of reaction progress with reaction rate analysis.

Kinetic analysis was performed using Prism 8.2.1 software on data collected from reaction monitoring experiments by ^{1}H-NMR. Nonlinear regression followed by straight line fit was performed using GraphPad Prism version 8.2.1 for Windows. Only data points after equilibrium were established between aryl ketone **43** and carbonyl-ene **44** were plotted. Nonlinear regression and straight-line fit were used to determine K_{obs} of product formation **29**. Specifically, we observed similar rates of metathesis product formation **29** from carbonyl-ene **44** compared to aryl ketone **43** of 0.246 and 0.247 respectively.

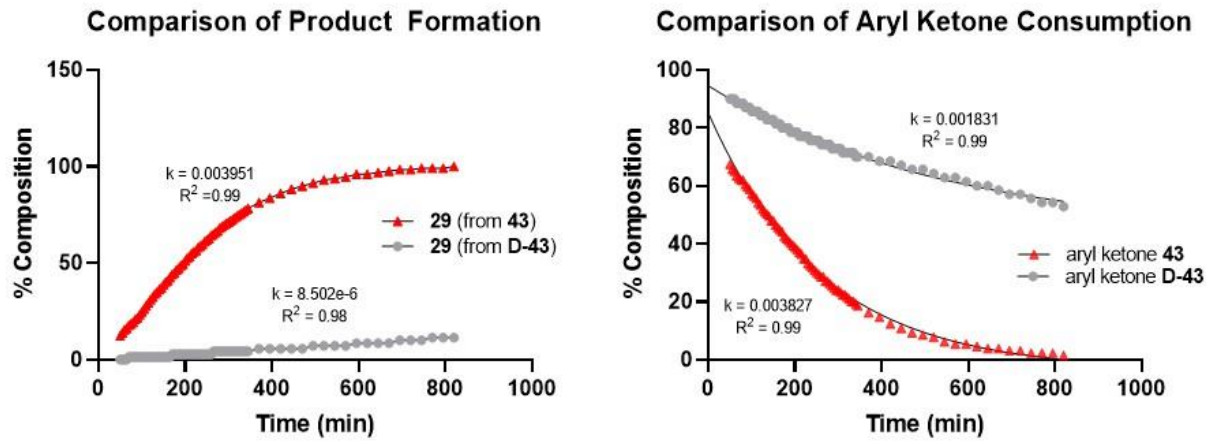

Figure 2.19. ^{1}H-NMR monitoring of reaction progress with KIE analysis.

KIE studies

Data points collected from reaction monitoring experiments using ^{1}H-NMR were plotted and analyzed using Prism 8.2.1software. Non-linear regression with exponential fitting was used to determine K_{obs} for formation of product **29** from either **43** or **D-43.** We have calculated the KIE value based on product **29** formation. When the protons on substrate **43** are replaced with deuterium atoms, the reaction effectively shuts down production of **29** which results in a very large KIE of 465 based on product formation (k_H/k_D = 3.95*10^{-3} /8.50*10^{-6} = 465). Since the rate of product formation with **D-43** is significantly inhibited, the KIE based on starting material consumption was reported in the text. Similar analysis was performed to determine K_{obs} for the consumption of aryl ketones **43** and **D-43**. A rate of 3.83*10^{-3} was observed for **43** and a rate of 1.83*10^{-3} was observed for **D-43**. The two values were then compared to calculate the reported primary KIE (k_H/k_D = 3.83*10^{-3} /1.83*10^{-3} = 2.09). Determining the KIE based on starting material consumption is standard practice and has also been used in previous studies in this area of

research.[31] These results suggest that carbonyl-ene formation is a key step for the overall transformation as it is expected to give a primary KIE while the concerted [2+2]-cycloaddition pathway would not.

2.5.7. ^{1}H and ^{13}C NMR Spectra

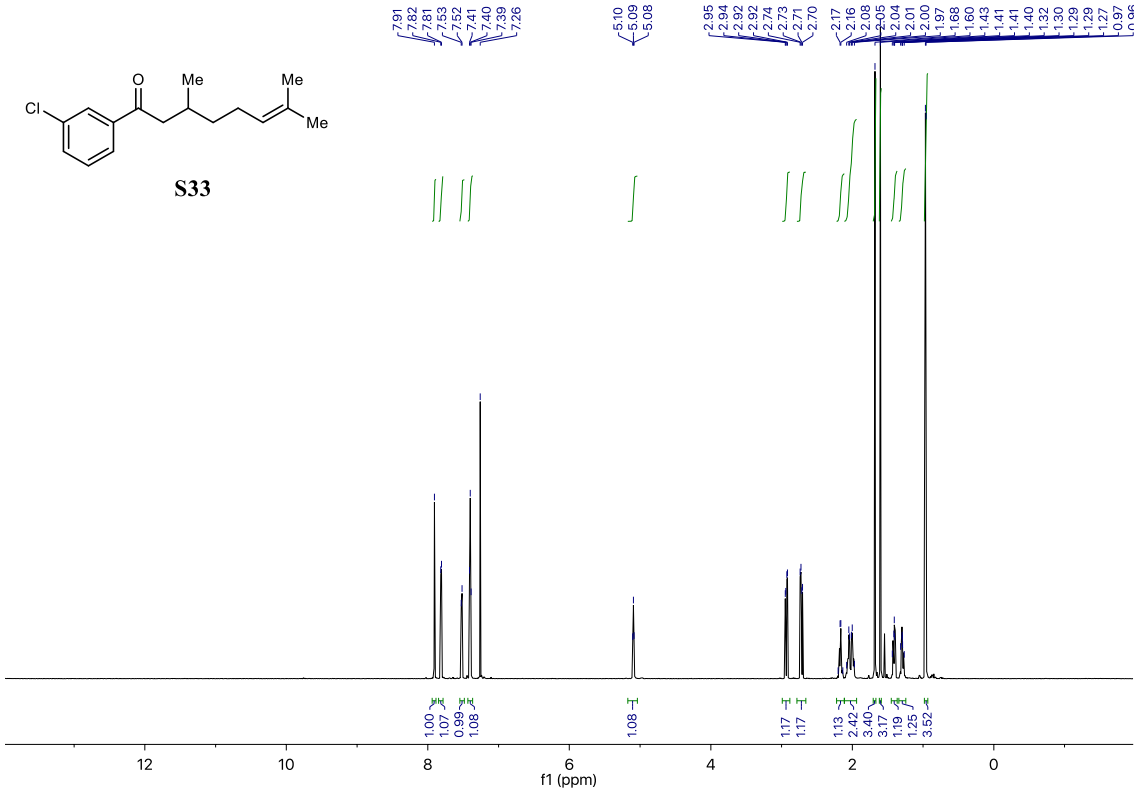

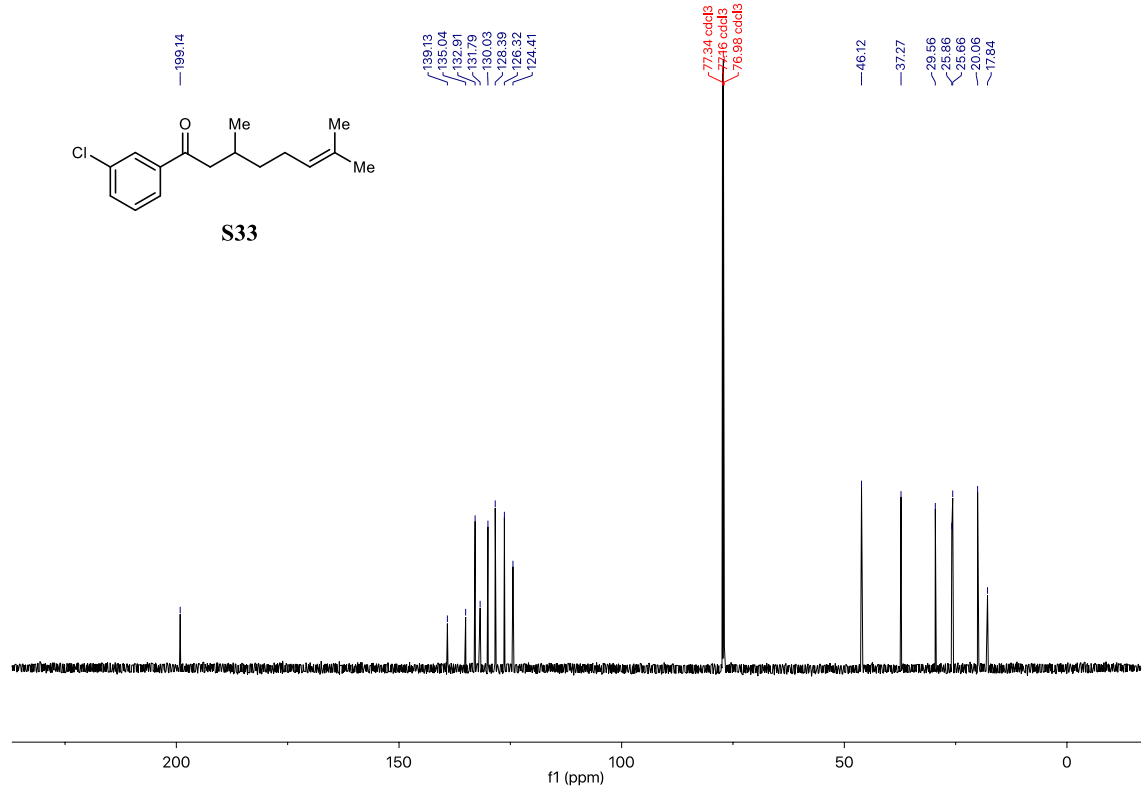

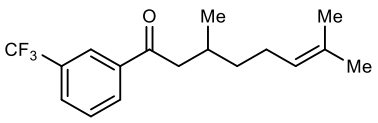
O
Me
Me
CF3
Me

S19

8.19
8.13
8.11
7.82
7.80
7.62
7.60
7.59
7.26
5.11
5.10
5.08
3.01
3.00
2.97
2.96
2.80
2.78
2.77
2.75
2.21
2.20
2.18
2.17
2.07
2.06
2.04
2.03
2.01
2.00
1.98
1.68
1.60
1.46
1.42
1.39
1.34
1.33
1.29
0.98
1.00
1.02
0.96
1.03
1.02
1.14
1.12
1.12
2.32
3.32
3.12
1.20
1.24
3.45
4
12
10
8
6
f1 (ppm)
4
2
0


198.98
138.05
131.84
131.50
131.37
131.37
131.24
129.45
129.42
129.40
129.38
127.13
125.11
125.08
125.05
125.02
124.96
124.35
122.79
120.63
77.41 cdcl3
77.16 cdcl3
76.91 cdcl3
46.09
37.25
29.51
25.83
25.66
20.06
17.82

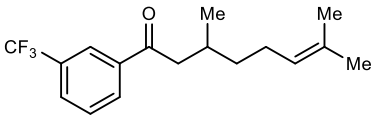
O
Me
Me
CF3
Me

S19

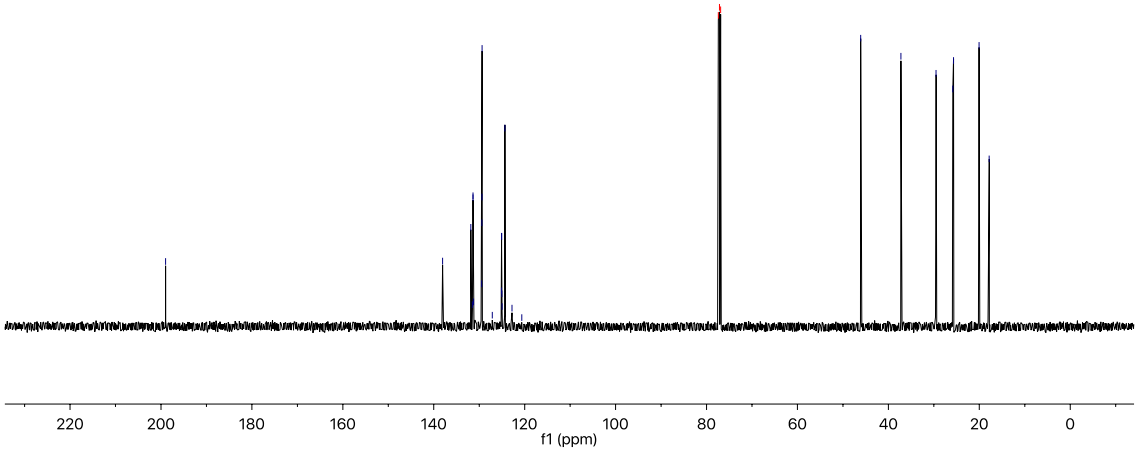
220
200
180
160
140
120
100
80
60
40
20
0
f1 (ppm)

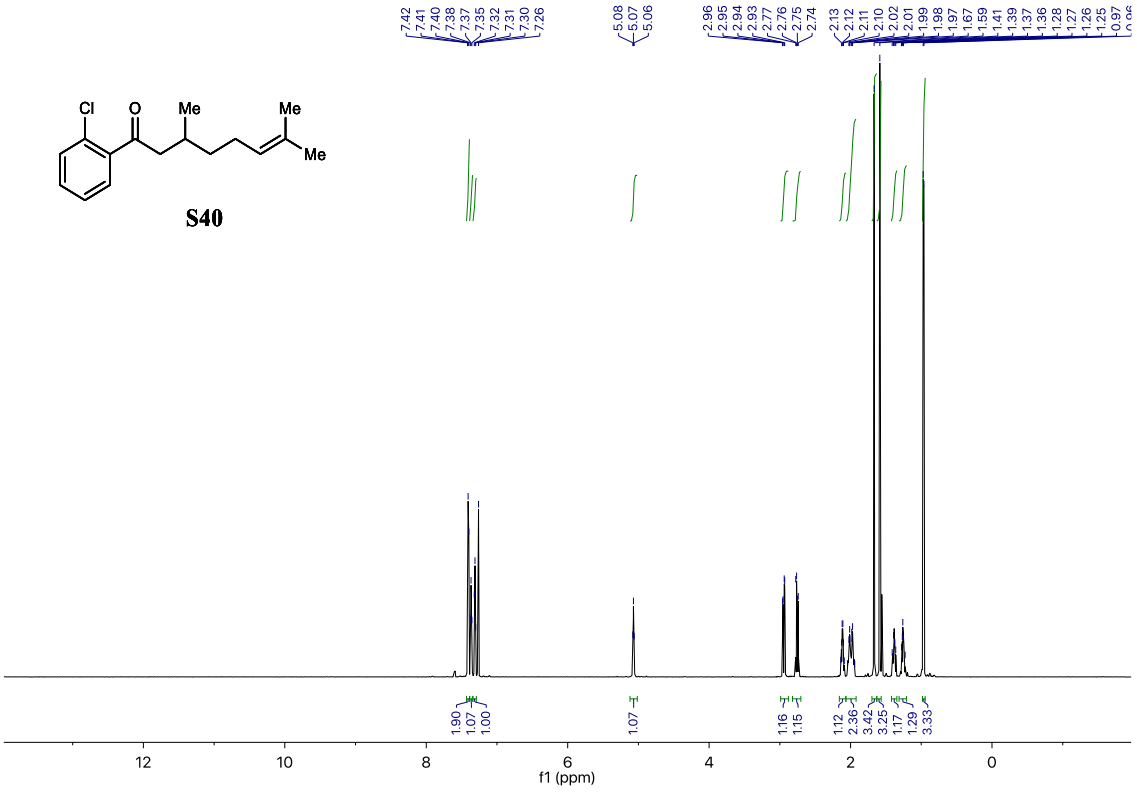
Cl
O
Me
Me
Me
S40
7.42
7.41
7.40
7.38
7.37
7.35
7.32
7.31
7.30
7.26
5.08
5.07
5.06
2.96
2.95
2.94
2.93
2.77
2.76
2.75
2.74
2.13
2.12
2.11
2.10
2.02
2.01
1.99
1.98
1.97
1.67
1.59
1.41
1.39
1.37
1.36
1.28
1.27
1.26
1.25
0.97
1.90
1.07
1.00
1.07
1.16
1.15
1.12
2.36
3.42
3.25
1.17
1.29
3.33
12
10
8
6
4
2
0
f1 (ppm)

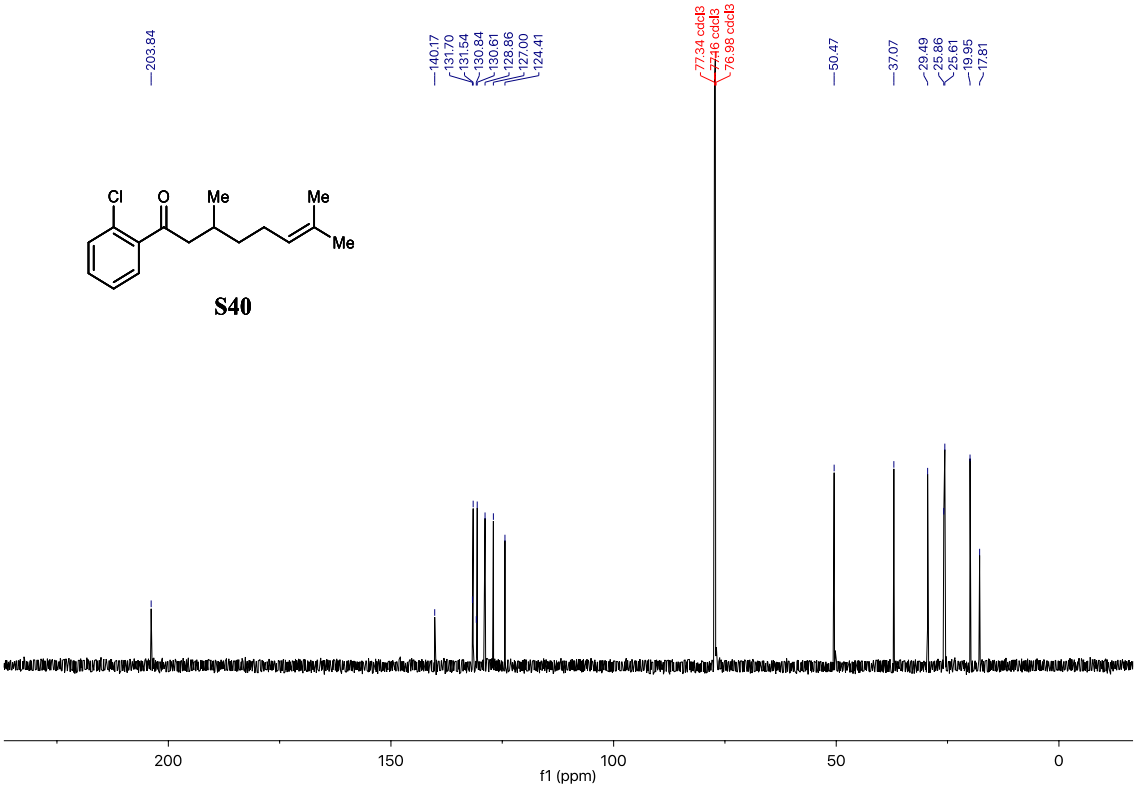
203.84
140.17
131.70
131.54
130.84
130.61
128.86
127.00
124.41
77.34 cdcl3
77.16 cdcl3
76.98 cdcl3
50.47
37.07
29.49
25.86
25.61
19.95
17.81
Cl
O
Me
Me
Me
S40
200
150
100
50
0
f1 (ppm)

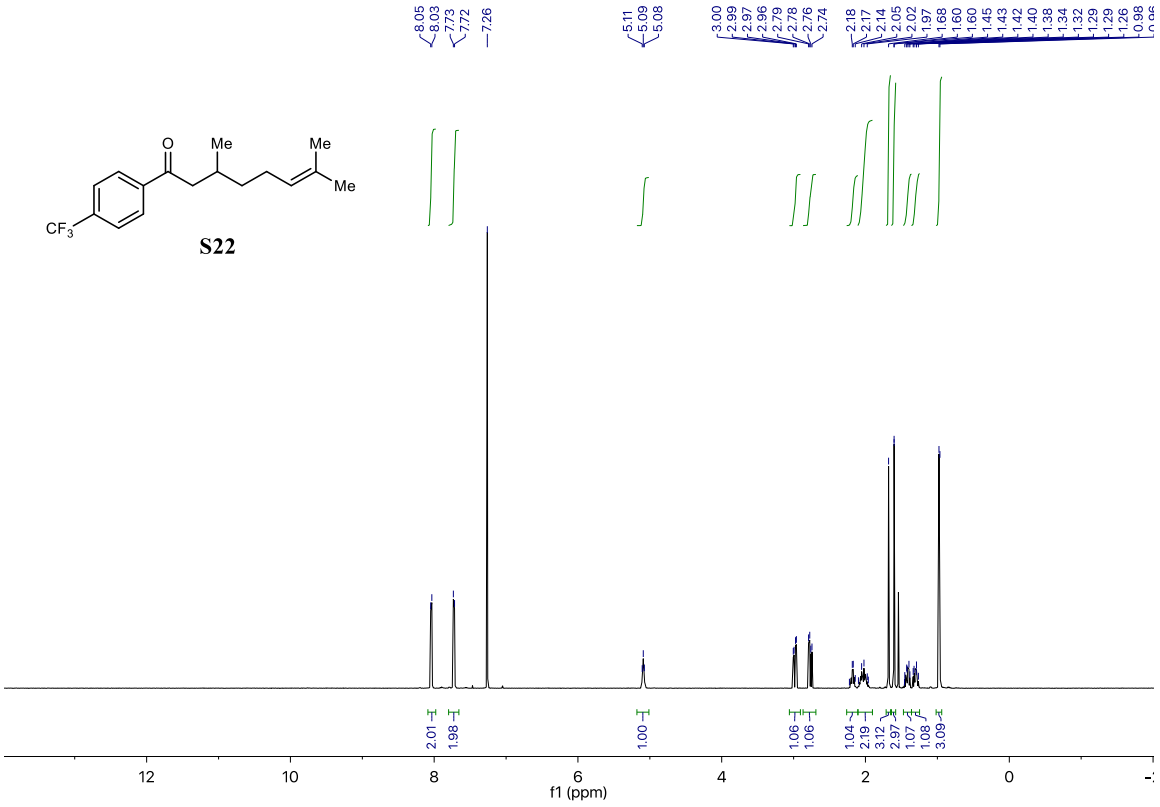
8.05
8.03
7.73
7.72
7.26
5.11
5.09
5.08
3.00
2.99
2.97
2.96
2.79
2.78
2.76
2.74
2.18
2.17
2.14
2.05
2.02
1.97
1.68
1.60
1.45
1.43
1.42
1.40
1.38
1.34
1.32
1.29
1.26
0.98
O
Me
Me
Me
CF3
2.01
1.98
1.00
1.06
1.06
1.04
2.19
3.12
2.97
1.07
1.08
3.09
12
10
8
6
4
2
0
f1 (ppm)

S22

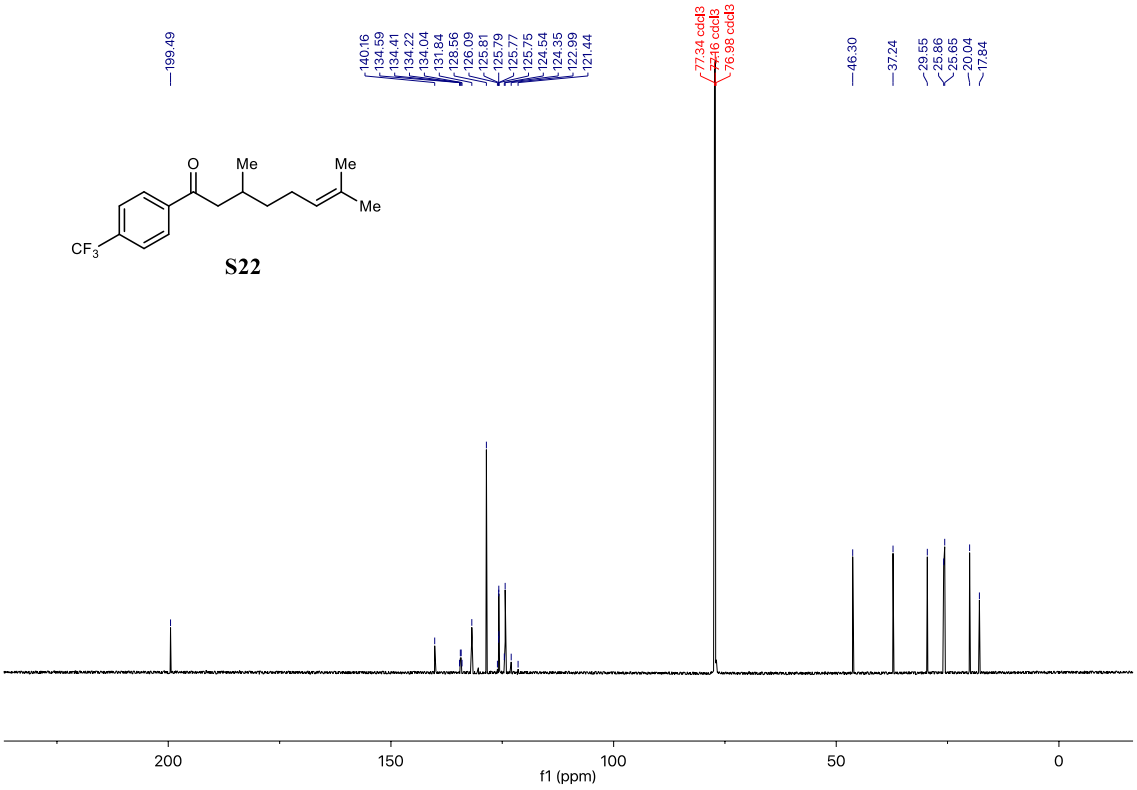
199.49
140.16
134.59
134.41
134.22
134.04
131.84
128.56
126.09
125.81
125.79
125.77
125.75
124.54
124.35
122.99
121.44
77.34 cdd3
77.16 cdd3
76.98 cdd3
46.30
37.24
29.55
25.86
25.65
20.04
17.84
O
Me
Me
Me
CF3
200
150
100
50
0
f1 (ppm)

S22

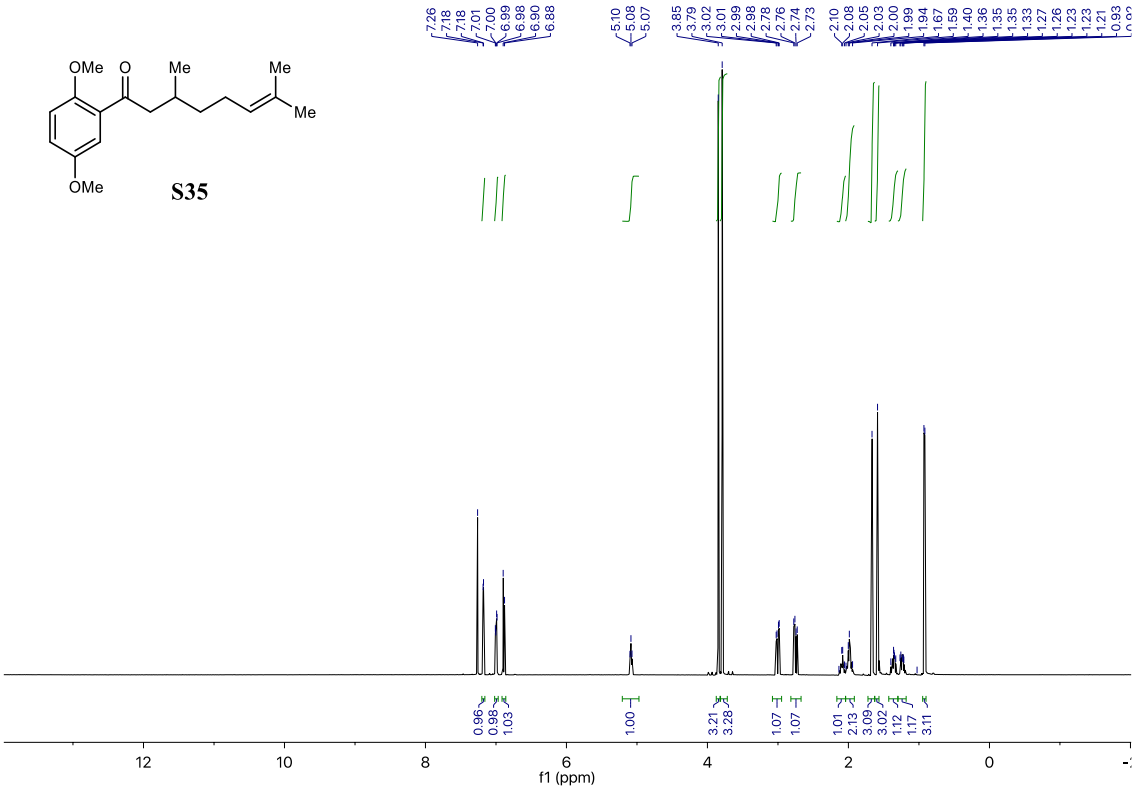
OMe
O
Me
Me
Me
OMe
S35
f1 (ppm)

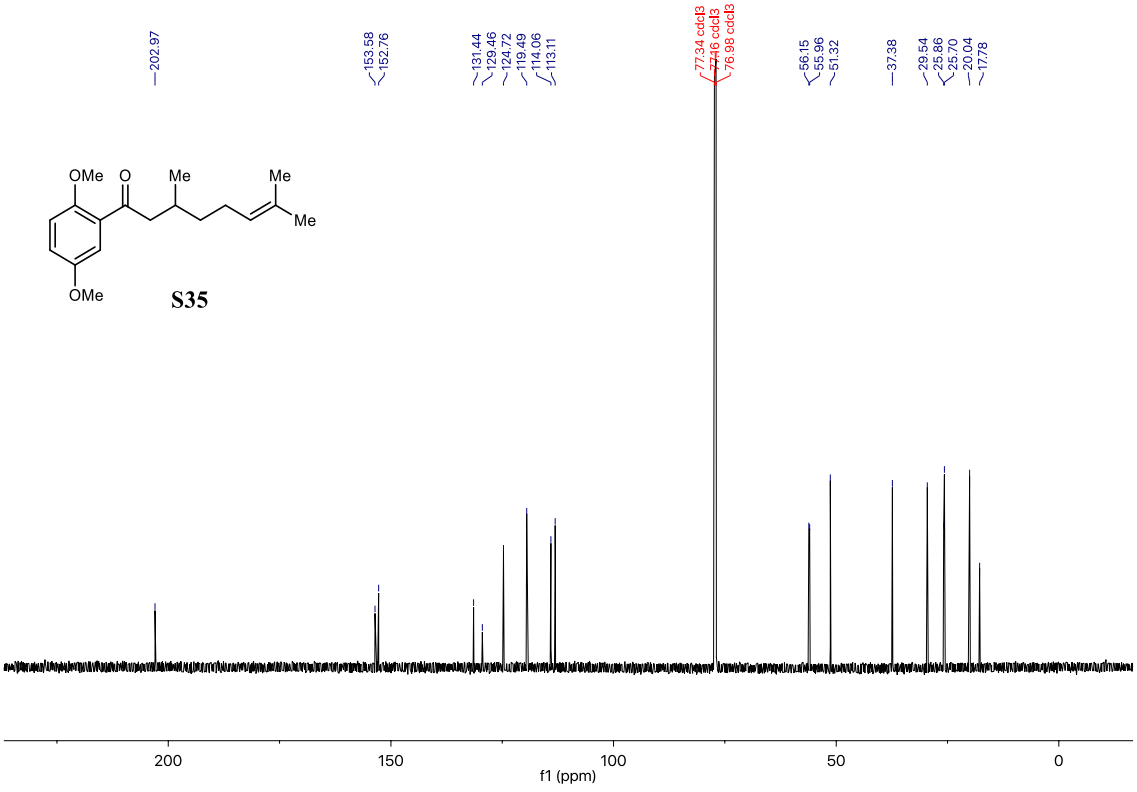
OMe
O
Me
Me
Me
OMe
S35
f1 (ppm)

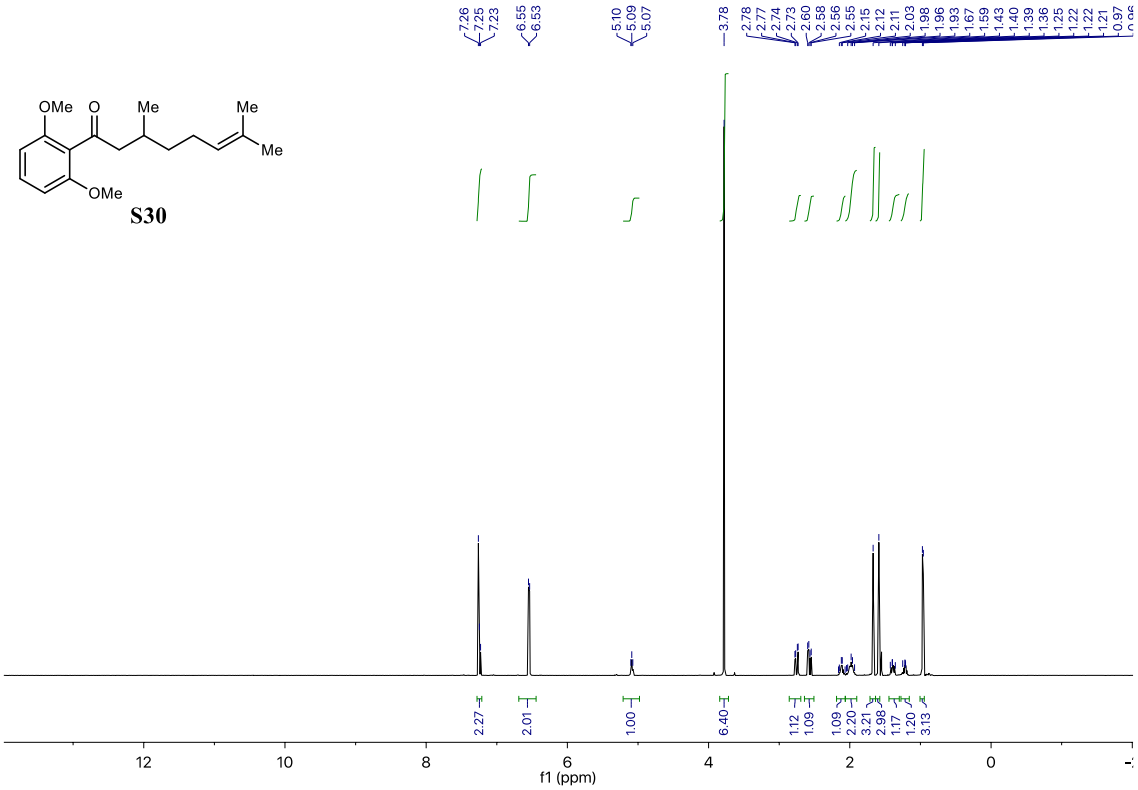
OMe
O
Me
Me
Me
OMe
S30
7.26
7.25
7.23
6.55
6.53
5.10
5.09
5.07
3.78
2.78
2.77
2.74
2.73
2.60
2.58
2.56
2.55
2.15
2.12
2.11
2.03
1.98
1.96
1.93
1.67
1.59
1.43
1.40
1.39
1.36
1.25
1.22
1.22
1.21
0.97
2.27
2.01
1.00
6.40
1.12
1.09
1.09
2.20
3.21
2.98
1.17
1.20
3.13
12
10
8
6
4
2
0
f1 (ppm)

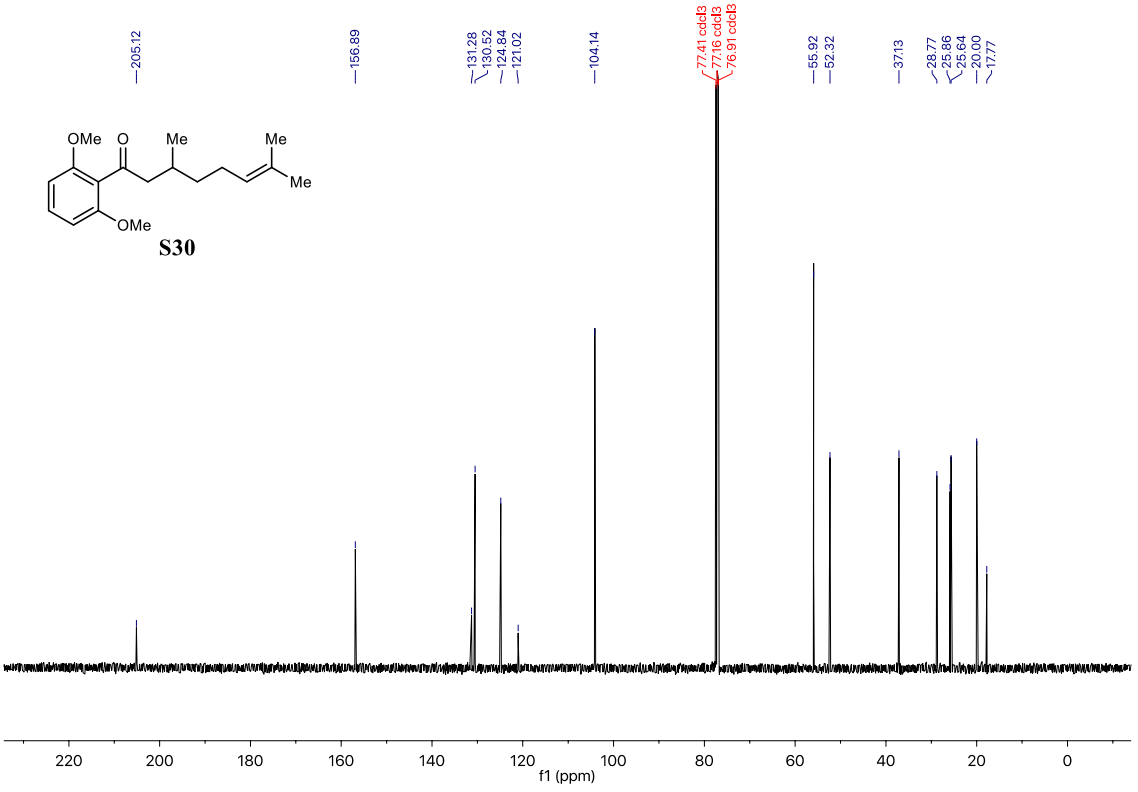
205.12
156.89
131.28
130.52
124.84
121.02
104.14
77.41 cdd3
77.16 cdd3
76.91 cdd3
55.92
52.32
37.13
28.77
25.86
25.64
20.00
17.77
OMe
O
Me
Me
Me
OMe
S30
220
200
180
160
140
120
100
80
60
40
20
0
f1 (ppm)

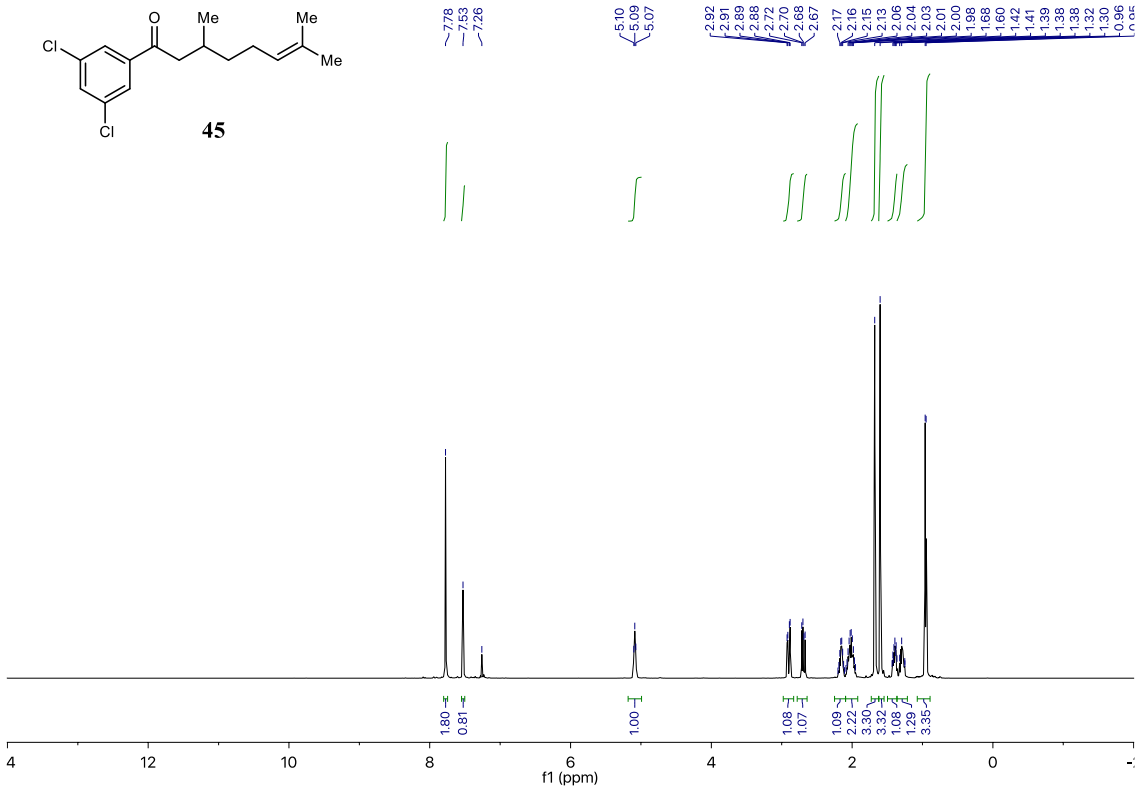
Cl
O
Me
Me
Cl
45
7.78
7.53
7.26
5.10
5.09
5.07
2.92
2.91
2.89
2.88
2.72
2.70
2.68
2.67
2.17
2.16
2.15
2.13
2.06
2.04
2.03
2.01
2.00
1.98
1.68
1.60
1.42
1.41
1.39
1.38
1.38
1.32
1.30
0.96
1.80
0.81
1.00
1.08
1.07
1.09
2.22
3.30
3.32
1.08
1.29
3.35
4
12
10
8
6
4
2
0
f1 (ppm)

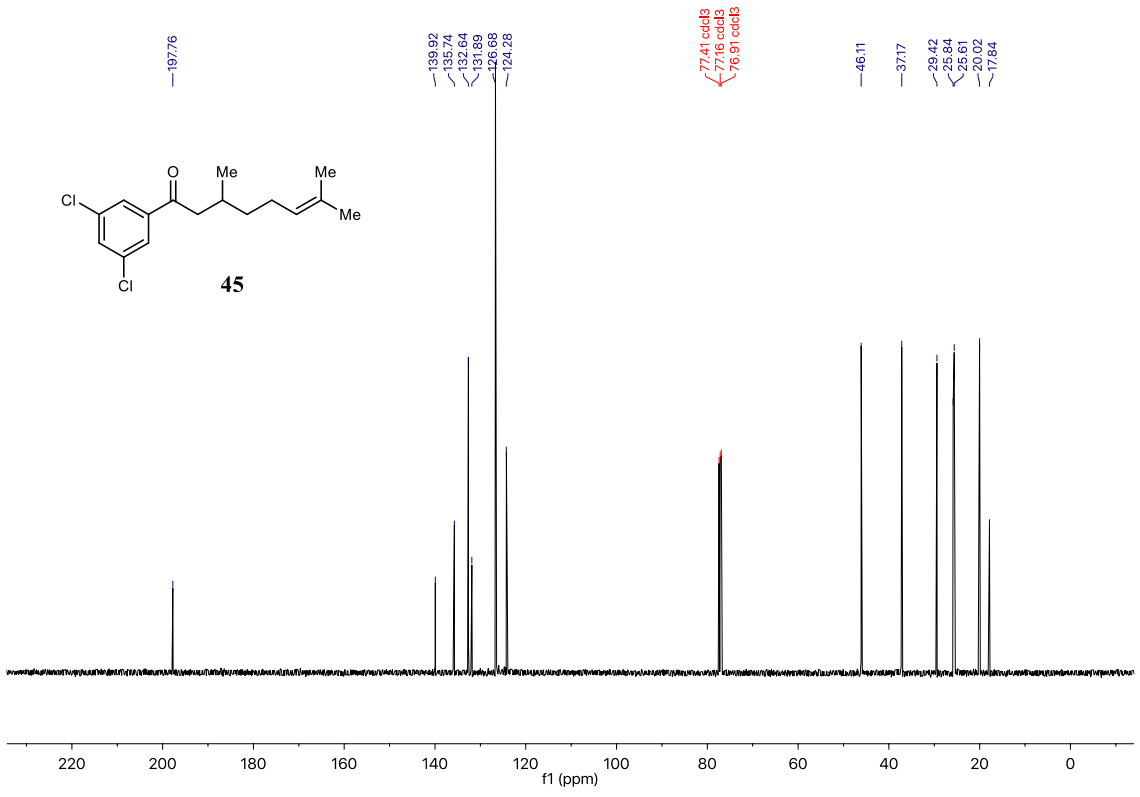
197.76
139.92
135.74
132.64
131.89
126.68
124.28
77.41 cdd3
77.16 cdd3
76.91 cdd3
46.11
37.17
29.42
25.84
25.61
20.02
17.84
Cl
O
Me
Me
Me
Cl
45
220
200
180
160
140
120
100
80
60
40
20
0
f1 (ppm)

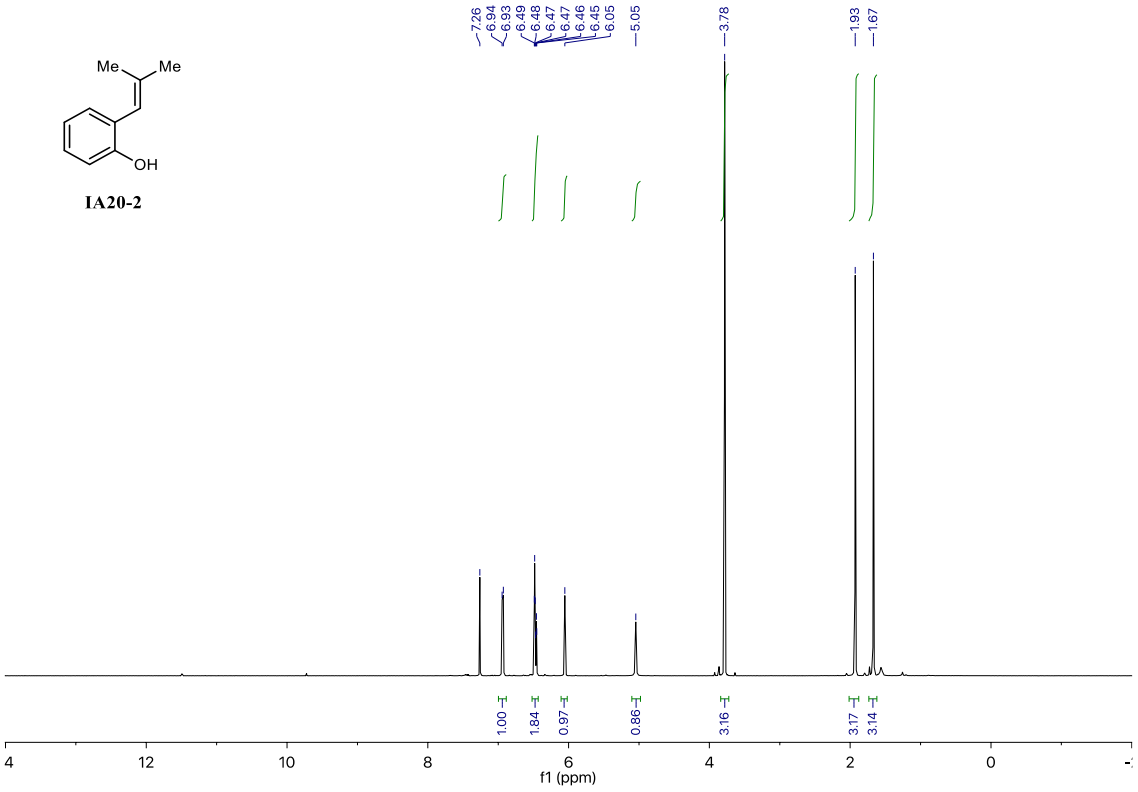
Me
Me
OH
IA20-2
7.26
6.94
6.93
6.49
6.48
6.47
6.47
6.46
6.45
6.05
5.05
3.78
1.93
1.67
1.00
1.84
0.97
0.86
3.16
3.17
3.14
4
12
10
8
6
4
2
0
f1 (ppm)

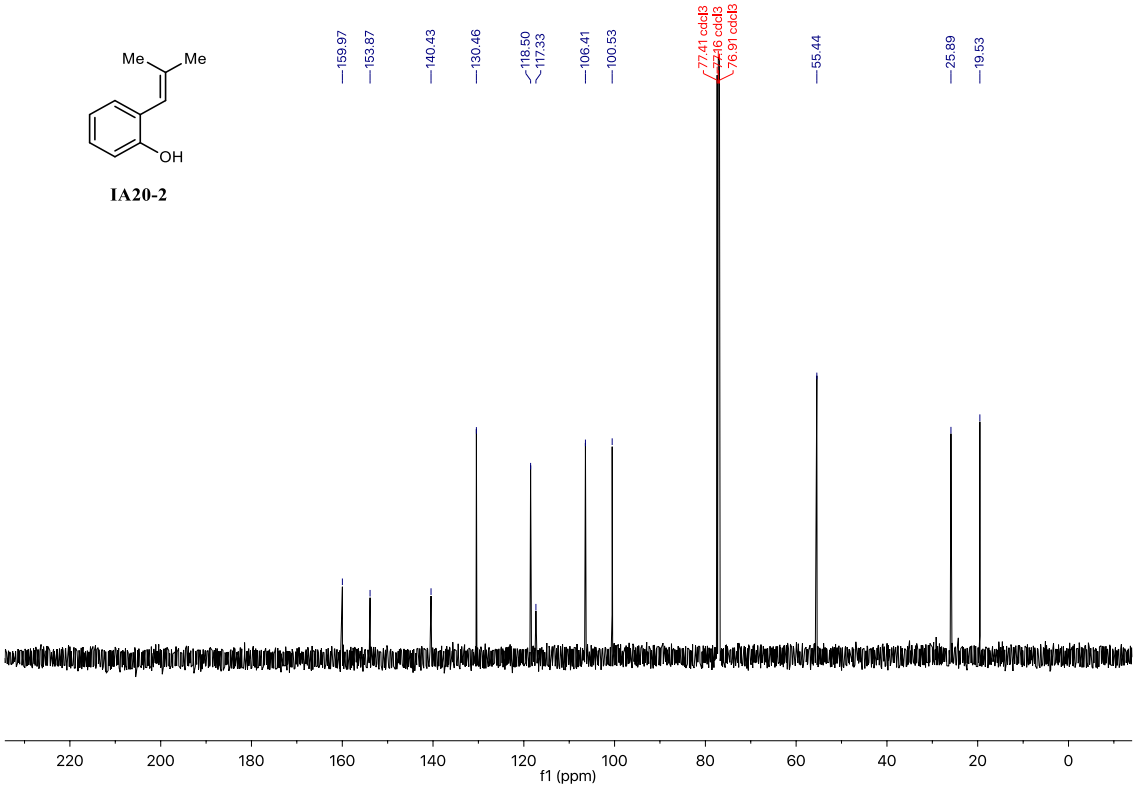
Me
Me
OH
IA20-2
159.97
153.87
140.43
130.46
118.50
117.33
106.41
100.53
77.41 cdcl3
77.16 cdcl3
76.91 cdcl3
55.44
25.89
19.53
220
200
180
160
140
120
100
80
60
40
20
0
f1 (ppm)

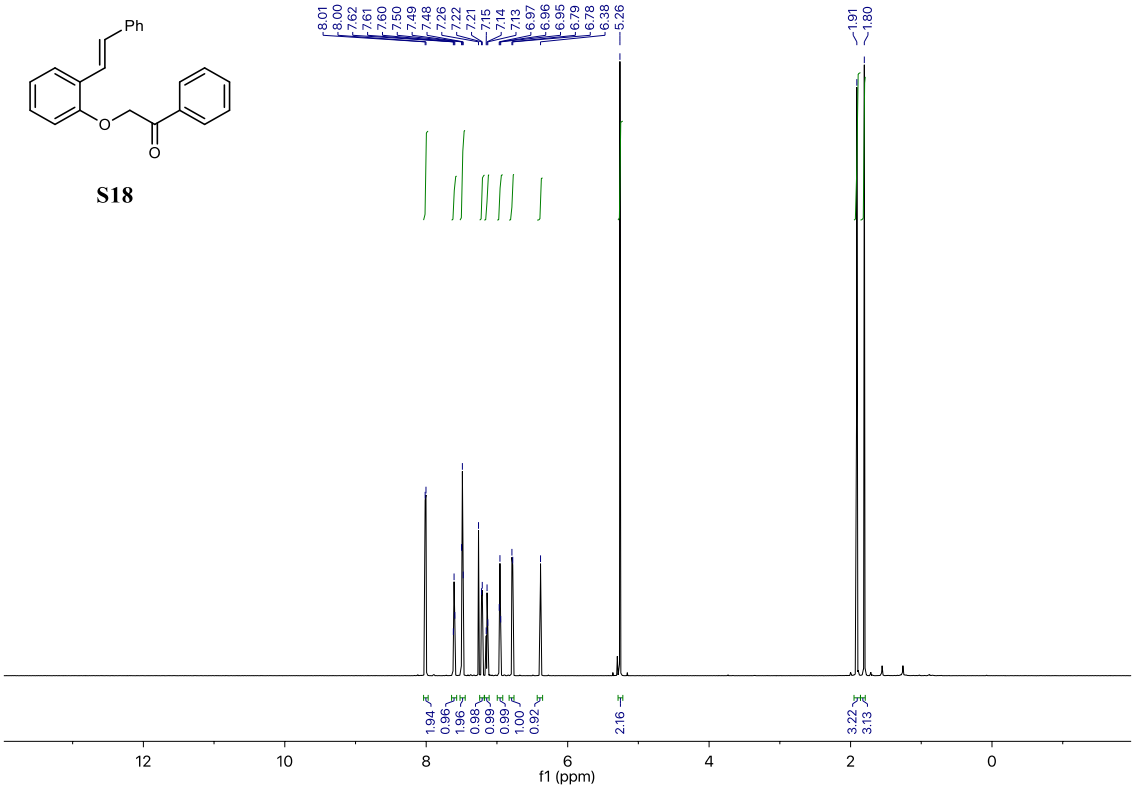
Ph
O
O
S18
8.01
8.00
7.62
7.61
7.60
7.50
7.49
7.48
7.26
7.22
7.21
7.15
7.14
7.13
6.97
6.96
6.95
6.79
6.78
6.38
5.26
1.91
1.80
1.94
0.96
1.96
0.98
0.99
0.99
1.00
0.92
2.16
3.22
3.13
12
10
8
6
4
2
0
f1 (ppm)

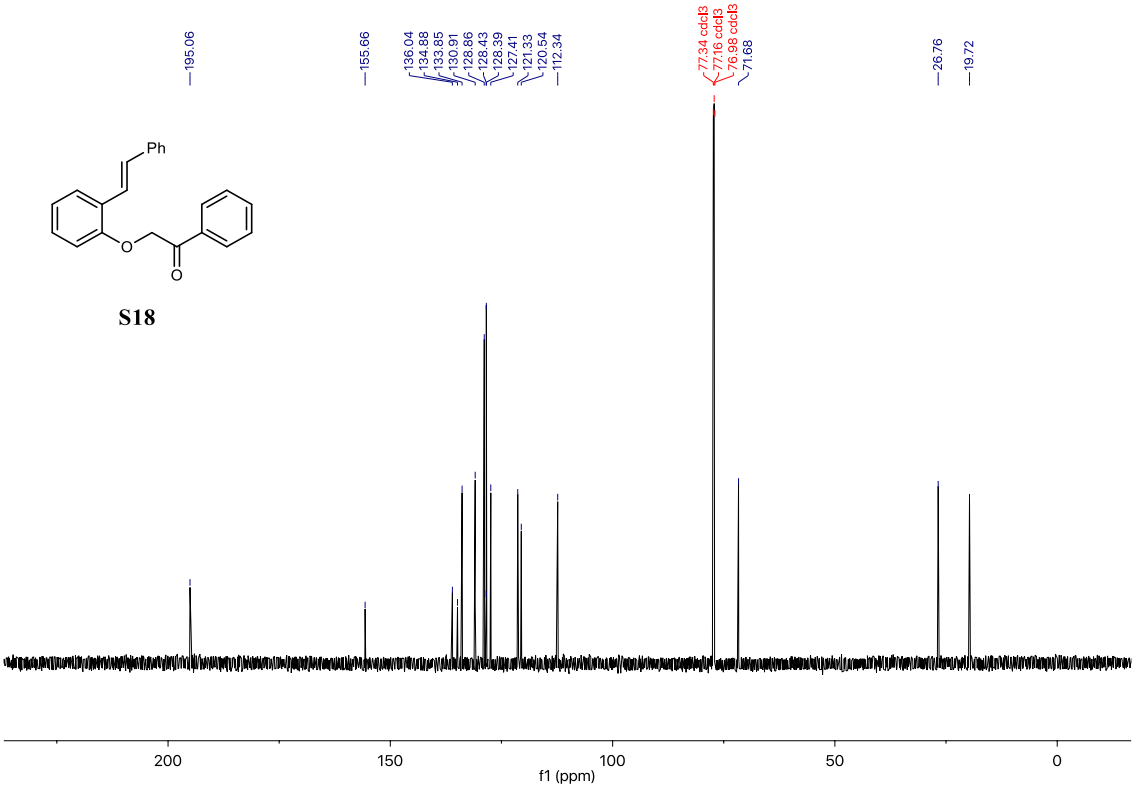
195.06
155.66
136.04
134.88
133.85
130.91
128.86
128.43
128.39
127.41
121.33
120.54
112.34
77.34 cdcl3
77.16 cdcl3
76.98 cdcl3
71.68
26.76
19.72
Ph
O
O
S18
200
150
100
50
0
f1 (ppm)

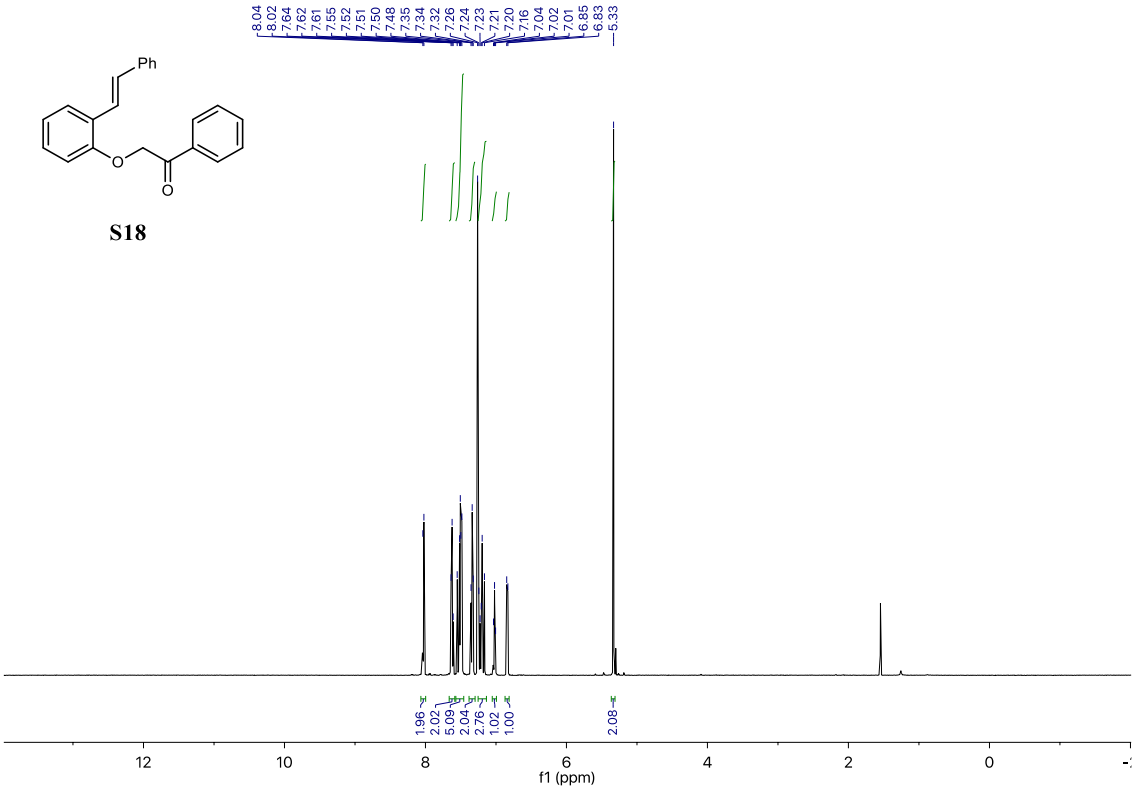
8.04
8.02
7.64
7.62
7.61
7.55
7.52
7.51
7.50
7.48
7.35
7.34
7.32
7.26
7.24
7.23
7.21
7.20
7.16
7.04
7.02
7.01
6.85
6.83
5.33
Ph
O
O
1.96
2.02
5.09
2.04
2.76
1.02
1.00
2.08
12
10
8
6
4
2
0
f1 (ppm)

S18

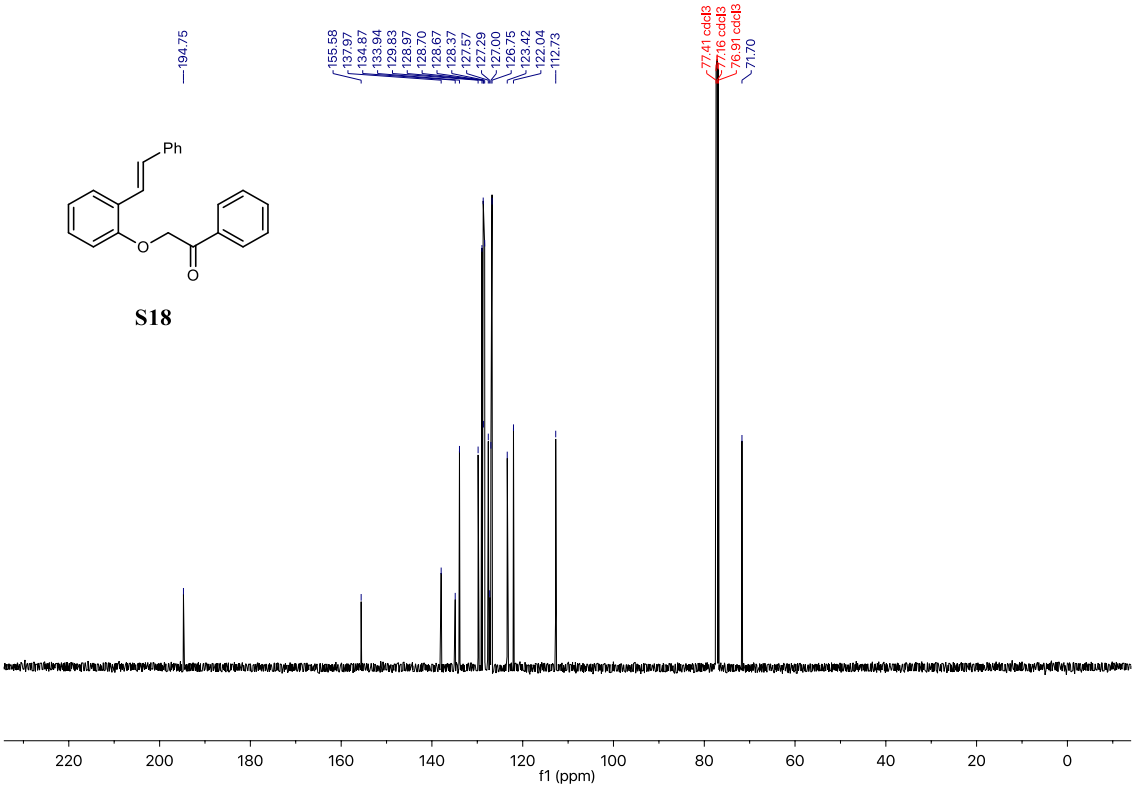
194.75
155.58
137.97
134.87
133.94
129.83
128.97
128.70
128.67
128.37
127.57
127.29
127.00
126.75
123.42
122.04
112.73
77.41 cdcl3
77.16 cdcl3
76.91 cdcl3
71.70
Ph
O
O
220
200
180
160
140
120
100
80
60
40
20
0
f1 (ppm)

S18

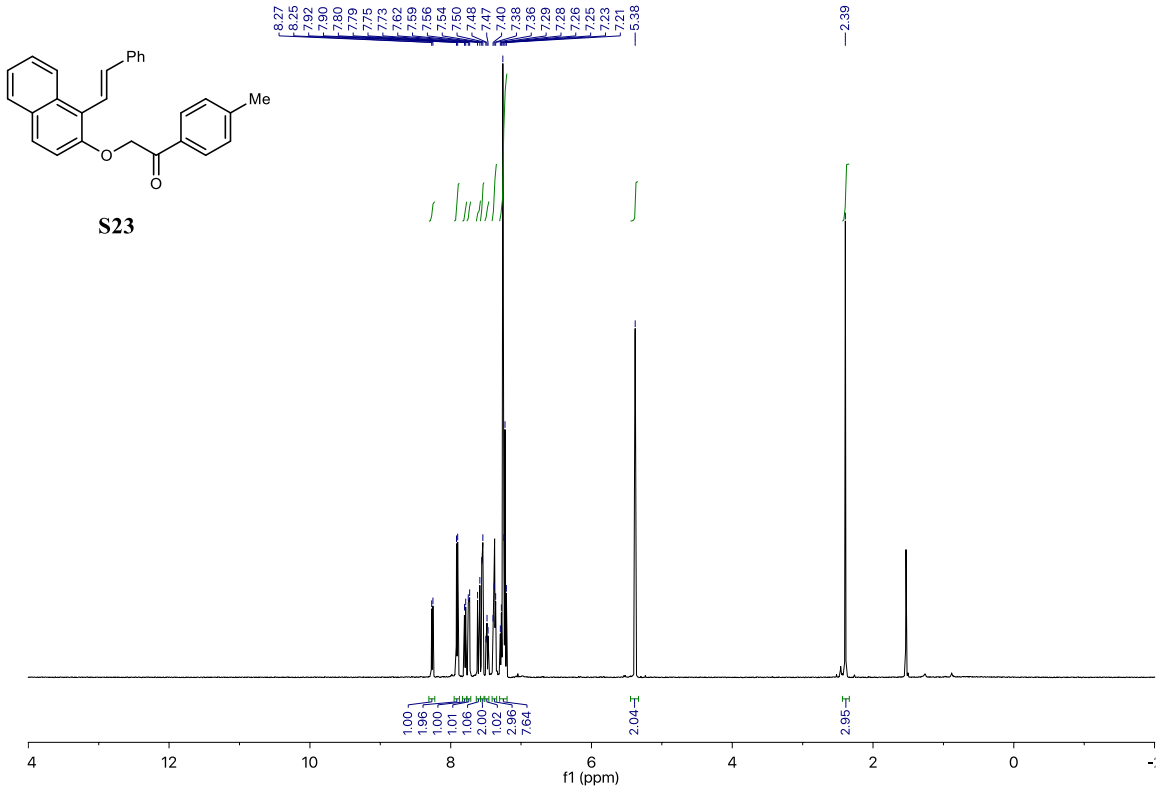
Ph
Me
O
O
S23
8.27
8.25
7.92
7.90
7.80
7.79
7.75
7.73
7.62
7.59
7.56
7.54
7.50
7.48
7.47
7.40
7.38
7.36
7.29
7.28
7.26
7.25
7.23
7.21
5.38
2.39
1.00
1.96
1.00
1.01
1.06
2.00
1.02
2.96
7.64
2.04
2.95
4
12
10
8
6
4
2
0
f1 (ppm)

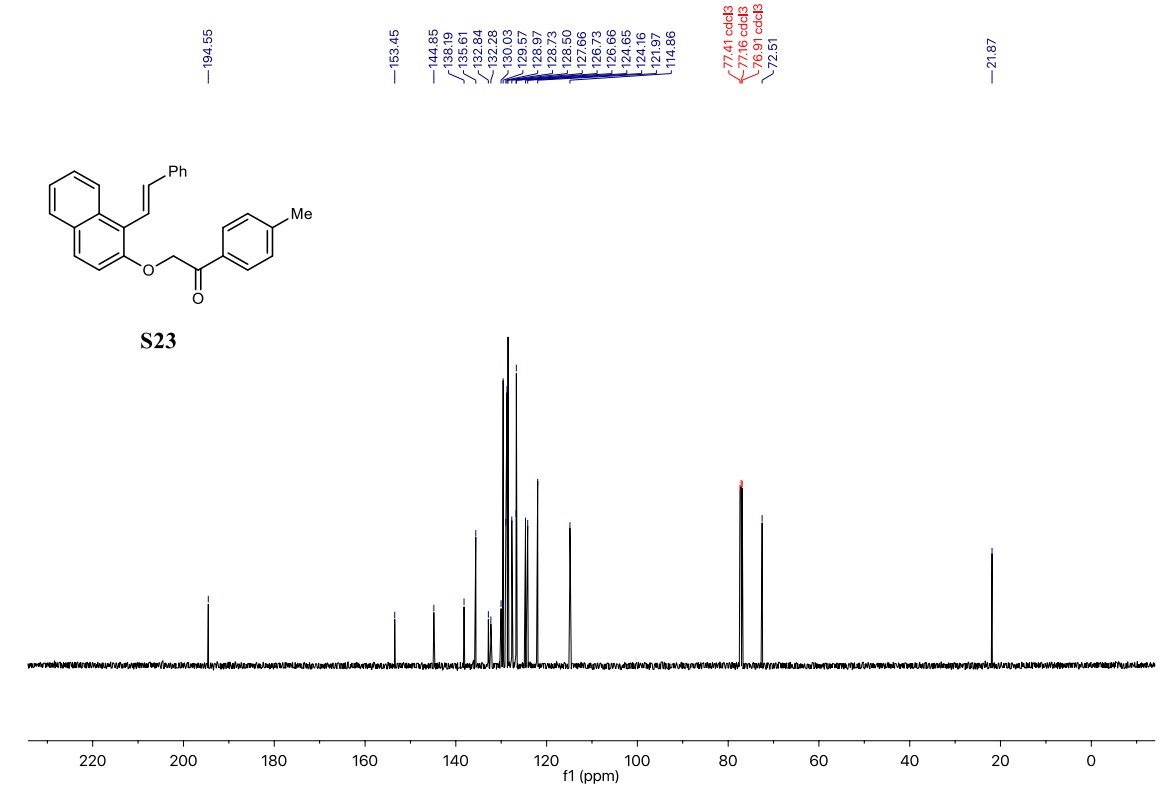
194.55
153.45
144.85
138.19
135.61
132.84
132.28
130.03
129.57
128.97
128.73
128.50
127.66
126.73
126.66
124.65
124.16
121.97
114.86
77.41 cdd3
77.16 cdd3
76.91 cdd3
72.51
21.87
Ph
Me
O
O
S23
220
200
180
160
140
120
100
80
60
40
20
0
f1 (ppm)

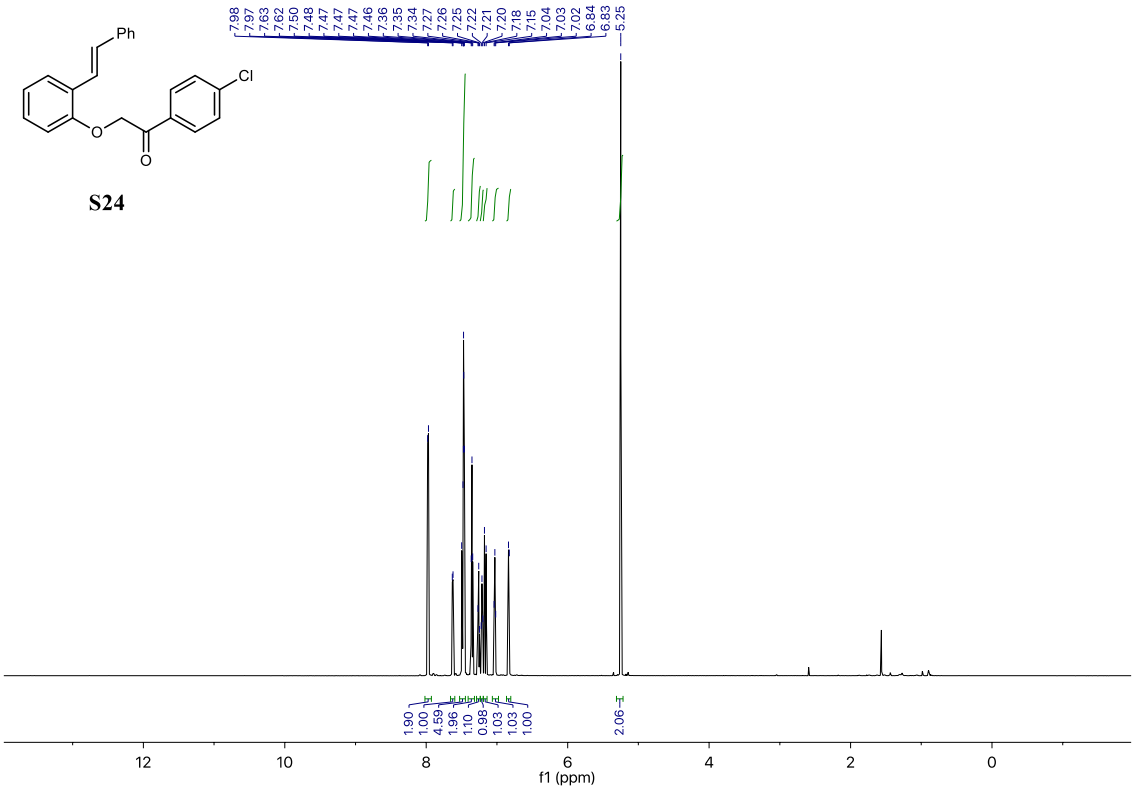
Ph
Cl
O
O
7.98
7.97
7.63
7.62
7.50
7.48
7.47
7.47
7.47
7.46
7.36
7.35
7.34
7.27
7.26
7.25
7.22
7.21
7.20
7.18
7.15
7.04
7.03
7.02
6.84
6.83
5.25
1.90
1.00
4.59
1.96
1.10
0.98
1.03
1.03
1.00
2.06
12
10
8
6
4
2
0
f1 (ppm)

S24

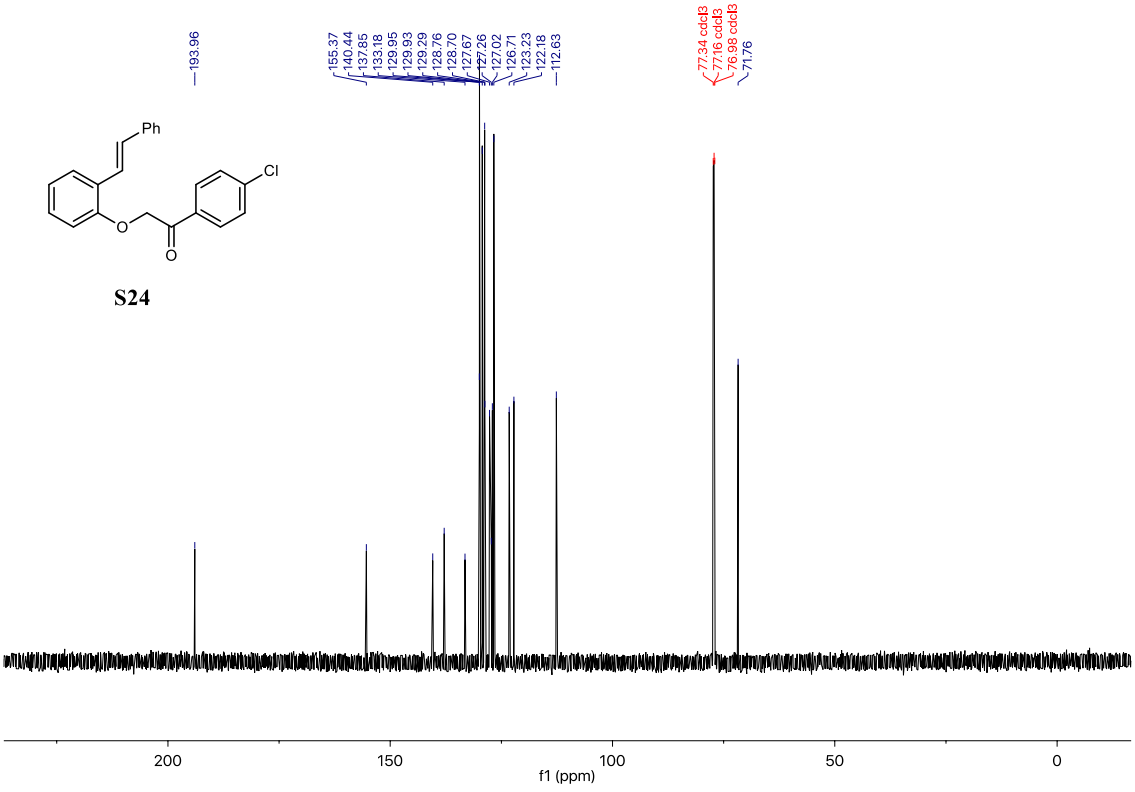
Ph
Cl
O
O
193.96
155.37
140.44
137.85
133.18
129.95
129.93
129.29
128.76
128.70
127.67
127.26
127.02
126.71
123.23
122.18
112.63
77.34 cdcl3
77.16 cdcl3
76.98 cdcl3
71.76
200
150
100
50
0
f1 (ppm)

S24

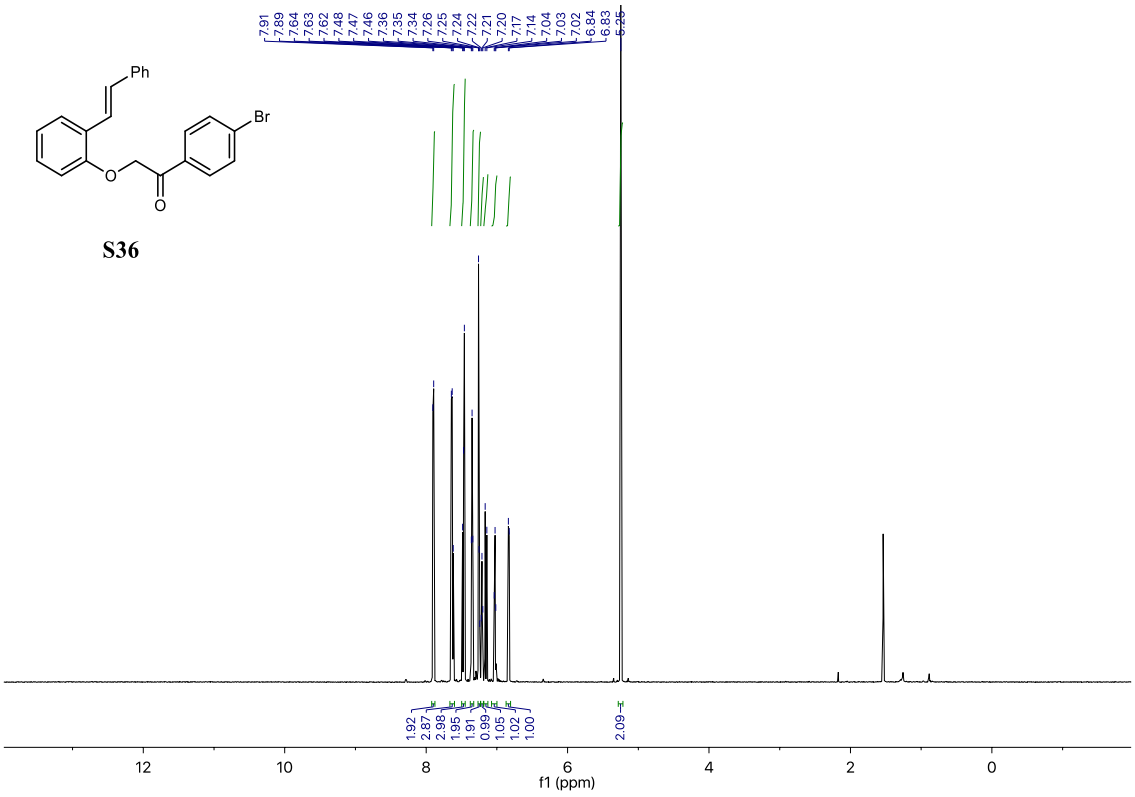
7.91
7.89
7.64
7.63
7.62
7.48
7.47
7.46
7.36
7.35
7.34
7.26
7.25
7.24
7.22
7.21
7.20
7.17
7.14
7.04
7.03
7.02
6.84
6.83
6.26
Ph
Br
O
O
1.92
2.87
2.98
1.95
1.91
0.99
1.05
1.02
1.00
2.09
12
10
8
6
4
2
0
f1 (ppm)

S36

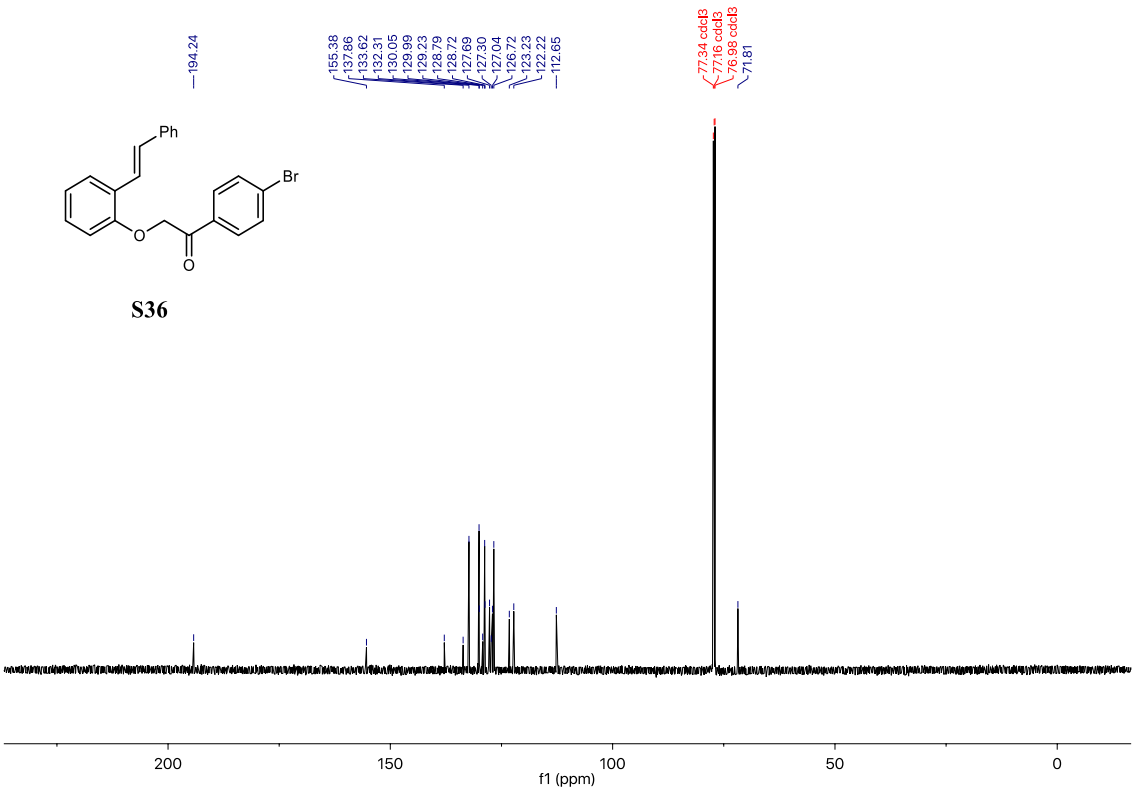
194.24
155.38
137.86
133.62
132.31
130.05
129.99
129.23
128.79
128.72
127.69
127.30
127.04
126.72
123.23
122.22
112.65
77.34 cdcl3
77.16 cdcl3
76.98 cdcl3
71.81
Ph
Br
O
O
200
150
100
50
0
f1 (ppm)

S36

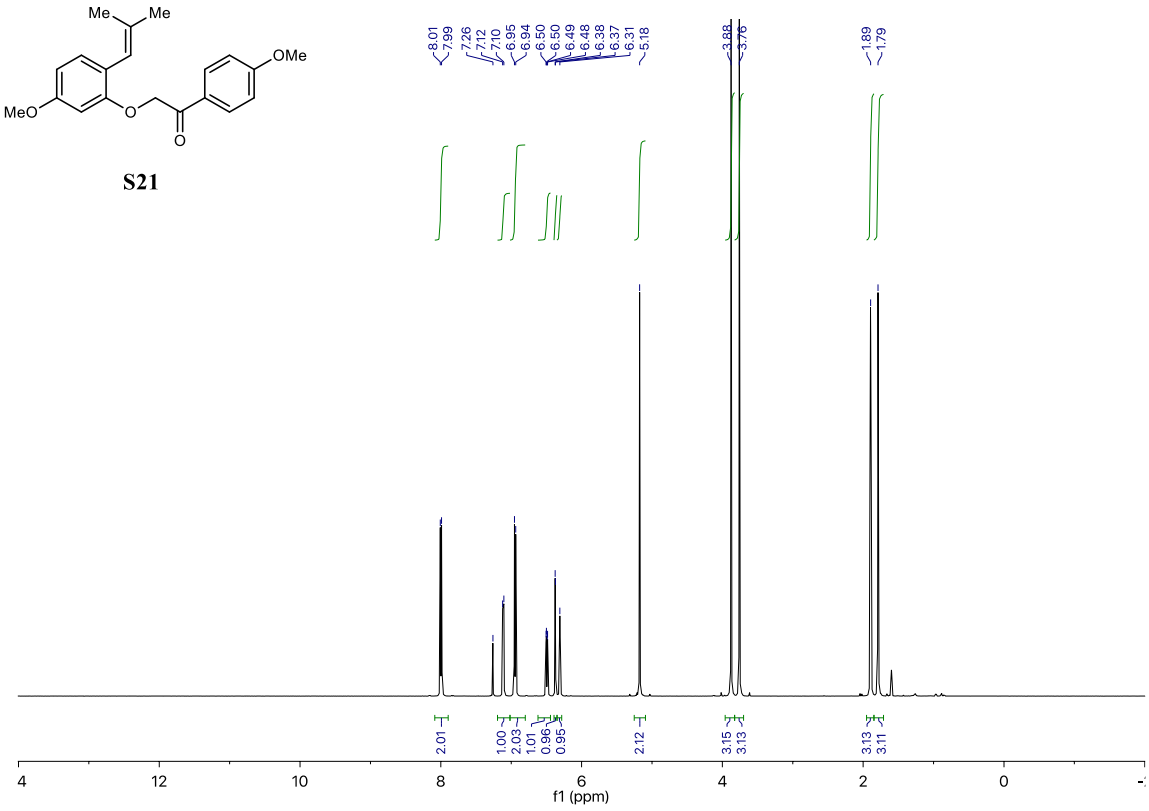
Me
Me
OMe
MeO
O
O
8.01
7.99
7.26
7.12
7.10
6.95
6.94
6.50
6.50
6.49
6.48
6.38
6.37
6.31
5.18
3.88
3.76
1.89
1.79
2.01
1.00
2.03
1.01
0.96
0.95
2.12
3.15
3.13
3.13
3.11
4
12
10
8
6
4
2
0
f1 (ppm)

S21

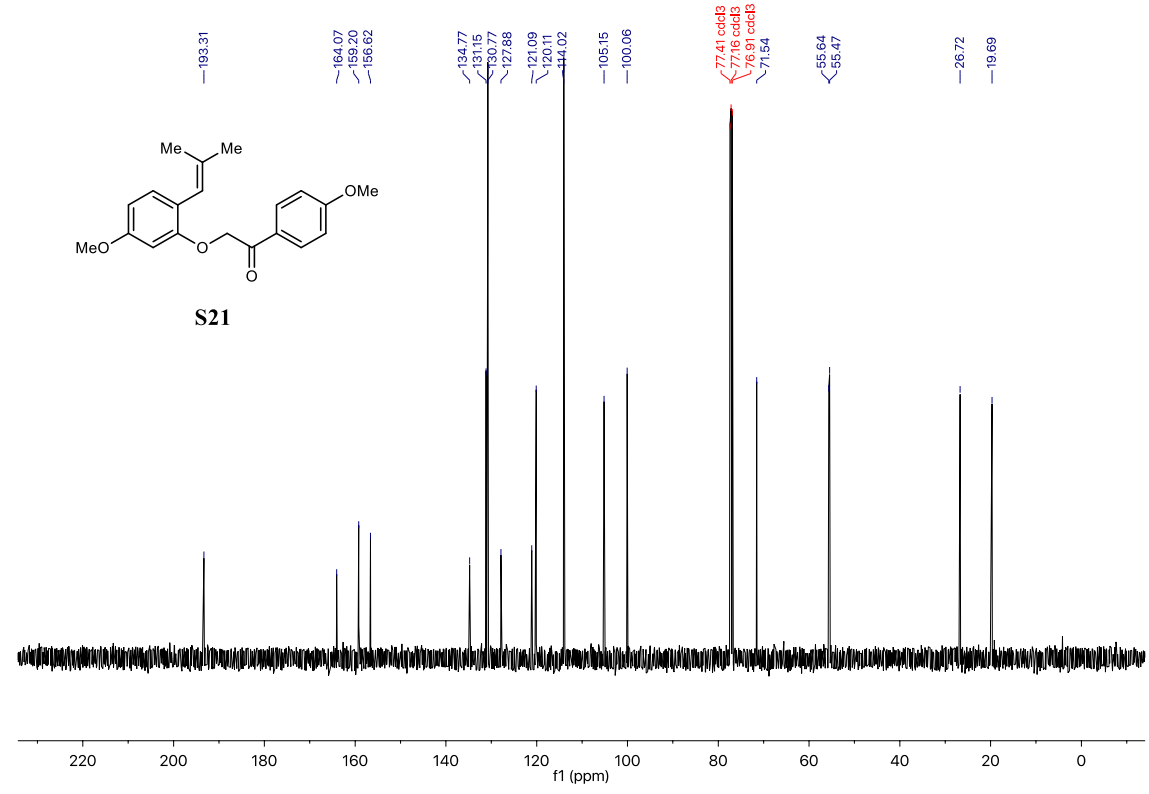
193.31
164.07
159.20
156.62
134.77
131.15
130.77
127.88
121.09
120.11
114.02
105.15
100.06
77.41 cdcl3
77.16 cdcl3
76.91 cdcl3
71.54
55.64
55.47
26.72
19.69
Me
Me
OMe
MeO
O
O
220
200
180
160
140
120
100
80
60
40
20
0
f1 (ppm)

S21

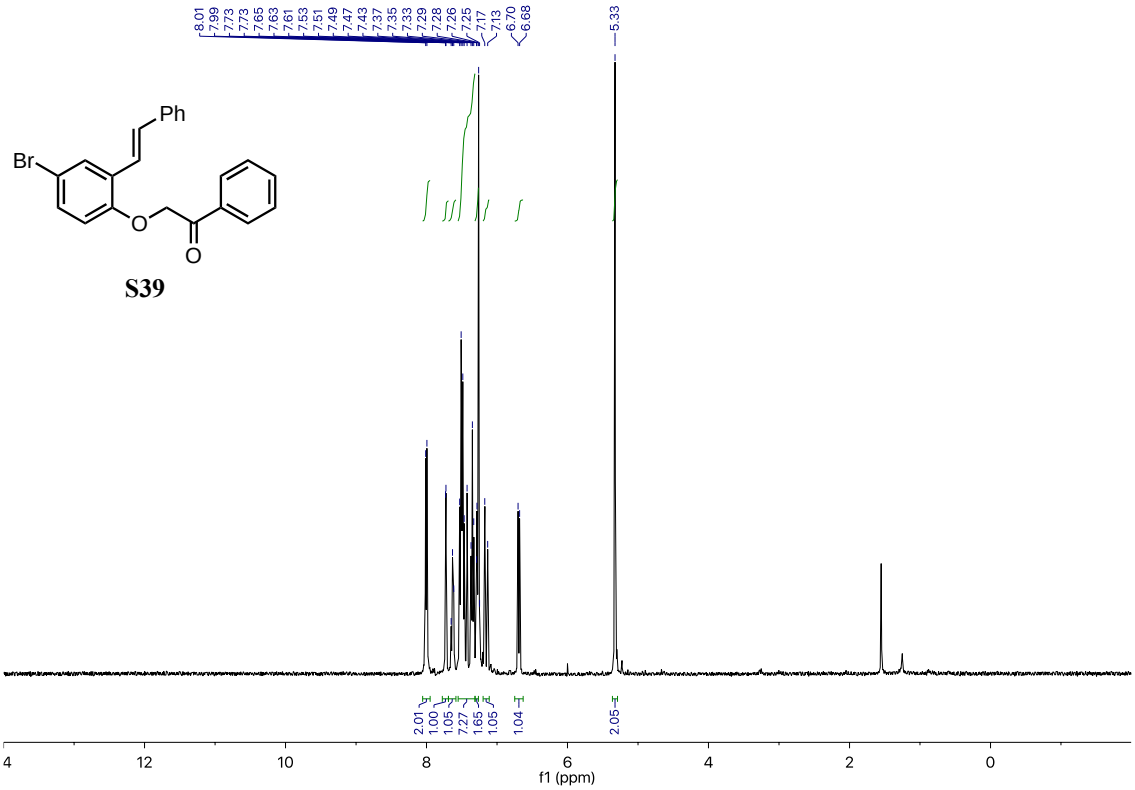
8.01
7.99
7.73
7.73
7.65
7.63
7.61
7.53
7.51
7.49
7.47
7.43
7.37
7.35
7.33
7.29
7.28
7.26
7.25
7.17
7.13
6.70
6.68
5.33
Ph
Br
O
O
2.01
1.00
1.05
1.05
7.27
1.65
1.05
1.04
2.05
4
12
10
8
6
4
2
0
f1 (ppm)

S39

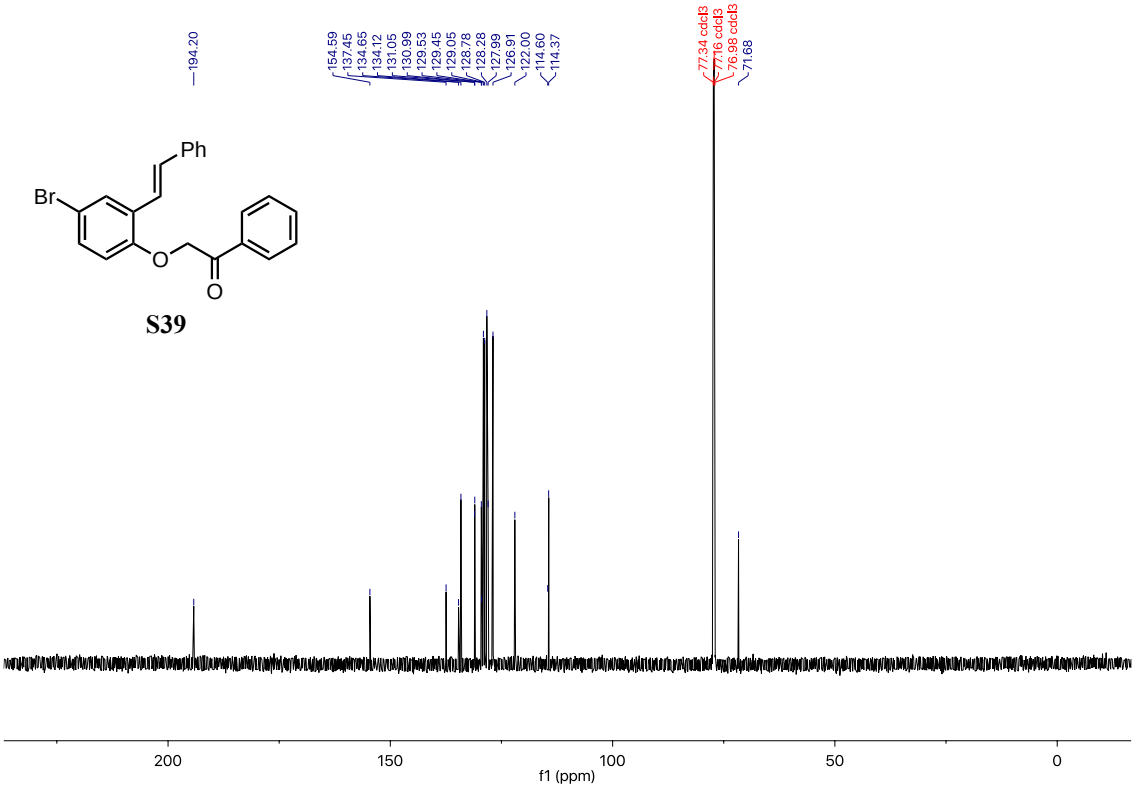
194.20
154.59
137.45
134.65
134.12
131.05
130.99
129.53
129.45
129.05
128.78
128.28
127.99
126.91
122.00
114.60
114.37
77.34 cdcl3
77.16 cdcl3
76.98 cdcl3
71.68
Ph
Br
O
O
200
150
100
50
0
f1 (ppm)

S39

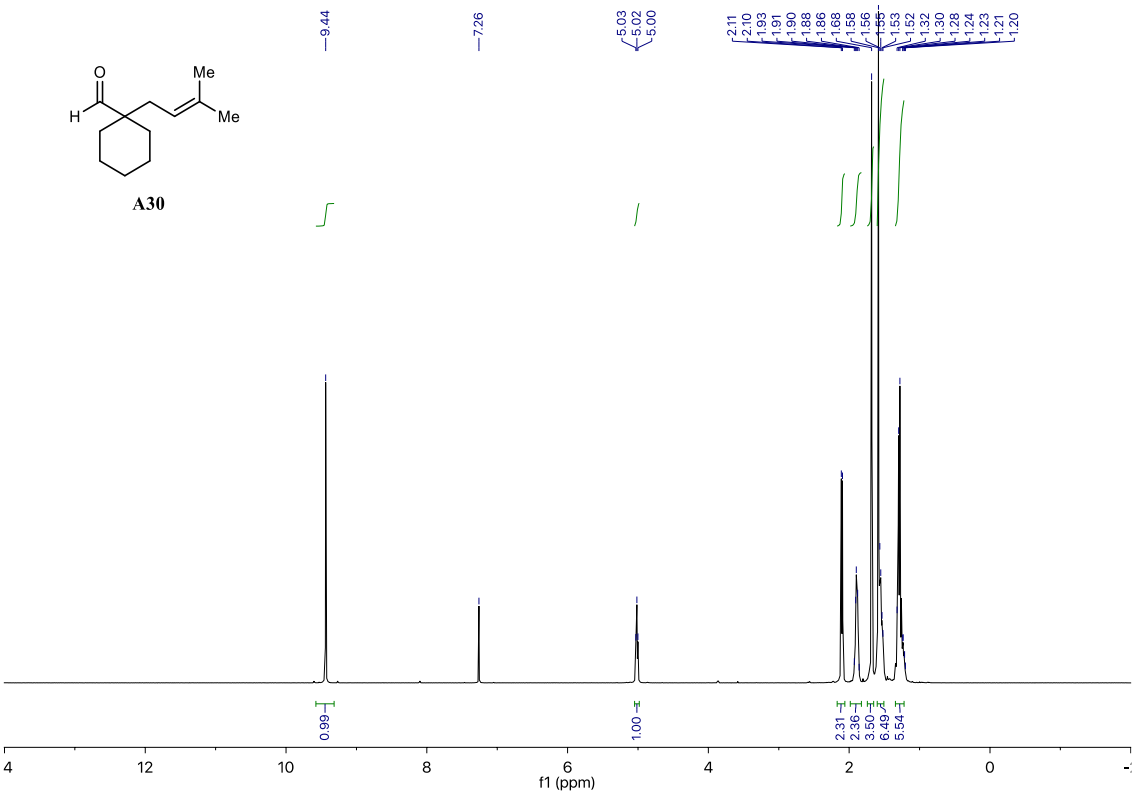
O
H
Me
Me
A30
9.44
7.26
5.03
5.02
5.00
2.11
2.10
1.93
1.91
1.90
1.88
1.86
1.68
1.58
1.56
1.55
1.53
1.52
1.32
1.30
1.28
1.24
1.23
1.21
1.20
0.99
1.00
2.31
2.36
3.50
6.49
5.54
f1 (ppm)

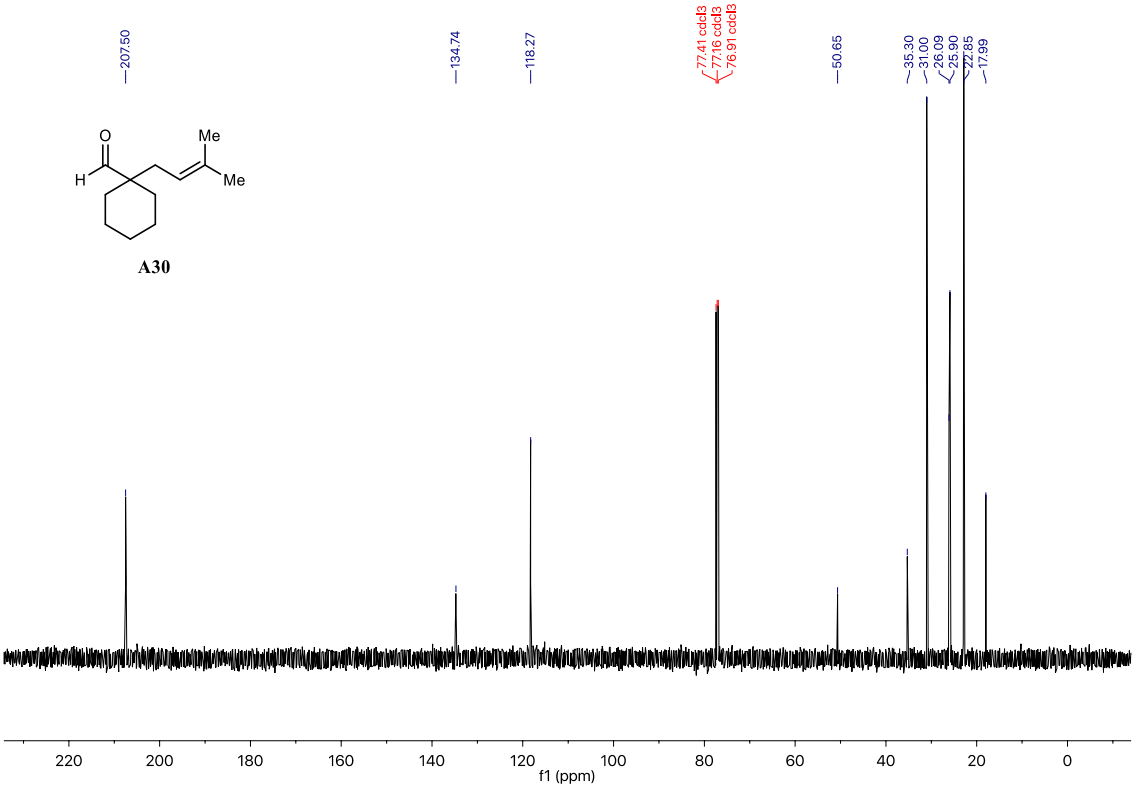
O
H
Me
Me
A30
207.50
134.74
118.27
77.41 cdcl3
77.16 cdcl3
76.91 cdcl3
50.65
35.30
31.00
26.09
25.90
22.85
17.99
f1 (ppm)

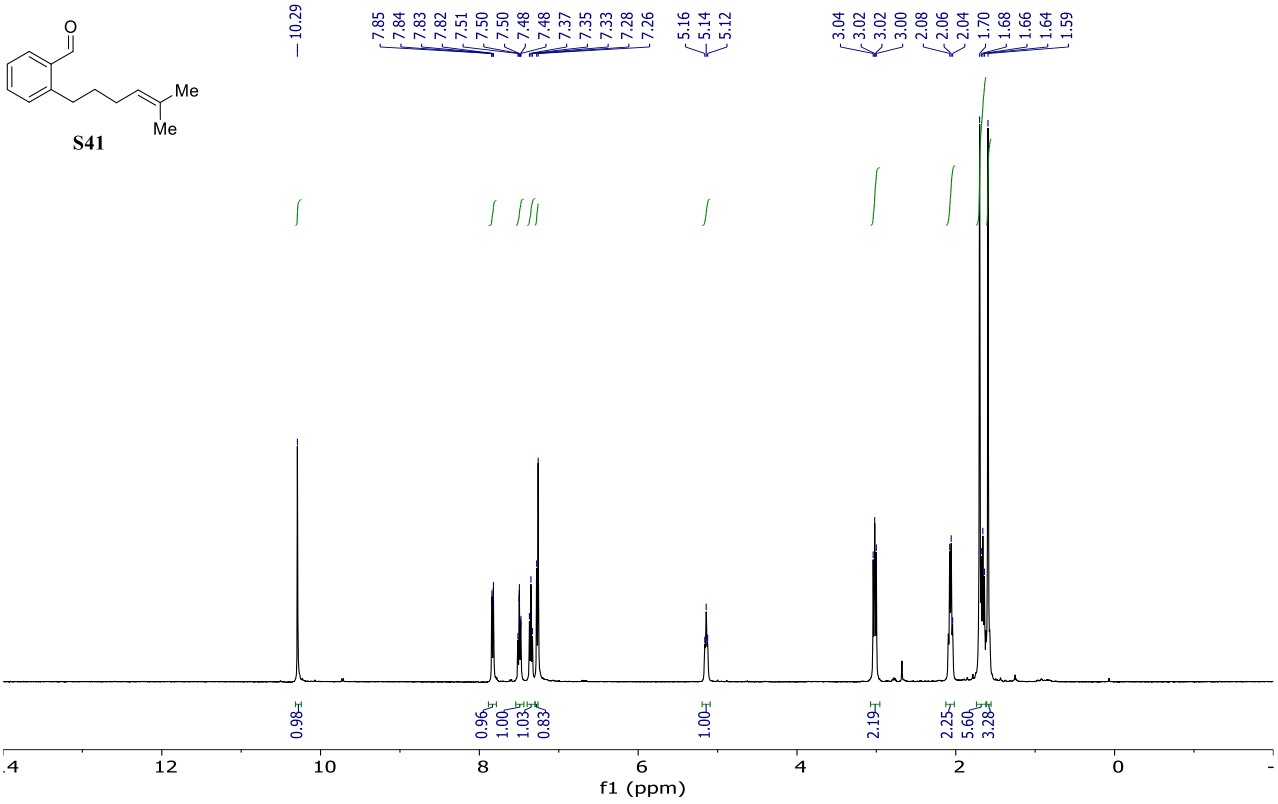
S41
10.29
7.85
7.84
7.83
7.82
7.51
7.50
7.50
7.48
7.48
7.37
7.35
7.33
7.28
7.26
5.16
5.14
5.12
3.04
3.02
3.02
3.00
2.08
2.06
2.04
1.70
1.68
1.66
1.64
1.59
0.98
0.96
1.00
1.03
0.83
1.00
2.19
2.25
5.60
3.28
f1 (ppm)

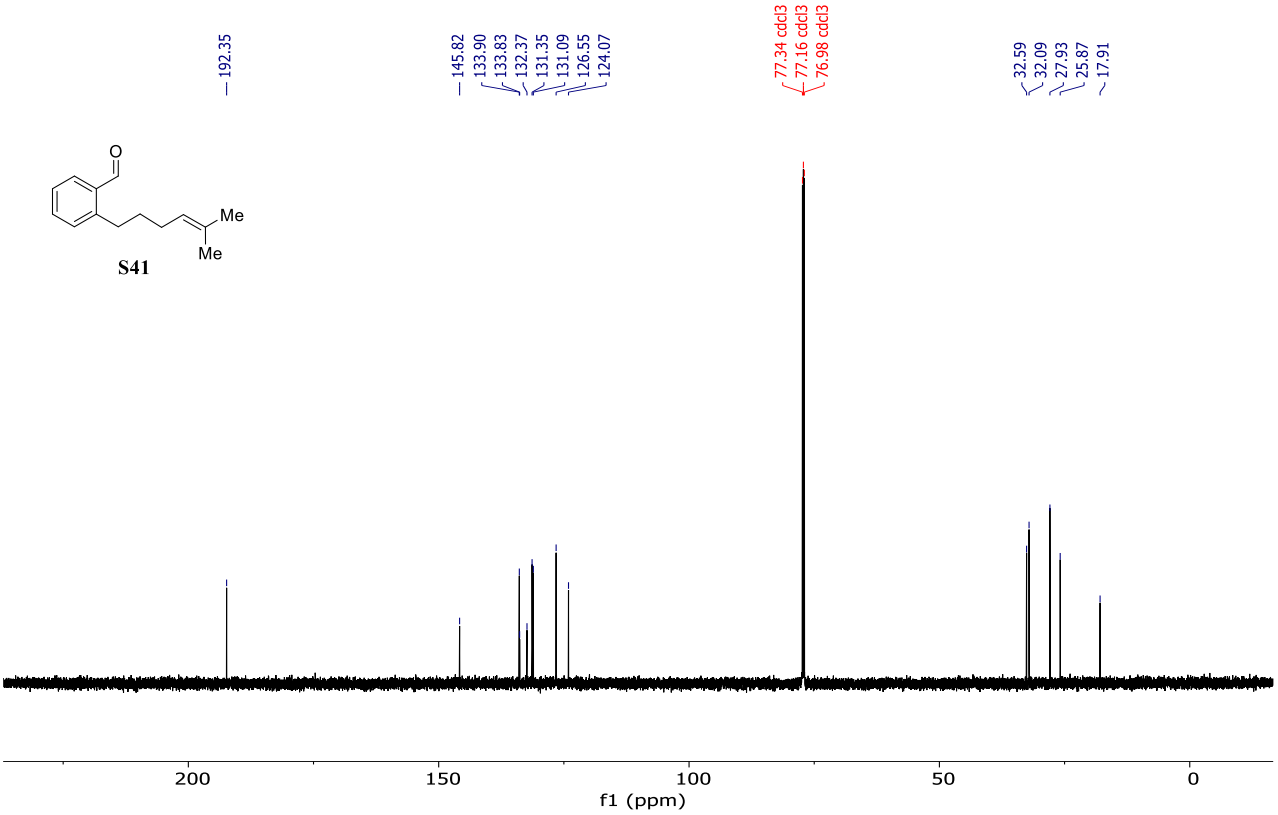
S41
192.35
145.82
133.90
133.83
132.37
131.35
131.09
126.55
124.07
77.34 cdcl3
77.16 cdcl3
76.98 cdcl3
32.59
32.09
27.93
25.87
17.91
f1 (ppm)

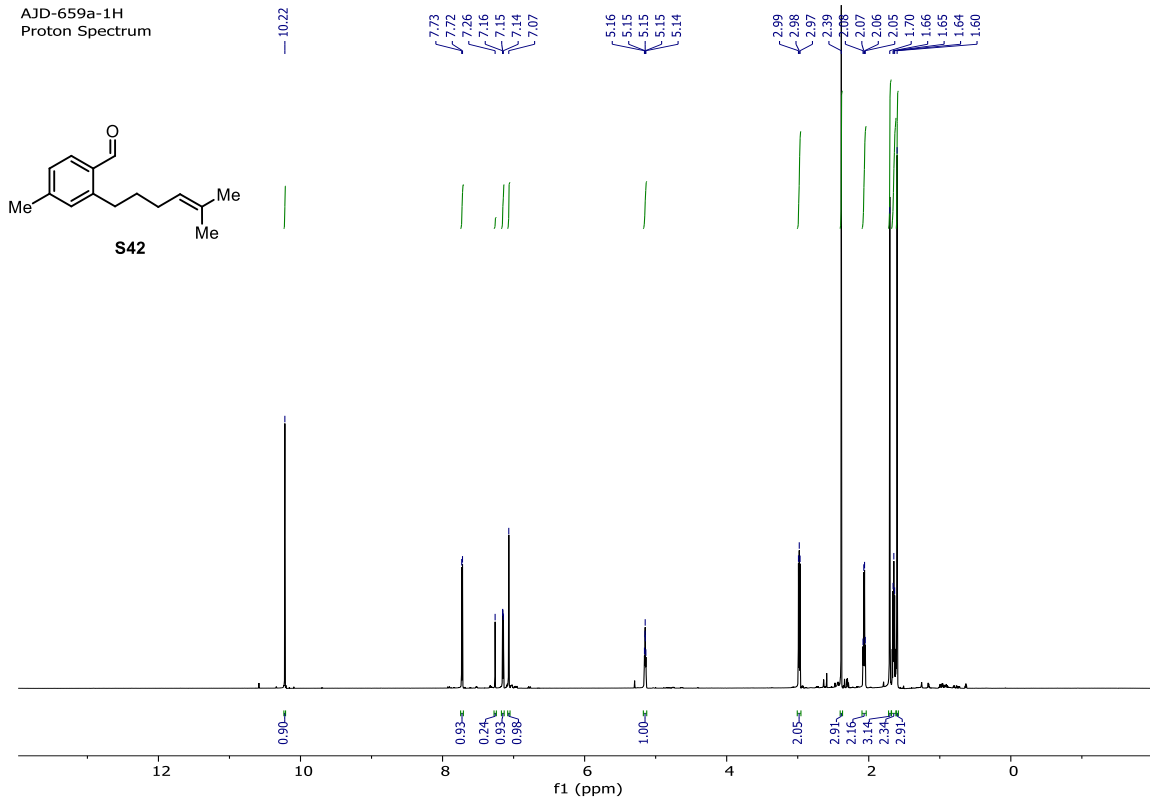
AJD-659a-1H
Proton Spectrum
10.22
7.73
7.72
7.26
7.16
7.15
7.14
7.07
5.16
5.15
5.15
5.15
5.14
2.99
2.98
2.97
2.39
2.08
2.07
2.06
2.05
1.70
1.66
1.65
1.64
1.60
O
Me
Me
Me
S42
0.90
0.93
0.24
0.93
0.98
1.00
2.05
2.91
2.16
3.14
2.34
2.91
12
10
8
6
4
2
0
f1 (ppm)

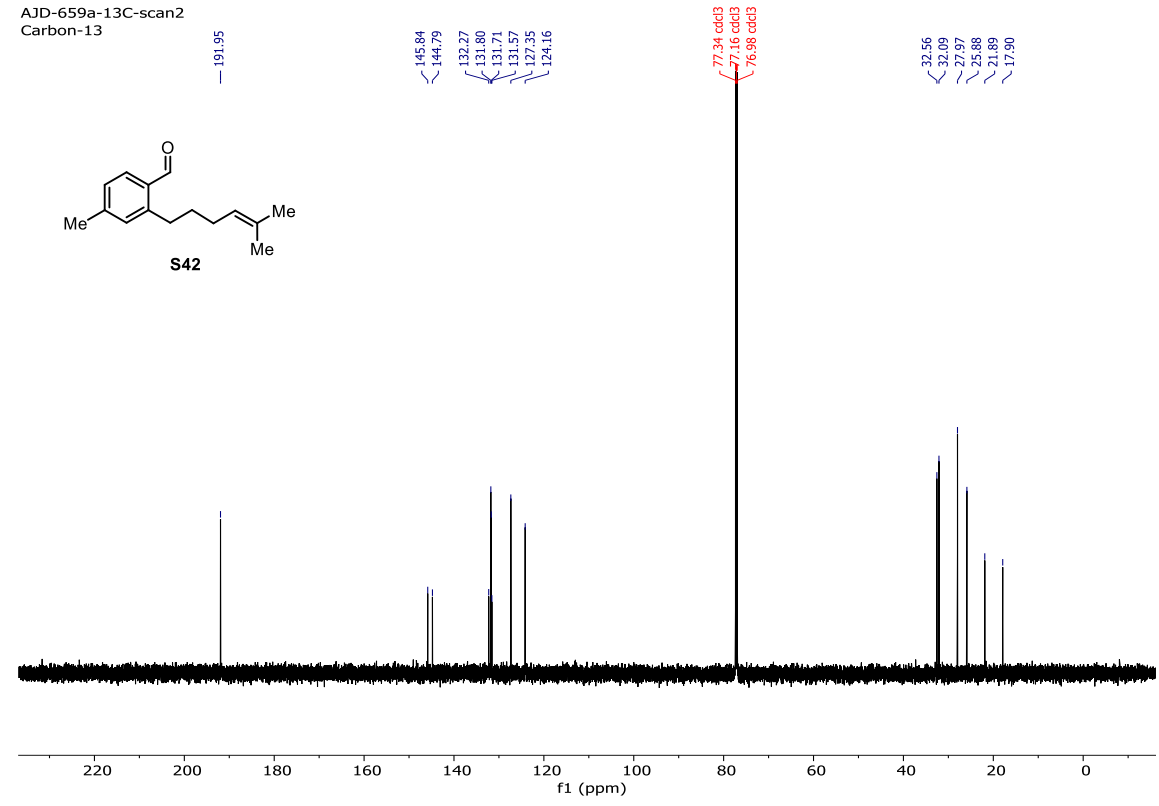
AJD-659a-13C-scan2
Carbon-13
191.95
145.84
144.79
132.27
131.80
131.71
131.57
127.35
124.16
77.34 cdcl3
77.16 cdcl3
76.98 cdcl3
32.56
32.09
27.97
25.88
21.89
17.90
O
Me
Me
Me
S42
220
200
180
160
140
120
100
80
60
40
20
0
f1 (ppm)

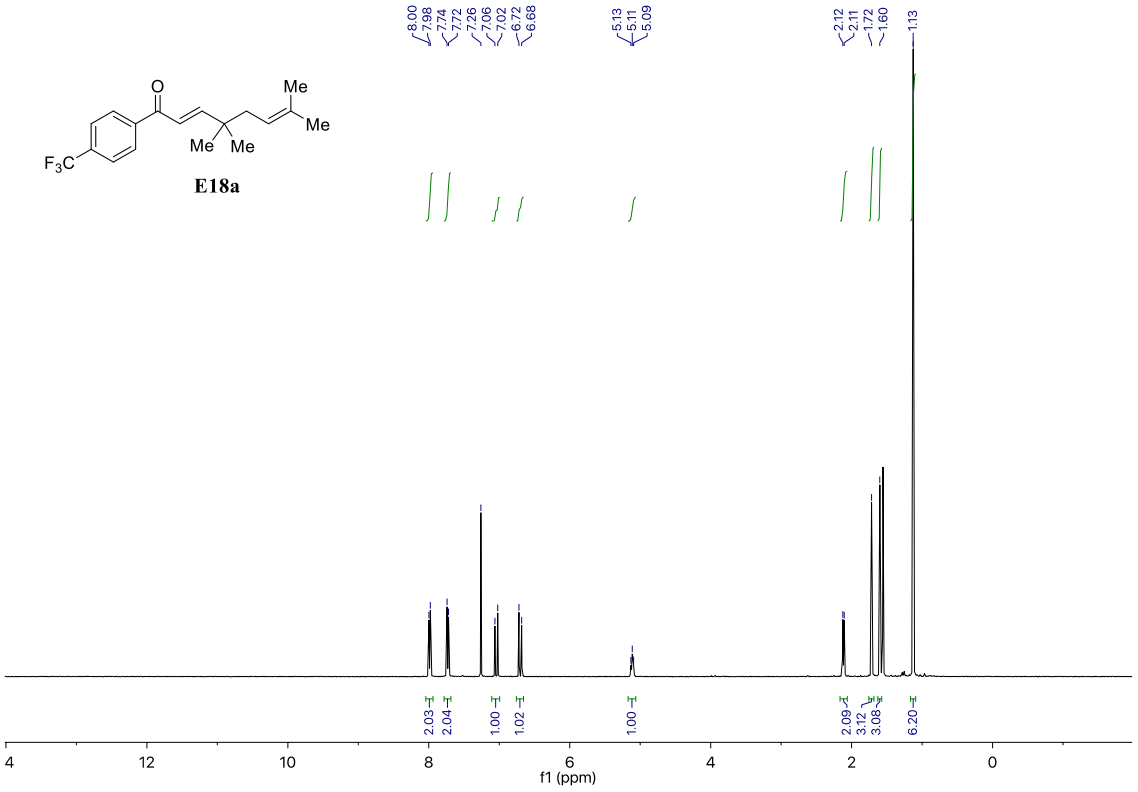
8.00
7.98
7.74
7.72
7.26
7.06
7.02
6.72
6.68
5.13
5.11
5.09
2.12
2.11
1.72
1.60
1.13
O
Me
Me
Me
Me
F3C
2.03
2.04
1.00
1.02
1.00
2.09
3.12
3.08
6.20
4
12
10
8
6
4
2
0
f1 (ppm)

E18a

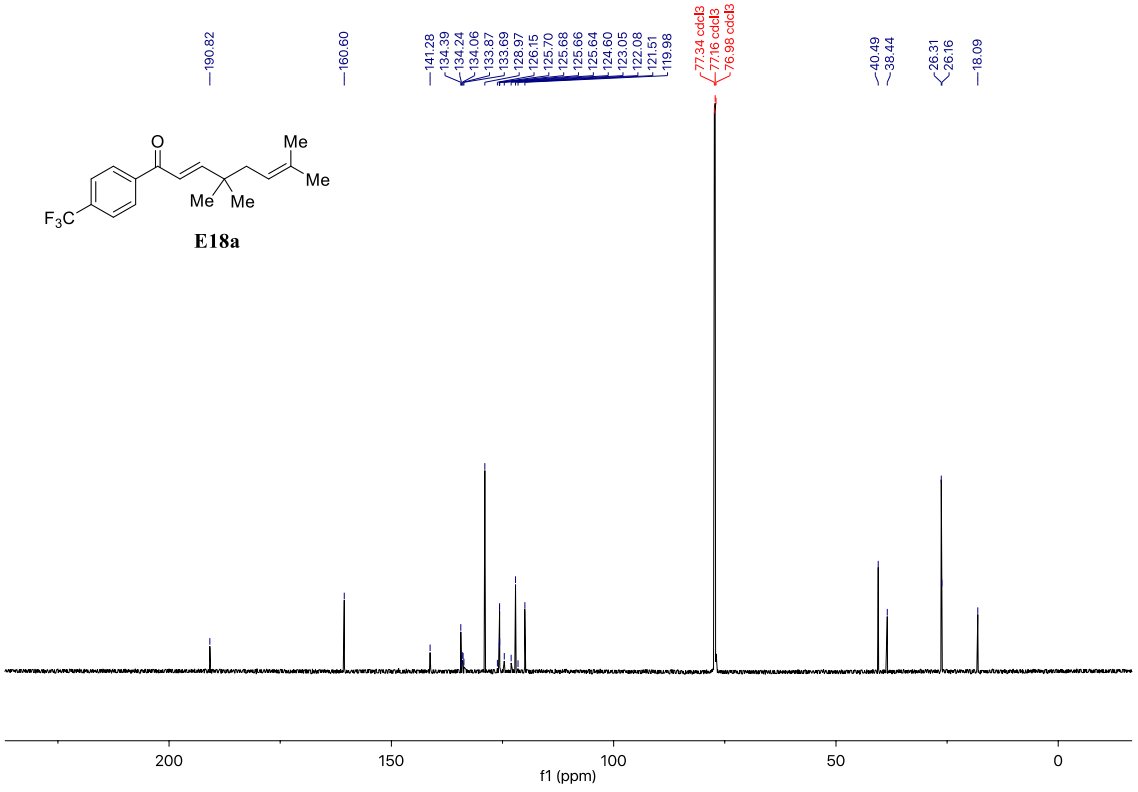
190.82
160.60
141.28
134.39
134.24
134.06
133.87
133.69
128.97
126.15
125.70
125.68
125.66
125.64
124.60
123.05
122.08
121.51
119.98
77.34 cdcl3
77.16 cdcl3
76.98 cdcl3
40.49
38.44
26.31
26.16
18.09
O
Me
Me
Me
Me
F3C
200
150
100
50
0
f1 (ppm)

E18a

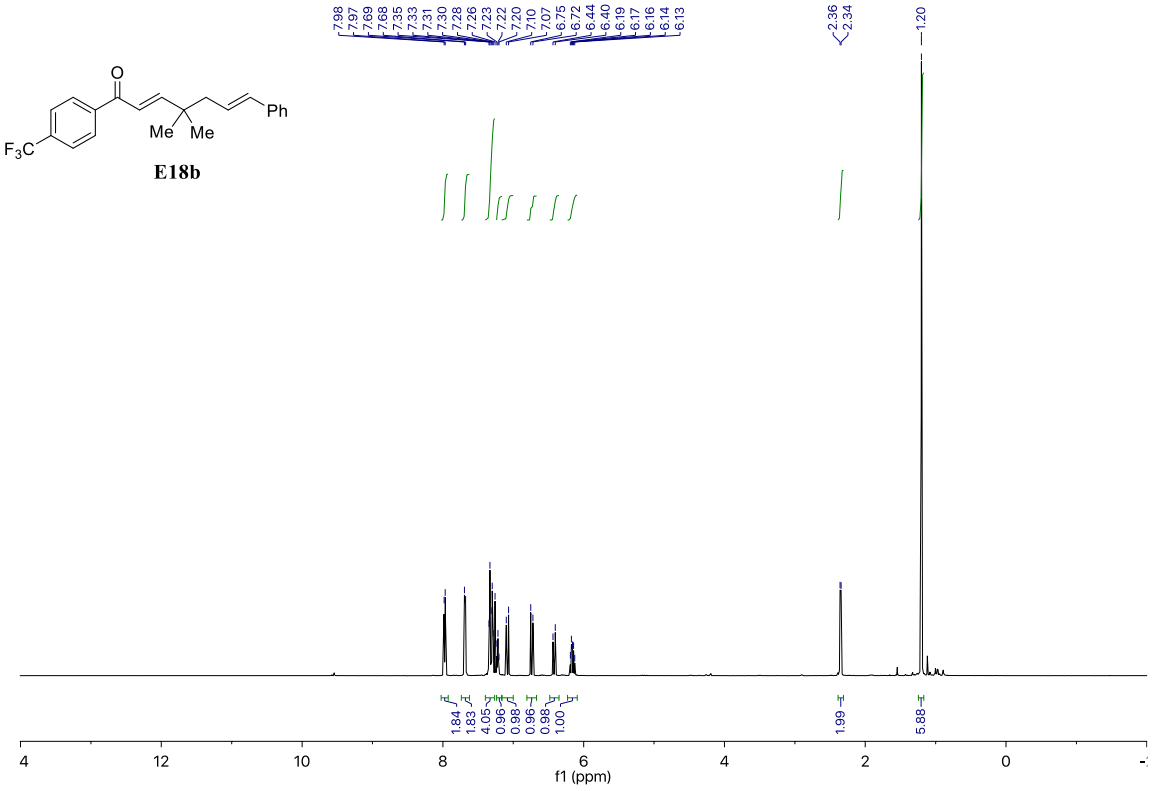
O
Ph
Me Me
F3C
E18b
7.98
7.97
7.69
7.68
7.35
7.33
7.31
7.30
7.28
7.26
7.23
7.22
7.20
7.10
7.07
6.75
6.72
6.44
6.40
6.19
6.17
6.16
6.14
6.13
2.36
2.34
1.20
1.84
1.83
4.05
0.96
0.98
0.96
0.98
1.00
1.99
5.88
f1 (ppm)

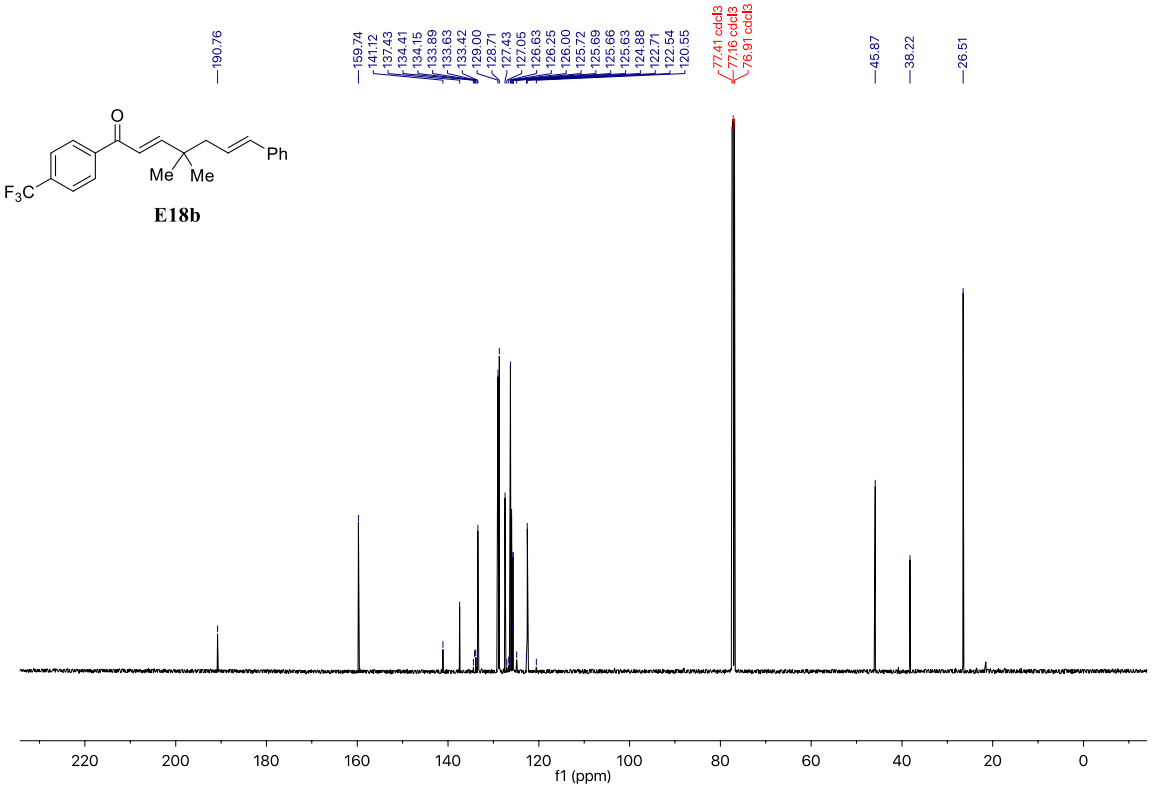
O
Ph
Me Me
F3C
E18b
190.76
159.74
141.12
137.43
134.41
134.15
133.89
133.63
133.42
129.00
128.71
127.43
127.05
126.63
126.25
126.00
125.72
125.69
125.66
125.63
124.88
122.71
122.54
120.55
77.41 cdd3
77.16 cdd3
76.91 cdd3
45.87
38.22
26.51
f1 (ppm)

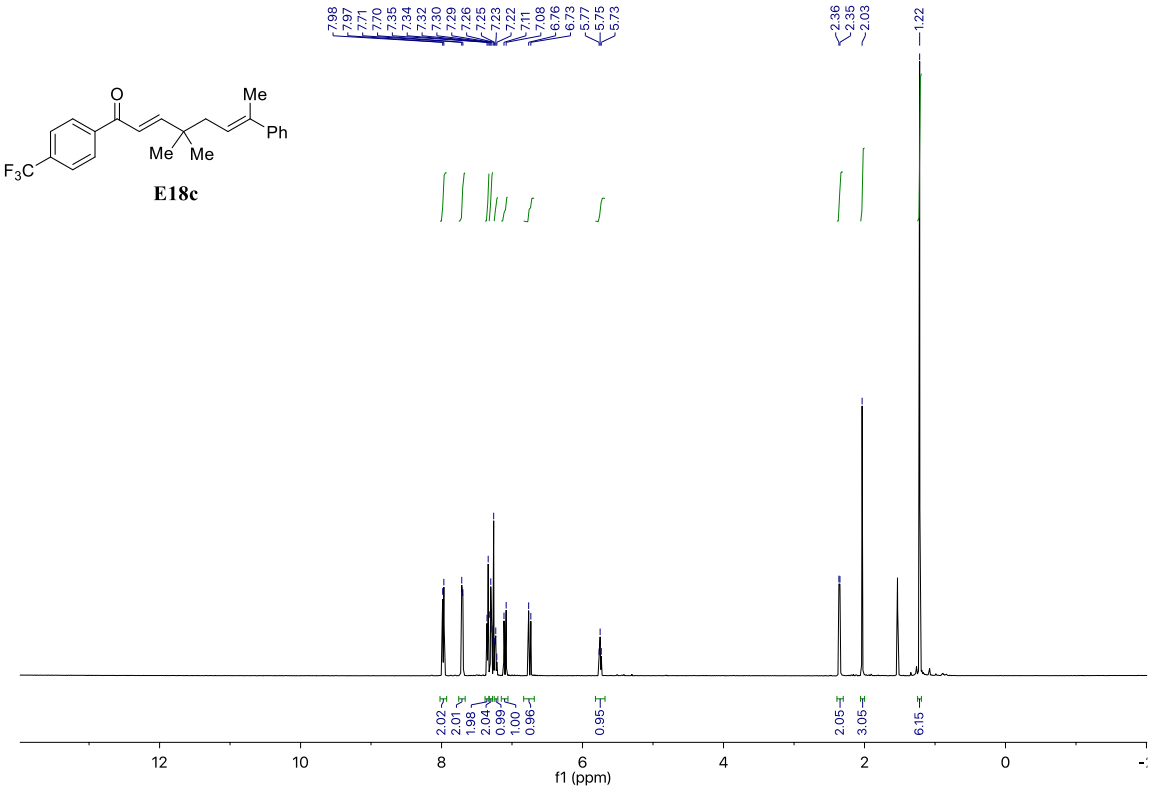
E18c
f1 (ppm)

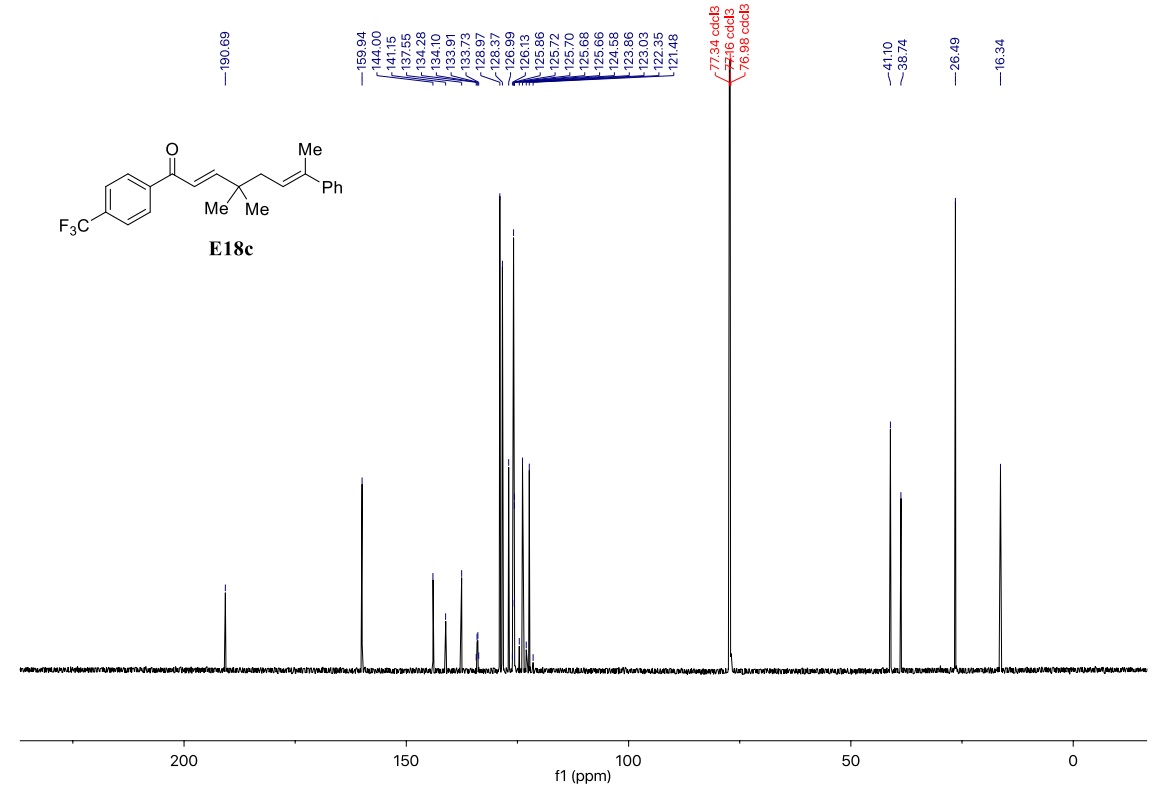
E18c
f1 (ppm)

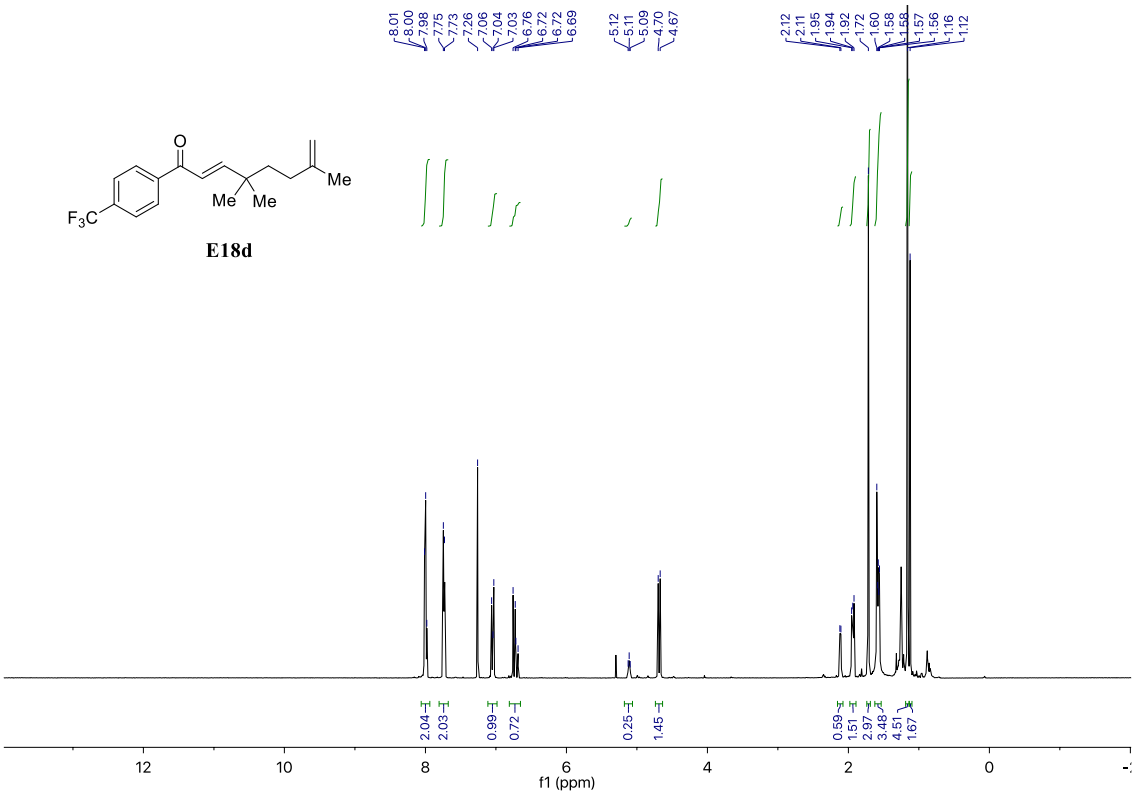
8.01
8.00
7.98
7.75
7.73
7.26
7.06
7.04
7.03
6.76
6.72
6.72
6.69
5.12
5.11
5.09
4.70
4.67
2.12
2.11
1.95
1.94
1.92
1.72
1.60
1.58
1.58
1.57
1.56
1.16
1.12
O
Me
Me
Me
F3C
E18d
2.04
2.03
0.99
0.72
0.25
1.45
0.59
1.51
2.97
3.48
4.51
1.67
12
10
8
6
4
2
0
f1 (ppm)

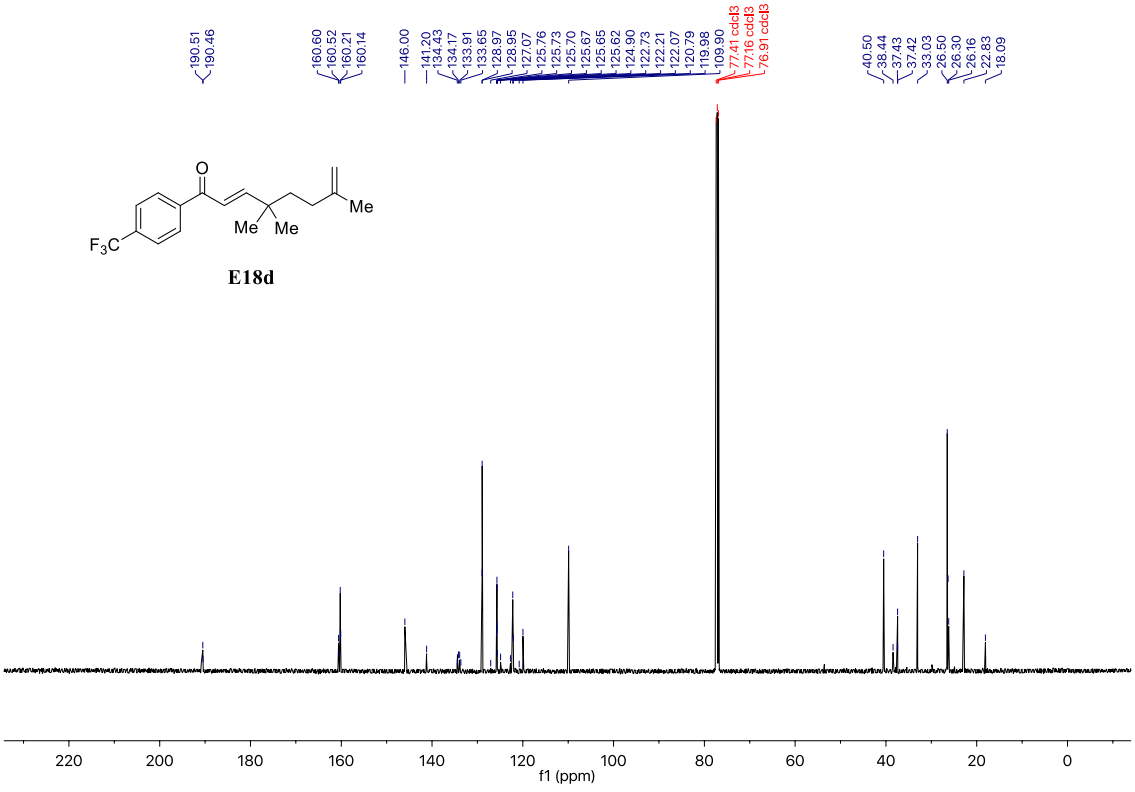
190.51
190.46
160.60
160.52
160.21
160.14
146.00
141.20
134.43
134.17
133.91
133.65
128.97
128.95
127.07
125.76
125.73
125.70
125.67
125.65
125.62
124.90
122.73
122.21
122.07
120.79
119.98
109.90
77.41 cdcl3
77.16 cdcl3
76.91 cdcl3
40.50
38.44
37.43
37.42
33.03
26.50
26.30
26.16
22.83
18.09
O
Me
Me
Me
F3C
E18d
220
200
180
160
140
120
100
80
60
40
20
0
f1 (ppm)

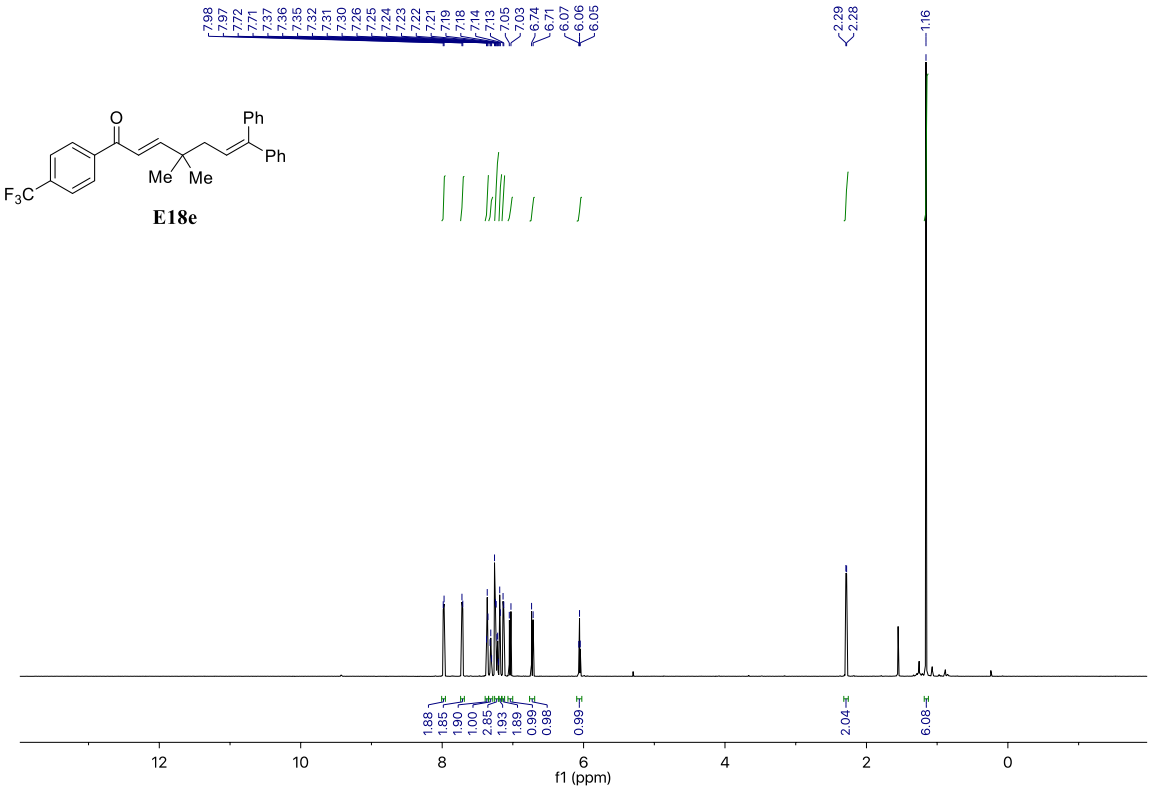
7.98
7.97
7.72
7.71
7.37
7.36
7.35
7.32
7.31
7.30
7.26
7.25
7.24
7.23
7.22
7.21
7.19
7.18
7.14
7.13
7.05
7.03
6.74
6.71
6.07
6.06
6.05
2.29
2.28
1.16
O
Ph
Ph
Me
Me
F3C
1.88
1.85
1.90
1.00
2.85
1.93
1.89
0.99
0.98
0.99
2.04
6.08
12
10
8
6
4
2
0
f1 (ppm)

E18e

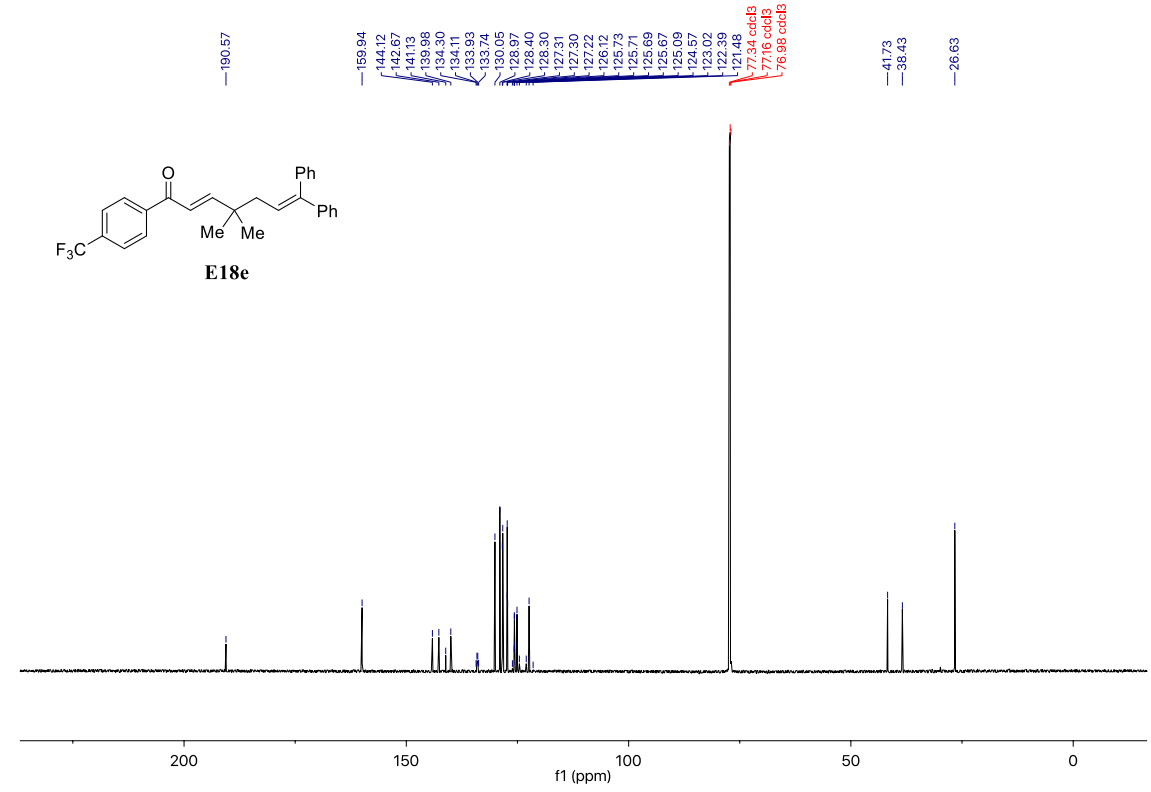
190.57
159.94
144.12
142.67
141.13
139.98
134.30
134.11
133.93
133.74
130.05
128.97
128.40
128.30
127.31
127.30
127.22
126.12
125.73
125.71
125.69
125.67
125.09
124.57
123.02
122.39
121.48
77.34 cdcl3
77.16 cdcl3
76.98 cdcl3
41.73
38.43
26.63
O
Ph
Ph
Me
Me
F3C
200
150
100
50
0
f1 (ppm)

E18e

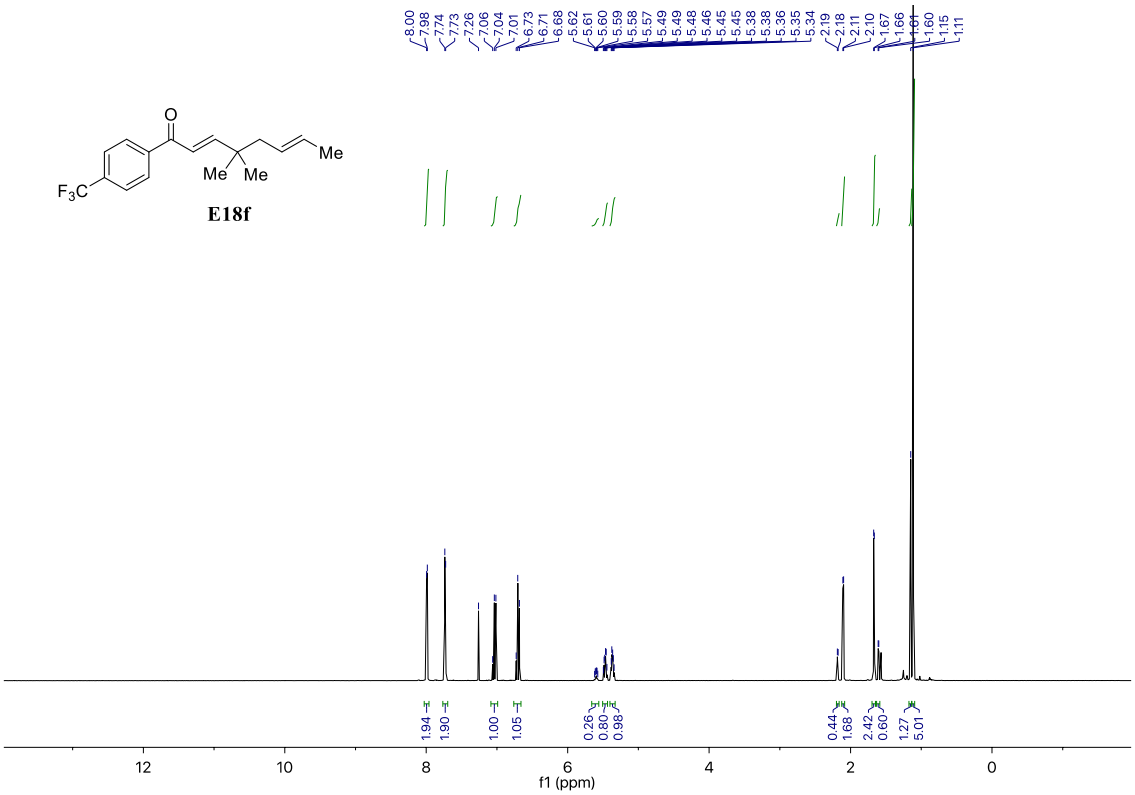
O
Me
Me
Me
F3C
E18f
8.00
7.98
7.74
7.73
7.26
7.06
7.04
7.01
6.73
6.71
6.68
5.62
5.61
5.60
5.59
5.58
5.57
5.49
5.49
5.48
5.46
5.45
5.45
5.38
5.38
5.36
5.35
5.34
2.19
2.18
2.11
2.10
1.67
1.66
1.61
1.60
1.15
1.11
1.94
1.90
1.00
1.05
0.26
0.80
0.98
0.44
1.68
2.42
0.60
1.27
5.01
12
10
8
6
4
2
0
f1 (ppm)

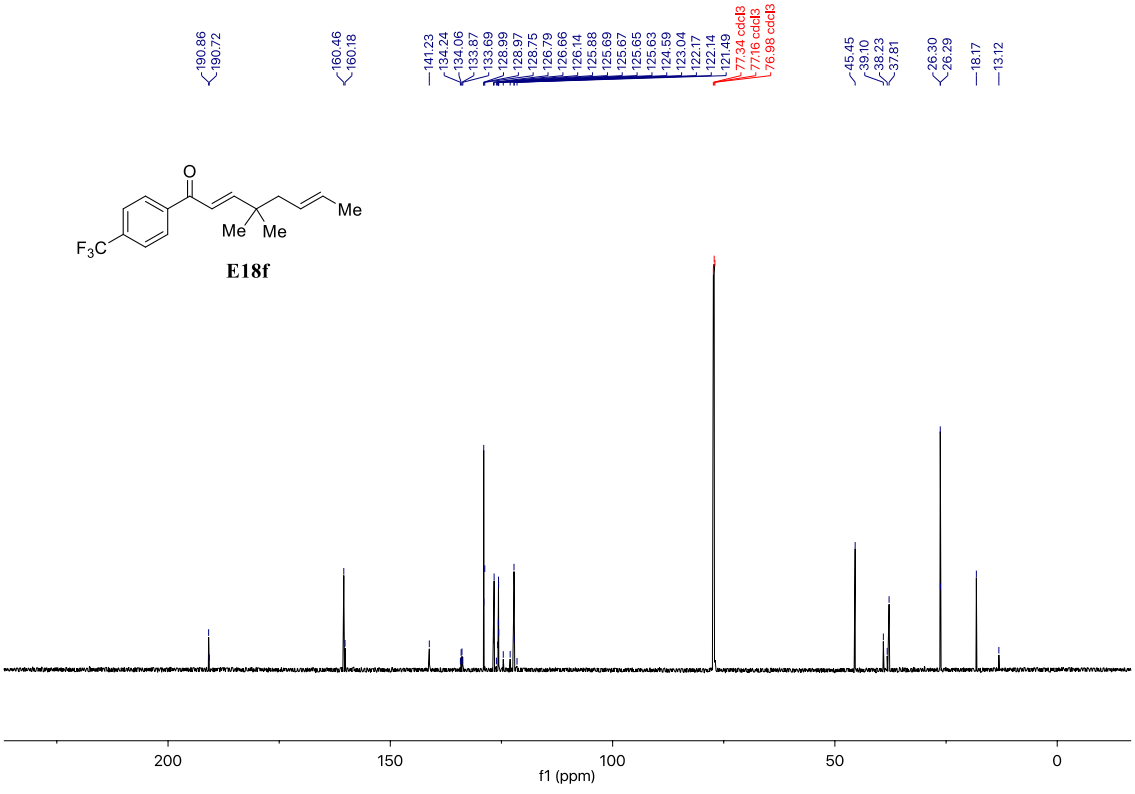
O
Me
Me
Me
F3C
E18f
190.86
190.72
160.46
160.18
141.23
134.24
134.06
133.87
133.69
128.99
128.97
128.75
126.79
126.66
126.14
125.88
125.69
125.67
125.65
125.63
124.59
123.04
122.17
122.14
121.49
77.34 cdcl3
77.16 cdcl3
76.98 cdcl3
45.45
39.10
38.23
37.81
26.30
26.29
18.17
13.12
200
150
100
50
0
f1 (ppm)

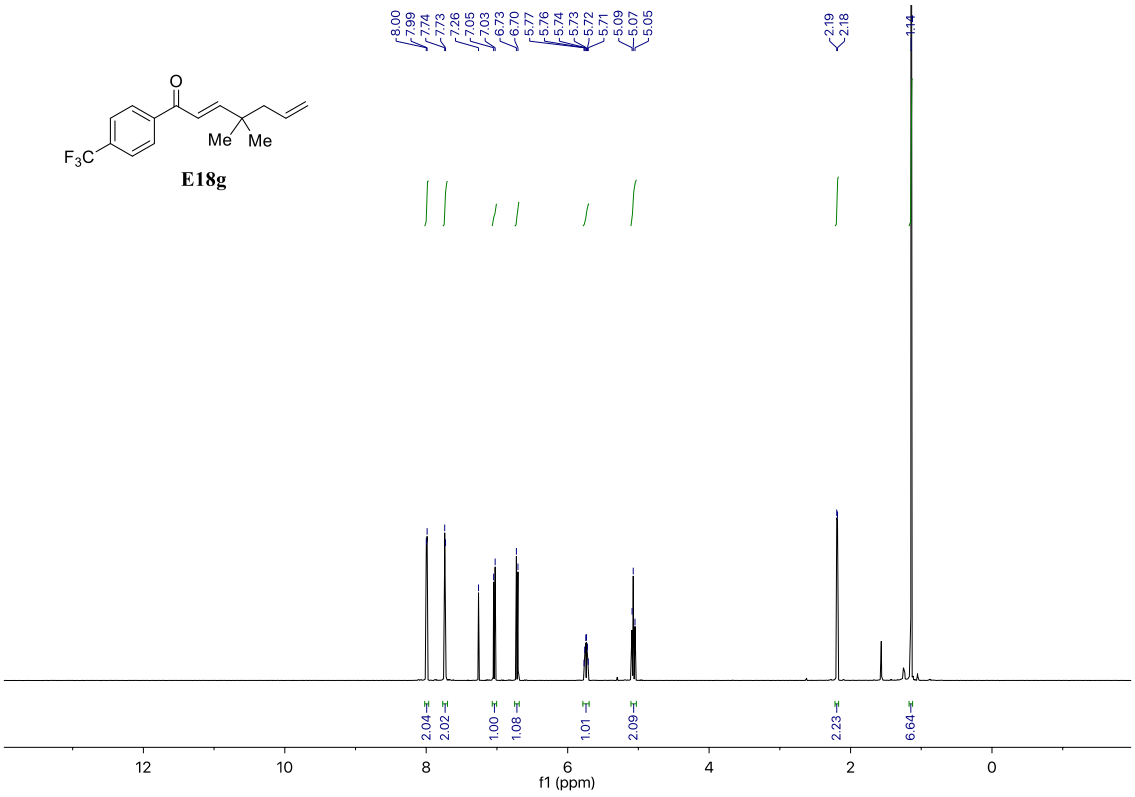
8.00
7.99
7.74
7.73
7.26
7.05
7.03
6.73
6.70
5.77
5.76
5.74
5.73
5.72
5.71
5.09
5.07
5.05
2.19
2.18
1.14
O
Me Me
F3C
E18g
2.04
2.02
1.00
1.08
1.01
2.09
2.23
6.64
12
10
8
6
4
2
0
f1 (ppm)

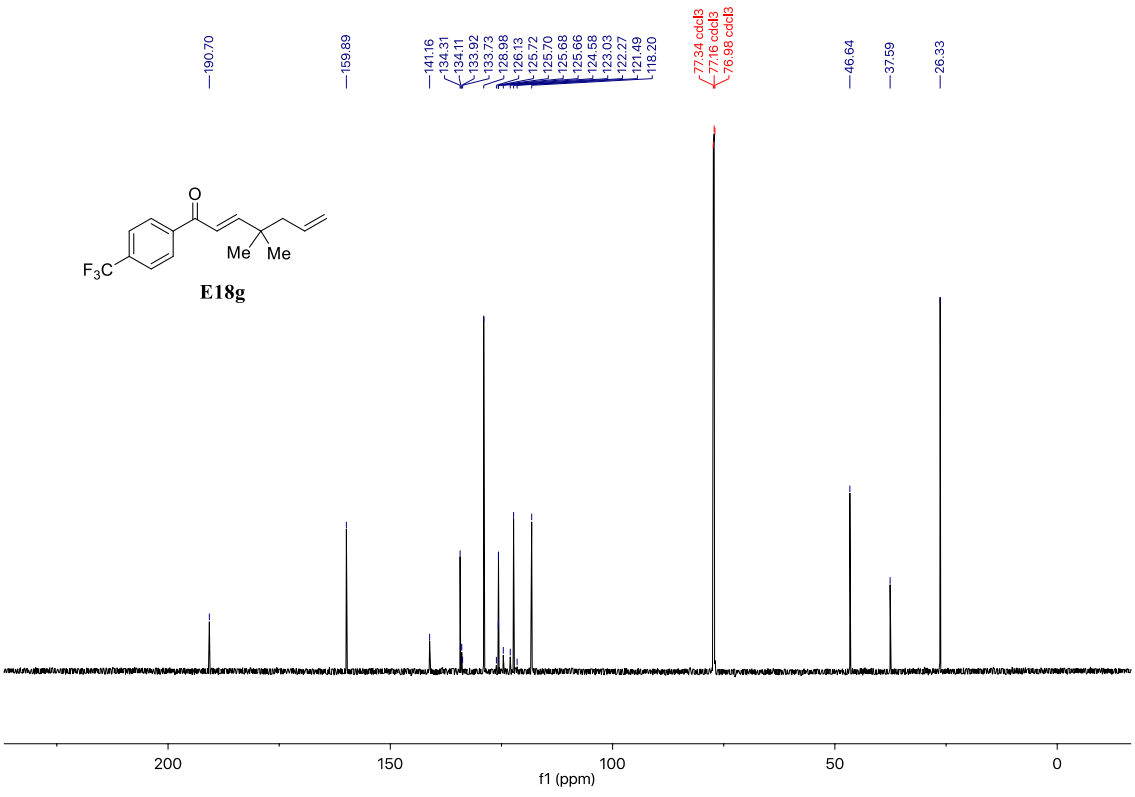
190.70
159.89
141.16
134.31
134.11
133.92
133.73
128.98
126.13
125.72
125.70
125.68
125.66
124.58
123.03
122.27
121.49
118.20
77.34 cdcl3
77.16 cdcl3
76.98 cdcl3
46.64
37.59
26.33
O
Me Me
F3C
E18g
200
150
100
50
0
f1 (ppm)

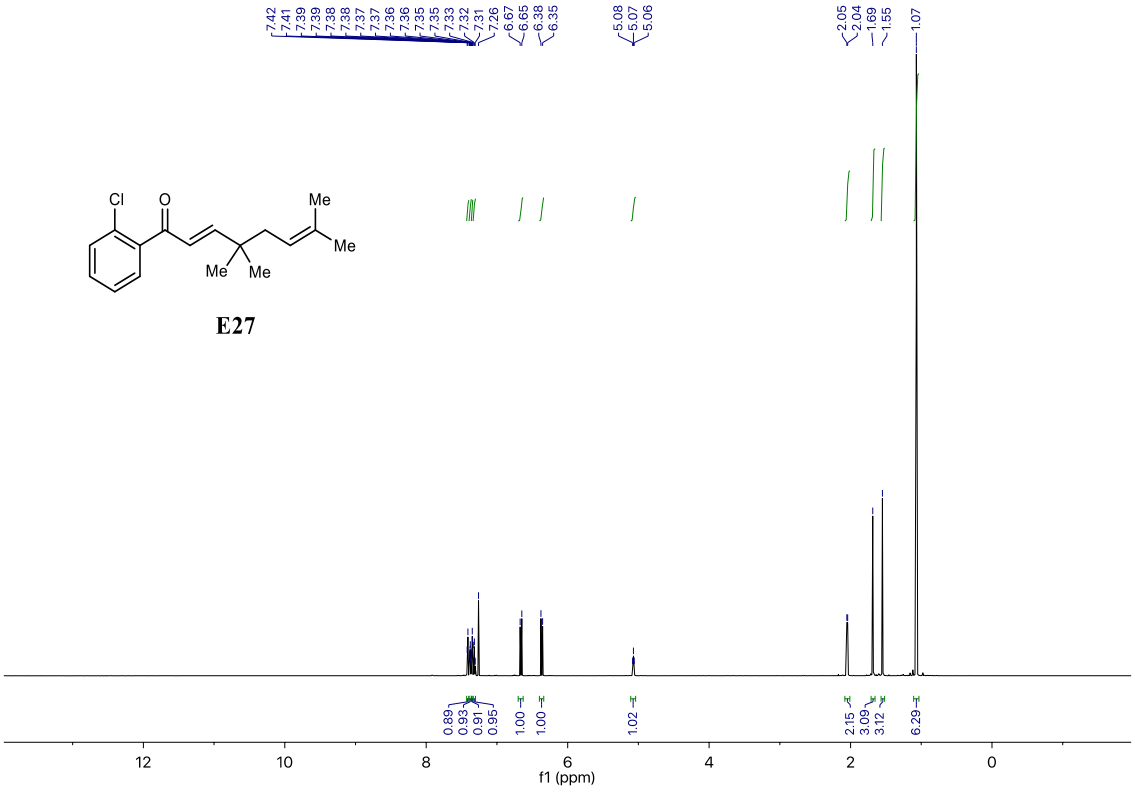
7.42
7.41
7.39
7.39
7.38
7.38
7.37
7.37
7.36
7.36
7.35
7.35
7.33
7.32
7.31
7.26
6.67
6.65
6.38
6.35
5.08
5.07
5.06
2.05
2.04
1.69
1.55
1.07
Cl
O
Me
Me
Me
Me
0.89
0.93
0.91
0.95
1.00
1.00
1.02
2.15
3.09
3.12
6.29
12
10
8
6
4
2
0
f1 (ppm)

E27

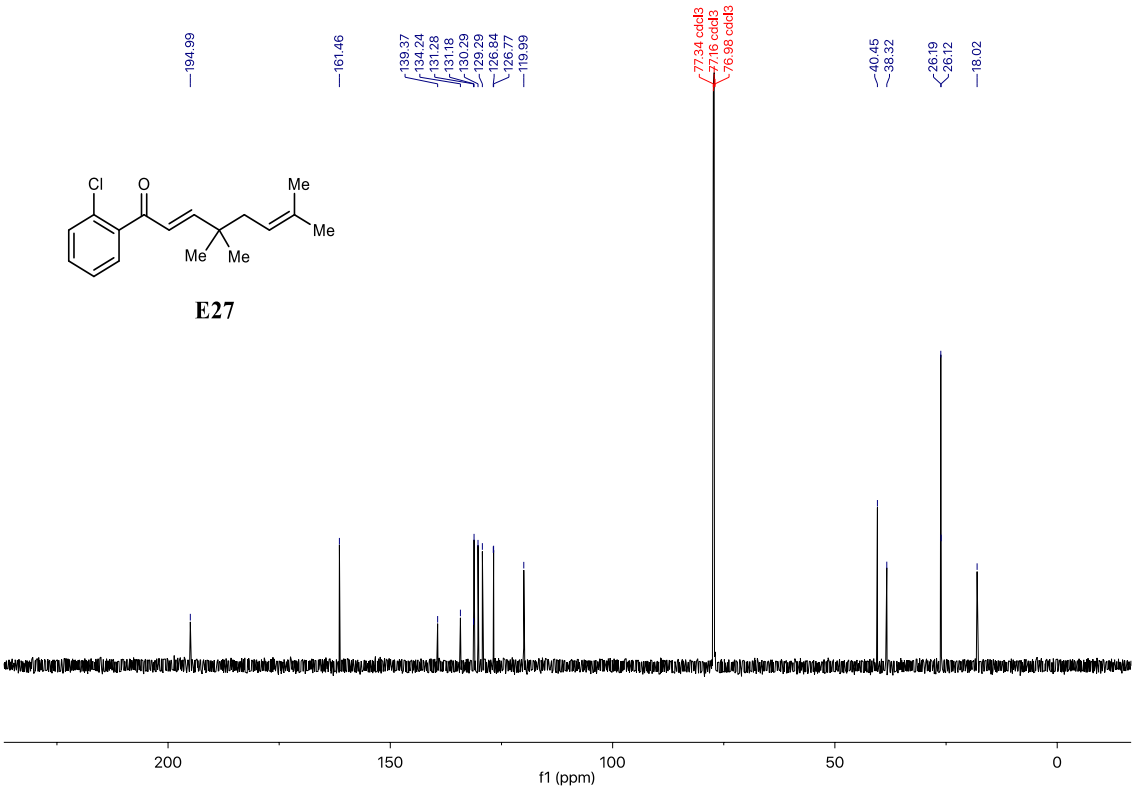
194.99
161.46
139.37
134.24
131.28
131.18
130.29
129.29
126.84
126.77
119.99
77.34 cdcl3
77.16 cdcl3
76.98 cdcl3
40.45
38.32
26.19
26.12
18.02
Cl
O
Me
Me
Me
Me
200
150
100
50
0
f1 (ppm)

E27

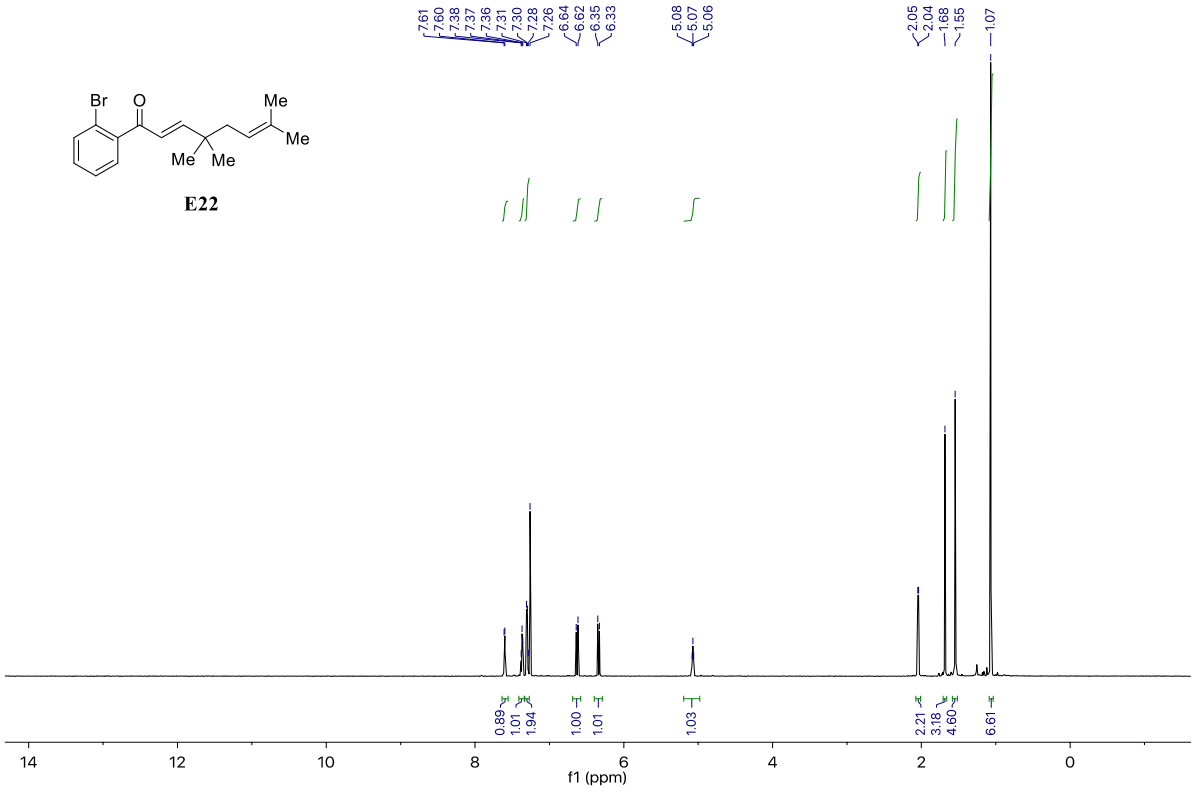
Br
O
Me
Me
Me
Me
E22
7.61
7.60
7.38
7.37
7.36
7.31
7.30
7.28
7.26
6.64
6.62
6.35
6.33
5.08
5.07
5.06
2.05
2.04
1.68
1.55
1.07
0.89
1.01
1.94
1.00
1.01
1.03
2.21
3.18
4.60
6.61
14
12
10
8
6
4
2
0
f1 (ppm)

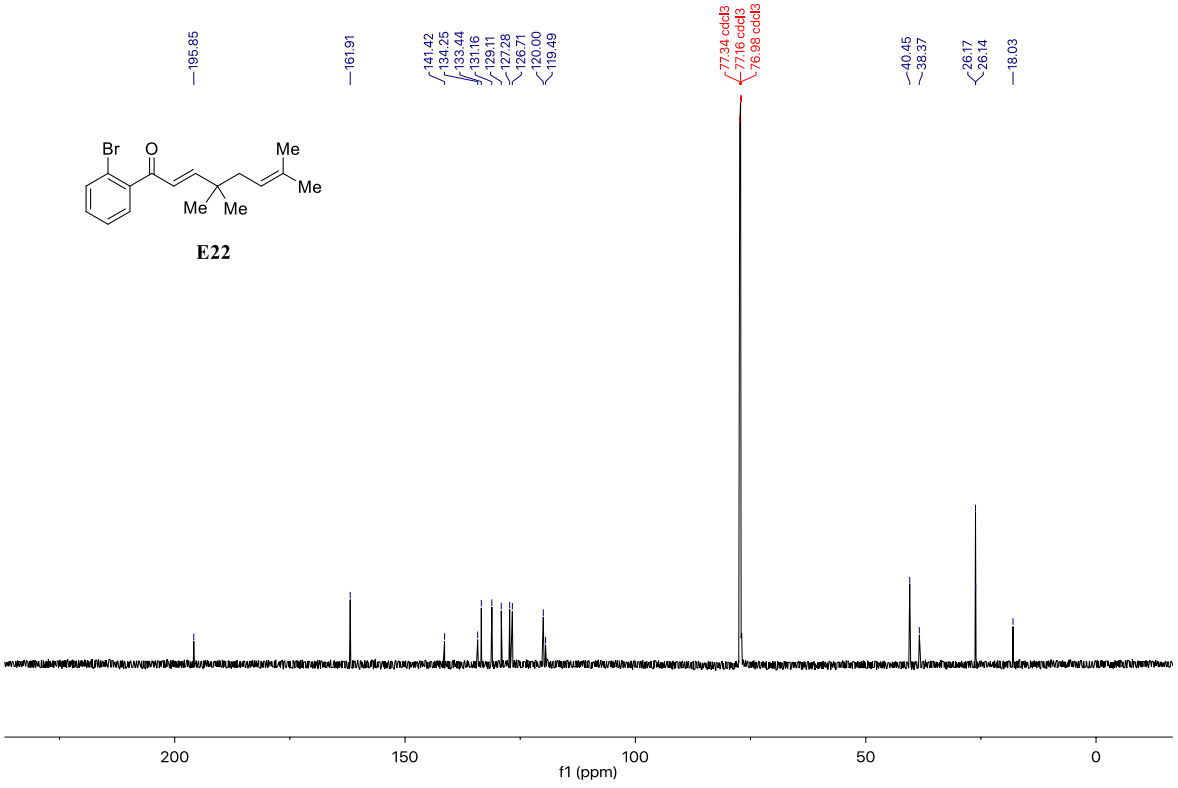
195.85
161.91
141.42
134.25
133.44
131.16
129.11
127.28
126.71
120.00
119.49
77.34 cdd3
77.16 cdd3
76.98 cdd3
40.45
38.37
26.17
26.14
18.03
Br
O
Me
Me
Me
Me
E22
200
150
100
50
0
f1 (ppm)

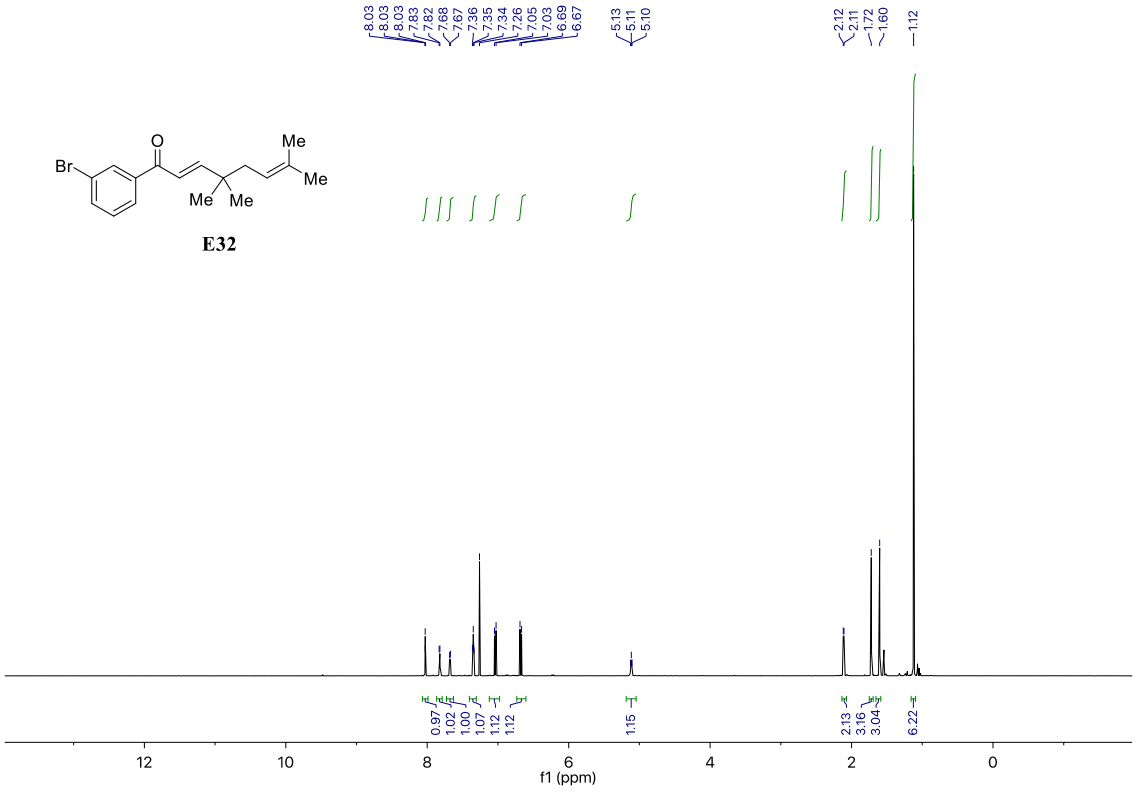
8.03
8.03
8.03
7.83
7.82
7.68
7.67
7.36
7.35
7.34
7.26
7.05
7.03
6.69
6.67
5.13
5.11
5.10
2.12
2.11
1.72
1.60
1.12
Br
O
Me
Me
Me
Me
0.97
1.02
1.00
1.07
1.12
1.12
1.15
2.13
3.16
3.04
6.22
12
10
8
6
4
2
0
f1 (ppm)

E32

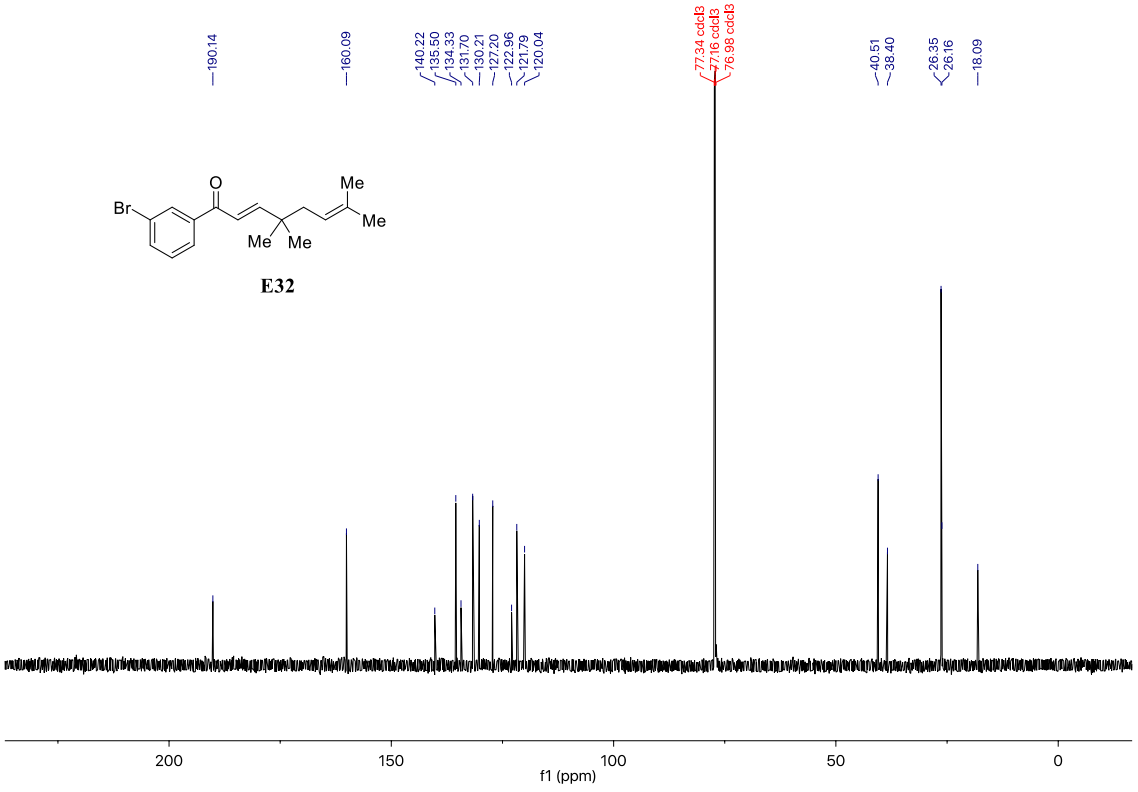
190.14
160.09
140.22
135.50
134.33
131.70
130.21
127.20
122.96
121.79
120.04
77.34 cdcl3
77.16 cdcl3
76.98 cdcl3
40.51
38.40
26.35
26.16
18.09
Br
O
Me
Me
Me
Me
200
150
100
50
0
f1 (ppm)

E32

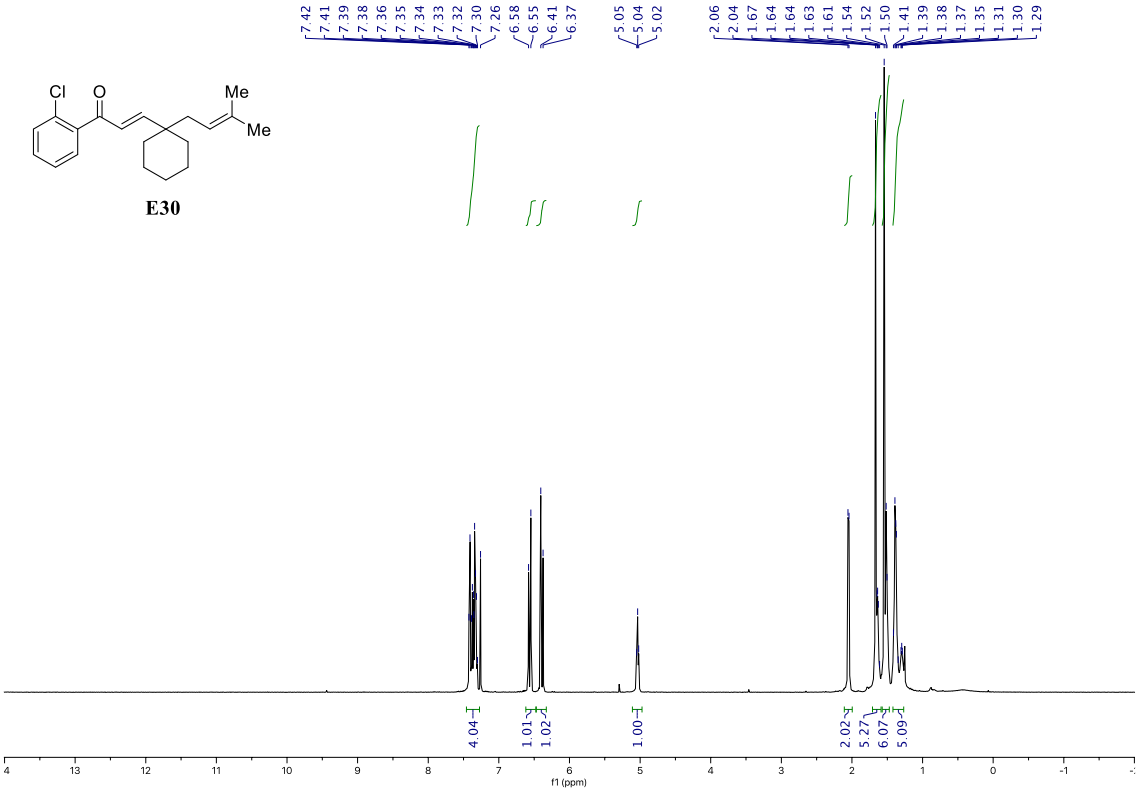
Cl
O
Me
Me
E30
7.42
7.41
7.39
7.38
7.36
7.35
7.34
7.33
7.32
7.30
7.26
6.58
6.55
6.41
6.37
5.05
5.04
5.02
2.06
2.04
1.67
1.64
1.64
1.63
1.61
1.54
1.52
1.50
1.41
1.39
1.38
1.37
1.35
1.31
1.30
1.29
4.04
1.01
1.02
1.00
2.02
5.27
6.07
5.09
f1 (ppm)

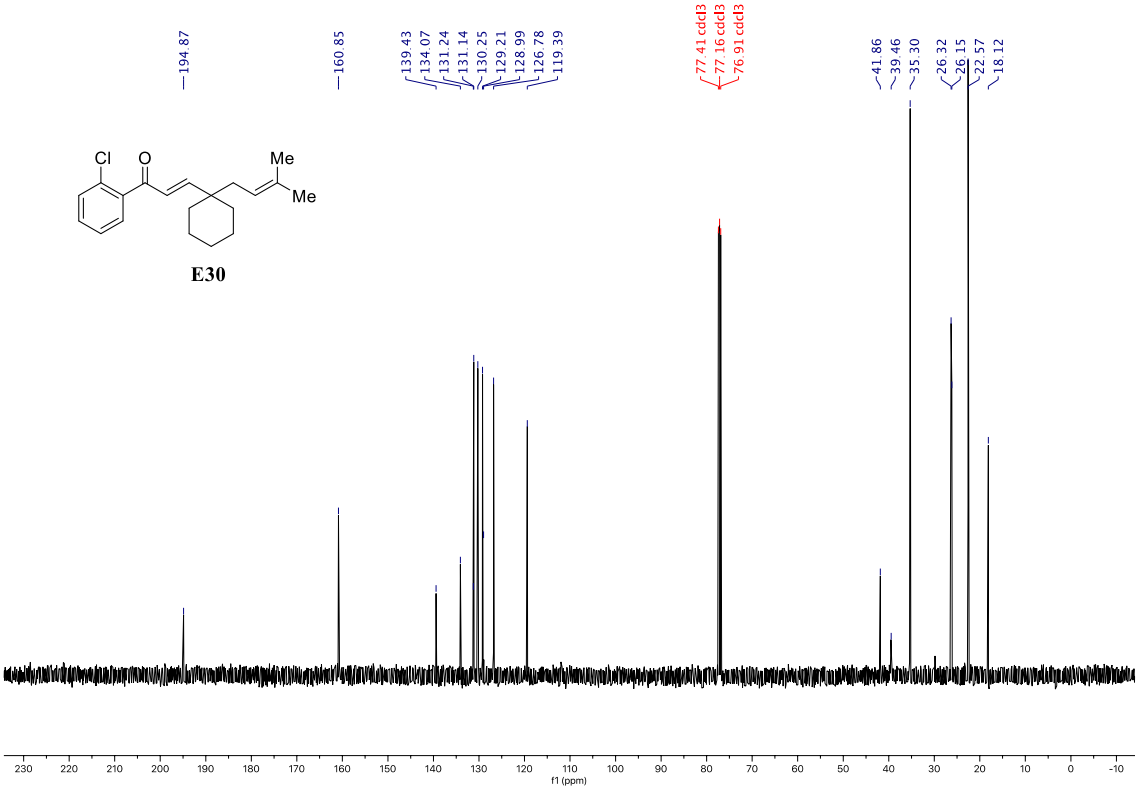
Cl
O
Me
Me
E30
194.87
160.85
139.43
134.07
131.24
131.14
130.25
129.21
128.99
126.78
119.39
77.41 cdcl3
77.16 cdcl3
76.91 cdcl3
41.86
39.46
35.30
26.32
26.15
22.57
18.12
f1 (ppm)

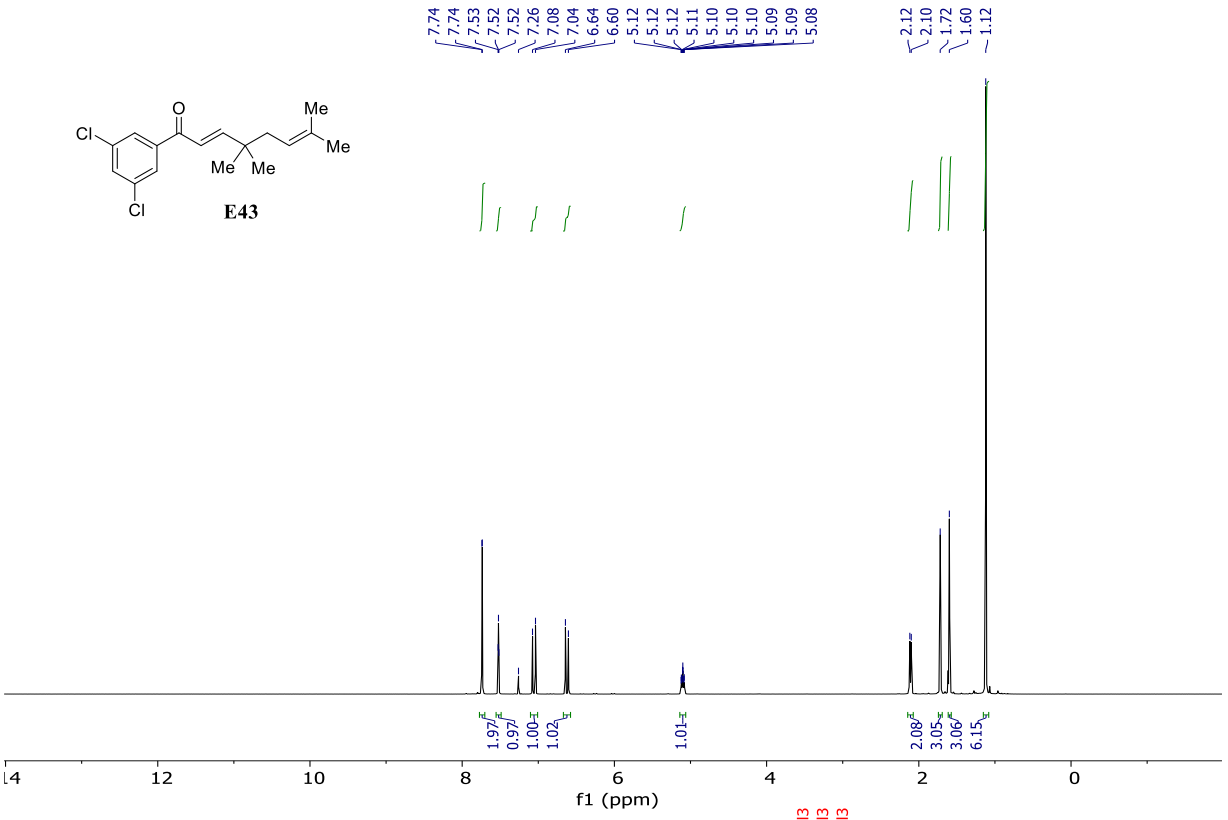
7.74
7.74
7.53
7.52
7.52
7.26
7.08
7.04
6.64
6.60
5.12
5.12
5.11
5.10
5.10
5.09
5.09
5.08
2.12
2.10
1.72
1.60
1.12
Cl
O
Me
Me
Me
Me
Cl
E43
1.97
0.97
1.00
1.02
1.01
2.08
3.05
3.06
6.15
f1 (ppm)

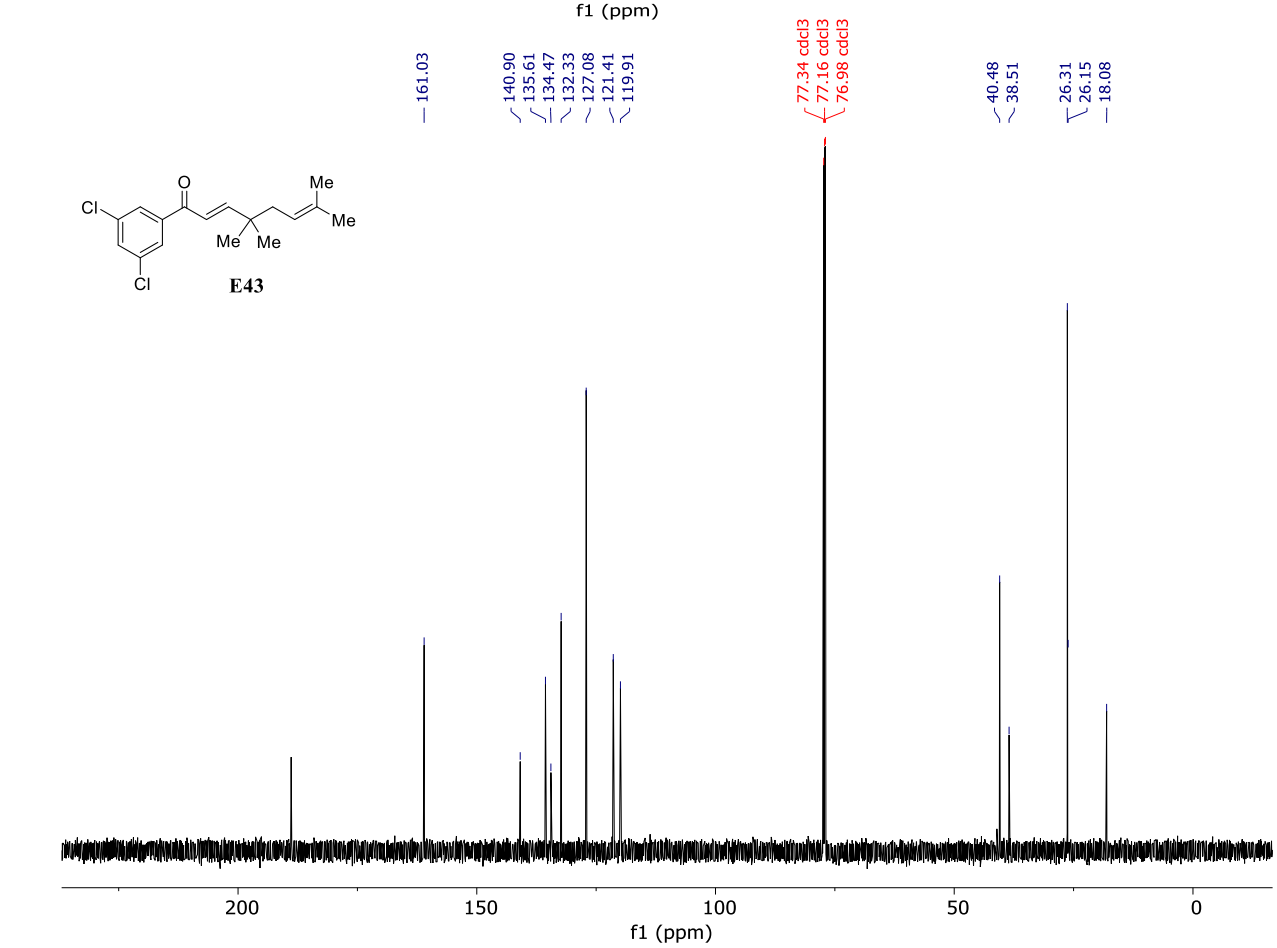
161.03
140.90
135.61
134.47
132.33
127.08
121.41
119.91
77.34 cdcl3
77.16 cdcl3
76.98 cdcl3
40.48
38.51
26.31
26.15
18.08
Cl
O
Me
Me
Me
Me
Cl
E43
f1 (ppm)

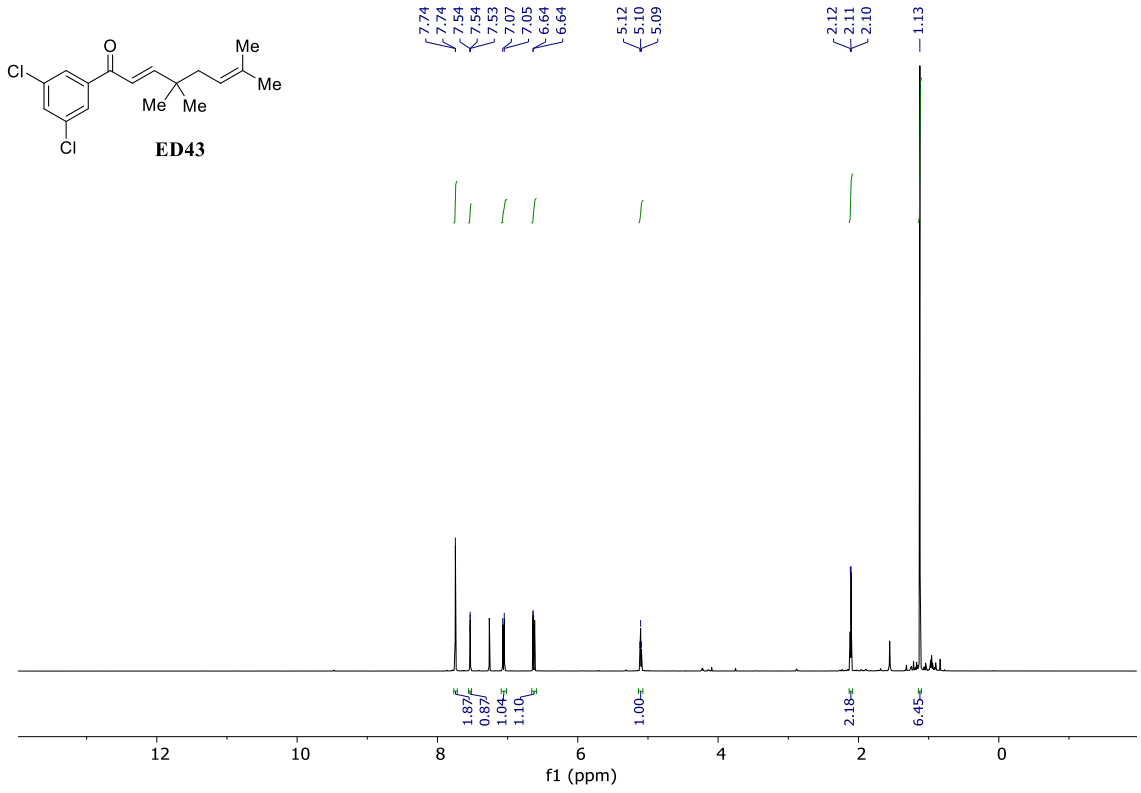
ED43
7.74
7.74
7.54
7.54
7.53
7.07
7.05
6.64
6.64
5.12
5.10
5.09
2.12
2.11
2.10
1.13
1.87
0.87
1.04
1.10
1.00
2.18
6.45
f1 (ppm)

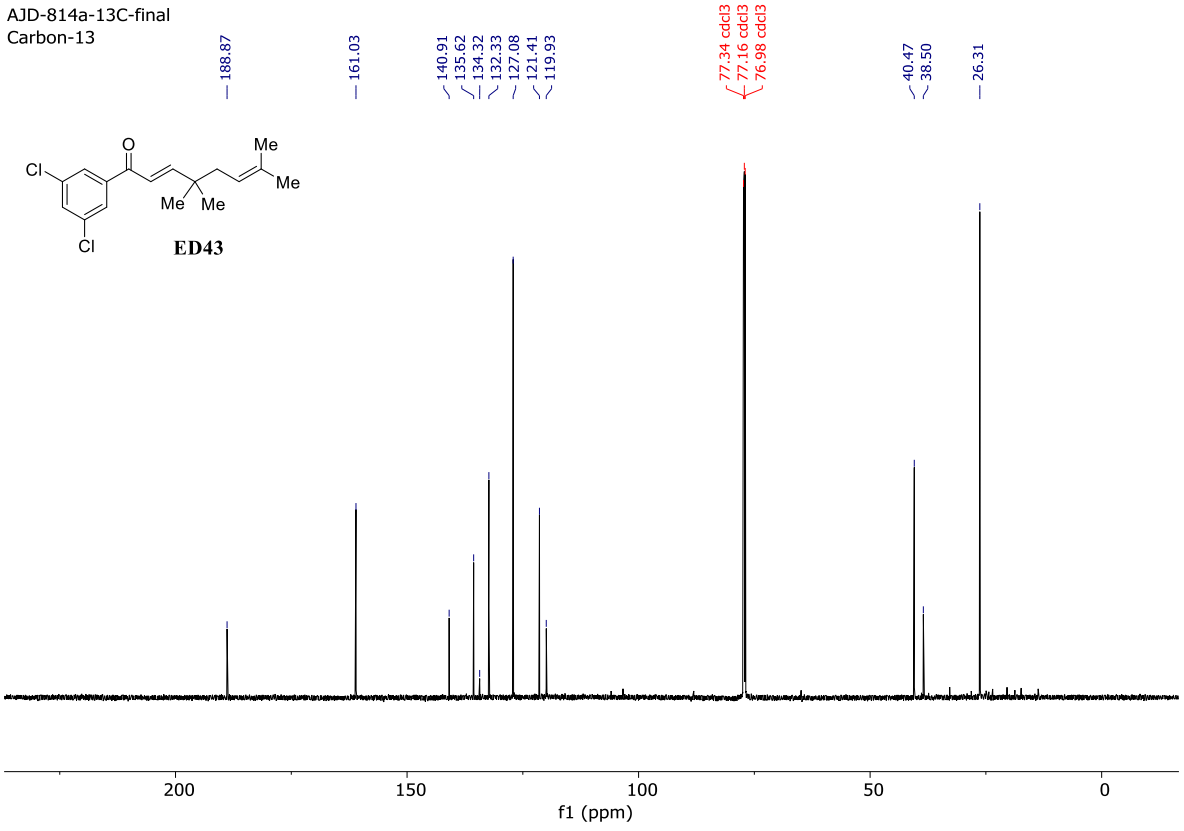
AJD-814a-13C-final
Carbon-13
ED43
188.87
161.03
140.91
135.62
134.32
132.33
127.08
121.41
119.93
77.34 cdcl3
77.16 cdcl3
76.98 cdcl3
40.47
38.50
26.31
f1 (ppm)

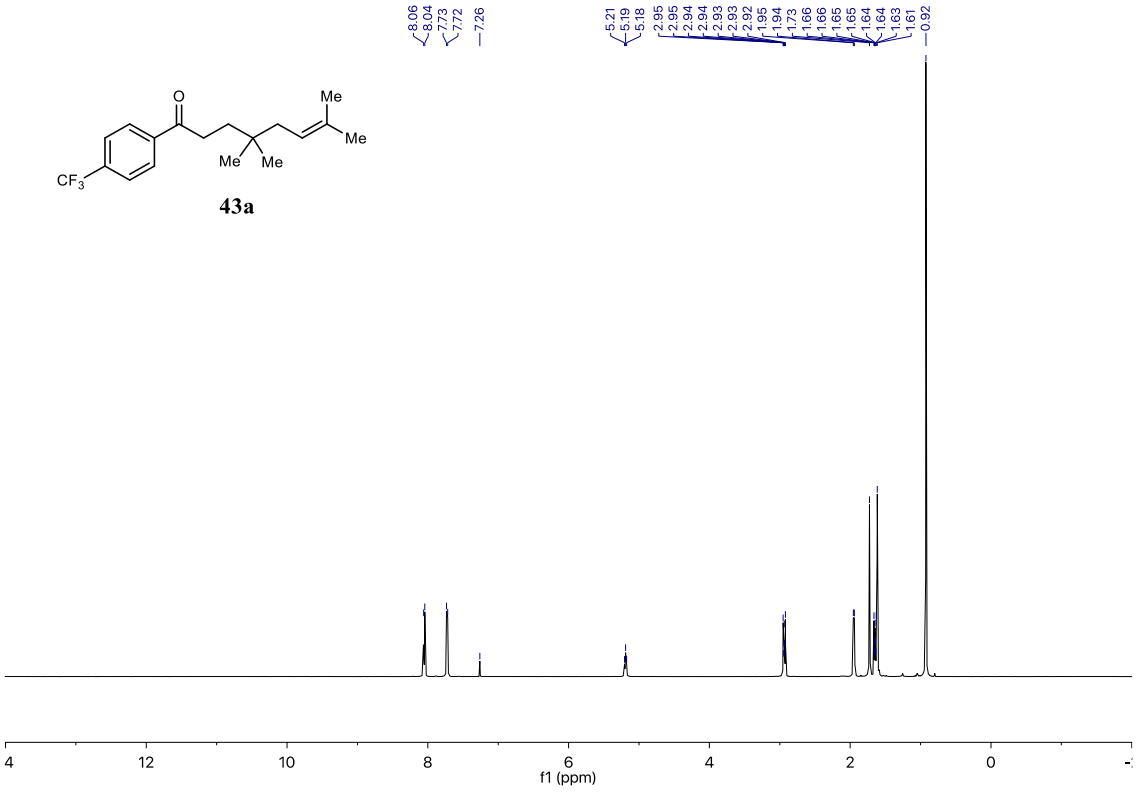
8.06
8.04
7.73
7.72
7.26
5.21
5.19
5.18
2.95
2.95
2.94
2.94
2.93
2.93
2.92
1.95
1.94
1.73
1.66
1.66
1.65
1.65
1.64
1.64
1.63
1.61
0.92
O
Me
Me
Me
Me
CF3
43a
f1 (ppm)

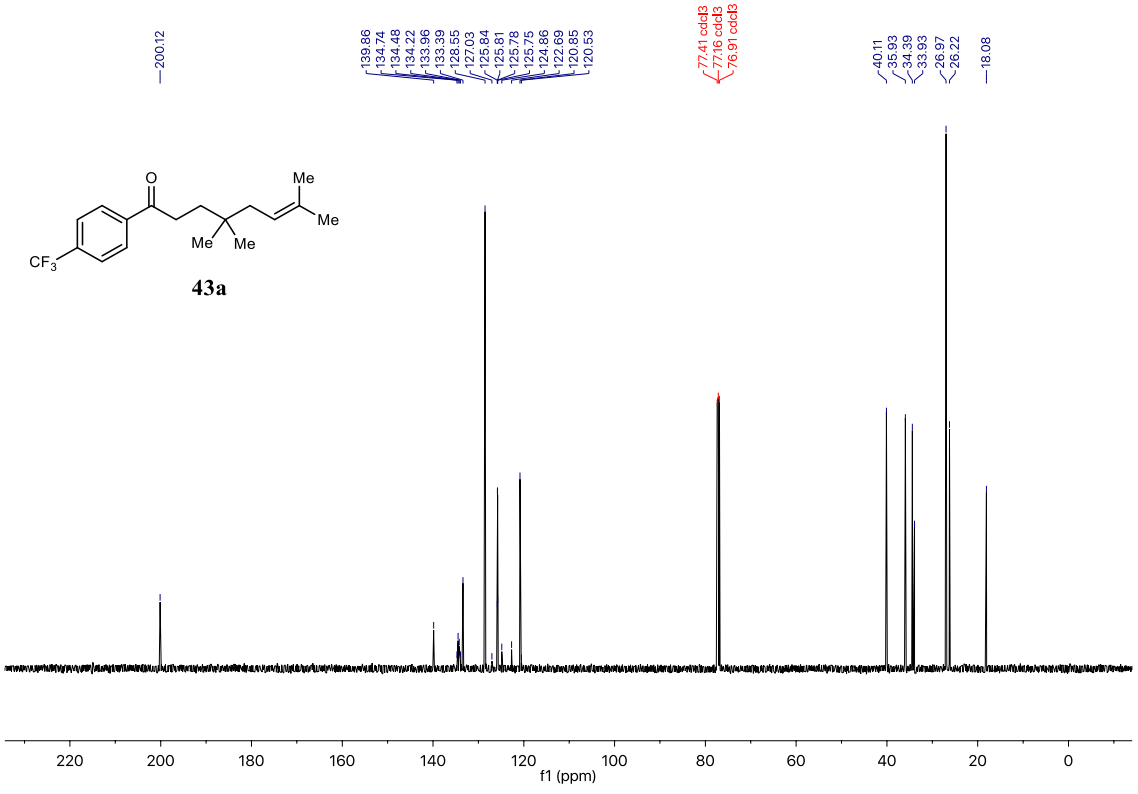
200.12
139.86
134.74
134.48
134.22
133.96
133.39
128.55
127.03
125.84
125.81
125.78
125.75
124.86
122.69
120.85
120.53
77.41 cdd3
77.16 cdd3
76.91 cdd3
40.11
35.93
34.39
33.93
26.97
26.22
18.08
O
Me
Me
Me
Me
CF3
43a
f1 (ppm)

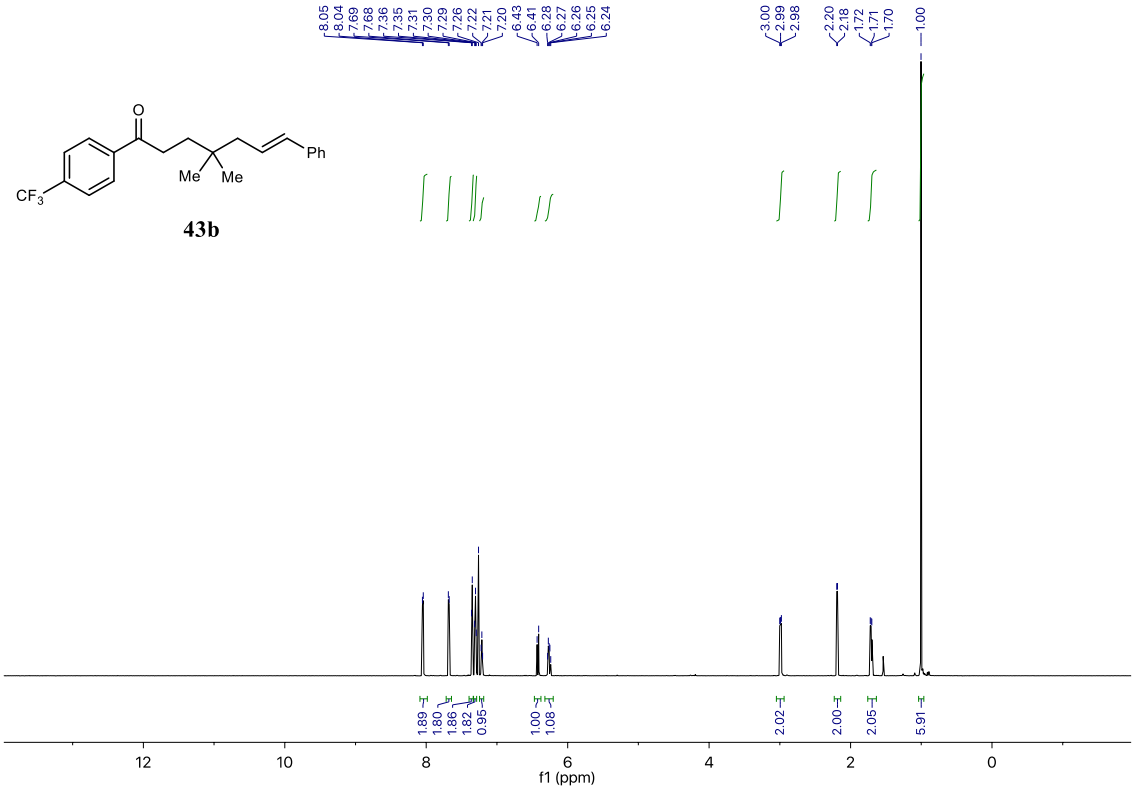
8.05
8.04
7.69
7.68
7.36
7.35
7.31
7.30
7.29
7.26
7.22
7.21
7.20
6.43
6.41
6.28
6.27
6.26
6.25
6.24
3.00
2.99
2.98
2.20
2.18
1.72
1.71
1.70
1.00
O
Me
Me
Ph
CF3
43b
1.89
1.80
1.86
1.82
0.95
1.00
1.08
2.02
2.00
2.05
5.91
12
10
8
6
4
2
0
f1 (ppm)

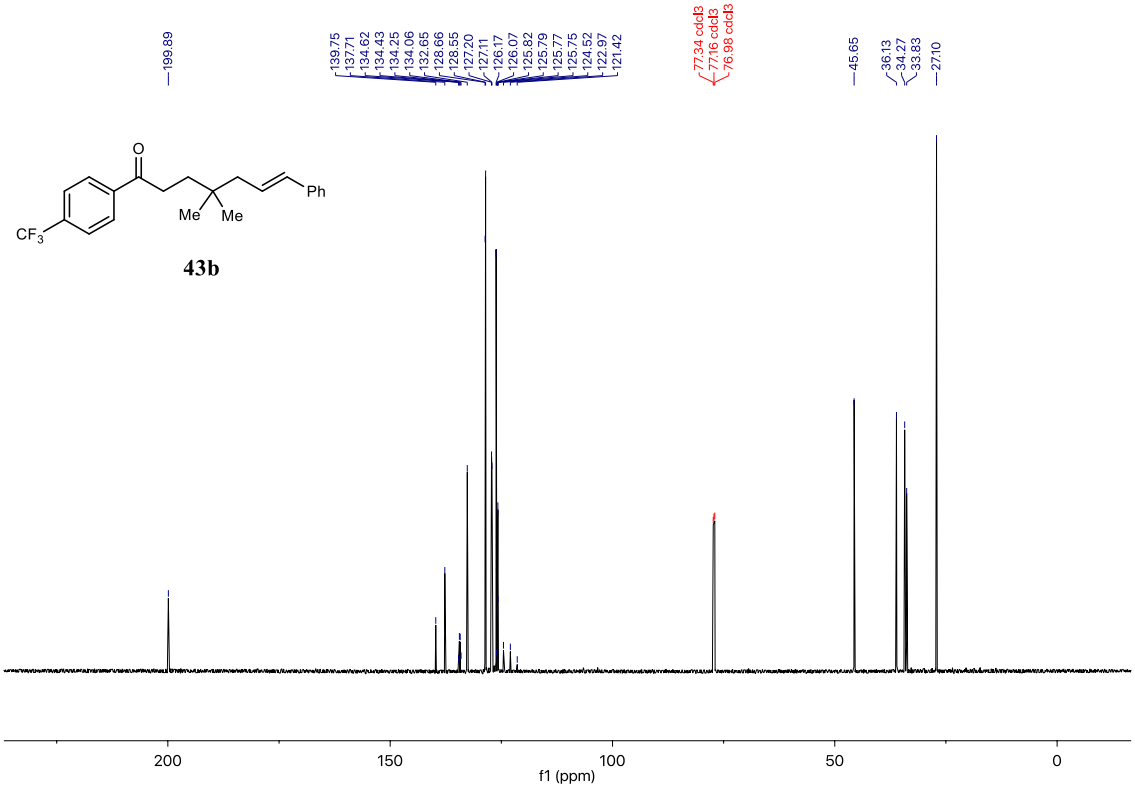
199.89
139.75
137.71
134.62
134.43
134.25
134.06
132.65
128.66
128.55
127.20
127.11
126.17
126.07
125.82
125.79
125.77
125.75
124.52
122.97
121.42
77.34 cdcl3
77.16 cdcl3
76.98 cdcl3
45.65
36.13
34.27
33.83
27.10
O
Me
Me
Ph
CF3
43b
200
150
100
50
0
f1 (ppm)

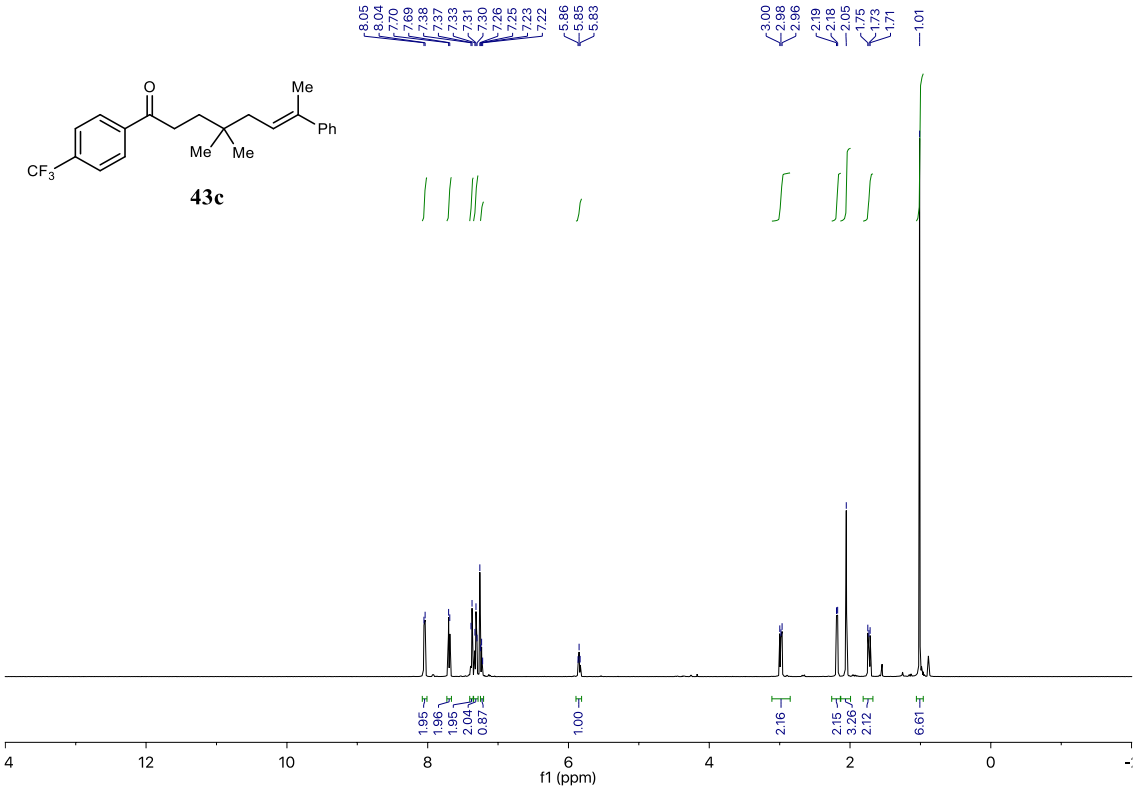
8.05
8.04
7.70
7.69
7.38
7.37
7.33
7.31
7.30
7.26
7.25
7.23
7.22
5.86
5.85
5.83
3.00
2.98
2.96
2.19
2.18
2.05
1.75
1.73
1.71
1.01
O
Me
Ph
Me
Me
CF3
43c
1.95
1.96
1.95
2.04
0.87
1.00
2.16
2.15
3.26
2.12
6.61
f1 (ppm)

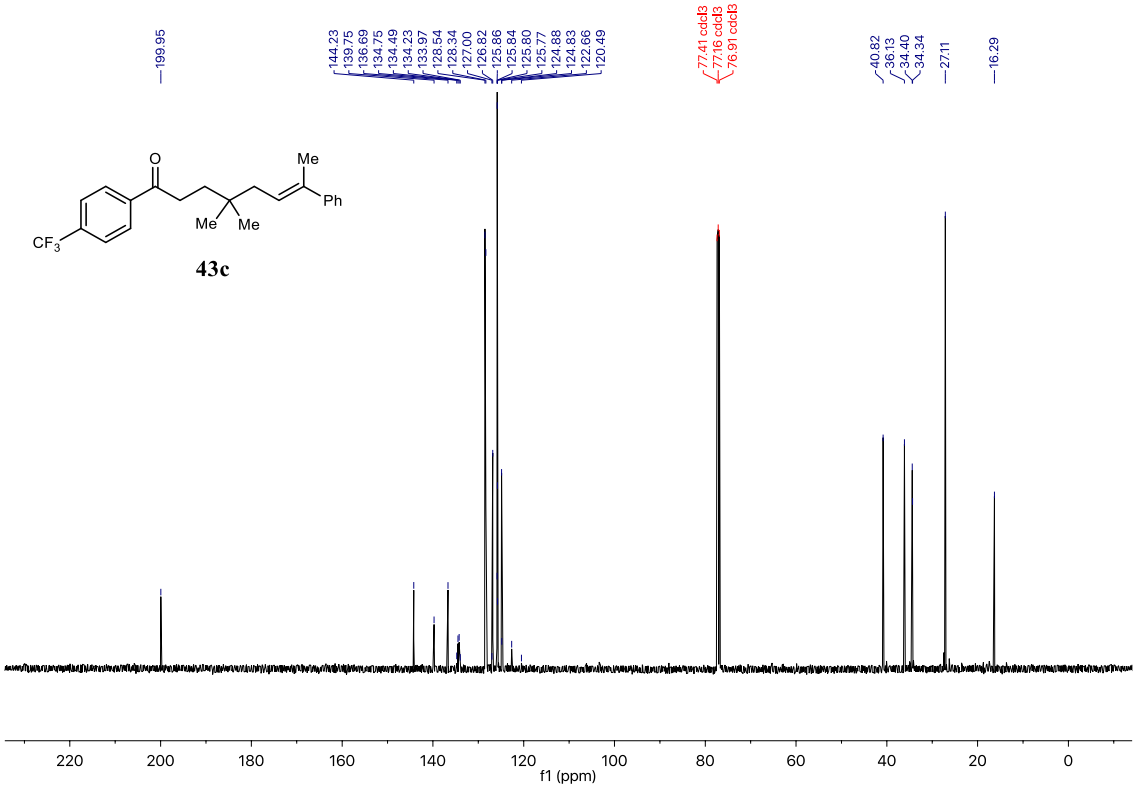
199.95
144.23
139.75
136.69
134.75
134.49
134.23
133.97
128.54
128.34
127.00
126.82
125.86
125.84
125.80
125.77
124.88
124.83
122.66
120.49
77.41 cdd3
77.16 cdd3
76.91 cdd3
40.82
36.13
34.40
34.34
27.11
16.29
O
Me
Ph
Me
Me
CF3
43c
f1 (ppm)

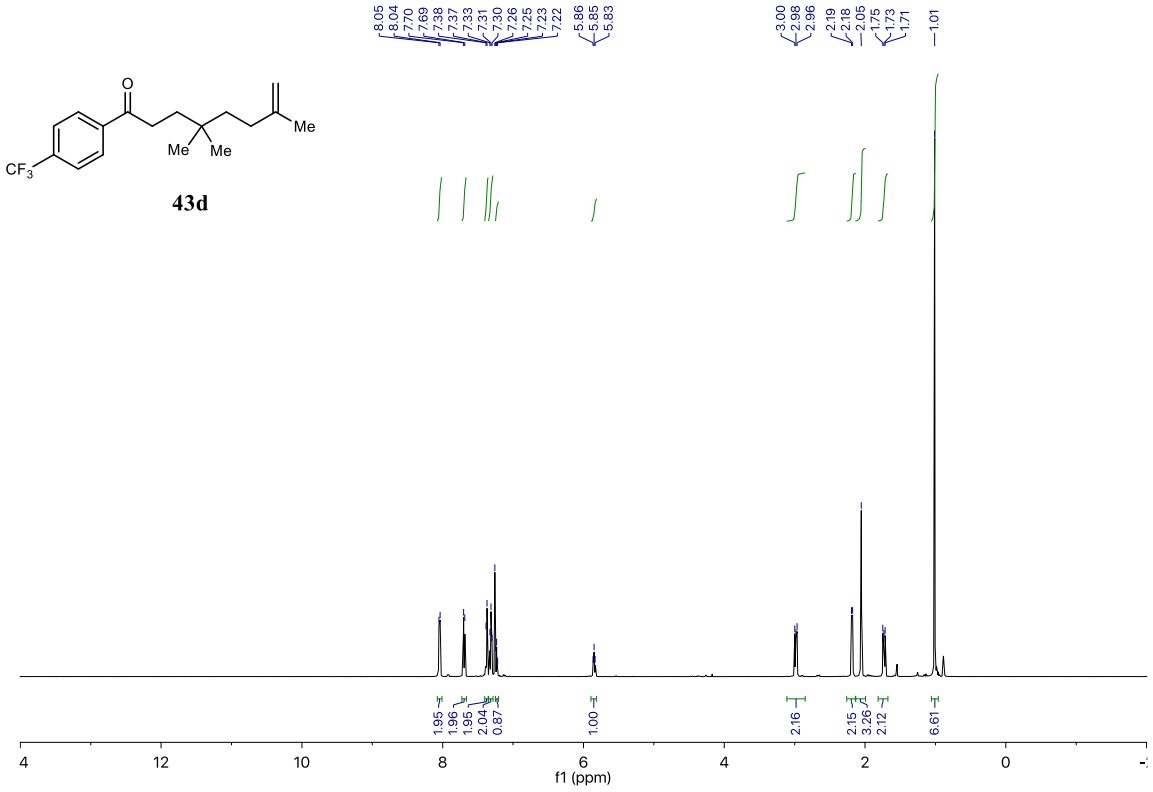
8.05
8.04
7.70
7.69
7.38
7.37
7.33
7.31
7.30
7.26
7.25
7.23
7.22
5.86
5.85
5.83
3.00
2.98
2.96
2.19
2.18
2.05
1.75
1.73
1.71
1.01
O
Me
Me
Me
CF3
1.95
1.96
1.95
2.04
0.87
1.00
2.16
2.15
3.26
2.12
6.61
f1 (ppm)

43d

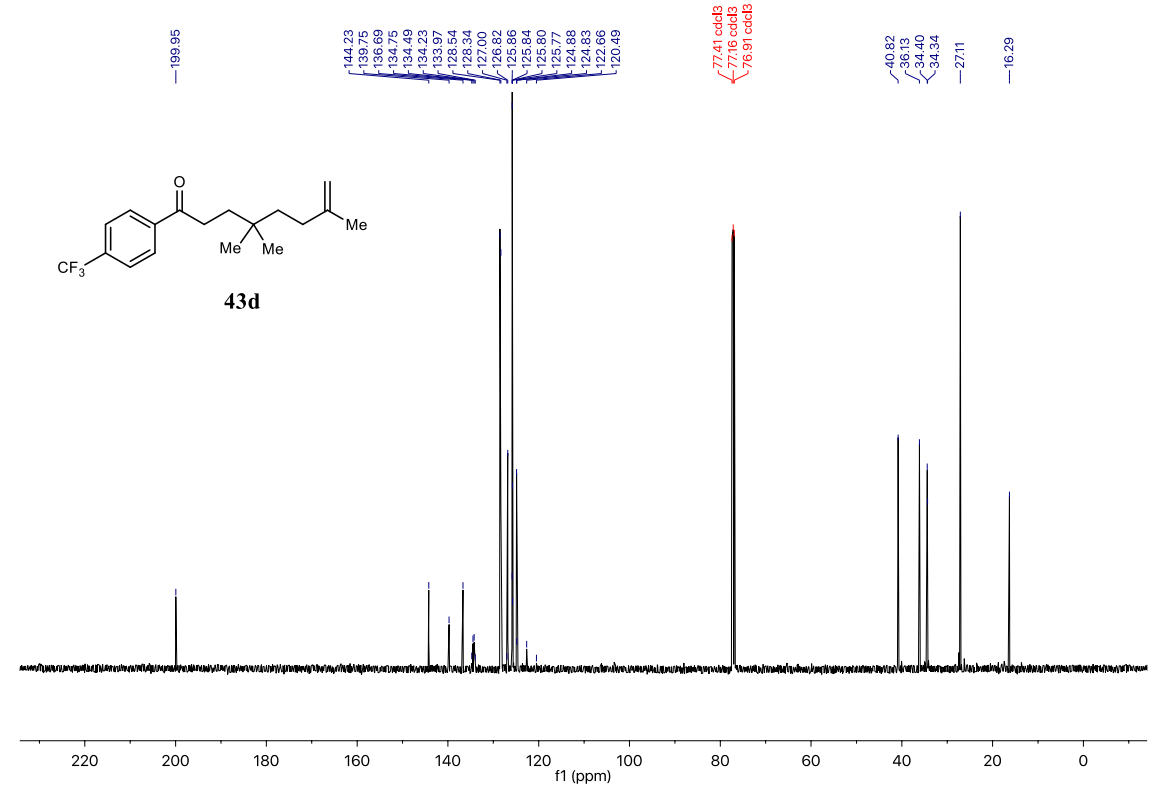
199.95
144.23
139.75
136.69
134.75
134.49
134.23
133.97
128.54
128.34
127.00
126.82
125.86
125.84
125.80
125.77
124.88
124.83
122.66
120.49
77.41 cdd3
77.16 cdd3
76.91 cdd3
40.82
36.13
34.40
34.34
27.11
16.29
O
Me
Me
Me
CF3
f1 (ppm)

43d

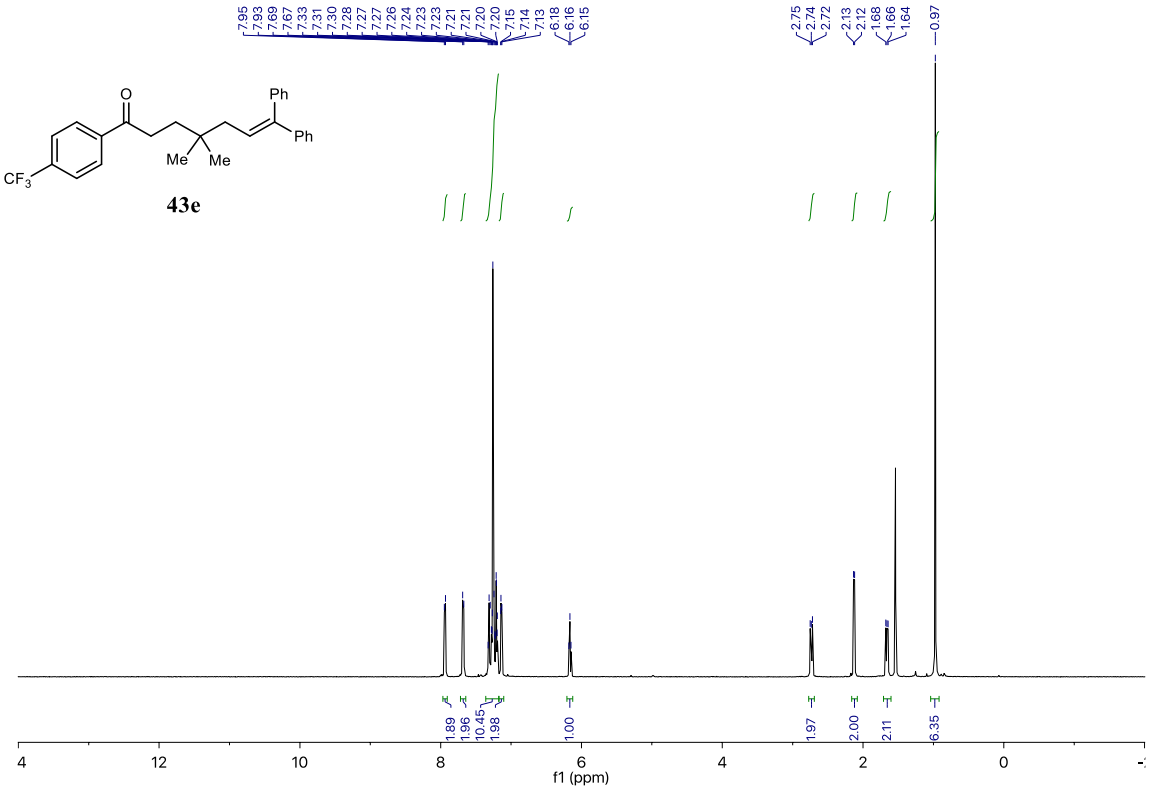
7.95
7.93
7.69
7.67
7.33
7.31
7.30
7.28
7.27
7.27
7.26
7.24
7.23
7.23
7.21
7.21
7.20
7.20
7.15
7.14
7.13
6.18
6.16
6.15
2.75
2.74
2.72
2.13
2.12
1.68
1.66
1.64
0.97
O
Ph
Ph
Me
Me
CF3
43e
1.89
1.96
10.45
1.98
1.00
1.97
2.00
2.11
6.35
f1 (ppm)

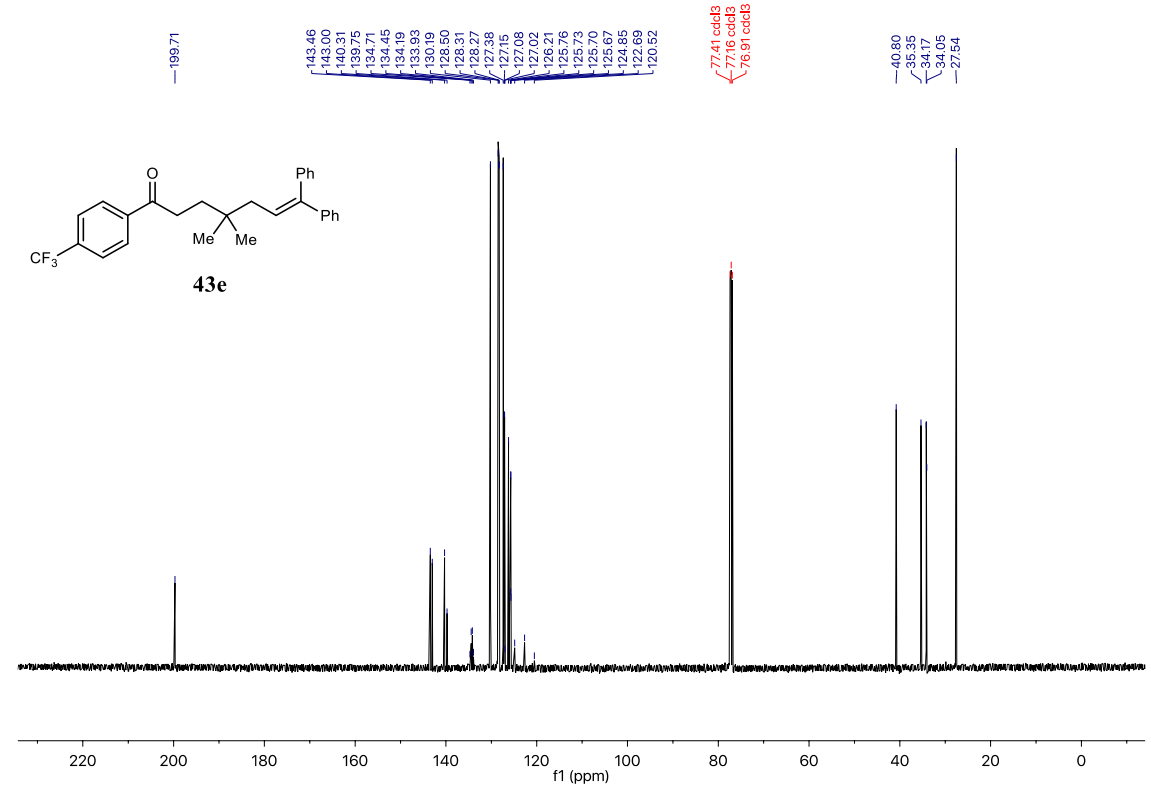
199.71
143.46
143.00
140.31
139.75
134.71
134.45
134.19
133.93
130.19
128.50
128.31
128.27
127.38
127.15
127.08
127.02
126.21
125.76
125.73
125.70
125.67
124.85
122.69
120.52
77.41 cdd3
77.16 cdd3
76.91 cdd3
40.80
35.35
34.17
34.05
27.54
O
Ph
Ph
Me
Me
CF3
43e
f1 (ppm)

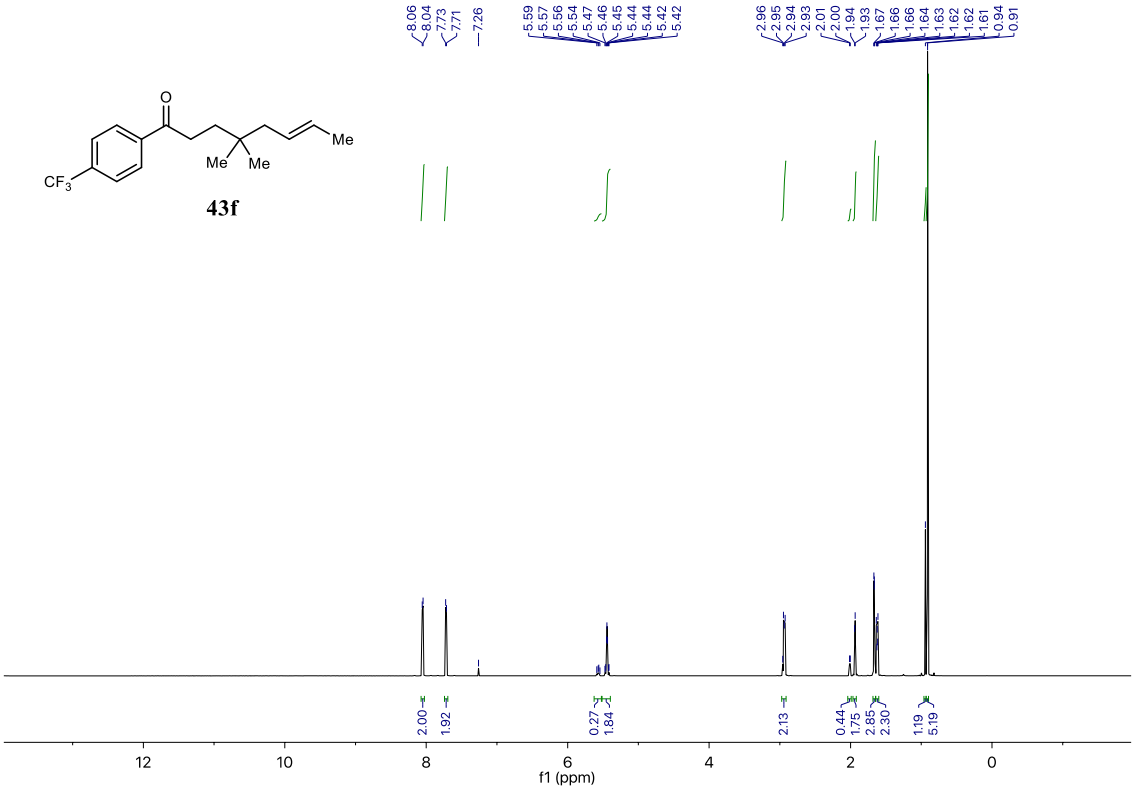
8.06
8.04
7.73
7.71
7.26
5.59
5.57
5.56
5.54
5.47
5.46
5.45
5.44
5.44
5.42
5.42
2.96
2.95
2.94
2.93
2.01
2.00
1.94
1.93
1.67
1.66
1.66
1.64
1.63
1.62
1.62
1.61
0.94
0.91
O
Me
Me
Me
CF3
43f
2.00
1.92
0.27
1.84
2.13
0.44
1.75
2.85
2.30
1.19
5.19
12
10
8
6
4
2
0
f1 (ppm)

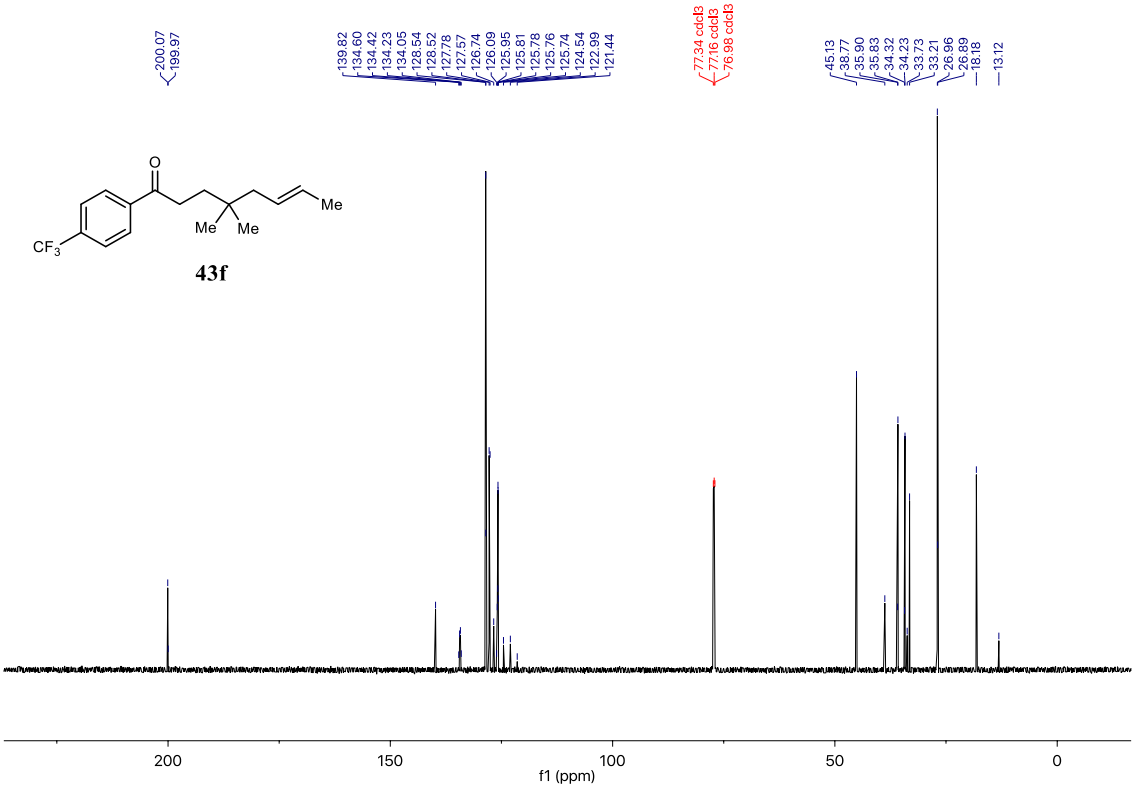
200.07
199.97
139.82
134.60
134.42
134.23
134.05
128.54
128.52
127.78
127.57
126.74
126.09
125.95
125.81
125.78
125.76
125.74
124.54
122.99
121.44
77.34 cdcl3
77.16 cdcl3
76.98 cdcl3
45.13
38.77
35.90
35.83
34.32
34.23
33.73
33.21
26.96
26.89
18.18
13.12
O
Me
Me
Me
CF3
43f
200
150
100
50
0
f1 (ppm)

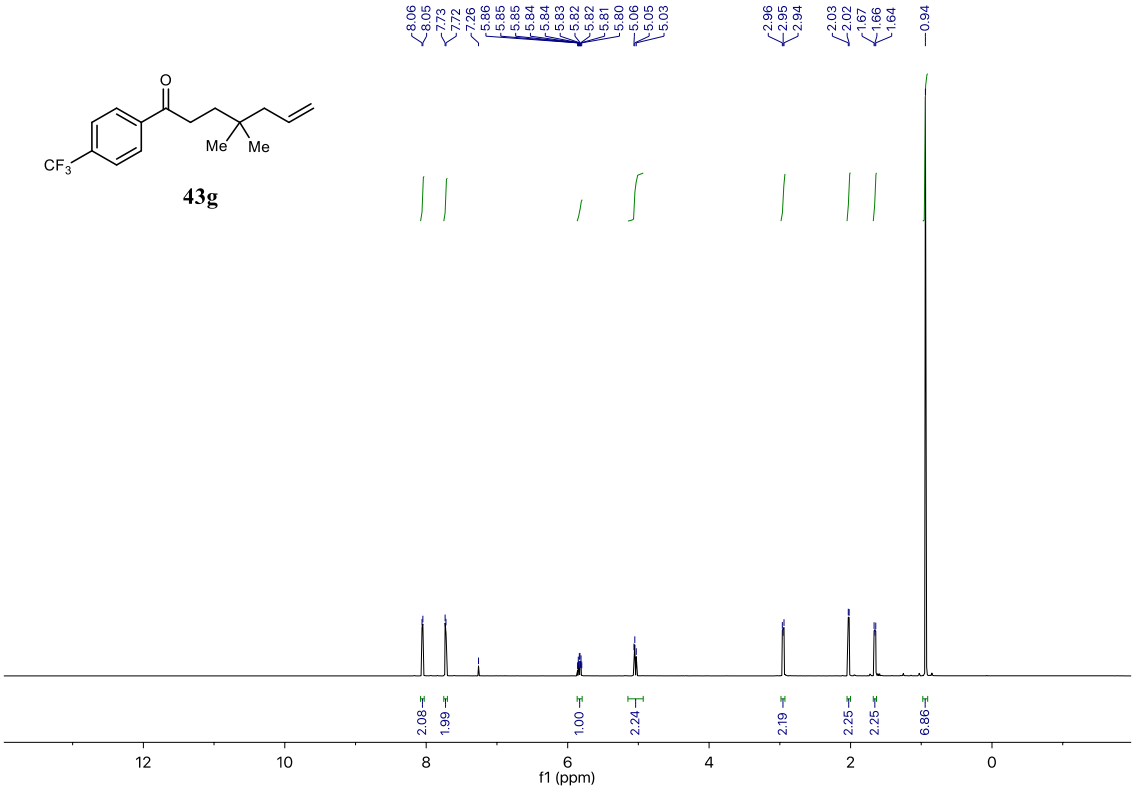
8.06
8.05
7.73
7.72
7.26
5.86
5.85
5.85
5.84
5.84
5.83
5.82
5.82
5.81
5.80
5.06
5.05
5.03
2.96
2.95
2.94
2.03
2.02
1.67
1.66
1.64
0.94
O
Me
Me
CF3
2.08
1.99
1.00
2.24
2.19
2.25
2.25
6.86
12
10
8
6
4
2
0
f1 (ppm)

43g

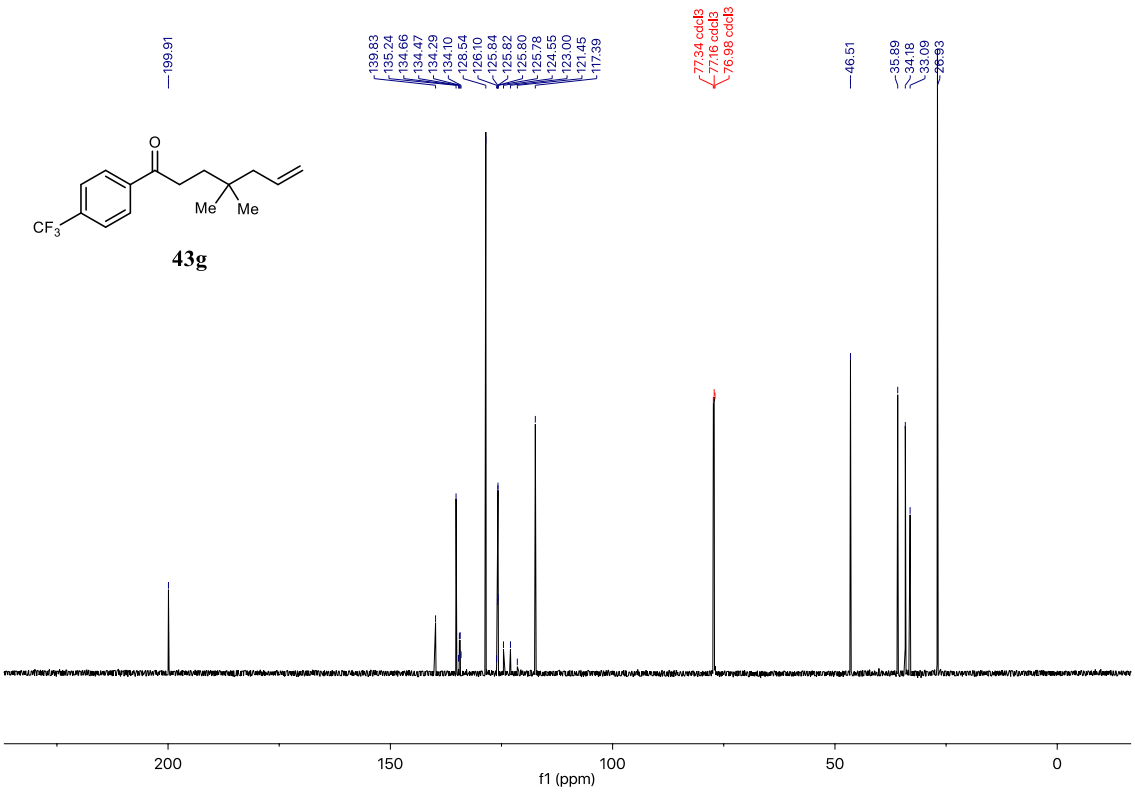
199.91
139.83
135.24
134.66
134.47
134.29
134.10
128.54
126.10
125.84
125.82
125.80
125.78
124.55
123.00
121.45
117.39
77.34 cdcl3
77.16 cdcl3
76.98 cdcl3
46.51
35.89
34.18
33.09
26.93
O
Me
Me
CF3
200
150
100
50
0
f1 (ppm)

43g

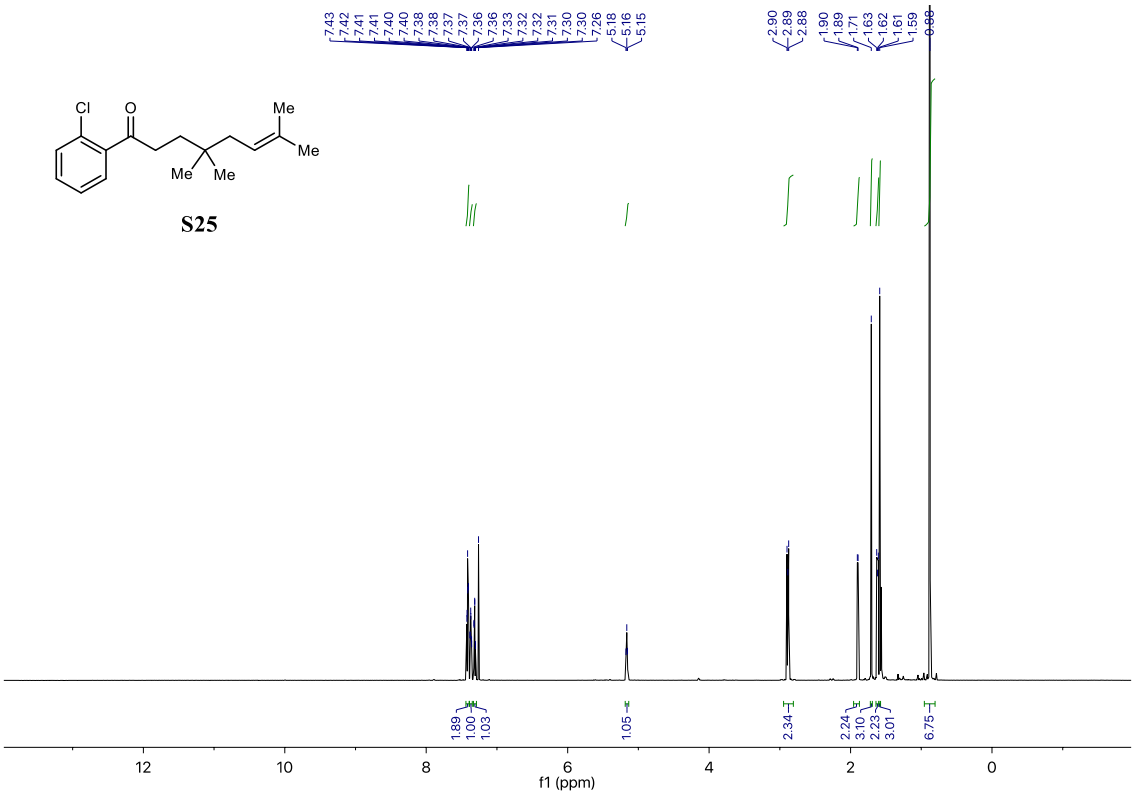
Cl
O
Me
Me
Me
Me
S25
7.43
7.42
7.41
7.41
7.40
7.40
7.38
7.38
7.37
7.37
7.36
7.36
7.33
7.32
7.32
7.31
7.30
7.30
7.26
5.18
5.16
5.15
2.90
2.89
2.88
1.90
1.89
1.71
1.63
1.62
1.61
1.59
0.88
1.89
1.00
1.03
1.05
2.34
2.24
3.10
2.23
3.01
6.75
12
10
8
6
4
2
0
f1 (ppm)

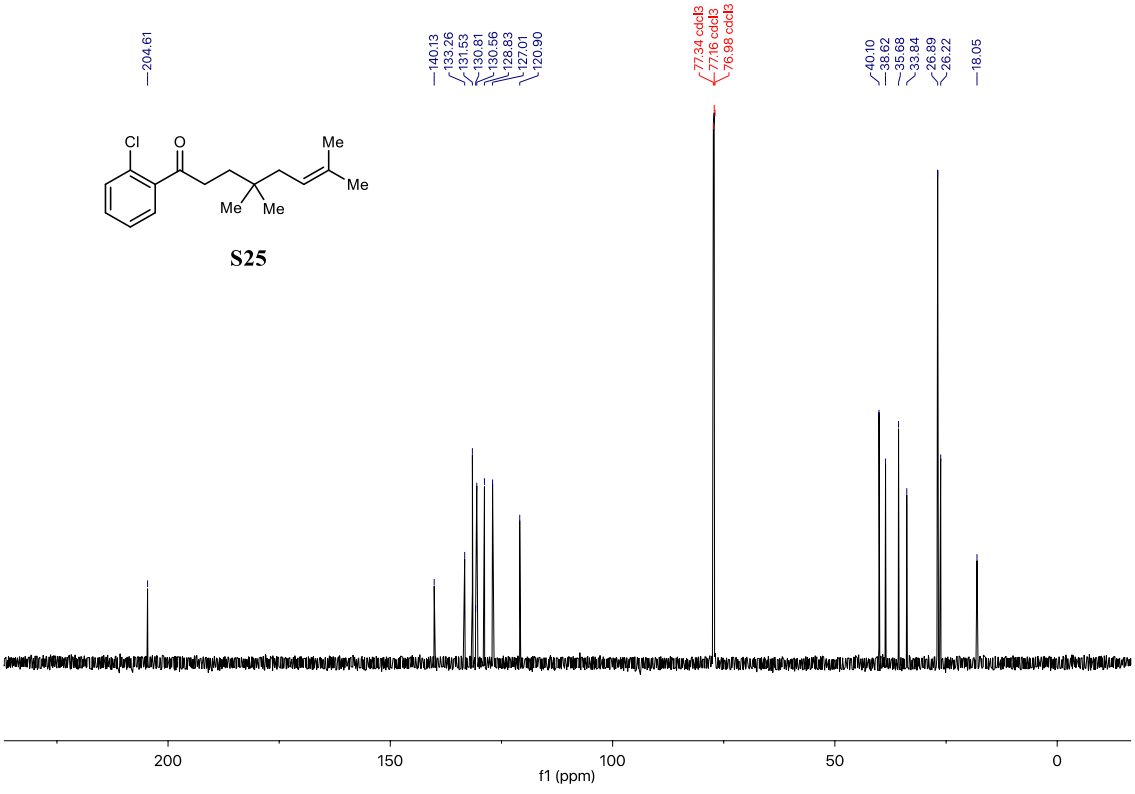
204.61
140.13
133.26
131.53
130.81
130.56
128.83
127.01
120.90
77.34 cdcl3
77.16 cdcl3
76.98 cdcl3
40.10
38.62
35.68
33.84
26.89
26.22
18.05
Cl
O
Me
Me
Me
Me
S25
200
150
100
50
0
f1 (ppm)

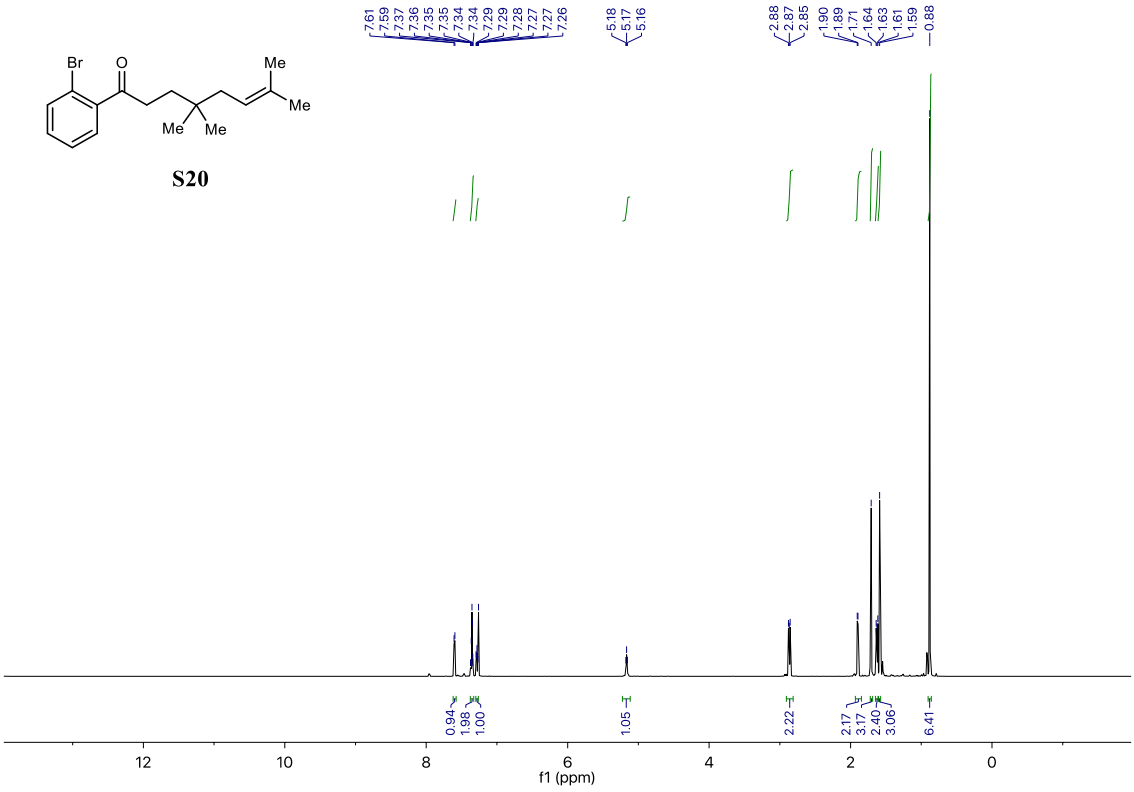
Br
O
Me
Me
Me
Me
S20
7.61
7.59
7.37
7.36
7.35
7.35
7.34
7.34
7.29
7.29
7.28
7.27
7.27
7.26
5.18
5.17
5.16
2.88
2.87
2.85
1.90
1.89
1.71
1.64
1.63
1.61
1.59
0.88
0.94
1.98
1.00
1.05
2.22
2.17
3.17
2.40
3.06
6.41
12
10
8
6
4
2
0
f1 (ppm)

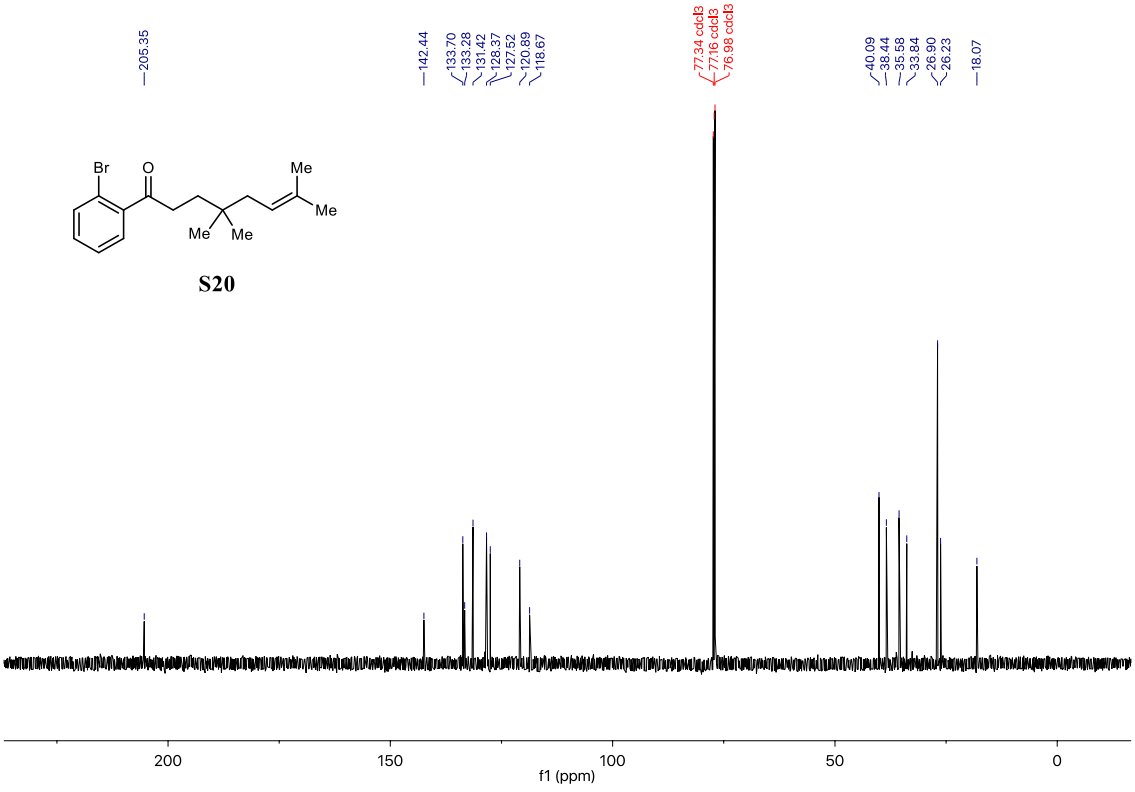
205.35
142.44
133.70
133.28
131.42
128.37
127.52
120.89
118.67
77.34 cdcl3
77.16 cdcl3
76.98 cdcl3
40.09
38.44
35.58
33.84
26.90
26.23
18.07
Br
O
Me
Me
Me
Me
S20
200
150
100
50
0
f1 (ppm)

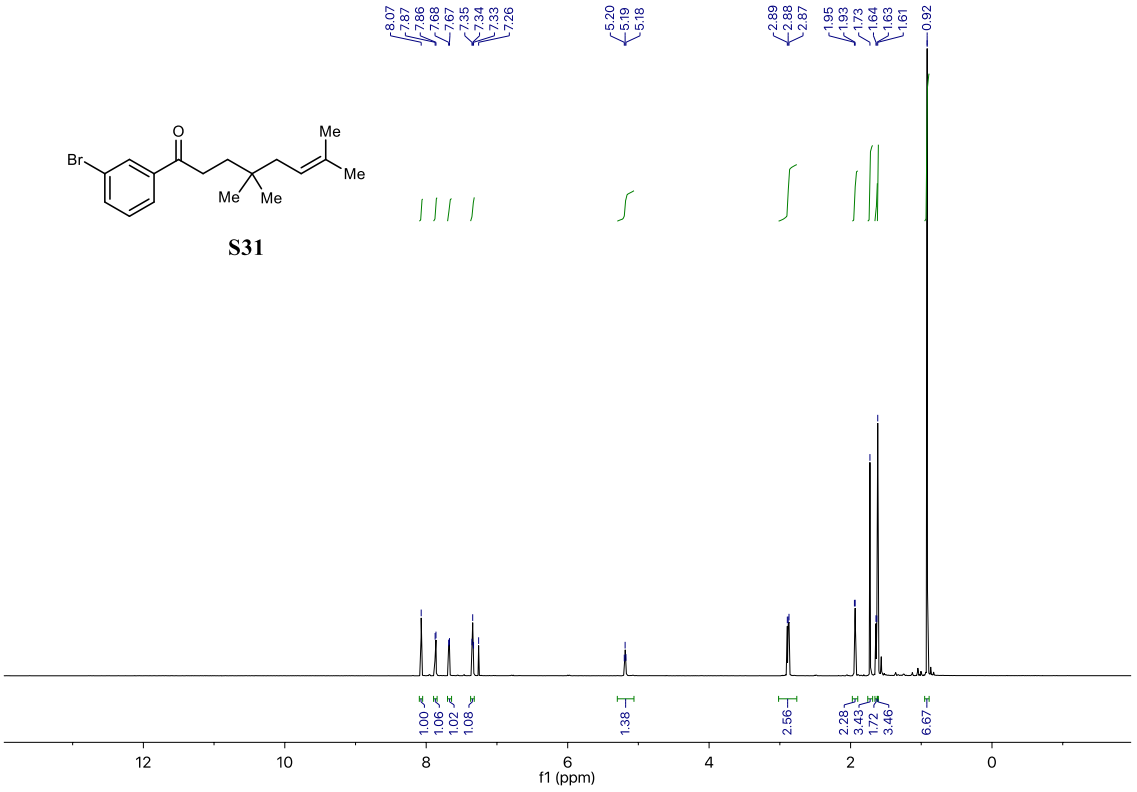
8.07
7.87
7.86
7.68
7.67
7.35
7.34
7.33
7.26
5.20
5.19
5.18
2.89
2.88
2.87
1.95
1.93
1.73
1.64
1.63
1.61
0.92
Br
O
Me
Me
Me
Me
1.00
1.06
1.02
1.08
1.38
2.56
2.28
3.43
1.72
3.46
6.67
12
10
8
6
4
2
0
f1 (ppm)

S31

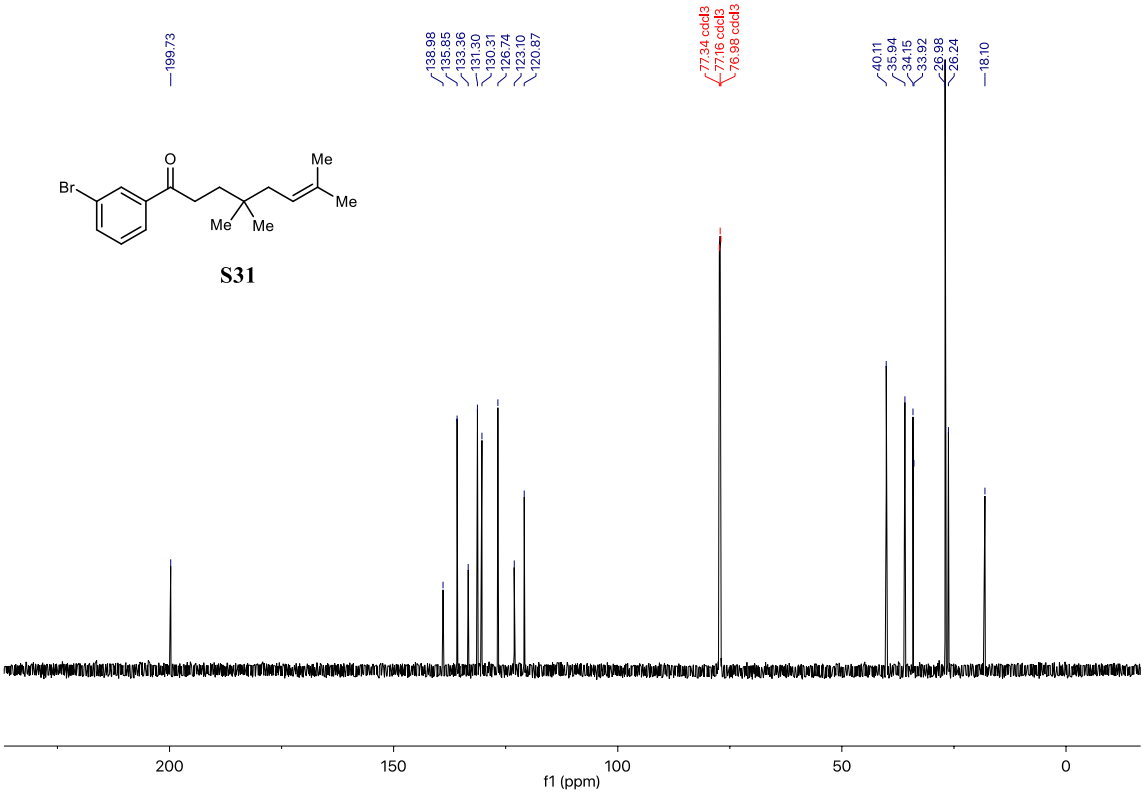
199.73
138.98
135.85
133.36
131.30
130.31
126.74
123.10
120.87
77.34 cdcl3
77.16 cdcl3
76.98 cdcl3
40.11
35.94
34.15
33.92
26.98
26.24
18.10
Br
O
Me
Me
Me
Me
200
150
100
50
0
f1 (ppm)

S31

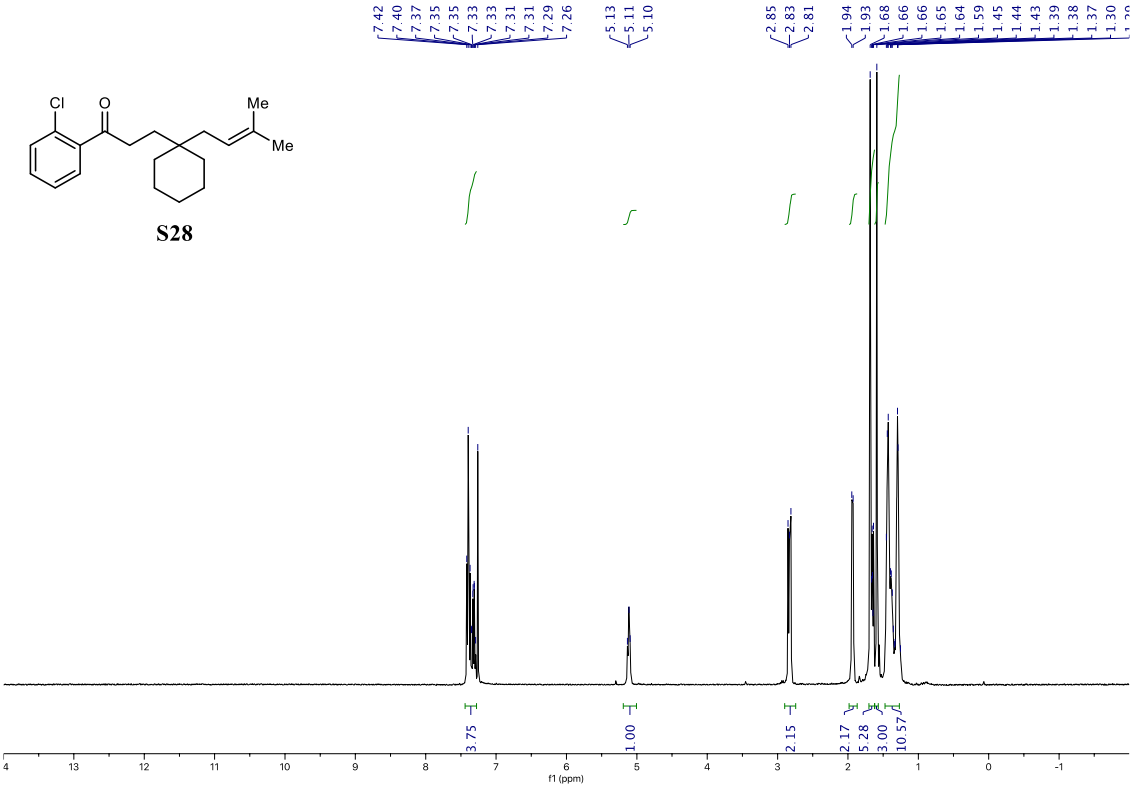
Cl
O
Me
Me
7.42
7.40
7.37
7.35
7.35
7.33
7.33
7.31
7.31
7.29
7.26
5.13
5.11
5.10
2.85
2.83
2.81
1.94
1.93
1.68
1.66
1.66
1.65
1.64
1.59
1.45
1.44
1.43
1.39
1.38
1.37
1.30
3.75
1.00
2.15
2.17
5.28
3.00
10.57
f1 (ppm)

S28

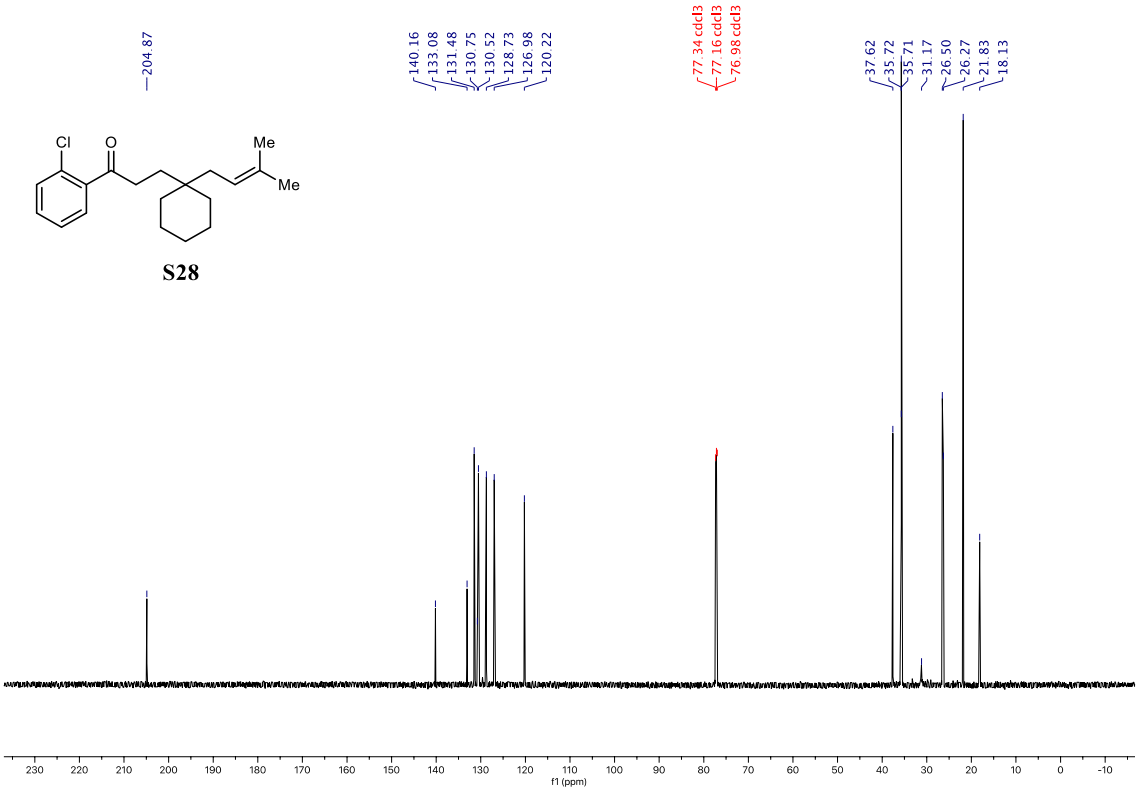
204.87
140.16
133.08
131.48
130.75
130.52
128.73
126.98
120.22
77.34 cdcl3
77.16 cdcl3
76.98 cdcl3
37.62
35.72
35.71
31.17
26.50
26.27
21.83
18.13
Cl
O
Me
Me
f1 (ppm)

S28

AJD-834a-1H
Proton Spectrum

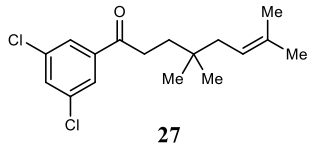

27

AJD-834a-13C-final
Carbon-13

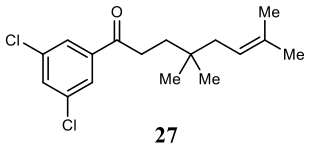

27

AJD-815a-1H
Proton Spectrum

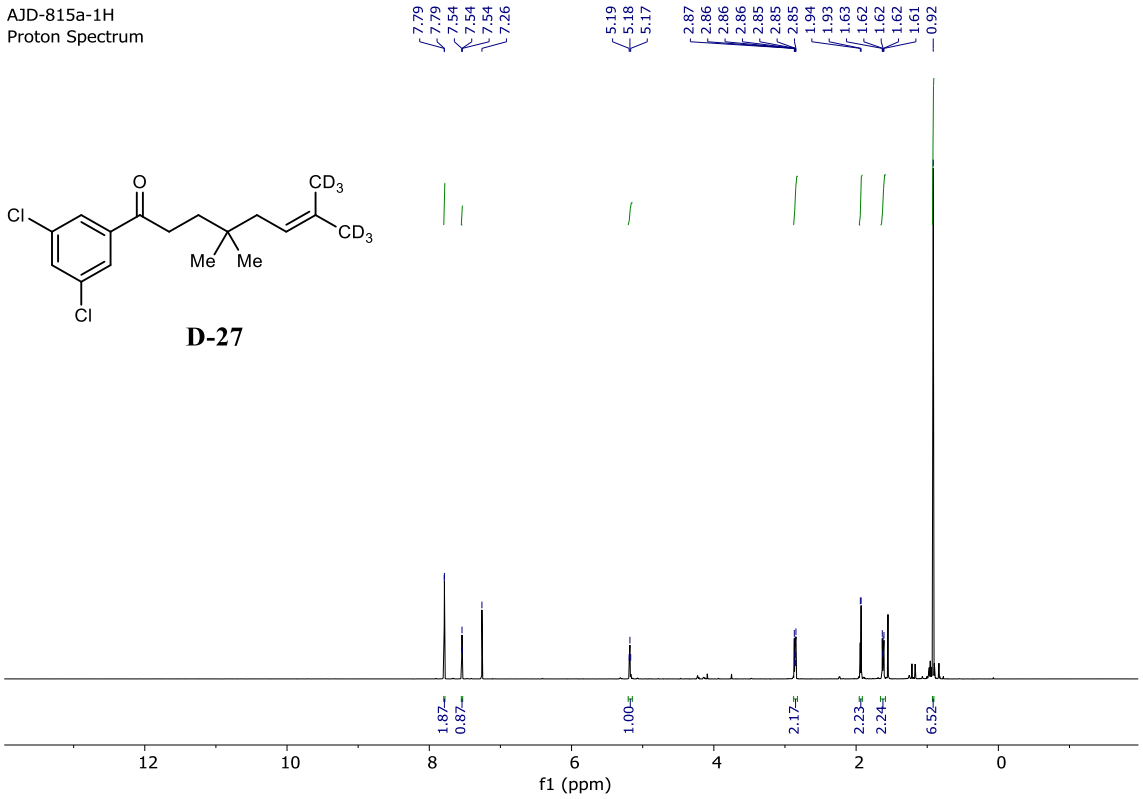

D-27

AJD-815a-13C-scan11
Carbon-13

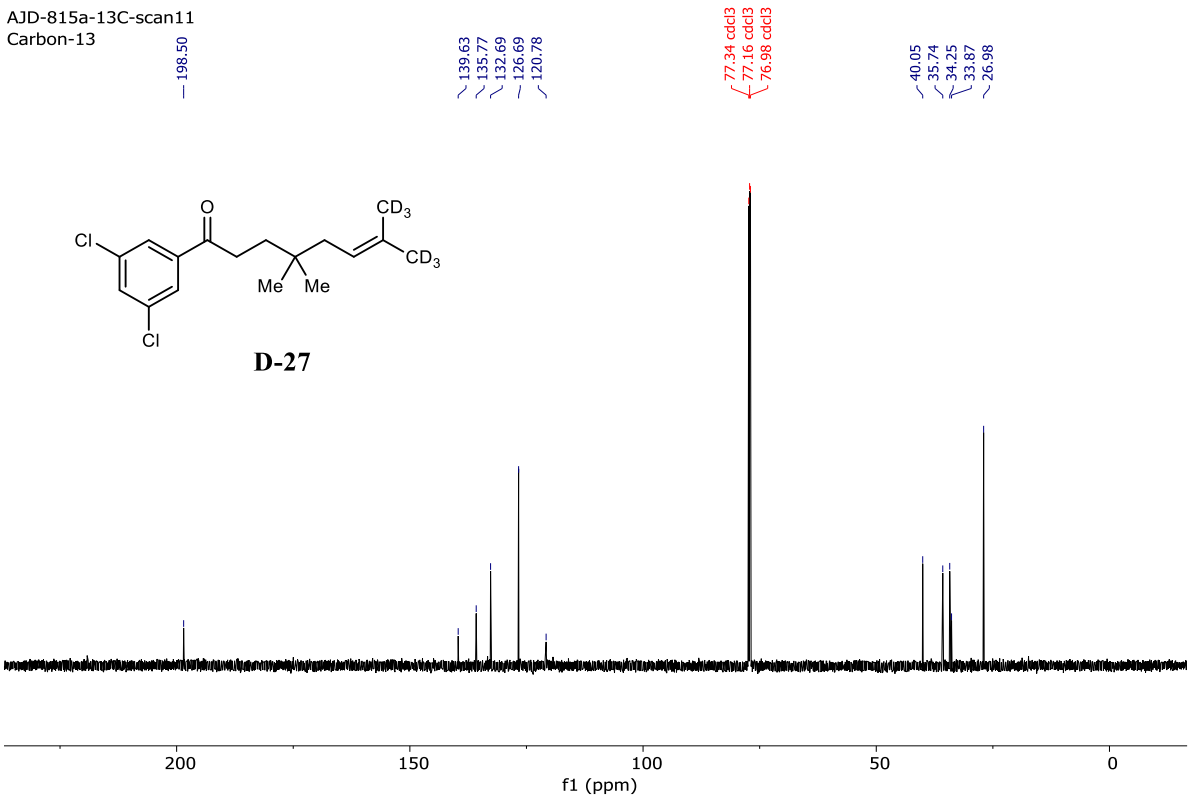

D-27

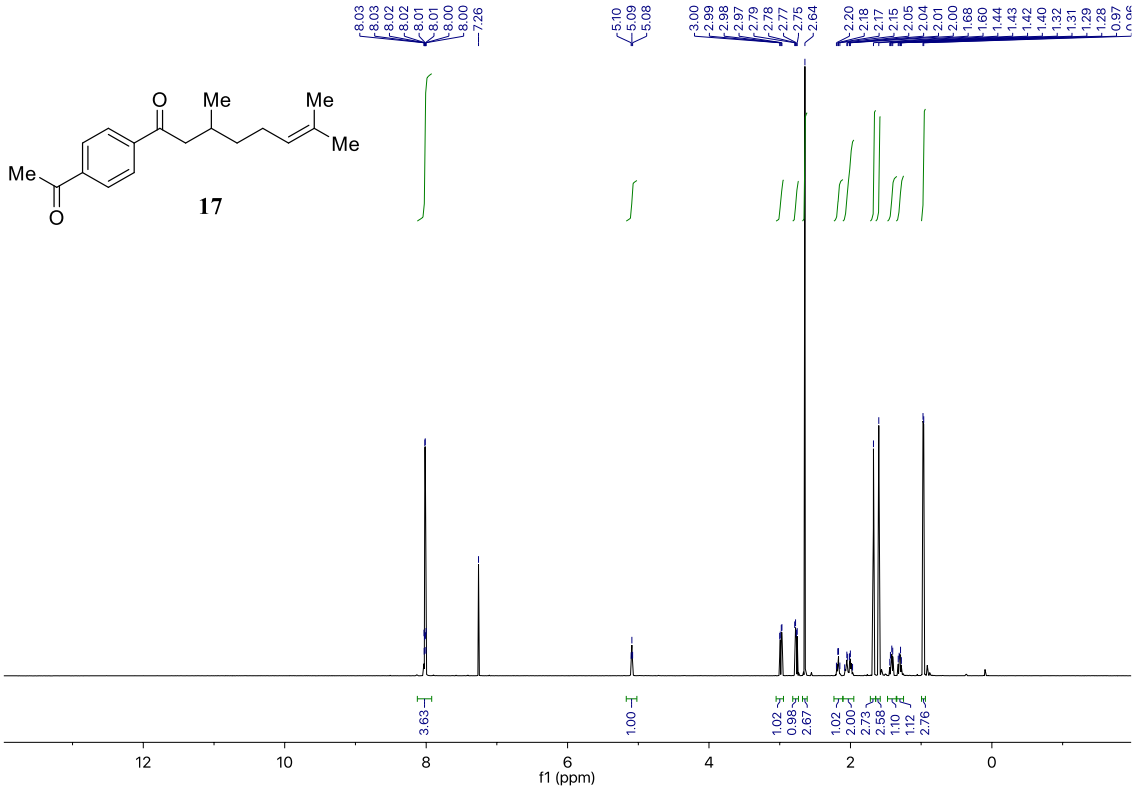
8.03
8.03
8.02
8.02
8.01
8.01
8.00
8.00
7.26
5.10
5.09
5.08
3.00
2.99
2.98
2.97
2.79
2.78
2.77
2.75
2.64
2.20
2.18
2.17
2.15
2.05
2.04
2.01
2.00
1.68
1.60
1.44
1.43
1.42
1.40
1.32
1.31
1.29
1.28
0.97
O
Me
Me
Me
O
17
3.63
1.00
1.02
0.98
2.67
1.02
2.00
2.73
2.58
1.10
1.12
2.76
12
10
8
6
4
2
0
f1 (ppm)

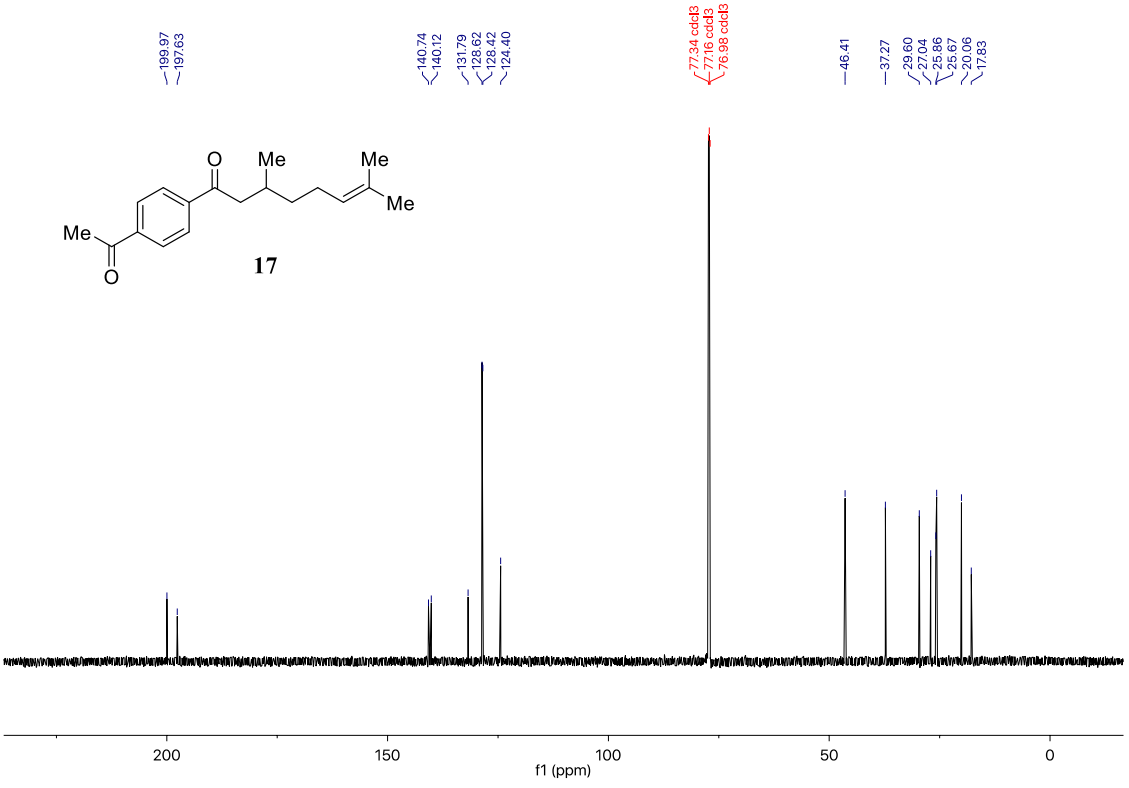
199.97
197.63
140.74
140.12
131.79
128.62
128.42
124.40
77.34 cdd3
77.16 cdd3
76.98 cdd3
46.41
37.27
29.60
27.04
25.86
25.67
20.06
17.83
O
Me
Me
Me
O
17
200
150
100
50
0
f1 (ppm)

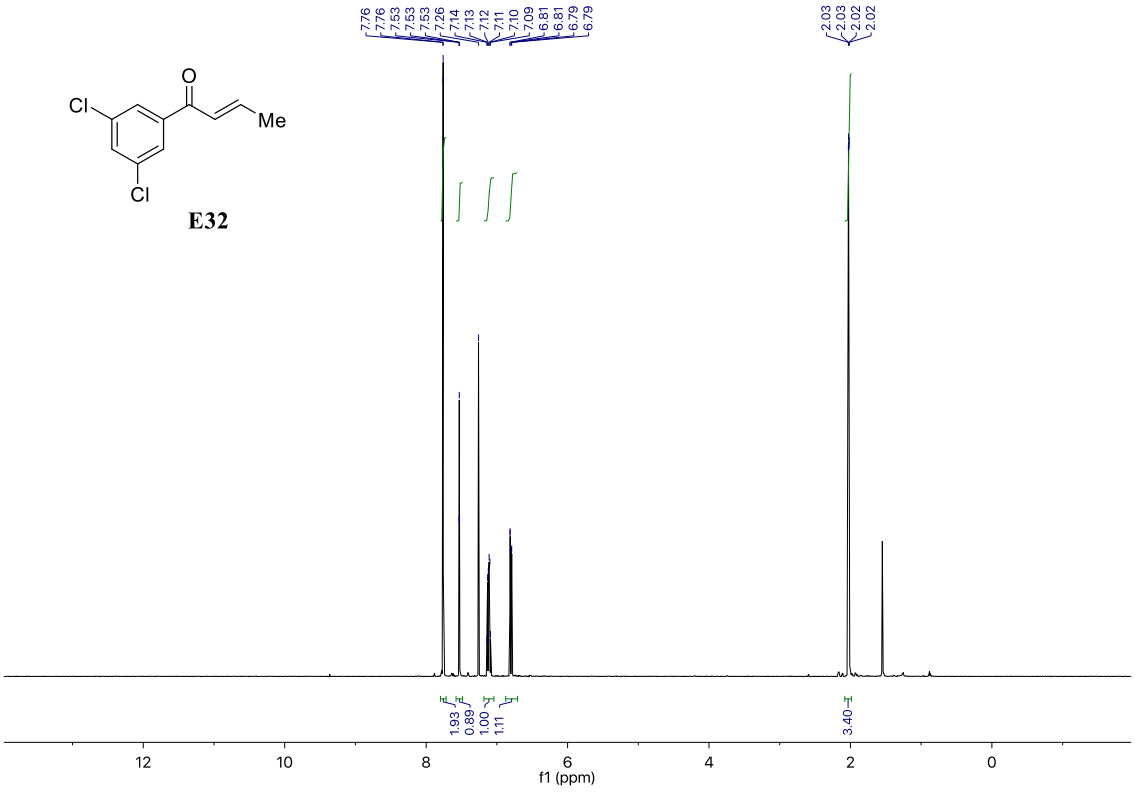
7.76
7.76
7.53
7.53
7.53
7.26
7.14
7.13
7.12
7.11
7.10
7.09
6.81
6.81
6.79
6.79
2.03
2.03
2.02
2.02
O
Cl
Me
Cl
E32
1.93
0.89
1.00
1.11
3.40
12
10
8
6
4
2
0
f1 (ppm)

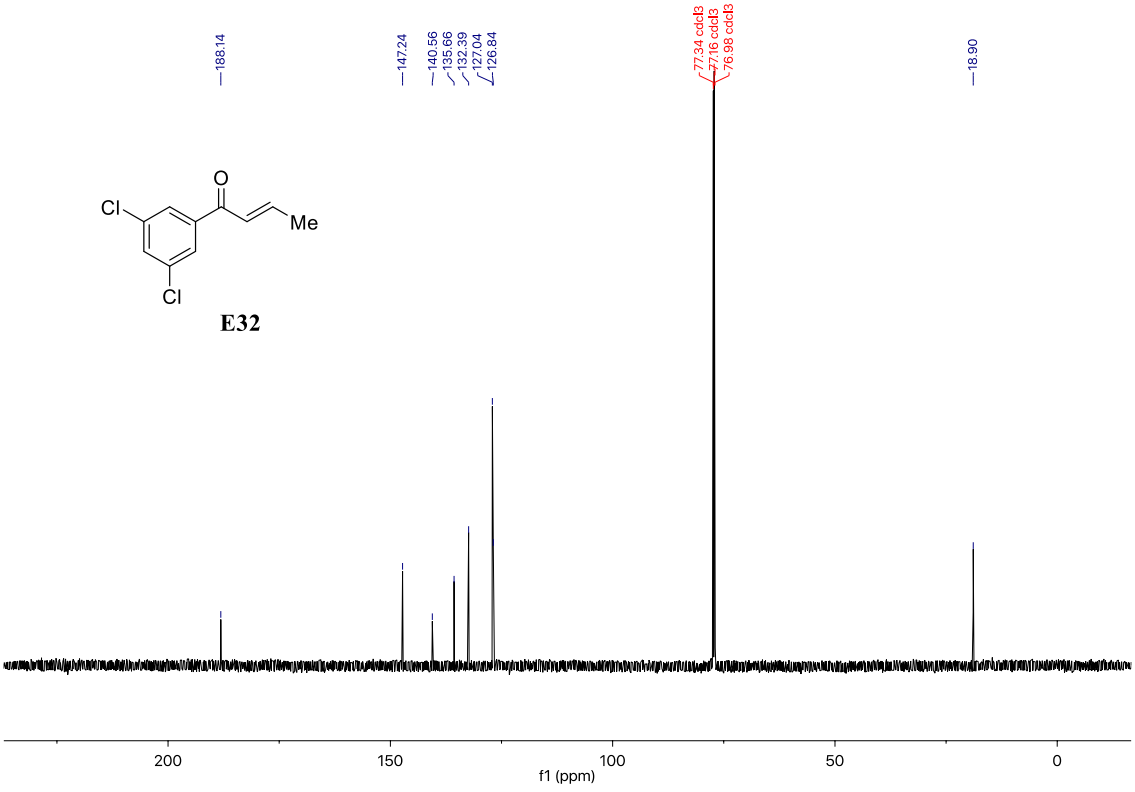
188.14
147.24
140.56
135.66
132.39
127.04
126.84
77.34 cdcl3
77.16 cdcl3
76.98 cdcl3
18.90
O
Cl
Me
Cl
E32
200
150
100
50
0
f1 (ppm)

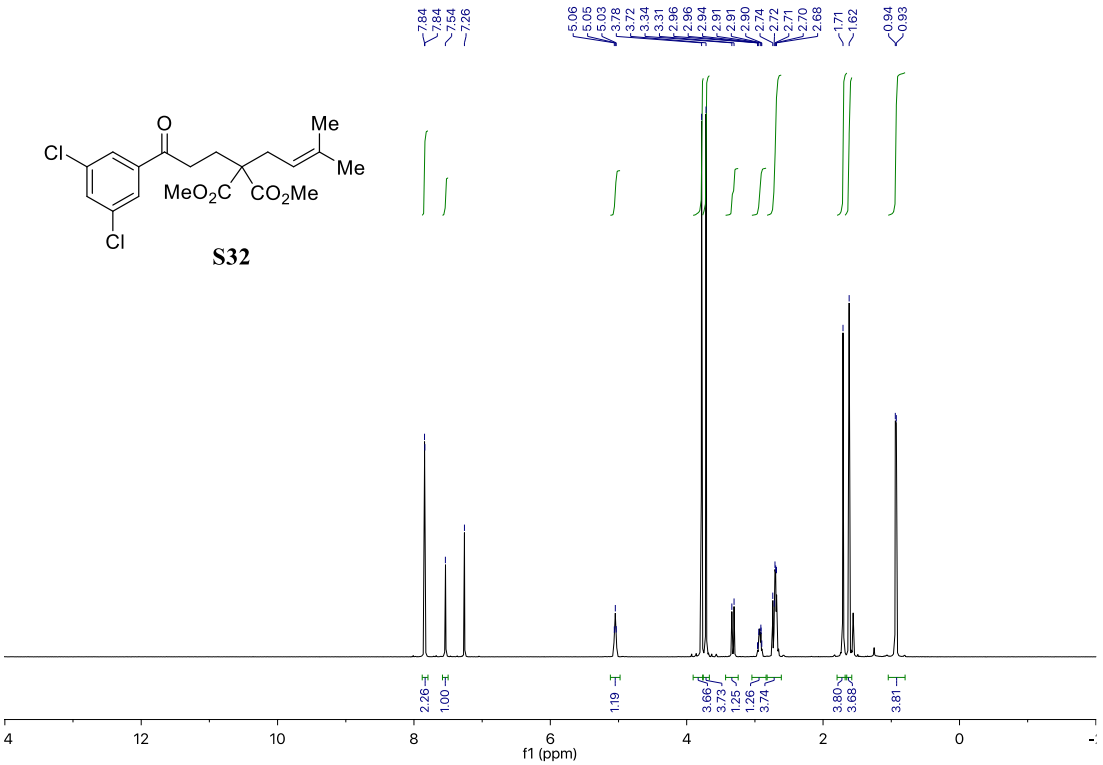
7.84
7.84
7.54
7.26
5.06
5.05
5.03
3.78
3.72
3.34
3.31
2.96
2.96
2.94
2.91
2.91
2.90
2.74
2.72
2.71
2.70
2.68
1.71
1.62
0.94
0.93
Cl
O
Me
Me
MeO2C
CO2Me
Cl
2.26
1.00
1.19
3.66
3.73
1.25
1.26
3.74
3.80
3.68
3.81
4
12
10
8
6
4
2
0
f1 (ppm)

S32

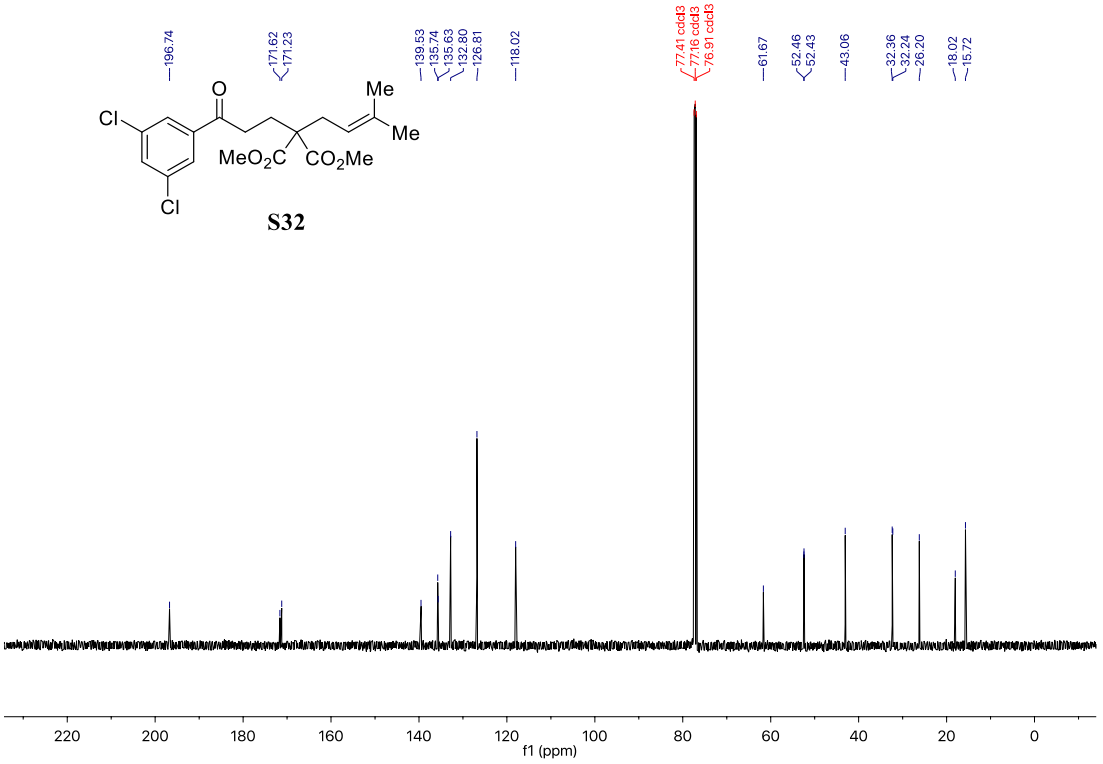
196.74
171.62
171.23
139.53
135.74
135.63
132.80
126.81
118.02
77.41 cdcl3
77.16 cdcl3
76.91 cdcl3
61.67
52.46
52.43
43.06
32.36
32.24
26.20
18.02
15.72
Cl
O
Me
Me
MeO2C
CO2Me
Cl
220
200
180
160
140
120
100
80
60
40
20
0
f1 (ppm)

S32

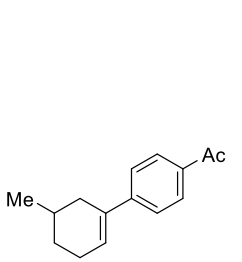
Ac
Me

17

7.91
7.89
7.47
7.45
7.26
6.25
6.10
2.59
2.50
2.49
2.46
2.45
2.34
2.28
2.27
2.26
2.25
2.24
2.09
2.08
2.06
2.03
2.02
1.85
1.80
1.78
1.75
1.74
1.32
1.29
1.26
1.25
1.23
1.21
1.08
1.06
2.17
2.19
1.00
0.08
3.37
1.08
2.38
1.12
2.34
1.88
3.48
4
12
10
8
6
4
2
0
f1 (ppm)

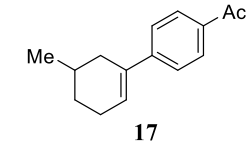
Ac
Me

17

197.91
147.27
135.62
135.32
128.57
127.20
125.06
77.34 cdcl3
77.16 cdcl3
76.98 cdcl3
35.84
30.30
29.04
26.72
26.27
22.12
200
150
100
50
0
f1 (ppm)

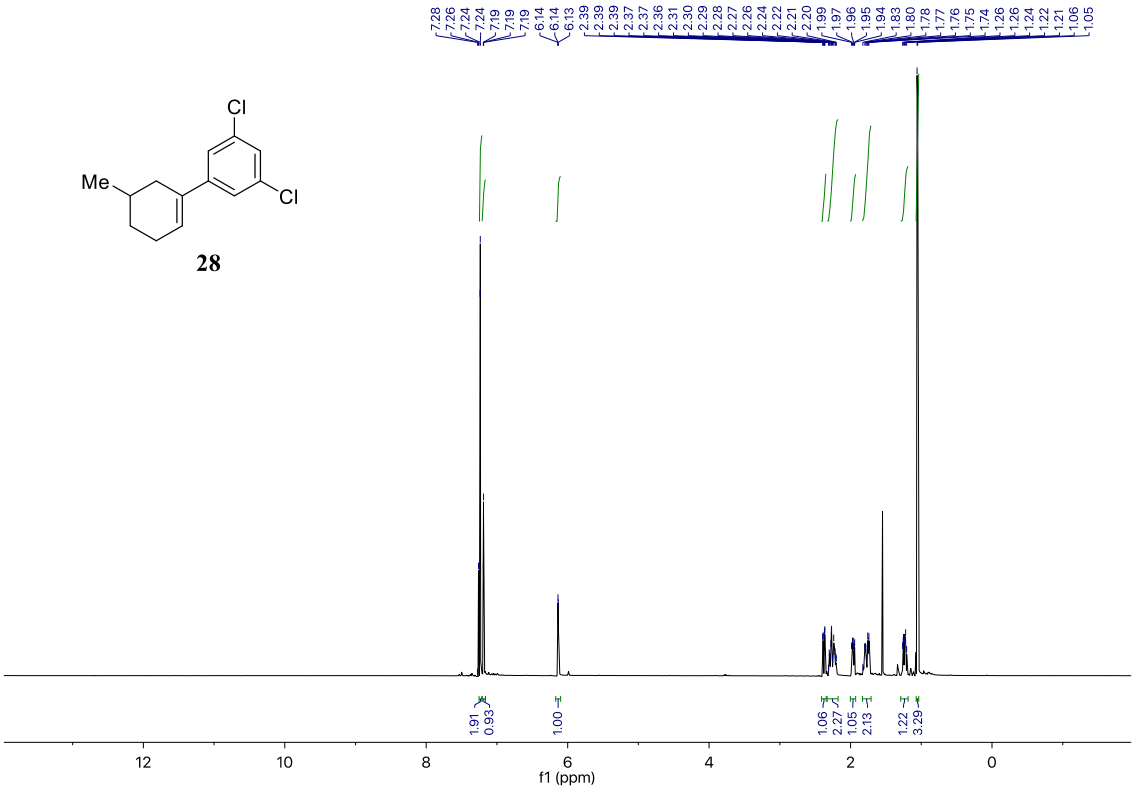
Cl
Me
Cl
28
7.28
7.26
7.24
7.24
7.19
7.19
7.19
6.14
6.14
6.13
2.39
2.39
2.39
2.37
2.37
2.36
2.31
2.30
2.29
2.28
2.27
2.26
2.24
2.22
2.21
2.20
1.99
1.97
1.96
1.95
1.94
1.83
1.80
1.78
1.77
1.76
1.75
1.74
1.26
1.26
1.24
1.22
1.21
1.06
1.05
1.91
0.93
1.00
1.06
2.27
1.05
2.13
1.22
3.29
12
10
8
6
4
2
0
f1 (ppm)

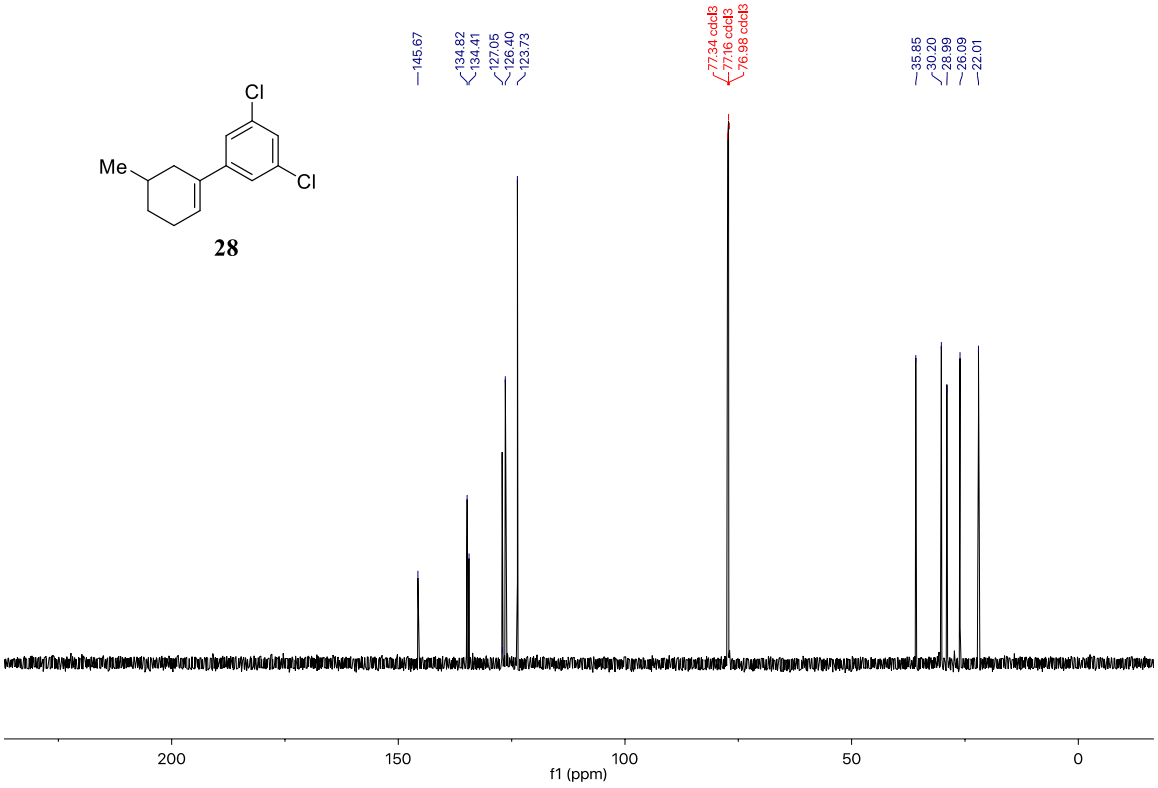
Cl
Me
Cl
28
145.67
134.82
134.41
127.05
126.40
123.73
77.34 cdcl3
77.16 cdcl3
76.98 cdcl3
35.85
30.20
28.99
26.09
22.01
200
150
100
50
0
f1 (ppm)

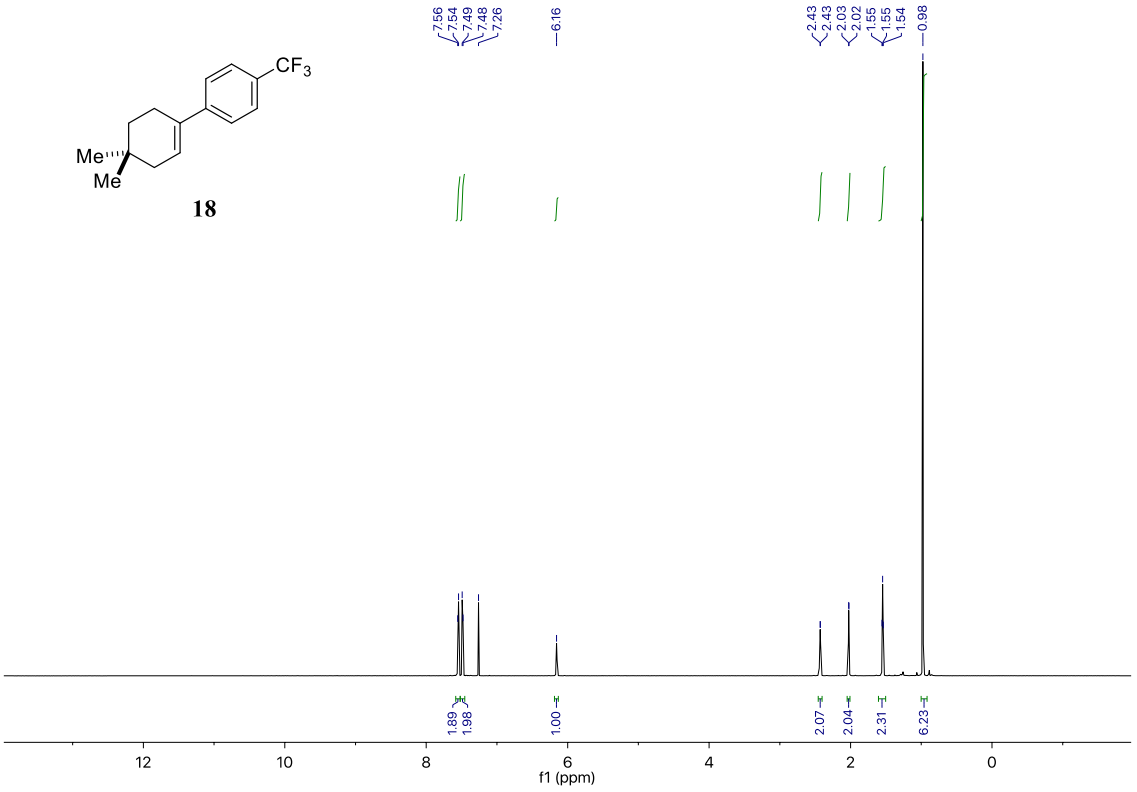
CF3
Me
Me
18
7.56
7.54
7.49
7.48
7.26
6.16
2.43
2.43
2.03
2.02
1.55
1.55
1.54
0.98
1.89
1.98
1.00
2.07
2.04
2.31
6.23
12
10
8
6
4
2
0
f1 (ppm)

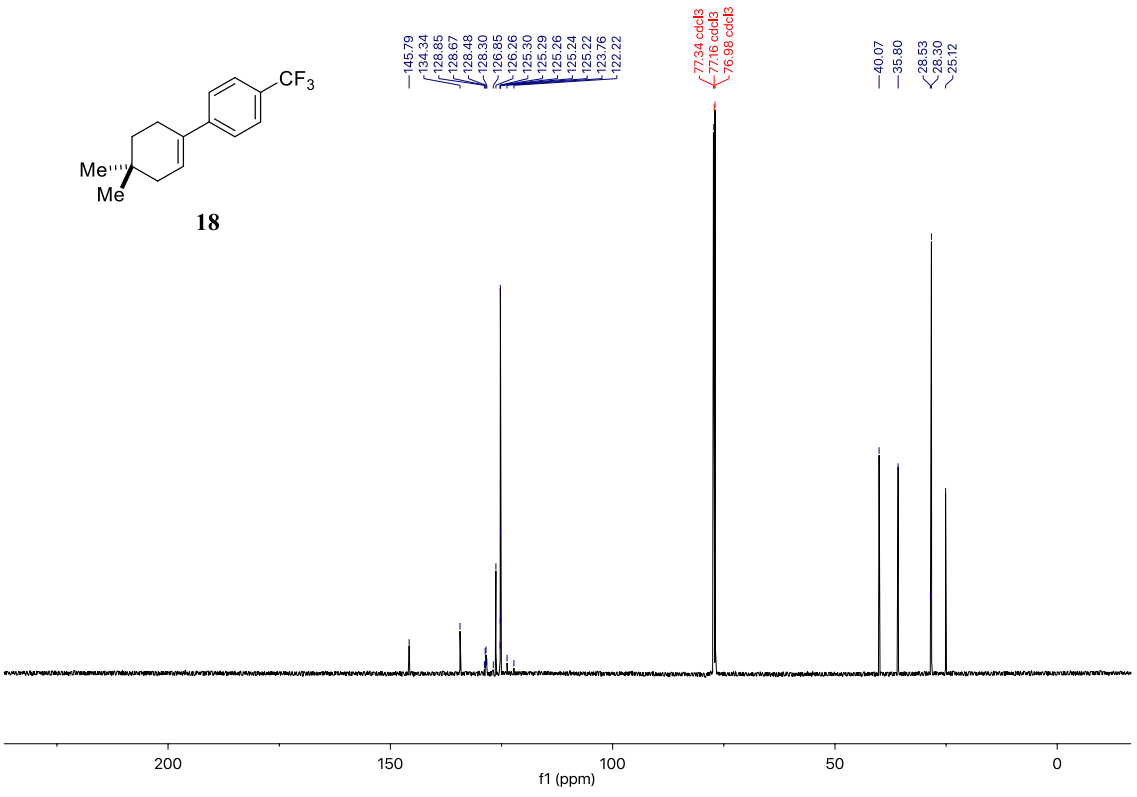
CF3
Me
Me
18
145.79
134.34
128.85
128.67
128.48
128.30
126.85
126.26
125.30
125.29
125.26
125.24
125.22
123.76
122.22
77.34 cdcl3
77.16 cdcl3
76.98 cdcl3
40.07
35.80
28.53
28.30
25.12
200
150
100
50
0
f1 (ppm)

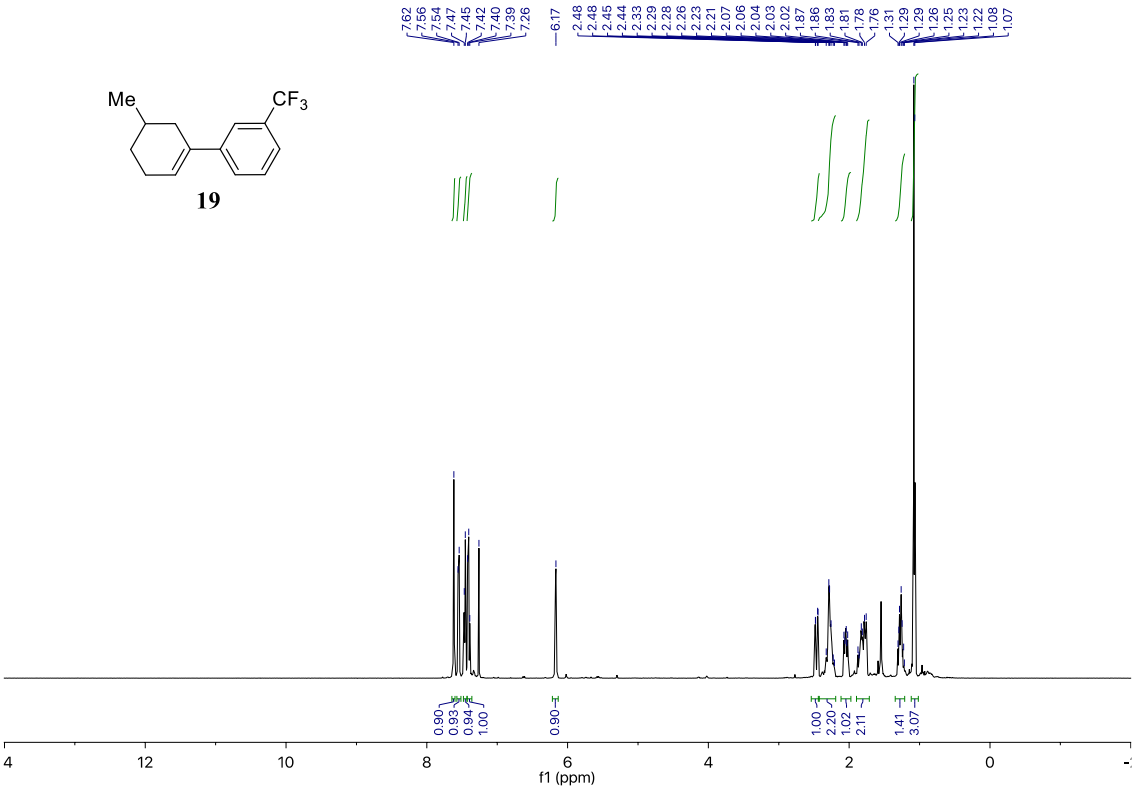
Me
CF3
19
f1 (ppm)

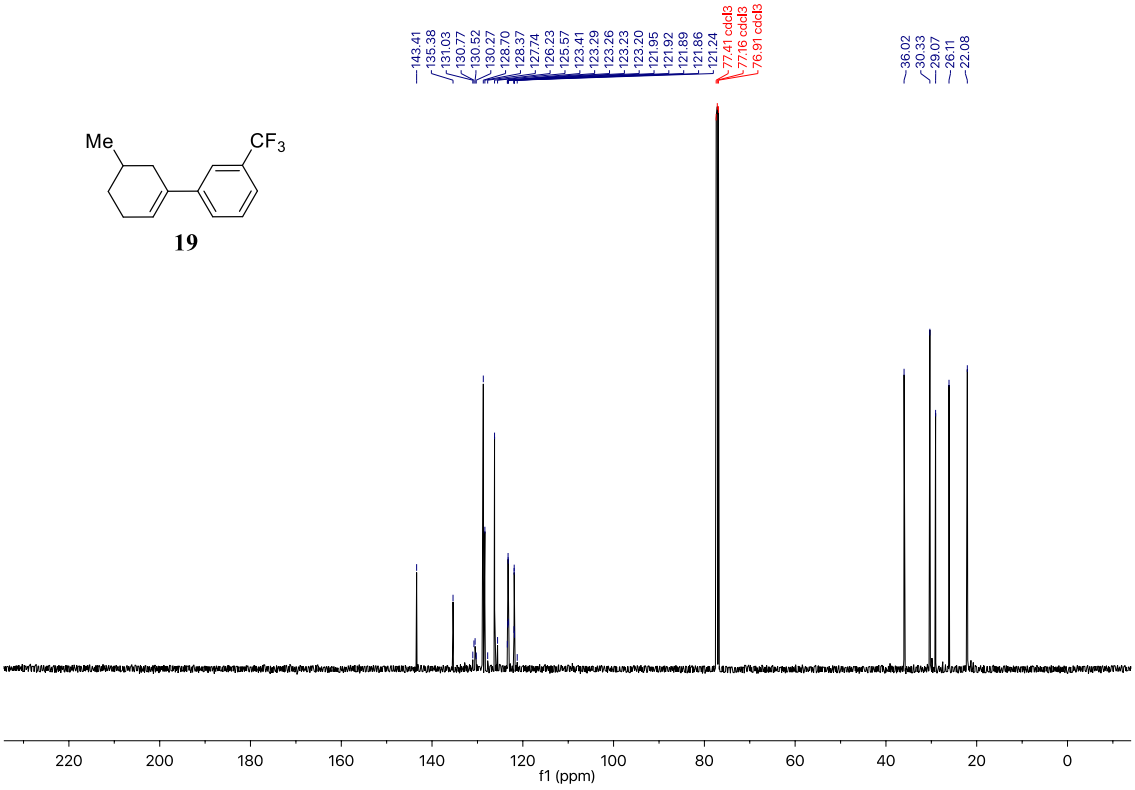
Me
CF3
19
f1 (ppm)

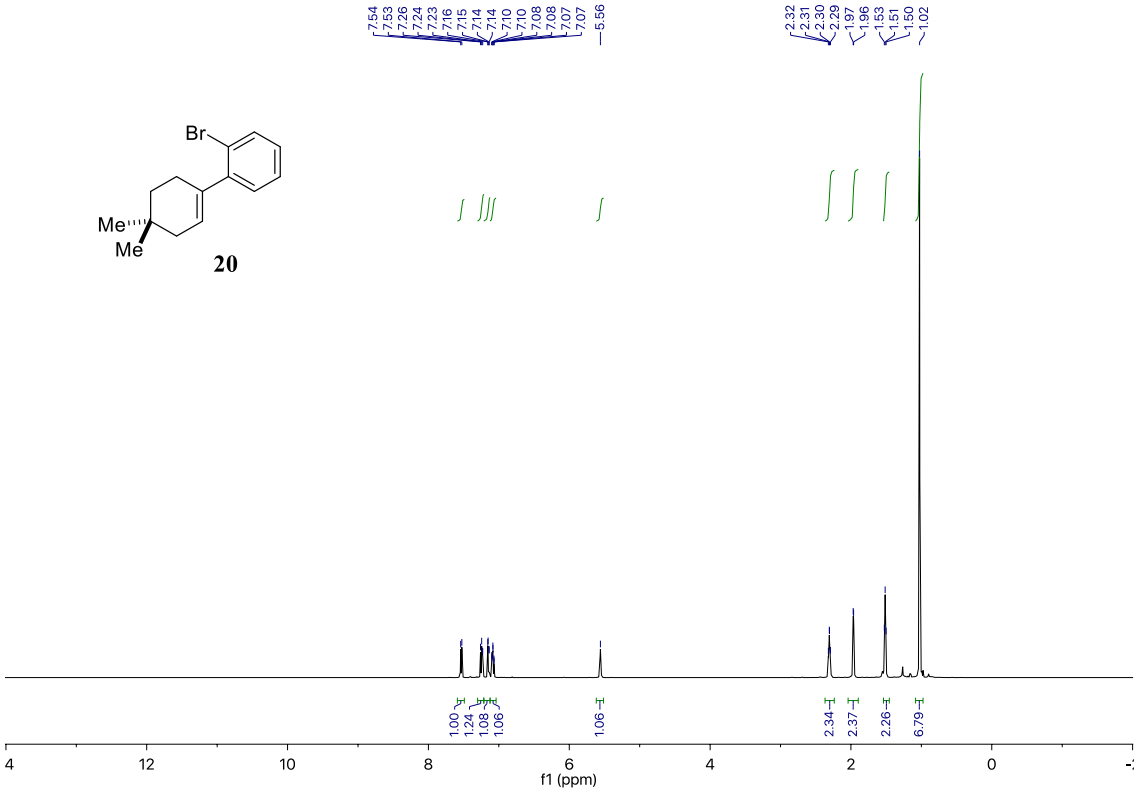
Br
Me
Me
20
7.54
7.53
7.26
7.24
7.23
7.16
7.15
7.14
7.14
7.10
7.08
7.08
7.07
7.07
5.56
2.32
2.31
2.30
2.29
1.97
1.96
1.53
1.51
1.50
1.02
1.00
1.24
1.08
1.06
1.06
2.34
2.37
2.26
6.79
f1 (ppm)

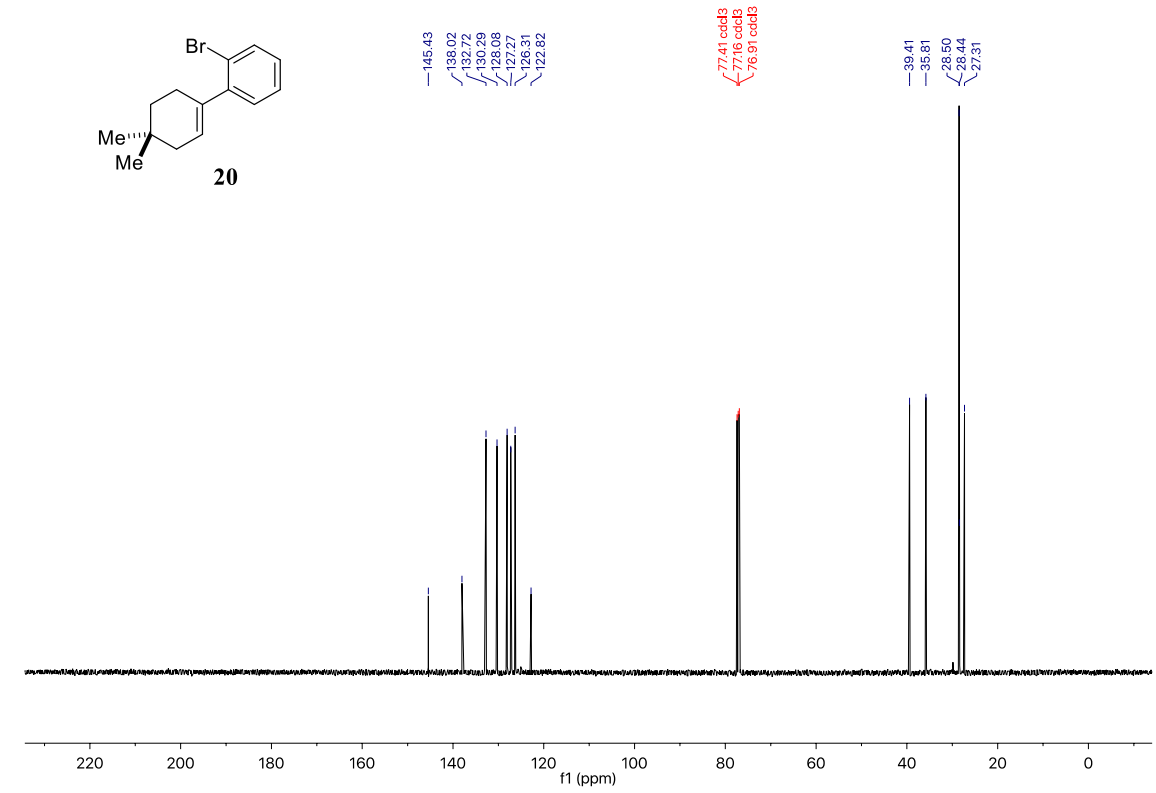
Br
Me
Me
20
145.43
138.02
132.72
130.29
128.08
127.27
126.31
122.82
77.41 cdcl3
77.16 cdcl3
76.91 cdcl3
39.41
35.81
28.50
28.44
27.31
f1 (ppm)

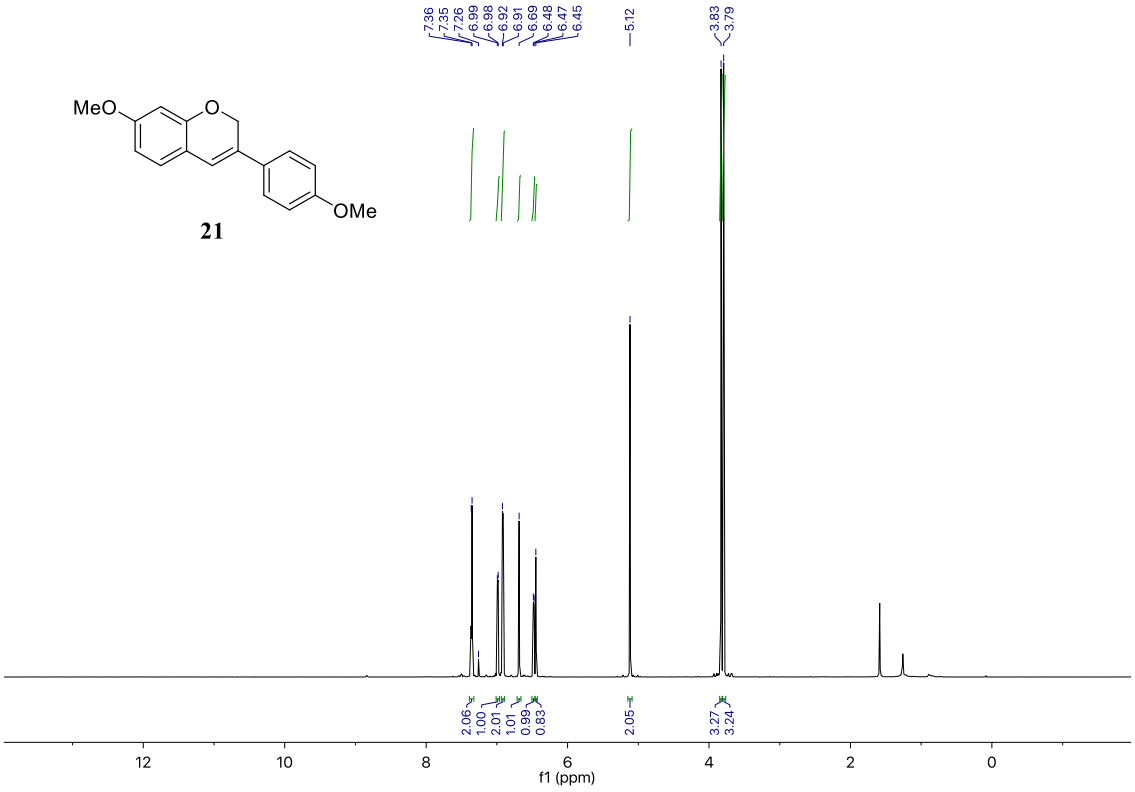
MeO
O
OMe
21
7.36
7.35
7.26
6.99
6.98
6.92
6.91
6.69
6.48
6.47
6.45
5.12
3.83
3.79
2.06
1.00
2.01
1.01
0.99
0.83
2.05
3.27
3.24
12
10
8
6
4
2
0
f1 (ppm)

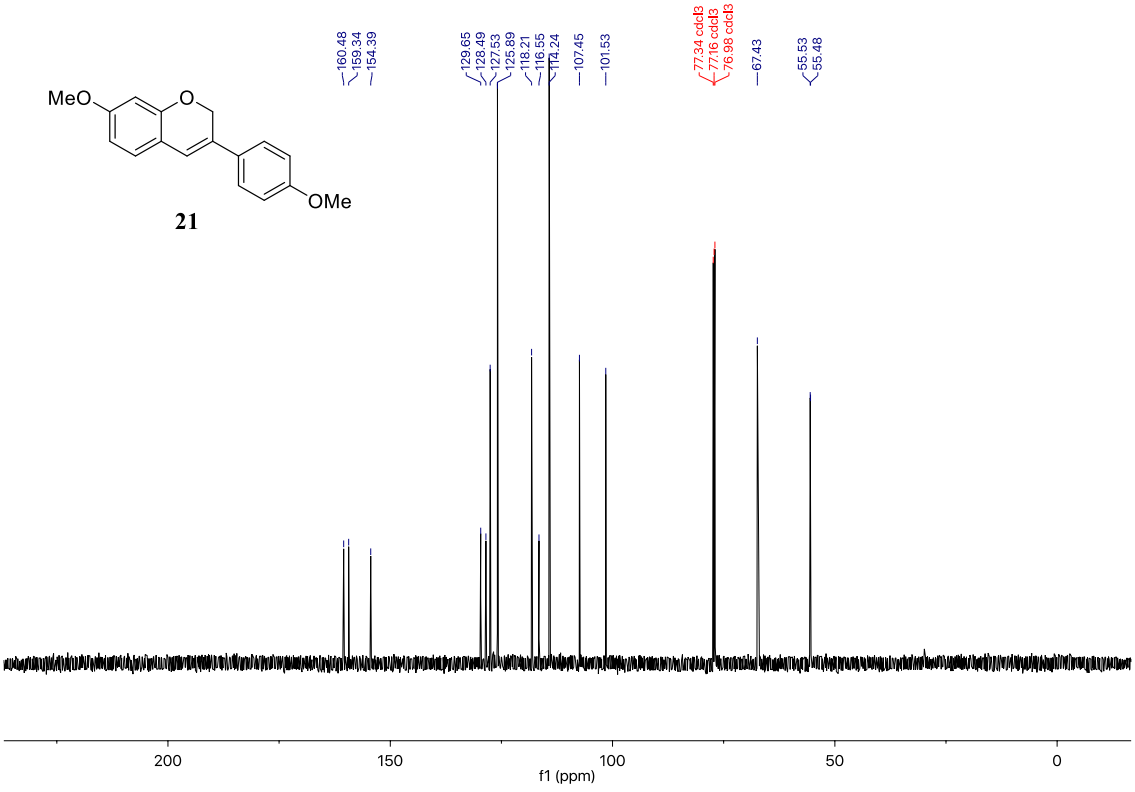
MeO
O
OMe
21
160.48
159.34
154.39
129.65
128.49
127.53
125.89
118.21
116.55
112.24
107.45
101.53
77.34 cdcl3
77.16 cdcl3
76.98 cdcl3
67.43
55.53
55.48
200
150
100
50
0
f1 (ppm)

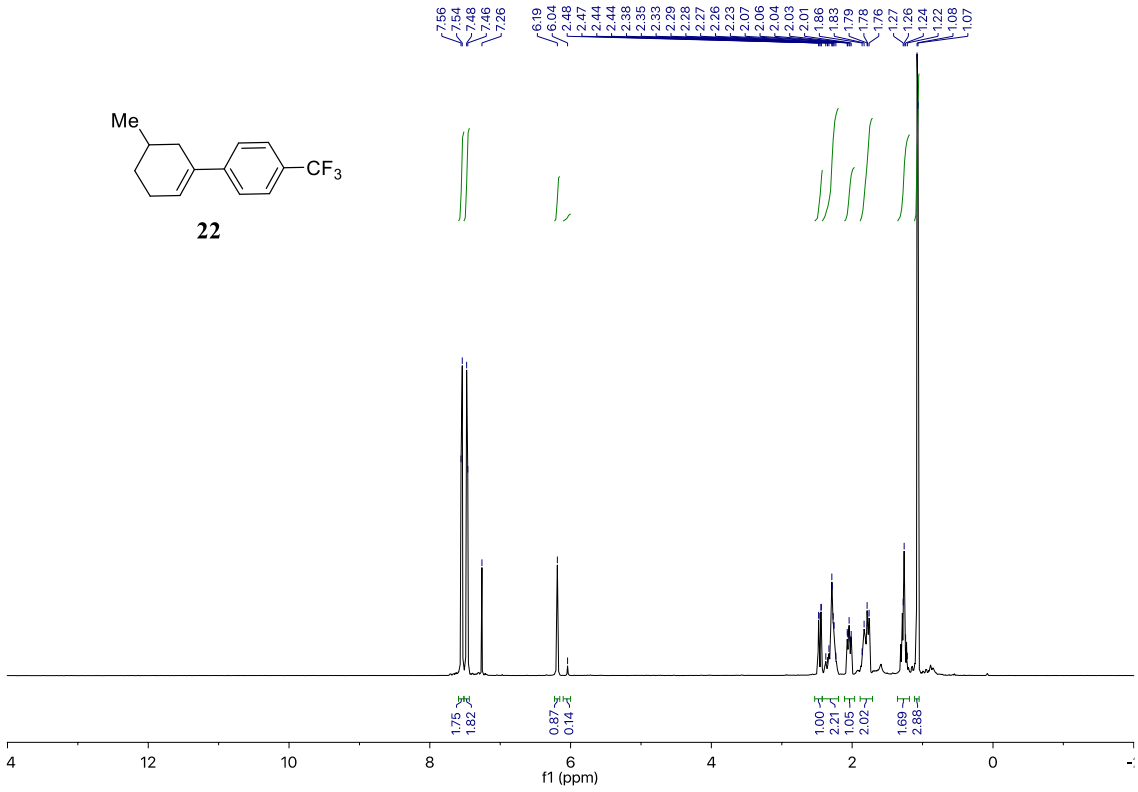
Me
CF3
22
7.56
7.54
7.48
7.46
7.26
6.19
6.04
2.48
2.47
2.44
2.44
2.38
2.35
2.33
2.29
2.28
2.27
2.26
2.23
2.07
2.06
2.04
2.03
2.01
1.86
1.83
1.79
1.78
1.76
1.27
1.26
1.24
1.22
1.08
1.07
1.75
1.82
0.87
0.14
1.00
2.21
1.05
2.02
1.69
2.88
f1 (ppm)

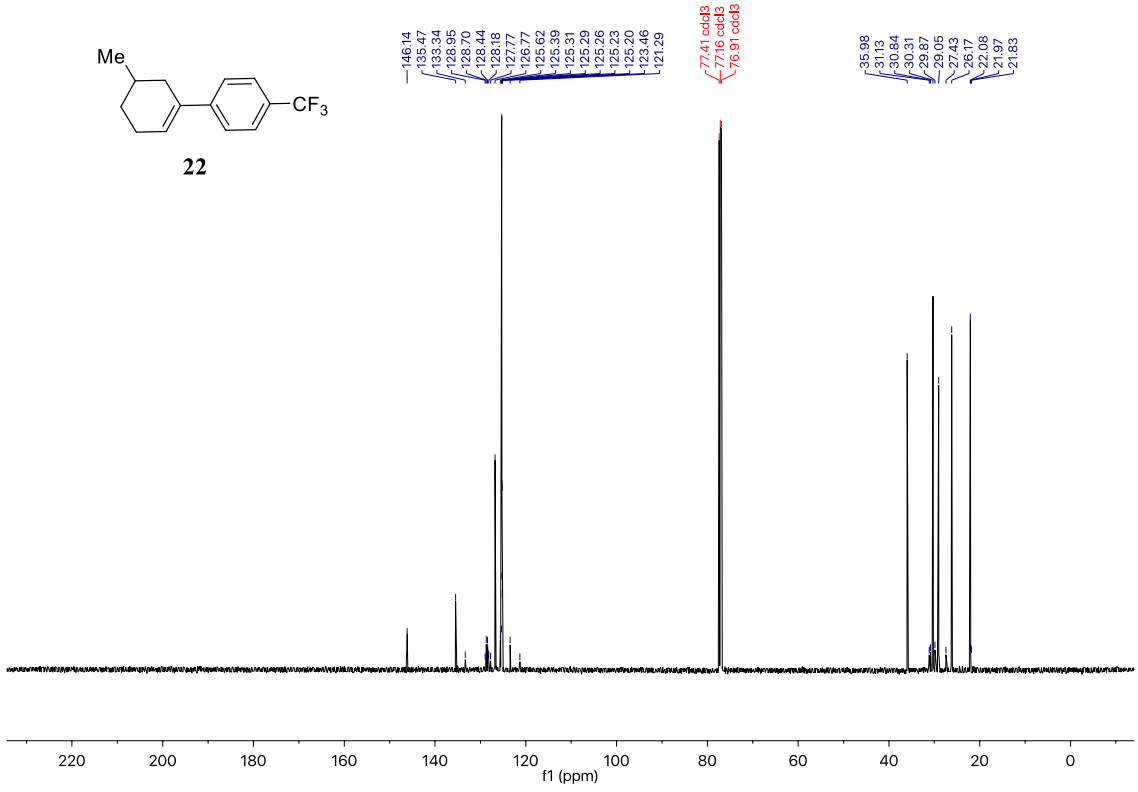
Me
CF3
22
146.14
135.47
133.34
128.95
128.70
128.44
128.18
127.77
126.77
125.62
125.39
125.31
125.29
125.26
125.23
125.20
123.46
121.29
77.41 cdd3
77.16 cdd3
76.91 cdd3
35.98
31.13
30.84
30.31
29.87
29.05
27.43
26.17
22.08
21.97
21.83
f1 (ppm)

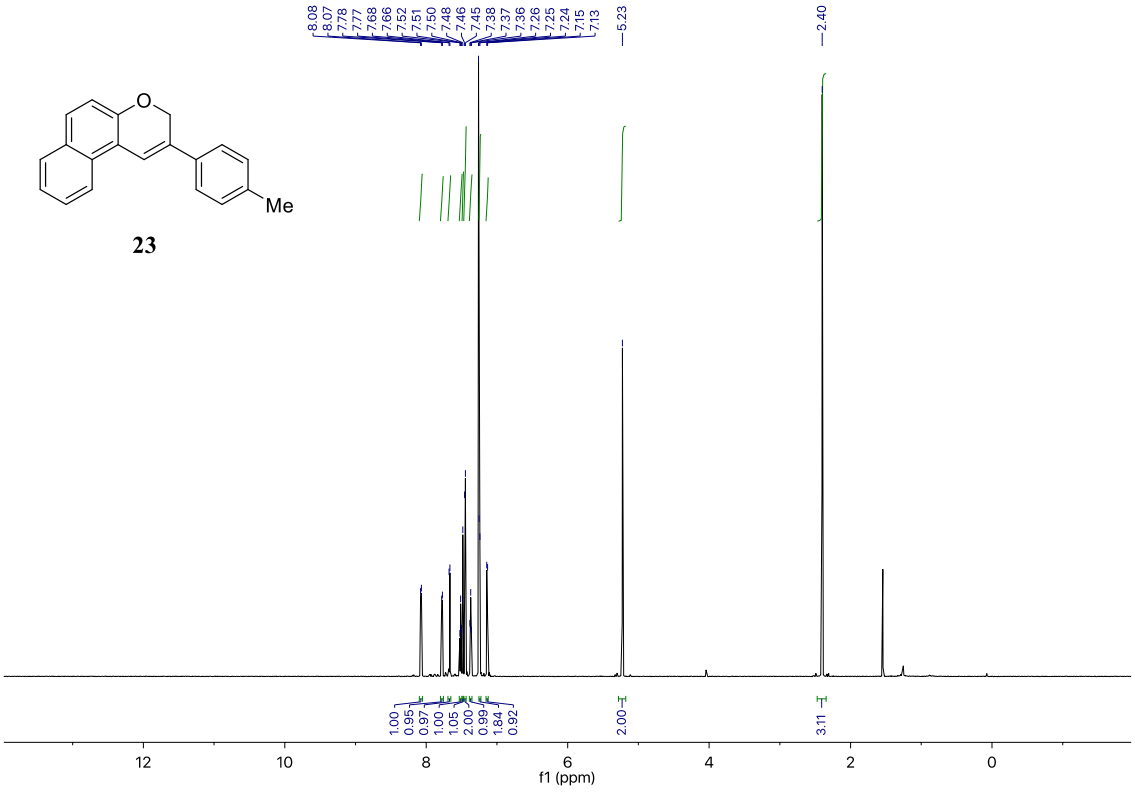
8.08
8.07
7.78
7.77
7.68
7.66
7.52
7.51
7.50
7.48
7.46
7.45
7.38
7.37
7.36
7.26
7.25
7.24
7.15
7.13
5.23
2.40
O
Me
23
1.00
0.95
0.97
1.00
1.05
2.00
0.99
1.84
0.92
2.00
3.11
12
10
8
6
4
2
0
f1 (ppm)

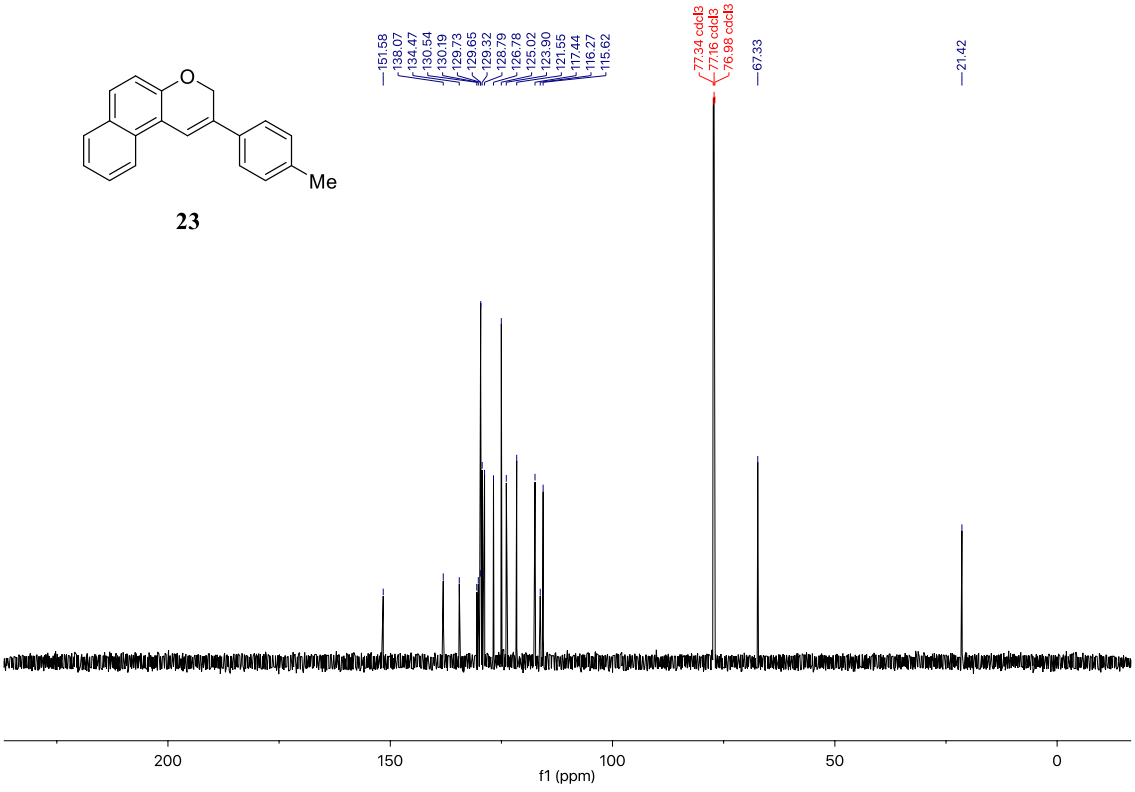
151.58
138.07
134.47
130.54
130.19
129.73
129.65
129.32
128.79
126.78
125.02
123.90
121.55
117.44
116.27
115.62
77.34 cdcl3
77.16 cdcl3
76.98 cdcl3
67.33
21.42
O
Me
23
200
150
100
50
0
f1 (ppm)

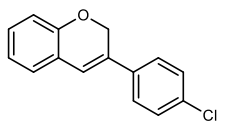
O
Cl

24

7.36
7.26
7.17
7.15
7.13
7.10
7.09
6.94
6.92
6.91
6.87
6.85
6.80
5.13
3.82
1.00
0.96
0.99
0.90
0.95
1.97
4
12
10
8
6
4
2
0
f1 (ppm)

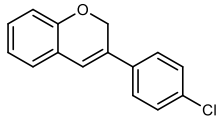
O
Cl

24

153.36
135.30
133.91
130.66
129.49
129.06
127.26
126.14
122.83
121.86
120.78
115.68
77.41 cdd3
77.16 cdd3
76.91 cdd3
67.08
220
200
180
160
140
120
100
80
60
40
20
0
f1 (ppm)

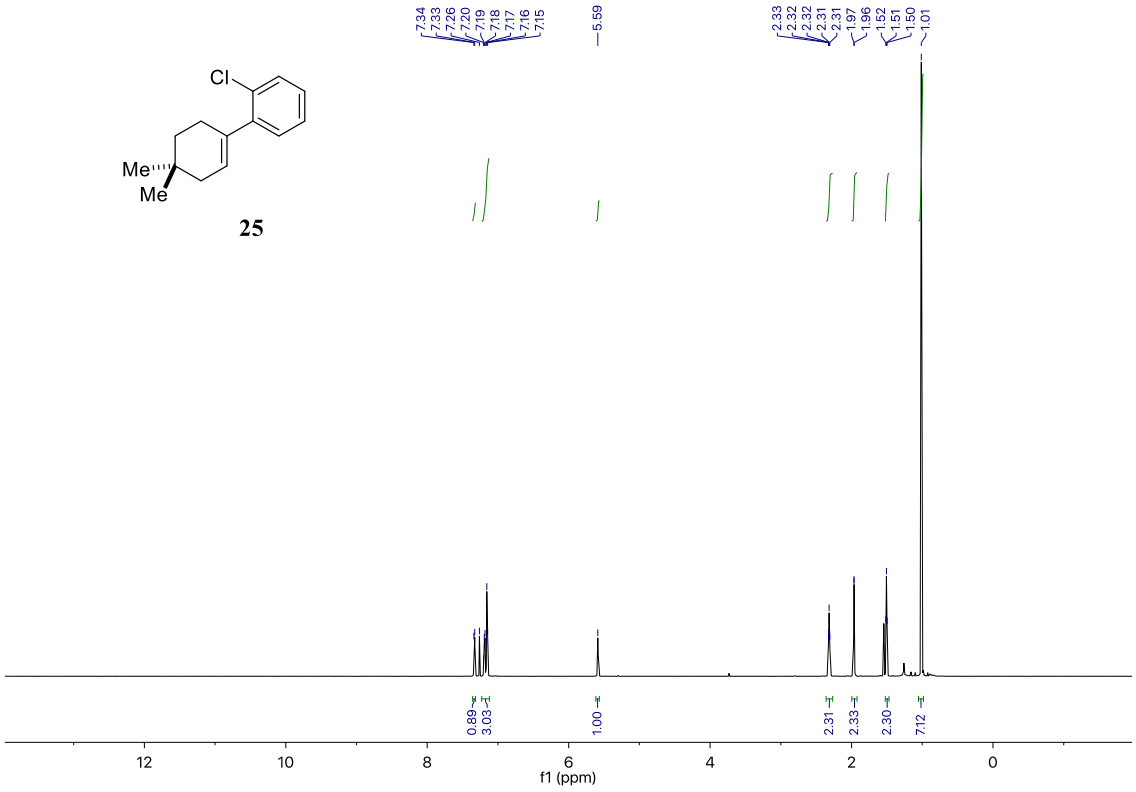
Cl
Me
Me
25
7.34
7.33
7.26
7.20
7.19
7.18
7.17
7.16
7.15
5.59
2.33
2.32
2.32
2.31
2.31
1.97
1.96
1.52
1.51
1.50
1.01
0.89
3.03
1.00
2.31
2.33
2.30
7.12
12
10
8
6
4
2
0
f1 (ppm)

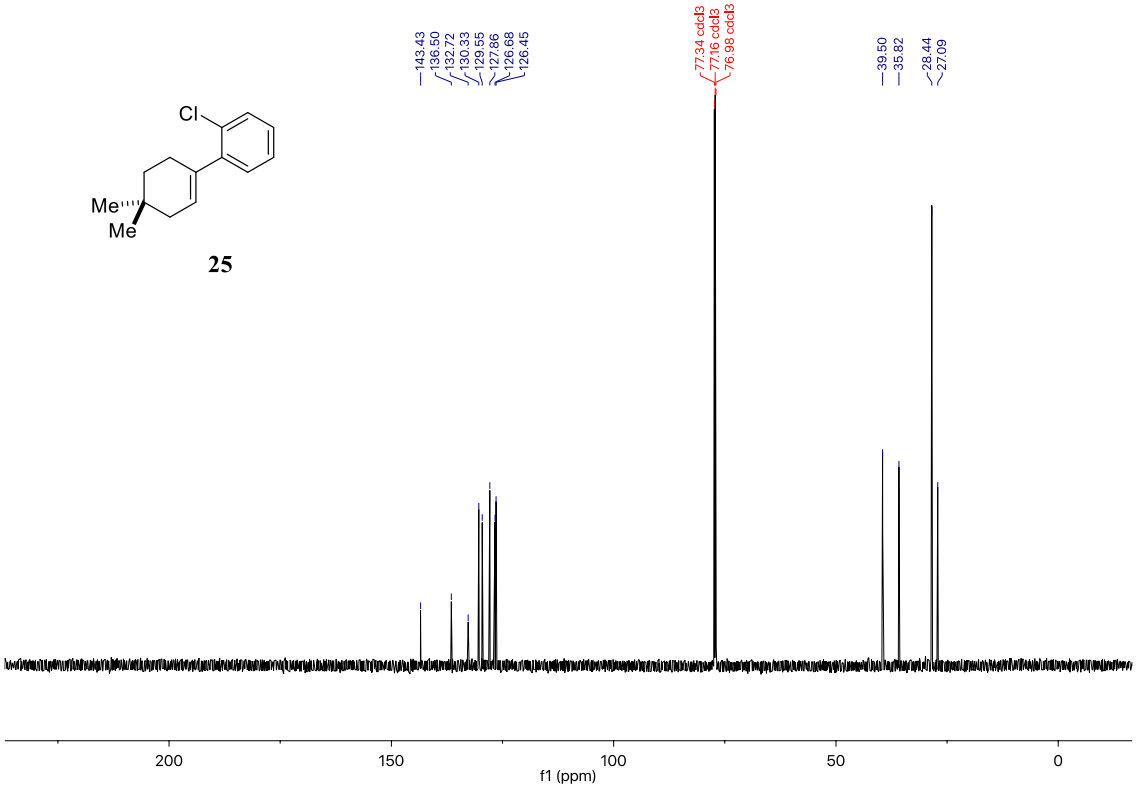
Cl
Me
Me
25
143.43
136.50
132.72
130.33
129.55
127.86
126.68
126.45
77.34 cdcl3
77.16 cdcl3
76.98 cdcl3
39.50
35.82
28.44
27.09
200
150
100
50
0
f1 (ppm)

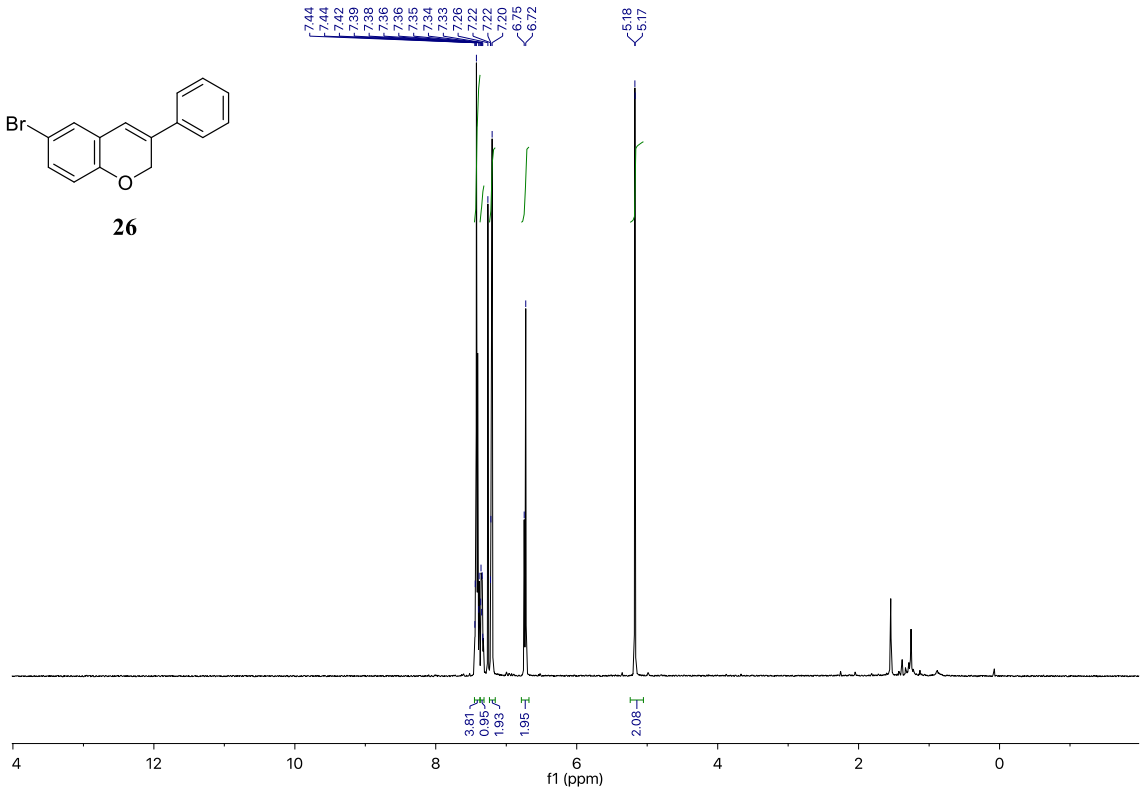
Br
O
26
7.44
7.44
7.42
7.39
7.38
7.36
7.36
7.35
7.34
7.33
7.26
7.22
7.22
7.20
6.75
6.72
5.18
5.17
3.81
0.95
1.93
1.95
2.08
4
12
10
8
6
4
2
0
f1 (ppm)

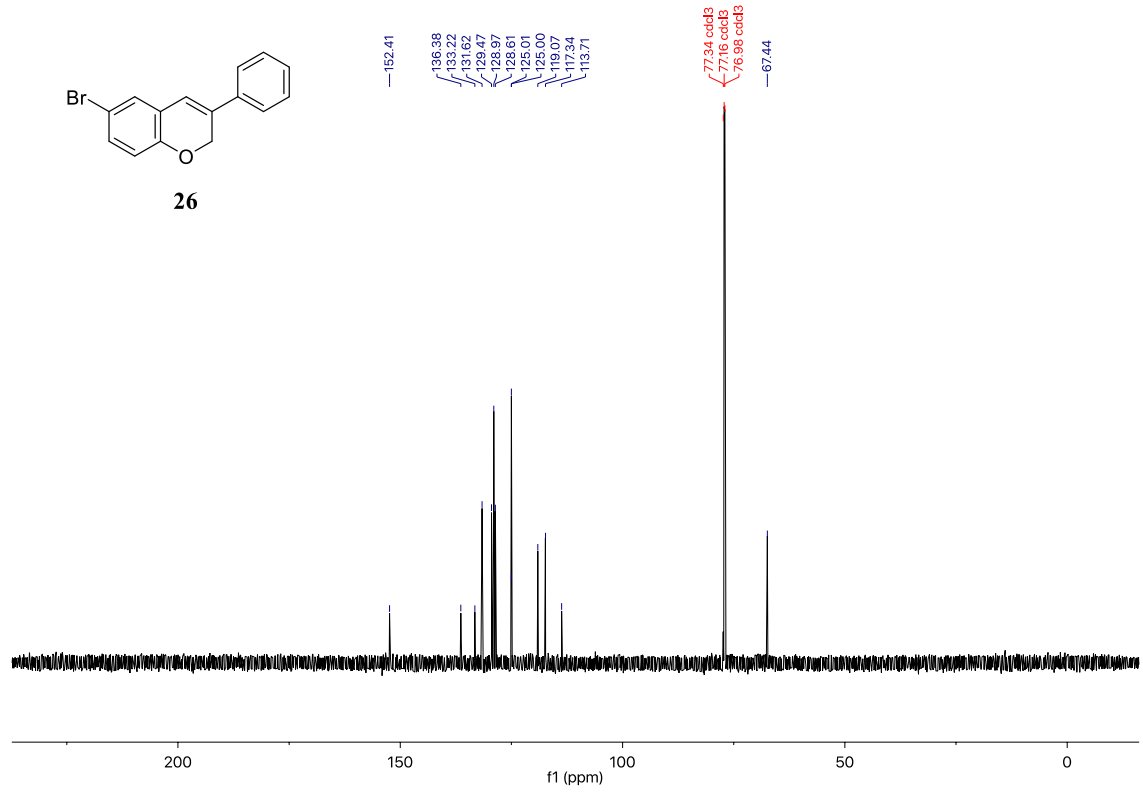
Br
O
26
152.41
136.38
133.22
131.62
129.47
128.97
128.61
125.01
125.00
119.07
117.34
113.71
77.34 cdcl3
77.16 cdcl3
76.98 cdcl3
67.44
200
150
100
50
0
f1 (ppm)

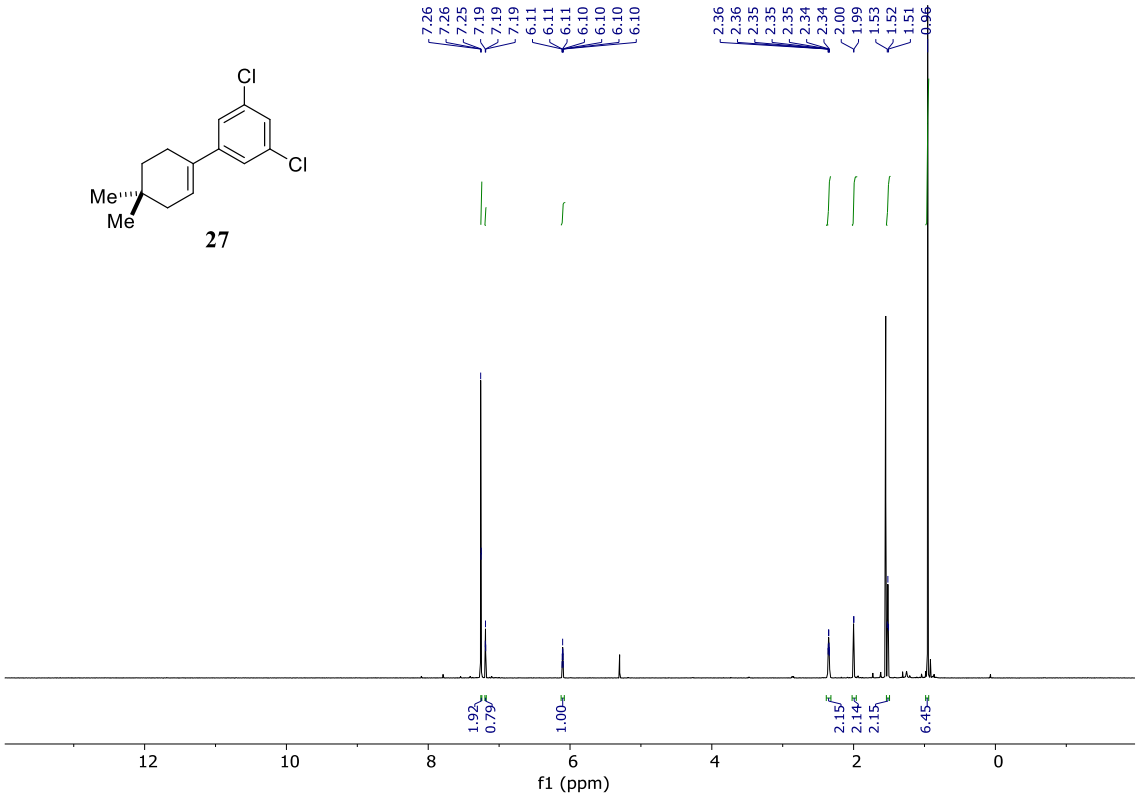
Cl
Cl
Me
Me
27
7.26
7.26
7.25
7.19
7.19
7.19
6.11
6.11
6.11
6.10
6.10
6.10
6.10
2.36
2.36
2.35
2.35
2.35
2.34
2.34
2.34
2.00
1.99
1.53
1.52
1.51
0.96
1.92
0.79
1.00
2.15
2.14
2.15
6.45
12
10
8
6
4
2
0
f1 (ppm)

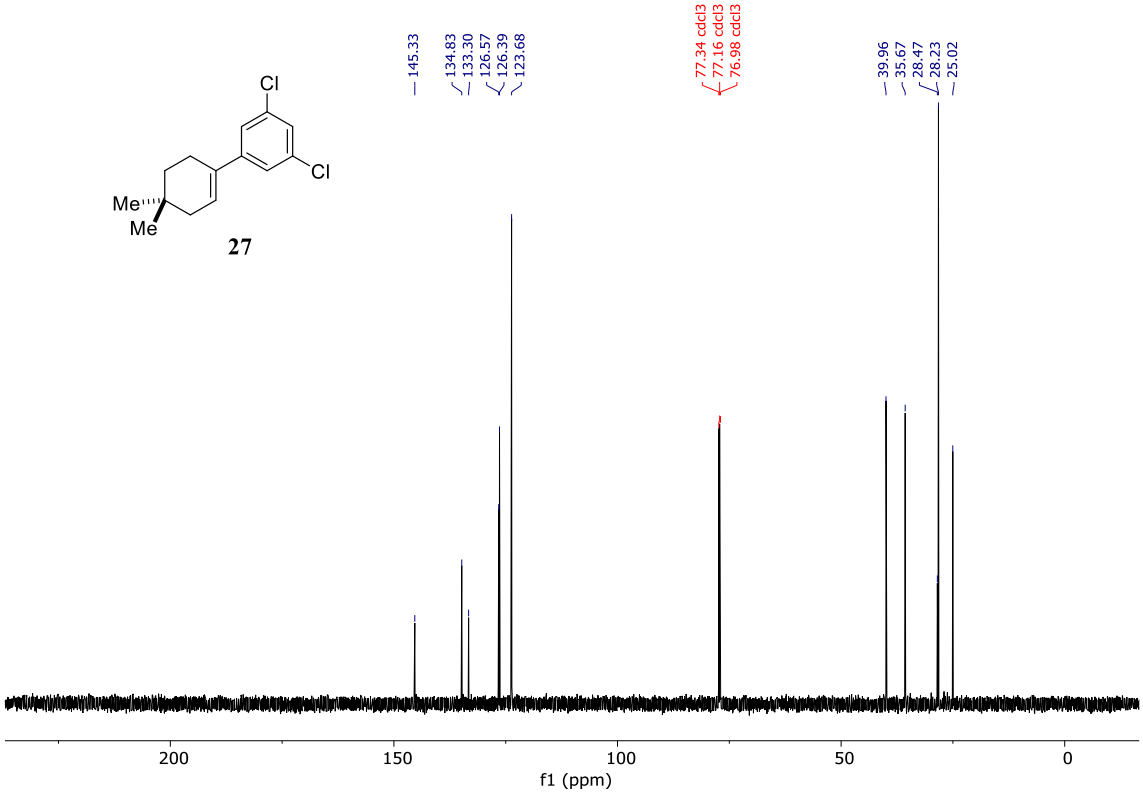
Cl
Cl
Me
Me
27
145.33
134.83
133.30
126.57
126.39
123.68
77.34 cdcl3
77.16 cdcl3
76.98 cdcl3
39.96
35.67
28.47
28.23
25.02
200
150
100
50
0
f1 (ppm)

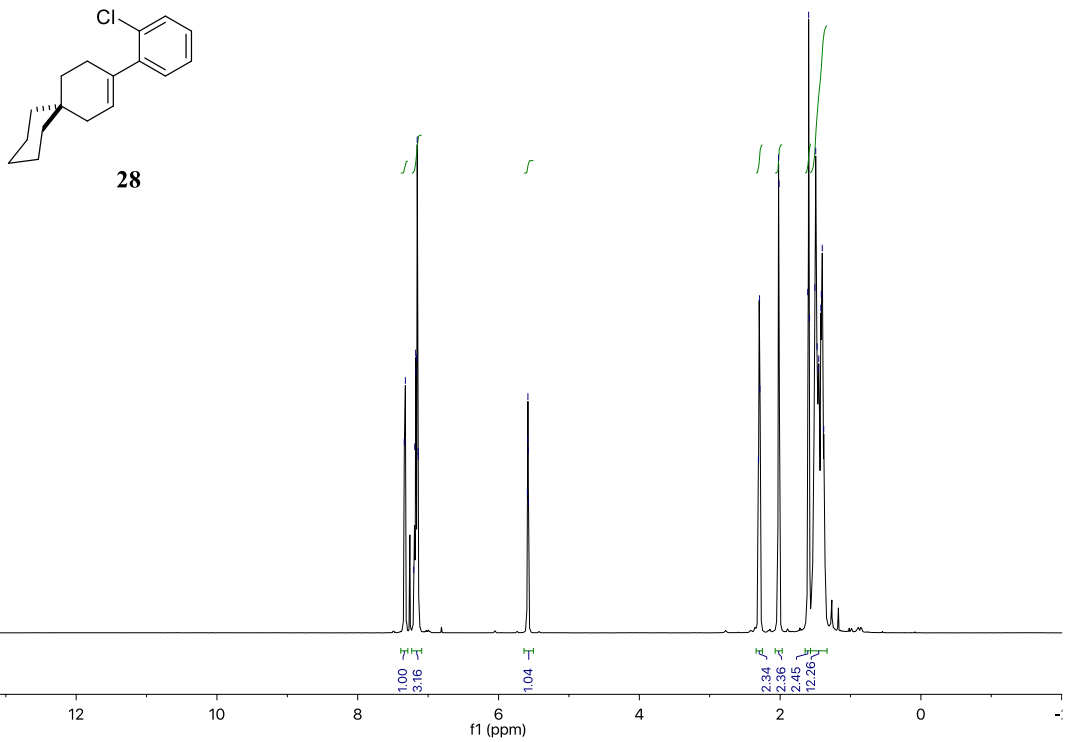
Cl
28
7.34
7.32
7.21
7.19
7.18
7.17
7.17
7.16
7.14
7.14
5.59
5.59
5.58
5.58
5.57
2.31
2.29
2.29
2.02
2.01
1.61
1.59
1.58
1.51
1.49
1.47
1.46
1.45
1.42
1.41
1.40
1.38
1.00
3.16
1.04
2.34
2.36
2.45
12.26
f1 (ppm)

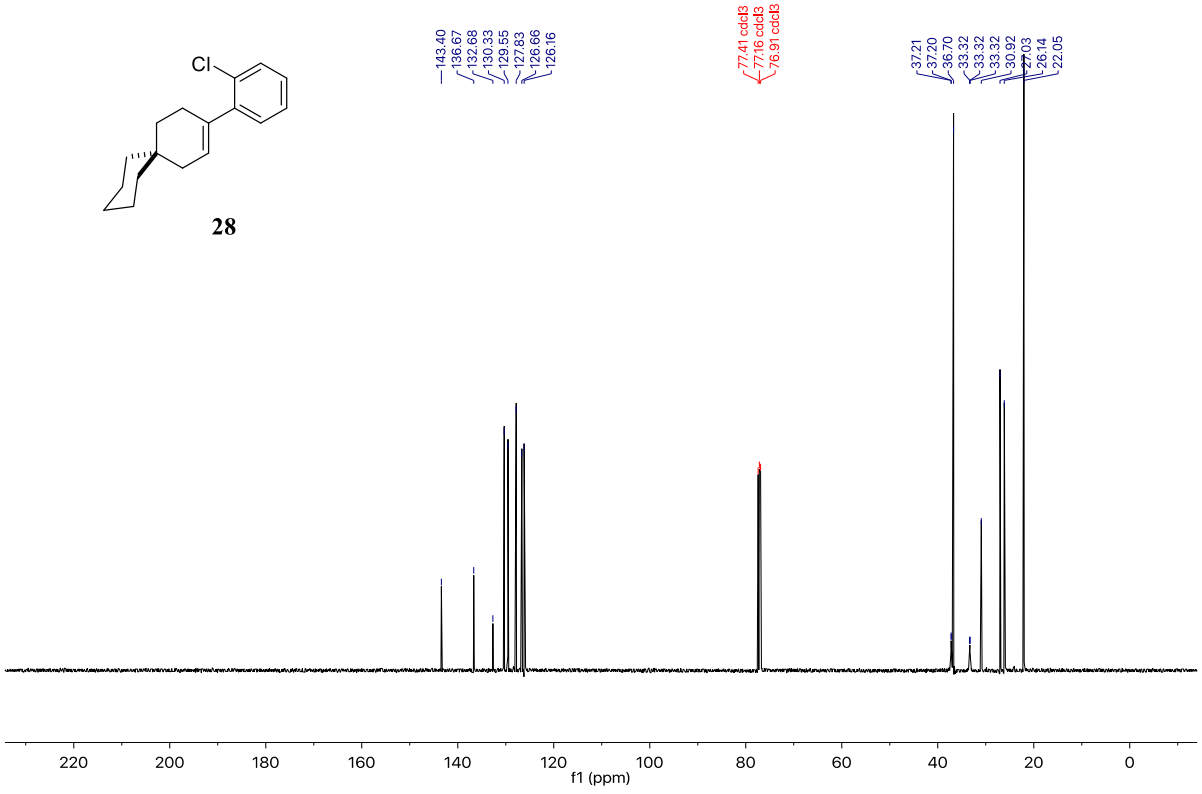
Cl
28
143.40
136.67
132.68
130.33
129.55
127.83
126.66
126.16
77.41 cdcl3
77.16 cdcl3
76.91 cdcl3
37.21
37.20
36.70
33.32
33.32
33.32
30.92
27.03
26.14
22.05
f1 (ppm)

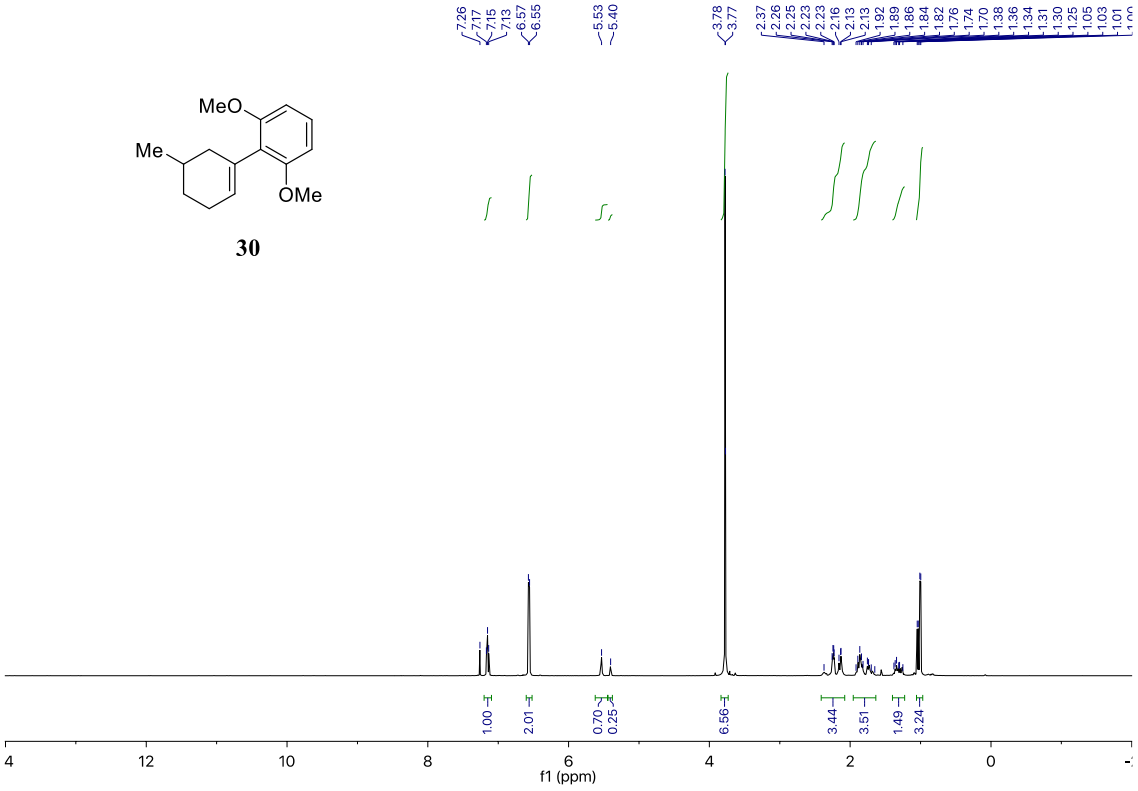
MeO
Me
OMe
7.26
7.17
7.15
7.13
6.57
6.55
5.53
5.40
3.78
3.77
2.37
2.26
2.25
2.23
2.23
2.16
2.13
2.13
1.92
1.89
1.86
1.84
1.82
1.76
1.74
1.70
1.38
1.36
1.34
1.31
1.30
1.25
1.05
1.03
1.01
1.00
2.01
0.70
0.25
6.56
3.44
3.51
1.49
3.24
4
12
10
8
6
4
2
0
f1 (ppm)

30

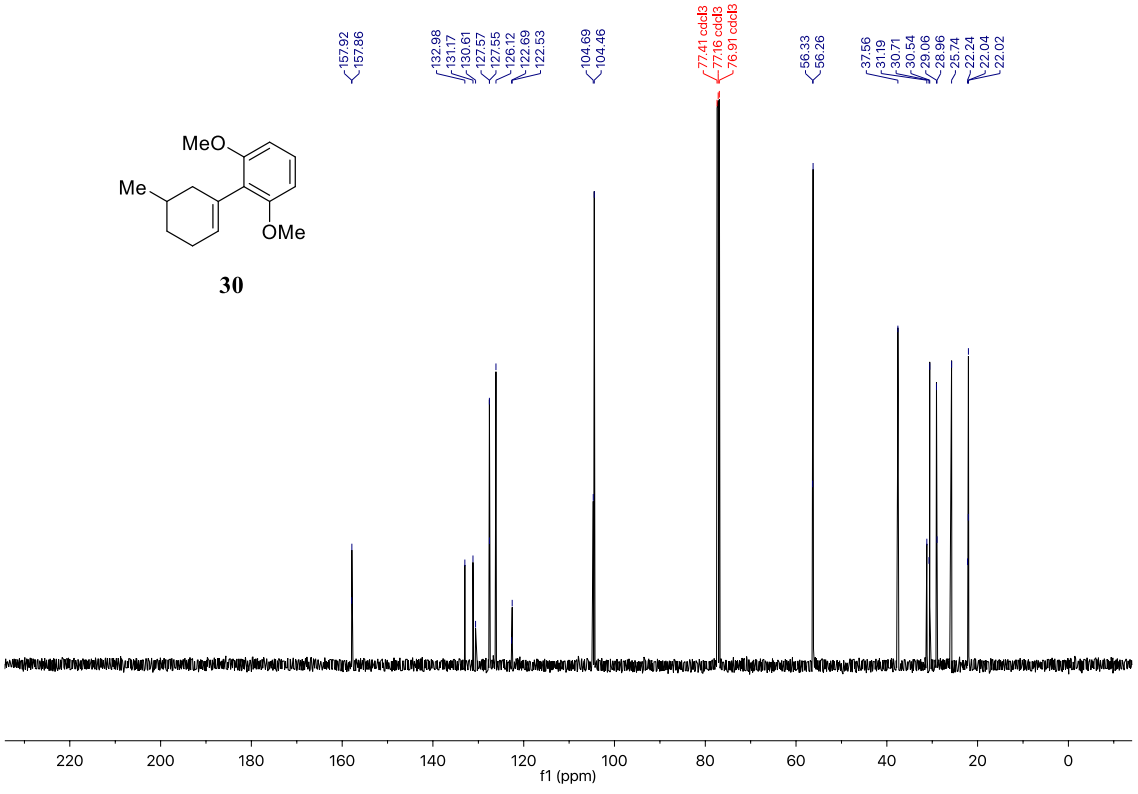
MeO
Me
OMe
157.92
157.86
132.98
131.17
130.61
127.57
127.55
126.12
122.69
122.53
104.69
104.46
77.41 cdd3
77.16 cdd3
76.91 cdd3
56.33
56.26
37.56
31.19
30.71
30.54
29.06
28.96
25.74
22.24
22.04
22.02
220
200
180
160
140
120
100
80
60
40
20
0
f1 (ppm)

30

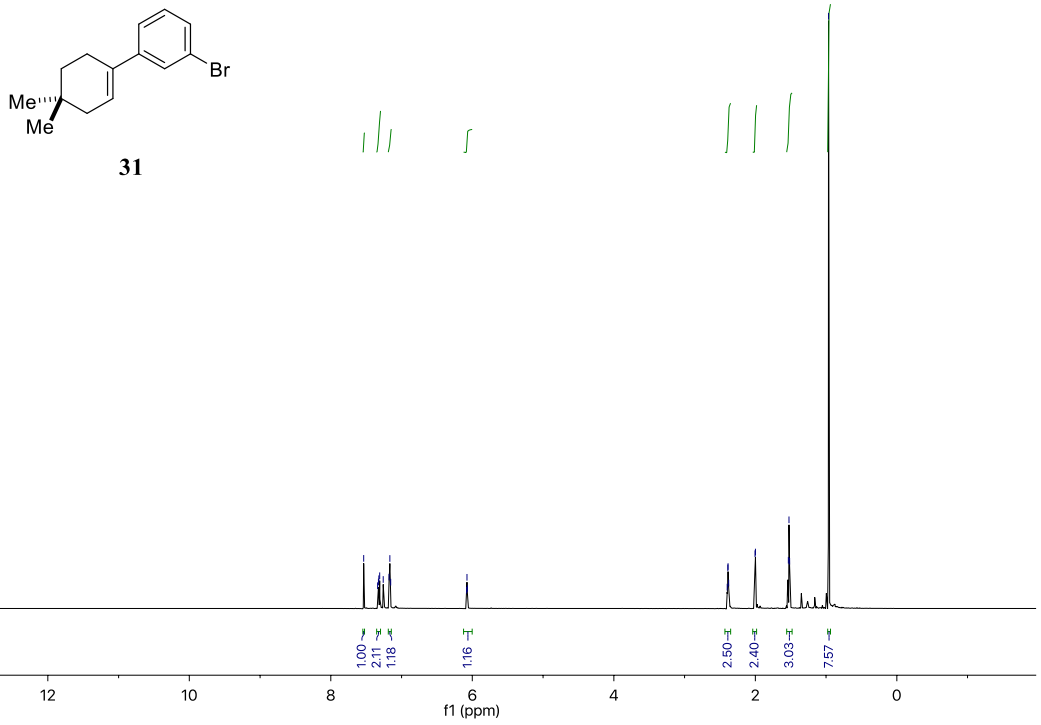
Br
Me
Me
7.54
7.34
7.33
7.32
7.31
7.26
7.18
7.17
7.15
6.08
6.08
6.07
2.40
2.39
2.38
2.38
2.00
2.00
1.53
1.52
1.51
0.96
1.00
2.11
1.18
1.16
2.50
2.40
3.03
7.57
12
10
8
6
4
2
0
f1 (ppm)

31

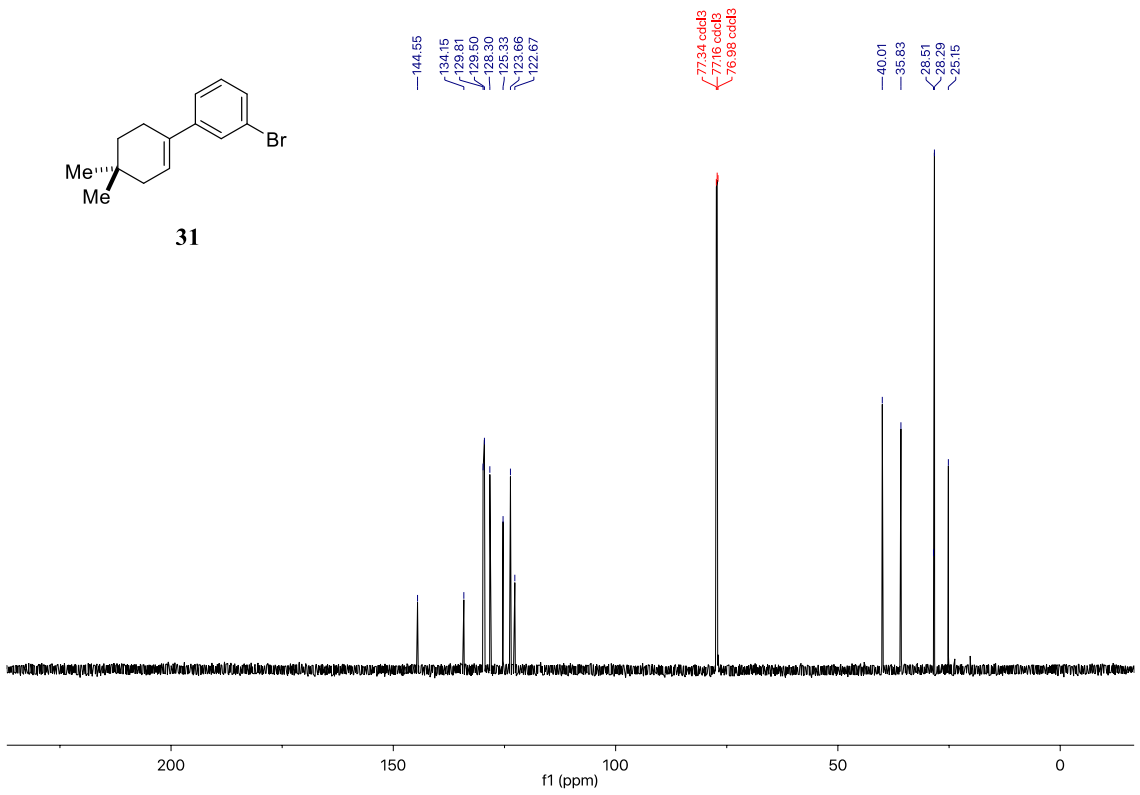
Br
Me
Me
144.55
134.15
129.81
129.50
128.30
125.33
123.66
122.67
77.34 cdcl3
77.16 cdcl3
76.98 cdcl3
40.01
35.83
28.51
28.29
25.15
200
150
100
50
0
f1 (ppm)

31

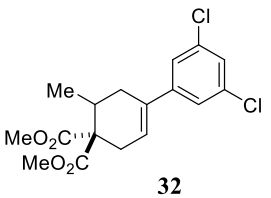
Cl
Me
Cl
MeO2C
MeO2C

32

7.26
7.22
7.22
7.21
7.21
7.21
6.09
6.09
6.08
6.08
6.08
3.74
3.73
2.84
2.84
2.84
2.83
2.76
2.75
2.74
2.73
2.71
2.70
2.70
2.24
2.24
2.23
2.22
2.21
1.08
1.07
2.69
1.00
5.99
1.99
2.10
1.10
3.12
12
10
8
6
4
2
0
f1 (ppm)

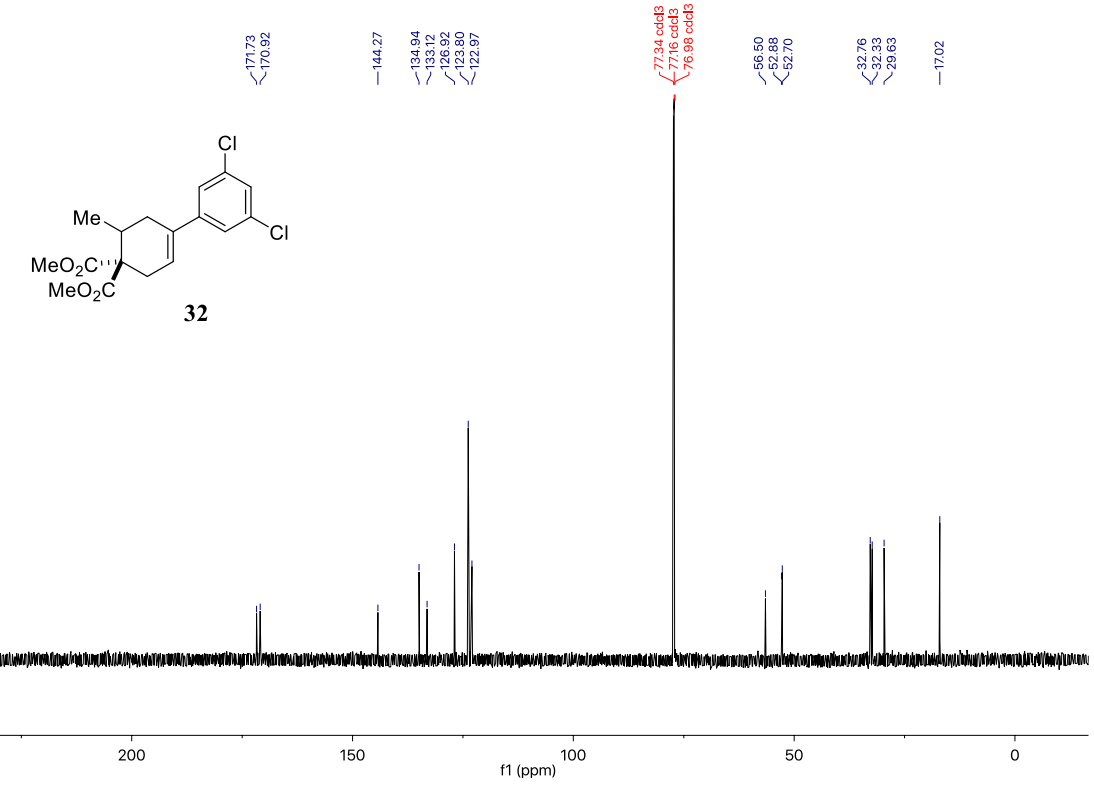
171.73
170.92
144.27
134.94
133.12
126.92
123.80
122.97
77.34 cdd3
77.16 cdd3
76.98 cdd3
56.50
52.88
52.70
32.76
32.33
29.63
17.02
200
150
100
50
0
f1 (ppm)

Cl
Me
Cl
MeO2C
MeO2C

32

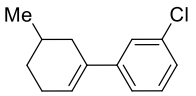
Me
Cl

33

1.00
3.40
0.84
0.17
0.92
2.50
0.96
2.22
1.40
3.19
f1 (ppm)

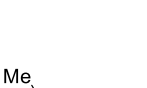
Me
Cl

33

144.56
135.32
135.01
134.28
132.40
129.48
126.63
126.57
125.79
125.45
125.38
123.31
123.24
77.41 cdd3
77.16 cdd3
76.91 cdd3
36.01
31.07
30.90
30.36
29.07
27.44
26.10
22.09
22.01
21.88
f1 (ppm)

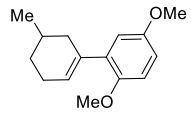
Me
OMe
MeO

35

7.26
6.79
6.78
6.74
6.74
6.72
5.77
5.64
3.78
3.77
3.77
3.76
2.38
2.38
2.37
2.34
2.32
2.24
2.24
2.23
2.22
2.22
2.04
2.03
2.01
1.83
1.79
1.75
1.72
1.30
1.27
1.26
1.25
1.05
1.04
1.02
1.00
1.70
0.71
0.34
5.11
1.62
1.39
0.79
2.06
1.36
0.91
1.89
f1 (ppm)

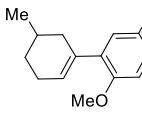
Me
OMe
MeO

35

153.68
153.66
151.23
151.13
137.02
136.76
134.89
134.87
132.83
126.11
115.86
115.72
112.45
112.26
112.08
112.05
77.41 cdd3
77.16 cdd3
76.91 cdd3
56.48
56.42
55.84
55.83
37.41
31.12
30.87
30.52
29.03
28.84
25.94
22.18
22.06
f1 (ppm)

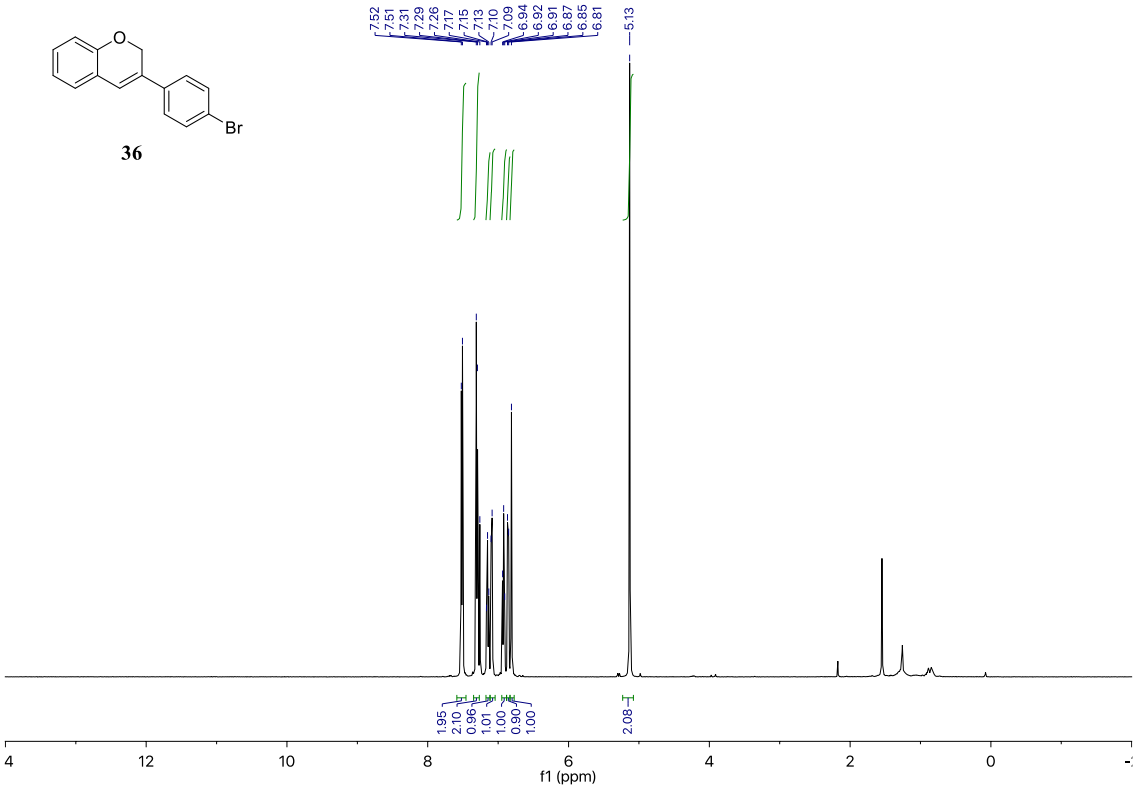
O
Br
36
7.52
7.51
7.31
7.29
7.26
7.17
7.15
7.13
7.10
7.09
6.94
6.92
6.91
6.87
6.85
6.81
5.13
1.95
2.10
0.96
1.01
1.00
0.90
1.00
2.08
f1 (ppm)

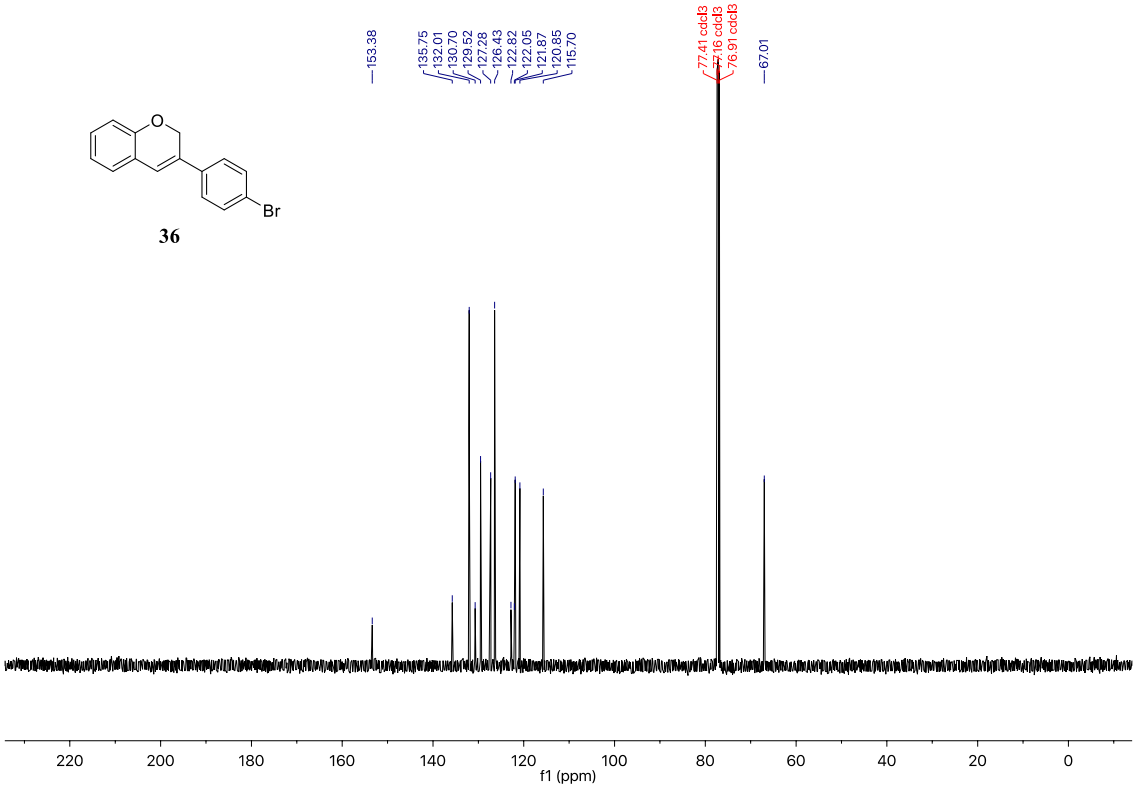
O
Br
36
153.38
135.75
132.01
130.70
129.52
127.28
126.43
122.82
122.05
121.87
120.85
115.70
77.41 cdd3
77.16 cdd3
76.91 cdd3
67.01
f1 (ppm)

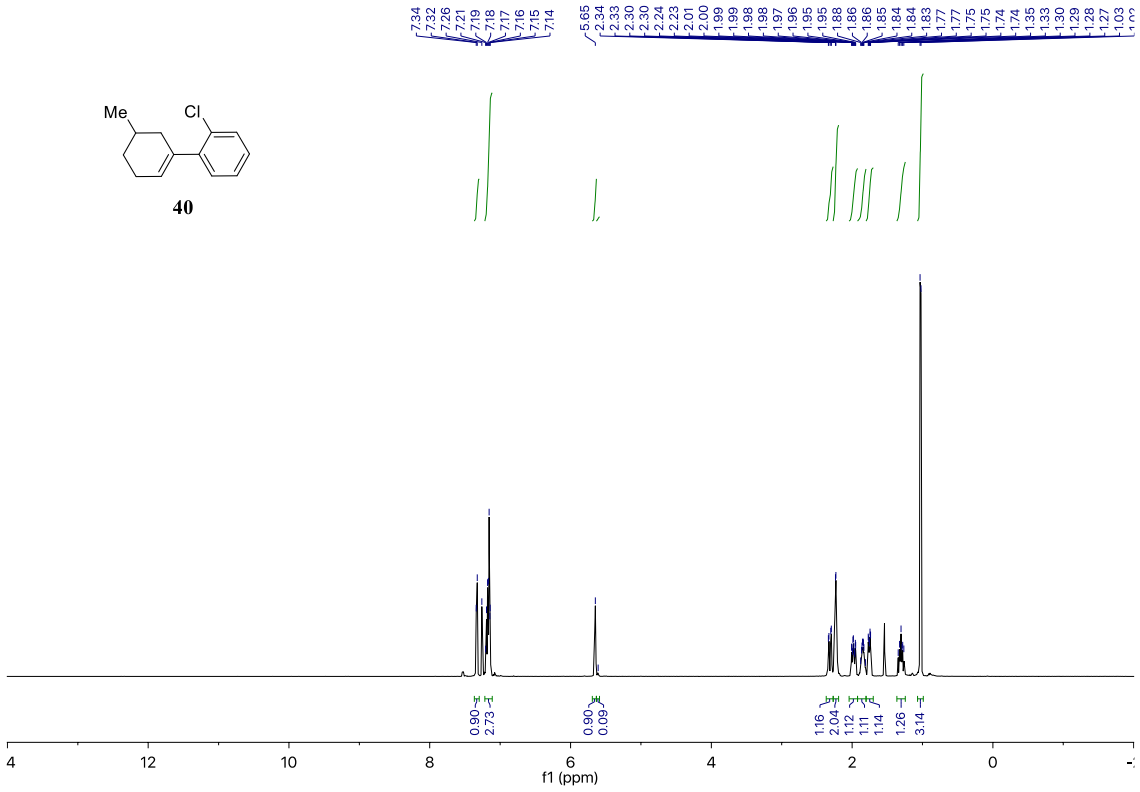
Me
Cl
40
7.34
7.32
7.26
7.21
7.19
7.18
7.17
7.16
7.15
7.14
5.65
2.34
2.33
2.30
2.24
2.23
2.01
2.00
1.99
1.99
1.98
1.98
1.97
1.96
1.95
1.95
1.88
1.86
1.86
1.85
1.84
1.84
1.83
1.77
1.77
1.75
1.75
1.74
1.74
1.35
1.33
1.30
1.29
1.28
1.27
1.03
0.90
2.73
0.90
0.09
1.16
2.04
1.12
1.11
1.14
1.26
3.14
4
12
10
8
6
4
2
0
f1 (ppm)

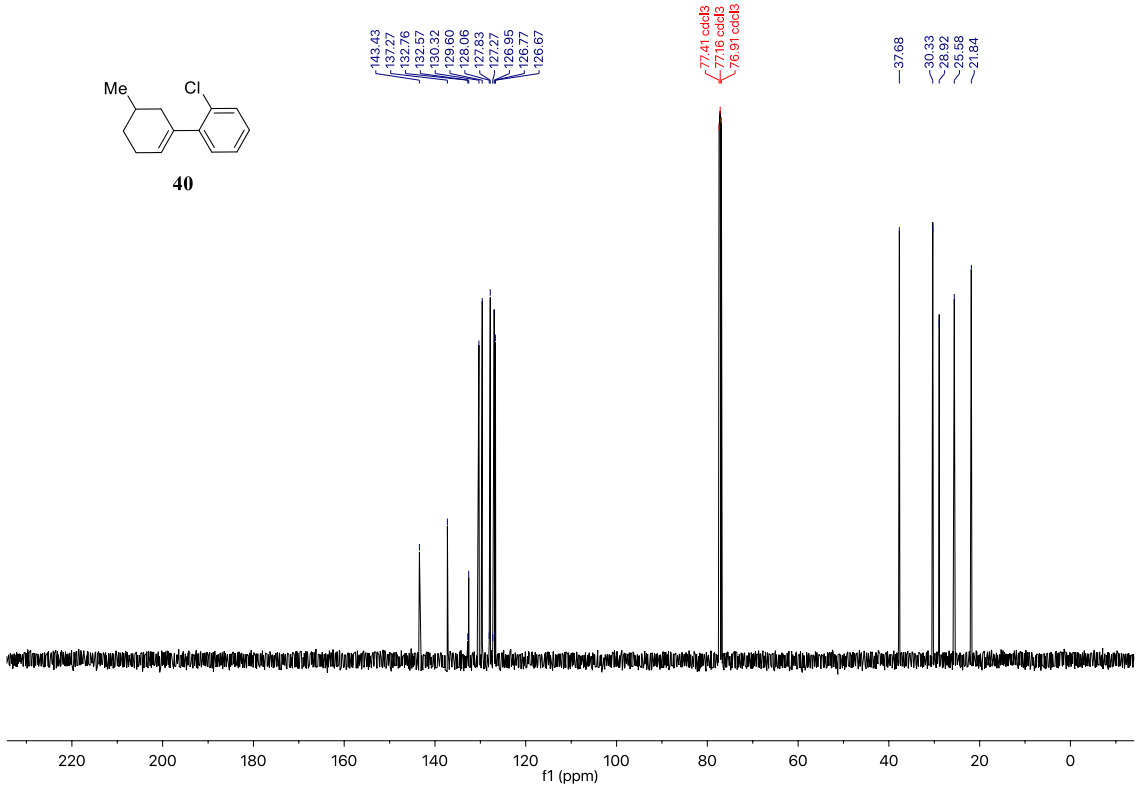
Me
Cl
40
143.43
137.27
132.76
132.57
130.32
129.60
128.06
127.83
127.27
126.95
126.77
126.67
77.41 cdd3
77.16 cdd3
76.91 cdd3
37.68
30.33
28.92
25.58
21.84
220
200
180
160
140
120
100
80
60
40
20
0
f1 (ppm)

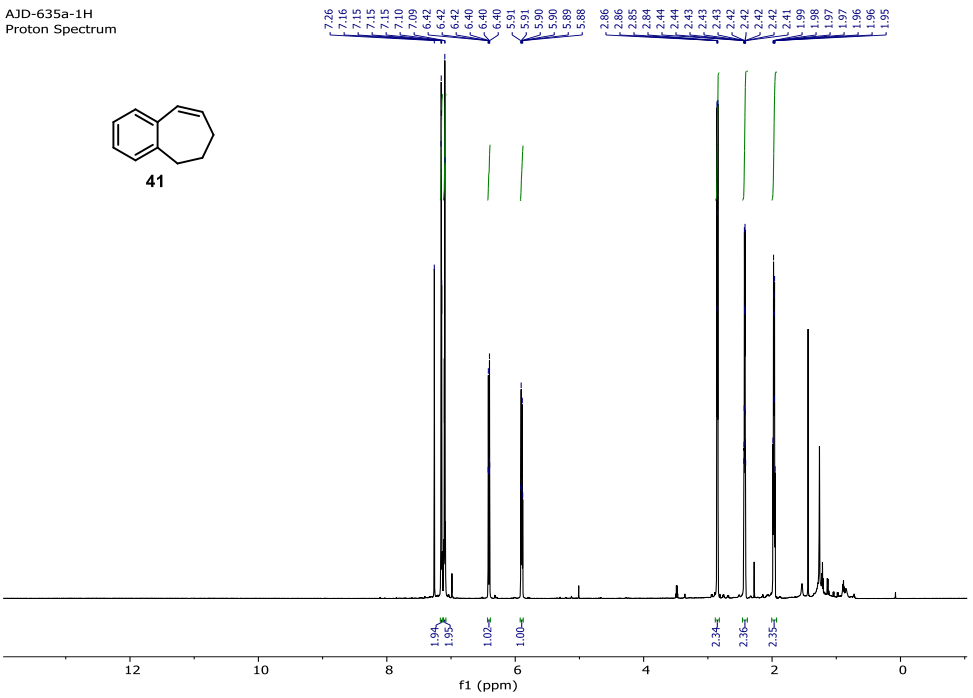
AJD-635a-1H
Proton Spectrum
41
f1 (ppm)

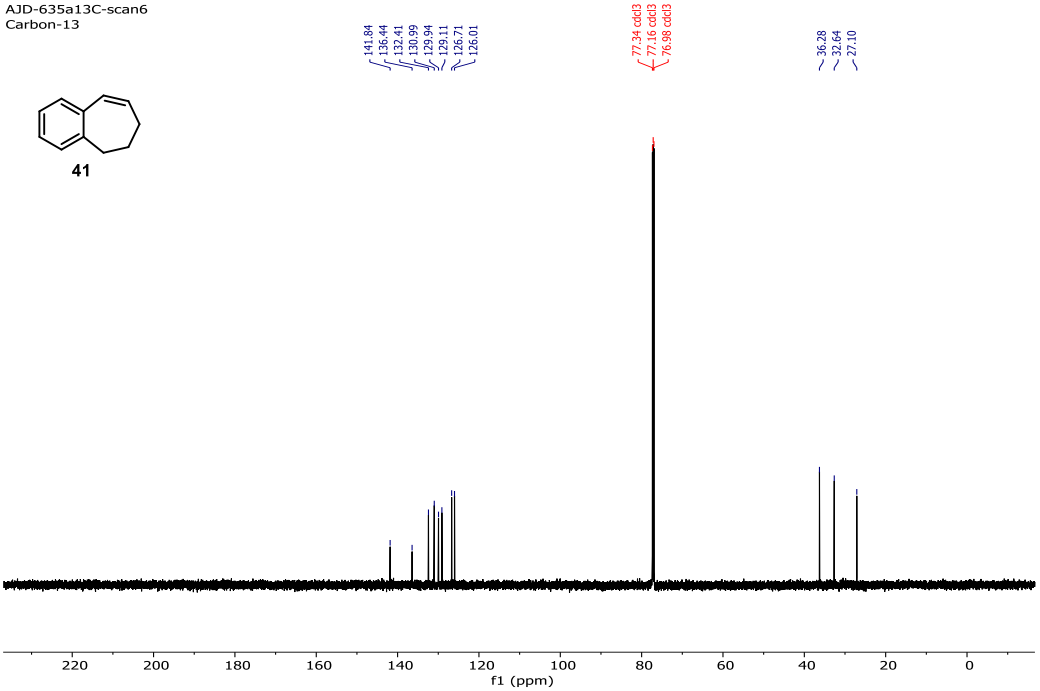
AJD-635a13C-scan6
Carbon-13
41
f1 (ppm)

AJD-662a-1H
Proton Spectrum

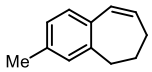

42

AJD-662a-13C-scan5
Carbon-13

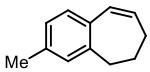

42

2.6 References

(1) Albright, H.; Davis, A. J.; Gomez-Lopez, J. L.; Vonesh, H. L.; Quach, P. K.; Lambert, T. H.; Schindler, C. S. Carbonyl-Olefin Metathesis. *Chemical Reviews*. American Chemical Society August 11, 2021, pp 9359–9406. https://doi.org/10.1021/acs.chemrev.0c01096.

(2) Angew Chem Int Ed Engl - October 2 1995 - Schwab - A Series of Well-Defined Metathesis Catalysts Synthesis of RuCl2 .

(3) Scholl, M.; Trnka, T. M.; Morgan, J. P.; Grubbs, R. H. *Increased Ring Closing Metathesis Activity of Ruthenium-Based Oiefin Metathesis Catalysts Coordinated with Imidazolin-2-Ylidene Ligands*; 1999; Vol. 40.

(4) Ho, T.-L.; Mcmurry, J. E.; Clive, D. L. J.; Zhang, C.; Murthy, K. S. K.; Hayward, W. D.; Daigneault, S.; Grubbs, R. H.; Turnas, W.; Hartley, F.; Pine, S. H. *C) Feast, W. J.; Gibson, V. C. In The Chemistry of the Metal-Carbon Bond*; UTC, 1993; Vol. 89.

(5) Helvetica Chimica Acta - 1 November 1971 - Demole - Applications Synth Tiques de La Cyclisation d Alcools Tertiaires -.

(6) Ludwig, J. R.; Zimmerman, P. M.; Gianino, J. B.; Schindler, C. S. Iron(III)-Catalysed Carbonyl-Olefin Metathesis. *Nature* **2016**, *533*, 374–379. https://doi.org/10.1038/nature17432.

(7) Jackson, A. C.; Goldman, B. E.; Snider, B. B. *Intramolecular and Intermolecular Lewis Acid Catalyzed Ene Reactions Using Ketones as Enophiles*; 1984; Vol. 49.

(8) *COM M UNlCATlONS.*

(9) Khripach, V. A.; Zhabinskii, V. N.; Kuchto, A. I.; Zhiburtovich, Y. Y.; Gromak, V. v.; Groen, M. B.; van der Louw, J.; de Groot, A. Intramolecular Cycloaddition/Cycloreversion of (E)-3β,17β-Diacetoxy-5,10-Secoandrost-1(10)-En-5-

One. *Tetrahedron Letters* **2006**, *47* (38), 6715–6718. https://doi.org/10.1016/j.tetlet.2006.07.096.

(10) Soicke, A.; Slavov, N.; Neudörfl, J. M.; Schmalz, H. G. Metal-Free Intramolecular Carbonyl-Olefin Metathesis of Ortho-Prenylaryl Ketones. *Synlett* **2011**, No. 17, 2487–2490. https://doi.org/10.1055/s-0030-1260320.

(11) Malakar, T.; Hanson, C. S.; Devery, J. J.; Zimmerman, P. M. Combined Theoretical and Experimental Investigation of Lewis Acid-Carbonyl Interactions for Metathesis. *ACS Catalysis* **2021**, *11* (8), 4381–4394. https://doi.org/10.1021/acscatal.0c05277.

(12) Hanson, C. S.; Psaltakis, M. C.; Cortes, J. J.; Devery, J. J. Catalyst Behavior in Metal-Catalyzed Carbonyl-Olefin Metathesis. *J Am Chem Soc* **2019**, *141* (30), 11870–11880. https://doi.org/10.1021/jacs.9b02613.

(13) Ludwig, J. R.; Phan, S.; McAtee, C. C.; Zimmerman, P. M.; Devery, J. J.; Schindler, C. S. Mechanistic Investigations of the Iron(III)-Catalyzed Carbonyl-Olefin Metathesis Reaction. *J Am Chem Soc* **2017**, *139* (31), 10832–10842. https://doi.org/10.1021/jacs.7b05641.

(14) Becker, M. Carbonyl-Olefin Metathesis for the Synthesis of Cyclic Olefins. *Organic Syntheses* **2018**, *95*, 472–485. https://doi.org/10.15227/orgsyn.095.0472.

(15) Ma, L.; Li, W.; Xi, H.; Bai, X.; Ma, E.; Yan, X.; Li, Z. FeCl 3 -Catalyzed Ring-Closing Carbonyl-Olefin Metathesis . *Angewandte Chemie* **2016**, *128* (35), 10566–10569. https://doi.org/10.1002/ange.201604349.

(16) Groso, E. J.; Golonka, A. N.; Harding, R. A.; Alexander, B. W.; Sodano, T. M.; Schindler, C. S. 3-Aryl-2,5-Dihydropyrroles via Catalytic Carbonyl-Olefin Metathesis. *ACS Catalysis* **2018**, *8* (3), 2006–2011. https://doi.org/10.1021/acscatal.7b03769.

(17) Rykaczewski, K. A.; Groso, E. J.; Vonesh, H. L.; Gaviria, M. A.; Richardson, A. D.; Zehnder, T. E.; Schindler, C. S. Tetrahydropyridines via FeCl3-Catalyzed Carbonyl-Olefin Metathesis. *Organic Letters* **2020**, *22* (7), 2844–2848. https://doi.org/10.1021/acs.orglett.0c00918.

(18) Ni, S.; Franzén, J. Carbocation Catalysed Ring Closing Aldehyde-Olefin Metathesis. *Chemical Communications* **2018**, *54* (92), 12982–12985. https://doi.org/10.1039/C8CC06734A.

(19) Wang, R.; Chen, Y.; Shu, M.; Zhao, W.; Tao, M.; Du, C.; Fu, X.; Li, A.; Lin, Z. AuCl3-Catalyzed Ring-Closing Carbonyl–Olefin Metathesis. *Chemistry - A European Journal* **2020**, *26* (9), 1941–1946. https://doi.org/10.1002/chem.201905199.

(20) Tran, U. P. N.; Oss, G.; Breugst, M.; Detmar, E.; Pace, D. P.; Liyanto, K.; Nguyen, T. v. Carbonyl-Olefin Metathesis Catalyzed by Molecular Iodine. *ACS Catalysis* **2019**, *9* (2), 912–919. https://doi.org/10.1021/acscatal.8b03769.

(21) Tran, U. P. N.; Oss, G.; Pace, D. P.; Ho, J.; Nguyen, T. v. Tropylium-Promoted Carbonyl-Olefin Metathesis Reactions. *Chemical Science* **2018**, *9* (23), 5145–5151. https://doi.org/10.1039/c8sc00907d.

(22) Djurovic, A.; Vayer, M.; Li, Z.; Guillot, R.; Baltaze, J. P.; Gandon, V.; Bour, C. Synthesis of Medium-Sized Carbocycles by Gallium-Catalyzed Tandem Carbonyl-Olefin Metathesis/Transfer Hydrogenation. *Organic Letters* **2019**, *21* (19), 8132–8137. https://doi.org/10.1021/acs.orglett.9b03240.

(23) McAtee, C. C.; Riehl, P. S.; Schindler, C. S. Polycyclic Aromatic Hydrocarbons via Iron(III)-Catalyzed Carbonyl-Olefin Metathesis. *J Am Chem Soc* **2017**, *139* (8), 2960–2963. https://doi.org/10.1021/jacs.7b01114.

(24) Albright, H.; Riehl, P. S.; McAtee, C. C.; Reid, J. P.; Ludwig, J. R.; Karp, L. A.; Zimmerman, P. M.; Sigman, M. S.; Schindler, C. S. Catalytic Carbonyl-Olefin Metathesis of Aliphatic Ketones: Iron(III) Homo-Dimers as Lewis Acidic Superelectrophiles. *J Am Chem Soc* **2019**, *141* (4), 1690–1700. https://doi.org/10.1021/jacs.8b11840.

(25) Olah, G. A. *International Edition in English Superelectrophiles***; 1993; Vol. 32.

(26) Negishi, E. *CONCEPTS*; 1999; Vol. 5.

(27) Albright, H.; Vonesh, H. L.; Becker, M. R.; Alexander, B. W.; Ludwig, J. R.; Wiscons, R. A.; Schindler, C. S. GaCl3-Catalyzed Ring-Opening Carbonyl-Olefin Metathesis. *Organic Letters* **2018**, *20* (16), 4954–4958. https://doi.org/10.1021/acs.orglett.8b02086.

(28) Naidu, V. R.; Bah, J.; Franzén, J. Direct Organocatalytic Oxo-Metathesis, a Trans-Selective Carbocation-Catalyzed Olefination of Aldehydes. *European Journal of Organic Chemistry* **2015**, *2015* (8), 1834–1839. https://doi.org/10.1002/ejoc.201403651.

(29) Albright, H.; Vonesh, H. L.; Schindler, C. S. Superelectrophilic Fe(III)-Ion Pairs as Stronger Lewis Acid Catalysts for (E)-Selective Intermolecular Carbonyl-Olefin Metathesis. *Organic Letters* **2020**, *22* (8), 3155–3160. https://doi.org/10.1021/acs.orglett.0c00917.

(30) Riehl, P. S.; Nasrallah, D. J.; Schindler, C. S. Catalytic, Transannular Carbonyl-Olefin Metathesis Reactions. *Chemical Science* **2019**, *10* (44), 10267–10274. https://doi.org/10.1039/c9sc03716k.

(31) Ni, S.; Franzén, J. Carbocation Catalysed Ring Closing Aldehyde-Olefin Metathesis. *Chemical Communications* **2018**, *54* (92), 12982–12985. https://doi.org/10.1039/C8CC06734A.

(32) Tran, U. P. N.; Oss, G.; Pace, D. P.; Ho, J.; Nguyen, T. v. Tropylium-Promoted Carbonyl-Olefin Metathesis Reactions. *Chemical Science* **2018**, *9* (23), 5145–5151. https://doi.org/10.1039/c8sc00907d.

(33) Naidu, V. R.; Bah, J.; Franzén, J. Direct Organocatalytic Oxo-Metathesis, a Trans-Selective Carbocation-Catalyzed Olefination of Aldehydes. *European Journal of Organic Chemistry* **2015**, *2015* (8), 1834–1839. https://doi.org/10.1002/ejoc.201403651.

(34) Hanson, C. S.; Psaltakis, M. C.; Cortes, J. J.; Devery, J. J. Catalyst Behavior in Metal-Catalyzed Carbonyl-Olefin Metathesis. *J Am Chem Soc* **2019**, *141* (30), 11870–11880. https://doi.org/10.1021/jacs.9b02613.

(35) Ma, L.; Li, W.; Xi, H.; Bai, X.; Ma, E.; Yan, X.; Li, Z. FeCl 3 -Catalyzed Ring-Closing Carbonyl-Olefin Metathesis . *Angewandte Chemie* **2016**, *128* (35), 10566–10569. https://doi.org/10.1002/ange.201604349.

(36) Riehl, P. S.; Nasrallah, D. J.; Schindler, C. S. Catalytic, Transannular Carbonyl-Olefin Metathesis Reactions. *Chemical Science* **2019**, *10* (44), 10267–10274. https://doi.org/10.1039/c9sc03716k.

(37) Albright, H.; Vonesh, H. L.; Becker, M. R.; Alexander, B. W.; Ludwig, J. R.; Wiscons, R. A.; Schindler, C. S. GaCl3-Catalyzed Ring-Opening Carbonyl-Olefin Metathesis. *Organic Letters* **2018**, *20* (16), 4954–4958. https://doi.org/10.1021/acs.orglett.8b02086.

(38) Groso, E. J.; Golonka, A. N.; Harding, R. A.; Alexander, B. W.; Sodano, T. M.; Schindler, C. S. 3-Aryl-2,5-Dihydropyrroles via Catalytic Carbonyl-Olefin Metathesis. *ACS Catalysis* **2018**, *8* (3), 2006–2011. https://doi.org/10.1021/acscatal.7b03769.

(39) Ludwig, J. R.; Phan, S.; McAtee, C. C.; Zimmerman, P. M.; Devery, J. J.; Schindler, C. S. Mechanistic Investigations of the Iron(III)-Catalyzed Carbonyl-Olefin Metathesis

Reaction. *J Am Chem Soc* **2017**, *139* (31), 10832–10842. https://doi.org/10.1021/jacs.7b05641.

(40) Ludwig, J. R.; Schindler, C. S. Lewis Acid Catalyzed Carbonyl-Olefin Metathesis. *Synlett* **2017**, *28* (13), 1501–1509. https://doi.org/10.1055/s-0036-1588827.

(41) Ludwig, J. R.; Zimmerman, P. M.; Gianino, J. B.; Schindler, C. S. Iron(III)-Catalysed Carbonyl-Olefin Metathesis. *Nature* **2016**, *533*, 374–379. https://doi.org/10.1038/nature17432.

(42) Albright, H.; Riehl, P. S.; McAtee, C. C.; Reid, J. P.; Ludwig, J. R.; Karp, L. A.; Zimmerman, P. M.; Sigman, M. S.; Schindler, C. S. Catalytic Carbonyl-Olefin Metathesis of Aliphatic Ketones: Iron(III) Homo-Dimers as Lewis Acidic Superelectrophiles. *J Am Chem Soc* **2019**, *141* (4), 1690–1700. https://doi.org/10.1021/jacs.8b11840.

(43) McAtee, C. C.; Riehl, P. S.; Schindler, C. S. Polycyclic Aromatic Hydrocarbons via Iron(III)-Catalyzed Carbonyl-Olefin Metathesis. *J Am Chem Soc* **2017**, *139* (8), 2960–2963. https://doi.org/10.1021/jacs.7b01114.

(44) Rykaczewski, K. A.; Groso, E. J.; Vonesh, H. L.; Gaviria, M. A.; Richardson, A. D.; Zehnder, T. E.; Schindler, C. S. Tetrahydropyridines via FeCl3-Catalyzed Carbonyl-Olefin Metathesis. *Organic Letters* **2020**, *22* (7), 2844–2848. https://doi.org/10.1021/acs.orglett.0c00918.

(45) Catti, L.; Tiefenbacher, K. Brønsted-Säure-Katalysierte Carbonyl-Olefin-Metathese in Einer Selbstorganisierten Supramolekularen Wirtstruktur. *Angewandte Chemie* **2018**, *130* (44), 14797–14800. https://doi.org/10.1002/ange.201712141.

(46) Zhu, Y.; Rebek, J.; Yu, Y. Cyclizations Catalyzed inside a Hexameric Resorcinarene Capsule. *Chemical Communications* **2019**, *55* (25), 3573–3577. https://doi.org/10.1039/c9cc01611b.

(47) Griffith, A. K.; Vanos, C. M.; Lambert, T. H. Organocatalytic Carbonyl-Olefin Metathesis. *J Am Chem Soc* **2012**, *134* (45), 18581–18584. https://doi.org/10.1021/ja309650u.

(48) Hong, X.; Liang, Y.; Griffith, A. K.; Lambert, T. H.; Houk, K. N. Distortion-Accelerated Cycloadditions and Strain-Release-Promoted Cycloreversions in the Organocatalytic Carbonyl-Olefin Metathesis. *Chemical Science* **2014**, *5* (2), 471–475. https://doi.org/10.1039/c3sc52882k.

(49) Zhang, Y.; Jermaks, J.; MacMillan, S. N.; Lambert, T. H. Synthesis of 2 H-Chromenes via Hydrazine-Catalyzed Ring-Closing Carbonyl-Olefin Metathesis. *ACS Catalysis* **2019**, *9* (10), 9259–9264. https://doi.org/10.1021/acscatal.9b03656.

(50) Zhang, Y.; Jermaks, J.; MacMillan, S. N.; Lambert, T. H. Synthesis of 2 H-Chromenes via Hydrazine-Catalyzed Ring-Closing Carbonyl-Olefin Metathesis. *ACS Catalysis* **2019**, *9* (10), 9259–9264. https://doi.org/10.1021/acscatal.9b03656.

(51) Albright, H.; Davis, A. J.; Gomez-Lopez, J. L.; Vonesh, H. L.; Quach, P. K.; Lambert, T. H.; Schindler, C. S. Carbonyl-Olefin Metathesis. *Chemical Reviews*. American Chemical Society August 11, 2021, pp 9359–9406. https://doi.org/10.1021/acs.chemrev.0c01096.

(52) Soicke, A.; Slavov, N.; Neudörfl, J. M.; Schmalz, H. G. Metal-Free Intramolecular Carbonyl-Olefin Metathesis of Ortho-Prenylaryl Ketones. *Synlett* **2011**, No. 17, 2487–2490. https://doi.org/10.1055/s-0030-1260320.

(53) Schopov, I. *A Carbonyl-Olefin Exchange Reaction-New Route to Polyconjugated Polymers, 1 A New Synthesis of Polyphenylacetylene*; 1983; Vol. 4.

(54) Ho, T.-L.; Mcmurry, J. E.; Clive, D. L. J.; Zhang, C.; Murthy, K. S. K.; Hayward, W. D.; Daigneault, S.; Grubbs, R. H.; Turnas, W.; Hartley, F.; Pine, S. H. *C) Feast, W. J.; Gibson, V. C. In The Chemistry of the Metal-Carbon Bond*; UTC, 1993; Vol. 89.

(55) Valiulin, R. A.; Arisco, T. M.; Kutateladze, A. G. Photoinduced Intramolecular Cyclopentanation vs Photoprotolytic Oxametathesis in Polycyclic Alkenes Outfitted with Conformationally Constrained Aroylmethyl Chromophores. *Journal of Organic Chemistry* **2013**, *78* (5), 2012–2025. https://doi.org/10.1021/jo301909j.

(56) Valiulin, R. A.; Arisco, T. M.; Kutateladze, A. G. Double-Tandem [4π+2π]·[2 Π+2π]·[4π+2π] ·[2π+2π] Synthetic Sequence with Photoprotolytic Oxametathesis and Photoepoxidation in the Chromone Series. *Journal of Organic Chemistry* **2011**, *76* (5), 1319–1332. https://doi.org/10.1021/jo102221q.

(57) Valiulin, R. A.; Kutateladze, A. G. Harvesting the Strain Installed by a Paternò-Büchi Step in a Synthetically Useful Way: High-Yielding Photoprotolytic Oxametathesis in Polycyclic Systems. *Organic Letters* **2009**, *11* (17), 3886–3889. https://doi.org/10.1021/ol901456m.

(58) Pérez-Ruiz, R.; Miranda, M. A.; Alle, R.; Meerholz, K.; Griesbeck, A. G. An Efficient Carbonyl-Alkene Metathesis of Bicyclic Oxetanes: Photoinduced Electron Transfer Reduction of the Paternò–Büchi Adducts from 2,3-Dihydrofuran and Aromatic Aldehydes. *Photochemical and Photobiological Sciences* **2006**, *5* (1), 51–55. https://doi.org/10.1039/b513875b.

(59) Pérez-Ruiz, R.; Gil, S.; Miranda, M. A. Stereodifferentiation in the Photochemical Cycloreversion of Diastereomeric Methoxynaphthalene-Oxetane Dyads. **2005**. https://doi.org/10.1021/jo048708.

(60) D'Auria, M.; Racioppi, R.; Viggiani, L. Paternò-Büchi Reaction between Furan and Heterocyclic Aldehydes: Oxetane Formation vs. Metathesis. *Photochemical and Photobiological Sciences* **2010**, *9* (8), 1134–1138. https://doi.org/10.1039/c0pp00076k.

(61) Guilford Jones, B.; Acquadro, M. A.; Carmody, M. A. *Long-Chain Enals Oia Carbonyl-Olefin Metathesis. An Application in Pheromone Synthesis*; 1975.

(62) Guilford Jones, B. I.; Schwartz, S. B.; Marton, M. T. *Regiospecific Thermal Cleavage of Some Oxetan Photoadducts : Carbonyl-Olefin Metathesis in Sequential Photochemical and Thermal Steps*; 1973.

(63) Albright, H.; Vonesh, H. L.; Schindler, C. S. Superelectrophilic Fe(III)-Ion Pairs as Stronger Lewis Acid Catalysts for (E)-Selective Intermolecular Carbonyl-Olefin Metathesis. *Organic Letters* **2020**, *22* (8), 3155–3160. https://doi.org/10.1021/acs.orglett.0c00917.

(64) Olah, G. A. *International Edition in English Superelectrophiles***; 1993; Vol. 32.

(65) Negishi, E. *CONCEPTS*; 1999; Vol. 5.

(66) Stephan, D. W.; Erker, G. Chemie Frustrierter Lewis-Paare: Entwicklung Und Perspektiven. *Angewandte Chemie* **2015**, *127* (22), 6498–6541. https://doi.org/10.1002/ange.201409800.

(67) Denmark, S. E.; Eklov, B. M.; Yao, P. J.; Eastgate, M. D. On the Mechanism of Lewis Base Catalyzed Aldol Addition Reactions: Kinetic and Spectroscopic Investigations Using

Rapid-Injection NMR. *J Am Chem Soc* **2009**, *131* (33), 11770–11787. https://doi.org/10.1021/ja902474j.

(68) Tomifuji, R.; Maeda, K.; Takahashi, T.; Kurahashi, T.; Matsubara, S. FeCl 3 as an Ion-Pairing Lewis Acid Catalyst. Formation of Highly Lewis Acidic FeCl 2+ and Thermodynamically Stable FeCl 4- to Catalyze the Aza-Diels-Alder Reaction with High Turnover Frequency. *Organic Letters* **2018**, *20* (23), 7474–7477. https://doi.org/10.1021/acs.orglett.8b03249.

(69) Ic00256a033.

(70) Davis, A. J.; Watson, R. B.; Nasrallah, D. J.; Gomez-Lopez, J. L.; Schindler, C. S. Superelectrophilic Aluminium(Iii)–Ion Pairs Promote a Distinct Reaction Path for Carbonyl–Olefin Ring-Closing Metathesis. *Nature Catalysis* **2020**, *3* (10), 787–796. https://doi.org/10.1038/s41929-020-00499-5.

(71) Strauss, S. H. *The Search for Larger and More Weakly Coordinating Anions*; 1993; Vol. 93.

(72) Beck, W.; Sunkel, K. Metal Complexes of Weakly Coordinating Anions. Precursors of Strong Cationic Organometallic Lewis Acids1^.

(73) Schottel, B. L.; Chifotides, H. T.; Shatruk, M.; Chouai, A.; Pérez, L. M.; Bacsa, J.; Dunbar, K. R. Anion-π Interactions as Controlling Elements in Self-Assembly Reactions of Ag(I) Complexes with π-Acidic Aromatic Rings. *J Am Chem Soc* **2006**, *128* (17), 5895–5912. https://doi.org/10.1021/ja0606273.

(74) Om50006a014.

(75) Mayfield, H. G.; Bull, W. E. *SECTION A I Norgan Ic, P Hysica I, and T Heoret Ica 1 Chemistry Co-Ordinating Tendencies of the Hexaf Luorophosphate Ion*.

(76) *Chapman et Al*.

(77) Bini, R.; Chiappe, C.; Marmugi, E.; Pieraccini, D. The “Non-Nucleophilic” Anion [Tf2N]- Competes with the Nucleophilic Br-: An Unexpected Trapping in the Dediazoniation Reaction in Ionic Liquids. *Chemical Communications* **2006**, No. 8, 897–899. https://doi.org/10.1039/b514988f.

(78) Hanson, C. S.; Psaltakis, M. C.; Cortes, J. J.; Siddiqi, S. S.; Devery, J. J. Investigation of Lewis Acid-Carbonyl Solution Interactions via Infrared-Monitored Titration. *Journal of Organic Chemistry* **2020**, *85* (2), 820–832. https://doi.org/10.1021/acs.joc.9b02822.

(79) Hanson, C. S.; Psaltakis, M. C.; Cortes, J. J.; Devery, J. J. Catalyst Behavior in Metal-Catalyzed Carbonyl-Olefin Metathesis. *J Am Chem Soc* **2019**, *141* (30), 11870–11880. https://doi.org/10.1021/jacs.9b02613.

(80) Malakar, T.; Hanson, C. S.; Devery, J. J.; Zimmerman, P. M. Combined Theoretical and Experimental Investigation of Lewis Acid-Carbonyl Interactions for Metathesis. *ACS Catalysis* **2021**, *11* (8), 4381–4394. https://doi.org/10.1021/acscatal.0c05277.

(81) Hull, S.; Keen, D. A. *Pressure-Induced Phase Transitions in AgCl, AgBr, and AgI*.

(82) Rodriguez-Ruiz, V.; Carlino, R.; Bezzenine-Lafollée, S.; Gil, R.; Prim, D.; Schulz, E.; Hannedouche, J. Recent Developments in Alkene Hydro-Functionalisation Promoted by Homogeneous Catalysts Based on Earth Abundant Elements: Formation of C-N, C-O and C-P Bond. *Dalton Transactions*. Royal Society of Chemistry July 21, 2015, pp 12029–12059. https://doi.org/10.1039/c5dt00280j.

(83) Ozawa, T.; Kurahashi, T.; Matsubara, S. Manganese Porphyrin Catalyzed Cycloisomerization of Enynes. *Organic Letters* **2012**, *14* (12), 3008–3011. https://doi.org/10.1021/ol301416f.

(84) Ic00219a025.

(85) Honeychuck, R. v; Hersh, W. H. *) And 1.954 (11) A (3b), 2.186 (3) and 1.979 (3) A (3c), 2.168 (7) and 1.500 (14) A (5*; 1989; Vol. 28.

(86) Gowik, P.; Klapiitke, T.; Thewalt, U. *Metallocen-Chemie Hochfluorierter Ligand-Systeme XI *. Synthese Und Charakterisierung von Cp,Ti(SbF,) 2 Und Cp,Ti(Sb, F,) 2; Struktur von Cp,Ti(SbF,) 2 Und Cp2V(SbF,) 2*; Elsevier Sequoia S.A, 1990.

(87) Dash, C.; Das, A.; Yousufuddin, M.; Dias, H. V. R. Isolable, Copper(I) Dicarbonyl Complexes Supported by N-Heterocyclic Carbenes. *Inorganic Chemistry* **2013**, *52* (3), 1584–1590. https://doi.org/10.1021/ic302455y.

(88) Smirnova, E. S.; Muñoz Molina, J. M.; Johnson, A.; Bandeira, N. A. G.; Bo, C.; Echavarren, A. M. Polynuclear Gold [Au I] 4 , [Au I] 8 , and Bimetallic [Au I 4 Ag I] Complexes: C−H Functionalization of Carbonyl Compounds and Homogeneous Carbonylation of Amines . *Angewandte Chemie* **2016**, *128* (26), 7613–7617. https://doi.org/10.1002/ange.201603200.

(89) Bour, C.; Monot, J.; Tang, S.; Guillot, R.; Farjon, J.; Gandon, V. Structure, Stability, and Catalytic Activity of Fluorine-Bridged Complexes IPr·GaCl2(μ-F)EFn -1 (EFn- = SbF6-, PF6-, or BF 4-). *Organometallics* **2014**, *33* (2), 594–599. https://doi.org/10.1021/om4012054.

(90) Kavoosi, A.; Fillion, E. Synthesis and Characterization of Tricarbastannatranes and Their Reactivity in B(C 6 F 5) 3 -Promoted Conjugate Additions . *Angewandte Chemie* **2015**, *127* (18), 5578–5582. https://doi.org/10.1002/ange.201500983.

(91) Michelet, B.; Colard-Itté, J. R.; Thiery, G.; Guillot, R.; Bour, C.; Gandon, V. Dibromoindium(Iii) Cations as a π-Lewis Acid: Characterization of [IPr·InBr2][SbF6] and

Its Catalytic Activity towards Alkynes and Alkenes. *Chemical Communications* **2015**, *51* (34), 7401–7404. https://doi.org/10.1039/c5cc00740b.

(92) Cornella, J.; Martin, R. Ni-Catalyzed Stereoselective Arylation of Inert C-O Bonds at Low Temperatures. *Organic Letters* **2013**, *15* (24), 6298–6301. https://doi.org/10.1021/ol4031815.

(93) Kshirsagar, U. A.; Regev, C.; Parnes, R.; Pappo, D. Iron-Catalyzed Oxidative Cross-Coupling of Phenols and Alkenes. *Organic Letters* **2013**, *15* (12), 3174–3177. https://doi.org/10.1021/ol401532a.

(94) Bao, L.-L.; Iu, Z.-Q. Tetrahydropyrrolization of Resveratrol and Other Stilbenes Improves Inhibitory Effects on DNA Oxidation. https://doi.org/10.1002/cmdc.201600205:NMR.

(95) Konishi, H.; Ueda, T.; Muto, T.; Manabe, K. Remarkable Improvement Achieved by Imidazole Derivatives in Ruthenium-Catalyzed Hydroesterification of Alkenes Using Formates. *Organic Letters* **2012**, *14* (18), 4722–4725. https://doi.org/10.1021/ol301850y.

(96) Yoo, K. S.; Yoon, C. H.; Jung, K. W. Oxidative Palladium(II) Catalysis: A Highly Efficient and Chemoselective Cross-Coupling Method for Carbon-Carbon Bond Formation under Base-Free and Nitrogenous-Ligand Conditions. *J Am Chem Soc* **2006**, *128* (50), 16384–16393. https://doi.org/10.1021/ja063710z.

(97) Kobayashi, K.; Ueno, M.; Kondo, Y. Phosphazene Base-Catalyzed Condensation of Trimethylsilylacetate with Carbonyl Compounds. *Chemical Communications* **2006**, No. 29, 3128–3130. https://doi.org/10.1039/b606056k.

(98) Charette, A. B.; Molinaro, C.; Brochu, C. Catalytic Asymmetric Cyclopropanation of Allylic Alcohols with Titanium-TADDOLate: Scope of the Cyclopropanation Reaction. *J Am Chem Soc* **2001**, *123* (49), 12168–12175. https://doi.org/10.1021/ja0108382.

(99) Hodgson, D. M.; Ying, K. C.; Nuzzo, I.; Freixas, G.; Kulikiewicz, K. K.; Cleator, E.; Paris, J. M. Intramolecular Cyclopropanation of Unsaturated Terminal Epoxides and Chlorohydrins. *J Am Chem Soc* **2007**, *129* (14), 4456–4462. https://doi.org/10.1021/ja0672932.

(100) Usui, I.; Schmidt, S.; Breit, B. Dual Palladium-and Proline-Catalyzed Allylic Alkylation of Enolizable Ketones and Aldehydes with Allylic Alcohols. *Organic Letters* **2009**, *11* (6), 1453–1456. https://doi.org/10.1021/ol9001812.

(101) Oppolzer, W.; Spivey, A. C.; Bochet, C. G. *1991,56, 2988 and References Mentioned Therein. Cf.\ Martin, S. F. The Amaryllidaceae Alkaloids*; Academic Press, 1994; Vol. 116.

(102) Daniel Little, R.; Carroll, G. L.; Petersen, J. L.; Tetrahedron Symp, K. Total Synthesis of the Marine Natural Product A9(12)-Capnellene. Reversal of Regiochemistry in the Intramolecular 1,3-Diyl Trapping Reaction. *Marine Natural Products, Chemical and Biological Perspectives* **1983**, *105* (2), 7129–7130.

(103) le Nôtre, J.; Touzani, R.; Lavastre, O.; Bruneau, C.; Dixneuf, P. H. Homologation of Monoterpenoids into New Sesquiterpenoids via Tandem Isomerisation/Claisen Rearrangement Reactions with Three-Component Ruthenium Catalysts, and Ru(Methallyl)2 (COD) Revealed by High Throughput Screening Techniques. *Advanced Synthesis and Catalysis* **2005**, *347* (6), 783–791. https://doi.org/10.1002/adsc.200404391.

(104) Aebi, J. D.; Deyo, D. T.; Sun, C. Q.; Guillaume, D.; Dunlap, B.; Rich, D. H. *Synthesis, Conformation, and Immunosuppressive Activities of Three Analogues of Cyclosporin A Modified in the 1-Position1 Both Conformations Have a Type IT 0-Tum for Residues 2-*· *5 and a Cis Amide Bond Between*; 1990; Vol. 33.

(105) Casey, C. P.; Bertz, S. H.; Burkhardt, T. J. *REACTION OF METAL-CARBENE COMPLEXES WITH OIAZOALKANES. A VERSATILE VINYL ETHER SYNTHESIS*; PequDon Pram, 1973.

(106) Banks, J. L.; Beard, H. S.; Cao, Y.; Cho, A. E.; Damm, W.; Farid, R.; Felts, A. K.; Halgren, T. A.; Mainz, D. T.; Maple, J. R.; Murphy, R.; Philipp, D. M.; Repasky, M. P.; Zhang, L. Y.; Berne, B. J.; Friesner, R. A.; Gallicchio, E.; Levy, R. M. Integrated Modeling Program, Applied Chemical Theory (IMPACT). *Journal of Computational Chemistry*. December 2005, pp 1752–1780. https://doi.org/10.1002/jcc.20292.

(107) Shao, Y.; Gan, Z.; Epifanovsky, E.; Gilbert, A. T. B.; Wormit, M.; Kussmann, J.; Lange, A. W.; Behn, A.; Deng, J.; Feng, X.; Ghosh, D.; Goldey, M.; Horn, P. R.; Jacobson, L. D.; Kaliman, I.; Khaliullin, R. Z.; Kuš, T.; Landau, A.; Liu, J.; Proynov, E. I.; Rhee, Y. M.; Richard, R. M.; Rohrdanz, M. A.; Steele, R. P.; Sundstrom, E. J.; Woodcock, H. L.; Zimmerman, P. M.; Zuev, D.; Albrecht, B.; Alguire, E.; Austin, B.; Beran, G. J. O.; Bernard, Y. A.; Berquist, E.; Brandhorst, K.; Bravaya, K. B.; Brown, S. T.; Casanova, D.; Chang, C. M.; Chen, Y.; Chien, S. H.; Closser, K. D.; Crittenden, D. L.; Diedenhofen, M.; Distasio, R. A.; Do, H.; Dutoi, A. D.; Edgar, R. G.; Fatehi, S.; Fusti-Molnar, L.; Ghysels, A.; Golubeva-Zadorozhnaya, A.; Gomes, J.; Hanson-Heine, M. W. D.; Harbach, P. H. P.; Hauser, A. W.; Hohenstein, E. G.; Holden, Z. C.; Jagau, T. C.; Ji, H.; Kaduk, B.; Khistyaev, K.; Kim, J.; Kim, J.; King, R. A.; Klunzinger, P.; Kosenkov, D.; Kowalczyk, T.; Krauter, C. M.; Lao, K. U.; Laurent, A. D.; Lawler, K. v.; Levchenko, S. v.; Lin, C. Y.; Liu, F.; Livshits, E.; Lochan, R. C.; Luenser, A.; Manohar, P.; Manzer, S. F.; Mao, S. P.; Mardirossian, N.; Marenich, A. v.; Maurer, S. A.; Mayhall, N. J.; Neuscamman, E.; Oana, C. M.; Olivares-Amaya, R.; Oneill, D. P.; Parkhill, J. A.; Perrine, T. M.; Peverati, R.;

Prociuk, A.; Rehn, D. R.; Rosta, E.; Russ, N. J.; Sharada, S. M.; Sharma, S.; Small, D. W.; Sodt, A.; Stein, T.; Stück, D.; Su, Y. C.; Thom, A. J. W.; Tsuchimochi, T.; Vanovschi, V.; Vogt, L.; Vydrov, O.; Wang, T.; Watson, M. A.; Wenzel, J.; White, A.; Williams, C. F.; Yang, J.; Yeganeh, S.; Yost, S. R.; You, Z. Q.; Zhang, I. Y.; Zhang, X.; Zhao, Y.; Brooks, B. R.; Chan, G. K. L.; Chipman, D. M.; Cramer, C. J.; Goddard, W. A.; Gordon, M. S.; Hehre, W. J.; Klamt, A.; Schaefer, H. F.; Schmidt, M. W.; Sherrill, C. D.; Truhlar, D. G.; Warshel, A.; Xu, X.; Aspuru-Guzik, A.; Baer, R.; Bell, A. T.; Besley, N. A.; Chai, J. da; Dreuw, A.; Dunietz, B. D.; Furlani, T. R.; Gwaltney, S. R.; Hsu, C. P.; Jung, Y.; Kong, J.; Lambrecht, D. S.; Liang, W.; Ochsenfeld, C.; Rassolov, V. A.; Slipchenko, L. v.; Subotnik, J. E.; van Voorhis, T.; Herbert, J. M.; Krylov, A. I.; Gill, P. M. W.; Head-Gordon, M. Advances in Molecular Quantum Chemistry Contained in the Q-Chem 4 Program Package. *Molecular Physics* **2015**, *113* (2), 184–215. https://doi.org/10.1080/00268976.2014.952696.

(108) Zimmerman, P. M. Single-Ended Transition State Finding with the Growing String Method. *Journal of Computational Chemistry* **2015**, *36* (9), 601–611. https://doi.org/10.1002/jcc.23833.

(109) Zimmerman, P. M. Growing String Method with Interpolation and Optimization in Internal Coordinates: Method and Examples. *Journal of Chemical Physics* **2013**, *138* (18). https://doi.org/10.1063/1.4804162.

(110) Jafari, M.; Zimmerman, P. M. Reliable and Efficient Reaction Path and Transition State Finding for Surface Reactions with the Growing String Method. *Journal of Computational Chemistry* **2017**, *38* (10), 645–658. https://doi.org/10.1002/jcc.24720.

(111) Zimmerman, P. Reliable Transition State Searches Integrated with the Growing String Method. *Journal of Chemical Theory and Computation* **2013**, *9* (7), 3043–3050. https://doi.org/10.1021/ct400319w.

(112) Metz, B.; Stoll, H.; Dolg, M. Small-Core Multiconfiguration-Dirac-Hartree-Fock-Adjusted Pseudopotentials for Post-d Main Group Elements: Application to PbH and PbO. *Journal of Chemical Physics* **2000**, *113* (7), 2563–2569. https://doi.org/10.1063/1.1305880.

(113) Peterson, K. A.; Figgen, D.; Goll, E.; Stoll, H.; Dolg, M. Systematically Convergent Basis Sets with Relativistic Pseudopotentials. II. Small-Core Pseudopotentials and Correlation Consistent Basis Sets for the Post-d Group 16-18 Elements. *Journal of Chemical Physics* **2003**, *119* (21), 11113–11123. https://doi.org/10.1063/1.1622924.

(114) Leininger, T.; Nicklass, A.; Kiichle, W.; Stoll, H.; Dolg, M.; Bergner, A. *PHYSICS LETTERS ELSEVIER The Accuracy of the Pseudopotential Approximation: Non-Frozen-Core Effects for Spectroscopic Constants of Alkali Fluorides XF (X = K, Rb, Cs)*; 1996; Vol. 255.

(115) Kaupp, M.; Schleyer, P. V. R.; Stoll, H.; Preuss, H. Pseudopotential Approaches to Ca, Sr, and Ba Hydrides. Why Are Some Alkaline Earth MX2 Compounds Bent? *The Journal of Chemical Physics* **1991**, *94* (2), 1360–1366. https://doi.org/10.1063/1.459993.

(116) Marenich, A. v.; Cramer, C. J.; Truhlar, D. G. Universal Solvation Model Based on Solute Electron Density and on a Continuum Model of the Solvent Defined by the Bulk Dielectric Constant and Atomic Surface Tensions. *Journal of Physical Chemistry B* **2009**, *113* (18), 6378–6396. https://doi.org/10.1021/jp810292n.

(117) Djurovic, A.; Vayer, M.; Li, Z.; Guillot, R.; Baltaze, J. P.; Gandon, V.; Bour, C. Synthesis of Medium-Sized Carbocycles by Gallium-Catalyzed Tandem Carbonyl-Olefin Metathesis/Transfer Hydrogenation. *Organic Letters* **2019**, *21* (19), 8132–8137. https://doi.org/10.1021/acs.orglett.9b03240.

(118) Catti, L.; Tiefenbacher, K. Brønsted-Säure-Katalysierte Carbonyl-Olefin-Metathese in Einer Selbstorganisierten Supramolekularen Wirtstruktur. *Angewandte Chemie* **2018**, *130* (44), 14797–14800. https://doi.org/10.1002/ange.201712141.

(119) Lambert, T. H. Development of a Hydrazine-Catalyzed Carbonyl-Olefin Metathesis Reaction. *Synlett* **2019**, *30* (17), 1954–1965. https://doi.org/10.1055/s-0039-1689924.

(120) Ohkubo, K.; Menon, S. C.; Orita, A.; Otera, J.; Fukuzumi, S. Quantitative Evaluation of Lewis Acidity of Metal Ions with Different Ligands and Counterions in Relation to the Promoting Effects of Lewis Acids on Electron Transfer Reduction of Oxygen. *Journal of Organic Chemistry* **2003**, *68* (12), 4720–4726. https://doi.org/10.1021/jo034258u.

(121) Evans, D. A.; Lectka, T.; Miller, S. J.; Murry, J. A.; Matt, P.; Norcross, R. D.; Johnson, J. S.; Kozlowski, M. C.; Ghosh, A. K.; Mathivanan, P.; Cappiello, J.; Krishnan, K.; Johannsen, M.; Jørgensen, K. A. *C 2-Symmetric Copper(II) Complexes as Chiral Lewis Acids. Enantioselective Catalysis of the Glyoxylate-Ene Reaction*; 1993; Vol. 115.

(122) Johnson, J. S.; Evans, D. A. Chiral Bis(Oxazoline) Copper(II) Complexes: Versatile Catalysts for Enantioselective Cycloaddition, Aldol, Michael, and Carbonyl Ene Reactions. *Accounts of Chemical Research* **2000**, *33* (6), 325–335. https://doi.org/10.1021/ar960062n.

(123) Hilt, G.; Pünner, F.; Möbus, J.; Naseri, V.; Bohn, M. A. A Lewis Acidity Scale in Relation to Rate Constants of Lewis Acid Catalyzed Organic Reactions. *European Journal of Organic Chemistry* **2011**, No. 30, 5962–5966. https://doi.org/10.1002/ejoc.201101029.

(124) *INFRARED SPECTRA OF XANTH0NE:LEWIS ACID COMPLEXES*?*

(125) Tran, U. P. N.; Oss, G.; Breugst, M.; Detmar, E.; Pace, D. P.; Liyanto, K.; Nguyen, T. v. Carbonyl-Olefin Metathesis Catalyzed by Molecular Iodine. *ACS Catalysis* **2019**, *9* (2), 912–919. https://doi.org/10.1021/acscatal.8b03769.

(126) Wang, R.; Chen, Y.; Shu, M.; Zhao, W.; Tao, M.; Du, C.; Fu, X.; Li, A.; Lin, Z. AuCl3-Catalyzed Ring-Closing Carbonyl–Olefin Metathesis. *Chemistry - A European Journal* **2020**, *26* (9), 1941–1946. https://doi.org/10.1002/chem.201905199.

(127) Jermaks, J.; Quach, P. K.; Seibel, Z. M.; Pomarole, J.; Lambert, T. H. Ring-Opening Carbonyl-Olefin Metathesis of Norbornenes. *Chemical Science* **2020**, *11* (30), 7884–7895. https://doi.org/10.1039/d0sc02243h.

(128) Lambert, T. H. Development of a Hydrazine-Catalyzed Carbonyl-Olefin Metathesis Reaction. *Synlett* **2019**, *30* (17), 1954–1965. https://doi.org/10.1055/s-0039-1689924.

(129) Zhang, Y.; Jermaks, J.; MacMillan, S. N.; Lambert, T. H. Synthesis of 2 H-Chromenes via Hydrazine-Catalyzed Ring-Closing Carbonyl-Olefin Metathesis. *ACS Catalysis* **2019**, *9* (10), 9259–9264. https://doi.org/10.1021/acscatal.9b03656.

(130) Hong, X.; Liang, Y.; Griffith, A. K.; Lambert, T. H.; Houk, K. N. Distortion-Accelerated Cycloadditions and Strain-Release-Promoted Cycloreversions in the Organocatalytic Carbonyl-Olefin Metathesis. *Chemical Science* **2014**, *5* (2), 471–475. https://doi.org/10.1039/c3sc52882k.

(131) Griffith, A. K.; Vanos, C. M.; Lambert, T. H. Organocatalytic Carbonyl-Olefin Metathesis. *J Am Chem Soc* **2012**, *134* (45), 18581–18584. https://doi.org/10.1021/ja309650u.

(132) Musacchio, A. J.; Nguyen, L. Q.; Beard, G. H.; Knowles, R. R. Catalytic Olefin Hydroamination with Aminium Radical Cations: A Photoredox Method for Direct C-N Bond Formation. *J Am Chem Soc* **2014**, *136* (35), 12217–12220. https://doi.org/10.1021/ja5056774.

(133) Fernández-Mateos, A.; Madrazo, S. E.; Teijón, P. H.; González, R. R. Radical Cyclization of Epoxy Vinyl- and Allylsulfones Promoted by Titanocene Chloride. *Journal of Organic Chemistry* **2015**, *80* (9), 4378–4391. https://doi.org/10.1021/acs.joc.5b00206.

(134) Kuriyama, Y.; Sasano, Y.; Hoshino, Y.; Uesugi, S. ichiro; Yamaichi, A.; Iwabuchi, Y. Highly Regioselective 5-Endo-Tet Cyclization of 3,4-Epoxy Amines into 3-Hydroxypyrrolidines Catalyzed by La(OTf)3. *Chemistry - A European Journal* **2021**, *27* (6), 1961–1965. https://doi.org/10.1002/chem.202004455.

(135) Johnson, L. A.; Dunbabin, A.; Benton, J. C. R.; Mart, R. J.; Allemann, R. K. Modular Chemoenzymatic Synthesis of Terpenes and Their Analogues. *Angewandte Chemie - International Edition* **2020**, *59* (22), 8486–8490. https://doi.org/10.1002/anie.202001744.

(136) Lucke, A. J.; Young, D. J. Electrophilic Cleavage of Cyclopropylmethystannanes: An Experimental Comparison of σ-σ and σ-π Conjugation. *Journal of Organic Chemistry* **2005**, *70* (9), 3579–3583. https://doi.org/10.1021/jo047822p.

(137) Cai, Z.; Yongpruksa, N.; Harmata, M. Total Synthesis of the Terpenoid Buddledone A: 11-Membered Ring-Closing Metathesis. *Organic Letters* **2012**, *14* (7), 1661–1663. https://doi.org/10.1021/ol300400x.

(138) Anderson, T. E.; Woerpel, K. A. Strain-Promoted Oxidation of Methylenecyclopropane Derivatives Using N-Hydroxyphthalimide and Molecular Oxygen in the Dark. *Organic Letters* **2020**, *22* (14), 5690–5694. https://doi.org/10.1021/acs.orglett.0c02075.

(139) Xu, B.; Shi, M. Ring-Opening Reactions of Methylenecyclopropanes Promoted by Metal Halides. *Organic Letters* **2003**, *5* (9), 1415–1418. https://doi.org/10.1021/ol034142k.

(140) Labes, R.; Battilocchio, C.; Mateos, C.; Cumming, G. R.; de Frutos, O.; Rincón, J. A.; Binder, K.; Ley, S. v. Chemoselective Continuous Ru-Catalyzed Hydrogen-Transfer Oppenauer-Type Oxidation of Secondary Alcohols. *Organic Process Research and Development* **2017**, *21* (9), 1419–1422. https://doi.org/10.1021/acs.oprd.7b00190.

(141) Labes, R.; González-Calderón, D.; Battilocchio, C.; Mateos, C.; Cumming, G. R.; de Frutos, O.; Rincón, J. A.; Ley, S. v. Rapid Continuous Ruthenium-Catalysed Transfer Hydrogenation of Aromatic Nitriles to Primary Amines. *Synlett* **2017**, *28* (20), 2855–2858. https://doi.org/10.1055/s-0036-1589096.

(142) Köckinger, M.; Hone, C. A.; Gutmann, B.; Hanselmann, P.; Bersier, M.; Torvisco, A.; Kappe, C. O. Scalable Continuous Flow Process for the Synthesis of Eflornithine Using Fluoroform as Difluoromethyl Source. *Organic Process Research and Development* **2018**, *22* (11), 1553–1563. https://doi.org/10.1021/acs.oprd.8b00318.

(143) Mata, A.; Hone, C. A.; Gutmann, B.; Moens, L.; Kappe, C. O. Continuous-Flow Pd-Catalyzed Carbonylation of Aryl Chlorides with Carbon Monoxide at Elevated Temperature and Pressure. *ChemCatChem* **2019**, *11* (3), 997–1001. https://doi.org/10.1002/cctc.201801974.

(144) Labes, R.; Mateos, C.; Battilocchio, C.; Chen, Y.; Dingwall, P.; Cumming, G. R.; Rincón, J. A.; Nieves-Remacha, M. J.; Ley, S. v. Fast Continuous Alcohol Amination Employing a

Hydrogen Borrowing Protocol. *Green Chemistry* **2019**, *21* (1), 59–63. https://doi.org/10.1039/c8gc03328e.

(145) Sagmeister, P.; Kaldre, D.; Sedelmeier, J.; Moessner, C.; Püntener, K.; Kummli, D.; Williams, J. D.; Kappe, C. O. Intensified Continuous Flow Synthesis and Workup of 1,5-Disubstituted Tetrazoles Enhanced by Real-Time Process Analytics. *Organic Process Research and Development* **2021**, *25* (5), 1206–1214. https://doi.org/10.1021/acs.oprd.1c00096.

(146) Sambiagio, C.; Ferrari, M.; van Beurden, K.; Ca', N. della; van Schijndel, J.; Noel, T. Continuous-Flow Synthesis of Pyrylium Tetrafluoroborates: Application to Synthesis of Katritzky Salts and Photoinduced Cationic RAFT Polymerization. *Organic Letters* **2021**, *23* (6), 2042–2047. https://doi.org/10.1021/acs.orglett.1c00178.

(147) Quesnel, J. S.; Kayser, L. v.; Fabrikant, A.; Arndtsen, B. A. Acid Chloride Synthesis by the Palladium-Catalyzed Chlorocarbonylation of Aryl Bromides. *Chemistry - A European Journal* **2015**, *21* (26), 9550–9555. https://doi.org/10.1002/chem.201500476.

(148) Schröder, N.; Wencel-Delord, J.; Glorius, F. High-Yielding, Versatile, and Practical [Rh(III)Cp*]-Catalyzed Ortho Bromination and Iodination of Arenes. *J Am Chem Soc* **2012**, *134* (20), 8298–8301. https://doi.org/10.1021/ja302631j.

(149) Mukhopadhyay, S.; Batra, S. Direct Transformation of Arylamines to Aryl Halides via Sodium Nitrite and N-Halosuccinimide. *Chemistry - A European Journal* **2018**, *24* (55), 14622–14626. https://doi.org/10.1002/chem.201803347.

(150) Moreira, J. A.; Corrêa, A. G. Enantioselective Synthesis of Three Stereoisomers of 5,9-Dimethylpentadecane, Sex Pheromone Component of Leucoptera Coffeella, from (-)-

Isopulegol. *Tetrahedron Asymmetry* **2003**, *14* (23), 3787–3795.

https://doi.org/10.1016/j.tetasy.2003.09.030.

Chapter 3 Bis(oxazoline) Iron Complexes Enable Tuning of Lewis Acidity for Catalytic Carbonyl-Olefin Metathesis

Gomez-Lopez, J. L.; Davis, A. J.; Watson, R. B.; Son, M.; Schindler, C. S. *unpublished.*

3.1 Introduction

Carbonyl-olefin metathesis has emerged as a powerful strategy for direct carbon-carbon bond formation from simple carbonyl and olefin precursors.[31–39,41–44,46,48–53,55,62,63,117–119] Early efforts for reaction development focused on the employment of catalytic amounts of $FeCl_3$ to access functionalized cyclopentene scaffolds (**4**) from aryl ketones (**Figure 3.1**).[40] Since this discovery, a variety of catalyst systems have been reported for ring-closing, ring-opening, and cross metathesis variations.[31–33,37,42,46,47,49,50,70] Notably, our group discovered that higher loadings of $FeCl_3$ promote the *in-situ* formation of singly-bridged Fe(III)-homodimers, which serve as Lewis acidic

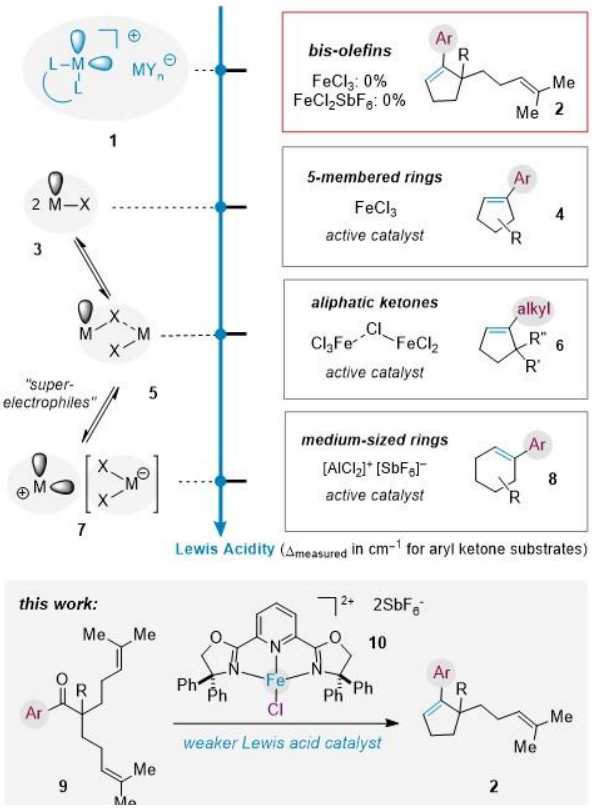

Figure 3.1. Current scope and limitations of carbonyl-olefin metathesis.

superelectrophiles to convert previously unreactive aliphatic ketones into the ring-closing metathesis products (**6**).[42] Additionally, the formation of heterobimetallic ion pairs enabled access to cyclohexene scaffolds (**8**),[70] further expanding the substrate scope for carbonyl-olefin metathesis. Despite these important advancements, several limitations remain within the field. Specifically, no catalyst systems exist which promote productive reactivity for sensitive substrates.

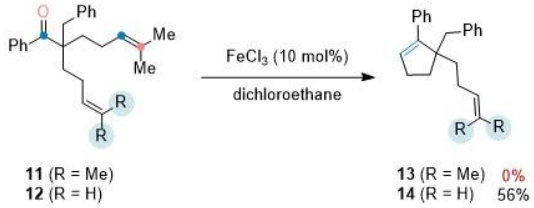

Figure 3.2. Olefin chain effect on reactivity.

For example, aryl ketones such **11**, which contain multiple olefin moieties, are prone to rapid decomposition when subjected to Lewis acids such as $FeCl_3$ and $[FeCl_2][SbF_6]$. For example, when **11**, bearing two identical prenylated olefin subunits, is subjected to catalytic $FeCl_3$, rapid decomposition is observed (**Figure 3.2**). We proposed that these decomposition pathways are with accessed via activation of the pendant olefin on the metathesis product. By replacing the second olefin subunit with an allylic fragment (**12**), these decomposition pathways are mitigated, and metathesis product **14** can be obtained in 56% yield. Therefore, there exists a distinct need for the development for new catalysts with controllable reactivity to convert these overreactive substrates in a general fashion. However, the reaction design relying on $FeCl_3$ as a simple Lewis acid raised concerns for the feasibility of designing tunable catalytic systems. Specifically, the Lewis acidic character of a metal center is known to reduce dramatically upon ligand-binding which renders the resulting metal complexes less efficient as catalysts.[120] The work presented in this chapter represents the development of Fe(III)-complexes utilizing bis(oxazoline) ligand scaffolds to promote carbonyl-olefin metathesis for overreactive bis-olefinic aryl ketones. Catalyst formation occurs *in situ* via ligand bind to the Lewis acid io pair upon halide abstraction. Importantly, the Lewis acidic nature of the catalyst can be tuned to access both more and less reactive catalytic species in a controllable fashion through additional halide abstraction. This method is demonstrated on 23 examples, providing the metathesis products in up to 91% yield.

3.2 Results and Discussion

Our initial investigation into the development of a metal complex focused on identifying a system to efficiently convert β-ketoester **15** to cyclopentene **16**. We selected substrate **15** as an ideal probe to benchmark catalytic activity due to its high reactivity profile (**Figure 3.3**, entry 1) in the presence of $FeCl_3$.[39,41] Bis(oxazoline) (BOX) ligands were initially selected for evaluation, as they have been established for related carbonyl-olefination reactions.[121,122] However, upon incorporation of ligand **18a**, the resulting pentacoordinated Fe(III)-complex failed to provide any of metathesis product **16** (entry 2). Addition of equimolar amounts of $AgSbF_6$ to promote halide abstraction was equally inefficient at promoting any reactivity (entry 3). In comparison, when two equivalents of $AgSbF_6$ are added to form the corresponding tricoordinated complex, **16** was formed in 20% yield (entry 4). Exploration of other Lewis acids including $AlCl_3$, $RuCl_3$, and $InCl_3$ in combination with BOX ligand **18a** failed to provide any of the desired product (entries 5-7). When $GaCl_3$ was employed as the Lewis acid, a dramatic increase of reactivity was observed, with

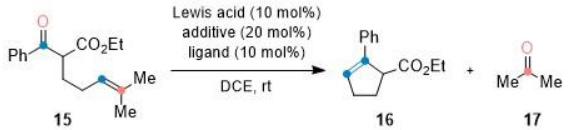

entry	Lewis acid	additive	ligand	yield **16** (%)
1	$FeCl_3$	-	-	99
2	$FeCl_3$	-	**18a**	0
3	$FeCl_3$	$AgSbF_6$ (10 mol%)	**18a**	0
4	$FeCl_3$	$AgSbF_6$	**18a**	20
5	$AlCl_3$	$AgSbF_6$	**18a**	0
6	$RuCl_3$	$AgSbF_6$	**18a**	0
7	$InCl_3$	$AgSbF_6$	**18a**	0
8	$GaCl_3$	$AgSbF_6$	**18a**	55
9	[GaCl((*S*,*S*)-Ph-box)]$(SbF_6)_2$	-	-	58
10	$GaCl_3$	AgOAc	**18a**	0
11	$GaCl_3$	AgOTf	**18a**	19
12	$GaCl_3$	$AgBF_4$	**18a**	4
13	$GaCl_3$	$AgPF_6$	**18a**	0
14	$GaCl_3$	$AgAsF_6$	**18a**	34
15	$GaCl_3$	$AgSbF_6$	**18b**	35
16	$GaCl_3$	$AgSbF_6$	**18c**	26
17	$GaCl_3$	$AgSbF_6$	**19**	78
18	$GaCl_3$	$AgSbF_6$	**20a**	8
19	$GaCl_3$	$AgSbF_6$	**20b**	16
20	$GaCl_3$	$AgSbF_6$ (30 mol%)	**18a**	98

Conditions: all reactions were performed using 0.09 mmol of the substrate in DCE (0.01 M) at room temperature for 1-24 h. Yields are reported as NMR yields with dimethyl terephthalate as an internal standard.

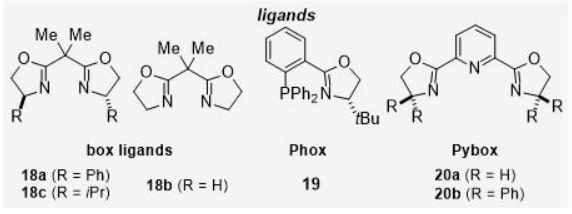

Figure 3.3. Catalyst optimization for carbonyl-olefin metathesis of **15**.

cyclopentene **16** formed in 55% yield (entry 8). Importantly, to confirm its role as the active catalyst [GaCl(*S,S*)-PhBOX][SbF_6]$_2$ formed *in situ* was isolated and used as a discrete catalyst for metathesis of substrate XX. This resulted in similar yield of 58% of **16**, confirming that the tricoordinated Ga(III)-complex is in fact catalyzing the reaction. Next, various Ag(I) salts were evaluated, including salts bearing strongly coordinated anions (entries 10,11) or weakly coordinating anions (entries 12-14), although these all resulted in inferior reactivity in comparison to $AgSbF_6$. Next, the steric effects of the ligand were evaluated. More sterically encumbered (*S,S*)-*i*PrBOX (**18c**) and unsubstituted BOX (**18b**) derived complexes both provided diminished yields of 35% and 26%, respectively, of the metathesis product (entries 15, 16), while bidentate PHOX ligand **19** promoted increased reactivity, resulting in 78% of **16** (entry 17). The use of tricoordinated bis(oxazoline)pyridine (PyBOX) ligands **20a** or **20b** yielded diminished product formation of 8% and 16%, respectively (entries 18-19). Ultimately, the use of 30 mol% of $AgSbF_6$, along with $GaCl_3$ and **18a**, resulted in an efficient catalyst, providing the metathesis product in 98% yield (entry 20).

To further support the *in-situ* generation of an active Ga(III)-complex, we utilized the diamagnetic nature of the catalyst to monitor its formation via ^{1}H NMR spectroscopy in CD_2Cl_2 (**Figure 3.4**). Specifically, when **18a** was subjected to an equimolar amount of $GaCl_3$, ligand

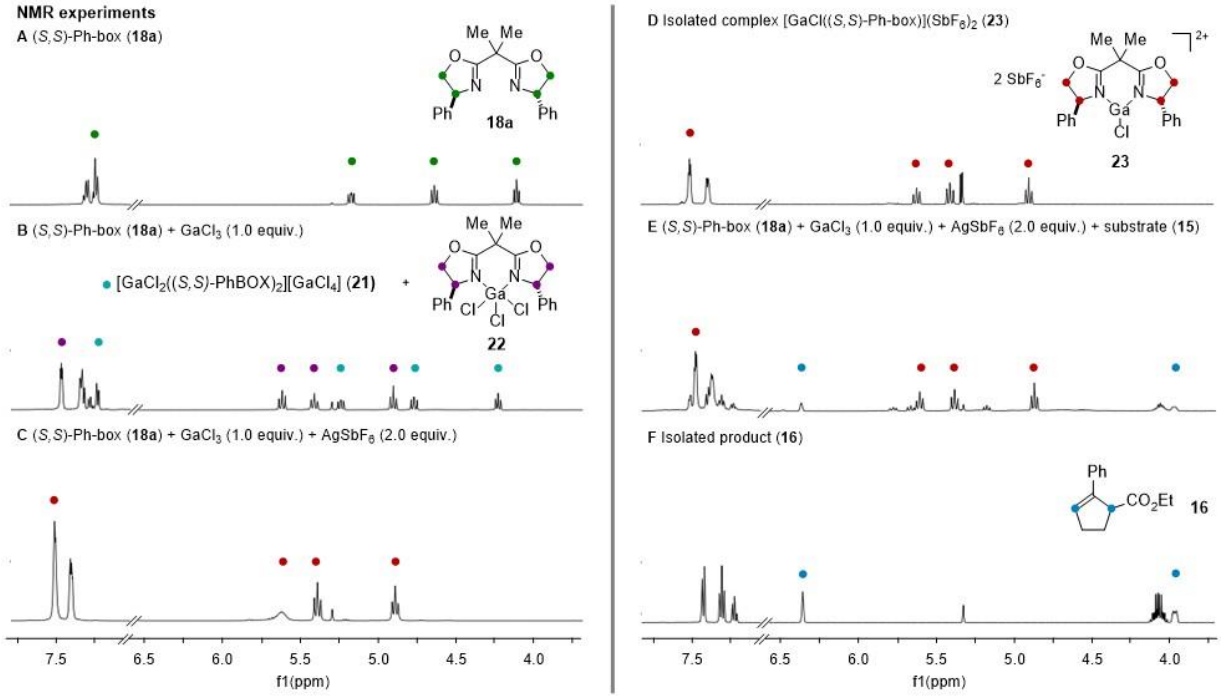

Figure 3.4. ^{1}H NMR Experiments to monitor the in-situ formation of Ga(III)-complex **23**.

coordiantion to the metal center was observed, along with the dimeric species **21** (panels A and B). Addition of 2.0 equivalents of $AgSbF_6$ resulted in the exclusive formation of active catalyst along with precipitation of AgCl as a white solid (panel C). Furthermore, **23** was isolated in 68% yield and the corresponding solid was analyzed by ^1H NMR, confirming its structure (panel D). This isolated complex could be used as a discrete catalyst for carbonyl-olefin metathesis, providing the metathesis product in 58% yield (panels E and F), comparable to the observed yield of 55% when the catalyst is formed *in situ* (**Figure 3.3,** entries 8-9).

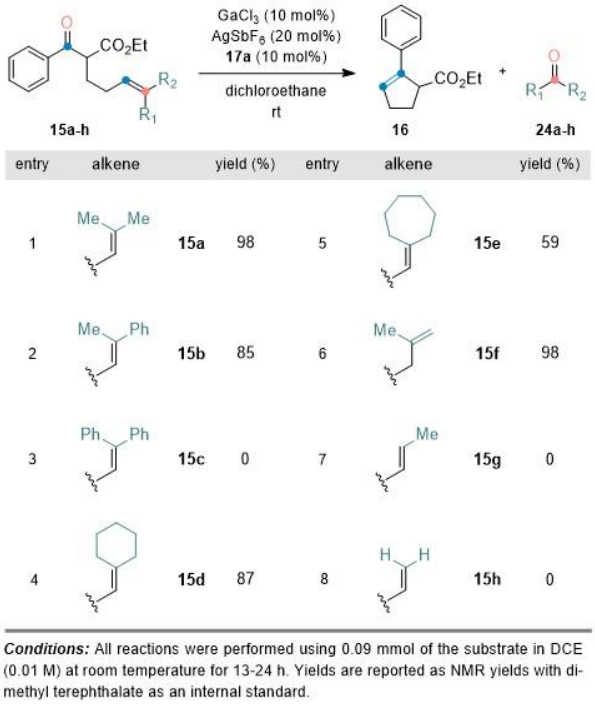

Figure 3.5. Olefin scope.

With suitable conditions for the formation of a catalytically active Ga(III)-complex for carbonyl-olefin metathesis of ketone **15**, we next sought to evaluate the scope of olefin substitution tolerated under this regime (**Figure 3.5**). The prenylated olefin provided excellent yield of 98% of the desired product (entry 1). Interestingly, ketone **15b**, which would form acetophenone as the carbonyl byproduct upon metathesis, was also efficiently converted to the corresponding products in 85% yield (entry 2) suggesting competitive binding of the carbonyl byproduct is not prevalent for this catalytic system. Diphenyl-substituted **15c** was unreactive under these conditions, likely due to the increased steric profile of the olefin coupling partner (entry 3). Exo-cyclic olefins **15d** and **15e** were also well tolerated, providing the metathesis product in good yields of 87% and 59%, respectively (entries 4-5), while terminal olefin **15f** was converted to cyclopentene **16** in excellent yield of 98% via *in situ* isomerization to the prenylated intermediate (entry 6). Olefins lacking

nucleophilic character such as crotyl (**15g**) and allyl (**15h**) alkenes were inactive under these reaction conditions, consistent with other Lewis acid-catalyzed carbonyl-olefin metathesis transformations (entries 7-8).[41,63,70]

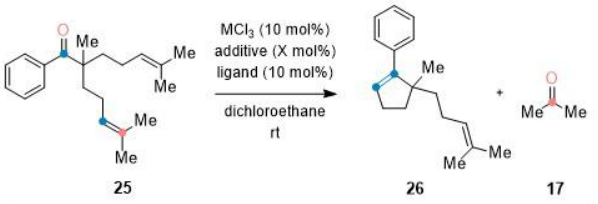

entry	Lewis acid	additive	mol %	ligand	yield **20** (%)
1	$FeCl_3$	-	-	-	0[a]
2	$FeCl_3$	$AgSbF_6$	10	-	0[a]
3	$GaCl_3$	$AgSbF_6$	30	**18a**	0[a]
4	$GaCl_3$	$AgSbF_6$	20	**18a**	49
5	$FeCl_3$	$AgSbF_6$	20	**18a**	68
6	$FeCl_3$	$AgSbF_6$	20	**18b**	46
7	$FeCl_3$	$AgSbF_6$	20	**18d**	39
8	$FeCl_3$	$AgSbF_6$	20	**20a**	80
9	$FeCl_3$	$AgSbF_6$	20	**20b**	91
10	$FeCl_3$	$AgSbF_6$	20	**20c**	47
11	$FeCl_3$	$AgSbF_6$	20	**20d**	66
12	$FeCl_3$	$AgSbF_6$	20	**27**	21

Conditions: All reactions were performed using 0.09 mmol of the substrate in DCE (0.01 M) at room temperature for 0.5 - 13 h. Yields are reported as NMR yields with dimethyl terephthalate as internal standard. [a]Decomposition observed.

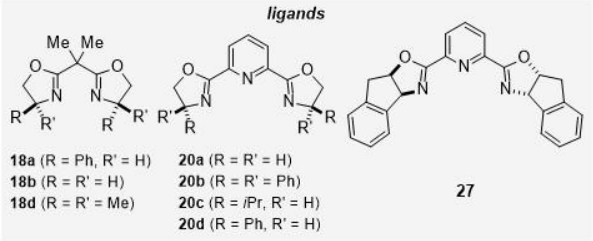

Figure 3.6. Evaluation of metal complexes for carbonyl-olefin metathesis of bis-olefin **25**.

Subsequent investigations focused on evaluating these metal complexes as active catalysts for carbonyl-olefin metathesis of sensitive substrates (**Figure 3.6**). Specifically, aryl ketones bearing two olefinic chains such as **25** are incompatible with established catalysts such as $FeCl_3$ or $FeCl_3$ combined with $AgSbF_6$ due to rapid decomposition of the substrate (entries 1-2). When subjected to reaction conditions that would form Ga(III)-complex **23**, similar decomposition pathways were observed (entry 3). However, reducing the Ag(I) salt loading to 20 mol% resulted in 49% formation of the metathesis product (entry 4), and switching from $GaCl_3$ to $FeCl_3$ as the Lewis acid further increased the yield to 68% (entry 5). The use of either unsubstituted BOX **18b** or MeBOX **18d** proved diminished yields of 46% and 39% of **26**, respectively (entries 6-7). Switching to a tricoordinate ligand scaffold such as **20a** resulted in a dramatic increase in

reactivity, forming **26** in 80% yield (entry 8). Diphenyl substituted **20b** proved to be optimal for converting bis-olefin **25**, providing **26** in excellent yield of 91% (entry 9). Monosubstituted ligands **20c** and **20d** resulted in loss of reactivity, forming **26** in inferior yields of 47% and 66%, respectively (entries 10-11), while sterically demanding IndenoPyBOX **27** similarly resulted in loss of reactivity, providing just 21% of cyclopentene **26** (entry 12).

With a catalyst system identified which could efficiently convert sensitive bis-olefinic ketones **28** to the corresponding ring-closing metathesis products, we next turned our attention to the overall scope of the transformation (**Figure 3.7**). Generally, aryl ketones bearing two identical prenylated side chains were well tolerated. Aryl rings bearing electron-poor substituents such as halides (**32-34**) were efficiently converted to the metathesis products in 72-89% yield. Similarly, electron-rich arenes bearing alkyl substituents provided cyclopentenes **35**, **37**, and **38**, in good yields of 65-86%. Importantly, **37** was obtained in good yield of 62%, despite containing a methoxy substituent, which could serve as a second Lewis basic site, reducing catalytic activity via competitive binding.

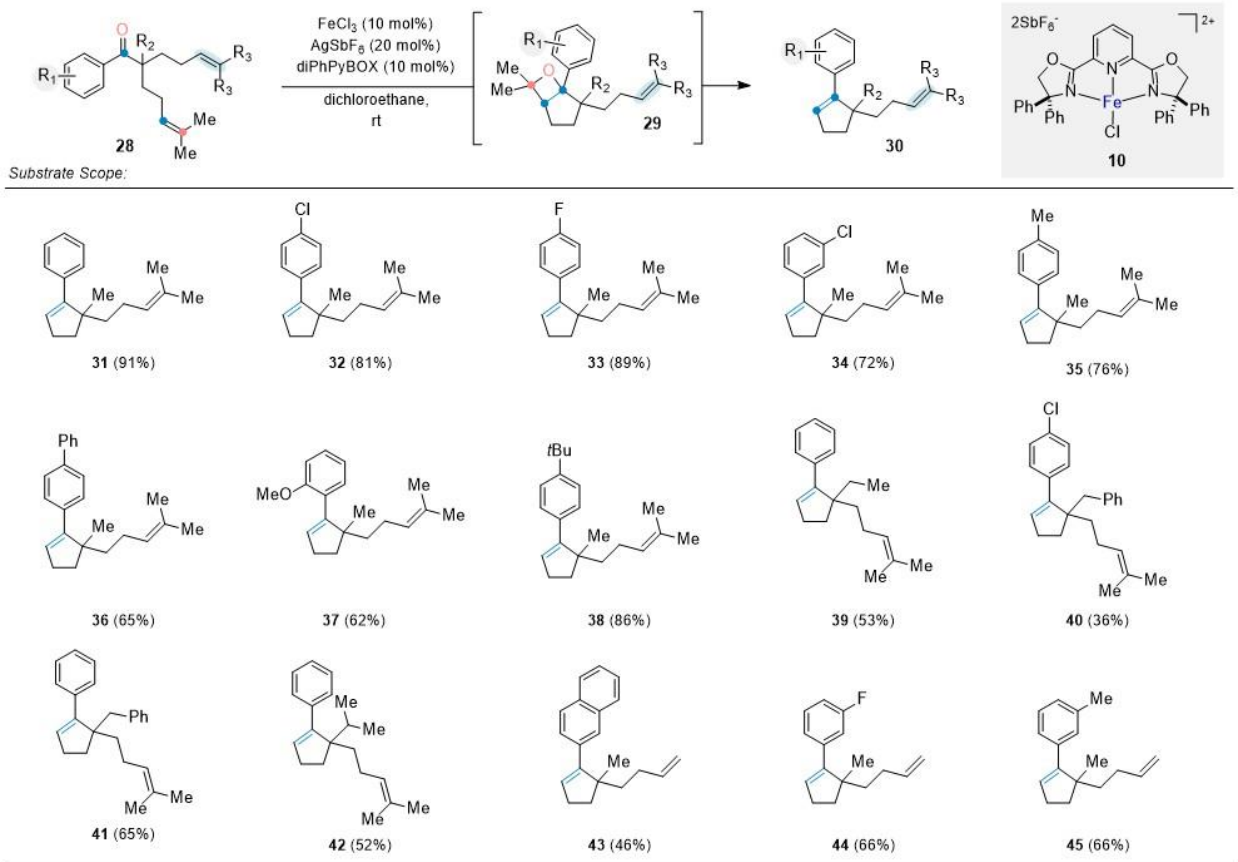

Conditions: all reactions were performed using 0.09 mmol of the substrate in DCE (0.01 M) at room temperature for 0.5-48 h. Yields are reported as NMR yields with dimethyl terephthalate as an internal standard.

Figure 3.7. Substrate scope.

Substrates containing more sterically encumbering side chains at the α-position were also suitable metathesis candidates. Specifically, ethyl substituted **39** was formed in 53% yield, while benzylated **40** and **41** were produced in moderate yields of 36% and 65%, respectively. Notably, bulky isopropyl groups did not appear to have an impact on reactivity, as **42** was formed in 52%, despites its proximity to the reactive ketone moiety. Finally, substrates bearing two electronically differentiated olefin side chains demonstrated high selectivity for activation of the more electron-rich alkene for carbonyl-olefin metathesis. This enabled access to compounds such as **43-45** with pendant allylic side chains in up to 66% yield. The development of these metal complexes as tunable Lewis acids for challenging substrates led us to explore their utility on another class of overreactivity. Specifically, substrates which undergo alkene isomerization have previously led to inseparable mixtures of olefin products, or exclusive formation of the incorrect isomer.[32,41] When conditions to form modified Fe(III)-complex **48** were used, cyclopentenes **47** containing both electron-rich and -poor substituents were formed as the exclusive isomer in up to 76% yield (**Figure 3.8**). Importantly, less than 5% of undesired, isomerized alkene was observed in each case, demonstrating these complexes unique ability to serve as potent catalysts for sensitive chemical transformations.

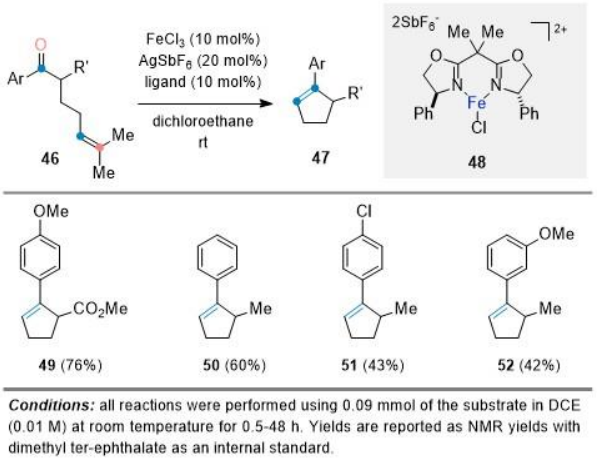

Figure 3.8. Fe(III)-complexes prevent alkene isomerization.

Our subsequent efforts focused on identifying a method for relating the relative Lewis acidity of these novel complexes to previously reported systems. We envisioned the development of a technique which would enable us to relate carbonyl activation to Lewis acid strength would further demonstrate that these catalysts serve as less Lewis acidic species quantitatively.[123] To this end, solution phase infrared (IR) spectroscopy was utilized to measure the shift of absorption frequency of the carbonyl moiety of **51** in the presence of various Lewis acids (**Figure 3.9**).[124]

When aryl ketone **51**, which lacks an olefin subunit and is therefore inactive for metathesis, was subjected to 1.0 equivalents of $FeCl_3$, a new absorption appeared 124 cm^{-1} up field from the unbound carbonyl stretch, consistent with previously observed reports for monomeric $FeCl_3$ activation.[39,42] Increasing the amount of $FeCl_3$ to 2.0 equivalents resulted in the appearance of a second band at 1494 cm^{-1}, an even larger shift of 187 cm^{-1} relative to the free carbonyl. This supports both the formation of a singly bridge dimeric $FeCl_3$ species, as well as its increased Lewis acidic character in comparison to monomeric $FeCl_3$ as was previously reported.[42] The use of $FeCl_3$ and $AgSbF_6$ together to form $[FeCl_2][SbF_6]$ *in situ* promoted a further increase in the shift of the carbonyl stretch of 219 cm^{-1}, supporting the formation of ion pairs as superelectrophilic species to activate substrates for carbonyl-olefin metathesis.[70] These three data points collectively demonstrated that this method for quantifying Lewis acidic as a function of carbonyl activation is viable for evaluating the relative strength of the metal complex systems. Preformed complex **53** was exposed to 1.0 equivalent of ketone **51**, which resulted in a shift of the carbonyl peak less than that observed with $FeCl_3$ alone (37 cm^{-1} vs. 124 cm^{-1}) signifying a dramatic decrease in Lewis acidity of the metal center upon ligand association. Similarly, the pentacoordinated cationic complex formed upon combination of $FeCl_3$, diPhPyBOX ligand, and 1.0 equivalent of $AgSbF_6$ is also less Lewis acidic than $FeCl_3$ alone, highlighted by a carbonyl shift of just 66 cm^{-1}. Interestingly, when 2.0 equivalents of $AgSbF_6$ are used, which would result in the corresponding

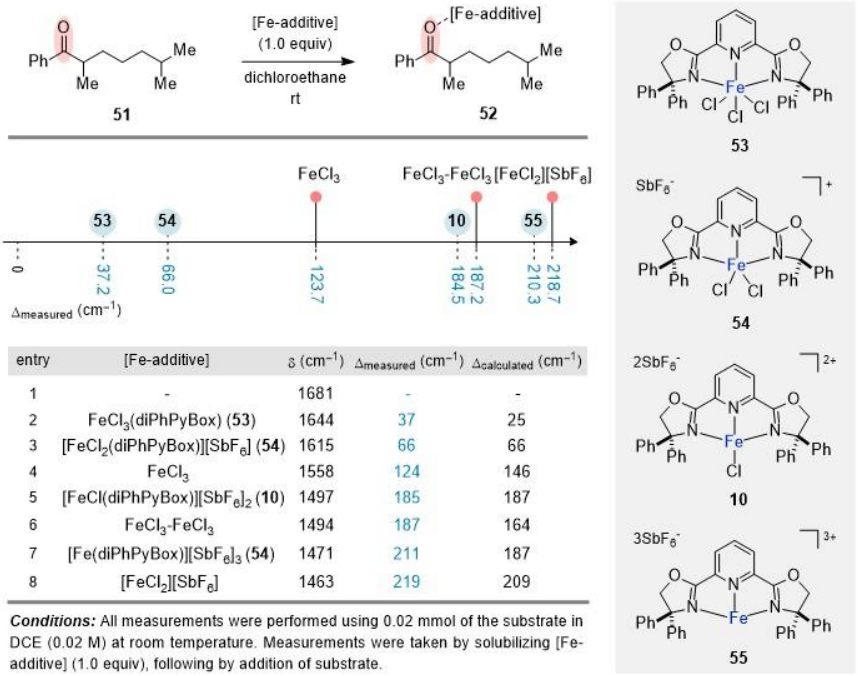

entry	[Fe-additive]	δ (cm^{-1})	$\Delta_{measured}$ (cm^{-1})	$\Delta_{calculated}$ (cm^{-1})
1	-	1681	-	-
2	$FeCl_3$(diPhPyBox) (**53**)	1644	37	25
3	$[FeCl_2$(diPhPyBox)$][SbF_6]$ (**54**)	1615	66	66
4	$FeCl_3$	1558	124	146
5	$[FeCl$(diPhPyBox)$][SbF_6]_2$ (**10**)	1497	185	187
6	$FeCl_3$-$FeCl_3$	1494	187	164
7	$[Fe$(diPhPyBox)$][SbF_6]_3$ (**54**)	1471	211	187
8	$[FeCl_2][SbF_6]$	1463	219	209

Conditions: All measurements were performed using 0.02 mmol of the substrate in DCE (0.02 M) at room temperature. Measurements were taken by solubilizing [Fe-additive] (1.0 equiv), following by addition of substrate.

Figure 3.9. IR studies of Lewis acidic Fe(III)-complexes.

tetracoordinated complex **10**, the carbonyl absorption peak experienced a shift of 185 cm^{-1}. Interestingly, this result suggests that the metal complex **10** has the potential to serve as an alternative to $FeCl_3$-dimers, as the formation of the active complex is irreversible, and therefore can be formed more efficiently. Finally complex **55**, which forms upon abstraction of all three halide substituents from the metal center, activates carbonyl **51** as represented by a shift of 211cm^{-1}, suggesting it can promote unreactive substrates is a fashion analogous to the corresponding ion pair catalyst system. Notably, computations for the activation of the carbonyl moiety by Lewis acid association is in good agreement with the experimentally obtained values. Specifically, density functional theory calculations at the B3LYP-D3/LACVP/6-31G** level of theory were employed to calculate the vibrational frequencies of ketone **51** in the presence of each catalyst system. The calculations support that the least Lewis acidic species **53** should least affect the shift in frequency, while superelectrophilic ion pairs should promote the largest shift in the carbonyl peak.

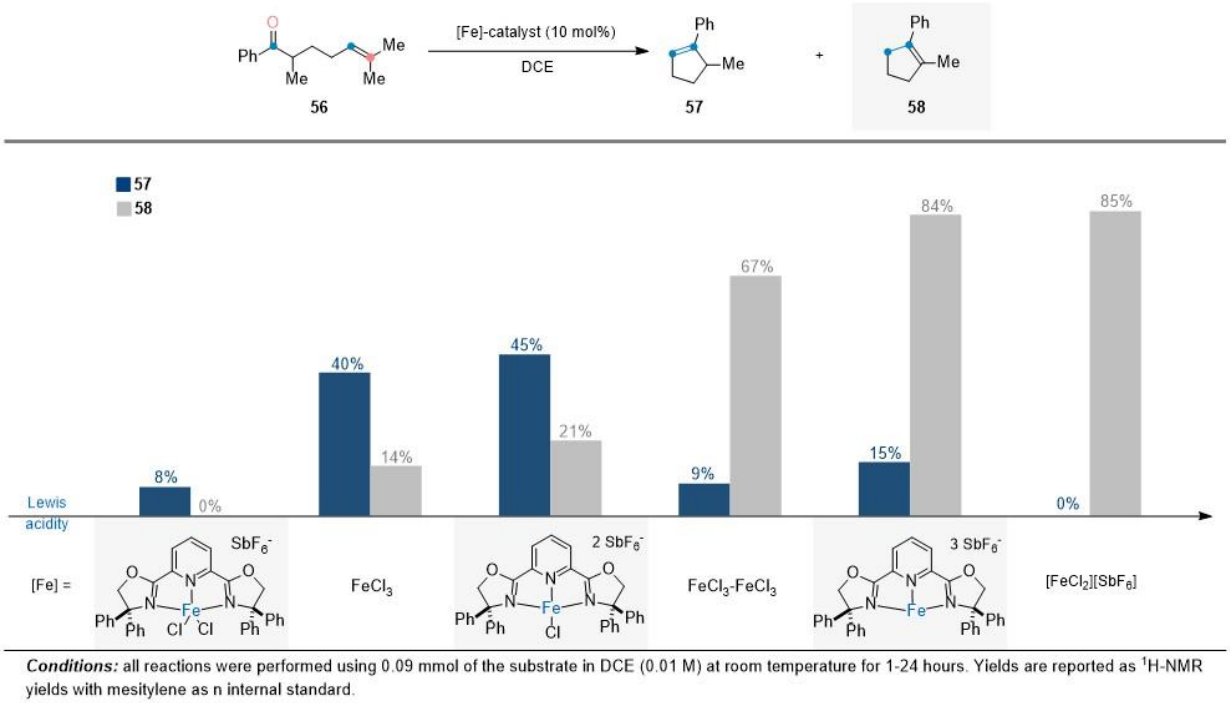

Figure 3.10. Correlation between Lewis acidity and reactivity profile for Fe(III)-catalysts.

To fully understand the relationship between Lewis acidic-activation of the carbonyl and the overall reactivity of these Fe(III)-catalysts, a reactivity profile for substrate **56** was conducted (**Figure 3.10**). When the weakest Lewis acid **53** was employed, the desired metathesis product was

formed in diminished yield of just 8% as the exclusive product. Increasing the potency of the Fe(III)-catalyst by using monomeric $FeCl_3$ provided more efficient product formation of **57** in 40%. However, this also resulted in the *in-situ* isomerization to form tetrasubstituted **58** as an inseparable diastereomer in 14%. Complex **54** provided the highest yield of the desired COM product, forming **57** in 45% yield, along with 21% yield of isomer **58**. The $FeCl_3$-dimer resulted in a dramatic shift in product formation, favoring the formation of the isomerized product as the major species, forming in 67%, while the trisubstituted olefin **57** was formed in just 9%. Complex **55**, which is the most Lewis acidic of the three Fe(III)-complexes evaluated providing quantitative formation of the COM product as a 5.6:1 ratio of the isomers favoring the isomerized product. Finally, the Fe(III)-ion pair, which displayed the strongest Lewis acidic character, provided isomerized **58** as the exclusive product in 85% yield.

3.3 Conclusions

In summary, we have developed a method for Lewis acid-catalyzed carbonyl-olefin metathesis of sensitive substrates relying on the use of Fe(III)-complexes. This strategy utilizes bis(oxazoline) and bis(oxazoline)pyridine ligand scaffolds to tune the overall Lewis acidity of metal center, enabling efficient conversion of substrates that were prone to decomposition or isomerization pathways under previously reported catalyst systems. Importantly, solution phase IR spectroscopy demonstrated that the strength of these metal complexes can controlled by iterative chloride abstraction to access catalysts with a range of Lewis acidic character. The results presented in this chapter are expected to guide the design of future catalyst systems to further broaden the scope of carbonyl-olefin metathesis transformations catalyzed by Lewis acids.

3.4 Experimental Procedures and Supplemental Information

3.4.1 General Information

General laboratory procedures. All moisture-sensitive reactions were performed in a nitrogen-filled glovebox or using Schlenk techniques in oven or flame-dried round bottom flasks fitted with

rubber septa. Stainless steel syringes were used to transfer air or moisture-sensitive liquids. Flash chromatography was performed using silica gel SiliaFlash® 40-63 micron (230-400 mesh) from SiliCycle.

Materials and instrumentation. All chemicals were purchased from commercial suppliers and were used as received unless otherwise stated. **(*S*,*S*)-2,2-Bis(4-phenyl-2-oxazolin-2-yl)propane (17a),**[1] 2,2'-(propane-2,2-diyl)bis(4,5-dihydrooxazole) (**17b**),[2a] 2,2'-(propane-2,2-diyl)bis(4,4-dimethyl-4,5-dihy-drooxazole) (**17c**),[2b] 2,6-bis(4,5-dihydrooxazol-2-yl)pyridine (**18a**),[3] 2,6-bis(4,4-diphenyl-4,5-dihydro-oxazol-2-yl)pyridine (**18b**),[4] ethyl 2-benzoyl-6-methylhept-5-enoate (**13**),[5] ethyl (*E*)-2-benzoyl-6-phenylhept-5-enoate (**24**),[5] ethyl (*E*)-2-benzoylhept-5-enoate (**29**),[5] ethyl 2-benzoylhex-5-enoate (**30**),[6] methyl 2-(4-methoxybenzoyl)-6-methylhept-5-enoate (**S47**),[5] and 2,6-dimethyl-1-phenylhept-5-en-1-one (**S48**)[5] were prepared according to literature procedures. Proton Nuclear Magnetic Resonance (^{1}H NMR) spectra and Carbon Nuclear Magnetic Resonance (^{13}C NMR) spectra were recorded on a Varian Unity Plus 400, Varian MR400, Varian vnmrs 500, Varian Inova 500, Varian Mercury 500, and Varian vnmrs 700 spectrometers. Chemical shifts for protons are reported in parts per million and are referenced to the NMR solvent peak ($CDCl_3$: δ 7.26). Chemical shifts for carbons are reported in parts per million and are referenced to the carbon resonances of the NMR solvent ($CDCl_3$: δ 77.16). Data is represented as follows: chemical shift, integration, multiplicity (br = broad, s = singlet, d = doublet, t = triplet, q = quartet, p = pentet, h = hexet, hept = heptet, m = multiplet), and coupling constants in Hertz (Hz). Mass spectroscopic (MS) data was recorded at the Mass Spectrometry Facility at the Department of Chemistry of the University of Michigan in Ann Arbor, MI on an Agilent Q-TOF HPLC-MS with ESI high resolution mass spectrometer. Infrared (IR) spectra were obtained using either an Avatar 360 FT-IR or Perkin Elmer Spectrum BX FT-IR spectrometer. IR data are represented as frequency of absorption (cm^{-1}).

Abbreviations used: $FeCl_3$ = iron(III) chloride, $AlCl_3$ = aluminum(III) chloride, $RuCl_3$ = ruthenium(III) chloride, $InCl_3$ = indium(III) chloride, $GaCl_3$ = gallium(III) chloride, (*S*,*S*)-Ph-BOX = **(*S*,*S*)-2,2-Bis(4-phenyl-2-oxazolin-2-yl)propane**, diPh-PyBOX = 2,6-bis(4,4-diphenyl-4,5-dihydro-oxazol-2-yl)pyridine, $AgSbF_6$ = silver hexafluoroantimonate(V), AgOAc = silver acetate, $AgBF_4$ = silver tetrafluoroborate, AgOTf = silver trifluoromethanesulfonate, $AgPF_6$ = silver

hexafluorophosphate, $AgAsF_6$ = silver hexafluoroarsenate(V), AgOTFA = silver trifluoroacetate, AgOTs = silver *p*-toluensulfonate, EtOAc = ethyl acetate, Et_2O = diethyl ether, DMF = dimethylformamide, DCM = dichloromethane, DCE = 1,2-dichloroethane, THF = tetrahydrofuran, DMSO = dimethylsulfoxide, NaH = sodium hydride, K_2CO_3 = potassium carbonate, KI = potassium iodide, Na_2SO_4 = sodium sulfate, TLC = thin layer chromatography, LDA = lithium diisopropylamine, *n*-BuLi = *n*-butyllithium, DIBAL = diisobutylaluminium hydride, IBX = 2-iodoxybenzoic acid, PCC = pyridinium chlorochromate.

3.4.2 Reaction Optimization

An oven-dried round bottom flask equipped with a magnetic stir bar was charged with the appropriate Lewis acid, ligand, additive and DCE (8 mL). The catalyst solution was allowed to stir for 30 min or 1 h when $FeCl_3$ was used as Lewis acid at room temperature. The β-ketoester or bisalkene substrate (0.09 mmol dissolved in 1 mL of DCE) was added in one portion to the catalyst solution. The reaction was allowed to stir for the indicated time at room temperature. After reaching completion as judged by TLC or 48 h, the reaction was filtered through a silica plug eluting with DCM. The filtrate was concentrated under reduced pressure to remove all volatile components. Yields were determined by ^1H NMR using dimethyl terephthalate as internal standard.

Table 3.1. Reaction optimization for β-ketoester or bisalkene.

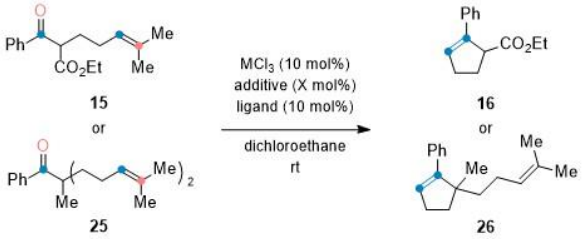

entry	substrate	Lewis acid	additive	mol %	ligand	yield (%)
1	**15**	$FeCl_3$	-	-	-	99
2	**15**	$FeCl_3$	$AgSbF_6$	10	-	90
3	**15**	-	$AgSbF_6$	10	-	0
4	**15**	$FeCl_3$	-	-	**18a**	0
5	**15**	$FeCl_3$	$AgSbF_6$	10	**18a**	0
6	**15**	$FeCl_3$	$AgSbF_6$	20	**18a**	20
7	**15**	$FeCl_3$	$AgSbF_6$	30	**18a**	68
8	**15**	$GaCl_3$	-	-	**18a**	0
9	**15**	$GaCl_3$	$AgSbF_6$	10	**18a**	0
10	**15**	$GaCl_3$	$AgSbF_6$	20	**18a**	97
11	**15**	$GaCl_3$	$AgSbF_6$	30	**18a**	98
12	**15**	[GaCl((*S*,*S*)-Ph-box)]$(SbF_6)_2$ (**20**)		-	-	98
13	**15**	$AlCl_3$	$AgSbF_6$	20	**18a**	0
14	**15**	$RuCl_3$	$AgSbF_6$	20	**18a**	0
15	**15**	$InCl_3$	$AgSbF_6$	20	**18a**	0
16	**15**	$GaCl_3$	AgOAc	20	**18a**	0
17	**15**	$GaCl_3$	$AgBF_4$	20	**18a**	4
18	**15**	$GaCl_3$	AgOTf	20	**18a**	19
19	**15**	$GaCl_3$	$AgPF_6$	20	**18a**	0
20	**15**	$GaCl_3$	$AgAsF_6$	20	**18a**	34
21	**25**	$FeCl_3$	-	-	-	0[a]
22	**25**	$FeCl_3$	$AgSbF_6$	10	-	0[a]
23	**25**	$GaCl_3$	$AgSbF_6$	20	**18a**	49
24	**25**	$FeCl_3$	$AgSbF_6$	20	**18a**	68
25	**25**	$FeCl_3$	$AgSbF_6$	20	**18a**	46
26	**25**	$FeCl_3$	$AgSbF_6$	20	**18c**	39
27	**25**	$FeCl_3$	$AgSbF_6$	20	**18a**	80
28	**25**	$FeCl_3$	$AgSbF_6$	20	**20b**	91
29	**25**	$FeCl_3$	$AgSbF_6$	20	**20c**	47
30	**25**	$FeCl_3$	$AgSbF_6$	20	**20d**	66
31	**25**	$FeCl_3$	$AgSbF_6$	20	**27**	21

Conditions: All reactions were performed using 0.09 mmol of the substrate in DCE (0.01 M) at room temperature for 0.5 - 24 h. Yields are reported as NMR yields with dimethyl terephthalate as internal standard. [a]Decomposition observed.

ligands

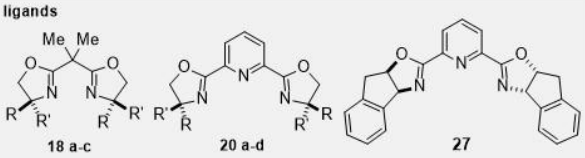

with **18a** (R = Ph, R' = H); **18b** (R, R' = H); **18c** (R, R' = Me); **20a** (R, R' = H); **20b** (R, R' = Ph), **20c** (R = iPr, R' = H); **20d** (R = Ph, R' = H).

3.4.3 Synthesis of [GaCl((*S*,*S*)-PhBOX)][SbF_6]$_2$

3.4.4. In situ formation: identification of precursors.

The mixture of (*S*,*S*)-PhBOX (1.0 equiv) with $GaCl_3$ (1.0 equiv) in CD_2Cl_2 at room temperature resulted in the formation of two new species in a ratio of 3:1 (Fig. 2). The minor species showed

^{1}H NMR chemical shifts slightly downfield compared to the free ligand. After several unsuccessful attempts to crystallize the complex, we decided to analyze the formation of complexes varying the ratio of ligand and metal by ^{1}H NMR and compare the spectra to determine the nature of the species. The structures were proposed based on reported literature of gallium complexes with bidentate ligands (nitrogen or phosphorus-based ligands)[7] and ^{71}Ga NMR spectroscopy. The ^{1}H NMR spectra of each complex obtained is showed in **Figure 3.11**.

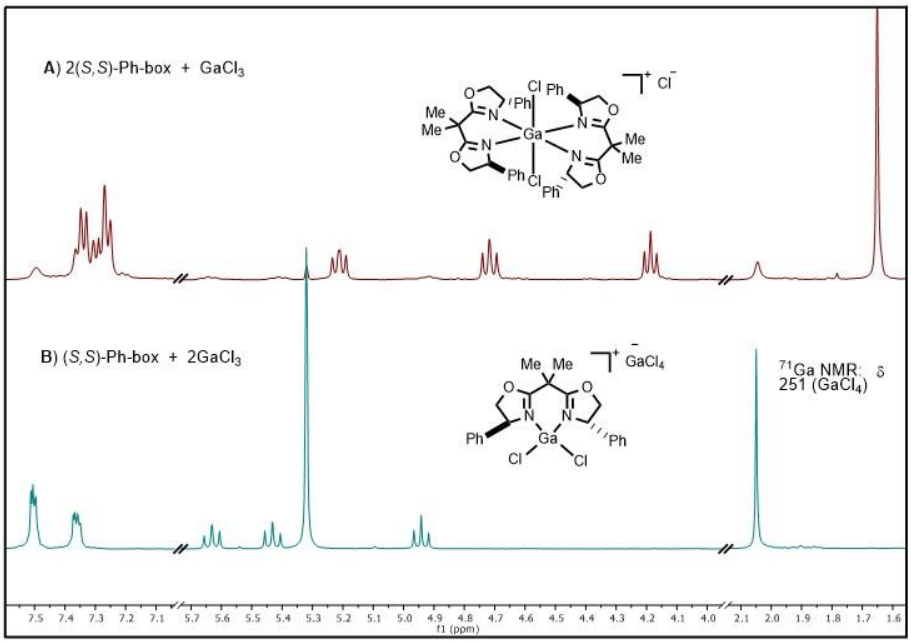

Figure 3.11. ^{1}H NMR spectra of gallium(III) complexes. A) Octahedral gallium complex obtained with 2.0 equiv of (S,S)-PhBOX. B) tetracoordinated gallium complex obtained after addition of 2.0 equiv of $GaCl_3$.

The cationic octahedral gallium complex chemical shifts (**Figure 3.11**) and the pattern in the aromatic region are similar to the minor species observed in a 1:1 mixture of $GaCl_3$ and (*S*,*S*)-Ph-box (Fig. S2). The proposed structure for the minor species corresponds to [Ga((*S*,*S*)-Ph-box)$_2$Cl$_2$][GaCl$_4$] due to the similarity on the NMR chemical shifts and the presence of tetrachloro gallate anion ($GaCl_4$) confirmed by ^{71}Ga NMR, which is a common counterion in gallium complexes.[7a-b]

The major species NMR chemical shifts are quite similar to the complex with one bidentate ligand (**Figure 3.12**). We proposed a pentacoordinated neutral complex structure, which experiments a rearrangement via PhBOX/chloride exchange to form the cationic minor species.

The addition of 2.0 equiv of $AgSbF_6$ to the mixture of complexes resulted in the exclusive formation of $[GaCl((S,S)\text{-Ph-box})][SbF_6]_2$ (**20**, **Figure 3.13**).

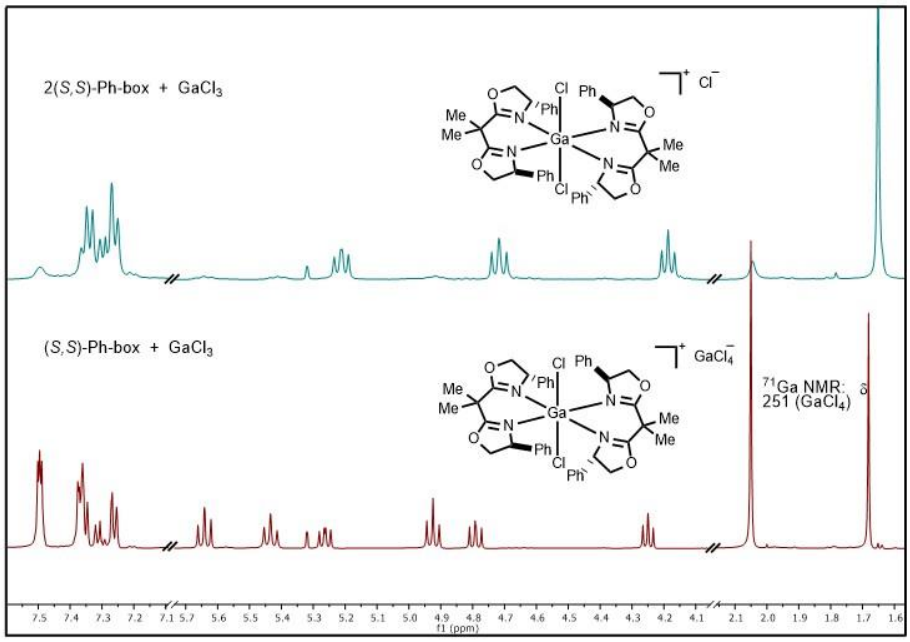

Figure 3.12. Comparison of ^{1}H NMR spectra of gallium(III) complexes and proposed structure for the minor species (bottom).

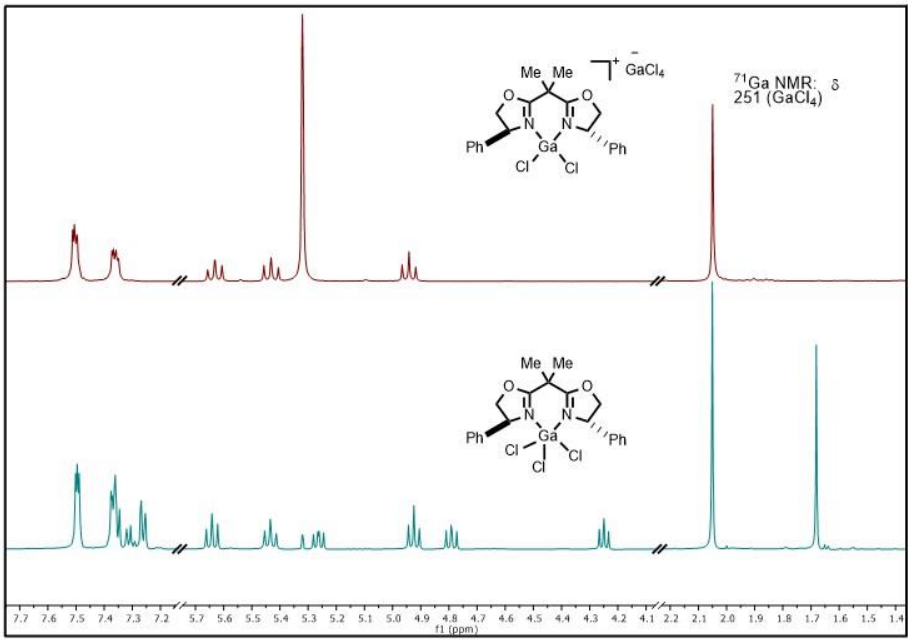

Figure 3.13. Comparison of ^{1}H NMR spectra of gallium(III) complexes and proposed structure for the major species (bottom).

3.2. Synthesis and isolation.

In a scintillation vial was added (*S*,*S*)-Ph-box (30.0 mg, 0.09 mmol), $GaCl_3$ (15.8 mg, 0.09 mmol) and 5 mL of DCM at room temperature. The mixture was stirred for 2 min and $AgSbF_6$ (62.9 mg, 0.18 mmol) was added in one portion. The mixture was stirred for 10 min and then filtered through a fiber glass filter. The solvent was removed under reduced pressure. The gallium complex **20** was obtained as a pale-yellow solid in 68% yield (55.7 mg). This complex is highly hygroscopic and has poor solubility in DCM after isolation. **^{1}H NMR** (500 MHz; CD_2Cl_2) δ 7.51-7.50 (m, 6H), 7.40-7.38 (m, 4H), 5.64-5.59 (m, 2H), 5.42-5.38 (m, 2H), 4.91-4.87 (m, 2H), 2.01 (s, 6H); **^{13}C NMR** (175 MHz; CD_2Cl_2) δ 179.0, 134.6, 130.4, 129.4, 129.2, 79.4, 67.4, 42.4, 25.2.

3.4.4. Synthesis of Substrates and Intermediates

General alkylation procedure for the synthesis of β-ketoester substrates.

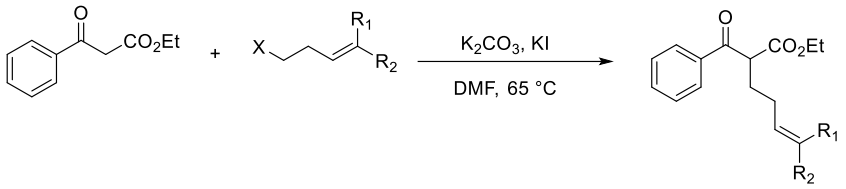

A 25 mL round bottom flask equipped with a magnetic stir bar was charged with K_2CO_3 (460 mg, 3.30 mmol) and KI (293 mg, 1.80 mmol). Dry DMF (11.0 mL) was then added, followed by starting ketone (2.20 mmol) and alkyl halide[8a-b] (1.47 mmol). The resulting mixture was heated to 65 °C and stirred for 3 h. The reaction flask was allowed to cool to room temperature, and then partitioned between EtOAc (20 mL) and water (10 mL). The organic phase was washed with water (3 × 10 mL) and saturated sodium chloride (1 × 10 mL), dried over Na_2SO_4 and concentrated under reduced pressure to remove all volatile components. The crude product was purified via column chromatography eluting with the indicated solvent to give the pure alkylated ketone.

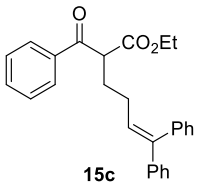

15c

ethyl 2-benzoyl-6,6-diphenylhex-5-enoate (15c): Purification by flash column chromatography eluting with DCM/hexanes (7:3) provided 151.0 mg (26% yield) of **25** as a clear oil. **^{1}H NMR**

(500 MHz; $CDCl_3$) δ 7.96-7.90 (m, 2H), 7.60-7.53 (m, 1H), 7.45 (t, *J* = 7.8 Hz, 2H), 7.35-7.26 (m, 4H), 7.25-7.17 (m, 4H), 7.12-7.04 (m, 2H), 6.08-6.05 (m, 1H), 4.27 (t, *J* =6.6 Hz, 1H), 4.08 (p, *J* = 7.1 Hz, 2H), 2.26-2.09 (m, 4H), 1.11 (t, *J* = 7.1 Hz, 3H); **^{13}C NMR** (125 MHz; $CDCl_3$) δ 195.1, 169.9, 143.1, 142.5, 139.9, 136.3, 133.6, 129.9, 128.8, 128.8, 128.3, 128.2, 128.1, 127.3, 127.2, 127.1, 61.5, 53.8, 29.2, 27.9, 14.1. **IR** (Neat) 2928, 1732, 1683, 1596, 1579, 1494, 1445, 1367, 1223, 1152, 1095, 1073, 1001, 975, 926, 862, 760, 734, 696, 629, 609; **HRMS** (ESI) *m/z*: $[M+Na]^+$ calcd for $C_{27}H_{26}O_3Na^+$ 421.1774; found 421.1776.

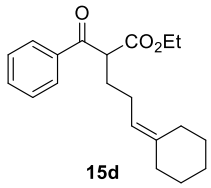

15d

ethyl 2-benzoyl-5-cyclohexylidenepentanoate (15d): Purification by flash column chromatography eluting with DCM/hexanes (9:1) provided 277.9 mg (67% yield) of **26** as a clear oil. **^{1}H NMR** (500 MHz; $CDCl_3$) δ 8.00-7.94 (m, 2H), 7.58 (t, *J* =7.4 Hz, 1H), 7.47 (t, *J* = 7.6 Hz, 2H), 5.07-5.05 (m, 1H), 4.32 (t, *J* =6.7 Hz, 1H), 4.15 (q, *J* = 7.1 Hz, 2H), 2.12-1.98 (m, 8H), 1.54-1.46 (m, 4H), 1.42 (d, *J* = 5.5 Hz, 2H), 1.18 (t, *J* = 7.1 Hz, 3H); **^{13}C NMR** (125 MHz; $CDCl_3$) δ 195.6, 170.2, 141.8, 136.4, 133.5, 128.8, 128.7, 119.7, 61.4, 53.5, 37.3, 29.4, 28.8, 27.9, 27.0, 25.1, 14.2. **IR** (Neat) 2925, 2852, 1735, 1684, 1447, 1231, 1180, 1152, 1095, 1024, 1001, 987, 775, 689, 661; **HRMS** (ESI) *m/z*: $[M+Na]^+$ calcd for $C_{20}H_{26}O_3Na^+$ 337.1774; found 337.1780.

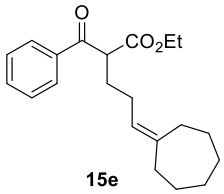

15e

ethyl 2-benzoyl-5-cycloheptylidenepentanoate (15e): Purification by flash column chromatography eluting with DCM/hexanes (9:1) provided 155.8 mg (33% yield) of **27** as a clear oil. **^{1}H NMR** (400 MHz; $CDCl_3$) δ 8.03-7.94 (m, 2H), 7.62-7.53 (m, 1H), 7.47 (td, *J* = 7.6, 7.2, 1.5 Hz, 2H), 5.12 (s, 1H), 4.34-4.31 (m, 1H), 4.19-4.09 (m, 2H), 2.17 (dd, *J* = 14.0, 7.6, Hz, 4H), 2.06 (bs, 4H), 1.52-1.46 (m, 8H), 1.18 (t, *J* = 7.1 Hz, 3H); **^{13}C NMR** (125 MHz; $CDCl_3$) δ 195.6, 170.2, 143.2, 136.5, 133.5, 128.8, 128.7, 123.4, 61.4, 53.7, 38.0, 30.1, 30.0, 29.5, 29.3, 29.2, 27.2,

25.7, 14.2. **IR** (Neat) 2920, 2850, 1734, 1684, 1447, 1230, 1181, 1149, 1095, 1026, 1001, 984, 776, 689, 661; **HRMS** (ESI) *m/z*: $[M+Na]^+$ calcd for $C_{21}H_{28}O_3Na^+$ 351.1931; found 351.1936.

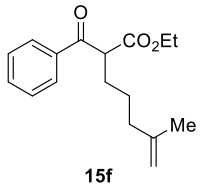

15f

ethyl 2-benzoyl-6-methylhept-6-enoate (15f): Purification by flash column chromatography eluting with DCM/hexanes (19:1) provided 92.8 mg (23% yield) of **28** as a clear oil. **^{1}H NMR** (500 MHz; $CDCl_3$) δ 8.02-7.95 (m, 2H), 7.58 (d, *J* =7.3 Hz, 1H), 7.48 (t, *J* = 7.6 Hz, 2H), 4.68 (d, *J* = 17.5 Hz, 2H), 4.30 (t, *J* = 7.1 Hz, 1H), 4.15 (qd, *J* = 7.1, 1.3 Hz, 2H), 2.06 (t, *J* =7.6 Hz, 2H), 2.03-1.94 (m, 2H), 1.69 (s, 3H), 1.54-1.45 (m, 2H), 1.17 (t, *J* = 7.1 Hz, 3H); **^{13}C NMR** (125 MHz; $CDCl_3$) δ 195.3, 170.1, 145.2, 136.5, 133.6, 128.9, 128.7, 110.5, 61.5, 54.4, 37.6, 28.7, 25.6, 22.4, 14.2. **IR** (Neat) 3071, 2935, 1733, 1684, 1649, 1597, 1581, 1448, 1369, 1261, 1219, 1182, 1146, 1095, 1026, 1001, 980, 886, 776, 689, 660, 606; **HRMS** (ESI) *m/z*: $[M+Na]^+$ calcd for $C_{17}H_{22}O_3Na^+$ 297.1461; found 297.1464.

General procedures for synthesis of bisalkene substrates.

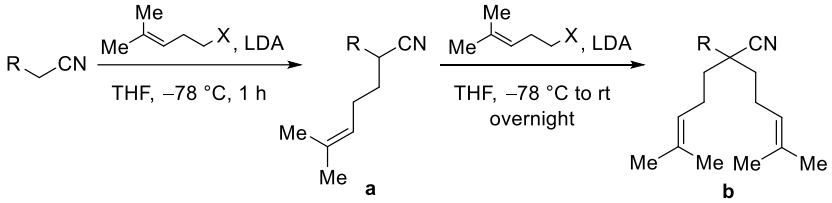

General procedure A: alkylation of nitriles to form intermediates (a and b).

A flame-dried round bottom flask equipped with a magnetic stir bar, was sealed with a rubber septum. The flask was charged with diisopropylamine (1.2 equiv) and THF (0.4 M). This solution was then cooled to −78 °C and *n*-BuLi (1.2 equiv, 2.5 M in hexanes) was slowly added. After 15 min of stirring at −78 °C, the corresponding nitrile (1.0 equiv) dissolved in THF (2.5 M) was added dropwise via syringe. After 15 min of stirring at −78 °C, 5-iodo-2-methylpent-2-ene[8c] (1.1 equiv) was added dropwise. The reaction solution was allowed to stir for 1 h at the same temperature (for **a**) or allowed to warm slowly to room temperature overnight (for **b**). The resulting reaction mixture

was quenched with saturated ammonium chloride and was extracted with EtOAc (3 × 60 mL). The combined organic layers were washed with brine, dried over Na_2SO_4 and concentrated under reduced pressure. The crude oil was purified via flash column chromatography eluting with the indicated solvent to afford intermediate **or b**.

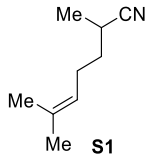

S1

2,6-dimethylhept-5-enenitrile (S1): General procedure A was followed employing propionitrile (36 mmol). Purification by flash column chromatography eluting with hexanes/EtOAc (19:1) provided 3.44 g (70% yield) of **S1** as a clear yellow oil. **^{1}H NMR** (500 MHz; $CDCl_3$) δ 5.07-5.04 (m, 1H), 2.61 (dqd, *J* = 9.2, 7.1, 5.6 Hz, 1H), 2.21-2.13 (m, 2H), 1.72-1.65 (m, 5H), 1.64 (s, 3H), 1.56-1.51 (m, 1H), 1.31 (d, *J* = 7.1 Hz, 3H); **^{13}C NMR** (125 MHz; $CDCl_3$) δ 133.8, 123.2, 122.4, 34.3, 25.9, 25.6, 25.0, 18.1, 17.9. **HRMS** (ESI) *m/z*: $[M+H]^+$ calcd for $C_9H_{16}N^+$ 138.1277; found 138.1275.

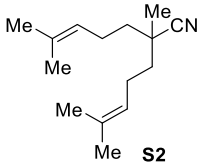

S2

2,6-dimethyl-2-(4-methylpent-3-en-1-yl)hept-5-enenitrile (S2): General procedure A was followed employing **S1** (25.1 mmol). Purification by flash column chromatography eluting with hexanes/EtOAc (19:1) provided 5.06 g (92% yield) of **15b** as a clear yellow oil. **^{1}H NMR** (500 MHz; $CDCl_3$) δ 5.11-5.07 (m, 2H), 2.15 (q, *J* = 7.9 Hz, 4H), 1.69 (s, 6H), 1.66-1.59 (m, 8H), 1.52-1.42 (m, 2H), 1.33 (s, 3H); **^{13}C NMR** (125 MHz; $CDCl_3$) δ 132.9, 124.5, 122.8, 39.4, 36.6, 25.8, 24.0, 23.7, 17.8. **HRMS** (EI) *m/z*: $[M]^+$ calcd for $C_{15}H_{25}N^+$ 219.1982; found 219.1984.

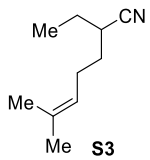

S3

2-ethyl-6-methylhept-5-enenitrile (S3): General procedure A was followed employing butyronitrile (15.0 mmol). Purification by flash column chromatography eluting with

hexanes/EtOAc (16:1) provided 1.90 g (84% yield) of **S3** as a clear oil. **^{1}H NMR** (500 MHz; $CDCl_3$) δ 5.10-5.03 (m, 1H), 2.47 (m, 1H), 2.16 (m, 2H), 1.81-1.41 (m, 10H), 1.08 (t, *J* = 7.4 Hz, 3H); **^{13}C NMR** (125 MHz; $CDCl_3$) δ 133.7, 122.4, 32.8, 32.2, 25.9, 25.8, 25.7, 17.9, 11.7. **HRMS** (EI) *m/z*: $[M]^+$ calcd for $C_{10}H_{17}N^+$ 151.1361; found 151.1365.

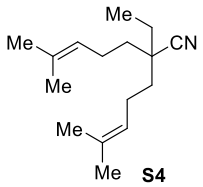

S4

2-ethyl-6-methyl-2-(4-methylpent-3-en-1-yl)hept-5-enenitrile (S4): General procedure A was followed employing **S3** (12.6 mmol). Purification by flash column chromatography eluting with hexanes/EtOAc (16:1) provided 2.20 g (75% yield) of **S4** as a clear oil. **^{1}H NMR** (500 MHz; $CDCl_3$) δ 5.15-5.04 (m, 2H), 2.09 (q, *J* = 7.5 Hz, 4H), 1.69 (s, 6H), 1.65 (q, *J* = 7.5 Hz, 2H), 1.63 (s, 6H), 1.61-1.51 (m, 4H), 1.02 (t, *J* = 7.5 Hz, 3H); **^{13}C NMR** (125 MHz; $CDCl_3$) δ 132.9, 122.9, 41.1, 35.7, 29.0, 25.8, 23.2, 17.8, 8.8. **HRMS** (ESI) *m/z*: $[M+H]^+$ calcd for $C_{16}H_{27}N^+$ 234.2216; found 234.2218.

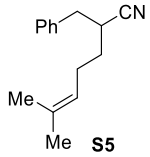

S5

2-benzyl-6-methylhept-5-enenitrile (S5): General procedure A was followed employing 3-phenylpropionitrile (18.0 mmol). Purification by flash column chromatography eluting with hexanes/EtOAc (19:1) provided 3.02 g (79% yield) of **S5** as a clear oil. **^{1}H NMR** (500 MHz; $CDCl_3$) δ 7.34 (dd, *J* = 8.1, 6.6 Hz, 2H), 7.30-7.27 (m, 1H), 7.24 (dd, *J* = 6.9, 1.7 Hz, 2H), 5.06-5.02 (m, 1H), 2.89 (qd, *J* = 13.7, 7.2 Hz, 2H), 2.78 (tt, *J* = 8.4, 5.6 Hz, 1H), 2.22-2.12 (m, 2H), 1.72-1.58 (m, 8H); **^{13}C NMR** (125 MHz; $CDCl_3$) δ 137.2, 133.9, 129.2, 128.9, 127.3, 122.2, 121.9, 38.5, 33.3, 32.1, 25.9, 25.7, 18.0. **HRMS** (ESI) *m/z*: $[M+H]^+$ calcd for $C_{15}H_{20}N^+$ 214.1590; found 214.1606.

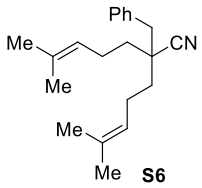

S6

2-benzyl-6-methyl-2-(4-methylpent-3-en-1-yl)hept-5-enenitrile (S6): General procedure A was followed employing **S5** (14.1 mmol). Purification by flash column chromatography eluting with hexanes/EtOAc (16:1) provided 3.80 g (91% yield) of **S6** as a clear yellow oil. **^{1}H NMR** (500 MHz; $CDCl_3$) δ 7.36-7.31 (m, 2H), 7.31-7.27 (m, 3H), 5.08-5.04 (m, 2H), 2.88 (s, 2H), 2.24-2.10 (m, 4H), 1.69 (s, 6H), 1.63 (s, 6H), 1.56 (ddd, *J* = 10.7, 6.6, 2.2 Hz, 4H); **^{13}C NMR** (125 MHz; $CDCl_3$) δ 135.6, 133.0, 130.5, 128.6, 127.4, 123.5, 122.7, 42.6, 41.9, 36.1, 25.8, 23.4, 17.9. **HRMS** (ESI) *m/z*: $[M+H]^+$ calcd for $C_{21}H_{30}N^+$ 296.2373; found 296.2391.

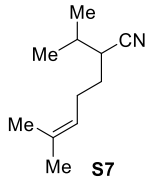

S7

2-isopropyl-6-methylhept-5-enenitrile (S7): General procedure A was followed employing Isovaleronitrile (24 mmol). Purification by flash column chromatography eluting with hexanes/EtOAc (19:1) provided 3.26 g (82% yield) of **S7** as a clear oil. **^{1}H NMR** (500 MHz; $CDCl_3$) δ 5.08-5.04 (m, 1H), 2.42 (dt, *J* = 10.3, 5.0 Hz, 1H), 2.25-2.09 (m, 2H), 1.87-1.80 (m, 1H), 1.72-1.64 (m, 7H), 1.55-1.49 (m, 1H), 1.06 (d, *J* = 2.6 Hz, 3H), 1.05 (d, *J* = 2.5 Hz, 3H); **^{13}C NMR** (125 MHz; $CDCl_3$) δ 133.8, 122.5, 121.4, 38.7, 30.4, 30.2, 26.0, 25.9, 21.2, 18.8, 17.9. **HRMS** (ESI) *m/z*: $[M+H]^+$ calcd for $C_{11}H_{20}N^+$ 166.1590; found 166.1583.

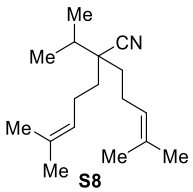

S8

2-isopropyl-6-methyl-2-(4-methylpent-3-en-1-yl)hept-5-enenitrile (S8): General procedure A was followed employing **S7** (19.7 mmol). Purification by flash column chromatography eluting with hexanes/diethyl ether (97:3) provided 3.26 g (67% yield) of **S8** as a clear yellow oil. **^{1}H NMR** (500 MHz; $CDCl_3$) δ 5.11-5.08 (m, 2H), 2.10-2.06 (m, 4H), 1.95 (hept, *J* = 6.9 Hz, 1H), 1.69 (s, 6H), 1.67-1.48 (m, 10H), 1.03 (d, *J* = 6.8 Hz, 6H); **^{13}C NMR** (125 MHz; $CDCl_3$) δ 132.9, 123.5,

123.0, 45.0, 33.0, 32.0, 25.8, 23.3, 17.9, 17.8. **HRMS** (ESI) *m/z*: $[M+H]^+$ calcd for $C_{17}H_{30}N^+$ 248.2373; found 248.2372.

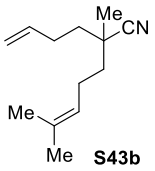

S43b

2-(but-3-en-1-yl)-2,6-dimethylhept-5-enenitrile (S9): General procedure A was followed employing **15a (**3.75 mmol). Purification by flash column chromatography eluting with hexanes/DCM (2:1) provided 683 mg (95% yield) of **S43b** as a clear yellow oil. **^{1}H NMR** (500 MHz; $CDCl_3$) δ 5.81 (dddd, *J* = 18.1, 10.2, 7.2, 5.9 Hz, 1H), 5.17-5.04 (m, 2H), 5.01 (dt, *J* = 10.2, 1.5 Hz, 1H), 2.23 (dddd, *J* = 12.3, 6.5, 2.9, 1.5 Hz, 2H), 2.15 (q, *J* = 8.0 Hz, 2H), 1.75-1.67 (m, 4H), 1.67-1.62 (m, 4H), 1.60-1.53 (m, 1H), 1.53-1.44 (m, 1H), 1.33 (s, 3H); **^{13}C NMR** (126 MHz, $CDCl_3$) δ 137.3, 133.1, 124.3, 122.8, 115.6, 39.5, 38.7, 36.6, 29.3, 25.8, 24.0, 23.7, 17.8. **HRMS** (APCI) *m/z*: $[M+H]^+$ calcd for $C_{13}H_{22}N^+$ 192.1747; found 192.1747.

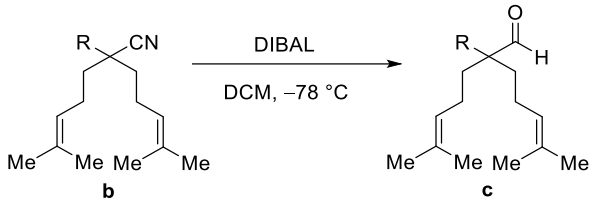

General procedure B: reduction of nitriles to aldehydes (c).

To a flame-dried round bottom flask was added starting nitrile **b** (1.0 equiv) and DCM (0.1 M). The solution was cooled to −78 °C and DIBAL (1.8 equiv) was added slowly via syringe. This temperature was maintained for 1 h and then warmed to 0 °C. The resulting mixture was quenched with 3 M HCl and stirred for an additional 1 h at 0 °C, and then 20 min at room temperature. The solution was extracted with DCM (3 × 50 mL). The combined organic extracts were washed with 1 M HCl, brine, dried over Na_2SO_4 and concentrated under reduced pressure. The crude aldehyde was purified via flash column chromatography eluting with the indicated solvent to afford intermediate **c**.

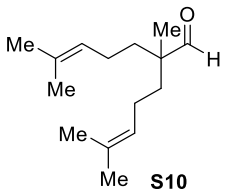

2,6-dimethyl-2-(4-methylpent-3-en-1-yl)hept-5-enal (S10): General procedure B was followed employing **S2** (23.1 mmol). Purification by flash column chromatography eluting with hexa-nes/EtOAc (13:1) provided 3.24 g (63% yield) of **15c** as a clear oil. **^{1}H NMR** (500 MHz; $CDCl_3$) δ 9.43 (s, 1H), 5.07-5.04 (m, 2H), 1.95-1.79 (m, 4H), 1.67 (s, 6H), 1.58 (s, 6H), 1.55-1.42 (m, 4H), 1.04 (s, 3H); **^{13}C NMR** (125 MHz; $CDCl_3$) δ 206.5, 132.3, 124.1, 49.2, 35.8, 25.8, 22.8, 18.1, 17.8. **HRMS** (EI) *m/z*: $[M]^+$ calcd for $C_{15}H_{22}O^+$ 222.1984; found 222.1986.

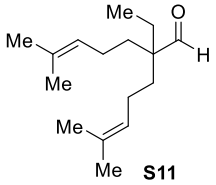

2-ethyl-6-methyl-2-(4-methylpent-3-en-1-yl)hept-5-enal (S11): General procedure B was followed employing **S4** (6.72 mmol). Purification by flash column chromatography eluting with hexa-nes/EtOAc (16:1) provided 960.0 mg (60% yield) of **S11** as a clear oil. **^{1}H NMR** (500 MHz; $CDCl_3$) δ 9.41 (s, 1H), 5.15-4.98 (m, 2H), 1.83 (q, *J* = 8.0 Hz, 4H), 1.67 (s, 6H), 1.58 (s, 6H), 1.57-1.46 (m, 6H), 0.80 (t, *J* = 7.6 Hz, 3H); **^{13}C NMR** (125 MHz; $CDCl_3$) δ 207.1, 132.20, 124.1, 52.3, 31.8, 25.8, 24.2, 22.4, 17.8, 8.0. **HRMS** (ESI) *m/z*: $[M+Na]^+$ calcd for $C_{16}H_{28}ONa^+$ 259.2032; found 259.2036.

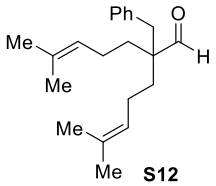

2-benzyl-6-methyl-2-(4-methylpent-3-en-1-yl)hept-5-enal (S12): General procedure B was followed employing **S6** (12.85 mmol). Purification by flash column chromatography eluting with hexa-nes/EtOAc (16:1) provided 2.80 g (73% yield) of **S12** as a clear oil. **^{1}H NMR** (400 MHz; $CDCl_3$) δ 9.56 (s, 1H), 7.30-7.18 (m, 3H), 7.12-7.01 (m, 2H), 5.12-4.97 (m, 2H), 2.86 (s, 2H), 1.99-1.93 (m, 4H), 1.67 (s, 6H), 1.59 (s, 6H), 1.56-1.39 (m, 4H); **^{13}C NMR** (125 MHz; $CDCl_3$) δ

206.7, 137.0, 132.3, 130.2, 128.4, 126.6, 123.9, 53.4, 39.0, 32.1, 25.8, 22.6, 17.9. **HRMS** (ESI) *m/z*: $[M+Na]^+$ calcd for $C_{21}H_{30}ONa^+$ 321.2189; found 321.2193.

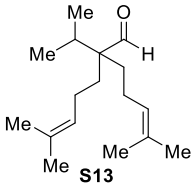

S13

2-isopropyl-6-methyl-2-(4-methylpent-3-en-1-yl)hept-5-enal (S13): General procedure B was followed employing **S8** (6.06 mmol). Purification by flash column chromatography eluting with hexa-nes/EtOAc (16:1) provided 760 Mg (50% yield) of **S13** as a clear oil. **^{1}H NMR** (400 MHz; $CDCl_3$) δ 9.60 (s, 1H), 5.12-5.08 (m, 2H), 1.97-1.79 (m, 5H), 1.68 (s, 6H), 1.65-1.51 (m, 10H), 0.96 (d, *J* = 7.1 Hz, 6H); **^{13}C NMR** (125 MHz; $CDCl_3$) δ 207.9, 132.0, 124.4, 53.7, 31.8, 30.2, 25.8, 22.6, 17.9, 17.8. **HRMS** (ESI) *m/z*: $[M+H]^+$ calcd for $C_{17}H_{31}O^+$ 251.2369; found 251.2370.

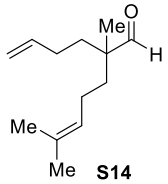

S14

2-(but-3-en-1-yl)-2,6-dimethylhept-5-enal (S14): General procedure B was followed employing **S9** (1.36 mmol). Purification by flash column chromatography eluting with hexanes/EtOAc (13:1) provided 87.0 mg (33% yield) of **S14** as a clear oil. **^{1}H NMR** (700 MHz, $CDCl_3$) δ 9.44 (s, 1H), 5.78 (ddt, *J* = 16.8, 10.2, 6.5 Hz, 1H), 5.08-5.04 (m, 1H), 5.01 (dd, *J* = 17.1, 1.7 Hz, 1H), 4.97-4.94 (m, 1H), 2.04-1.96 (m, 1H), 1.96-1.81 (m, 3H), 1.67 (s, 3H), 1.63-1.44 (m, 7H), 1.05 (s, 3H); **^{13}C NMR** (176 MHz, $CDCl_3$) δ 206.4, 138.4, 132.4, 123.9, 115.0, 49.0, 35.8, 34.8, 28.4, 25.8, 22.8, 18.2, 17.8. **HRMS** (APCI) *m/z*: $[M+H]^+$ calcd for $C_{13}H_{23}O^+$ 195.1743; found 195.1740.

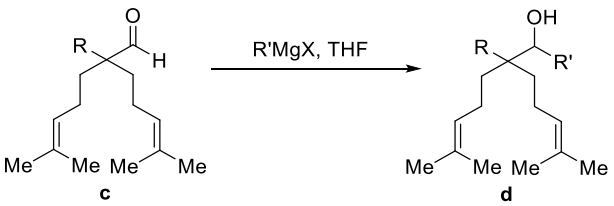

c **d**

General procedure C1: Grignard addition to intermediates (d).

A flame-dried round bottom flask equipped with a magnetic stir bar was charged with starting aldehyde **c** (1.0 equiv) and dry THF (0.2 M). The solution was cooled to 0 °C and arylmagnesium halide (1.5 equiv) was added slowly via syringe. The reaction mixture was stirred for 1 h at 0 °C. The resulting mixture was quenched with saturated ammonium chloride. After stirring for 20 min, the reaction was extracted with EtOAc (3 x 50 mL). The organic phase was washed with brine, dried over Na_2SO_4, filtered and concentrated under reduced pressure to remove all volatile components. The crude product was purified via flash column chromatography eluting with the indicated solvent to afford intermediate **d**.

General procedure C2: Grignard addition to intermediates (d).

A flame-dried round bottom flask equipped with a magnetic stir bar was charged with magnesium turnings (3.0 equiv), a small iodine crystal and was sealed under a nitrogen atmosphere. Dry THF (0.2 M) was added via syringe, followed by the desired aryl bromide (3.2 equiv). The solution was allowed to stir until all magnesium turnings dissolved. The resulting mixture was added dropwise to a solution of **c** (1.0 equiv) in THF (0.2 M) at 0 °C and stirred for 1 h at the same temperature. The reaction mixture was quenched with addition of saturated ammonium chloride. After stirring for 20 min, the reaction mixture was extracted with EtOAc (3 x 50 mL). The organic phase was washed with brine, dried over Na_2SO_4, filtered and concentrated under reduced pressure to remove all volatile components. The crude product was purified via flash column chromatography eluting with the indicated solvent to afford intermediate **d**.

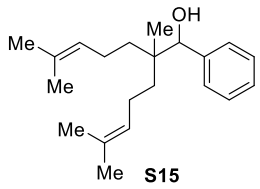

S15

2,6-dimethyl-2-(4-methylpent-3-en-1-yl)-1-phenylhept-5-en-1-ol (S15): General procedure C2 was followed employing bromobenzene and **S10** (10.7 mmol). Purification by flash column chromatography eluting with hexanes/EtOAc (9:1) provided 2.94 g (91% yield) of **S15** as a clear oil. **^{1}H NMR** (500 MHz; $CDCl_3$) δ 7.36-7.29 (m, 4H), 7.27 (t, *J* = 2.8 Hz, 1H), 5.16-5.09 (m, 1H), 5.09-5.02 (m, 1H), 4.60 (s, 1H), 2.12-1.94 (m, 4H), 1.69 (s, 3H), 1.67 (s, 3H), 1.65-1.52 (m, 7H), 1.34-1.13 (m, 3H), 0.84 (s, 3H); **^{13}C NMR** (125 MHz; $CDCl_3$) δ 142.2, 131.2, 128.1, 127.7, 127.4,

125.3, 125.2, 79.4, 40.5, 35.9, 35.4, 25.9, 25.8, 22.5, 22.4, 20.5, 17.9, 17.8. **HRMS** (ESI) *m/z*: $[M+Na]^+$ calcd for $C_{21}H_{32}ONa^+$ 323.2345; found 323.2346.

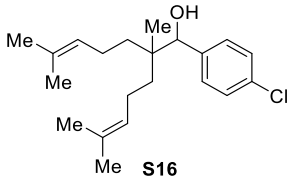

S16

1-(4-chlorophenyl)-2,6-dimethyl-2-(4-methylpent-3-en-1-yl)hept-5-en-1-ol (S16): General proce-dure C1 was followed employing 4-chlorophenylmagnesium bromide (1.0 M solution in diethyl ether) and **S10** (5.44 mmol). Purification by flash column chromatography eluting with hexanes/EtOAc (9:1) provided 1.54 g (85% yield) of **S16** as a clear oil. **^{1}H NMR** (500 MHz; $CDCl_3$) δ 7.30-7.24 (m, 4H), 5.12-5.09 (m, 1H), 5.06-5.03 (m, 1H), 4.58 (d, *J* = 3.0 Hz, 1H), 2.07-1.90 (m, 4H), 1.69 (s, 3H), 1.67 (s, 3H), 1.62 (s, 3H), 1.60 (s, 3H), 1.54 (ddd, *J* = 13.9, 11.6, 5.2 Hz, 1H), 1.30-1.20 (m, 2H), 1.15 (ddd, *J* = 13.7, 11.4, 5.9 Hz, 1H), 0.82 (s, 3H); **^{13}C NMR** (125 MHz; $CDCl_3$) δ 140.6, 133.1, 131.4, 129.4, 127.9, 125.0, 124.9, 78.7, 40.5, 35.8, 35.3, 25.9, 25.8, 22.4, 22.3, 20.4, 17.9, 17.8. **HRMS** (ESI) *m/z*: $[M+H-H_2O]^+$ calcd for $C_{21}H_{30}Cl^+$ 317.2031; found 317.2026.

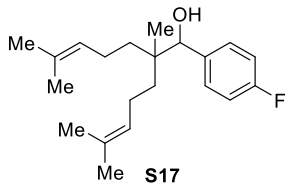

S17

1-(4-fluorophenyl)-2,6-dimethyl-2-(4-methylpent-3-en-1-yl)hept-5-en-1-ol (S17): General proce-dure C2 was followed employing 1-bromo-4-fluorobenzene and **S10** (6.29 mmol). Purification by flash column chromatography eluting with hexanes/EtOAc (19:1) provided 1.87 g (93% yield) of **S17** as a clear oil. **^{1}H NMR** (500 MHz; $CDCl_3$) δ 7.32-7.26 (m, 2H), 7.05-6.95 (m, 2H), 5.13-5.09 (m, 1H), 5.06-5.03 (m, 1H), 4.59 (d, *J* = 2.9 Hz, 1H), 2.08-1.90 (m, 4H), 1.69 (s, 3H), 1.67 (s, 3H), 1.62 (s, 3H), 1.59 (s, 3H), 1.58-1.50 (m, 1H), 1.30-1.11 (m, 3H), 0.82 (s, 3H); **^{13}C NMR** (125 MHz; $CDCl_3$) δ 162.2 (d, *J* = 245.3 Hz), 137.8 (d, *J* = 3.2 Hz), 131.4, 129.5 (d, *J* = 8.0 Hz), 125.1, 125.0, 114.6 (d, *J* = 21.2 Hz), 78.7, 40.5, 35.9, 35.3, 25.9, 25.8, 22.4, 22.3, 20.4, 17.9, 17.8. **HRMS** (ESI) *m/z*: $[M+Na]^+$ calcd for $C_{21}H_{31}FONa^+$ 341.2251; found 341.2222.

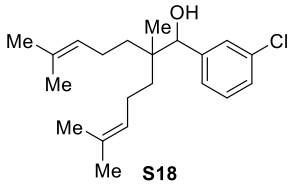

S18

1-(3-chlorophenyl)-2,6-dimethyl-2-(4-methylpent-3-en-1-yl)hept-5-en-1-ol (S18): General proce-dure C2 was followed employing 1-bromo-3-chlorobenzene and **S10** (1.35 mmol). Purification by flash column chromatography eluting with hexanes/EtOAc (5:1) provided 334.0 mg (74% yield) of **S18** as a clear oil. **^{1}H NMR** (400 MHz; $CDCl_3$) δ 7.33 (s, 1H), 7.25-7.17 (m, 3H), 5.17-5.01 (m, 2H), 4.57 (d, *J* = 3.0 Hz, 1H), 2.12-1.85 (m, 4H), 1.78 (d, *J* = 3.1 Hz, 1H), 1.68 (d, *J* = 5.9 Hz, 6H), 1.62 (d, *J* = 9.9 Hz, 6H), 1.35-1.11 (m, 4H), 0.84 (s, 3H); **^{13}C NMR** (125 MHz; $CDCl_3$) δ 133.8, 131.5, 129.0, 128.2, 127.6, 126.3, 125.0, 124.9, 40.6, 35.8, 35.3, 25.9, 22.4, 20.5, 17.8. **HRMS** (ESI) *m/z*: $[M+Na]^+$ calcd for $C_{21}H_{31}ClONa^+$ 357.1956; found 357.1960.

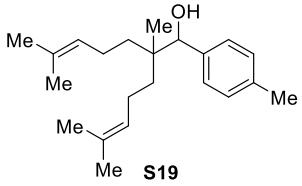

S19

2,6-dimethyl-2-(4-methylpent-3-en-1-yl)-1-(*p*-tolyl)hept-5-en-1-ol (S19): General procedure C1 was followed employing *p*-tolylmagnesium bromide (0.5 M solution in diethyl ether) and **S10** (6.29 mmol). Purification by flash column chromatography eluting with hexanes/EtOAc (16:1) provided 1.90 g (96% yield) of **S19** as a clear oil. **^{1}H NMR** (500 MHz; $CDCl_3$) δ 7.24-7.18 (m, 2H), 7.12 (d, *J* = 7.9 Hz, 2H), 5.13-5.10 (m, 1H), 5.07-5.04 (m, 1H), 4.57 (d, *J* = 2.7 Hz, 1H), 2.34 (s, 3H), 2.10-1.89 (m, 4H), 1.69 (s, 3H), 1.67 (s, 3H), 1.62 (s, 3H), 1.60 (s, 3H), 1.58-1.55 (m, 1H), 1.33-1.13 (m, 3H), 0.84 (s, 3H); **^{13}C NMR** (125 MHz; $CDCl_3$) δ 139.2, 137.0, 131.2, 131.1, 128.5, 128.0, 125.3, 125.2, 79.3, 40.5, 35.9, 35.4, 25.9, 25.8, 22.5, 22.4, 21.2, 20.5, 17.9, 17.8. **HRMS** (ESI) *m/z*: $[M+H-H_2O]^+$ calcd for $C_{22}H_{33}^+$ 297.2577; found 297.2594.

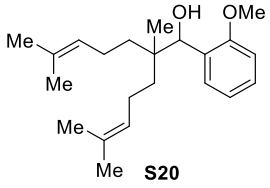

S20

1-(2-methoxyphenyl)-2,6-dimethyl-2-(4-methylpent-3-en-1-yl)hept-5-en-1-ol (S20): General procedure C2 was followed employing 2-bromoanisole and **S10** (2.43 mmol). Purification by flash column chromatography eluting with hexanes/EtOAc (16:1) provided 552.7 mg (60% yield) of **S20** as a clear oil. **^{1}H NMR** (400 MHz; $CDCl_3$) δ 7.32 (d, *J* = 7.5 Hz, 1H), 7.26-7.18 (m, 2H), 6.95 (t, *J* = 7.5 Hz, 1H), 6.87 (d, *J* = 2.8 Hz, 1H), 5.17-5.08 (m, 1H), 5.08-5.00 (m, 1H), 4.94 (d, *J* = 5.9 Hz 1H), 3.81 (s, 3H) 2.54 (d, *J* = 5.9 Hz, 1H), 2.09-1.93 (m, 4H)1.68 (s, 3H), 1.66 (s, 3H), 1.62 (s, 3H), 1.59 (s, 3H), 1.41-1.09 (m, 4H), 0.83 (s, 3H); **^{13}C NMR** (125 MHz; $CDCl_3$) δ 157.3, 131.0, 130.9, 130.2, 129.9, 128.2, 125.6, 125.5, 120.3, 110.7, 55.3, 41.6, 35.7, 35.5, 25.9, 25.8, 22.6, 22.5, 20.5, 17.9, 17.8. **HRMS** (ESI) *m/z*: $[M+H-H_2O]^+$ calcd for $C_{22}H_{33}O^+$ 313.2526; found 313.2549.

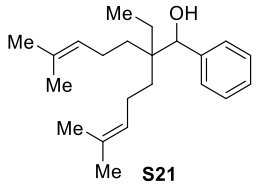

S21

2-ethyl-6-methyl-2-(4-methylpent-3-en-1-yl)-1-phenylhept-5-en-1-ol (S21): General procedure C2 was followed employing bromobenzene and **S11** (1.27 mmol). Purification by flash column chromatography eluting with hexanes/EtOAc (5:1) provided 252.0 mg (63% yield) of **S21** as a clear oil. **^{1}H NMR** (500 MHz; $CDCl_3$)) δ 7.38-7.26 (m, 4H), 5.10-5.01 (m, 2H), 4.64 (d, *J* = 2.9 Hz, 1H), 2.05-1.88 (m, 4H), 1.70 (d, *J* = 2.9 Hz, 1H), 1.66 (s, 6H), 1.59 (s, 6H), 1.40-1.28 (m, 7H), 0.87 (t, *J* = 7.5 Hz, 3H); **^{13}C NMR** (125 MHz; $CDCl_3$) δ 142.6, 131.0, 128.0, 127.9, 127.4, 125.4, 79.7, 42.7, 33.9, 33.8, 26.6, 25.9, 22.9, 22.8, 17.9, 8.7 **HRMS** (ESI) *m/z*: $[M+Na]^+$ calcd for $C_{21}H_{30}Cl^+$ 379.2971; found 379.2975.

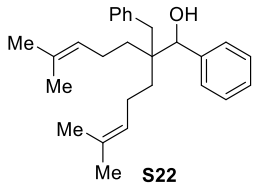

S22

2-benzyl-6-methyl-2-(4-methylpent-3-en-1-yl)-1-phenylhept-5-en-1-ol (S22): General procedure C2 was followed employing bromobenzene and **S12** (9.38 mmol). Purification by flash column chromatography eluting with hexanes/EtOAc (13:1) provided 3.45 g (98% yield) of **S22** as a clear oil. **^{1}H NMR** (500 MHz; $CDCl_3$) δ 7.39-7.28 (m, 5H), 7.29-7.27 (m, 4H), 7.23-7.20 (m, 1H), 5.11-5.03 (m, 1H), 5.01-4.91 (m, 1H), 4.54 (d, *J* = 2.7 Hz, 1H), 2.94 (d, *J* = 13.2 Hz, 1H), 2.66 (d, *J* = 13.2 Hz, 1H), 2.11-1.94 (m, 2H), 1.90-1.80 (m, 2H), 1.69 (s, 3H), 1.65 (s, 3H), 1.61 (s, 3H), 1.55-1.47 (m, 4H), 1.45-1.36 (m, 1H), 1.34-1.25 (m, 4H); **^{13}C NMR** (125 MHz; $CDCl_3$) δ

142.4, 139.3, 131.1, 131.0, 130.9, 128.4, 128.0, 127.9, 127.6, 126.1, 125.3, 125.1, 78.9, 44.4, 40.8, 34.4, 33.0, 25.9, 25.8, 23.2, 22.9, 18.0, 17.9. **HRMS** (ESI) *m/z*: $[M+H-H_2O]^+$ calcd for $C_{27}H_{35}^+$ 359.2733; found 359.2750.

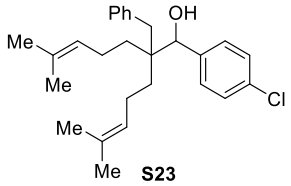

S23

2-benzyl-1-(4-chlorophenyl)-6-methyl-2-(4-methylpent-3-en-1-yl)hept-5-en-1-ol (S23): General procedure C1 was followed employing 4-chlorophenylmagnesium bromide (1.0 M solution in diethyl ether) and **S12** (3.0 mmol). Purification by flash column chromatography eluting with hexanes/EtOAc (13:1) provided 1.18 g (95% yield) of **S23** as a clear oil. **^{1}H NMR** (500 MHz; $CDCl_3$) δ 7.33-7.26 (m, 6H), 7.25-7.17 (m, 4H), 5.08-5.03 (m, 1H), 4.97-4.93 (m, 1H), 4.49 (d, *J* = 2.9 Hz, 1H), 2.90 (d, *J* = 13.3 Hz, 1H), 2.63 (d, *J* = 13.3 Hz, 1H), 2.10-1.80 (m, 4H), 1.69 (s, 3H), 1.65 (s, 3H), 1.60 (s, 3H), 1.53 (s, 3H), 1.51-1.44 (m, 1H), 1.40-1.33 (m, 1H), 1.33-1.19 (m, 2H); **^{13}C NMR** (125 MHz; $CDCl_3$) δ 140.8, 139.0, 133.3, 131.3, 131.2, 130.9, 129.7, 128.1, 128.0, 126.2, 125.1, 124.9, 78.3, 44.4, 40.6, 34.3, 32.9, 25.9, 25.8, 23.2, 22.9, 18.0, 17.9. **HRMS** (ESI) *m/z*: $[M+H-H_2O]^+$ calcd for $C_{27}H_{34}Cl^+$ 393.2344; found 393.2350.

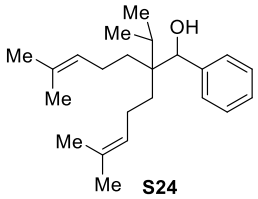

S24

2-isopropyl-6-methyl-2-(4-methylpent-3-en-1-yl)-1-phenylhept-5-en-1-ol (S24): General procedure C2 was followed employing bromobenzene and **S13** (2.4 mmol). Purification by flash column chromatography eluting with hexanes/EtOAc (13:1) provided 496 mg (63% yield) of **S24** as a clear oil. **^{1}H NMR** (500 MHz; $CDCl_3$) δ 7.38 (d, *J* = 7.1 Hz, 2H), 7.32 (d, *J* = 7.4 Hz, 2H), 7.28-7.26 (m, 1H), 5.11-5.07 (m, 1H), 4.97-4.94 (m, 1H), 4.75 (d, *J* = 2.8 Hz, 1H), 2.19-1.91 (m, 3H), 1.84-1.76 (m, 1H), 1.69 (s, 3H), 1.66-1.64 (m, 4H), 1.62 (s, 3H), 1.58-1.49 (m, 4H), 1.42-1.23 (m, 3H), 1.00 (d, *J* = 7.0 Hz, 3H), 0.93 (d, *J* = 6.9 Hz, 3H); **^{13}C NMR** (125 MHz; $CDCl_3$) δ 143.6, 130.9, 130.8, 128.2, 128.0, 127.5, 125.7, 125.5, 79.5, 44.7, 33.8, 31.9, 31.7, 25.9, 25.8, 23.4,

23.2, 18.9, 18.4, 17.9, 17.8. **HRMS** (ESI) *m/z*: $[M+H-H_2O]^+$ calcd for $C_{23}H_{35}^+$ 311.2733; found 311.2735.

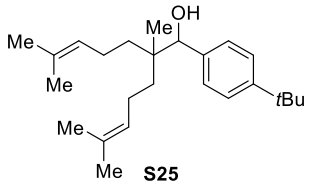

S25

1-(4-(tert-butyl)phenyl)-2,6-dimethyl-2-(4-methylpent-3-en-1-yl)hept-5-en-1-ol (S25): General procedure C2 was followed employing 1-bromo-4-*tert*-butylbenzene and **S10** (1.35 mmol). Purification by flash column chromatography eluting with hexanes/EtOAc (5:1) provided 380.0 mg (79% yield) of **S25** as a clear oil. **^{1}H NMR** (500 MHz; $CDCl_3$) δ 7.33 (d, *J* = 8.1 Hz, 2H), 7.26 (d, *J* = 8.1 Hz, 2H), 5.18-5.10 (m, 1H), 5.07 (dt, *J* = 8.0, 4.2 Hz, 1H), 4.57 (s, 1H), 2.09-1.92 (m, 4H), 1.69 (s, 3H), 1.68 (s, 3H) 1.63 (s, 3H), 1.60 (s, 3H) 1.33 (s, 9H), 1.31-1.15 (m, 4H), 0.85 (s, 3H); **^{13}C NMR** (125 MHz; $CDCl_3$) δ 150.2, 139.3, 131.2, 127.8, 125.4, 124.7, 79.3, 40.5,

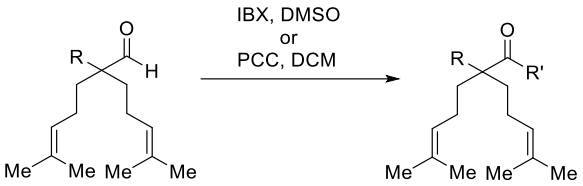

c **S**

35.8, 35.5, 34.6, 31.5, 25.9, 22.5, 22.4, 20.6, 17.9, 17.8. **HRMS** (ESI) *m/z*: $[M+Na]^+$ calcd for $C_{25}H_{40}ONa^+$ 379.2971; found 379.2975.

General procedure D1: Oxidation of intermediate d.

A round bottom flask equipped with a magnetic stir bar was charged with starting alcohol **d** (1.0 equiv) and dry DMSO (0.2 M). IBX (1.2 equiv) was added slowly to the reaction mixture at room temperature. The reaction mixture was stirred for 2-4 hours. The reaction was quenched with addition of water. After stirring overnight, the reaction mixture was filtered over Celite and extracted with EtOAc (3 x 50 mL). The organic phase was washed with brine, dried over Na_2SO_4, filtered and concentrated under reduced pressure to remove all volatile components. The crude product was purified via column chromatography eluting with the indicated solvent to afford pure ketone substrate (**S**).

General Procedure D2: Oxidation of intermediate d.

A round bottom flask equipped with a magnetic stir bar was charged with PCC (1.5 equiv) and dry DCM (0.2 M). Starting alcohol **d** (1.0 equiv) was added at room temperature and the reaction mixture was allowed to stir for 2 h. Et_2O was added, and the reaction mixture was filtered over a plug of silica, eluting with Et_2O. The mixture was concentrated under reduced pressure to remove all volatile components. The crude product was purified via column chromatography eluting with the indicated solvent to afford pure ketone substrate (**S**).

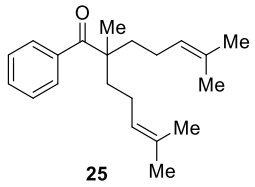

25

2,6-dimethyl-2-(4-methylpent-3-en-1-yl)-1-phenylhept-5-en-1-one (25): General procedure D2 was followed employing **S15** (9.80 mmol). Purification by flash column chromatography eluting with hexanes/EtOAc (19:1) provided 2.38 g (81% yield) of **15** as a clear oil. **^{1}H NMR** (500 MHz; $CDCl_3$) δ 7.71-7.66 (m, 2H), 7.47-7.42 (m, 1H), 7.39 (dd, *J* = 8.2, 6.7 Hz, 2H), 5.04-5.00 (m, 2H), 2.01-1.77 (m, 6H), 1.64-1.62 (m, 8H), 1.47 (s, 6H), 1.29 (s, 3H); **^{13}C NMR** (125 MHz; $CDCl_3$) δ 208.6, 139.7, 132.0, 131.0, 128.3, 127.7, 124.1, 51.6, 39.9, 25.8, 23.4, 22.7, 17.6. **IR** (Neat) 2968, 2914, 2856, 1670, 1597, 1444, 1377, 1255, 1220, 1194, 1177, 1103, 1002, 956, 831, 787, 716, 697, 632, 609. **HRMS** (ESI) *m/z*: $[M+H]^+$ calcd for $C_{21}H_{31}O^+$ 299.2369; found 299.2368.

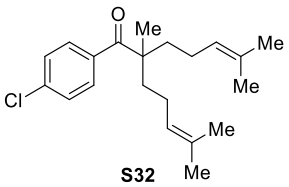

S32

1-(4-chlorophenyl)-2,6-dimethyl-2-(4-methylpent-3-en-1-yl)hept-5-en-1-one (S32): General proce-dure D2 was followed employing **S16** (3.92 mmol). Purification by flash column chromatography eluting with hexanes/DCM (2:3) provided 323.0 mg (25% yield) of **S32** as a clear oil. **^{1}H NMR** (500 MHz; $CDCl_3$) δ 7.69-7.63 (m, 2H), 7.37 (d, *J* = 8.6 Hz, 2H), 5.02-4.99 (m, 2H), 2.00-1.74 (m, 6H), 1.65-1.58 (m, 8H), 1.48 (s, 6H), 1.28 (s, 3H); **^{13}C NMR** (125 MHz; $CDCl_3$) δ 207.0, 137.6, 137.4, 132.2, 129.4, 128.6, 123.9, 51.7, 40.0, 25.8, 23.4, 22.7, 17.7. **IR** (Neat) 2967, 2915, 2856, 1670, 1588, 1567, 1487, 1450, 1377, 1279, 1254, 1219, 1192, 1173, 1092, 1013, 981,

959, 841, 761, 738, 692, 634. **HRMS** (ESI) *m/z*: $[M+H]^+$ calcd for $C_{21}H_{30}OCl^+$ 333.1980; found 333.1982.

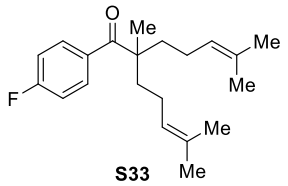

S33

1-(4-fluorophenyl)-2,6-dimethyl-2-(4-methylpent-3-en-1-yl)hept-5-en-1-one (S33): General proce-dure D1 was followed employing **S17** (5.87 mmol). Purification by flash column chromatography eluting with hexanes/EtOAc (19:1) provided 1.46 g (79% yield) of **S33** as a clear oil. **^{1}H NMR** (500 MHz; $CDCl_3$) δ 7.78 (dd, *J* = 8.8, 5.4 Hz, 2H), 7.07 (t, *J* = 8.6 Hz, 2H), 5.02-4.99 (m, 2H), 1.99-1.88 (m, 4H), 1.81-1.75 (m, 2H), 1.65-1.58 (m, 8H), 1.46 (s, 6H), 1.29 (s, 3H); **^{13}C NMR** (125 MHz; $CDCl_3$) δ 206.5, 164.4 (d, *J* = 252.4 Hz), 135.4 (d, *J* = 3.4 Hz), 132.2, 130.5 (d, *J* = 8.8 Hz), 124.0, 115.3 (d, *J* = 21.6 Hz), 51.6, 40.2, 25.8, 23.4, 22.8, 17.6. **IR** (Neat) 2968, 2917, 1670, 1599, 1505, 1450, 1377, 1295, 1229, 1190, 1156, 1099, 1013, 982, 959, 846, 767, 696, 631. **HRMS** (ESI) *m/z*: $[M+Na]^+$ calcd for $C_{21}H_{29}OFNa^+$ 339.2095; found 339.2099.

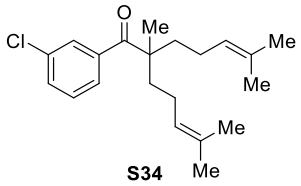

S34

1-(3-chlorophenyl)-2,6-dimethyl-2-(4-methylpent-3-en-1-yl)hept-5-en-1-one (S34): General proce-dure D1 was followed employing **S18** (0.717 mmol). Purification by flash column chromatography eluting with hexanes/EtOAc (19:1) provided 99.0 mg (41% yield) of **S34** as a clear oil. **^{1}H NMR** (500 MHz; $CDCl_3$) δ 7.63 (t, *J* = 1.9 Hz, 1H), 7.55 (dt, *J* = 7.9, 1.3 Hz, 1H), 7.43 (ddd, *J* = 7.9, 2.2, 1.3 Hz, 1H), 7.33 (t, *J* = 7.9 Hz), 5.04-5.00 (m, 2H), 2.01-1.78 (m, 6H), 1.64-1.58 (m, 8H), 1.50 (s, 6H), 1.28 (s, 3H); **^{13}C NMR** (125 MHz; $CDCl_3$) δ 207.3, 141.2, 134.5, 132.3, 131.0, 129.6, 127.9, 125.6, 123.9, 51.8, 39.8, 25.8, 23.4, 22.6, 17.7. **IR** (Neat) 2968, 2925, 2855, 1674, 1567, 1450, 1410, 1377, 1279, 1218, 1185, 1098, 1079, 985, 883, 832, 796, 743, 680, 631, 608. **HRMS** (ESI) *m/z*: $[M+Na]^+$ calcd for $C_{21}H_{29}OClNa^+$ 355.1799; found 355.1804.

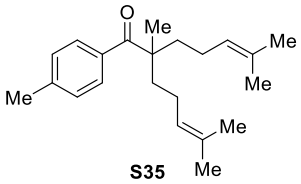

S35

2,6-dimethyl-2-(4-methylpent-3-en-1-yl)-1-(p-tolyl)hept-5-en-1-one (S19): General procedure D1 was followed employing **S35d** (6.05 mmol). Purification by flash column chromatography eluting with hexanes/EtOAc (19:1) provided 1.59 g (84% yield) of **S35** as a clear oil. **^{1}H NMR** (500 MHz; $CDCl_3$) δ 7.65 (d, *J* = 8.0 Hz, 2H), 7.19 (d, *J* = 8.0 Hz, 2H), 5.05-4.97 (m, 2H), 2.38 (s, 3H), 1.99-1.88 (m, 4H), 1.85-1.73 (m, 2H), 1.68-1.57 (m, 9H), 1.47 (s, 6H), 1.28 (s, 3H); **^{13}C NMR** (125 MHz; $CDCl_3$) δ 207.8, 141.6, 136.7, 131.9, 128.9, 128.1, 124.2, 51.6, 40.2, 25.8, 23.4, 22.8, 21.6, 17.7. **IR** (Neat) 2967, 2919, 2857, 1667, 1608, 1569, 1449, 1376, 1308, 1279, 1256, 1222, 1197, 1175, 1121, 959, 823, 756, 697, 640. **HRMS** (ESI) *m/z*: $[M+Na]^+$ calcd for $C_{22}H_{32}ONa^+$ 335.2345; found 335.2341.

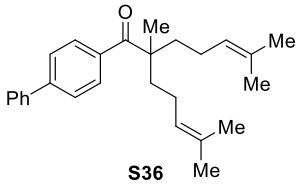

S36

1-([1,1'-biphenyl]-4-yl)-2,6-dimethyl-2-(4-methylpent-3-en-1-yl)hept-5-en-1-one (S36): General procedure D2 was followed using crude alcohol (0.701 mmol). Purification by flash column chromatography eluting with DCM/hexanes (3:1) provided 177.0 mg (67% yield) of **S36** as a clear oil. **^{1}H NMR** (500 MHz; $CDCl_3$) δ 7.86-7.77 (m, 2H), 7.63 (ddd, *J* = 6.8, 4.7, 2.5 Hz, 4H), 7.47 (td, *J* = 7.7, 1.8 Hz, 2H), 7.39 (td, *J* = 7.3, 1.5 Hz, 2H), 5.05 (d, *J* = 6.9 Hz, 2H), 2.06-1.94 (m, 4H), 1.85 (dt, *J* = 14.3, 6.9 Hz, 2H), 1.75-1.66 (m, 2H), 1.64 (s, 6H), 1.49 (s, 6H), 1.33 (d, *J* = 4.8 Hz, 3H); **^{13}C NMR** (125 MHz; $CDCl_3$) δ 207.9, 143.9, 140.3, 138.1, 132.1, 129.1, 128.5, 128.5, 128.1, 127.3, 126.9, 124.2, 124.1, 51.7, 40.1, 25.8, 23.4, 22.8, 17.7. **IR** (Neat) 3061, 3033, 2968, 2915, 2857, 1667, 1603, 1557, 1486, 1447, 1377, 1222, 1177, 1117, 1076, 1007, 960, 849, 748, 695. **HRMS** (ESI) *m/z*: $[M+Na]^+$ calcd for $C_{27}H_{34}ONa^+$ 397.2505; found 397.2496.

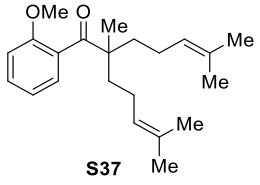

S37

1-(2-methoxyphenyl)-2,6-dimethyl-2-(4-methylpent-3-en-1-yl)hept-5-en-1-one (S37): General procedure D1 was followed employing **S20** (1.67 mmol). Purification by flash column chromatography eluting with hexanes/EtOAc (16:1) provided 450.2 mg (82% yield) of S**37** as a clear oil. **^{1}H NMR** (500 MHz; $CDCl_3$) δ 7.32 (ddd, *J* = 8.6, 7.5, 1.7 Hz, 1H), 7.01 (dd, *J* = 7.5, 1.7 Hz, 1H), 6.94 (t, *J* = 7.5 Hz, 1H), 6.89 (d, *J* = 8.6 Hz, 1H), 5.10-5.07 (m, 2H), 3.79 (s, 3H), 1.96 (q, *J* = 8.0 Hz, 4H), 1.72-1.63 (m, 8H), 1.63-1.56 (m, 8H), 1.16 (s, 3H); **^{13}C NMR** (125 MHz; $CDCl_3$) δ 212.7, 155.7, 131.7, 130.0, 126.2, 124.6, 120.4, 111.2, 55.5, 51.6, 37.6, 25.9, 23.2, 22.0, 17.8. **IR** (Neat) 2966, 2915, 1688, 1598, 1582, 1488, 1463, 1434, 1376, 1285, 1245, 1181, 1162, 1113, 1050, 1025, 956, 928, 832, 795, 750, 675, 628. **HRMS** (ESI) *m/z*: $[M+Na]^+$ calcd for $C_{22}H_{32}O_2Na^+$ 351.2295; found 351.2292.

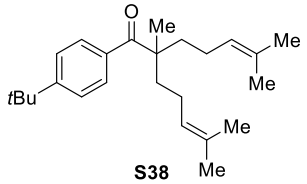

S38

1-(4-(tert-butyl)phenyl)-2,6-dimethyl-2-(4-methylpent-3-en-1-yl)hept-5-en-1-one (S38): General procedure D1 was followed employing **S25** (0.917 mmol). Purification by flash column chromatography eluting with hexanes/EtOAc (19:1) provided 173.0 mg (42% yield) of **S38** as a clear oil. **^{1}H NMR** (500 MHz; $CDCl_3$) δ 7.69 (d, *J* = 8.5 Hz, 2H), 7.40 (d, *J* = 8.5 Hz, 2H), 5.06-4.98 (m, 2H), 2.00-1.89 (m, 4H), 1.85-1.73 (m, 2H), 1.67-1.60 (m, 8H), 1.45 (s, 6H), 1.33 (s, 9H), 1.29 (s, 3H); **^{13}C NMR** (125 MHz; $CDCl_3$) δ 207.9, 154.6, 136.6, 132.0, 127.9, 125.2, 124.2, 51.6, 40.2, 35.0, 31.2, 25.8, 23.4, 22.8, 17.6. **IR** (Neat) 2964, 2926, 2866, 1733, 1667, 1605, 1562, 1462, 1403, 1376, 1364, 1269, 1223, 1182, 1108, 982, 961, 848, 830, 773, 738, 713, 648, 608. **HRMS** (ESI) *m/z*: $[M+H]^+$ calcd for $C_{25}H_{39}O^+$ 355.2995; found 355.3015.

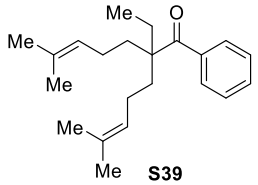

S39

2-ethyl-6-methyl-2-(4-methylpent-3-en-1-yl)-1-phenylhept-5-en-1-one (S39): General procedure D1 was followed employing **S21** (0.801 mmol). Purification by flash column chromatography eluting with hexanes/EtOAc (16:1) provided 158.0 mg (63% yield) of **S39** as a clear oil. **^{1}H NMR** (500 MHz; $CDCl_3$) δ 7.62 (d, *J* = 7.5 Hz, 2H), 7.44 (t, *J* = 7.3 Hz, 1H), 7.41-7.35 (m, 2H), 5.06-5.03 (m, 2H), 1.85-1.78 (m, 6H), 1.76-1.72 (m, 4H), 1.65 (s, 6H), 1.51 (s, 6H),

0.82 (t, *J* = 7.5 Hz, 3H); **^{13}C NMR** (125 MHz; $CDCl_3$) δ 209.4, 140.4, 131.9, 130.7, 128.3, 127.3, 124.2, 54.9, 34.5, 26.9, 25.8, 22.9, 17.7, 8.5. **IR** (Neat) 2966, 2927, 1670, 1597, 1443, 1376, 1220, 1176, 1106, 1002, 960, 833, 771, 714, 697, 627. **HRMS** (ESI) *m/z*: $[M+H]^+$ calcd for $C_{22}H_{32}ONa^+$ 335.2345; found 335.2350.

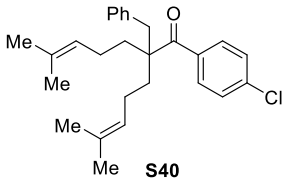

S40

2-benzyl-1-(4-chlorophenyl)-6-methyl-2-(4-methylpent-3-en-1-yl)hept-5-en-1-one (S40): General procedure D1 was followed employing **S23** (2.19 mmol). Purification by flash column chromatography eluting with hexanes/EtOAc (16:1) provided 766.8 mg (86% yield) of **S40** as a clear oil. **^{1}H NMR** (500 MHz; $CDCl_3$) δ 7.43-7.41 (m, 2H), 7.34-7.32 (m, 2H), 7.29-7.21 (m, 3H), 7.12-7.10 (m, 2H), 5.02-4.99 (m, 2H), 3.10 (s, 2H), 2.05-1.87 (m, 4H), 1.77-1.65 (m, 4H), 1.65 (s, 6H), 1.51 (s, 6H); **^{13}C NMR** (125 MHz; $CDCl_3$) δ 207.7, 138.4, 137.9, 137.2, 132.2, 130.6, 129.0, 128.5, 128.4, 126.7, 123.7, 56.0, 40.2, 35.4, 25.8, 23.2, 17.8. **IR** (Neat) 3029, 2926, 2857, 1670, 1587, 1487, 1452, 1395, 1376, 1253, 1219, 1172, 1093, 1031, 1013, 960, 841, 769, 730, 701, 603. **HRMS** (ESI) *m/z*: $[M+H]^+$ calcd for $C_{27}H_{34}ClO^+$ 409.2293; found 409.2297.

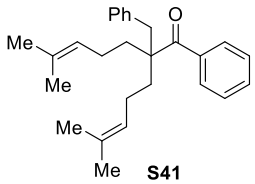

S41

2-benzyl-6-methyl-2-(4-methylpent-3-en-1-yl)-1-phenylhept-5-en-1-one (S41): General procedure D1 was followed employing **S22** (9.16 mmol). Purification by flash column chromatography eluting with hexanes/EtOAc (16:1) provided 2.81 g (82% yield) of **S41** as a clear oil. **^{1}H NMR** (500 MHz; $CDCl_3$) δ 7.52-7.46 (m, 2H), 7.46-7.40 (m, 1H), 7.35 (dd, *J* = 8.3, 7.0 Hz, 2H), 7.28-7.20 (m, 3H), 7.15-7.08 (m, 2H), 5.01-4.98 (m, 2H), 3.12 (s, 2H), 2.05-1.87 (m, 4H), 1.75-1.68 (m, 4H), 1.64 (s, 6H), 1.49 (s, 6H); **^{13}C NMR** (125 MHz; $CDCl_3$) δ 209.0, 140.3, 138.1, 132.0, 130.9, 130.6, 128.3, 128.2, 127.5, 126.5, 123.8, 55.9, 40.0, 35.5, 25.8, 23.2, 17.8. **IR**

(Neat) 3028, 2926, 1669, 1597, 1496, 1452, 1376, 1254, 1220, 1175, 1111, 1031, 1002, 959, 913, 840, 730, 699, 630. **HRMS** (ESI) *m/z*: $[M+H]^+$ calcd for $C_{27}H_{35}O^+$ 375.2682; found 375.2682.

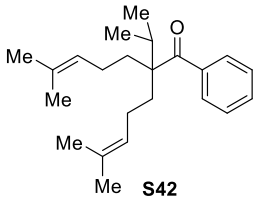

S42

2-isopropyl-6-methyl-2-(4-methylpent-3-en-1-yl)-1-phenylhept-5-en-1-one (S42): General proce-dure D1 was followed employing **S24** (1.49 mmol). Purification by flash column chromatography eluting with hexanes/EtOAc (16:1) provided 412 mg (85% yield) of **S42** as a clear oil. **^{1}H NMR** (500 MHz; $CDCl_3$) δ 7.66-7.60 (m, 2H), 7.46-7.41 (m, 1H), 7.38 (dd, *J* = 8.2, 6.8 Hz, 2H), 5.09-5.06 (m, 2H), 2.29 (hept, *J* = 6.9 Hz, 1H), 2.03-1.81 (m, 6H), 1.76-1.64 (m, 8H), 1.53 (s, 6H), 0.94 (d, *J* = 7.0 Hz, 6H); **^{13}C NMR** (125 MHz; $CDCl_3$) δ 209.1, 141.2, 131.7, 130.6, 128.3, 127.6, 124.7, 57.4, 34.4, 34.1, 25.9, 24.1, 18.6, 17.8. **IR** (Neat) 2966, 2927, 2879, 1670, 1597, 1444, 1375, 1220, 1176, 1108, 1002, 963, 835, 776, 714, 697. **HRMS** (ESI) *m/z*: $[M+H]^+$ calcd for $C_{23}H_{35}O^+$ 327.2682; found 327.2677.

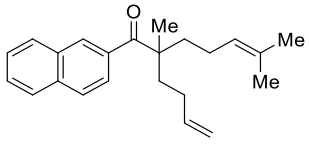

S43

2-(but-3-en-1-yl)-2,6-dimethyl-1-(naphthalen-2-yl)hept-5-en-1-one (S43): General procedure C2 was followed employing 2-bromonaphthalene and **S14**. General procedure D2 was followed using crude alcohol (0.675 mmol). Purification by flash column chromatography eluting with DCM/hexanes (3:1) provided 82.3 mg (38% yield) of **S43** as a clear oil. **^{1}H NMR** (500 MHz; $CDCl_3$) δ 8.21 (s, 1H), 7.91 (d, *J* = 8.1 Hz, 1H), 7.86 (d, *J* = 8.3 Hz, 2H), 7.76 (d, *J* = 8.6 Hz, 1H), 7.55 (dt, *J* = 20.6, 7.2 Hz, 2H), 5.76 (td, *J* = 10.5, 4.9 Hz, 1H), 5.04 (s, 1H), 4.97 (d, *J* = 17.2 Hz, 1H), 4.91 (d, *J* = 10.2 Hz, 1H), 2.13-2.05 (m, 2H), 2.05-1.92 (m, 3H), 1.89-1.82 (m, 1H), 1.79-1.68 (m, 2H), 1.63 (s, 3H), 1.47 (s, 3H), 1.36 (s, 3H); **^{13}C NMR** (125 MHz; $CDCl_3$) δ 208.4, 138.6, 136.8, 134.5, 132.5, 132.2, 129.3, 128.1, 128.0, 127.8, 127.8, 126.8, 124.8, 124.0, 114.8, 51.7, 40.1, 39.1, 29.1, 25.8, 23.5, 22.9, 17.7. **IR** (Neat) 3060, 2970, 2927, 2858, 1668. 1640, 1627, 1596,

1464, 1377, 1274, 1213, 1168, 1121, 1020, 991, 937, 861, 909, 861, 818, 778, 757. **HRMS** (ESI) *m/z*: $[M+Na]^+$ calcd for $C_{23}H_{28}ONa^+$ 343.2032; found 343.2022.

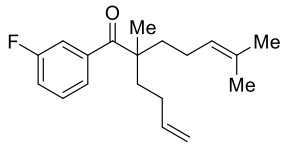

S44

2-(but-3-en-1-yl)-1-(3-fluorophenyl)-2,6-dimethylhept-5-en-1-one (S44): General procedure C2 was followed employing 1-bromo-3-fluorobenzene and **S14** (0.200 mmol). General procedure D2 was followed using crude alcohol. Purification by flash column chromatography eluting with DCM/hexanes (3:1) provided 32.9 mg (57% yield) of **S44** as a clear oil. **^{1}H NMR** (500 MHz; $CDCl_3$) δ 7.48-7.42 (m, 1H), 7.38 (dd, *J* = 8.0, 5.7 Hz, 1H), 7.36-7.34 (m, 1H), 7.19-7.10 (m, 1H), 5.75 (ddt, *J* = 16.7, 10.1, 6.4 Hz, 1H), 5.01 (t, *J* = 7.1 Hz, 1H), 4.97 (dd, *J* = 17.1, 1.7 Hz, 1H), 4.94-4.91 (m, 1H), 2.13-2.02 (m, 1H), 2.01-1.92 (m, 2H), 1.92-1.85 (m, 2H), 1.82 (tt, *J* = 12.2, 5.5 Hz, 1H), 1.73-1.67 (m, 2H), 1.66-1.60 (m, 4H), 1.49 (s, 3H), 1.28 (s, 3H); **^{13}C NMR** (125 MHz; $CDCl_3$) δ 207.2 (d, *J* = 1.8 Hz), 162.5 (d, *J* = 247.4 Hz), 141.5 (d, *J* = 5.9 Hz), 138.3, 132.3, 130.0 (d, *J* = 7.8 Hz), 123.8, 123.3 (d, *J* = 3.1 Hz), 118.0 (d, *J* = 21.2 Hz), 114.9, 114.8, 51.6, 39.6, 38.8, 29.0, 25.8, 23.4, 22.6, 17.7. **IR** (Neat) 3079, 2973, 2930, 2857, 1679 1641, 1585, 1483, 1431, 1378, 1259, 1239, 1145, 993, 911, 875, 789, 755, 678. **HRMS** (ESI) *m/z*: $[M+Na]^+$ calcd for $C_{19}H_{25}FONa^+$ 311.1782; found 311.1789.

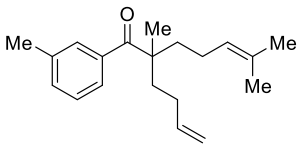

S45

2-(but-3-en-1-yl)-2,6-dimethyl-1-(m-tolyl)hept-5-en-1-one (S45): General procedure C2 was followed employing 1-bromo-3-methylbenzene and **S14** (0.2 mmol). General procedure D2 was followed using crude alcohol. Purification by flash column chromatography eluting with DCM/hexanes (3:1) provided 48.3 mg (85% yield) of **S45** as a clear oil. **^{1}H NMR** (500 MHz; $CDCl_3$) δ 7.46-7.44 (m, 1H), 7.43 (s, 1H), 7.27 (m, 2H), 5.76 (ddt, *J* = 16.6, 10.1, 6.4 Hz, 1H), 5.05-5.00 (m, 1H), 4.97 (dd, *J* = 17.1, 1.7 Hz, 1H), 4.92 (dd, *J* = 10.3, 1.6 Hz, 1H), 2.38 (s, 3H), 2.10-2.01 (m, 1H), 2.04-1.88 (m, 4H), 1.88-1.77 (m, 1H), 1.74-1.66 (m, 1H), 1.64 (s, 3H), 1.63-

1.59 (m, 1H), 1.49 (s, 3H), 1.28 (s, 3H); **^{13}C NMR** (125 MHz; $CDCl_3$) δ 209.1, 139.8, 138.6, 138.1, 132.1, 131.7, 128.3, 128.1, 124.4, 124.1, 114.7, 51.5, 39.8, 38.9, 29.0, 25.8, 23.4, 22.8, 21.6, 17.6. **IR** (Neat) 3079, 2971, 2924, 2857, 1671, 1641, 1601, 1584, 1451, 1377, 1260, 1160, 994, 909, 787, 748, 695. **HRMS** (ESI) *m/z*: $[M+Na]^+$ calcd for $C_{20}H_{28}ONa^+$ 307.2032; found 307.2026.

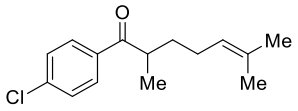

S51

1-(4-chlorophenyl)-2,6-dimethylhept-5-en-1-one (S51): General procedure C1 was followed employing 4-chlorophenylmagnesium bromide (1 M solution in diethyl ether) and 2,6-dimethyl-5-heptenal (3.15 mmol). General procedure D2 was followed using crude alcohol. Purification by flash column chromatography eluting with hexanes:EtOAc (19:1) provided 273 mg (35% yield) of **S51** as a clear oil. **^{1}H NMR** (700 MHz; $CDCl_3$) δ 7.88 (d, *J* = 8.6 Hz, 2H), 7.43 (d, *J* = 8.5 Hz, 2H), 5.08-5.06 (m, 1H), 3.41 (h, *J* = 6.8 Hz, 1H), 2.00 (q, *J* = 7.6 Hz, 2H), 1.86 (dq, *J* = 14.9, 7.5 Hz, 1H), 1.65 (s, 3H), 1.51 (s, 3H), 1.49-1.42 (m, 1H), 1.18 (d, *J* = 6.8 Hz, 3H); **^{13}C NMR** (176 MHz; $CDCl_3$) δ 203.3, 139.3, 135.2, 132.6, 129.8, 129.0, 123.9, 40.1, 33.8, 25.9, 25.8, 17.8, 17.3. **IR** (Neat) 2969, 2930, 2877, 2856, 1682, 1589, 1570, 1400, 1212, 1092, 971, 841, 749, 686. **HRMS** (APCI) *m/z*: $[M+H]^+$ calcd for $C_{15}H_{20}ClO^+$ 251.1197; found 251.1190.

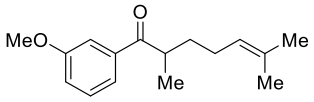

S52

1-(3-methoxyphenyl)-2,6-dimethylhept-5-en-1-one (S52): General procedure C2 was followed employing 3-bromoanisole and 2,6-dimethyl-5-heptenal (3.57 mmol). General procedure D2 was followed using crude alcohol. Purification by flash column chromatography eluting with hexanes:EtOAc (11:1) provided 430 mg (49% yield) of **S52** as a clear oil. **^{1}H NMR** (700 MHz; $CDCl_3$) δ 7.52 (d, *J* = 7.6 Hz, 1H), 7.48 (s, 1H), 7.36 (t, *J* = 7.9 Hz, 1H), 5.10-5.08 (m, 1H), 3.86 (s, 3H), 3.45 (h, *J* = 6.8 Hz, 1H), 2.01 (q, *J* = 8.3, 7.8 Hz, 2H), 1.87 (dq, *J* = 14.5, 7.3 Hz, 1H), 1.66 (s, 3H), 1.52 (s, 3H), 1.46 (dq, *J* = 14.2, 6.9 Hz, 1H), 1.19 (d, *J* = 6.8 Hz, 3H); **^{13}C NMR** (176 MHz; $CDCl_3$) δ 204.4, 160.0, 138.3, 132.5, 129.7, 124.1, 120.9, 119.4, 112.8, 55.6, 40.2, 33.9,

25.9, 25.8, 17.8, 17.5; **IR** (Neat) 2967, 2931, 2856, 1682, 1597, 1582, 1487, 1428, 1258, 1045, 995, 879, 795, 745, 682. **HRMS** (APCI) *m/z*: $[M+H]^+$ calcd for $C_{16}H_{23}O_2^+$ 247.1693; found 247.1689.

Synthesis of ketone 51.

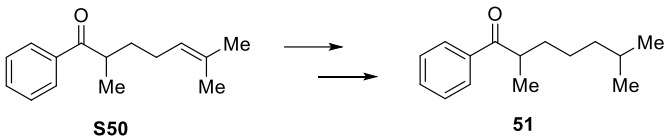

S50 **51**

To a flame-dried 25 mL round-bottom flask equipped with a magnetic stir bar was added Pd/C (110 mg, 0.0518 mmol, 5% w/w). A stream of MeOH (5 mL) was then added slowly down the side of the flask. Next, the suspension was sparged with a balloon of H_2 gas for 30 min. At this time, sparging was ceased and **S50**[5] (160 mg, 0.74 mmol) dissolved in MeOH (1 mL) was added dropwise to the reaction mixture. The flask was equipped with a balloon of H_2 and allowed to stir at room temperature for 2 h. The reaction was then filtered through a Celite® plug eluting with DCM (10 mL). The eluent was concentrated under reduced pressure and the resultant crude residue was purified via flash column chromatography over silica eluting with hexanes/EtOAc (9:1) to afford 106 mg (65%) of the completely reduced alcohol as a clear oil. Ratio of diastereomers ~1:1 by NMR. ^{1}H NMR (500 MHz; $CDCl_3$) δ 7.35-7.26 (m, 10H), 4.54 (dd, *J* = 5.7, 3.6 Hz, 1H), 4.44 (dd, *J* = 7.1, 3.2 Hz, 1H), 1.89-1.76 (m, 1H), 1.69-1.57 (m, 1H), 1.55-1.45 (m, 2H), 1.44-1.03 (m, 12H), 0.92-0.83 (m, 15H), 0.75 (d, *J* = 6.3 Hz, 3H). The alcohol (0.48 mmol, 1 equiv) and dry DMSO (0.2M) were added in a round-bottom flask equipped with a magnetic stir bar. IBX was added (1.2 equiv) slowly to the reaction mixture at room temperature. The reaction mixture was stirred for 3 hours. The reaction was quenched with addition of water and EtOAc. After stirring for 45 minutes, the reaction was filtered through a Celite® plug and extracted with EtOAc (3 x 10 mL). The organic phase was washed with brine and dried over Na_2SO_4, filtered and concentrated under reduced pressure to remove all volatile components. The crude product was purified via column chromatography eluting with the hexanes/EtOAc (9:1) to give 80 mg (76%) of the pure ketone **51**. **^{1}H NMR** (500 MHz; $CDCl_3$) δ 7.95 (d, *J* =7.0 Hz, 2H), 7.56 (t, *J* = 7.3 Hz, 1H), 7.47 (t, *J* = 7.6 Hz, 2H), 3.47 (h, *J* = 6.8 Hz, 1H), 1.82-1.75 (m, 1H), 1.53-1.46 (m, 1H), 1.45-1.38 (m, 1H), 1.34-1.24 (m, 2H), 1.20-1.10 (m, 5H), 0.84 (d, *J* =6.6 Hz, 6H); **^{13}C NMR** (125 MHz; $CDCl_3$) δ 204.7, 136.9, 132.9, 128.8, 128.4, 40.8, 39.2, 34.1, 27.9, 25.3, 22.8, 22.7, 17.4. **IR** (Neat) 2954,

2933, 2869, 1682, 1597, 1580, 1460, 1448, 1366, 1223, 1196, 1182, 1158, 1002, 969, 792, 701, 687, 654. **HRMS** (ESI) *m/z*: $[M+H]^+$ calcd for $C_{15}H_{23}O^+$ 219.1743; found 219.1743.

3.4.5. Synthesis of products

General procedure for Carbonyl-Olefin Metathesis of bisalkene substrates.

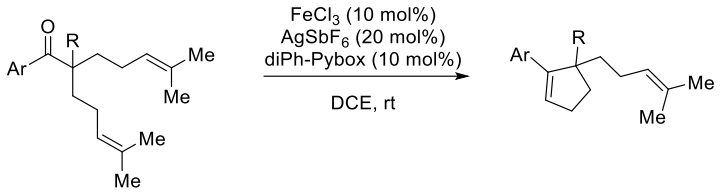

An oven-dried round bottom flask equipped with a magnetic stir bar was charged with $FeCl_3$ (0.009 mmol), $AgSbF_6$ (0.018 mmol), diPh-Pybox (0.009 mmol) and dry DCE (8.0 mL). The catalyst solution was allowed to stir for 1 h at room temperature. The bisalkene substrate (0.09 mmol dissolved in 1 mL of dry DCE) was added in one portion to the catalyst solution. The reaction mixture was allowed to stir for the indicated time at room temperature. After reaching completion as judged by TLC or 48 h, the reaction was filtered through a silica plug eluting with DCM (25 mL). The filtrate was concentrated under reduced pressure to remove all volatile components. Yield and conversion were determined either by ^{1}H NMR using dimethyl terephthalate as an internal standard, or by isolation via column chromatography with the indicated eluent to give the pure metathesis products.

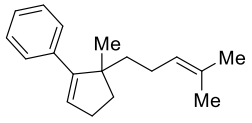

31

(5-methyl-5-(4-methylpent-3-en-1-yl)cyclopent-1-en-1-yl)benzene (31): The cyclization of **25** was performed according to the general procedure for metathesis with a reaction time of 5 h (91% yield, 100% conversion by ^{1}H NMR). Purification by flash column chromatography eluting with pentane provided 19.3 mg (89%) of **31** as a clear oil. **^{1}H NMR** (500 MHz; $CDCl_3$) δ 7.35-7.26 (m, 4H), 7.25-7.20 (m, 1H), 5.79 (t, *J* = 2.5 Hz, 1H), 5.08-5.04 (m, 1H), 2.43-2.31 (m, 2H), 2.08-1.72 (m, 4H), 1.64 (s, 3H), 1.52-1.46 (m, 5H), 1.22 (s, 3H); **^{13}C NMR** (125 MHz; $CDCl_3$) δ 150.8, 138.4, 131.1, 128.6, 128.1, 127.6, 126.7, 125.1, 50.4, 40.5, 38.8, 30.1, 26.8, 25.8, 23.8, 17.6. **IR**

(Neat) 2927, 1688, 1496, 1447, 1376, 1155, 1071, 1028, 974, 919, 752, 699. **HRMS** (EI) *m/z*: $[M]^+$ calcd for $C_{18}H_{24}^+$ 240.1873; found 240.1892.

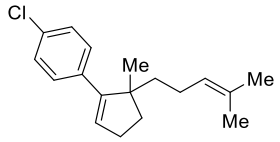

32

1-chloro-4-(5-methyl-5-(4-methylpent-3-en-1-yl)cyclopent-1-en-1-yl)benzene (32): The cyclization of **S32** was performed according to the general procedure for metathesis with a reaction time of 30 min (81% yield, 100% conversion by ^{1}H NMR). Purification by flash column chromatography eluting with pentane provided 19.5 mg (79%) of **32** as a clear oil. **^{1}H NMR** (500 MHz; $CDCl_3$) δ 7.25 (s, 4H), 5.79 (t, *J* = 2.5 Hz, 1H), 5.06-5.03 (m, 1H), 2.44-2.29 (m, 2H), 2.06-1.72 (m, 4H), 1.64 (s, 3H), 1.51 (s, 3H), 1.49-1.43 (m, 2H), 1.20 (s, 3H); **^{13}C NMR** (125 MHz; $CDCl_3$) δ 149.7, 136.8, 132.5, 131.3, 129.3, 128.9, 128.2, 124.9, 50.4, 40.4, 38.7, 30.1, 26.7, 25.8, 23.8, 17.7. **IR** (Neat) 2962, 1687, 1592, 1492, 1458, 1398, 1377, 1265, 1092, 1015, 921, 815, 735, 703, 680, 630, 604. **HRMS** (EI) *m/z*: $[M]^+$ calcd for $C_{18}H_{23}Cl^+$ 274.1483; found 274.1490.

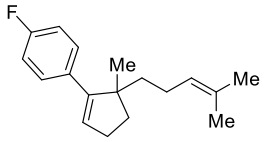

33

1-fluoro-4-(5-methyl-5-(4-methylpent-3-en-1-yl)cyclopent-1-en-1-yl)benzene (33): The cyclization of **S33** was performed according to the general procedure for metathesis with a reaction time of 30 min (89% yield, 100% conversion by ^{1}H NMR). Purification by flash column chromatography eluting with pentane provided 20.0 mg (86%) of **33** as a clear oil. **^{1}H NMR** (500 MHz; $CDCl_3$) δ 7.29-7.25 (m, 2H), 6.99-6.95 (m, 2H), 5.74 (t, *J* = 2.5 Hz, 1H), 5.07-5.03 (m, 1H), 2.42-2.29 (m, 2H), 2.05-1.73 (m, 4H), 1.64 (s, 3H), 1.51 (s, 3H), 1.49-1.42 (m, 2H), 1.20 (s, 3H); **^{13}C NMR** (125 MHz; $CDCl_3$) δ 162.0 (d, *J* = 245.1 Hz), 149.9, 134.4, 131.3, 129.1 (d, *J* = 7.7 Hz), 128.8, 125.0, 114.9 (d, *J* = 21.0 Hz), 50.4, 40.4, 38.6, 30.1, 26.8, 25.8, 23.8, 17.7. **IR** (Neat) 2963, 1688, 1604, 1513, 1459, 1408, 1377, 1266, 1223, 1158, 1095, 1015, 921, 838, 815, 735, 703. **HRMS** (EI) *m/z*: $[M]^+$ calcd for $C_{18}H_{23}F^+$ 258.1778; found 258.1790.

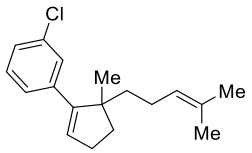

34

1-chloro-3-(5-methyl-5-(4-methylpent-3-en-1-yl)cyclopent-1-en-1-yl)benzene (34): The cyclization of **S34** was performed according to the general procedure for metathesis with a reaction time of 48 h (72% yield, 84% conversion by ^{1}H NMR). Purification by flash column chromatography eluting with pentane provided 16.5 mg (67%) of **34** as a clear oil. **^{1}H NMR** (500 MHz; $CDCl_3$) δ 7.30-7.29 (m, 1H), 7.22-7.18 (m, 3H), 5.81 (t, *J* = 2.6 Hz, 1H), 5.08-5.04 (m, 1H), 2.45-2.30 (m, 2H), 2.06-1.73 (m, 4H), 1.65 (s, 3H), 1.52 (s, 3H), 1.50-1.46 (m, 2H), 1.21 (s, 3H); **^{13}C NMR** (125 MHz; $CDCl_3$) δ 149.7, 140.3, 133.9, 131.3, 129.9, 129.3, 127.7, 126.8, 125.7, 124.9, 50.5, 40.4, 38.7, 30.2, 26.8, 25.8, 23.8, 17.6. **IR** (Neat) 2963, 1690, 1570, 1456, 1377, 1265, 1080, 999, 924, 886, 787, 735, 696. **HRMS** (EI) *m/z*: $[M]^+$ calcd for $C_{18}H_{23}Cl^+$ 274.1483; found 274.1501.

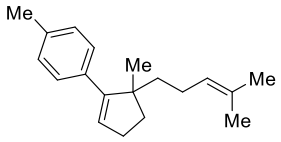

35

1-methyl-4-(5-methyl-5-(4-methylpent-3-en-1-yl)cyclopent-1-en-1-yl)benzene (35): The cyclization of **S35** was performed according to the general procedure for metathesis with a reaction time of 5 h (76% yield, 100% conversion by ^{1}H NMR). Purification by flash column chromatography eluting with pentane provided 15.1 mg (66%) of **35** as a clear oil. **^{1}H NMR** (500 MHz; $CDCl_3$) δ 7.21 (d, *J* = 8.0 Hz, 2H), 7.10 (d, *J* = 8.0 Hz, 2H), 5.75 (t, *J* = 2.5 Hz, 1H), 5.08-5.04 (m, 1H), 2.43-2.27 (m, 5H), 2.05-1.73 (m, 4H), 1.64 (s, 3H), 1.54-1.45 (m, 5H), 1.21 (s, 3H); **^{13}C NMR** (125 MHz; $CDCl_3$) δ 150.7, 136.3, 135.4, 131.1, 128.8, 128.0, 127.5, 125.2, 50.3, 40.6, 38.8, 30.1, 26.8, 25.8, 23.9, 21.2, 17.7. **IR** (Neat) 2960, 1687, 1609, 1516, 1454, 1409, 1377, 1267, 1179, 1111, 974, 919, 811, 734, 702, 681. **HRMS** (EI) *m/z*: $[M]^+$ calcd for $C_{19}H_{26}^+$ 254.2029; found 254.2044.

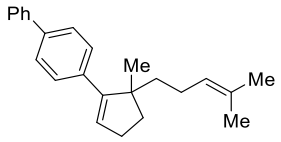

36

4-(5-methyl-5-(4-methylpent-3-en-1-yl)cyclopent-1-en-1-yl)-1,1'-biphenyl (36): The cyclization of **S36** was performed according to the general procedure for metathesis with a reaction time of 16 h. Purification by flash column chromatography eluting with hexanes provided 18.0 mg (65% yield) of **36** as a clear oil. **^{1}H NMR** (500 MHz; $CDCl_3$) δ 7.61 (d, *J* = 7.0 Hz, 2H), 7.53 (d, *J* = 8.3 Hz, 2H), 7.43 (q, *J* = 7.8 Hz, 4H), 7.34 (t, *J* = 7.4 Hz, 1H), 5.88 (t, *J* = 2.6 Hz, 1H), 5.15-5.05 (m, 1H), 2.40 (dddd, *J* = 13.5, 8.3, 5.8, 2.6 Hz, 2H), 2.13-1.97 (m, 2H), 1.92 (dq, *J* = 14.1, 6.9 Hz, 1H), 1.80 (ddd, *J* = 12.4, 8.6, 5.4 Hz, 1H), 1.65 (s, 3H), 1.60-1.54 (m, 2H), 1.53 (s, 3H), 1.28 (s, 3H); **^{13}C NMR** (125 MHz; $CDCl_3$) δ 150.4, 141.1, 139.5, 137.4, 131.2, 128.9, 127.9, 127.3, 127.1, 126.8, 126.6, 125.1, 50.4, 40.6, 38.9, 30.2, 26.9, 25.8, 23.9, 17.7. **IR** (Neat) 3054, 3032, 2925, 2850, 1597, 1579, 1486, 1447, 1404, 1374, 1339, 1324, 1202, 1158, 1122, 1102, 1004, 986, 953, 908, 883, 829, 811, 724, 690. **HRMS** (EI) *m/z*: $[M]^+$ calcd for $C_{24}H_{28}^+$ 316.2191; found 316.2187.

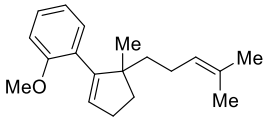

37

1-methoxy-2-(5-methyl-5-(4-methylpent-3-en-1-yl)cyclopent-1-en-1-yl)benzene (37): The cycliza-tion of **S37** was performed according to the general procedure for metathesis with a reaction time of 24 h (62% yield, 92% conversion by ^{1}H NMR). Purification by flash column chromatography eluting with pentane:DCM (9:1) provided 14.8 mg (61%) of **37** as a clear oil. **^{1}H NMR** (500 MHz; $CDCl_3$) δ 7.22 (td, *J* = 7.5, 1.8 Hz, 1H), 7.03 (dd, *J* = 7.5, 1.8 Hz, 1H), 6.91-8.86 (m, 2H), 5.61 (t, *J* = 2.4 Hz, 1H), 5.07-5.04 (m, 1H), 3.76 (s, 3H), 2.47-2.33 (m, 2H), 2.03-1.90 (m, 3H), 1.80-1.75 (m, 1H), 1.66 (s, 3H), 1.56 (s, 3H), 1.43-1.28 (m, 2H), 1.08 (s, 3H); **^{13}C NMR** (125 MHz; $CDCl_3$) δ 157.7, 148.1, 131.0, 130.8, 129.1, 128.0, 127.8, 125.6, 120.0, 110.9, 55.5, 51.7, 40.3, 37.8, 30.7, 25.9, 25.8, 23.8, 17.8. **IR** (Neat) 2926, 2851, 1684, 1595, 1578, 1489, 1453, 1434, 1375, 1291, 1249, 1180, 1162, 1113, 1051, 1028, 834, 785, 751, 704, 663, 608. **HRMS** (ESI) *m/z*: $[M+Na]^+$ calcd for $C_{19}H_{26}ONa^+$ 293.1876; found 293.1881.

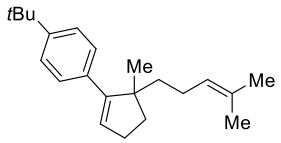

38

1-(tert-butyl)-4-(5-methyl-5-(4-methylpent-3-en-1-yl)cyclopent-1-en-1-yl)benzene (38): The cycli-zation of **S38** was performed according to the general procedure for metathesis with a reaction time of 20 h (86% yield, 100% conversion by ^{1}H NMR). Purification by flash column chromatography eluting with pentane provided 20.4 mg (77%) of **38** as a clear oil. **^{1}H NMR** (500 MHz; $CDCl_3$) δ 7.30 (d, *J* = 8.5 Hz, 2H), 7.27 (d, *J* = 8.5 Hz, 2H), 5.78 (t, *J* = 2.5 Hz, 1H), 5.09-5.05 (m, 1H), 2.42-2.29 (m, 2H), 2.05-1.70 (m, 4H), 1.64 (s, 3H), 1.54-1.46 (m, 5H), 1.31 (s, 9H), 1.23 (s, 3H); **^{13}C NMR** (125 MHz; $CDCl_3$) δ 150.6, 149.5, 135.3, 131.1, 128.1, 127.2, 125.2, 125.0, 50.3, 40.5, 38.8, 34.6, 31.5, 30.1, 26.9, 25.9, 23.9, 17.6. **IR** (Neat) 2961, 2867, 1680, 1606, 1514, 1460, 1398, 1376, 1363, 1268, 1202, 1107, 999, 921, 833, 817, 736, 704, 681, 637, 606. **HRMS** (EI) *m/z*: $[M]^+$ calcd for $C_{22}H_{32}^+$ 296.2499; found 296.2515.

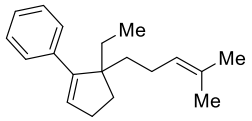

39

(5-ethyl-5-(4-methylpent-3-en-1-yl)cyclopent-1-en-1-yl)benzene (39): The cyclization of **S39** was performed according to the general procedure for metathesis with a reaction time of 48 h (28% yield, 43% conversion by ^{1}H NMR) or 2 h using 0.027 mmol of $AgSbF_6$ (53% yield, 100% conversion by ^{1}H NMR). Purification by flash column chromatography eluting with pentane provided 11.3 mg (49%) of **39** as a clear oil. **^{1}H NMR** (500 MHz; $CDCl_3$) δ 7.34-7.30 (m, 2H), 7.30-7.26 (m, 2H), 7.25-7.19 (m, 1H), 5.89 (t, *J* = 2.6 Hz, 1H), 5.09-5.05 (m, 1H), 2.39-2.33 (m, 2H), 2.03-1.85 (m, 4H), 1.64 (s, 3H), 1.63-1.51 (m, 4H), 1.50 (s, 3H), 0.84 (t, *J* = 7.4 Hz, 3H); **^{13}C NMR** (125 MHz; $CDCl_3$) δ 147.9, 138.7, 131.1, 130.4, 128.2, 127.4, 126.7, 125.2, 54.9, 40.5, 34.8, 32.8, 31.1, 25.9, 23.6, 17.7, 9.1. **IR** (Neat) 2962, 2922, 2850, 1598, 1492, 1442, 1376, 1101, 1075, 1033, 984, 908, 886, 834, 758, 696, 607. **HRMS** (EI) *m/z*: $[M]^+$ calcd for $C_{19}H_{26}^+$ 254.2029; found 254.2044.

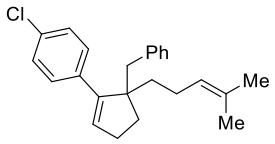

40

1-(5-benzyl-5-(4-methylpent-3-en-1-yl)cyclopent-1-en-1-yl)-4-chlorobenzene (40): The cyclization of **S40** was performed according to the general procedure for metathesis with a reaction time of 48 h (36% yield, 58% conversion by ^{1}H NMR). Purification by flash column chromatography eluting with pentane provided 10.8 mg (34%) of **40** as a clear oil. **^{1}H NMR** (500 MHz; $CDCl_3$) δ 7.42-7.36 (m, 2H), 7.33-7.28 (m, 2H), 7.19 (d, *J* = 6.6 Hz, 3H), 7.12-7.07 (m, 2H), 5.91 (t, *J* = 2.6 Hz, 1H), 5.04 (t, *J* = 7.3 Hz, 1H), 2.95 (d, *J* = 13.4 Hz, 1H), 2.77 (d, *J* = 13.4 Hz, 1H), 2.15-2.02 (m, 2H), 2.01-1.93 (m, 1H), 1.91-1.67 (m, 4H), 1.64 (s, 3H), 1.61-1.57 (m, 1H), 1.46 (s, 3H); **^{13}C NMR** (125 MHz; $CDCl_3$) δ 146.3, 139.1, 136.8, 132.6, 132.4, 131.4, 130.6, 128.6, 128.5, 127.7, 126.1, 124.7, 55.1, 46.1, 39.9, 35.0, 30.5, 25.9, 23.6, 17.6. **IR** (Neat) 3027, 2919, 2849, 1602, 1490, 1453, 1375, 1094, 1030, 1012, 826, 761, 725, 717, 701. **HRMS** (EI) *m/z*: $[M]^+$ calcd for $C_{24}H_{27}Cl^+$ 350.1796; found 350.1802.

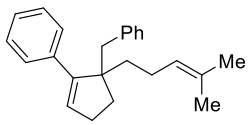

41

(5-benzyl-5-(4-methylpent-3-en-1-yl)cyclopent-1-en-1-yl)benzene (41): The cyclization of **S41** was performed according to the general procedure for metathesis with a reaction time of 48 h (65% yield, 73% conversion by ^{1}H NMR). Purification by flash column chromatography eluting with pentane provided 16.9 mg (59%) of **41** as a clear oil. **^{1}H NMR** (500 MHz; $CDCl_3$) δ 7.51-7.46 (m, 2H), 7.34 (dd, *J* = 8.4, 6.8 Hz, 2H), 7.29-7.26 (m, 1H), 7.18 (td, *J* = 5.8, 2.7 Hz, 3H), 7.13 (dd, J = 7.6, 1.9 Hz, 2H), 5.91 (t, *J* = 2.6 Hz, 1H), 5.09-5.00 (m, 1H), 3.00 (d, *J* = 13.4 Hz, 1H), 2.79 (d, *J* = 13.4 Hz, 1H), 2.17-1.67 (m, 7H), 1.64 (s, 3H), 1.61-1.54 (m, 1H), 1.44 (s, 3H); **^{13}C NMR** (125 MHz; $CDCl_3$) δ 147.4, 139.3, 138.4, 131.7, 131.3, 130.7, 128.4, 127.7, 127.3, 126.9, 125.9, 124.9, 55.1, 46.2, 39.9, 35.0, 30.5, 25.9, 23.6, 17.6. **IR** (Neat) 3028, 2926, 1690, 1602, 1495, 1447, 1377, 1265, 1030, 922, 841, 759, 734, 699. **HRMS** (EI) *m/z*: $[M]^+$ calcd for $C_{24}H_{28}^+$ 316.2186; found 316.2189.

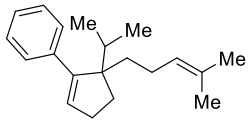

42

(5-isopropyl-5-(4-methylpent-3-en-1-yl)cyclopent-1-en-1-yl)benzene (42): The cyclization of **S42** was performed according to the general procedure for metathesis with a reaction time of 45 h (52% yield, 81% conversion by ^{1}H NMR). Purification by flash column chromatography eluting with pentane provided 12.4 mg (51%) of **42** as a clear oil. **^{1}H NMR** (500 MHz; $CDCl_3$) δ 7.37-7.33 (m, 2H), 7.28 (t, *J* = 7.6 Hz, 2H), 7.24-7.20 (m, 1H), 5.91 (t, *J* = 2.6 Hz, 1H), 5.16-5.09 (m, 1H), 2.43-2.26 (m, 2H), 2.10-2.03 (m, 1H), 1.99-1.87 (m, 3H), 1.72-1.58 (m, 6H), 1.52 (s, 3H), 0.89 (d, *J* = 6.8 Hz, 3H), 0.71 (d, *J* = 6.8 Hz, 3H); **^{13}C NMR** (125 MHz; $CDCl_3$) δ 147.5, 138.9, 131.1, 130.7, 128.2, 127.5, 126.7, 125.3, 58.3, 40.4, 34.4, 31.4, 30.2, 25.9, 24.0, 18.6, 17.8, 17.7. **IR** (Neat) 3035, 2955, 2925, 2848, 1494, 1468, 1443, 1385, 1105, 1075, 1034, 833, 759, 696. **HRMS** (EI) *m/z*: $[M]^+$ calcd for $C_{20}H_{28}^+$ 268.2191; found 268.2195.

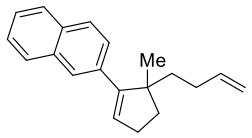

43

2-(5-(but-3-en-1-yl)-5-methylcyclopent-1-en-1-yl)naphthalene (43): The cyclization of **S43** was performed according to the general procedure for metathesis with a reaction time of 18 h. Purification by flash column chromatography eluting with hexanes provided 12.1 mg (46% yield) of **43** as a clear oil. **^{1}H NMR** (500 MHz; $CDCl_3$) δ7.82 (d, *J* = 8.0 Hz, 2H), 7.78-7.77 (m, 2H), 7.49-7.43 (m, 3H), 5.95 (s, 1H), 5.83-5.77 (m, 1H), 4.97 (d, *J* = 17.1 Hz, 1H), 4.90 (d, *J* = 10.2 Hz, 1H), 2.49-2.39 (m, 2H), 2.16-2.02 (m, 3H), 1.86-1.83 (m, 1H), 1.74-1.64 (m, 2H), 1.33 (s, 3H); **^{13}C NMR** (125 MHz; $CDCl_3$) δ 150.5, 139.6, 135.7, 133.4, 132.5, 129.5, 128.2, 127.6, 127.5, 126.6, 126.1, 125.7, 125.6, 114.0, 50.5, 39.8, 38.9, 30.2, 29.6, 26.9. **IR** (Neat) 3057, 2929, 2847, 1639, 1596, 152, 1453, 1373, 1317, 1271, 1191, 1123, 1018, 993, 945, 907, 891, 856, 675. **HRMS** (EI) *m/z*: $[M]^+$ calcd for $C_{20}H_{22}^+$ 262.1722; found 262.1716.

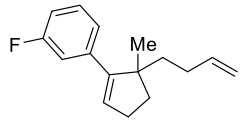

44

1-(5-(but-3-en-1-yl)-5-methylcyclopent-1-en-1-yl)-3-fluorobenzene (44): The cyclization of **S44** was performed according to the general procedure for metathesis with a reaction time of 16 h. Purification by flash column chromatography eluting with hexanes provided 7.6 mg (66% yield) of **44** as a clear o il. **^{1}H NMR** (500 MHz; $CDCl_3$) δ 7.29-7.19 (m, 1H), 7.08 (dd, *J* = 7.8, 1.4 Hz, 1H), 7.01 (dd, *J* = 10.7, 2.2 Hz, 1H), 6.96-6.89 (m, 1H), 5.83 (t, *J* = 2.2 Hz, 1H), 5.82-5.71 (m, 1H), 4.95 (dd, *J* = 17.1, 1.8 Hz, 1H), 4.89 (d, *J* = 10.2 Hz, 1H), 2.50-2.25 (m, 2H), 2.19-1.86 (m, 3H), 1.86-1.69 (m, 1H), 1.69-1.54 (m, 2H), 1.22 (s, 3H); **^{13}C NMR** (125 MHz; $CDCl_3$) δ 162.7 (d, *J* = 244.6 Hz), 149.6, 140.5 (d, *J* = 7.9 Hz), 139.4, 129.9, 129.5 (d, *J* = 8.5 Hz), 123.3 (d, *J* = 2.8 Hz), 114.4 (d, *J* = 21.6 Hz), 114.1, 113.6 (d, *J* = 21.0 Hz), 50.4, 39.6, 38.7, 30.1, 29.5, 26.8. **IR** (Neat) 2929, 2850, 1640, 1610, 1579, 1486, 1455, 1378, 1264, 112, 1157, 1075, 994, 908, 872, 844, 780, 695, 661. **HRMS** (EI) *m/z*: $[M]^+$ calcd for $C_{16}H_{19}F^+$ 230.1471; found 230.1475.

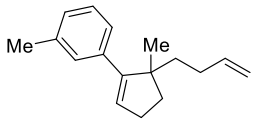

45

1-(5-(but-3-en-1-yl)-5-methylcyclopent-1-en-1-yl)-3-methylbenzene (45): The cyclization of **S45** was performed according to the general procedure for metathesis with a reaction time of 16 h. Purification by flash column chromatography eluting with hexanes provided 13.2 mg (66% yield) of **45** as a clear oil. **^{1}H NMR** (500 MHz; $CDCl_3$) δ 7.19 (t, *J* = 7.6 Hz, 1H), 7.16-7.10 (m, 2H), 7.07 (d, *J* = 6.9 Hz, 1H), 5.81 (ddd, *J* = 17.0, 10.2, 6.6 Hz, 1H), 5.78 (t, *J* = 2.5 Hz, 1H), 4.98 (dd, *J* = 17.1, 1.9 Hz, 1H), 4.90 (dd, *J* = 10.2, 1.1 Hz, 1H), 2.48-2.32 (m, 5H), 2.15-2.05 (m, 1H), 2.01 (ddd, *J* = 12.8, 8.9, 5.9 Hz, 2H), 1.78 (ddd, *J* = 12.5, 8.7, 5.6 Hz, 1H), 1.59 (dt, *J* = 11.1, 5.3 Hz, 2H), 1.23 (s, 3H); **^{13}C NMR** (125 MHz; $CDCl_3$) δ 150.8, 139.7, 138.3, 137.5, 128.6, 128.5, 128.0, 127.5, 124.7, 113.9, 50.4, 39.7, 38.7, 30.1, 29.6, 26.8, 21.7. **IR** (Neat) 3040, 2925, 2849, 1640, 1602, 1581, 1486, 1453, 1372, 1322, 1094, 993, 907, 882, 842, 780, 703, 661. **HRMS** (EI) *m/z*: $[M]^+$ calcd for $C_{17}H_{22}^+$ 226.1722; found 226.1729.

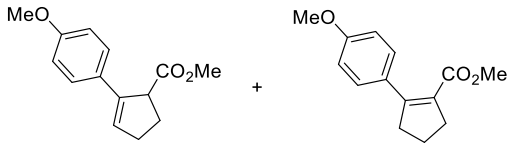

49 **I49** (trace)

methyl 2-(4-methoxyphenyl)cyclopent-2-ene-1-carboxylate (49): The cyclization of **S49**[5] was performed according to the general procedure for metathesis employing (*S*,*S*)-Ph-box as ligand with a reaction time of 24 h (76% yield of **49** + **I49**, 76% conversion by ^{1}H NMR). Purification by flash column chromatography eluting with DCM provided 13 mg (62%) of **49** as a clear oil. The ^{1}H, ^{13}C NMR, IR and HRMS data are consistent with literature reported data.[5]

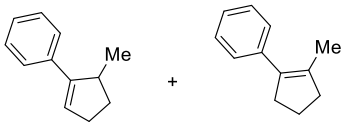

50 **I50**

methyl 2-(4-methoxyphenyl)cyclopent-2-ene-1-carboxylate (50): The cyclization of **S50**[5] was performed according to the general procedure for metathesis employing (*S*,*S*)-Ph-box as ligand with a reaction time of 19 h (60% yield of **50** + **I50** as a 11:1 mixture, 71% conversion by ^{1}H NMR). Purification by flash column chromatography eluting with hexanes provided 7.3 mg (51%) of **50 + I50** as a clear oil. The ^{1}H NMR data of **I50** is consistent with reported data.[5] Characterization data for **50**: **^{1}H NMR** (700 MHz; $CDCl_3$) δ 7.41 (d, *J* = 8.3 Hz, 2H), 7.31 (t, *J* = 7.5 Hz, 2H), 7.24-7.19 (m, 1H), 6.08-6.00 (m, 1H), 3.28-3.17 (m, 1H), 2.56-2.47 (m, 1H), 2.47-2.39 (m, 1H), 2.24 (dddd, *J* = 15.9, 12.3, 8.1, 2.2 Hz, 1H), 1.67-1.63 (m, 1H), 1.09 (d, *J* = 7.0 Hz, 3H); **^{13}C NMR** (176 MHz; $CDCl_3$) δ 148.0, 136.6, 128.4, 126.8, 126.3, 126.0, 39.6, 32.9, 31.3, 19.9. **IR** (Neat) 3036, 2955, 2925, 2848, 1599, 1494, 1468, 1443, 1385, 1106, 1075, 1034, 833, 759, 696. **HRMS** (EI) *m/z*: $[M]^+$ calcd for $C_{12}H_{14}^+$ 158.1096; found 158.1101.

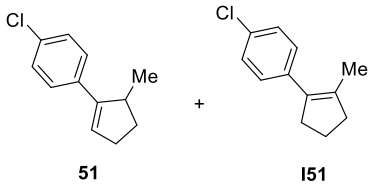

51 **I51**

methyl 2-(4-methoxyphenyl)cyclopent-2-ene-1-carboxylate (51): The cyclization of **S51** was performed according to the general procedure for metathesis employing (*S*,*S*)-Ph-box as ligand

with a reaction time of 19 h (43% yield of **51** + **I51** as a 16:1 mixture, 45% conversion by ^{1}H NMR). Purification by flash column chromatography eluting with hexanes provided 6 mg (35%) of **51 + I51** as a clear oil. Characterization data for **49**: **^{1}H NMR** (700 MHz; $CDCl_3$) δ 7.33 (d, *J* = 8.5 Hz, 2H), 7.27 (d, *J* = 8.6 Hz, 2H), 6.02 (q, *J* = 2.2 Hz, 1H), 3.22-3.12 (m, 1H), 2.57-2.46 (m, 1H), 2.46-2.37 (m, 1H), 2.24 (dtd, *J* = 12.7, 8.8, 7.2 Hz, 1H), 1.65 (ddt, *J* = 12.5, 8.2, 4.0 Hz, 1H), 1.06 (d, *J* = 6.9 Hz, 3H); **^{13}C NMR** (176 MHz; $CDCl_3$) δ 146.9, 135.1, 132.4, 128.6, 127.6, 126.8, 39.6, 32.8, 31.4, 19.8. **IR** (Neat) 3030, 2955, 2867, 2845, 1594, 1490, 1402, 1372, 1331, 1298, 1092, 1012, 966, 919, 820, 804, 775, 719, 671. **HRMS** (EI) *m/z*: $[M]^+$ calcd for $C_{12}H_{13}Cl^+$ 192.0706; found 192.0705.

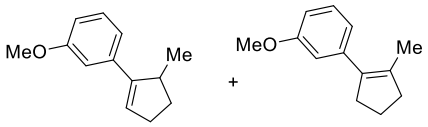

52 I52

methyl 2-(4-methoxyphenyl)cyclopent-2-ene-1-carboxylate (52): The cyclization of **S52** was performed according to the general procedure for metathesis employing (*S,S*)-Ph-box as ligand with a reaction time of 17 h (42% yield of **52** + **I52** as a 20:1 mixture, 68% conversion by ^{1}H NMR). Purification by flash column chromatography eluting with DCM provided 6.1 mg (36%) of **52 + I52** as a clear oil. The ^{1}H NMR data of **I52** is consistent with reported data.[9] Characterization data for **50**: **^{1}H NMR** (700 MHz; $CDCl_3$) δ 7.23 (t, *J* = 7.9 Hz, 1H), 7.01 (d, *J* = 7.6 Hz, 1H), 6.95 (t, *J* = 2.1 Hz, 1H), 6.77 (dd, *J* = 7.8, 2.6 Hz, 1H), 6.04 (td, *J* = 2.7, 1.4 Hz, 1H), 3.82 (s, 3H), 3.20 (dddd, *J* = 10.9, 5.2, 2.6, 1.3 Hz, 1H), 2.56-2.47 (m, 1H), 2.46-2.38 (m, 1H), 2.24 (dddt, *J* = 15.4, 9.7, 7.4, 4.9 Hz, 1H), 1.64 (ddt, *J* = 12.5, 8.3, 4.0 Hz, 1H), 1.09 (d, *J* = 6.9 Hz, 3H); **^{13}C NMR** (176 MHz; $CDCl_3$) δ 159.7, 147.9, 138.1, 129.4, 126.5, 118.9, 112.2, 112.1, 55.3, 39.7, 32.8, 31.3, 19.9. **IR** (Neat) 2953, 2865, 2843, 1599, 1577, 1486, 1452, 1430, 1287, 1265, 1214, 1050, 981, 874, 819, 774, 692. **HRMS** (APCI) *m/z*: $[M+H]^+$ calcd for $C_{13}H_{17}O^+$ 189.1274; found 189.1272.

3.4.6 FT-IR Experiments

Transmission IR spectra were recorded on PerkinElmer Frontier MIR spectrometer using ATR FlowThru attachment.

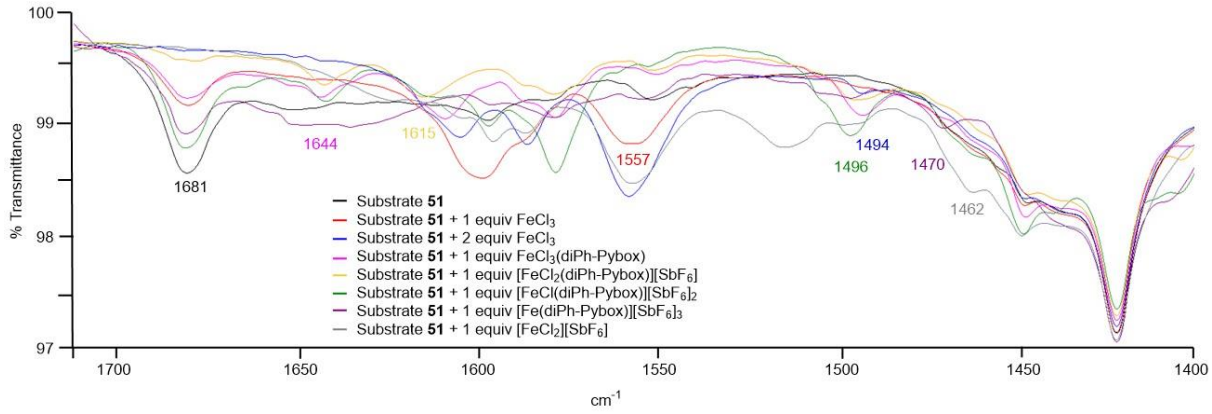

Figure 3.14. FT-IR data for Lewis acid carbonyl activation of **51**.

Figure 3.14 Details: IR measurements of compound X with A) no additive; B) 1 equiv. of $FeCl_3$; C) 2 equiv. $FeCl_3$; D) 1 equiv $FeCl_3$ + 1 equiv ligand **18b**; E) 1 equiv $FeCl_3$ + 1 equiv ligand **18b** + 1 equiv $AgSbF_6$; F) 1 equiv $FeCl_3$ + 1 equiv ligand **18b** + 2 equiv $AgSbF_6$; G) 1 equiv $FeCl_3$ + 1 equiv ligand **18b** + 3 equiv $AgSbF_6$; H) 1 equiv $FeCl_3$ + 1 equiv $AgSbF_6$.

A) Compound 51 with no additive: To a 1-dram vial was added **51** (5.0 mg, 0.02 mmol) along with 1 mL DCM. Then 150 µL was transferred via syringe into ATR FlowThru attachment and the spectrum was taken immediately.

B) Compound 51 with 1 equiv $FeCl_3$: $FeCl_3$ (3.7 mg, 0.02 mmol) was dissolved in 0.5 mL DCM inside of a 1-dram vial. In a second 1-dram vial was added **51** (5.0 mg, 0.02 mmol) along with 0.5 mL DCM. The resulting solution was added to the vial containing dissolved $FeCl_3$ and the solution was mixed. Then 150 µL was transferred via syringe into ATR FlowThru attachment and the spectrum was taken immediately.

C) Compound 51 with 2 equiv $FeCl_3$: $FeCl_3$ (7.4 mg, 0.04 mmol) was dissolved in 0.5 mL DCM inside of a 1-dram vial. In a second 1-dram vial was added **51** (5.0 mg, 0.02 mmol) along with 0.5 mL DCM. The resulting solution was added to the vial containing dissolved $FeCl_3$ and the solution was mixed. Then 150 µL was transferred via syringe into ATR FlowThru attachment and the spectrum was taken immediately.

D) Compound 51 with 1 equiv $FeCl_3$ + 1 equiv diPh-Pybox (18b): $FeCl_3$ (3.7 mg, 0.02 mmol) and ligand **18b** (12.0 mg, 0.02 mmol) were dissolved in 0.5 mL DCM inside of a 1-dram vial. In a second 1-dram vial was added **51** (5.0 mg, 0.02 mmol) along with 0.5 mL DCM. The

resulting solution was added to the vial containing dissolved $FeCl_3$ and the solution was mixed. Then 150 μL was transferred via syringe into ATR FlowThru attachment and the spectrum was taken immediately.

E) Compound 51 with 1 equiv $FeCl_3$ + 1 equiv diPh-Pybox (18b) + 1 equiv $AgSbF_6$: $FeCl_3$ (3.7 mg, 0.02 mmol), ligand **18b** (12.0 mg, 0.02 mmol) and $AgSbF_6$ (7.9 mg, 0.02 mmol) were dissolved in 0.5 mL DCM inside of a 1-dram vial. In a second 1-dram vial was added **51** (5.0 mg, 0.02 mmol) along with 0.5 mL DCM. The resulting solution was added to the vial containing dissolved $FeCl_3$ and the solution was mixed. Then 150 μL was transferred via syringe into ATR FlowThru attachment and the spectrum was taken immediately.

F) Compound 51 with 1 equiv $FeCl_3$ + 1 equiv diPh-Pybox (18b) + 2 equiv $AgSbF_6$: $FeCl_3$ (3.7 mg, 0.02 mmol), ligand **18b** (12.0 mg, 0.02 mmol) and $AgSbF_6$ (15.8 mg, 0.04 mmol) were dissolved in 0.5 mL DCM inside of a 1-dram vial. In a second 1-dram vial was added **51** (5.0 mg, 0.02 mmol) along with 0.5 mL DCM. The resulting solution was added to the vial containing dissolved $FeCl_3$ and the solution was mixed. Then 150 μL was transferred via syringe into ATR FlowThru attachment and the spectrum was taken immediately.

G) Compound 51 with 1 equiv $FeCl_3$ + 1 equiv diPh-Pybox (18b) + 3 equiv $AgSbF_6$: $FeCl_3$ (3.7 mg, 0.02 mmol), ligand **18b** (12.0 mg, 0.02 mmol) and $AgSbF_6$ (23.7 mg, 0.06 mmol) were dissolved in 0.5 mL DCM inside of a 1-dram vial. In a second 1-dram vial was added **51** (5.0 mg, 0.02 mmol) along with 0.5 mL DCM. The resulting solution was added to the vial containing dissolved $FeCl_3$ and the solution was mixed. Then 150 μL was transferred via syringe into ATR FlowThru attachment and the spectrum was taken immediately.

H) Compound 51 with 1 equiv $FeCl_3$ + 1 equiv $AgSbF_6$: $FeCl_3$ (3.7 mg, 0.02 mmol) and $AgSbF_6$ (7.9 mg, 0.02 mmol) were dissolved in 0.5 mL DCM inside of a 1-dram vial. In a second 1-dram vial was added **51** (5.0 mg, 0.02 mmol) along with 0.5 mL DCM. The resulting solution was added to the vial containing dissolved $FeCl_3$ and the solution was mixed. Then 150 μL was transferred via syringe into ATR FlowThru attachment and the spectrum was taken immediately.

3.4.7 ^{1}H and ^{13}C NMR Spectra

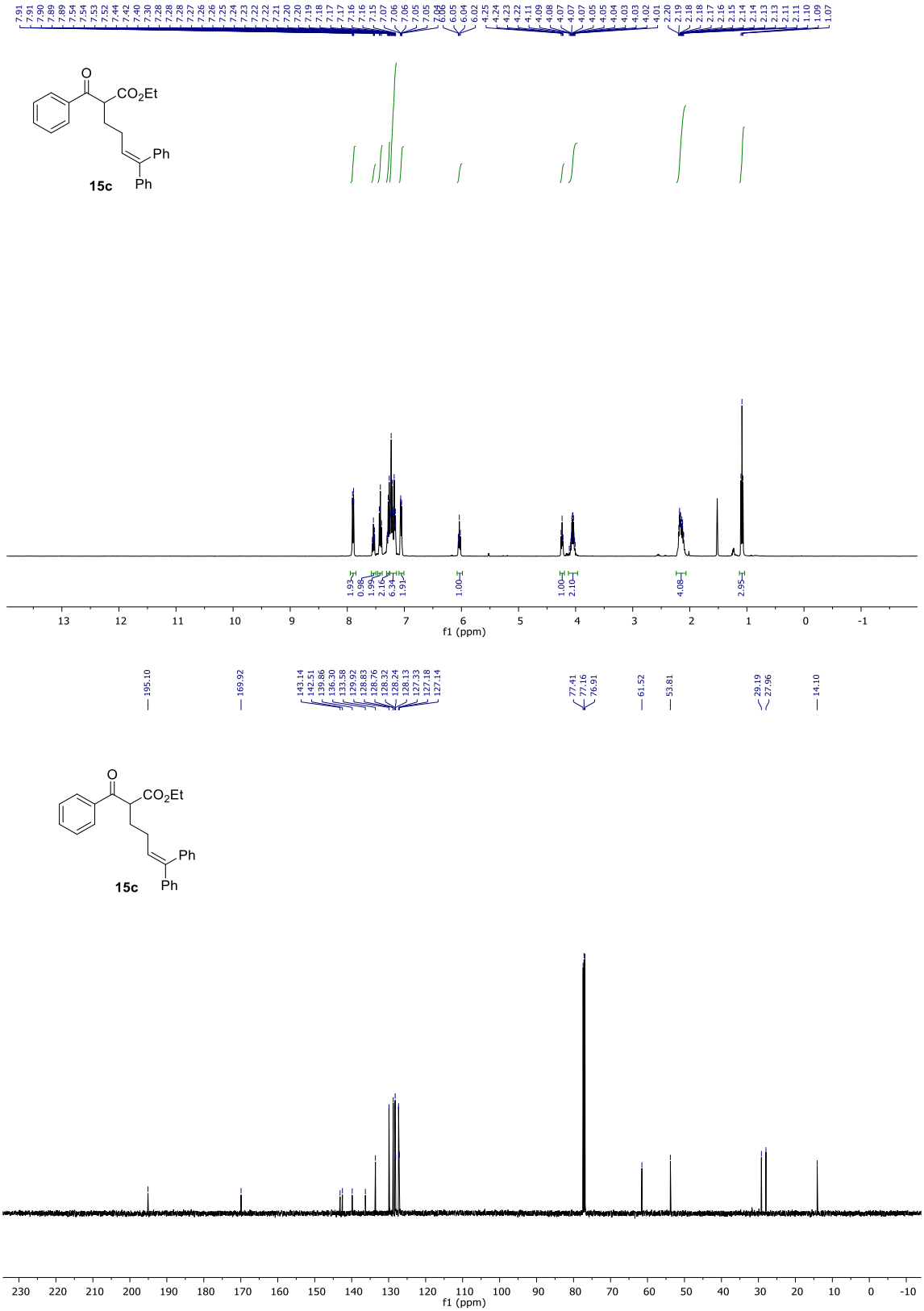

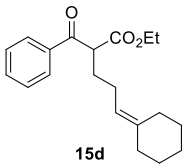
O
CO2Et

15d

7.98
7.97
7.97
7.59
7.58
7.56
7.49
7.47
7.46
7.26
5.07
5.06
5.05
4.33
4.32
4.31
4.31
4.17
4.17
4.16
4.14
4.13
2.09
2.08
2.08
2.07
2.07
2.06
2.05
2.04
2.03
2.02
2.02
2.01
2.01
2.00
2.00
1.51
1.51
1.50
1.43
1.42
1.19
1.18
1.16
1.90
1.13
1.97
1.00
1.02
1.93
8.48
4.43
2.25
2.83
f1 (ppm)


195.60
170.22
141.77
136.42
133.52
128.82
128.77
119.73
77.42
77.16
76.91
61.43
53.53
37.32
29.44
28.78
27.90
27.00
25.11
14.18

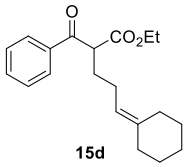
O
CO2Et

15d

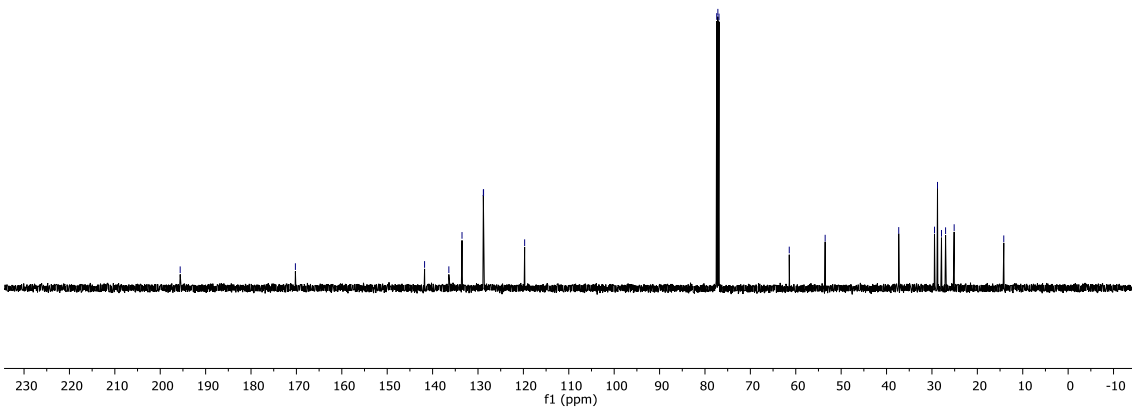
f1 (ppm)

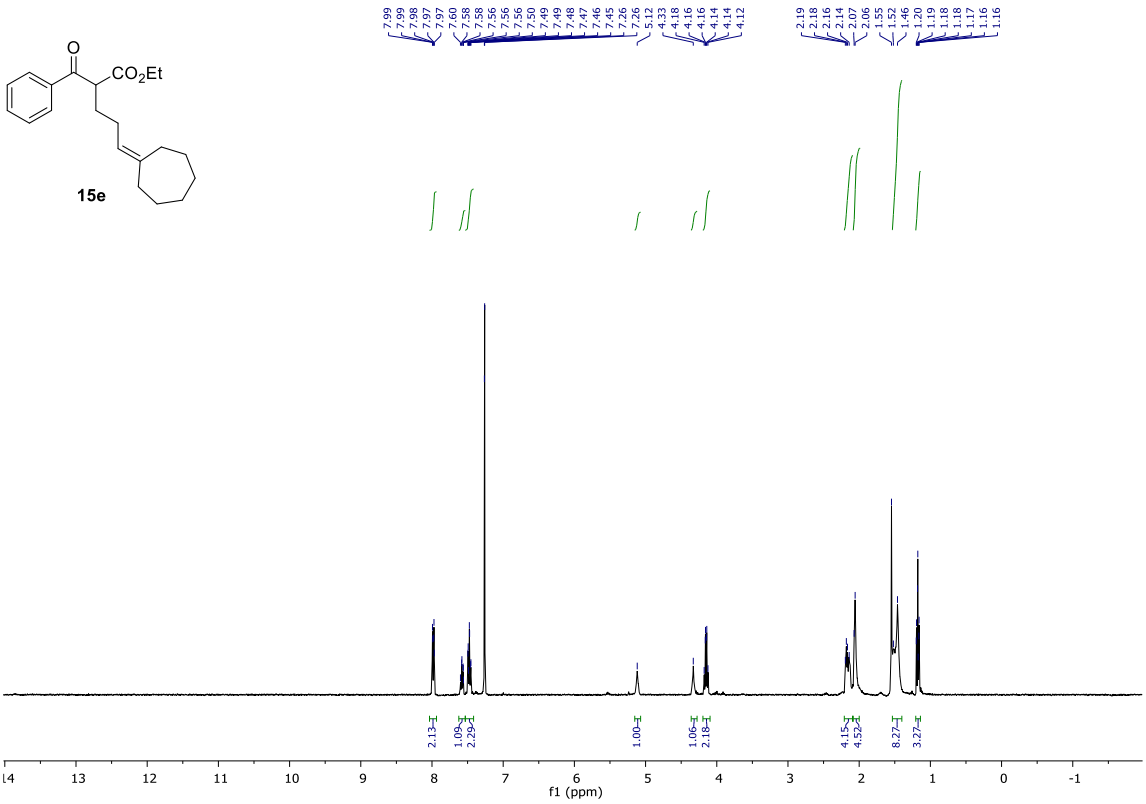
O
CO2Et
15e
7.99
7.99
7.98
7.97
7.97
7.60
7.58
7.58
7.56
7.56
7.56
7.50
7.49
7.49
7.48
7.47
7.46
7.45
7.26
5.12
4.33
4.18
4.16
4.16
4.14
4.14
4.12
2.19
2.18
2.16
2.14
2.07
2.06
1.55
1.52
1.46
1.20
1.19
1.18
1.18
1.17
1.16
1.16
2.13
1.09
2.29
1.00
1.06
2.18
4.15
4.52
8.27
3.27
f1 (ppm)

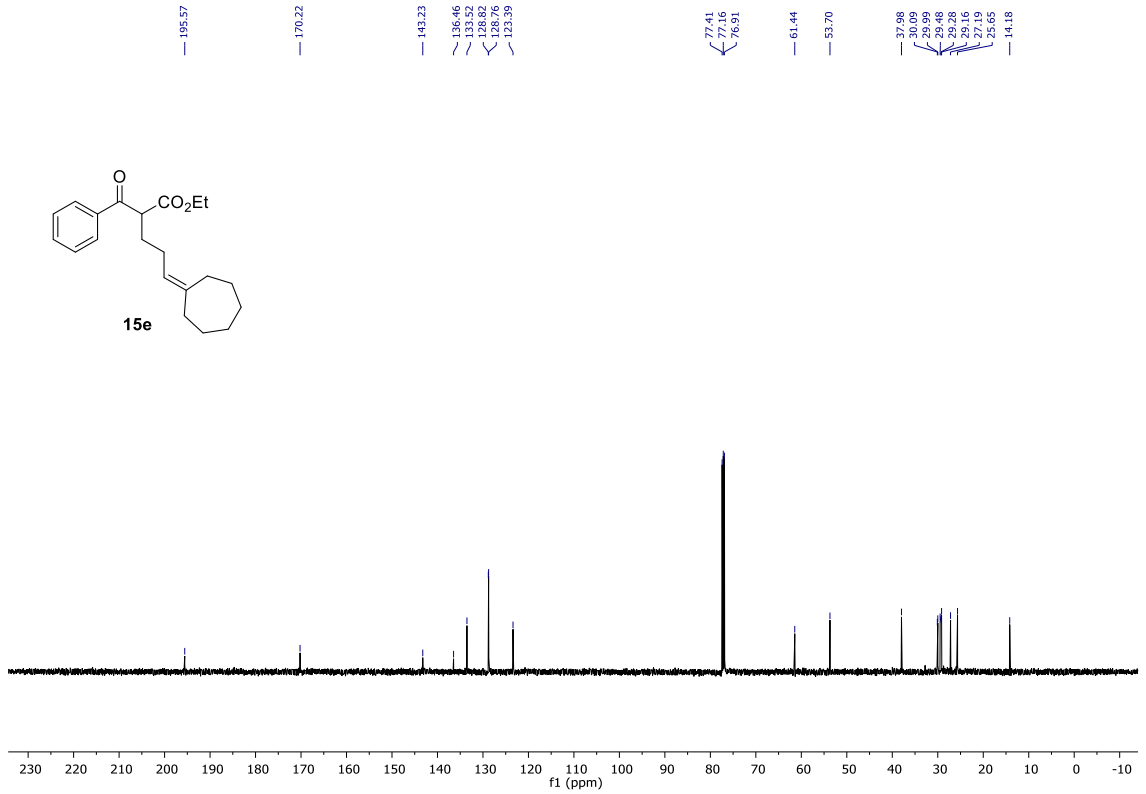
195.57
170.22
143.23
136.46
133.52
128.82
128.76
123.39
77.41
77.16
76.91
61.44
53.70
37.98
30.09
29.99
29.48
29.28
29.16
27.19
25.65
14.18
O
CO2Et
15e
f1 (ppm)

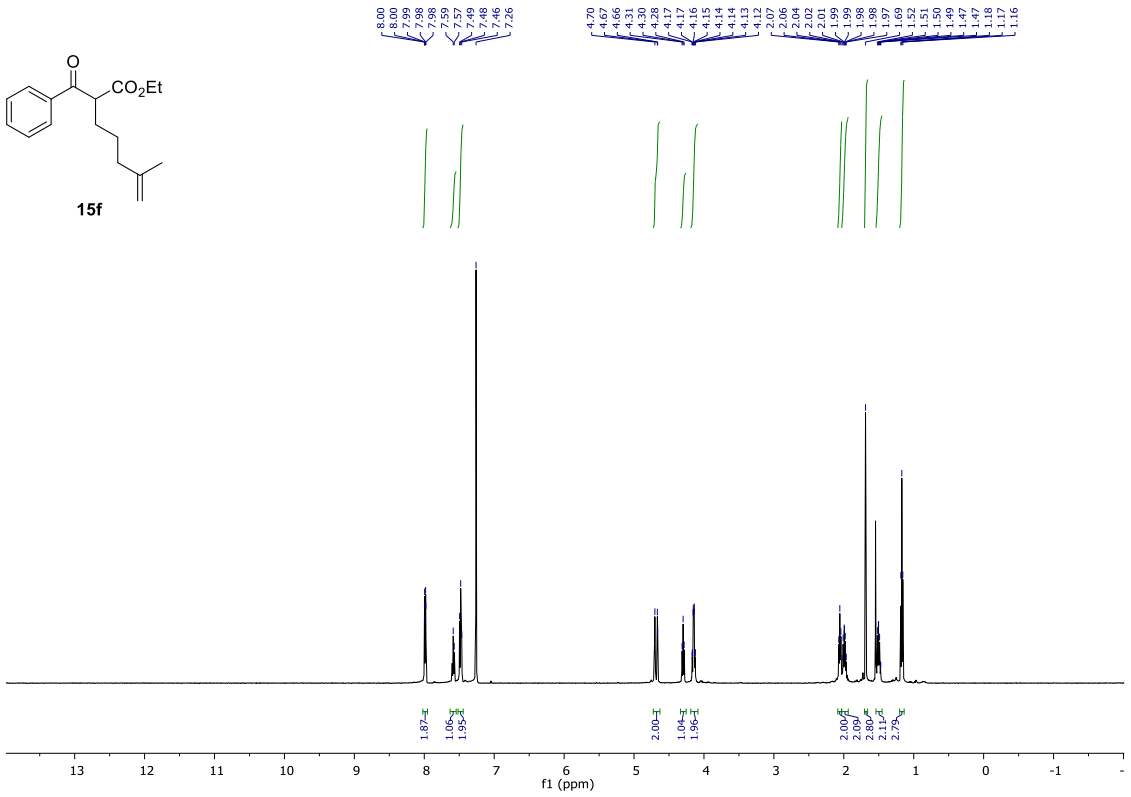
8.00
8.00
7.99
7.98
7.98
7.59
7.57
7.49
7.48
7.46
7.26
4.70
4.67
4.66
4.31
4.30
4.28
4.17
4.17
4.16
4.15
4.14
4.14
4.13
4.12
2.07
2.06
2.04
2.02
2.01
1.99
1.99
1.98
1.98
1.97
1.69
1.52
1.51
1.50
1.49
1.47
1.47
1.18
1.17
1.16
O
CO2Et
15f
1.87
1.06
1.95
2.00
1.04
1.96
2.00
2.09
2.80
2.11
2.79
13 12 11 10 9 8 7 6 5 4 3 2 1 0 -1
f1 (ppm)

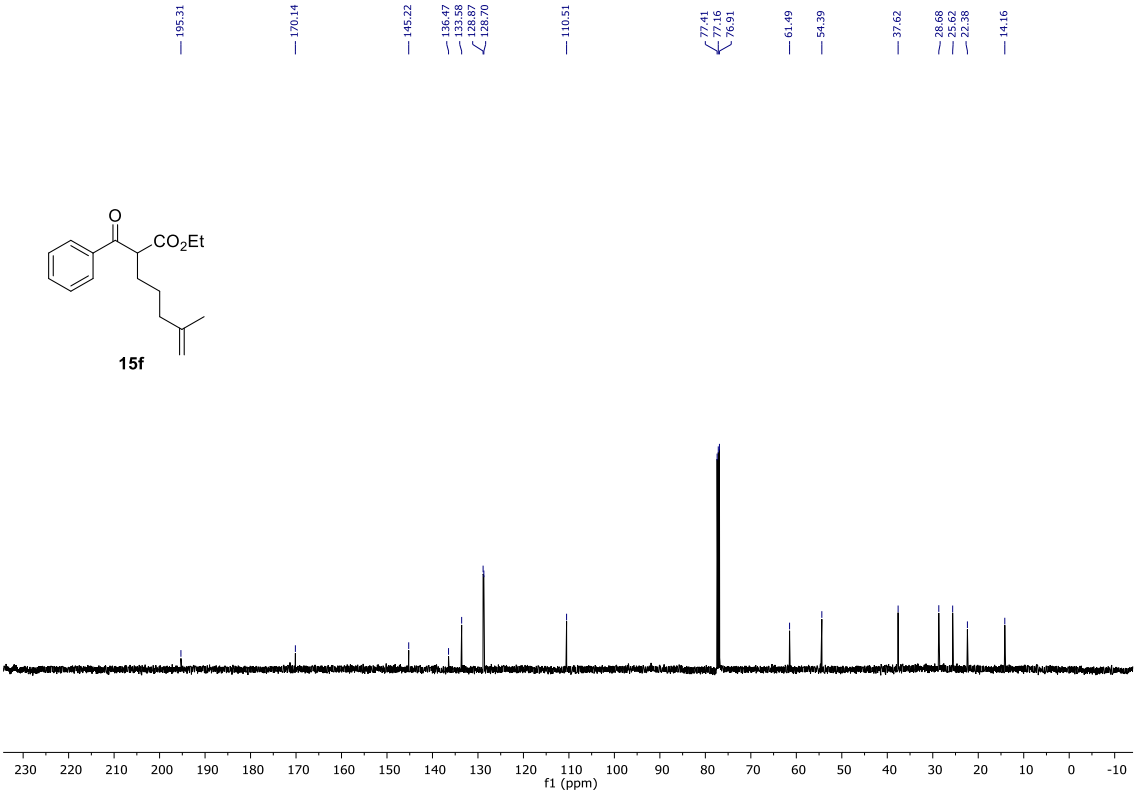
195.31
170.14
145.22
136.47
133.58
128.87
128.70
110.51
77.41
77.16
76.91
61.49
54.39
37.62
28.68
25.62
22.38
14.16
O
CO2Et
15f
230 220 210 200 190 180 170 160 150 140 130 120 110 100 90 80 70 60 50 40 30 20 10 0 -10
f1 (ppm)

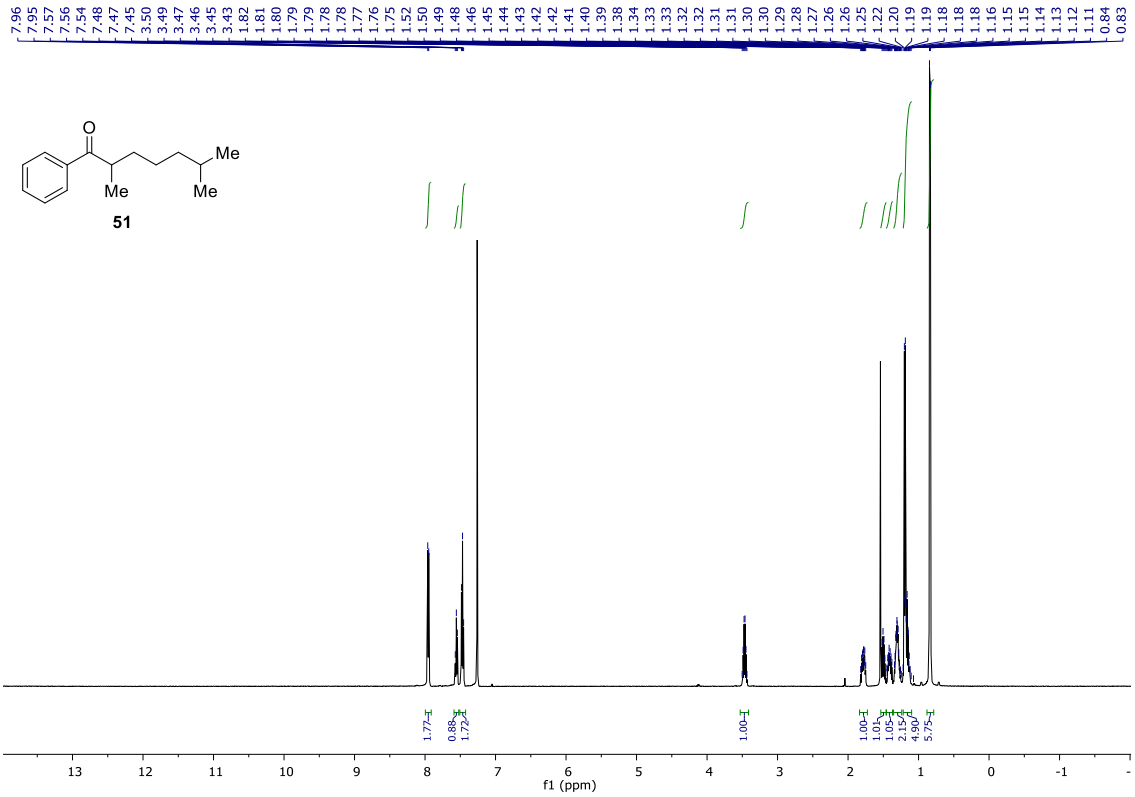
7.96 7.95 7.57 7.56 7.54 7.48 7.47 7.45 3.50 3.49 3.47 3.46 3.45 3.43 1.82 1.81 1.80 1.79 1.79 1.78 1.78 1.77 1.76 1.75 1.52 1.50 1.49 1.48 1.46 1.45 1.44 1.43 1.42 1.42 1.41 1.40 1.39 1.38 1.34 1.33 1.33 1.32 1.32 1.31 1.31 1.30 1.30 1.29 1.28 1.27 1.26 1.26 1.25 1.22 1.20 1.19 1.19 1.18 1.18 1.18 1.16 1.15 1.15 1.14 1.13 1.12 1.11 0.84 0.83
O
Me
Me
Me
51
1.77
0.88
1.72
1.00
1.00
1.01
1.05
2.15
4.90
5.75
13 12 11 10 9 8 7 6 5 4 3 2 1 0 -1
f1 (ppm)

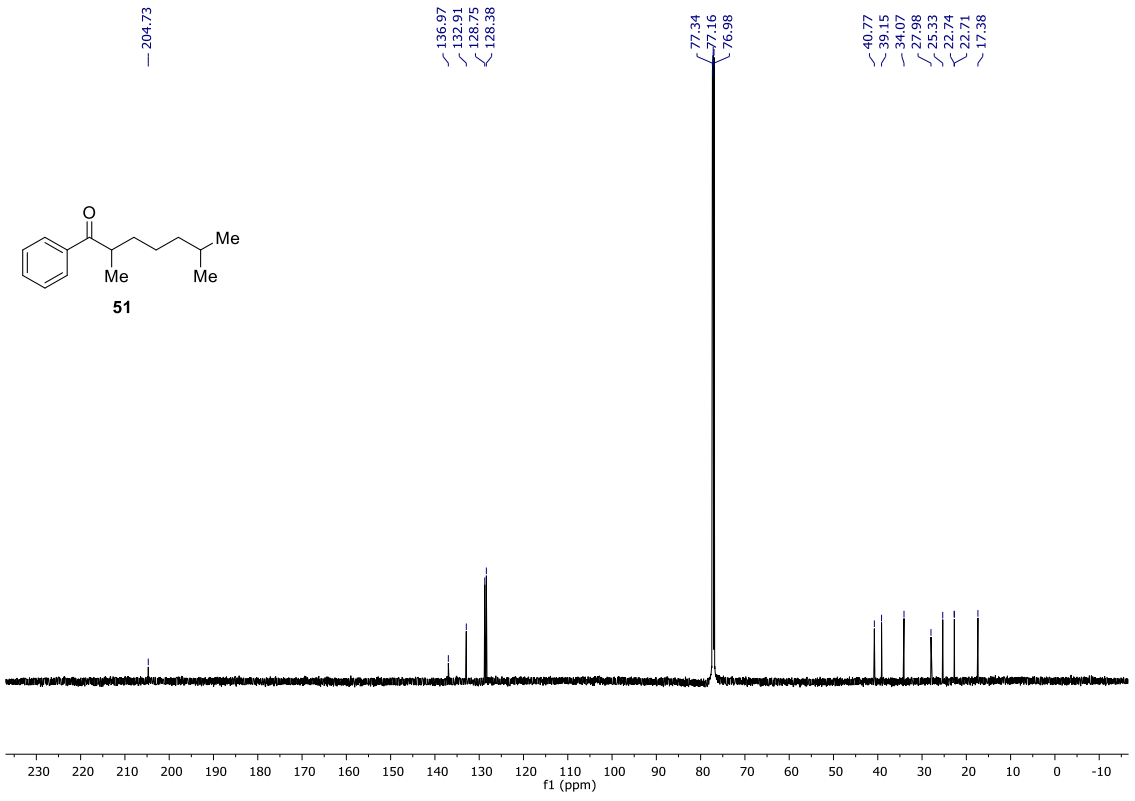
204.73
136.97
132.91
128.75
128.38
77.34
77.16
76.98
40.77
39.15
34.07
27.98
25.33
22.74
22.71
17.38
O
Me
Me
Me
51
230 220 210 200 190 180 170 160 150 140 130 120 110 100 90 80 70 60 50 40 30 20 10 0 -10
f1 (ppm)

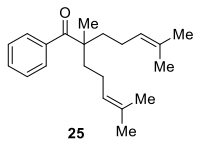
O
Me
Me
Me
Me
Me

25

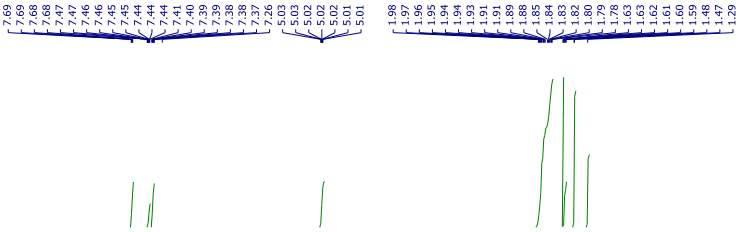
7.69
7.69
7.68
7.68
7.47
7.47
7.46
7.46
7.45
7.45
7.44
7.44
7.44
7.41
7.40
7.39
7.39
7.38
7.38
7.37
7.26
5.03
5.02
5.02
5.01
5.01
1.98
1.97
1.96
1.95
1.94
1.94
1.93
1.91
1.91
1.89
1.88
1.85
1.84
1.83
1.82
1.80
1.79
1.78
1.65
1.65
1.62
1.61
1.60
1.59
1.48
1.47
1.29

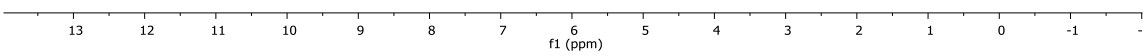
2.00
1.04
1.93
2.00
6.52
6.61
2.01
6.00
3.20
13
12
11
10
9
8
7
6
5
4
3
2
1
0
-1
f1 (ppm)


208.64
139.66
132.01
130.99
128.26
127.66
124.11
77.41
77.16
76.91
51.61
39.95
25.79
23.39
22.69
17.63

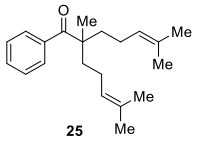
O
Me
Me
Me
Me
Me

25

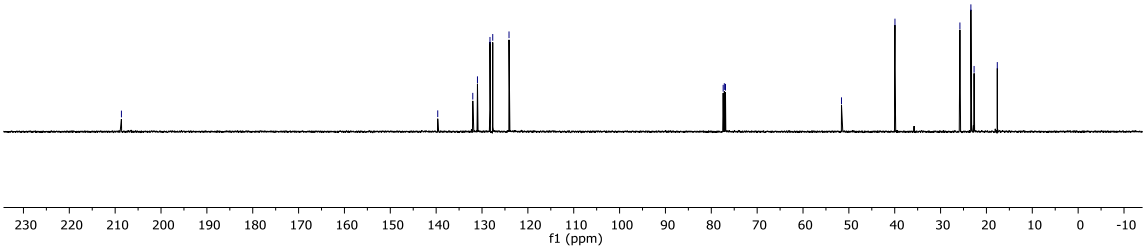
230
220
210
200
190
180
170
160
150
140
130
120
110
100
90
80
70
60
50
40
30
20
10
0
-10
f1 (ppm)

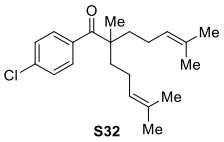
O
Me
Me
Me
Cl
Me
Me

S32

7.68
7.67
7.66
7.66
7.38
7.38
7.36
7.36
7.26
5.02
5.02
5.01
5.01
5.00
5.00
4.99
4.99
4.99
1.97
1.96
1.94
1.93
1.92
1.92
1.91
1.89
1.88
1.87
1.86
1.81
1.80
1.79
1.78
1.77
1.76
1.76
1.65
1.63
1.63
1.62
1.61
1.60
1.59
1.48
1.46
1.28
2.00
1.87
1.95
6.49
8.95
6.02
3.61
13
12
11
10
9
8
7
6
5
4
3
2
1
0
-1
f1 (ppm)


207.04
137.63
137.37
132.21
129.27
128.56
123.94
77.41
77.16
76.91
51.67
40.03
25.79
23.38
22.68
17.67

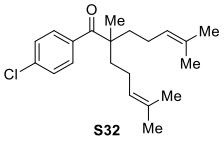
O
Me
Me
Me
Cl
Me
Me

S32

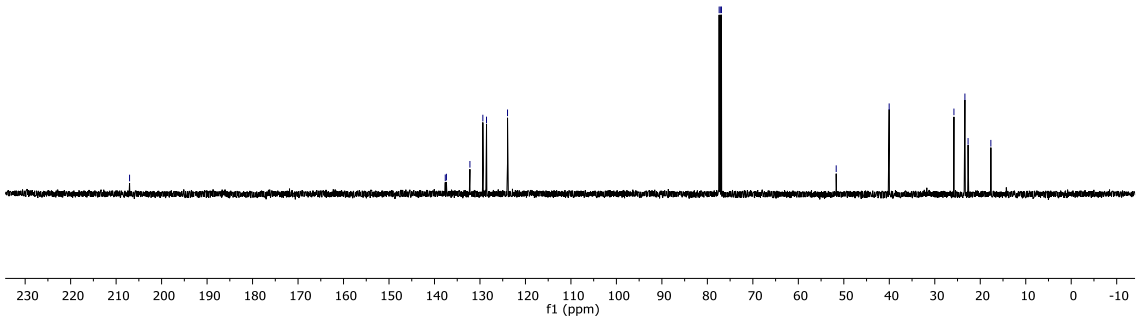
230
220
210
200
190
180
170
160
150
140
130
120
110
100
90
80
70
60
50
40
30
20
10
0
-10
f1 (ppm)

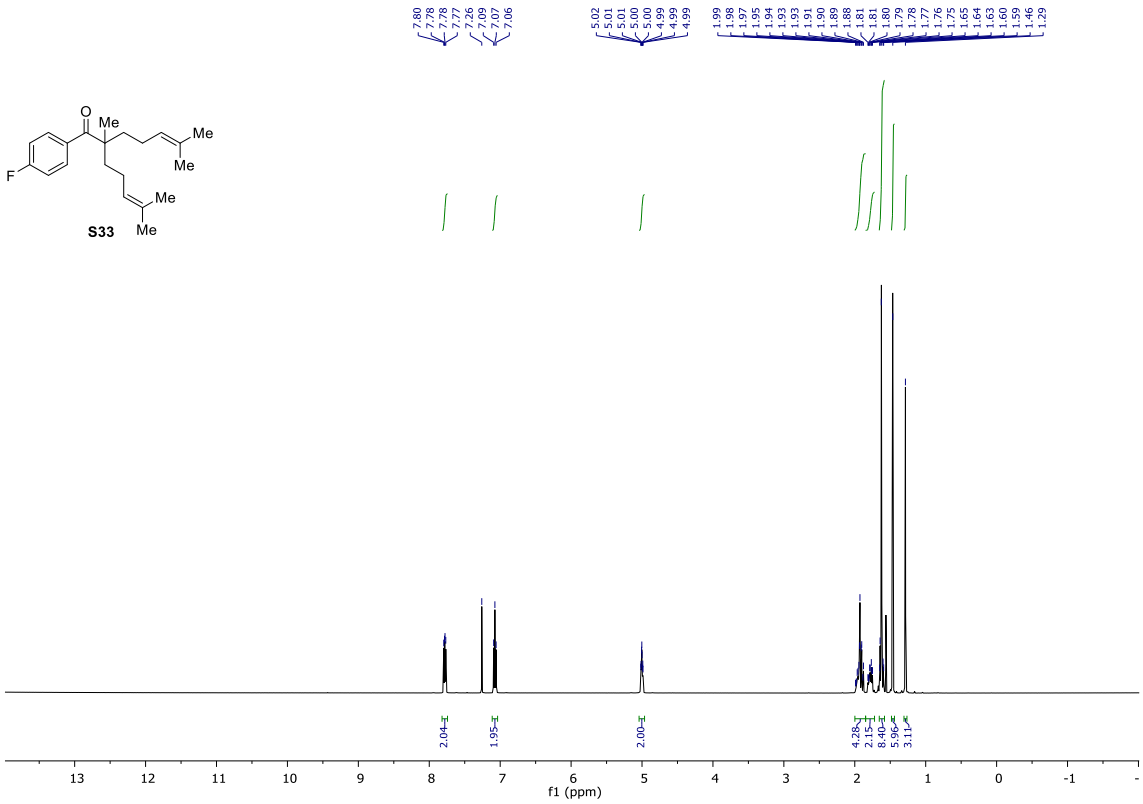
7.80
7.78
7.78
7.77
7.26
7.09
7.07
7.06
5.02
5.01
5.01
5.00
5.00
4.99
4.99
4.99
1.99
1.98
1.97
1.95
1.94
1.93
1.93
1.91
1.90
1.89
1.88
1.81
1.80
1.79
1.78
1.77
1.76
1.75
1.65
1.64
1.63
1.60
1.59
1.46
1.29
O
Me
Me
Me
F
Me
Me
S33
2.04
1.95
2.00
4.28
2.15
8.40
5.96
3.11
f1 (ppm)

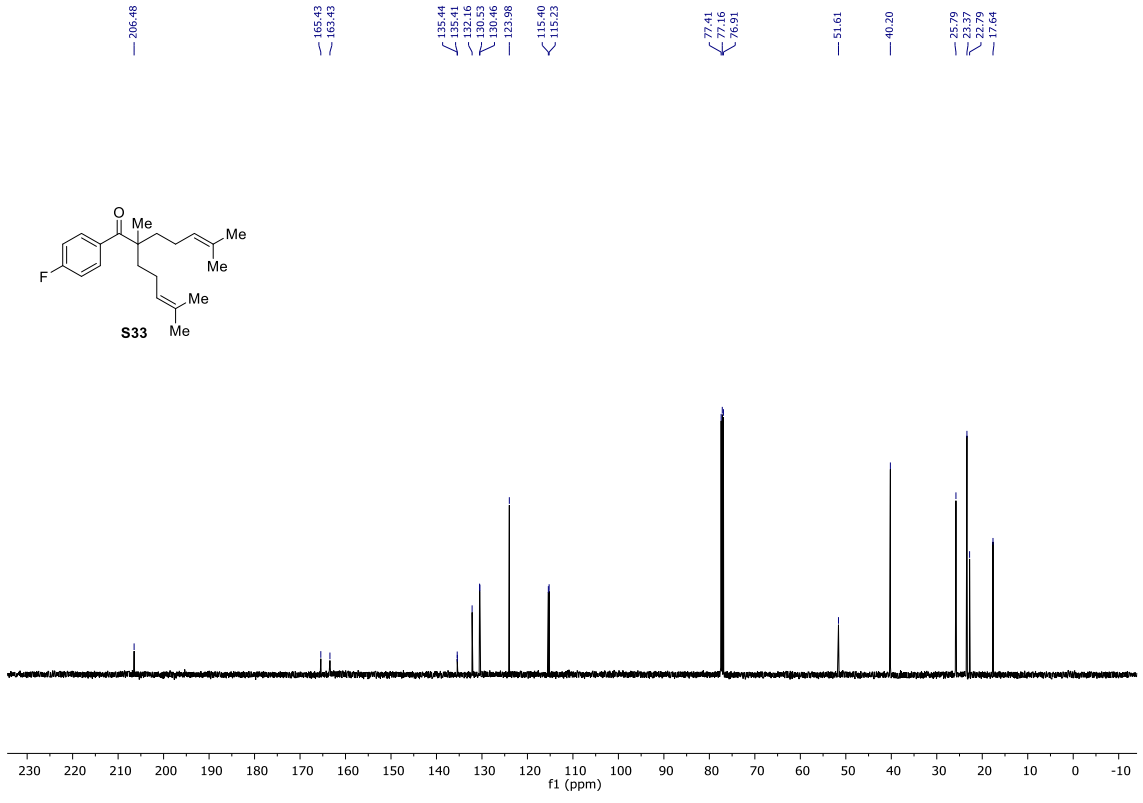
206.48
165.43
163.43
135.44
135.41
132.16
130.53
130.46
123.98
115.40
115.23
77.41
77.16
76.91
51.61
40.20
25.79
23.37
22.79
17.64
O
Me
Me
Me
F
Me
Me
S33
f1 (ppm)

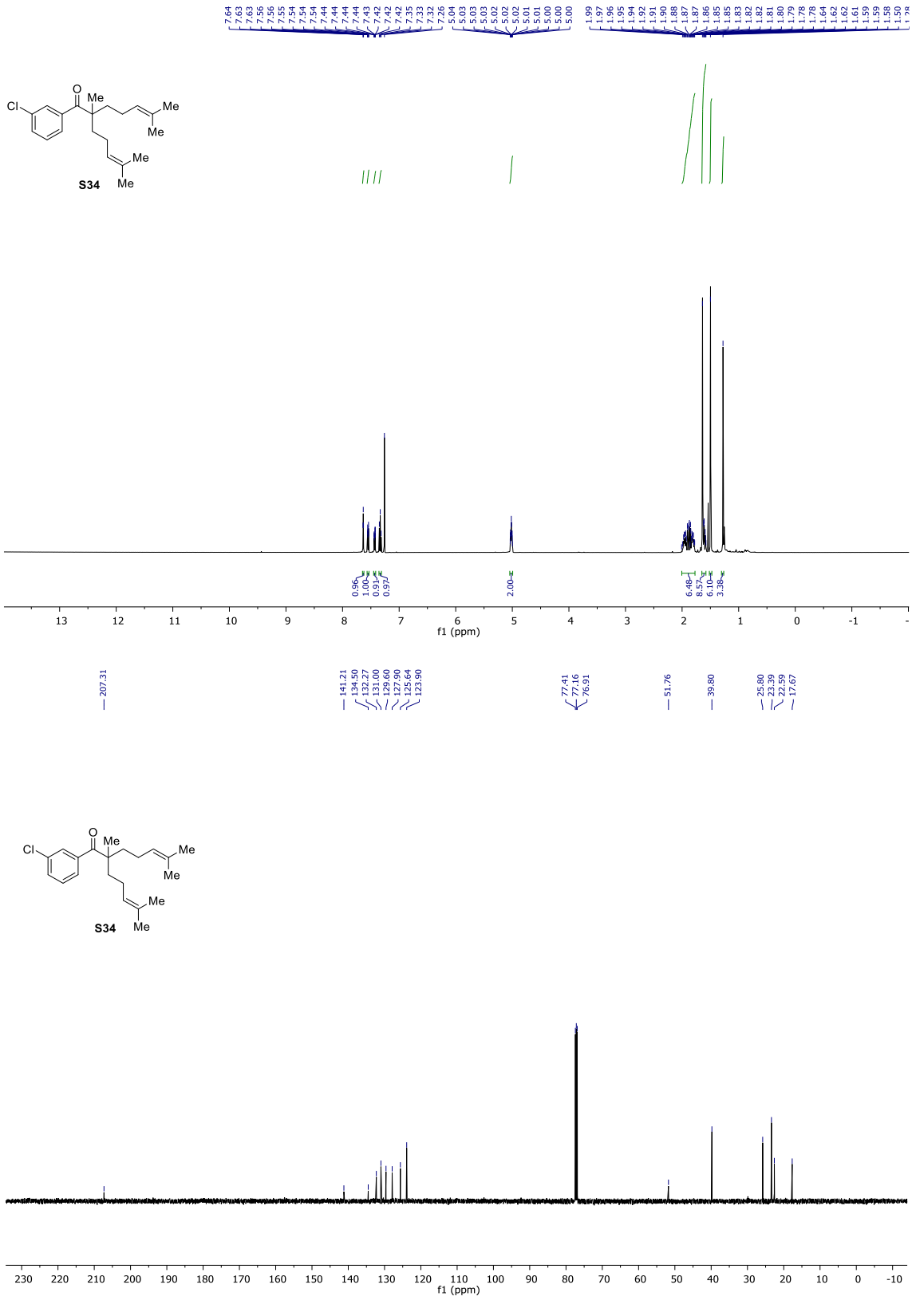
S34
f1 (ppm)
S34
f1 (ppm)

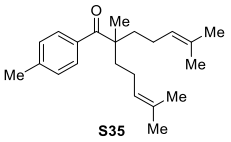
O
Me
Me
Me
Me
Me
Me

S35

7.65
7.64
7.26
7.20
7.18
5.02
5.01
5.01
5.00
2.38
1.94
1.93
1.92
1.92
1.81
1.80
1.78
1.77
1.63
1.63
1.62
1.61
1.59
1.47
1.28
2.04
1.99
2.00
3.09
4.19
2.06
8.66
6.06
3.16
13
12
11
10
9
8
7
6
5
4
3
2
1
0
-1
f1 (ppm)

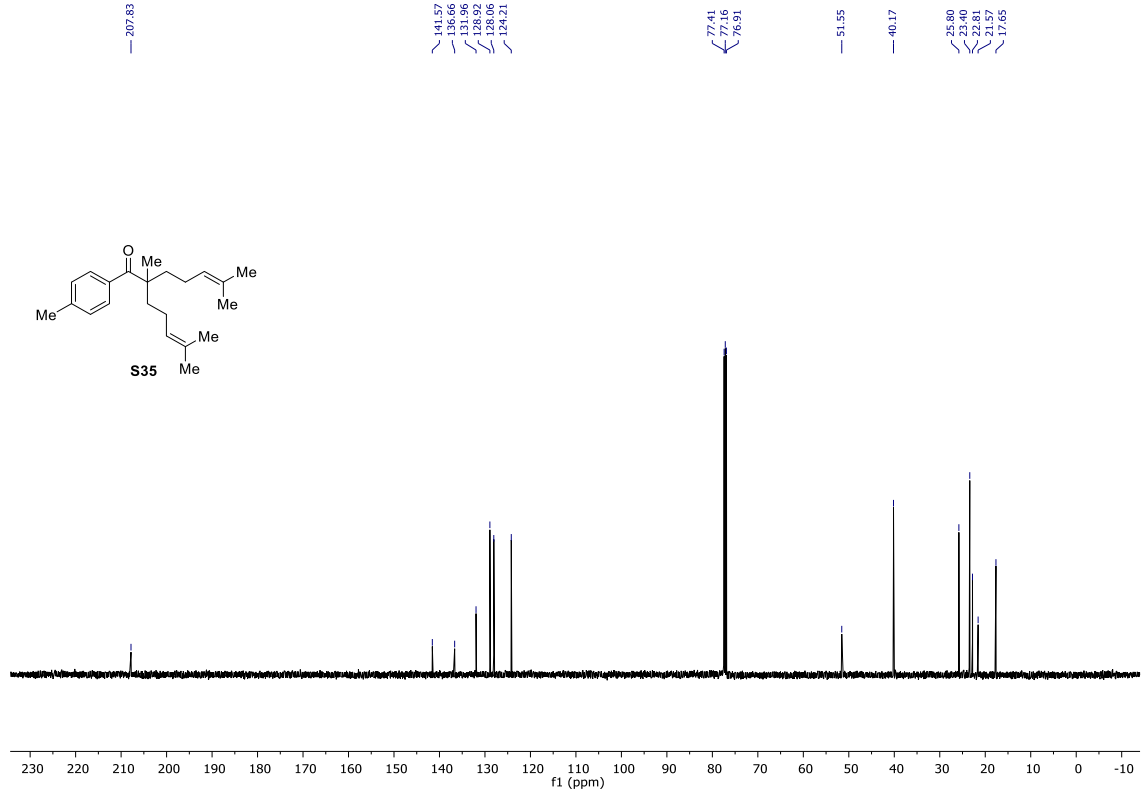
207.83
141.57
136.66
131.96
128.92
128.06
124.21
77.41
77.16
76.91
51.55
40.17
25.80
23.40
21.81
21.57
17.65
230
220
210
200
190
180
170
160
150
140
130
120
110
100
90
80
70
60
50
40
30
20
10
0
-10
f1 (ppm)

O
Me
Me
Me
Me
Me
Me

S35

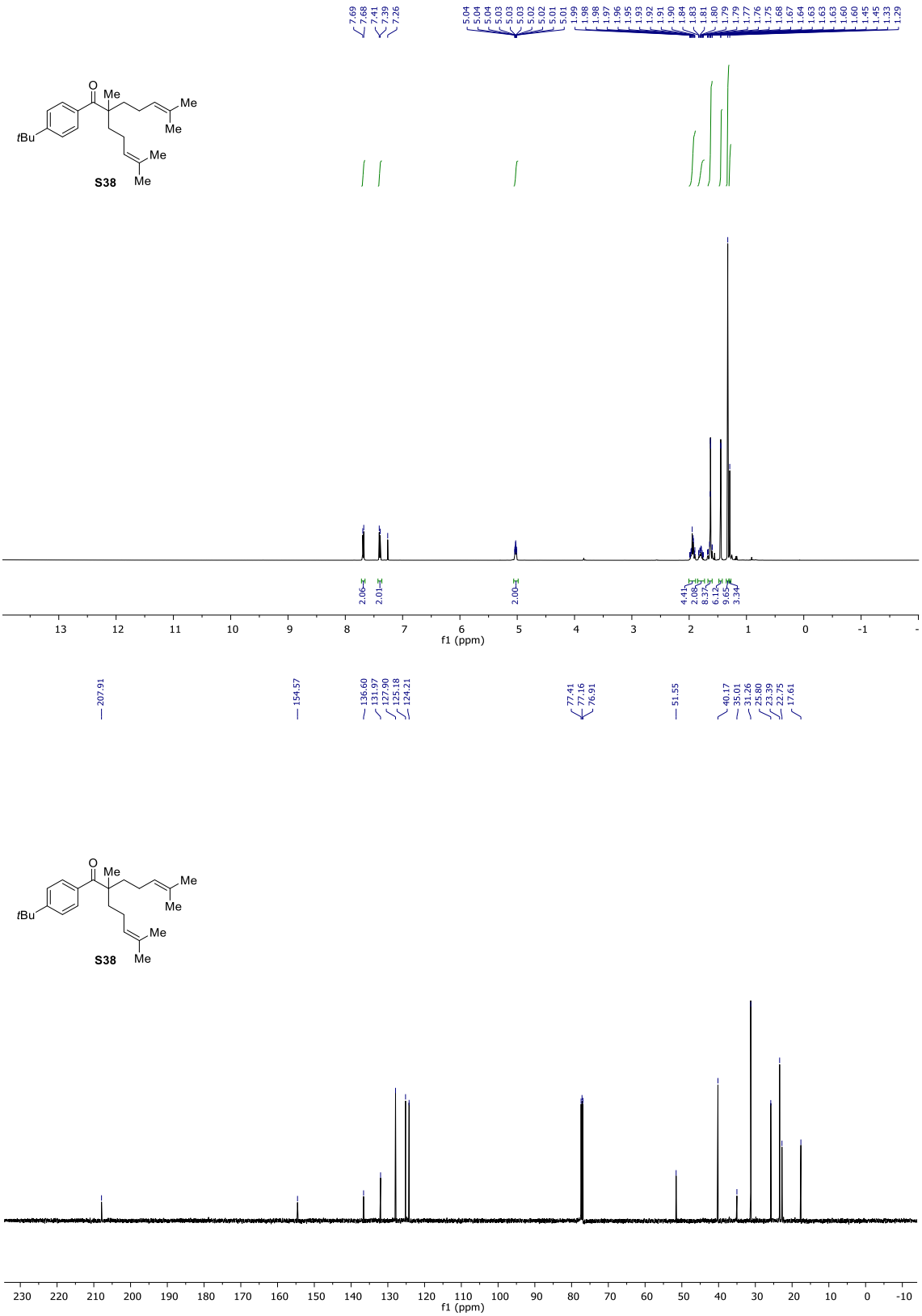
S38
f1 (ppm)
S38
f1 (ppm)

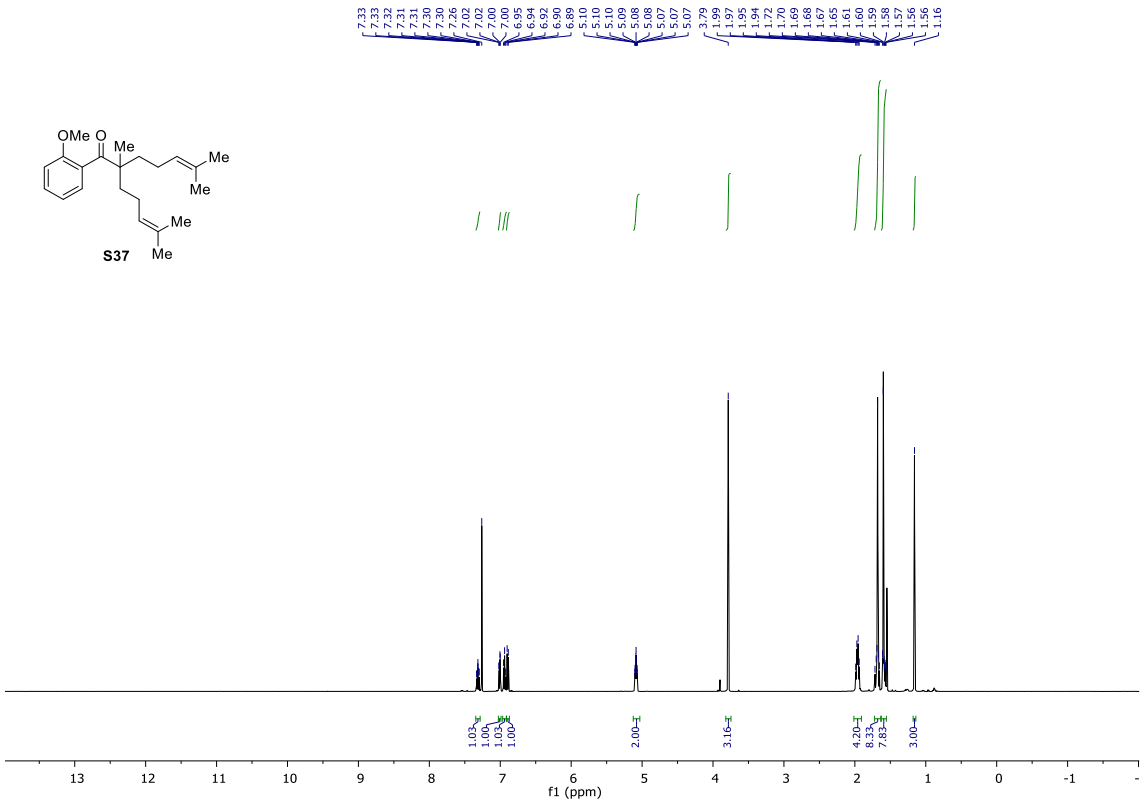
OMe O
Me
Me
Me
Me
Me
S37
7.33 7.33 7.32 7.31 7.31 7.30 7.30 7.26 7.02 7.02 7.00 7.00 6.95 6.94 6.92 6.90 6.89
5.10 5.10 5.10 5.09 5.08 5.08 5.07 5.07 5.07
3.79
1.99 1.97 1.95 1.94 1.72 1.70 1.69 1.68 1.67 1.65 1.61 1.60 1.59 1.58 1.57 1.56 1.56 1.16
1.03 1.00 1.03 1.00 2.00 3.16 4.20 8.33 7.83 3.00
f1 (ppm)

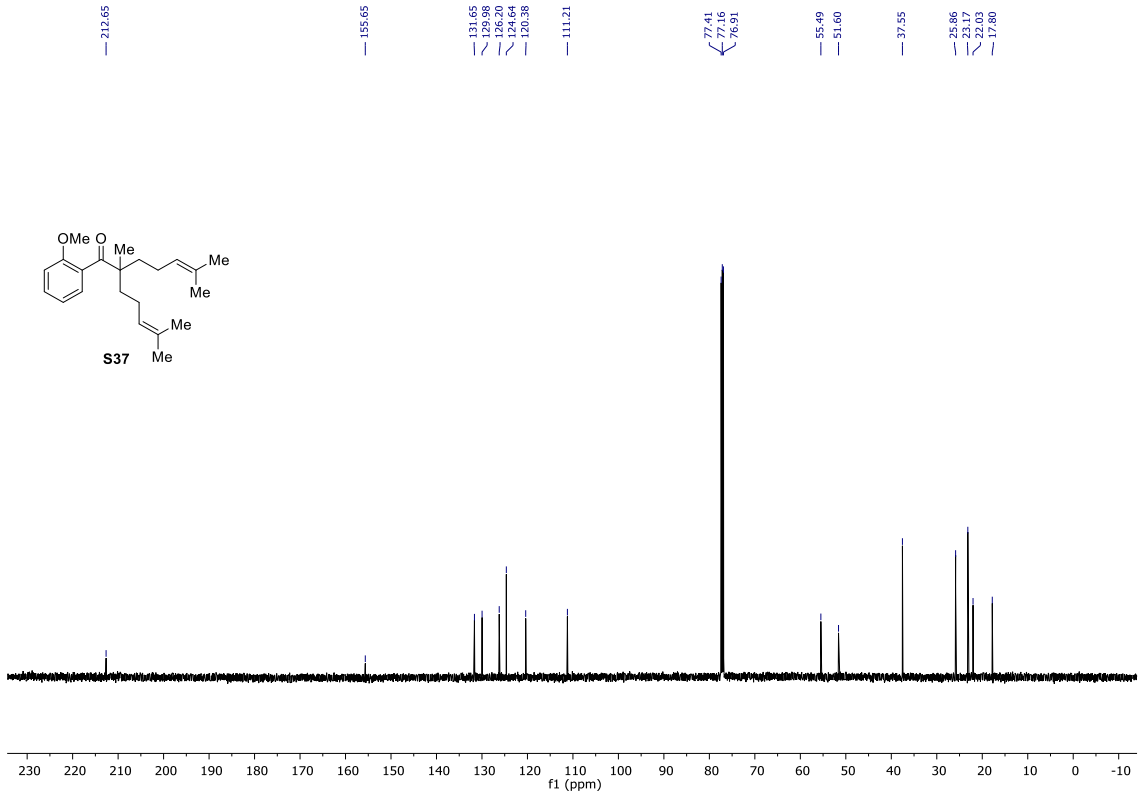
OMe O
Me
Me
Me
Me
Me
S37
212.65
155.65
131.65 129.98 126.20 124.64 120.38
111.21
77.41 77.16 76.91
55.49
51.60
37.55
25.86 23.17 22.03 17.80
f1 (ppm)

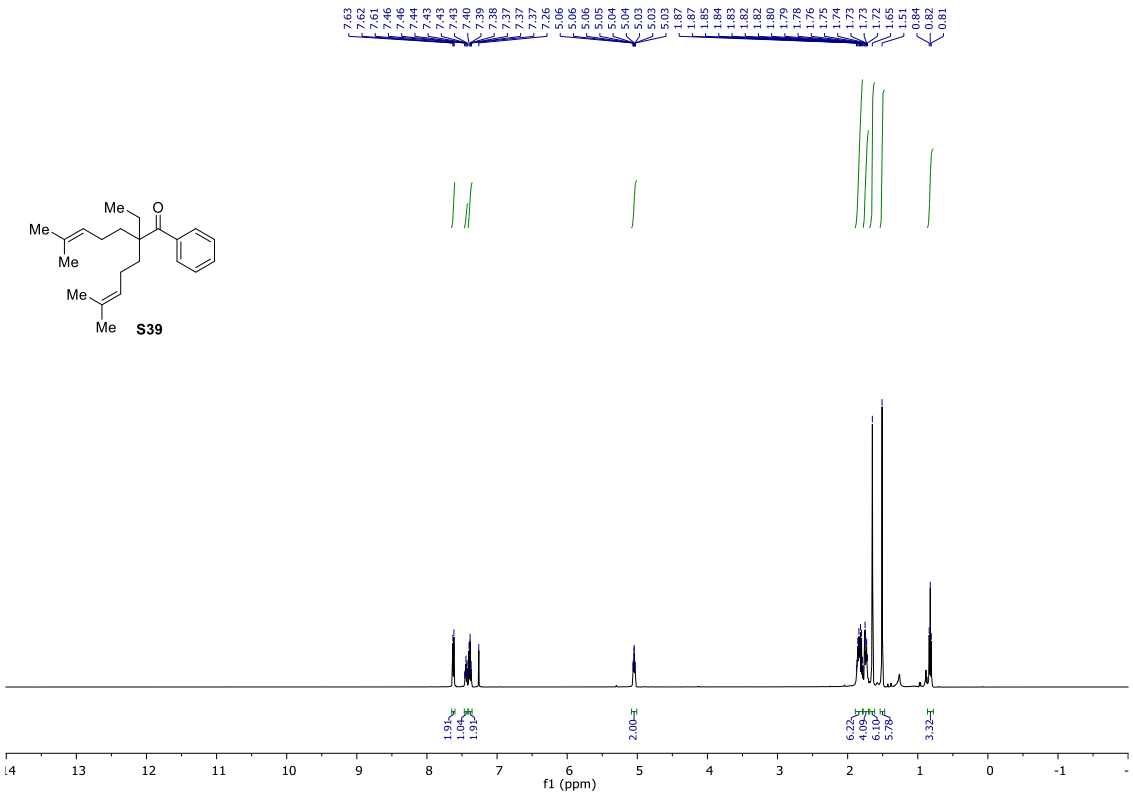
7.63
7.62
7.61
7.46
7.46
7.44
7.43
7.43
7.40
7.39
7.38
7.37
7.37
7.37
7.26
5.06
5.06
5.05
5.04
5.04
5.03
5.03
5.03
1.87
1.87
1.85
1.84
1.83
1.82
1.82
1.80
1.79
1.78
1.76
1.75
1.74
1.73
1.73
1.72
1.65
1.51
0.84
0.82
0.81
Me
O
Me
Me
Me
Me
S39
1.91
1.04
1.91
2.00
6.22
4.09
6.10
5.78
3.32
f1 (ppm)

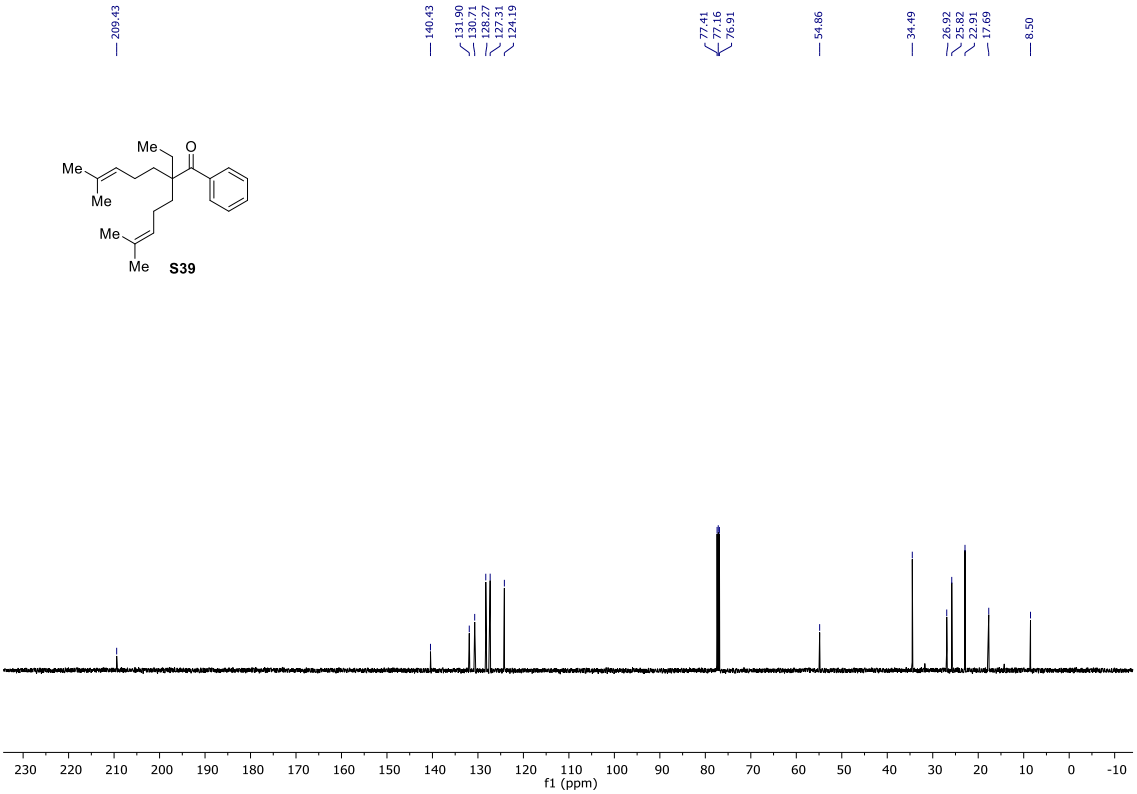
209.43
140.43
131.90
130.71
128.27
127.31
124.19
77.41
77.16
76.91
54.86
34.49
26.92
25.82
22.91
17.69
8.50
Me
O
Me
Me
Me
Me
S39
f1 (ppm)

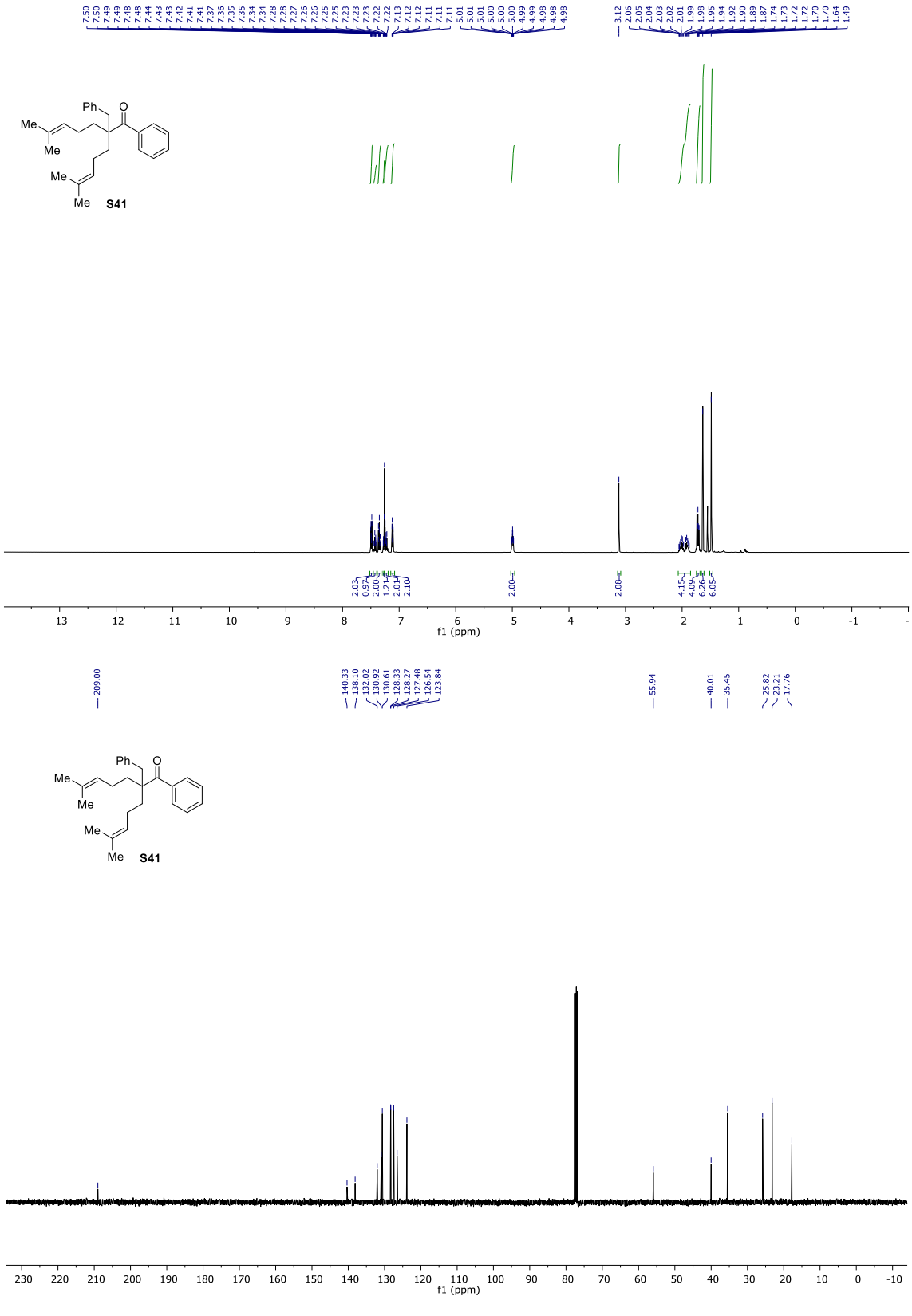
Ph
O
Me
Me
Me
Me
S41
f1 (ppm)
f1 (ppm)

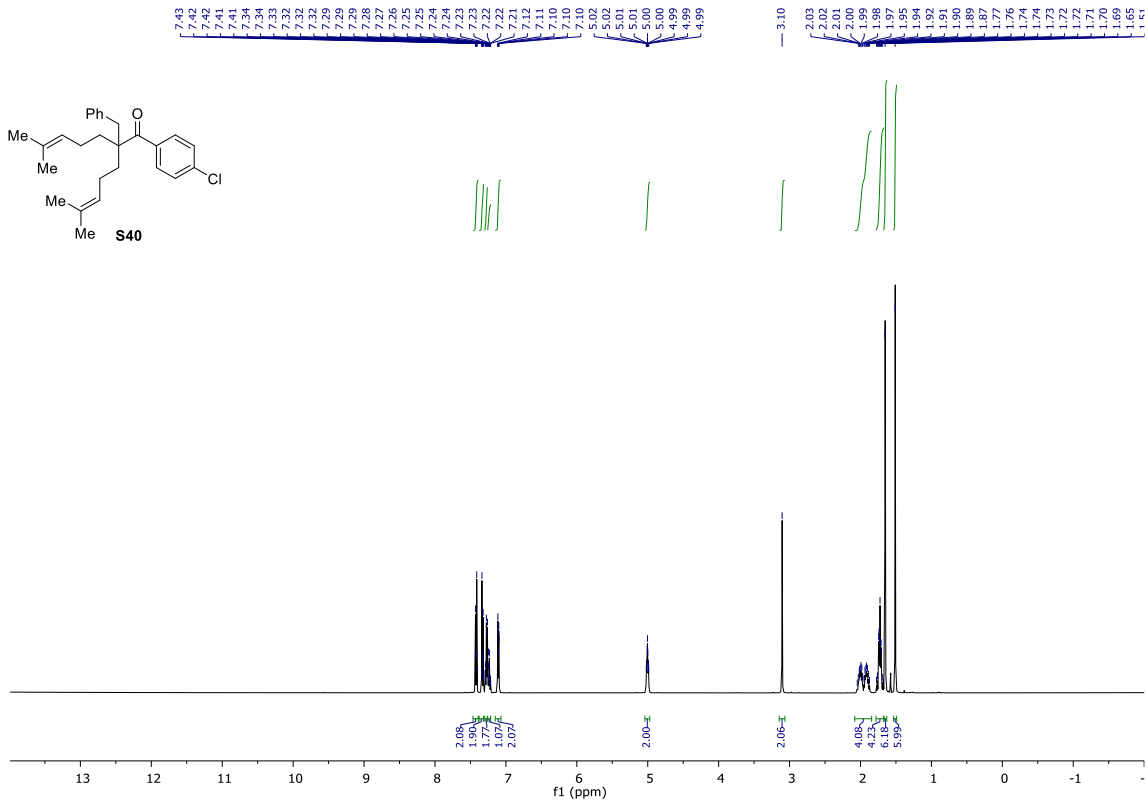
Ph
O
Me
Me
Me
Me
Cl
S40
f1 (ppm)

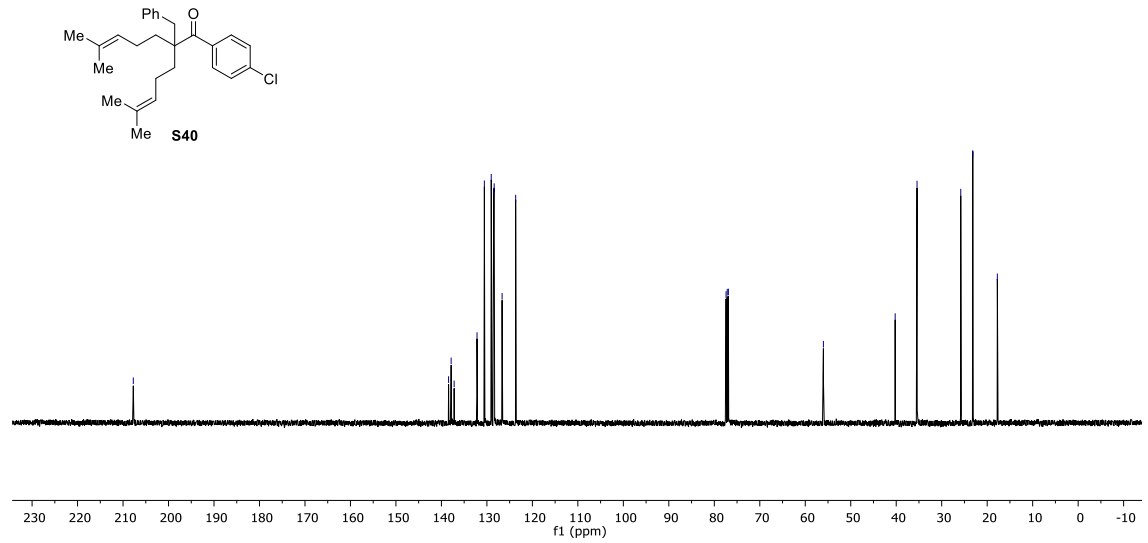
Ph
O
Me
Me
Me
Me
Cl
S40
f1 (ppm)

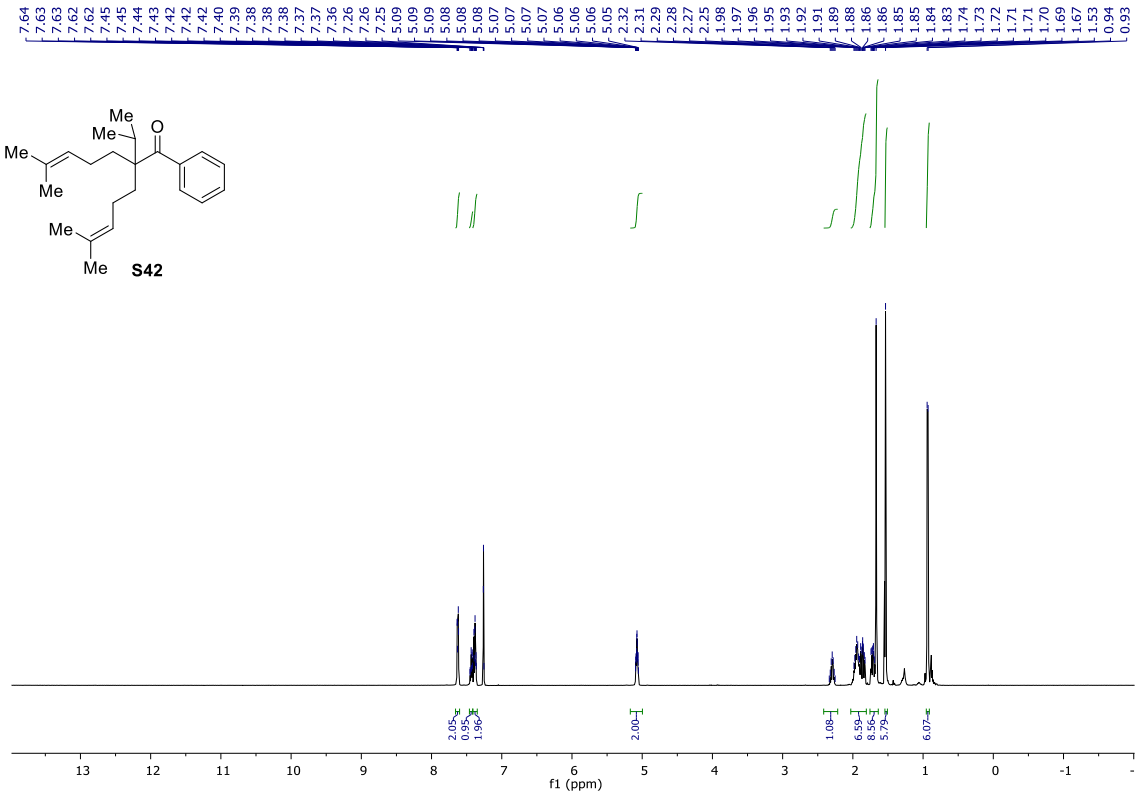
Me
Me
O
Me
Me
Me
Me
S42
f1 (ppm)

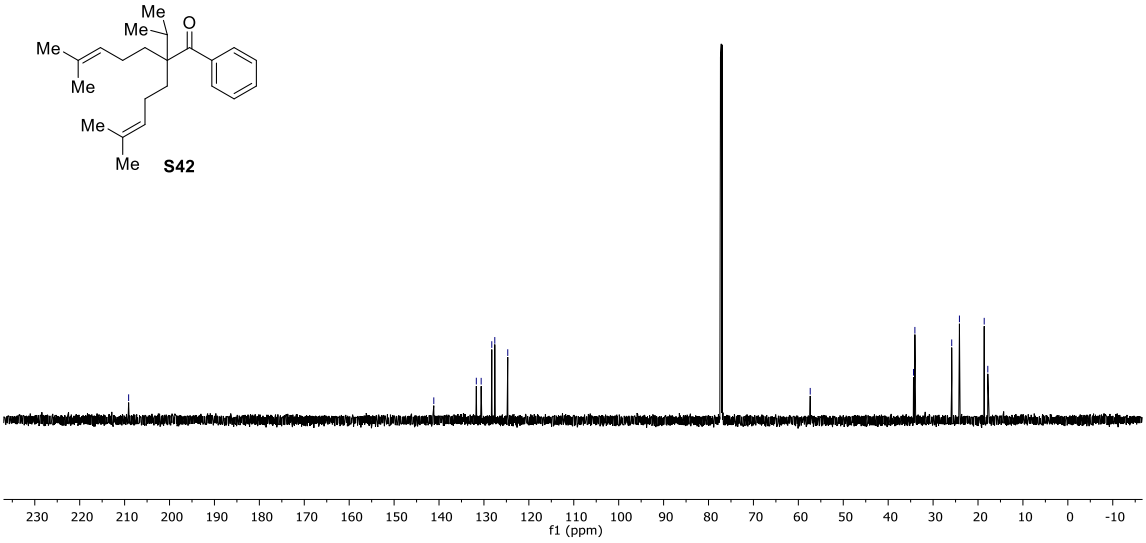
Me
Me
O
Me
Me
Me
Me
S42
f1 (ppm)

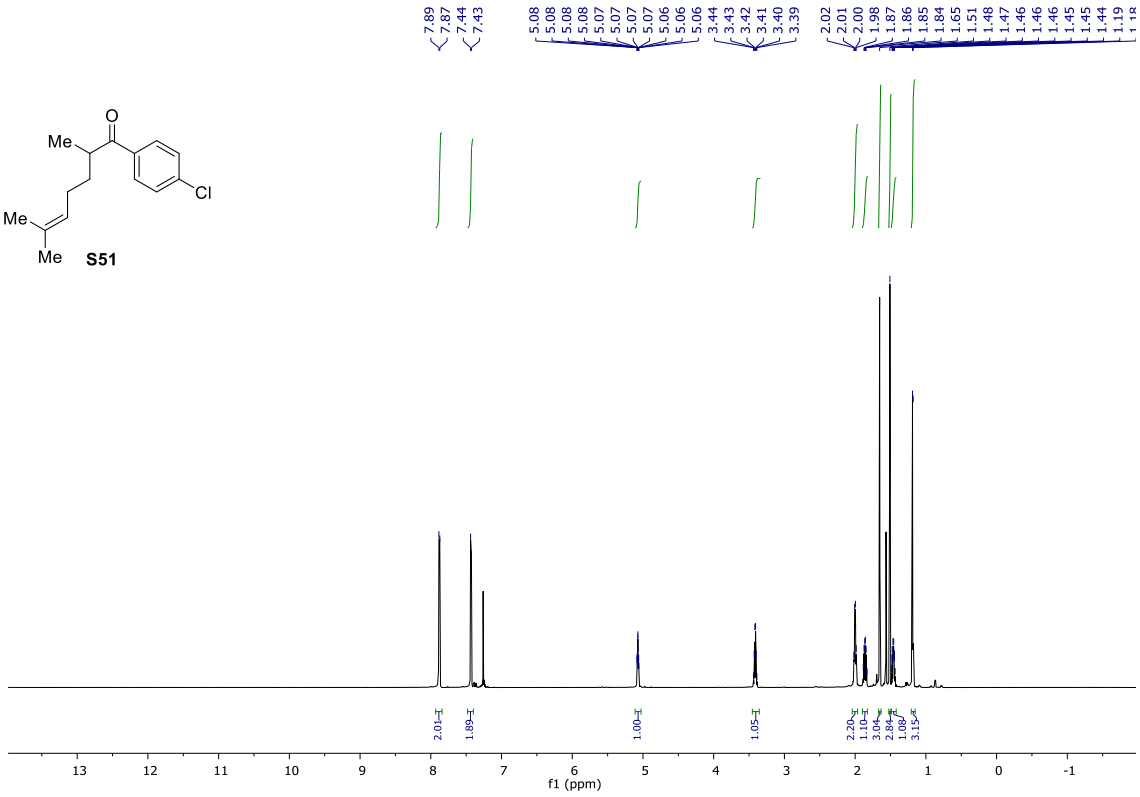
Me
O
Cl
Me
Me
S51
7.89
7.87
7.44
7.43
5.08
5.08
5.08
5.08
5.07
5.07
5.07
5.07
5.07
5.06
5.06
5.06
3.44
3.43
3.42
3.41
3.40
3.39
2.02
2.01
2.00
1.98
1.87
1.86
1.85
1.84
1.65
1.51
1.48
1.47
1.46
1.46
1.46
1.45
1.45
1.44
1.19
2.01
1.89
1.00
1.05
2.20
1.10
3.04
3.04
1.08
3.15
f1 (ppm)

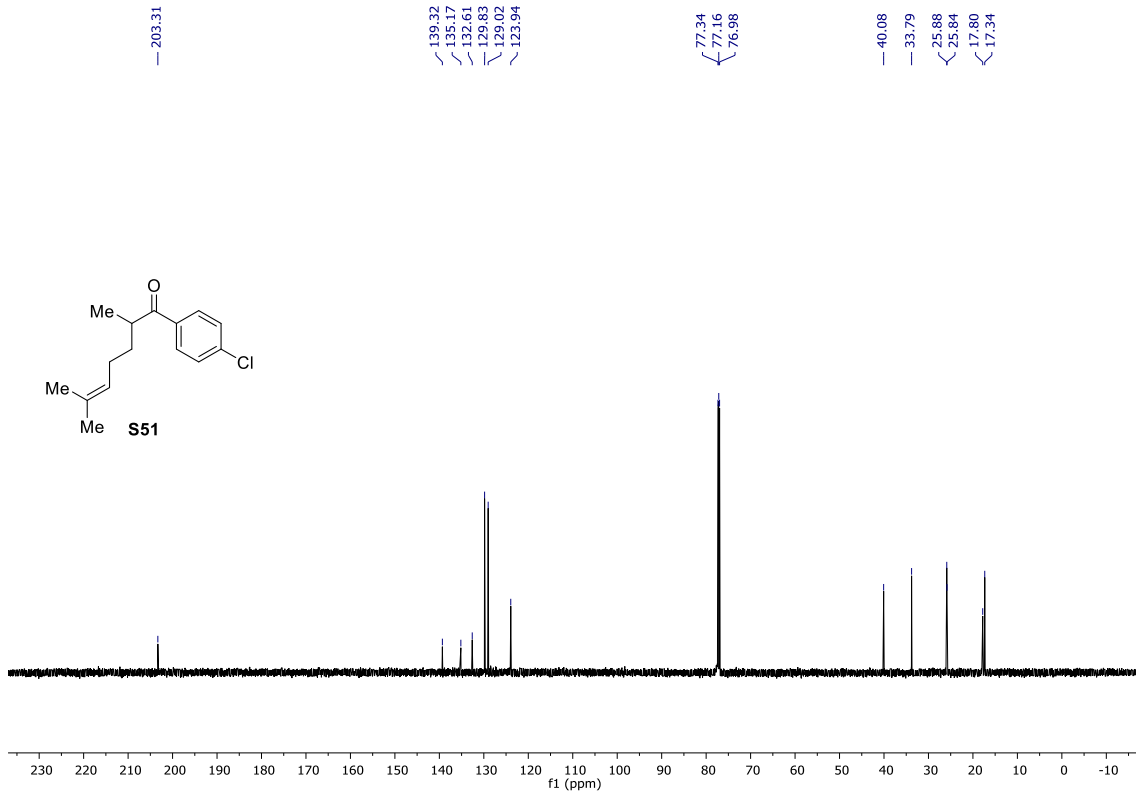
203.31
139.32
135.17
132.61
129.83
129.02
123.94
77.34
77.16
76.98
40.08
33.79
25.88
25.84
17.80
17.34
Me
O
Cl
Me
Me
S51
f1 (ppm)

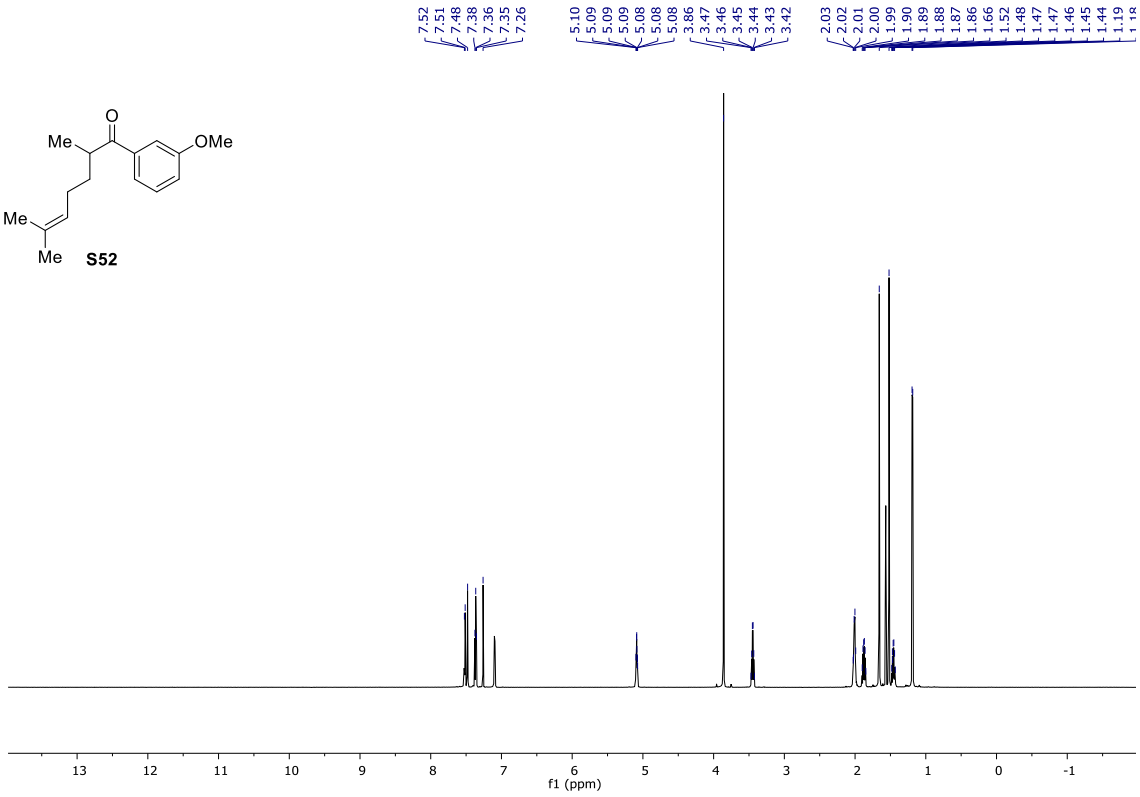
7.52
7.51
7.48
7.38
7.36
7.35
7.26
5.10
5.09
5.09
5.09
5.08
5.08
5.08
3.86
3.47
3.46
3.45
3.44
3.43
3.42
2.03
2.02
2.01
2.00
1.99
1.90
1.89
1.88
1.87
1.86
1.66
1.52
1.48
1.47
1.47
1.46
1.45
1.44
1.19
O
Me
OMe
Me
Me
S52
13
12
11
10
9
8
7
6
5
4
3
2
1
0
-1
f1 (ppm)

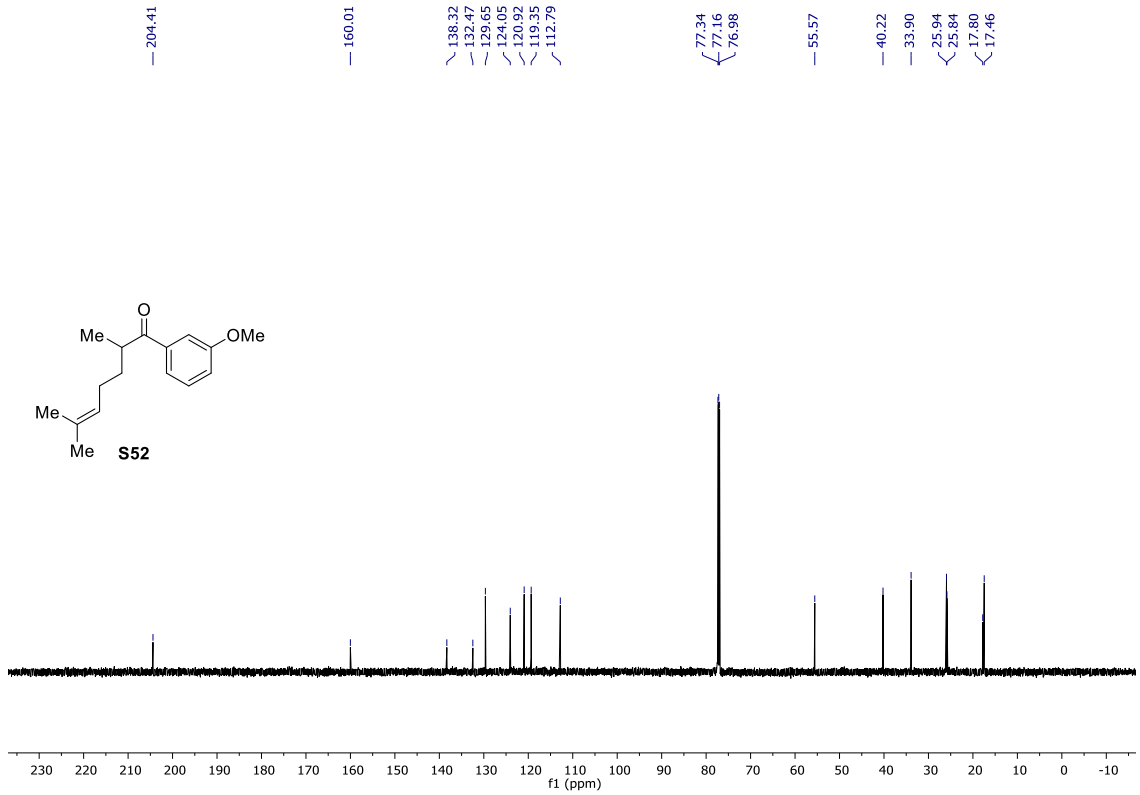
204.41
160.01
138.32
132.47
129.65
124.05
120.92
119.35
112.79
77.34
77.16
76.98
55.57
40.22
33.90
25.94
25.84
17.80
17.46
O
Me
OMe
Me
Me
S52
230
220
210
200
190
180
170
160
150
140
130
120
110
100
90
80
70
60
50
40
30
20
10
0
-10
f1 (ppm)

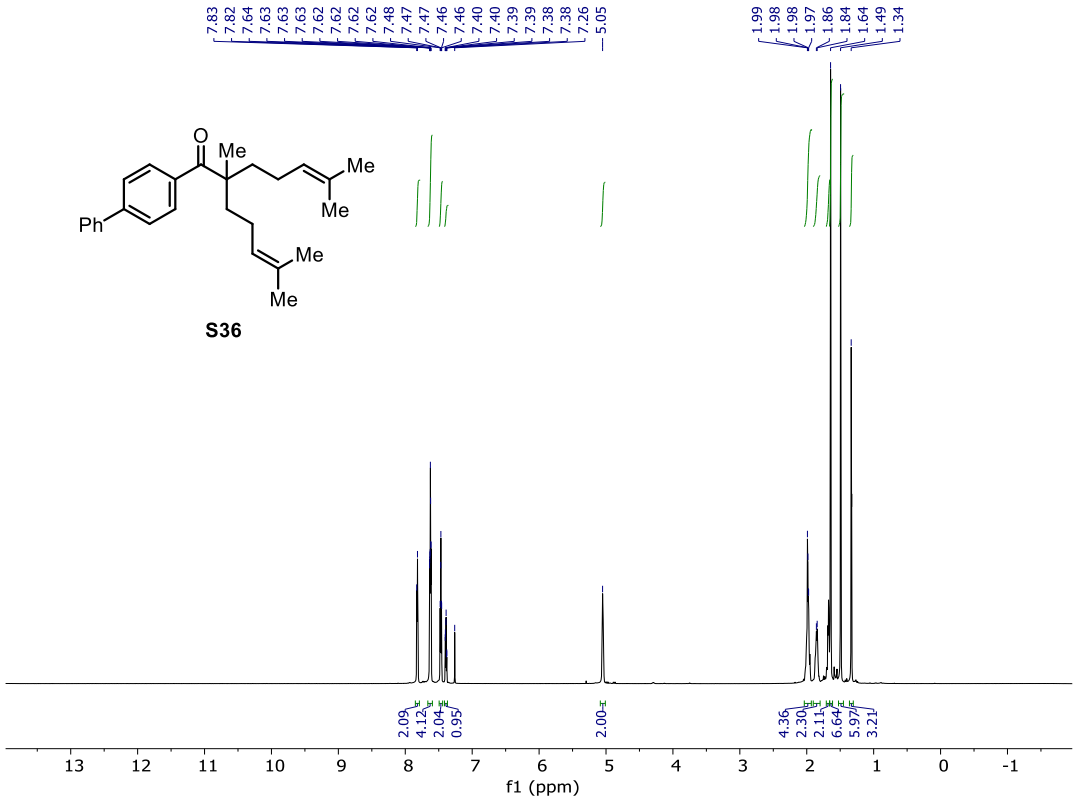
7.83
7.82
7.64
7.63
7.63
7.63
7.62
7.62
7.62
7.62
7.48
7.47
7.47
7.46
7.46
7.40
7.40
7.39
7.39
7.38
7.38
7.26
5.05
1.99
1.98
1.98
1.97
1.86
1.84
1.64
1.49
1.34
O
Me
Me
Me
Me
Me
Ph
2.09
4.12
2.04
0.95
2.00
4.36
2.30
2.11
6.64
5.97
3.21
13 12 11 10 9 8 7 6 5 4 3 2 1 0 -1
f1 (ppm)

S36

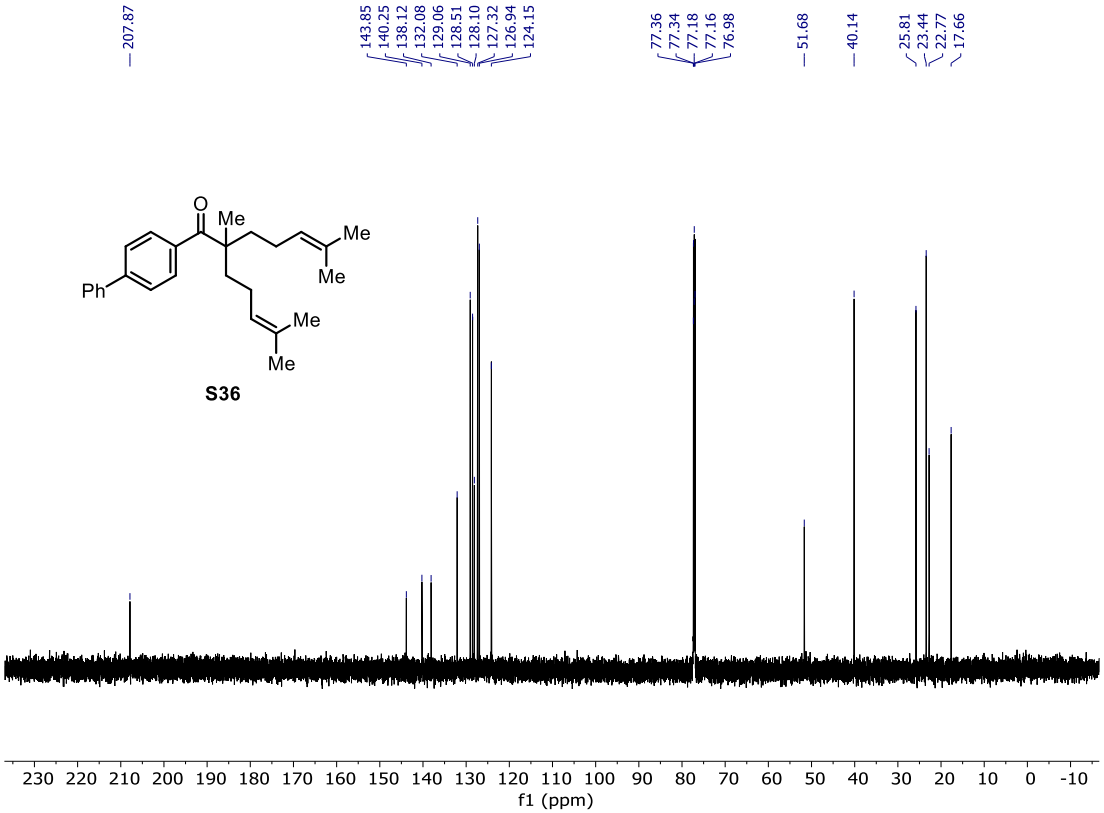
207.87
143.85
140.25
138.12
132.08
129.06
128.51
128.10
127.32
126.94
124.15
77.36
77.34
77.18
77.16
76.98
51.68
40.14
25.81
23.44
22.77
17.66
O
Me
Me
Me
Me
Me
Ph
230 220 210 200 190 180 170 160 150 140 130 120 110 100 90 80 70 60 50 40 30 20 10 0 -10
f1 (ppm)

S36

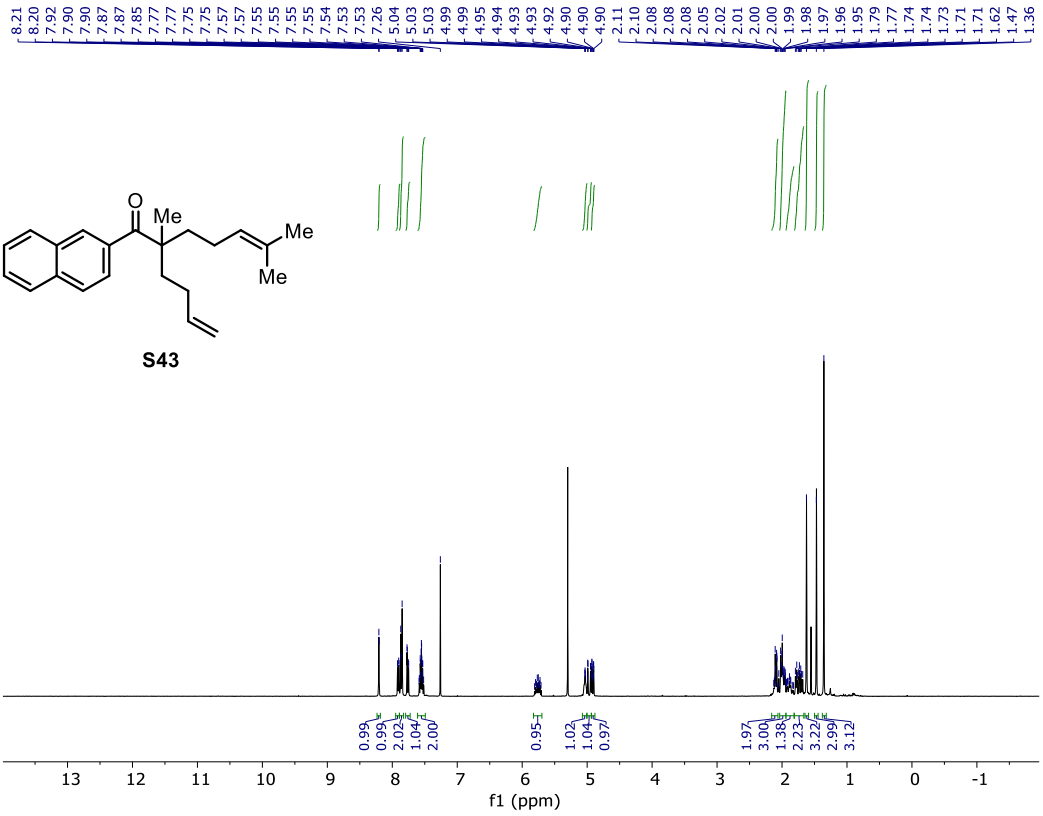
8.21 8.20 7.92 7.90 7.90 7.87 7.87 7.85 7.77 7.77 7.75 7.75 7.57 7.57 7.55 7.55 7.55 7.55 7.54 7.53 7.53 7.26 5.04 5.03 5.03 4.99 4.99 4.95 4.94 4.93 4.93 4.92 4.90 4.90 4.90 2.11 2.10 2.08 2.08 2.08 2.05 2.02 2.01 2.00 2.00 1.99 1.98 1.97 1.96 1.95 1.79 1.77 1.74 1.74 1.73 1.71 1.71 1.62 1.47 1.36
O
Me
Me
Me
S43
0.99 0.99 2.02 1.04 2.00 0.95 1.02 1.04 0.97 1.97 3.00 1.38 2.23 3.22 2.99 3.12
13 12 11 10 9 8 7 6 5 4 3 2 1 0 -1
f1 (ppm)

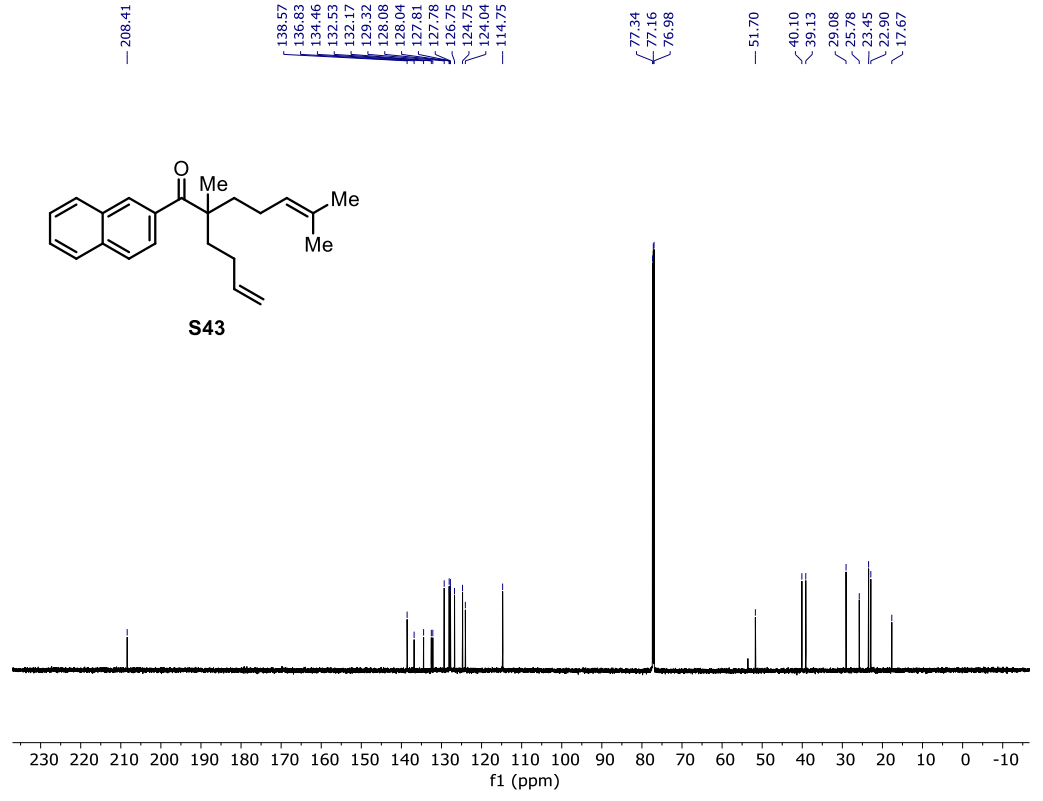
208.41
138.57 136.83 134.46 132.53 132.17 129.32 128.08 128.04 127.81 127.78 126.75 124.75 124.04 114.75
77.34 77.16 76.98
51.70
40.10 39.13 29.08 25.78 23.45 22.90 17.67
O
Me
Me
Me
S43
230 220 210 200 190 180 170 160 150 140 130 120 110 100 90 80 70 60 50 40 30 20 10 0 -10
f1 (ppm)

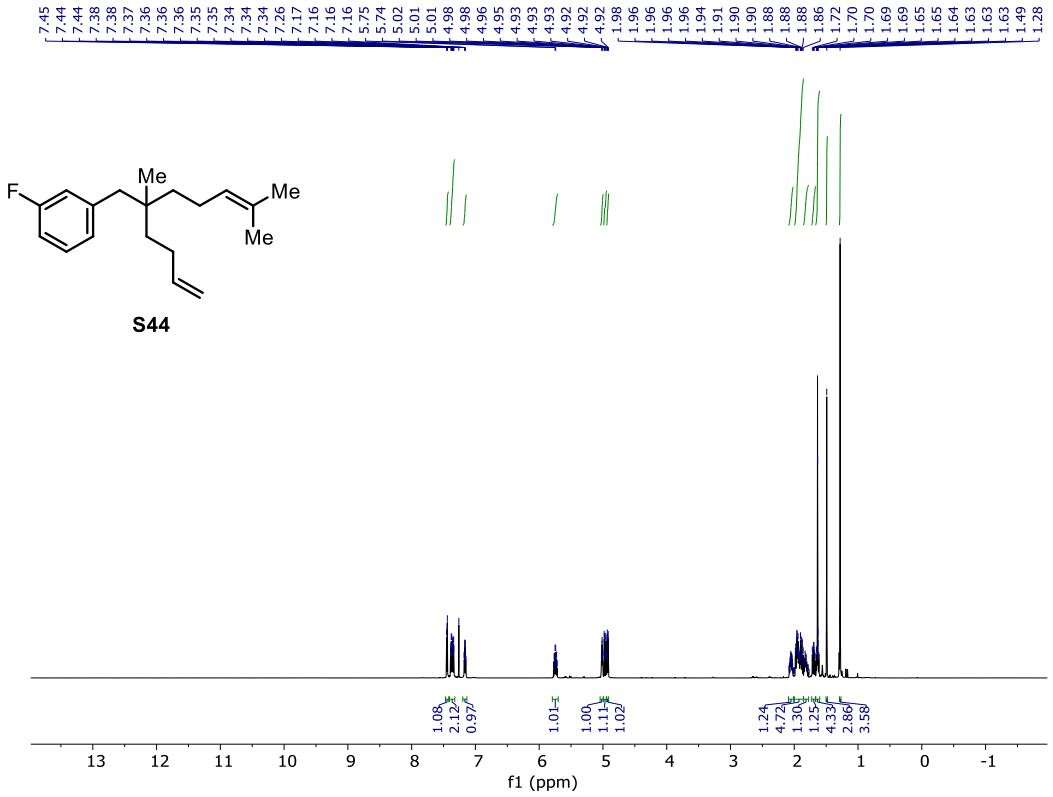
F
Me
Me
Me
S44
f1 (ppm)

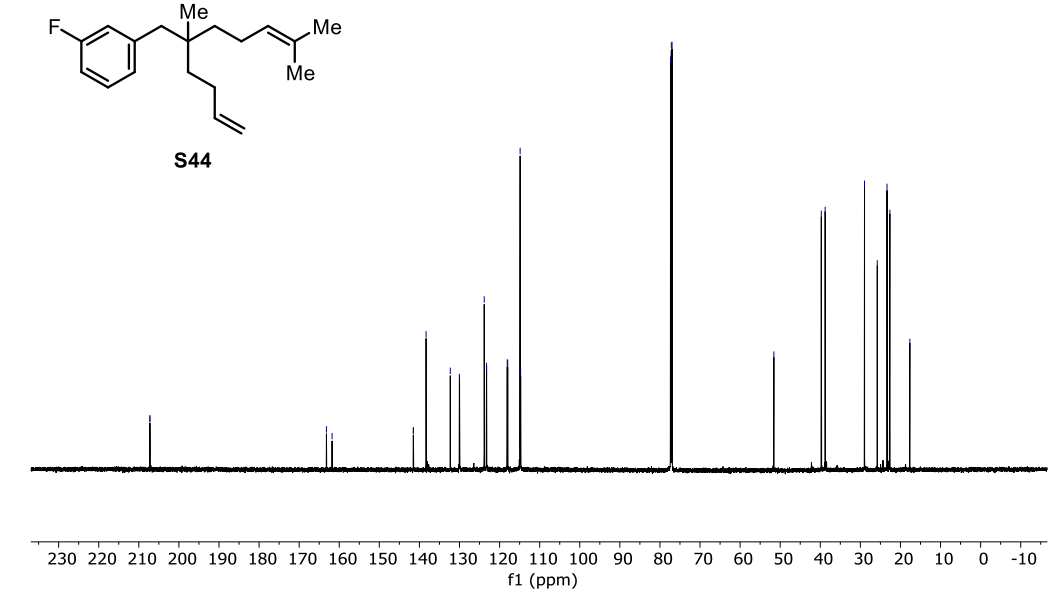
F
Me
Me
Me
S44
f1 (ppm)

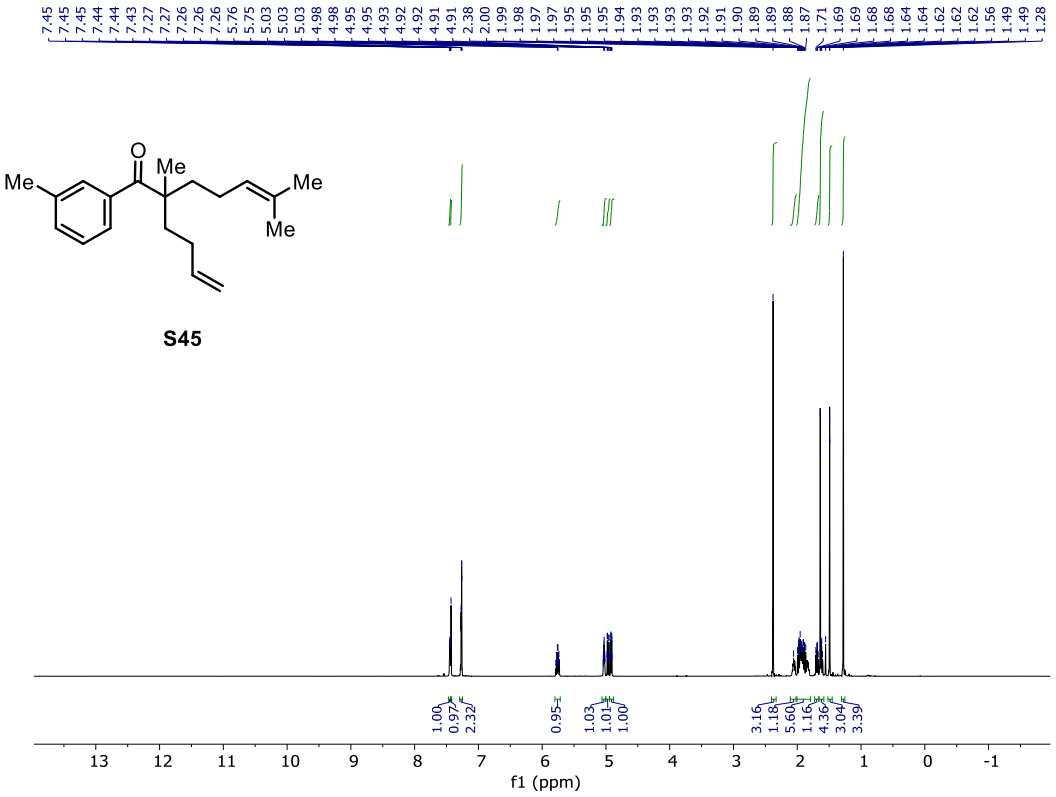
7.45 7.45 7.45 7.44 7.44 7.43 7.27 7.27 7.26 7.26 7.26 5.76 5.75 5.03 5.03 5.03 4.98 4.98 4.95 4.95 4.93 4.92 4.92 4.91 4.91 2.38 2.00 1.99 1.98 1.97 1.97 1.95 1.95 1.95 1.94 1.93 1.93 1.93 1.93 1.92 1.91 1.90 1.89 1.89 1.88 1.87 1.71 1.69 1.69 1.68 1.68 1.64 1.64 1.62 1.62 1.62 1.56 1.49 1.49 1.28
O
Me
Me
Me
Me
1.00 0.97 2.32 0.95 1.03 1.01 1.00 3.16 1.18 5.60 1.16 4.36 3.04 3.39
13 12 11 10 9 8 7 6 5 4 3 2 1 0 -1
f1 (ppm)

S45

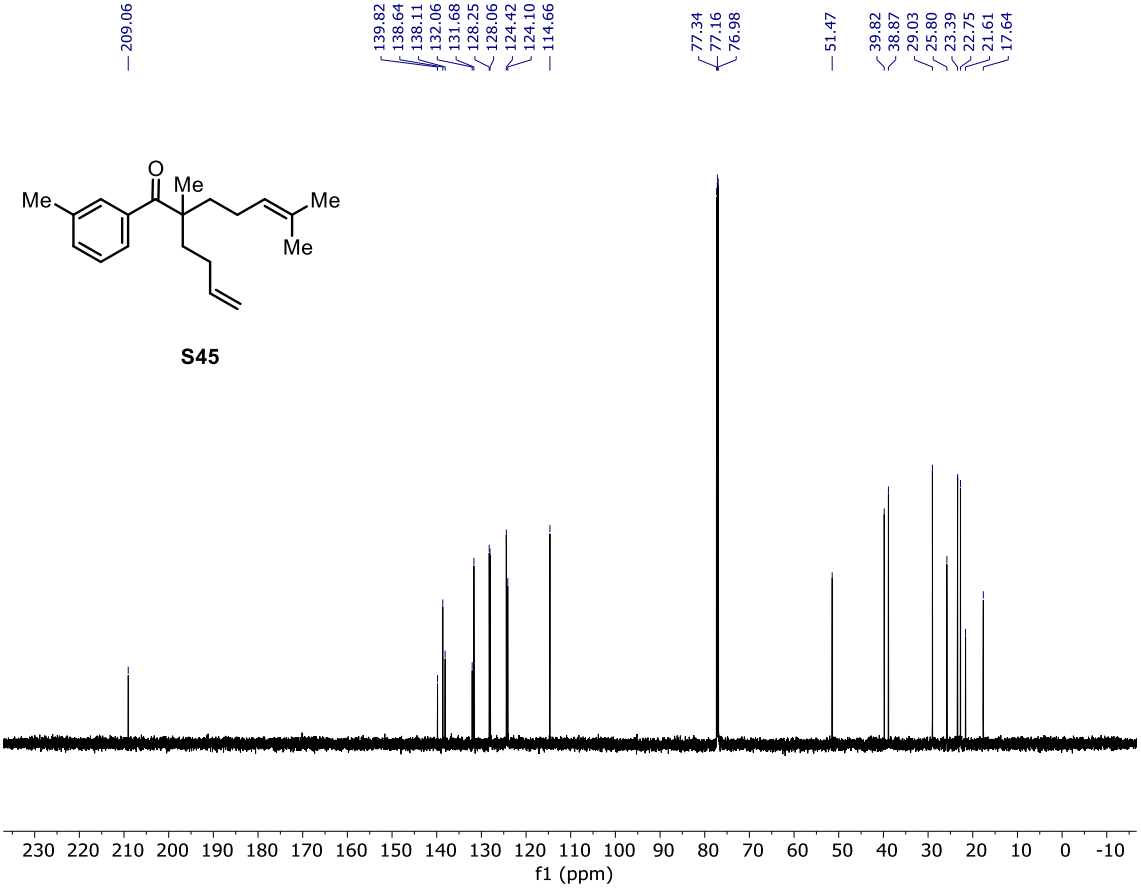
209.06
139.82 138.64 138.11 132.06 131.68 128.25 128.06 124.42 124.10 114.66
77.34 77.16 76.98
51.47
39.82 38.87 29.03 25.80 23.39 22.75 21.61 17.64
O
Me
Me
Me
Me
230 220 210 200 190 180 170 160 150 140 130 120 110 100 90 80 70 60 50 40 30 20 10 0 -10
f1 (ppm)

S45

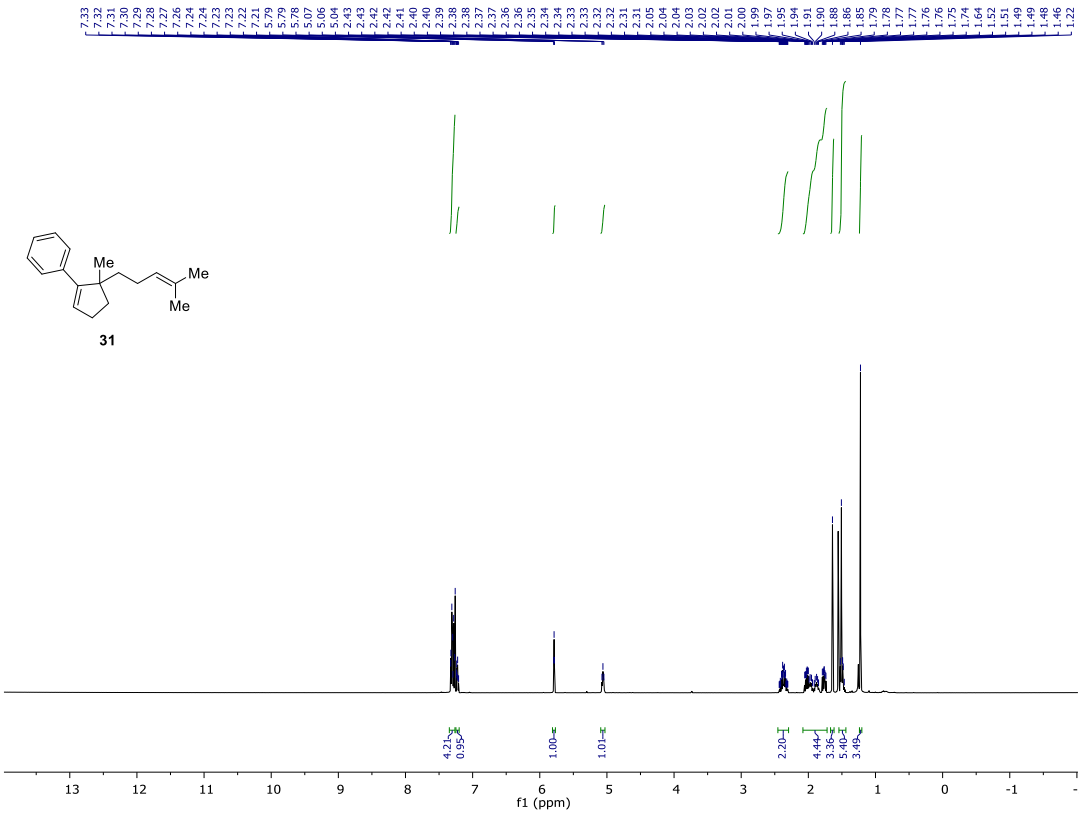
Me
Me
Me
31
f1 (ppm)

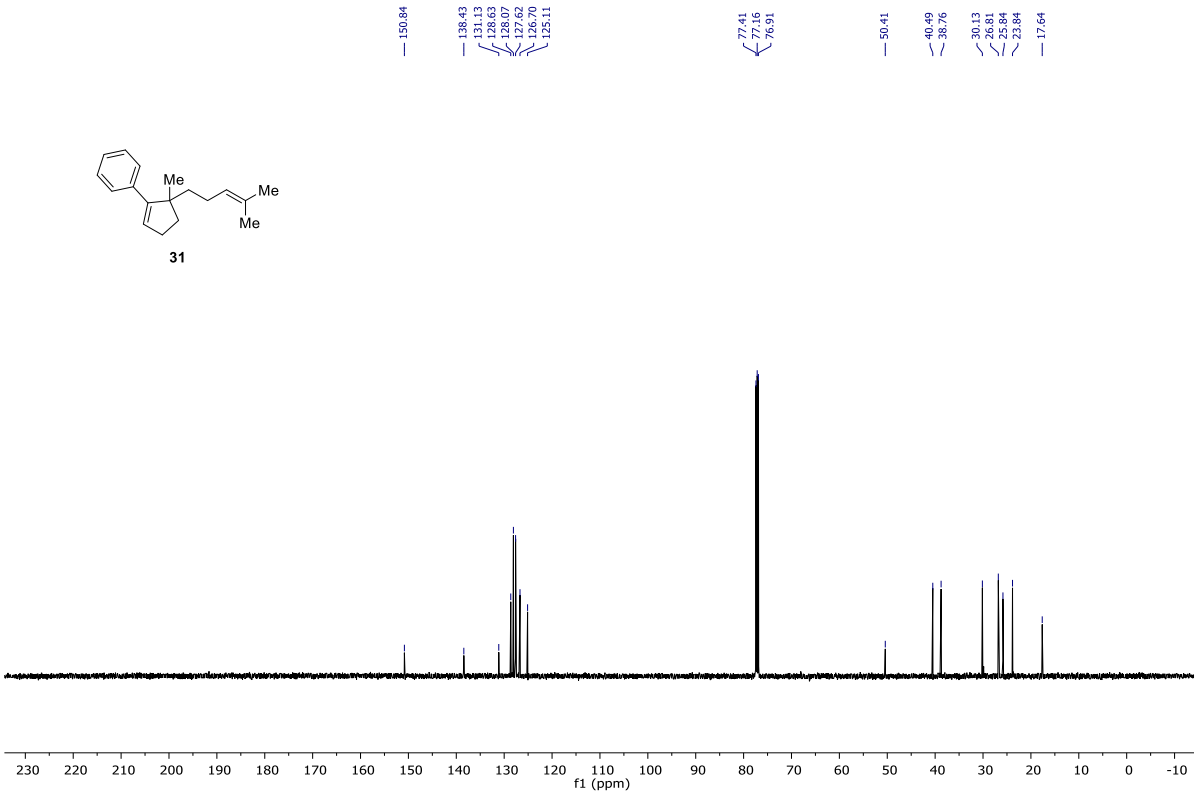
Me
Me
Me
31
f1 (ppm)

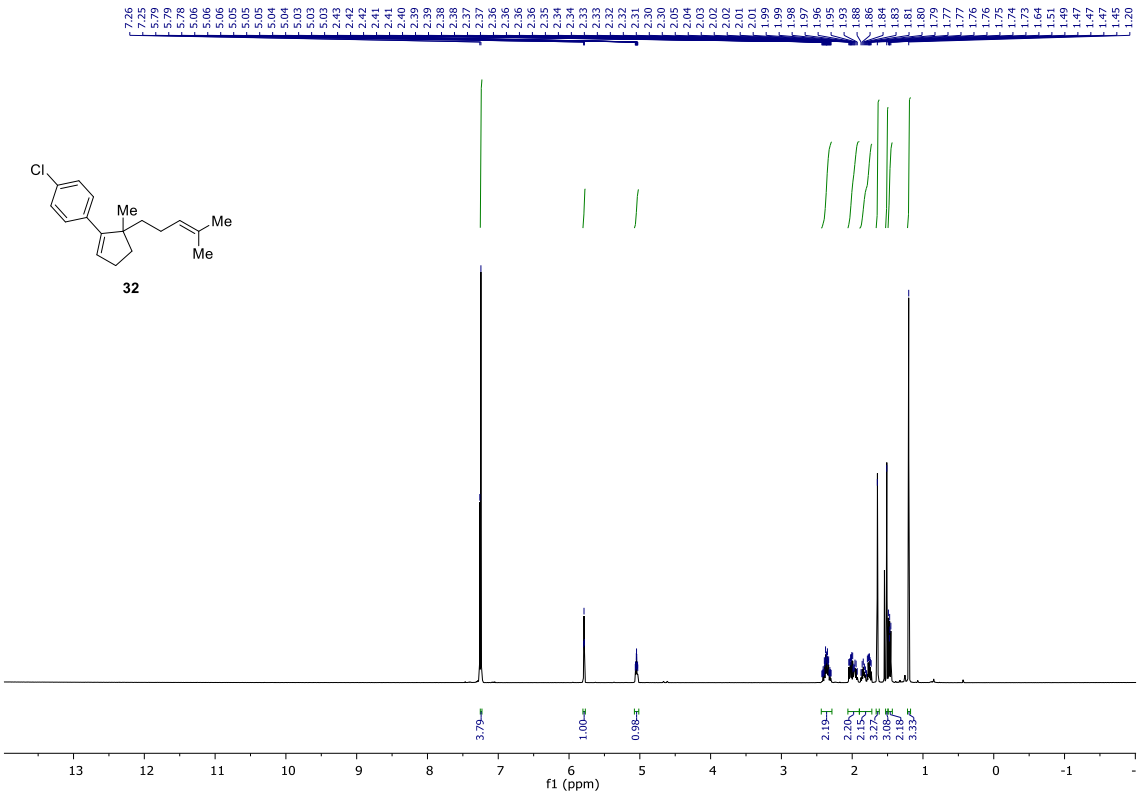
Cl
Me
Me
Me
32
f1 (ppm)

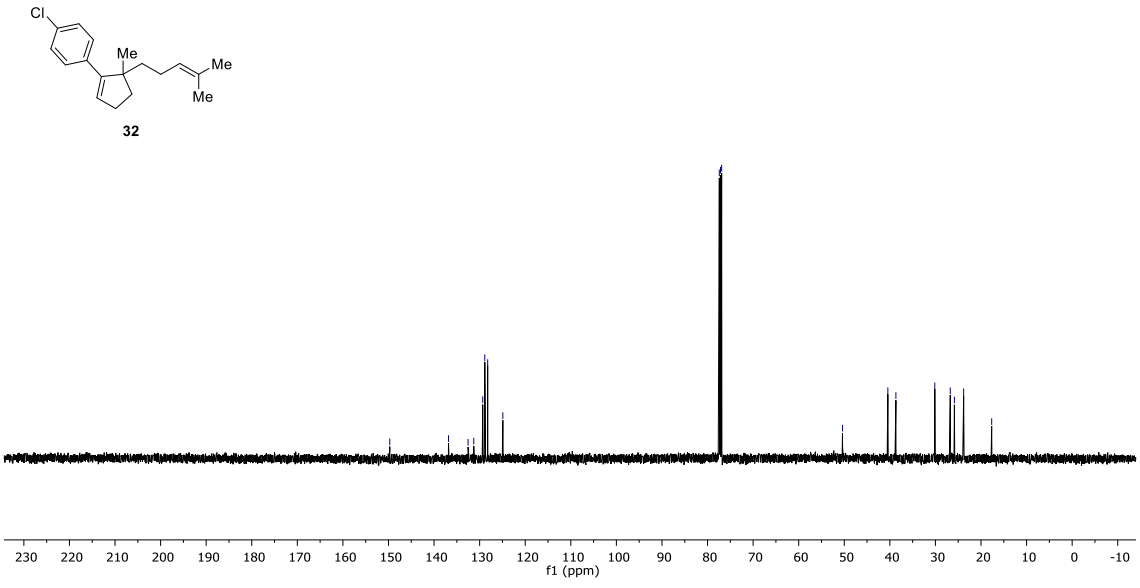
Cl
Me
Me
Me
32
f1 (ppm)

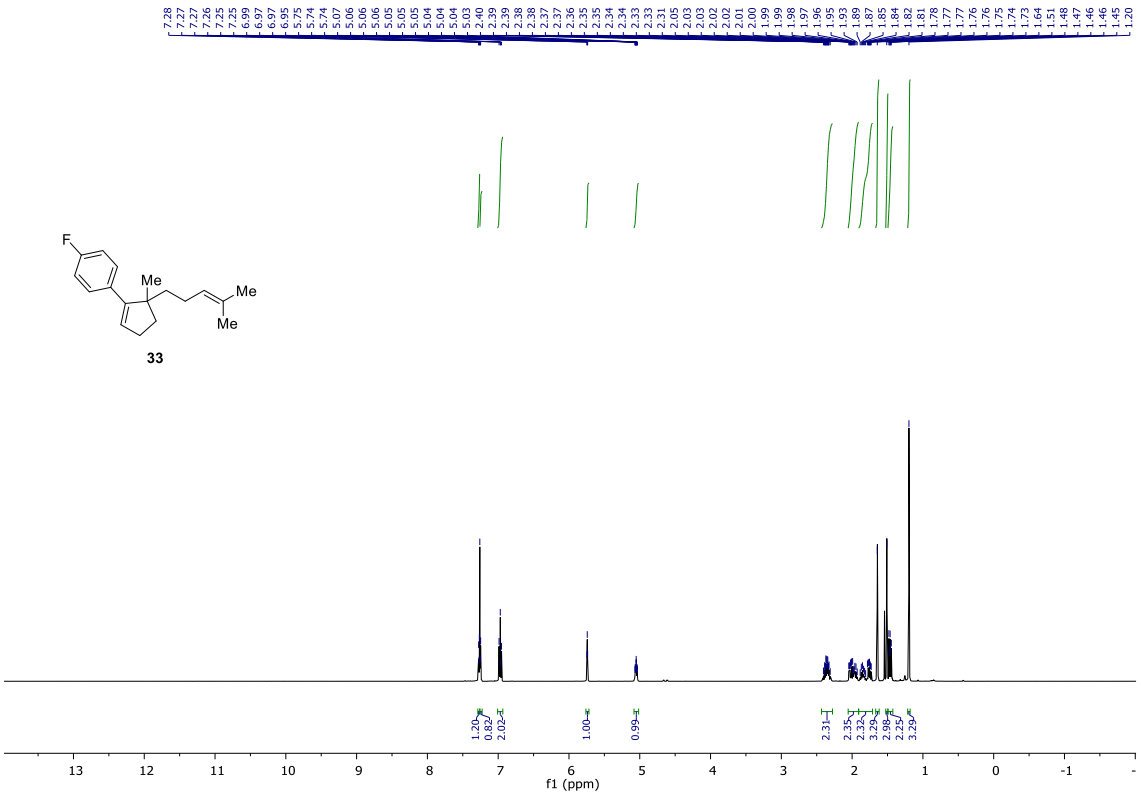
F
Me
Me
Me
33
f1 (ppm)

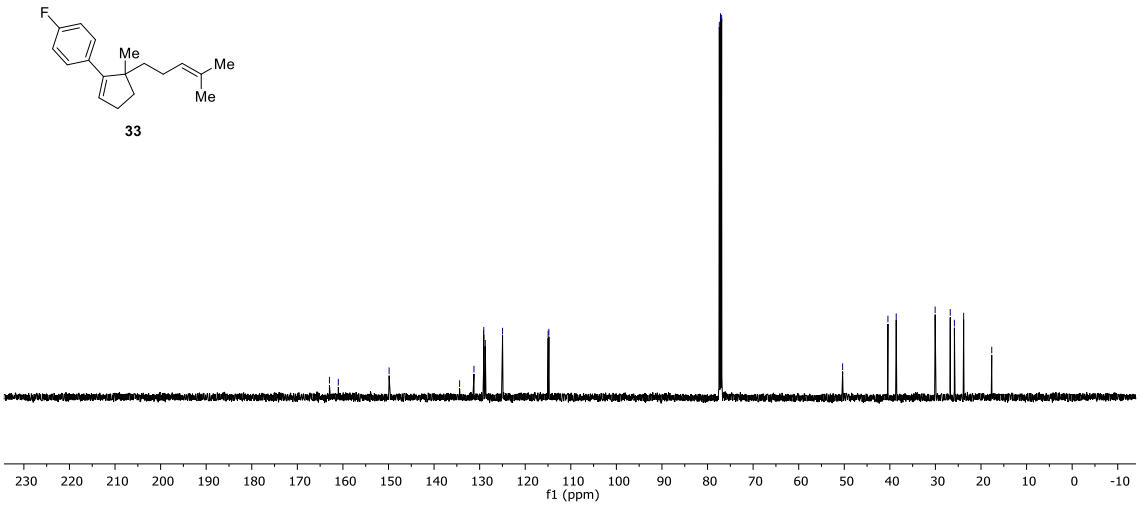
F
Me
Me
Me
33
f1 (ppm)

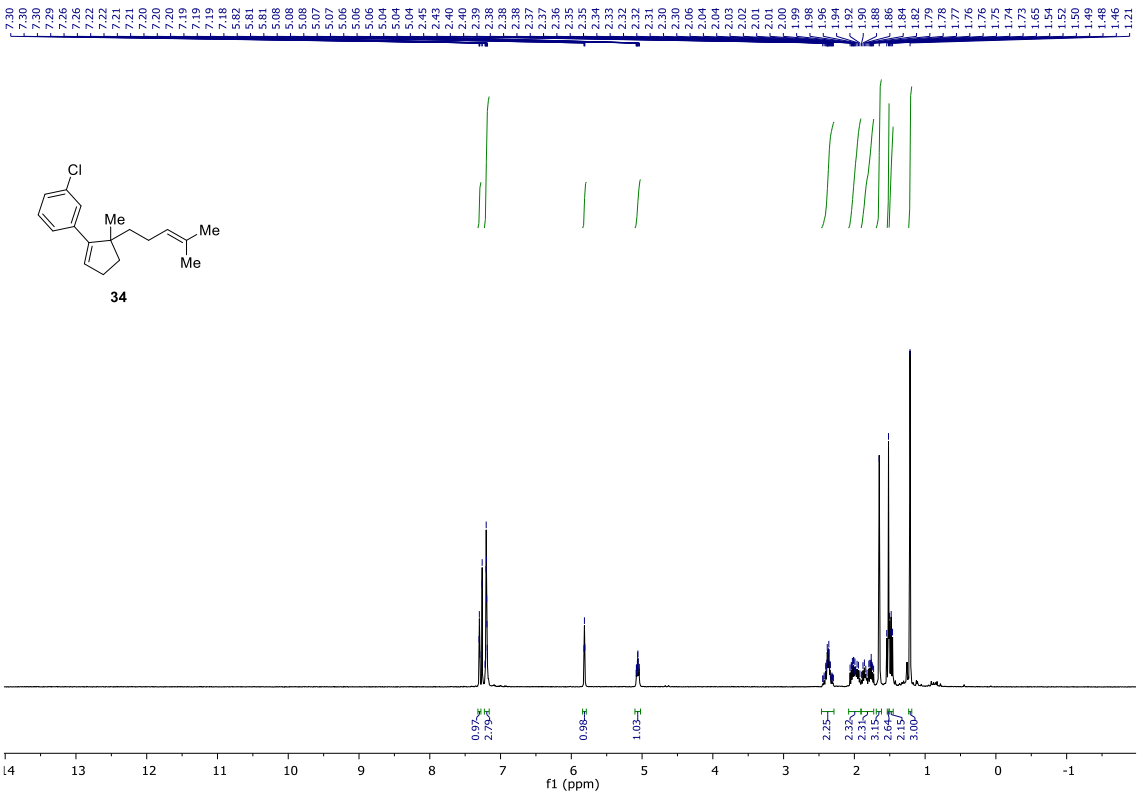
Cl
Me
Me
Me
34
f1 (ppm)

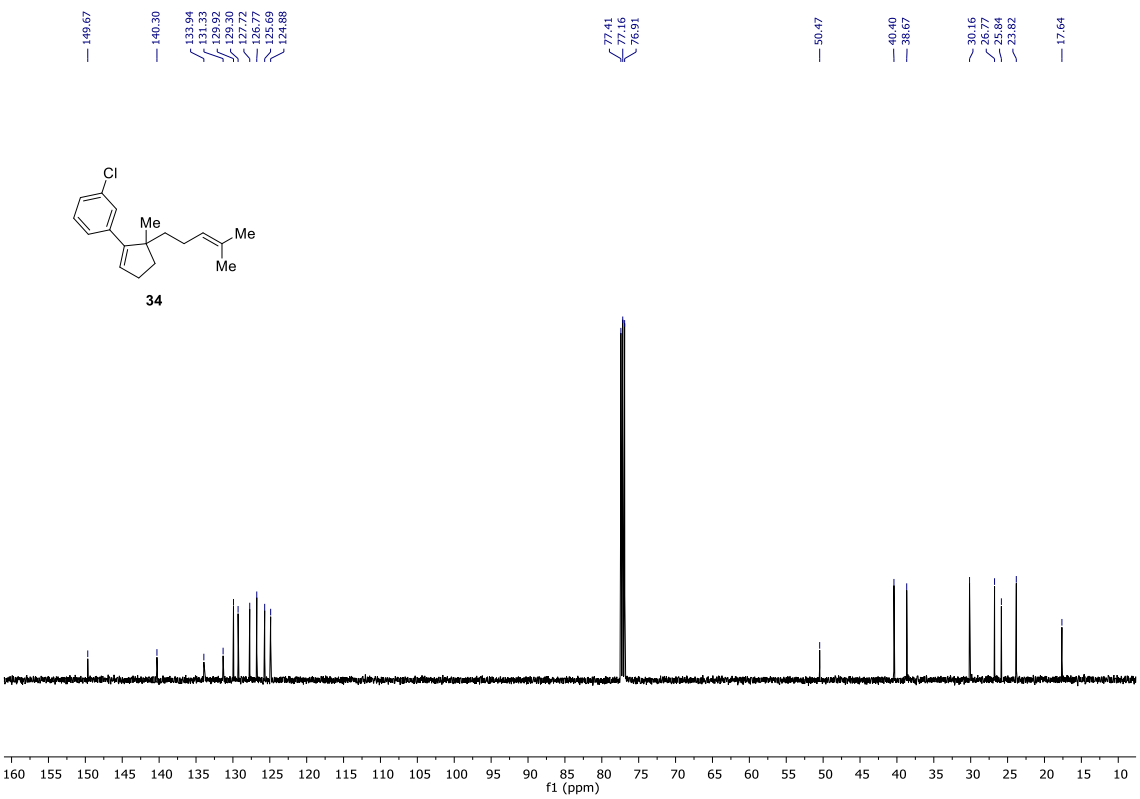
Cl
Me
Me
Me
34
f1 (ppm)

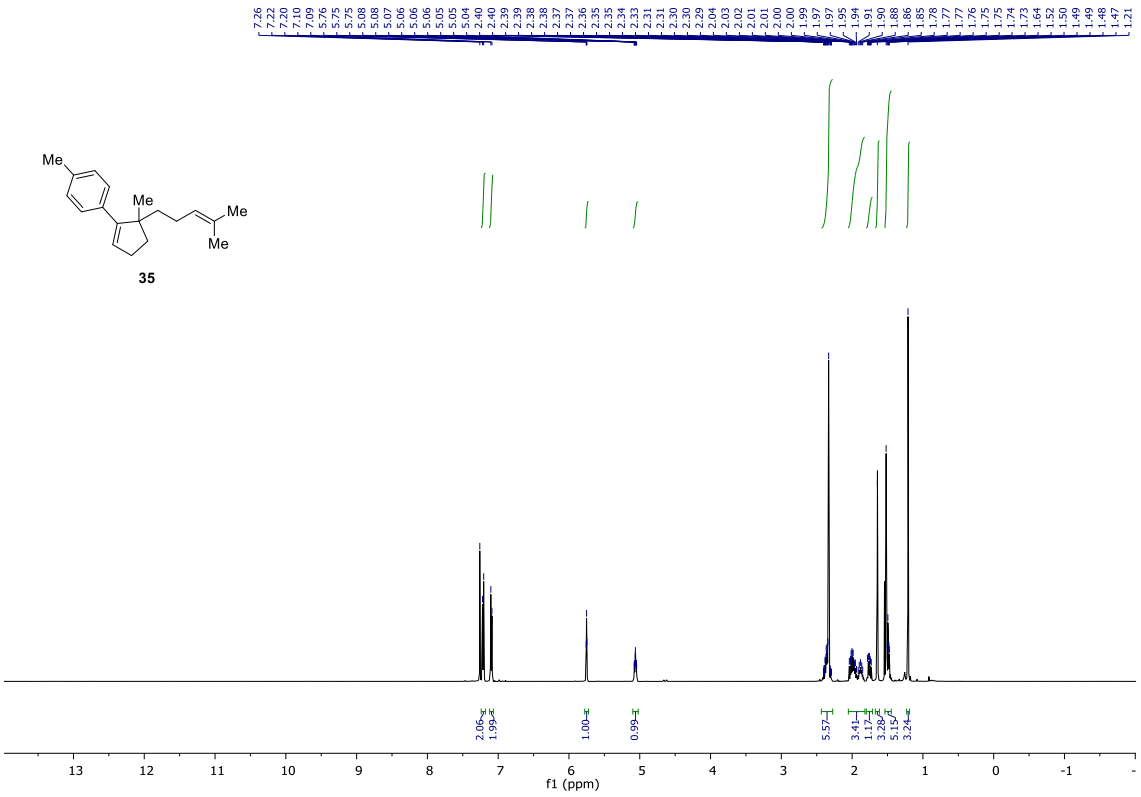
Me
Me
Me
Me
35
f1 (ppm)

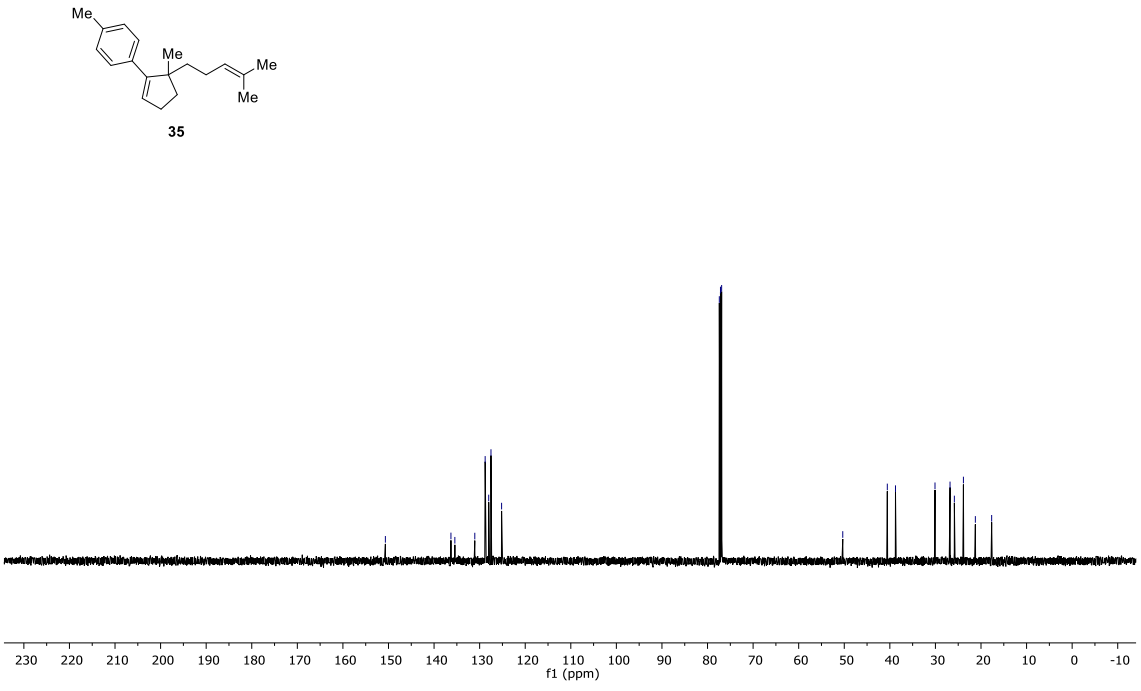
Me
Me
Me
Me
35
f1 (ppm)

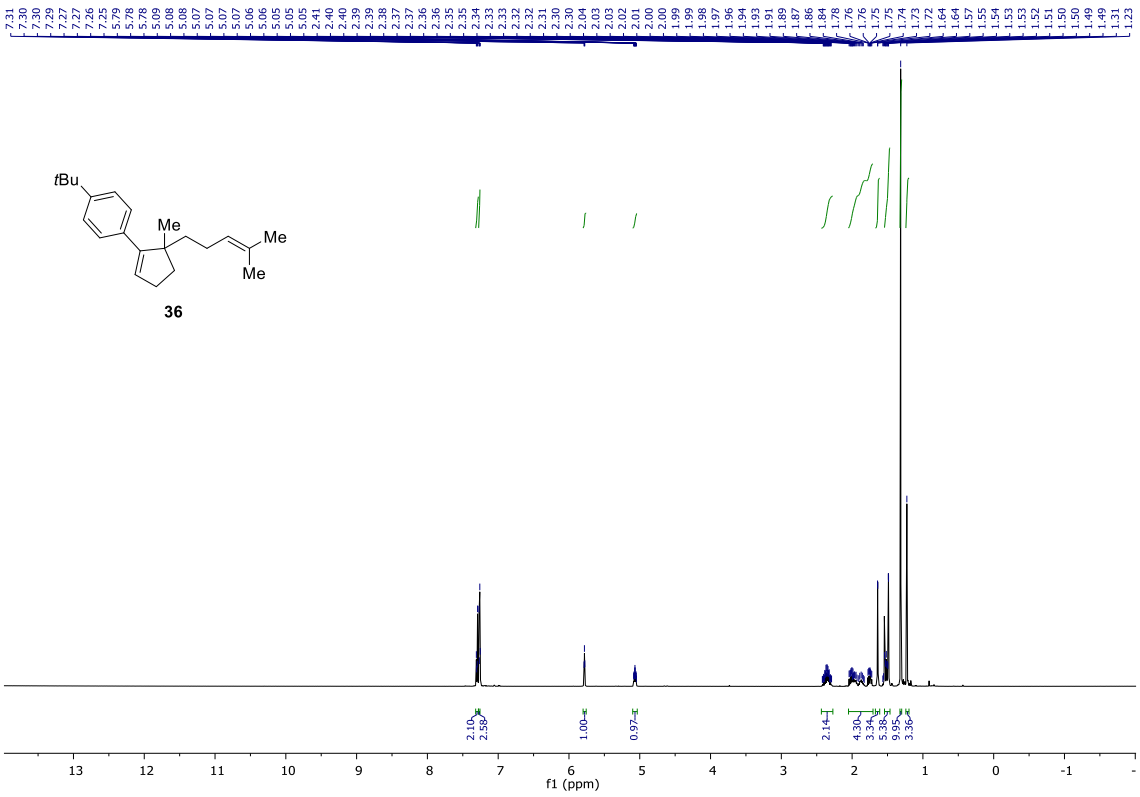
tBu
Me
Me
Me
36
f1 (ppm)

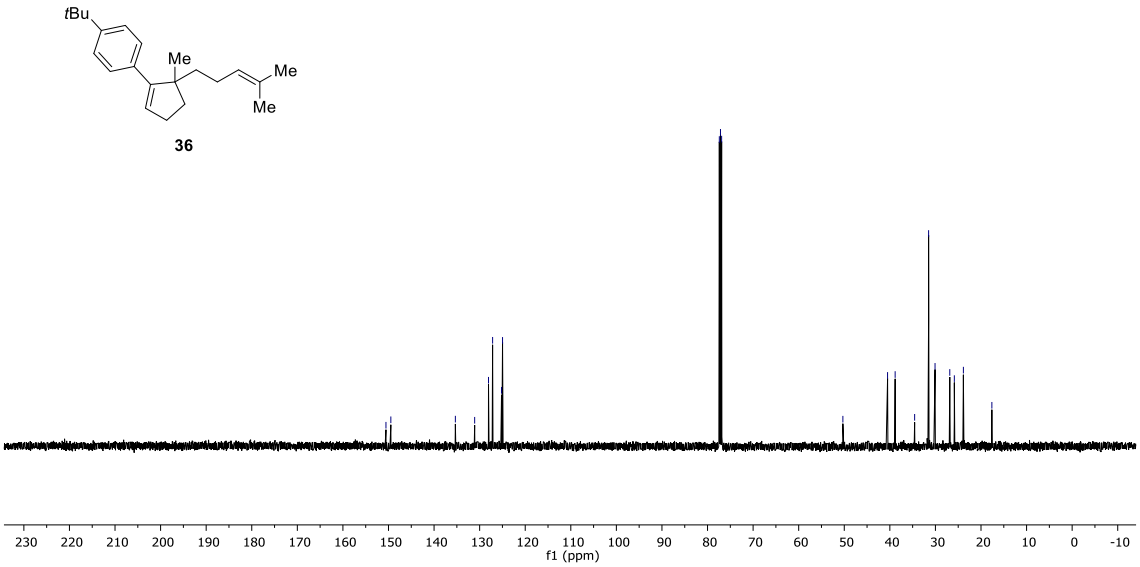
tBu
Me
Me
Me
36
f1 (ppm)

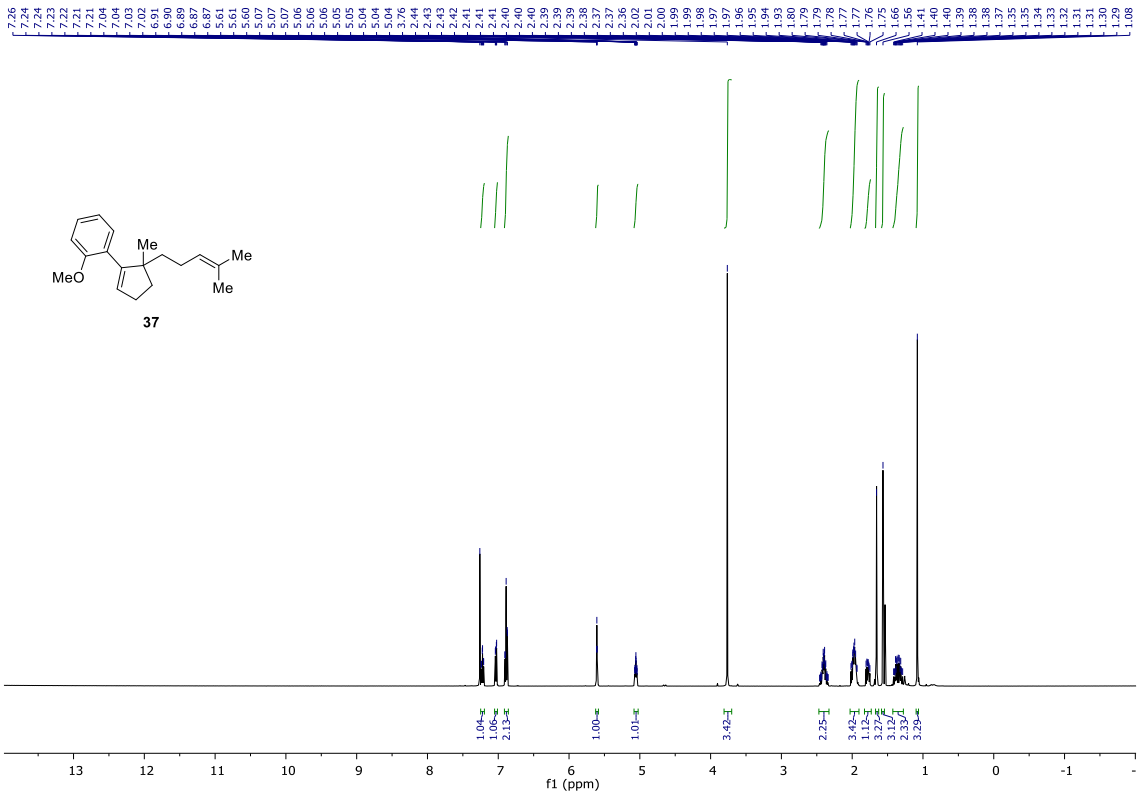
MeO
Me
Me
Me
37
f1 (ppm)

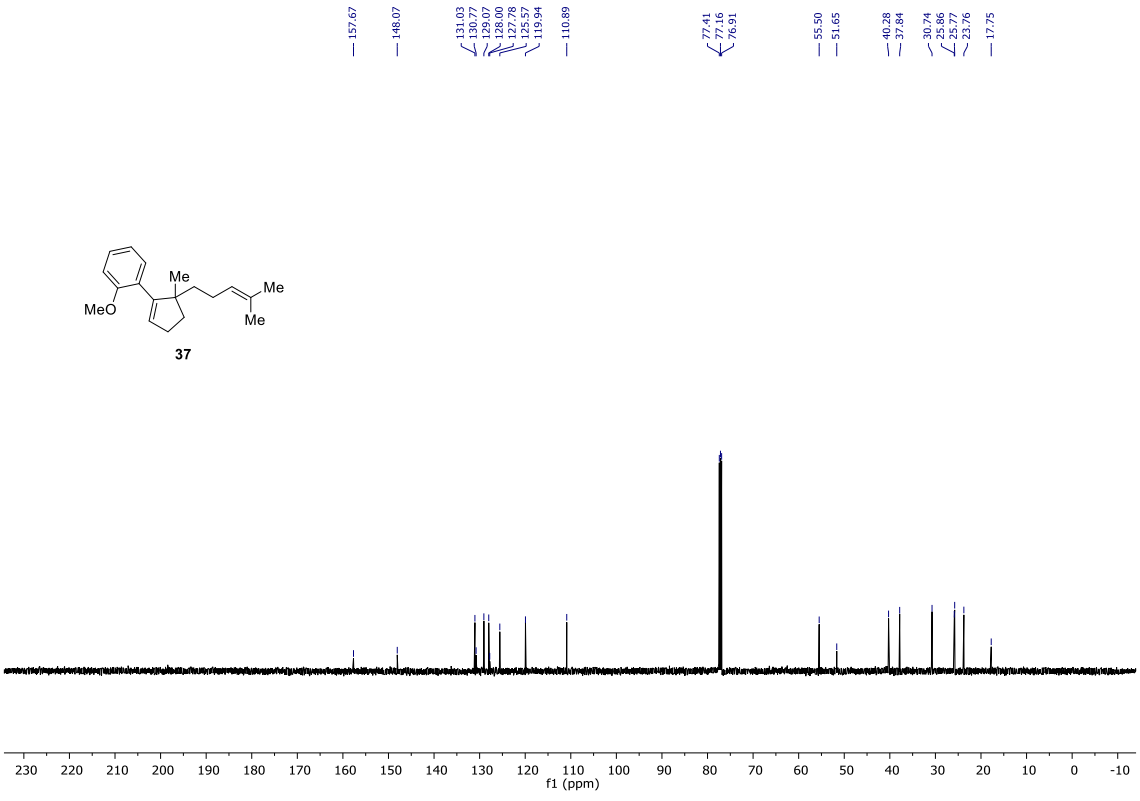
MeO
Me
Me
Me
37
f1 (ppm)

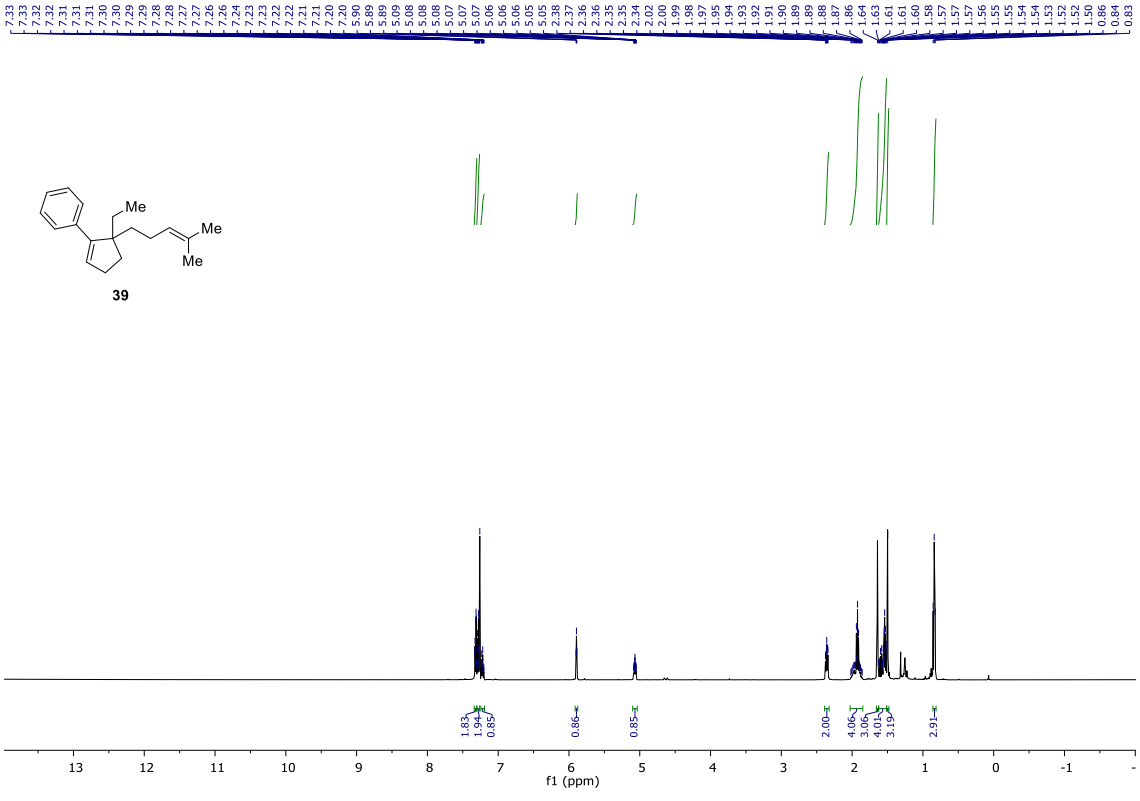
Me
Me
Me
39
1.83
1.94
0.89
0.86
0.85
2.00
4.06
3.06
4.01
3.19
2.91
f1 (ppm)

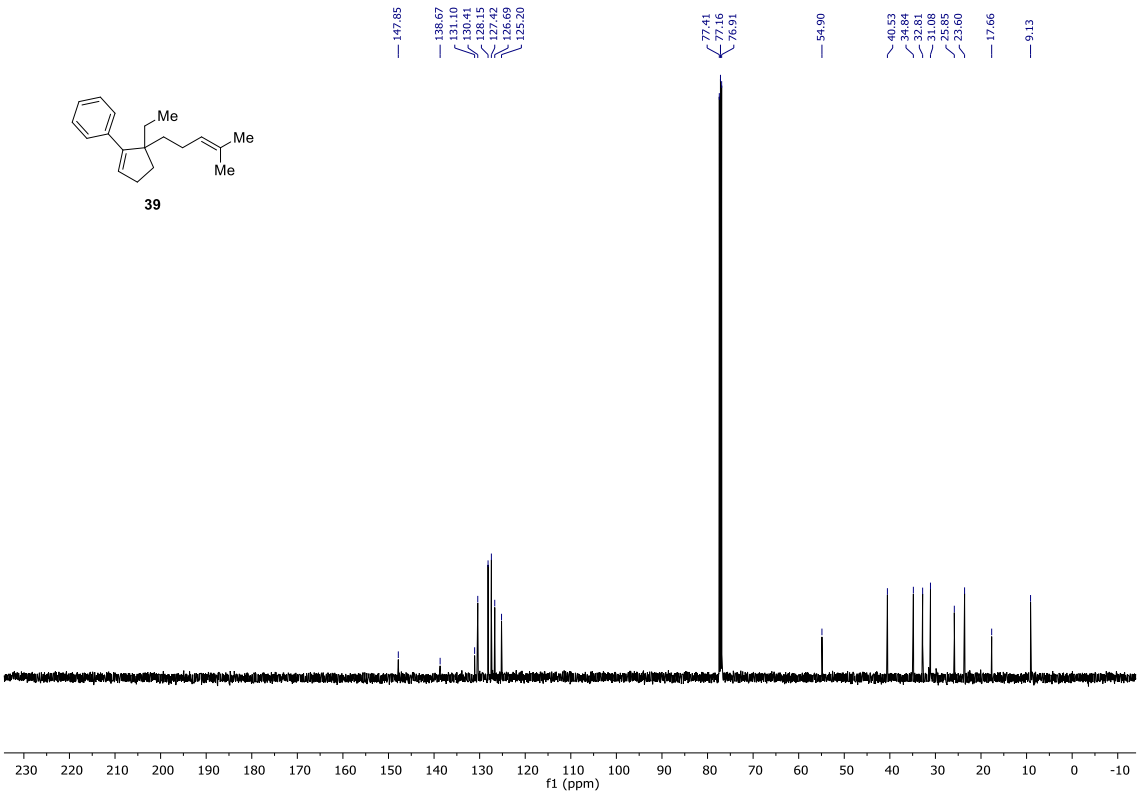
147.85
138.67
131.10
130.41
128.15
127.42
126.69
125.20
77.41
77.16
76.91
54.90
40.53
34.84
32.81
31.08
25.85
23.60
17.66
9.13
Me
Me
Me
39
f1 (ppm)

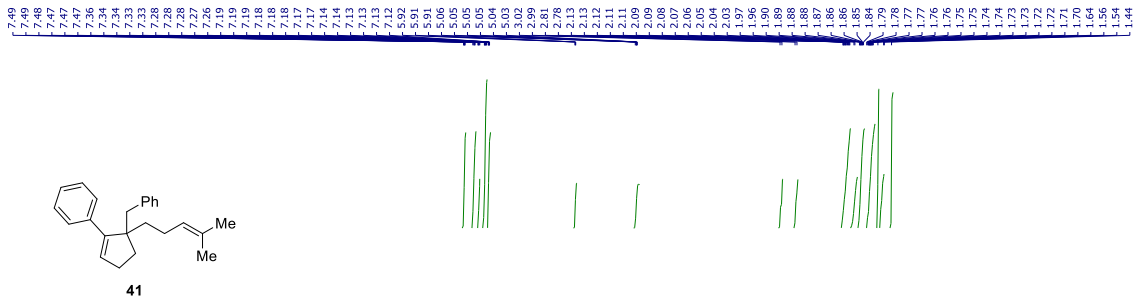

41

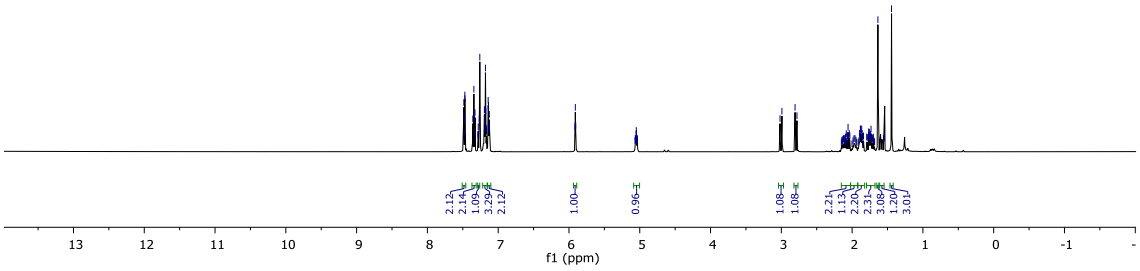

41

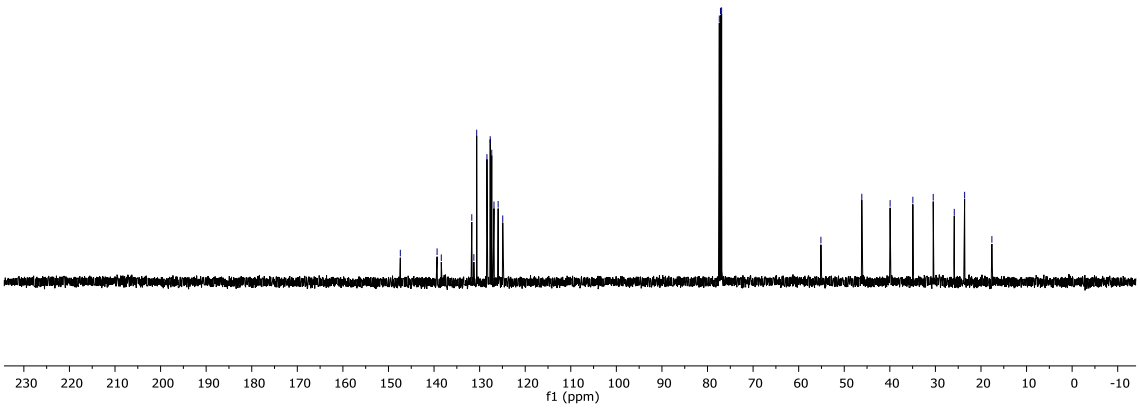

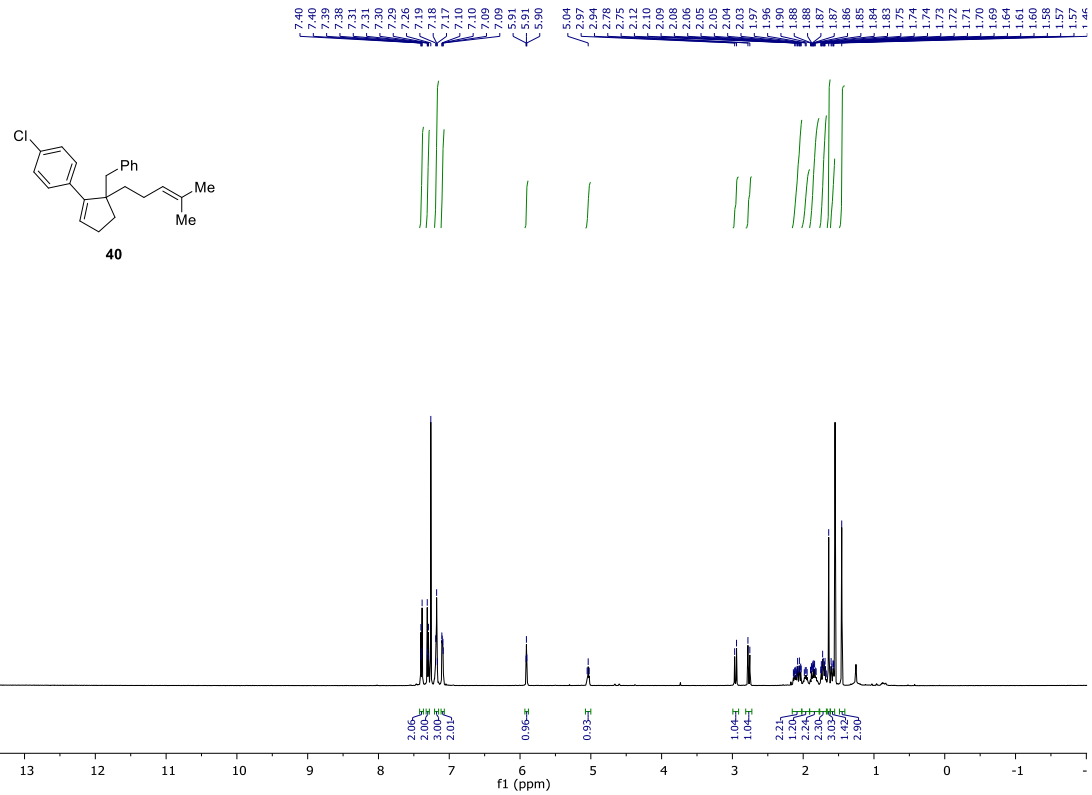
Cl
Ph
Me
Me
40
f1 (ppm)

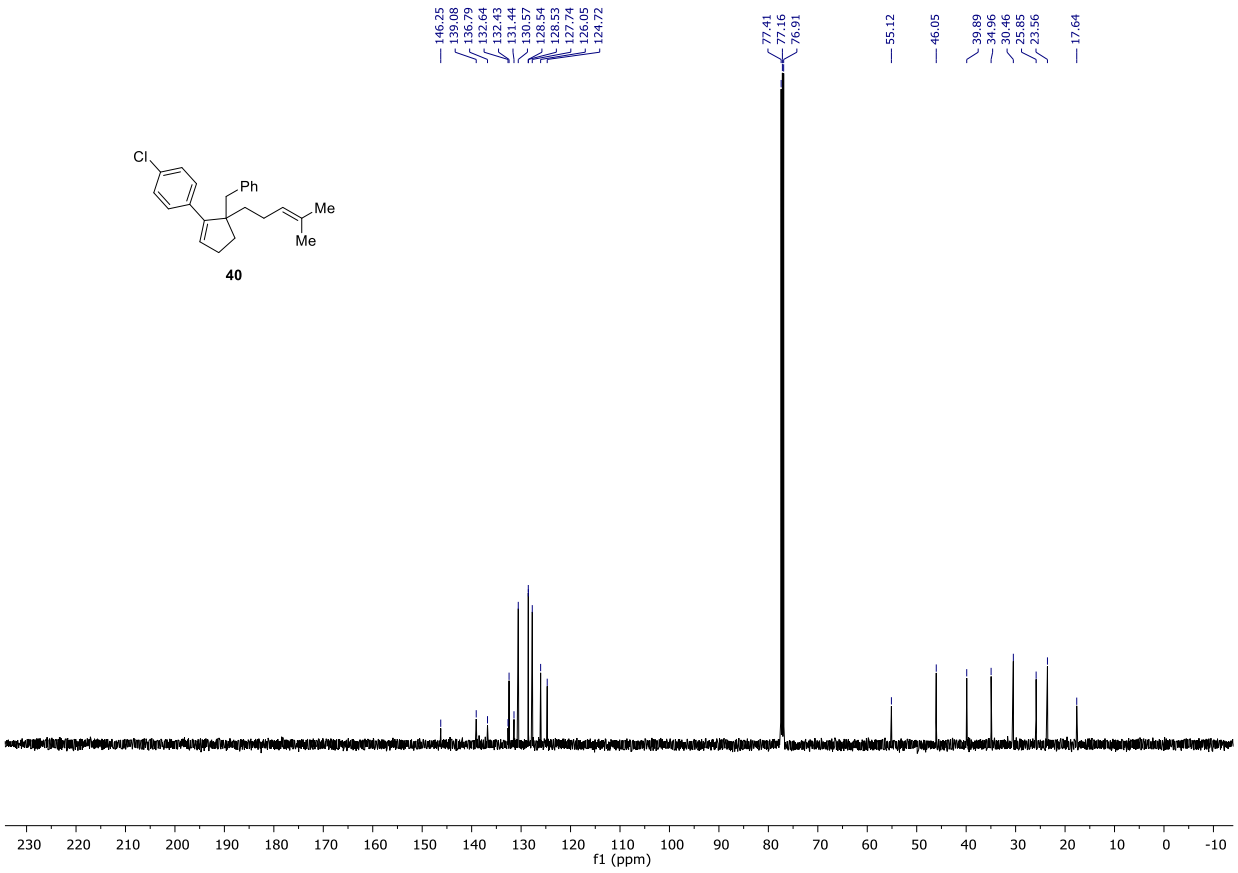
Cl
Ph
Me
Me
40
f1 (ppm)

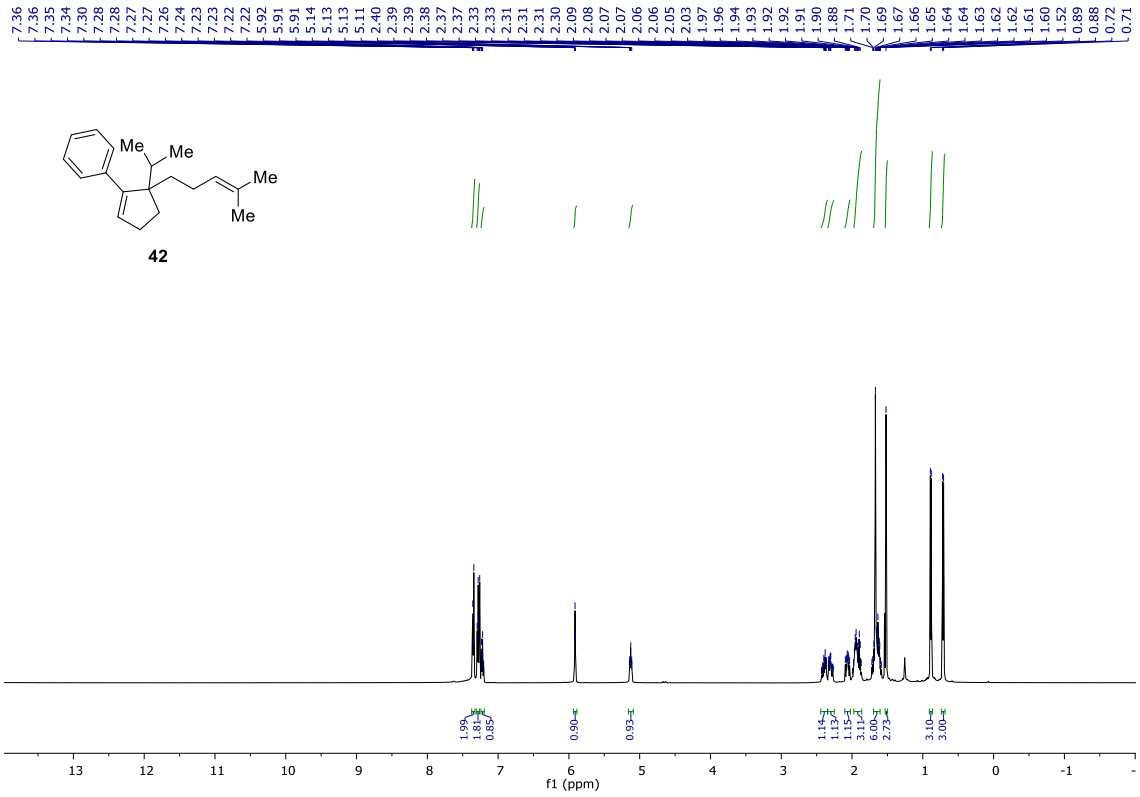
Me
Me
Me
Me
42
f1 (ppm)

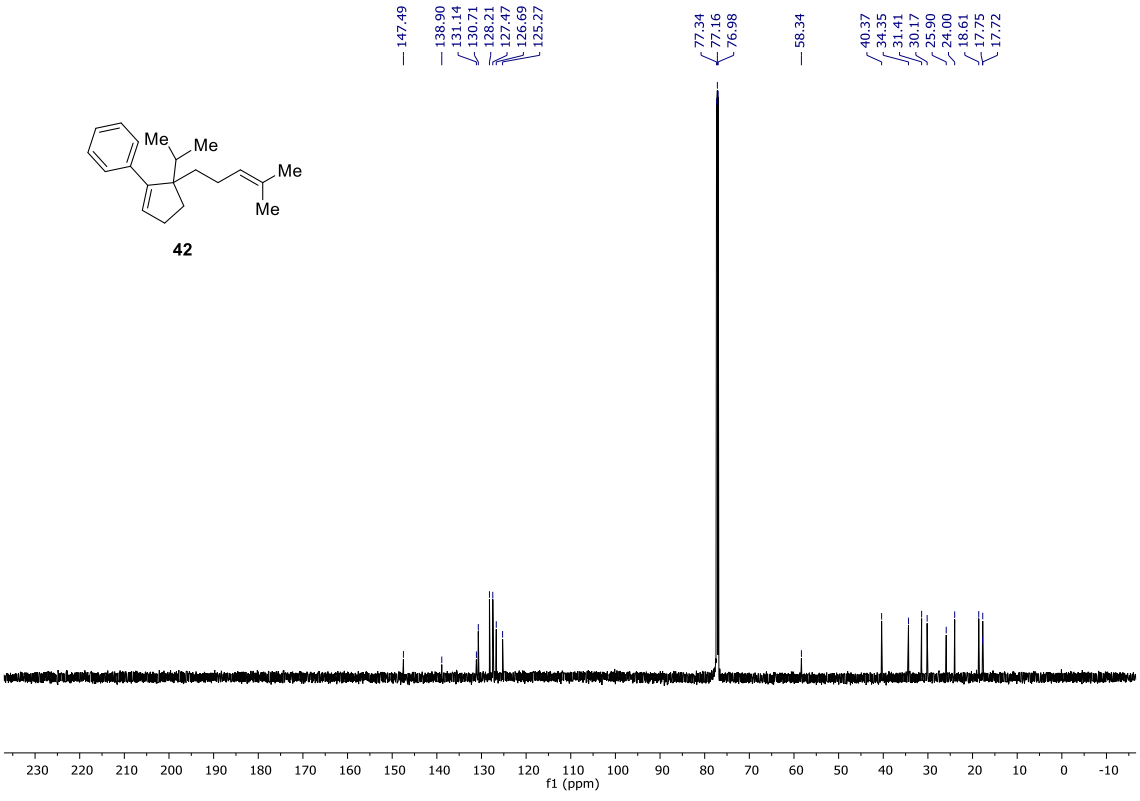
Me
Me
Me
Me
42
f1 (ppm)


7.36
7.35
7.26
6.85
6.83
6.22
6.22
6.22
6.21
3.96
3.96
3.96
3.96
3.95
3.95
3.95
3.94
3.94
3.80
3.63
2.71
2.70
2.69
2.69
2.55
2.54
2.54
2.53
2.35
2.35
2.34
2.34
2.33
2.32
2.32
2.25
2.24
2.24
2.23
2.22

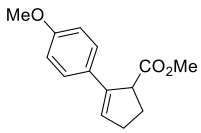
MeO
CO2Me

49

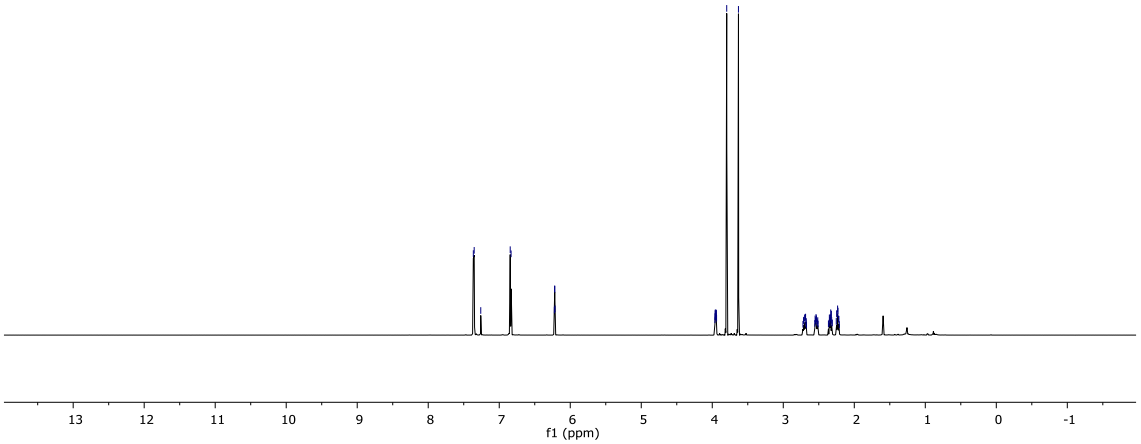
13
12
11
10
9
8
7
6
5
4
3
2
1
0
-1
f1 (ppm)


176.02
158.99
140.43
128.27
128.20
127.05
113.93
77.34
77.16
76.98
55.37
52.04
51.30
32.54
29.53

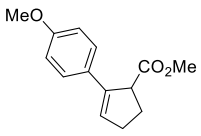
MeO
CO2Me

49

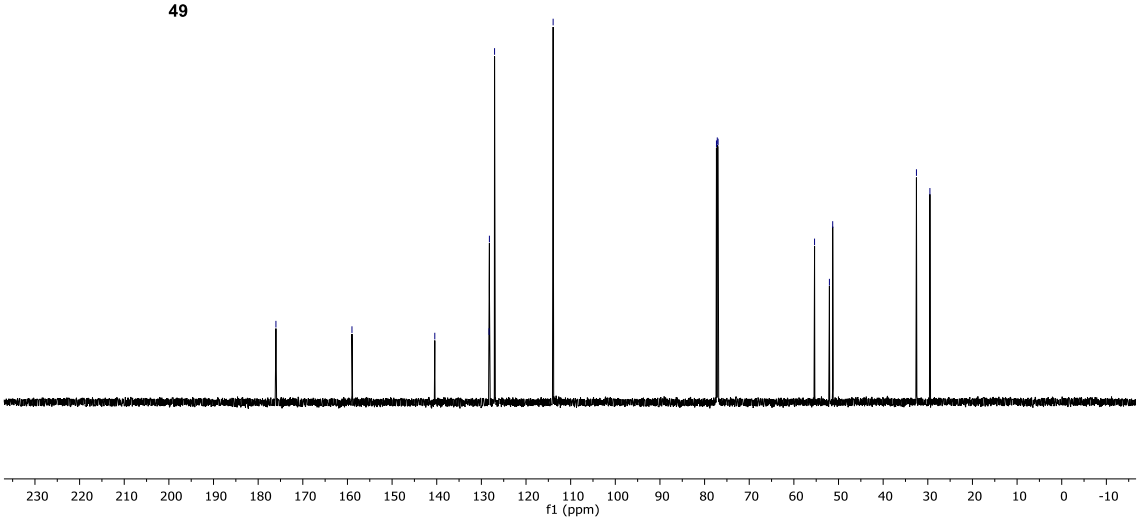
230
220
210
200
190
180
170
160
150
140
130
120
110
100
90
80
70
60
50
40
30
20
10
0
-10
f1 (ppm)

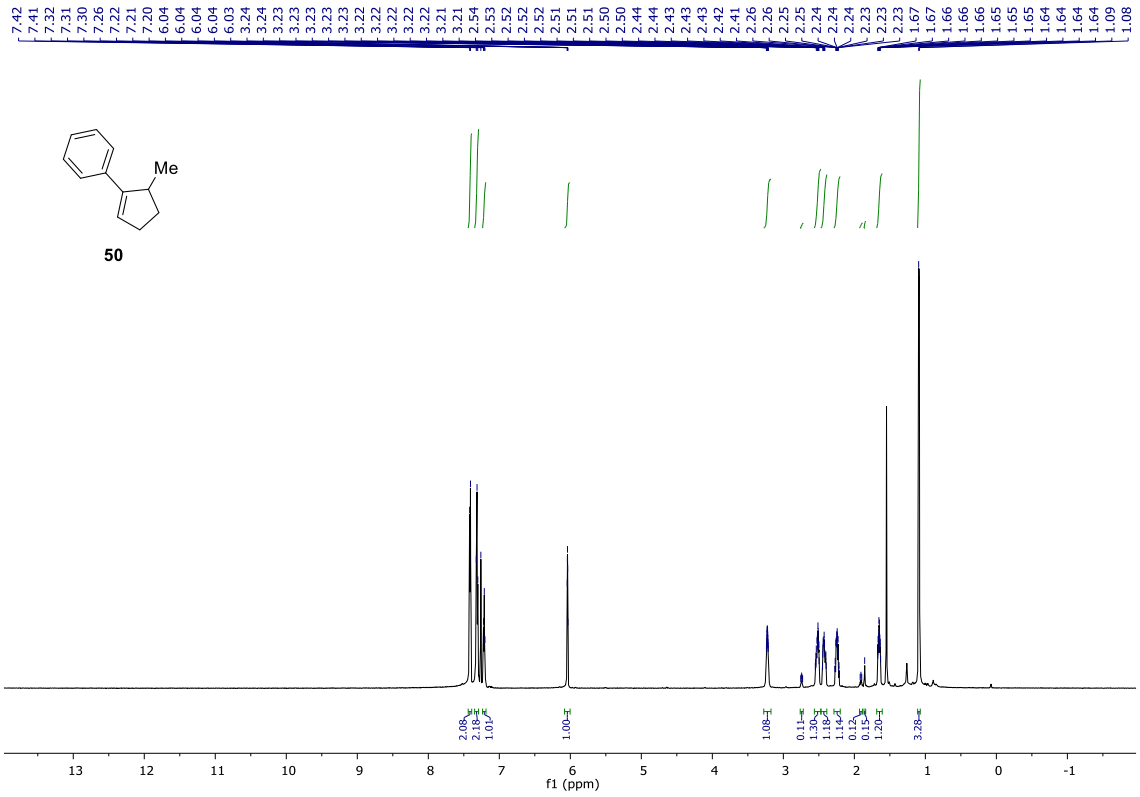
Me
50
f1 (ppm)

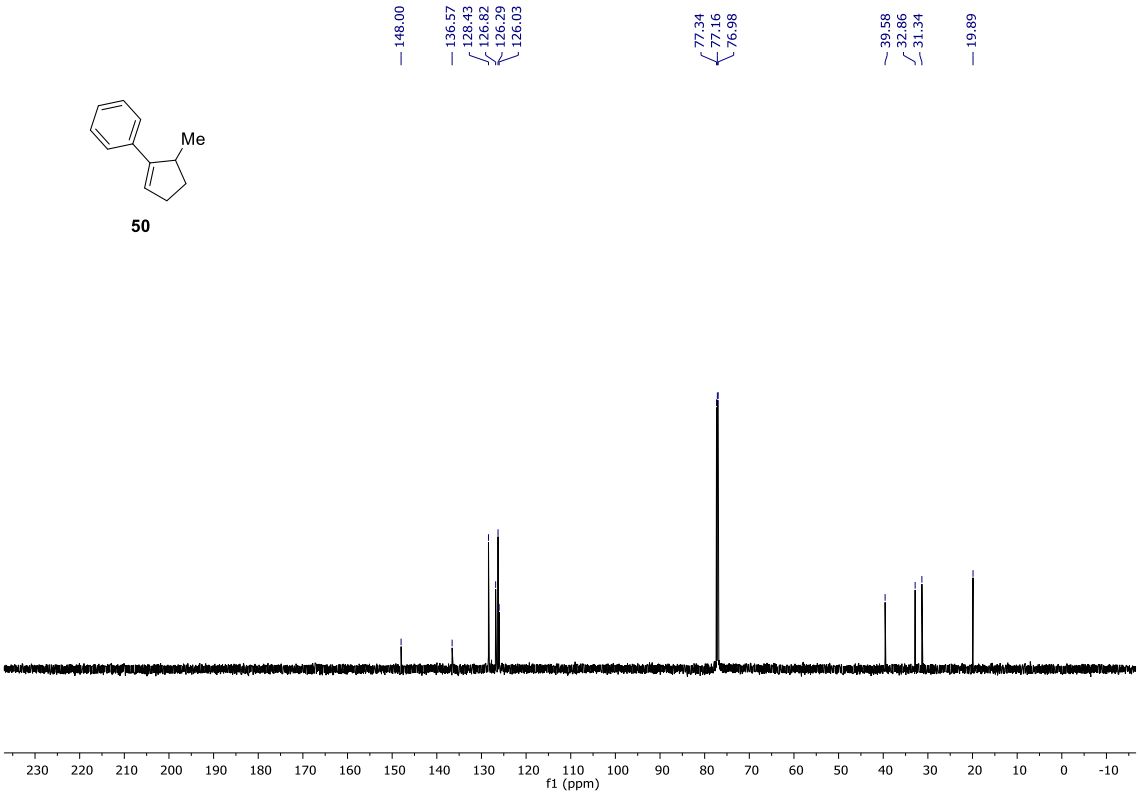
Me
50
f1 (ppm)

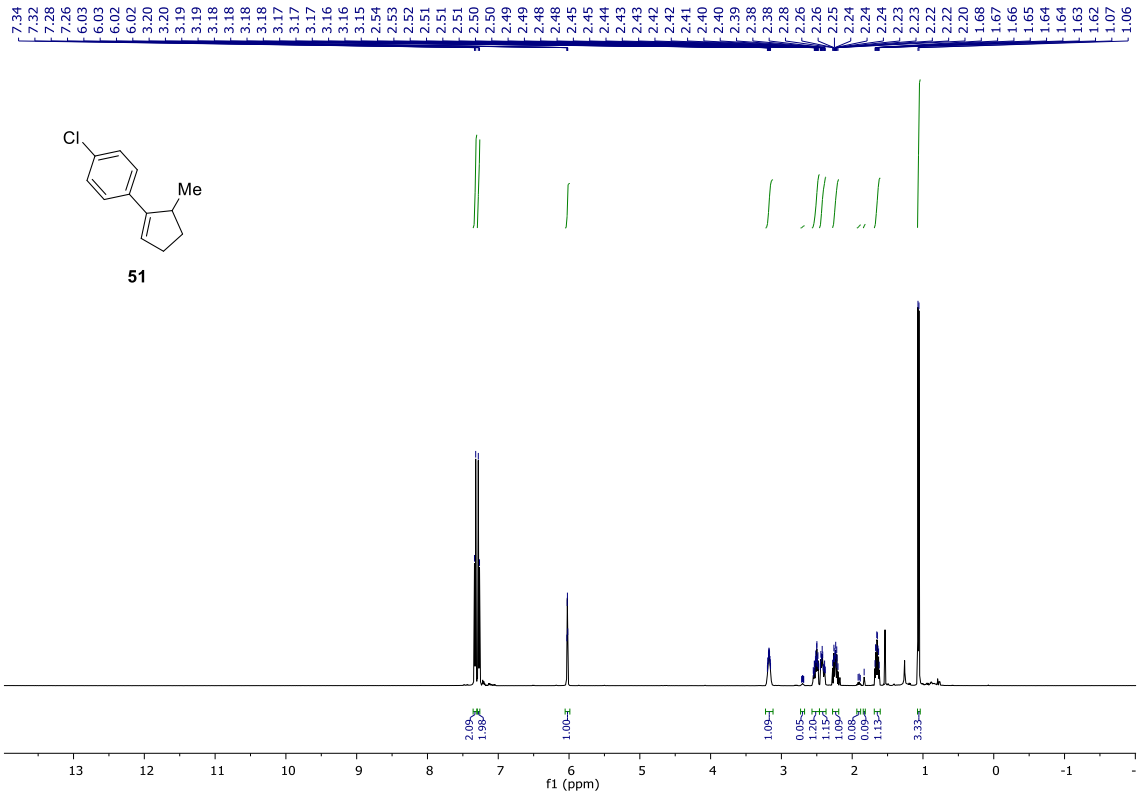
7.34 7.32 7.28 7.26 6.03 6.03 6.02 6.02 6.02 3.20 3.20 3.19 3.19 3.18 3.18 3.18 3.18 3.17 3.17 3.17 3.16 3.16 3.15 2.54 2.53 2.52 2.51 2.51 2.51 2.50 2.50 2.49 2.49 2.48 2.48 2.45 2.45 2.44 2.43 2.43 2.42 2.42 2.41 2.40 2.40 2.40 2.39 2.38 2.38 2.28 2.26 2.26 2.25 2.24 2.24 2.24 2.23 2.23 2.22 2.22 2.20 1.68 1.67 1.66 1.65 1.64 1.64 1.63 1.62 1.07 1.06
Cl
Me
51
2.09
1.98
1.00
1.09
0.05
1.20
1.15
1.09
0.08
0.09
1.13
3.33
f1 (ppm)

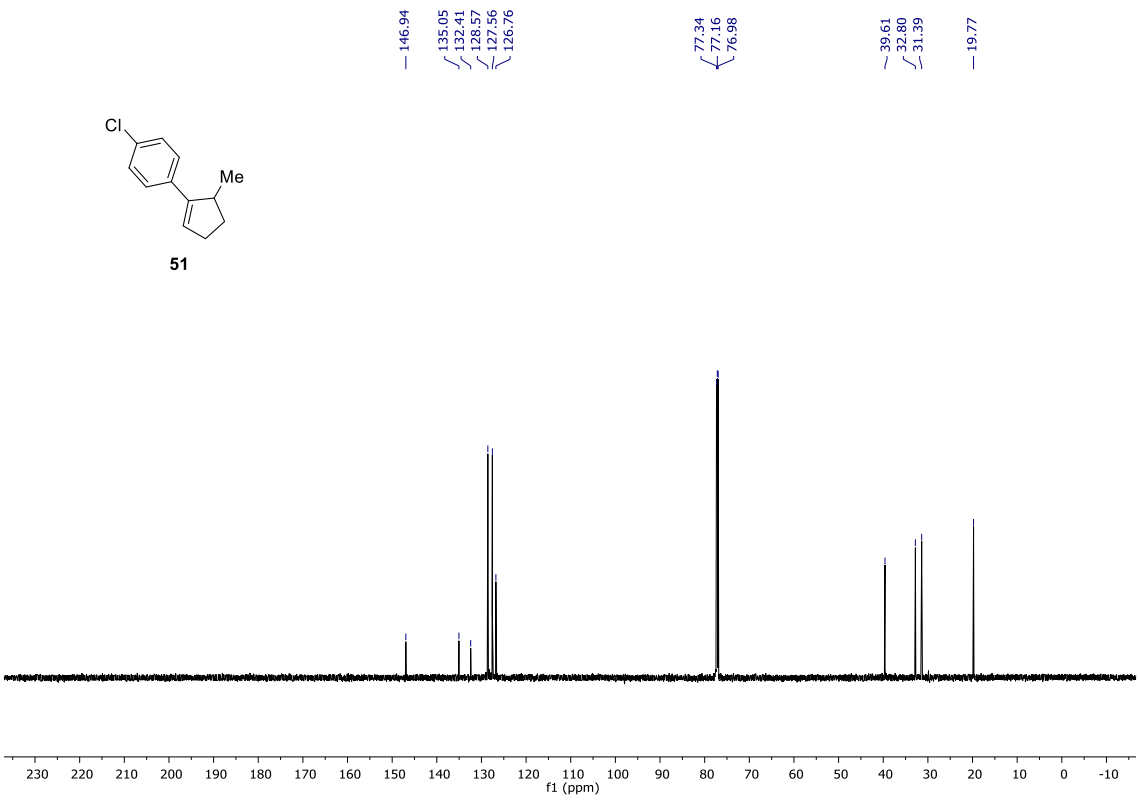
146.94
135.05
132.41
128.57
127.56
126.76
77.34
77.16
76.98
39.61
32.80
31.39
19.77
Cl
Me
51
f1 (ppm)

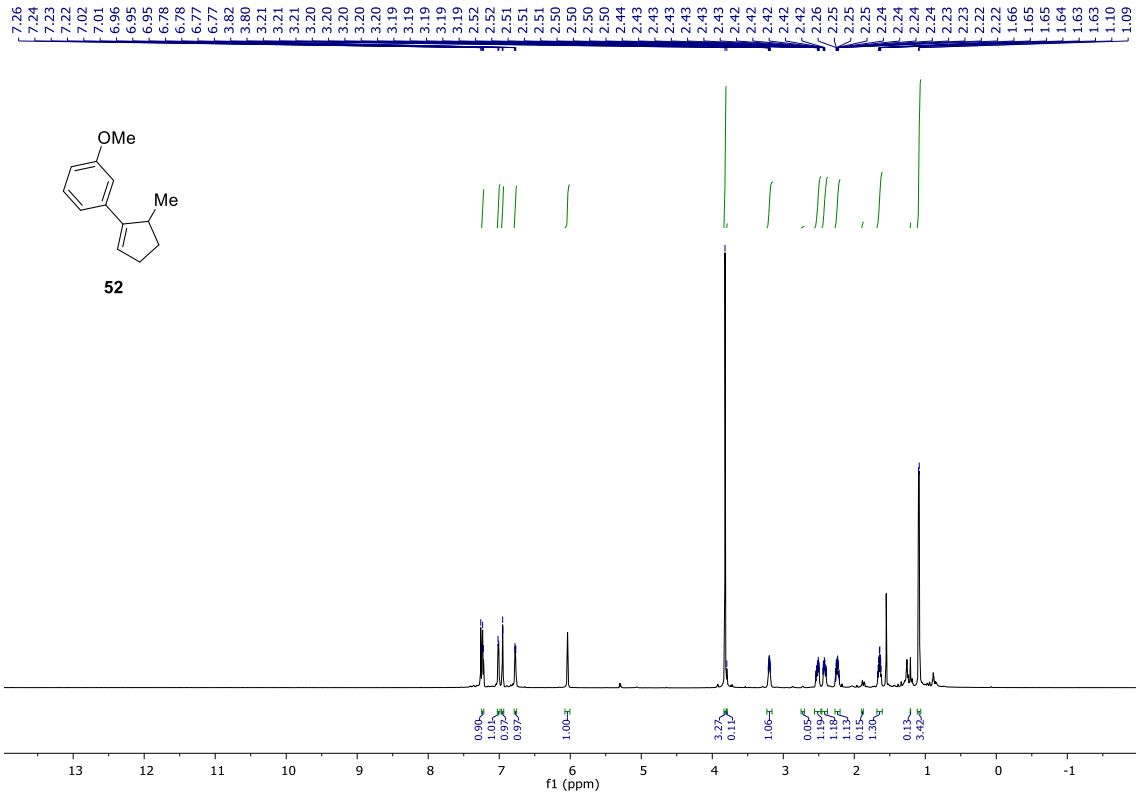
OMe
Me
52
f1 (ppm)

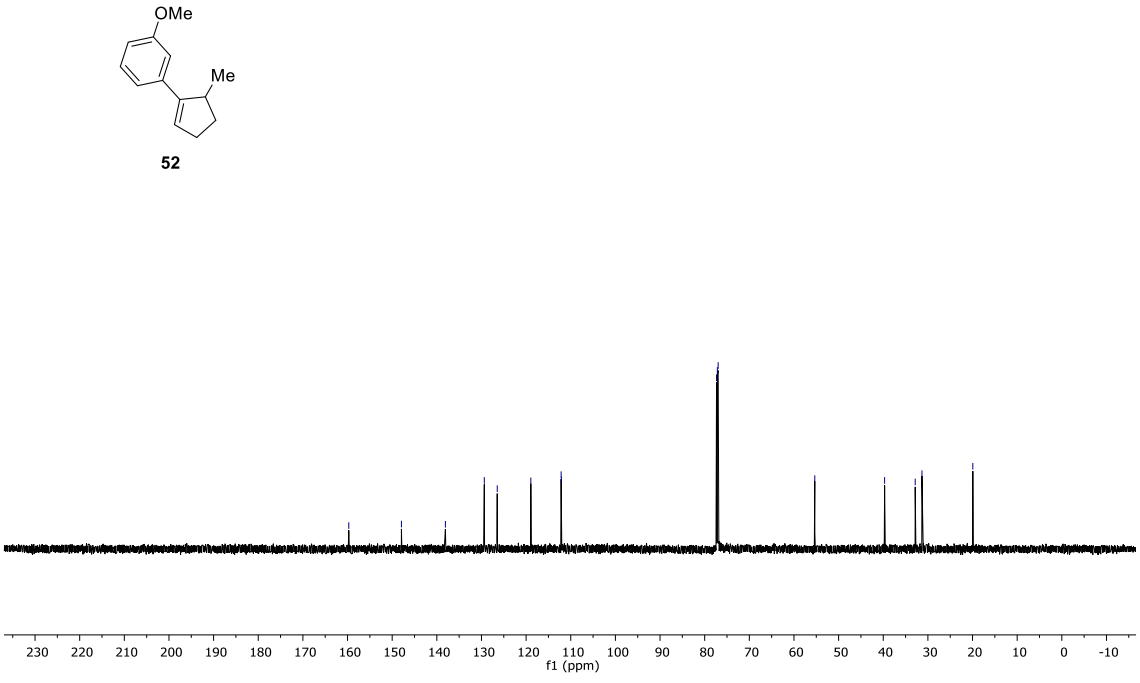
OMe
Me
52
f1 (ppm)

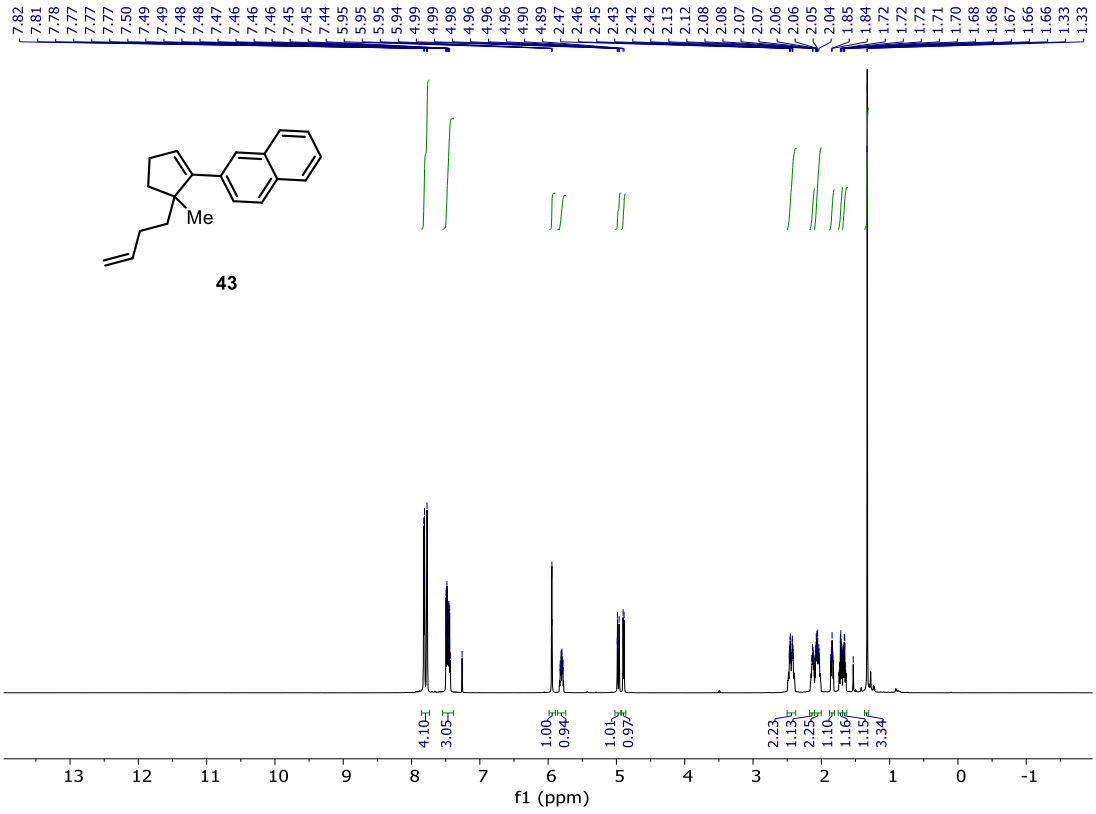
Me
43
f1 (ppm)

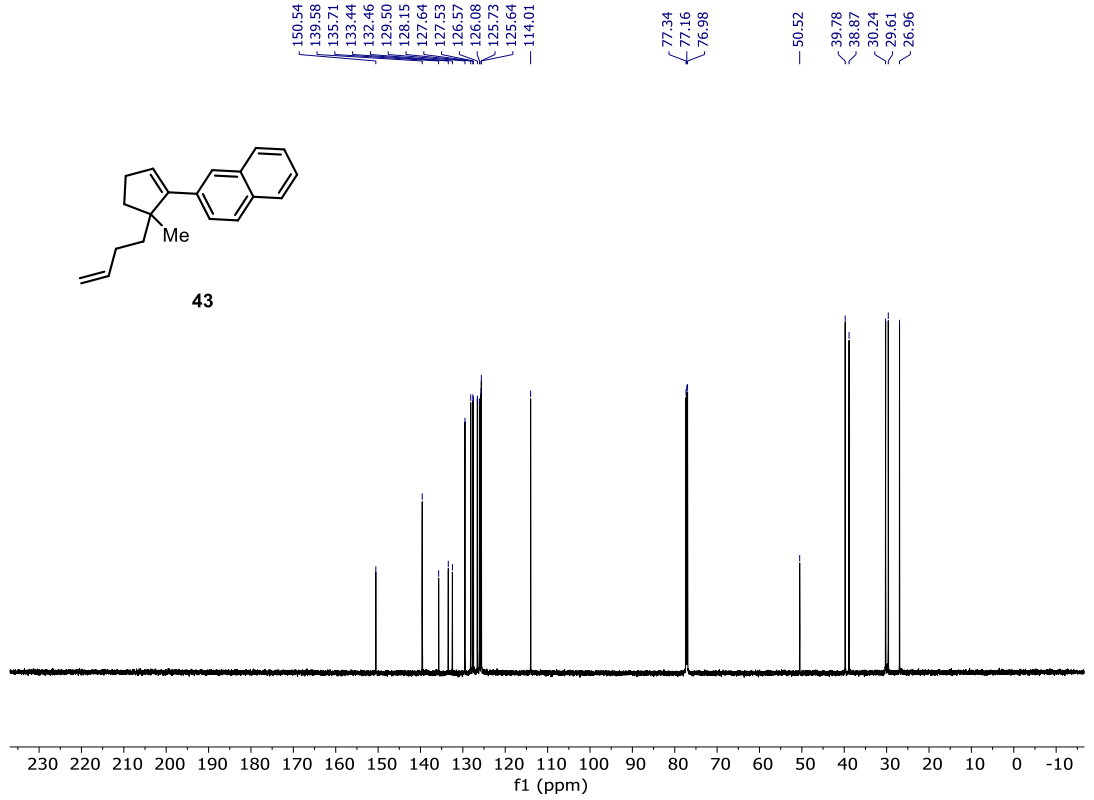
Me
43
f1 (ppm)

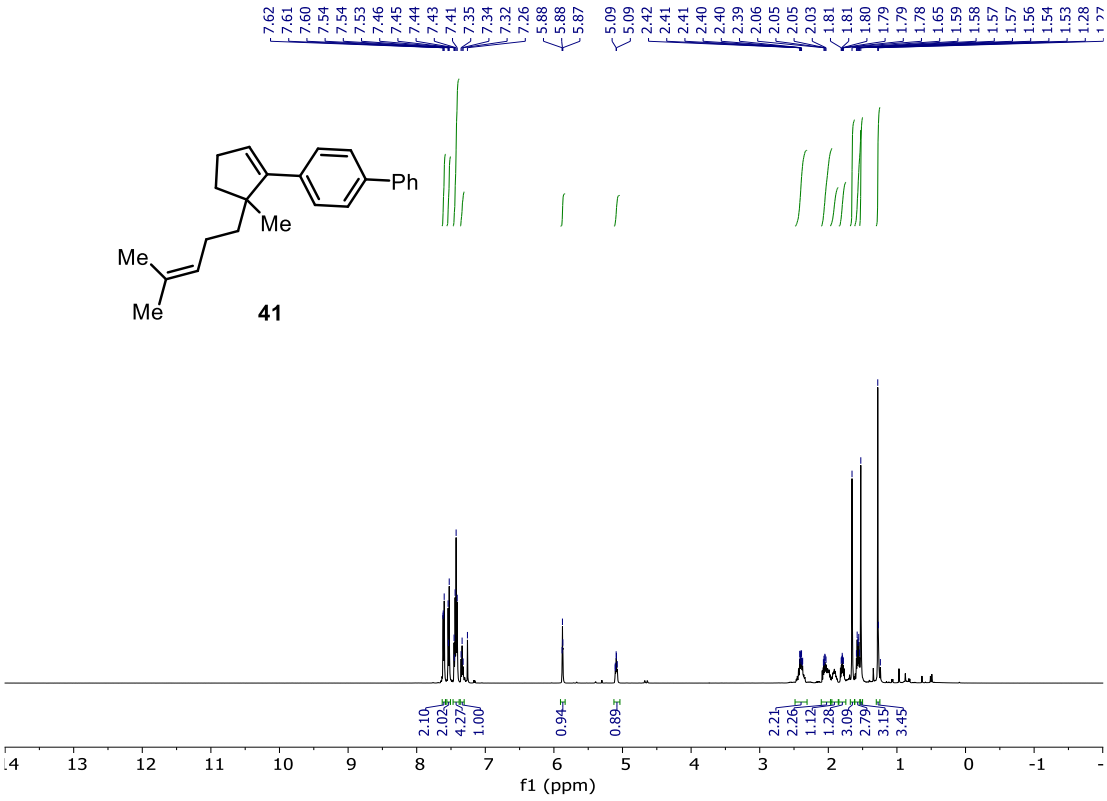
Ph
Me
Me
Me
41
f1 (ppm)

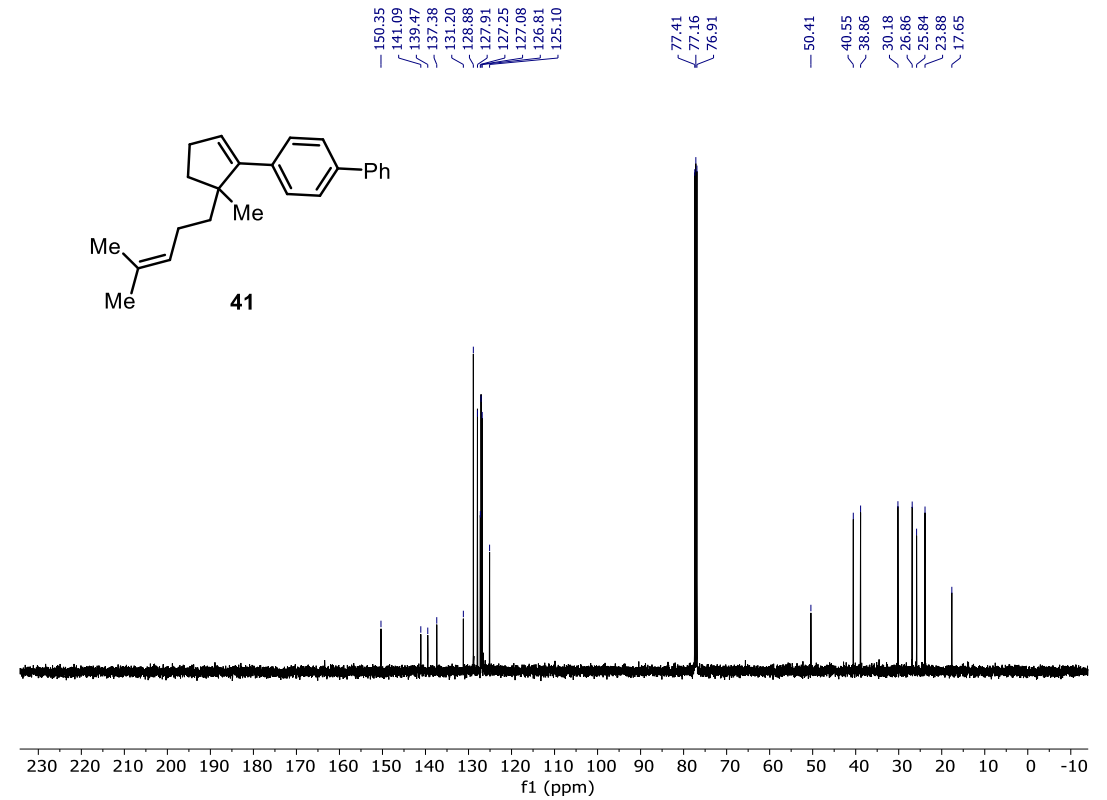
Ph
Me
Me
Me
41
f1 (ppm)

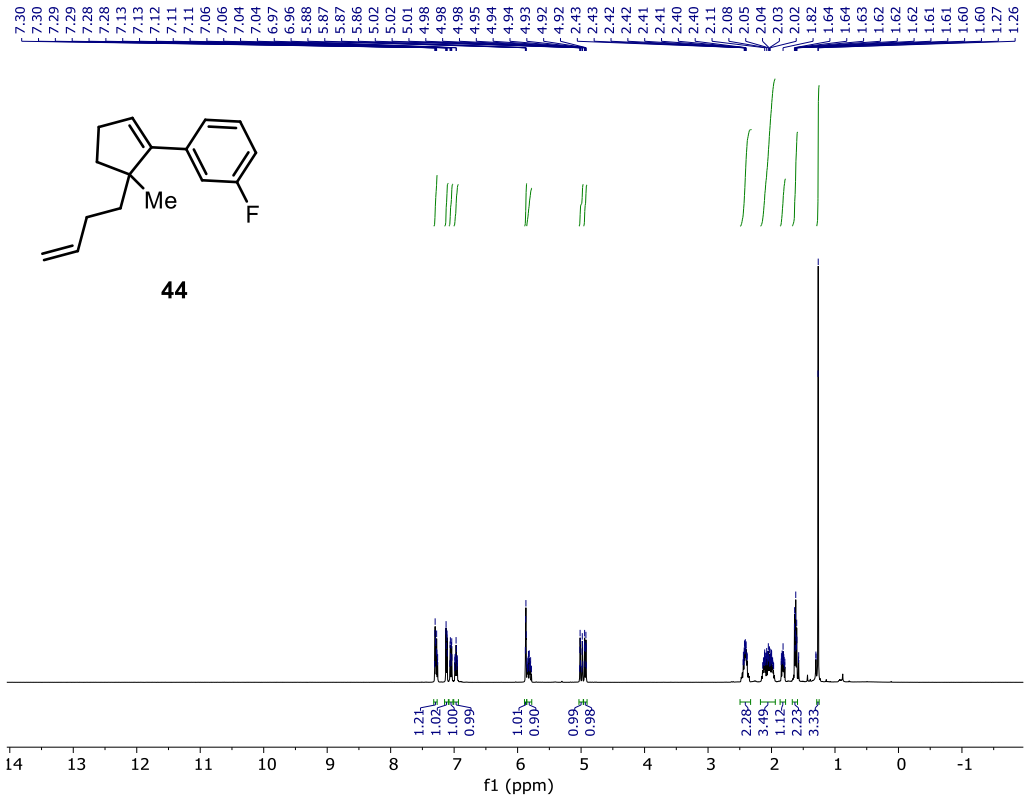
Me
F
44
f1 (ppm)

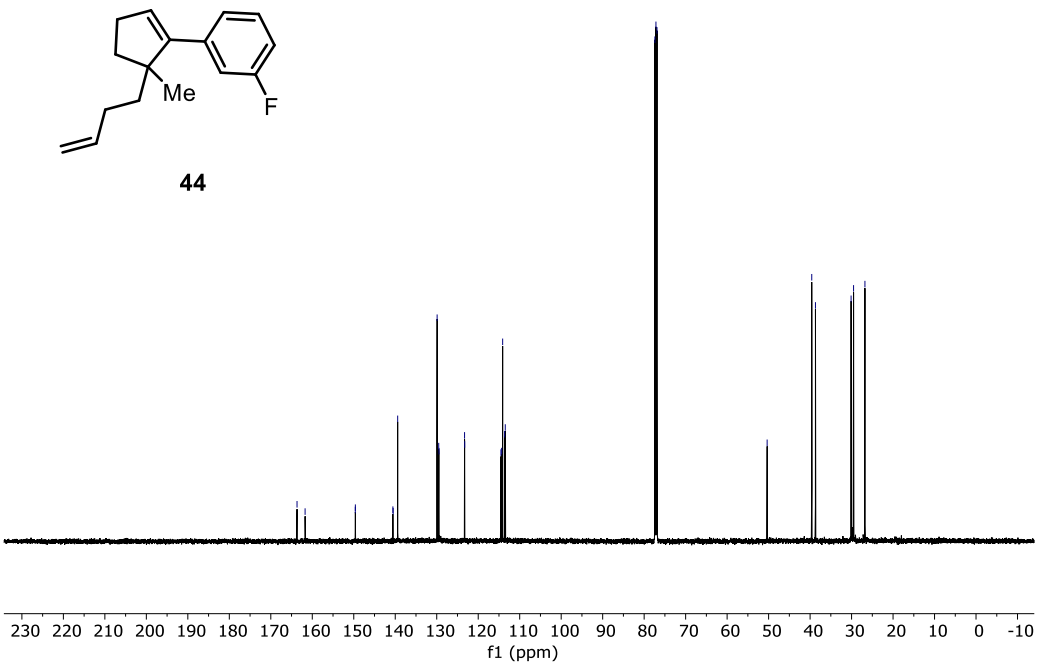
Me
F
44
f1 (ppm)

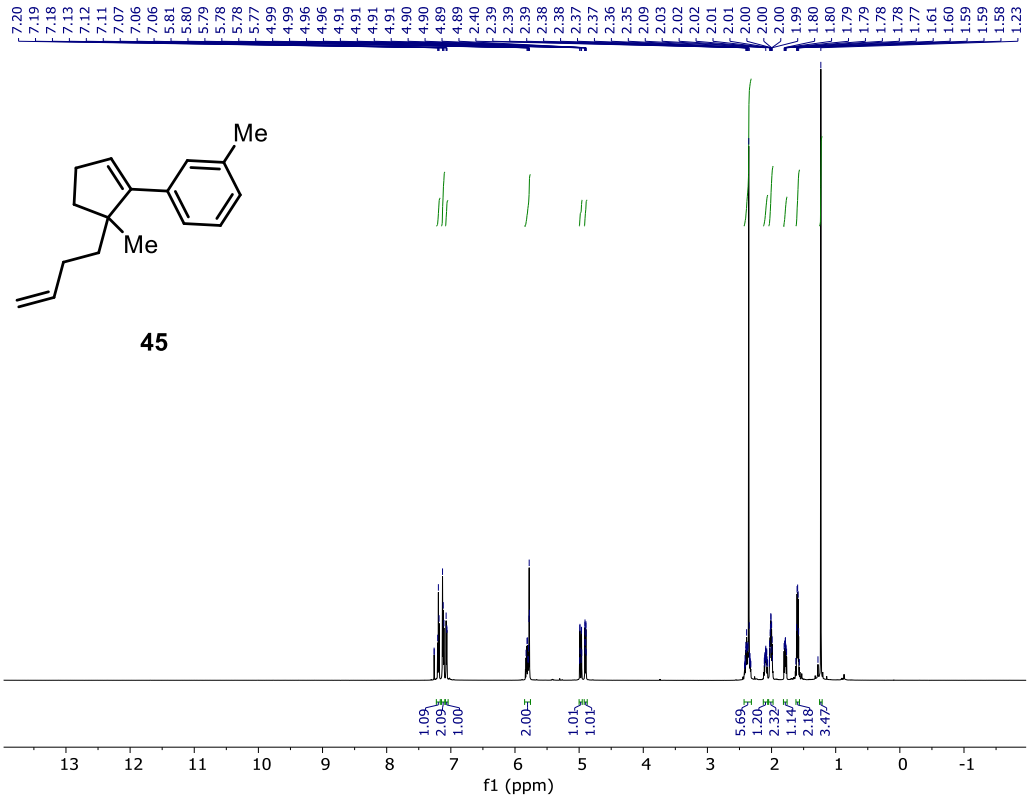
Me
Me
45
f1 (ppm)

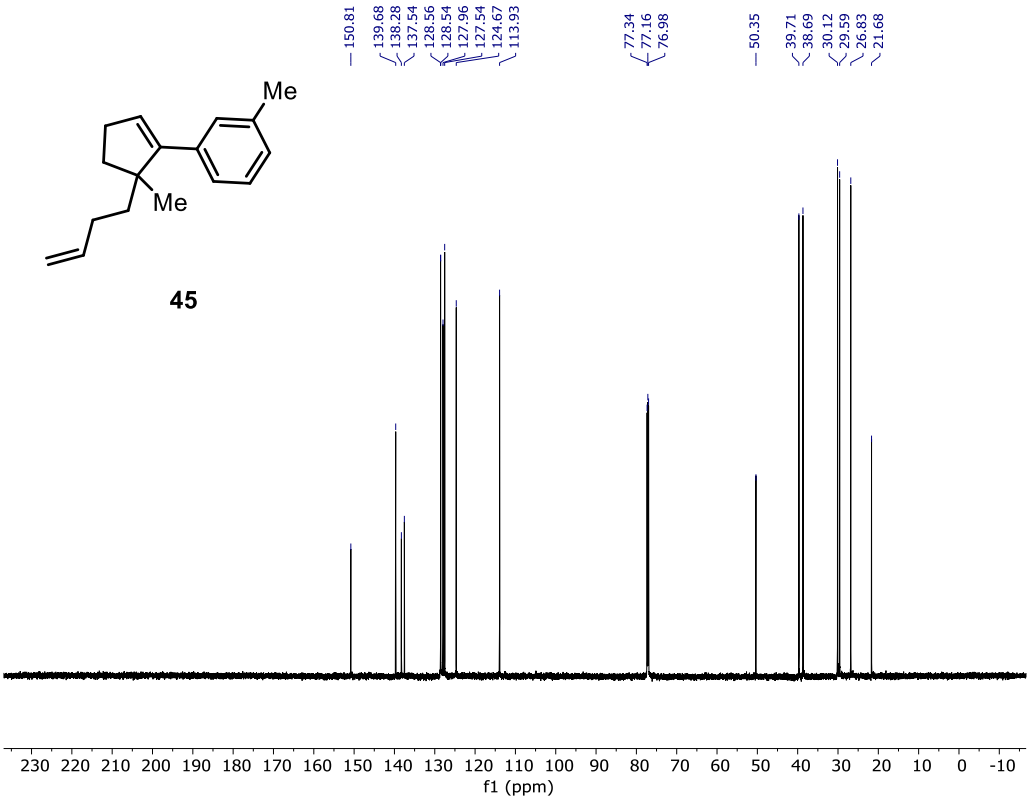
Me
Me
45
f1 (ppm)

3.5 References

(1) Albright, H.; Davis, A. J.; Gomez-Lopez, J. L.; Vonesh, H. L.; Quach, P. K.; Lambert, T. H.; Schindler, C. S. Carbonyl-Olefin Metathesis. *Chemical Reviews*. American Chemical Society August 11, 2021, pp 9359–9406. https://doi.org/10.1021/acs.chemrev.0c01096.

(2) Angew Chem Int Ed Engl - October 2 1995 - Schwab - A Series of Well-Defined Metathesis Catalysts Synthesis of RuCl2 .

(3) Scholl, M.; Trnka, T. M.; Morgan, J. P.; Grubbs, R. H. *Increased Ring Closing Metathesis Activity of Ruthenium-Based Oiefin Metathesis Catalysts Coordinated with Imidazolin-2-Ylidene Ligands*; 1999; Vol. 40.

(4) Ho, T.-L.; Mcmurry, J. E.; Clive, D. L. J.; Zhang, C.; Murthy, K. S. K.; Hayward, W. D.; Daigneault, S.; Grubbs, R. H.; Turnas, W.; Hartley, F.; Pine, S. H. *C) Feast, W. J.; Gibson, V. C. In The Chemistry of the Metal-Carbon Bond*; UTC, 1993; Vol. 89.

(5) Helvetica Chimica Acta - 1 November 1971 - Demole - Applications Synth Tiques de La Cyclisation d Alcools Tertiaires -.

(6) Ludwig, J. R.; Zimmerman, P. M.; Gianino, J. B.; Schindler, C. S. Iron(III)-Catalysed Carbonyl-Olefin Metathesis. *Nature* **2016**, *533*, 374–379. https://doi.org/10.1038/nature17432.

(7) Jackson, A. C.; Goldman, B. E.; Snider, B. B. *Intramolecular and Intermolecular Lewis Acid Catalyzed Ene Reactions Using Ketones as Enophiles*; 1984; Vol. 49.

(8) *COM M UNlCATlONS.*

(9) Khripach, V. A.; Zhabinskii, V. N.; Kuchto, A. I.; Zhiburtovich, Y. Y.; Gromak, V. v.; Groen, M. B.; van der Louw, J.; de Groot, A. Intramolecular Cycloaddition/Cycloreversion of (E)-3β,17β-Diacetoxy-5,10-Secoandrost-1(10)-En-5-

One. *Tetrahedron Letters* **2006**, *47* (38), 6715–6718. https://doi.org/10.1016/j.tetlet.2006.07.096.

(10) Soicke, A.; Slavov, N.; Neudörfl, J. M.; Schmalz, H. G. Metal-Free Intramolecular Carbonyl-Olefin Metathesis of Ortho-Prenylaryl Ketones. *Synlett* **2011**, No. 17, 2487–2490. https://doi.org/10.1055/s-0030-1260320.

(11) Malakar, T.; Hanson, C. S.; Devery, J. J.; Zimmerman, P. M. Combined Theoretical and Experimental Investigation of Lewis Acid-Carbonyl Interactions for Metathesis. *ACS Catalysis* **2021**, *11* (8), 4381–4394. https://doi.org/10.1021/acscatal.0c05277.

(12) Hanson, C. S.; Psaltakis, M. C.; Cortes, J. J.; Devery, J. J. Catalyst Behavior in Metal-Catalyzed Carbonyl-Olefin Metathesis. *J Am Chem Soc* **2019**, *141* (30), 11870–11880. https://doi.org/10.1021/jacs.9b02613.

(13) Ludwig, J. R.; Phan, S.; McAtee, C. C.; Zimmerman, P. M.; Devery, J. J.; Schindler, C. S. Mechanistic Investigations of the Iron(III)-Catalyzed Carbonyl-Olefin Metathesis Reaction. *J Am Chem Soc* **2017**, *139* (31), 10832–10842. https://doi.org/10.1021/jacs.7b05641.

(14) Becker, M. Carbonyl-Olefin Metathesis for the Synthesis of Cyclic Olefins. *Organic Syntheses* **2018**, *95*, 472–485. https://doi.org/10.15227/orgsyn.095.0472.

(15) Ma, L.; Li, W.; Xi, H.; Bai, X.; Ma, E.; Yan, X.; Li, Z. FeCl 3 -Catalyzed Ring-Closing Carbonyl-Olefin Metathesis . *Angewandte Chemie* **2016**, *128* (35), 10566–10569. https://doi.org/10.1002/ange.201604349.

(16) Groso, E. J.; Golonka, A. N.; Harding, R. A.; Alexander, B. W.; Sodano, T. M.; Schindler, C. S. 3-Aryl-2,5-Dihydropyrroles via Catalytic Carbonyl-Olefin Metathesis. *ACS Catalysis* **2018**, *8* (3), 2006–2011. https://doi.org/10.1021/acscatal.7b03769.

(17) Rykaczewski, K. A.; Groso, E. J.; Vonesh, H. L.; Gaviria, M. A.; Richardson, A. D.; Zehnder, T. E.; Schindler, C. S. Tetrahydropyridines via FeCl3-Catalyzed Carbonyl-Olefin Metathesis. *Organic Letters* **2020**, *22* (7), 2844–2848. https://doi.org/10.1021/acs.orglett.0c00918.

(18) Ni, S.; Franzén, J. Carbocation Catalysed Ring Closing Aldehyde-Olefin Metathesis. *Chemical Communications* **2018**, *54* (92), 12982–12985. https://doi.org/10.1039/C8CC06734A.

(19) Wang, R.; Chen, Y.; Shu, M.; Zhao, W.; Tao, M.; Du, C.; Fu, X.; Li, A.; Lin, Z. AuCl3-Catalyzed Ring-Closing Carbonyl–Olefin Metathesis. *Chemistry - A European Journal* **2020**, *26* (9), 1941–1946. https://doi.org/10.1002/chem.201905199.

(20) Tran, U. P. N.; Oss, G.; Breugst, M.; Detmar, E.; Pace, D. P.; Liyanto, K.; Nguyen, T. v. Carbonyl-Olefin Metathesis Catalyzed by Molecular Iodine. *ACS Catalysis* **2019**, *9* (2), 912–919. https://doi.org/10.1021/acscatal.8b03769.

(21) Tran, U. P. N.; Oss, G.; Pace, D. P.; Ho, J.; Nguyen, T. v. Tropylium-Promoted Carbonyl-Olefin Metathesis Reactions. *Chemical Science* **2018**, *9* (23), 5145–5151. https://doi.org/10.1039/c8sc00907d.

(22) Djurovic, A.; Vayer, M.; Li, Z.; Guillot, R.; Baltaze, J. P.; Gandon, V.; Bour, C. Synthesis of Medium-Sized Carbocycles by Gallium-Catalyzed Tandem Carbonyl-Olefin Metathesis/Transfer Hydrogenation. *Organic Letters* **2019**, *21* (19), 8132–8137. https://doi.org/10.1021/acs.orglett.9b03240.

(23) McAtee, C. C.; Riehl, P. S.; Schindler, C. S. Polycyclic Aromatic Hydrocarbons via Iron(III)-Catalyzed Carbonyl-Olefin Metathesis. *J Am Chem Soc* **2017**, *139* (8), 2960–2963. https://doi.org/10.1021/jacs.7b01114.

(24) Albright, H.; Riehl, P. S.; McAtee, C. C.; Reid, J. P.; Ludwig, J. R.; Karp, L. A.; Zimmerman, P. M.; Sigman, M. S.; Schindler, C. S. Catalytic Carbonyl-Olefin Metathesis of Aliphatic Ketones: Iron(III) Homo-Dimers as Lewis Acidic Superelectrophiles. *J Am Chem Soc* **2019**, *141* (4), 1690–1700. https://doi.org/10.1021/jacs.8b11840.

(25) Olah, G. A. *International Edition in English Superelectrophiles***; 1993; Vol. 32.

(26) Negishi, E. *CONCEPTS*; 1999; Vol. 5.

(27) Albright, H.; Vonesh, H. L.; Becker, M. R.; Alexander, B. W.; Ludwig, J. R.; Wiscons, R. A.; Schindler, C. S. GaCl3-Catalyzed Ring-Opening Carbonyl-Olefin Metathesis. *Organic Letters* **2018**, *20* (16), 4954–4958. https://doi.org/10.1021/acs.orglett.8b02086.

(28) Naidu, V. R.; Bah, J.; Franzén, J. Direct Organocatalytic Oxo-Metathesis, a Trans-Selective Carbocation-Catalyzed Olefination of Aldehydes. *European Journal of Organic Chemistry* **2015**, *2015* (8), 1834–1839. https://doi.org/10.1002/ejoc.201403651.

(29) Albright, H.; Vonesh, H. L.; Schindler, C. S. Superelectrophilic Fe(III)-Ion Pairs as Stronger Lewis Acid Catalysts for (E)-Selective Intermolecular Carbonyl-Olefin Metathesis. *Organic Letters* **2020**, *22* (8), 3155–3160. https://doi.org/10.1021/acs.orglett.0c00917.

(30) Riehl, P. S.; Nasrallah, D. J.; Schindler, C. S. Catalytic, Transannular Carbonyl-Olefin Metathesis Reactions. *Chemical Science* **2019**, *10* (44), 10267–10274. https://doi.org/10.1039/c9sc03716k.

(31) Ni, S.; Franzén, J. Carbocation Catalysed Ring Closing Aldehyde-Olefin Metathesis. *Chemical Communications* **2018**, *54* (92), 12982–12985. https://doi.org/10.1039/C8CC06734A.

(32) Tran, U. P. N.; Oss, G.; Pace, D. P.; Ho, J.; Nguyen, T. v. Tropylium-Promoted Carbonyl-Olefin Metathesis Reactions. *Chemical Science* **2018**, *9* (23), 5145–5151. https://doi.org/10.1039/c8sc00907d.

(33) Naidu, V. R.; Bah, J.; Franzén, J. Direct Organocatalytic Oxo-Metathesis, a Trans-Selective Carbocation-Catalyzed Olefination of Aldehydes. *European Journal of Organic Chemistry* **2015**, *2015* (8), 1834–1839. https://doi.org/10.1002/ejoc.201403651.

(34) Hanson, C. S.; Psaltakis, M. C.; Cortes, J. J.; Devery, J. J. Catalyst Behavior in Metal-Catalyzed Carbonyl-Olefin Metathesis. *J Am Chem Soc* **2019**, *141* (30), 11870–11880. https://doi.org/10.1021/jacs.9b02613.

(35) Ma, L.; Li, W.; Xi, H.; Bai, X.; Ma, E.; Yan, X.; Li, Z. FeCl 3 -Catalyzed Ring-Closing Carbonyl-Olefin Metathesis . *Angewandte Chemie* **2016**, *128* (35), 10566–10569. https://doi.org/10.1002/ange.201604349.

(36) Riehl, P. S.; Nasrallah, D. J.; Schindler, C. S. Catalytic, Transannular Carbonyl-Olefin Metathesis Reactions. *Chemical Science* **2019**, *10* (44), 10267–10274. https://doi.org/10.1039/c9sc03716k.

(37) Albright, H.; Vonesh, H. L.; Becker, M. R.; Alexander, B. W.; Ludwig, J. R.; Wiscons, R. A.; Schindler, C. S. GaCl3-Catalyzed Ring-Opening Carbonyl-Olefin Metathesis. *Organic Letters* **2018**, *20* (16), 4954–4958. https://doi.org/10.1021/acs.orglett.8b02086.

(38) Groso, E. J.; Golonka, A. N.; Harding, R. A.; Alexander, B. W.; Sodano, T. M.; Schindler, C. S. 3-Aryl-2,5-Dihydropyrroles via Catalytic Carbonyl-Olefin Metathesis. *ACS Catalysis* **2018**, *8* (3), 2006–2011. https://doi.org/10.1021/acscatal.7b03769.

(39) Ludwig, J. R.; Phan, S.; McAtee, C. C.; Zimmerman, P. M.; Devery, J. J.; Schindler, C. S. Mechanistic Investigations of the Iron(III)-Catalyzed Carbonyl-Olefin Metathesis

Reaction. *J Am Chem Soc* **2017**, *139* (31), 10832–10842. https://doi.org/10.1021/jacs.7b05641.

(40) Ludwig, J. R.; Schindler, C. S. Lewis Acid Catalyzed Carbonyl-Olefin Metathesis. *Synlett* **2017**, *28* (13), 1501–1509. https://doi.org/10.1055/s-0036-1588827.

(41) Ludwig, J. R.; Zimmerman, P. M.; Gianino, J. B.; Schindler, C. S. Iron(III)-Catalysed Carbonyl-Olefin Metathesis. *Nature* **2016**, *533*, 374–379. https://doi.org/10.1038/nature17432.

(42) Albright, H.; Riehl, P. S.; McAtee, C. C.; Reid, J. P.; Ludwig, J. R.; Karp, L. A.; Zimmerman, P. M.; Sigman, M. S.; Schindler, C. S. Catalytic Carbonyl-Olefin Metathesis of Aliphatic Ketones: Iron(III) Homo-Dimers as Lewis Acidic Superelectrophiles. *J Am Chem Soc* **2019**, *141* (4), 1690–1700. https://doi.org/10.1021/jacs.8b11840.

(43) McAtee, C. C.; Riehl, P. S.; Schindler, C. S. Polycyclic Aromatic Hydrocarbons via Iron(III)-Catalyzed Carbonyl-Olefin Metathesis. *J Am Chem Soc* **2017**, *139* (8), 2960–2963. https://doi.org/10.1021/jacs.7b01114.

(44) Rykaczewski, K. A.; Groso, E. J.; Vonesh, H. L.; Gaviria, M. A.; Richardson, A. D.; Zehnder, T. E.; Schindler, C. S. Tetrahydropyridines via FeCl3-Catalyzed Carbonyl-Olefin Metathesis. *Organic Letters* **2020**, *22* (7), 2844–2848. https://doi.org/10.1021/acs.orglett.0c00918.

(45) Catti, L.; Tiefenbacher, K. Brønsted-Säure-Katalysierte Carbonyl-Olefin-Metathese in Einer Selbstorganisierten Supramolekularen Wirtstruktur. *Angewandte Chemie* **2018**, *130* (44), 14797–14800. https://doi.org/10.1002/ange.201712141.

(46) Zhu, Y.; Rebek, J.; Yu, Y. Cyclizations Catalyzed inside a Hexameric Resorcinarene Capsule. *Chemical Communications* **2019**, *55* (25), 3573–3577. https://doi.org/10.1039/c9cc01611b.

(47) Griffith, A. K.; Vanos, C. M.; Lambert, T. H. Organocatalytic Carbonyl-Olefin Metathesis. *J Am Chem Soc* **2012**, *134* (45), 18581–18584. https://doi.org/10.1021/ja309650u.

(48) Hong, X.; Liang, Y.; Griffith, A. K.; Lambert, T. H.; Houk, K. N. Distortion-Accelerated Cycloadditions and Strain-Release-Promoted Cycloreversions in the Organocatalytic Carbonyl-Olefin Metathesis. *Chemical Science* **2014**, *5* (2), 471–475. https://doi.org/10.1039/c3sc52882k.

(49) Zhang, Y.; Jermaks, J.; MacMillan, S. N.; Lambert, T. H. Synthesis of 2 H-Chromenes via Hydrazine-Catalyzed Ring-Closing Carbonyl-Olefin Metathesis. *ACS Catalysis* **2019**, *9* (10), 9259–9264. https://doi.org/10.1021/acscatal.9b03656.

(50) Zhang, Y.; Jermaks, J.; MacMillan, S. N.; Lambert, T. H. Synthesis of 2 H-Chromenes via Hydrazine-Catalyzed Ring-Closing Carbonyl-Olefin Metathesis. *ACS Catalysis* **2019**, *9* (10), 9259–9264. https://doi.org/10.1021/acscatal.9b03656.

(51) Albright, H.; Davis, A. J.; Gomez-Lopez, J. L.; Vonesh, H. L.; Quach, P. K.; Lambert, T. H.; Schindler, C. S. Carbonyl-Olefin Metathesis. *Chemical Reviews*. American Chemical Society August 11, 2021, pp 9359–9406. https://doi.org/10.1021/acs.chemrev.0c01096.

(52) Soicke, A.; Slavov, N.; Neudörfl, J. M.; Schmalz, H. G. Metal-Free Intramolecular Carbonyl-Olefin Metathesis of Ortho-Prenylaryl Ketones. *Synlett* **2011**, No. 17, 2487–2490. https://doi.org/10.1055/s-0030-1260320.

(53) Schopov, I. *A Carbonyl-Olefin Exchange Reaction-New Route to Polyconjugated Polymers, 1 A New Synthesis of Polyphenylacetylene*; 1983; Vol. 4.

(54) Ho, T.-L.; Mcmurry, J. E.; Clive, D. L. J.; Zhang, C.; Murthy, K. S. K.; Hayward, W. D.; Daigneault, S.; Grubbs, R. H.; Turnas, W.; Hartley, F.; Pine, S. H. *C) Feast, W. J.; Gibson, V. C. In The Chemistry of the Metal-Carbon Bond*; UTC, 1993; Vol. 89.

(55) Valiulin, R. A.; Arisco, T. M.; Kutateladze, A. G. Photoinduced Intramolecular Cyclopentanation vs Photoprotolytic Oxametathesis in Polycyclic Alkenes Outfitted with Conformationally Constrained Aroylmethyl Chromophores. *Journal of Organic Chemistry* **2013**, *78* (5), 2012–2025. https://doi.org/10.1021/jo301909j.

(56) Valiulin, R. A.; Arisco, T. M.; Kutateladze, A. G. Double-Tandem [4π+2π]·[2 Π+2π]·[4π+2π] ·[2π+2π] Synthetic Sequence with Photoprotolytic Oxametathesis and Photoepoxidation in the Chromone Series. *Journal of Organic Chemistry* **2011**, *76* (5), 1319–1332. https://doi.org/10.1021/jo102221q.

(57) Valiulin, R. A.; Kutateladze, A. G. Harvesting the Strain Installed by a Paternò-Büchi Step in a Synthetically Useful Way: High-Yielding Photoprotolytic Oxametathesis in Polycyclic Systems. *Organic Letters* **2009**, *11* (17), 3886–3889. https://doi.org/10.1021/ol901456m.

(58) Pérez-Ruiz, R.; Miranda, M. A.; Alle, R.; Meerholz, K.; Griesbeck, A. G. An Efficient Carbonyl-Alkene Metathesis of Bicyclic Oxetanes: Photoinduced Electron Transfer Reduction of the Paternò–Büchi Adducts from 2,3-Dihydrofuran and Aromatic Aldehydes. *Photochemical and Photobiological Sciences* **2006**, *5* (1), 51–55. https://doi.org/10.1039/b513875b.

(59) Pérez-Ruiz, R.; Gil, S.; Miranda, M. A. Stereodifferentiation in the Photochemical Cycloreversion of Diastereomeric Methoxynaphthalene-Oxetane Dyads. **2005**. https://doi.org/10.1021/jo048708.

(60) D'Auria, M.; Racioppi, R.; Viggiani, L. Paternò-Büchi Reaction between Furan and Heterocyclic Aldehydes: Oxetane Formation vs. Metathesis. *Photochemical and Photobiological Sciences* **2010**, *9* (8), 1134–1138. https://doi.org/10.1039/c0pp00076k.

(61) Guilford Jones, B.; Acquadro, M. A.; Carmody, M. A. *Long-Chain Enals Oia Carbonyl-Olefin Metathesis. An Application in Pheromone Synthesis*; 1975.

(62) Guilford Jones, B. I.; Schwartz, S. B.; Marton, M. T. *Regiospecific Thermal Cleavage of Some Oxetan Photoadducts : Carbonyl-Olefin Metathesis in Sequential Photochemical and Thermal Steps*; 1973.

(63) Albright, H.; Vonesh, H. L.; Schindler, C. S. Superelectrophilic Fe(III)-Ion Pairs as Stronger Lewis Acid Catalysts for (E)-Selective Intermolecular Carbonyl-Olefin Metathesis. *Organic Letters* **2020**, *22* (8), 3155–3160. https://doi.org/10.1021/acs.orglett.0c00917.

(64) Olah, G. A. *International Edition in English Superelectrophiles***; 1993; Vol. 32.

(65) Negishi, E. *CONCEPTS*; 1999; Vol. 5.

(66) Stephan, D. W.; Erker, G. Chemie Frustrierter Lewis-Paare: Entwicklung Und Perspektiven. *Angewandte Chemie* **2015**, *127* (22), 6498–6541. https://doi.org/10.1002/ange.201409800.

(67) Denmark, S. E.; Eklov, B. M.; Yao, P. J.; Eastgate, M. D. On the Mechanism of Lewis Base Catalyzed Aldol Addition Reactions: Kinetic and Spectroscopic Investigations Using

Rapid-Injection NMR. *J Am Chem Soc* **2009**, *131* (33), 11770–11787. https://doi.org/10.1021/ja902474j.

(68) Tomifuji, R.; Maeda, K.; Takahashi, T.; Kurahashi, T.; Matsubara, S. FeCl 3 as an Ion-Pairing Lewis Acid Catalyst. Formation of Highly Lewis Acidic FeCl 2+ and Thermodynamically Stable FeCl 4- to Catalyze the Aza-Diels-Alder Reaction with High Turnover Frequency. *Organic Letters* **2018**, *20* (23), 7474–7477. https://doi.org/10.1021/acs.orglett.8b03249.

(69) Ic00256a033.

(70) Davis, A. J.; Watson, R. B.; Nasrallah, D. J.; Gomez-Lopez, J. L.; Schindler, C. S. Superelectrophilic Aluminium(Iii)–Ion Pairs Promote a Distinct Reaction Path for Carbonyl–Olefin Ring-Closing Metathesis. *Nature Catalysis* **2020**, *3* (10), 787–796. https://doi.org/10.1038/s41929-020-00499-5.

(71) Strauss, S. H. *The Search for Larger and More Weakly Coordinating Anions*; 1993; Vol. 93.

(72) Beck, W.; Sunkel, K. Metal Complexes of Weakly Coordinating Anions. Precursors of Strong Cationic Organometallic Lewis Acids1^.

(73) Schottel, B. L.; Chifotides, H. T.; Shatruk, M.; Chouai, A.; Pérez, L. M.; Bacsa, J.; Dunbar, K. R. Anion-π Interactions as Controlling Elements in Self-Assembly Reactions of Ag(I) Complexes with π-Acidic Aromatic Rings. *J Am Chem Soc* **2006**, *128* (17), 5895–5912. https://doi.org/10.1021/ja0606273.

(74) Om50006a014.

(75) Mayfield, H. G.; Bull, W. E. *SECTION A I Norgan Ic, P Hysica I, and T Heoret Ica 1 Chemistry Co-Ordinating Tendencies of the Hexaf Luorophosphate Ion*.

(76) *Chapman et Al*.

(77) Bini, R.; Chiappe, C.; Marmugi, E.; Pieraccini, D. The “Non-Nucleophilic” Anion [Tf2N]- Competes with the Nucleophilic Br-: An Unexpected Trapping in the Dediazoniation Reaction in Ionic Liquids. *Chemical Communications* **2006**, No. 8, 897–899. https://doi.org/10.1039/b514988f.

(78) Hanson, C. S.; Psaltakis, M. C.; Cortes, J. J.; Siddiqi, S. S.; Devery, J. J. Investigation of Lewis Acid-Carbonyl Solution Interactions via Infrared-Monitored Titration. *Journal of Organic Chemistry* **2020**, *85* (2), 820–832. https://doi.org/10.1021/acs.joc.9b02822.

(79) Hanson, C. S.; Psaltakis, M. C.; Cortes, J. J.; Devery, J. J. Catalyst Behavior in Metal-Catalyzed Carbonyl-Olefin Metathesis. *J Am Chem Soc* **2019**, *141* (30), 11870–11880. https://doi.org/10.1021/jacs.9b02613.

(80) Malakar, T.; Hanson, C. S.; Devery, J. J.; Zimmerman, P. M. Combined Theoretical and Experimental Investigation of Lewis Acid-Carbonyl Interactions for Metathesis. *ACS Catalysis* **2021**, *11* (8), 4381–4394. https://doi.org/10.1021/acscatal.0c05277.

(81) Hull, S.; Keen, D. A. *Pressure-Induced Phase Transitions in AgCl, AgBr, and AgI*.

(82) Rodriguez-Ruiz, V.; Carlino, R.; Bezzenine-Lafollée, S.; Gil, R.; Prim, D.; Schulz, E.; Hannedouche, J. Recent Developments in Alkene Hydro-Functionalisation Promoted by Homogeneous Catalysts Based on Earth Abundant Elements: Formation of C-N, C-O and C-P Bond. *Dalton Transactions*. Royal Society of Chemistry July 21, 2015, pp 12029–12059. https://doi.org/10.1039/c5dt00280j.

(83) Ozawa, T.; Kurahashi, T.; Matsubara, S. Manganese Porphyrin Catalyzed Cycloisomerization of Enynes. *Organic Letters* **2012**, *14* (12), 3008–3011. https://doi.org/10.1021/ol301416f.

(84) Ic00219a025.

(85) Honeychuck, R. v; Hersh, W. H. *) And 1.954 (11) A (3b), 2.186 (3) and 1.979 (3) A (3c), 2.168 (7) and 1.500 (14) A (5*; 1989; Vol. 28.

(86) Gowik, P.; Klapiitke, T.; Thewalt, U. *Metallocen-Chemie Hochfluorierter Ligand-Systeme XI *. Synthese Und Charakterisierung von Cp,Ti(SbF,) 2 Und Cp,Ti(Sb, F,) 2; Struktur von Cp,Ti(SbF,) 2 Und Cp2V(SbF,) 2*; Elsevier Sequoia S.A, 1990.

(87) Dash, C.; Das, A.; Yousufuddin, M.; Dias, H. V. R. Isolable, Copper(I) Dicarbonyl Complexes Supported by N-Heterocyclic Carbenes. *Inorganic Chemistry* **2013**, *52* (3), 1584–1590. https://doi.org/10.1021/ic302455y.

(88) Smirnova, E. S.; Muñoz Molina, J. M.; Johnson, A.; Bandeira, N. A. G.; Bo, C.; Echavarren, A. M. Polynuclear Gold [Au I] 4 , [Au I] 8 , and Bimetallic [Au I 4 Ag I] Complexes: C−H Functionalization of Carbonyl Compounds and Homogeneous Carbonylation of Amines . *Angewandte Chemie* **2016**, *128* (26), 7613–7617. https://doi.org/10.1002/ange.201603200.

(89) Bour, C.; Monot, J.; Tang, S.; Guillot, R.; Farjon, J.; Gandon, V. Structure, Stability, and Catalytic Activity of Fluorine-Bridged Complexes IPr·GaCl2(μ-F)EFn -1 (EFn- = SbF6-, PF6-, or BF 4-). *Organometallics* **2014**, *33* (2), 594–599. https://doi.org/10.1021/om4012054.

(90) Kavoosi, A.; Fillion, E. Synthesis and Characterization of Tricarbastannatranes and Their Reactivity in B(C 6 F 5) 3 -Promoted Conjugate Additions . *Angewandte Chemie* **2015**, *127* (18), 5578–5582. https://doi.org/10.1002/ange.201500983.

(91) Michelet, B.; Colard-Itté, J. R.; Thiery, G.; Guillot, R.; Bour, C.; Gandon, V. Dibromoindium(Iii) Cations as a π-Lewis Acid: Characterization of [IPr·InBr2][SbF6] and

Its Catalytic Activity towards Alkynes and Alkenes. *Chemical Communications* **2015**, *51* (34), 7401–7404. https://doi.org/10.1039/c5cc00740b.

(92) Cornella, J.; Martin, R. Ni-Catalyzed Stereoselective Arylation of Inert C-O Bonds at Low Temperatures. *Organic Letters* **2013**, *15* (24), 6298–6301. https://doi.org/10.1021/ol4031815.

(93) Kshirsagar, U. A.; Regev, C.; Parnes, R.; Pappo, D. Iron-Catalyzed Oxidative Cross-Coupling of Phenols and Alkenes. *Organic Letters* **2013**, *15* (12), 3174–3177. https://doi.org/10.1021/ol401532a.

(94) Bao, L.-L.; Iu, Z.-Q. Tetrahydropyrrolization of Resveratrol and Other Stilbenes Improves Inhibitory Effects on DNA Oxidation. https://doi.org/10.1002/cmdc.201600205:NMR.

(95) Konishi, H.; Ueda, T.; Muto, T.; Manabe, K. Remarkable Improvement Achieved by Imidazole Derivatives in Ruthenium-Catalyzed Hydroesterification of Alkenes Using Formates. *Organic Letters* **2012**, *14* (18), 4722–4725. https://doi.org/10.1021/ol301850y.

(96) Yoo, K. S.; Yoon, C. H.; Jung, K. W. Oxidative Palladium(II) Catalysis: A Highly Efficient and Chemoselective Cross-Coupling Method for Carbon-Carbon Bond Formation under Base-Free and Nitrogenous-Ligand Conditions. *J Am Chem Soc* **2006**, *128* (50), 16384–16393. https://doi.org/10.1021/ja063710z.

(97) Kobayashi, K.; Ueno, M.; Kondo, Y. Phosphazene Base-Catalyzed Condensation of Trimethylsilylacetate with Carbonyl Compounds. *Chemical Communications* **2006**, No. 29, 3128–3130. https://doi.org/10.1039/b606056k.

(98) Charette, A. B.; Molinaro, C.; Brochu, C. Catalytic Asymmetric Cyclopropanation of Allylic Alcohols with Titanium-TADDOLate: Scope of the Cyclopropanation Reaction. *J Am Chem Soc* **2001**, *123* (49), 12168–12175. https://doi.org/10.1021/ja0108382.

(99) Hodgson, D. M.; Ying, K. C.; Nuzzo, I.; Freixas, G.; Kulikiewicz, K. K.; Cleator, E.; Paris, J. M. Intramolecular Cyclopropanation of Unsaturated Terminal Epoxides and Chlorohydrins. *J Am Chem Soc* **2007**, *129* (14), 4456–4462. https://doi.org/10.1021/ja0672932.

(100) Usui, I.; Schmidt, S.; Breit, B. Dual Palladium-and Proline-Catalyzed Allylic Alkylation of Enolizable Ketones and Aldehydes with Allylic Alcohols. *Organic Letters* **2009**, *11* (6), 1453–1456. https://doi.org/10.1021/ol9001812.

(101) Oppolzer, W.; Spivey, A. C.; Bochet, C. G. *1991,56, 2988 and References Mentioned Therein. Cf.\ Martin, S. F. The Amaryllidaceae Alkaloids*; Academic Press, 1994; Vol. 116.

(102) Daniel Little, R.; Carroll, G. L.; Petersen, J. L.; Tetrahedron Symp, K. Total Synthesis of the Marine Natural Product A9(12)-Capnellene. Reversal of Regiochemistry in the Intramolecular 1,3-Diyl Trapping Reaction. *Marine Natural Products, Chemical and Biological Perspectives* **1983**, *105* (2), 7129–7130.

(103) le Nôtre, J.; Touzani, R.; Lavastre, O.; Bruneau, C.; Dixneuf, P. H. Homologation of Monoterpenoids into New Sesquiterpenoids via Tandem Isomerisation/Claisen Rearrangement Reactions with Three-Component Ruthenium Catalysts, and Ru(Methallyl)2 (COD) Revealed by High Throughput Screening Techniques. *Advanced Synthesis and Catalysis* **2005**, *347* (6), 783–791. https://doi.org/10.1002/adsc.200404391.

(104) Aebi, J. D.; Deyo, D. T.; Sun, C. Q.; Guillaume, D.; Dunlap, B.; Rich, D. H. *Synthesis, Conformation, and Immunosuppressive Activities of Three Analogues of Cyclosporin A Modified in the 1-Position1 Both Conformations Have a Type IT 0-Tum for Residues 2-*· *5 and a Cis Amide Bond Between*; 1990; Vol. 33.

(105) Casey, C. P.; Bertz, S. H.; Burkhardt, T. J. *REACTION OF METAL-CARBENE COMPLEXES WITH OIAZOALKANES. A VERSATILE VINYL ETHER SYNTHESIS*; PequDon Pram, 1973.

(106) Banks, J. L.; Beard, H. S.; Cao, Y.; Cho, A. E.; Damm, W.; Farid, R.; Felts, A. K.; Halgren, T. A.; Mainz, D. T.; Maple, J. R.; Murphy, R.; Philipp, D. M.; Repasky, M. P.; Zhang, L. Y.; Berne, B. J.; Friesner, R. A.; Gallicchio, E.; Levy, R. M. Integrated Modeling Program, Applied Chemical Theory (IMPACT). *Journal of Computational Chemistry*. December 2005, pp 1752–1780. https://doi.org/10.1002/jcc.20292.

(107) Shao, Y.; Gan, Z.; Epifanovsky, E.; Gilbert, A. T. B.; Wormit, M.; Kussmann, J.; Lange, A. W.; Behn, A.; Deng, J.; Feng, X.; Ghosh, D.; Goldey, M.; Horn, P. R.; Jacobson, L. D.; Kaliman, I.; Khaliullin, R. Z.; Kuš, T.; Landau, A.; Liu, J.; Proynov, E. I.; Rhee, Y. M.; Richard, R. M.; Rohrdanz, M. A.; Steele, R. P.; Sundstrom, E. J.; Woodcock, H. L.; Zimmerman, P. M.; Zuev, D.; Albrecht, B.; Alguire, E.; Austin, B.; Beran, G. J. O.; Bernard, Y. A.; Berquist, E.; Brandhorst, K.; Bravaya, K. B.; Brown, S. T.; Casanova, D.; Chang, C. M.; Chen, Y.; Chien, S. H.; Closser, K. D.; Crittenden, D. L.; Diedenhofen, M.; Distasio, R. A.; Do, H.; Dutoi, A. D.; Edgar, R. G.; Fatehi, S.; Fusti-Molnar, L.; Ghysels, A.; Golubeva-Zadorozhnaya, A.; Gomes, J.; Hanson-Heine, M. W. D.; Harbach, P. H. P.; Hauser, A. W.; Hohenstein, E. G.; Holden, Z. C.; Jagau, T. C.; Ji, H.; Kaduk, B.; Khistyaev, K.; Kim, J.; Kim, J.; King, R. A.; Klunzinger, P.; Kosenkov, D.; Kowalczyk, T.; Krauter, C. M.; Lao, K. U.; Laurent, A. D.; Lawler, K. v.; Levchenko, S. v.; Lin, C. Y.; Liu, F.; Livshits, E.; Lochan, R. C.; Luenser, A.; Manohar, P.; Manzer, S. F.; Mao, S. P.; Mardirossian, N.; Marenich, A. v.; Maurer, S. A.; Mayhall, N. J.; Neuscamman, E.; Oana, C. M.; Olivares-Amaya, R.; Oneill, D. P.; Parkhill, J. A.; Perrine, T. M.; Peverati, R.;

Prociuk, A.; Rehn, D. R.; Rosta, E.; Russ, N. J.; Sharada, S. M.; Sharma, S.; Small, D. W.; Sodt, A.; Stein, T.; Stück, D.; Su, Y. C.; Thom, A. J. W.; Tsuchimochi, T.; Vanovschi, V.; Vogt, L.; Vydrov, O.; Wang, T.; Watson, M. A.; Wenzel, J.; White, A.; Williams, C. F.; Yang, J.; Yeganeh, S.; Yost, S. R.; You, Z. Q.; Zhang, I. Y.; Zhang, X.; Zhao, Y.; Brooks, B. R.; Chan, G. K. L.; Chipman, D. M.; Cramer, C. J.; Goddard, W. A.; Gordon, M. S.; Hehre, W. J.; Klamt, A.; Schaefer, H. F.; Schmidt, M. W.; Sherrill, C. D.; Truhlar, D. G.; Warshel, A.; Xu, X.; Aspuru-Guzik, A.; Baer, R.; Bell, A. T.; Besley, N. A.; Chai, J. da; Dreuw, A.; Dunietz, B. D.; Furlani, T. R.; Gwaltney, S. R.; Hsu, C. P.; Jung, Y.; Kong, J.; Lambrecht, D. S.; Liang, W.; Ochsenfeld, C.; Rassolov, V. A.; Slipchenko, L. v.; Subotnik, J. E.; van Voorhis, T.; Herbert, J. M.; Krylov, A. I.; Gill, P. M. W.; Head-Gordon, M. Advances in Molecular Quantum Chemistry Contained in the Q-Chem 4 Program Package. *Molecular Physics* **2015**, *113* (2), 184–215. https://doi.org/10.1080/00268976.2014.952696.

(108) Zimmerman, P. M. Single-Ended Transition State Finding with the Growing String Method. *Journal of Computational Chemistry* **2015**, *36* (9), 601–611. https://doi.org/10.1002/jcc.23833.

(109) Zimmerman, P. M. Growing String Method with Interpolation and Optimization in Internal Coordinates: Method and Examples. *Journal of Chemical Physics* **2013**, *138* (18). https://doi.org/10.1063/1.4804162.

(110) Jafari, M.; Zimmerman, P. M. Reliable and Efficient Reaction Path and Transition State Finding for Surface Reactions with the Growing String Method. *Journal of Computational Chemistry* **2017**, *38* (10), 645–658. https://doi.org/10.1002/jcc.24720.

(111) Zimmerman, P. Reliable Transition State Searches Integrated with the Growing String Method. *Journal of Chemical Theory and Computation* **2013**, *9* (7), 3043–3050. https://doi.org/10.1021/ct400319w.

(112) Metz, B.; Stoll, H.; Dolg, M. Small-Core Multiconfiguration-Dirac-Hartree-Fock-Adjusted Pseudopotentials for Post-d Main Group Elements: Application to PbH and PbO. *Journal of Chemical Physics* **2000**, *113* (7), 2563–2569. https://doi.org/10.1063/1.1305880.

(113) Peterson, K. A.; Figgen, D.; Goll, E.; Stoll, H.; Dolg, M. Systematically Convergent Basis Sets with Relativistic Pseudopotentials. II. Small-Core Pseudopotentials and Correlation Consistent Basis Sets for the Post-d Group 16-18 Elements. *Journal of Chemical Physics* **2003**, *119* (21), 11113–11123. https://doi.org/10.1063/1.1622924.

(114) Leininger, T.; Nicklass, A.; Kiichle, W.; Stoll, H.; Dolg, M.; Bergner, A. *PHYSICS LETTERS ELSEVIER The Accuracy of the Pseudopotential Approximation: Non-Frozen-Core Effects for Spectroscopic Constants of Alkali Fluorides XF (X = K, Rb, Cs)*; 1996; Vol. 255.

(115) Kaupp, M.; Schleyer, P. V. R.; Stoll, H.; Preuss, H. Pseudopotential Approaches to Ca, Sr, and Ba Hydrides. Why Are Some Alkaline Earth MX2 Compounds Bent? *The Journal of Chemical Physics* **1991**, *94* (2), 1360–1366. https://doi.org/10.1063/1.459993.

(116) Marenich, A. v.; Cramer, C. J.; Truhlar, D. G. Universal Solvation Model Based on Solute Electron Density and on a Continuum Model of the Solvent Defined by the Bulk Dielectric Constant and Atomic Surface Tensions. *Journal of Physical Chemistry B* **2009**, *113* (18), 6378–6396. https://doi.org/10.1021/jp810292n.

(117) Djurovic, A.; Vayer, M.; Li, Z.; Guillot, R.; Baltaze, J. P.; Gandon, V.; Bour, C. Synthesis of Medium-Sized Carbocycles by Gallium-Catalyzed Tandem Carbonyl-Olefin Metathesis/Transfer Hydrogenation. *Organic Letters* **2019**, *21* (19), 8132–8137. https://doi.org/10.1021/acs.orglett.9b03240.

(118) Catti, L.; Tiefenbacher, K. Brønsted-Säure-Katalysierte Carbonyl-Olefin-Metathese in Einer Selbstorganisierten Supramolekularen Wirtstruktur. *Angewandte Chemie* **2018**, *130* (44), 14797–14800. https://doi.org/10.1002/ange.201712141.

(119) Lambert, T. H. Development of a Hydrazine-Catalyzed Carbonyl-Olefin Metathesis Reaction. *Synlett* **2019**, *30* (17), 1954–1965. https://doi.org/10.1055/s-0039-1689924.

(120) Ohkubo, K.; Menon, S. C.; Orita, A.; Otera, J.; Fukuzumi, S. Quantitative Evaluation of Lewis Acidity of Metal Ions with Different Ligands and Counterions in Relation to the Promoting Effects of Lewis Acids on Electron Transfer Reduction of Oxygen. *Journal of Organic Chemistry* **2003**, *68* (12), 4720–4726. https://doi.org/10.1021/jo034258u.

(121) Evans, D. A.; Lectka, T.; Miller, S. J.; Murry, J. A.; Matt, P.; Norcross, R. D.; Johnson, J. S.; Kozlowski, M. C.; Ghosh, A. K.; Mathivanan, P.; Cappiello, J.; Krishnan, K.; Johannsen, M.; Jørgensen, K. A. *C 2-Symmetric Copper(II) Complexes as Chiral Lewis Acids. Enantioselective Catalysis of the Glyoxylate-Ene Reaction*; 1993; Vol. 115.

(122) Johnson, J. S.; Evans, D. A. Chiral Bis(Oxazoline) Copper(II) Complexes: Versatile Catalysts for Enantioselective Cycloaddition, Aldol, Michael, and Carbonyl Ene Reactions. *Accounts of Chemical Research* **2000**, *33* (6), 325–335. https://doi.org/10.1021/ar960062n.

(123) Hilt, G.; Pünner, F.; Möbus, J.; Naseri, V.; Bohn, M. A. A Lewis Acidity Scale in Relation to Rate Constants of Lewis Acid Catalyzed Organic Reactions. *European Journal of Organic Chemistry* **2011**, No. 30, 5962–5966. https://doi.org/10.1002/ejoc.201101029.

(124) *INFRARED SPECTRA OF XANTH0NE:LEWIS ACID COMPLEXES*?*

(125) Tran, U. P. N.; Oss, G.; Breugst, M.; Detmar, E.; Pace, D. P.; Liyanto, K.; Nguyen, T. v. Carbonyl-Olefin Metathesis Catalyzed by Molecular Iodine. *ACS Catalysis* **2019**, *9* (2), 912–919. https://doi.org/10.1021/acscatal.8b03769.

(126) Wang, R.; Chen, Y.; Shu, M.; Zhao, W.; Tao, M.; Du, C.; Fu, X.; Li, A.; Lin, Z. AuCl3-Catalyzed Ring-Closing Carbonyl–Olefin Metathesis. *Chemistry - A European Journal* **2020**, *26* (9), 1941–1946. https://doi.org/10.1002/chem.201905199.

(127) Jermaks, J.; Quach, P. K.; Seibel, Z. M.; Pomarole, J.; Lambert, T. H. Ring-Opening Carbonyl-Olefin Metathesis of Norbornenes. *Chemical Science* **2020**, *11* (30), 7884–7895. https://doi.org/10.1039/d0sc02243h.

(128) Lambert, T. H. Development of a Hydrazine-Catalyzed Carbonyl-Olefin Metathesis Reaction. *Synlett* **2019**, *30* (17), 1954–1965. https://doi.org/10.1055/s-0039-1689924.

(129) Zhang, Y.; Jermaks, J.; MacMillan, S. N.; Lambert, T. H. Synthesis of 2 H-Chromenes via Hydrazine-Catalyzed Ring-Closing Carbonyl-Olefin Metathesis. *ACS Catalysis* **2019**, *9* (10), 9259–9264. https://doi.org/10.1021/acscatal.9b03656.

(130) Hong, X.; Liang, Y.; Griffith, A. K.; Lambert, T. H.; Houk, K. N. Distortion-Accelerated Cycloadditions and Strain-Release-Promoted Cycloreversions in the Organocatalytic Carbonyl-Olefin Metathesis. *Chemical Science* **2014**, *5* (2), 471–475. https://doi.org/10.1039/c3sc52882k.

(131) Griffith, A. K.; Vanos, C. M.; Lambert, T. H. Organocatalytic Carbonyl-Olefin Metathesis. *J Am Chem Soc* **2012**, *134* (45), 18581–18584. https://doi.org/10.1021/ja309650u.

(132) Musacchio, A. J.; Nguyen, L. Q.; Beard, G. H.; Knowles, R. R. Catalytic Olefin Hydroamination with Aminium Radical Cations: A Photoredox Method for Direct C-N Bond Formation. *J Am Chem Soc* **2014**, *136* (35), 12217–12220. https://doi.org/10.1021/ja5056774.

(133) Fernández-Mateos, A.; Madrazo, S. E.; Teijón, P. H.; González, R. R. Radical Cyclization of Epoxy Vinyl- and Allylsulfones Promoted by Titanocene Chloride. *Journal of Organic Chemistry* **2015**, *80* (9), 4378–4391. https://doi.org/10.1021/acs.joc.5b00206.

(134) Kuriyama, Y.; Sasano, Y.; Hoshino, Y.; Uesugi, S. ichiro; Yamaichi, A.; Iwabuchi, Y. Highly Regioselective 5-Endo-Tet Cyclization of 3,4-Epoxy Amines into 3-Hydroxypyrrolidines Catalyzed by La(OTf)3. *Chemistry - A European Journal* **2021**, *27* (6), 1961–1965. https://doi.org/10.1002/chem.202004455.

(135) Johnson, L. A.; Dunbabin, A.; Benton, J. C. R.; Mart, R. J.; Allemann, R. K. Modular Chemoenzymatic Synthesis of Terpenes and Their Analogues. *Angewandte Chemie - International Edition* **2020**, *59* (22), 8486–8490. https://doi.org/10.1002/anie.202001744.

(136) Lucke, A. J.; Young, D. J. Electrophilic Cleavage of Cyclopropylmethystannanes: An Experimental Comparison of σ-σ and σ-π Conjugation. *Journal of Organic Chemistry* **2005**, *70* (9), 3579–3583. https://doi.org/10.1021/jo047822p.

(137) Cai, Z.; Yongpruksa, N.; Harmata, M. Total Synthesis of the Terpenoid Buddledone A: 11-Membered Ring-Closing Metathesis. *Organic Letters* **2012**, *14* (7), 1661–1663. https://doi.org/10.1021/ol300400x.

(138) Anderson, T. E.; Woerpel, K. A. Strain-Promoted Oxidation of Methylenecyclopropane Derivatives Using N-Hydroxyphthalimide and Molecular Oxygen in the Dark. *Organic Letters* **2020**, *22* (14), 5690–5694. https://doi.org/10.1021/acs.orglett.0c02075.

(139) Xu, B.; Shi, M. Ring-Opening Reactions of Methylenecyclopropanes Promoted by Metal Halides. *Organic Letters* **2003**, *5* (9), 1415–1418. https://doi.org/10.1021/ol034142k.

(140) Labes, R.; Battilocchio, C.; Mateos, C.; Cumming, G. R.; de Frutos, O.; Rincón, J. A.; Binder, K.; Ley, S. v. Chemoselective Continuous Ru-Catalyzed Hydrogen-Transfer Oppenauer-Type Oxidation of Secondary Alcohols. *Organic Process Research and Development* **2017**, *21* (9), 1419–1422. https://doi.org/10.1021/acs.oprd.7b00190.

(141) Labes, R.; González-Calderón, D.; Battilocchio, C.; Mateos, C.; Cumming, G. R.; de Frutos, O.; Rincón, J. A.; Ley, S. v. Rapid Continuous Ruthenium-Catalysed Transfer Hydrogenation of Aromatic Nitriles to Primary Amines. *Synlett* **2017**, *28* (20), 2855–2858. https://doi.org/10.1055/s-0036-1589096.

(142) Köckinger, M.; Hone, C. A.; Gutmann, B.; Hanselmann, P.; Bersier, M.; Torvisco, A.; Kappe, C. O. Scalable Continuous Flow Process for the Synthesis of Eflornithine Using Fluoroform as Difluoromethyl Source. *Organic Process Research and Development* **2018**, *22* (11), 1553–1563. https://doi.org/10.1021/acs.oprd.8b00318.

(143) Mata, A.; Hone, C. A.; Gutmann, B.; Moens, L.; Kappe, C. O. Continuous-Flow Pd-Catalyzed Carbonylation of Aryl Chlorides with Carbon Monoxide at Elevated Temperature and Pressure. *ChemCatChem* **2019**, *11* (3), 997–1001. https://doi.org/10.1002/cctc.201801974.

(144) Labes, R.; Mateos, C.; Battilocchio, C.; Chen, Y.; Dingwall, P.; Cumming, G. R.; Rincón, J. A.; Nieves-Remacha, M. J.; Ley, S. v. Fast Continuous Alcohol Amination Employing a

Hydrogen Borrowing Protocol. *Green Chemistry* **2019**, *21* (1), 59–63. https://doi.org/10.1039/c8gc03328e.

(145) Sagmeister, P.; Kaldre, D.; Sedelmeier, J.; Moessner, C.; Püntener, K.; Kummli, D.; Williams, J. D.; Kappe, C. O. Intensified Continuous Flow Synthesis and Workup of 1,5-Disubstituted Tetrazoles Enhanced by Real-Time Process Analytics. *Organic Process Research and Development* **2021**, *25* (5), 1206–1214. https://doi.org/10.1021/acs.oprd.1c00096.

(146) Sambiagio, C.; Ferrari, M.; van Beurden, K.; Ca', N. della; van Schijndel, J.; Noel, T. Continuous-Flow Synthesis of Pyrylium Tetrafluoroborates: Application to Synthesis of Katritzky Salts and Photoinduced Cationic RAFT Polymerization. *Organic Letters* **2021**, *23* (6), 2042–2047. https://doi.org/10.1021/acs.orglett.1c00178.

(147) Quesnel, J. S.; Kayser, L. v.; Fabrikant, A.; Arndtsen, B. A. Acid Chloride Synthesis by the Palladium-Catalyzed Chlorocarbonylation of Aryl Bromides. *Chemistry - A European Journal* **2015**, *21* (26), 9550–9555. https://doi.org/10.1002/chem.201500476.

(148) Schröder, N.; Wencel-Delord, J.; Glorius, F. High-Yielding, Versatile, and Practical [Rh(III)Cp*]-Catalyzed Ortho Bromination and Iodination of Arenes. *J Am Chem Soc* **2012**, *134* (20), 8298–8301. https://doi.org/10.1021/ja302631j.

(149) Mukhopadhyay, S.; Batra, S. Direct Transformation of Arylamines to Aryl Halides via Sodium Nitrite and N-Halosuccinimide. *Chemistry - A European Journal* **2018**, *24* (55), 14622–14626. https://doi.org/10.1002/chem.201803347.

(150) Moreira, J. A.; Corrêa, A. G. Enantioselective Synthesis of Three Stereoisomers of 5,9-Dimethylpentadecane, Sex Pheromone Component of Leucoptera Coffeella, from (-)-

Isopulegol. *Tetrahedron Asymmetry* **2003**, *14* (23), 3787–3795.

https://doi.org/10.1016/j.tetasy.2003.09.030.

Chapter 4 Benzo-Fused O-Heterocycles via Carbonyl-Olefin Metathasis

Gomez-Lopez, J. L.; Davis, A. J.; Schindler, C. S. *unpublished*.

4.1 Introduction

Carbonyl-olefin metathesis has emerged in recent years as a powerful reaction for converting carbonyl and olefin functionalities into high-value olefinic products.[1] The Schindler lab pioneered these efforts, reporting ring-closing carbonyl-olefin metathesis of aryl ketones to form cyclopentenes **8** (**Figure 4.1**).[39,41] Importantly, this strategy was enabled by catalytic amounts of Earth-abundant $FeCl_3$ (**7**) as a Lewis acid monomer for the activation of the ketone starting materials. This report was followed with a protocol which expanded the use of $FeCl_3$ to transform less reactive aliphatic ketones to the ring-closed products **10**.[42] Comprehensive mechanistic investigations revealed that the reaction was catalyzed by Fe(III)-homodimer (**9**) formed *in-situ*. These homodimers serve as more potent Lewis acid superelelectrophiles,[64] making them

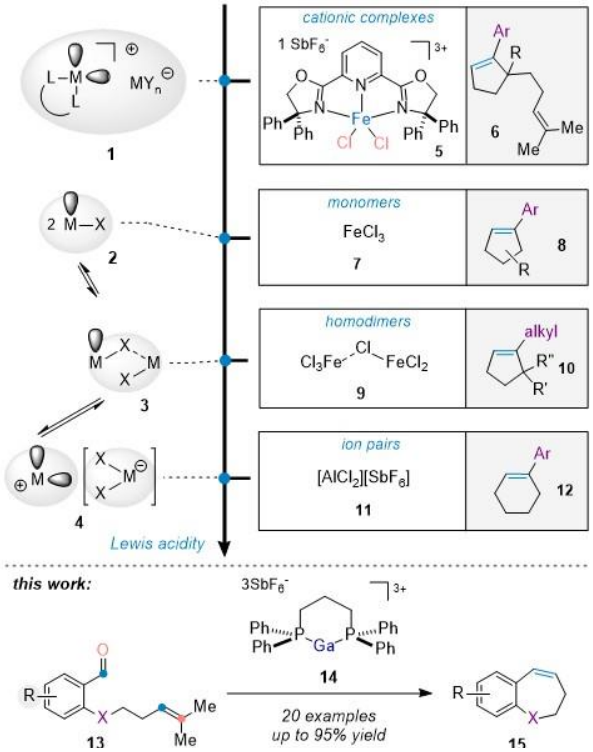

Figure 4.1. Development of Lewis acid catalysts for carbonyl-olefin metathesis.

particularly well suited for the activation of unreactive aliphatic ketones. The Schindler lab was able to further build upon the use of superelectrophiles as catalysts for unreactive substrates, identifying Al(III)-ion pair **11** as a powerful Lewis acid capable of converting chain extended aryl ketones into the corresponding cyclohexenes **12**.[70] This work represented for the general protocol for the formation of simple cyclohexenes from aryl ketones, proceeding through a unique carbonyl-ene/hydroalkoxylation pathway. While these two reports expanded access to structural motifs previously unavailable due to the unreactive nature of the starting materials, there remained no protocols for accessing products which suffer from high levels of decomposition or competing olefin isomerization reactions. To address this, the Schindler lab developed novel Fe(III)-metal complex **5** which functioned as a less Lewis acidic catalyst, converting bis-olefinic ketones into the ring-closed products **6** bearing a pendant olefin side-chain. They were also able to demonstrate that this weaker Lewis acid could efficiently promote carbonyl-olefin metathesis while avoiding alkene isomerization of the products. Additionally, a broad range of catalytic strategies have also been reported by other groups relying on both Lewis and Brønsted acid catalysts, for ring-closing,[32,34–36,38,39,41–44,47,49,50,52,61,79,117,118,125,126] ring-opening,[32,37,125] and cross metathesis reactions.[1,31,32,63,125] Additionally, a variety of organocatalytic approaches have been reported.[127–131] Despite these important advancements, several challenges persist within the field. For example, access to larger ring systems, such as 7-membered rings, remain limited in scope.[70,126] Additionally, substrates bearing additional Lewis sites vary in reactivity, with no general protocol available capable of converting this class of substrates smoothly.[38,41,44,70]

We envisioned that by building off the knowledge gained during our exploration of the development of metal complexes as Lewis acid catalysts, we could strategically design a complex potent enough to address these concerns. Specifically, the metal center could be tuned to achieve a high level of Lewis acidic character through the correct combination of ligand incorporation and halide abstraction to select for high reaction efficiency for carbonyl-olefin metathesis of 7-membered rings. Herein, we report the development of a Ga(III)-complex capable of forming benzo-fused *O*-heterocycles and carbocycles from aryl aldehydes via ring-closing carbonyl-olefin metathesis.

4.2 Results and Discussion

Our investigations began by identifying suitable reaction conditions to convert unsubstituted aryl aldehyde **16** to the corresponding metathesis product **18** (**Figure 4.2**). Initial conditions included evaluated previously reported catalyst systems for ring-closing carbonyl-olefin metathesis including $FeCl_3$, $AuCl_3$, and $[AlCl_2][SbF_6]$ (entries 1-3). However, these conditions all resulted in low yields of 12-36%, despite high consumption of the starting material. Importantly, previous studies have demonstrated that the Al(III)-ion pair catalyst acts as a superelectrophile, with increased Lewis acidic character to active unreactive substrates. The high level of decomposition observed under these conditions led us to evaluate the incorporation of ligands to selectively tune the reactivity to favor metathesis while avoiding decomposition pathways. The use of $[FeBOX][SbF_6]_3$ formed in situ upon addition of 30mol% of $AgSbF_6$ failed to promote the formation of **18** (entry 4). Although the analogous $[GaBOX][SbF_6]_3$ complex did provide the metathesis product in 25% yield, high levels of decomposition were again observed, suggesting the use of $GaCl_3$ forms a more reactive complex (entry 5). A similar yield of 22% was observed for the tricoordinate complex $[Ga(diPhPyBOX)][SbF_6]_3$ (entry 6). Failure to promote

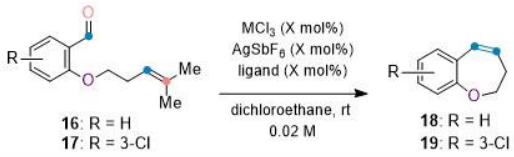

entry	substrate	MCl_3 (mol%)	$AgSbF_6$ (mol%)	ligand (mol%)	yield (%)	conv (%)
1	16	$FeCl_3$ (10)	-	-	21	96
2	16	$AuCl_3$ (5)	-	-	12	32
3	16	$AlCl_3$ (10)	10	-	36	99
4	16	$FeCl_3$ (10)	30	Box (10)	trace	47
5	16	$GaCl_3$ (10)	30	Box (10)	25	99
6	16	$GaCl_3$ (10)	30	diPhPyBox (10)	22	91
7	16	$GaCl_3$ (10)	30	dppe (10)	30	99
8	16	$GaCl_3$ (10)	30	dppp (10)	35	99
9	16	$GaCl_3$ (10)	30	dcpe (10)	25	99
10	16	$GaCl_3$ (10)	20	dppp (10)	2	67
11	16	$GaCl_3$ (20)	60	dppp (20)	37	99
12	16	$GaCl_3$ (4)	12	dppp (4)	30	95
13	**17**	**$GaCl_3$ (2)**	**6**	**dppp (2)**	**82**	**99**
14	17	$FeCl_3$ (5)	-	-	54	98
15	17	$AuCl_3$ (5)	-	-	68	81
16	17	$AlCl_3$ (10)	10	-	86	99

Conditions: All reactions were performed using 0.18 mmol of the substrate in DCE (0.02 M) at room temperature for 10 min-20 h. Yields are reported as NMR yields with mesitylene as internal standard. [a]Reaction performed in 0.01 M.

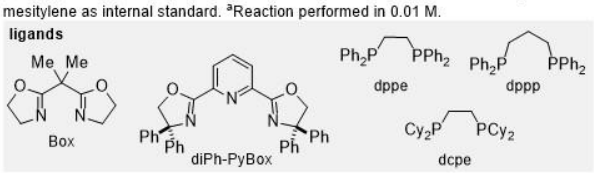

Figure 4.2. Reaction optimization.

metathesis using ligand scaffolds derived from bis(oxazolines) led us to explore another class of ligands – bidentate phosphines. Both the ethyl- and propyl-derived bisphosphines, along with 10 mol% of $GaCl_3$ and 30 mol% of SbF_6 resulted in increased yields of up to 35% (entries 7-8), although the more nucleophilic dcpe ligand resulted in higher decomposition (entry 9). Reducing the loading of silver to 20 mol% was also inefficient at catalyzing the desired reaction, providing just 2% of metathesis product **18** (entry 10). Finally, neither increasing the loading the of Ga(III) complex to 20 mol% or decreasing it to just 4 mol% did not show any change in reactivity, providing similar yields to that when 10 mol% was employed (entries 11-12 vs entry 8). These results indicate that unsubstituted **16** is particularly challenging to activate for COM selectively, likely due to the Lewis basic nature of both the starting material and product. By adding electron-withdrawing substituents near to the Lewis basic oxygen functionality, we hypothesized that combined electronics and sterics could overcome the undesired Lewis acid/base complexation and promote metathesis more selectively. Indeed, by switching to **17**, bearing a chloride substituent at the 3-position of the aromatic ring, ring-closed product **19** was formed in 82% when just 2 mol% of the dicoordinate Ga(III)-complex was employed (entry 13). Other reported Lewis acids were also evaluated on this substrate, with monomeric Lewis acids $FeCl_3$ and $AuCl_3$ providing 54% and 68% of **19** respectively, while the more potent Al(III)-ion pair resulted in 86% yield of **19** (entries 14-16).

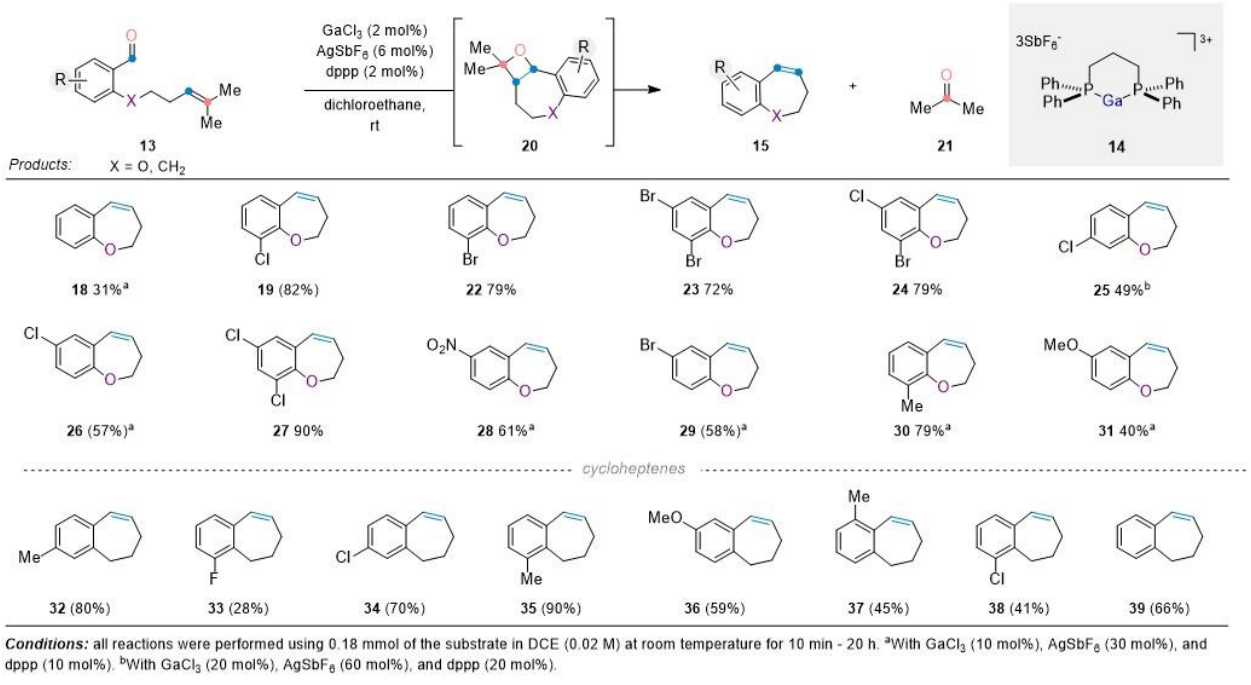

Conditions: all reactions were performed using 0.18 mmol of the substrate in DCE (0.02 M) at room temperature for 10 min - 20 h. [a]With $GaCl_3$ (10 mol%), $AgSbF_6$ (30 mol%), and dppp (10 mol%). [b]With $GaCl_3$ (20 mol%), $AgSbF_6$ (60 mol%), and dppp (20 mol%).

Figure 4.3. Evaluation of substrate scope for carbonyl-olefin metathesis employing Ga(III)-complex **14**.

With optimal conditions in hand, we next sought to explore the reactivity employing the Ga(III)-complex for the formation of and *O*-heterocyclic metathesis products (**Figure 4.3**). Unsubstituted **18** was formed in a moderate yield of 31%, although this required a higher loading of 10 mol% of the active catalyst **14**. Halogenated ring-closed products were achieved in moderate to excellent yields of 49-90%. (19-27, 29). Chlorinated products **26** and **25** required slightly increased loadings of 10 and 20 mol%, respectively. Interestingly, **28** which contains a pendant nitro group, was well tolerated, forming in 61% when 10 mol% of **14** was employed. Due to their strong Lewis basic character, nitro groups are generally not tolerated under Lewis-acid catalysis, with just a few examples in the literature of successful carbonyl-olefin metathesis of nitrated compounds.[42,43] Importantly, electron-rich substrates were also well tolerated under the reaction conditions, with methylated **32** formed in good yield of 79%. This represents a clear advantage of using the Ga(III)-complex for Lewis-acid catalyzed carbonyl-olefin metathesis of larger ring systems, as previously reported catalysts resulted in diminished yields. Additionally, anisole derived **30** bearing an additional Lewis basic site was achieved in 40%. To further explore the tolerance of Ga(III)-complex **14**, we next evaluated a variety of aryl aldehydes bearing hydrocarbon side chains for the formation of cycloheptyl ring-closed products. Indeed, a variety of electronically differentiated products could be reached in moderate to excellent yields of 28-

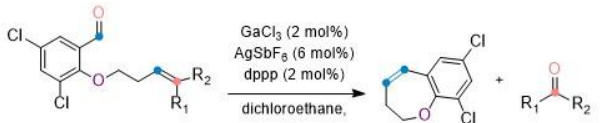

entry	substrate	yield **24** (%)	entry	substrate	yield **24** (%)
1	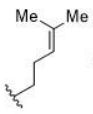 **40a**	95	4	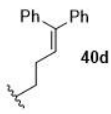 **40d**	10
2	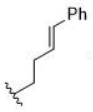 **40b**	90	5	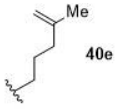 **40e**	8
3	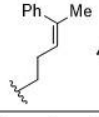 **40c**	51	6 7	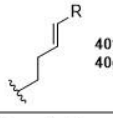 **40f** R = H **40g** R = Me	0 0

Conditions: all reactions were performed using 0.18 mmol of the substrate in DCE (0.02 M) at room temperature for 10 min - 20 h. Yields are reported as NMR yields with mesitylene as an internal standard.

Figure 4.4. Alkene scope for carbonyl-olefin metathesis employing Ga(III)-complex **14**.

90% (**32-39**). Again, electron-rich aromatics were tolerated with methylated **32** and **35** formed in 80% and 90%, respectively, and methoxy-substituted **36** formed in 59%. Interestingly, unsubstituted **39** had an improved yield of 66% relative to heterocyclic analog **18**, suggesting that the removal of the competitive Lewis basic site unlocked improved reactivity for substrates that do not exhibit any steric or electronic influence on the reactivity. The scope of the alkene functionality was explored next (**Figure 4.4**). Prenylated **40a** and styrenyl **40b** performed well, providing 95% and 90%, respectively, of metathesis product **24**. Increasing the steric profile of the olefin moiety resulted in a decrease in reactivity, with methyl, phenyl-substituted **40c** providing a diminished yield of 51%. Further steric influence from diphenyl **40d** yielded just 10% of the metathesis product. Interestingly, terminal olefin **40e**, which could provide **24** *via* an in-situ isomerization to form prenyl **40a** as an intermediate was unreactive, providing just 8% of **24**.

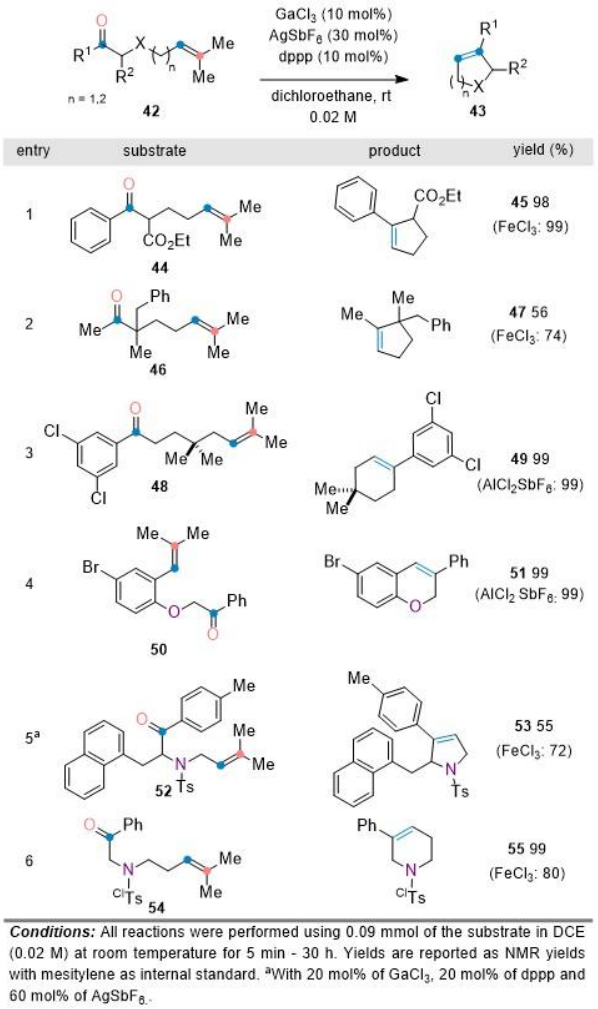

Figure 4.5. Ga(III)-complex enables ring-closing carbonyl-olefin metathesis for previously reported systems.

Finally, both crotyl-and allyl-derived olefins (**40e, 40f**) were both unsuited for metathesis, likely due to the lack of nucleophilic character of the olefin coupling partner, consistent with previous studies.

Subsequent efforts focused on the application of the superelectrophilic Ga(III)-complex for a variety of previously reported metathesis substrates (**Figure 4.5**). Cyclopentenes **45** and **47** were achieved in 98% and 56% yield respectively, demonstrating similar reactivity profiles for $FeCl_3$-catalyzed reactions for smaller ring systems (entries 1 and 2).[39,41,42] Cyclohexene **49** and chroman **51**, which could be formed quantitatively using the more potent Al(III)-ion pair catalyst,[70] was also produced in 99% yield using the Ga(III)-complex, highlighting the reactive nature of this catalyst system (entries 3 and 4). Dihydropyrrole **53**, which previously required an increased catalyst loading of 50 mol% was formed in 56% with a reduced loading of just 10 mol% of the Ga(III)-complex (entry 5).[38] Additionally, tetrahydropyridine **55** was formed in 99% yield, outperforming $FeCl_3$ without the need for extended reaction times or thermal activation (entry 6).[44]

4.3. Conclusions

This work presents the development of a novel Ga(III)-complex that serves as an efficient catalyst for ring-closing carbonyl-olefin metathesis for 7-membered ring systems. Electron-poor and -rich substrates are easily converted to the cyclic products, representing an important advancement in the field, as previously available catalyst systems were limited to electron-poor systems for larger rings. Importantly, the Ga(III)dppp-complex enables the formation of cyclopentene and cyclohexene products in similar or improved yields obtained under currently available protocols. The increased Lewis acidity of the catalyst promotes more efficient catalysis of particularly unreactive substrates such as *N*-heterocyclic motifs under milder reactions conditions. These findings are expected to enable further advances in carbonyl-olefin metathesis to further broaden the scope of structural scaffolds accessible by this strategy, therefore unlocking access to molecules of biological and pharmaceutical relevance.

4.4 Experimental Procedures and Supplemental Information

4.4.1 General Information

General laboratory procedures. All moisture-sensitive reactions were performed in a nitrogen-filled glovebox or using Schlenk techniques in oven-dried round bottom flasks fitted with rubber septa. Stainless steel syringes were used to transfer air or moisture-sensitive liquids. Flash chromatography was performed using silica gel SiliaFlash® 40-63 micron (230-400 mesh) from SiliCycle.

Materials and instrumentation. All chemicals were purchased from commercial suppliers and were used as received unless otherwise stated. 2,2'-(propane-2,2-diyl)bis(4,5-dihydrooxazole) **(box),**[1] 2,6-bis(4,4-diphenyl-4,5-dihydro-oxazol-2-yl)pyridine (diPh-PyBox),[2] and 2-alkyl benzaldehydes[3] were prepared according to literature procedures. Proton Nuclear Magnetic Resonance (^{1}H NMR) spectra and Carbon Nuclear Magnetic Resonance (^{13}C NMR) spectra were recorded on a Varian Inova 500, Varian Mercury 500, and Varian vnmrs 700 spectrometers. Chemical shifts for protons are reported in parts per million and are referenced to the NMR solvent peak ($CDCl_3$: δ 7.26). Chemical shifts for carbons are reported in parts per million and are referenced to the carbon resonances of the NMR solvent ($CDCl_3$: δ 77.16). Data is represented as follows: chemical shift, integration, multiplicity (br = broad, s = singlet, d = doublet, t = triplet, q = quartet, p = pentet, m = multiplet), and coupling constants in Hertz (Hz). Mass spectroscopic (MS) data was recorded at the Mass Spectrometry Facility at the Department of Chemistry of the University of Michigan in Ann Arbor, MI on an Agilent Q-TOF HPLC-MS with ESI or APCI high resolution mass spectrometer. Infrared (IR) spectra were obtained using Perkin Elmer Spectrum BX FT-IR spectrometer. IR data are represented as frequency of absorption (cm^{-1}).

Abbreviations used: $FeCl_3$ = iron(III) chloride, $AlCl_3$ = aluminum(III) chloride, $AuCl_3$ = gold(III) chloride, box = 2,2'-(propane-2,2-diyl)bis(4,5-dihydrooxazole), diPh-Pybox = 2,6-bis(4,4-diphenyl-4,5-dihydro-oxazol-2-yl)pyridine, dppe = 1,2-Bis(diphenylphosphino)ethane, dppp = 1,3-Bis(diphenylphosphino)propane, dcpe = 1,2-Bis(dicyclohexylphosphino)ethane, $AgSbF_6$ = silver hexafluoroantimonate(V), EtOAc = ethyl acetate, DMF = dimethylformamide, DCM = dichloromethane, DCE = 1,2-dichloroethane, K_2CO_3 = potassium carbonate, Na_2SO_4 = sodium

sulfate, Ts = tosyl protecting group, ^{Cl}Ts = 4-(chloro)benzenesulfonyl protecting group, TLC = thin layer chromatography.

4.4.2 Optimization of Reaction Conditions

An oven-dried round bottom flask equipped with a magnetic stir bar was charged with the appropriate Lewis acid, ligand and/or $AgSbF_6$ and DCE (3.5 mL). The catalyst solution was allowed to stir for 30 min or 1 h when $FeCl_3$ was used as Lewis acid at room temperature. The substrate (0.09 mmol dissolved in 1 mL of DCE) was added in one portion to the catalyst solution. The reaction was allowed to stir for the indicated time at room temperature. After reaching completion as judged by TLC or 20 h, the reaction was filtered through a silica plug eluting with DCM. The filtrate was concentrated under reduced pressure to remove all volatile components. Yields were determined by ^{1}H NMR using mesitylene as internal standard.

Table 4.1. Full reaction optimization.

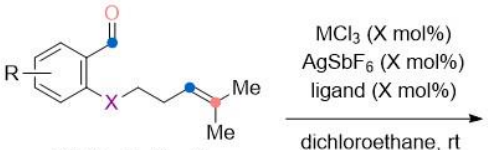

16: R = H, X = O
17: R = 3-Cl, X = O
S34: R = 4-Cl, X = CH_2
S35: R = 3-Me, X = CH_2

18: R = H, X = O
19: R = 3-Cl, X = O
34: R = 4-Cl, X = CH_2
35: R = 3-Me, X = CH_2

entry	substrate	MCl_3 (mol%)	$AgSbF_6$ (mol%)	ligand (mol%)	yield (%)	conv (%)
1	**16**	$FeCl_3$ (10)	-	-	21	96
2	**16**	$AuCl_3$ (5)	-	-	12	32
3	**16**	$AlCl_3$ (10)	10	-	36	99
4	**16**	$FeCl_3$ (10)	30	Box (10)	trace	47
5	**16**	$GaCl_3$ (10)	30	Box (10)	25	99
6	**16**	$GaCl_3$ (10)	30	diPh-PyBox (10)	22	91
7	**16**	$GaCl_3$ (10)	30	dppe(10)	30	99
8	**16**	$GaCl_3$ (10)	30	dppp (10)	35	99
9	**16**	$GaCl_3$ (10)	30	dcpe (10)	25	99
10	**16**	$GaCl_3$ (10)	20	dppp (10)	2	67
11	**16**	$GaCl_3$ (20)	60	dppp (20)	37	99
12	**16**	$GaCl_3$ (4)	12	dppp (4)	30	95
13	**16**	$FeCl_3$ (10)	30	dppp (10)	26	99
14	**17**	$GaCl_3$ (2)	6	dppp (2)	82	99
15	**17**	$FeCl_3$ (5)	-	-	54	98
16	**17**	$AuCl_3$ (5)	-	-	68	81
17	**17**	$AlCl_3$ (10)	10	-	86	99
18	**S34**	$GaCl_3$ (2)	6	dppp (2)	70	99
19	**S34**	$AlCl_3$ (10)	10	-	72	90
20	**S34**	$AuCl_3$ (5)	-	-	37	44
21	**S35**	$GaCl_3$ (2)	6	dppp (2)	90	99
22	**S35**	$AlCl_3$ (10)	10	-	75	99
23	**S35**	$AlCl_3$ (2)	2	-	49	65
24	**S35**	$GaCl_3$ (2)	2	-	69	99
25	**S35**	$GaCl_3$ (2)	6	-	60	99

Conditions: All reactions were performed using 0.18 mmol of the substrate in DCE (0.02 M) at room temperature for 10 min-20 h. Yields are reported as NMR yields with mesitylene as internal standard. [a]Reaction performed in 0.01 M.

ligands

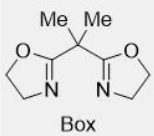

Box

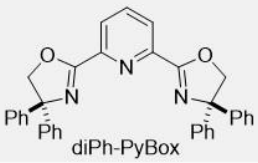

diPh-PyBox

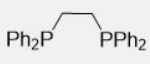

dppe

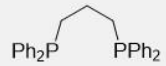

dppp

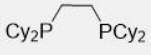

dcpe

4.4.3 Synthesis of Substrates and Intermediates

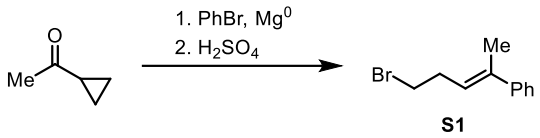

S1

(*E*)-(5-bromopent-2-en-2-yl)benzene (S1): A flame-dried 100 mL round bottom flask equipped with a stir bar was charged with THF (35 mL), bromobenzene (2.5 equiv.) magnesium metal (2.0 equiv) and a single crystal of iodine. The system was placed under an N2 atmosphere, and the heated until boiling, then allowed to cool to room temperature. Once the magnesium was fully dissolved, cyclopropyl methyl ketone (1.0 equiv) was added dropwise via syringe. Once judged complete by TLC, the reaction was quenched with saturated NH_4Cl. The layers were partitioned, and the aqueous layer was further extracted with Et_2O (2x30 mL). The combined organics were washed with saturated NaCl, dried over Mg_2SO_4, and concentrated under reduced pressure. Purification via flash chromatography eluting with 100% hexanes afforded 1.25g (83%) of **S1** as a clear oil. Spectral data was in accordance with literature data.[132]

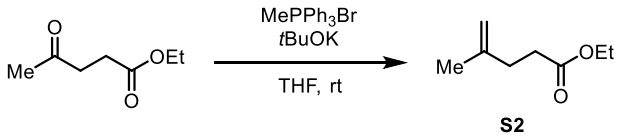

S2

ethyl 4-methylpent-4-enoate (S2): Substrate S2 was prepared following a modified literature procedure. Bromo(methyl)triphenyl-l5-phosphane (1.2 equiv) was added to a flame dried 250 mL round bottom flask equipped with a stir bar and the system was placed under an N_2 atmosphere. THF (150 mL) was added. KOtBu (1.8 equiv) was added in three portions over a 10 minute period. The resulting solution was stirred at room temperature for 2 hours. Ethyl 40xopentanoate (1 equiv) was added dropwise via syringe. The resulting mixture was stirred overnight at room temperature. The reaction was quenched with water (80 mL), and the layers partitioned. The aqueous layer was further extracted with Et_2O (2x30 mL), and the combined organics washed with saturated NaCl, dried over Mg2SO4, and concentrated under reduced pressure. Purification via flash chromatography eluting with DCM/hexanes (30:70) provided 993 mg (78%) of **S2** as a clear oil. Spectral data was in accordance with literature data.[133]

General Procedure for $LiAlH_4$ Reduction

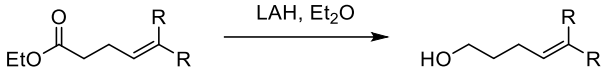

An oven-dried round bottom flask equipped with a stir bar was charged with $LiAlH_4$ (1.25 equiv.). Dry Et_2O (100 mL) added, and the system was placed under an atmosphere of nitrogen and cooled to 0°C. Substrate (1 equiv.) was diluted in Et_2O (2 mL) and added dropwise via syringe and warmed to room temperature. Once reaction was judged complete by TLC, the reaction was cooled to 0°C, and quenched by dropwise addition of water (2 mL), 4M NaOH (2 mL) and water (6 mL) sequentially. The solution was warmed to room temperature, anhydrous $MgSO_4$ was added and the heterogenous solution was stirred for 1 hour. The white solid was filtered, rinsing with Et_2O. The filtrate was concentrated under reduced pressure to remove all volatile components, and the resulting residue was used without further purification.

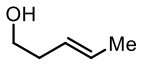

S3

(E)-pent-3-en-1-ol (S3): Substrate **S3** was prepared following general reduction procedure employing methyl (*E*)-pent-3-enoate. Crude alcohol was used without further purification, and the spectral data was in accordance with literature data.[134]

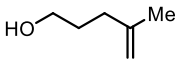

S4

4-methylpent-4-en-1-ol (S4): Substrate **S4** was prepared following the general reduction procedure employing XXX. The crude alcohol was used without further purification, and the spectral data was in accordance with literature data.[135]

General Procedure A. Tosylation and Nucleophilic Substitution to Form Alkyl Iodides.

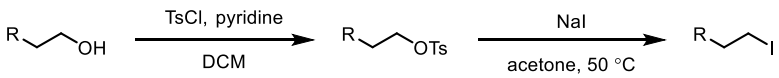

A flame-dried round bottom flask equipped with a stir bar was charged with crude alcohol (1 equiv.), triethylamine (3 equiv.), and DCM (0.2M). The reaction was cooled to 0 C, and TsCl (1.1

equiv.) was added in a single portion. The reaction was warmed to room temperature and stirred until judged complete by TLC. The reaction was quenched by addition of aq. NH_4Cl and extracted with DCM (3x15 mL). The combined organics were washed with saturated NaCl, dried over Mg_2SO_4, and concentrated under reduced pressure. The crude residue was collected in a round bottom flask equipped with a stir bar and dissolved in acetone (1.0M). NaI (1.5 equiv.) was added in a single portion, and the system was capped with a N_2-flushed reflux condenser. The reaction was stirred at 50 °C until judged complete by TLC analysis. The solution was filtered through a pad of Celite, rinsing with hexanes. The solution was concentrated under reduced pressure, and the residue was purified via column chromatography with the indicated solvent to give the pure alkyl iodide.

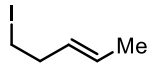

S5

(*E*)-5-iodopent-2-ene (S5): Iodide **S5** was prepared according to procedure A employing alcohol XX as the starting material. Purification by flash chromatography eluting with pentanes provided 1.78 g (78% yield over three steps) of **S5** as a clear oil. Spectral data was in accordance with literature data.[136]

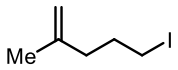

S6

5-iodo-2-methylpent-1-ene (S6): Iodide **S6** was prepared according to procedure A employing alcohol XX as the starting material. Purification by flash chromatography eluting with pentanes provided 341 mg (24% over three steps) off **S6** as a clear oil. Spectral data was in accordance with literature data.[137]

General Procedure for Preparation of Alkyl Iodides

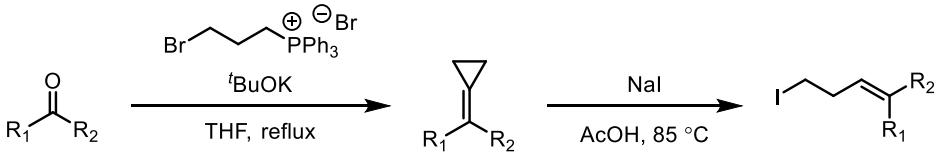

Procedure B. A flame-dried round bottom flask equipped with a stir bar was charged with (3-bromopropyl)triphenylphosphonium bromide (1 equiv.) in THF (0.1M) and KO^{t}Bu (2.2 equiv.) was added in three portions. The resulting mixture was placed under and atmosphere of N2 and stirred at room temperature for 30 minutes and refluxed for 2.5 hours. The corresponding carbonyl (1 equiv.) was added dropwise via syringe and the reaction was refluxed overnight. The reaction was cooled to room temperature and diluted with water extracted with hexanes (3x20 mL). The combined organics were washed with saturated NaCl, dried over Na_2SO_4, and concentrated under reduced pressure. The crude residue was used without further purification unless otherwise stated.

Procedure C. Methylenecyclopropane (1 equiv.) was dissolved in glacial acetic acid (0.5M) in a round bottom flask equipped with a stir bar. NaI (1.5 equiv.) was added in a single portion, and the reaction was heated to 80 °C. Once judged complete by TLC, the reaction was cooled to room temperature, and water (40 mL) and Et_2O (40 mL) were added. The aqueous phase was further extracted with Et_2O (2x20 mL). The combined organics were washed with aq. $Na_2S_2O_3$, followed by saturated NaCl, dried over Na_2SO_4, and concentrated under reduced pressure. The crude residue was purified via column chromatography with the indicated solvent to give the pure alkyl iodide.

(cyclopropylidenemethylene)dibenzene (S7): Intermediate **S7** was prepared according to

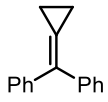

S7

procedure B employing benzophenone as the carbonyl unit. The crude material was used without further purification, and the spectral data was in accordance with literature data.[138]

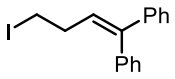

S8

(4-iodobut-1-ene-1,1-diyl)dibenzene (S8): Iodide **S8** was prepared according to procedure C employing **S**7. Purification by flash chromatography eluting with DCM/hex (10:90) provided 2.62 g (22% yield over two steps) of **S8** as a yellow oil. Spectral data was in accordance with literature data.[139]

General *O*-alkylation procedure.

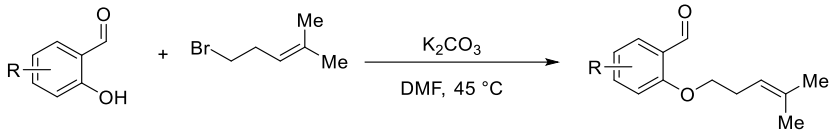

A 25 mL round bottom flask equipped with a magnetic stir bar was charged with K_2CO_3 (519 mg, 3.76 mmol). Dry DMF (8.0 mL) was then added, followed by starting aldehyde (3.13 mmol) and 5-bromo-2-methylpent-2-ene[4] (3.76 mmol). The resulting mixture was heated to 45 °C and stirred overnight. The reaction flask was allowed to cool to room temperature, and then water (10 mL) and EtOAc (20 mL) were added. The organic phase was separated and washed with water (3 × 10 mL) and saturated sodium chloride (1 × 10 mL), dried over Na_2SO_4 and concentrated under reduced pressure to remove all volatile components. The crude product was purified via column chromatography eluting with the indicated solvent to give the pure *O*-alkylated aldehyde.

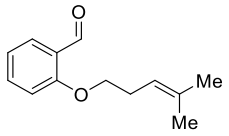

16

2-((4-methylpent-3-en-1-yl)oxy)benzaldehyde (16): Purification by flash column chromatography eluting with DCM/hexanes (3:7) provided 287.8 mg (45% yield) of **16** as a clear oil. **^{1}H NMR** (500 MHz; $CDCl_3$) δ 10.50 (s, 1H), 7.83 (dd, *J*= 7.7, 1.8 Hz, 1H), 7.52 (ddd, *J*= 8.8, 7.4, 1.9 Hz, 1H), 7.05-6.91 (m, 2H), 5.24-5.20 (m, 1H), 4.06 (t, *J*= 6.8 Hz, 2H), 2.54 (q, *J*= 7.0 Hz, 2H), 1.74 (s, 3H), 1.67 (s, 3H); **^{13}C NMR** (176 MHz; $CDCl_3$) δ 190.1, 161.6, 136.0, 135.0, 128.3, 125.1, 120.7, 119.4, 112.7, 68.4, 28.3, 25.9, 18.0. **IR** (Neat) 2970, 2929, 2860, 1686, 1598, 1457, 1383, 1286, 1240, 1161, 1018, 831, 754, 654; **HRMS** (APCI) *m/z*: $[M+H]^+$ calcd for $C_{13}H_{17}O_2^+$ 205.1223; found 205.1214.

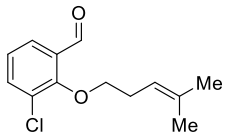

17

3-chloro-2-((4-methylpent-3-en-1-yl)oxy)benzaldehyde (17): Purification by flash column chromatography eluting with DCM/hexanes (3:7) provided 708.6 mg (95% yield) of **17** as a clear oil. **^{1}H NMR** (500 MHz; $CDCl_3$) δ 10.38 (s, 1H), 7.75 (dd, *J*= 7.8, 1.6 Hz, 1H), 7.62 (dd, *J*= 7.9, 1.6 Hz, 1H), 7.16 (t, *J*= 7.8 Hz, 1H), 5.21 (t, *J*= 7.2 Hz, 1H), 4.10 (t, *J*= 6.9 Hz, 2H), 2.56 (q, *J*=

7.1 Hz, 2H), 1.73 (s, 3H), 1.66 (s, 3H); **^{13}C NMR** (176 MHz; $CDCl_3$) δ 189.5, 158.4, 136.5, 135.3, 131.2, 128.9, 126.8, 125.0, 119.2, 75.8, 29.0, 25.9, 18.0. **IR** (Neat) 2970, 2916, 2873, 1690, 1586, 1445, 1371, 1235, 1171, 1135, 1073, 977, 783, 725; **HRMS** (APCI) *m/z*: $[M+H]^+$ calcd for $C_{13}H_{16}O_2Cl^+$ 239.0833; found 239.0828.

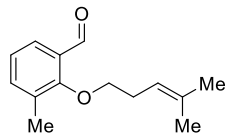

S35

3-methyl-2-((4-methylpent-3-en-1-yl)oxy)benzaldehyde (S35): Purification by flash column chromatography eluting with DCM/hexanes (1:4) provided 309.3 mg (45% yield) of **S35** as a yellow oil. **^{1}H NMR** (700 MHz; $CDCl_3$) δ 10.39 (s, 1H), 7.68 (dd, *J*= 7.8, 1.7 Hz, 1H), 7.43 (d, *J*= 7.5 Hz, 1H), 7.12 (t, *J*= 7.6 Hz, 1H), 5.25-5.20 (m, 1H), 3.91 (t, *J*= 6.9 Hz, 2H), 2.54 (q, *J*= 7.0 Hz, 2H), 2.33 (s, 3H), 1.74 (s, 3H), 1.67 (s, 3H); **^{13}C NMR** (176 MHz; $CDCl_3$) δ 190.7, 161.0, 137.7, 135.1, 132.5, 129.5, 126.3, 124.3, 119.5, 75.9, 29.1, 25.9, 18.0, 16.0. **IR** (Neat) 2970, 2916, 2873, 1690, 1586, 1445, 1371, 1235, 1171, 1135, 1073, 977, 783, 725; **HRMS** (APCI) *m/z*: $[M+H]^+$ calcd for $C_{14}H_{19}O_2^+$ 219.1380; found 219.1373.

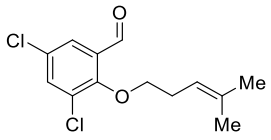

S27

3,5-dichloro-2-((4-methylpent-3-en-1-yl)oxy)benzaldehyde (S27): Purification by flash column chromatography eluting with DCM/hexanes (1:4) provided 211.4 mg (25% yield) of **S27** as a clear oil. **^{1}H NMR** (700 MHz; $CDCl_3$) δ 10.30 (s, 1H), 7.70 (s, 1H), 7.61 (s, 1H), 5.22-5.16 (m, 1H), 4.09 (t, *J*= 6.9 Hz, 2H), 2.54 (q, *J*= 7.0 Hz, 2H), 1.72 (s, 3H), 1.65 (s, 3H); **^{13}C NMR** (176 MHz; $CDCl_3$) δ 188.1, 157.0, 135.9, 135.5, 131.6, 130.4, 130.0, 126.6, 119.1, 76.1, 28.9, 25.9, 18.1. **IR** (Neat) 3073, 2970, 2916, 2873, 1694, 1582, 1439, 1369, 1238, 1212, 1166, 974, 875, 836, 778, 667; **HRMS** (APCI) *m/z*: $[M+H]^+$ calcd for $C_{13}H_{15}O_2Cl_2^+$ 273.0444; found 273.0431.

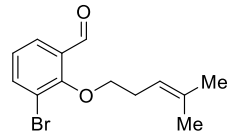

S22

3-bromo-2-((4-methylpent-3-en-1-yl)oxy)benzaldehyde (S22): Purification by flash column chromatography eluting with DCM/hexanes (1:3) provided 796.5 mg (90% yield) of **S22** as a clear oil. **^{1}H NMR** (700 MHz; $CDCl_3$) δ 10.36 (s, 1H), 7.85-7.74 (m, 2H), 7.11 (t, *J*= 7.8 Hz, 1H), 5.27-5.18 (m, 1H), 4.07 (t, *J*= 7.0 Hz, 2H), 2.58 (q, *J*= 7.1 Hz, 2H), 1.73 (s, 3H), 1.67 (s, 3H); **^{13}C NMR** (176 MHz; $CDCl_3$) δ 189.5, 159.5, 139.6, 135.3, 131.3, 127.7, 125.6, 119.2, 118.5, 76.3, 29.0, 25.9, 18.1. **IR** (Neat) 2969, 2915, 2869, 2739, 1706, 1685, 1586, 1440, 1370, 1241, 1118, 1071, 979, 781, 704; **HRMS** (APCI) *m/z*: $[M+H]^+$ calcd for $C_{13}H_{16}O_2{}^{81}Br^+$ 285.0308; found 285.0316.

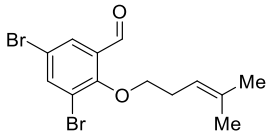

S23

3,5-dibromo-2-((4-methylpent-3-en-1-yl)oxy)benzaldehyde (S23): Purification by flash column chromatography eluting with DCM/hexanes (1:4) provided 891.4 mg (79% yield) of **S23** as a white solid. **^{1}H NMR** (700 MHz; $CDCl_3$) δ 10.27 (s, 1H), 7.93 (d, *J*= 2.5 Hz, 1H), 7.89 (d, *J*= 2.4 Hz, 1H), 5.21 (t, *J*= 7.1 Hz, 1H), 4.05 (t, *J*= 6.9 Hz, 2H), 2.57 (q, *J*= 7.0 Hz, 2H), 1.73 (s, 3H), 1.66 (s, 3H); **^{13}C NMR** (176 MHz; $CDCl_3$) δ 188.1, 158.6, 141.5, 135.6, 132.0, 130.5, 119.5, 119.0, 118.0, 76.5, 28.9, 25.9, 18.1. **IR** (Neat) 3065, 2974, 2934, 2908, 2886, 1688, 1572, 1445, 1433, 1391, 1371, 1212, 1149, 876, 725, 656; **HRMS** (APCI) *m/z*: $[M+H]^+$ calcd for $C_{13}H_{15}O_2{}^{79}Br{}^{81}Br^+$ 362.9413; found 362.9418.

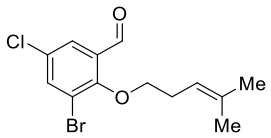

S24

3-bromo-5-chloro-2-((4-methylpent-3-en-1-yl)oxy)benzaldehyde (S24): Purification by flash column chromatography eluting with DCM/hexanes (3:7) provided 961.0 mg (97% yield) of **S24** as a white solid. **^{1}H NMR** (700 MHz; $CDCl_3$) δ 10.28 (s, 1H), 7.78 (dd, *J*= 2.7, 1.2 Hz, 1H), 7.75 (dd, *J*= 2.7, 1.2 Hz, 1H), 5.22-5.19 (m, 1H), 4.05 (t, *J*= 6.9 Hz, 2H), 2.57 (q, *J*= 7.1 Hz, 2H), 1.73

(s, 3H), 1.66 (s, 3H); **^{13}C NMR** (176 MHz; $CDCl_3$) δ 188.2, 158.1, 138.8, 135.5, 131.6, 130.9, 127.4, 119.2, 119.0, 76.5, 28.9, 25.9, 18.1. **IR** (Neat) 3070, 2970, 2915, 2889, 1692, 1579, 1555, 1436, 1368, 1236, 1213, 1155, 974, 876, 725, 662; **HRMS** (APCI) *m/z*: $[M+H]^+$ calcd for $C_{13}H_{15}O_2Cl\,^{81}Br^+$ 318.9918; found 318.9911.

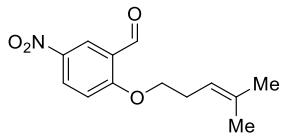

S28

2-((4-methylpent-3-en-1-yl)oxy)-5-nitrobenzaldehyde (S28): Purification by flash column chromatography eluting with DCM/hexanes (1:1) provided 154.5 mg (20% yield) of **S28** as a white solid. **^{1}H NMR** (700 MHz; $CDCl_3$) δ 10.46 (s, 1H), 8.70 (s, 1H), 8.41 (dd, *J*= 9.2, 2.9 Hz, 1H), 7.09 (d, *J*= 9.1, 1H), 5.20 (t, *J*= 7.5 Hz, 1H), 4.19 (t, *J*= 6.7 Hz, 2H), 2.60 (q, *J*= 7.0 Hz, 2H), 1.74 (s, 3H), 1.68 (s, 3H); **^{13}C NMR** (176 MHz; $CDCl_3$) δ 187.8, 165.3, 141.6, 135.9, 130.7, 124.8, 124.7, 118.5, 113.1, 69.6, 28.0, 25.9, 18.1. **IR** (neat) 3078, 2975, 2893, 1691, 1607, 1586, 1519, 1485, 1338, 1275, 1179, 1002, 942, 825, 748, 662; **HRMS** (APCI) *m/z*: $[M+H]^+$ calcd for $C_{13}H_{16}NO_4^+$ 250.1074; found 250.1071.

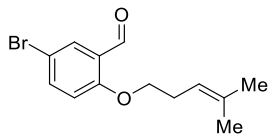

S29

5-bromo-2-((4-methylpent-3-en-1-yl)oxy)benzaldehyde (S29): Purification by flash column chromatography eluting with DCM/hexanes (1:4) provided 326.6 mg (37% yield) of **S29** as a clear oil. **^{1}H NMR** (700 MHz; $CDCl_3$) δ 10.39 (s, 1H), 7.92 (d, *J*= 2.5 Hz, 1H), 7.60 (dd, *J*= 8.9, 2.6 Hz, 1H), 6.87 (d, *J*= 8.8, 1H), 5.22-5.16 (m, 1H), 4.04 (t, *J*= 6.8 Hz, 2H), 2.53 (q, *J*= 7.0 Hz, 2H), 1.73 (s, 3H), 1.66 (s, 3H); **^{13}C NMR** (176 MHz; $CDCl_3$) δ 188.7, 160.5, 138.4, 135.3, 130.9, 126.4, 119.1, 114.8, 113.5, 68.8, 28.2, 25.9, 18.0. **IR** (neat) 2969, 2928, 2867, 1682, 1590, 1482, 1464, 1382, 1269, 1240, 1177, 1121, 1015, 806, 657; **HRMS** (APCI) *m/z*: $[M+H]^+$ calcd for $C_{13}H_{16}O_2Br^+$ 283.0328; found 283.0314.

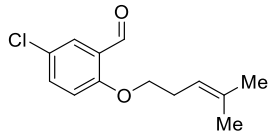

S26

5-chloro-2-((4-methylpent-3-en-1-yl)oxy)benzaldehyde (S26): Purification by flash column chromatography eluting with DCM/hexanes (1:4) provided 374.7 mg (50% yield) of **S26** as a clear oil. **^{1}H NMR** (700 MHz; $CDCl_3$) δ 10.41 (s, 1H), 7.77 (d, *J*= 2.6 Hz, 1H), 7.46 (dd, *J*= 8.9, 2.6 Hz, 1H), 6.93 (d, *J*= 8.9, 1H), 5.24-5.15 (m, 1H), 4.04 (t, *J*= 6.8 Hz, 2H), 2.53 (q, *J*= 7.0 Hz, 2H), 1.73 (s, 3H), 1.66 (s, 3H); **^{13}C NMR** (176 MHz; $CDCl_3$) δ 188.8, 160.0, 135.5, 135.2, 127.9, 126.4, 125.9, 119.1, 114.4, 68.9, 28.2, 25.9, 18.0. **IR** (neat) 2971, 2930, 2870, 1683, 1596, 1484, 1465, 1383, 1269, 1236, 1179, 1127, 1015, 898, 810, 669; **HRMS** (APCI) *m/z*: $[M+H]^+$ calcd for $C_{13}H_{16}O_2Cl^+$ 239.0833; found 239.0834.

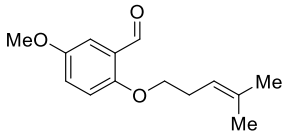

S31

5-methoxy-2-((4-methylpent-3-en-1-yl)oxy)benzaldehyde (S31): Purification by flash column chromatography eluting with DCM/hexanes (7:13) provided 175.0 mg (24% yield) of **S31** as a clear oil. **^{1}H NMR** (700 MHz; $CDCl_3$) δ 10.45 (s, 1H), 7.32 (d, *J*= 3.2 Hz, 1H), 7.11 (dd, *J*= 9.1, 3.3 Hz, 1H), 6.93 (d, *J*= 9.0, 1H), 5.23-5.17 (m, 1H), 4.01 (t, *J*= 6.8 Hz, 2H), 3.80 (s, 3H), 2.51 (q, *J*= 7.0 Hz, 2H), 1.73 (s, 3H), 1.66 (s, 3H); **^{13}C NMR** (176 MHz; $CDCl_3$) δ 189.9, 156.5, 153.7, 134.9, 125.3, 123.7, 119.5, 114.8, 110.1, 69.1, 55.9, 28.4, 25.9, 18.0. **IR** (neat) 2965, 2928, 2860, 1682, 1493, 1467, 1422, 1276, 1215, 1158, 1039, 812, 711; **HRMS** (APCI) *m/z*: $[M+H]^+$ calcd for $C_{14}H_{19}O_3^+$ 235.1329; found 235.1330.

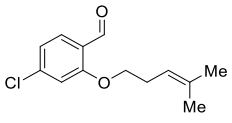

S25

4-chloro-2-((4-methylpent-3-en-1-yl)oxy)benzaldehyde (S25): Purification by flash column chromatography eluting with DCM/hexanes (3:17) provided 383.0 mg (51% yield) of **S25** as a white solid. **^{1}H NMR** (700 MHz; $CDCl_3$) δ 10.40 (s, 1H), 7.76 (d, *J*= 8.3 Hz, 1H), 6.99 (d, *J*= 8.4

Hz, 1H), 6.97 (s, 1H), 5.21-5.19 (m, 1H), 4.04 (t, *J*= 6.8 Hz, 2H), 2.55 (q, *J*= 7.0 Hz, 2H), 1.73 (s, 3H), 1.67 (s, 3H); **^{13}C NMR** (176 MHz; $CDCl_3$) δ 188.9, 161.9, 142.0, 135.3, 129.5, 123.6, 121.2, 119.0, 113.4, 68.8, 28.1, 25.9, 18.0. **IR** (neat) 3078, 2975, 2939, 2891, 1691, 1607, 1587, 1520, 1338, 1275, 1242, 1179, 1079, 1003, 942, 825, 748, 663; **HRMS** (APCI) *m/z*: $[M+H]^+$ calcd for $C_{13}H_{16}O_2Cl^+$ 239.0833; found 239.0828.

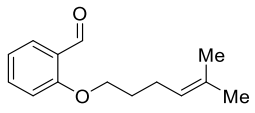

16

2-((5-methylhex-4-en-1-yl)oxy)benzaldehyde (16): Using 6-iodo-2-methylhex-2-ene[5] and 15.0 mmol of salicylaldehyde. Purification by flash column chromatography eluting with DCM/hexanes (1:9 to 2:1) provided 1.54 g (47% yield) of **16** as a clear oil. **^{1}H NMR** (700 MHz; $CDCl_3$) δ 10.53 (s, 1H), 7.83 (d, *J*= 7.7 Hz, 1H), 7.52 (t, *J*= 7.8 Hz, 1H), 7.00 (t, *J*= 7.5 Hz, 1H), 6.97 (d, *J*= 8.4 Hz, 1H), 5.19-5.11 (m, 1H), 4.07 (t, *J*= 6.3 Hz, 2H), 2.20 (q, *J*= 7.4 Hz, 2H), 1.89 (p, *J*= 6.5 Hz, 1H), 1.70 (s, 3H), 1.60 (s, 3H); **^{13}C NMR** (176 MHz; $CDCl_3$) δ 190.0, 161.7, 136.0, 133.0, 128.4, 125.1, 123.2, 120.6, 112.6, 68.0, 29.3, 25.9, 24.5, 17.8. **IR** (Neat) 2966, 2930, 2857, 1687, 1598, 1486, 1457, 1384, 1285, 1241, 1188, 1160, 1042, 842, 756, 652; **HRMS** (ESI) *m/z*: $[M+H]^+$ calcd for $C_{14}H_{19}O_2^+$ 219.1380; found 219.1375.

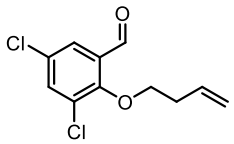

40g

2-(but-3-en-1-yloxy)-3,5-dichlorobenzaldehyde (40g): Substrate **40g** was synthesized following general O-alkylation procedure employing 4-bromo-1-butene as the electrophile. Purification by flash chromatography eluting with EtOAc/hex (3:97) provided 425.7 mg (59% yield) of **40g** as a yellow oil. **^{1}H NMR** (700 MHz; $CDCl_3$) δ10.31 (s, 1H), 7.71 (d, *J*= 2.6 Hz, 1H), 7.62 (d, *J*= 2.6 Hz, 1H), 5.91 (ddt, *J*= 17.1, 10.2, 6.7 Hz, 1H), 5.21 (d, *J*= 17.1 Hz, 1H), 5.16 (d, *J*= 8.6 Hz, 1H), 4.15 (t, *J*= 6.6 Hz, 2H), 2.62 (q, *J*= 6.4 Hz, 2H). ; **^{13}C NMR** (176 MHz; $CDCl_3$) δ 188.06, 156.92, 135.92, 133.74, 131.53, 130.56, 129.99, 126.79, 118.13, 75.58, 34.37. **IR** (Neat) 3076, 2952, 2873,

1693, 1642, 1582, 1439, 1370, 1237, 1212, 1165, 979, 917, 827, 768, 668; **HRMS** (APCI) *m/z*: $[M+H]^+$ calcd for $C_{11}H_{10}Cl_2O_2^+$: 245.0131; found 245.1023.

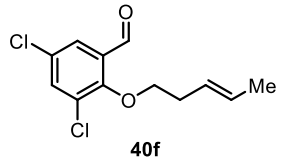

40f

(E)-3,5-dichloro-2-(pent-3-en-1-yloxy)benzaldehyde (40f): Substrate **40f** was synthesized following general O-alkylation procedure employing (E)-5-iodo-2-pentene as the electrophile. Purification by flash chromatography eluting with EtOAc/hex (3:97) provided 541.5 mg (65% yield) of **XX** as a yellow oil. **^{1}H NMR** (700 MHz; $CDCl_3$) δ 10.31 (s, 1H), 7.70 (d, *J* = 2.7 Hz, 1H), 7.61 (d, *J*= 2.6 Hz, 1H), 5.68 – 5.56 (m, 1H), 5.54 – 5.43 (m, 1H), 4.10 (t, *J*= 6.7 Hz, 2H), 2.55 – 2.52 (m, 2H), 1.69 (dd, *J*= 6.4, 1.5 Hz, 3H); **^{13}C NMR** (176 MHz; $CDCl_3$) δ188.12, 157.05, 135.89, 131.53, 130.42, 129.96, 128.91, 126.69, 126.06, 76.14, 33.27, 18.15. **IR** (Neat) 3073, 2938, 2874, 2737, 1693, 1581, 1438, 1369, 1236, 1212, 966, 875, 771, 666; **HRMS** (EI) *m/z*: $[M]^+$ calcd for $C_{12}H_{12}Cl_2O_2^+$: 258.0214; found 258.0222.

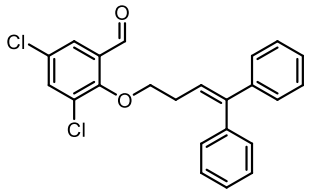

40d

3,5-dichloro-2-((4,4-diphenylbut-3-en-1-yl)oxy)benzaldehyde (40d): Substrate XX was synthesized following general O-alkylation procedure employing (4-iodobut-1-ene-1,1-diyl)dibenzene as the electrophile. Purification by flash chromatography eluting with DCM/hex (25:75) provided 345.2 mg (17% yield) of **40d** as a yellow oil. **^{1}H NMR** (700 MHz; $CDCl_3$) δ 10.25 (s, 1H), 7.70 (d, *J*= 2.6 Hz, 1H), 7.61 (d, *J*= 2.6 Hz, 2H), 7.39 (t, *J*= 7.0 Hz, 1H), 7.34 (t, *J*= 7.4 Hz, 3H), 7.30 – 7.18 (m, 4H), 6.22 (t, *J*= 7.3 Hz, 1H), 4.15 (t, *J*= 6.6 Hz, 2H), 2.69 (q, *J*= 6.9 Hz, 2H); **^{13}C NMR** (176 MHz; $CDCl_3$) δ 187.86, 156.89, 144.97, 142.21, 139.68, 135.90, 131.54, 130.54, 130.01, 129.86, 128.51, 128.34, 127.47, 127.37, 126.81, 123.77, 75.99, 30.61. **IR** (Neat) 3057, 3024, 2871, 1693, 1494, 1440, 1365, 1237, 1213, 1166, 998, 980, 875, 735, 761, 697; **HRMS** (ESI) *m/z*: $[M+H]^+$ calcd for $C_{23}H_{22}Cl_2O_2N^+$: 414.1022; found 414.1016.

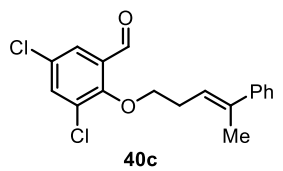

40c

(E)-3,5-dichloro-2-((4-phenylpent-3-en-1-yl)oxy)benzaldehyde (40c): Substrate XX was synthesized following general O-alkylation procedure employing (E)-(5-bromopent-2-en-2-yl)benzene as the electrophile. Purification by flash chromatography eluting with DCM/hexanes (35:65) provided 876 mgs (60%) of **40c** as a clear oil. **^{1}H NMR** (700 MHz; $CDCl_3$) δ10.36 (s, 1H), 7.74 (d, *J*= 2.6 Hz, 1H), 7.65 (d, *J*= 2.6 Hz, 1H), 7.40 (d, *J*= 8.0 Hz, 2H), 7.35 (t, *J*= 7.7 Hz, 2H), 7.28 (d, *J*= 7.6 Hz, 1H), 5.87 (t, *J*= 7.2 Hz, 1H), 4.23 (t, *J*= 6.8 Hz, 2H), 2.80 (q, *J*= 6.9 Hz, 2H), 2.12 (s, 3H); **^{13}C NMR** (176 MHz; $CDCl_3$) δ 187.95, 156.90, 143.47, 138.37, 135.93, 131.60, 130.55, 130.04, 128.42, 127.15, 126.84, 125.82, 122.47, 77.34, 77.16, 76.98, 75.78, 29.65, 16.31. **IR** (Neat) 3072, 2951, 2851, 1693, 1494, 1439, 1369, 1212, 980, 875, 756, 666; **HRMS** (+ESI) *m/z*: $[M+NH_4]^+$ calcd for $C_{18}H_{20}Cl_2O_2N^+$: 352.0866; found 352.0862.

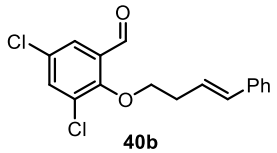

40b

(E)-3,5-dichloro-2-((4-phenylbut-3-en-1-yl)oxy)benzaldehyde (40b): Substrate **40b** was synthesized following general O-alkylation procedure employing (E)-(4-iodobut-1-en-1-yl)benzene as the electrophile. Purification by flash chromatography eluting with DCM/hexanes (35:65) provided 658 mgs (41%) of **40b** as a clear oil. **^{1}H NMR** (700 MHz; $CDCl_3$) δ 10.33 (s, 1H), 7.72 (d, *J*= 2.6 Hz, 1H), 7.63 (d, *J*= 2.6 Hz, 1H), 7.36 (d, *J*= 7.0 Hz, 2H), 7.32 (t, *J*= 7.5 Hz, 2H), 7.23 (t, *J*= 7.1 Hz, 1H), 6.56 (d, *J*= 15.8 Hz, 1H), 6.29 (dt, *J*= 15.7, 7.0 Hz, 1H), 4.22 (t, *J*= 6.6 Hz, 2H), 2.78 (q, *J*= 6.8 Hz, 2H); **^{13}C NMR** (176 MHz; $CDCl_3$) δ 187.91, 156.86, 137.19, 135.91, 133.23, 131.54, 130.58, 130.00, 128.73, 127.59, 126.87, 126.26, 125.06, 75.81, 33.67. **IR** (Neat) 3066, 2956, 2885, 1694, 1582, 1439, 1378, 1212, 1164, 977, 963, 878, 773, 73, 688, 665; **HRMS** (+ESI) *m/z*: $[M+NH_4]^+$ calcd; found.

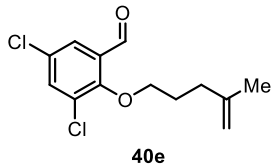

40e

3,5-dichloro-2-((4-methylpent-4-en-1-yl)oxy)benzaldehydebenzaldehyde (40e): Substrate **40e** was synthesized following general O-alkylation procedure employing 5-iodo-2-methylpent-1-ene as the electrophile. Purification by flash chromatography eluting with DCM/hexanes (35:65)

provided 319 mgs (87%) of **40e** as a clear oil. **^{1}H NMR** (700 MHz; $CDCl_3$) δ 10.31 (s, 1H), 7.71 (d, *J*= 2.6 Hz, 1H), 7.62 (d, *J*= 2.7 Hz, 1H), 4.78 (s, 1H), 4.74 (s, 1H), 4.08 (t, *J*= 6.5 Hz, 2H), 2.24 (t, *J*= 7.7 Hz, 2H), 2.02 (dd, *J*= 8.5, 6.6 Hz, 2H), 1.76 (s, 3H); **^{13}C NMR** (176 MHz; $CDCl_3$) δ 188.00, 157.15, 144.60, 135.92, 131.57, 130.48, 130.11, 126.79, 110.87, 76.46, 33.93, 27.93, 22.51. **IR** (Neat) 3074, 2940, 2873, 1694, 1582, 1439, 1373, 1212, 985, 887, 876, 736, 666; **HRMS** (+ESI) *m/z*: $[M+H]^+$ calcd for $C_{13}H_{15}Cl_2O_2^+$: 273.0444; found 273.0443.

4.4.5 Synthesis of Products

General procedure for Carbonyl-Olefin Metathesis.

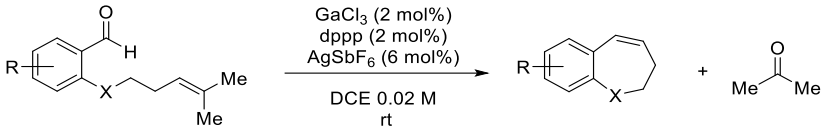

An oven-dried round bottom flask equipped with a magnetic stir bar was charged with $GaCl_3$ (0.0036 mmol), dppp (0.0036 mmol), $AgSbF_6$ (0.0108 mmol), and dry DCE (8.0 mL). The catalyst solution was allowed to stir for 20 min at room temperature. The benzaldehyde substrate (0.18 mmol dissolved in 1 mL of dry DCE) was added in one portion to the catalyst solution. The reaction mixture was allowed to stir for the indicated time at room temperature. After reaching completion as judged by TLC or 20 h, the reaction was filtered through a silica plug eluting with DCM (25 mL). The filtrate was concentrated under reduced pressure to remove all volatile components. Yield and conversion were determined either by ^{1}H NMR using mesitylene as an internal standard, or by isolation via column chromatography with the indicated eluent to give the pure metathesis products.

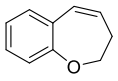

18

2,3-dihydrobenzo[*b*]oxepine (18): The cyclization of **16** was performed according to the general procedure for metathesis with 10 mol% of $GaCl_3$, 10 mol% of dppp and 30 mol% of $AgSbF_6$ with a reaction time of 10 min (35% yield, 99% conversion by ^{1}H NMR). Purification by flash column chromatography eluting with DCM/hexanes (1:19) provided 8.1 mg (31%) of **18** as a clear oil. **^{1}H NMR** (700 MHz; $CDCl_3$) δ 7.17 (d, *J*= 7.6 Hz, 1H), 7.12 (t, *J*= 7.6 Hz, 1H), 7.00-6.94 (m, 2H), 6.33 (d, *J*= 11.8 Hz, 1H), 5.97 (dt, *J*= 11.8, 4.5 Hz, 1H), 4.24 (t, *J*= 4.9 Hz, 2H), 2.71-2.63 (m,

2H); **^{13}C NMR** (176 MHz; $CDCl_3$) δ 159.1, 132.9, 130.4, 128.9, 128.1, 127.0, 122.5, 120.1, 69.7, 34.4. **IR** (Neat) 3064, 3023, 2961, 2930, 2891, 1601, 1569, 1489, 1245, 1213, 1111, 996, 938, 771, 754, 708, 681. **HRMS** (APCI) *m/z*: $[M+H]^+$ calcd for $C_{10}H_{11}O^+$ 147.0804; found 147.0807.

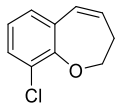

19

9-chloro-2,3-dihydrobenzo[*b*]oxepine (19): The cyclization of **17** was performed according to the general procedure for metathesis with a reaction time of 20 min (82% yield, 99% conversion by ^{1}H NMR). Purification by flash column chromatography eluting with DCM/hexanes (1:19) provided 25.4 mg (78%) of **19** as a clear oil. **^{1}H NMR** (700 MHz; $CDCl_3$) δ 7.23 (d, *J*= 7.9 Hz, 1H), 7.07 (d, *J*= 7.8 Hz, 1H), 6.90 (t, *J*= 7.7 Hz, 1H), 6.32 (d, *J*= 11.4 Hz, 1H), 6.03 (dt, *J*= 11.7, 4.5 Hz, 1H), 4.33 (t, *J*= 5.0 Hz, 2H), 2.71 (q, *J*= 5.0 Hz, 2H); **^{13}C NMR** (176 MHz; $CDCl_3$) δ 154.6, 131.6, 131.3, 128.7, 128.6, 128.2, 125.3, 122.7, 70.5, 34.1. **IR** (Neat) 3066, 3025, 2967, 2893, 1560, 1471, 1442, 1278, 1256, 1227, 1085, 992, 880, 793, 732, 695. **HRMS** (APCI) *m/z*: $[M+H]^+$ calcd for $C_{10}H_{10}OCl^+$ 181.0415; found 181.0417.

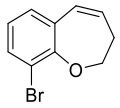

22

9-bromo-2,3-dihydrobenzo[*b*]oxepine (22): The cyclization of **S22** was performed according to the general procedure for metathesis with a reaction time of 20 min (83% yield, 99% conversion by ^{1}H NMR). Purification by flash column chromatography eluting with DCM/hexanes (1:19) provided 31.9 mg (79%) of **22** as a clear oil. **^{1}H NMR** (700 MHz; $CDCl_3$) δ 7.40 (d, *J*= 7.2 Hz, 1H), 7.11 (d, *J*= 7.5 Hz, 1H), 6.84 (t, *J*= 7.8 Hz, 1H), 6.31 (d, *J*= 11.5 Hz, 1H), 6.02 (dt, *J*= 11.7, 4.5 Hz, 1H), 4.32 (t, *J*= 5.0 Hz, 2H), 2.72 (q, *J*= 5.6 Hz, 2H); **^{13}C NMR** (176 MHz; $CDCl_3$) δ 155.4, 132.1, 131.7, 131.6, 128.7, 128.2, 123.3, 115.0, 70.5, 34.1. **IR** (Neat) 3062, 3024, 2966, 2892, 1555, 1469, 1439, 1411, 1278, 1254, 1226, 1085, 1034, 991, 864, 791, 731, 692. **HRMS** (APCI) *m/z*: $[M+H]^+$ calcd for $C_{10}H_{10}OBr^+$ 224.9910; found 224.9911.

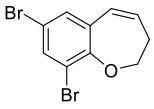

23

7,9-dibromo-2,3-dihydrobenzo[*b*]oxepine (23): The cyclization of **S23** was performed according to the general procedure for metathesis with a reaction time of 40 min (76% yield, 99% conversion by ^{1}H NMR). Purification by flash column chromatography eluting with DCM/hexanes (1:19) provided 39.4 mg (72%) of **23** as a white solid. **^{1}H NMR** (700 MHz; $CDCl_3$) δ 7.52 (d, *J*= 2.3 Hz, 1H), 7.24 (d, *J*= 2.3 Hz, 1H), 6.21 (d, *J*= 11.8 Hz, 1H), 6.07 (dt, *J*= 11.8, 4.5 Hz, 1H), 4.29 (t, *J*= 4.9 Hz, 2H), 2.76-2.67 (m, 2H); **^{13}C NMR** (176 MHz; $CDCl_3$) δ 154.7, 134.3, 133.5, 133.2, 130.0, 127.1, 115.8, 114.6, 70.6, 34.0. **IR** (Neat) 3099, 3070, 3021, 2958, 2892, 1461, 1445, 1368, 1258, 1160, 1040, 995, 877, 853, 802, 691, 673. **HRMS** (APCI) *m/z*: $[M+H]^+$ calcd for $C_{10}H_9OBr_2^+$ 302.9015; found 302.9016.

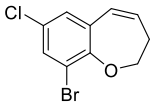

24

9-bromo-7-chloro-2,3-dihydrobenzo[*b*]oxepine (24): The cyclization of **S24** was performed according to the general procedure for metathesis with a reaction time of 40 min (82% yield, 99% conversion by ^{1}H NMR). Purification by flash column chromatography eluting with DCM/hexanes (1:19) provided 37.0 mg (79%) of **24** as a white solid. **^{1}H NMR** (500 MHz; $CDCl_3$) δ 7.39 (d, *J*= 2.5 Hz, 1H), 7.10 (d, *J*= 2.6 Hz, 1H), 6.22 (d, *J*= 11.9 Hz, 1H), 6.08 (dt, *J*= 11.8, 4.4 Hz, 1H), 4.29 (t, *J*= 4.9 Hz, 2H), 2.72 (qd, *J*= 4.8, 1.8 Hz, 2H); **^{13}C NMR** (176 MHz; $CDCl_3$) δ 154.2, 133.2, 131.4, 130.8, 129.5, 127.5, 127.2, 115.4, 70.6, 34.0. **IR** (Neat) 3070, 3021, 2958, 2892, 1461, 1444, 1368, 1258, 1160, 1041, 995, 876, 853, 802, 692, 673. **HRMS** (APCI) *m/z*: $[M+H]^+$ calcd for $C_{10}H_9OBrCl^+$ 258.9520; found 258.9519.

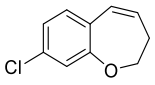

25

8-chloro-2,3-dihydrobenzo[*b*]oxepine (25): The cyclization of **S25** was performed according to the general procedure for metathesis with 20 mol% of $GaCl_3$, 20 mol% of dppp and 60 mol% of $AgSbF_6$ with a reaction time of 10 min (50% yield, 99% conversion by ^{1}H NMR). Purification by flash column chromatography eluting with DCM/hexanes (1:19) provided 15.8 mg (49%) of **25** as a clear oil. **^{1}H NMR** (700 MHz; $CDCl_3$) δ 7.07 (d, *J*= 8.2 Hz, 1H), 6.99-6.92 (m, 2H), 6.28 (d, *J*=

11.6 Hz, 1H), 5.97 (dt, *J*= 11.7, 4.6 Hz, 1H), 4.23 (t, *J*= 4.9 Hz, 2H), 2.67 (qd, *J*= 4.7, 1.5 Hz, 2H); **^{13}C NMR** (176 MHz; $CDCl_3$) δ 159.5, 133.5, 133.0, 130.8, 128.0, 125.6, 122.7, 120.4, 69.9, 34.3. **IR** (Neat) 3026, 2965, 2931, 2893, 2815, 1594, 1558, 1482, 1238, 1082, 1037, 998, 947, 889, 865, 815, 684. **HRMS** (APCI) *m/z*: $[M+H]^+$ calcd for $C_{10}H_{10}OCl^+$ 181.0415; found 181.0414.

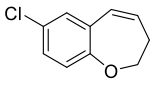

26

7-chloro-2,3-dihydrobenzo[*b*]oxepine (26): The cyclization of **S26** was performed according to the general procedure for metathesis with 10 mol% of $GaCl_3$, 10 mol% of dppp and 30 mol% of $AgSbF_6$ with a reaction time of 10 min (57% yield, 99% conversion by ^{1}H NMR). Purification by flash column chromatography eluting with DCM/hexanes (1:19) provided 16.8 mg (52%) of **26** as a clear oil. **^{1}H NMR** (500 MHz; $CDCl_3$) δ 7.13 (d, *J*= 2.6 Hz, 1H), 7.06 (dd, *J*= 8.6, 2.5 Hz, 1H), 6.88 (d, *J*= 8.6 Hz, 1H), 6.23 (d, *J*= 11.8 Hz, 1H), 6.02 (dt, *J*= 11.8, 4.5 Hz, 1H), 4.21 (t, *J*= 4.9 Hz, 2H), 2.72-2.63 (m, 2H); **^{13}C NMR** (126 MHz; $CDCl_3$) δ 157.7, 132.0, 131.9, 128.5, 127.8, 127.7, 127.3, 121.4, 69.8, 34.3. **IR** (Neat) 3027, 2963, 2928, 2892, 1483, 1282, 1244, 1214, 1168, 1116, 1038, 864, 820, 769, 690. **HRMS** (EI) *m/z*: $[M]^+$ calcd for $C_{10}H_{10}OCl^+$ 180.0342; found 180.0346.

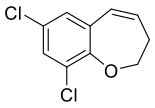

27

7,9-dichloro-2,3-dihydrobenzo[*b*]oxepine (27): The cyclization of **S27** was performed according to the general procedure for metathesis with a reaction time of 15 min (95% yield, 99% conversion by ^{1}H NMR). Purification by flash column chromatography eluting with DCM/hexanes (1:32) provided 35.0 mg (90%) of **27** as a white solid. **^{1}H NMR** (700 MHz; $CDCl_3$) δ 7.22 (s, 1H), 7.05 (s, 1H), 6.23 (d, *J*= 11.8 Hz, 1H), 6.08 (dt, *J*= 11.8, 4.5 Hz, 1H), 4.30 (t, *J*= 4.9 Hz, 2H), 2.72 (q, *J*= 4.9 Hz, 2H); **^{13}C NMR** (176 MHz; $CDCl_3$) δ 153.4, 133.2, 130.6, 129.6, 128.0, 127.2, 127.0, 126.0, 70.6, 34.1. **IR** (Neat) 3078, 3023, 2974, 2919, 2897, 1684, 1590, 1463, 1447, 1339, 1258, 1230, 1166, 1082, 996, 853, 826, 695, 681. **HRMS** (APCI) *m/z*: $[M+H]^+$ calcd for $C_{10}H_9OCl_2^+$ 215.0025; found 215.0029.

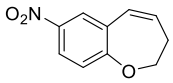

28

7-nitro-2,3-dihydrobenzo[*b*]oxepine (28): The cyclization of **S28** was performed according to the general procedure for metathesis with 10 mol% of $GaCl_3$, 10 mol% of dppp and 30 mol% of $AgSbF_6$ with a reaction time of 40 min (62% yield, 99% conversion by ^{1}H NMR). Purification by flash column chromatography eluting with DCM/hexanes (1:4) provided 20.9 mg (61%) of **28** as a white solid. **^{1}H NMR** (700 MHz; $CDCl_3$) δ 8.10 (d, *J*= 2.8 Hz, 1H), 7.98 (dd, *J*= 8.9, 2.8 Hz, 1H), 7.03 (d, *J*= 8.9 Hz, 1H), 6.36 (d, *J*= 11.7 Hz, 1H), 6.15 (dt, *J*= 11.7, 4.7 Hz, 1H), 4.32 (t, *J*= 4.8 Hz, 2H), 2.73 (qd, *J*= 4.7, 1.6 Hz, 2H); **^{13}C NMR** (176 MHz; $CDCl_3$) δ 164.0, 142.8, 133.3, 128.6, 127.7, 127.0, 123.4, 120.9, 70.1, 33.9. **IR** (Neat) 3077, 2975, 2937, 2890, 1686, 1608, 1588, 1520, 1485, 1338, 1275, 1243, 1179, 1078, 1001, 942, 826, 748, 663. **HRMS** (APCI) *m/z*: $[M+H]^+$ calcd for $C_{10}H_{10}NO_3^+$ 192.0655; found 192.0661.

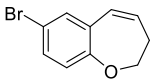

29

7-bromo-2,3-dihydrobenzo[*b*]oxepine (29): The cyclization of **S29** was performed according to the general procedure for metathesis with 10 mol% of $GaCl_3$, 10 mol% of dppp and 30 mol% of $AgSbF_6$ with a reaction time of 10 min (58% yield, 99% conversion by ^{1}H NMR). Purification by flash column chromatography eluting with DCM/hexanes (1:19) provided 22.2 mg (55%) of **29** as a clear oil. **^{1}H NMR** (700 MHz; $CDCl_3$) δ 7.28 (d, *J*= 2.4 Hz, 1H), 7.19 (dd, *J*= 8.6, 2.4 Hz, 1H), 6.83 (d, *J*= 8.6 Hz, 1H), 6.22 (d, *J*= 11.7 Hz, 1H), 6.02 (dt, *J*= 11.8, 4.5 Hz, 1H), 4.21 (t, *J*= 4.9 Hz, 2H), 2.67 (qd, *J*= 4.8, 1.7 Hz, 2H); **^{13}C NMR** (176 MHz; $CDCl_3$) δ 158.2, 139.9, 132.0, 130.6, 129.0, 127.7, 121.9, 114.7, 69.8, 34.3. **IR** (Neat) 3026, 2962, 2926, 2890, 2815, 1482, 1425, 1281, 1243, 1213, 1168, 1075, 1036, 846, 818, 764, 687. **HRMS** (APCI) *m/z*: $[M+H]^+$ calcd for $C_{10}H_{10}OBr^+$ 224.9910; found 224.9909.

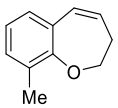

30

9-methyl-2,3-dihydrobenzo[*b*]oxepine (30): The cyclization of **S30** was performed according to the general procedure for metathesis with a reaction time of 10 min (85% yield, 99% conversion

by ^{1}H NMR). Purification by flash column chromatography eluting with DCM/hexanes (1:19) provided 22.7 mg (79%) of **30** as a clear oil. **^{1}H NMR** (700 MHz; $CDCl_3$) δ 7.02 (d, *J*= 7.5 Hz, 2H), 6.88 (t, *J*= 7.5 Hz, 1H), 6.32 (d, *J*= 11.9 Hz, 1H), 5.95 (dt, *J*= 11.8, 4.5 Hz, 1H), 4.26 (t, *J*= 4.9 Hz, 2H), 2.68 (q, *J*= 5.4 Hz, 2H), 2.26 (s, 3H); **^{13}C NMR** (176 MHz; $CDCl_3$) δ 157.5, 130.7, 130.0, 129.5, 129.0, 128.8, 126.9, 122.1, 69.8, 34.5, 16.7. **IR** (Neat) 3021, 2956, 2921, 2892, 1476, 1449, 1413, 1359, 1281, 1248, 1195, 1093, 995, 792, 736, 699. **HRMS** (APCI) *m/z*: $[M+H]^+$ calcd for $C_{11}H_{13}O^+$ 161.0961; found 161.0962.

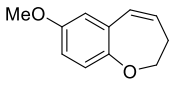

31

7-methoxy-2,3-dihydrobenzo[*b*]oxepine (31): The cyclization of **S31** was performed according to the general procedure for metathesis with 10 mol% of $GaCl_3$, 10 mol% of dppp and 30 mol% of $AgSbF_6$ with a reaction time of 40 min (42% yield, 99% conversion by ^{1}H NMR). Purification by flash column chromatography eluting with DCM/hexanes (1:4) provided 12.6 mg (40%) of **31** as a clear oil. **^{1}H NMR** (700 MHz; $CDCl_3$) δ 6.88 (d, *J*= 9.7 Hz, 1H), 6.69-6.67 (m, 2H), 6.27 (d, *J*= 11.8 Hz, 1H), 5.98 (dt, *J*= 11.7, 4.5 Hz, 1H), 4.19 (t, *J*= 4.9 Hz, 2H), 3.77 (s, 3H), 2.66 (tt, *J*= 4.8, 3.1 Hz, 2H); **^{13}C NMR** (176 MHz; $CDCl_3$) δ 154.9, 153.3, 131.1, 128.6, 127.9, 120.7, 117.0, 113.6, 69.9, 55.8, 34.5. **IR** (Neat) 3022, 3000, 2954, 2931, 2893, 2834, 1496, 1463, 1429, 1268, 1243, 1196, 1045, 1035, 818, 761, 691. **HRMS** (APCI) *m/z*: $[M+H]^+$ calcd for $C_{11}H_{13}O_2^+$ 177.0910; found 177.0909.

4.4.6 ^{1}H and ^{13}C NMR Spectra

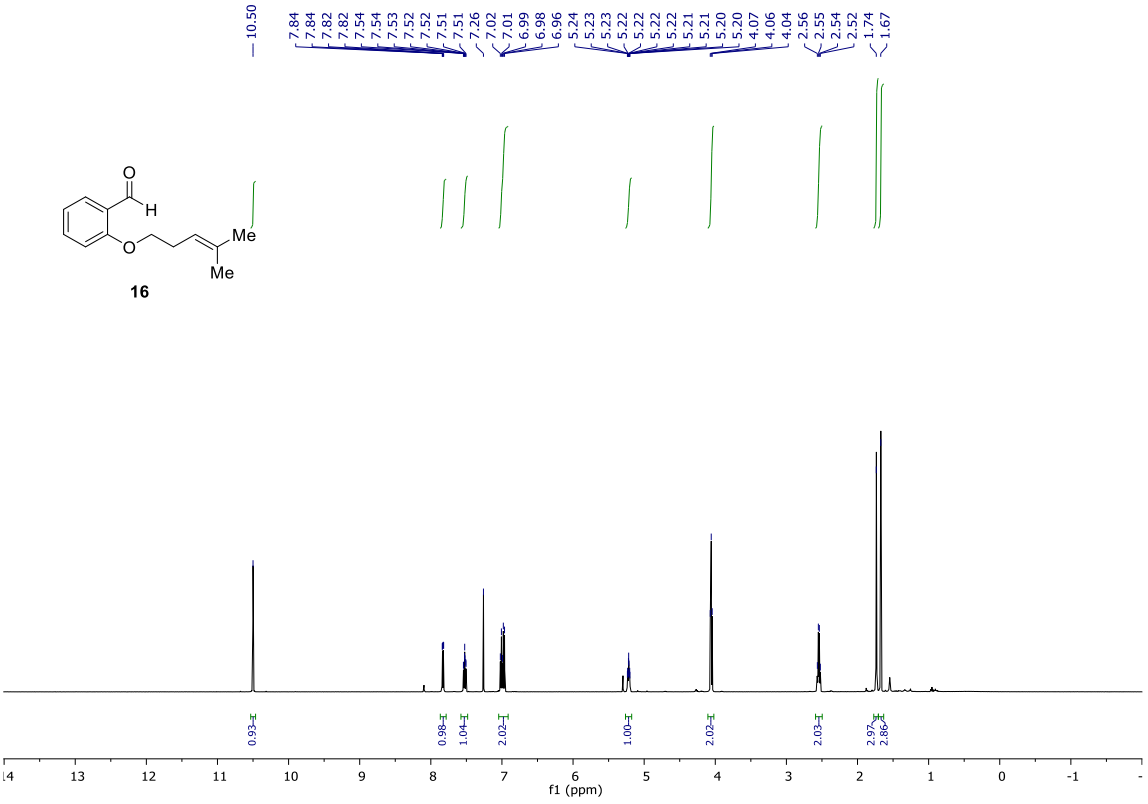

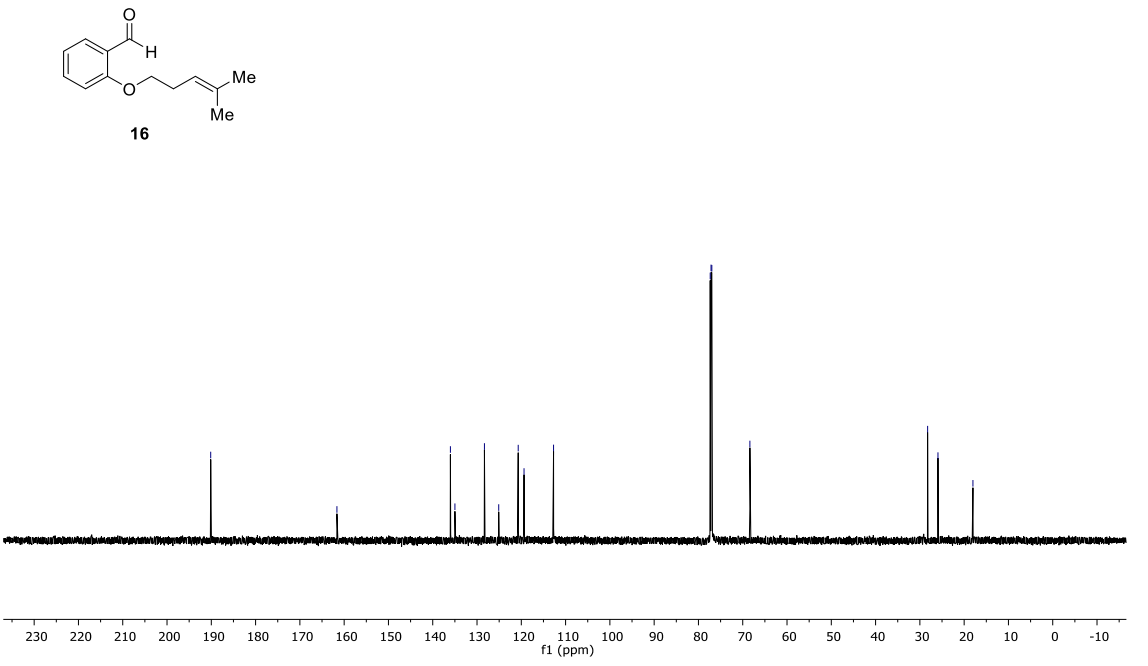

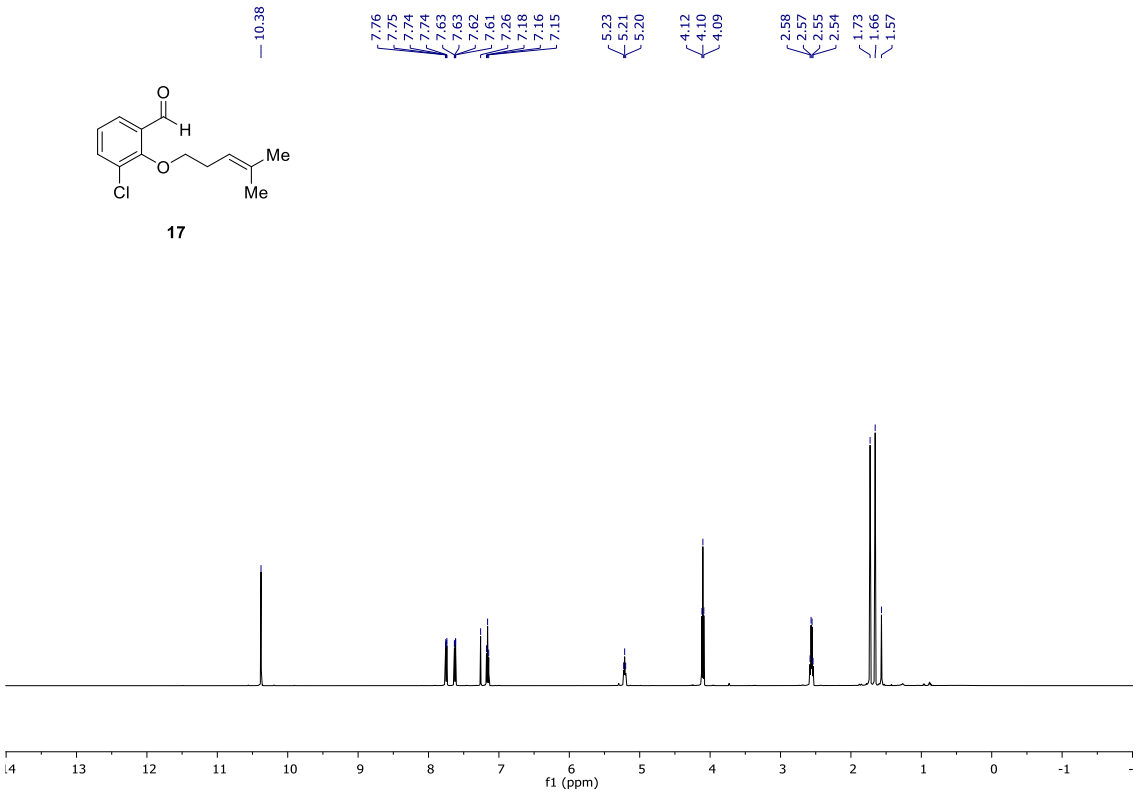
10.38
7.76
7.75
7.74
7.74
7.63
7.63
7.62
7.61
7.26
7.18
7.16
7.15
5.23
5.21
5.20
4.12
4.10
4.09
2.58
2.57
2.55
2.54
1.73
1.66
1.57
O
H
O
Me
Cl
Me
f1 (ppm)

17

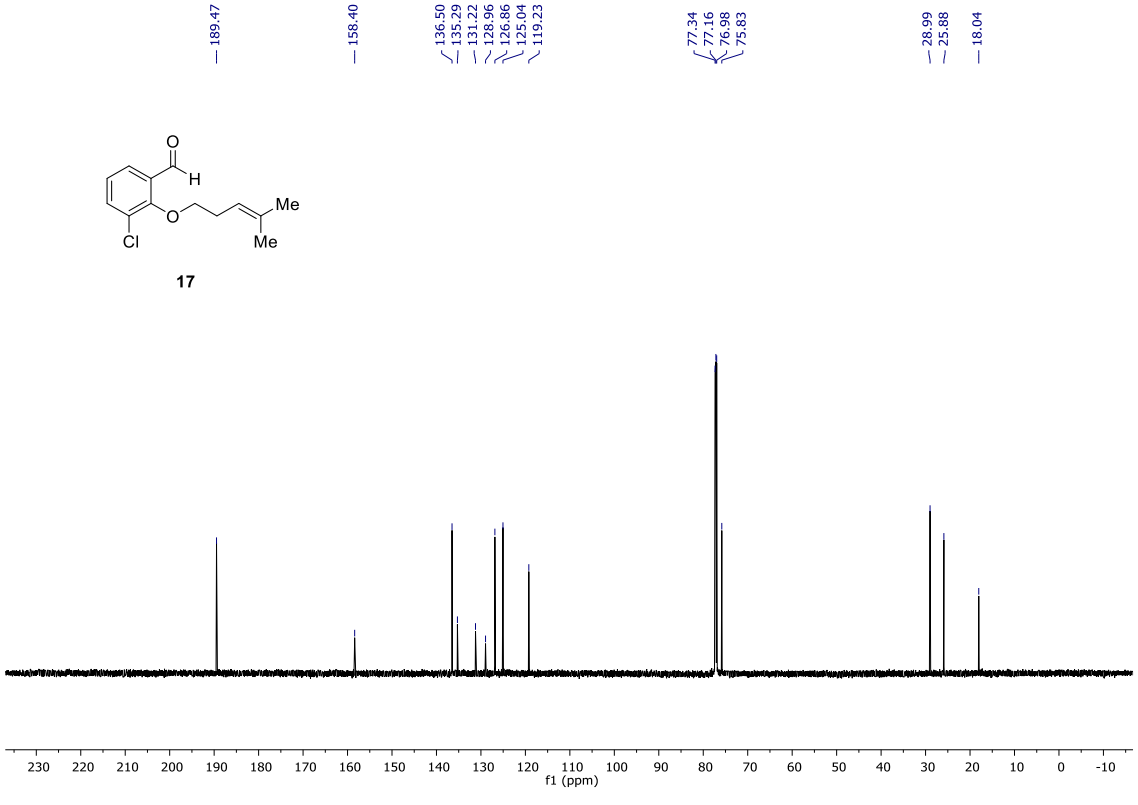
189.47
158.40
136.50
135.29
131.22
128.96
126.86
125.04
119.23
77.34
77.16
76.98
75.83
28.99
25.88
18.04
O
H
O
Me
Cl
Me
f1 (ppm)

17

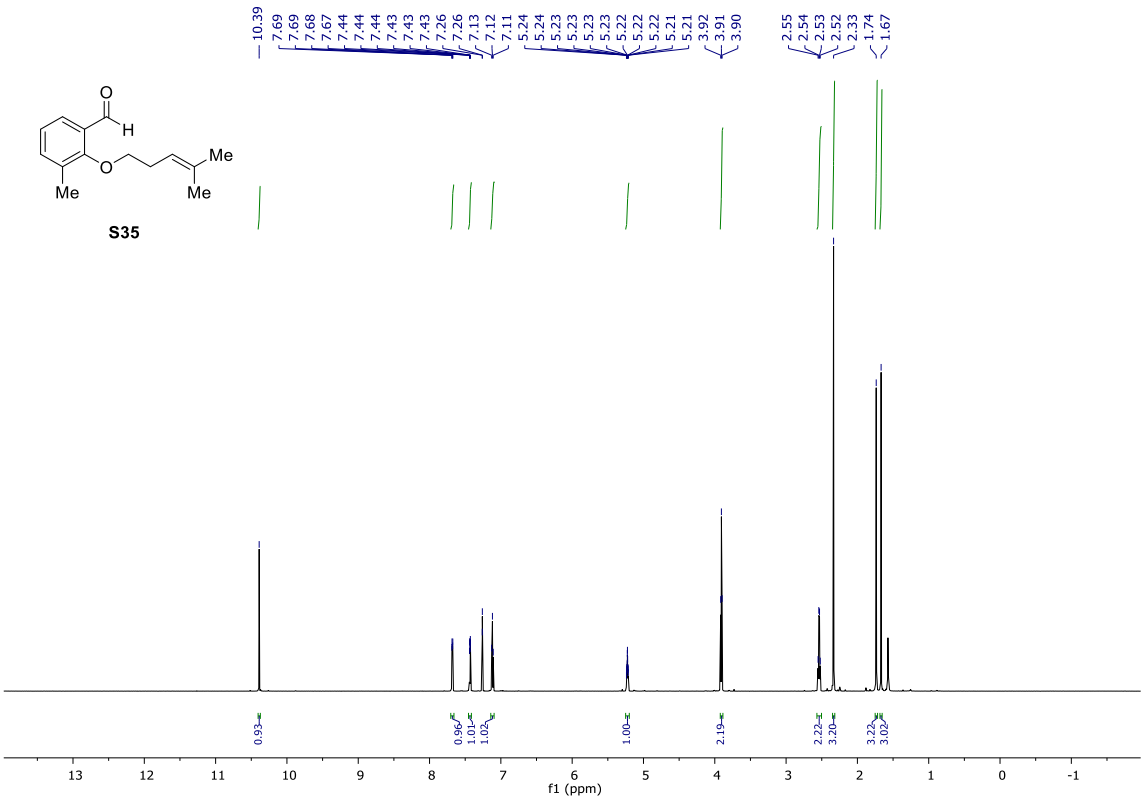
10.39
7.69
7.69
7.68
7.67
7.44
7.44
7.44
7.43
7.43
7.43
7.26
7.13
7.12
7.11
5.24
5.24
5.23
5.23
5.23
5.23
5.22
5.22
5.22
5.21
5.21
3.92
3.91
3.90
2.55
2.54
2.53
2.52
2.33
1.74
1.67
O
H
O
Me
Me
Me
S35
0.93
0.96
1.01
1.02
1.00
2.19
2.22
3.26
3.22
3.02
13
12
11
10
9
8
7
6
5
4
3
2
1
0
-1
f1 (ppm)

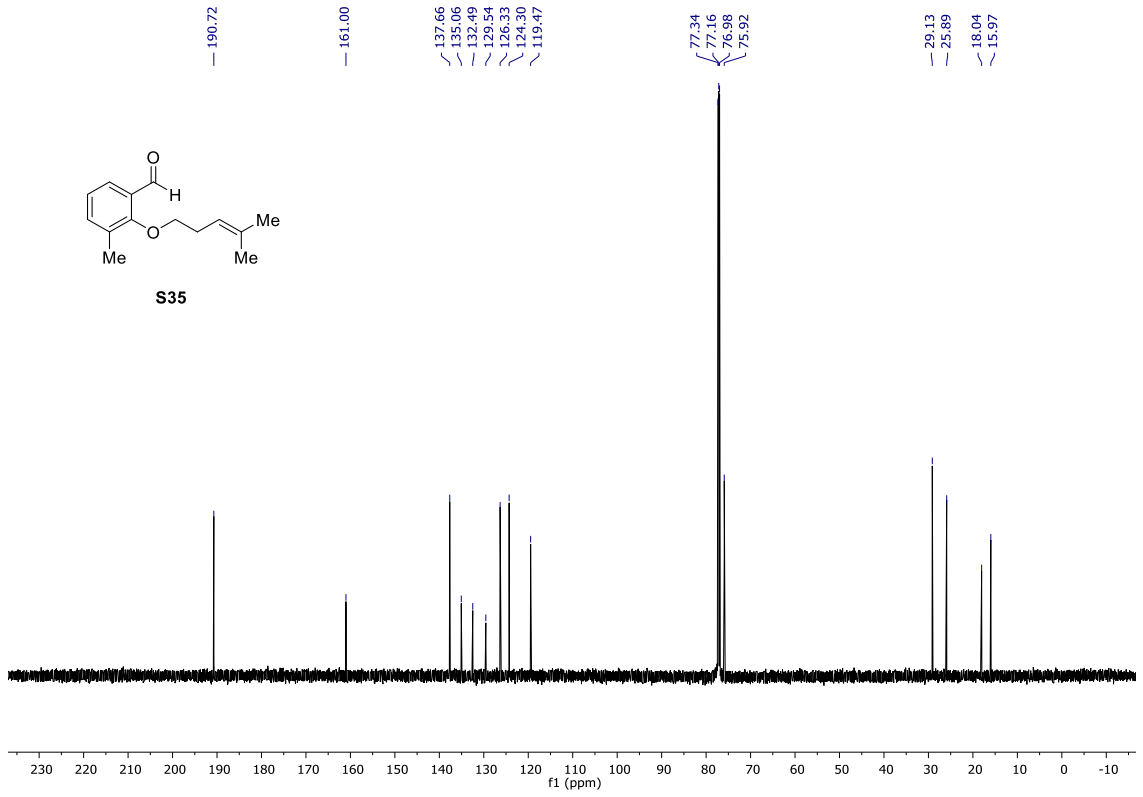
190.72
161.00
137.66
135.06
132.49
129.54
126.33
124.30
119.47
77.34
77.16
76.98
75.92
29.13
25.89
18.04
15.97
O
H
O
Me
Me
Me
S35
230
220
210
200
190
180
170
160
150
140
130
120
110
100
90
80
70
60
50
40
30
20
10
0
-10
f1 (ppm)

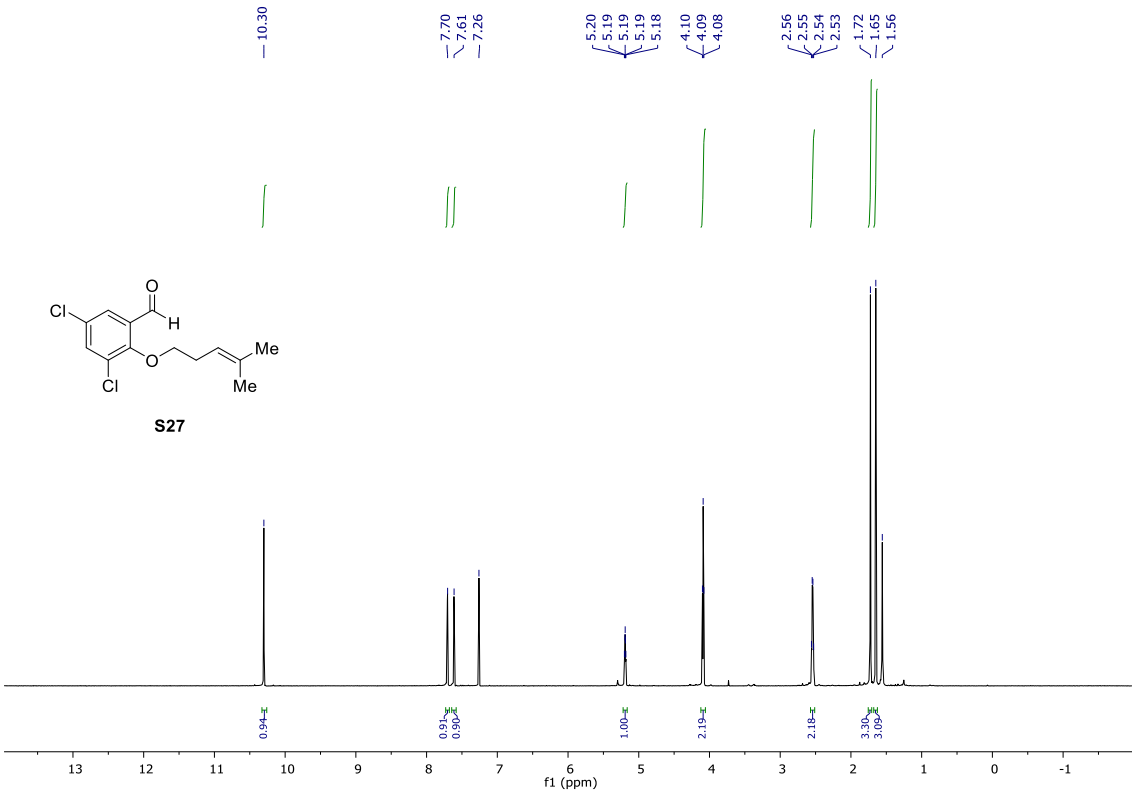
10.30
7.70
7.61
7.26
5.20
5.19
5.19
5.19
5.18
4.10
4.09
4.08
2.56
2.55
2.54
2.53
1.72
1.65
1.56
Cl
O
H
O
Me
Cl
Me
0.94
0.91
0.90
1.00
2.19
2.18
3.30
3.09
13 12 11 10 9 8 7 6 5 4 3 2 1 0 -1
f1 (ppm)

S27

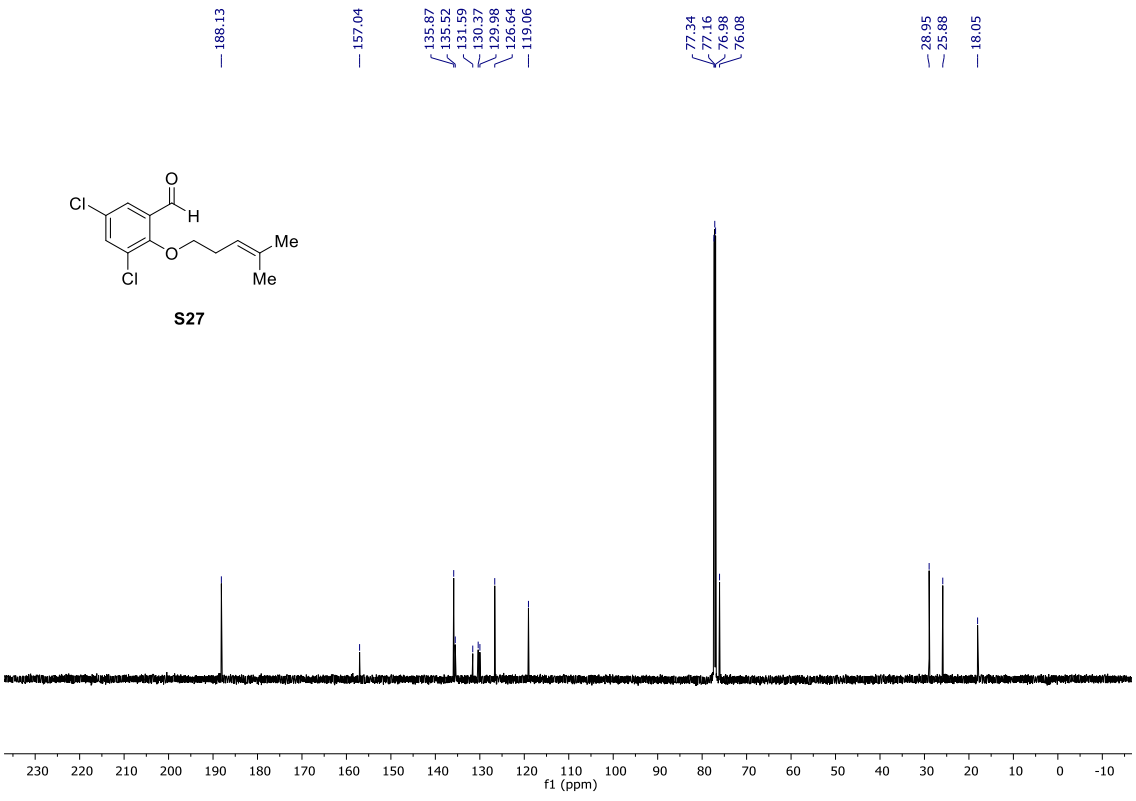
188.13
157.04
135.87
135.52
131.59
130.37
129.98
126.64
119.06
77.34
77.16
76.98
76.08
28.95
25.88
18.05
Cl
O
H
O
Me
Cl
Me
230 220 210 200 190 180 170 160 150 140 130 120 110 100 90 80 70 60 50 40 30 20 10 0 -10
f1 (ppm)

S27

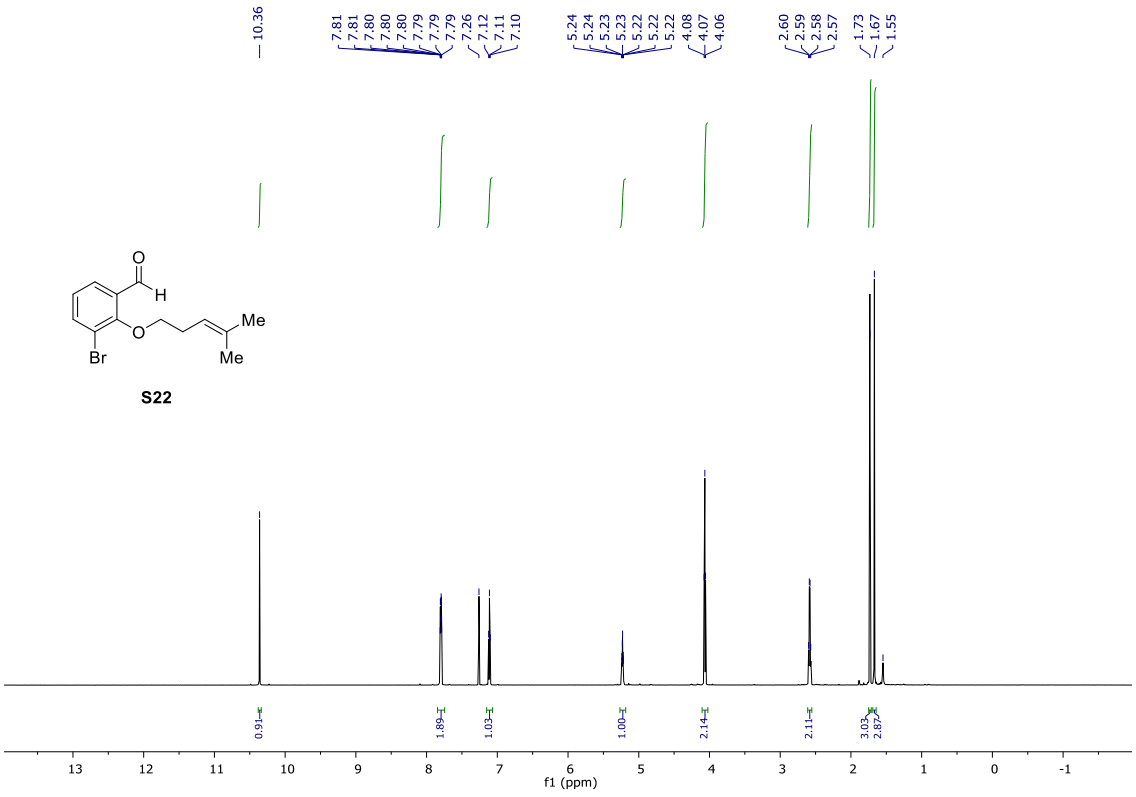
10.36
7.81
7.81
7.80
7.80
7.80
7.79
7.79
7.79
7.26
7.12
7.11
7.10
5.24
5.24
5.23
5.23
5.22
5.22
5.22
4.08
4.07
4.06
2.60
2.59
2.58
2.57
1.73
1.67
1.55
O
H
O
Me
Br
Me
0.91
1.89
1.03
1.00
2.14
2.11
3.03
2.87
13
12
11
10
9
8
7
6
5
4
3
2
1
0
-1
f1 (ppm)

S22

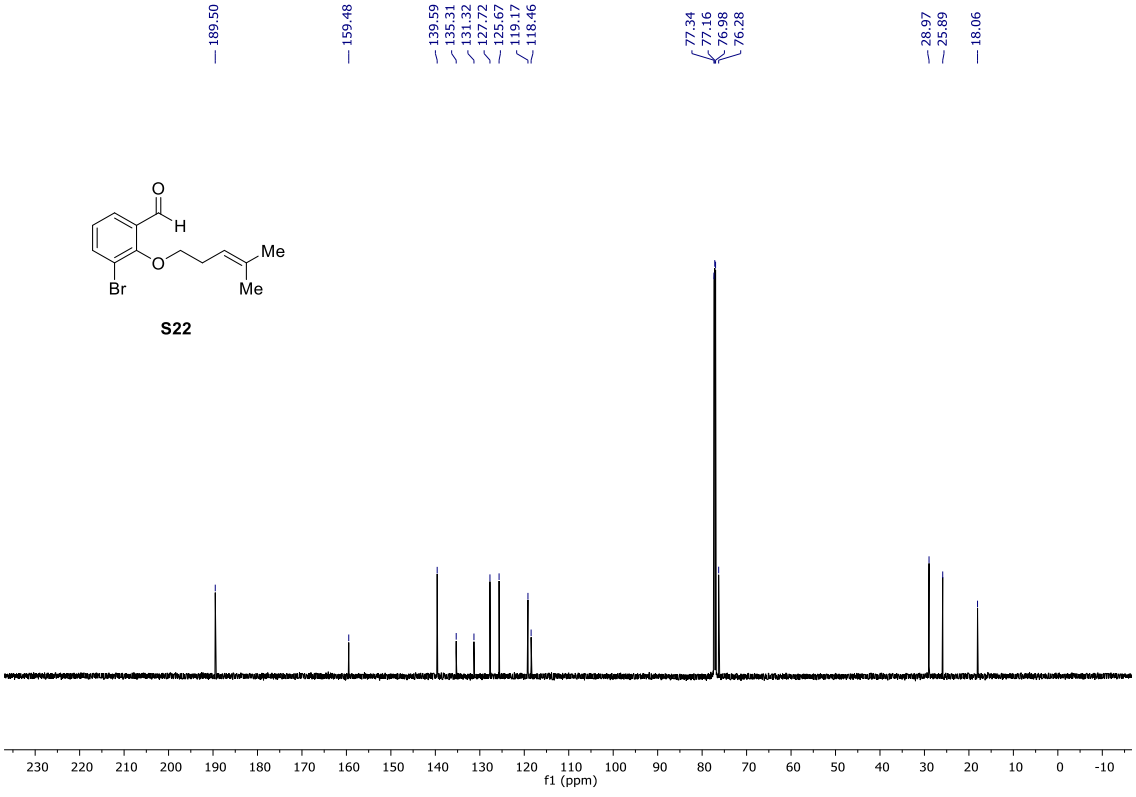
189.50
159.48
139.59
135.31
131.32
127.72
125.67
119.17
118.46
77.34
77.16
76.98
76.28
28.97
25.89
18.06
O
H
O
Me
Br
Me
230
220
210
200
190
180
170
160
150
140
130
120
110
100
90
80
70
60
50
40
30
20
10
0
-10
f1 (ppm)

S22

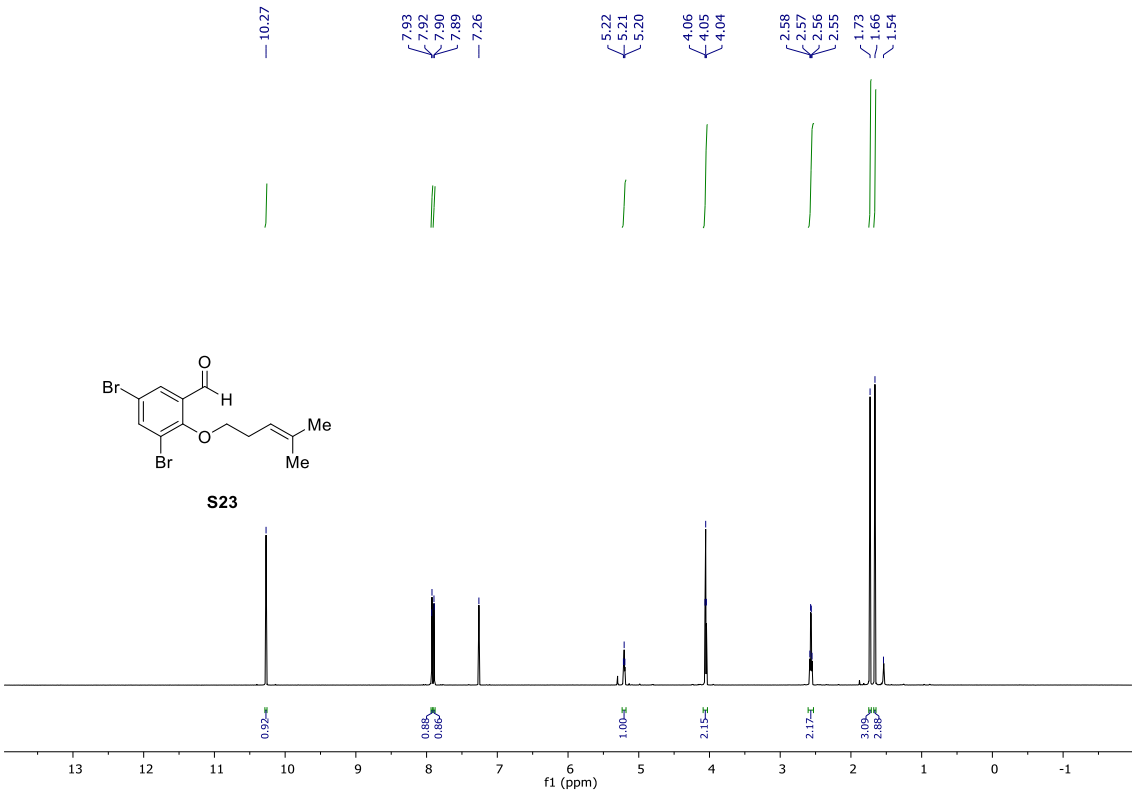
10.27
7.93
7.92
7.90
7.89
7.26
5.22
5.21
5.20
4.06
4.05
4.04
2.58
2.57
2.56
2.55
1.73
1.66
1.54
Br
O
H
Me
O
Br
Me
0.92
0.88
0.86
1.00
2.15
2.17
3.09
2.86
13 12 11 10 9 8 7 6 5 4 3 2 1 0 -1
f1 (ppm)

S23

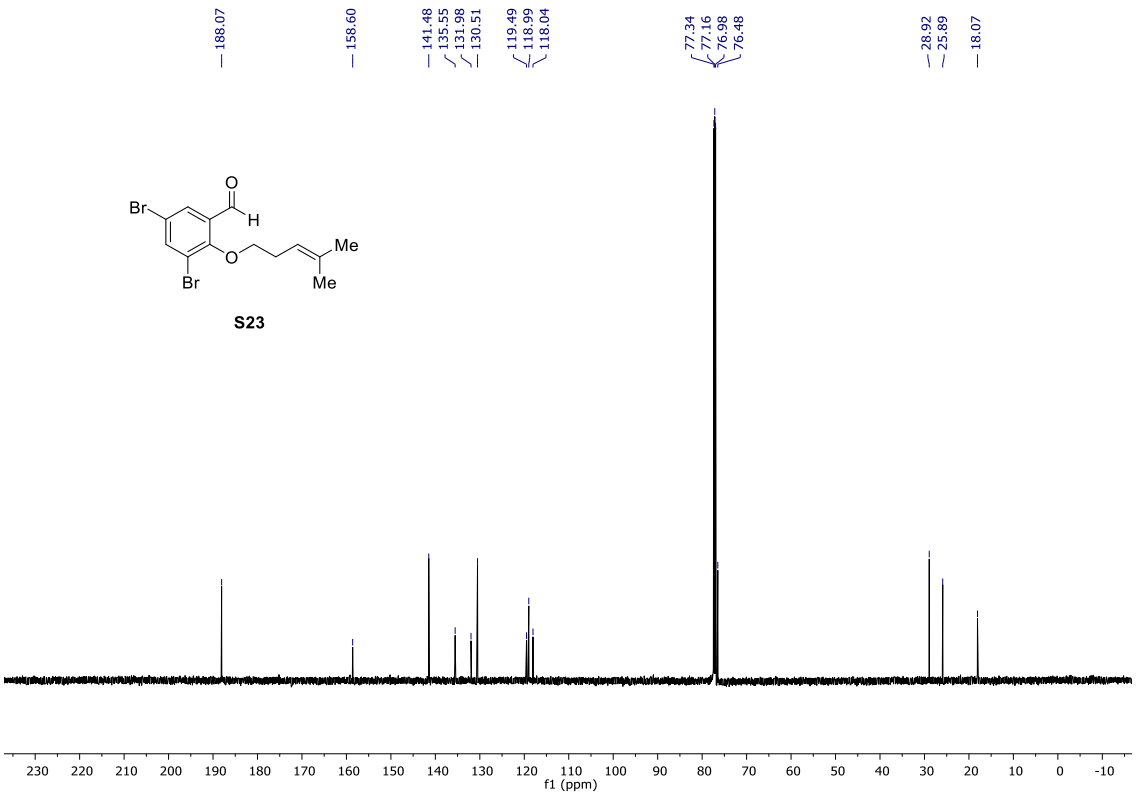
188.07
158.60
141.48
135.55
131.98
130.51
119.49
118.99
118.04
77.34
77.16
76.98
76.48
28.92
25.89
18.07
Br
O
H
Me
O
Br
Me
230 220 210 200 190 180 170 160 150 140 130 120 110 100 90 80 70 60 50 40 30 20 10 0 -10
f1 (ppm)

S23

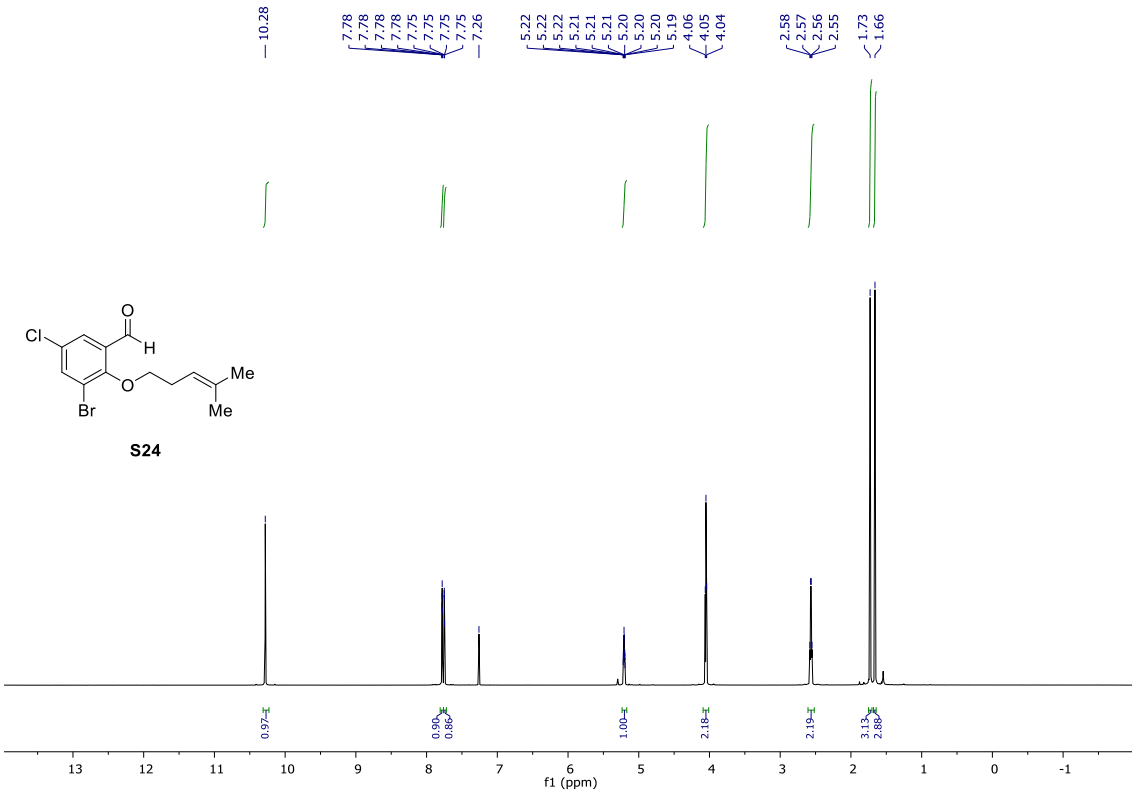
10.28
7.78
7.78
7.78
7.78
7.75
7.75
7.75
7.75
7.26
5.22
5.22
5.22
5.21
5.21
5.21
5.20
5.20
5.20
5.19
4.06
4.05
4.04
2.58
2.57
2.56
2.55
1.73
1.66
Cl
O
H
Br
O
Me
Me
0.97
0.90
0.85
1.00
2.18
2.19
3.13
2.86
13
12
11
10
9
8
7
6
5
4
3
2
1
0
-1
f1 (ppm)

S24

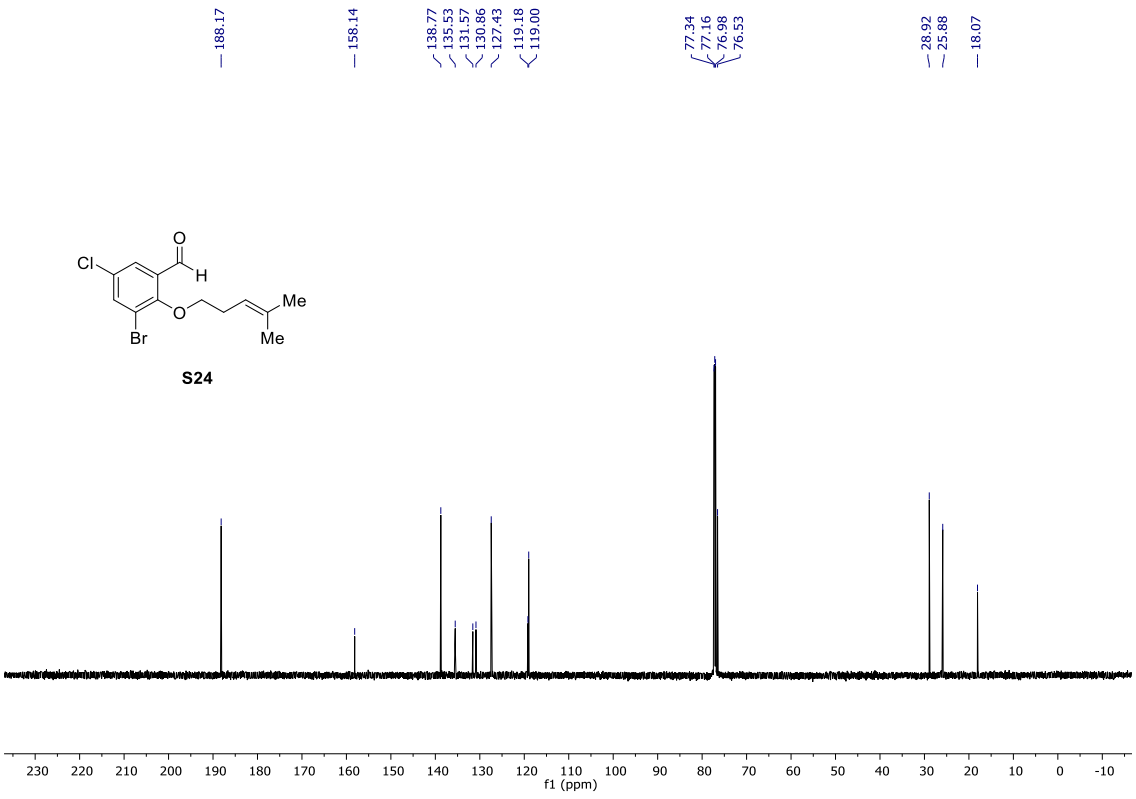
188.17
158.14
138.77
135.53
131.57
130.86
127.43
119.18
119.00
77.34
77.16
76.98
76.53
28.92
25.88
18.07
Cl
O
H
Br
O
Me
Me
230
220
210
200
190
180
170
160
150
140
130
120
110
100
90
80
70
60
50
40
30
20
10
0
-10
f1 (ppm)

S24

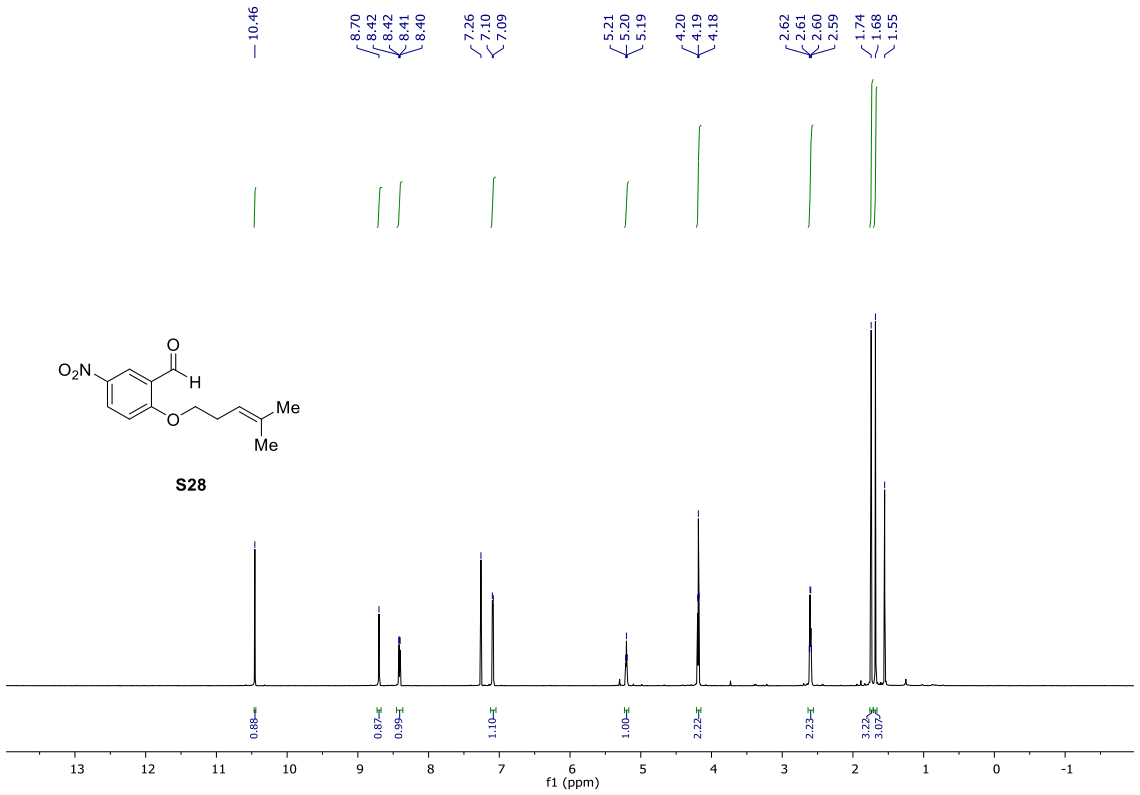
10.46
8.70
8.42
8.42
8.41
8.40
7.26
7.10
7.09
5.21
5.20
5.19
4.20
4.19
4.18
2.62
2.61
2.60
2.59
1.74
1.68
1.55
O2N
O
H
O
Me
Me
0.88
0.87
0.99
1.10
1.00
2.22
2.23
3.22
3.07
f1 (ppm)

S28

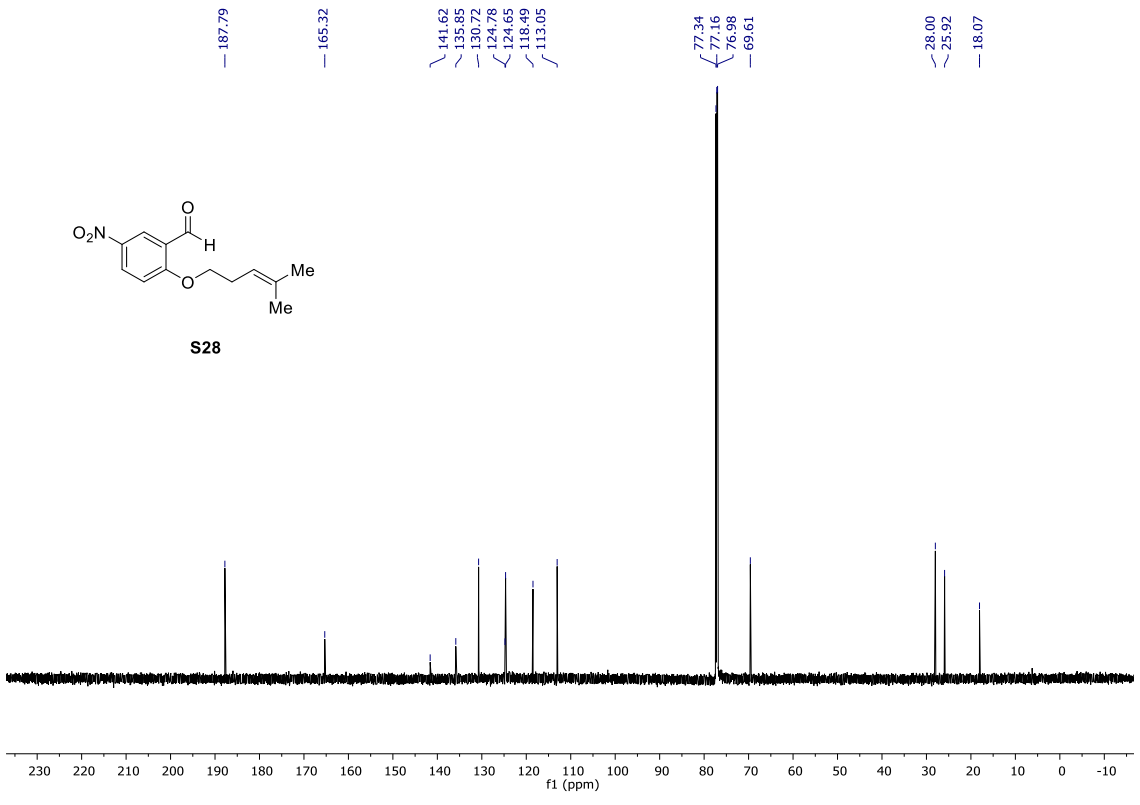
187.79
165.32
141.62
135.85
130.72
124.78
124.65
118.49
113.05
77.34
77.16
76.98
69.61
28.00
25.92
18.07
O2N
O
H
O
Me
Me
f1 (ppm)

S28

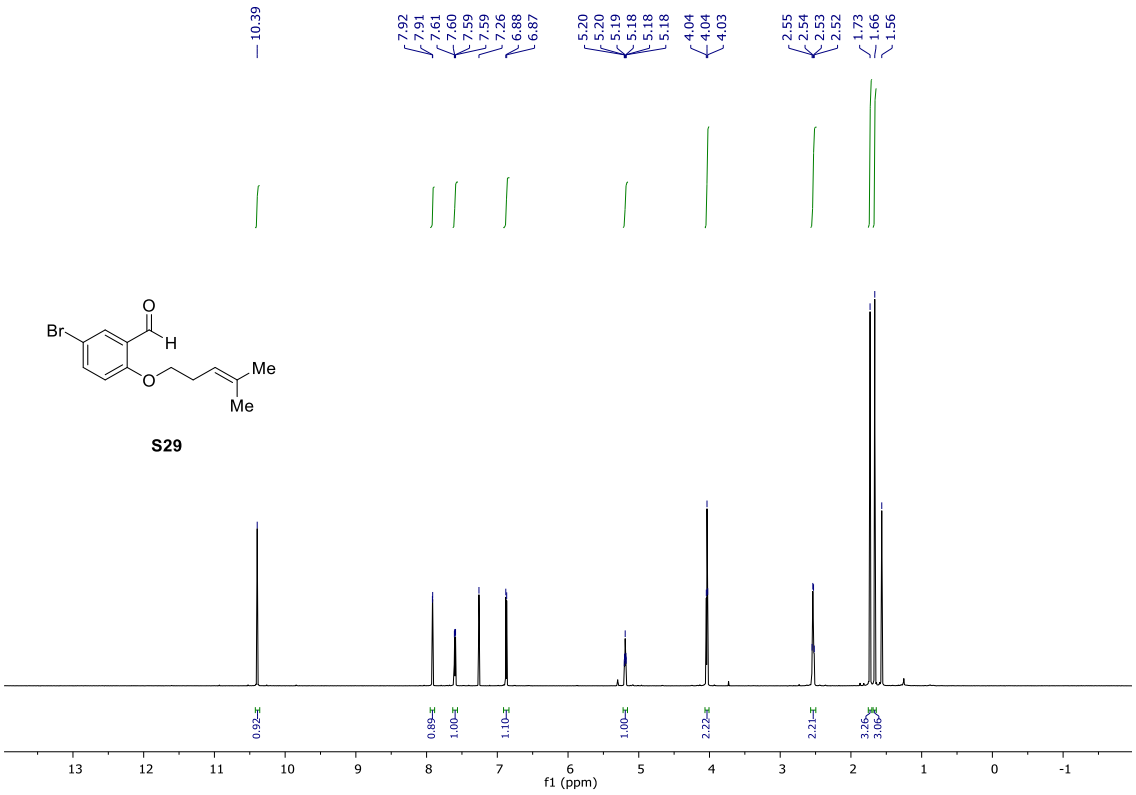
10.39
7.92
7.91
7.61
7.60
7.59
7.59
7.26
6.88
6.87
5.20
5.20
5.19
5.18
5.18
5.18
4.04
4.04
4.03
2.55
2.54
2.53
2.52
1.73
1.66
1.56
Br
O
H
O
Me
Me
0.92
0.89
1.00
1.10
1.00
2.22
2.21
3.26
3.06
f1 (ppm)

S29

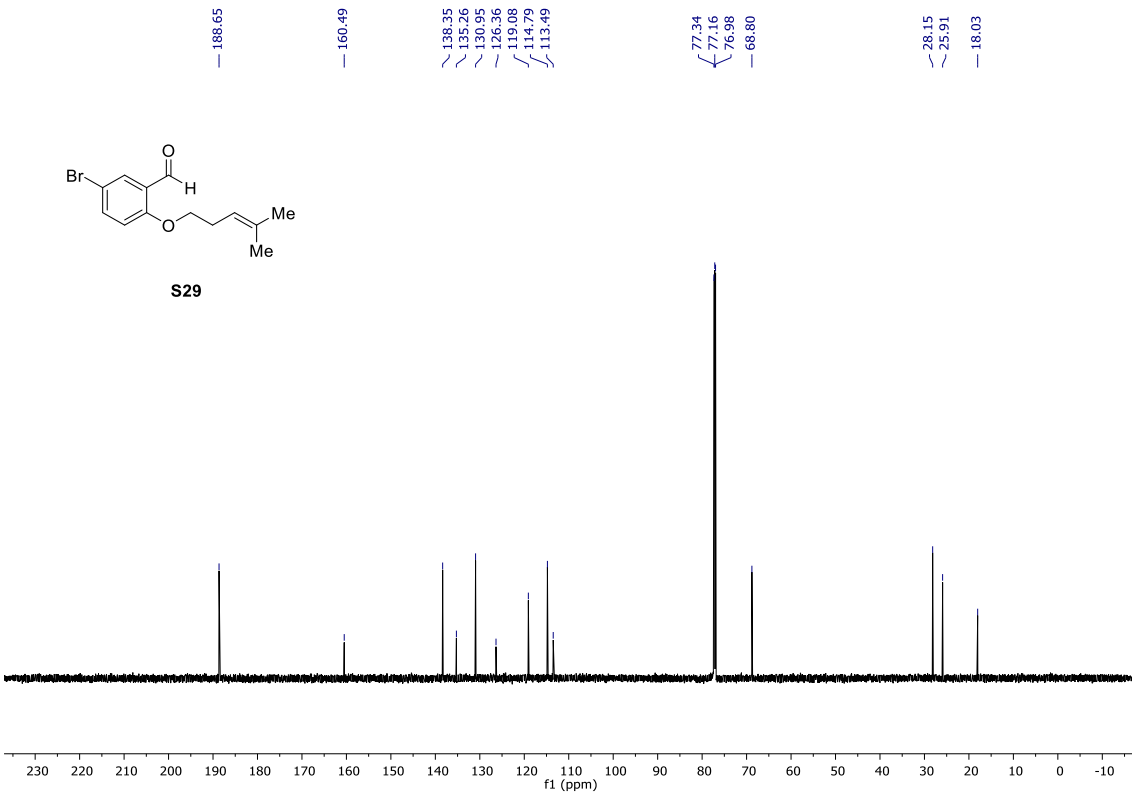
188.65
160.49
138.35
135.26
130.95
126.36
119.08
114.79
113.49
77.34
77.16
76.98
68.80
28.15
25.91
18.03
Br
O
H
O
Me
Me
f1 (ppm)

S29

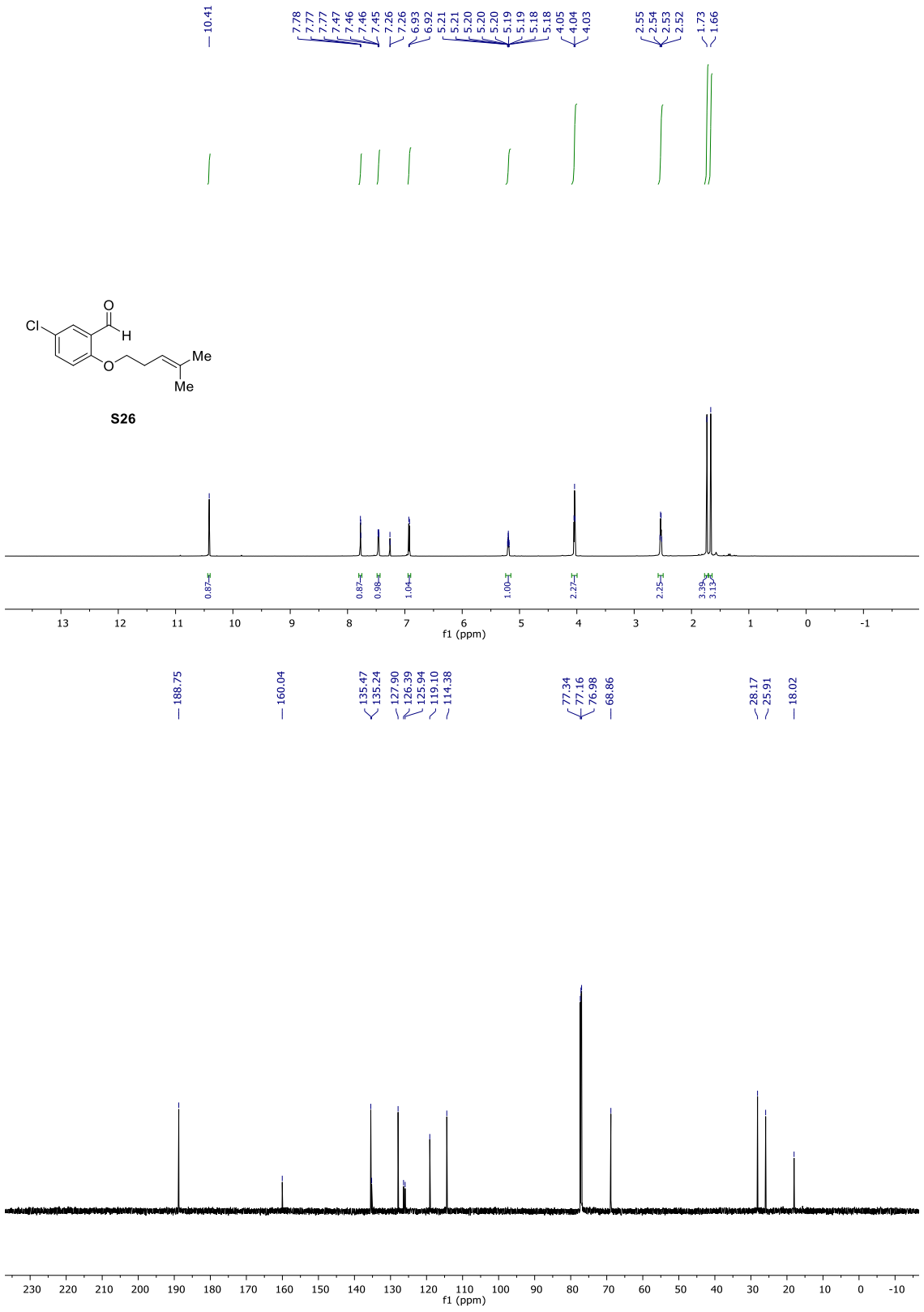
10.41
7.78
7.77
7.77
7.47
7.46
7.46
7.45
7.26
7.26
6.93
6.92
5.21
5.21
5.20
5.20
5.20
5.19
5.19
5.18
5.18
4.05
4.04
4.03
2.55
2.54
2.53
2.52
1.73
1.66
Cl
O
H
O
Me
Me
S26
0.87
0.87
0.98
1.04
1.00
2.27
2.25
3.39
3.13
13 12 11 10 9 8 7 6 5 4 3 2 1 0 -1
f1 (ppm)
188.75
160.04
135.47
135.24
127.90
126.39
125.94
119.10
114.38
77.34
77.16
76.98
68.86
28.17
25.91
18.02
230 220 210 200 190 180 170 160 150 140 130 120 110 100 90 80 70 60 50 40 30 20 10 0 -10
f1 (ppm)

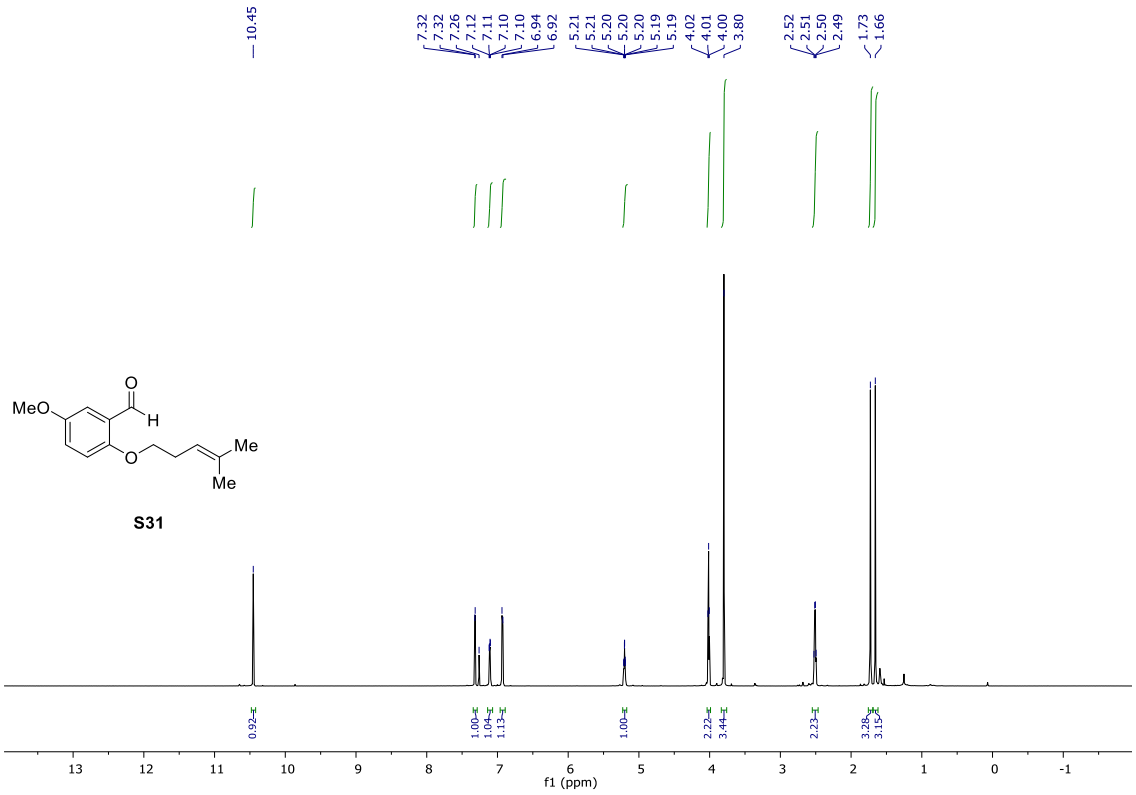
10.45
7.32
7.32
7.26
7.12
7.11
7.10
7.10
6.94
6.92
5.21
5.21
5.20
5.20
5.19
5.19
4.02
4.01
4.00
3.80
2.52
2.51
2.50
2.49
1.73
1.66
MeO
O
H
O
Me
Me
0.92
1.00
1.04
1.13
1.00
2.22
3.44
2.23
3.28
3.15
f1 (ppm)

S31

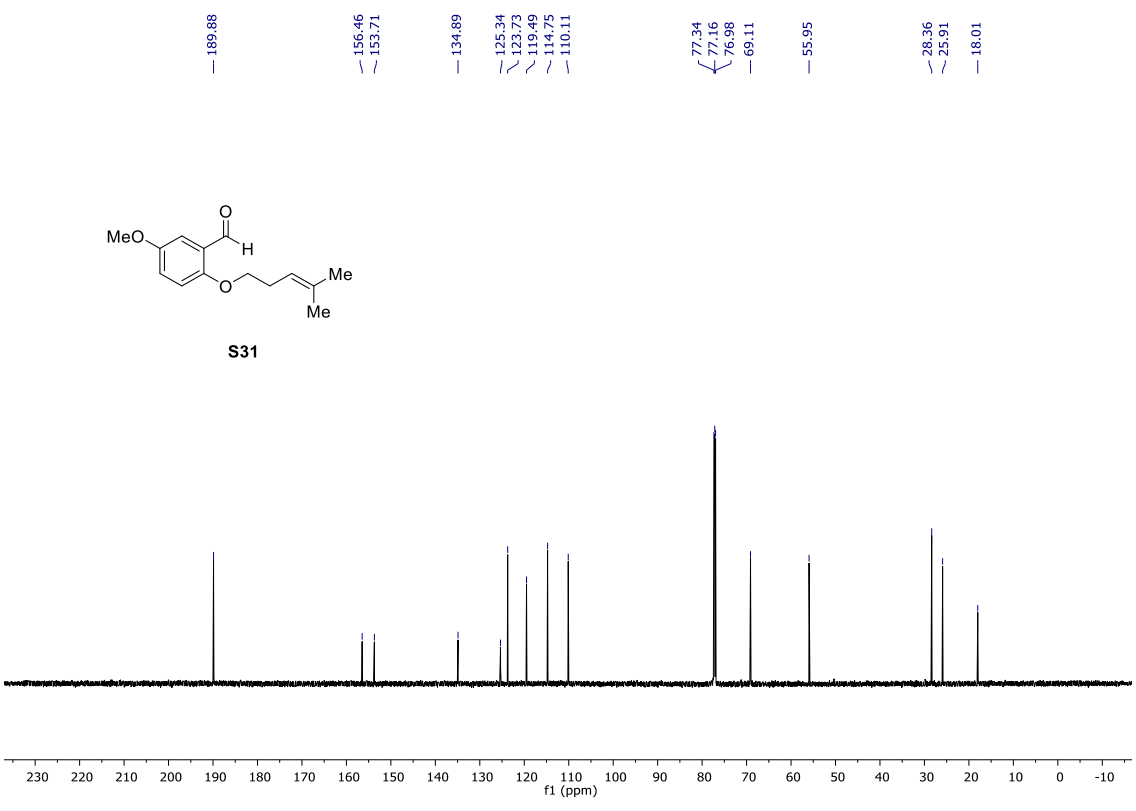
189.88
156.46
153.71
134.89
125.34
123.73
119.49
114.75
110.11
77.34
77.16
76.98
69.11
55.95
28.36
25.91
18.01
MeO
O
H
O
Me
Me
f1 (ppm)

S31

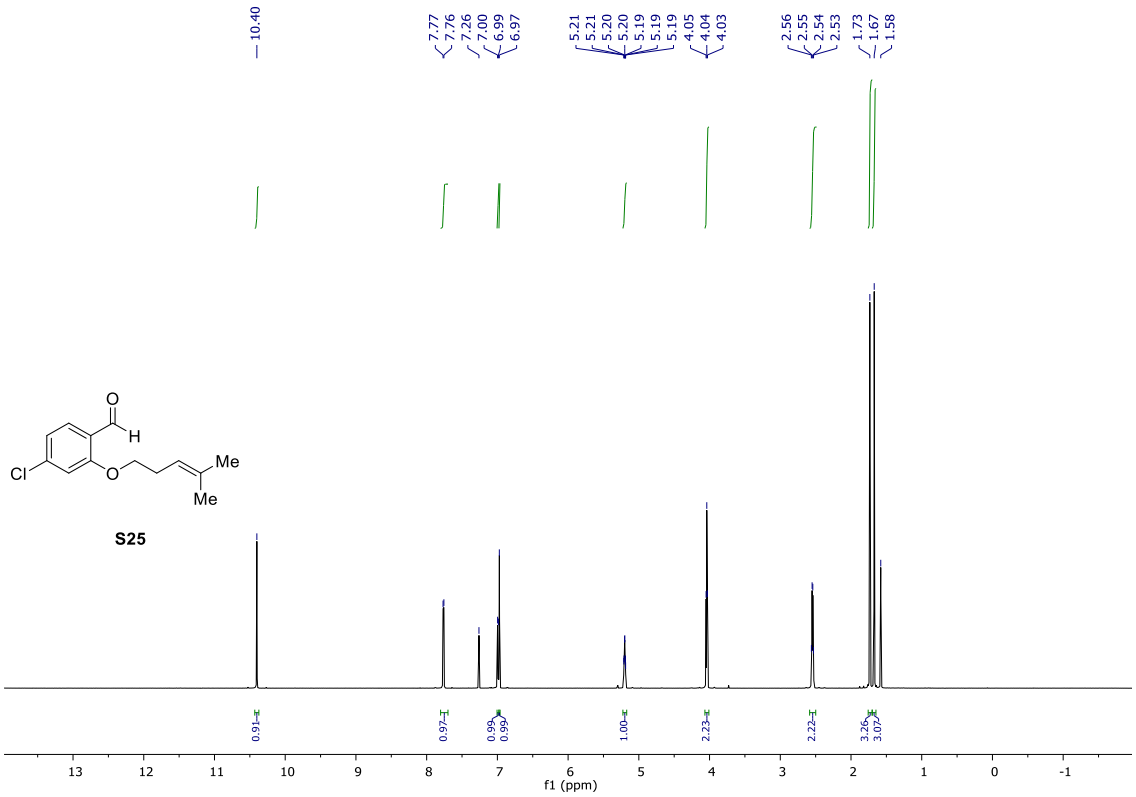
10.40
7.77
7.76
7.26
7.00
6.99
6.97
5.21
5.21
5.20
5.20
5.19
5.19
5.19
4.05
4.04
4.03
2.56
2.55
2.54
2.53
1.73
1.67
1.58
O
H
Cl
O
Me
Me
0.91
0.97
0.99
0.99
1.00
2.23
2.22
3.26
3.07
13
12
11
10
9
8
7
6
5
4
3
2
1
0
-1
f1 (ppm)

S25

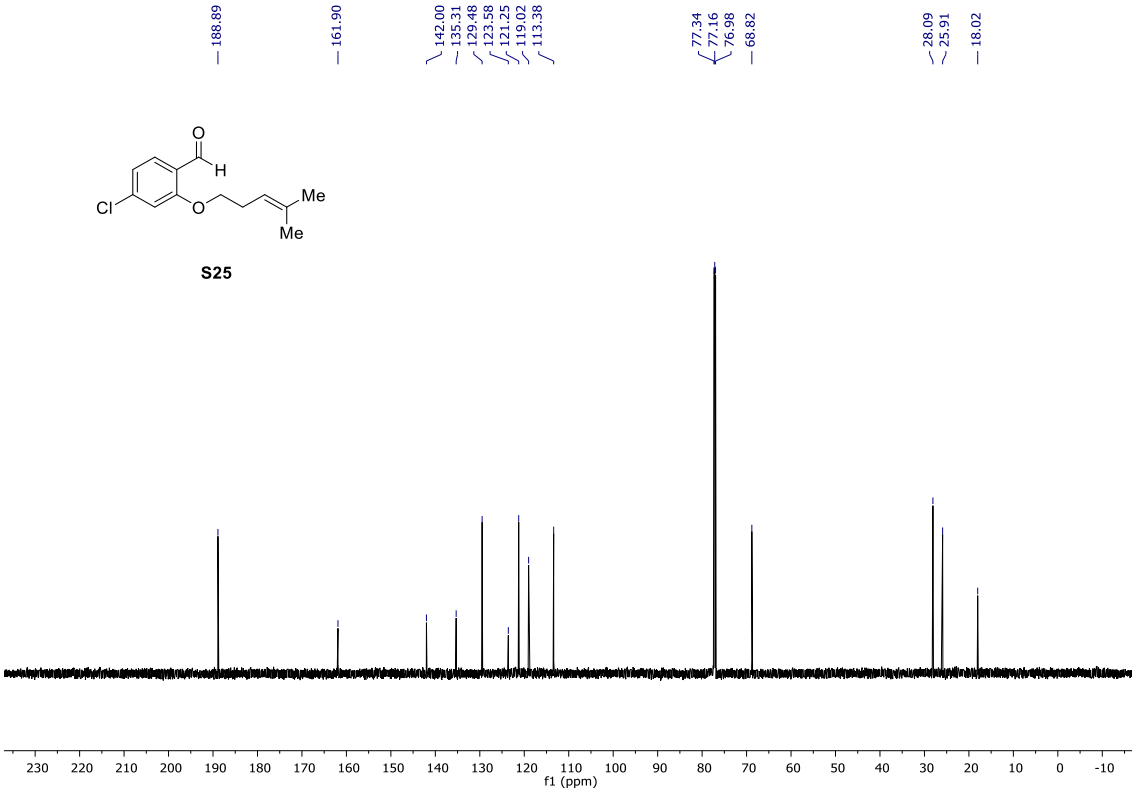
188.89
161.90
142.00
135.31
129.48
123.58
121.25
119.02
113.38
77.34
77.16
76.98
68.82
28.09
25.91
18.02
O
H
Cl
O
Me
Me
230
220
210
200
190
180
170
160
150
140
130
120
110
100
90
80
70
60
50
40
30
20
10
0
-10
f1 (ppm)

S25

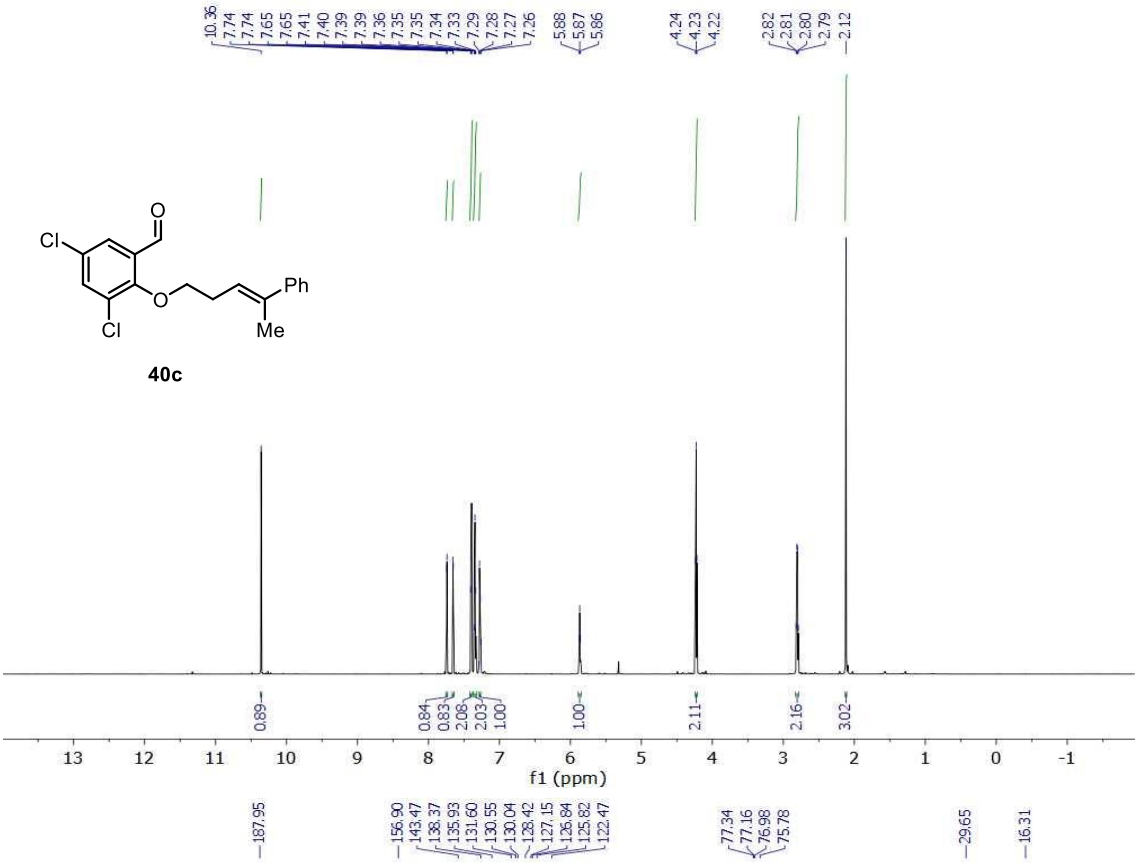
10.36
7.74
7.74
7.65
7.65
7.41
7.40
7.39
7.39
7.36
7.35
7.35
7.34
7.33
7.29
7.28
7.27
7.26
5.88
5.87
5.86
4.24
4.23
4.22
2.82
2.81
2.80
2.79
2.12
Cl
O
Cl
O
Ph
Me
40c
0.89
0.84
0.83
2.08
2.03
1.00
1.00
2.11
2.16
3.02
13 12 11 10 9 8 7 6 5 4 3 2 1 0 -1
f1 (ppm)

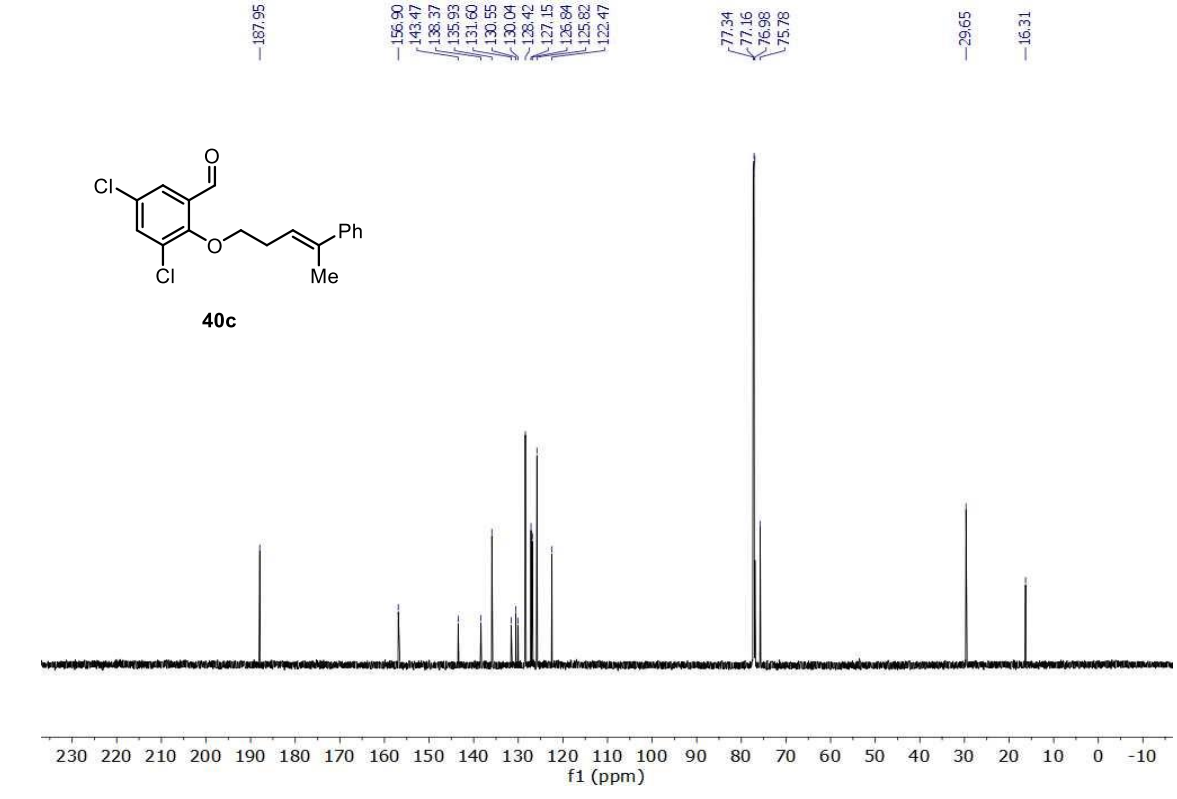
187.95
156.90
143.47
138.37
135.93
131.60
130.55
130.04
128.42
127.15
126.84
125.82
122.47
77.34
77.16
76.98
75.78
29.65
16.31
Cl
O
Cl
O
Ph
Me
40c
230 220 210 200 190 180 170 160 150 140 130 120 110 100 90 80 70 60 50 40 30 20 10 0 -10
f1 (ppm)

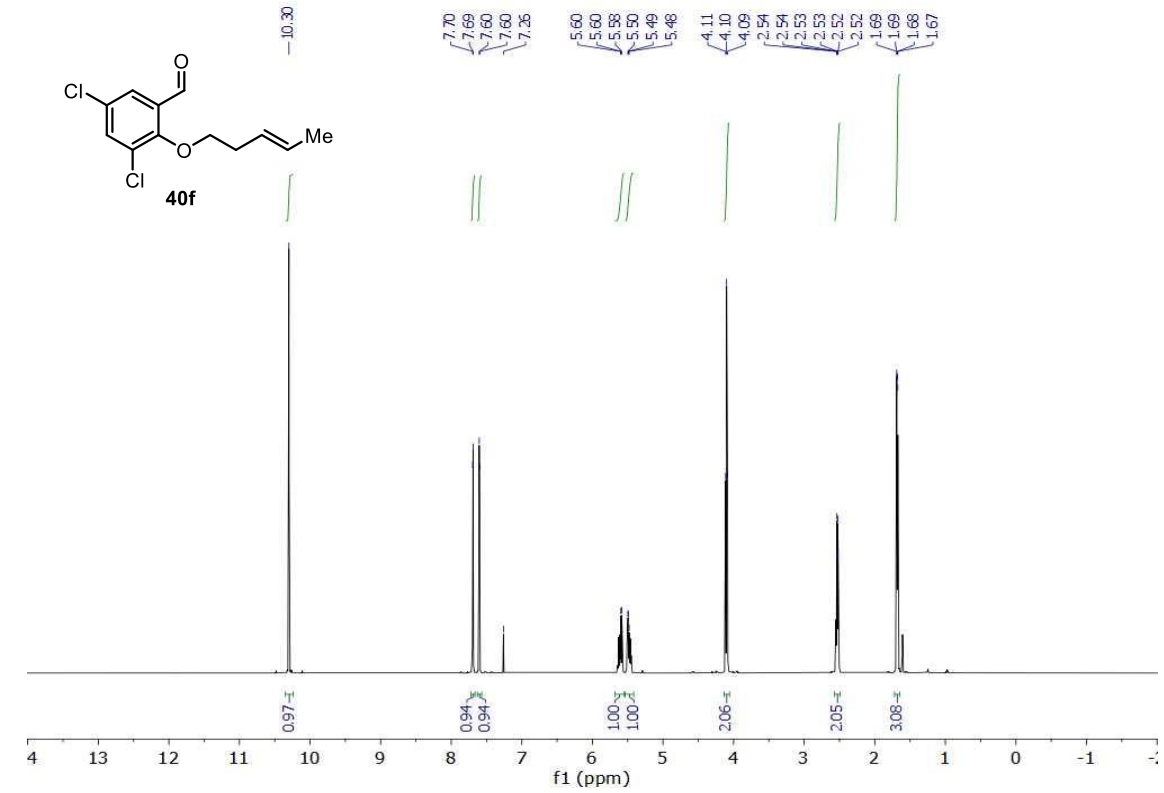
10.30
7.70
7.69
7.60
7.60
7.26
5.60
5.60
5.58
5.50
5.49
5.48
4.11
4.10
4.09
2.54
2.54
2.53
2.53
2.52
2.52
1.69
1.69
1.68
1.67
Cl
O
Me
O
Cl
40f
0.97
0.94
0.94
1.00
1.00
2.06
2.05
3.08
f1 (ppm)

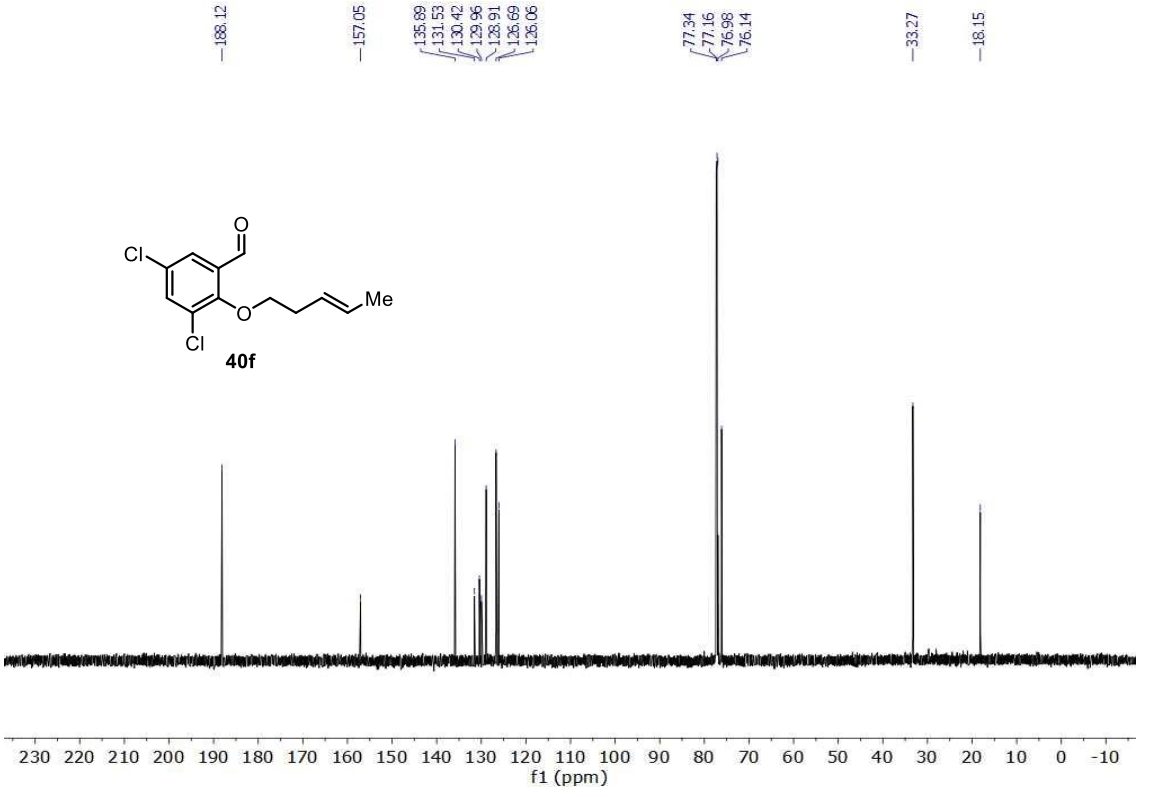
188.12
157.05
135.89
131.53
130.42
129.96
128.91
126.69
126.06
77.34
77.16
76.98
76.14
33.27
18.15
Cl
O
Me
O
Cl
40f
f1 (ppm)

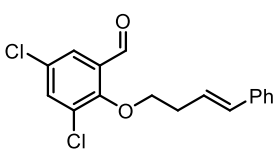
Cl
O
Ph
O
Cl

40b

f1 (ppm)

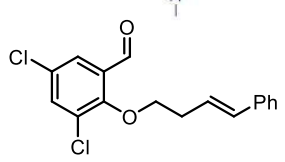
Cl
O
Ph
O
Cl

40b

187.86
156.89
144.98
142.21
139.68
135.90
131.54
130.54
130.01
129.86
128.51
128.34
127.47
127.37
126.81
123.77
77.41
77.36
77.16
76.91
75.99
30.61
f1 (ppm)

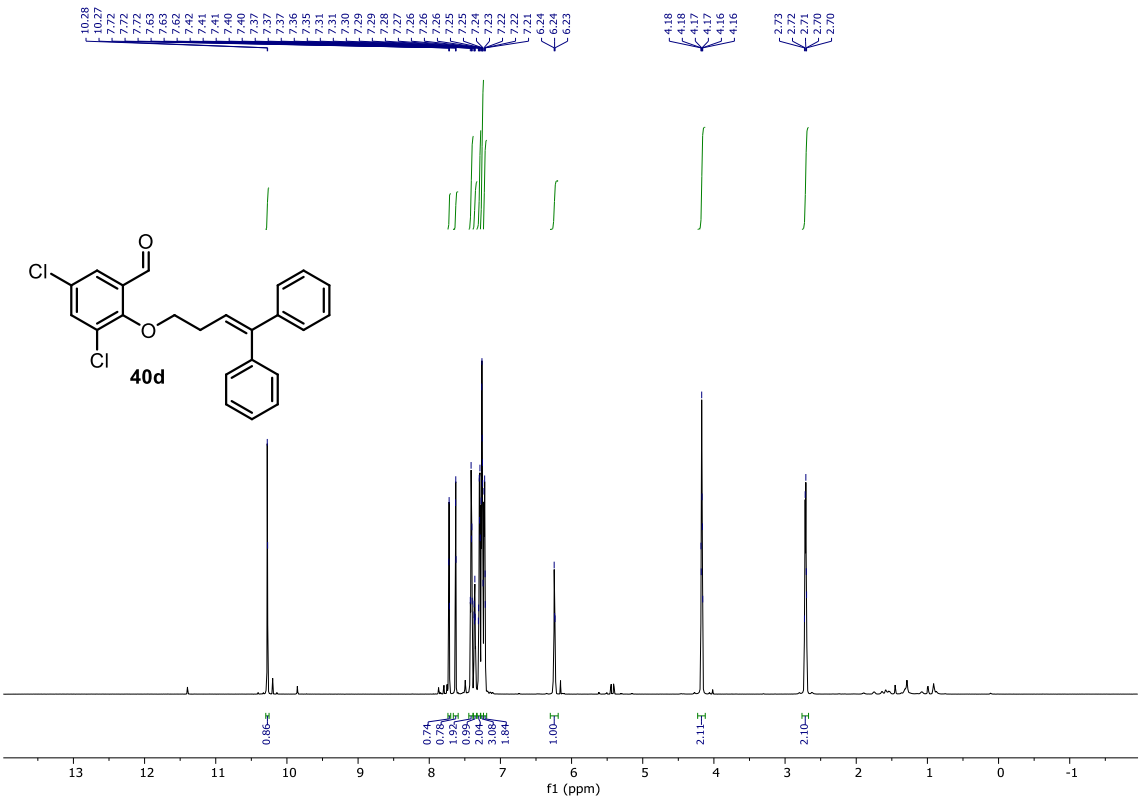
10.28
10.27
7.72
7.72
7.72
7.72
7.63
7.63
7.62
7.42
7.41
7.41
7.40
7.40
7.37
7.37
7.37
7.36
7.35
7.31
7.31
7.30
7.29
7.29
7.28
7.27
7.26
7.26
7.26
7.25
7.25
7.24
7.23
7.22
7.22
7.21
6.24
6.24
6.23
4.18
4.18
4.17
4.17
4.16
4.16
2.73
2.72
2.71
2.70
2.70
Cl
O
O
Cl
40d
0.86
0.74
0.78
1.92
0.99
2.04
3.08
1.84
1.00
2.11
2.10
f1 (ppm)

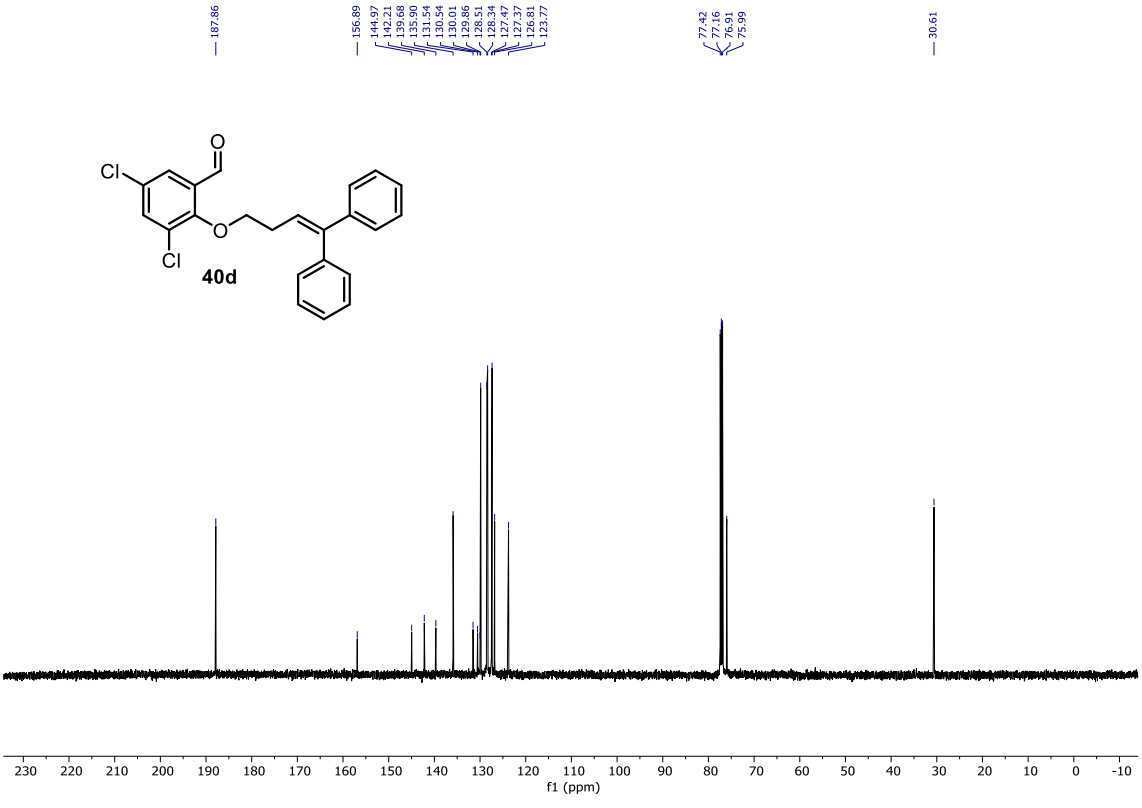
187.86
156.89
144.97
142.21
139.68
135.90
131.54
130.54
130.01
129.86
128.51
128.34
127.47
127.37
126.81
123.77
77.42
77.16
76.91
75.99
30.61
Cl
O
O
Cl
40d
f1 (ppm)

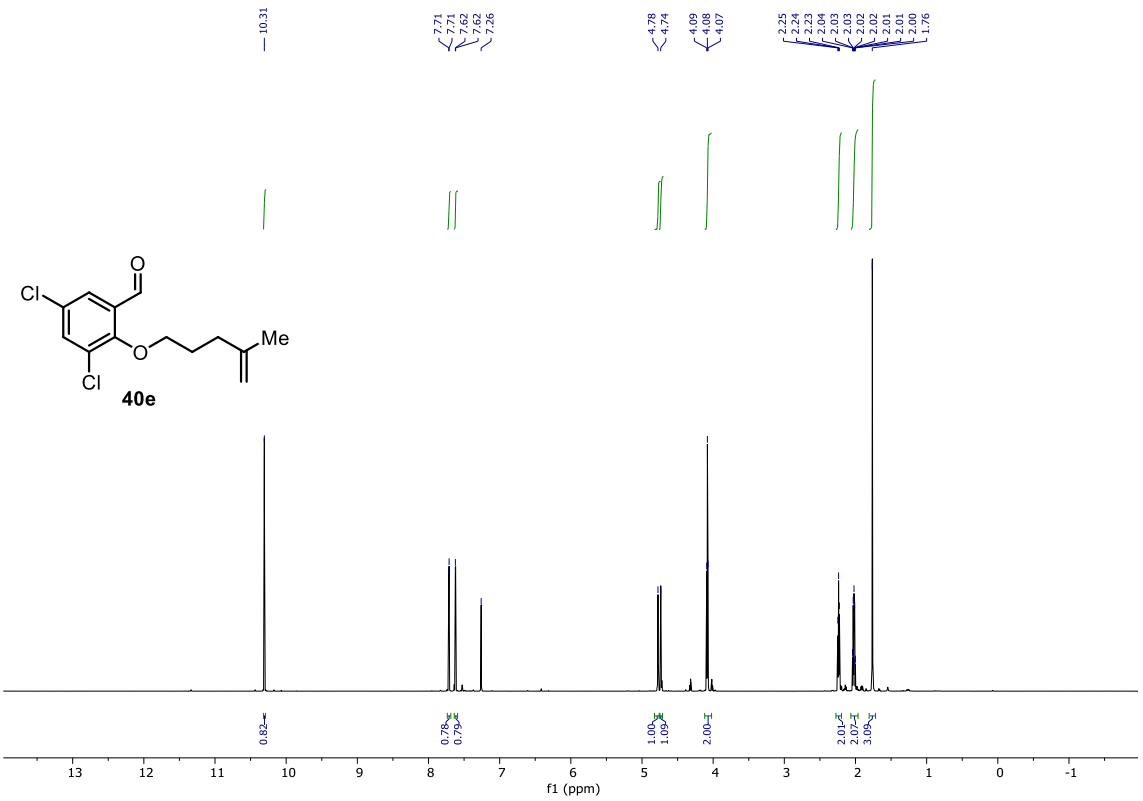
10.31
7.71
7.71
7.62
7.62
7.26
4.78
4.74
4.09
4.08
4.07
2.25
2.24
2.23
2.04
2.03
2.03
2.02
2.01
2.01
2.00
1.76
O
Cl
Me
O
Cl
40e
0.82
0.78
0.79
1.00
1.09
2.00
2.01
2.07
3.09
13
12
11
10
9
8
7
6
5
4
3
2
1
0
-1
f1 (ppm)

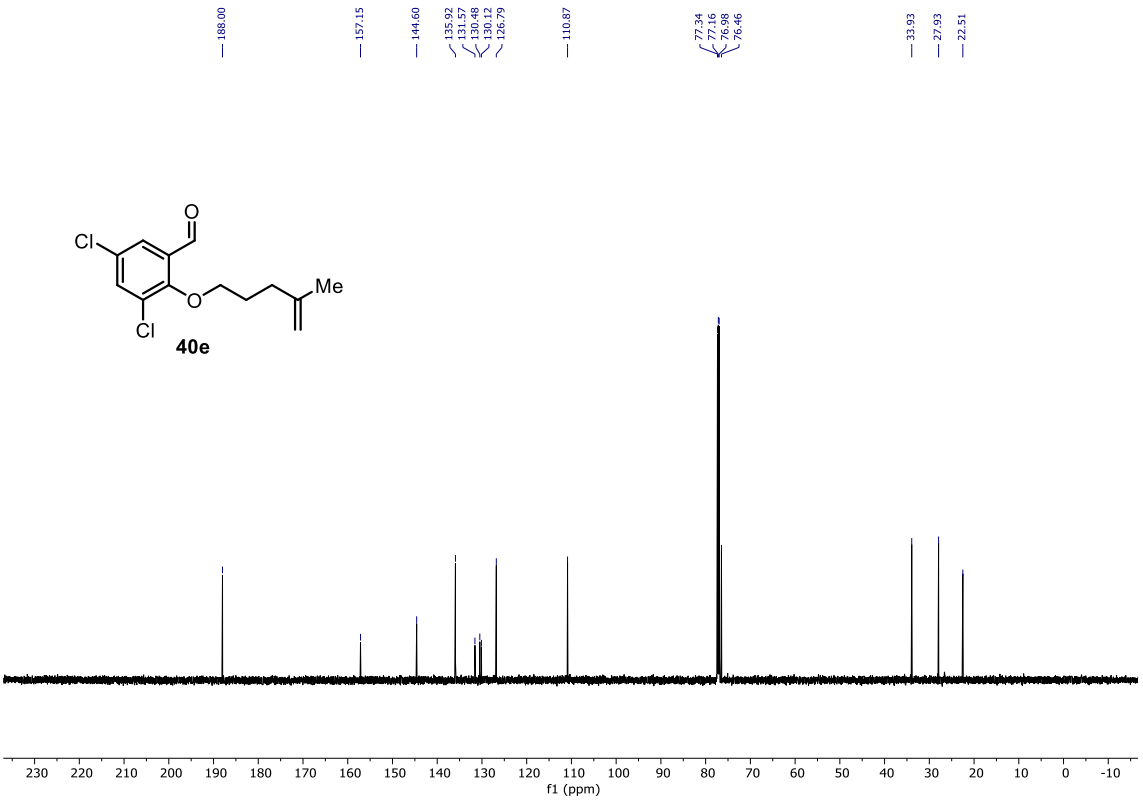
188.00
157.15
144.60
135.92
131.57
130.48
130.12
126.79
110.87
77.34
77.16
76.98
76.46
33.93
27.93
22.51
O
Cl
Me
O
Cl
40e
230
220
210
200
190
180
170
160
150
140
130
120
110
100
90
80
70
60
50
40
30
20
10
0
-10
f1 (ppm)

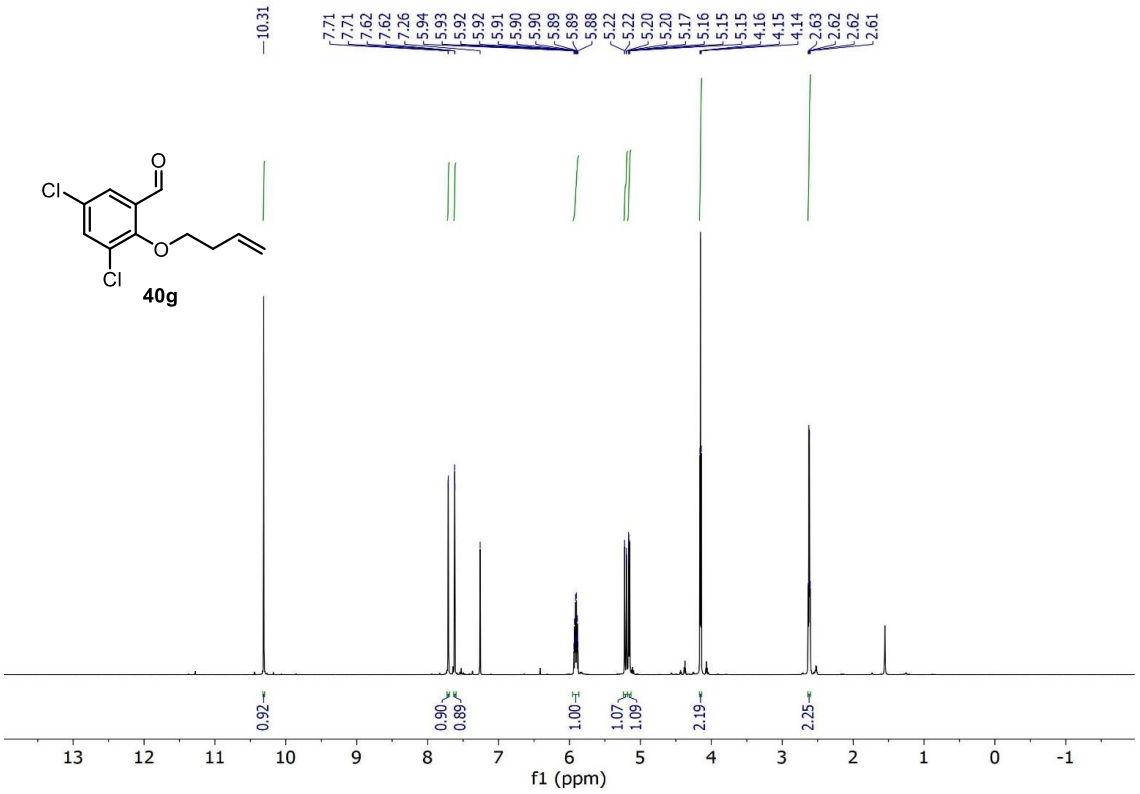
10.31
7.71
7.71
7.62
7.62
7.26
5.94
5.93
5.92
5.92
5.91
5.90
5.90
5.89
5.89
5.88
5.22
5.22
5.20
5.20
5.17
5.16
5.15
5.15
4.16
4.15
4.14
2.63
2.62
2.62
2.61
Cl
O
O
Cl
40g
0.92
0.90
0.89
1.00
1.07
1.09
2.19
2.25
13 12 11 10 9 8 7 6 5 4 3 2 1 0 -1
f1 (ppm)

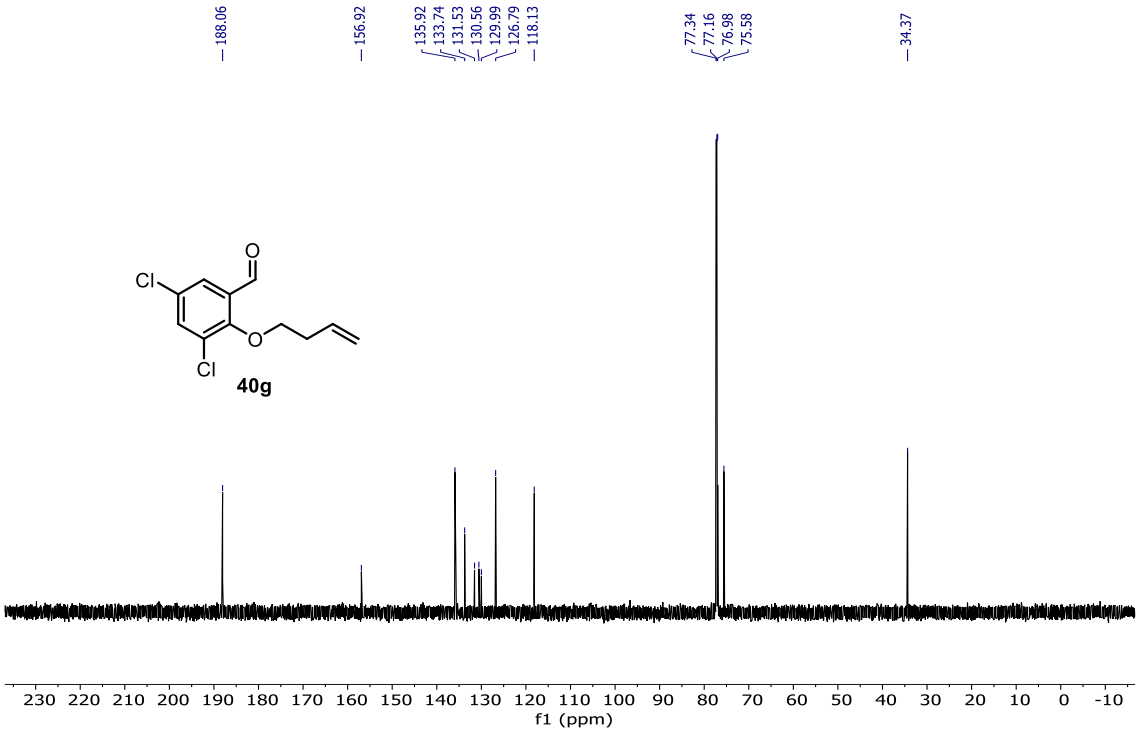
188.06
156.92
135.92
133.74
131.53
130.56
129.99
126.79
118.13
77.34
77.16
76.98
75.58
34.37
Cl
O
O
Cl
40g
230 220 210 200 190 180 170 160 150 140 130 120 110 100 90 80 70 60 50 40 30 20 10 0 -10
f1 (ppm)

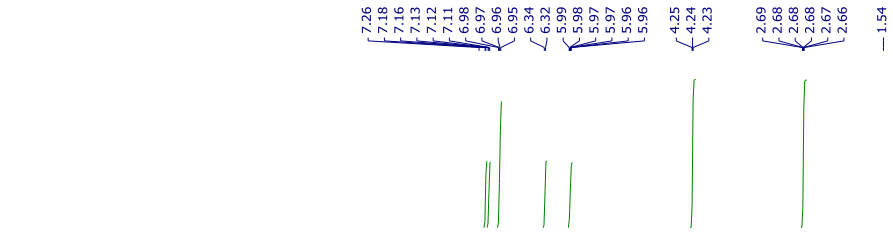
7.26
7.18
7.16
7.13
7.12
7.11
6.98
6.97
6.96
6.95
6.34
6.32
5.99
5.98
5.97
5.97
5.96
5.96
4.25
4.24
4.23
2.69
2.68
2.68
2.68
2.67
2.66
1.54

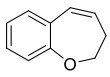

18

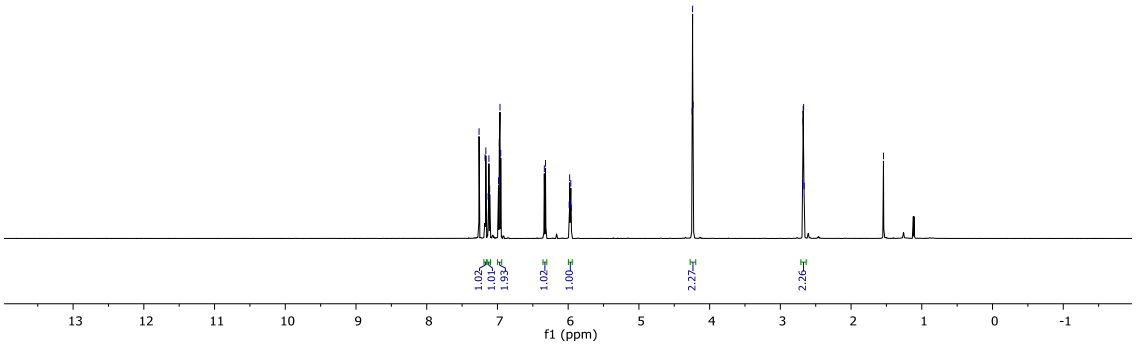
1.02
1.01
1.93
1.02
1.00
2.27
2.26
13
12
11
10
9
8
7
6
5
4
3
2
1
0
-1
f1 (ppm)

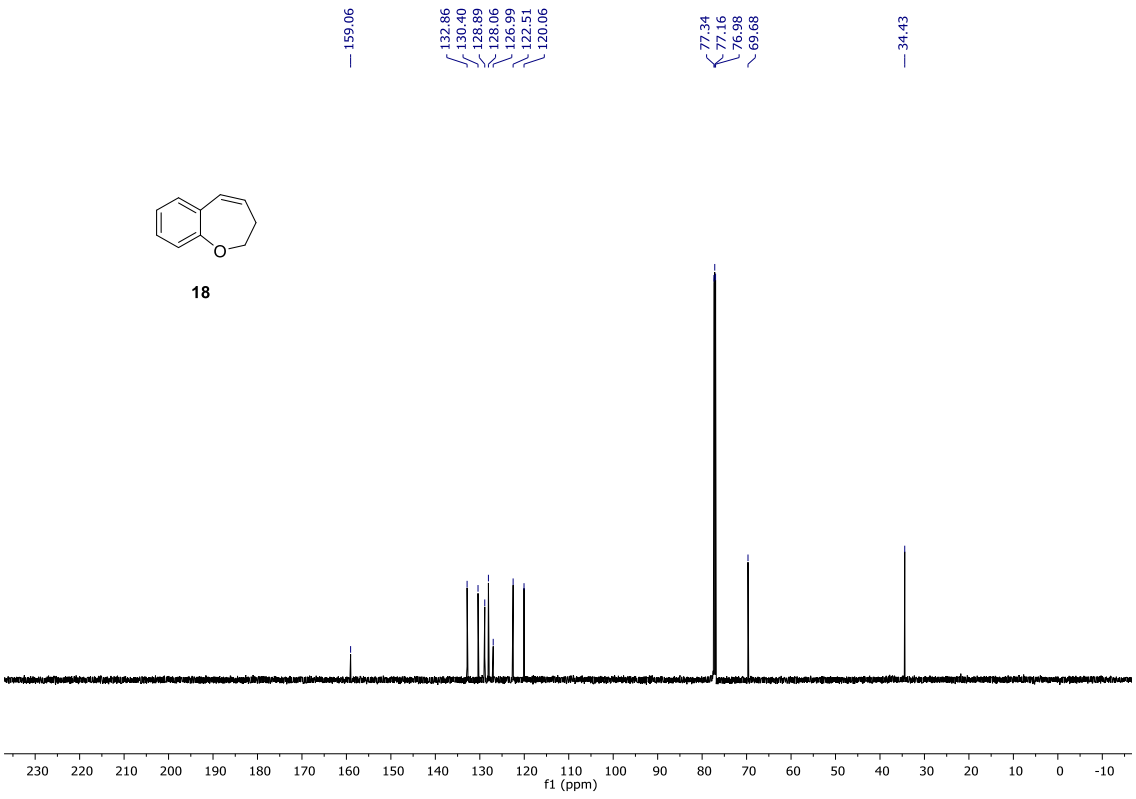
159.06
132.86
130.40
128.89
128.06
126.99
122.51
120.06
77.34
77.16
76.98
69.68
34.43
230
220
210
200
190
180
170
160
150
140
130
120
110
100
90
80
70
60
50
40
30
20
10
0
-10
f1 (ppm)

18

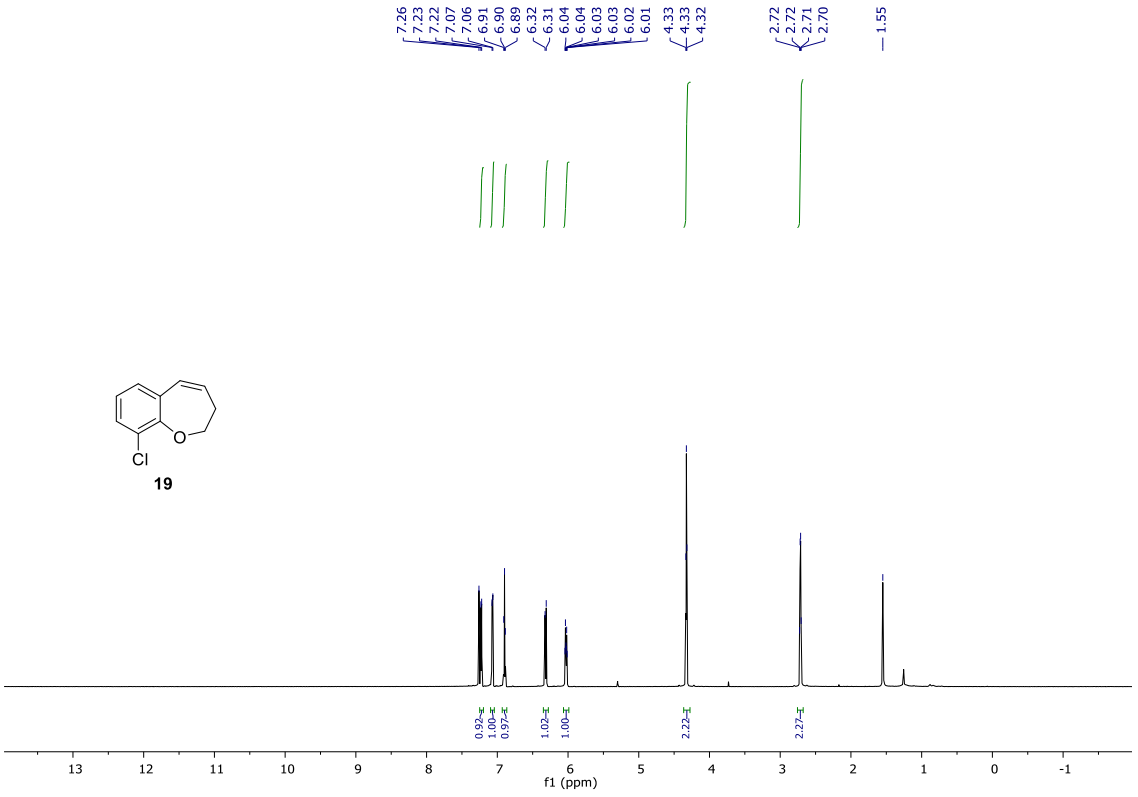
7.26
7.23
7.22
7.07
7.06
6.91
6.90
6.89
6.32
6.31
6.04
6.04
6.03
6.03
6.02
6.01
4.33
4.33
4.32
2.72
2.72
2.71
2.70
1.55
Cl
O
19
0.92
1.00
0.97
1.02
1.00
2.22
2.27
13
12
11
10
9
8
7
6
5
4
3
2
1
0
-1
f1 (ppm)

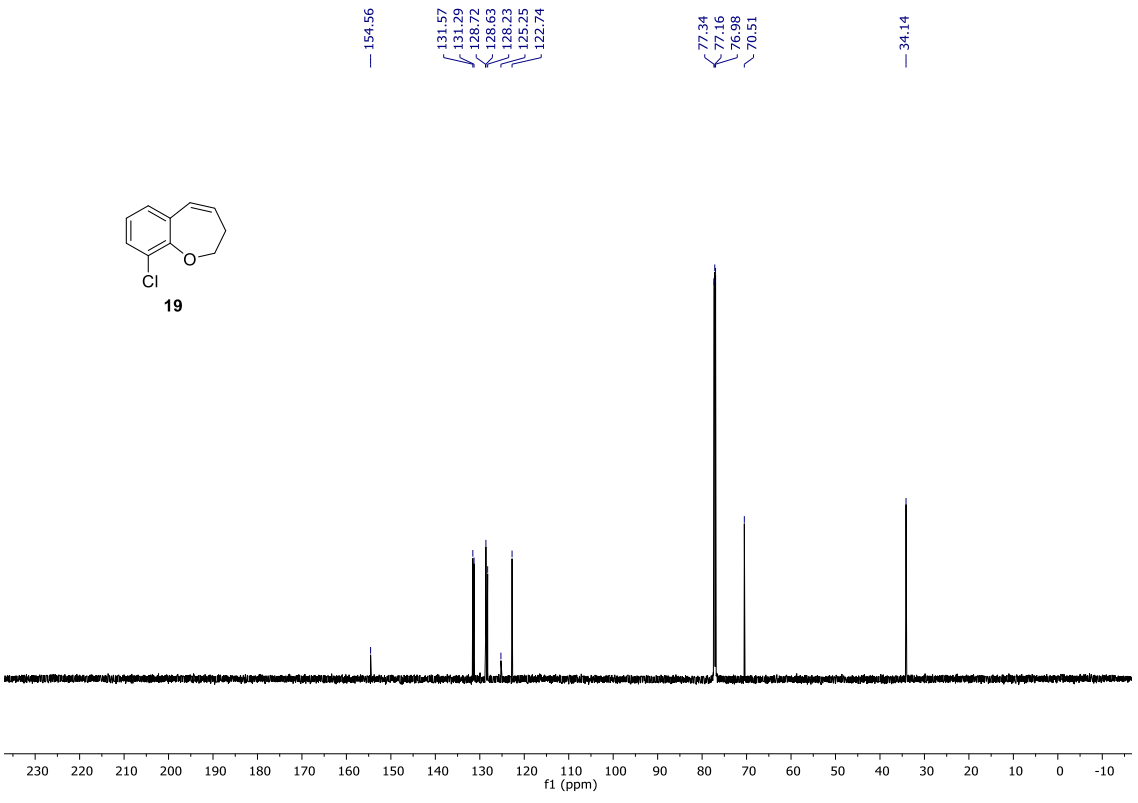
154.56
131.57
131.29
128.72
128.63
128.23
125.25
122.74
77.34
77.16
76.98
70.51
34.14
Cl
O
19
230
220
210
200
190
180
170
160
150
140
130
120
110
100
90
80
70
60
50
40
30
20
10
0
-10
f1 (ppm)

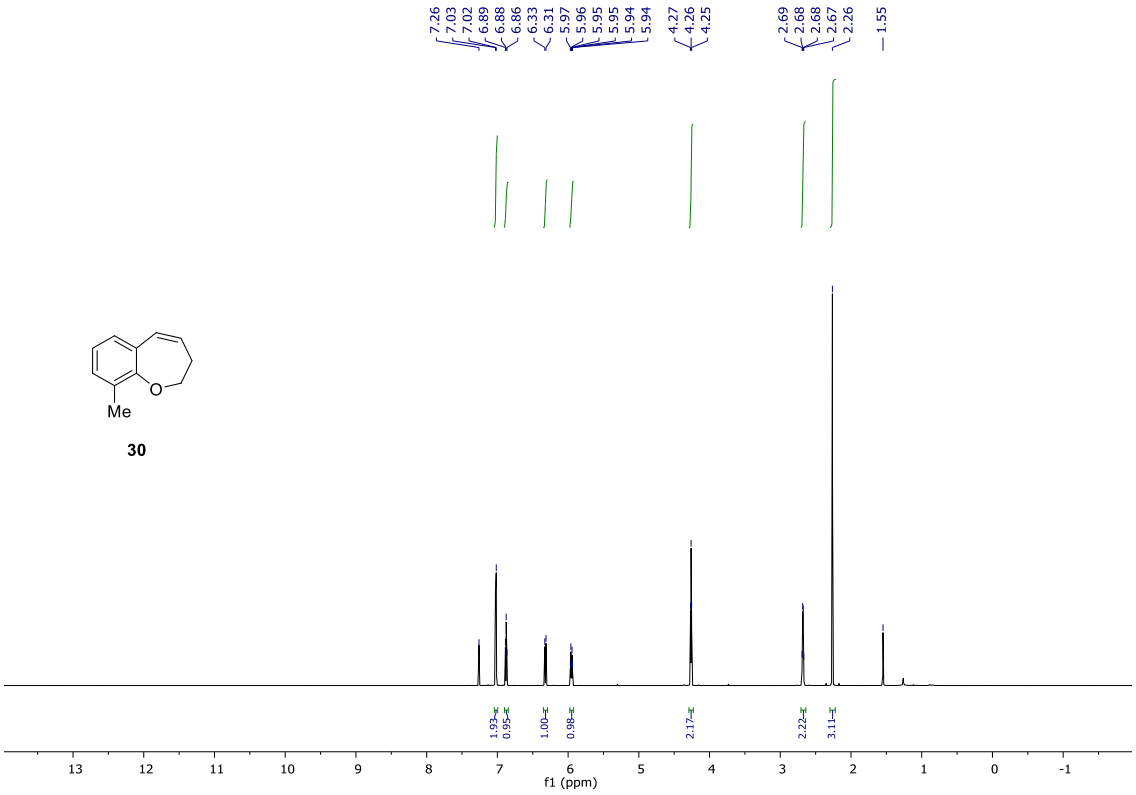
7.26
7.03
7.02
6.89
6.88
6.86
6.33
6.31
5.97
5.96
5.95
5.95
5.94
5.94
4.27
4.26
4.25
2.69
2.68
2.68
2.67
2.26
1.55
O
Me
1.93
0.95
1.00
0.98
2.17
2.22
3.11
f1 (ppm)

30

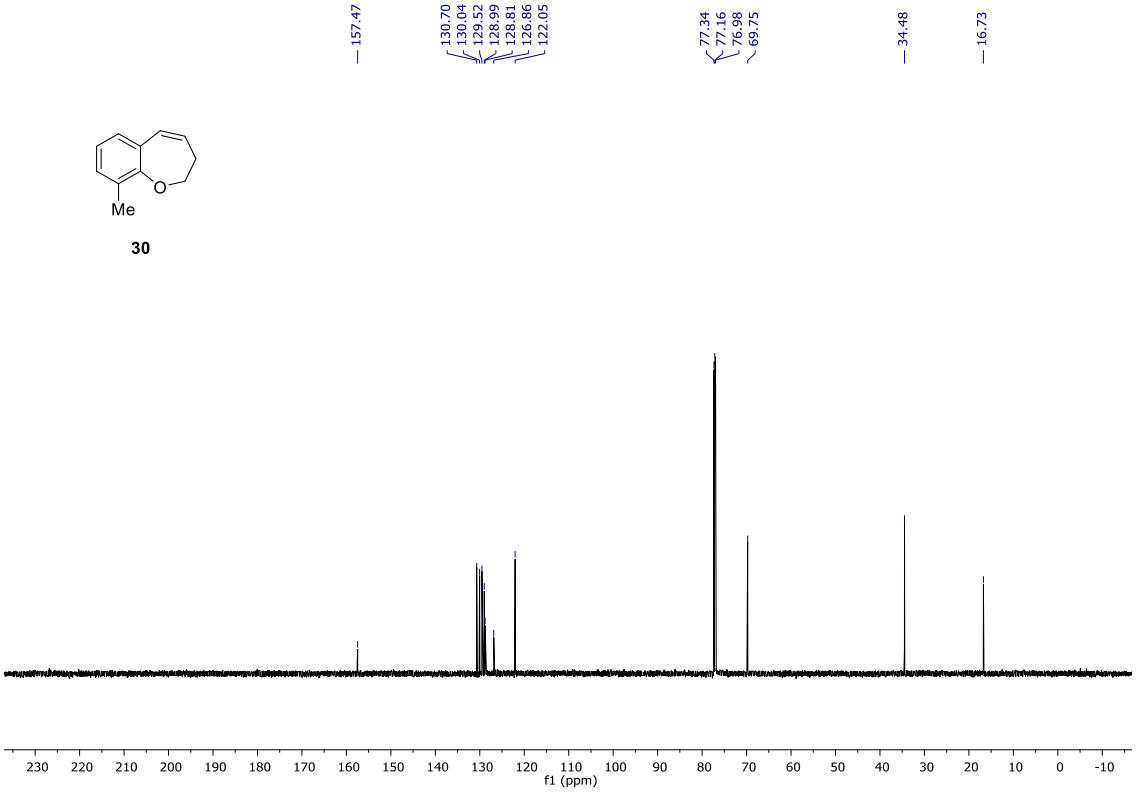
157.47
130.70
130.04
129.52
128.99
128.81
126.86
122.05
77.34
77.16
76.98
69.75
34.48
16.73
O
Me
f1 (ppm)

30

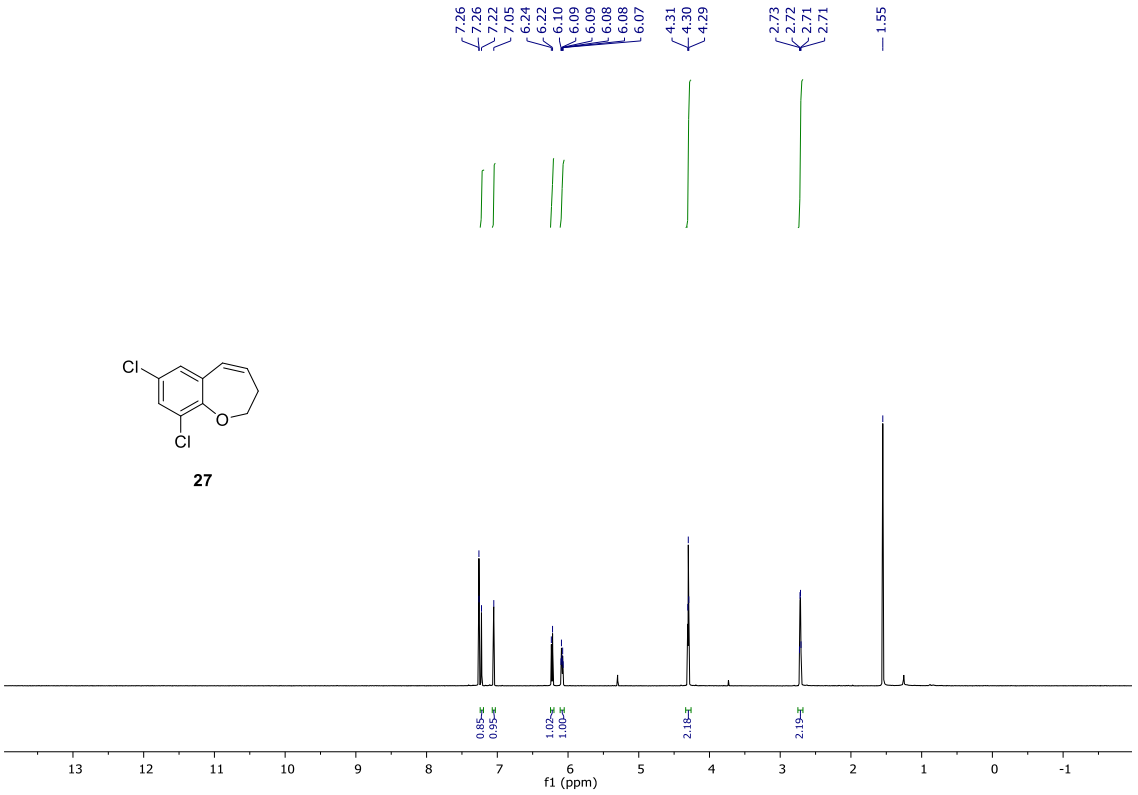
7.26
7.26
7.22
7.05
6.24
6.22
6.10
6.09
6.09
6.08
6.08
6.07
4.31
4.30
4.29
2.73
2.72
2.71
2.71
1.55
Cl
O
Cl
0.85
0.95
1.02
1.00
2.18
2.19
13
12
11
10
9
8
7
6
5
4
3
2
1
0
-1
f1 (ppm)

27

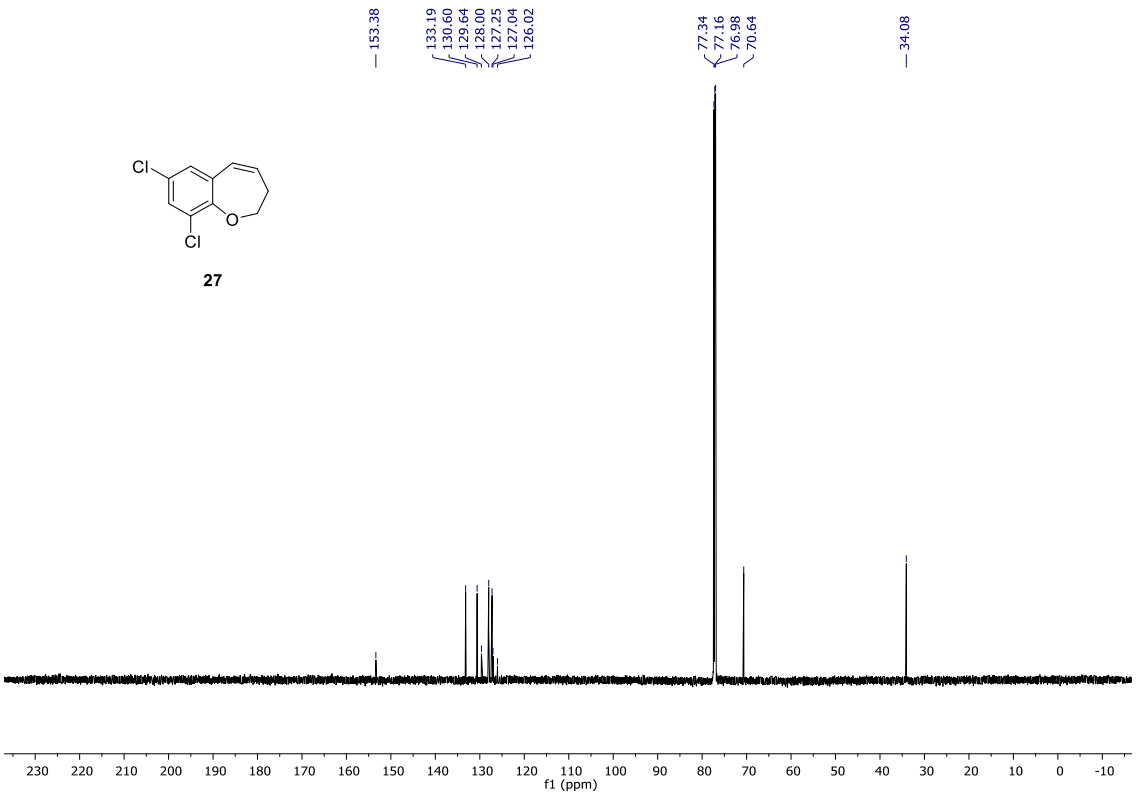
153.38
133.19
130.60
129.64
128.00
127.25
127.04
126.02
77.34
77.16
76.98
70.64
34.08
Cl
O
Cl
230
220
210
200
190
180
170
160
150
140
130
120
110
100
90
80
70
60
50
40
30
20
10
0
-10
f1 (ppm)

27

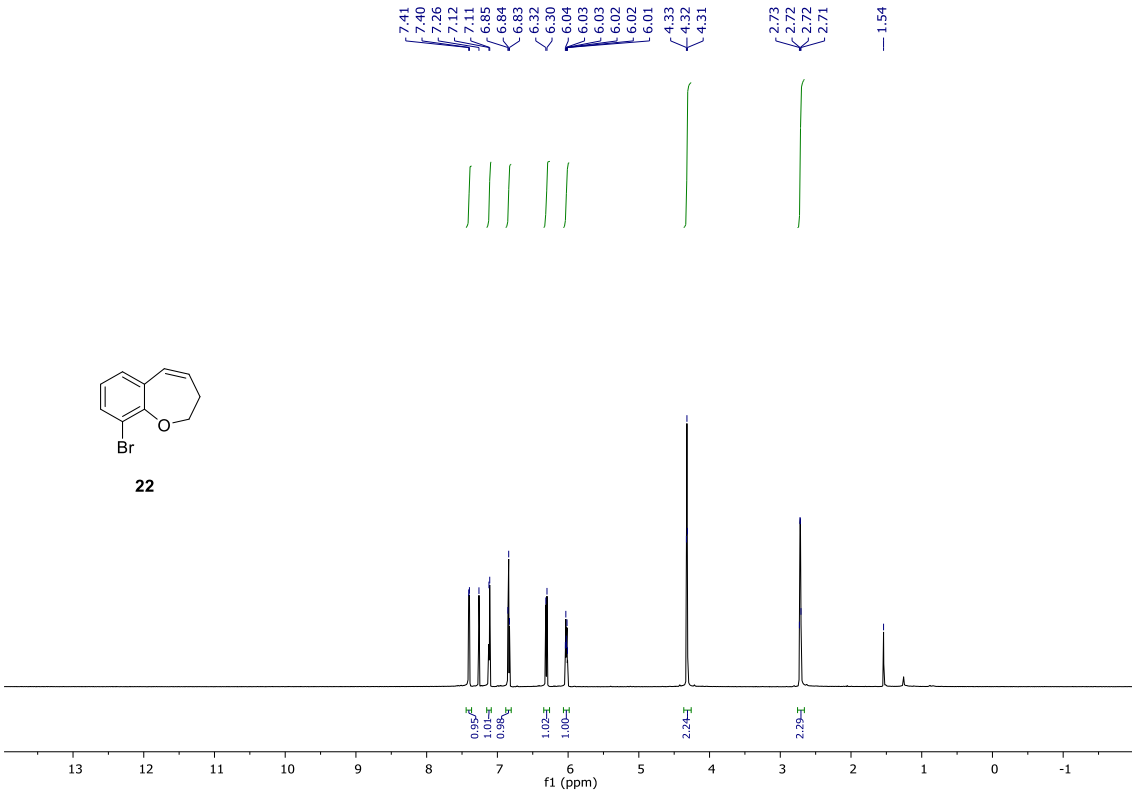
7.41
7.40
7.26
7.12
7.11
6.85
6.84
6.83
6.32
6.30
6.04
6.03
6.03
6.02
6.02
6.01
4.33
4.32
4.31
2.73
2.72
2.72
2.71
1.54
Br
O
22
0.95
1.01
0.98
1.02
1.00
2.24
2.29
f1 (ppm)

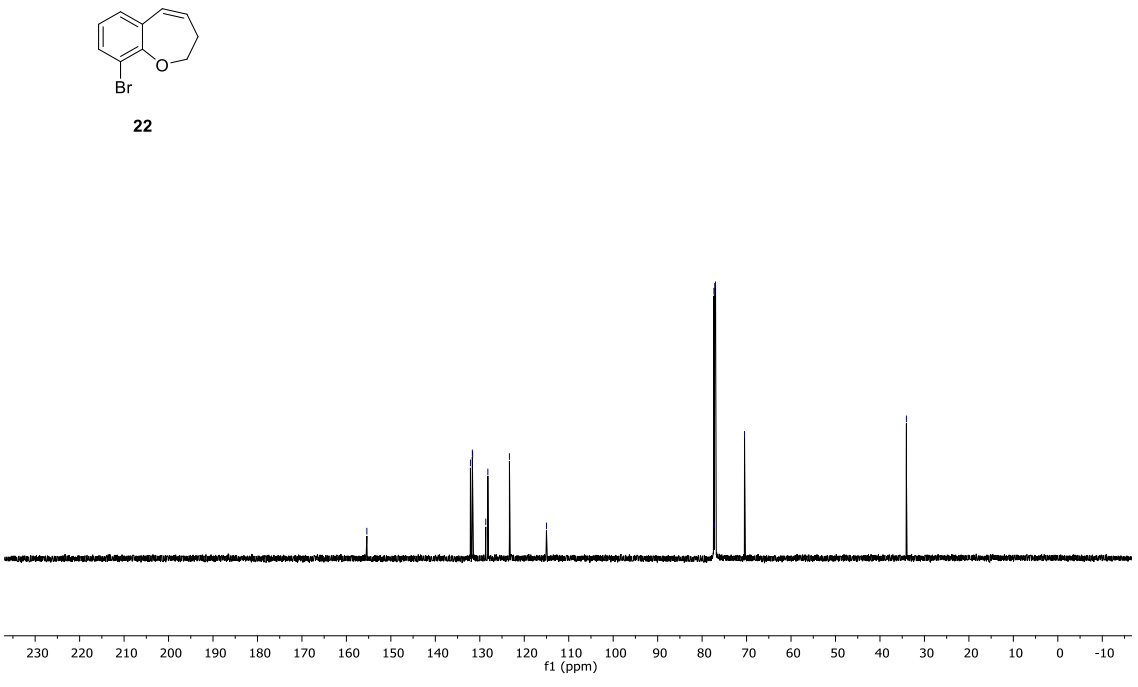
155.40
132.11
131.67
131.61
128.66
128.19
123.33
115.01
77.34
77.30
77.16
76.98
70.46
34.05
Br
O
22
f1 (ppm)

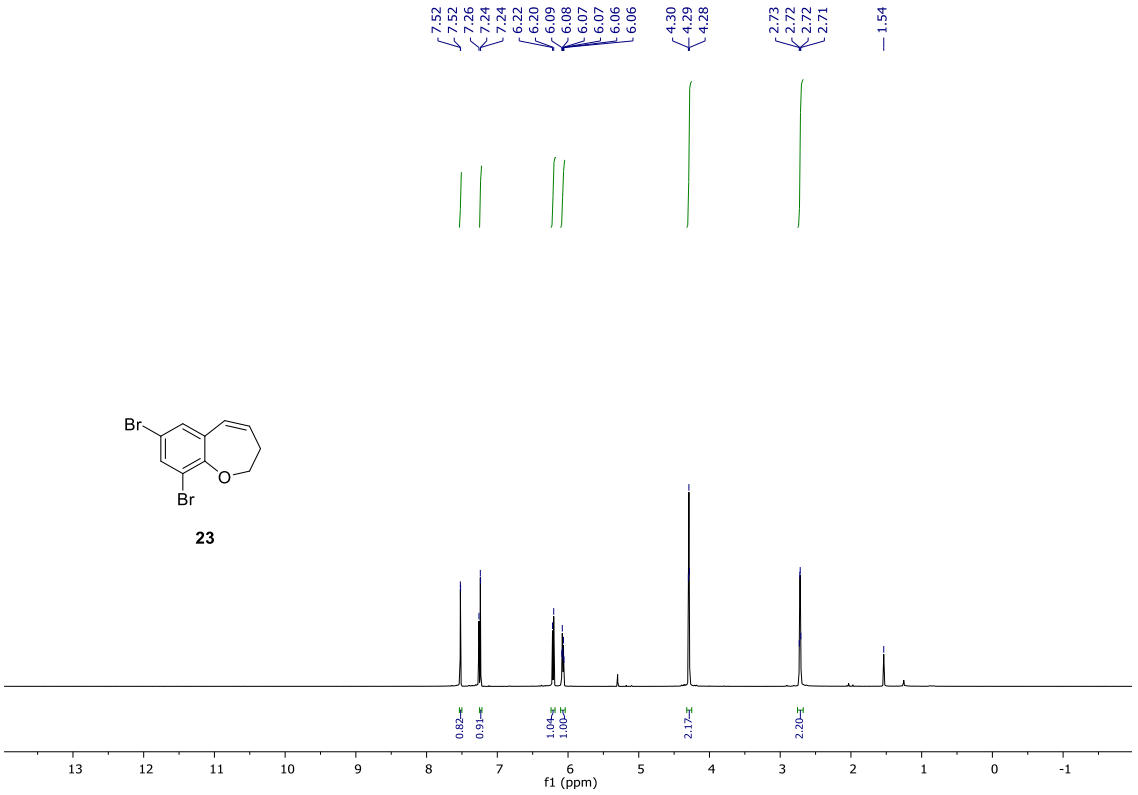
7.52
7.52
7.26
7.24
7.24
6.22
6.20
6.09
6.08
6.07
6.07
6.06
6.06
4.30
4.29
4.28
2.73
2.72
2.72
2.71
1.54
Br
O
Br
23
0.82
0.91
1.04
1.00
2.17
2.20
13
12
11
10
9
8
7
6
5
4
3
2
1
0
-1
f1 (ppm)

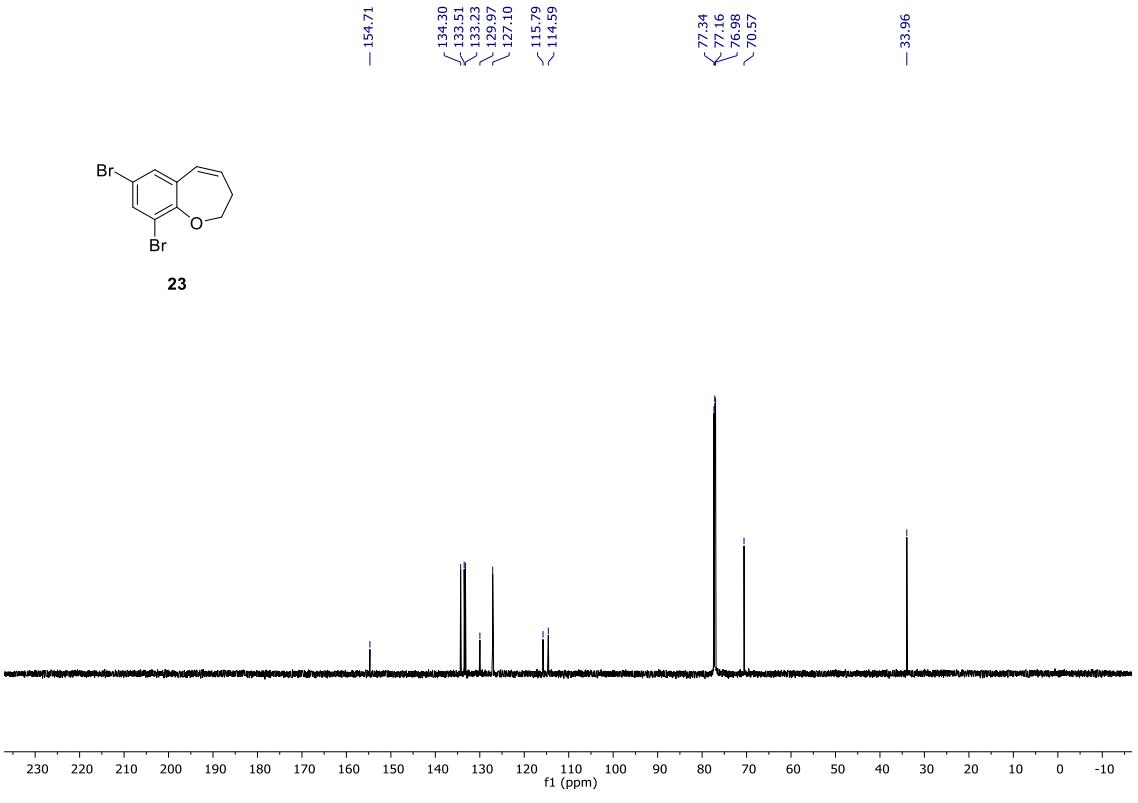
154.71
134.30
133.51
133.23
129.97
127.10
115.79
114.59
77.34
77.16
76.98
70.57
33.96
Br
O
Br
23
230
220
210
200
190
180
170
160
150
140
130
120
110
100
90
80
70
60
50
40
30
20
10
0
-10
f1 (ppm)

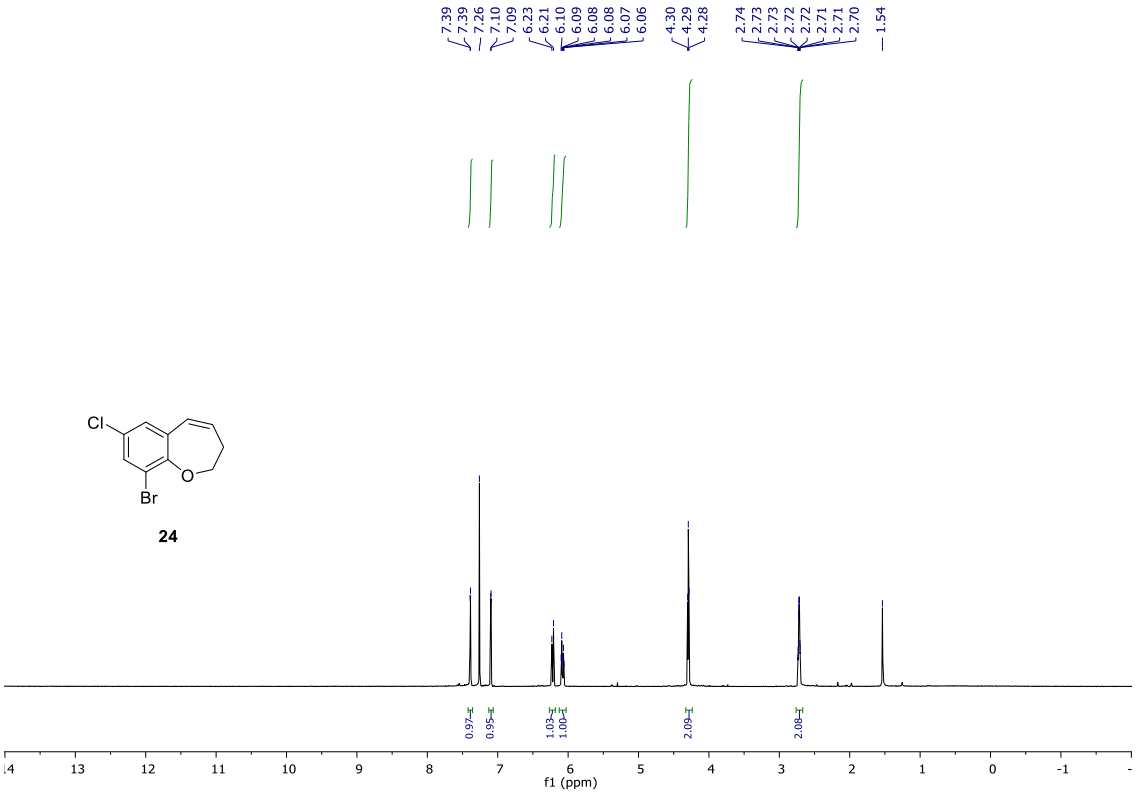
7.39
7.39
7.26
7.10
7.09
6.23
6.21
6.10
6.09
6.08
6.08
6.07
6.06
4.30
4.29
4.28
2.74
2.73
2.73
2.72
2.72
2.71
2.71
2.70
1.54
Cl
O
Br
24
0.97
0.95
1.03
1.00
2.09
2.08
f1 (ppm)

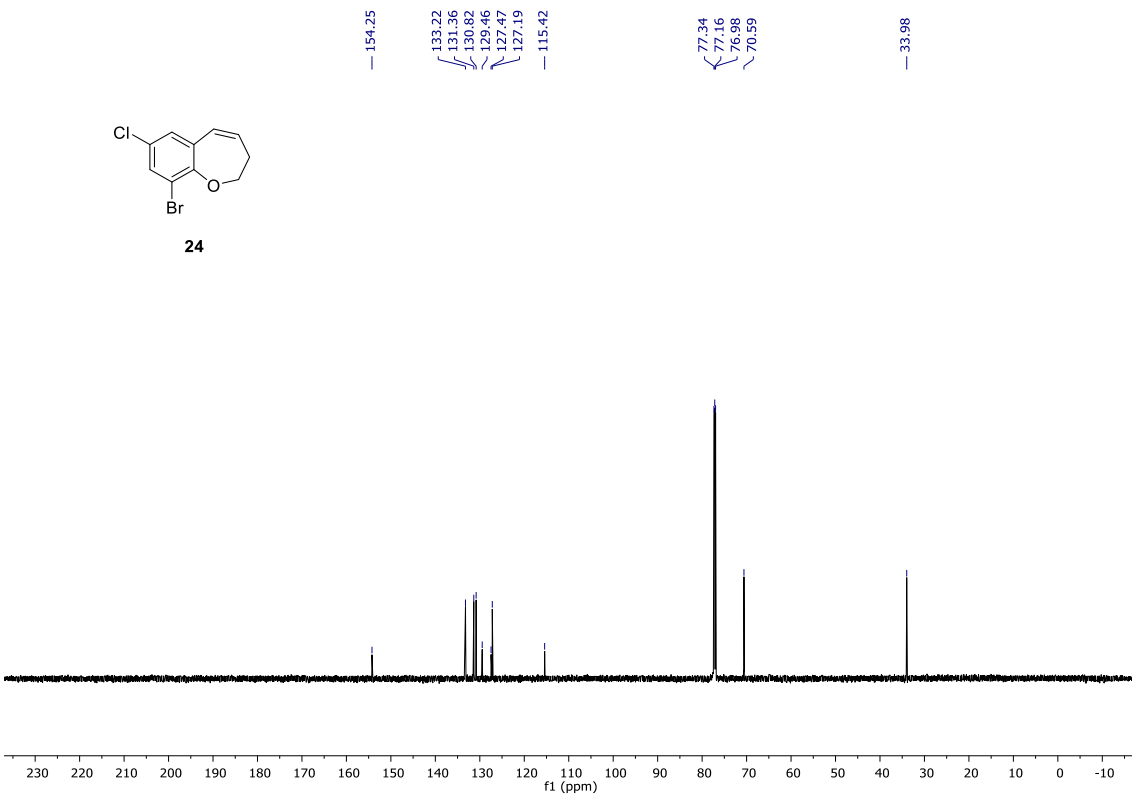
154.25
133.22
131.36
130.82
129.46
127.47
127.19
115.42
77.34
77.16
76.98
70.59
33.98
Cl
O
Br
24
f1 (ppm)

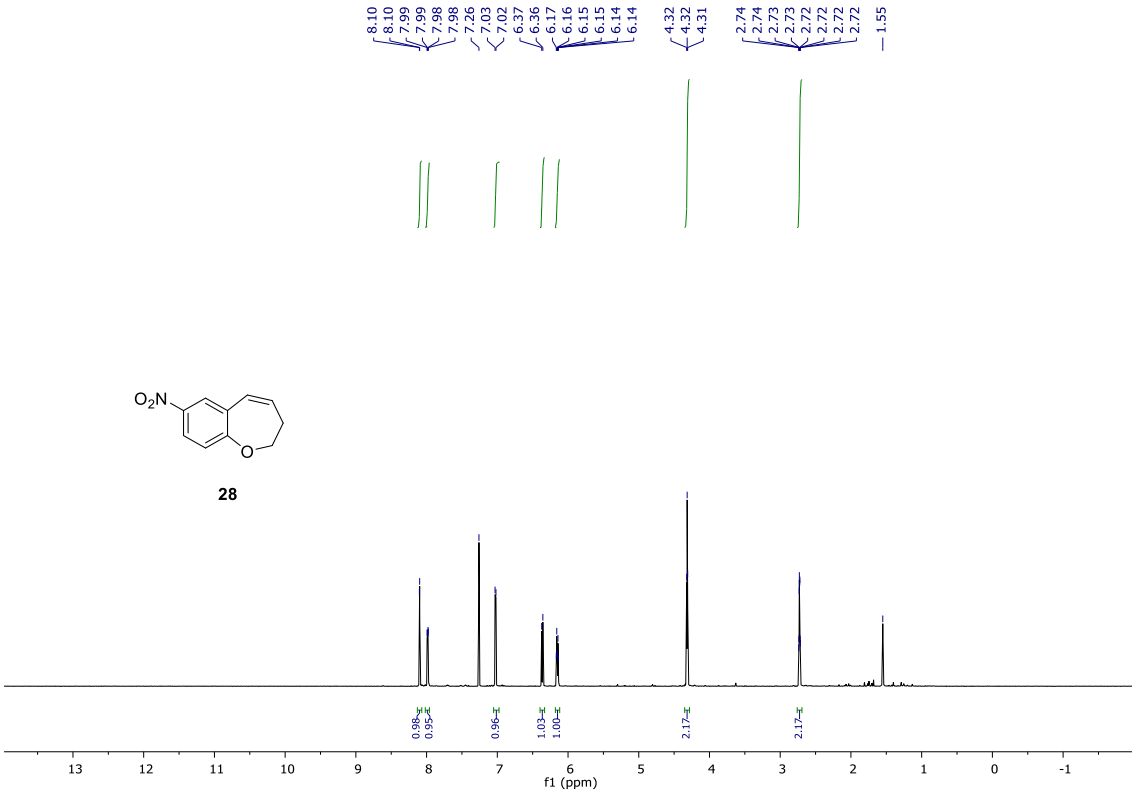
8.10
8.10
7.99
7.99
7.98
7.98
7.26
7.03
7.02
6.37
6.36
6.17
6.16
6.15
6.15
6.14
6.14
4.32
4.32
4.31
2.74
2.74
2.73
2.73
2.72
2.72
2.72
2.72
1.55
O2N
O
28
0.98
0.95
0.96
1.03
1.00
2.17
2.17
13 12 11 10 9 8 7 6 5 4 3 2 1 0 -1
f1 (ppm)

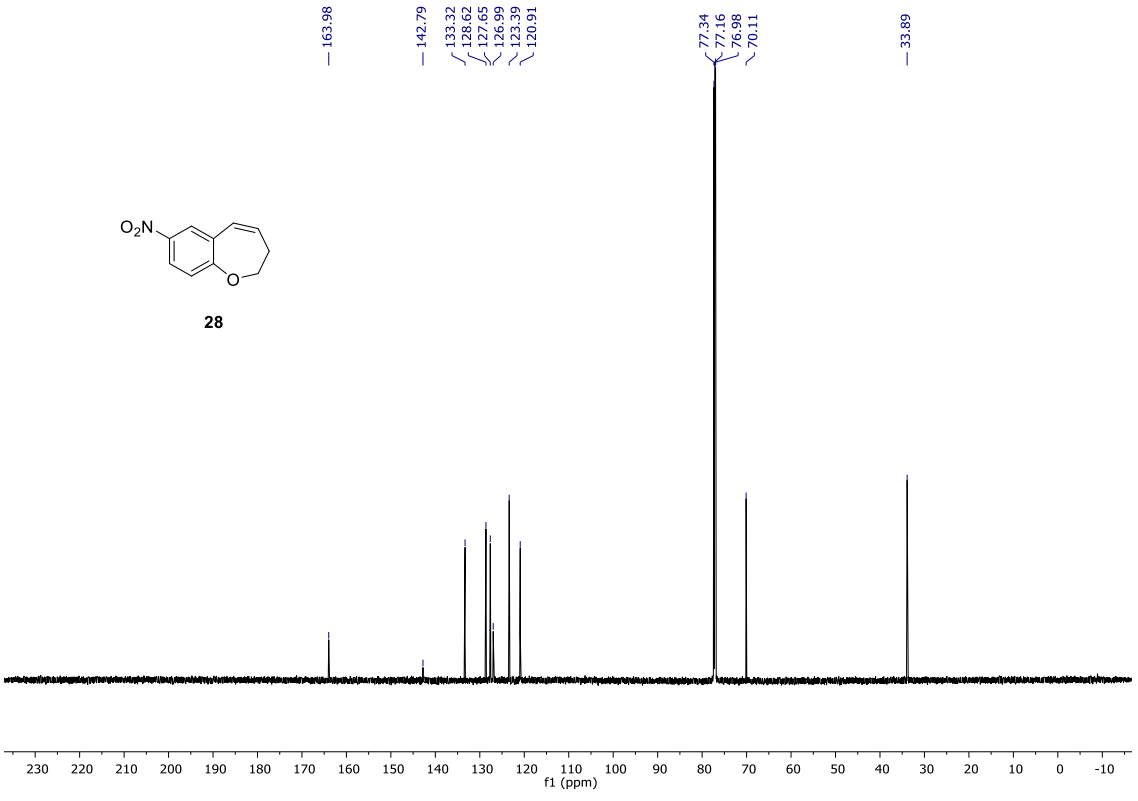
163.98
142.79
133.32
128.62
127.65
126.99
123.39
120.91
77.34
77.16
76.98
70.11
33.89
O2N
O
28
230 220 210 200 190 180 170 160 150 140 130 120 110 100 90 80 70 60 50 40 30 20 10 0 -10
f1 (ppm)

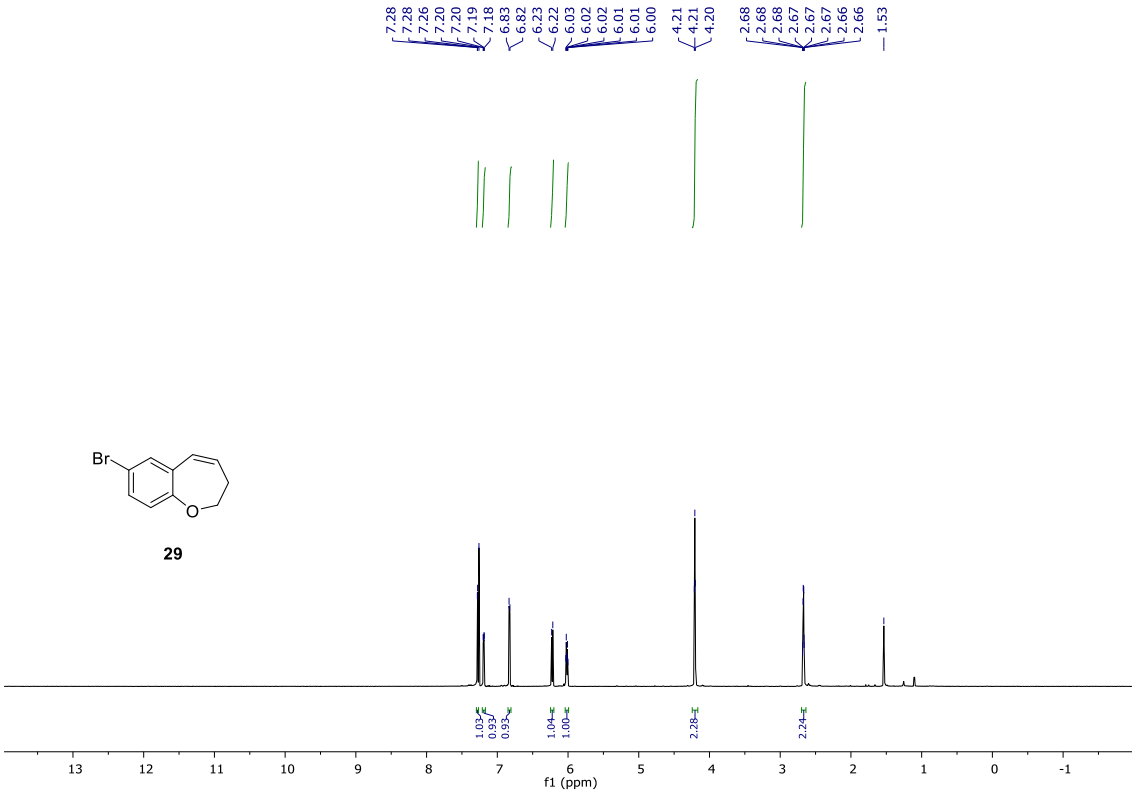
7.28
7.28
7.26
7.20
7.20
7.19
7.18
6.83
6.82
6.23
6.22
6.03
6.02
6.02
6.01
6.01
6.00
4.21
4.21
4.20
2.68
2.68
2.68
2.67
2.67
2.67
2.66
2.66
1.53
Br
O
29
1.03
0.93
0.93
1.04
1.00
2.28
2.24
13 12 11 10 9 8 7 6 5 4 3 2 1 0 -1
f1 (ppm)

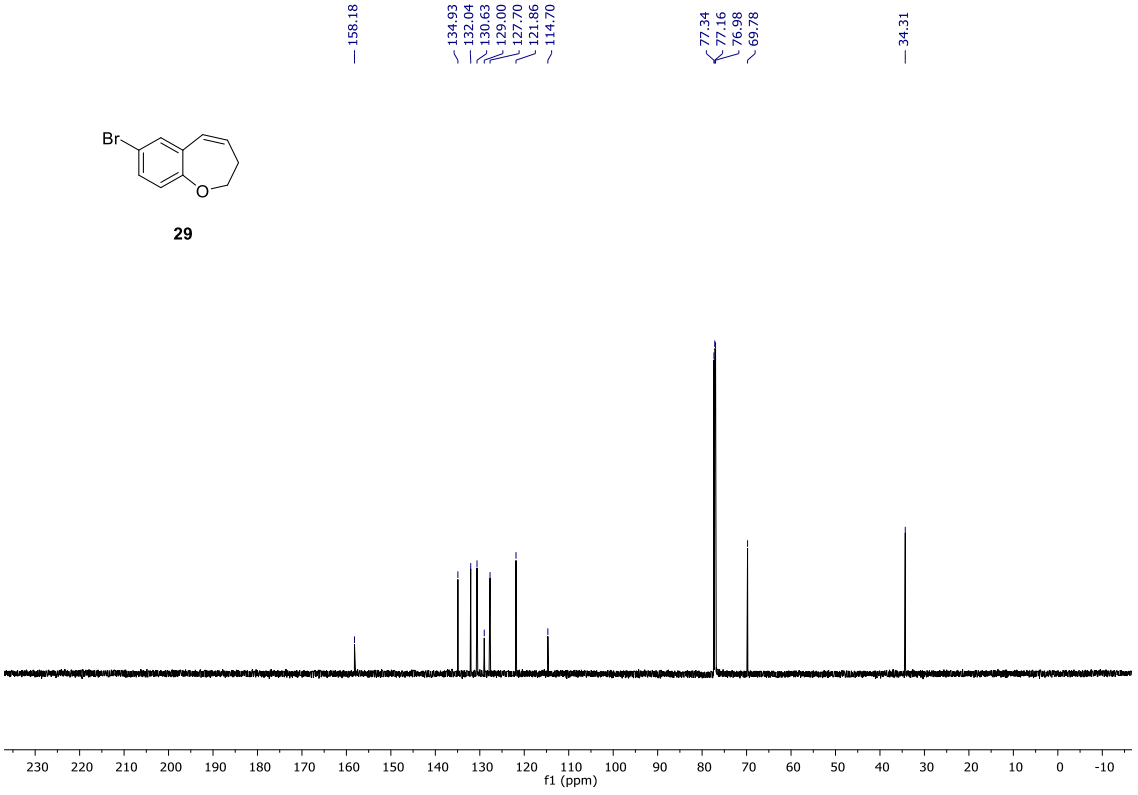
158.18
134.93
132.04
130.63
129.00
127.70
121.86
114.70
77.34
77.16
76.98
69.78
34.31
Br
O
29
230 220 210 200 190 180 170 160 150 140 130 120 110 100 90 80 70 60 50 40 30 20 10 0 -10
f1 (ppm)

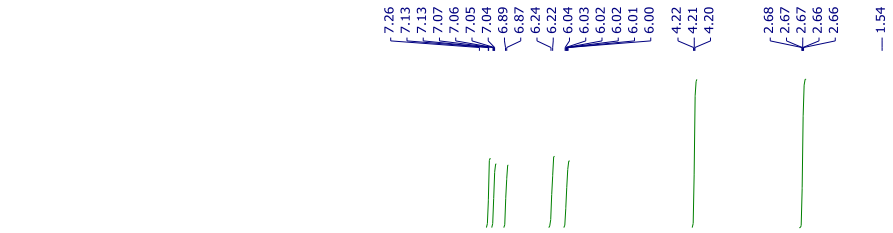
7.26
7.13
7.13
7.07
7.06
7.05
7.04
6.89
6.87
6.24
6.22
6.04
6.03
6.02
6.02
6.01
6.00
4.22
4.21
4.20
2.68
2.67
2.67
2.66
2.66
1.54

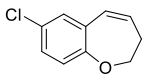
Cl
O

26

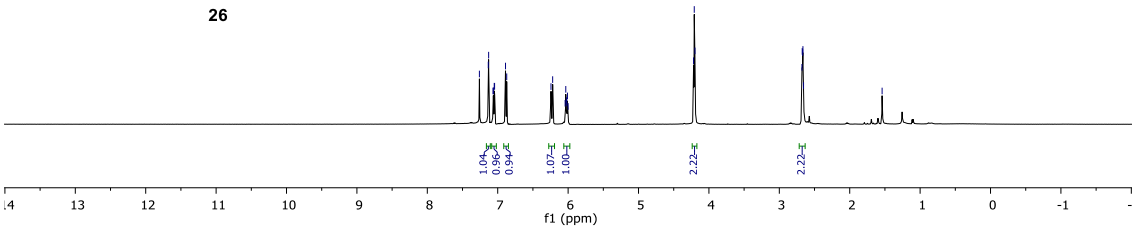
1.04
0.98
0.94
1.07
1.00
2.22
2.22
f1 (ppm)


157.68
132.02
131.97
128.49
127.78
127.70
127.26
121.43
77.41
77.16
76.91
69.80
34.33

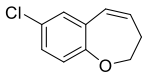
Cl
O

26

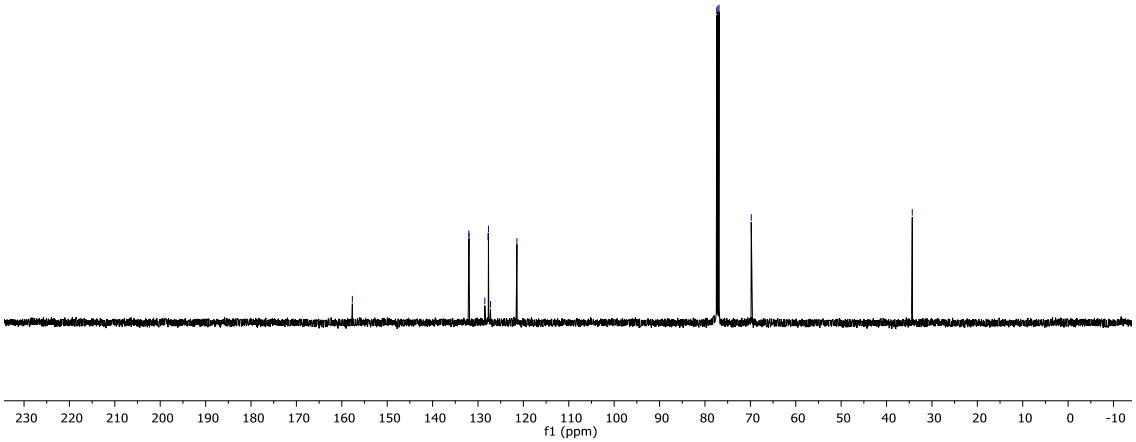
f1 (ppm)

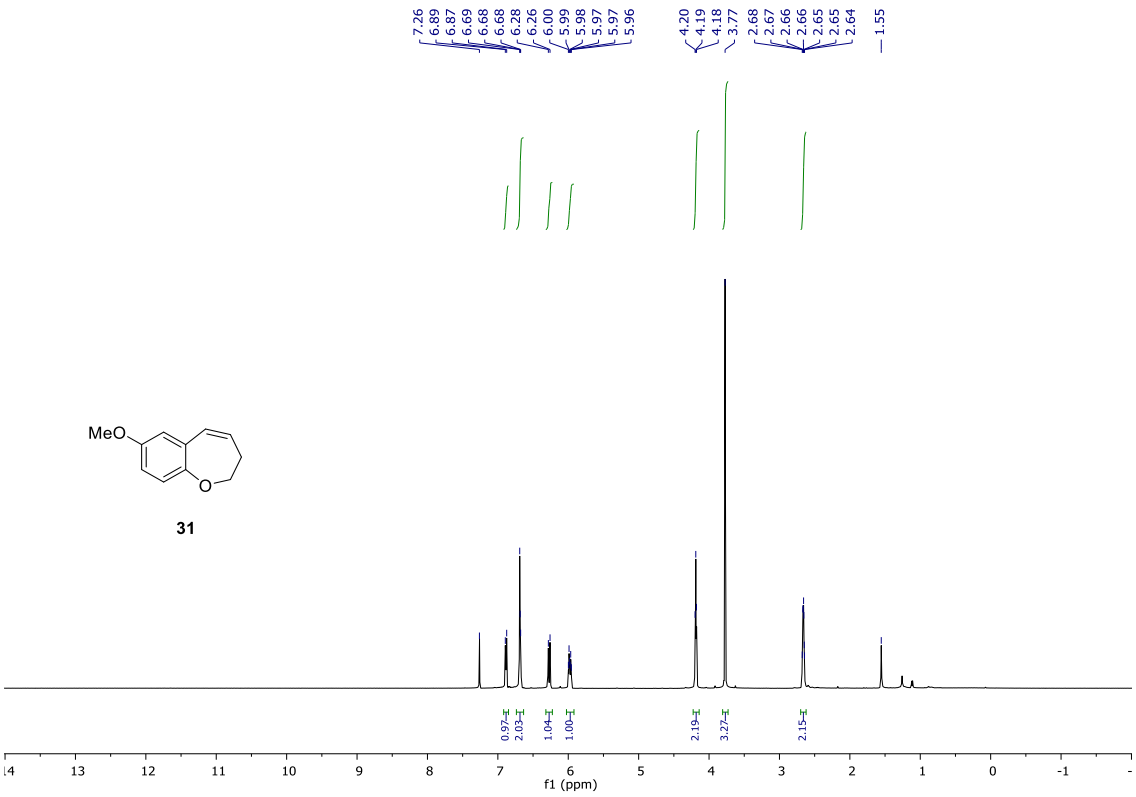
7.26
6.89
6.87
6.69
6.68
6.68
6.28
6.26
6.00
5.99
5.98
5.97
5.97
5.96
4.20
4.19
4.18
3.77
2.68
2.67
2.66
2.66
2.65
2.65
2.64
1.55
MeO
O
0.97
2.03
1.04
1.00
2.19
3.27
2.15
f1 (ppm)

31

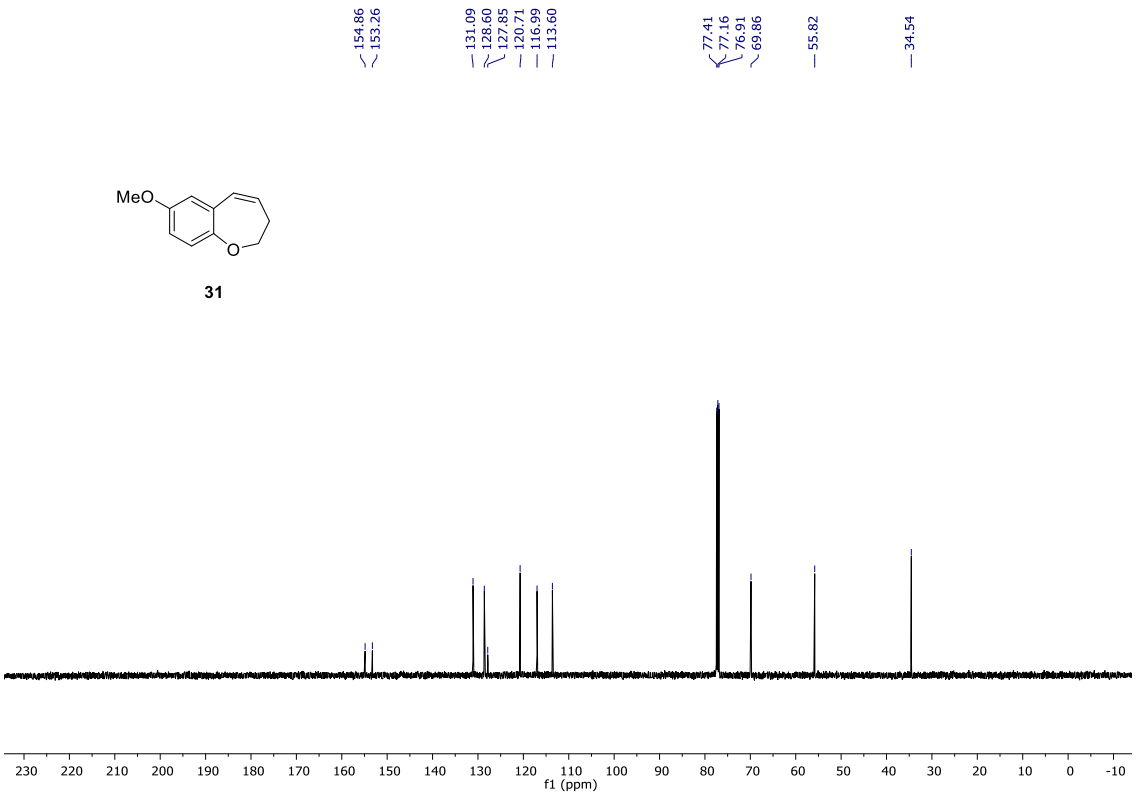
154.86
153.26
131.09
128.60
127.85
120.71
116.99
113.60
77.41
77.16
76.91
69.86
55.82
34.54
MeO
O
f1 (ppm)

31

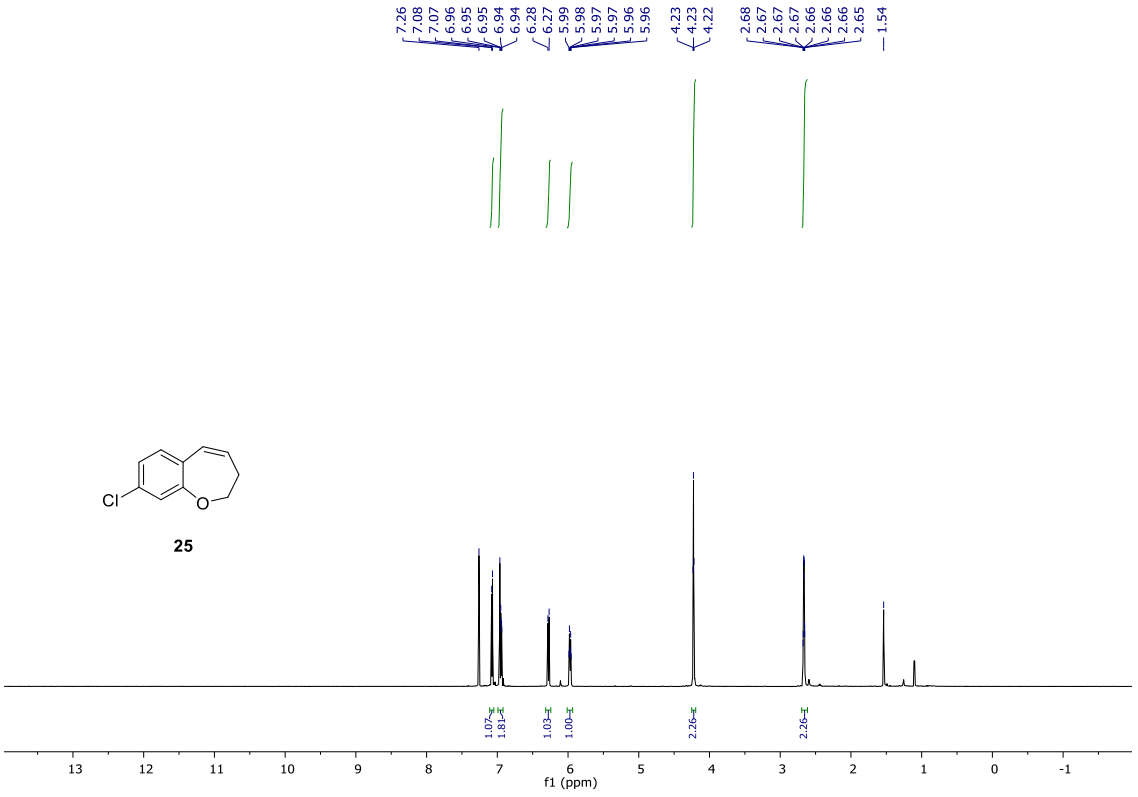
7.26
7.08
7.07
6.96
6.95
6.95
6.94
6.94
6.28
6.27
5.99
5.98
5.97
5.97
5.96
5.96
4.23
4.23
4.22
2.68
2.67
2.67
2.67
2.66
2.66
2.66
2.65
1.54
Cl
O
25
1.07
1.81
1.03
1.00
2.26
2.26
13
12
11
10
9
8
7
6
5
4
3
2
1
0
-1
f1 (ppm)

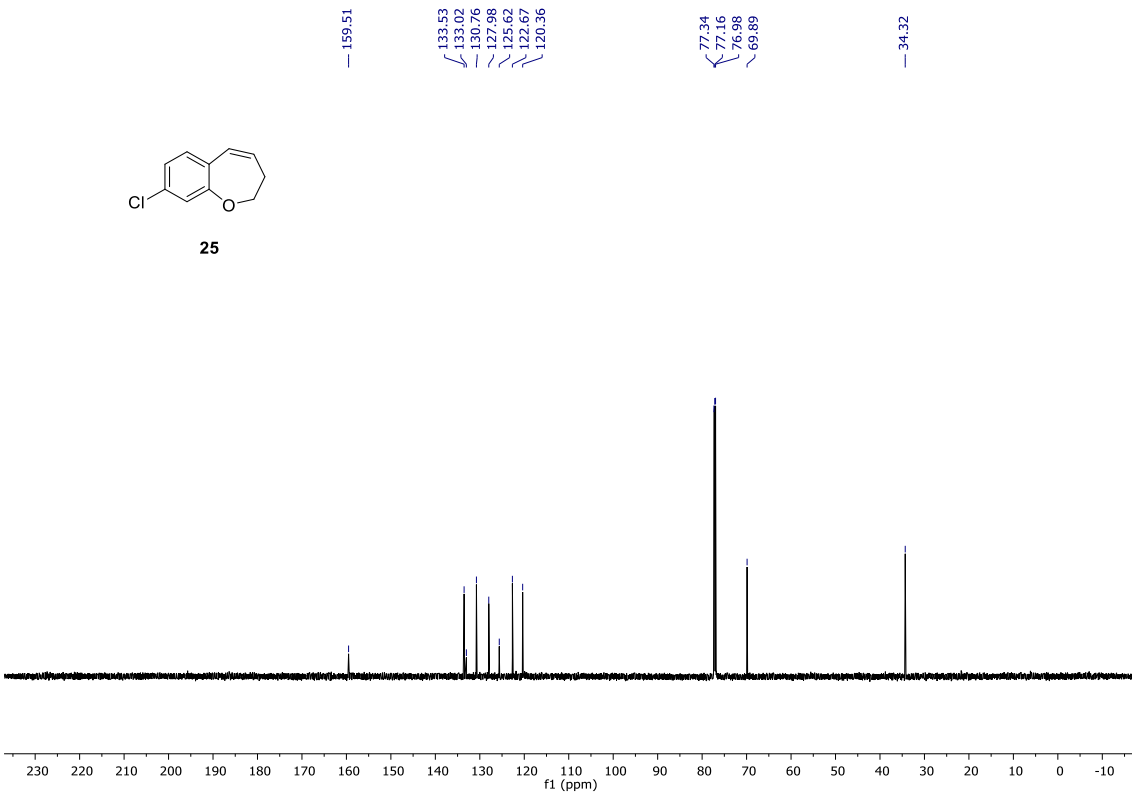
159.51
133.53
133.02
130.76
127.98
125.62
122.67
120.36
77.34
77.16
76.98
69.89
34.32
Cl
O
25
230
220
210
200
190
180
170
160
150
140
130
120
110
100
90
80
70
60
50
40
30
20
10
0
-10
f1 (ppm)

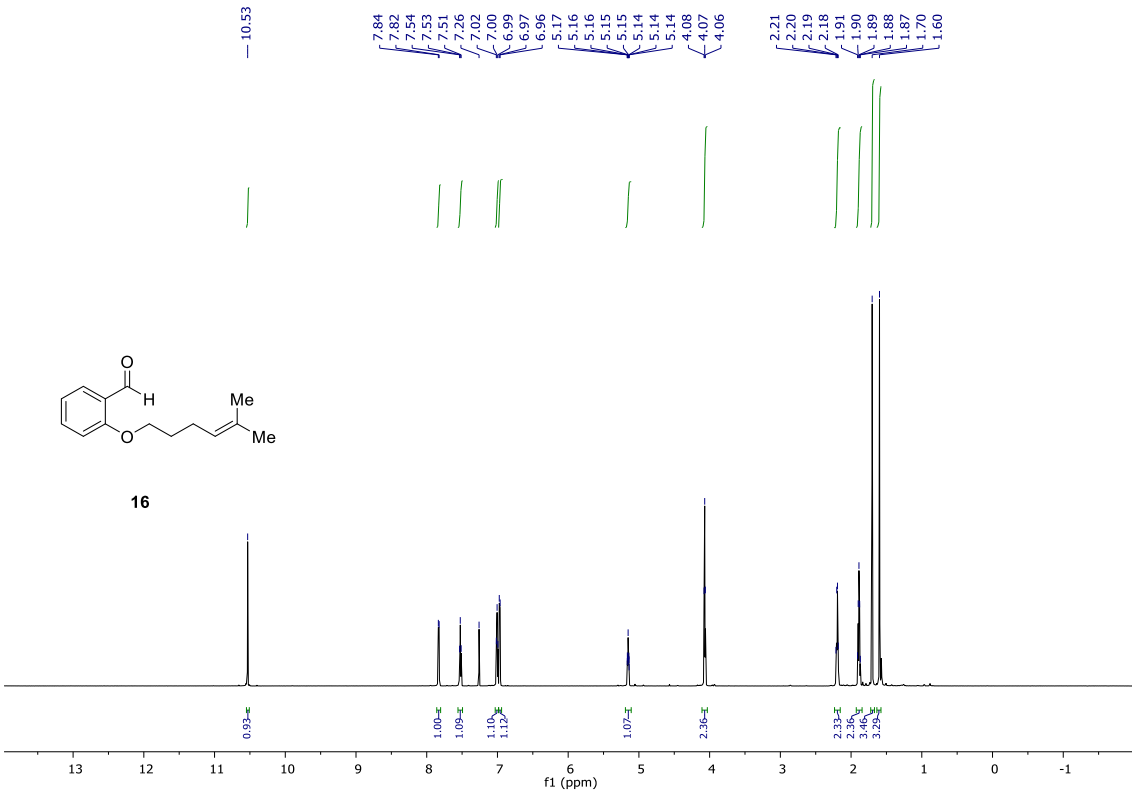
10.53
7.84
7.82
7.54
7.53
7.51
7.26
7.02
7.00
6.99
6.97
6.96
5.17
5.16
5.16
5.15
5.15
5.14
5.14
5.14
4.08
4.07
4.06
2.21
2.20
2.19
2.18
1.91
1.90
1.89
1.88
1.87
1.70
1.60
O
H
O
Me
Me
0.93
1.00
1.09
1.10
1.12
1.07
2.36
2.33
2.36
3.46
3.25
13
12
11
10
9
8
7
6
5
4
3
2
1
0
-1
f1 (ppm)

16

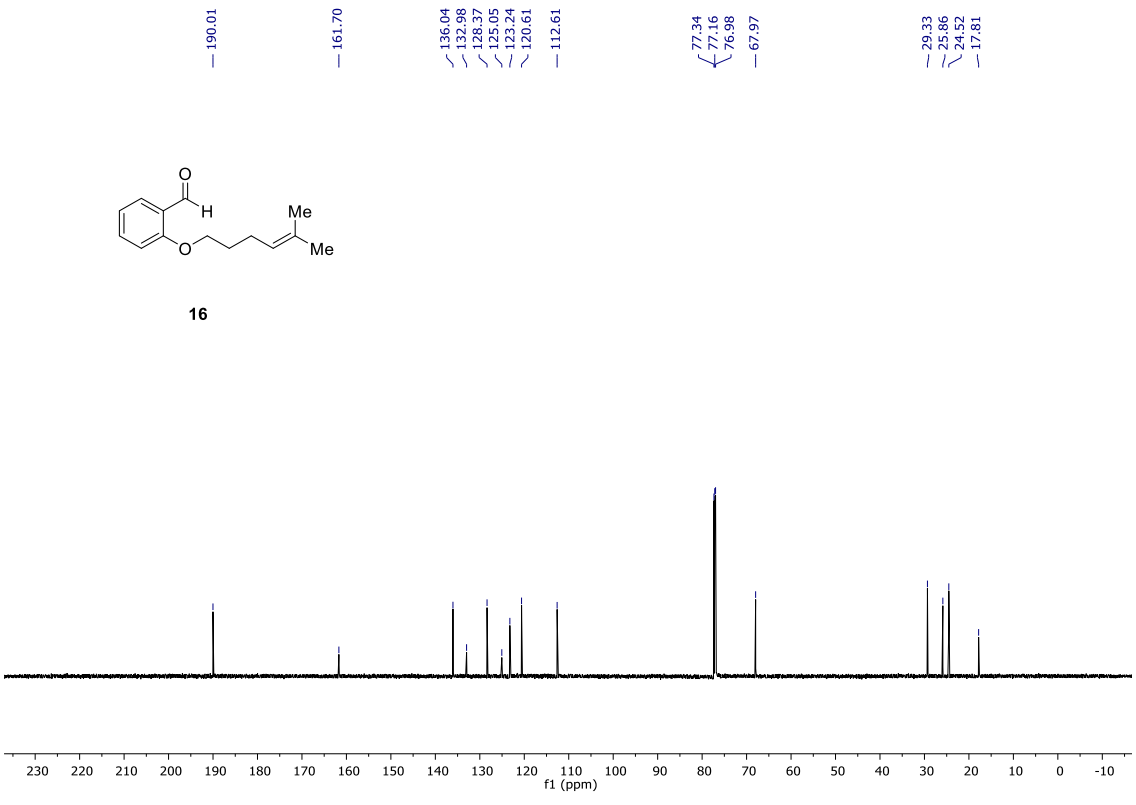
190.01
161.70
136.04
132.98
128.37
125.05
123.24
120.61
112.61
77.34
77.16
76.98
67.97
29.33
25.86
24.52
17.81
O
H
O
Me
Me
230
220
210
200
190
180
170
160
150
140
130
120
110
100
90
80
70
60
50
40
30
20
10
0
-10
f1 (ppm)

16

4.5. References

(1) Albright, H.; Davis, A. J.; Gomez-Lopez, J. L.; Vonesh, H. L.; Quach, P. K.; Lambert, T. H.; Schindler, C. S. Carbonyl-Olefin Metathesis. *Chemical Reviews*. American Chemical Society August 11, 2021, pp 9359–9406. https://doi.org/10.1021/acs.chemrev.0c01096.

(2) Angew Chem Int Ed Engl - October 2 1995 - Schwab - A Series of Well-Defined Metathesis Catalysts Synthesis of RuCl2 .

(3) Scholl, M.; Trnka, T. M.; Morgan, J. P.; Grubbs, R. H. *Increased Ring Closing Metathesis Activity of Ruthenium-Based Oiefin Metathesis Catalysts Coordinated with Imidazolin-2-Ylidene Ligands*; 1999; Vol. 40.

(4) Ho, T.-L.; Mcmurry, J. E.; Clive, D. L. J.; Zhang, C.; Murthy, K. S. K.; Hayward, W. D.; Daigneault, S.; Grubbs, R. H.; Turnas, W.; Hartley, F.; Pine, S. H. *C) Feast, W. J.; Gibson, V. C. In The Chemistry of the Metal-Carbon Bond*; UTC, 1993; Vol. 89.

(5) Helvetica Chimica Acta - 1 November 1971 - Demole - Applications Synth Tiques de La Cyclisation d Alcools Tertiaires -.

(6) Ludwig, J. R.; Zimmerman, P. M.; Gianino, J. B.; Schindler, C. S. Iron(III)-Catalysed Carbonyl-Olefin Metathesis. *Nature* **2016**, *533*, 374–379. https://doi.org/10.1038/nature17432.

(7) Jackson, A. C.; Goldman, B. E.; Snider, B. B. *Intramolecular and Intermolecular Lewis Acid Catalyzed Ene Reactions Using Ketones as Enophiles*; 1984; Vol. 49.

(8) *COM M UNlCATlONS.*

(9) Khripach, V. A.; Zhabinskii, V. N.; Kuchto, A. I.; Zhiburtovich, Y. Y.; Gromak, V. v.; Groen, M. B.; van der Louw, J.; de Groot, A. Intramolecular Cycloaddition/Cycloreversion of (E)-3β,17β-Diacetoxy-5,10-Secoandrost-1(10)-En-5-

One. *Tetrahedron Letters* **2006**, *47* (38), 6715–6718. https://doi.org/10.1016/j.tetlet.2006.07.096.

(10) Soicke, A.; Slavov, N.; Neudörfl, J. M.; Schmalz, H. G. Metal-Free Intramolecular Carbonyl-Olefin Metathesis of Ortho-Prenylaryl Ketones. *Synlett* **2011**, No. 17, 2487–2490. https://doi.org/10.1055/s-0030-1260320.

(11) Malakar, T.; Hanson, C. S.; Devery, J. J.; Zimmerman, P. M. Combined Theoretical and Experimental Investigation of Lewis Acid-Carbonyl Interactions for Metathesis. *ACS Catalysis* **2021**, *11* (8), 4381–4394. https://doi.org/10.1021/acscatal.0c05277.

(12) Hanson, C. S.; Psaltakis, M. C.; Cortes, J. J.; Devery, J. J. Catalyst Behavior in Metal-Catalyzed Carbonyl-Olefin Metathesis. *J Am Chem Soc* **2019**, *141* (30), 11870–11880. https://doi.org/10.1021/jacs.9b02613.

(13) Ludwig, J. R.; Phan, S.; McAtee, C. C.; Zimmerman, P. M.; Devery, J. J.; Schindler, C. S. Mechanistic Investigations of the Iron(III)-Catalyzed Carbonyl-Olefin Metathesis Reaction. *J Am Chem Soc* **2017**, *139* (31), 10832–10842. https://doi.org/10.1021/jacs.7b05641.

(14) Becker, M. Carbonyl-Olefin Metathesis for the Synthesis of Cyclic Olefins. *Organic Syntheses* **2018**, *95*, 472–485. https://doi.org/10.15227/orgsyn.095.0472.

(15) Ma, L.; Li, W.; Xi, H.; Bai, X.; Ma, E.; Yan, X.; Li, Z. FeCl 3 -Catalyzed Ring-Closing Carbonyl-Olefin Metathesis . *Angewandte Chemie* **2016**, *128* (35), 10566–10569. https://doi.org/10.1002/ange.201604349.

(16) Groso, E. J.; Golonka, A. N.; Harding, R. A.; Alexander, B. W.; Sodano, T. M.; Schindler, C. S. 3-Aryl-2,5-Dihydropyrroles via Catalytic Carbonyl-Olefin Metathesis. *ACS Catalysis* **2018**, *8* (3), 2006–2011. https://doi.org/10.1021/acscatal.7b03769.

(17) Rykaczewski, K. A.; Groso, E. J.; Vonesh, H. L.; Gaviria, M. A.; Richardson, A. D.; Zehnder, T. E.; Schindler, C. S. Tetrahydropyridines via FeCl3-Catalyzed Carbonyl-Olefin Metathesis. *Organic Letters* **2020**, *22* (7), 2844–2848. https://doi.org/10.1021/acs.orglett.0c00918.

(18) Ni, S.; Franzén, J. Carbocation Catalysed Ring Closing Aldehyde-Olefin Metathesis. *Chemical Communications* **2018**, *54* (92), 12982–12985. https://doi.org/10.1039/C8CC06734A.

(19) Wang, R.; Chen, Y.; Shu, M.; Zhao, W.; Tao, M.; Du, C.; Fu, X.; Li, A.; Lin, Z. AuCl3-Catalyzed Ring-Closing Carbonyl–Olefin Metathesis. *Chemistry - A European Journal* **2020**, *26* (9), 1941–1946. https://doi.org/10.1002/chem.201905199.

(20) Tran, U. P. N.; Oss, G.; Breugst, M.; Detmar, E.; Pace, D. P.; Liyanto, K.; Nguyen, T. v. Carbonyl-Olefin Metathesis Catalyzed by Molecular Iodine. *ACS Catalysis* **2019**, *9* (2), 912–919. https://doi.org/10.1021/acscatal.8b03769.

(21) Tran, U. P. N.; Oss, G.; Pace, D. P.; Ho, J.; Nguyen, T. v. Tropylium-Promoted Carbonyl-Olefin Metathesis Reactions. *Chemical Science* **2018**, *9* (23), 5145–5151. https://doi.org/10.1039/c8sc00907d.

(22) Djurovic, A.; Vayer, M.; Li, Z.; Guillot, R.; Baltaze, J. P.; Gandon, V.; Bour, C. Synthesis of Medium-Sized Carbocycles by Gallium-Catalyzed Tandem Carbonyl-Olefin Metathesis/Transfer Hydrogenation. *Organic Letters* **2019**, *21* (19), 8132–8137. https://doi.org/10.1021/acs.orglett.9b03240.

(23) McAtee, C. C.; Riehl, P. S.; Schindler, C. S. Polycyclic Aromatic Hydrocarbons via Iron(III)-Catalyzed Carbonyl-Olefin Metathesis. *J Am Chem Soc* **2017**, *139* (8), 2960–2963. https://doi.org/10.1021/jacs.7b01114.

(24) Albright, H.; Riehl, P. S.; McAtee, C. C.; Reid, J. P.; Ludwig, J. R.; Karp, L. A.; Zimmerman, P. M.; Sigman, M. S.; Schindler, C. S. Catalytic Carbonyl-Olefin Metathesis of Aliphatic Ketones: Iron(III) Homo-Dimers as Lewis Acidic Superelectrophiles. *J Am Chem Soc* **2019**, *141* (4), 1690–1700. https://doi.org/10.1021/jacs.8b11840.

(25) Olah, G. A. *International Edition in English Superelectrophiles***; 1993; Vol. 32.

(26) Negishi, E. *CONCEPTS*; 1999; Vol. 5.

(27) Albright, H.; Vonesh, H. L.; Becker, M. R.; Alexander, B. W.; Ludwig, J. R.; Wiscons, R. A.; Schindler, C. S. GaCl3-Catalyzed Ring-Opening Carbonyl-Olefin Metathesis. *Organic Letters* **2018**, *20* (16), 4954–4958. https://doi.org/10.1021/acs.orglett.8b02086.

(28) Naidu, V. R.; Bah, J.; Franzén, J. Direct Organocatalytic Oxo-Metathesis, a Trans-Selective Carbocation-Catalyzed Olefination of Aldehydes. *European Journal of Organic Chemistry* **2015**, *2015* (8), 1834–1839. https://doi.org/10.1002/ejoc.201403651.

(29) Albright, H.; Vonesh, H. L.; Schindler, C. S. Superelectrophilic Fe(III)-Ion Pairs as Stronger Lewis Acid Catalysts for (E)-Selective Intermolecular Carbonyl-Olefin Metathesis. *Organic Letters* **2020**, *22* (8), 3155–3160. https://doi.org/10.1021/acs.orglett.0c00917.

(30) Riehl, P. S.; Nasrallah, D. J.; Schindler, C. S. Catalytic, Transannular Carbonyl-Olefin Metathesis Reactions. *Chemical Science* **2019**, *10* (44), 10267–10274. https://doi.org/10.1039/c9sc03716k.

(31) Ni, S.; Franzén, J. Carbocation Catalysed Ring Closing Aldehyde-Olefin Metathesis. *Chemical Communications* **2018**, *54* (92), 12982–12985. https://doi.org/10.1039/C8CC06734A.

(32) Tran, U. P. N.; Oss, G.; Pace, D. P.; Ho, J.; Nguyen, T. v. Tropylium-Promoted Carbonyl-Olefin Metathesis Reactions. *Chemical Science* **2018**, *9* (23), 5145–5151. https://doi.org/10.1039/c8sc00907d.

(33) Naidu, V. R.; Bah, J.; Franzén, J. Direct Organocatalytic Oxo-Metathesis, a Trans-Selective Carbocation-Catalyzed Olefination of Aldehydes. *European Journal of Organic Chemistry* **2015**, *2015* (8), 1834–1839. https://doi.org/10.1002/ejoc.201403651.

(34) Hanson, C. S.; Psaltakis, M. C.; Cortes, J. J.; Devery, J. J. Catalyst Behavior in Metal-Catalyzed Carbonyl-Olefin Metathesis. *J Am Chem Soc* **2019**, *141* (30), 11870–11880. https://doi.org/10.1021/jacs.9b02613.

(35) Ma, L.; Li, W.; Xi, H.; Bai, X.; Ma, E.; Yan, X.; Li, Z. FeCl 3 -Catalyzed Ring-Closing Carbonyl-Olefin Metathesis . *Angewandte Chemie* **2016**, *128* (35), 10566–10569. https://doi.org/10.1002/ange.201604349.

(36) Riehl, P. S.; Nasrallah, D. J.; Schindler, C. S. Catalytic, Transannular Carbonyl-Olefin Metathesis Reactions. *Chemical Science* **2019**, *10* (44), 10267–10274. https://doi.org/10.1039/c9sc03716k.

(37) Albright, H.; Vonesh, H. L.; Becker, M. R.; Alexander, B. W.; Ludwig, J. R.; Wiscons, R. A.; Schindler, C. S. GaCl3-Catalyzed Ring-Opening Carbonyl-Olefin Metathesis. *Organic Letters* **2018**, *20* (16), 4954–4958. https://doi.org/10.1021/acs.orglett.8b02086.

(38) Groso, E. J.; Golonka, A. N.; Harding, R. A.; Alexander, B. W.; Sodano, T. M.; Schindler, C. S. 3-Aryl-2,5-Dihydropyrroles via Catalytic Carbonyl-Olefin Metathesis. *ACS Catalysis* **2018**, *8* (3), 2006–2011. https://doi.org/10.1021/acscatal.7b03769.

(39) Ludwig, J. R.; Phan, S.; McAtee, C. C.; Zimmerman, P. M.; Devery, J. J.; Schindler, C. S. Mechanistic Investigations of the Iron(III)-Catalyzed Carbonyl-Olefin Metathesis

Reaction. *J Am Chem Soc* **2017**, *139* (31), 10832–10842. https://doi.org/10.1021/jacs.7b05641.

(40) Ludwig, J. R.; Schindler, C. S. Lewis Acid Catalyzed Carbonyl-Olefin Metathesis. *Synlett* **2017**, *28* (13), 1501–1509. https://doi.org/10.1055/s-0036-1588827.

(41) Ludwig, J. R.; Zimmerman, P. M.; Gianino, J. B.; Schindler, C. S. Iron(III)-Catalysed Carbonyl-Olefin Metathesis. *Nature* **2016**, *533*, 374–379. https://doi.org/10.1038/nature17432.

(42) Albright, H.; Riehl, P. S.; McAtee, C. C.; Reid, J. P.; Ludwig, J. R.; Karp, L. A.; Zimmerman, P. M.; Sigman, M. S.; Schindler, C. S. Catalytic Carbonyl-Olefin Metathesis of Aliphatic Ketones: Iron(III) Homo-Dimers as Lewis Acidic Superelectrophiles. *J Am Chem Soc* **2019**, *141* (4), 1690–1700. https://doi.org/10.1021/jacs.8b11840.

(43) McAtee, C. C.; Riehl, P. S.; Schindler, C. S. Polycyclic Aromatic Hydrocarbons via Iron(III)-Catalyzed Carbonyl-Olefin Metathesis. *J Am Chem Soc* **2017**, *139* (8), 2960–2963. https://doi.org/10.1021/jacs.7b01114.

(44) Rykaczewski, K. A.; Groso, E. J.; Vonesh, H. L.; Gaviria, M. A.; Richardson, A. D.; Zehnder, T. E.; Schindler, C. S. Tetrahydropyridines via FeCl3-Catalyzed Carbonyl-Olefin Metathesis. *Organic Letters* **2020**, *22* (7), 2844–2848. https://doi.org/10.1021/acs.orglett.0c00918.

(45) Catti, L.; Tiefenbacher, K. Brønsted-Säure-Katalysierte Carbonyl-Olefin-Metathese in Einer Selbstorganisierten Supramolekularen Wirtstruktur. *Angewandte Chemie* **2018**, *130* (44), 14797–14800. https://doi.org/10.1002/ange.201712141.

(46) Zhu, Y.; Rebek, J.; Yu, Y. Cyclizations Catalyzed inside a Hexameric Resorcinarene Capsule. *Chemical Communications* **2019**, *55* (25), 3573–3577. https://doi.org/10.1039/c9cc01611b.

(47) Griffith, A. K.; Vanos, C. M.; Lambert, T. H. Organocatalytic Carbonyl-Olefin Metathesis. *J Am Chem Soc* **2012**, *134* (45), 18581–18584. https://doi.org/10.1021/ja309650u.

(48) Hong, X.; Liang, Y.; Griffith, A. K.; Lambert, T. H.; Houk, K. N. Distortion-Accelerated Cycloadditions and Strain-Release-Promoted Cycloreversions in the Organocatalytic Carbonyl-Olefin Metathesis. *Chemical Science* **2014**, *5* (2), 471–475. https://doi.org/10.1039/c3sc52882k.

(49) Zhang, Y.; Jermaks, J.; MacMillan, S. N.; Lambert, T. H. Synthesis of 2 H-Chromenes via Hydrazine-Catalyzed Ring-Closing Carbonyl-Olefin Metathesis. *ACS Catalysis* **2019**, *9* (10), 9259–9264. https://doi.org/10.1021/acscatal.9b03656.

(50) Zhang, Y.; Jermaks, J.; MacMillan, S. N.; Lambert, T. H. Synthesis of 2 H-Chromenes via Hydrazine-Catalyzed Ring-Closing Carbonyl-Olefin Metathesis. *ACS Catalysis* **2019**, *9* (10), 9259–9264. https://doi.org/10.1021/acscatal.9b03656.

(51) Albright, H.; Davis, A. J.; Gomez-Lopez, J. L.; Vonesh, H. L.; Quach, P. K.; Lambert, T. H.; Schindler, C. S. Carbonyl-Olefin Metathesis. *Chemical Reviews*. American Chemical Society August 11, 2021, pp 9359–9406. https://doi.org/10.1021/acs.chemrev.0c01096.

(52) Soicke, A.; Slavov, N.; Neudörfl, J. M.; Schmalz, H. G. Metal-Free Intramolecular Carbonyl-Olefin Metathesis of Ortho-Prenylaryl Ketones. *Synlett* **2011**, No. 17, 2487–2490. https://doi.org/10.1055/s-0030-1260320.

(53) Schopov, I. *A Carbonyl-Olefin Exchange Reaction-New Route to Polyconjugated Polymers, 1 A New Synthesis of Polyphenylacetylene*; 1983; Vol. 4.

(54) Ho, T.-L.; Mcmurry, J. E.; Clive, D. L. J.; Zhang, C.; Murthy, K. S. K.; Hayward, W. D.; Daigneault, S.; Grubbs, R. H.; Turnas, W.; Hartley, F.; Pine, S. H. *C) Feast, W. J.; Gibson, V. C. In The Chemistry of the Metal-Carbon Bond*; UTC, 1993; Vol. 89.

(55) Valiulin, R. A.; Arisco, T. M.; Kutateladze, A. G. Photoinduced Intramolecular Cyclopentanation vs Photoprotolytic Oxametathesis in Polycyclic Alkenes Outfitted with Conformationally Constrained Aroylmethyl Chromophores. *Journal of Organic Chemistry* **2013**, *78* (5), 2012–2025. https://doi.org/10.1021/jo301909j.

(56) Valiulin, R. A.; Arisco, T. M.; Kutateladze, A. G. Double-Tandem [4π+2π]·[2 Π+2π]·[4π+2π] ·[2π+2π] Synthetic Sequence with Photoprotolytic Oxametathesis and Photoepoxidation in the Chromone Series. *Journal of Organic Chemistry* **2011**, *76* (5), 1319–1332. https://doi.org/10.1021/jo102221q.

(57) Valiulin, R. A.; Kutateladze, A. G. Harvesting the Strain Installed by a Paternò-Büchi Step in a Synthetically Useful Way: High-Yielding Photoprotolytic Oxametathesis in Polycyclic Systems. *Organic Letters* **2009**, *11* (17), 3886–3889. https://doi.org/10.1021/ol901456m.

(58) Pérez-Ruiz, R.; Miranda, M. A.; Alle, R.; Meerholz, K.; Griesbeck, A. G. An Efficient Carbonyl-Alkene Metathesis of Bicyclic Oxetanes: Photoinduced Electron Transfer Reduction of the Paternò–Büchi Adducts from 2,3-Dihydrofuran and Aromatic Aldehydes. *Photochemical and Photobiological Sciences* **2006**, *5* (1), 51–55. https://doi.org/10.1039/b513875b.

(59) Pérez-Ruiz, R.; Gil, S.; Miranda, M. A. Stereodifferentiation in the Photochemical Cycloreversion of Diastereomeric Methoxynaphthalene-Oxetane Dyads. **2005**. https://doi.org/10.1021/jo048708.

(60) D'Auria, M.; Racioppi, R.; Viggiani, L. Paternò-Büchi Reaction between Furan and Heterocyclic Aldehydes: Oxetane Formation vs. Metathesis. *Photochemical and Photobiological Sciences* **2010**, *9* (8), 1134–1138. https://doi.org/10.1039/c0pp00076k.

(61) Guilford Jones, B.; Acquadro, M. A.; Carmody, M. A. *Long-Chain Enals Oia Carbonyl-Olefin Metathesis. An Application in Pheromone Synthesis*; 1975.

(62) Guilford Jones, B. I.; Schwartz, S. B.; Marton, M. T. *Regiospecific Thermal Cleavage of Some Oxetan Photoadducts : Carbonyl-Olefin Metathesis in Sequential Photochemical and Thermal Steps*; 1973.

(63) Albright, H.; Vonesh, H. L.; Schindler, C. S. Superelectrophilic Fe(III)-Ion Pairs as Stronger Lewis Acid Catalysts for (E)-Selective Intermolecular Carbonyl-Olefin Metathesis. *Organic Letters* **2020**, *22* (8), 3155–3160. https://doi.org/10.1021/acs.orglett.0c00917.

(64) Olah, G. A. *International Edition in English Superelectrophiles***; 1993; Vol. 32.

(65) Negishi, E. *CONCEPTS*; 1999; Vol. 5.

(66) Stephan, D. W.; Erker, G. Chemie Frustrierter Lewis-Paare: Entwicklung Und Perspektiven. *Angewandte Chemie* **2015**, *127* (22), 6498–6541. https://doi.org/10.1002/ange.201409800.

(67) Denmark, S. E.; Eklov, B. M.; Yao, P. J.; Eastgate, M. D. On the Mechanism of Lewis Base Catalyzed Aldol Addition Reactions: Kinetic and Spectroscopic Investigations Using

Rapid-Injection NMR. *J Am Chem Soc* **2009**, *131* (33), 11770–11787. https://doi.org/10.1021/ja902474j.

(68) Tomifuji, R.; Maeda, K.; Takahashi, T.; Kurahashi, T.; Matsubara, S. FeCl 3 as an Ion-Pairing Lewis Acid Catalyst. Formation of Highly Lewis Acidic FeCl 2+ and Thermodynamically Stable FeCl 4- to Catalyze the Aza-Diels-Alder Reaction with High Turnover Frequency. *Organic Letters* **2018**, *20* (23), 7474–7477. https://doi.org/10.1021/acs.orglett.8b03249.

(69) Ic00256a033.

(70) Davis, A. J.; Watson, R. B.; Nasrallah, D. J.; Gomez-Lopez, J. L.; Schindler, C. S. Superelectrophilic Aluminium(Iii)–Ion Pairs Promote a Distinct Reaction Path for Carbonyl–Olefin Ring-Closing Metathesis. *Nature Catalysis* **2020**, *3* (10), 787–796. https://doi.org/10.1038/s41929-020-00499-5.

(71) Strauss, S. H. *The Search for Larger and More Weakly Coordinating Anions*; 1993; Vol. 93.

(72) Beck, W.; Sunkel, K. Metal Complexes of Weakly Coordinating Anions. Precursors of Strong Cationic Organometallic Lewis Acids1^.

(73) Schottel, B. L.; Chifotides, H. T.; Shatruk, M.; Chouai, A.; Pérez, L. M.; Bacsa, J.; Dunbar, K. R. Anion-π Interactions as Controlling Elements in Self-Assembly Reactions of Ag(I) Complexes with π-Acidic Aromatic Rings. *J Am Chem Soc* **2006**, *128* (17), 5895–5912. https://doi.org/10.1021/ja0606273.

(74) Om50006a014.

(75) Mayfield, H. G.; Bull, W. E. *SECTION A I Norgan Ic, P Hysica I, and T Heoret Ica 1 Chemistry Co-Ordinating Tendencies of the Hexaf Luorophosphate Ion*.

(76) *Chapman et Al*.

(77) Bini, R.; Chiappe, C.; Marmugi, E.; Pieraccini, D. The “Non-Nucleophilic” Anion [Tf2N]- Competes with the Nucleophilic Br-: An Unexpected Trapping in the Dediazoniation Reaction in Ionic Liquids. *Chemical Communications* **2006**, No. 8, 897–899. https://doi.org/10.1039/b514988f.

(78) Hanson, C. S.; Psaltakis, M. C.; Cortes, J. J.; Siddiqi, S. S.; Devery, J. J. Investigation of Lewis Acid-Carbonyl Solution Interactions via Infrared-Monitored Titration. *Journal of Organic Chemistry* **2020**, *85* (2), 820–832. https://doi.org/10.1021/acs.joc.9b02822.

(79) Hanson, C. S.; Psaltakis, M. C.; Cortes, J. J.; Devery, J. J. Catalyst Behavior in Metal-Catalyzed Carbonyl-Olefin Metathesis. *J Am Chem Soc* **2019**, *141* (30), 11870–11880. https://doi.org/10.1021/jacs.9b02613.

(80) Malakar, T.; Hanson, C. S.; Devery, J. J.; Zimmerman, P. M. Combined Theoretical and Experimental Investigation of Lewis Acid-Carbonyl Interactions for Metathesis. *ACS Catalysis* **2021**, *11* (8), 4381–4394. https://doi.org/10.1021/acscatal.0c05277.

(81) Hull, S.; Keen, D. A. *Pressure-Induced Phase Transitions in AgCl, AgBr, and AgI*.

(82) Rodriguez-Ruiz, V.; Carlino, R.; Bezzenine-Lafollée, S.; Gil, R.; Prim, D.; Schulz, E.; Hannedouche, J. Recent Developments in Alkene Hydro-Functionalisation Promoted by Homogeneous Catalysts Based on Earth Abundant Elements: Formation of C-N, C-O and C-P Bond. *Dalton Transactions*. Royal Society of Chemistry July 21, 2015, pp 12029–12059. https://doi.org/10.1039/c5dt00280j.

(83) Ozawa, T.; Kurahashi, T.; Matsubara, S. Manganese Porphyrin Catalyzed Cycloisomerization of Enynes. *Organic Letters* **2012**, *14* (12), 3008–3011. https://doi.org/10.1021/ol301416f.

(84) Ic00219a025.

(85) Honeychuck, R. v; Hersh, W. H. *) And 1.954 (11) A (3b), 2.186 (3) and 1.979 (3) A (3c), 2.168 (7) and 1.500 (14) A (5*; 1989; Vol. 28.

(86) Gowik, P.; Klapiitke, T.; Thewalt, U. *Metallocen-Chemie Hochfluorierter Ligand-Systeme XI *. Synthese Und Charakterisierung von Cp,Ti(SbF,) 2 Und Cp,Ti(Sb, F,) 2; Struktur von Cp,Ti(SbF,) 2 Und Cp2V(SbF,) 2*; Elsevier Sequoia S.A, 1990.

(87) Dash, C.; Das, A.; Yousufuddin, M.; Dias, H. V. R. Isolable, Copper(I) Dicarbonyl Complexes Supported by N-Heterocyclic Carbenes. *Inorganic Chemistry* **2013**, *52* (3), 1584–1590. https://doi.org/10.1021/ic302455y.

(88) Smirnova, E. S.; Muñoz Molina, J. M.; Johnson, A.; Bandeira, N. A. G.; Bo, C.; Echavarren, A. M. Polynuclear Gold [Au I] 4 , [Au I] 8 , and Bimetallic [Au I 4 Ag I] Complexes: C−H Functionalization of Carbonyl Compounds and Homogeneous Carbonylation of Amines . *Angewandte Chemie* **2016**, *128* (26), 7613–7617. https://doi.org/10.1002/ange.201603200.

(89) Bour, C.; Monot, J.; Tang, S.; Guillot, R.; Farjon, J.; Gandon, V. Structure, Stability, and Catalytic Activity of Fluorine-Bridged Complexes IPr·GaCl2(μ-F)EFn -1 (EFn- = SbF6-, PF6-, or BF 4-). *Organometallics* **2014**, *33* (2), 594–599. https://doi.org/10.1021/om4012054.

(90) Kavoosi, A.; Fillion, E. Synthesis and Characterization of Tricarbastannatranes and Their Reactivity in B(C 6 F 5) 3 -Promoted Conjugate Additions . *Angewandte Chemie* **2015**, *127* (18), 5578–5582. https://doi.org/10.1002/ange.201500983.

(91) Michelet, B.; Colard-Itté, J. R.; Thiery, G.; Guillot, R.; Bour, C.; Gandon, V. Dibromoindium(Iii) Cations as a π-Lewis Acid: Characterization of [IPr·InBr2][SbF6] and

Its Catalytic Activity towards Alkynes and Alkenes. *Chemical Communications* **2015**, *51* (34), 7401–7404. https://doi.org/10.1039/c5cc00740b.

(92) Cornella, J.; Martin, R. Ni-Catalyzed Stereoselective Arylation of Inert C-O Bonds at Low Temperatures. *Organic Letters* **2013**, *15* (24), 6298–6301. https://doi.org/10.1021/ol4031815.

(93) Kshirsagar, U. A.; Regev, C.; Parnes, R.; Pappo, D. Iron-Catalyzed Oxidative Cross-Coupling of Phenols and Alkenes. *Organic Letters* **2013**, *15* (12), 3174–3177. https://doi.org/10.1021/ol401532a.

(94) Bao, L.-L.; Iu, Z.-Q. Tetrahydropyrrolization of Resveratrol and Other Stilbenes Improves Inhibitory Effects on DNA Oxidation. https://doi.org/10.1002/cmdc.201600205:NMR.

(95) Konishi, H.; Ueda, T.; Muto, T.; Manabe, K. Remarkable Improvement Achieved by Imidazole Derivatives in Ruthenium-Catalyzed Hydroesterification of Alkenes Using Formates. *Organic Letters* **2012**, *14* (18), 4722–4725. https://doi.org/10.1021/ol301850y.

(96) Yoo, K. S.; Yoon, C. H.; Jung, K. W. Oxidative Palladium(II) Catalysis: A Highly Efficient and Chemoselective Cross-Coupling Method for Carbon-Carbon Bond Formation under Base-Free and Nitrogenous-Ligand Conditions. *J Am Chem Soc* **2006**, *128* (50), 16384–16393. https://doi.org/10.1021/ja063710z.

(97) Kobayashi, K.; Ueno, M.; Kondo, Y. Phosphazene Base-Catalyzed Condensation of Trimethylsilylacetate with Carbonyl Compounds. *Chemical Communications* **2006**, No. 29, 3128–3130. https://doi.org/10.1039/b606056k.

(98) Charette, A. B.; Molinaro, C.; Brochu, C. Catalytic Asymmetric Cyclopropanation of Allylic Alcohols with Titanium-TADDOLate: Scope of the Cyclopropanation Reaction. *J Am Chem Soc* **2001**, *123* (49), 12168–12175. https://doi.org/10.1021/ja0108382.

(99) Hodgson, D. M.; Ying, K. C.; Nuzzo, I.; Freixas, G.; Kulikiewicz, K. K.; Cleator, E.; Paris, J. M. Intramolecular Cyclopropanation of Unsaturated Terminal Epoxides and Chlorohydrins. *J Am Chem Soc* **2007**, *129* (14), 4456–4462. https://doi.org/10.1021/ja0672932.

(100) Usui, I.; Schmidt, S.; Breit, B. Dual Palladium-and Proline-Catalyzed Allylic Alkylation of Enolizable Ketones and Aldehydes with Allylic Alcohols. *Organic Letters* **2009**, *11* (6), 1453–1456. https://doi.org/10.1021/ol9001812.

(101) Oppolzer, W.; Spivey, A. C.; Bochet, C. G. *1991,56, 2988 and References Mentioned Therein. Cf.\ Martin, S. F. The Amaryllidaceae Alkaloids*; Academic Press, 1994; Vol. 116.

(102) Daniel Little, R.; Carroll, G. L.; Petersen, J. L.; Tetrahedron Symp, K. Total Synthesis of the Marine Natural Product A9(12)-Capnellene. Reversal of Regiochemistry in the Intramolecular 1,3-Diyl Trapping Reaction. *Marine Natural Products, Chemical and Biological Perspectives* **1983**, *105* (2), 7129–7130.

(103) le Nôtre, J.; Touzani, R.; Lavastre, O.; Bruneau, C.; Dixneuf, P. H. Homologation of Monoterpenoids into New Sesquiterpenoids via Tandem Isomerisation/Claisen Rearrangement Reactions with Three-Component Ruthenium Catalysts, and Ru(Methallyl)2 (COD) Revealed by High Throughput Screening Techniques. *Advanced Synthesis and Catalysis* **2005**, *347* (6), 783–791. https://doi.org/10.1002/adsc.200404391.

(104) Aebi, J. D.; Deyo, D. T.; Sun, C. Q.; Guillaume, D.; Dunlap, B.; Rich, D. H. *Synthesis, Conformation, and Immunosuppressive Activities of Three Analogues of Cyclosporin A Modified in the 1-Position1 Both Conformations Have a Type IT 0-Tum for Residues 2-*· *5 and a Cis Amide Bond Between*; 1990; Vol. 33.

(105) Casey, C. P.; Bertz, S. H.; Burkhardt, T. J. *REACTION OF METAL-CARBENE COMPLEXES WITH OIAZOALKANES. A VERSATILE VINYL ETHER SYNTHESIS*; PequDon Pram, 1973.

(106) Banks, J. L.; Beard, H. S.; Cao, Y.; Cho, A. E.; Damm, W.; Farid, R.; Felts, A. K.; Halgren, T. A.; Mainz, D. T.; Maple, J. R.; Murphy, R.; Philipp, D. M.; Repasky, M. P.; Zhang, L. Y.; Berne, B. J.; Friesner, R. A.; Gallicchio, E.; Levy, R. M. Integrated Modeling Program, Applied Chemical Theory (IMPACT). *Journal of Computational Chemistry*. December 2005, pp 1752–1780. https://doi.org/10.1002/jcc.20292.

(107) Shao, Y.; Gan, Z.; Epifanovsky, E.; Gilbert, A. T. B.; Wormit, M.; Kussmann, J.; Lange, A. W.; Behn, A.; Deng, J.; Feng, X.; Ghosh, D.; Goldey, M.; Horn, P. R.; Jacobson, L. D.; Kaliman, I.; Khaliullin, R. Z.; Kuš, T.; Landau, A.; Liu, J.; Proynov, E. I.; Rhee, Y. M.; Richard, R. M.; Rohrdanz, M. A.; Steele, R. P.; Sundstrom, E. J.; Woodcock, H. L.; Zimmerman, P. M.; Zuev, D.; Albrecht, B.; Alguire, E.; Austin, B.; Beran, G. J. O.; Bernard, Y. A.; Berquist, E.; Brandhorst, K.; Bravaya, K. B.; Brown, S. T.; Casanova, D.; Chang, C. M.; Chen, Y.; Chien, S. H.; Closser, K. D.; Crittenden, D. L.; Diedenhofen, M.; Distasio, R. A.; Do, H.; Dutoi, A. D.; Edgar, R. G.; Fatehi, S.; Fusti-Molnar, L.; Ghysels, A.; Golubeva-Zadorozhnaya, A.; Gomes, J.; Hanson-Heine, M. W. D.; Harbach, P. H. P.; Hauser, A. W.; Hohenstein, E. G.; Holden, Z. C.; Jagau, T. C.; Ji, H.; Kaduk, B.; Khistyaev, K.; Kim, J.; Kim, J.; King, R. A.; Klunzinger, P.; Kosenkov, D.; Kowalczyk, T.; Krauter, C. M.; Lao, K. U.; Laurent, A. D.; Lawler, K. v.; Levchenko, S. v.; Lin, C. Y.; Liu, F.; Livshits, E.; Lochan, R. C.; Luenser, A.; Manohar, P.; Manzer, S. F.; Mao, S. P.; Mardirossian, N.; Marenich, A. v.; Maurer, S. A.; Mayhall, N. J.; Neuscamman, E.; Oana, C. M.; Olivares-Amaya, R.; Oneill, D. P.; Parkhill, J. A.; Perrine, T. M.; Peverati, R.;

Prociuk, A.; Rehn, D. R.; Rosta, E.; Russ, N. J.; Sharada, S. M.; Sharma, S.; Small, D. W.; Sodt, A.; Stein, T.; Stück, D.; Su, Y. C.; Thom, A. J. W.; Tsuchimochi, T.; Vanovschi, V.; Vogt, L.; Vydrov, O.; Wang, T.; Watson, M. A.; Wenzel, J.; White, A.; Williams, C. F.; Yang, J.; Yeganeh, S.; Yost, S. R.; You, Z. Q.; Zhang, I. Y.; Zhang, X.; Zhao, Y.; Brooks, B. R.; Chan, G. K. L.; Chipman, D. M.; Cramer, C. J.; Goddard, W. A.; Gordon, M. S.; Hehre, W. J.; Klamt, A.; Schaefer, H. F.; Schmidt, M. W.; Sherrill, C. D.; Truhlar, D. G.; Warshel, A.; Xu, X.; Aspuru-Guzik, A.; Baer, R.; Bell, A. T.; Besley, N. A.; Chai, J. da; Dreuw, A.; Dunietz, B. D.; Furlani, T. R.; Gwaltney, S. R.; Hsu, C. P.; Jung, Y.; Kong, J.; Lambrecht, D. S.; Liang, W.; Ochsenfeld, C.; Rassolov, V. A.; Slipchenko, L. v.; Subotnik, J. E.; van Voorhis, T.; Herbert, J. M.; Krylov, A. I.; Gill, P. M. W.; Head-Gordon, M. Advances in Molecular Quantum Chemistry Contained in the Q-Chem 4 Program Package. *Molecular Physics* **2015**, *113* (2), 184–215. https://doi.org/10.1080/00268976.2014.952696.

(108) Zimmerman, P. M. Single-Ended Transition State Finding with the Growing String Method. *Journal of Computational Chemistry* **2015**, *36* (9), 601–611. https://doi.org/10.1002/jcc.23833.

(109) Zimmerman, P. M. Growing String Method with Interpolation and Optimization in Internal Coordinates: Method and Examples. *Journal of Chemical Physics* **2013**, *138* (18). https://doi.org/10.1063/1.4804162.

(110) Jafari, M.; Zimmerman, P. M. Reliable and Efficient Reaction Path and Transition State Finding for Surface Reactions with the Growing String Method. *Journal of Computational Chemistry* **2017**, *38* (10), 645–658. https://doi.org/10.1002/jcc.24720.

(111) Zimmerman, P. Reliable Transition State Searches Integrated with the Growing String Method. *Journal of Chemical Theory and Computation* **2013**, *9* (7), 3043–3050. https://doi.org/10.1021/ct400319w.

(112) Metz, B.; Stoll, H.; Dolg, M. Small-Core Multiconfiguration-Dirac-Hartree-Fock-Adjusted Pseudopotentials for Post-d Main Group Elements: Application to PbH and PbO. *Journal of Chemical Physics* **2000**, *113* (7), 2563–2569. https://doi.org/10.1063/1.1305880.

(113) Peterson, K. A.; Figgen, D.; Goll, E.; Stoll, H.; Dolg, M. Systematically Convergent Basis Sets with Relativistic Pseudopotentials. II. Small-Core Pseudopotentials and Correlation Consistent Basis Sets for the Post-d Group 16-18 Elements. *Journal of Chemical Physics* **2003**, *119* (21), 11113–11123. https://doi.org/10.1063/1.1622924.

(114) Leininger, T.; Nicklass, A.; Kiichle, W.; Stoll, H.; Dolg, M.; Bergner, A. *PHYSICS LETTERS ELSEVIER The Accuracy of the Pseudopotential Approximation: Non-Frozen-Core Effects for Spectroscopic Constants of Alkali Fluorides XF (X = K, Rb, Cs)*; 1996; Vol. 255.

(115) Kaupp, M.; Schleyer, P. V. R.; Stoll, H.; Preuss, H. Pseudopotential Approaches to Ca, Sr, and Ba Hydrides. Why Are Some Alkaline Earth MX2 Compounds Bent? *The Journal of Chemical Physics* **1991**, *94* (2), 1360–1366. https://doi.org/10.1063/1.459993.

(116) Marenich, A. v.; Cramer, C. J.; Truhlar, D. G. Universal Solvation Model Based on Solute Electron Density and on a Continuum Model of the Solvent Defined by the Bulk Dielectric Constant and Atomic Surface Tensions. *Journal of Physical Chemistry B* **2009**, *113* (18), 6378–6396. https://doi.org/10.1021/jp810292n.

(117) Djurovic, A.; Vayer, M.; Li, Z.; Guillot, R.; Baltaze, J. P.; Gandon, V.; Bour, C. Synthesis of Medium-Sized Carbocycles by Gallium-Catalyzed Tandem Carbonyl-Olefin Metathesis/Transfer Hydrogenation. *Organic Letters* **2019**, *21* (19), 8132–8137. https://doi.org/10.1021/acs.orglett.9b03240.

(118) Catti, L.; Tiefenbacher, K. Brønsted-Säure-Katalysierte Carbonyl-Olefin-Metathese in Einer Selbstorganisierten Supramolekularen Wirtstruktur. *Angewandte Chemie* **2018**, *130* (44), 14797–14800. https://doi.org/10.1002/ange.201712141.

(119) Lambert, T. H. Development of a Hydrazine-Catalyzed Carbonyl-Olefin Metathesis Reaction. *Synlett* **2019**, *30* (17), 1954–1965. https://doi.org/10.1055/s-0039-1689924.

(120) Ohkubo, K.; Menon, S. C.; Orita, A.; Otera, J.; Fukuzumi, S. Quantitative Evaluation of Lewis Acidity of Metal Ions with Different Ligands and Counterions in Relation to the Promoting Effects of Lewis Acids on Electron Transfer Reduction of Oxygen. *Journal of Organic Chemistry* **2003**, *68* (12), 4720–4726. https://doi.org/10.1021/jo034258u.

(121) Evans, D. A.; Lectka, T.; Miller, S. J.; Murry, J. A.; Matt, P.; Norcross, R. D.; Johnson, J. S.; Kozlowski, M. C.; Ghosh, A. K.; Mathivanan, P.; Cappiello, J.; Krishnan, K.; Johannsen, M.; Jørgensen, K. A. *C 2-Symmetric Copper(II) Complexes as Chiral Lewis Acids. Enantioselective Catalysis of the Glyoxylate-Ene Reaction*; 1993; Vol. 115.

(122) Johnson, J. S.; Evans, D. A. Chiral Bis(Oxazoline) Copper(II) Complexes: Versatile Catalysts for Enantioselective Cycloaddition, Aldol, Michael, and Carbonyl Ene Reactions. *Accounts of Chemical Research* **2000**, *33* (6), 325–335. https://doi.org/10.1021/ar960062n.

(123) Hilt, G.; Pünner, F.; Möbus, J.; Naseri, V.; Bohn, M. A. A Lewis Acidity Scale in Relation to Rate Constants of Lewis Acid Catalyzed Organic Reactions. *European Journal of Organic Chemistry* **2011**, No. 30, 5962–5966. https://doi.org/10.1002/ejoc.201101029.

(124) *INFRARED SPECTRA OF XANTH0NE:LEWIS ACID COMPLEXES*?*

(125) Tran, U. P. N.; Oss, G.; Breugst, M.; Detmar, E.; Pace, D. P.; Liyanto, K.; Nguyen, T. v. Carbonyl-Olefin Metathesis Catalyzed by Molecular Iodine. *ACS Catalysis* **2019**, *9* (2), 912–919. https://doi.org/10.1021/acscatal.8b03769.

(126) Wang, R.; Chen, Y.; Shu, M.; Zhao, W.; Tao, M.; Du, C.; Fu, X.; Li, A.; Lin, Z. AuCl3-Catalyzed Ring-Closing Carbonyl–Olefin Metathesis. *Chemistry - A European Journal* **2020**, *26* (9), 1941–1946. https://doi.org/10.1002/chem.201905199.

(127) Jermaks, J.; Quach, P. K.; Seibel, Z. M.; Pomarole, J.; Lambert, T. H. Ring-Opening Carbonyl-Olefin Metathesis of Norbornenes. *Chemical Science* **2020**, *11* (30), 7884–7895. https://doi.org/10.1039/d0sc02243h.

(128) Lambert, T. H. Development of a Hydrazine-Catalyzed Carbonyl-Olefin Metathesis Reaction. *Synlett* **2019**, *30* (17), 1954–1965. https://doi.org/10.1055/s-0039-1689924.

(129) Zhang, Y.; Jermaks, J.; MacMillan, S. N.; Lambert, T. H. Synthesis of 2 H-Chromenes via Hydrazine-Catalyzed Ring-Closing Carbonyl-Olefin Metathesis. *ACS Catalysis* **2019**, *9* (10), 9259–9264. https://doi.org/10.1021/acscatal.9b03656.

(130) Hong, X.; Liang, Y.; Griffith, A. K.; Lambert, T. H.; Houk, K. N. Distortion-Accelerated Cycloadditions and Strain-Release-Promoted Cycloreversions in the Organocatalytic Carbonyl-Olefin Metathesis. *Chemical Science* **2014**, *5* (2), 471–475. https://doi.org/10.1039/c3sc52882k.

(131) Griffith, A. K.; Vanos, C. M.; Lambert, T. H. Organocatalytic Carbonyl-Olefin Metathesis. *J Am Chem Soc* **2012**, *134* (45), 18581–18584. https://doi.org/10.1021/ja309650u.

(132) Musacchio, A. J.; Nguyen, L. Q.; Beard, G. H.; Knowles, R. R. Catalytic Olefin Hydroamination with Aminium Radical Cations: A Photoredox Method for Direct C-N Bond Formation. *J Am Chem Soc* **2014**, *136* (35), 12217–12220. https://doi.org/10.1021/ja5056774.

(133) Fernández-Mateos, A.; Madrazo, S. E.; Teijón, P. H.; González, R. R. Radical Cyclization of Epoxy Vinyl- and Allylsulfones Promoted by Titanocene Chloride. *Journal of Organic Chemistry* **2015**, *80* (9), 4378–4391. https://doi.org/10.1021/acs.joc.5b00206.

(134) Kuriyama, Y.; Sasano, Y.; Hoshino, Y.; Uesugi, S. ichiro; Yamaichi, A.; Iwabuchi, Y. Highly Regioselective 5-Endo-Tet Cyclization of 3,4-Epoxy Amines into 3-Hydroxypyrrolidines Catalyzed by La(OTf)3. *Chemistry - A European Journal* **2021**, *27* (6), 1961–1965. https://doi.org/10.1002/chem.202004455.

(135) Johnson, L. A.; Dunbabin, A.; Benton, J. C. R.; Mart, R. J.; Allemann, R. K. Modular Chemoenzymatic Synthesis of Terpenes and Their Analogues. *Angewandte Chemie - International Edition* **2020**, *59* (22), 8486–8490. https://doi.org/10.1002/anie.202001744.

(136) Lucke, A. J.; Young, D. J. Electrophilic Cleavage of Cyclopropylmethystannanes: An Experimental Comparison of σ-σ and σ-π Conjugation. *Journal of Organic Chemistry* **2005**, *70* (9), 3579–3583. https://doi.org/10.1021/jo047822p.

(137) Cai, Z.; Yongpruksa, N.; Harmata, M. Total Synthesis of the Terpenoid Buddledone A: 11-Membered Ring-Closing Metathesis. *Organic Letters* **2012**, *14* (7), 1661–1663. https://doi.org/10.1021/ol300400x.

(138) Anderson, T. E.; Woerpel, K. A. Strain-Promoted Oxidation of Methylenecyclopropane Derivatives Using N-Hydroxyphthalimide and Molecular Oxygen in the Dark. *Organic Letters* **2020**, *22* (14), 5690–5694. https://doi.org/10.1021/acs.orglett.0c02075.

(139) Xu, B.; Shi, M. Ring-Opening Reactions of Methylenecyclopropanes Promoted by Metal Halides. *Organic Letters* **2003**, *5* (9), 1415–1418. https://doi.org/10.1021/ol034142k.

(140) Labes, R.; Battilocchio, C.; Mateos, C.; Cumming, G. R.; de Frutos, O.; Rincón, J. A.; Binder, K.; Ley, S. v. Chemoselective Continuous Ru-Catalyzed Hydrogen-Transfer Oppenauer-Type Oxidation of Secondary Alcohols. *Organic Process Research and Development* **2017**, *21* (9), 1419–1422. https://doi.org/10.1021/acs.oprd.7b00190.

(141) Labes, R.; González-Calderón, D.; Battilocchio, C.; Mateos, C.; Cumming, G. R.; de Frutos, O.; Rincón, J. A.; Ley, S. v. Rapid Continuous Ruthenium-Catalysed Transfer Hydrogenation of Aromatic Nitriles to Primary Amines. *Synlett* **2017**, *28* (20), 2855–2858. https://doi.org/10.1055/s-0036-1589096.

(142) Köckinger, M.; Hone, C. A.; Gutmann, B.; Hanselmann, P.; Bersier, M.; Torvisco, A.; Kappe, C. O. Scalable Continuous Flow Process for the Synthesis of Eflornithine Using Fluoroform as Difluoromethyl Source. *Organic Process Research and Development* **2018**, *22* (11), 1553–1563. https://doi.org/10.1021/acs.oprd.8b00318.

(143) Mata, A.; Hone, C. A.; Gutmann, B.; Moens, L.; Kappe, C. O. Continuous-Flow Pd-Catalyzed Carbonylation of Aryl Chlorides with Carbon Monoxide at Elevated Temperature and Pressure. *ChemCatChem* **2019**, *11* (3), 997–1001. https://doi.org/10.1002/cctc.201801974.

(144) Labes, R.; Mateos, C.; Battilocchio, C.; Chen, Y.; Dingwall, P.; Cumming, G. R.; Rincón, J. A.; Nieves-Remacha, M. J.; Ley, S. v. Fast Continuous Alcohol Amination Employing a

Hydrogen Borrowing Protocol. *Green Chemistry* **2019**, *21* (1), 59–63. https://doi.org/10.1039/c8gc03328e.

(145) Sagmeister, P.; Kaldre, D.; Sedelmeier, J.; Moessner, C.; Püntener, K.; Kummli, D.; Williams, J. D.; Kappe, C. O. Intensified Continuous Flow Synthesis and Workup of 1,5-Disubstituted Tetrazoles Enhanced by Real-Time Process Analytics. *Organic Process Research and Development* **2021**, *25* (5), 1206–1214. https://doi.org/10.1021/acs.oprd.1c00096.

(146) Sambiagio, C.; Ferrari, M.; van Beurden, K.; Ca', N. della; van Schijndel, J.; Noel, T. Continuous-Flow Synthesis of Pyrylium Tetrafluoroborates: Application to Synthesis of Katritzky Salts and Photoinduced Cationic RAFT Polymerization. *Organic Letters* **2021**, *23* (6), 2042–2047. https://doi.org/10.1021/acs.orglett.1c00178.

(147) Quesnel, J. S.; Kayser, L. v.; Fabrikant, A.; Arndtsen, B. A. Acid Chloride Synthesis by the Palladium-Catalyzed Chlorocarbonylation of Aryl Bromides. *Chemistry - A European Journal* **2015**, *21* (26), 9550–9555. https://doi.org/10.1002/chem.201500476.

(148) Schröder, N.; Wencel-Delord, J.; Glorius, F. High-Yielding, Versatile, and Practical [Rh(III)Cp*]-Catalyzed Ortho Bromination and Iodination of Arenes. *J Am Chem Soc* **2012**, *134* (20), 8298–8301. https://doi.org/10.1021/ja302631j.

(149) Mukhopadhyay, S.; Batra, S. Direct Transformation of Arylamines to Aryl Halides via Sodium Nitrite and N-Halosuccinimide. *Chemistry - A European Journal* **2018**, *24* (55), 14622–14626. https://doi.org/10.1002/chem.201803347.

(150) Moreira, J. A.; Corrêa, A. G. Enantioselective Synthesis of Three Stereoisomers of 5,9-Dimethylpentadecane, Sex Pheromone Component of Leucoptera Coffeella, from (-)-

Isopulegol. *Tetrahedron Asymmetry* **2003**, *14* (23), 3787–3795.

https://doi.org/10.1016/j.tetasy.2003.09.030.

Chapter 5 Pushing the Limits of Fe(III)-Catalysis: A Distinct Mechanistic Pathway Enables Additive-Free Reactivity

Davis, A. J.; Ferry, E. K.; Breen, C. P.; Zhang, J.; Reid, J. P.; Jamison, T. F.; Schindler, C. S.

unpublished.

5.1 Introduction

Over the last decade, carbonyl-olefin metathesis has materialized as a powerful strategy for the formation of carbon-carbon double bonds.[1] The Schindler lab pioneered these efforts, identifying $FeCl_3$ as an Earth-abundant Lewis acid catalyst capable of converting aryl ketones **1** to the corresponding cyclopentenes **3** (**Figure 5.1a**).[6,13] Although this original report targeted aryl ketones as the starting materials, the method was quickly adapted for the synthesis of trialkyl-substituted cyclopentenes **4** from aliphatic ketones.[24] Further advances have since been reported

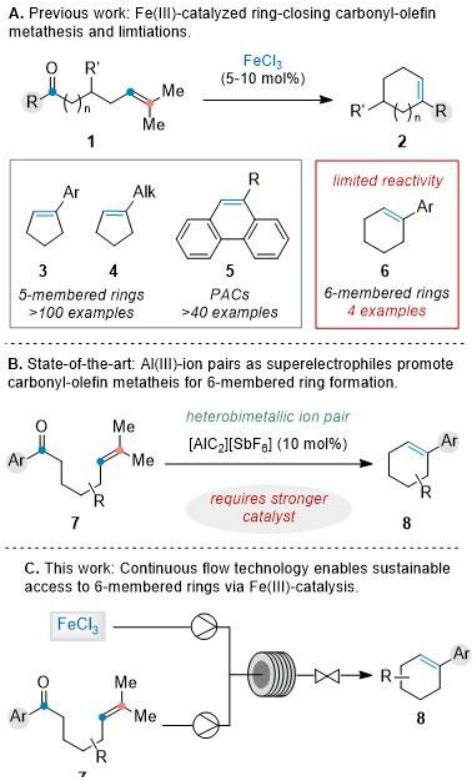

Figure 5.1. Strategies for 6-membered ring formation by carbonyl-olefin metathesis.

for the Lewis acid-catalyzed production of heterocyclic motifs,[15–17] as well as intermolecular ring-opening[20,21,27] and cross metathesis.[21,28,29] Despite these advances, most ring-closing methods were limited to the formation of 5-membered rings. Although a few catalysts could form 6-membered rings (**6**), these were limited to just a few examples,[6,17,21,22] as the unreactive nature of the starting materials led to diminished yields. The only reported general method for the formation of cyclohexenes was developed by the Schindler lab, which utilized $FeCl_3$ for the formation of polycycles **5**.[23] However, this method relied on the use of styrenyl aryl ketones, as prenylated olefins led to competing carbonyl-ene/elimination byproducts. To address the need for a more generalized method, the Schindler group identified an Al(III)-ion pair catalyst as a superelectrophilic Lewis acid that could promote cyclohexene formation (**8**) by carbonyl-olefin metathesis (**Figure 5.1b**).[70] Mechanistic investigations revealed that the ion pair, formed *in situ* from $AlCl_3$ and $AgSbF_6$, enabled a distinct mechanism following a carbonyl-ene/hydroalkoxylation pathway to provide the desired products. Although this report addressed an inherent limitation within the field, the use of Ag(I) additives represents a departure from the use of sustainable catalysts previously reported.[6,39,43] Additionally, the method required a glovebox setup to form the active catalyst species, limiting its overall accessibility.

We envisioned that transferring this reactivity from batch to a continuous flow process could enable a shift back to the use of a more sustainable catalyst system, while increasing the overall reaction efficiency (**Figure 5.1c**). Specifically, the use of a plug-flow reactor could allow for the reaction to take place under extreme thermal conditions,[140–146] enabling efficient catalyst turnover with $FeCl_3$. Importantly, this strategy would eliminate the need for precious metal additives, resulting in a more sustainable and accessible approach for the synthesis of larger ring systems. The results discussed in this chapter focus the development of a benchtop continuous flow approach for ring-closing carbonyl-olefin metathesis, including the overall scope and stability of the reactor. Mechanistic insights reveals that a distinct and unprecedented bimolecular pathway enables the return to monomeric $FeCl_3$ as the Lewis acid catalyst.

5.2 Results and Discussion

Our initial efforts focused on identifying suitable conditions for the incorporation flow technology to convert dichlorinated aryl ketone **9** to metathesis product **10** (**Figure 5.2**). To this end, we designed a tubular plug flow reactor outlined in **Figure 5.2**. Substrate and catalyst feeds

were introduced into the reactor *via* independent syringe pumps, and the combined reaction mixture was then flowed through a heated 1 mL reactor coil before exiting through a back pressure regulator. The outlet stream then enters a quench flask containing triethylamine, effectively terminating the reaction. A variety of Lewis acids were evaluated for their ability to promote the reaction in flow. $FeCl_3$ was the most efficient, providing 22% of **10** with a residence time of 7.1 minutes (entry 1).[6] Under identical conditions, both $GaCl_3$[37] and $InCl_3$ proved inferior as catalysts, producing just 6% and 3%, respectively, of the desired cyclohexene (entries 2-3). With $FeCl_3$ identified as the suitable Lewis acid, the catalyst loading was next considered. Increasing the loading from 10 mol% to 20 mol% resulted in a significant increase in productivity, with **10** formed in 87% with a residence time of 8.3 minutes (entry 4). Further extension of the residence time to 13.9 minutes resulted in a slightly reduced yield of 70%, likely due to thermal decomposition of **10** (entry 5). Next, a variety of solvents were evaluated for their ability to promote the metathesis reaction. Chlorinated solvents worked best, with 1,2-DCE proving optimal. Lower boiling DCM worked, providing a diminished yield of 22% of metathesis product **10** (entry 6). In an effort to move toward more sustainable reaction solvents, nonhalogenated solvents were also considered. However, polar solvents MeCN and THF resulted in complete inhibition of the reaction, likely due to competing Lewis acid/base interactions with the catalyst (entries 7-8). Nonpolar toluene also failed to provide any of **10** (entry 9). Lastly, temperature was evaluated. Temperatures below the boiling point of DCE (86 °C) resulted in reduced yields of **10** (entries 10-11).

With established conditions for the continuous synthesis of cyclohexenes, we evaluated the overall scope of the transformation (). Substrates bearing halogenated aryl rings worked

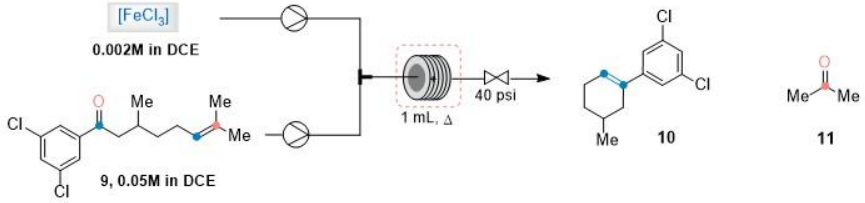

entry	Lewis acid	catalyst loading (mol%)	solvent	temperature (°C)	t_R (min)	yield **10** (%)	conv. **9** (%)
1	$FeCl_3$	10	DCE	110	7.1	22	48
2	$GaCl_3$	10	DCE	110	7.1	6	28
3	$InCl_3$	10	DCE	110	7.1	3	29
4	**$FeCl_3$**	**20**	**DCE**	**110**	**8.3**	**87**	**93**
5	$FeCl_3$	20	DCE	110	13.9	70	96
6[a]	$FeCl_3$	20	DCM	110	8.3	21	44
7	$FeCl_3$	20	MeCN	110	8.3	0	0
8	$FeCl_3$	20	THF	110	8.3	0	0
9	$FeCl_3$	20	Toluene	110	8.3	0	40
10	$FeCl_3$	20	DCE	80	8.3	11	42
11	$FeCl_3$	20	DCE	60	8.3	31	77

All runs were equilibrated for $3t_R$ before sample collection. Yields and conversions determined by ^{1}H NMR against 1,4-dinitrobenzene as internal standard. [a]Back pressure regulator set to 100 psi.

Figure 5.2. Reaction optimization.

exceptionally well, providing 64-99% of the metathesis products (**10, 14-17**). Interestingly, the residence time could be shortened to roughly 5 minutes without diminishing product formation. 4-Acylated **18** required a longer processing time of 16.7 minutes due to the additional Lewis basic carbonyl unit but was ultimately formed in 81%. 2-Brominated **19** also required a longer residence time and was formed in 63%. Cyclohexenes **20-22** were formed in 52-86% under a reduced catalyst loading of 10 mol%. To directly compare the efficiency of the plug-flow reactor, batch controls were ran using a 10 mol% loading of $FeCl_3$ for each substrate evaluated. 4-Trifluoromethylated **14** had the most dramatic increase in productivity, with an 85% increase in yield in flow over the batch process. In fact, every substrate evaluated benefitted from the translation to a continuous process, with reaction efficiency ranging from 26-201 times more productive than the corresponding batch processes. Electron-rich aryl ketones **23** and **24** were formed in 62% and 91% respectively, and required less thermal activation, proceeding at just 60 °C. Other electron-rich aryl fragments (**25-27**) failed to perform under either batch or continuous conditions, a limitation unresolved even under optimal Al(III)-ion pair catalysis.[6,70]

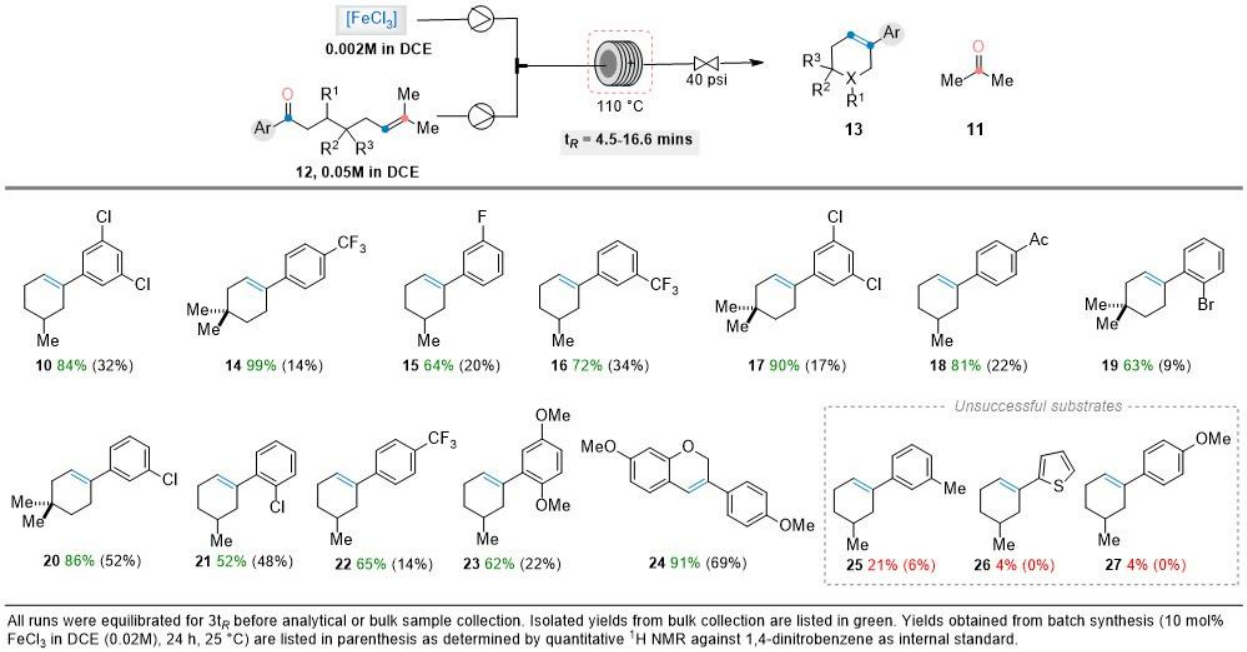

All runs were equilibrated for $3t_R$ before analytical or bulk sample collection. Isolated yields from bulk collection are listed in green. Yields obtained from batch synthesis (10 mol% $FeCl_3$ in DCE (0.02M), 24 h, 25 °C) are listed in parenthesis as determined by quantitative ^1H NMR against 1,4-dinitrobenzene as internal standard.

Figure 5.3. Substrate scope and limitations of continuous carbonyl-olefin metathesis.

To evaluate the stability of our plug-flow reactor, a longevity study was conducted to convert **28** to metathesis product **14** (**Figure 5.4**). After an equilibration period, the reaction mixture was collected over a 130-minute period (theoretical yield: 1.05 mmol), equating to a throughput of 99.8 mg/hr (entry 1). Batch controls using both $FeCl_3$[6] and $[AlCl_2][SbF_6]$[70] were

also performed on a 1.00 mmol scale for direct comparison and resulted in formation of **14** in 82% and 81%, respectively (entries 2-3). Batch synthesis of **14** employing $FeCl_3$ as the catalyst had the lowest throughput of just 9.5 mg/hr, while the Al(III)-ion pair had a slightly improved throughput

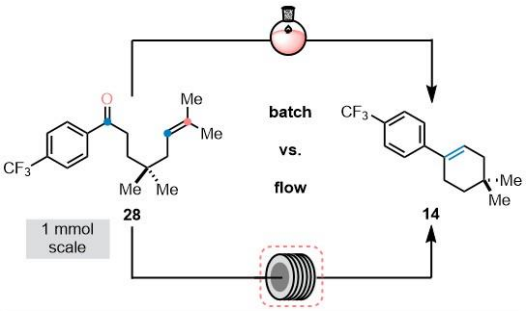

entry	reactor	catalyst	isolated yield (%)	throughput (mg/hr)
1	flow	$FeCl_3$	72	99.8
2	batch	$FeCl_3$	82	9.5
3	batch	$[AlCl_2][SbF_6]$	81	25.8

Conditions: Batch synthesis was performed on 1.0 mmol of **28** using 10 mol% $FeCl_3$ or 10 mol% $[AlCl_2][SbF_6]$ in DCE (0.02M). Continuous flow synthesis of **28** was performed by equilibrating reactor for $3t_R$, followed by a timed collection to produce a theoretical yield of 1.05 mmol of **29** based on molar flow rates.

Figure 5.4. Stability study for scaled-out synthesis of **14**.

of 25.8 mg/hr. Ultimately, the continuous process demonstrated superior productivity over both batch processes, with 10 times increase in product formation when iron was used, and roughly quadrupled improvement over the optimal batch catalyst.

5.3 Mechanistic Investigations

We next sought to explore the use of the plug-flow reactor to access metathesis products from differentially substituted olefins. Previous studies have demonstrated although the prenylated aryl ketones are converted to the metathesis product through a carbonyl-ene/hydroalkoxylation mechanism as the predominant path under Al(III)-ion pair catalysis.[70] However, styrenyl derived substrates such as **29** can also be converted to the cyclic product, suggesting that a direct [2+2]-cycloaddition/cycloreversion pathway is still possible as a secondary mechanism. However, when $FeCl_3$ was used as the Lewis acid catalyst under batch conditions, none of the desired product is observed. Additionally, when aryl ketone **29** is subjected to $FeCl_3$-catalyzed continuous flow

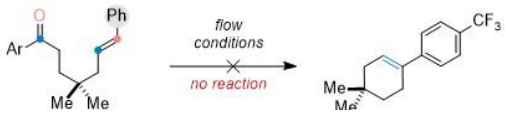

Figure 5.5. Styrenyl substrates fail to fail under continuous catalysis.

conditions, complete recovery of the starting material is achieved (**Figure 5.5**). This result represents a clear departure from previously observed reactivity trends in batch employing Al(III)-ion pair and suggests that formation of **14** is prohibitively high in energy when $FeCl_3$ is used as the active catalyst. To explore this possibility, we conducted computational investigations into the Fe(III)-catalyzed transformation.

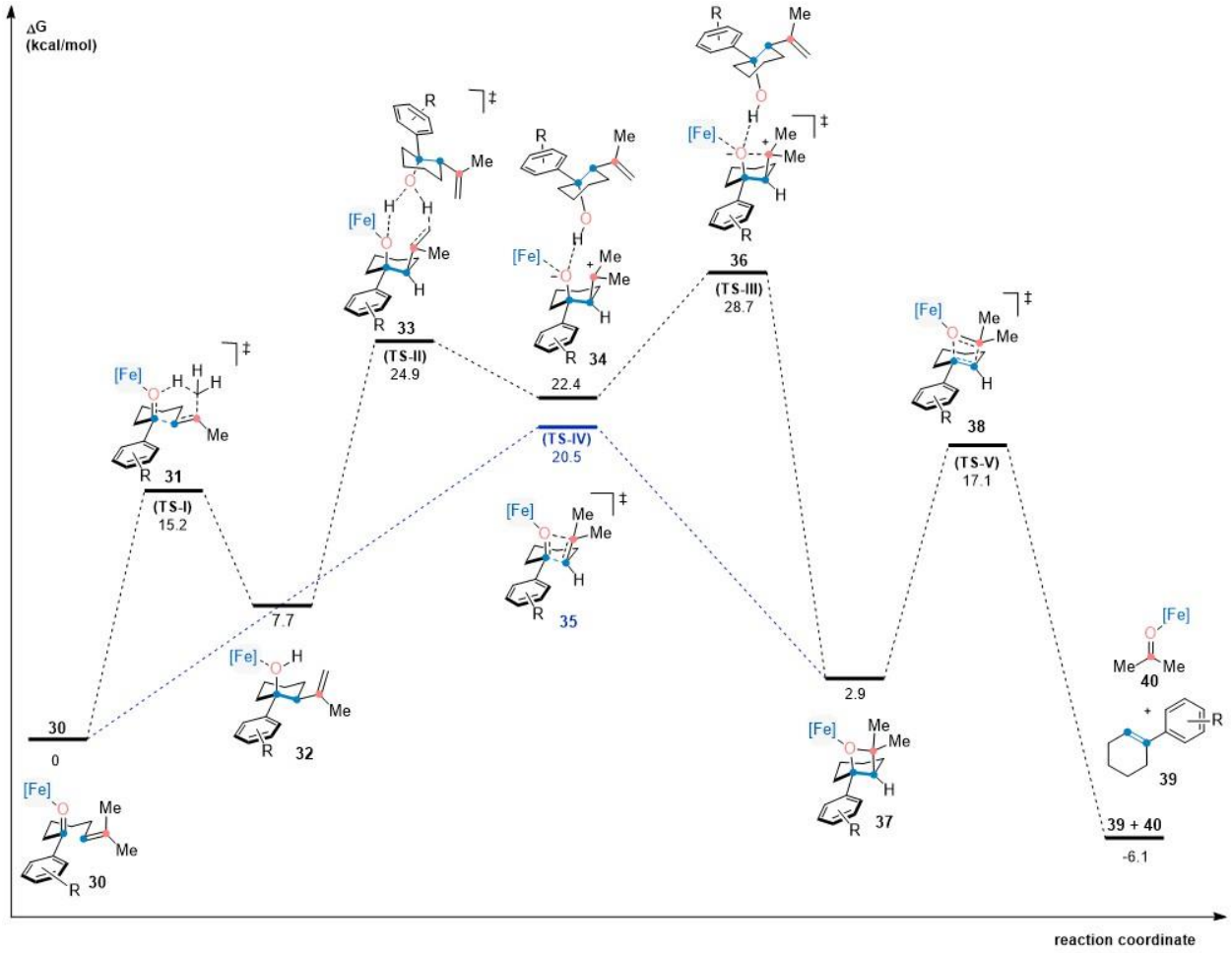

Figure 5.6. Computational pathways for continuous Fe(III)-catalysis.

Two distinct mechanistic pathways were identified from these computational studies (**Figure 5.6**). The first pathway (highlighted in blue) involves the direct [2+2]-cycloaddition of coordinated ketone **30** to from oxetane **37** directly. This was found to proceed via **35** (**TS-IV**) with a corresponding activation energy of +20.5 kcal/mol. The second pathway proceeds *via* a reversible carbonyl-ene reaction (**TS-I**) to form homoallylic alcohol **32**. Once formed, **32** is then converted to oxetane **37** through an unprecedented stepwise cycloaddition to form **37**. **33** (**TS-II**) is promoted *via* bimolecular activation of **32** to form cationic **34**, with an energy barrier of 22.4 kcal/mol. Importantly, this step represents the rate-limiting step of this pathway and is 3.3 kcal/mol

lower in energy that the direct [2+2]-cycloaddition (**TS-IV**). Hydrogen-bond assisted collapse of cation **34** (**TS-III**) leads to formation of oxetane **37**. Once formed, oxetane **37** - common to both mechanistic pathways - undergoes retro-[2+2]-cycloaddition (**TS-V**) to form the thermodynamically favored metathesis product **39** and carbonyl byproduct **40**. These computational findings corroborate the experimental evidence that direct [2+2]-cycloaddition is prohibitively costly in energy and does not serve as the active mechanism for cyclohexene formation under continuous Fe(III)-catalysis.

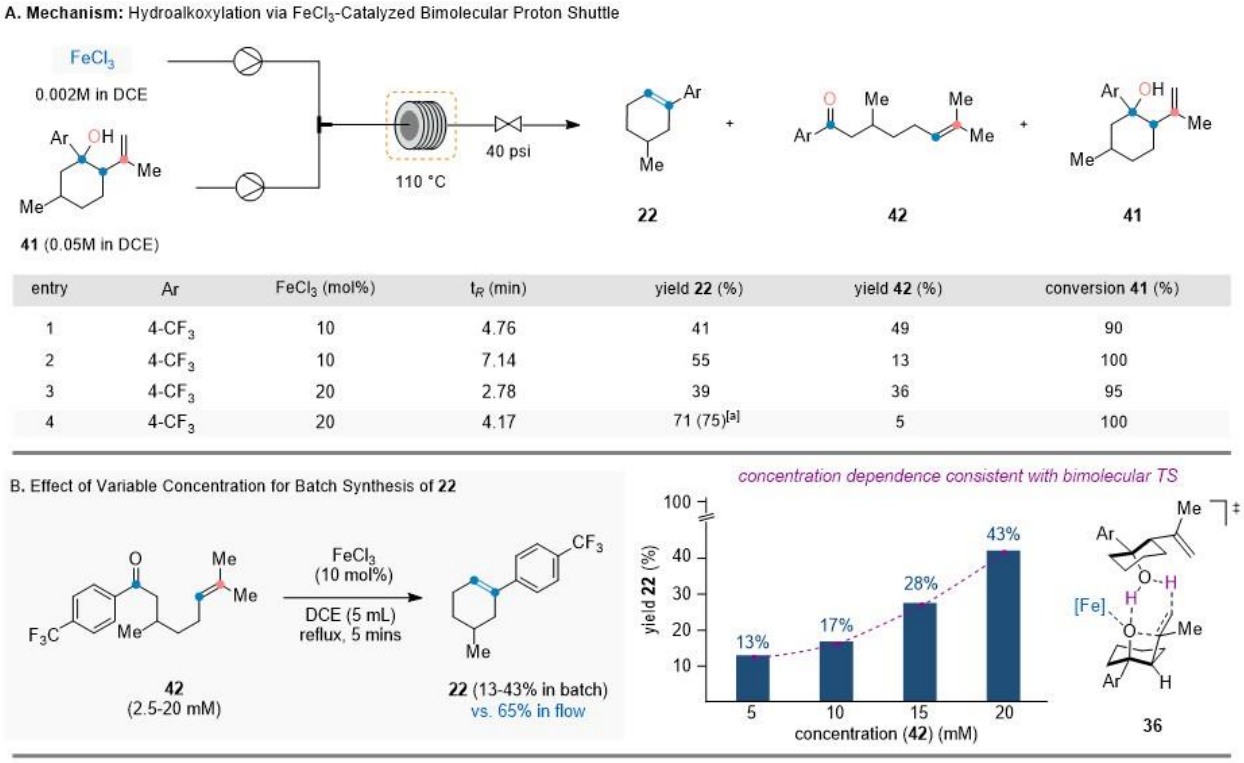

entry	Ar	$FeCl_3$ (mol%)	t_R (min)	yield **22** (%)	yield **42** (%)	conversion **41** (%)
1	4-CF_3	10	4.76	41	49	90
2	4-CF_3	10	7.14	55	13	100
3	4-CF_3	20	2.78	39	36	95
4	4-CF_3	20	4.17	71 (75)[a]	5	100

Figure 5.7. Mechanistic investigations for $FeCl_3$-catalyzed carbonyl-olefin metathesis in flow.

To gain additional support for the computationally suggested reaction pathway, we explored the reversible formation of carbonyl-ene product **22** under continuous conditions (**Figure 5.7A**). When the catalyst loading was reduced to 10 mol%, a residence times 4.76 minutes resulted in 90% conversion of carbonyl-ene **41**. Metathesis product **22** was formed in 41%, with the mass balance being the corresponding aryl ketone **42** (entry 1). This supports the computational findings that under $FeCl_3$-catalyzed conditions, there exists an equilibrium between the aryl ketones and carbonyl-ene adducts that heavily favors the former under the elevated temperatures. However, under more forcing conditions, such as extended the residence times (entry 2) and increased

catalyst loadings of 20 mol% (entries 3 and 4), the reaction is pushed toward formation of **19**, consistent with the higher energetic barriers observed computationally.

To probe the bimolecular nature of the transformation, batch reactions employing a range of concentrations of **42** were set up in refluxing DCE and quenched after 5 minutes (**Figure 5.7B**). At a concentration of 0.005M, metathesis product **22** was formed in just 13%. However, when the concentration was increased up to 0.02M under otherwise identical conditions, **22** was achieved in increasing yields of 17-43%. These results suggest a clear dependence on the concentration of the aryl ketone, consistent with a non-zero order substrate kinetics

5.4 Conclusions

The results contained within this chapter represent the successful translation of Fe(III)-catalyzed carbonyl-olefin metathesis from batch to a continuous flow platform. The plug-flow reactor design serves as an operationally simple and benchtop amenable alternative for the synthesis of larger ring systems while avoiding the use of unstable metal additives and costly tools and techniques. Longevity studies highlight the excellent stability of the reactor and increased throughput in comparison to traditional batch reactors. Computations revealed that an unprecedented pathway for metathesis *via* a preliminary carbonyl-ene reaction, followed by a unique bimolecular stepwise hydroalkoxylation serve as the active mechanism for Fe(III)-catalyzed reactivity, a stark departure from previously reported methods. Ultimately, this work marks a key first step in applying enabling technology to overcome the current challenges within the field of carbonyl-olefin metathesis and is expected to significantly alter the ways in which chemists address these outstanding limitations.

5.5 Experimental Procedures and Supplemental Information

5.5.1 General Information

Materials and instrumentation

All chemicals were purchased from commercial suppliers and were used as received unless otherwise stated. Proton Nuclear Magnetic Resonance (^{1}H NMR) spectra and Carbon Nuclear Magnetic Resonance (^{13}C NMR) spectra were recorded on a Varian Unity Plus 400, Varian MR400, Varian vnmrs 500, Varian Inova 500, Varian Mercury 500, and Varian vnmrs 700

spectrometers. Chemical shifts for protons are reported in parts per million and are referenced to the NMR solvent peak ($CDCl_3$: δ 7.26). Chemical shifts for carbons are reported in parts per million and are referenced to the carbon resonances of the NMR solvent ($CDCl_3$: δ 77.16). Data is represented as follows: chemical shift, integration, multiplicity (br = broad, s = singlet, d = doublet, t = triplet, q = quartet, p = pentet, m = multiplet), and coupling constants in Hertz (Hz). Mass spectroscopic (MS) data was recorded at the Mass Spectrometry Facility at the Department of Chemistry of the University of Michigan in Ann Arbor, MI on an Agilent Q-TOF HPLC-MS with EI high resolution mass spectrometer. Infrared (IR) spectra were obtained using either an Avatar 360 FT-IR or Perkin Elmer Spectrum BX FT-IR spectrometer. IR data are represented as frequency of absorption (cm^{-1}).

Continuous Flow Equipment and Supplies

Liquid reagents were delivered by syringe pumps sourced from Harvard Apparatus (,Part # 70-3007Holliston, MA) utilizing stainless steel syringes with PTFE sealed plungers also purchased from Harvard Apparatus (Part # 70-2267, 70-2251). Tubular reactors were constructed by hand using high-purity perfluoroalkyl (PFA) tubing (ID = 0.020",OD = 1/16") and PEEK fittings were sourced from IDEX Health & Science, LLC (Oak Harbor, WA). Stainless steel fittings were sourced from Swagelok (Solon, OH) were also used to construct tubular reactors. An adjustable pack pressure regulator (BPR) was purchased from Zaiput Flow Technologies (Part # BPR-10,Waltham, MA).

Abbreviations used

THF = tetrahydrofuran, TLC = thin layer chromatography, IBX = 2-iodoxybenzoic acid, DMSO = dimethylsulfoxide, Na_2SO_4 = sodium sulfate, EtOAc = ethyl acetate, DMF = dimethylformamide, DCM = dichloromethane, K_2CO_3 = potassium carbonate, KI = potassium iodide, NaH = sodium hydride, *t*BuOK = potassium *tert*-butoxide, DCE = 1,2-dichloroethane, Et_2O = diethyl ether, PBr_3 = phosphorus tribromide, $FeCl_3$ = iron(III) chloride, $InCl_3$ = indium(III) chloride, $GaCl_3$ = gallium(III) chloride, adjustable back pressure regulator = BPR, PCC = pyridinium chlorochromate, TMSCl = chlorotrimethylsilane

5.5.2. Synthesis of Substrates and Intermediates

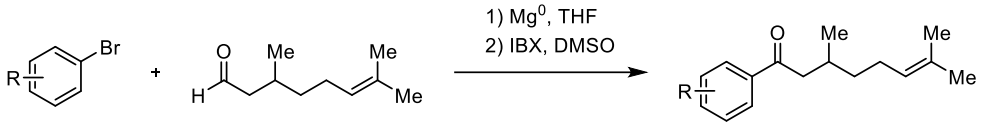

General Procedure A. Grignard Protocol and IBX Oxidation of Citronellal-derived Substrates

A flame-dried round-bottom flask containing a stir bar was charged with 2,6-dimethyl-5-heptanal (1.0 equiv.) and dry DCM (0.2M). The solution was cooled to 0°C and KOtBu (1.3 equiv.) was added in 3 portions. The resulting solution was stirred at 0°C for 15 minutes. Benzylic halide (1.3 equiv.) was added dropwise via syringe. The reaction was warmed to room temperature and stirred until judged complete by TLC analysis. The reaction was quenched with aq. NH_4Cl and diluted with DCM. The aqueous solution was extracted with DCM three times, and the combined organics were washed with brine, dried over Na_2SO_4, filtered and concentrated under reduced pressure. The crude alcohol was added to a round bottom flask equipped with a stir bar and DMSO (0.2M) was added. IBX (1.2 equiv.) was added, and the reaction was stirred at room temperature until judged complete by TLC analysis. The reaction was then quenched by the addition of water and EtOAc and allowed to stir an addition hour. The resulting mixture was filtered over Celite, and the aqueous layer was extracted three times with EtOAc. The combined organics were washed with brine, dried over Na_2SO_4, filtered, and concentrated under reduced pressure. The crude product was purified by column chromatography to afford pure metathesis substrate.

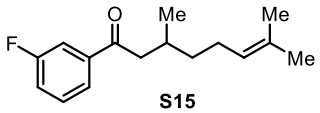

S15

1-(3-fluorophenyl)-3,7-dimethyloct-6-en-1-one (S15): The Grignard addition and IBX oxidation protocol was performed on 15.0 mmol scale. Purification by flash chromatography eluting with hexanes/EtOAc (93:7) provided 2.41g (65%) of S15 as a clear, colorless oil. **^{1}H NMR** (500MHz; $CDCl_3$): δ 7.72 (dd, *J* = 7.8, 1.3 Hz, 1H), 7.62 (dt, *J* = 9.6, 2.1 Hz, 1H), 7.43 (td, *J* = 8.0, 5.5 Hz,

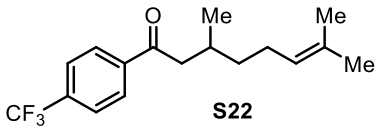

S22

1H), 7.30 – 7.20 (m, 1H), 5.09 (t, *J* = 7.1 Hz, 1H), 2.94 (dd, *J* = 15.9, 5.5 Hz, 1H), 2.72 (dd, *J* = 15.9, 8.1 Hz, 1H), 2.17 (m, 1H), 2.02 (m, 2H), 1.68 (s, 3H), 1.60 (s, 3H), 1.41 (m, 1H), 1.29 (m, 2H), 0.96 (d, *J* = 6.6 Hz, 4H); **^{13}C NMR** (126 MHz, $CDCl_3$): δ 199.1 (d, *J* = 2.1 Hz), 163.9 (d, *J* = 247.7 Hz), 139.7 (d, *J* = 5.9 Hz), 131.7, 130.3 (d, *J* = 7.6 Hz), 124.4, 123.9 (d, *J* = 3.0 Hz), 119.9 (d, *J* = 21.5 Hz), 114.9 (d, *J* = 22.2 Hz), 46.1, 37.2, 29.6, 25.8, 25.6, 20.0, 17.8. **IR:** 2964, 2916, 2855, 1687, 1589, 1441, 1244, 785, 682; **HRMS:** calcd for $C_{16}H_{21}FO^+$: 248.1576; found: 248.1586

3,7-dimethyl-1-(4-(trifluoromethyl)phenyl)oct-6-en-1-one (S22): The Grignard addition and IBX oxidation protocol was performed on 8.32 mmol scale. Purification by flash chromatography eluting with hexanes/EtOAc (93:7) provided 1.93 (78%) of S22 as a clear, colorless oil. Spectral data was found to be in accordance with literature spectra.[70] **^{1}H NMR**: (500 MHz; CDCl3) δ 8.04 (d, *J* = 8.1 Hz, 2H), 7.73 (d, *J* = 8.2 Hz, 2H), 5.09 (t, *J* = 7.1 Hz, 1H), 2.98 (dd, *J* = 16.0, 5.5 Hz, 1H), 2.77 (dd, *J* = 16.0, 8.1 Hz, 1H), 2.28 – 2.11 (m, *J* = 6.5 Hz, 1H), 2.01 (ddt, *J* = 21.9, 14.6, 7.2 Hz, 2H), 1.68 (s, 3H), 1.60 (s, 3H), 1.48 – 1.36 (m, 1H), 1.36 – 1.24 (m, 1H), 0.97 (d, *J* = 6.6 Hz, 3H).

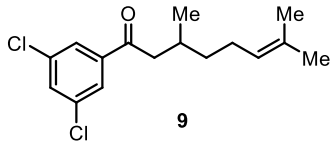

9

1-(3,5-dichlorophenyl)-3,7-dimethyloct-6-en-1-one (9): The Grignard addition and IBX oxidation protocol was performed on 5.40 mmol scale. Purification by flash chromatography eluting with hexanes/EtOAc (93:7) provided 1.11 (69%) of **9** as a clear, colorless oil. Spectral data was found to be in accordance with literature spectra.[70] **^{1}H NM**R (500 MHz; $CDCl_3$) δ 7.78 (s, 2H), 7.53 (s, 1H), 5.09 (t, *J* = 6.8 Hz, 1H), 2.90 (dd, *J* = 16.1, 5.5 Hz, 1H), 2.69 (dd, *J* = 16.1, 8.1 Hz, 1H), 2.15 (dq, *J* = 13.3, 6.7 Hz, 1H), 2.02 (ddt, *J* = 22.5, 14.5, 7.4 Hz, 2H), 1.68 (s, 3H), 1.60 (s, 3H), 1.45 – 1.35 (m, 1H), 1.34 – 1.23 (m,1H), 0.96 (d, *J* = 6.6 Hz, 3H).

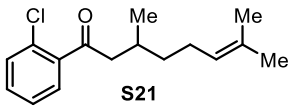

S21

1-(2-chlorophenyl)-3,7-dimethyloct-6-en-1-one (S21): The Grignard addition and IBX oxidation protocol was performed on 4.86 mmol scale. Purification by flash chromatography eluting with hexanes/EtOAc (93:7) provided 1.06 (82%) of **S21** as a clear, colorless oil. Spectral data was found to be in accordance with literature spectra.[70] **^{1}H NMR** (500 MHz; $CDCl_3$) δ 7.48 – 7.28 (m, 4H), 5.07 (t, *J* = 6.2 Hz, 1H), 2.95 (dd, *J* = 16.3, 5.7 Hz, 1H), 2.75 (dd, *J* = 16.3, 8.1 Hz, 1H), 2.11 (h, *J* = 6.8 Hz, 1H), 1.99 (hept, *J* = 7.5 Hz, 2H), 1.66 (s, 3H), 1.58 (s, 3H), 1.38 (ddt, *J* = 16.7, 13.4, 6.7 Hz, 1H), 1.31 – 1.17 (m, 1H), 0.97 (d, *J* = 6.6 Hz, 3H).

ethyl 3,5-dichlorobenzoate (E1): A flame-dried 500 mL RBF equipped with a stir bar was charged with anhydrous DCM (200 mL, 0.2M), ethanol (4.67 mL, 80.0 mmol, 2.0 equiv.) and

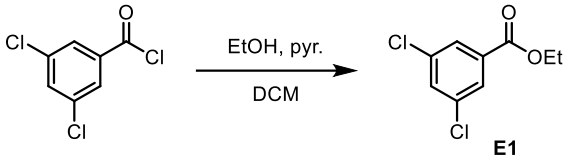

E1

pyridine (3.87 mL, 1.2 mmol, 1.2 equiv.). The solution was then cooled to 0°C, 3,5-dichlorobenzoyl chloride (8.38 g, 40.0 mmol 1.0 equiv.) was added as a single portion. The reaction was warmed to room temperature and stirred until judged complete by TLC analysis. The reaction was then quenched with aq. NH_4Cl and extracted with DCM (3 x 25 mL). The combined organics were washed with brine, dried over Na_2SO_4, and concentrated under reduced pressure. The crude ester was used without further purification. Spectral data was found to be in accordance with literature data.[147] **^{1}H NMR**: (500 MHz; $CDCl_3$): δ 7.90 (s, 2H), 7.53 (d, *J* = 1.9 Hz, 1H), 4.39 (q, *J* = 7.2 Hz, 2H), 1.40 (t, *J* = 7.1 Hz, 3H).

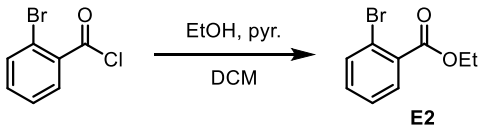

E2

ethyl 2-bromobenzoate (E2): A flame-dried 250 mL RBF equipped with a stir bar was charged with anhydrous DCM (120 mL, 0.17M), ethanol (2.22 mL, 38.1 mmol, 2.0 equiv.) and pyridine (1.85 mL, 22.9 mmol, 1.2 equiv.). The solution was then cooled to 0°C, 2-bromobenzoyl chloride (4.39 g, 20.0 mmol, 1.0 equiv.) was added as a single portion. The reaction was warmed to room

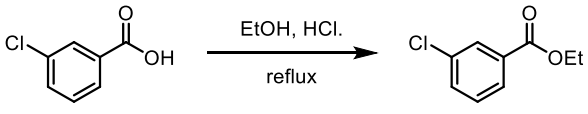

E3

temperature and stirred until judged complete by TLC analysis. The reaction was then quenched with aq. NH_4Cl and extracted with DCM (3 x 10 mL). The combined organics were washed with brine, dried over Na_2SO_4, and concentrated under reduced pressure. The crude ester was used without further purification. Spectral data was found to be in accordance with literature data.[148] **^{1}H NMR**: (500 MHz; $CDCl_3$) δ 7.78 (dd, *J* = 7.7, 1.8 Hz, 1H), 7.66 (d, *J* = 8.2 Hz, 1H), 7.55 – 7.28 (m, 2H), 4.41 (q, *J* = 7.2 Hz, 2H), 1.41 (t, *J* = 7.1 Hz, 3H).

ethyl 3-chlorobenzoate (E3): A 250 mL RBF equipped with a stir bar was charged with EtOH (66 mL, 0.3 M), 3-chlorobenzoic acid (3.13 g, 20.0 mmol, 1 equiv.) and 0.50 mL of aq. HCl. The flask was sealed with a N_2-flushed reflux condenser and refluxed overnight. The reaction was cooled to room temperature and washed with aq. $NaHCO_3$, then extracted 3 x 25 mL EtOAc. The combined organics were washed with brine, dried over Na_2SO_4, and concentrated under reduced pressure. The crude ester was used without further purification. Spectral data was found to be in accordance with literature data.[149] **^{1}H NMR** (500 MHz; $CDCl_3$): δ 8.02 (s, 1H), 7.93 (d, *J* = 7.8 Hz, 1H), 7.52 (d, *J* = 8.0 Hz, 1H), 7.38 (t, *J* = 7.8 Hz, 1H), 4.38 (q, *J* = 7.2 Hz, 2H), 1.40 (t, *J* = 7.1 Hz, 3H).

General Procedure B. Synthesis of Aryl-Substituted Phosphonate Esters

A flame-dried RBF equipped with a stir bar was charged with anhydrous THF (0.2 M) and placed under N_2 atmosphere. Diisopropylamine (1.2 equiv.) was added via syringe, and the solution was cooled to -78 °C. *n*-Butyllithium (1.2 equiv, 1.6M solution in hexanes) was added dropwise, and the solution was stirred at the same temperature for 20 minutes. At this time, dimethyl methyl phosphonate (1.1 equiv.) was added dropwise via syringe, and the reaction was stirred at the same temperature for 20 minutes. Aryl ester (1.0 equiv.) was added dropwise via syringe, and the

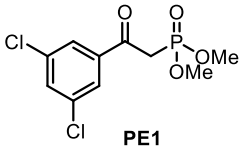

PE1

reaction was warmed to room temperature and stirred until judged completed by TLC analysis. The reaction was quenched with aq. NH_4Cl and extracted with EtOAc (3 x 20 mL). The combined organics were washed with brine, dried over Na_2SO_4, and concentrated under reduced pressure. Purification by flash chromatography eluting with 100% EtOAc provided the pure phosphonate ester.

dimethyl (2-(3,5-dichlorophenyl)-2-oxoethyl)phosphonate (PE1): General procedure B was performed on 9.13 mmol scale using ethyl 3,5-dichlorobenzoate. Purification by flash chromatography eluting with 100% EtOAc provided 2.34 g (86%) of **PE1** as a white solid. **^{1}H NMR** (500 MHz; $CDCl_3$): δ 7.86 (d, *J* = 1.9 Hz, 2H), 7.58 (t, *J* = 1.9 Hz, 1H), 3.81 (s, 3H), 3.79 (s, 3H), 3.58 (d, *J* = 22.7 Hz, 2H); **^{13}C NMR** (176 MHz, $CDCl_3$): δ 189.6, 138.8, 135.9, 133.6, 127.6, 53.5, 38.3, 37.6; **IR:** 3071, 2959, 2934, 2855, 1680, 1252, 1027, 830, 796; **HRMS:** calcd for $C_{10}H_{11}Cl_2O_4P^+$: 295.9772; found 295.9782.

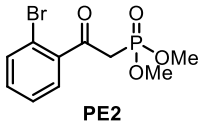

PE2

dimethyl (2-(2-bromophenyl)-2-oxoethyl)phosphonate (PE2): General procedure B was performed on 12.8 mmol scale using ethyl 2-bromobenzoate. Purification by flash chromatography eluting with 100% EtOAc provided 2.72 g (69%) of **PE2** as a white solid. **^{1}H NMR** (500 MHz; $CDCl_3$): δ 7.96 (t, *J* = 1.9 Hz, 1H), 7.91 – 7.82 (m, 1H), 7.64 – 7.51 (m, 1H), 7.43 (t, *J* = 7.9 Hz, 1H), 3.79 (s, 3H), 3.77 (s, 3H), 3.61 (d, *J* = 22.7 Hz, 2H); **^{13}C NMR** (176 MHz, $CDCl_3$): δ 190.7 (d, $^2J_{C,P}$ = 6.7 Hz), 138.0 (d, $^3J_{C,P}$ = 2.4 Hz), 135.2, 133.8, 130.2, 129.0, 127.3, 53.4 (d, $^1J_{C,P}$ = 6.6 Hz), 38.3, 37.3; **IR:** 3465, 2963, 2917, 1690, 1251, 1215, 1044, 1020, 1000, 781; **HRMS:** calcd for $C_{10}H_{13}BrPO_4^+$: 306.9726; found 306.9735.

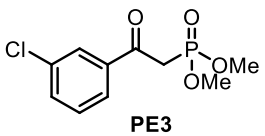

PE3

dimethyl (2-(3-chlorophenyl)-2-oxoethyl)phosphonate (PE3): General procedure B was performed on 16.9 mmol scale using ethyl 3-chlorobenzoate. Purification by flash chromatography eluting with 100% EtOAc provided 4.15 g (94%) of **PE3** as a green oil**^{1}H NMR**(500 MHz; $CDCl_3$): δ 7.62 (dd, *J* = 8.0, 1.2 Hz, 1H), 7.55 (dd, *J* = 7.7, 1.7 Hz, 1H), 7.40 (td, *J* = 7.5, 1.2 Hz,

1H), 7.32 (td, *J* = 7.7, 1.7 Hz, 1H), 3.77 (s, 3H), 3.75 (s, 3H), 3.70 (d, *J* = 22.2 Hz, 2H); **^{13}C NMR** (176 MHz, $CDCl_3$): δ 195.1 (d, $^2J_{C,P}$ = 6.8 Hz), 140.7 (d, $^3J_{C,P}$ = 2.3 Hz), 133.9, 132.5, 129.8, 127.7, 119.1, 53.3 (d, $^1J_{C,P}$ = 6.4 Hz), 41.6, 40.6; **IR:** 3068, 2957, 2854, 1736, 1683, 1251, 1023, 813, 788, 676; **HRMS:** calcd for $C_{10}H_{13}ClPO_4^+$: 263.0234; found 263.0244.

General Procedure C. Synthesis of Alkylated Aldehyde Intermediates

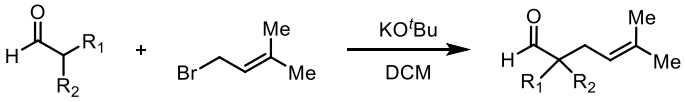

A flame-dried RBF equipped with a stir bar was charged with dry DCM (0.1M) and KO^{t}Bu (1.3 equiv.). The mixture was placed under N_2 atmosphere and cooled to 0°C, and the aldehyde (1.0 equiv.) was added dropwise via syringe. After stirring for 15 minutes at the same temperature, 3,3-dimethyl bromide (1.3 equiv.) was added dropwise via syringe. The resulting mixture was warmed to room temperature and stirred until judged complete by TLC analysis. The reaction was quenched with aq. NH_4Cl and extracted with DCM (3x10 mL). The combined organics were washed with brine, dried over Na_2SO_4, and concentrated under reduced pressure. Purification by flash chromatography provided the pure aldehyde.

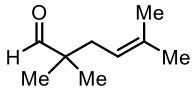

A1

2,2,5-trimethylhex-4-enal (A1): General procedure C was performed on 60.0 mmol scale using isobutyraldehyde. Purification by flash chromatography eluting with 75:25 hexanes/DCM provided 4.99 g (59%) of **A1** as a clear oil. Spectral data was found to be in accordance with literature data.[70] **^{1}H NMR** (500 MHz; $CDCl_3$): δ 9.47 (s, 1H), 5.05 (t, *J* = 7.6 Hz, 1H), 2.15 (d, *J* = 7.6 Hz, 2H), 1.70 (s, 3H), 1.60 (s, 3H), 1.04 (s, 6H).

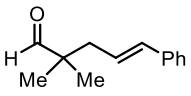

A2

(*E*)-2,2-dimethyl-5-phenylpent-4-enal (A2): General procedure C was performed on 41.6 mmol scale using isobutyraldehyde. Purification by flash chromatography eluting with 75:25 hexanes/DCM provided 7.16 g (91%) of **A2** as a clear oil. Spectral data was found to be in accordance with literature data.[70] **^{1}H NMR** (500 MHz; $CDCl_3$): 9.54 (s, 1H), 7.40 – 7.27 (m, 4H), 7.22 (t, *J* = 7.0 Hz, 1H), 6.43 (d, *J* = 15.7 Hz, 1H), 6.12 (dt, *J* = 15.5, 7.6 Hz, 1H), 2.38 (d, *J* = 7.6 Hz, 2H), 1.12 (s, 6H).

General Procedure D. Horner-Wadsworth-Emmons Olefination

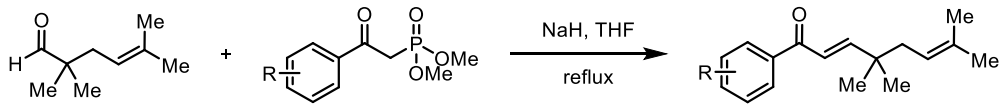

A flame-dried RBF equipped with a stir bar was charged with NaH (1.2 equiv., 60% dispersion in mineral oil) and anhydrous THF and placed under N_2 atmosphere. The solution was cooled to 0 °C, and phosphonate ester (1.1 equiv.) was added dropwise via syringe. The reaction was warmed to room temperature and stirred for 20 minutes. Aldehyde XX (1.0 equiv.) was added dropwise

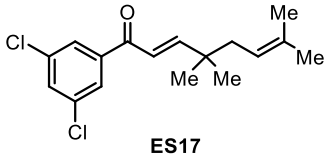

ES17

via syringe. The reaction was capped with a N_2-flushed reflux condenser and heated to 80 °C. Once judged complete by TLC analysis, the reaction was cooled to room temperature and quenched with aq. NH_4Cl, then extracted with 3 x 15 mL EtOAc. The combined organics were washed with brine, dried over Na_2SO_4, and concentrated under reduced pressure. Purification by flash chromatography provided pure enone.

(E)-1-(3,5-dichlorophenyl)-4,4,7-trimethylocta-2,6-dien-1-one (ES17): General procedure D was performed on 6.06 mmol scale. Purification by flash chromatography eluting with 95:5 hexanes/EtOAc provided 1.34 g (71%) of **ES17** as a green oil. Spectral data was found to be in accordance with literature data.[70] **^{1}H NMR** (500 MHz; $CDCl_3$): δ 7.74 (d, *J* = 1.9 Hz, 2H), 7.54 (t, *J* = 1.8 Hz, 1H), 7.06 (d, *J* = 15.7 Hz, 1H), 6.63 (d, *J* = 15.7 Hz, 1H), 5.11 (ddt, *J* = 7.6, 6.1, 1.5 Hz, 1H), 2.11 (d, *J* = 7.6 Hz, 2H), 1.73 (s, 3H), 1.61 (s, 3H), 1.13 (s, 6H).

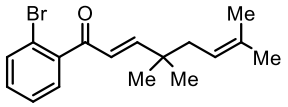

ES19

(E)-1-(2-bromophenyl)-4,4,7-trimethylocta-2,6-dien-1-one (ES19): General procedure D was performed on 5.37 mmol scale. Purification by flash chromatography eluting with 95:5 hexanes/EtOAc provided 1.50 g (87%) of **ES19** as a green oil. Spectral data was found to be in accordance with literature data.[70] **^{1}H NMR** (500 MHz; $CDCl_3$): δ 7.60 (d, *J* = 8.0 Hz, 1H), 7.36 (d, *J* = 7.2 Hz, 1H), 7.30 (m, 2H), 6.62 (d, *J* = 16.1 Hz, 1H), 6.33 (d, *J* = 16.1 Hz, 1H), 5.07 (t, *J* = 8.0 Hz, 1H), 2.04 (d, *J* = 7.6 Hz, 2H), 1.68 (s, 3H), 1.54 (s, 3H), 1.06 (s, 6H).

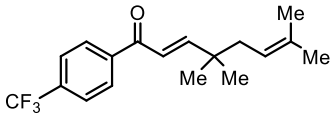

ES28

(E)-4,4,7-trimethyl-1-(4-(trifluoromethyl)phenyl)octa-2,6-dien-1-one (ES28): General procedure D was performed on 4.28 mmol scale. Purification by flash chromatography eluting with 96:4 hexanes/EtOAc provided 1.12 g (75%) of **ES28** as a green oil. Spectral data was found to be in accordance with literature data.[70] **^{1}H NMR** (500 MHz; $CDCl_3$): δ 7.99 (d, *J* = 8.1 Hz, 2H), 7.73 (d, *J* = 8.1 Hz,20H), 7.04 (d, *J* = 15.8 Hz, 1H), 6.70 (d, *J* = 15.8 Hz, 1H), 5.11 (t, *J* = 7.5 Hz, 1H), 2.11 (d, *J* = 7.6 Hz, 2H), 1.72 (s, 3H), 1.60 (s, 3H), 1.13 (s, 6H).

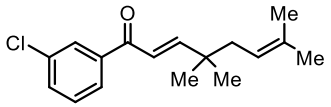

ES20

(E)-1-(3-chlorophenyl)-4,4,7-trimethylocta-2,6-dien-1-one (ES20): General procedure D was performed on 5.35 mmol scale. Purification by flash chromatography eluting with 95:5 hexanes/EtOAc provided 1.17 g (71%) of **ES20** as a green oil. **^{1}H NMR** (500 MHz; $CDCl_3$): δ 7.87 (s, 1H), 7.78 (d, *J* = 7.8 Hz, 1H), 7.52 (d, *J* = 7.9 Hz, 1H), 7.41 (t, *J* = 7.8 Hz, 1H), 7.04 (d, *J* = 15.7 Hz, 1H), 6.68 (d, *J* = 15.7 Hz, 1H), 5.11 (t, *J* = 7.6 Hz, 1H), 2.11 (d, *J* = 7.6 Hz, 2H), 1.72 (s, 3H), 1.60 (s, 3H), 1.12 (s, 6H); **^{13}C NMR** (176 MHz, $CDCl_3$): δ 190.3, 160.1, 134.0, 134.9,

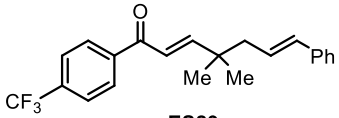

ES29

134.3, 132.6, 130.0, 128.8, 126.8, 121.8, 120.0, 40.5, 38.4, 26.3, 26.2, 18; **IR:** 3542, 3078, 2949, 2926, 1637, 1605, 1508, 1223, 1156, 830, 820; **HRMS**: calcd for $C_{17}H_{21}ClO^{+}$: 276.1281; found: 276.1281.

(2E,6E)-4,4-dimethyl-7-phenyl-1-(4-(trifluoromethyl)phenyl)hepta-2,6-dien-1-one (ES29): General procedure D was performed on 6.00 mmol scale. Purification by flash chromatography eluting with 95:5 hexanes/EtOAc provided 1.60 g (74%) of **ES29** as a green oil. Spectral data was found to be in accordance with literature data.[70] **^{1}H NMR** (500 MHz; $CDCl_3$): δ 7.97 (d, *J* = 8.0 Hz, 2H), 7.69 (d, *J* = 8.1 Hz, 2H), 7.34 (d, *J* = 7.4 Hz, 2H), 7.30 (t, *J* = 7.6 Hz, 2H), 7.22 (t, *J* = 7.3 Hz, 1H), 7.08 (d, *J* = 15.8 Hz, 1H), 6.74 (d, *J* = 15.8 Hz, 1H), 6.42 (d, *J* = 15.7 Hz, 1H), 6.16 (dt, *J* = 15.4, 7.6 Hz, 1H), 2.35 (d, *J* = 7.6 Hz, 2H), 1.20 (s, 6H).

General Procedure E. 1,4-Reduction of Enones for Synthesis of Aryl Ketone Substrates:

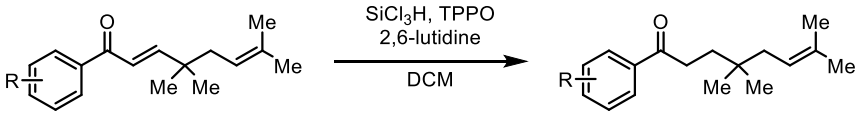

A flame-dried RBF equipped with a stir bar was charged with anhydrous DCM (0.1M) enone (1.0 equiv.) and triphenylphosphine oxide (0.2 equiv.). The flask was placed under N_2 atmosphere and cooled to 0 °C. At this temperature, 2,6-lutidine (2.0 equiv.) was added dropwise via syringe, followed by trichlorosilane (2.0 equiv.). The reaction was then warmed to room temperature and

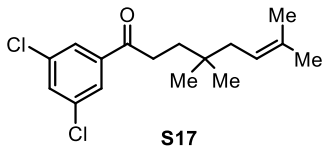

S17

stirred until judged complete by TLC analysis. The reaction was quenched by cooling to 0°C and adding a few drops of water. The crude mixture was then adsorbed to Celite and purified by flash chromatography to provide pure metathesis substrate.

1-(3,5-dichlorophenyl)-4,4,7-trimethyloct-6-en-1-one (S17): General procedure E was performed on 4.67 mmol scale. Purification by flash chromatography eluting with 95:5 hexanes/EtOAc provided 1.01 g (75%) of **S17** as a green oil. Spectral data was found to be in accordance with literature data.[70] **^{1}H NMR** (500 MHz; $CDCl_3$): δ 7.79 (d, *J* = 1.7 Hz, 2H), 7.54 (s,

1H), 5.18 (t, *J* = 7.1 Hz, 1H), 2.94 – 2.76 (m, 2H), 1.94 (d, *J* = 7.6 Hz, 2H), 1.73 (s, 3H), 1.69 – 1.51 (m, 5H), 0.92 (s, 6H).

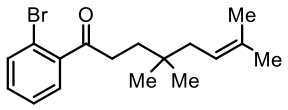

S19

1-(2-bromophenyl)-4,4,7-trimethyloct-6-en-1-one (S19): General procedure E was performed on 4.31 mmol scale. Purification by flash chromatography eluting with 75:25 hexanes/DCM provided 864 mg (57%) of **S19** as a green oil. Spectral data was found to be in accordance with literature data.[70] **^{1}H NMR** (500 MHz; $CDCl_3$): δ 7.60 (d, *J* = 7.5 Hz, 1H), 7.45 – 7.33 (m, 2H), 7.28 (m, 1H), 5.17 (t, *J* = 7.6 Hz1H), 2.94 – 2.78 (m, 2H), 1.90 (d, *J* = 7.6 Hz, 2H), 1.71 (s, 3H), 1.68 – 1.60 (m, 2H), 1.59 (s, 3H), 0.88 (s, 6H).

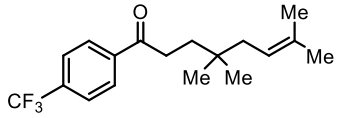

28

4,4,7-trimethyl-1-(4-(trifluoromethyl)phenyl)oct-6-en-1-one (28): General procedure E was performed on mmol scale. Purification by flash chromatography eluting with 70:30 hexanes/DCM provided 855 g (73%) of **28** as a green oil. Spectral data was found to be in accordance with literature data.[70] **^{1}H NMR** (500 MHz; $CDCl_3$): δ 8.05 (d, *J* = 8.6 Hz, 2H), 7.73 (d, *J* = 8.2 Hz, 2H), 5.19 (tt, *J* = 7.5, 1.5 Hz, 1H), 2.99 – 2.90 (m, 2H), 1.95 (d, *J* = 7.6 Hz, 2H), 1.73 (s, 3H), 1.68 – 1.62 (m, 2H), 1.61 (s, 3H), 0.92 (s, 6H).

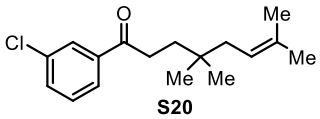

S20

1-(3-chlorophenyl)-4,4,7-trimethyloct-6-en-1-one (S20): General procedure E was performed on 4.05 mmol scale. Purification by flash chromatography eluting with 96:4 hexanes/DCM provided 836 mg (74%) of **S20** as a green oil. **^{1}H NMR** (500 MHz; $CDCl_3$): δ 7.91 (s, 1H), 7.82 (d, *J* = 7.9 Hz, 1H), 7.57 – 7.48 (m, 1H), 7.40 (t, *J* = 7.8 Hz, 1H), 5.19 (t, *J* = 7.5 Hz, 1H), 3.00 – 2.74 (m, 2H), 1.94 (d, *J* = 7.6 Hz, 2H), 1.73 (s, 3H), 1.67 – 1.59 (m, 5H), 0.92 (s, 6H).; **^{13}C NMR** (176 MHz, $CDCl_3$): δ 199.8, 138.8, 135.1, 133.4, 132.9, 130.1, 128.4, 126.3, 120.9, 40.1, 36.0, 34.2, 33.9, 27.0, 26.2, 18.1. **IR:** 3538, 3076, 2949, 2926, 1634, 1605, 1508, 1223, 1159, 830, 820 **HRMS:** calcd for $C_{17}H_{23}ClO^+$: 278.1437; found 278.1446.

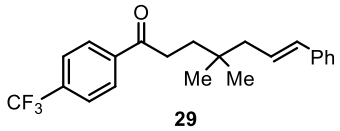

29

(E)-4,4-dimethyl-7-phenyl-1-(4-(trifluoromethyl)phenyl)hept-6-en-1-one (29): General procedure E was performed on 4.46 mmol scale. Purification by flash chromatography eluting with 90:10 hexanes/EtOAc provided 1.01 g (63%) of **29** as a green oil. Spectral data was found to be in accordance with literature data.[70] **^{1}H NMR** (500 MHz; $CDCl_3$): δ 8.05 (d, *J* = 8.1 Hz, 2H), 7.68 (d, *J* = 8.2 Hz, 2H), 7.35 (d, *J* = 6.8 Hz, 2H), 7.30 (t, *J* = 7.6 Hz, 2H), 7.21 (t, *J* = 7.2 Hz, 1H), 6.42 (d, *J* = 15.8 Hz, 1H), 6.26 (dt, *J* = 15.4, 7.4 Hz, 1H), 3.04 – 2.87 (m, 2H), 2.19 (d, *J* = 7.5 Hz, 2H), 1.79 – 1.63 (m, 2H), 1.00 (s, 6H).

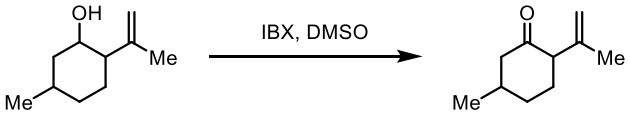

I1

5-methyl-2-(prop-1-en-2-yl)cyclohexan-1-one (I1): A flame-dried 500mL flask equipped with a stir bar was charged with isopulegol (8.77 mL, 51.9 mmol, 1 equiv.), and dry DMSO (260 mL, 0.2M). IBX (17.4 g, 62.2 mmol, 1.2 equiv.). The reaction was stirred at room temperature until judged complete by TLC analysis. The reaction was then diluted with Et_2O and water, then stirred overnight. The mixture was then filtered over Celite. The filtrate was partitioned, and the aqueous layer was extracted 3x25 mL Et_2O. The combined organics were washed with brine, dried over Na_2SO_4, and concentrated under reduced pressure. Purification by flash chromatography eluting with 70:30 hexanes/DCM provided 5.87 g (74%) of **I1** as a clear oil. Spectral data was found to be in accordance with literature data.[150] **^{1}H NMR** (500 MHz; $CDCl_3$): δ 4.93 (s, 1H), 4.72 (s, 1H),

2.95 (dd, *J* = 13.0, 5.4 Hz, 1H), 2.56 – 2.30 (m, 1H), 2.11 – 1.98 (m, 2H), 1.98 – 1.83 (m, 2H), 1.79 (m, 1H), 1.74 (s, 3H), 1.42 (m, 1H), 1.03 (d, *J* = 6.3 Hz, 3H).

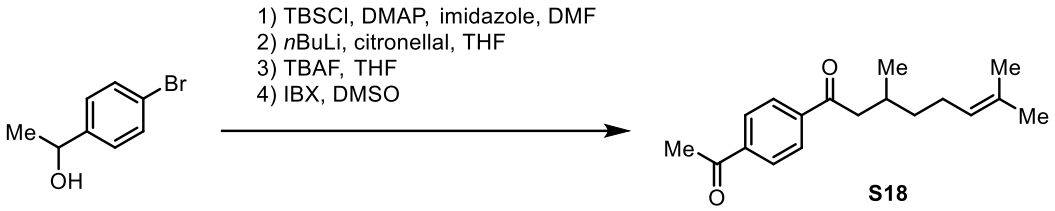

S18

1-(4-acetylphenyl)-3,7-dimethyloct-6-en-1-one (S18): A flame-dried flask was charged with 4-Bromo-α-methylbenzyl alcohol (8.04 g, 40.0 mmol, 1.0 equiv.), 4-(dimethylamino)pyridine (1.47 g, 12.0 mmol, 0.3 equiv.), and imidazole (8.17 g, 120.0 mmol, 3.0 equiv.) and DMF (120 mL, 0.3M). The mixture was cooled to 0 °C, and *tert*-butyldimethylsilyl chloride (12.1 g, 80.0 mmol, 2.0 equiv.) was added as a single portion. The reaction was warmed to room temperature and stirred until judged complete by TLC analysis. The reaction was quenched with aq. NH_4Cl and extracted 3x50 mL of EtOAc. The combined organics were washed with 3x50 mL aq. LiCl solution, brine, dried over Na_2SO_4, and concentrated under reduced pressure. The crude aryl bromide was used without further purification. A flame-dried flask was charged with aryl bromide (6.31 g, 20.0 mmol, 1.1 equiv.) and THF (90 mL, 0.2 M). The mixture was placed under N_2 atmosphere and cooled to -78 °C, and *n*BuLi (14.8 mL, 1.6M in hexanes, 1.3 equiv.) was added dropwise via syringe. After stirring for 40 minutes at the same temperature, citronellal (2.80 g, 18.2 mmol, 1.0 equiv.) was added dropwise via syringe. The reaction was warmed to room temperature and stirred until judged complete by TLC analysis. The reaction was quenched with aq. NH_4Cl and extracted with 3x25 mL of EtOAc. The combined organics were washed with brine, dried over Na_2SO_4, and concentrated under reduced pressure. The crude alcohol was used without further purification. The crude alcohol was dissolved in THF (67 mL, 0.3 M). The mixture was cooled to 0 °C, and tetrabutylammonium fluoride (5.71 g, 1.0M in THF) was added dropwise. The reaction was warmed to room temperature and stirred until judged complete by TLC analysis. The reaction was quenched with aq. NH_4Cl and extracted with 3x15 mL of EtOAc. The combined organics were washed with brine, dried over Na_2SO_4, and concentrated under reduced pressure. The crude diol was used without further purification. The diol was dissolve in DMSO (40 mL, 0.3 M) and IBX (13.3 g, 47.3 mmol, 2.6 equiv.) was added as a single portion. The reaction was stirred

at room temperature until judged complete by TLC analysis. The reaction was diluted with EtOAc and quenched with water, stirred for 1 hour, then filtered over Celite. The filtrate was extracted 3x20 mL, of EtOAc, the combined organics were washed with brine, dried over Na_2SO_4, and concentrated under reduced pressure. Purification by flash chromatography eluting with 90:10 hexanes/EtOAc provided 800 mg (XX% over 4 steps) of **S18** as a clear oil. Spectral data was found to be in accordance with literature data.[70] **^{1}H NMR** (500 MHz; $CDCl_3$): δ 8.02 (m, 4H), 5.09 (t, *J* = 7.0 Hz, 1H), 2.99 (dd, *J* = 15.9, 5.5 Hz, 1H), 2.77 (dd, *J* = 16.0, 8.1 Hz, 1H), 2.64 (s, 3H), 2.17 (m, 1H), 2.03 (tt, *J* = 14.4, 7.4 Hz, 2H), 1.68 (s, 3H), 1.60 (s, 3H), 1.42 (ddt, *J* = 12.4, 9.3, 6.1 Hz, 1H), 1.29 (dddd, *J* = 14.1, 10.5, 7.5, 5.5 Hz, 1H), 0.97 (d, *J* = 6.6 Hz, 3H).

General Procedure F. Grignard Addition for Synthesis of Carbonyl-Ene Substrates:

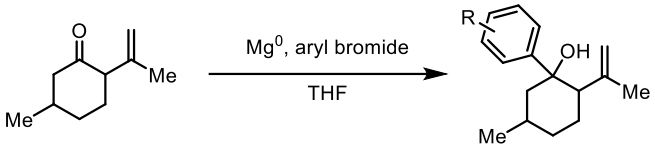

A flame-dried RBF equipped with a stir bar was charged with magnesium turnings (2 equiv.), aryl bromide (2.5 equiv.), dry THF (0.1M) and a catalytic amount of iodine. The reaction was placed under an N_2 atmosphere and initiated by heating with a heat gun until the solvent began to reflux. Once the magnesium was fully dissolved, the flask was cooled to 0C, and XX (1.0 equiv.) was added dropwise via syringe. The reaction was then warmed to room temperature and stirred until judged complete by TLC analysis. The reaction was quenched by added aq. NH_4Cl and extracted with 3x10mL EtOAc. The combined organics were washed with brine, dried over Na_2SO_4, and concentrated under reduced pressure. Purification by flash chromatography provided pure carbonyl-ene substrate.

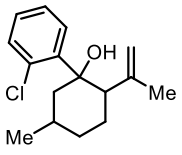

CE21

1-(2-chlorophenyl)-5-methyl-2-(prop-1-en-2-yl)cyclohexan-1-ol (CE21): General procedure F was performed in 3.28 mmol scale. Purification by flash chromatography eluting with 65:35 hexanes/DCM provided 592 mg (68%) of **CE21** as a clear oil. **^{1}H NMR** (500 MHz; $CDCl_3$): δ 7.42 (s, 1H), 7.28 (d, *J* = 8.0 Hz, 1H), 7.23 (t, *J* = 7.9 Hz, 1H), 7.18 (d, *J* = 7.9 Hz, 1H), 4.80 (s, 1H), 4.73 (s, 1H), 2.42 (d, *J* = 12.9 Hz, 1H), 2.25 (s, 1H), 1.95 – 1.84 (m, 2H), 1.81 (d, *J* = 12.3 Hz, 2H), 1.60 (d, *J* = 13.4 Hz, 1H), 1.46 (t, *J* = 13.0 Hz, 1H), 1.21 (s, 3H), 1.17 – 1.03 (m, 1H), 0.92 (d, *J* = 6.6 Hz, 3H); **^{13}C NMR** (176 MHz, $CDCl_3$): δ 150.8, 147.8, 134.2, 129.3, 126.6, 125.4, 123.3, 112.8, 74.6, 52.9, 49.1, 34.9, 28.1, 27.9, 25.4, 22.2; **IR:** 3535, 3074, 2949, 2926, 2868, 2845, 1636, 1595, 1455, 1071, 897, 783, 698; **HRMS:** calcd for $C_{16}H_{21}ClO^+$: 264.1281; found 264.1279.

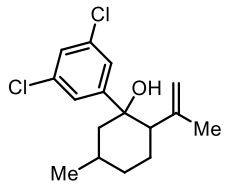

CE10

1-(3,5-dichlorophenyl)-5-methyl-2-(prop-1-en-2-yl)cyclohexan-1-ol (CE10): General procedure F was performed in 3.28 mmol scale. Purification by flash chromatography eluting with 65:35 hexanes/DCM provided 688 mg (70%) of **CE10** as a clear oil. **^{1}H NMR** (500 MHz; $CDCl_3$): δ 7.30 (s, 2H), 7.21 (d, *J* = 1.7 Hz, 1H), 4.87 – 4.78 (m, 1H), 4.73 (s, 1H), 2.39 (dd, *J* = 12.6, 3.7 Hz, 1H), 2.23 (s, 1H), 2.07 – 1.72 (m, 4H), 1.66 – 1.57 (m, 1H), 1.41 (t, *J* = 12.8 Hz, 1H), 1.28 (s, 3H), 1.08 (qd, *J* = 13.3, 4.0 Hz, 1H), 0.92 (d, *J* = 6.5 Hz, 3H); **^{13}C NMR** (176 MHz, $CDCl_3$): δ 152.3, 147.2, 134.7, 126.6, 124.0, 113.3, 74.7, 52.7, 49.0, 34.8, 28.0, 27.9, 25.3, 22.2; **IR:** 3531, 3081, 2950, 2926, 1636, 1587, 1565, 1413, 905, 851, 797, 733, 691; **HRMS:** calcd for $C_{16}H_{20}Cl_2O^+$: 298.0891; found 298.0901.

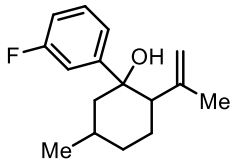

CE15

1-(3-fluorophenyl)-5-methyl-2-(prop-1-en-2-yl)cyclohexan-1-ol (CE15): General procedure F was performed in 3.28 mmol scale. Purification by flash chromatography eluting with 65:35 hexanes/DCM provided 488 mg (60%) of **CE15** as a clear oil. **^{1}H NMR** (500 MHz; $CDCl_3$): δ 7.32 – 7.23 (m, 1H), 7.17 (dt, *J* = 7.9, 1.1 Hz, 1H), 7.14 (dt, *J* = 10.8, 2.2 Hz, 1H), 6.89 (td, *J* = 8.3, 2.6 Hz, 1H), 4.81 (s, 1H), 4.74 (s, 1H), 1.97 – 1.85 (m, 1H), 1.83 (dtd, *J* = 15.9, 5.6, 2.6 Hz, 1H), 1.61 (dq, *J* = 13.4, 3.4 Hz, 2H), 1.48 (dd, *J* = 14.0, 12.1 Hz, 2H), 1.20 (s, 1H), 1.09 (qd, *J* = 13.0, 3.5 Hz, 1zH), 0.92 (d, *J* = 6.6 Hz, 1H); **^{13}C NMR** (176 MHz, $CDCl_3$): δ 163.0 (d, *J* = 244.8 Hz), 151.51= (d, *J* = 6.3 Hz), 147.9, 129.4 (d, *J* = 8.0 Hz), 120.7 (d, *J* = 2.7 Hz), 113.2 (d, *J* = 21.1 Hz), 112.7, 112.3 (d, *J* = 22.6 Hz), 74.5 (d, *J* = 1.7 Hz), 52.9, 49.0, 35.0, 28.2, 27.9, 25.4, 22.2; **IR:** 3536, 3077, 2949, 2926, 1635, 1614, 1588, 1439, 1253, 891, 782, 702; **HRMS:** calcd for $C_{16}H_{21}FO^+$: 248.1576; found: 248.1585.

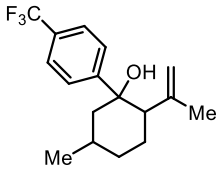

CE22

5-methyl-2-(prop-1-en-2-yl)-1-(4-(trifluoromethyl)phenyl)cyclohexan-1-ol (CE22): General procedure F was performed in 3.28 mmol scale. Purification by flash chromatography eluting with 65:35 hexanes/DCM provided 744 mg (76%) of **CE22** as a clear oil. **^{1}H NMR** (500 MHz; $CDCl_3$): δ 7.56 (d, *J* = 8.4 Hz, 1H), 7.54 (d, *J* = 8.4 Hz, 2H), 4.79 (s, 1H), 4.73 (s, 1H), 2.46 (d, *J* = 12.7 Hz, 1H), 2.29 (s, 1H), 1.91 (m, 2H), 1.83 (m, 2H), 1.63 (d, *J* = 13.4 Hz, 1H), 1.49 (t, *J* = 13.0 Hz, 1H), 1.18 (s, 3H), 1.11 (q, *J* = 12.9 Hz, 1H), 0.92 (d, *J* = 6.6 Hz, 3H); **^{13}C NMR** (176 MHz, $CDCl_3$): 152.5, 147.6, 128.8 (q, *J* = 32.3 Hz), 125.5, 125.0 (q, *J* = 3.8 Hz), 124.4 (q, *J* = 271.9 Hz), 113.0, 74.8, 52.9, 49.1, 34.9, 28.11, 27.90, 25.31, 22.20; **IR:** 3537, 3078, 2951, 2928, 1619, 1324, 1122, 1067, 832; **HRMS:** calcd for $C_{17}H_{21}F_3O^+$: 298.1545; found 298.1553.

5.5.3. General Procedure for Continuous Flow Carbonyl-Olefin Metathesis from Aryl Ketone Substrates and Additional Optimization Data

Substrate **9** was prepared as a 0.05M solution in anhydrous DCE by adding 75.0 mg (0.500 mmol) of substrate to a 5.0 mL volumetric flask and diluting to the mark with DCE. $FeCl_3$ was prepared as a 0.002M solution in anhydrous DCE by adding 3.24 mg (0.02 mmol) of anhydrous $FeCl_3$ to a 10.0 mL volumetric flask and diluting to the mark with DCE, followed by sonication to achieve full dissolution of $FeCl_3$. Solutions were drawn up into individual syringes and loaded into syringe pumps. Flow rates were adjusted to achieve various catalyst loadings and reaction concentration. Reactions were equilibrated for 3 t_R before a timed sample was collected in a vial containing triethylamine, which results in immediate quenching of the Lewis acid catalyst. The crude reaction mixture was then filtered through a silica plug, eluting with DCM and concentrated. Yields and conversions were determined by comparison of the theoretical yield set by the substrate molar flow rate and sample collection period and quantified by ^{1}H NMR against mesitylene as internal standard. A schematic of the reactor is depicted in **Figure 5.8**, optimization data is contained in **Table 5.1**, and an image of the reactor setup is shown in **Figure 5.9**.

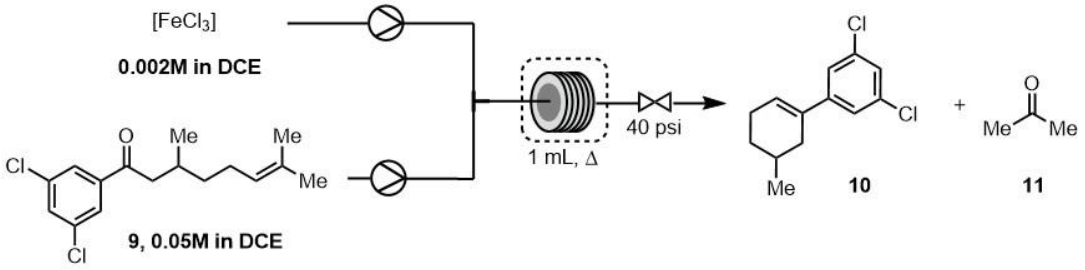

Figure 5.8. Schematic of reactor configuration for ring-closing COM for **10**.

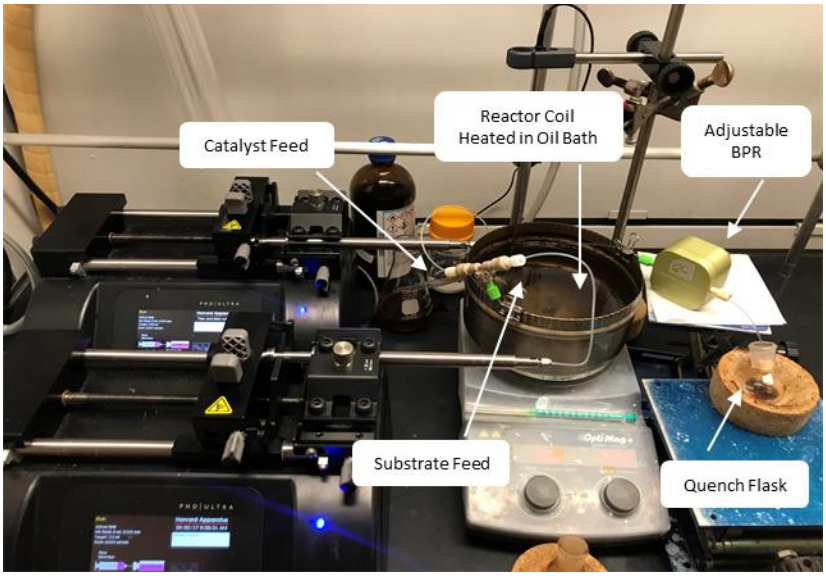

Figure 5.9. Image of reactor for ring-closing COM for **10**.

Table 5.1. Optimization data for continuous flow ring-closing COM for **10**.

Entry	ketone flow (mL/min)	Lewis Acid	[LA] (mol%)	Solvent	t_R (min)	BPR (psi)	Temp (C°)	Yield X (%)	Conv. X (%)
1	0.04	$FeCl_3$	10	1,2-DCE	7.14	40	110	22	48
2	0.02	$FeCl_3$	10	1,2-DCE	14.29	40	110	41	68
3	0.02	$FeCl_3$	20	1,2-DCE	8.33	40	110	87	93
4	0.012	$FeCl_3$	20	1,2-DCE	13.89	40	110	70	96
5	0.04	$GaCl_3$	10	1,2-DCE	7.14	40	110	6	28
6	0.04	$InCl_3$	10	1,2-DCE	7.14	40	110	3	29
7	0.02	$FeCl_3$	20	DCM	8.33	100	110	21	44
8	0.02	$FeCl_3$	20	MeCN	8.33	40	110	0	0
9	0.02	$FeCl_3$	20	THF	8.33	40	110	0	0
10	0.02	$FeCl_3$	20	Toluene	8.33	40	110	0	40
11	0.02	$FeCl_3$	20	1,2-DCE	8.33	40	60	11	42
12	0.02	$FeCl_3$	20	1,2-DCE	8.33	40	80	31	77

5.5.4 Characterization Data for COM Products Prepared in Flow and Additional Optimization Data

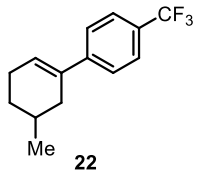

22

3-methyl-4'-(trifluoromethyl)-2,3,4,5-tetrahydro-1,1'-biphenyl (22): Trials were conducted in a continuous flow reactor similarly to the procedure described for the synthesis of **22** using the reactor configuration shown in **Figure 5.9**. Optimization data for the synthesis of **22** from ketone **S22** is shown in **Table 5.2**. Optimal conditions provided 64% of **22** by quantitative ^{1}H NMR analysis of a sample collected over one hour (theoretical yield: 0.060 mmol) against 1,4-dinitrobenzene as internal standard. A bulk sample was then collected for 45 minutes (theoretical yield: 0.090 mmol) and concentrated under reduced pressure. Purification by flash chromatography eluting with 100% pentane provided 14.0 mg (65%) of **22** as a clear oil. Spectral data was found to be in accordance with literature data.[70] **^{1}H NMR** (500 MHz; $CDCl_3$): δ 7.55 (d, *J* = 8.2 Hz, 2H), 7.47 (d, *J* = 8.2 Hz, 3H), 6.19 (s, 1H), 2.53 – 2.41 (m, 1H), 2.42 – 2.22 (m, 2H), 2.15 – 1.93 (m, 1H), 1.99 – 1.70 (m, 2H), 1.27 (m, 1H), 1.07 (d, *J* = 6.5 Hz, 3H).

Table 5.2. Optimization data for the continuous synthesis of **22**.

Entry	ketone flow (mL/min)	$FeCl_3$ Loading (%)		$FeCl_3$ Flow (mL/min)	t_R (min)	BPR (psi)	Temp (C°)	Yield (%)	Conversion (%)
1	0.02	10		0.05	14.29	40	110	64	88
2	0.04	10		0.1	7.14	40	110	61	85
3	0.16	10		0.4	1.79	40	110	26	45
4	0.04	6		0.06	10.00	40	110	46	60
5	.024	20		.12	6.94	40	110	53	72

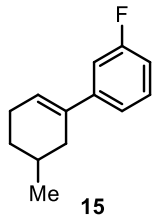

15

3'-fluoro-3-methyl-2,3,4,5-tetrahydro-1,1'-biphenyl (15): Trials were conducted in a continuous flow reactor similarly to the procedure described for the synthesis of **15** using the reactor configuration shown in **Figure 5.9**. Optimization data for the synthesis of **15** from ketone **S15** is shown in **Table 5.3**. Optimal conditions provided 64% of **15** (theoretical yield: 0.050 mmol) against 1,4-dinitrobenzene as internal standard. A bulk sample was then collected for 100 minutes (theoretical yield: 0.100 mmol) and concentrated under reduced pressure. Purification by flash chromatography eluting with 100% pentane provided 12.0 mg (64%) of **15** as a 1.0:0.45 mixture of olefin isomers a clear oil. **^{1}H NMR** (500 MHz, $CDCl_3$): δ 7.25 (q, *J* = 7.5, 7.0 Hz, 2H), 7.17 (t, *J* = 6.6 Hz, 2H), 7.07 (d, *J* = 11.1 Hz, 2H), 6.90 (t, *J* = 8.4 Hz, 2H), 6.13 (s, 1H), 6.00 (s, 0.45H), 2.48 – 2.40 (m, 1H), 2.39 – 2.32 (m, 2H), 2.31 – 2.16 (m, 3H), 2.05 – 1.97 (m, 1H), 1.97 – 1.88 (m, 1H), 1.88 – 1.78 (m, 1H), 1.78 – 1.71 (m, 1H), 1.39 – 1.21 (m, 1H), 1.07 (t, *J* = 6.9 Hz, 5H); **^{13}C NMR** (125 MHz, $CDCl_3$): δ 163.1 (d, *J* = 244.7 Hz), 145.0 (d, *J* = 7.4 Hz), 135.4 (d, *J* = 2.1 Hz), 129.6 (d, *J* = 8.5 Hz), 125.6, 120.7 (d, *J* = 2.7 Hz), 113.3 (d, *J* = 21.2 Hz), 112.0 (d, *J* = 21.7 Hz), 36.0, 30.4, 29.1, 26.1, 22.1; **IR:** 2952, 2924, 1611, 1583, 1489, 1434, 1265, 1173, 837, 777; **HRMS:** calcd for $C_{13}H_{15}F^{+}$: 190.1158; found 190.1165.

Table 5.3. Optimization data for the continuous synthesis of **15**.

Entry	ketone flow (mL/min)	$FeCl_3$ Loading (%)	$FeCl_3$ Flow (mL/min)	t_R (min)	BPR (psi)	Temp (C°)	Yield (%)	Conversion (%)
1	0.02	20	0.100	8.33	40	110	64	100
2	0.04	10	0.05	7.14	40	110	50	50
3	0.04	20	0.200	4.17	40	110	38	91
4	0.04	15	0.15	7.15	40	110	50	100
5	.02	10	.050	14.29	40	110	29	89

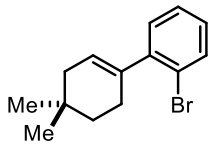

19

2'-bromo-4,4-dimethyl-2,3,4,5-tetrahydro-1,1'-biphenyl (19): Trials were conducted in a continuous flow reactor similarly to the procedure described for the synthesis of **19** using the reactor configuration shown in **Figure 5.9**. Optimization data for the synthesis of **19** from ketone **S19** is shown in **Table 5.4**. Optimal conditions provided 64% of **19** by quantitative ^{1}H NMR analysis of a sample collected over 80 minutes (theoretical yield: 0.040 mmol) against 1,4-dinitrobenzene as internal standard. A bulk sample was then collected for 158 minutes (theoretical yield: 0.079 mmol) and concentrated under reduced pressure. Purification by flash chromatography eluting with 100% pentane provided 13.3 (64%) of **19** as a clear oil. **^{1}H NMR** (500 MHz, $CDCl_3$): δ 7.53 (dd, *J* = 8.0, 1.2 Hz, 1H), 7.24 (td, *J* = 7.5, 1.2 Hz, 1H), 7.14 (dd, *J* = 7.6, 1.8 Hz, 1H), 7.08 (ddd, *J* = 8.0, 7.3, 1.8 Hz, 1H), 5.55 (dt, *J* = 3.9, 2.0 Hz, 1H), 2.30 (m, 2H), 1.96 (d, *J* = 4.0, 2.6 Hz, 2H), 1.51 (t, *J* = 6.4 Hz, 32H), 1.02 (s, 6H); **^{13}C NMR** (125 MHz, $CDCl_3$): δ 145.4, 138.0, 132.7, 130.3, 128.1, 127.3, 126.3, 122.8, 39., 35.8, 28.5, 27.3; **IR:** 3325, 2951, 2916, 2866, 1593, 1565, 1472, 1457, 1029, 772, 742, 685; **HRMS:** calcd for $C_{14}H_{17}Br^{+}$: 264.0514; found 264.0513.

Table 5.4. Optimization data for the continuous synthesis of **19.**

Entry	ketone flow (mL/min)	$FeCl_3$ Loading (%)	$FeCl_3$ Flow (mL/min)	t_R (min)	BPR (psi)	Temp (C°)	Yield (%)	Conversion (%)
1	0.05	10	0.125	5.71	40	110	22	24
2	0.034	10	0.085	8.40	40	110	32	50
3	0.02	20	0.10	8.33	40	110	26	77
4	0.01	20	0.05	16.67	40	110	60	80

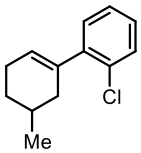

21

2'-chloro-3-methyl-2,3,4,5-tetrahydro-1,1'-biphenyl (21): Trials were conducted in a continuous flow reactor similarly to the procedure described for the synthesis of **21** using the reactor configuration shown in **Figure 5.9**. Optimization data for the synthesis of **21** from ketone **S21** is shown in **Table 5.5**. Optimal conditions provided 66% of **21** by quantitative ^{1}H NMR analysis of a sample collected over 25 minutes (theoretical yield: 0.0625 mmol) against 1,4-dinitrobenzene as internal standard. A bulk sample was then collected for one hour (theoretical yield: 0.150 mmol) and concentrated under reduced pressure. Purification by flash chromatography eluting with 100% pentane provided 16.1 (52%) of **21** as a clear oil. Spectral data was found to be in accordance with literature data.[70] **^{1}H NMR** (500 MHz, $CDCl_3$): 7.33 (d, *J* = 7.1 Hz, 1H), 7.19 (d, *J* = 7.8 Hz, 1H), 7.16 (t, *J* = 7.0 Hz, 1H), 5.91 – 5.36 (m, 1H), 2.31 (dd, *J* = 17.3, 5.0 Hz, 1H), 2.30 – 2.15 (m, 2H), 2.02 – 1.92 (m, 1H), 1.84 (tdd, *J* = 13.9, 7.6, 3.9 Hz, 1H), 1.80 – 1.67 (m, 1H), 1.38 – 1.27 (m, 1H), 1.03 (d, *J* = 6.6 Hz, 3H).

Table 5.5. Optimization data for continuous synthesis of **21**.

Entry	ketone flow (mL/min)	$FeCl_3$ Loading (%)	$FeCl_3$ Flow (mL/min)	t_R (min)	BPR (psi)	Temp (C°)	Yield (%)	Conversion (%)
1	0.02	20	0.100	8.33	40	110	53	100
2	0.035	20	0.175	4.76	40	110	39	100
3	0.05	10	0.125	5.71	40	110	66	83

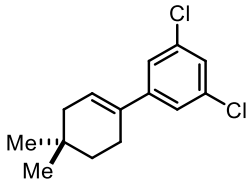

17

3',5'-dichloro-4,4-dimethyl-2,3,4,5-tetrahydro-1,1'-biphenyl (17): Trials were conducted in a continuous flow reactor similarly to the procedure described for the synthesis of **17** using the reactor configuration shown in **Figure 5.9**. Optimization data for the synthesis of **17** from ketone **S17** is shown in **Table 5.6**. Optimal conditions provided 86% of **17** by quantitative ^{1}H NMR analysis of a sample collected over 25 minutes (theoretical yield: 0.05 mmol) against mesitylene as internal standard. A bulk sample was then collected for 60 minutes (theoretical yield: 0.120 mmol) and concentrated under reduced pressure. Purification by flash chromatography eluting with 100% pentane provided 24.9 mg (85%) of **17** as a clear oil. Spectral data was found to be in

accordance with literature data.[70] **^{1}H NMR (700 MHz, $CDCl_3$)**: δ 7.26 (t, *J* = 2.1 Hz, 2H), 7.20 (d, *J* = 1.8 Hz, 1H), 6.11 (q, *J* = 2.1 Hz, 1H), 2.36 (t, *J* = 7.9 Hz, 2H), 2.00 (d, *J* = 2.3 Hz, 2H), 1.52 (t, *J* = 6.4 Hz, 2H), 0.96 (s, 6H).

Table 5.6. Optimization data for the continuous synthesis of **17**.

Entry	ketone flow (mL/min)	$FeCl_3$ Loading (%)	$FeCl_3$ Flow (mL/min)	t_R (min)	BPR (psi)	Temp (C°)	Yield (%)	Conversion (%)
1	0.06	10	0.150	4.76	40	110	45	60
2	0.04	20	0.200	4.17	40	110	86	85
3	0.04	20	0.150	5.56	40	110	85	100

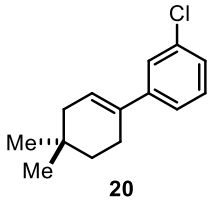

20

3'-chloro-4,4-dimethyl-2,3,4,5-tetrahydro-1,1'-biphenyl (20): Trials were conducted in a continuous flow reactor similarly to the procedure described for the synthesis of **20** using the reactor configuration shown in **Figure 5.9**. Optimization data for the synthesis of **20** from ketone **S20** is shown in **Table 5.7**. Optimal conditions provided 75% of **20** by quantitative ^{1}H NMR analysis of a sample collected over 11 minutes (theoretical yield: 0.033 mmol) against mesitylene as internal standard. A bulk sample was then collected for 50 minutes (theoretical yield: 0.150 mmol) and concentrated under reduced pressure. Purification by flash chromatography eluting with 100% pentane provided 28.4 mg (86%) of **20** as a clear oil. **^{1}H NMR** (500 MHz, $CDCl_3$): δ 7.38 (s, 1H), 7.28 (d, *J* = 7.6 Hz, 1H), 7.23 (t, *J* = 7.7 Hz, 1H), 7.19 (d, *J* = 6.3 Hz, 1H), 6.12 – 6.06 (m, 1H), 2.46 – 2.38 (m, 2H), 2.01 (s, 2H), 1.53 (t, *J* = 6.4 Hz, 2H), 0.97 (s, 6H); **^{13}C NMR** (125 MHz, $CDCl_3$): δ 144.2, 134.3, 134.2, 129.5, 126.6, 125.4, 125.2, 123.2, 40.0, 35.8, 28.5, 28.3, 25.1; **IR:** 2950, 2866, 1466, 1431, 1363, 1024, 749, 726, 689; **HRMS:** calcd for $C_{14}H_{17}Cl^+$: 220.1019; found 220.1015.

Table 5.7. Optimization data for the continuous synthesis of **20**.

Entry	ketone flow (mL/min)	$FeCl_3$ Loading (%)	$FeCl_3$ Flow (mL/min)	t_R (min)	BPR (psi)	Temp (C°)	Yield (%)	Conversion (%)
1	0.06	10	0.150	5.71	40	110	75	100
2	0.036	10	0.09	7.94	40	110	65	100
3	0.02	20	0.10	8.33	40	110	40	100

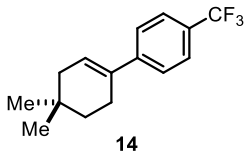

14

4,4-dimethyl-4'-(trifluoromethyl)-2,3,4,5-tetrahydro-1,1'-biphenyl (14): Trials were conducted in a continuous flow reactor similarly to the procedure described for the synthesis of **14** using the reactor configuration shown in **Figure 5.9**. Optimization data for the synthesis of **14** from ketone **S14** is shown in **Table 5.8**. Optimal conditions provided 99% of **14** by quantitative ^{1}H NMR analysis of a sample collected over 25 minutes (theoretical yield: 0.05 mmol) against mesitylene as internal standard. A bulk sample was then collected for 75 minutes (theoretical yield: 0.150 mmol) and concentrated under reduced pressure. Purification by flash chromatography eluting with 100% pentane provided 37.4 mg (99%) of **14** as a clear oil. Spectral data was found to be in accordance with literature data.[70] **^{1}H NMR** (500 MHz, $CDCl_3$): δ 7.56 (d, *J* = 8.1 Hz, 2H), 7.49 (d, *J* = 8.1 Hz, 2H), 6.16 (s, 1H), 2.43 (t, *J* = 6.3 Hz, 2H), 2.03 (d, *J* = 3.3 Hz, 2H), 1.55 (t, *J* = 6.4 Hz, 2H), 0.98 (s, 6H).

Table 5.8. Optimization data for continuous synthesis of **14**.

Entry	ketone flow (mL/min)	$FeCl_3$ Loading (%)	$FeCl_3$ Flow (mL/min)	t_R (min)	BPR (psi)	Temp (C°)	Yield (%)	Conversion (%)
1	0.04	20	0.20	4.17	40	110	99	99
2	0.02	20	0.10	8.33	40	110	99	99

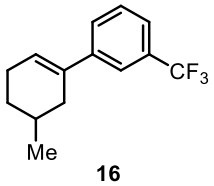

16

3-methyl-3'-(trifluoromethyl)-2,3,4,5-tetrahydro-1,1'-biphenyl (16): Trials were conducted in a continuous flow reactor similarly to the procedure described for the synthesis of **16** using the reactor configuration shown in **Figure 5.9**. Optimization data for the synthesis of **16** from ketone **S16** is shown in **Table 5.9**. Optimal conditions provided 71% of **16** by quantitative ^{1}H NMR analysis of a sample collected over 25 minutes (theoretical yield: 0.05 mmol) against mesitylene as internal standard. A bulk sample was then collected for 180 minutes (theoretical yield: 0.128 mmol) and concentrated under reduced pressure. Purification by flash chromatography eluting with 100% pentane provided 22.1 mg (72%) of **16** as a clear oil. Spectral data was found to be in accordance with literature data.[70] **^{1}H NMR (700 MHz, $CDCl_3$)**: δ 7.62 (s, 1H), 7.55 (d, *J* = 7.7 Hz, 1H), 7.46 (d, *J* = 7.6 Hz, 1H), 7.40 (t, *J* = 7.7 Hz, 1H), 6.17 (s, 1H), 2.54 – 2.41 (m, 1H), 2.37 – 2.14 (m, 2H), 2.09 – 1.96 (m, 1H), 1.90 – 1.72 (m, 2H), 1.35 – 1.21 (m, 1H), 1.07 (d, *J* = 6.5 Hz, 3H).

Table 5.9. Optimization data for the continuous synthesis of **16**.

Entry	ketone flow (mL/min)	$FeCl_3$ Loading (%)	$FeCl_3$ Flow (mL/min)	t_R (min)	BPR (psi)	Temp (C°)	Yield (%)	Conversion (%)
1	0.024	20	0.12	6.94	40	110	40	51
2	0.04	10	0.10	7.14	40	110	8	12
3	0.02	20	0.1	8.33	40	110	48	82
4	0.017	20	0.085	9.80	40	110	71	78

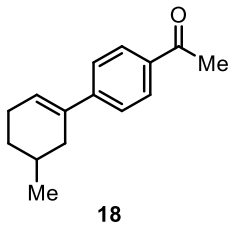

18

1-(3'-methyl-2',3',4',5'-tetrahydro-[1,1'-biphenyl]-4-yl)ethan-1-one (18): Trials were conducted in a continuous flow reactor similarly to the procedure described for the synthesis of **18**

using the reactor configuration shown in **Figure 5.8**. Optimization data for the synthesis of **18** from ketone **S18** is shown in **Table 5.10**. Optimal conditions provided 78% of **18** by quantitative ^{1}H NMR analysis of a sample collected over XX minutes (theoretical yield: XX mmol) against mesitylene as internal standard. A bulk sample was then collected for 210 minutes (theoretical yield: 0.105 mmol) and concentrated under reduced pressure. Purification by flash chromatography eluting with 60:40 DCM/hexanes provided 18.3 mg (81%) of **18** as a clear oil. Spectral data was found to be in accordance with literature data.[70] **^{1}H NMR (700 MHz, CDCl$_3$)**: δ 7.90 (d, J = 8.5 Hz, 2H), 7.46 (d, J = 8.5 Hz, 2H), 6.25 (s, 0.9H), 6.10 (s, 0.1H), 2.59 (s, 3H), 2.47 (dd, J = 16.7, 3.8 Hz, 1H), 2.35 – 2.23 (m, 2H), 2.12 – 1.99 (m, 1H), 1.88 – 1.71 (m, 2H), 1.34 – 1.16 (m, 1H), 1.07 (d, J = 6.5 Hz, 3H).

Table 5.10. Optimization data for continuous synthesis of **18**.

Entry	ketone flow (mL/min)	$FeCl_3$ Loading (%)	$FeCl_3$ Flow (mL/min)	t_R (min)	BPR (psi)	Temp (C°)	Yield (%)	Conversion (%)
1	0.02	20	0.1	8.33	40	110	58	83
2	0.015	20	0.075	11.11	40	110	48	76
3	0.01	20	0.05	16.67	80	130	78	96

5.5.5 Batch Synthesis of 29: 1.0 mmol Scale Up

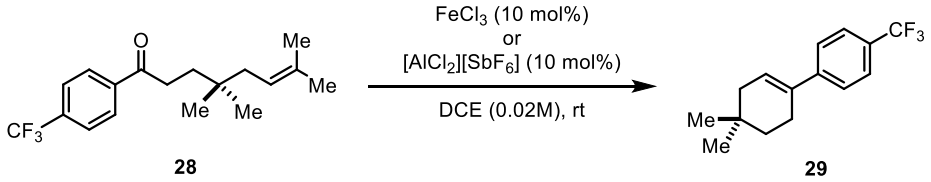

28 **29**

A flame-dried 100mL RBF equipped with a stir bar was charged with $FeCl_3$ (16.2 mg, 0.10 mmol, 0.1 equiv.) and DCE (40 mL). The flask was capped with a septum and placed under N_2 atmosphere. Substrate **28** (312 mg, 1.00 mmol, 1.0 equiv) was dissolved in 10 mL of DCE, and the solution was added via syringe at room temperature. The reaction was stirred at the same temperature until judged complete by TLC analysis (22 hours). The reaction was filtered over a silica plug, eluting with DCM and concentrated. The crude residue was purified by flash chromatography eluting with 100% pentanes to provide 210 mg (82%) of **29** as a yellow oil. The overall throughput was calculated to be 210 mg/22 hr = 9.5 mg/hr.

A similar procedure was followed employing $AlCl_3$ (13.3 mg, 0.10 mmol, 0.1 equiv.) and $AgSbF_6$ (34.4 mg, 0.10 mmol, 0.10 equiv) as the Lewis acid precatalyst. Reaction was monitored by TLC analysis, reaching full conversion at 8 hours. Purification by flash chromatography eluting with 100% pentanes provided 206 mg (81%) of **29** as a clear oil. The overall throughput was calculated to be 206 mg/8 hr = 25.8 mg/hr.

5.5.6 Procedure for 1 mmol Scale Out Experiment for Continuous Synthesis of 28.

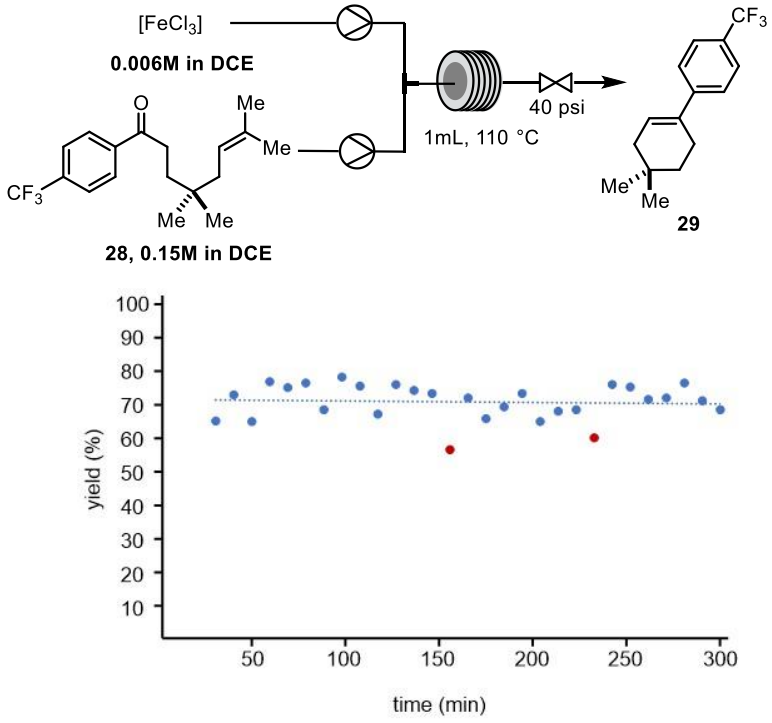

Figure 5.10. Longevity study on flow reactor for continuous synthesis of **29**.

Substrate **28** was prepared as a 0.15M solution in anhydrous DCE by dissolving 703 mg (2.25 mmol) of substrate in 15.0 mL of DCE. $FeCl_3$ was prepared as a 0.006M solution in anhydrous DCE by dissolving 77.9 mg (0.480 mmol) in 80 mL of DCE, followed by sonication to achieve full dissolution of $FeCl_3$. Solutions were drawn up into individual syringes and loaded into syringe pumps. Flow rates were adjusted to 50 uL/min and 250 uL/min for substrate and catalyst feeds, respectively (t_R = 3.33 minutes). The system was equilibrated for 3 t_R (10 minutes) followed by collection of samples every 10 minutes (theoretical yield: 0.075 mmol) over a period of 5 hours. Each aliquot was filtered through a silica plug, eluting with DCM and concentrated. Yields and conversions were determined by comparison of the theoretical yield set by the substrate molar flow

rate and sample collection period and quantified by ^{1}H NMR against mesitylene as internal standard. The first 14 samples (combined theoretical yield: 1.05 mmol) were then combined and purified by flash chromatography, eluting with 100% pentanes to provided 192 mg (72%) of **28** as a clear oil. A plot of the yield vs. time graph for the scale out experiment is depicted in **Figure 5.10**. The red data points indicate time points when the catalyst solution syringe was refilled, and so the observed yield reflects the equilibration period of the reactor.

5.5.7 General Procedure for Continuous Carbonyl-Olefin Metathesis from Carbonyl-Ene Substrates.

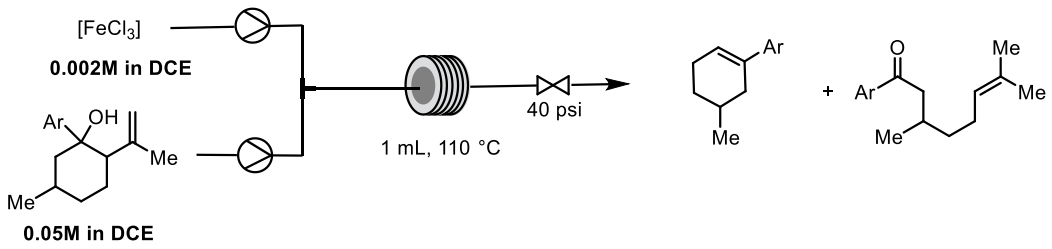

Substrates were prepared as a 0.05M solution in anhydrous DCE by adding 0.500 mmol of substrate to a 5.0 mL volumetric flask and diluting to the mark with DCE. $FeCl_3$ was prepared as a 0.002M solution in anhydrous DCE by adding 3.24 mg (0.02 mmol) of anhydrous $FeCl_3$ to a 10.0 mL volumetric flask and diluting to the mark with DCE, followed by sonication to achieve full dissolution of $FeCl_3$. Solutions were drawn up into individual syringes and loaded into syringe pumps. Flow rates were adjusted to achieve various catalyst loadings and reaction concentration. Reactions were equilibrated for 3 t_R before a timed sample was collected in a vial containing triethylamine, which results in immediate quenching of the Lewis acid catalyst. The crude reaction mixture was then filtered through a silica plug, eluting with DCM and concentrated. Yields and conversions were determined by comparison of the theoretical yield set by the substrate molar flow rate and sample collection period and quantified by ^{1}H NMR against mesitylene as internal standard.

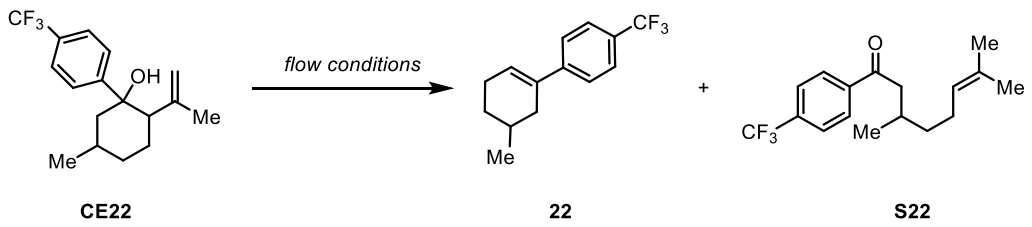

CE22 **22** **S22**

Trials were conducted in a continuous flow reactor similarly to the procedure described for the synthesis of **22** using the reactor configuration shown in **Figure 5.9**. Optimization data for the synthesis of **22** from **CE22** is shown in **Table 5.11**. Optimal conditions provided 59% of **22** by quantitative ^{1}H NMR analysis of a sample collected over 25 minutes (theoretical yield: 0.05 mmol) against mesitylene as internal standard. A bulk sample was then collected for 75 minutes (theoretical yield: 0.150 mmol) and concentrated under reduced pressure. Purification by flash chromatography eluting with 100% pentane provided 27.0 mg (75%) of **75** as a clear oil.

Table 5.11. Optimization data for continuous synthesis of **22** from **CE22**.

Entry	ketone flow (mL/min)	$FeCl_3$ Loading (%)	$FeCl_3$ Flow (mL/min)	t_R (min)	BPR (psi)	Temp (C°)	COM (%)	Ketone (%)	Conv. (%)
1	0.04	20	0.20	4.17	40	110	59	5	100
2	0.06	10	0.15	4.76	40	110	41	49	90
3	0.04	10	0.10	7.14	40	110	55	13	100
4	0.06	20	0.30	2.78	40	100	39	36	95

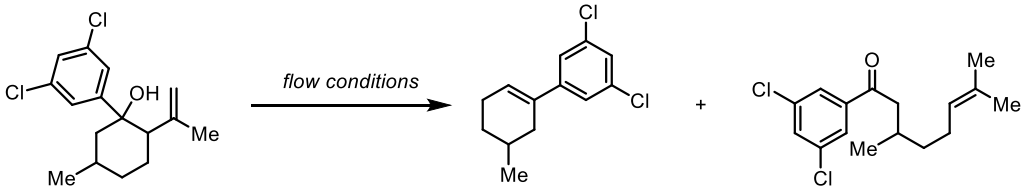

CE10 **10** **9**

Trials were conducted in a continuous flow reactor similarly to the procedure described for the synthesis of **10** using the reactor configuration shown in **Figure 5.9**. Optimization data for the synthesis of **10** from ketone XX is shown in **Table 5.12**. Optimal conditions provided 59% of **10** by quantitative ^{1}H NMR analysis of a sample collected over 36 minutes (theoretical yield: 0.047

mmol) against mesitylene as internal standard. A bulk sample was then collected for 110 minutes (theoretical yield: 0.143 mmol) and concentrated under reduced pressure. Purification by flash chromatography eluting with 100% pentane provided 31.0 mg (90%) of **10** as a clear oil.

Table 5.12. Optimization data for continuous synthesis of **10** from **CE10**.

Entry	ketone flow (mL/min)	$FeCl_3$ Loading (%)	$FeCl_3$ Flow (mL/min)	t_R (min)	BPR (psi)	Temp (C°)	COM (%)	Ketone (%)	Conversion (%)
1	0.04	20	0.20	4.17	40	110	76	11	100
2	0.06	10	0.15	4.76	40	110	69	25	96
3	0.026	20	0.13	6.41	40	110	86	4	99

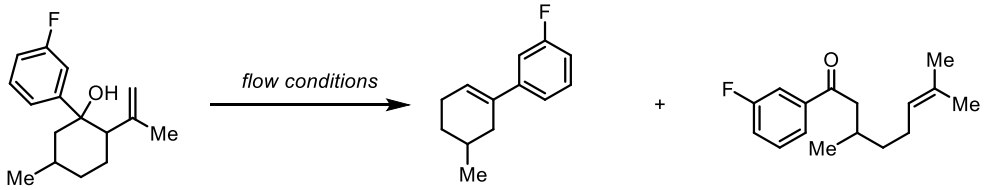

CE15 **15** **S15**

Trials were conducted in a continuous flow reactor similarly to the procedure described for the synthesis of **10** using the reactor configuration shown in **Figure 5.9**. Optimization data for the synthesis of **15** is shown in **Table 5.13**. Optimal conditions provided 59% of **15** by quantitative ^1H NMR analysis of a sample collected over 36 minutes (theoretical yield: 0.047 mmol) against mesitylene as internal standard.

Table 5.13. Optimization data for continuous synthesis of **15** from **CE15**.

Entry	ketone flow (mL/min)	$FeCl_3$ Loading (%)	$FeCl_3$ Flow (mL/min)	t_R (min)	BPR (psi)	Temp (C°)	COM (%)	Ketone (%)	Conversion (%)
1	0.04	20	0.20	4.17	40	110	37	6	99
2	0.04	10	0.10	7.14	40	110	35	8	99
3	0.132	10	0.330	2.16	40	110	31	13	98

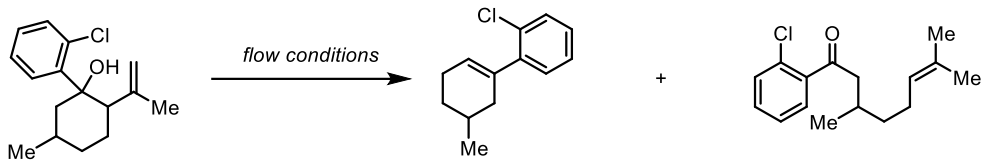

CE21 **21** **S21**

Trials were conducted in a continuous flow reactor similarly to the procedure described for the synthesis of **10** using the reactor configuration shown in **Figure 5.9**. Optimization data for the synthesis of **21** from **CE21** is shown in **Table 5.14**. Optimal conditions provided 39% of **21** by quantitative ^{1}H NMR analysis of a sample collected over 36 minutes (theoretical yield: 0.047 mmol) against mesitylene as internal standard.

Table 5.14. Optimization data for continuous synthesis of **21** from **CE21**.

Entry	ketone flow (mL/min)	$FeCl_3$ Loading (%)	$FeCl_3$ Flow (mL/min)	t_R (min)	BPR (psi)	Temp (C°)	COM (%)	Ketone (%)	Conversion (%)
1	0.034	10	0.085	8.40	40	110	27	33	96
2	0.0.06	10	0.15	4.76	40	110	39	12	100
3	0.120	10	0.30	2.38	40	110	24	46	93
4	0.06	10	0.15	4.76	40	80	21	53	93
5	0.04	20	0.20	4.17	40	80	23	41	96

5.5.8 Computational Data

5.5.9 ^{1}H and ^{13}C NMR Spectra

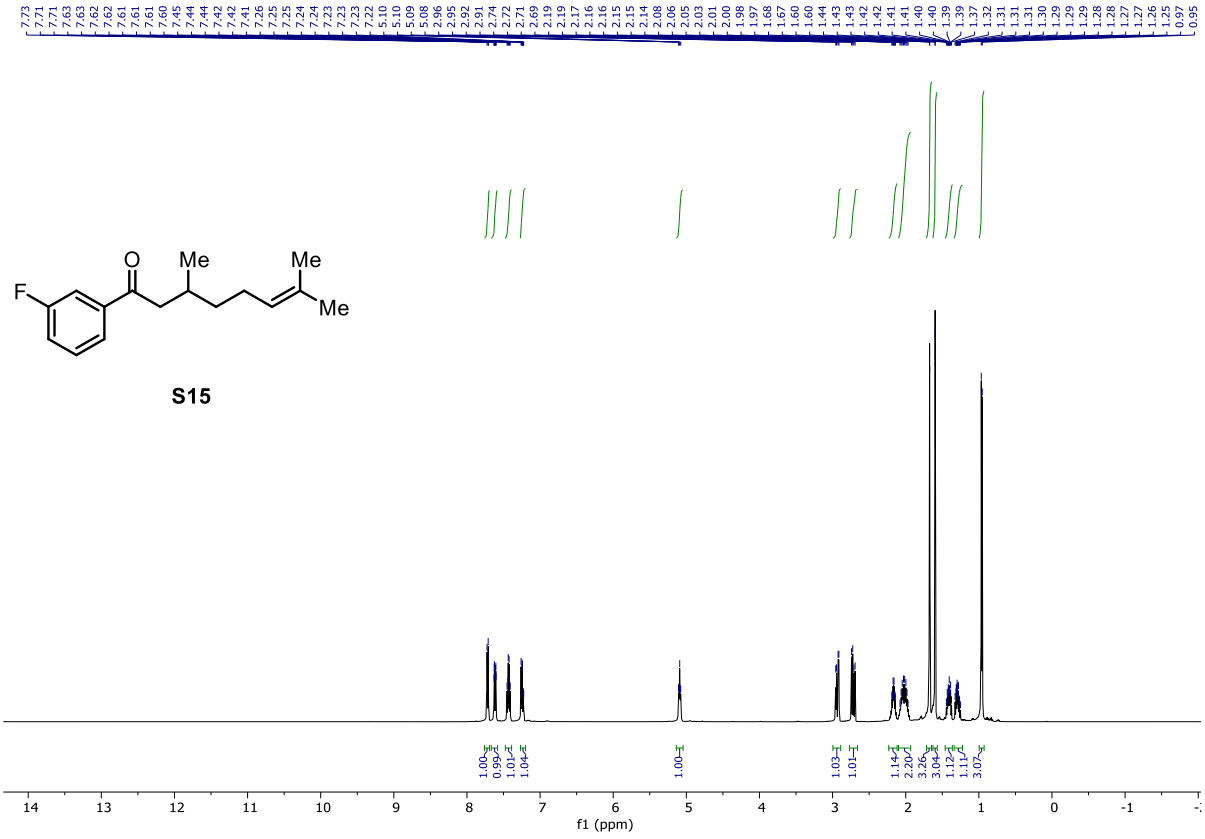

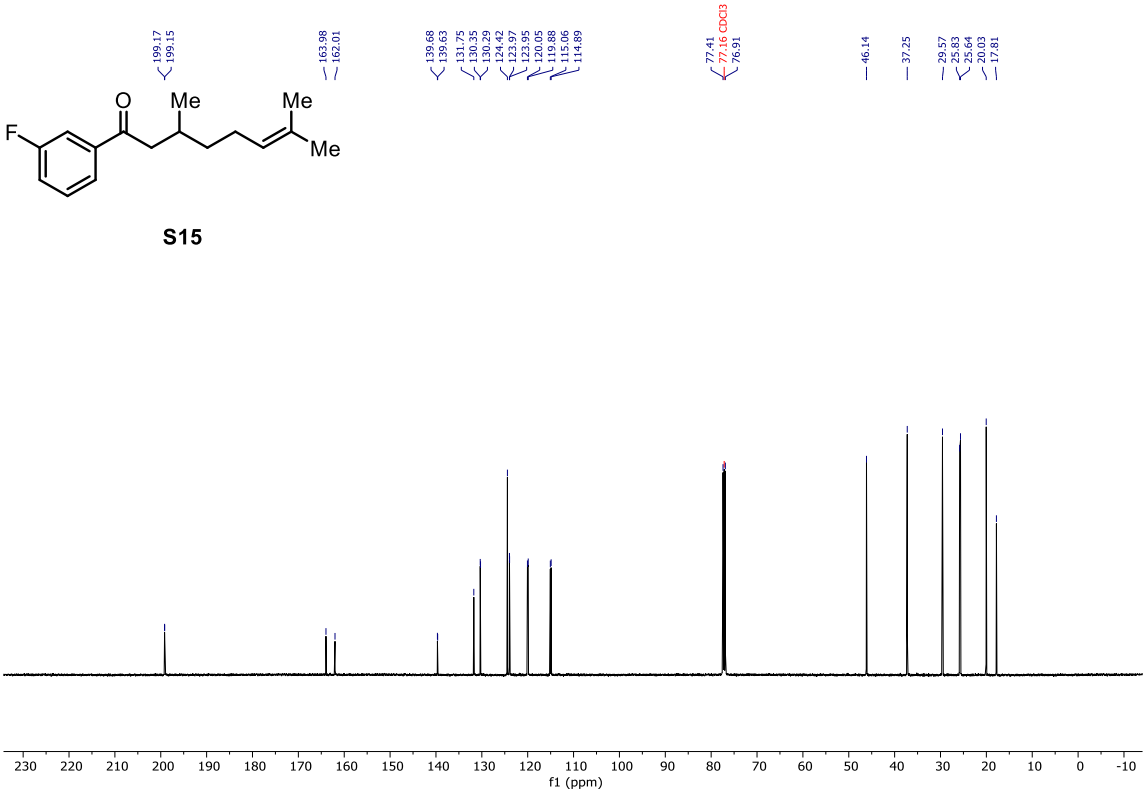
199.17
199.15
163.98
162.01
139.68
139.63
131.75
130.35
130.29
124.42
124.37
123.95
120.05
119.88
115.06
114.89
77.41
77.16
76.91
CDCl3
46.14
37.25
29.57
25.83
25.64
20.03
17.81
O
Me
Me
F
Me
230 220 210 200 190 180 170 160 150 140 130 120 110 100 90 80 70 60 50 40 30 20 10 0 -10
f1 (ppm)

S15

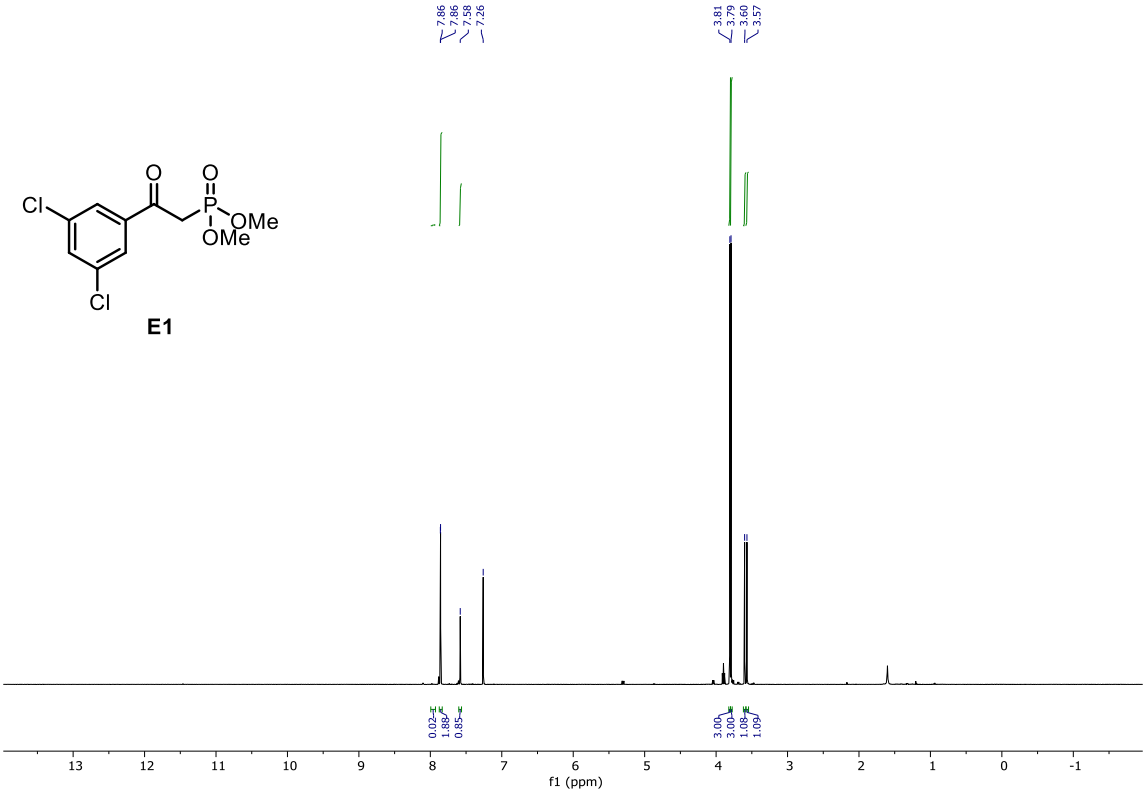
7.86
7.86
7.58
7.26
3.81
3.79
3.60
3.57
O
O
P
OMe
OMe
Cl
Cl
0.02
1.88
0.85
3.00
3.00
1.08
1.09
13 12 11 10 9 8 7 6 5 4 3 2 1 0 -1
f1 (ppm)

E1

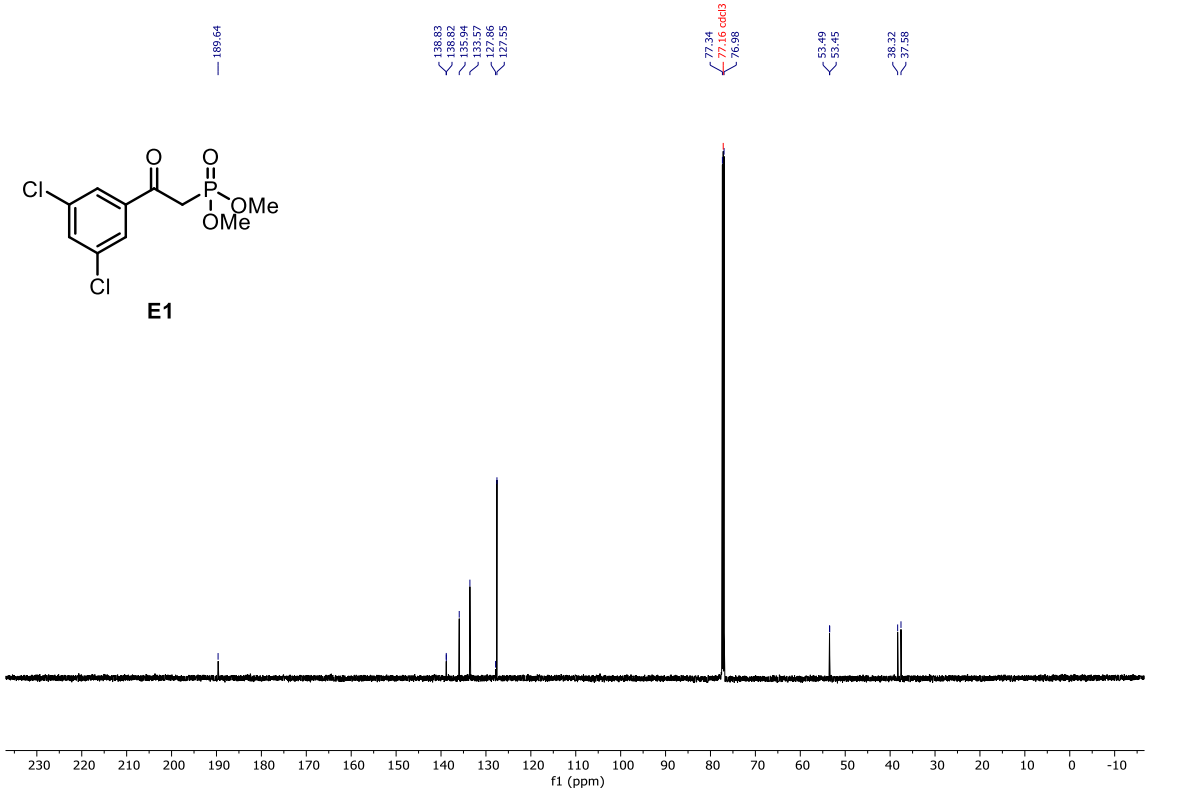
189.64
138.83
138.82
135.94
133.57
127.86
127.55
77.34
77.16 cdcl3
76.98
53.49
53.45
38.32
37.58
Cl
O
O
P
OMe
OMe
Cl
E1
230 220 210 200 190 180 170 160 150 140 130 120 110 100 90 80 70 60 50 40 30 20 10 0 -10
f1 (ppm)

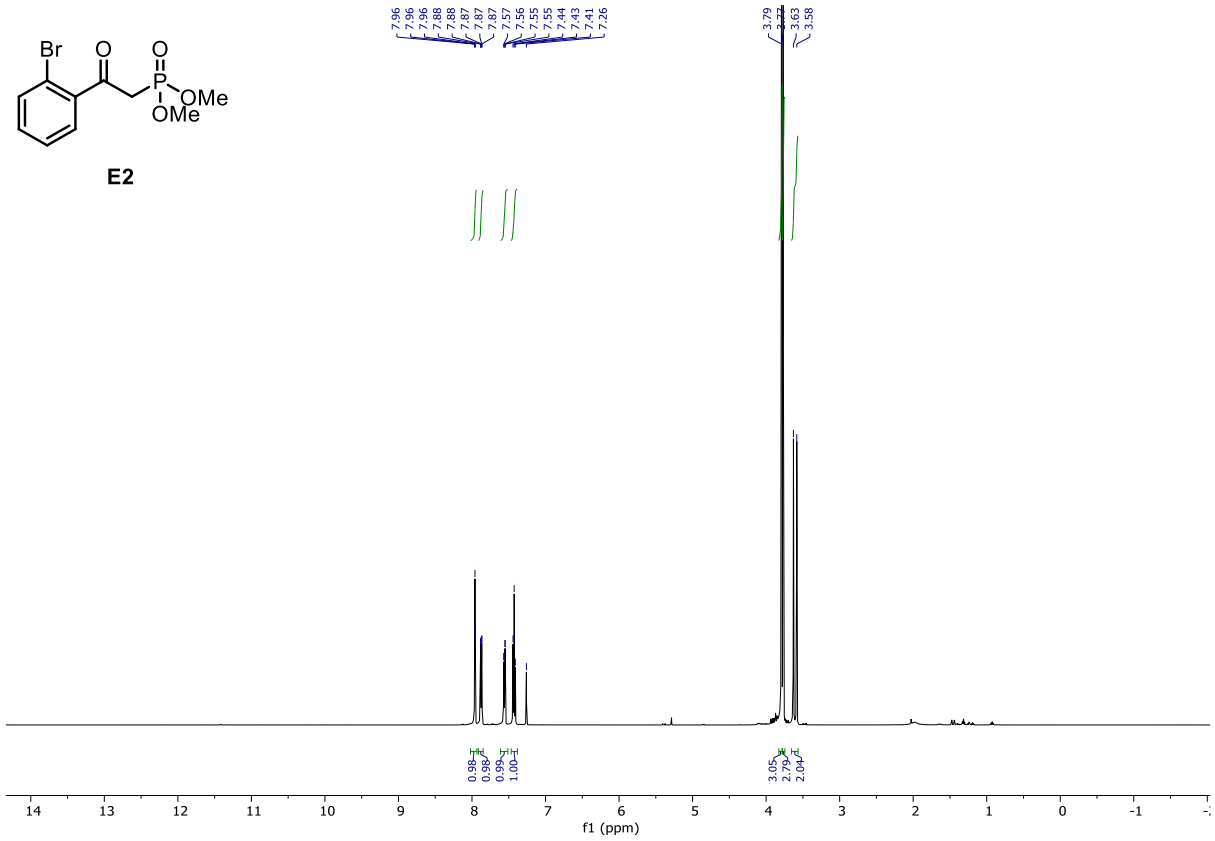
7.96
7.96
7.96
7.88
7.88
7.87
7.87
7.87
7.57
7.56
7.55
7.55
7.44
7.43
7.41
7.26
3.79
3.77
3.63
3.58
Br
O
O
P
OMe
OMe
E2
0.98
0.98
0.99
1.00
3.05
2.79
2.04
14 13 12 11 10 9 8 7 6 5 4 3 2 1 0 -1
f1 (ppm)

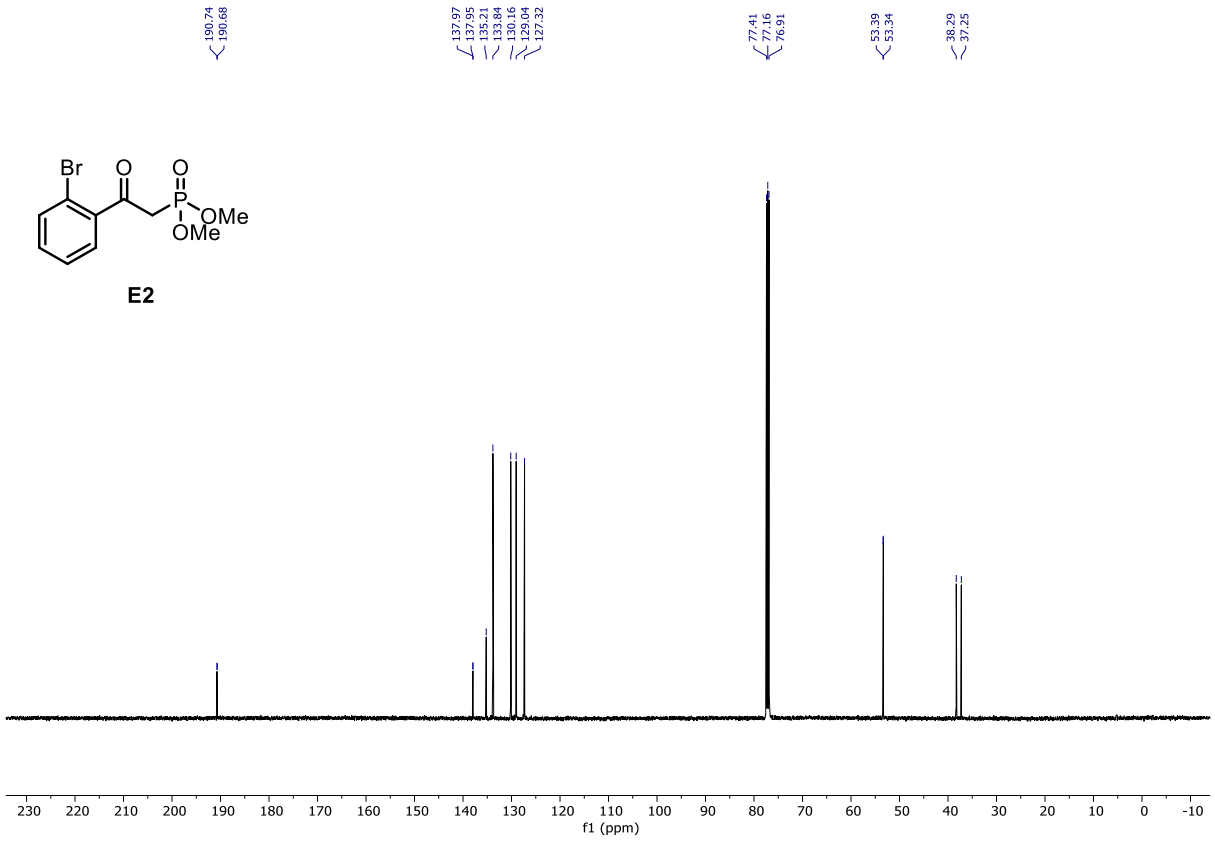
190.74
190.68
137.97
137.95
135.21
133.84
130.16
129.04
127.32
77.41
77.16
76.91
53.39
53.34
38.29
37.25
Br
O
O
P
OMe
OMe
E2
230 220 210 200 190 180 170 160 150 140 130 120 110 100 90 80 70 60 50 40 30 20 10 0 -10
f1 (ppm)

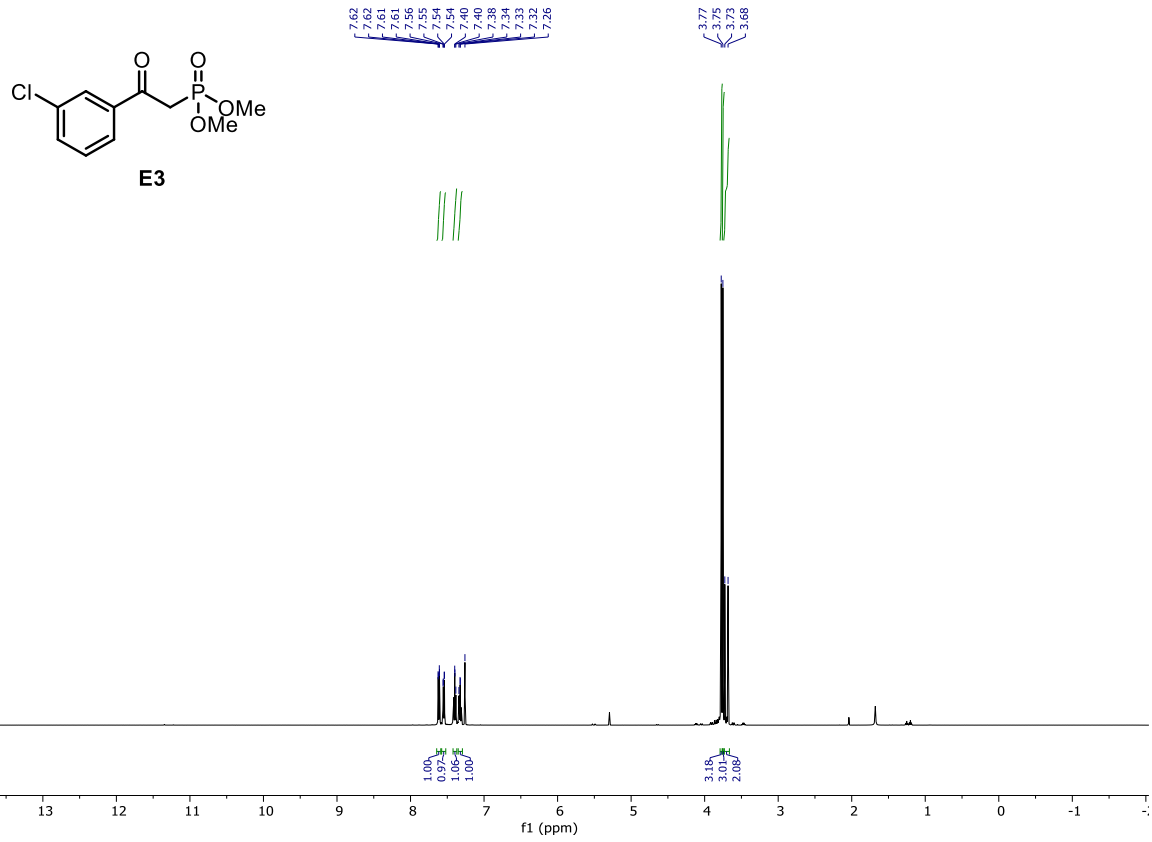
E3
7.62
7.62
7.61
7.61
7.56
7.55
7.54
7.54
7.40
7.38
7.34
7.33
7.32
7.26
3.77
3.75
3.73
3.68
1.00
0.97
1.06
1.00
3.18
3.01
2.08
f1 (ppm)

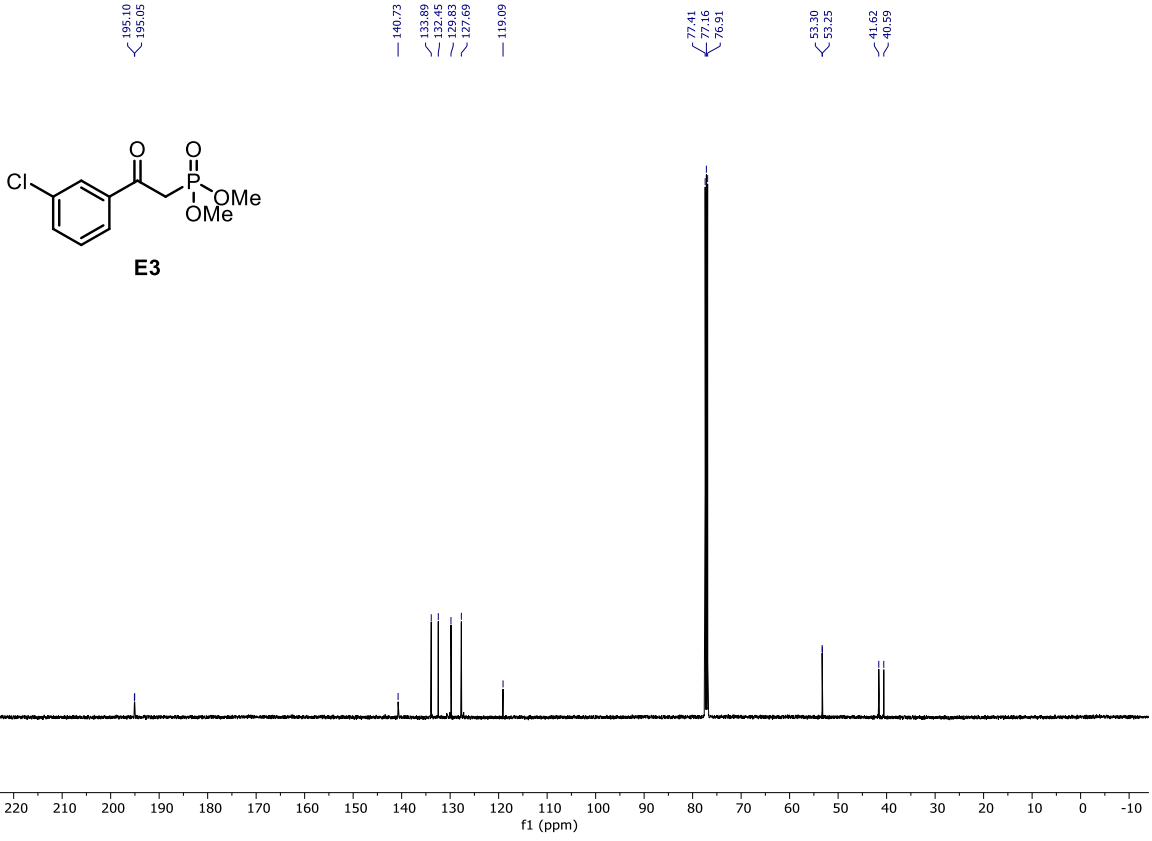
E3
195.10
195.05
140.73
133.89
132.45
129.83
127.69
119.09
77.41
77.16
76.91
53.30
53.25
41.62
40.59
f1 (ppm)

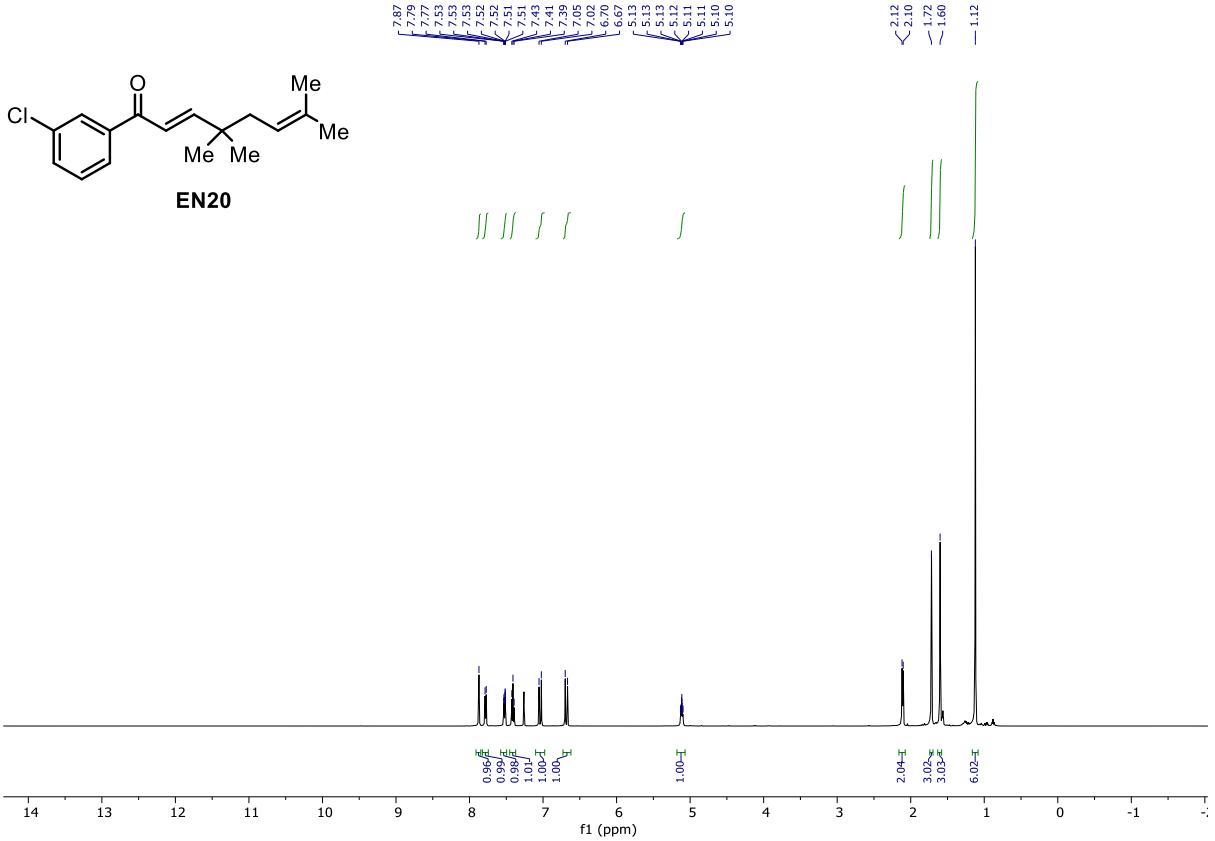
Cl
O
Me
Me
Me
Me
EN20
f1 (ppm)

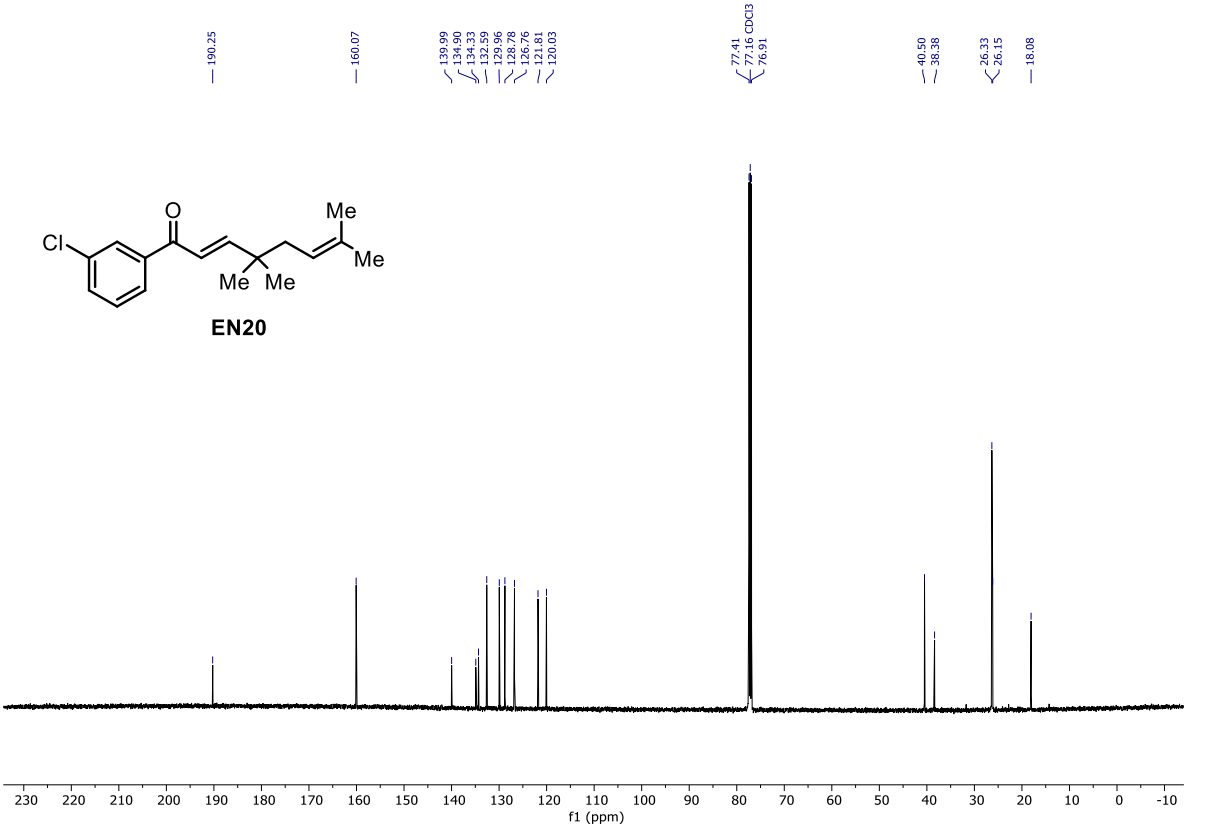
Cl
O
Me
Me
Me
Me
EN20
f1 (ppm)

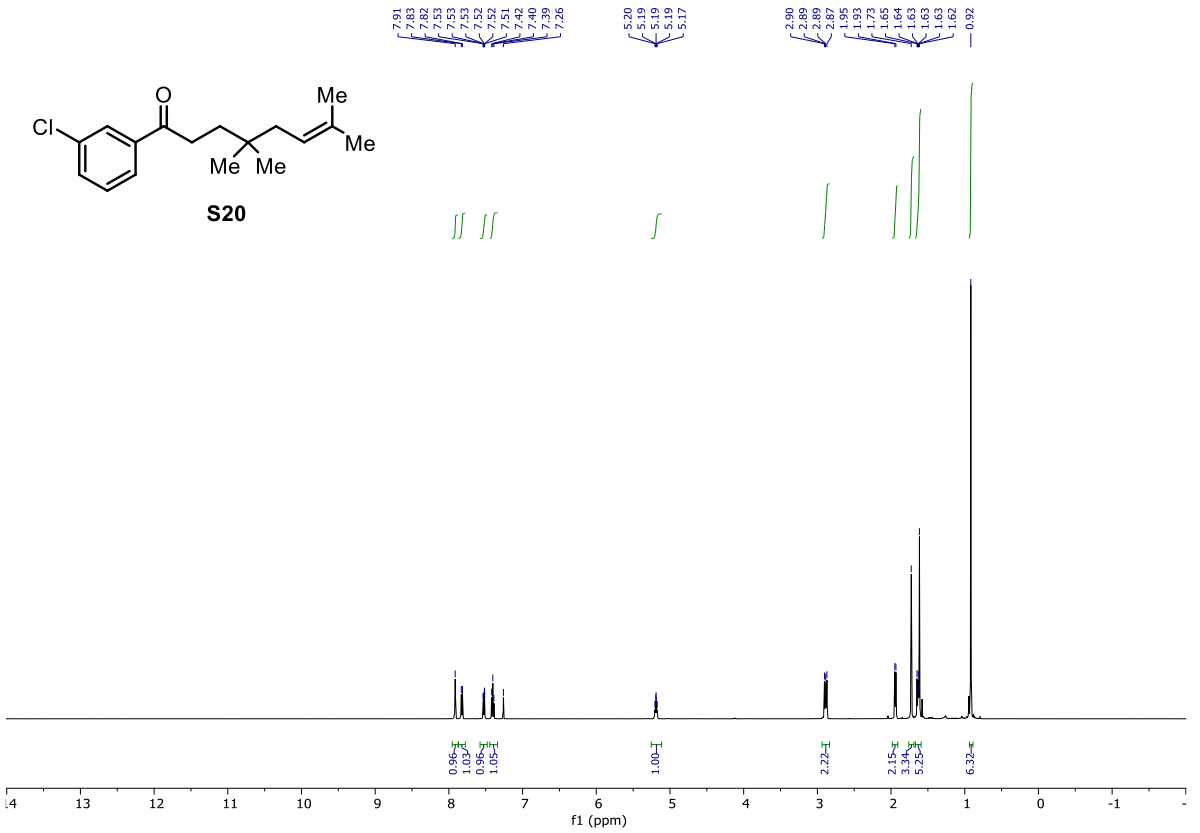
7.91
7.83
7.82
7.55
7.53
7.53
7.52
7.52
7.51
7.42
7.40
7.39
7.26
5.20
5.19
5.19
5.19
5.17
2.90
2.89
2.89
2.87
1.95
1.93
1.73
1.65
1.64
1.63
1.63
1.63
1.62
0.92
Cl
O
Me
Me
Me
Me
S20
0.96
1.03
0.96
1.05
1.00
2.22
2.15
3.34
5.25
6.32
f1 (ppm)

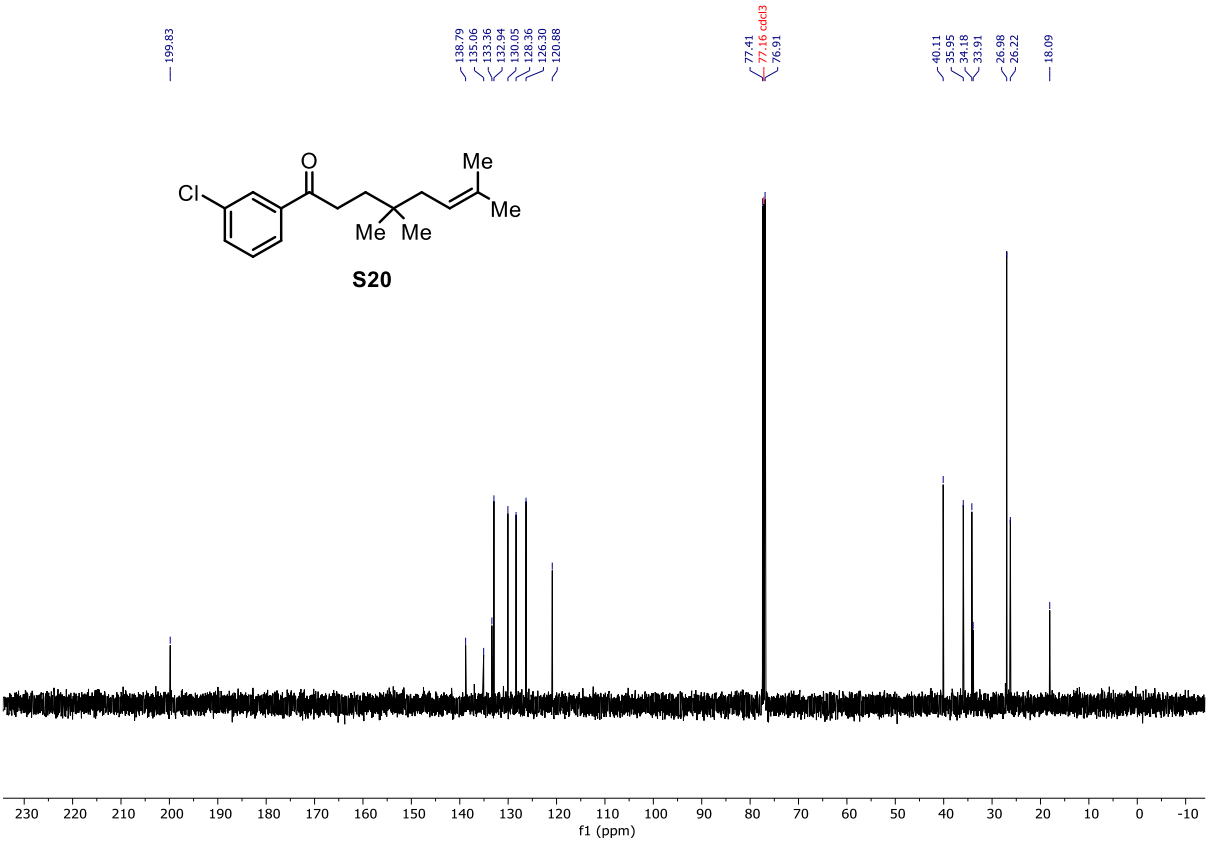
199.83
138.79
135.06
133.36
132.94
130.05
128.36
126.30
120.88
77.41
77.16 cdcl3
76.91
40.11
35.55
34.18
33.91
26.98
26.22
18.09
Cl
O
Me
Me
Me
Me
S20
f1 (ppm)

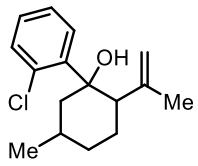
OH
Cl
Me
Me

CE21

7.42
7.29
7.28
7.26
7.24
7.24
7.23
7.22
7.18
7.17
4.80
4.73
2.43
2.41
2.25
1.91
1.91
1.89
1.89
1.87
1.85
1.84
1.83
1.82
1.80
1.79
1.61
1.61
1.59
1.48
1.46
1.44
1.21
1.11
1.11
1.10
1.09
1.08
1.07
1.06
0.92
0.91
0.93
0.95
0.92
0.87
0.98
1.00
0.98
0.94
2.03
2.00
1.01
1.02
2.94
1.03
3.02
13
12
11
10
9
8
7
6
5
4
3
2
1
0
-1
f1 (ppm)

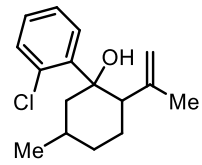
OH
Cl
Me
Me

CE21

150.75
147.76
134.15
129.26
126.59
125.44
123.33
112.83
77.34
77.16 cdcl3
76.98
74.56
52.85
49.06
34.93
28.14
27.92
25.41
22.21
230
220
210
200
190
180
170
160
150
140
130
120
110
100
90
80
70
60
50
40
30
20
10
0
-10
f1 (ppm)

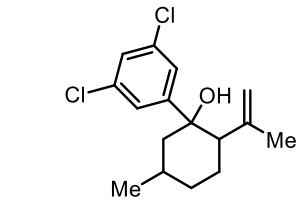
Cl
Cl
OH
Me
Me

CE10

7.31
7.30
7.30
7.26
7.21
7.20
4.83
4.83
4.82
4.73
2.41
2.40
2.38
2.37
2.23
1.92
1.91
1.90
1.88
1.88
1.85
1.82
1.81
1.80
1.80
1.78
1.77
1.76
1.63
1.63
1.60
1.44
1.41
1.37
1.28
1.14
1.13
1.10
1.09
1.07
1.06
1.04
0.93
1.85
0.79
0.99
1.00
0.98
0.93
4.05
1.05
1.04
2.97
1.06
3.03
f1 (ppm)

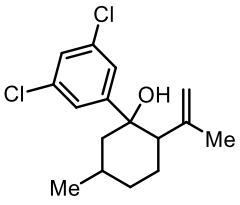
Cl
Cl
OH
Me
Me

CE10

152.30
147.18
134.73
126.62
123.99
113.32
77.34
77.16 cdcl3
76.98
74.68
52.73
49.01
34.79
28.04
27.90
25.30
22.15
f1 (ppm)

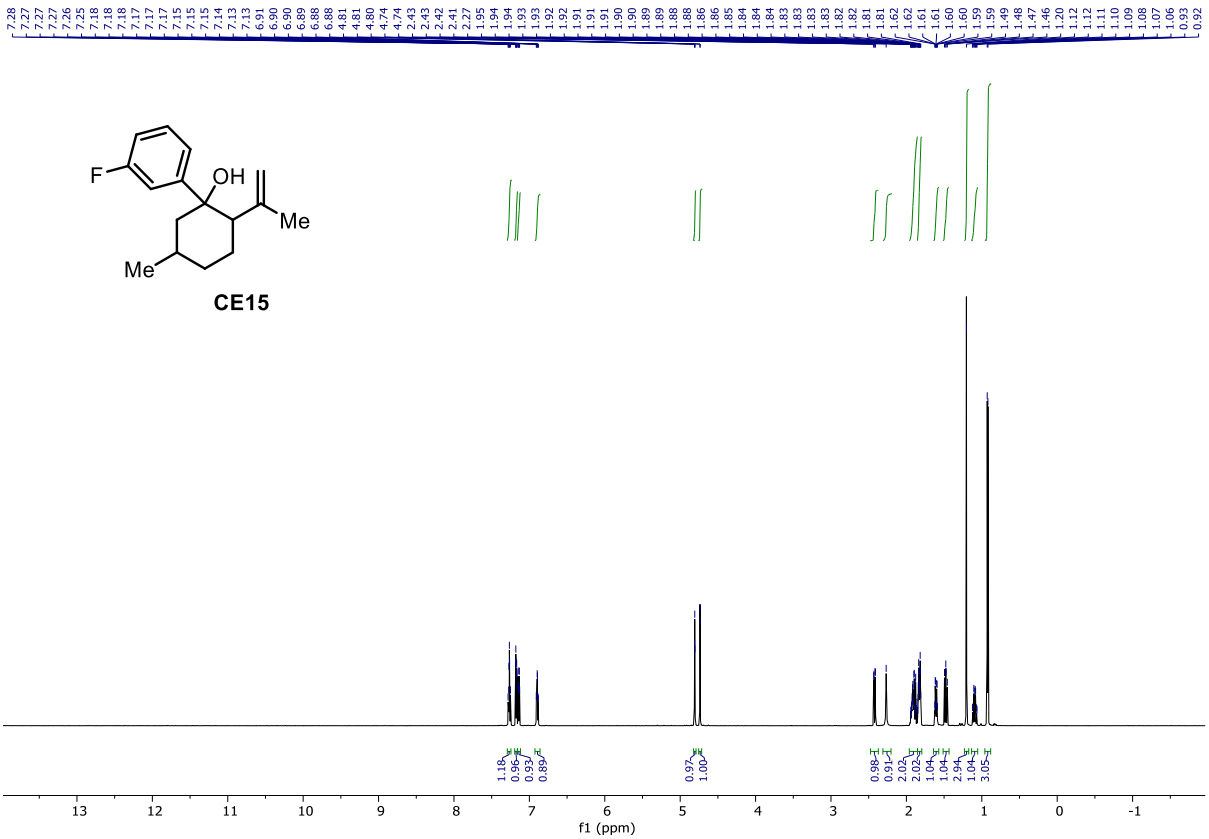
F
OH
Me
Me
CE15
f1 (ppm)

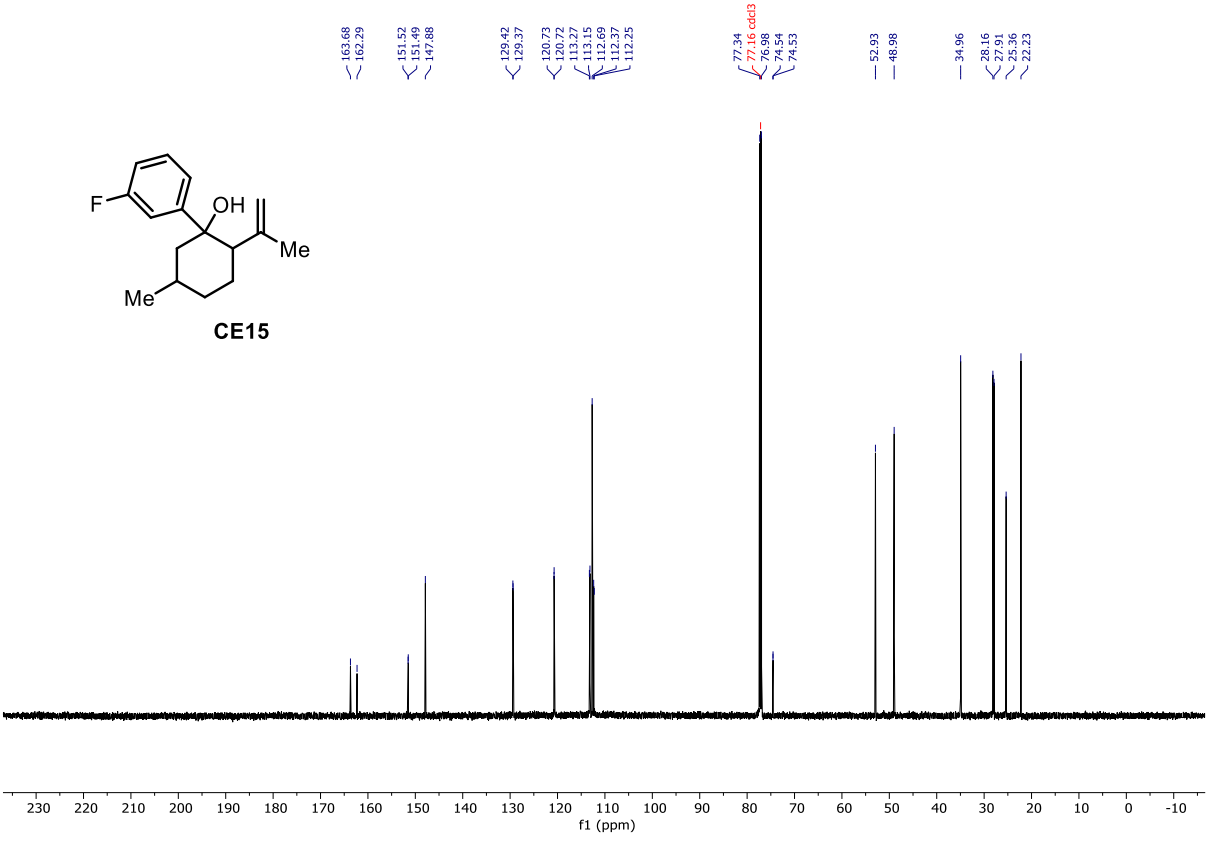
F
OH
Me
Me
CE15
f1 (ppm)

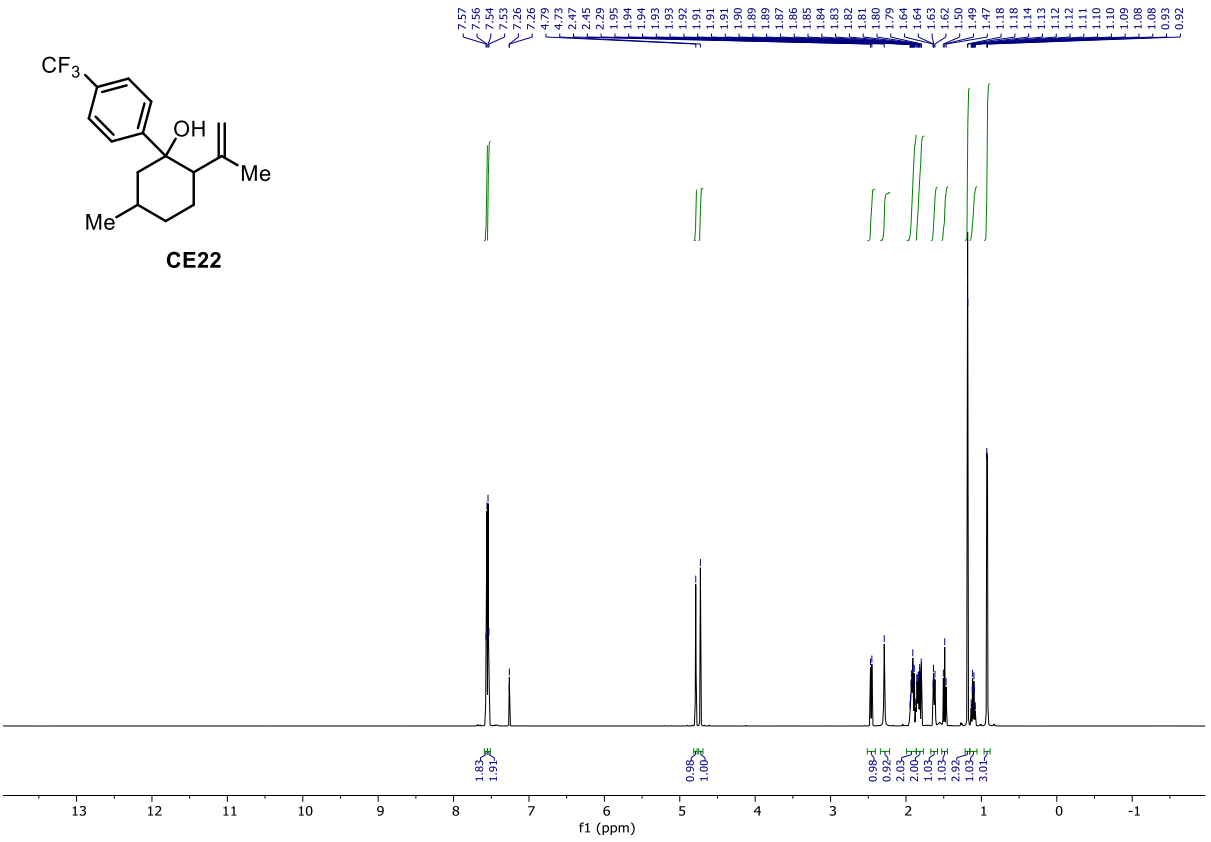
CF3
OH
Me
Me
CE22
f1 (ppm)

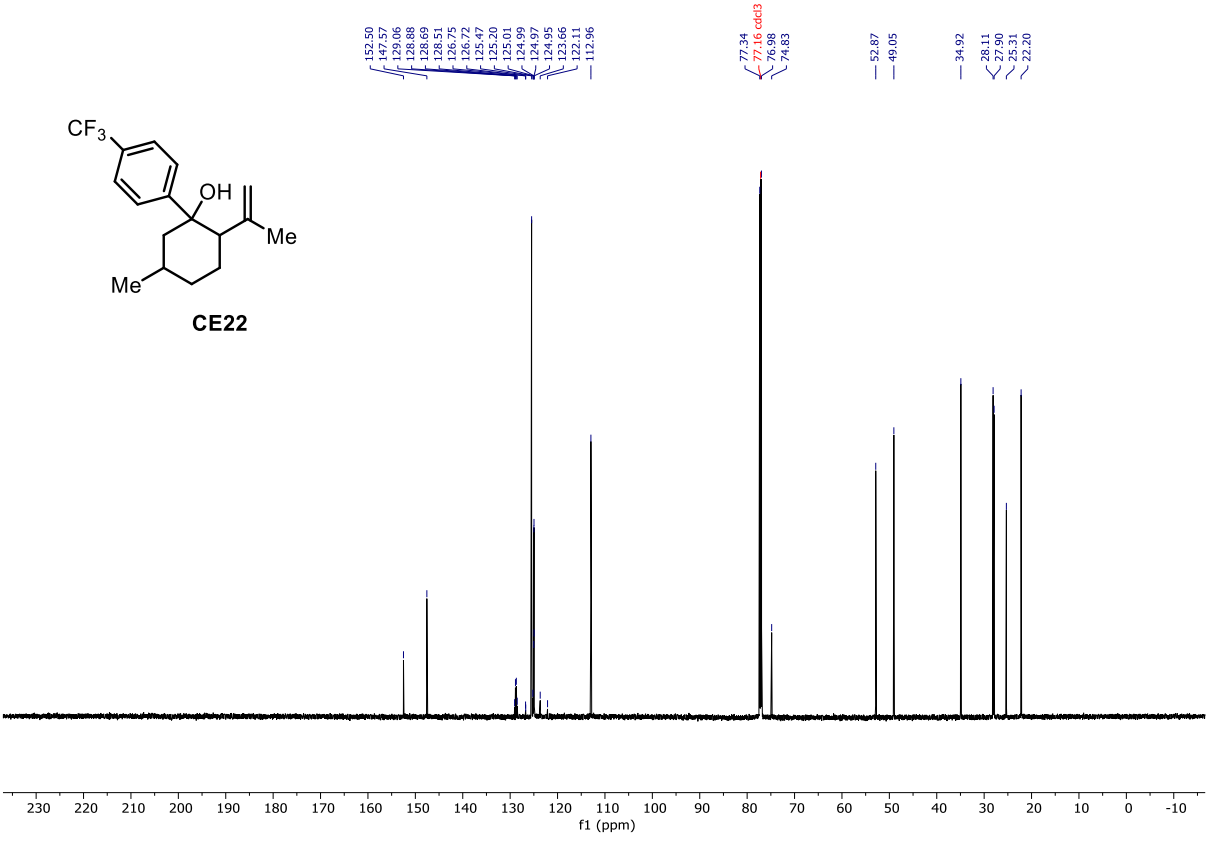
CF3
OH
Me
Me
CE22
f1 (ppm)

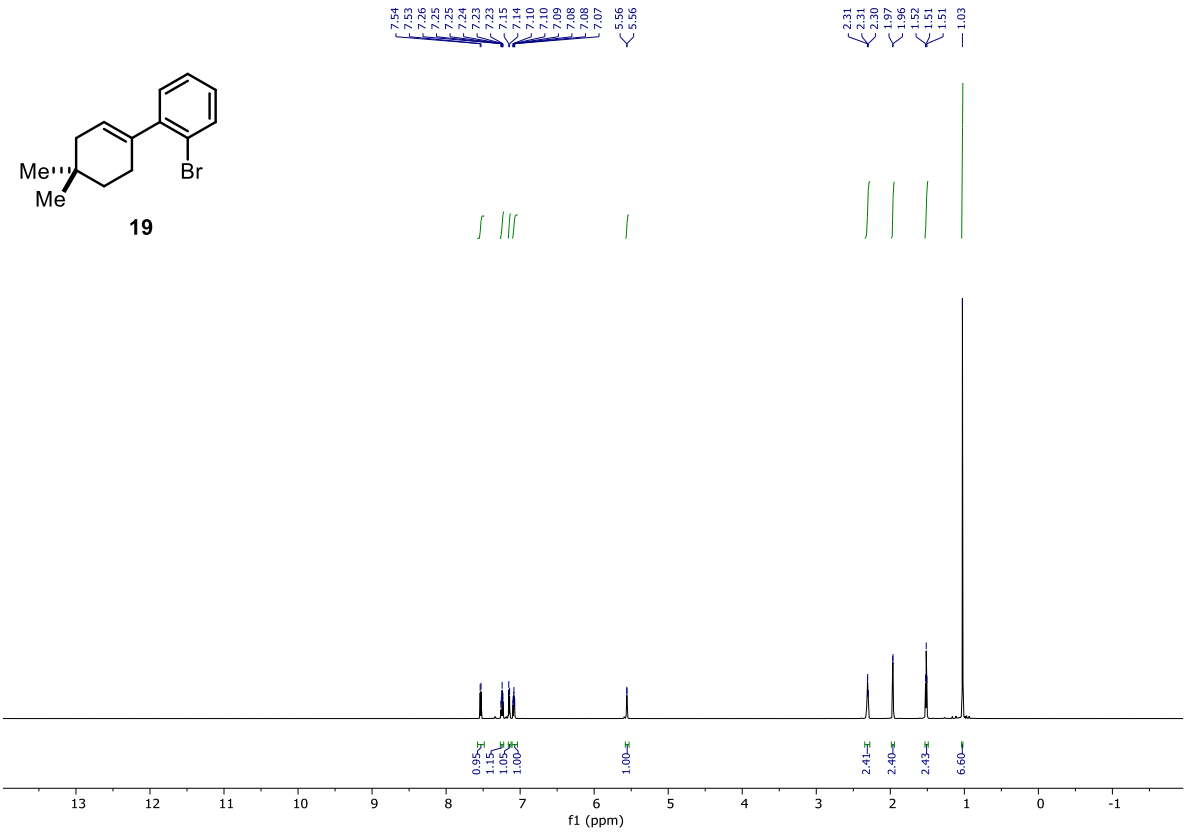
Me
Me
Br
19
f1 (ppm)

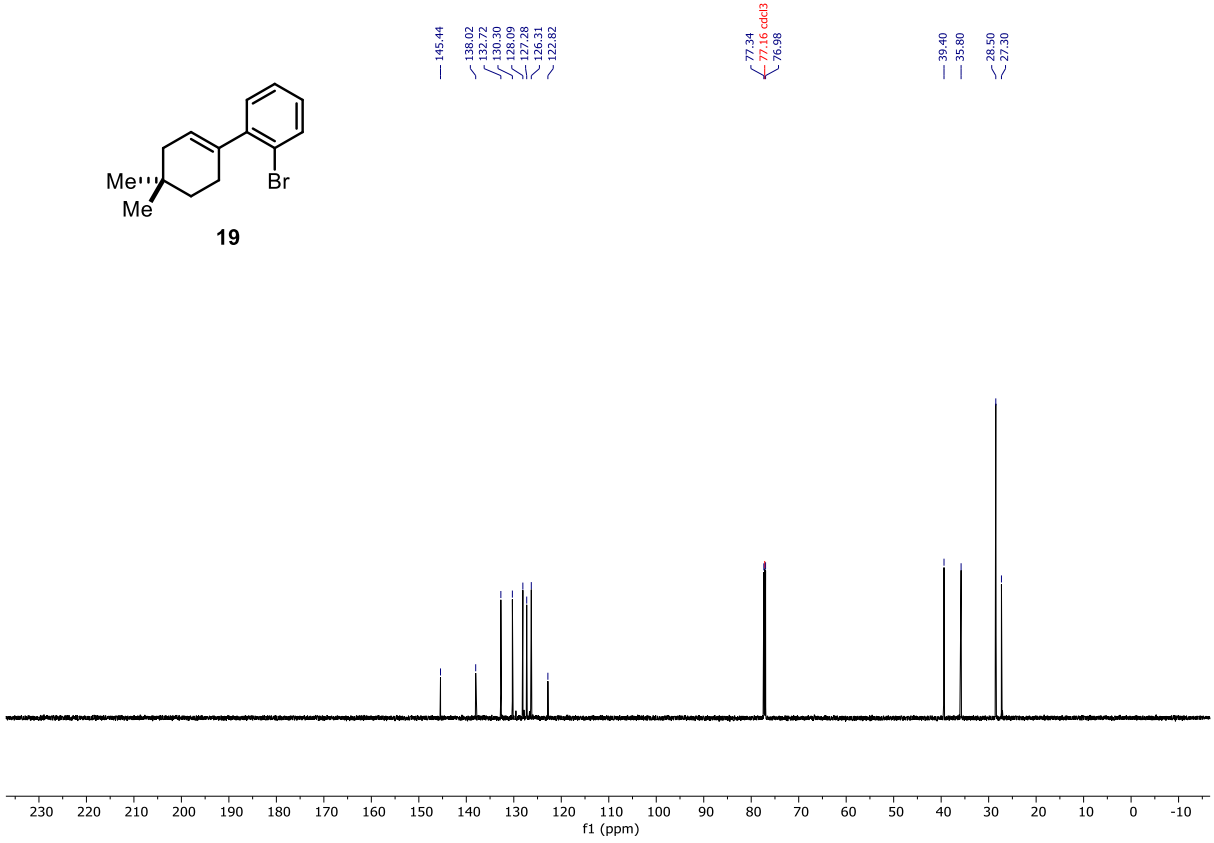
Me
Me
Br
19
f1 (ppm)

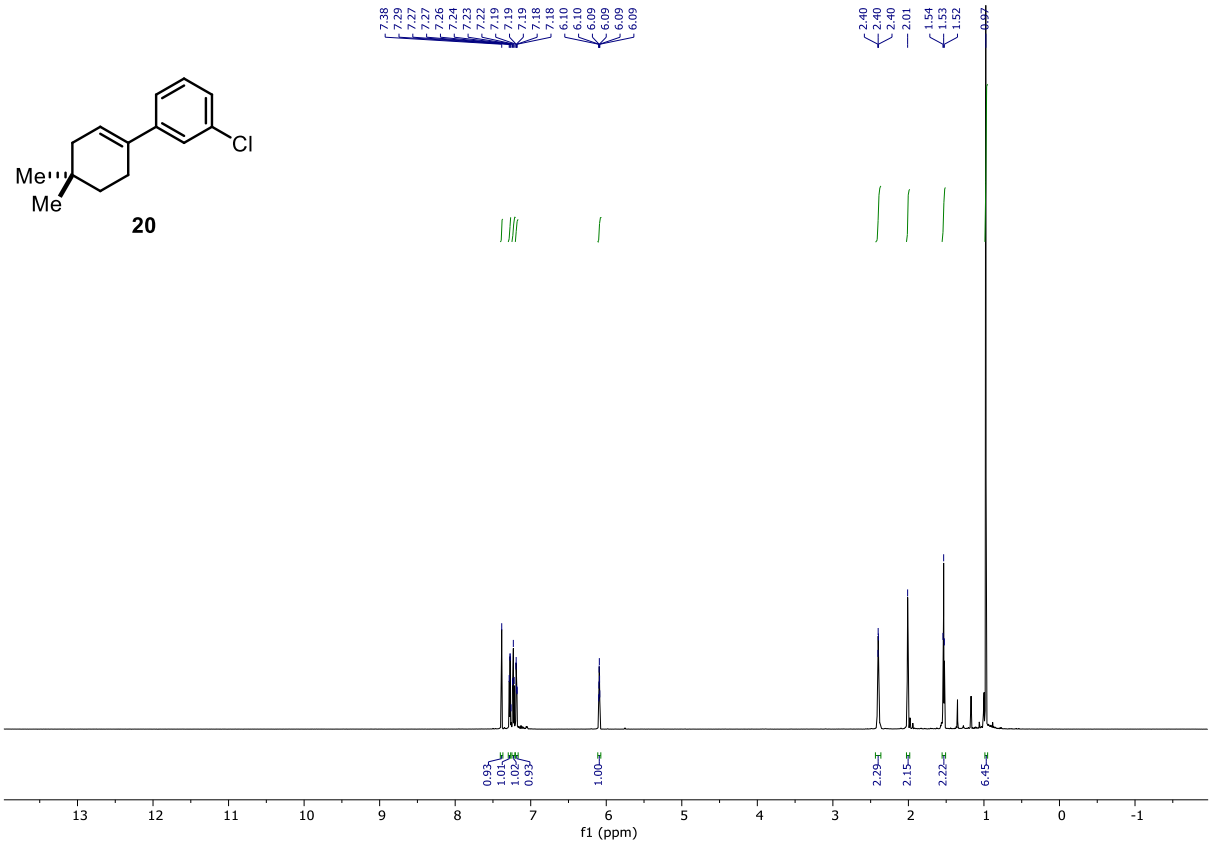
Cl
Me
Me
20
f1 (ppm)

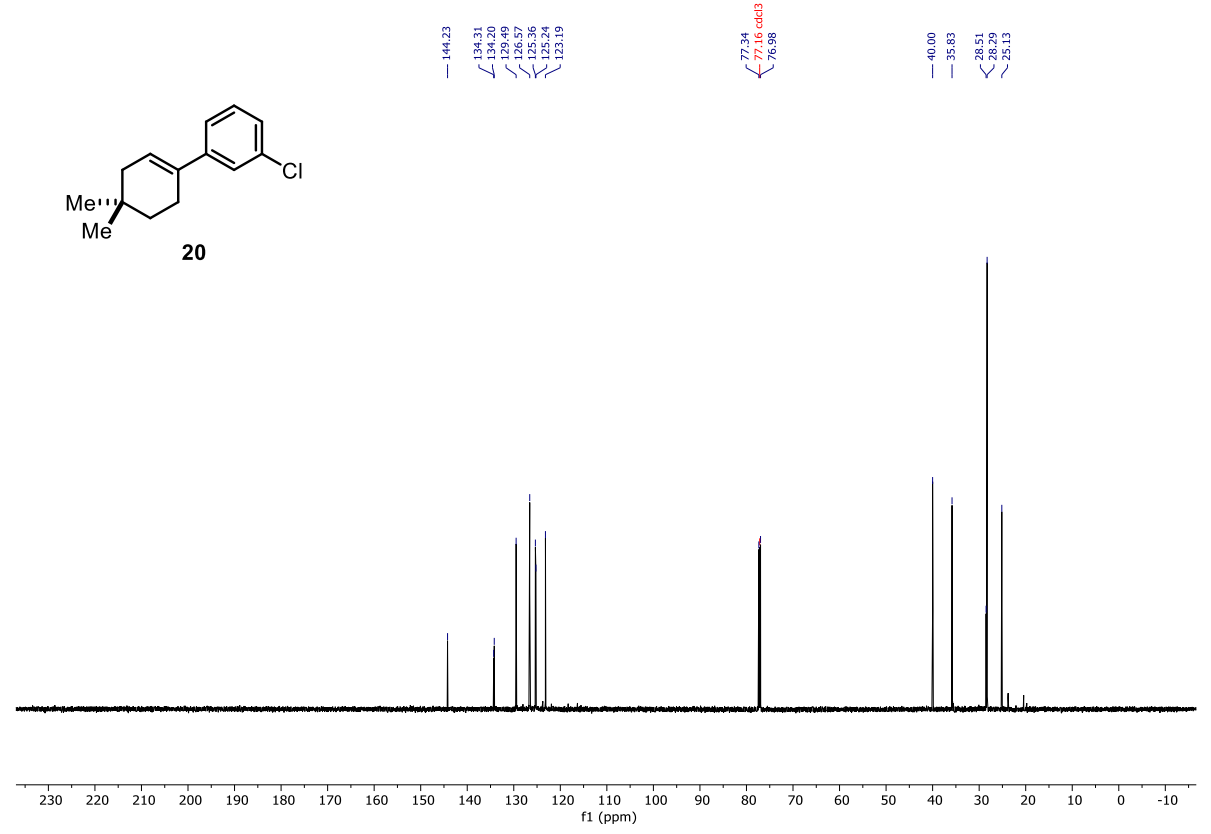
Cl
Me
Me
20
f1 (ppm)

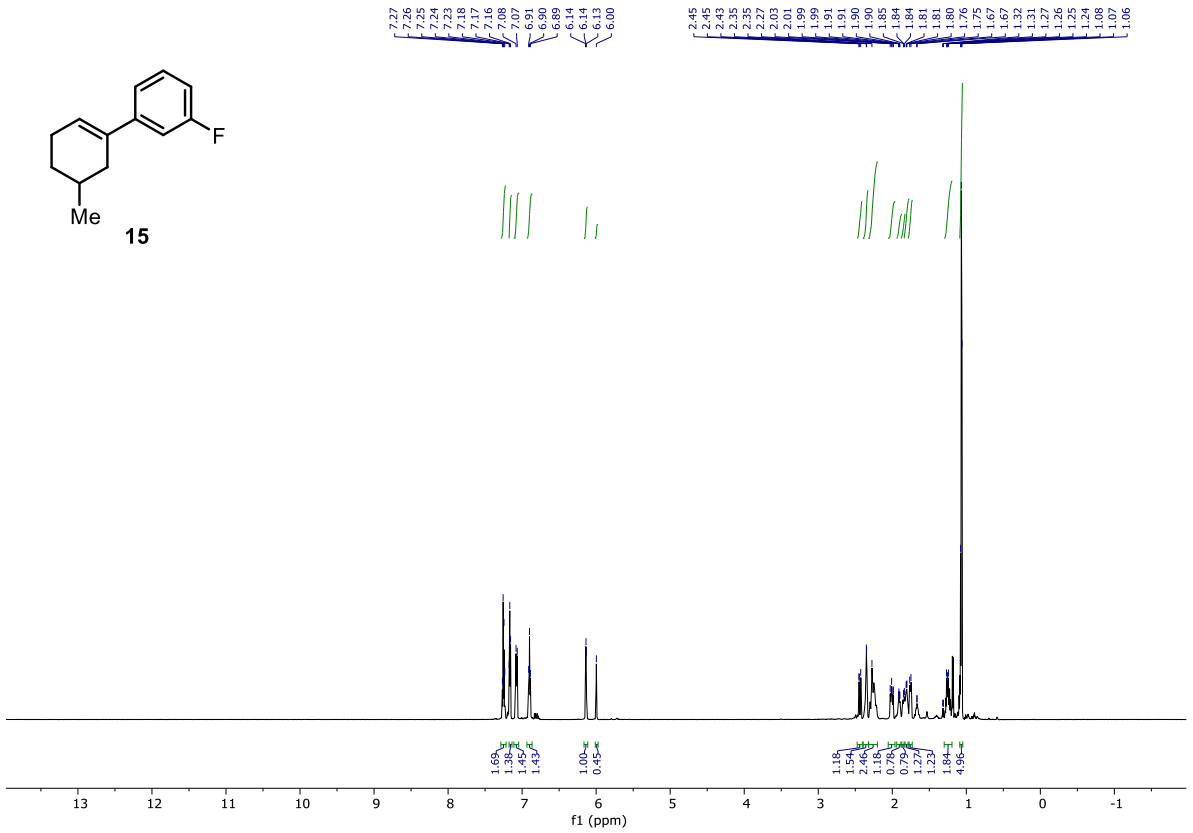
F
Me
15
f1 (ppm)

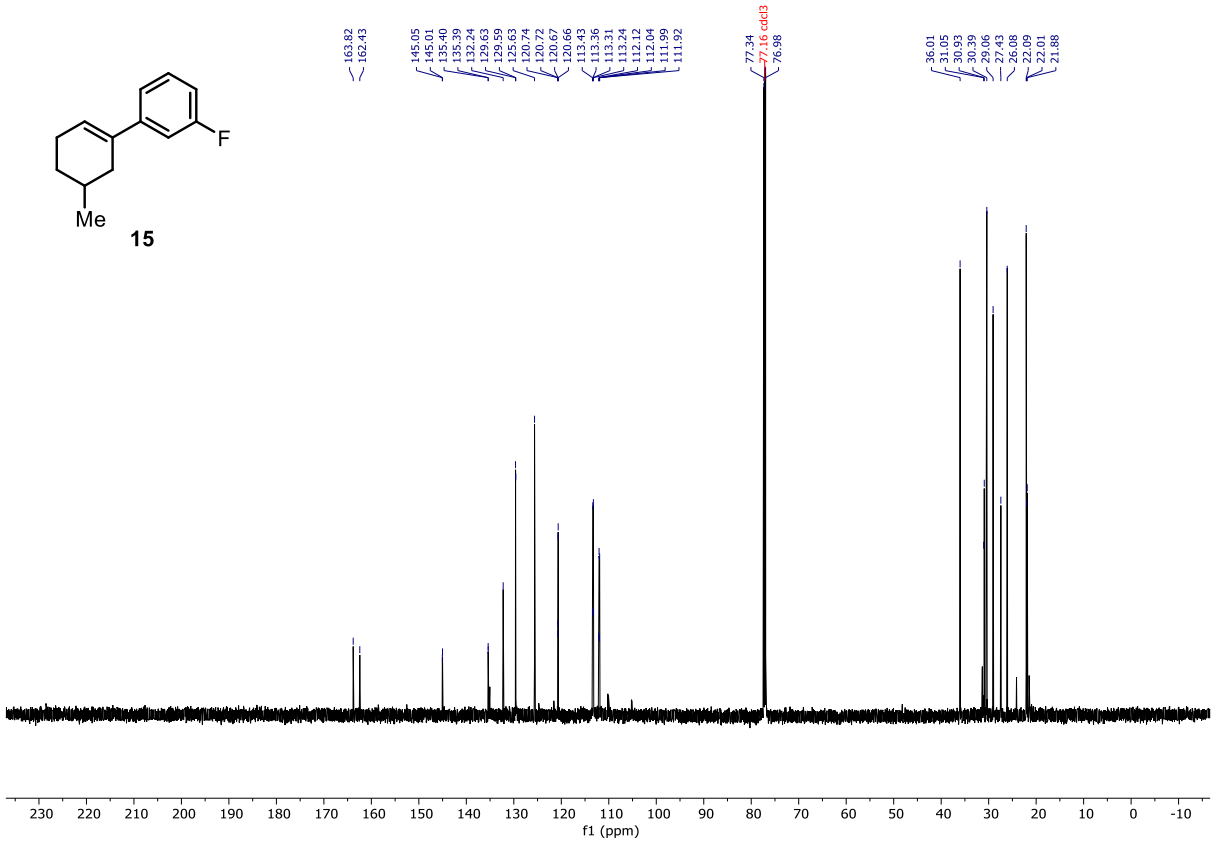
F
Me
15
f1 (ppm)

5.6 References

(1) Albright, H.; Davis, A. J.; Gomez-Lopez, J. L.; Vonesh, H. L.; Quach, P. K.; Lambert, T. H.; Schindler, C. S. Carbonyl-Olefin Metathesis. *Chemical Reviews*. American Chemical Society August 11, 2021, pp 9359–9406. https://doi.org/10.1021/acs.chemrev.0c01096.

(2) Angew Chem Int Ed Engl - October 2 1995 - Schwab - A Series of Well-Defined Metathesis Catalysts Synthesis of RuCl2 .

(3) Scholl, M.; Trnka, T. M.; Morgan, J. P.; Grubbs, R. H. *Increased Ring Closing Metathesis Activity of Ruthenium-Based Oiefin Metathesis Catalysts Coordinated with Imidazolin-2-Ylidene Ligands*; 1999; Vol. 40.

(4) Ho, T.-L.; Mcmurry, J. E.; Clive, D. L. J.; Zhang, C.; Murthy, K. S. K.; Hayward, W. D.; Daigneault, S.; Grubbs, R. H.; Turnas, W.; Hartley, F.; Pine, S. H. *C) Feast, W. J.; Gibson, V. C. In The Chemistry of the Metal-Carbon Bond*; UTC, 1993; Vol. 89.

(5) Helvetica Chimica Acta - 1 November 1971 - Demole - Applications Synth Tiques de La Cyclisation d Alcools Tertiaires -.

(6) Ludwig, J. R.; Zimmerman, P. M.; Gianino, J. B.; Schindler, C. S. Iron(III)-Catalysed Carbonyl-Olefin Metathesis. *Nature* **2016**, *533*, 374–379. https://doi.org/10.1038/nature17432.

(7) Jackson, A. C.; Goldman, B. E.; Snider, B. B. *Intramolecular and Intermolecular Lewis Acid Catalyzed Ene Reactions Using Ketones as Enophiles*; 1984; Vol. 49.

(8) *COM M UNlCATlONS.*

(9) Khripach, V. A.; Zhabinskii, V. N.; Kuchto, A. I.; Zhiburtovich, Y. Y.; Gromak, V. v.; Groen, M. B.; van der Louw, J.; de Groot, A. Intramolecular Cycloaddition/Cycloreversion of (E)-3β,17β-Diacetoxy-5,10-Secoandrost-1(10)-En-5-

One. *Tetrahedron Letters* **2006**, *47* (38), 6715–6718. https://doi.org/10.1016/j.tetlet.2006.07.096.

(10) Soicke, A.; Slavov, N.; Neudörfl, J. M.; Schmalz, H. G. Metal-Free Intramolecular Carbonyl-Olefin Metathesis of Ortho-Prenylaryl Ketones. *Synlett* **2011**, No. 17, 2487–2490. https://doi.org/10.1055/s-0030-1260320.

(11) Malakar, T.; Hanson, C. S.; Devery, J. J.; Zimmerman, P. M. Combined Theoretical and Experimental Investigation of Lewis Acid-Carbonyl Interactions for Metathesis. *ACS Catalysis* **2021**, *11* (8), 4381–4394. https://doi.org/10.1021/acscatal.0c05277.

(12) Hanson, C. S.; Psaltakis, M. C.; Cortes, J. J.; Devery, J. J. Catalyst Behavior in Metal-Catalyzed Carbonyl-Olefin Metathesis. *J Am Chem Soc* **2019**, *141* (30), 11870–11880. https://doi.org/10.1021/jacs.9b02613.

(13) Ludwig, J. R.; Phan, S.; McAtee, C. C.; Zimmerman, P. M.; Devery, J. J.; Schindler, C. S. Mechanistic Investigations of the Iron(III)-Catalyzed Carbonyl-Olefin Metathesis Reaction. *J Am Chem Soc* **2017**, *139* (31), 10832–10842. https://doi.org/10.1021/jacs.7b05641.

(14) Becker, M. Carbonyl-Olefin Metathesis for the Synthesis of Cyclic Olefins. *Organic Syntheses* **2018**, *95*, 472–485. https://doi.org/10.15227/orgsyn.095.0472.

(15) Ma, L.; Li, W.; Xi, H.; Bai, X.; Ma, E.; Yan, X.; Li, Z. FeCl 3 -Catalyzed Ring-Closing Carbonyl-Olefin Metathesis . *Angewandte Chemie* **2016**, *128* (35), 10566–10569. https://doi.org/10.1002/ange.201604349.

(16) Groso, E. J.; Golonka, A. N.; Harding, R. A.; Alexander, B. W.; Sodano, T. M.; Schindler, C. S. 3-Aryl-2,5-Dihydropyrroles via Catalytic Carbonyl-Olefin Metathesis. *ACS Catalysis* **2018**, *8* (3), 2006–2011. https://doi.org/10.1021/acscatal.7b03769.

(17) Rykaczewski, K. A.; Groso, E. J.; Vonesh, H. L.; Gaviria, M. A.; Richardson, A. D.; Zehnder, T. E.; Schindler, C. S. Tetrahydropyridines via FeCl3-Catalyzed Carbonyl-Olefin Metathesis. *Organic Letters* **2020**, *22* (7), 2844–2848. https://doi.org/10.1021/acs.orglett.0c00918.

(18) Ni, S.; Franzén, J. Carbocation Catalysed Ring Closing Aldehyde-Olefin Metathesis. *Chemical Communications* **2018**, *54* (92), 12982–12985. https://doi.org/10.1039/C8CC06734A.

(19) Wang, R.; Chen, Y.; Shu, M.; Zhao, W.; Tao, M.; Du, C.; Fu, X.; Li, A.; Lin, Z. AuCl3-Catalyzed Ring-Closing Carbonyl–Olefin Metathesis. *Chemistry - A European Journal* **2020**, *26* (9), 1941–1946. https://doi.org/10.1002/chem.201905199.

(20) Tran, U. P. N.; Oss, G.; Breugst, M.; Detmar, E.; Pace, D. P.; Liyanto, K.; Nguyen, T. v. Carbonyl-Olefin Metathesis Catalyzed by Molecular Iodine. *ACS Catalysis* **2019**, *9* (2), 912–919. https://doi.org/10.1021/acscatal.8b03769.

(21) Tran, U. P. N.; Oss, G.; Pace, D. P.; Ho, J.; Nguyen, T. v. Tropylium-Promoted Carbonyl-Olefin Metathesis Reactions. *Chemical Science* **2018**, *9* (23), 5145–5151. https://doi.org/10.1039/c8sc00907d.

(22) Djurovic, A.; Vayer, M.; Li, Z.; Guillot, R.; Baltaze, J. P.; Gandon, V.; Bour, C. Synthesis of Medium-Sized Carbocycles by Gallium-Catalyzed Tandem Carbonyl-Olefin Metathesis/Transfer Hydrogenation. *Organic Letters* **2019**, *21* (19), 8132–8137. https://doi.org/10.1021/acs.orglett.9b03240.

(23) McAtee, C. C.; Riehl, P. S.; Schindler, C. S. Polycyclic Aromatic Hydrocarbons via Iron(III)-Catalyzed Carbonyl-Olefin Metathesis. *J Am Chem Soc* **2017**, *139* (8), 2960–2963. https://doi.org/10.1021/jacs.7b01114.

(24) Albright, H.; Riehl, P. S.; McAtee, C. C.; Reid, J. P.; Ludwig, J. R.; Karp, L. A.; Zimmerman, P. M.; Sigman, M. S.; Schindler, C. S. Catalytic Carbonyl-Olefin Metathesis of Aliphatic Ketones: Iron(III) Homo-Dimers as Lewis Acidic Superelectrophiles. *J Am Chem Soc* **2019**, *141* (4), 1690–1700. https://doi.org/10.1021/jacs.8b11840.

(25) Olah, G. A. *International Edition in English Superelectrophiles***; 1993; Vol. 32.

(26) Negishi, E. *CONCEPTS*; 1999; Vol. 5.

(27) Albright, H.; Vonesh, H. L.; Becker, M. R.; Alexander, B. W.; Ludwig, J. R.; Wiscons, R. A.; Schindler, C. S. GaCl3-Catalyzed Ring-Opening Carbonyl-Olefin Metathesis. *Organic Letters* **2018**, *20* (16), 4954–4958. https://doi.org/10.1021/acs.orglett.8b02086.

(28) Naidu, V. R.; Bah, J.; Franzén, J. Direct Organocatalytic Oxo-Metathesis, a Trans-Selective Carbocation-Catalyzed Olefination of Aldehydes. *European Journal of Organic Chemistry* **2015**, *2015* (8), 1834–1839. https://doi.org/10.1002/ejoc.201403651.

(29) Albright, H.; Vonesh, H. L.; Schindler, C. S. Superelectrophilic Fe(III)-Ion Pairs as Stronger Lewis Acid Catalysts for (E)-Selective Intermolecular Carbonyl-Olefin Metathesis. *Organic Letters* **2020**, *22* (8), 3155–3160. https://doi.org/10.1021/acs.orglett.0c00917.

(30) Riehl, P. S.; Nasrallah, D. J.; Schindler, C. S. Catalytic, Transannular Carbonyl-Olefin Metathesis Reactions. *Chemical Science* **2019**, *10* (44), 10267–10274. https://doi.org/10.1039/c9sc03716k.

(31) Ni, S.; Franzén, J. Carbocation Catalysed Ring Closing Aldehyde-Olefin Metathesis. *Chemical Communications* **2018**, *54* (92), 12982–12985. https://doi.org/10.1039/C8CC06734A.

(32) Tran, U. P. N.; Oss, G.; Pace, D. P.; Ho, J.; Nguyen, T. v. Tropylium-Promoted Carbonyl-Olefin Metathesis Reactions. *Chemical Science* **2018**, *9* (23), 5145–5151. https://doi.org/10.1039/c8sc00907d.

(33) Naidu, V. R.; Bah, J.; Franzén, J. Direct Organocatalytic Oxo-Metathesis, a Trans-Selective Carbocation-Catalyzed Olefination of Aldehydes. *European Journal of Organic Chemistry* **2015**, *2015* (8), 1834–1839. https://doi.org/10.1002/ejoc.201403651.

(34) Hanson, C. S.; Psaltakis, M. C.; Cortes, J. J.; Devery, J. J. Catalyst Behavior in Metal-Catalyzed Carbonyl-Olefin Metathesis. *J Am Chem Soc* **2019**, *141* (30), 11870–11880. https://doi.org/10.1021/jacs.9b02613.

(35) Ma, L.; Li, W.; Xi, H.; Bai, X.; Ma, E.; Yan, X.; Li, Z. FeCl 3 -Catalyzed Ring-Closing Carbonyl-Olefin Metathesis . *Angewandte Chemie* **2016**, *128* (35), 10566–10569. https://doi.org/10.1002/ange.201604349.

(36) Riehl, P. S.; Nasrallah, D. J.; Schindler, C. S. Catalytic, Transannular Carbonyl-Olefin Metathesis Reactions. *Chemical Science* **2019**, *10* (44), 10267–10274. https://doi.org/10.1039/c9sc03716k.

(37) Albright, H.; Vonesh, H. L.; Becker, M. R.; Alexander, B. W.; Ludwig, J. R.; Wiscons, R. A.; Schindler, C. S. GaCl3-Catalyzed Ring-Opening Carbonyl-Olefin Metathesis. *Organic Letters* **2018**, *20* (16), 4954–4958. https://doi.org/10.1021/acs.orglett.8b02086.

(38) Groso, E. J.; Golonka, A. N.; Harding, R. A.; Alexander, B. W.; Sodano, T. M.; Schindler, C. S. 3-Aryl-2,5-Dihydropyrroles via Catalytic Carbonyl-Olefin Metathesis. *ACS Catalysis* **2018**, *8* (3), 2006–2011. https://doi.org/10.1021/acscatal.7b03769.

(39) Ludwig, J. R.; Phan, S.; McAtee, C. C.; Zimmerman, P. M.; Devery, J. J.; Schindler, C. S. Mechanistic Investigations of the Iron(III)-Catalyzed Carbonyl-Olefin Metathesis

Reaction. *J Am Chem Soc* **2017**, *139* (31), 10832–10842. https://doi.org/10.1021/jacs.7b05641.

(40) Ludwig, J. R.; Schindler, C. S. Lewis Acid Catalyzed Carbonyl-Olefin Metathesis. *Synlett* **2017**, *28* (13), 1501–1509. https://doi.org/10.1055/s-0036-1588827.

(41) Ludwig, J. R.; Zimmerman, P. M.; Gianino, J. B.; Schindler, C. S. Iron(III)-Catalysed Carbonyl-Olefin Metathesis. *Nature* **2016**, *533*, 374–379. https://doi.org/10.1038/nature17432.

(42) Albright, H.; Riehl, P. S.; McAtee, C. C.; Reid, J. P.; Ludwig, J. R.; Karp, L. A.; Zimmerman, P. M.; Sigman, M. S.; Schindler, C. S. Catalytic Carbonyl-Olefin Metathesis of Aliphatic Ketones: Iron(III) Homo-Dimers as Lewis Acidic Superelectrophiles. *J Am Chem Soc* **2019**, *141* (4), 1690–1700. https://doi.org/10.1021/jacs.8b11840.

(43) McAtee, C. C.; Riehl, P. S.; Schindler, C. S. Polycyclic Aromatic Hydrocarbons via Iron(III)-Catalyzed Carbonyl-Olefin Metathesis. *J Am Chem Soc* **2017**, *139* (8), 2960–2963. https://doi.org/10.1021/jacs.7b01114.

(44) Rykaczewski, K. A.; Groso, E. J.; Vonesh, H. L.; Gaviria, M. A.; Richardson, A. D.; Zehnder, T. E.; Schindler, C. S. Tetrahydropyridines via FeCl3-Catalyzed Carbonyl-Olefin Metathesis. *Organic Letters* **2020**, *22* (7), 2844–2848. https://doi.org/10.1021/acs.orglett.0c00918.

(45) Catti, L.; Tiefenbacher, K. Brønsted-Säure-Katalysierte Carbonyl-Olefin-Metathese in Einer Selbstorganisierten Supramolekularen Wirtstruktur. *Angewandte Chemie* **2018**, *130* (44), 14797–14800. https://doi.org/10.1002/ange.201712141.

(46) Zhu, Y.; Rebek, J.; Yu, Y. Cyclizations Catalyzed inside a Hexameric Resorcinarene Capsule. *Chemical Communications* **2019**, *55* (25), 3573–3577. https://doi.org/10.1039/c9cc01611b.

(47) Griffith, A. K.; Vanos, C. M.; Lambert, T. H. Organocatalytic Carbonyl-Olefin Metathesis. *J Am Chem Soc* **2012**, *134* (45), 18581–18584. https://doi.org/10.1021/ja309650u.

(48) Hong, X.; Liang, Y.; Griffith, A. K.; Lambert, T. H.; Houk, K. N. Distortion-Accelerated Cycloadditions and Strain-Release-Promoted Cycloreversions in the Organocatalytic Carbonyl-Olefin Metathesis. *Chemical Science* **2014**, *5* (2), 471–475. https://doi.org/10.1039/c3sc52882k.

(49) Zhang, Y.; Jermaks, J.; MacMillan, S. N.; Lambert, T. H. Synthesis of 2 H-Chromenes via Hydrazine-Catalyzed Ring-Closing Carbonyl-Olefin Metathesis. *ACS Catalysis* **2019**, *9* (10), 9259–9264. https://doi.org/10.1021/acscatal.9b03656.

(50) Zhang, Y.; Jermaks, J.; MacMillan, S. N.; Lambert, T. H. Synthesis of 2 H-Chromenes via Hydrazine-Catalyzed Ring-Closing Carbonyl-Olefin Metathesis. *ACS Catalysis* **2019**, *9* (10), 9259–9264. https://doi.org/10.1021/acscatal.9b03656.

(51) Albright, H.; Davis, A. J.; Gomez-Lopez, J. L.; Vonesh, H. L.; Quach, P. K.; Lambert, T. H.; Schindler, C. S. Carbonyl-Olefin Metathesis. *Chemical Reviews*. American Chemical Society August 11, 2021, pp 9359–9406. https://doi.org/10.1021/acs.chemrev.0c01096.

(52) Soicke, A.; Slavov, N.; Neudörfl, J. M.; Schmalz, H. G. Metal-Free Intramolecular Carbonyl-Olefin Metathesis of Ortho-Prenylaryl Ketones. *Synlett* **2011**, No. 17, 2487–2490. https://doi.org/10.1055/s-0030-1260320.

(53) Schopov, I. *A Carbonyl-Olefin Exchange Reaction-New Route to Polyconjugated Polymers, 1 A New Synthesis of Polyphenylacetylene*; 1983; Vol. 4.

(54) Ho, T.-L.; Mcmurry, J. E.; Clive, D. L. J.; Zhang, C.; Murthy, K. S. K.; Hayward, W. D.; Daigneault, S.; Grubbs, R. H.; Turnas, W.; Hartley, F.; Pine, S. H. *C) Feast, W. J.; Gibson, V. C. In The Chemistry of the Metal-Carbon Bond*; UTC, 1993; Vol. 89.

(55) Valiulin, R. A.; Arisco, T. M.; Kutateladze, A. G. Photoinduced Intramolecular Cyclopentanation vs Photoprotolytic Oxametathesis in Polycyclic Alkenes Outfitted with Conformationally Constrained Aroylmethyl Chromophores. *Journal of Organic Chemistry* **2013**, *78* (5), 2012–2025. https://doi.org/10.1021/jo301909j.

(56) Valiulin, R. A.; Arisco, T. M.; Kutateladze, A. G. Double-Tandem [4π+2π]·[2 Π+2π]·[4π+2π] ·[2π+2π] Synthetic Sequence with Photoprotolytic Oxametathesis and Photoepoxidation in the Chromone Series. *Journal of Organic Chemistry* **2011**, *76* (5), 1319–1332. https://doi.org/10.1021/jo102221q.

(57) Valiulin, R. A.; Kutateladze, A. G. Harvesting the Strain Installed by a Paternò-Büchi Step in a Synthetically Useful Way: High-Yielding Photoprotolytic Oxametathesis in Polycyclic Systems. *Organic Letters* **2009**, *11* (17), 3886–3889. https://doi.org/10.1021/ol901456m.

(58) Pérez-Ruiz, R.; Miranda, M. A.; Alle, R.; Meerholz, K.; Griesbeck, A. G. An Efficient Carbonyl-Alkene Metathesis of Bicyclic Oxetanes: Photoinduced Electron Transfer Reduction of the Paternò–Büchi Adducts from 2,3-Dihydrofuran and Aromatic Aldehydes. *Photochemical and Photobiological Sciences* **2006**, *5* (1), 51–55. https://doi.org/10.1039/b513875b.

(59) Pérez-Ruiz, R.; Gil, S.; Miranda, M. A. Stereodifferentiation in the Photochemical Cycloreversion of Diastereomeric Methoxynaphthalene-Oxetane Dyads. **2005**. https://doi.org/10.1021/jo048708.

(60) D'Auria, M.; Racioppi, R.; Viggiani, L. Paternò-Büchi Reaction between Furan and Heterocyclic Aldehydes: Oxetane Formation vs. Metathesis. *Photochemical and Photobiological Sciences* **2010**, *9* (8), 1134–1138. https://doi.org/10.1039/c0pp00076k.

(61) Guilford Jones, B.; Acquadro, M. A.; Carmody, M. A. *Long-Chain Enals Oia Carbonyl-Olefin Metathesis. An Application in Pheromone Synthesis*; 1975.

(62) Guilford Jones, B. I.; Schwartz, S. B.; Marton, M. T. *Regiospecific Thermal Cleavage of Some Oxetan Photoadducts : Carbonyl-Olefin Metathesis in Sequential Photochemical and Thermal Steps*; 1973.

(63) Albright, H.; Vonesh, H. L.; Schindler, C. S. Superelectrophilic Fe(III)-Ion Pairs as Stronger Lewis Acid Catalysts for (E)-Selective Intermolecular Carbonyl-Olefin Metathesis. *Organic Letters* **2020**, *22* (8), 3155–3160. https://doi.org/10.1021/acs.orglett.0c00917.

(64) Olah, G. A. *International Edition in English Superelectrophiles***; 1993; Vol. 32.

(65) Negishi, E. *CONCEPTS*; 1999; Vol. 5.

(66) Stephan, D. W.; Erker, G. Chemie Frustrierter Lewis-Paare: Entwicklung Und Perspektiven. *Angewandte Chemie* **2015**, *127* (22), 6498–6541. https://doi.org/10.1002/ange.201409800.

(67) Denmark, S. E.; Eklov, B. M.; Yao, P. J.; Eastgate, M. D. On the Mechanism of Lewis Base Catalyzed Aldol Addition Reactions: Kinetic and Spectroscopic Investigations Using

Rapid-Injection NMR. *J Am Chem Soc* **2009**, *131* (33), 11770–11787. https://doi.org/10.1021/ja902474j.

(68) Tomifuji, R.; Maeda, K.; Takahashi, T.; Kurahashi, T.; Matsubara, S. FeCl 3 as an Ion-Pairing Lewis Acid Catalyst. Formation of Highly Lewis Acidic FeCl 2+ and Thermodynamically Stable FeCl 4- to Catalyze the Aza-Diels-Alder Reaction with High Turnover Frequency. *Organic Letters* **2018**, *20* (23), 7474–7477. https://doi.org/10.1021/acs.orglett.8b03249.

(69) Ic00256a033.

(70) Davis, A. J.; Watson, R. B.; Nasrallah, D. J.; Gomez-Lopez, J. L.; Schindler, C. S. Superelectrophilic Aluminium(Iii)–Ion Pairs Promote a Distinct Reaction Path for Carbonyl–Olefin Ring-Closing Metathesis. *Nature Catalysis* **2020**, *3* (10), 787–796. https://doi.org/10.1038/s41929-020-00499-5.

(71) Strauss, S. H. *The Search for Larger and More Weakly Coordinating Anions*; 1993; Vol. 93.

(72) Beck, W.; Sunkel, K. Metal Complexes of Weakly Coordinating Anions. Precursors of Strong Cationic Organometallic Lewis Acids1^.

(73) Schottel, B. L.; Chifotides, H. T.; Shatruk, M.; Chouai, A.; Pérez, L. M.; Bacsa, J.; Dunbar, K. R. Anion-π Interactions as Controlling Elements in Self-Assembly Reactions of Ag(I) Complexes with π-Acidic Aromatic Rings. *J Am Chem Soc* **2006**, *128* (17), 5895–5912. https://doi.org/10.1021/ja0606273.

(74) Om50006a014.

(75) Mayfield, H. G.; Bull, W. E. *SECTION A I Norgan Ic, P Hysica I, and T Heoret Ica 1 Chemistry Co-Ordinating Tendencies of the Hexaf Luorophosphate Ion*.

(76) *Chapman et Al*.

(77) Bini, R.; Chiappe, C.; Marmugi, E.; Pieraccini, D. The “Non-Nucleophilic” Anion [Tf2N]- Competes with the Nucleophilic Br-: An Unexpected Trapping in the Dediazoniation Reaction in Ionic Liquids. *Chemical Communications* **2006**, No. 8, 897–899. https://doi.org/10.1039/b514988f.

(78) Hanson, C. S.; Psaltakis, M. C.; Cortes, J. J.; Siddiqi, S. S.; Devery, J. J. Investigation of Lewis Acid-Carbonyl Solution Interactions via Infrared-Monitored Titration. *Journal of Organic Chemistry* **2020**, *85* (2), 820–832. https://doi.org/10.1021/acs.joc.9b02822.

(79) Hanson, C. S.; Psaltakis, M. C.; Cortes, J. J.; Devery, J. J. Catalyst Behavior in Metal-Catalyzed Carbonyl-Olefin Metathesis. *J Am Chem Soc* **2019**, *141* (30), 11870–11880. https://doi.org/10.1021/jacs.9b02613.

(80) Malakar, T.; Hanson, C. S.; Devery, J. J.; Zimmerman, P. M. Combined Theoretical and Experimental Investigation of Lewis Acid-Carbonyl Interactions for Metathesis. *ACS Catalysis* **2021**, *11* (8), 4381–4394. https://doi.org/10.1021/acscatal.0c05277.

(81) Hull, S.; Keen, D. A. *Pressure-Induced Phase Transitions in AgCl, AgBr, and AgI*.

(82) Rodriguez-Ruiz, V.; Carlino, R.; Bezzenine-Lafollée, S.; Gil, R.; Prim, D.; Schulz, E.; Hannedouche, J. Recent Developments in Alkene Hydro-Functionalisation Promoted by Homogeneous Catalysts Based on Earth Abundant Elements: Formation of C-N, C-O and C-P Bond. *Dalton Transactions*. Royal Society of Chemistry July 21, 2015, pp 12029–12059. https://doi.org/10.1039/c5dt00280j.

(83) Ozawa, T.; Kurahashi, T.; Matsubara, S. Manganese Porphyrin Catalyzed Cycloisomerization of Enynes. *Organic Letters* **2012**, *14* (12), 3008–3011. https://doi.org/10.1021/ol301416f.

(84) Ic00219a025.

(85) Honeychuck, R. v; Hersh, W. H. *) And 1.954 (11) A (3b), 2.186 (3) and 1.979 (3) A (3c), 2.168 (7) and 1.500 (14) A (5*; 1989; Vol. 28.

(86) Gowik, P.; Klapiitke, T.; Thewalt, U. *Metallocen-Chemie Hochfluorierter Ligand-Systeme XI *. Synthese Und Charakterisierung von Cp,Ti(SbF,) 2 Und Cp,Ti(Sb, F,) 2; Struktur von Cp,Ti(SbF,) 2 Und Cp2V(SbF,) 2*; Elsevier Sequoia S.A, 1990.

(87) Dash, C.; Das, A.; Yousufuddin, M.; Dias, H. V. R. Isolable, Copper(I) Dicarbonyl Complexes Supported by N-Heterocyclic Carbenes. *Inorganic Chemistry* **2013**, *52* (3), 1584–1590. https://doi.org/10.1021/ic302455y.

(88) Smirnova, E. S.; Muñoz Molina, J. M.; Johnson, A.; Bandeira, N. A. G.; Bo, C.; Echavarren, A. M. Polynuclear Gold [Au I] 4 , [Au I] 8 , and Bimetallic [Au I 4 Ag I] Complexes: C−H Functionalization of Carbonyl Compounds and Homogeneous Carbonylation of Amines . *Angewandte Chemie* **2016**, *128* (26), 7613–7617. https://doi.org/10.1002/ange.201603200.

(89) Bour, C.; Monot, J.; Tang, S.; Guillot, R.; Farjon, J.; Gandon, V. Structure, Stability, and Catalytic Activity of Fluorine-Bridged Complexes IPr·GaCl2(μ-F)EFn -1 (EFn- = SbF6-, PF6-, or BF 4-). *Organometallics* **2014**, *33* (2), 594–599. https://doi.org/10.1021/om4012054.

(90) Kavoosi, A.; Fillion, E. Synthesis and Characterization of Tricarbastannatranes and Their Reactivity in B(C 6 F 5) 3 -Promoted Conjugate Additions . *Angewandte Chemie* **2015**, *127* (18), 5578–5582. https://doi.org/10.1002/ange.201500983.

(91) Michelet, B.; Colard-Itté, J. R.; Thiery, G.; Guillot, R.; Bour, C.; Gandon, V. Dibromoindium(Iii) Cations as a π-Lewis Acid: Characterization of [IPr·InBr2][SbF6] and

Its Catalytic Activity towards Alkynes and Alkenes. *Chemical Communications* **2015**, *51* (34), 7401–7404. https://doi.org/10.1039/c5cc00740b.

(92) Cornella, J.; Martin, R. Ni-Catalyzed Stereoselective Arylation of Inert C-O Bonds at Low Temperatures. *Organic Letters* **2013**, *15* (24), 6298–6301. https://doi.org/10.1021/ol4031815.

(93) Kshirsagar, U. A.; Regev, C.; Parnes, R.; Pappo, D. Iron-Catalyzed Oxidative Cross-Coupling of Phenols and Alkenes. *Organic Letters* **2013**, *15* (12), 3174–3177. https://doi.org/10.1021/ol401532a.

(94) Bao, L.-L.; Iu, Z.-Q. Tetrahydropyrrolization of Resveratrol and Other Stilbenes Improves Inhibitory Effects on DNA Oxidation. https://doi.org/10.1002/cmdc.201600205:NMR.

(95) Konishi, H.; Ueda, T.; Muto, T.; Manabe, K. Remarkable Improvement Achieved by Imidazole Derivatives in Ruthenium-Catalyzed Hydroesterification of Alkenes Using Formates. *Organic Letters* **2012**, *14* (18), 4722–4725. https://doi.org/10.1021/ol301850y.

(96) Yoo, K. S.; Yoon, C. H.; Jung, K. W. Oxidative Palladium(II) Catalysis: A Highly Efficient and Chemoselective Cross-Coupling Method for Carbon-Carbon Bond Formation under Base-Free and Nitrogenous-Ligand Conditions. *J Am Chem Soc* **2006**, *128* (50), 16384–16393. https://doi.org/10.1021/ja063710z.

(97) Kobayashi, K.; Ueno, M.; Kondo, Y. Phosphazene Base-Catalyzed Condensation of Trimethylsilylacetate with Carbonyl Compounds. *Chemical Communications* **2006**, No. 29, 3128–3130. https://doi.org/10.1039/b606056k.

(98) Charette, A. B.; Molinaro, C.; Brochu, C. Catalytic Asymmetric Cyclopropanation of Allylic Alcohols with Titanium-TADDOLate: Scope of the Cyclopropanation Reaction. *J Am Chem Soc* **2001**, *123* (49), 12168–12175. https://doi.org/10.1021/ja0108382.

(99) Hodgson, D. M.; Ying, K. C.; Nuzzo, I.; Freixas, G.; Kulikiewicz, K. K.; Cleator, E.; Paris, J. M. Intramolecular Cyclopropanation of Unsaturated Terminal Epoxides and Chlorohydrins. *J Am Chem Soc* **2007**, *129* (14), 4456–4462. https://doi.org/10.1021/ja0672932.

(100) Usui, I.; Schmidt, S.; Breit, B. Dual Palladium-and Proline-Catalyzed Allylic Alkylation of Enolizable Ketones and Aldehydes with Allylic Alcohols. *Organic Letters* **2009**, *11* (6), 1453–1456. https://doi.org/10.1021/ol9001812.

(101) Oppolzer, W.; Spivey, A. C.; Bochet, C. G. *1991,56, 2988 and References Mentioned Therein. Cf.\ Martin, S. F. The Amaryllidaceae Alkaloids*; Academic Press, 1994; Vol. 116.

(102) Daniel Little, R.; Carroll, G. L.; Petersen, J. L.; Tetrahedron Symp, K. Total Synthesis of the Marine Natural Product A9(12)-Capnellene. Reversal of Regiochemistry in the Intramolecular 1,3-Diyl Trapping Reaction. *Marine Natural Products, Chemical and Biological Perspectives* **1983**, *105* (2), 7129–7130.

(103) le Nôtre, J.; Touzani, R.; Lavastre, O.; Bruneau, C.; Dixneuf, P. H. Homologation of Monoterpenoids into New Sesquiterpenoids via Tandem Isomerisation/Claisen Rearrangement Reactions with Three-Component Ruthenium Catalysts, and Ru(Methallyl)2 (COD) Revealed by High Throughput Screening Techniques. *Advanced Synthesis and Catalysis* **2005**, *347* (6), 783–791. https://doi.org/10.1002/adsc.200404391.

(104) Aebi, J. D.; Deyo, D. T.; Sun, C. Q.; Guillaume, D.; Dunlap, B.; Rich, D. H. *Synthesis, Conformation, and Immunosuppressive Activities of Three Analogues of Cyclosporin A Modified in the 1-Position1 Both Conformations Have a Type IT 0-Tum for Residues 2-*·*5 and a Cis Amide Bond Between*; 1990; Vol. 33.

(105) Casey, C. P.; Bertz, S. H.; Burkhardt, T. J. *REACTION OF METAL-CARBENE COMPLEXES WITH OIAZOALKANES. A VERSATILE VINYL ETHER SYNTHESIS*; PequDon Pram, 1973.

(106) Banks, J. L.; Beard, H. S.; Cao, Y.; Cho, A. E.; Damm, W.; Farid, R.; Felts, A. K.; Halgren, T. A.; Mainz, D. T.; Maple, J. R.; Murphy, R.; Philipp, D. M.; Repasky, M. P.; Zhang, L. Y.; Berne, B. J.; Friesner, R. A.; Gallicchio, E.; Levy, R. M. Integrated Modeling Program, Applied Chemical Theory (IMPACT). *Journal of Computational Chemistry*. December 2005, pp 1752–1780. https://doi.org/10.1002/jcc.20292.

(107) Shao, Y.; Gan, Z.; Epifanovsky, E.; Gilbert, A. T. B.; Wormit, M.; Kussmann, J.; Lange, A. W.; Behn, A.; Deng, J.; Feng, X.; Ghosh, D.; Goldey, M.; Horn, P. R.; Jacobson, L. D.; Kaliman, I.; Khaliullin, R. Z.; Kuš, T.; Landau, A.; Liu, J.; Proynov, E. I.; Rhee, Y. M.; Richard, R. M.; Rohrdanz, M. A.; Steele, R. P.; Sundstrom, E. J.; Woodcock, H. L.; Zimmerman, P. M.; Zuev, D.; Albrecht, B.; Alguire, E.; Austin, B.; Beran, G. J. O.; Bernard, Y. A.; Berquist, E.; Brandhorst, K.; Bravaya, K. B.; Brown, S. T.; Casanova, D.; Chang, C. M.; Chen, Y.; Chien, S. H.; Closser, K. D.; Crittenden, D. L.; Diedenhofen, M.; Distasio, R. A.; Do, H.; Dutoi, A. D.; Edgar, R. G.; Fatehi, S.; Fusti-Molnar, L.; Ghysels, A.; Golubeva-Zadorozhnaya, A.; Gomes, J.; Hanson-Heine, M. W. D.; Harbach, P. H. P.; Hauser, A. W.; Hohenstein, E. G.; Holden, Z. C.; Jagau, T. C.; Ji, H.; Kaduk, B.; Khistyaev, K.; Kim, J.; Kim, J.; King, R. A.; Klunzinger, P.; Kosenkov, D.; Kowalczyk, T.; Krauter, C. M.; Lao, K. U.; Laurent, A. D.; Lawler, K. v.; Levchenko, S. v.; Lin, C. Y.; Liu, F.; Livshits, E.; Lochan, R. C.; Luenser, A.; Manohar, P.; Manzer, S. F.; Mao, S. P.; Mardirossian, N.; Marenich, A. v.; Maurer, S. A.; Mayhall, N. J.; Neuscamman, E.; Oana, C. M.; Olivares-Amaya, R.; Oneill, D. P.; Parkhill, J. A.; Perrine, T. M.; Peverati, R.;

Prociuk, A.; Rehn, D. R.; Rosta, E.; Russ, N. J.; Sharada, S. M.; Sharma, S.; Small, D. W.; Sodt, A.; Stein, T.; Stück, D.; Su, Y. C.; Thom, A. J. W.; Tsuchimochi, T.; Vanovschi, V.; Vogt, L.; Vydrov, O.; Wang, T.; Watson, M. A.; Wenzel, J.; White, A.; Williams, C. F.; Yang, J.; Yeganeh, S.; Yost, S. R.; You, Z. Q.; Zhang, I. Y.; Zhang, X.; Zhao, Y.; Brooks, B. R.; Chan, G. K. L.; Chipman, D. M.; Cramer, C. J.; Goddard, W. A.; Gordon, M. S.; Hehre, W. J.; Klamt, A.; Schaefer, H. F.; Schmidt, M. W.; Sherrill, C. D.; Truhlar, D. G.; Warshel, A.; Xu, X.; Aspuru-Guzik, A.; Baer, R.; Bell, A. T.; Besley, N. A.; Chai, J. da; Dreuw, A.; Dunietz, B. D.; Furlani, T. R.; Gwaltney, S. R.; Hsu, C. P.; Jung, Y.; Kong, J.; Lambrecht, D. S.; Liang, W.; Ochsenfeld, C.; Rassolov, V. A.; Slipchenko, L. v.; Subotnik, J. E.; van Voorhis, T.; Herbert, J. M.; Krylov, A. I.; Gill, P. M. W.; Head-Gordon, M. Advances in Molecular Quantum Chemistry Contained in the Q-Chem 4 Program Package. *Molecular Physics* **2015**, *113* (2), 184–215. https://doi.org/10.1080/00268976.2014.952696.

(108) Zimmerman, P. M. Single-Ended Transition State Finding with the Growing String Method. *Journal of Computational Chemistry* **2015**, *36* (9), 601–611. https://doi.org/10.1002/jcc.23833.

(109) Zimmerman, P. M. Growing String Method with Interpolation and Optimization in Internal Coordinates: Method and Examples. *Journal of Chemical Physics* **2013**, *138* (18). https://doi.org/10.1063/1.4804162.

(110) Jafari, M.; Zimmerman, P. M. Reliable and Efficient Reaction Path and Transition State Finding for Surface Reactions with the Growing String Method. *Journal of Computational Chemistry* **2017**, *38* (10), 645–658. https://doi.org/10.1002/jcc.24720.

(111) Zimmerman, P. Reliable Transition State Searches Integrated with the Growing String Method. *Journal of Chemical Theory and Computation* **2013**, *9* (7), 3043–3050. https://doi.org/10.1021/ct400319w.

(112) Metz, B.; Stoll, H.; Dolg, M. Small-Core Multiconfiguration-Dirac-Hartree-Fock-Adjusted Pseudopotentials for Post-d Main Group Elements: Application to PbH and PbO. *Journal of Chemical Physics* **2000**, *113* (7), 2563–2569. https://doi.org/10.1063/1.1305880.

(113) Peterson, K. A.; Figgen, D.; Goll, E.; Stoll, H.; Dolg, M. Systematically Convergent Basis Sets with Relativistic Pseudopotentials. II. Small-Core Pseudopotentials and Correlation Consistent Basis Sets for the Post-d Group 16-18 Elements. *Journal of Chemical Physics* **2003**, *119* (21), 11113–11123. https://doi.org/10.1063/1.1622924.

(114) Leininger, T.; Nicklass, A.; Kiichle, W.; Stoll, H.; Dolg, M.; Bergner, A. *PHYSICS LETTERS ELSEVIER The Accuracy of the Pseudopotential Approximation: Non-Frozen-Core Effects for Spectroscopic Constants of Alkali Fluorides XF (X = K, Rb, Cs)*; 1996; Vol. 255.

(115) Kaupp, M.; Schleyer, P. V. R.; Stoll, H.; Preuss, H. Pseudopotential Approaches to Ca, Sr, and Ba Hydrides. Why Are Some Alkaline Earth MX2 Compounds Bent? *The Journal of Chemical Physics* **1991**, *94* (2), 1360–1366. https://doi.org/10.1063/1.459993.

(116) Marenich, A. v.; Cramer, C. J.; Truhlar, D. G. Universal Solvation Model Based on Solute Electron Density and on a Continuum Model of the Solvent Defined by the Bulk Dielectric Constant and Atomic Surface Tensions. *Journal of Physical Chemistry B* **2009**, *113* (18), 6378–6396. https://doi.org/10.1021/jp810292n.

(117) Djurovic, A.; Vayer, M.; Li, Z.; Guillot, R.; Baltaze, J. P.; Gandon, V.; Bour, C. Synthesis of Medium-Sized Carbocycles by Gallium-Catalyzed Tandem Carbonyl-Olefin Metathesis/Transfer Hydrogenation. *Organic Letters* **2019**, *21* (19), 8132–8137. https://doi.org/10.1021/acs.orglett.9b03240.

(118) Catti, L.; Tiefenbacher, K. Brønsted-Säure-Katalysierte Carbonyl-Olefin-Metathese in Einer Selbstorganisierten Supramolekularen Wirtstruktur. *Angewandte Chemie* **2018**, *130* (44), 14797–14800. https://doi.org/10.1002/ange.201712141.

(119) Lambert, T. H. Development of a Hydrazine-Catalyzed Carbonyl-Olefin Metathesis Reaction. *Synlett* **2019**, *30* (17), 1954–1965. https://doi.org/10.1055/s-0039-1689924.

(120) Ohkubo, K.; Menon, S. C.; Orita, A.; Otera, J.; Fukuzumi, S. Quantitative Evaluation of Lewis Acidity of Metal Ions with Different Ligands and Counterions in Relation to the Promoting Effects of Lewis Acids on Electron Transfer Reduction of Oxygen. *Journal of Organic Chemistry* **2003**, *68* (12), 4720–4726. https://doi.org/10.1021/jo034258u.

(121) Evans, D. A.; Lectka, T.; Miller, S. J.; Murry, J. A.; Matt, P.; Norcross, R. D.; Johnson, J. S.; Kozlowski, M. C.; Ghosh, A. K.; Mathivanan, P.; Cappiello, J.; Krishnan, K.; Johannsen, M.; Jørgensen, K. A. *C 2-Symmetric Copper(II) Complexes as Chiral Lewis Acids. Enantioselective Catalysis of the Glyoxylate-Ene Reaction*; 1993; Vol. 115.

(122) Johnson, J. S.; Evans, D. A. Chiral Bis(Oxazoline) Copper(II) Complexes: Versatile Catalysts for Enantioselective Cycloaddition, Aldol, Michael, and Carbonyl Ene Reactions. *Accounts of Chemical Research* **2000**, *33* (6), 325–335. https://doi.org/10.1021/ar960062n.

(123) Hilt, G.; Pünner, F.; Möbus, J.; Naseri, V.; Bohn, M. A. A Lewis Acidity Scale in Relation to Rate Constants of Lewis Acid Catalyzed Organic Reactions. *European Journal of Organic Chemistry* **2011**, No. 30, 5962–5966. https://doi.org/10.1002/ejoc.201101029.

(124) *INFRARED SPECTRA OF XANTH0NE:LEWIS ACID COMPLEXES*?*

(125) Tran, U. P. N.; Oss, G.; Breugst, M.; Detmar, E.; Pace, D. P.; Liyanto, K.; Nguyen, T. v. Carbonyl-Olefin Metathesis Catalyzed by Molecular Iodine. *ACS Catalysis* **2019**, *9* (2), 912–919. https://doi.org/10.1021/acscatal.8b03769.

(126) Wang, R.; Chen, Y.; Shu, M.; Zhao, W.; Tao, M.; Du, C.; Fu, X.; Li, A.; Lin, Z. AuCl3-Catalyzed Ring-Closing Carbonyl–Olefin Metathesis. *Chemistry - A European Journal* **2020**, *26* (9), 1941–1946. https://doi.org/10.1002/chem.201905199.

(127) Jermaks, J.; Quach, P. K.; Seibel, Z. M.; Pomarole, J.; Lambert, T. H. Ring-Opening Carbonyl-Olefin Metathesis of Norbornenes. *Chemical Science* **2020**, *11* (30), 7884–7895. https://doi.org/10.1039/d0sc02243h.

(128) Lambert, T. H. Development of a Hydrazine-Catalyzed Carbonyl-Olefin Metathesis Reaction. *Synlett* **2019**, *30* (17), 1954–1965. https://doi.org/10.1055/s-0039-1689924.

(129) Zhang, Y.; Jermaks, J.; MacMillan, S. N.; Lambert, T. H. Synthesis of 2 H-Chromenes via Hydrazine-Catalyzed Ring-Closing Carbonyl-Olefin Metathesis. *ACS Catalysis* **2019**, *9* (10), 9259–9264. https://doi.org/10.1021/acscatal.9b03656.

(130) Hong, X.; Liang, Y.; Griffith, A. K.; Lambert, T. H.; Houk, K. N. Distortion-Accelerated Cycloadditions and Strain-Release-Promoted Cycloreversions in the Organocatalytic Carbonyl-Olefin Metathesis. *Chemical Science* **2014**, *5* (2), 471–475. https://doi.org/10.1039/c3sc52882k.

(131) Griffith, A. K.; Vanos, C. M.; Lambert, T. H. Organocatalytic Carbonyl-Olefin Metathesis. *J Am Chem Soc* **2012**, *134* (45), 18581–18584. https://doi.org/10.1021/ja309650u.

(132) Musacchio, A. J.; Nguyen, L. Q.; Beard, G. H.; Knowles, R. R. Catalytic Olefin Hydroamination with Aminium Radical Cations: A Photoredox Method for Direct C-N Bond Formation. *J Am Chem Soc* **2014**, *136* (35), 12217–12220. https://doi.org/10.1021/ja5056774.

(133) Fernández-Mateos, A.; Madrazo, S. E.; Teijón, P. H.; González, R. R. Radical Cyclization of Epoxy Vinyl- and Allylsulfones Promoted by Titanocene Chloride. *Journal of Organic Chemistry* **2015**, *80* (9), 4378–4391. https://doi.org/10.1021/acs.joc.5b00206.

(134) Kuriyama, Y.; Sasano, Y.; Hoshino, Y.; Uesugi, S. ichiro; Yamaichi, A.; Iwabuchi, Y. Highly Regioselective 5-Endo-Tet Cyclization of 3,4-Epoxy Amines into 3-Hydroxypyrrolidines Catalyzed by La(OTf)3. *Chemistry - A European Journal* **2021**, *27* (6), 1961–1965. https://doi.org/10.1002/chem.202004455.

(135) Johnson, L. A.; Dunbabin, A.; Benton, J. C. R.; Mart, R. J.; Allemann, R. K. Modular Chemoenzymatic Synthesis of Terpenes and Their Analogues. *Angewandte Chemie - International Edition* **2020**, *59* (22), 8486–8490. https://doi.org/10.1002/anie.202001744.

(136) Lucke, A. J.; Young, D. J. Electrophilic Cleavage of Cyclopropylmethystannanes: An Experimental Comparison of σ-σ and σ-π Conjugation. *Journal of Organic Chemistry* **2005**, *70* (9), 3579–3583. https://doi.org/10.1021/jo047822p.

(137) Cai, Z.; Yongpruksa, N.; Harmata, M. Total Synthesis of the Terpenoid Buddledone A: 11-Membered Ring-Closing Metathesis. *Organic Letters* **2012**, *14* (7), 1661–1663. https://doi.org/10.1021/ol300400x.

(138) Anderson, T. E.; Woerpel, K. A. Strain-Promoted Oxidation of Methylenecyclopropane Derivatives Using N-Hydroxyphthalimide and Molecular Oxygen in the Dark. *Organic Letters* **2020**, *22* (14), 5690–5694. https://doi.org/10.1021/acs.orglett.0c02075.

(139) Xu, B.; Shi, M. Ring-Opening Reactions of Methylenecyclopropanes Promoted by Metal Halides. *Organic Letters* **2003**, *5* (9), 1415–1418. https://doi.org/10.1021/ol034142k.

(140) Labes, R.; Battilocchio, C.; Mateos, C.; Cumming, G. R.; de Frutos, O.; Rincón, J. A.; Binder, K.; Ley, S. v. Chemoselective Continuous Ru-Catalyzed Hydrogen-Transfer Oppenauer-Type Oxidation of Secondary Alcohols. *Organic Process Research and Development* **2017**, *21* (9), 1419–1422. https://doi.org/10.1021/acs.oprd.7b00190.

(141) Labes, R.; González-Calderón, D.; Battilocchio, C.; Mateos, C.; Cumming, G. R.; de Frutos, O.; Rincón, J. A.; Ley, S. v. Rapid Continuous Ruthenium-Catalysed Transfer Hydrogenation of Aromatic Nitriles to Primary Amines. *Synlett* **2017**, *28* (20), 2855–2858. https://doi.org/10.1055/s-0036-1589096.

(142) Köckinger, M.; Hone, C. A.; Gutmann, B.; Hanselmann, P.; Bersier, M.; Torvisco, A.; Kappe, C. O. Scalable Continuous Flow Process for the Synthesis of Eflornithine Using Fluoroform as Difluoromethyl Source. *Organic Process Research and Development* **2018**, *22* (11), 1553–1563. https://doi.org/10.1021/acs.oprd.8b00318.

(143) Mata, A.; Hone, C. A.; Gutmann, B.; Moens, L.; Kappe, C. O. Continuous-Flow Pd-Catalyzed Carbonylation of Aryl Chlorides with Carbon Monoxide at Elevated Temperature and Pressure. *ChemCatChem* **2019**, *11* (3), 997–1001. https://doi.org/10.1002/cctc.201801974.

(144) Labes, R.; Mateos, C.; Battilocchio, C.; Chen, Y.; Dingwall, P.; Cumming, G. R.; Rincón, J. A.; Nieves-Remacha, M. J.; Ley, S. v. Fast Continuous Alcohol Amination Employing a

Hydrogen Borrowing Protocol. *Green Chemistry* **2019**, *21* (1), 59–63. https://doi.org/10.1039/c8gc03328e.

(145) Sagmeister, P.; Kaldre, D.; Sedelmeier, J.; Moessner, C.; Püntener, K.; Kummli, D.; Williams, J. D.; Kappe, C. O. Intensified Continuous Flow Synthesis and Workup of 1,5-Disubstituted Tetrazoles Enhanced by Real-Time Process Analytics. *Organic Process Research and Development* **2021**, *25* (5), 1206–1214. https://doi.org/10.1021/acs.oprd.1c00096.

(146) Sambiagio, C.; Ferrari, M.; van Beurden, K.; Ca', N. della; van Schijndel, J.; Noel, T. Continuous-Flow Synthesis of Pyrylium Tetrafluoroborates: Application to Synthesis of Katritzky Salts and Photoinduced Cationic RAFT Polymerization. *Organic Letters* **2021**, *23* (6), 2042–2047. https://doi.org/10.1021/acs.orglett.1c00178.

(147) Quesnel, J. S.; Kayser, L. v.; Fabrikant, A.; Arndtsen, B. A. Acid Chloride Synthesis by the Palladium-Catalyzed Chlorocarbonylation of Aryl Bromides. *Chemistry - A European Journal* **2015**, *21* (26), 9550–9555. https://doi.org/10.1002/chem.201500476.

(148) Schröder, N.; Wencel-Delord, J.; Glorius, F. High-Yielding, Versatile, and Practical [Rh(III)Cp*]-Catalyzed Ortho Bromination and Iodination of Arenes. *J Am Chem Soc* **2012**, *134* (20), 8298–8301. https://doi.org/10.1021/ja302631j.

(149) Mukhopadhyay, S.; Batra, S. Direct Transformation of Arylamines to Aryl Halides via Sodium Nitrite and N-Halosuccinimide. *Chemistry - A European Journal* **2018**, *24* (55), 14622–14626. https://doi.org/10.1002/chem.201803347.

(150) Moreira, J. A.; Corrêa, A. G. Enantioselective Synthesis of Three Stereoisomers of 5,9-Dimethylpentadecane, Sex Pheromone Component of Leucoptera Coffeella, from (-)-

Isopulegol. *Tetrahedron Asymmetry* **2003**, *14* (23), 3787–3795.

https://doi.org/10.1016/j.tetasy.2003.09.030.